

- 1 N. D. Coggeshall, "A Mass Spectrometer of Wide Versatility", (Abstract) Physical Review 61, 738 (1942)
- 2 E. B. Jordan & N. D. Coggeshall, "Measurement of Relative Abundance with the Mass Spectrometer," Journal of Applied Physics, 13, 539 (1942)
- 3 N. D. Coggeshall, "Discrimination in Mass Spectrometer Ion Sources," Journal of Chemical Physics, 12, 19 (1944)
- 4 N. D. Coggeshall & E. B. Jordan, "An Experimental Mass Spectrometer," Review of Scientific Instruments, 14, 125 (1943)
- 5 N. D. Coggeshall & M. Muskat, "The Paths of Ions and Electrons in Non-Uniform Magnetic Fields," Physical Review (Abstract), 65, 325 (1944)
- 6 N. D. Coggeshall & M. Muskat, "The Paths of Ions and Electrons in Non-Uniform Magnetic Fields," Physical Review, 66, 187 (1944)
- 7 N. D. Coggeshall, "Gas Cell for Beckman Quartz Spectrophotometer," Industrial & Engineering Chemistry, Analytical Edition, 17, 513 (1945)
- 8 N. D. Coggeshall, "The Paths of Ions and Electrons in Non-Uniform, Crossed Electric and Magnetic Fields," (Abstract) Physical Review, 68, 98 (1945)
- 9 E. Topanelian & N. D. Coggeshall, "A Metal Packless Vacuum Valve," Review of Scientific Instruments, 17, 38 (1946)
- 10 N. D. Coggeshall "Intra-Red Spectroscopy," Chemical Industries, 58, 256 (1946)
- 11 N. D. Coggeshall, "The Mass Spectrometer," Chemical Industries, 58, 420 (1946)

- 12 N. D. Coggeshall & J. A. Hipple Jr. "The Mass Spectrometer and Its Applications", Colloid Chemistry Vol. VI, edited by Jerome Alexander, Reinhold Publishing Corp. New York, 1946
- 13 R. G. Russell & N. D. Coggeshall, "Ultra-Violet and Visible Spectroscopy", Chemical Industries, 58, 586 (1946)
- 14 N. D. Coggeshall & E. L. Saier, "The Infra-Red Absorption of Methane as Influenced by Foreign Gases", ~~Physical Review~~ (Abstract), Physical Review, 69, 257 (1946)
- 15 N. D. Coggeshall & E. L. Saier, "Analyses of Light Gases by Infra-Red Absorption", Journal of Applied Physics, 17, 450 (1946)
- 16 N. D. Coggeshall, "Infra-Red Absorption Cell For Liquids" Review of Scientific Instruments, 17, 343 (1946)
- 17 N. D. Coggeshall, "The Paths of Ions and Electrons in ~~Non-Uniform~~ Non-Uniform Crossed Electric and Magnetic Fields", Physical Review, 70, 270 (1946)
- 18 N. D. Coggeshall & E. L. Saier, "The Pressure Broadening in the Infra-Red and Optical Collision Diameters" Journal of Chemical Physics, 15, 65 (1947)
- 19 N. D. Coggeshall, "Fringing Flux Corrections for Magnetic Focussing Devices", Physical Review, 71, 482 (1947) (Abstract)
- 20 N. D. Coggeshall, "Infra-Red Spectroscopic Investigations of Hydrogen Bonding in Hindered and Unhindered Phenols", J. A. C. S., 69, 1620 (1947)
- 21 N. D. Coggeshall, "Fringing Flux Corrections for Magnetic Focusing Devices", J. Applied Physics, 18, 855 (1947)
- 22 Eleanor L. Saier & N. D. Coggeshall, "Infrared Analysis of Organic Mixtures Using C-H Band Structure Resolved by a Lithium Fluoride Prism", Analytical Chemistry, 20, 812 (1948)

23¹ "Method of Cementing Wells", U.S. Patent 2,451,472
6 Oct. 12, 1948, N.D. Coggeshall

24¹ "Influence of Solvents, Hydrogen Bonding, Temperature
and Conjugation on the Ultraviolet Spectra of Phenols
and Aromatic Hydrocarbons", N.D. Coggeshall & E.M. Lang,
J. A. C. S., 70, 3283 (1948)

25¹ M. Muskat & N.D. Coggeshall, "Method of Geophysical Exploration
6 by Microwaves", U.S. Patent 2,455,940. 2

26¹ M. Muskat & N.D. Coggeshall, "Geophysical Prospecting in Bore
6 Holes by Microwaves", U.S. Patent 2,455,941. 3

27¹ N.D. Coggeshall & M. Muskat, "Geophysical Exploration &
6 of Bore Holes by Microwaves", U.S. Patent 2,455,942.

28¹ M. Muskat & N.D. Coggeshall, "Method of and Apparatus for
Measuring the Electrical Properties and Surface
6 Characteristics of Materials", U.S. Patent 2,456,012.

29¹ N.D. Coggeshall & N.F. Kerr, "Electron Gun for Mass
6 Spectrometers", U.S. Patent 2,457,530.

30¹ M. Muskat & N.D. Coggeshall, "Method of Determining
6 the Fluid Content of Well Cores", U.S. Patent 2,458,093

31¹ N.D. Coggeshall & M. Muskat, "Automatic System of Process
Control by Infrared Spectrometry" U.S. Patent 2,462,946

32¹ M. Muskat & N.D. Coggeshall, "Apparatus for Testing Insulating
6 Materials", U.S. Patent 2,463,297.

33¹ N.D. Coggeshall & A.S. Glessner Jr., "Ultraviolet Absorption
Analysis for Naphthalenes", Analytical Chemistry, 21,
550 (1949)

34¹ N.D. Coggeshall & M. Muskat, "Method and Apparatus for
Separating Charged Particles of Different Masses", U.S.
Patent 2,471,935

- 35^o N. D. Coggeshall, "Hydrogen Bonding and Isomeric Forms in Bis-Phenols" (Abstract), *Phys. Rev.*, 76, 174 (1949)
- 36^o N. D. Coggeshall and A. S. Glessner, "Ultraviolet Absorption Study of the Ionization of Substituted Phenols in Ethanol", *J. A. C. S.*, 71, 3150 (1949)
- 37^o M. Muskat and N. D. Coggeshall, "Method of Detecting Mud Films on Exposed Rock Strata", U.S. Patent 2,484,422.
- 38^o N. D. Coggeshall & N. F. Kerr, "Mass Spectrometer Studies of Thermal Decomposition Products from Hydrocarbon", *J. Chemical Physics*, 17, 1016 (1949)
- 39^o N. D. Coggeshall, "Electrical Logarithm Computer", U.S. Patent 2,497,208.
- 40^o "Optical Properties of Hydrocarbons; Infrared Absorption, Raman, and Ultraviolet Absorption Spectroscopy", - Chapt. 4 of Physical Chemistry of Hydrocarbons, vol. I, edited by A. Farkas, Academic Press, N.Y., 1950
- 41^o "Optical Methods of Hydrocarbon Analysis" - Chapt. 5 of Physical Chemistry of Hydrocarbons, Vol. I, edited by A. Farkas, Academic Press, N.Y., 1950.
- 42^o ~~xxx~~ N. D. Coggeshall, "Determination of Organic Functionality by Molecular Spectroscopy", *Analytical Chemistry*, 22, 381 (1950)
- 43^o "Instrumentation and ~~Automatic~~ Auxiliary Equipment for Automatic Infrared Gas Analyzers", W. J. Happel + N. D. Coggeshall, *Instruments*, 23, 552 (1950)
- 44^o "Electrostatic Interaction in Hydrogen Bonding", N. D. Coggeshall, *Journal of Chemical Physics*, 18, 978 (1950)
- 45^o "Absorption Spectroscopic Studies of Hydrogen Bonding and Isomeric Forms in Bis-phenol Alkanes", *J. A. C. S.*, 72, 2836 (1950)
- 46^o "Solvent Induced Frequency Shifts for Cata-Condensed Aromatics" N. D. Coggeshall + A. Pozefsky, *J. Chem. Phys.* 19, 980 (1951)

- V
- 47¹ "Infrared Absorption Study of Hydrogen Bonding Equilibria"
N.D. Coggeshall & E.L. Saier, J.A.C.S., 23, 5414 (1951)
- 48¹ "Infrared Absorption Studies of Carbon-Hydrogen Stretching
Frequencies in Sulfurized and Oxygenated Materials", A. Pozelsky
& N.D. Coggeshall, Anal. Chem., 23, 1611 (1951)
- 49¹ "Ultraviolet Absorption Determination of C₉ and C₁₀ Aromatics"
M.S. Norris & N.D. Coggeshall, Anal. Chem., 25, 183 (1953)
- 50¹ "Spectroscopic Functional Group Analysis in the Petroleum
Industry", N.D. Coggeshall - Chapter in Vol. I of
Organic Analysis, Interscience Publishers, N.Y., 1953, p. 403.
- 51¹ "Determination of Olefin Group Types - Chromatographic and
Infrared Absorption Techniques", E.L. Saier, A. Pozelsky and
N.D. Coggeshall, Anal. Chem., 26, 1258 (1954)
- 52¹ "Temperature Dependence of Infrared Absorption" R.H. Hughes,
R.J. Martin & N.D. Coggeshall, J. Chem. Phys., 24, 489 (1956)
- 53¹ "Gas Partition Analysis of Light Ends in Gasolines", D.H. Lichtentels,
S.A. Fleck, F.H. Borow & N.D. Coggeshall, Analytical Chemistry,
1376, ~~1375~~ 28 (1956).
- 54¹ N.D. Coggeshall & W.E. Hanson, "Method of Geochemical Prospecting",
U.S. Patent No. 2,767,320 13
- 55¹ "Application of Total Ionization Principles to Mass Spectrometric
Analysis", R.F. Crable & N.D. Coggeshall, Anal. Chem., 310, ~~310~~ 30 (1958)
- 56¹ N.D. Coggeshall, "Chromatographic Method and Apparatus"
U.S. Patent 2,841,005. 14
- 57¹ N.D. Coggeshall, "Multiple-Column Chromatographic Apparatus"
U.S. Patent 2,868,011. 15
- 58¹ N.D. Coggeshall, "Ionization of n-Paraffin Molecules"
J. Chem. Physics, 30, 595 (1959)
- 59¹ J.S. Mathews & N.D. Coggeshall, "Concentration of Impurities From Organic Compounds
by Progressive Freezing", Analytical Chemistry, 31, 1124 (1959)

- Process"
- 60' N.D. Coggeshall, "Continuous Separation ~~Process~~"
 U.S. Patent No. 3,893,955 16
- 61' "Ionization Potentials and Electrostatic Polarization"
 N.D. Coggeshall, J. Chem. Phys., 32, 1265 (1960)
- 62' "The Combination of Methods in the Analysis of Complex Hydrocarbon
 Systems", N.D. Coggeshall & W. Hubis, ASTM Special Technical
 Publication 269 - Symposium on Spectroscopy, 1960 6
- 63' "Quantitative Relations in the Mass Spectra of n-Paraffins",
 N.D. Coggeshall, J. Chem. Phys., 33, 1247 (1960)
- 64' "Effect of Dissolved Oxygen on the Spin-Lattice Relaxation Time
 of Free Radicals in Petroleum Oils", A. J. Saraceno and N.D.
 Coggeshall, J. Chem. Phys., 34, 260 (1961) FPR
- 65' "An Electron Paramagnetic Resonance Investigation of Vanadium
 in Petroleum Oils", A. J. Saraceno, D. T. Fanale and N.D.
 Coggeshall, Analytical Chemistry, 33, 500 (1961) EPR
- 66' N.D. Coggeshall & B. M. Wedner, "Recording Integrator",
 U.S. Patent 2,998,291 17
- 67' "Note on the Statistical Theory of Mass Spectra", J. G. Schug
 and N.D. Coggeshall, J. Chem. Phys., 35, 1146 (1961)
- 68' "Initial ~~Energy~~ Kinetic Energy Discrimination Effects in Crossed-
 Field Ion Sources", N.D. Coggeshall, J. Chem. Physics, 36, 1640 (1962)
 also Advances in Mass Spectrometry, Edited by R. M. Elliott,
 Vol. II, Pergamon Press, 1963, p. 51
- 69' "Sorption-Desorption Method and Apparatus", U.S. Patent
 3,059,478, N.D. Coggeshall, O.K. Doolen & R.D. Wyckoff. 18
- 70' "Studies of Metastable Ion Transitions with a 180°
 Mass Spectrometer", N.D. Coggeshall, J. Chem. Phys., 37, 2167 (1962)
- 71' "Comparison of Mass Spectral Regularities for n-Paraffins and n-Terminal
 Olefins", N.D. Coggeshall, J. Phys. Chem. 67, 183 (1963)

- 19
- 72 N.D. Coggeshall + M.S. Norris, U.S. Patent 3,121,677
"Process For Controlling Carbon Residue Content of Oil"
- 73 " N.D. Coggeshall, F.A. Nelson, O.K. Doolen + G.A. Baker
"A Process Analyzer for Vanadium in Gas Oils"
Proc. of Am. Petr. Institute, Vol. 43, Section III, page 229 (1963)
- 74 N.D. Coggeshall + O.K. Doolen, U.S. Patent 3,203,250
"Sampling Apparatus"
- 75 W.M. Zarella, R.J. Mousseau, N.D. Coggeshall, M.S. Norris +
G.J. Schroyer, "Analysis and Significance of Hydrocarbons
in Subsurface Brines", *Geochimica et Cosmochimica*, 31,
1155 (1967)
- 76 W.F. Benusa + N.D. Coggeshall, U.S. Patent 3,349,625
"Adsorption Measuring Apparatus and Method"

Measurement of Relative Abundance with the Mass Spectrometer

BY E. B. JORDAN AND N. D. COGGESHALL
University of Illinois, Urbana, Illinois

This paper covers the general methods employed in mass spectrometry, machine design, and possible sources of error in relative-abundance measurements which are inherently associated with instrument design. Also included are graphs for determining the critical constants of the usual types of instruments.

INTRODUCTION

THE variety of problems which have recently been studied with the aid of a "relative-abundance" spectrometer makes apparent the growing importance of this instrument in a modern physics laboratory. Not only as an instrument for measuring the natural abundances^{1,2} of the isotopes of an element and for studying the products of ionization and dissociation by electron impact³ may it be used, but also to study the fine variations⁴ in isotopic abundances as related to the origin of the element, to search for faint missing isotopes, and to separate isotopes⁵ in quantities sufficient for disintegration experiments. It is also an indispensable instrument in the study of methods of separating isotopes⁶ and in problems involving the use of separated isotopes as tracers.⁷

As is well known, the mass spectrograph as well as the mass spectrometer can be used for making abundance measurements, and indeed the majority of isotopes as now known were first discovered and their abundances measured by Dr. Aston using a mass spectrograph. Since the problems have now become more specialized, it is more satisfactory to use a spectrometer for abundance measurements and to design a mass spectrograph* primarily for mass measurements, the latter instrument being of inestimable value for this purpose alone. On the other hand, the

abundance spectrometer, although it cannot in any way be used for mass measurements, is designed primarily for the types of problems listed above and is a much simpler instrument to construct, easier to use, and much less expensive.

When used for abundance measurements, a mass spectrograph is inconvenient since a photographic plate is employed to record the different isotopic ions and the procedure of determining abundances from the plate tracks is both more tedious and less reliable than the direct measurements made with a mass spectrometer. This is the case since the density of the image produced on the plate is an unknown function of the intensity of the corresponding ion beam, and it is necessary to make a number of tests, none of which is conclusive separately, before a correct interpretation may be reached. In addition, the ions follow entirely different paths and consequently corrections have to be made for the line breadths.

The abundance spectrometer method of making these measurements, however, is both comparatively easy and quite reliable once the apparatus is set up and working. In this method the isotopic ions are made to follow approximately the same paths and the isotopes are recorded electrically by means of an electrometer tube, the relative heights of the peaks indicating the relative numbers of the isotopes present. With this instrument, it is also possible to measure the ionization potential and the shape of the ionization probability curve for any particular ion, information which is important as evidence for or against the existence of a particular species.

* Recently, when money was granted by the Graduate School Research Board of Illinois for building up a research laboratory in mass spectroscopy, it thus appeared more desirable, in view of these considerations, to build a separate machine for making relative abundance measurements and to use the new mass spectrograph (see reference 8) exclusively for mass measurements. A description of this new spectrometer will be published shortly.

Since the peaks are plotted one at a time and several minutes are required to record the complete spectrum of an element, it does, however, require a steady source of ions.

ION SOURCES

A survey of existing spectrometers⁹⁻¹³ revealed the interesting fact that in every case the ions are drawn from a region in which there is a crossed electric and magnetic field. In most cases the source region is in the same uniform magnetic field that is used to resolve the ions after they leave the source. In those instruments¹² in which this is not the case, an auxiliary magnetic field is supplied by means of a small horseshoe magnet. Even when it does not occur naturally, the presence of a magnetic field in this region is essential to the particular arrangements used. On the other hand, its presence leads to a number of inconveniences, especially in the case of the sector type magnetic field instruments, as well as to a number of small systematic errors, which combined probably amount to no more than one or two percent, depending of course upon the magnitude of the isotopic abundance ratio and the mass difference. For comparison, a brief

description of the different arrangements in common use is included.

The most general arrangement is that shown in Fig. 1. The ions are created by means of an electron beam BB which is moving in a direction perpendicular to the plane of the figure and parallel to the magnetic field. A gas pressure of approximately 10^{-4} mm Hg is usually maintained within this region. The longer sides of the slits S_1 , S_2 are also parallel to the magnetic field and thus to the direction in which the electrons are moving. Ions which are formed in the region BB are accelerated towards the slit S_1 , by means of a weak electric field E_1 (20 to 30 volts/cm). A second acceleration then takes place between the plates P_1 and P_2 in which region they acquire from 300 to 1000 electron-volts energy. After passing through S_2 , the ions may either be bent in a circle by the same uniform magnetic field H , coming to a focus at different positions along the plane S_2F a distance away equal to twice the radius of curvature, or else they may be directed through a neutral region into a V-shaped magnetic field, the focusing properties of which have been discussed by Barber,¹⁴ and Stephens and Hughes.¹⁵

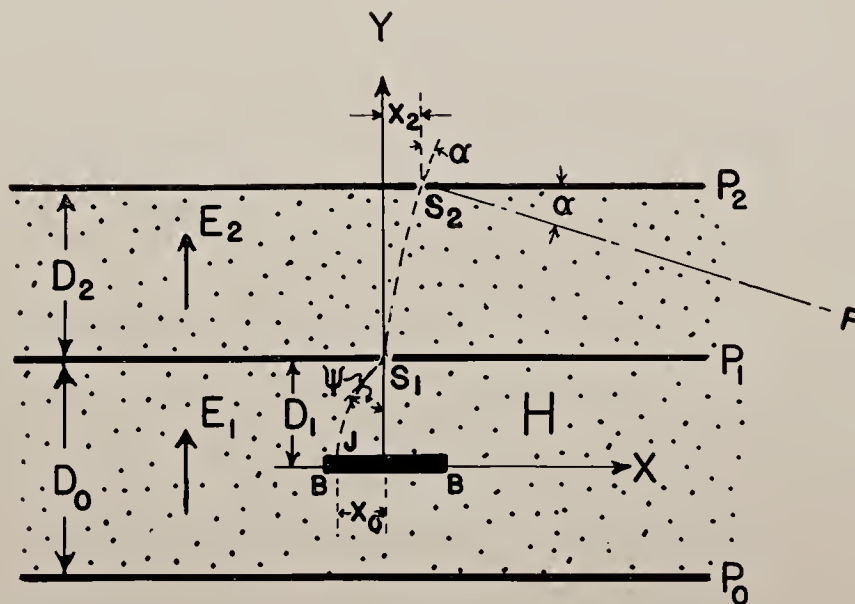


FIG. 1. Schematic cross-section diagram of a crossed field spectrometer source: BB represents the cross section of the electron beam which is used to create the ions; D_1 represents the perpendicular distance from the plane of the beam to the plane of the slit S_1 ; P_0 , P_1 , and P_2 are the plates across which the accelerating potentials are placed; JS_1S_2 is an exaggerated representation of the path of an ion starting from rest in the plane of the electron beam. The magnetic field H is assumed to be pointing out of the paper.

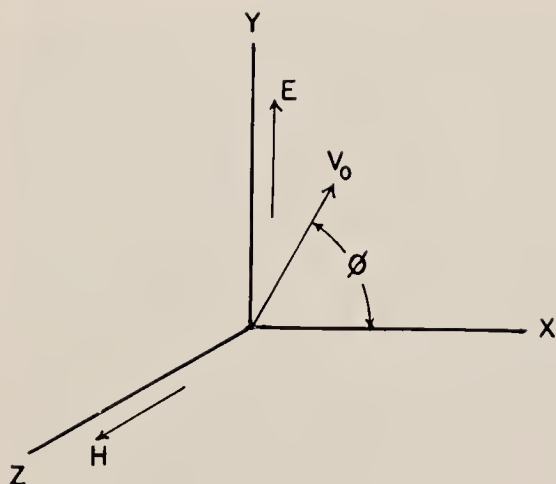


FIG. 2. Arrangement of fields in the source region.

A. Electron Beam

The first problem which is of interest is to find the shape of the electron beam *BB* which is used to create the ions. It is important to know the shape of this beam and whether or not it is influenced appreciably by the electric and magnetic fields since it determines the origin and the conditions under which the ions originate.

Figure 2 is a diagram showing the particular arrangement of fields in the source region. V_0 represents the component of the initial velocity of a charged particle in the *xy* plane, and ϕ the angle that V_0 makes with the *x* axis. The path of a charged particle in such a combination of fields has been discussed by a number of authors.^{16,17} As is well known, its projection on

the *xy* plane is a cycloid, the particular type of cycloid being determined by the initial conditions. The parametric solutions of the differential equations representing this motion are:

$$x = -\frac{V_0}{\gamma} \sin(\phi - \gamma t) + \frac{1}{\gamma} \left(V_0 \sin \phi - \frac{Ec}{H} \sin \gamma t \right) + \frac{Ec}{H} t + x_0, \quad (1)$$

$$y = \frac{V_0}{\gamma} \cos(\phi - \gamma t) - \frac{1}{\gamma} \left(V_0 \cos \phi + \frac{Ec}{H} \cos \gamma t - \frac{Ec}{H} \right) + y_0. \quad (2)$$

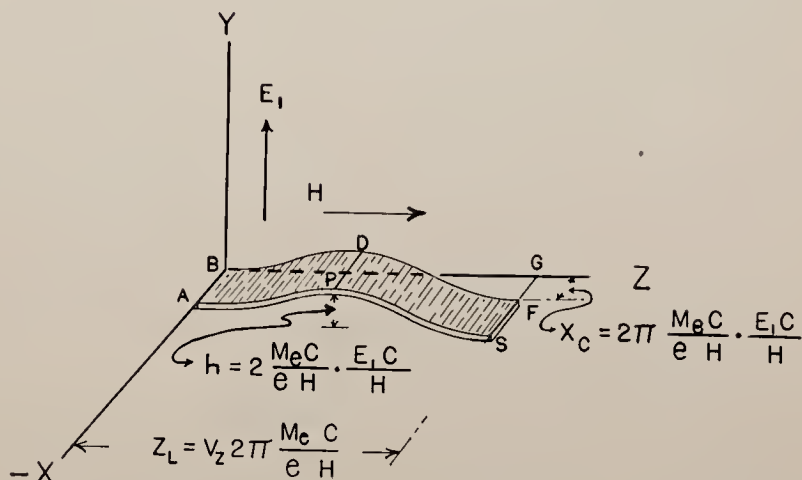
E represents the electric field strength in e.s.u., H the magnetic field strength in e.m.u., t the time in seconds, and γ is defined by the relation

$$\gamma = eH/Mc, \quad (3)$$

where e , M , and c represent the charge in e.s.u., M the mass of the charged particle in grams, and c the velocity of light in cm/sec.

For convenience, let us assume that the incident electron beam is not diverging and that it is moving parallel to the magnetic field H . As no force is exerted in the direction of the magnetic lines of force and since there is no component of the electric field in this direction, the motion of the electrons parallel to the *Z* axis is one of constant velocity. By letting $V_0 = 0$ in Eqs. (1) and (2), which is the case for a non-diverging beam, we see that the projected path of the

FIG. 3. Diagrammatic sketch of one loop of electron beam. The maximum height " h " of the beam as shown is greatly exaggerated in comparison to other dimensions.



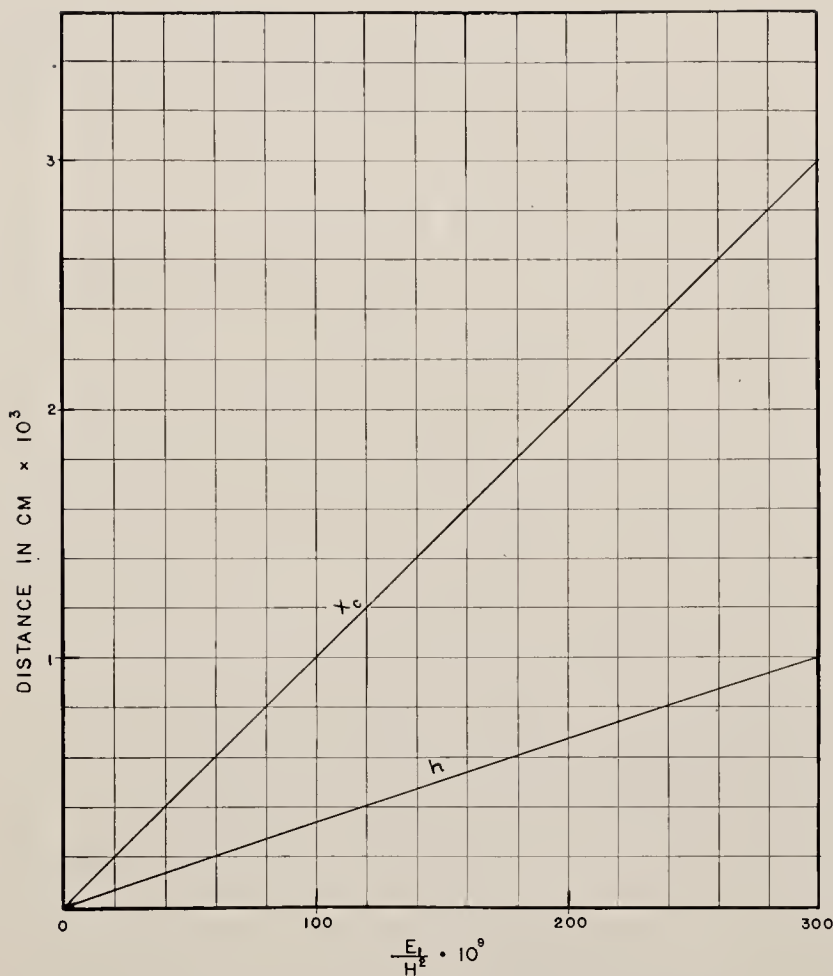


FIG. 4. Plot showing variation in x_c and h as a function of E_1/H^2 .

beam on the xy plane is that of a common cycloid with cusps in the xz plane. The distance between the cusps of the projected paths is

$$x_c = 2\pi \cdot \frac{M_e c}{eH} \cdot \frac{E_1 c}{H} \text{ cm} \quad (4)$$

and its maximum deviation from the xz plane is

$$h = 2 \cdot \frac{M_e c}{eH} \cdot \frac{E_1 c}{H} \text{ cm.} \quad (5)$$

Here M_e represents the mass of the electron and other symbols have their usual significance.

A rough sketch of one loop of a very narrow portion of this beam is shown in Fig. 3. We thus see that the beam not only shifts in position, i.e., x_c changes when either H or E (Fig. 3) is altered,

but also that h and Z_L change. These variations are quite small, however, as can be seen by referring to Fig. 4 in which the magnitudes of " x_c " and " h " are plotted as a function of the field strengths. E.g., if E_1/H^2 is altered by a factor of 300, the changes in " x_c " and " h " are 0.003 cm and 0.001 cm, respectively. In practice, the variation in this factor is no more than a few percent. Variations in the beam position of this order of magnitude introduce small errors in a relative abundance measurement which, for the most part, are negligible.

The distance " BG " (Fig. 3) can be determined from the expression " BG " = Z_L = $V_z 2\pi M_e c / eH$, where V_z is the component of the initial velocity along the Z axis. For 100-volt electrons and a field strength $H = 2000$ gauss, " Z_L " = 1 mm. Thus there are several of these loops in a distance equal to the length of slit S_1 (Fig. 1),

which as mentioned previously is parallel to the beam direction.

In reality, the electron beam is not uniform in thickness as shown in Fig. 3, but varies from point to point since the incident beam is diverging ($V_0 \neq 0$). Assuming that V_0 is finite, small, and has a component in the y direction only, and that the beam is diverging from a line source AB in the xz plane, then under these conditions, it diverges and comes to a focus twice, once along the line PD (Fig. 3) and the second time along the line SF .

B. Ion Paths

The main characteristics of this type of source depend primarily upon the paths of the positive ions which originate within the electron beam and

which, under the influence of the field E_1 (Fig. 1), move toward the plate P_1 . If second-order errors are present due to selective effects, they depend upon these paths as well as space charge conditions, and thus it is necessary to know if, for a given set of operating conditions, ions having different M/e values originate at the same point, and travel along identical paths.

If, for example, the magnetic field H or the electric field E_1 is changed in order to collect different ions, and if as a consequence the ions do not travel the same paths throughout, the effective solid angles for collection subtended by the defining slit S_1 (Fig. 1) will be different and the abundance ratio will be in error.

Furthermore, when ions of different M/e values originate at different points, then in addition to the above effect, space charge conditions, if present, will also be different.

As has been pointed out by Bainbridge,¹⁸ when space charge conditions exist, a number of

selective factors enter in, even if all the ions come from the same point.

The position x_0 (Fig. 1) of the point from which an ion of mass M will start from rest and pass through the center of slit S_1 for a given value of E_1 and H , can also be determined by means of Eqs. (1) and (2), since these equations hold for ions as well as for slow electrons if the proper value of M is used.

To find x_0 the following conditions must be satisfied; i.e., $y_0=0$ at $t=0$, $V_0=0$; and after a time t_1 , $x=0$ and $y=D_1$. Putting $U_1=\gamma t_1$ in Eqs. (1) and (2), the resulting expressions are:

$$x_0/(Mc/eH) \cdot (E_1c/H) = \sin U_1 - U_1, \quad (6)$$

$$\cos U_1 = 1 - D_1/(Mc/eH) \cdot (E_1c/H). \quad (7)$$

Plots of $-x_0/(Mc/eH) \cdot (E_1c/H)$ and U_1 as functions of $D_1/(Mc/eH) \cdot (E_1c/H)$ are shown in Figs. 5 and 6. A plot of x_0 as a function of M for several sets of values of D_1 , E_1 , and H is shown in Fig. 7.

Thus, if E_1 and H both remain fixed, the

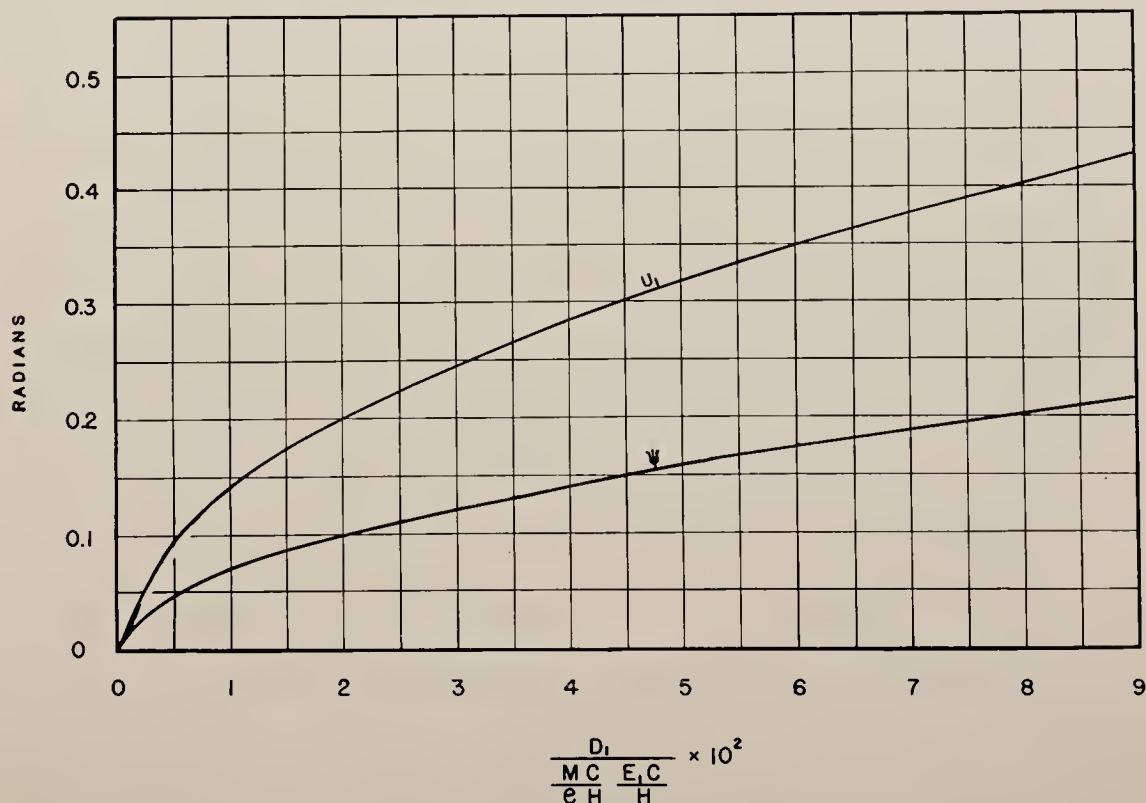


FIG. 5. Plot showing U_1 and ψ as a function of $D_1/(Mc/eH) \cdot (E_1c/H)$.

different isotopic ions which pass through slit S_1 originate at different positions x_0 depending upon their mass M . In one sense this feature may be considered a disadvantage of this type of instrument since if the method¹⁹ of comparing two isotopic peaks at the same time is used it is subject to criticism, the positions at which the different ions originate being slightly different.

For isotopic ions, however, ΔM is seldom greater than four or five units, and thus the difference in position of ion origin is seldom more than a thousandth of a cm. The corresponding error introduced into an abundance measurement is difficult to calculate if varying space charge conditions are present. However, considering selective effects alone, it is only a small fraction of one percent.

In this connection, it is worth noting that when the method of simultaneous comparison of two isotopic beams is used, extreme caution must be exercised that there are no limiting slits between the last source slit and the collector

slits, since the paths of the ions are quite different after they leave the source.

When the ion beams are studied one at a time, however, it is possible to make the starting points x_0 the same for ions having different values of M/e by varying H or E_1 in a given manner. If, for example, the magnetic method of collection is used and different isotopic beams are brought to the collector by varying the magnetic field H , E_1 , and D_1 having fixed values, and H is varied in such a way that H^2/M remains constant, then $(Mc/eH) \cdot (E_1c/H)$ (Eqs. (6) and (7)) also remains a constant and consequently the ions which are collected, although they have different masses, originate at the same position x_0 . In those instruments in which the entire apparatus (i.e., source region and analyzer) is in the same uniform magnetic field, the condition that H^2/M be a constant is automatically satisfied since the final energy of the ions is always the same. All of the earlier instruments used by Tate, Bleakney, and Nier were of this type.

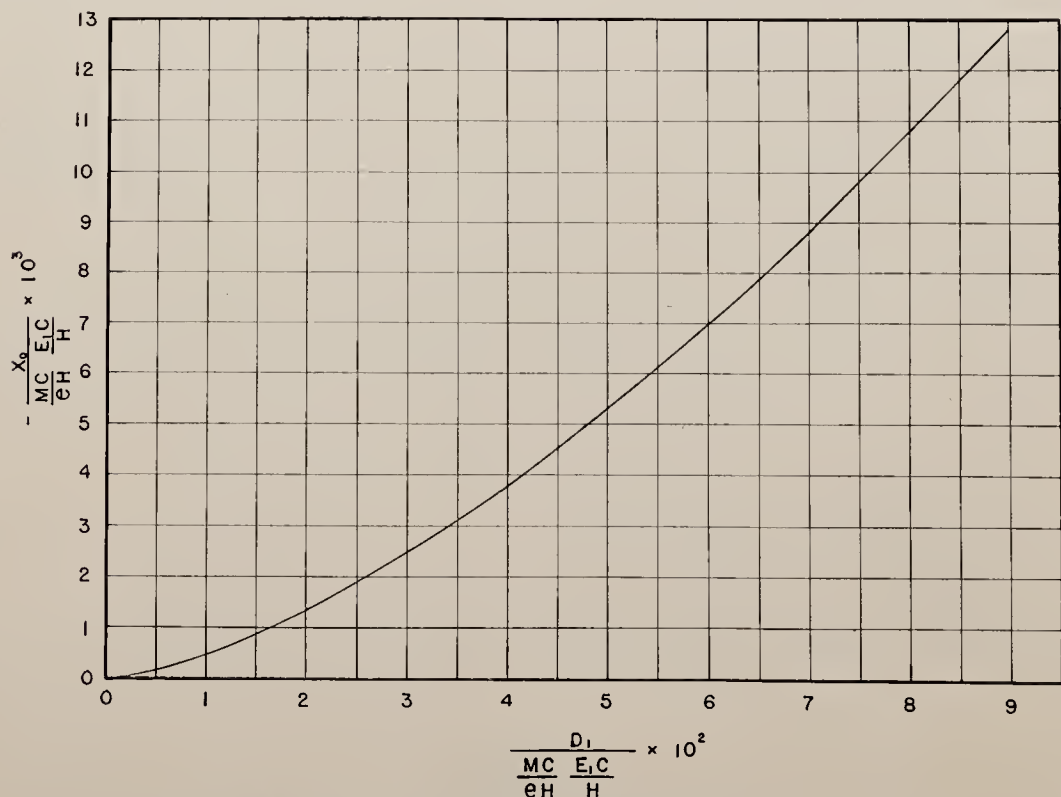


FIG. 6. Plot showing $-x_0/(Mc/eH) \cdot (E_1c/H)$ as a function of $D_1/(Mc/eH) \cdot (E_1c/H)$. x_0 is in cm, if E_1 is in e.s.u., H in e.m.u., M in grams, and D_1 in cm.

In practice the isotopes of a given element are seldom studied using this procedure, since it is difficult to vary the magnetic field in uniform steps (except in the case of a solenoid) and thus to plot the peak shapes. Usually the magnetic field is set at a given value depending on the element to be studied and the different isotopes are brought to the collector by varying the electric fields E_1 and E_2 .

In this latter method, it is also possible to insure that ions of different M/e values follow identical paths, by keeping the factor $E_1 M$ a constant. If this condition is satisfied, then assuming that D_1 , the perpendicular distance from the point where the ions originate to the plane of the slit S_1 , remains fixed, the factor $D_1/(Mc/eH) \cdot (E_1 c/H)$ (Fig. 6) also remains invariant, H being fixed, and consequently x_0 is the same for different isotopes. While this method satisfies the requirements for identical paths, it does involve the variation of the electrical field strength E_1 in the source region and possible attendant variations in space charge conditions. In addition, if the space charge conditions are altered, then D_1 is changed slightly and the paths of different ions will not be identical.

Although it is impossible to calculate such effects, they can at the most, introduce very small systematic errors only, since in practice the abundance ratio of two isotopes is always checked as a function of the electron beam current density and gas pressure within the source chamber. Also as shown previously, the effect of any reasonable change in E_1 on the shape and position of the electron beam is quite small.

Another factor which is important in this type

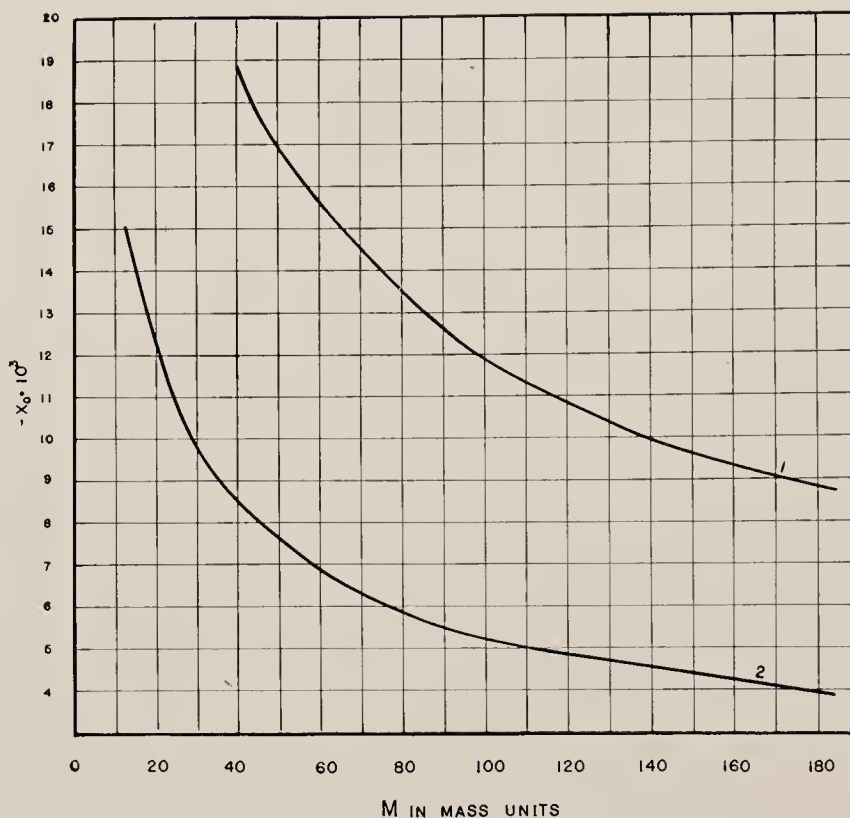


FIG. 7. Plot showing x_0 as a function of M for two sets of values of D_1 , E_1 , and H . For curve one, the values of these quantities are: $E_1=25$ volts/cm; $D_1=0.1$ cm; and $H=4000$ gauss. For curve two: $E_1=30$ volts/cm; $D_1=0.1$ cm; and $H=2000$ gauss.

of source is the angle ψ , (Fig. 1) between the direction of the ion motion at S_1 and the y axis. This angle not only determines the effective aperture of the slit S_1 , but also is an important factor in the expression for the position of slit S_2 and for the final angle α at slit S_2 , which determines the orientation of the focal plane of the instrument.

Differentiating the equations of motion (1), (2), and substituting the proper initial conditions, the expression for ψ is found to be

$$\psi = \frac{1}{2} U_1, \quad (8)$$

where U_1 is the parameter corresponding to the coordinates of slit S_1 and may be determined from Eq. (7). Values of ψ as a function of $D_1/(Mc/eH) \cdot (E_1 c/H)$ can be obtained from the lower curve in Fig. 5. The limiting conditions that the ions just reach the slit ($\psi=90^\circ$, and effective aperture equal to zero) is $D_1=2(Mc/eH)(E_1 c/H)$.

The fields are always chosen so that ψ is as small as possible and yet so that E_1 is not great enough to influence the electron beam appreciably. For $D_1=0.1$ cm, $E_1=25$ volts/cm, $H=4000$ gauss, and $M=100$ mass units, ψ is equal to $10^\circ 6'$, and the effective aperture $S_1 \cos \psi$ is 98.5 per cent of its maximum value.

As has been pointed out in a very simple way by Bleakney,²⁰ the paths of the ions between plates P_1 and P_2 introduce no additional errors providing certain conditions are satisfied. Substituting the expression found for ψ and putting $\phi=90-\psi$, $x_0=0$, $y_0=D_1$ in Eqs. (1) and (2), the parametric expressions for the ion paths become:

$$\frac{x}{\frac{Mc}{eH} \cdot \frac{E_2 c}{H}} - \frac{E_1}{E_2} \sin 2\psi = \left(-\frac{E_1}{E_2} \sin 2\psi \right) \cos U + \left[\frac{D_1}{\frac{Mc}{eH} \cdot \frac{E_2 c}{H}} - 1 \right] \sin U + U, \quad (9)$$

$$\left[\frac{D_1}{\frac{Mc}{eH} \cdot \frac{E_2 c}{H}} - 1 \right] \cos U + \left[\frac{E_1}{E_2} \sin 2\psi \right] \sin U = \frac{y}{\frac{Mc}{eH} \cdot \frac{E_2 c}{H}} - 1. \quad (10)$$

From these equations, we see that the paths between plates P_1 and P_2 of ions having different M/e values are identical if the two factors $(Mc/eH) \cdot (E_2 c/H)$ and (E_1/E_2) are held constant when either the electric or magnetic field is varied in order to collect different ions. This is the case since $(Mc/eH) \cdot (E_1 c/H)$ and thus ψ (Eqs. (7) and (8)) also remain fixed under these conditions.

Both sets of conditions, i.e., for the paths between P_0 and P_1 as well as between P_1 and P_2 , are automatically satisfied when the magnetic

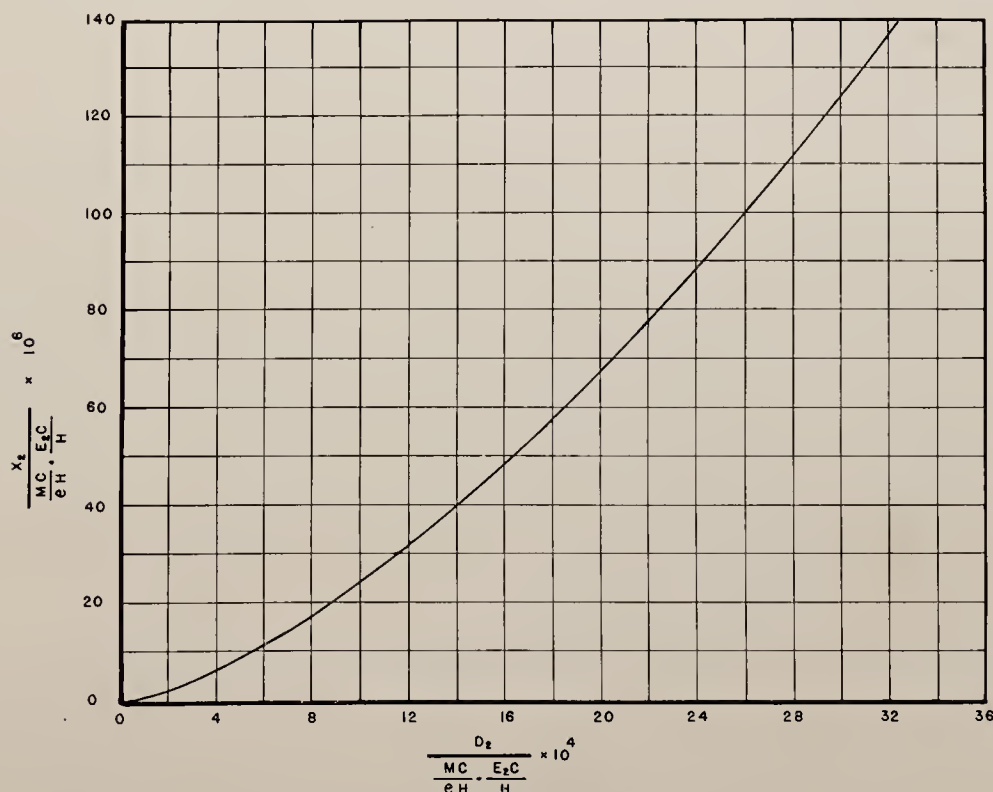


FIG. 8. Plot showing $x_2/(Mc/eH) \cdot (E_2 c/H)$ as a function of $D_2/(Mc/eH) \cdot (E_2 c/H)$. For the special case $D_2=2D_1$, X_2 is in cm if E_2 and e are in e.s.u., H in e.m.u., M in grams, c in cm/sec., and D_2 in cm. The curve is valid for values of E_2/E_1 from 50 to 300, within the limits of error of the plot.

method of collection previously discussed is used, since H is varied in such a way that H^2/M is a constant and none of the other factors is varied. When the electrical method of collection is used, however, H being fixed, both sets of conditions are satisfied only if E_1 and E_2 are varied in such a way that E_1M and E_2M remain constant. This is equivalent to keeping E_2/E_1 a constant, which condition is easily satisfied experimentally by using a divided potential arrangement.

Another factor which is essential for a description of this type of spectrometer is the displacement x_2 . It can be determined from Eqs. (9) and (10) by substituting the values $x=x_2$, $y=D_1+D_2$. In Fig. 8, $x_2/(Mc/eH) \cdot (E_2c/H)$ is plotted as a function of $D_2/(Mc/eH) \cdot (E_2c/H)$ for the special case $D_2=2D_1$. This curve is valid for values of E_2/E_1 from 50 to 300 within the limits of error of the plot.

A corresponding plot for the parameter U_2 (value of U corresponding to $x=x_2$) for the

special case $D_2=2D_1$ and for different values of E_2/E_1 is shown in Fig. 9.

" α " the angle which determines the position of the focal plane of the analyzer can be determined in the same way that ψ was determined. The expression for $\tan \alpha$ is

$$\tan \alpha = \frac{1}{\frac{Mc}{eH} \cdot \frac{E_2c}{H} U_2 + \frac{E_1}{E_2} \sin 2\psi - \frac{x_2}{\frac{Mc}{eH} \cdot \frac{E_2c}{H}}} \cdot \frac{D_1+D_2}{\frac{Mc}{eH} \cdot \frac{E_2c}{H}} \quad (11)$$

In general, U_2 and $x_2/(Mc/eH) \cdot (E_2c/H)$ can be determined by means of Eqs. (9) and (10) in the same way that they were calculated for the case $D_2=2D_1$ previously discussed. $\psi=U_1/2$ can be obtained from Eq. (7) since $(Mc/eH) \cdot (E_1c/H)$ is fixed by the values chosen for E_2/E_1 and $(Mc/eH) \cdot (E_2c/H)$. For the special case $D_2=2D_1$, U_2 and $x_2/(Mc/eH) \cdot (E_2c/H)$ may be obtained

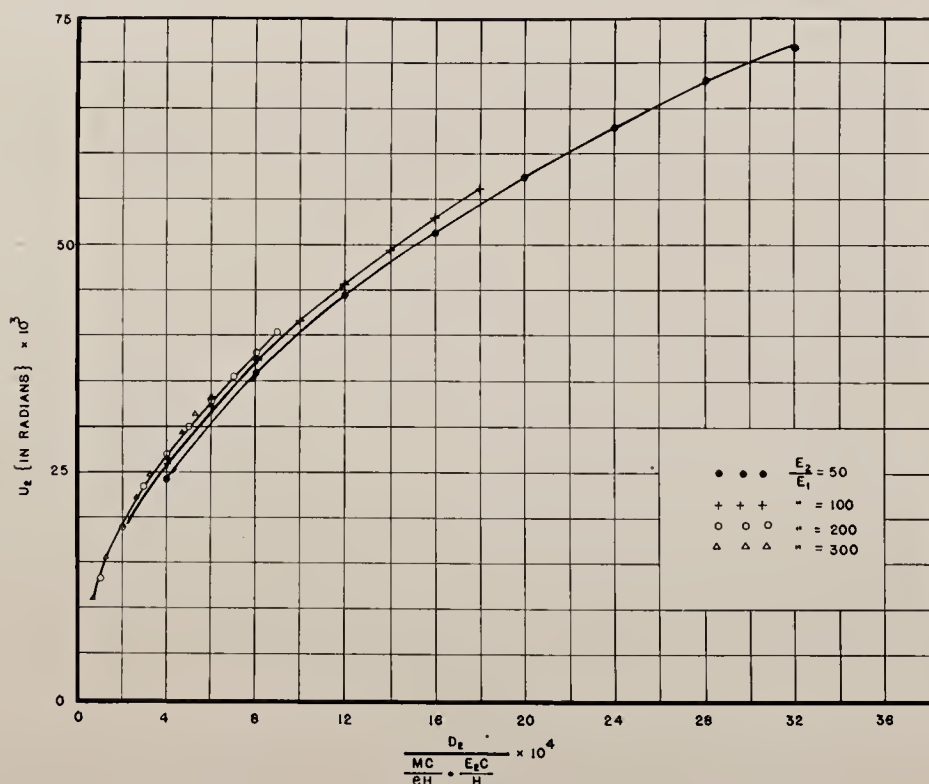


FIG. 9. Plot showing U_2 as a function of $D_2/(Mc/eH) \cdot (E_2c/H)$ for different values of E_2/E_1 and for $D_2=2D_1$.

from the plots shown in Figs. 8 and 9, and for this case " α " is plotted as a function of $D_2/(Mc/eH) \cdot (E_2c/H)$ for different values of E_2/E_1 in Fig. 10.

Although the value of " α " is in most cases quite small, it is important to take it into consideration in the over-all design of an instrument, if the maximum resolving power is to be attained.

The values of these various constants are listed below for an instrument which is designed to handle 1002.5-volt ions of mass number 100, $H=5000$ gauss, $D_2=2D_1=0.2$ cm, and $E_2/E_1=200$. For this case $(Mc/eH)(E_2c/H)=324.0$, $(Mc/eH)(E_1c/H)=1.62$.^{**} Making use of these values and the graphs, the following constants

^{**} E_1 can always be found from the energy relation $e(E_1D_1+E_2D_2)=\text{ion energy}$, and the value for E_2/E_1 .

are obtained:

$$x_0 = -0.012 \text{ cm}, \quad \psi = 10^\circ 6', \\ x_2 = 0.0035 \text{ cm}, \quad \text{and} \quad \alpha = 1^\circ 30'.$$

The values of H , E_1 , and E_2 which would be used in this case to study ions of another mass number could then be found from the conditions for identical paths, i.e., $E_1'/E_1=E_2'/E_2$ and $M'E_2'/(H')^2=ME_2/H^2$, which conditions must be satisfied at all times if the abundance measurements are to be free from error.

INSTRUMENT DESIGN

The over-all design of a spectrometer will depend upon many different factors such as size of magnet available, power, dispersion desired, and the particular use for which the instrument is intended. There are two general types in use at the present time which for convenience may

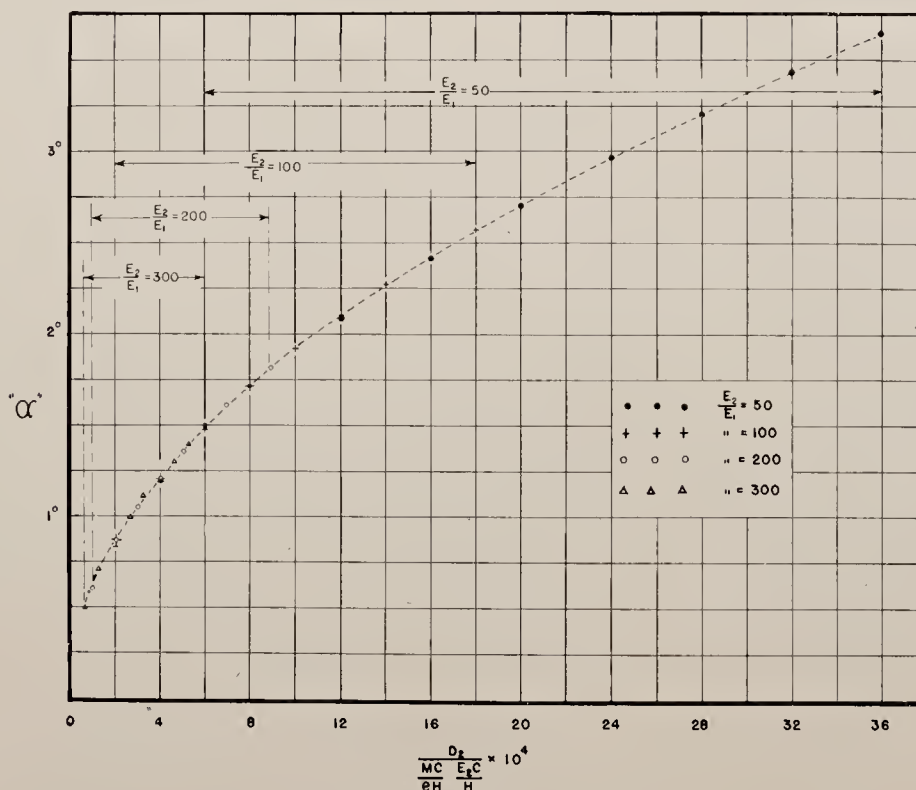


FIG. 10. Plot showing " α " as a function of $D_2/(Mc/eH) \cdot (E_2c/H)$ for the special case $D_2=2D_1$. The region of the curve which is valid for a given value of E_2/E_1 is indicated by the corresponding arrowed line in the upper left-hand corner. It is very possible that the overlapping values are identical for even greater ranges than shown. However, calculations were made only within the limits indicated.

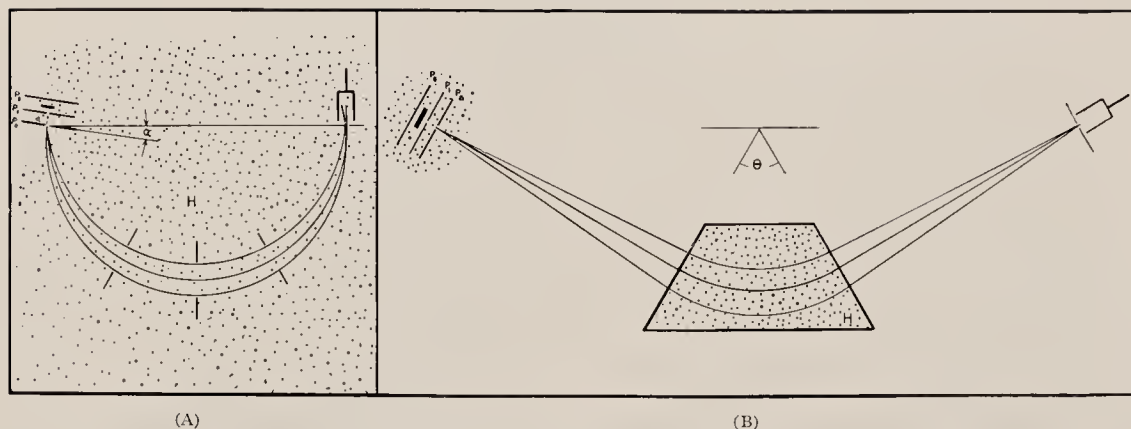


FIG. 11. General types of mass spectrometers: (A) π radian design; (B) sector type magnetic field design.

be classified as the π radian design shown schematically in Fig. 11A and the sector type magnetic field design shown in Fig. 11B.

In both cases, the type of ion source most generally used is that described in the preceding section. In the previous discussion, however, it was assumed that the magnetic field was uniform between the plates P_0 , P_1 , and P_2 , Figs. 1 and 11. This is true only in the case of the π radian type of instrument in which the mass analyzer and source are both in the same uniform magnetic field, and only in this case are the values obtained for " α " (Figs. 10 and 11), and for x_2 (Fig. 8) valid. Other advantages of the π radian instrument include ease of alignment (the conditions within the source being known), maximum effective use of the slit widths and a uniform electron beam shape. It is doubtful if measurements made with this type of instrument under the conditions requisite for identical ion trajectories are in error by more than one or two percent.

Since the same type of source is used in the sector magnetic field type of instrument and since the source region is outside and some distance from the analyzer magnetic field, an auxiliary field, supplied by a bar magnet in most cases, is necessary. In this arrangement, the equations previously obtained no longer apply since the magnetic field is not uniform throughout the source region, and is in fact distorted in those instruments in which magnetic materials are used to fabricate the source.

This also applies to the π radian type of instru-

ment when semicircular pole faces are used and the source is just outside the pole edges in a stray field region. In these cases, it is difficult to calculate the critical constants necessary for the proper orientation of the source relative to the magnetic field and alignment must be made experimentally by trial and error. In addition, if the magnetic field is distorted appreciably in the region traversed by the electron beam near slit S_1 (Fig. 1), one can also expect a loss of resolving power.

It is important to note, however, that although these factors may decrease the intensity and reduce the resolving power insofar as the source is concerned, they do not in any way invalidate the results obtained providing that E_1M and E_2M are always kept constant while making relative abundance measurements. These conditions are the same as those for the uniform magnetic field case, and can be shown to be the requisite conditions for identical ion paths in the source region in the case of a non-uniform magnetic field by the method of Bleakney.²⁰

Under these conditions, measurements made with a sector instrument are just as accurate as those obtained with the π radian type of instrument discussed above and the results, in point of view of accumulative errors inherently associated with machine design, are probably accurate to one or two percent.

We wish to express our appreciation to Professors Serber and Morrison for reading the manuscript.

BIBLIOGRAPHY

- (1) A. O. Nier, Phys. Rev. **52**, 933 (1937); **54**, 275 (1938).
- (2) M. B. Sampson and W. Bleakney, Phys. Rev. **50**, 732 (1936).
- (3) See, for example, H. D. Hagstrum and J. T. Tate, Phys. Rev. **59**, 354 (1941).
- (4) A. O. Nier, J. Am. Chem. Soc. **60**, 1571 (1938).
- (5) A. O. Nier, E. T. Booth, J. R. Dunning, and A. V. Grosse, Phys. Rev. **57**, 546 (1940).
- (6) H. C. Urey, J. R. Huffman, H. G. Thode, and M. Fox, J. Chem. Phys. **5**, 856 (1937).
- (7) D. Rittenberg, A. S. Keston, F. Rosebury, and R. Schoenheimer, J. Biol. Chem. **127**, 291 (1931).
- (8) E. B. Jordan, Phys. Rev. **57**, 1072A (1940).
- (9) W. Bleakney, Phys. Rev. **34**, 157 (1929); **40**, 496 (1932).
- (10) A. O. Nier, Phys. Rev. **50**, 1041 (1936).
- (11) J. T. Tate, P. T. Smith, and A. L. Vaughan, Phys. Rev. **48**, 525 (1935).
- (12) A. O. Nier, Rev. Sci. Inst. **11**, 212 (1940).
- (13) H. Brown, J. J. Mitchell, and R. D. Fowler, Rev. Sci. Inst. **12**, 435 (1941).
- (14) N. F. Barber, Proc. Leeds Phil. Soc. **2**, 247 (1933).
- (15) W. E. Stephens, A. L. Hughes, Phys. Rev. **45**, 123A (1934); W. E. Stephens, Phys. Rev. **45**, 513 (1934).
- (16) W. Bleakney and J. A. Hipple, Jr., Phys. Rev. **53**, 521 (1938).
- (17) Hannes Alfvén, Arkiv f. Matematik, Astronomi och Fysik **A27**, No. 22, 1 (1940).
- (18) K. T. Bainbridge, J. Frank. Inst. **212**, 317 (1931).
- (19) H. A. Straus, Phys. Rev. **59**, 102 (1941).
- (20) W. Bleakney, Am. Phys. T. **4**, 12 (1936).

An Experimental Mass Spectrometer

N. D. COGGESHALL AND E. B. JORDAN
University of Illinois, Urbana, Illinois

(Received March 5, 1943)

A mass spectrometer, designed for investigating different source arrangements with great ease, has been completed. It is an all metal, sector-shaped magnetic field type, constructed so that it may be disassembled, repaired, or modified without altering its focusing properties in any way. An important feature of the design is a removable ion source unit. A new source arrangement, investigated with this instrument, is discussed.

INTRODUCTION

MANY of the applications of the mass spectrometer, instrument design, and methods of operation have been discussed in previous articles.^{1,2} The present paper is a description of a mass spectrometer designed to permit the investigation of different source arrangements of possible use in smaller all-glass instruments; for investigating sources of ions of the heavier elements of possible use in the large mass spectrograph;³ for collecting small quantities of isotopes for disintegration purposes; and for measuring the abundances of those elements whose isotopes occur at positions not contaminated by hydrides. One source arrangement has already been reported in abstract form,⁴ and another is being investigated at the present time. The instrument has proven convenient and of considerable value for these purposes.

GENERAL ARRANGEMENT

A picture of the spectrometer has already appeared in the *Journal of Applied Physics*. Figure 1 is a drawing which shows the arrangement of its component parts. It is the sector-shaped magnetic field type now in common use.⁵

Except for glass insulators used to bring in necessary electrical connections, the hull of the instrument was constructed entirely of metal. Accurate machine work was thus possible, and as a consequence, no trouble was encountered in focusing the instrument. This latter was accomplished by lengthening (screw attachment) or shortening the two arms; which arms, in turn, determine the positions of the entrance and exit slits (see Fig. 2).

The ion source, including the insulators, was also constructed entirely of machinable parts; and is a unit complete within itself. Accurate construction and alignment of the source parts was thus possible; in addition, the unit, as a

¹ E. B. Jordan and N. D. Coggeshall, *J. App. Phys.* **13**, 539 (1942).

² E. B. Jordan and L. B. Young, *J. App. Phys.* **18**, 526 (1942).

³ E. B. Jordan, *Phys. Rev.* **57**, 1072 (1940).

⁴ N. D. Coggeshall, *Phys. Rev.* **61**, 738 (1942).

⁵ *J. App. Phys.* Special issue on Mass Spectrometry, Vol. **13**, No. 9 (September, 1942).

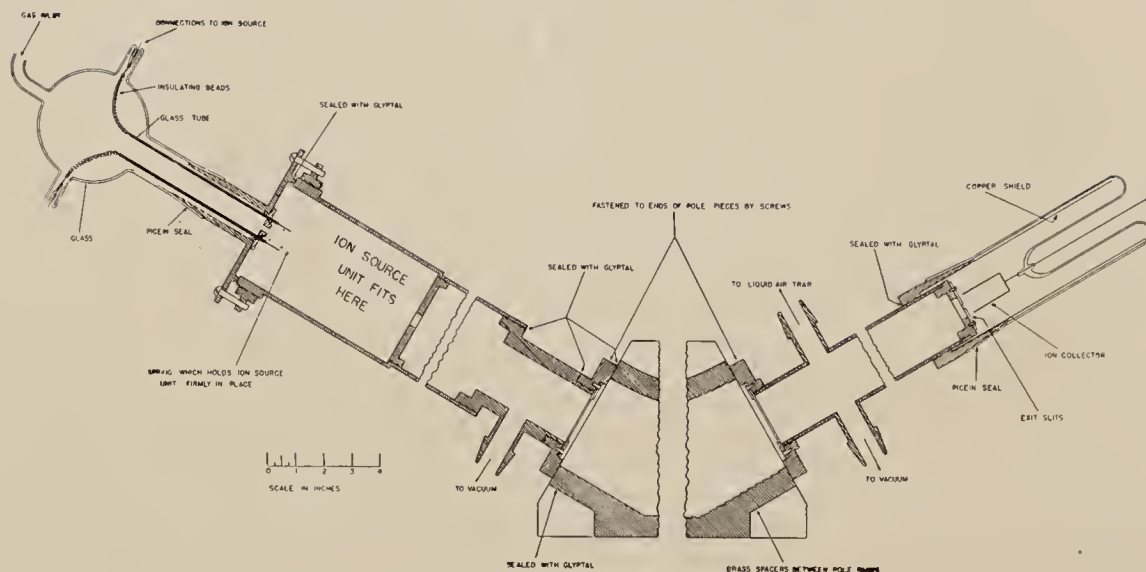


FIG. 1. Detailed drawing showing mechanical arrangement of the different parts of the spectrometer. With the exception of the magnet poles, all parts were made of brass or copper.

whole, is easily removed for replacement of parts or modification. The focusing conditions are not altered in any way by its removal and replacement. Although the unit itself is not shown in Fig. 1, the housing into which it fits is indicated. The plate at the bottom of this region serves as a stop to locate its position accurately. It is held firmly against this stop by means of a strong spring attached to the removable top.

The positive ion collimating system consists of five slits; two within the source unit itself, the positions of which are located by means of the stop just mentioned. Then there are slit jaws at each end of the pole pieces as well as an exit slit adjacent to the Faraday cage. The slit jaws next to the pole faces project into the gap region a sixteenth of an inch on either side to prevent scattering from the pole faces. These slits, 1.75 inches long, also limit the height of the beam within the magnetic field or pole gap region. Although only one exit slit (slit 5) is shown in the diagram, an additional one has recently been inserted in order to prevent the escape of secondary electrons from the Faraday cage.

All metal to metal joints were made vacuum tight with Glyptal; the metal to glass joints with Picein. Two, two-stage mercury diffusion pumps backed by a Cenco Megavac pump constituted

the vacuum system. Differential pumping between the source unit and the rest of the system was possible since the clearance between it and the housing into which it fits (Fig. 1) is not more than two thousandths of an inch.

ION SOURCE

A cross-sectional view of the ion source unit previously mentioned is shown in Fig. 2.

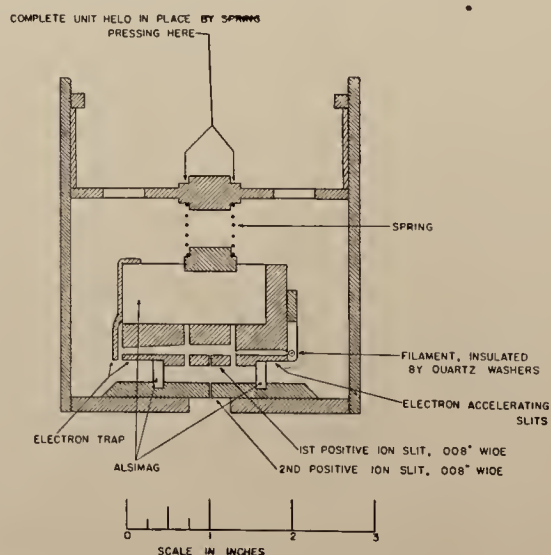


FIG. 2. Cross-sectional view of ion source unit.

The source filament, electron collimating slits, condenser plates, and electron trap were all mounted on a carefully machined block of AlSiMag by means of small copper bolts. Their relative sizes and positions are shown in Fig. 2 (central unit), and the mounting arrangement used is shown in Fig. 3. For clarity in this latter figure, part of the AlSiMag block is not shown.

An oxide-coated cathode, insulated from the support by small pieces of quartz tubing, was used. Details of the assembly may be seen in Fig. 3. The spacing between the filament and the first electron collimating slit was 1.5 mm and the two collimating slits, each 0.5 mm by 20 mm, were spaced 15 mm apart. As may be seen in Figs. 2 and 3, the collimating slits were formed by milling out the region between the outer edges of the plane of contact between two copper surfaces. Spacers were then inserted at each end to give the proper slit width.

After passing through the two collimating slits, the thin, wide, flat electron beam next passed into the region of the first positive ion accelerating field. The ions were created in this region by electron impact in the usual manner. This first accelerating field was maintained between two condenser plates, the lower one of which contained the so-called first positive ion slit.

These condenser plates were made wide enough compared to their separation so that the electric field was uniform for a distance of several mm

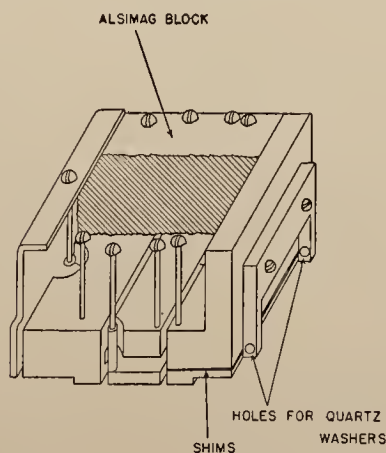


FIG. 3. Mounting arrangement for filament, collimating slits, condenser plates, and electron trap. The AlSiMag block is shown in section.

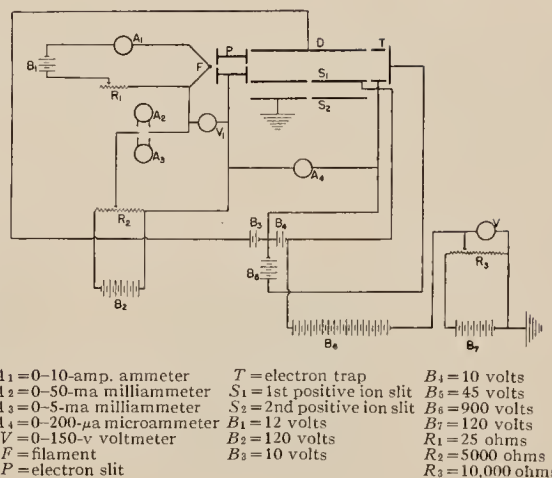


FIG. 4. Circuit diagram.

in the region just above the slit. Also, by making one jaw of the slit a carefully machined portion of the plate itself, it was possible to keep both the upper and lower surfaces of the plate plane, and thus to prevent any undue distortion of the fields.

In order to prevent the formation of ghost lines due to electron reflection back into the ionizing region, a relatively long, narrow, electron trap was used. The back plate of this trap was maintained at a positive potential relative to the side walls.

This source arrangement is different from that used in previous instruments in two respects. Firstly, no magnetic field is employed in the source region to keep the electron beam in alignment; secondly, the electron beam moves in a direction perpendicular, rather than parallel, to the first positive ion slit. One is a consequence of the other for, in order to dispense with a magnetic field in this region and at the same time retain a narrow, well-resolved, isotopic beam width at the collector end of the spectrometer, it was necessary to orientate the electron beam in this manner. The resolved positive ion beam width in this case depends upon the width of the region from which the positive ions are drawn; and this in turn is a function of the width of the electron beam in the ionizing region. Since in this type of instrument the electron beam is deflected slightly by the weak positive ion accelerating field, it is necessary that the electron speed and

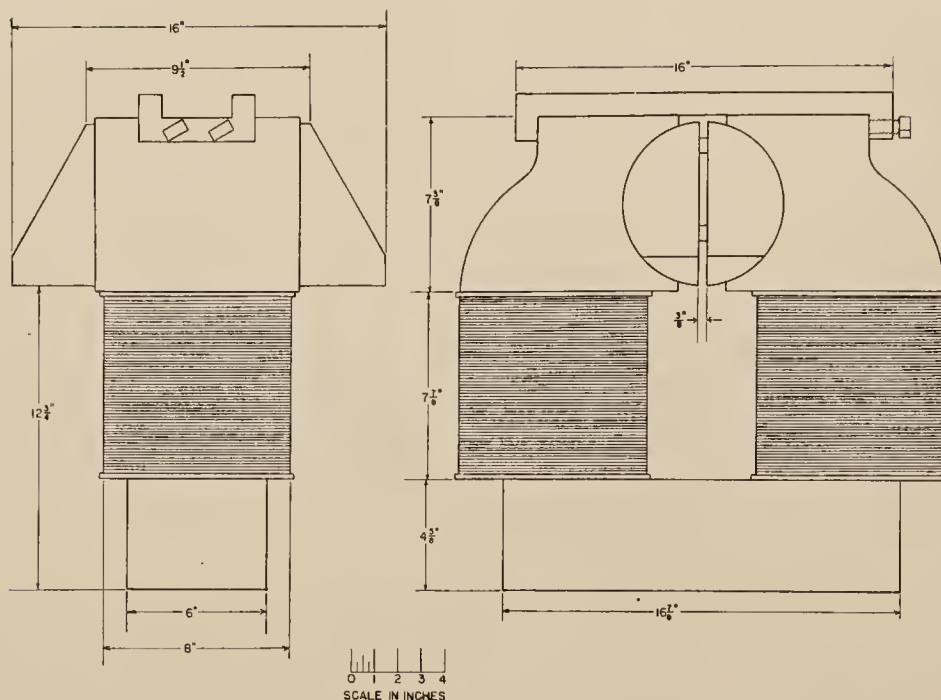


FIG. 5. Scale drawing of magnet.

thus the deflection be the same at all points. This was accomplished by using an oxide coated unipotential/cathode. Actually, in practice, tungsten filaments were also used; and for the light elements (up to $M/e=40$) the resolving power was still high enough to yield well-defined, narrow peaks.

With this source arrangement, it is also necessary, if peak distortion and resulting errors are to be eliminated, to keep this first positive ion accelerating field fixed. Different isotopic peaks may be investigated either by varying the second positive ion accelerating field (between slits 1 and 2) or else by varying the magnetic field. For abundance measurements, the latter method is the most accurate, although difficult in procedure. When the first method is used, the efficiency of collection for positive ions having difficult values of e/m (effectively a variation in solid angle of collection) is a function of this second positive ion accelerating field strength, and thus small errors are introduced when measurements are made in this way. For collecting isotopes and for many other uses of the spectrometer, these errors need not be considered.

Since, in operation, the portion of the source just described had to be maintained at a potential difference of 800 to 2000 volts (second positive ion accelerating field) relative to the base plate (Fig. 2), i.e., the plate containing the second positive ion slit, some form of insulated support was indispensable. Also, the accurate alignment of the two positive ion slits as well as convenience in dismantling was necessary. To accomplish this, two short, straight bars of AlSiMag were used to insulate the two units. The lower surfaces of these bars were embedded in the second positive ion slit plate (Fig. 2). Their upper surfaces were fitted into milled steps on the under surfaces of the electron trap and electron collimating slit units. A well-insulated bronze spring, mounted as shown in Fig. 2, held the two parts together.

Except for the spring, all metal parts in this unit were made of copper.

As previously mentioned, the complete unit (Fig. 2) was made to fit, with small clearance, in the source arm of the instrument in the position indicated in Fig. 1. Index lines served as guides for orientating it. To hold it firmly in place, a

spring (Fig. 1) fastened to the vacuum lid, was compressed against its top plate. Details of this arrangement as well as the lid attachment may be seen in Fig. 1.

Figure 4 is a diagram of the circuit.

THE MAGNET

The magnet consisted of two semi-circular pole pieces, separated by brass spacers, inserted in the armature space of an old Edison bipolar dynamo. The pole pieces were machined from separate forgings of Armco iron. The brass strips used as spacers between the pole pieces were $\frac{3}{8}$ " thick. They, as well as the pole faces, were plane to ± 0.002 ".

Since the radius of curvature of the central ion beam in the magnetic field was ~ 35 cm, field strengths of 2000 oersteds or less were sufficient for most purposes and could be obtained with a power consumption of less than 12 watts. The original dynamo field coils were found to be quite adequate.

A scale drawing of the magnet is shown in Fig. 5.

PERFORMANCE

For measuring the ion beam currents, the Penick balanced bridge circuit arrangement in which a Western Electric D-96475 electrometer tube was employed, was used. The tube was housed in a vacuum chamber and a vacuum

switching arrangement was used for grounding its grid through any one of three high resistances.

Figure 6 is a plot of the neon isotopic ion currents corresponding to data taken with this spectrometer. As may be seen, the peaks are well resolved, flat topped, and widely separated.

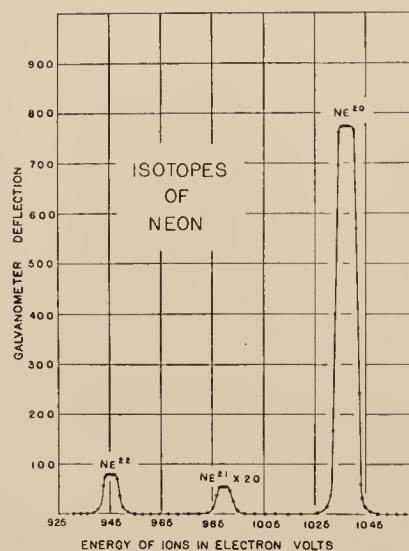


FIG. 6. The neon spectrum.

We wish to express our appreciation to Mr. Richard Burke who constructed part of the apparatus, and to the members of the physics department shop.

Discrimination in Mass Spectrometer Ion Sources

NORMAN D. COGGESHALL

Reprinted from THE JOURNAL OF CHEMICAL PHYSICS, Vol. 12, No. 1, pp. 19-27, January, 1944

Discrimination in Mass Spectrometer Ion Sources

NORMAN D. COGGESHALL

Gulf Research and Development Company, Pittsburgh, Pennsylvania

(Received October 13, 1943)

An analysis is made of the collection and definition of a beam of ions by an ion source. It is found that the first slit of the source has no discriminating effect but the second slit does have. This is due to the fact that ions of certain values of initial energy, angle of velocity vector, and position of striking the plane of the first slit cannot get through the second one. An efficiency of collection of a source for ions of a certain initial energy is defined as the ratio of the number with that initial energy that get through the second slit to the number with that initial energy which get through the first slit. An expression for this efficiency is derived and it is applied to rather typical data to show how an abundance ratio obtained by taking the ratio of peak heights may be in error several percent. The method of measuring isotopic abundances is recommended wherein the focusing conditions are changed only by varying the magnetic analyzer field.

FOR some time it has been believed that it is possible for the accelerating slit system in a mass spectrometer ion source to discriminate between ions of different mass, i.e., to collect ions of one mass more effectively than those of another. This would lead to different values of the isotopic abundances measured with different instruments.

One possible source of discrimination is the fact that the solid angle of collection, i.e., the angle in which ions are collected, may vary from one ion to the next during a determination of isotopic abundances. It is the purpose of this paper to analyze the reason for this discrimination and to calculate the magnitude of its effect. The effect of this change of solid angle of collection on peak shape for ions from dissociating molecules has been considered by Hagstrum and Tate.¹

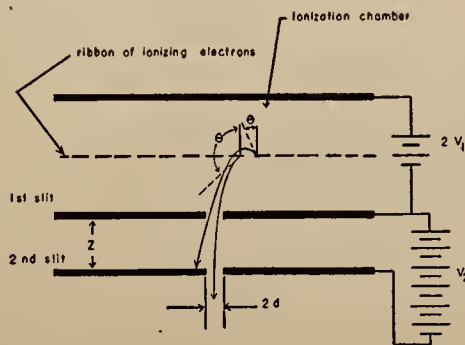


FIG. 1.

Let us consider an ion source such as shown schematically in Fig. 1 where the ions are formed by a beam of electrons coming into the ionization region parallel to the plane of the first slit. In this figure are shown two ions originating in the region of the electron beam with different values of θ , one ion being able to traverse the second slit and one not being able to. Let us further restrict ourselves to an ion source which is magnetic field free.² Since all ions are formed with an initial velocity (either thermal or due to dissociation energy, as for ions from molecules), let us denote this velocity by c and denote the angles of its vector by θ and Φ . Let us denote by c' , θ' , Φ' the corresponding quantities for the ion as it passes through the first slit, and by c'' , θ'' , Φ'' the corresponding quantities as it passes through the second slit. Let V_1 be the potential difference between the first slit and the position traversed by the electron beam. Let V_2 be the potential difference between the first and second slits. Let the separation between the first and second slits be z and the slit width in each case be $2d$. We shall consider an ion source in which no magnetic field is present, and we shall assume that the electric field is uniform both in the region above the first slit and in the region between the first and second slits.

If the area of the first slit is small compared to the area of the electron beam and if the first slit is located well away from any of the edges of the electron beam, it is clear that there can

¹ H. D. Hagstrum and J. T. Tate, Phys. Rev. 59, 354 (1941).

² N. D. Coggeshall and E. B. Jordan, Rev. Sci. Instr. 14, 125 (1943).

be no selective influence due to the first slit alone. For, consider ions of any mass, there will be created in the electron beam a definite number per unit area; and since the electric field is uniform, the number arriving per unit area on the plane of the first slit will be equal to this, so the number collected by the first slit is proportional only to its area and the number created per unit area in the electron beam.

The second slit, however, does have a selective influence as can be seen from Fig. 1. This is because only part of the ions going through the first slit get through the second slit and this fraction depends upon the initial velocity of the ions and upon the accelerating voltages used.

Let us consider ions of mass m . We shall denote by $\rho(c)$ the number of ions of mass m and initial velocity c which are created per second, per unit area in the electron beam. Now since the first slit gathers as many, per unit area, as are created per unit area in the electron beam we have:

$$f(\theta', \Phi', c') d\omega' = \rho(c) (d\omega/4\pi), \quad (1)$$

where $f(\theta', \Phi', c')$ is the number of ions of coordinates θ', Φ' , and velocity c' , contained within unit solid angle ω' at the plane of the first slit; $d\omega$ refers to solid angle in the electron beam. We assume that the ions have initial velocities randomly distributed. Using $d\Phi = d\Phi'$ and $c \sin \theta = c' \sin \theta'$, $f(\theta', \Phi', c')$ turns out to be:

$$f(\theta', \Phi', c') = \frac{\rho(c)}{2\pi} \frac{c'^2 \cos \theta'}{c(c^2 - c'^2 \sin^2 \theta')^{\frac{1}{2}}}. \quad (2)$$

We may now evaluate the selective influence of the second slit by defining an efficiency of collection $p(c)$. We define $p(c)$ as being the ratio of ions of mass m and initial velocity c getting through the second slit to the number getting through the first slit. From previous consideration we know that this is equal also to the ratio of the number of ions of mass m and initial velocity c in the final ion beam to the number created in the electron beam in an area equal to the area of the first slit.

$$p(c) = \frac{\rho(c)A' - \int \int f(\theta', \Phi', c') d\omega' da'}{\rho(c)A'}, \quad (3)$$

where A' is the area of the first slit. The integral

is integrated over those portions of solid angle ω' , such that ions striking the first slit in those portions of solid angle do not get through the second slit; also it is integrated over the area of the slit.

In order to evaluate the above integral, let us consider the limiting values of θ', Φ' that an ion of initial velocity c may have at the first slit and still get through the second slit. Let an ion strike the first slit, at a distance s from one edge and with a given Φ' and initial velocity c . Then one limiting value of θ' must satisfy the following relationships:

$$s = \frac{c' \sin \bar{\theta}' \cos \Phi' z}{H_{Nv}},$$

where H_{Nv} is the average value of the component of the ion's velocity perpendicular to the planes of the slits, while the ion is between the first and second slits, if $V_2 \gg V_1$ as is usually the case, we may write $H_{Nv} = c''/2$ since $2eV_2/m \gg c^2$, where c is initial thermal velocity or even dissociation velocity of a few volts.

This gives:

$$s = (2c'/c'') \sin \bar{\theta}' \cos \Phi' z. \quad (4)$$

The other limiting value of θ' is given by:

$$\bar{\theta}' = \sin^{-1}(c/c'), \quad (5)$$

which is the case when all the initial velocity c is parallel to the plane of the first slit. The limits of Φ' are:

$$\pm \cos^{-1} \frac{sc''}{2zc'}$$

so $p(c)$ becomes, neglecting end effects:

$$p(c) = \frac{\rho(c)2Ld - f(c)}{\rho(c)2Ld}, \quad (6)$$

where L is the length of the slits and $f(c)$ is given by:

$$f(c) = \frac{2\rho(c)}{\pi} L \frac{c'^2}{c} \int_0^{2d} ds \int_0^{\cos^{-1}(sc''/2zc')} d\Phi' \times \int_{\sin^{-1}(sc''/2zc' \cos \Phi')}^{\sin^{-1}(c/c')} \frac{\cos \theta' \sin \theta' d\theta'}{(c^2 - c'^2 \sin^2 \theta')^{\frac{1}{2}}}$$

The factor 2 appearing in $f(c)$ is the alternative to setting up an additional integral where instead of having ds we have $d(2d-s)$, i.e., the integral to take care of ions having Φ' differing by 180° from the values considered.

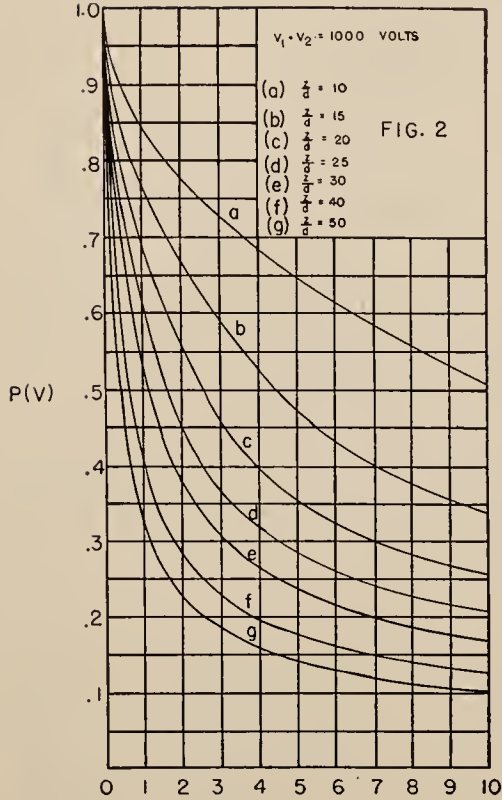


FIG. 2. Energy in electron volts.

Integrating with respect to θ' and inserting the limits we obtain:

$$f(c) = \frac{2\rho(c)L}{\pi} \int_0^{2d} \int_0^{\cos^{-1}(sc''/2zc)} \times \left(1 - \left(\frac{sc''}{2zc}\right)^2 \frac{1}{\cos^2 \Phi'}\right)^{\frac{1}{2}} d\Phi' ds.$$

Suppose we let $(sc''/2zc) = a$

$$f(c) = \frac{2\rho(c)L}{\pi} \int_0^{2d} \int_0^{\cos^{-1}a} \times \frac{1}{\cos \Phi'} (\cos^2 \Phi' - a^2)^{\frac{1}{2}} d\Phi' ds.$$

Suppose we next let

$$\frac{\cos^2 \Phi' - a^2}{1 - \cos^2 \Phi'} = v^2;$$

we obtain:

$$f(c) = \frac{2\rho(c)L}{\pi} \int_0^{2d} \int_0^{\infty} \frac{v^2(1-a^2)dv ds}{(1+v^2)(v^2+a^2)}$$

which can be integrated by partial fractions to

yield:

$$f(c) = \rho(c)L \int_0^{2d} (1-a) ds; \quad (7)$$

or using value of a and inserting in (7) we get:

$$f(c) = 2\rho(c)Ld \left(1 - \frac{d}{z} \frac{1}{2} \frac{c''}{c}\right). \quad (8)$$

Now this expression for $f(c)$ has been derived for values of c such that the second slit was operative in cutting out ions regardless of where they struck the first slit. However, for small values of c there are regions of the first slit where the ions may strike and be free of the discriminating effects of the second slit. For such values of c the integral $f(c)$ becomes

$$f(c) = \rho(c)L \int_0^{\bar{s}} (1-a) ds \quad \text{where} \quad \bar{s} = \frac{2zc}{c''}$$

or

$$f(c) = \rho(c)Lz(c/c''). \quad (9)$$

The value of c for which $f(c)$ changes from form (8) to form (9) is of course given by $d = zc/c''$, i.e., it will be given by the root of the equation:

$$d \left(c^2 + \frac{2e}{m} (V_1 + V_2) \right)^{\frac{1}{2}} = zc.$$

Let us call this transition value \bar{c} . Then our efficiency of collection is given by:

$$p(c) = 1 - [(1/2)(z/d)(c/c'')] \quad \text{for } c < \bar{c}, \quad (10)$$

$$p(c) = [(1/2)(d/z)(c''/c)] \quad \text{for } c > \bar{c}. \quad (11)$$

Or if we express the initial velocities in terms of electron volts of energy V we obtain:

$$p(V) = 1 - \frac{z}{2d} \left(\frac{V}{V + V_1 + V_2} \right)^{\frac{1}{2}} \quad \text{for } V < \bar{V}, \quad (12)$$

$$p(V) = \frac{d}{2z} \left(\frac{V + V_1 + V_2}{V} \right)^{\frac{1}{2}} \quad \text{for } V > \bar{V}. \quad (13)$$

As they should, the two expressions for $p(V)$ agree in value and slope for $V = \bar{V}$. Graphs of $p(V)$ for various values of z/d and for $V_1 + V_2 = 1000$ volts may be seen in Fig. 2. These curves agree in general over-all characteristics with those obtained by Hagstrum and Tate.¹ However, in the important region of small initial velocities the curves differ radically.

As the function $p(V)$ is independent of the mass of the ion being collected, true values of isotopic abundance ratios should be obtained if

all the ions are collected with voltage conditions remaining the same in the ion source. The only way this can be realized, of course, is by bringing first one ion beam and then another into focus by varying the magnetic field only.

Let us assume that the ions when formed from a monatomic gas will have a Maxwellian energy distribution. Then the density of ions of isotope M_α , in the path of the electron beam, as a function of energy will be

$$\rho_\alpha(V)dV = K p_\alpha A \epsilon^{-eV/300kT} V^{\frac{1}{2}} dV, \quad (14)$$

where p_α = partial pressure of isotope M_α

$$A = \pi N \left(\frac{e}{\pi k T} \right)^{\frac{1}{2}} \frac{1}{(300)^{\frac{1}{2}}},$$

V = energy in electron volts, N = total density of atoms of all isotopes, e = electronic charge, m_α = mass of isotope M_α .

K represents the fraction of atoms present in electron beam which are ionized; i.e., it represents ionization efficiency. We shall assume K to be the same for all isotopes of same element.

The intensity of the ion current for isotope M_α will then be proportional to I_α where:

$$I_\alpha = \int_0^\infty \rho_\alpha(V) P(V) dV.$$

Since $\epsilon^{-eV/300kT} \ll 1$ for V of the order 1 volt and for temperatures of the order of 500°C we may use the expression for $P(V)$ which was obtained for small values of V , i.e., (12):

$$I_\alpha = K p_\alpha A \int_0^\infty \epsilon^{-eV/300kT} V^{\frac{1}{2}} \times \left(1 - \frac{z}{2d} \left[\frac{V}{V_1 + V_2 + V} \right]^{\frac{1}{2}} \right) dV.$$

Since for operating conditions $V \ll (V_1 + V_2)$ we have

$$I_\alpha = K p_\alpha A \int_0^\infty \epsilon^{-eV/300kT} V^{\frac{1}{2}} (1 - g_\alpha V^{\frac{1}{2}}) dV,$$

where

$$g_\alpha = \frac{1}{2} \frac{1}{(V_1 + V_2)^{\frac{1}{2}}} \frac{z}{d},$$

$$I_\alpha = K p_\alpha A \left\{ \frac{1}{2} \left(\frac{(300)^{\frac{3}{2}} \pi k^{\frac{3}{2}} T^{\frac{3}{2}}}{e^{\frac{3}{2}}} \right)^{\frac{1}{2}} - g_\alpha \left(\frac{300kT}{e} \right)^{\frac{2}{2}} \right\}, \quad (15)$$

$$I_\alpha = p_\alpha \bar{A} \left\{ \frac{1}{2} \frac{\pi e}{300kT} - g_\alpha \right\},$$

where

$$\bar{A} = K A \left(\frac{300kT}{e} \right)^{\frac{2}{2}}.$$

Suppose $T = 450^\circ\text{K}$, then

$$I_\alpha = p_\alpha \bar{A} \{4.46 - g_\alpha\}. \quad (16)$$

By a similar calculation we can show that the ion beam intensity of an isotope M_b would be proportional to I_b where:

$$I_b = p_b \bar{A} \{4.46 - g_b\}.$$

Using the usual practice of taking ratios of peak heights to get isotopic abundances, the observed abundance ratio of isotope M_α to M_b would be:

$$I_\alpha/I_b = [(p_\alpha)(4.46 - g_\alpha)/(p_b)(4.46 - g_b)]$$

instead of p_α/p_b which would be the true abundance ratio.

As a test of the order of magnitude of the error introduced by such discrimination let us consider the neon isotopes Ne^{20} and Ne^{22} . Let us suppose in our instrument that the ions are focused for a path with radius of curvature 5". Further, let us suppose that we have a magnetic field of 800 gauss and the two slits in the ion source are $\frac{1}{4}$ " apart and 0.007" in width. It would be necessary to accelerate the Ne^{20} ions through a voltage $V_1 + V_2 = 965$ volts and the Ne^{22} ions through $V_1 + V_2 = 877$ volts. Using these values in our expression for I_α/I_b we obtain:

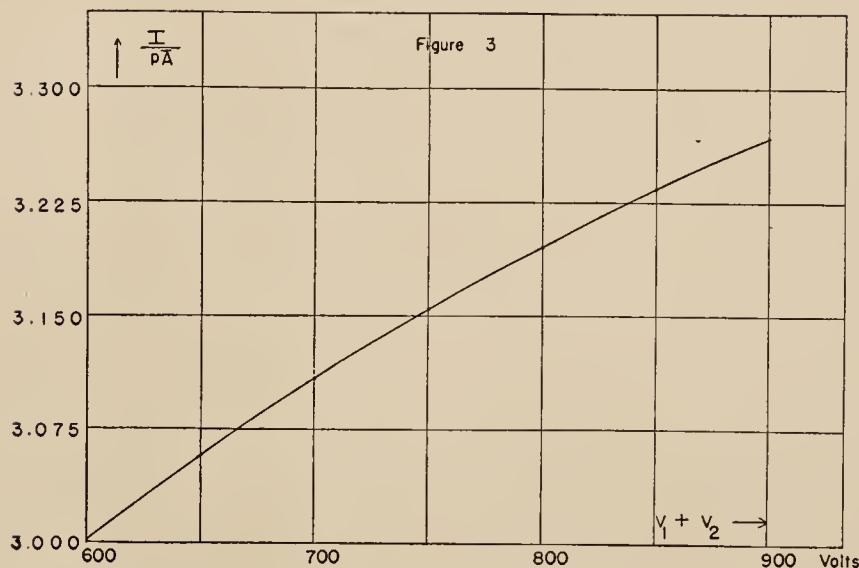
$$\frac{I(\text{Ne}^{20})}{I(\text{Ne}^{22})} = \frac{p(\text{Ne}^{20})}{p(\text{Ne}^{22})} \times 1.02.$$

In other words, the value obtained by taking a ratio of the peak heights would be 2 percent in error. This is much larger than the usual experimental error and it is certainly outside the limits of accuracy some investigators claim.

DISCUSSION

In Fig. 2 are to be seen graphs for $P(V)$ for values of V up to 10 volts and for $V_1 + V_2 = 1000$ volts with different values of z/d . As can be seen from them, the smaller the value of z/d the less discrimination an ion source will have;

FIG. 3.



that is, the less the separation between slits as compared to slit width. When working with ions originating in dissociation processes we would expect the characteristics of the ion source strongly to affect the shape of the peaks. The dependence is through the $P(V)$ curve and is discussed by Hagstrum and Tate.¹ From our Fig. 2 we can see that the $P(V)$ curve would strongly affect the peak shape due to the steepness of the curve for energy values of the order of one electron volt.

It is to be remembered that the analysis above is for a rather simplified ion source, i.e., one in which the electric fields are uniform and one which is free of a magnetic field. The latter condition is not hard to meet but the first condition is one which in practice could only be approximated. This is because of the fringing of the fields near the slits and the penetration of the strong field into the weaker field region through the first slit.

In view of the simplified ion source analyzed, the numerical results and the expression for $P(V)$ should not be taken as exact for any ion source. However, it is reasonable to believe that the qualitative implications are true and that the expressions obtained are good as a first approximation for any actual case. Actually it is expected that the discrimination would be worse since the penetration of the high voltage field through the first slit can give the ions an added

amount of velocity in a direction parallel to the planes of the slits and in this way decrease their chances of getting through the second slit. However, the method recommended above for getting abundance ratios, i.e., focusing by varying the magnetic field only, would be expected to give the best answer as this would not vary the discrimination for the different ions as their peaks were measured.

From Eq. (16) one would expect the peak height of any ion to grow if it were focused using progressively higher values for $V_1 + V_2$. This is illustrated in Fig. 3. In this figure not the peak height is plotted, but a quantity to which the peak height is proportional, namely, I/pA . In the plotting directly of the peak the slope would be greater or less depending upon units used. As may be seen the curve, which is for any ion focused for values of $V_1 + V_2$ between 600 and 900 volts, is slightly concave downwards but could be represented quite accurately by a straight line.

It would be desirable to have a similar analysis for the type of ion source in which there is a magnetic field present in the ion source, usually for the purpose of aligning the ionizing electrons. Some discussion has been made of this type of source³ but the amount of discrimination is not calculated.

³ E. B. Jordan and N. D. Coggeshall, J. App. Phys. **13**, 539 (1942).

The Paths of Ions and Electrons in Non-Uniform Magnetic Fields

NORMAN D. COGGESHALL AND MORRIS MUSKAT

Reprinted from THE PHYSICAL REVIEW, Vol. 66, Nos. 7 and 8, pp. 187-198, October 1 and 15, 1944

The Paths of Ions and Electrons in Non-Uniform Magnetic Fields*

NORMAN D. COGGESHALL AND MORRIS MUSKAT

Gulf Research and Development Company, Pittsburgh, Pennsylvania

(Received July 29, 1944)

The integration of the Lorentz force equations to give electron or ion paths has been reduced to simple quadratures for systems in which the electric field is zero and the magnetic field is a function of one Cartesian or cylindrical coordinate. For several interesting types of magnetic field variation the quadrature can be carried through analytically; and even for complicated magnetic fields, or such as are known only empirically, the numerical integration can be effected without difficulty. From general considerations of the functions involved, it is possible to determine the extension and periodicity of the orbits for any set of initial conditions. The representation used is also convenient for obtaining information regarding the dispersion and focusing characteristics of the trajectories, some of which have unique properties of promise for use in specific instrument design such as mass spectrometers, beta-ray spectrographs, etc. Schematic designs of such instruments are proposed, and a discussion is given of their advantages and special properties.

INTRODUCTION

THE focusing and dispersing properties of a uniform magnetic field have been applied with great success in recent years to mass spectrographs, mass spectrometers, and β -ray spectrometers, as well as to more special uses.

Many instruments have been built and described which employ either 180° focusing or the focusing properties of sector-shaped magnetic fields. All are generically of the same class, of which the 360° analyzer is the only one having the property of perfect focusing. However, it is not practical to attempt to utilize the latter because of the physical impossibility of locating both a source of ions and a collector at exactly the same place.

In contrast to the wide application of the focusing and dispersing properties of a uniform magnetic field, little use has been made of the focusing properties of non-uniform fields. The problem of calculating paths, dispersion, and focusing characteristics for a general type of non-uniform field is one of great mathematical difficulty.¹ There are, however, some cases of considerable physical interest in which the magnetic field varies in a fairly simple manner, and for which it is possible to calculate exactly the paths, dispersion, and focusing properties.

In all cases where the pole faces of a magnet or an electromagnet are symmetrically located with respect to a median plane, the magnetic field at any point on the plane will be perpendicular to it. For an ion or electron moving in this plane the problem of describing its path reduces to a two-dimensional one.

For those cases where the magnetic field in the median plane can be expressed as a function only of one Cartesian coordinate, or as a function only of the radial distance from the axis of symmetry, for cases of circular symmetry, the equations describing the ion or electron paths admit of a simple treatment. Even if the dependence of the field upon such coordinates is known only experimentally, the complete solution may be determined by simple numerical integration to an accuracy equal to that with which the magnetic field is known. The general theory will be outlined and discussed below and certain cases analyzed in detail.

GENERAL THEORY

The Lorentz force equation for a charged particle in the presence of a magnetic field H and the absence of an electric field, is:

$$\mathbf{F} = \frac{e}{c} \mathbf{v} \times \mathbf{H}, \quad (1)$$

where e = charge of particle in e.s.u.; c = velocity of light; and \mathbf{v} = velocity of particle in cm/sec.

* For an abstract of a preliminary report of this work see Phys. Rev. 65, 352 (1944).

¹ While there is a vast literature on the general optics of charged particles moving in magnetic fields, applications of the type considered here do not appear to have been given specific treatment.

In addition to Eq. (1), we have the equation: However, from Eq. (2), we have:

$$(\dot{x})^2 + (\dot{y})^2 + (\dot{z})^2 = v^2 = \text{const.},$$

$$\dot{x} = \pm (v^2 - \dot{y}^2)^{\frac{1}{2}} = \pm v(1 - f^2)^{\frac{1}{2}}. \quad (7)$$

since the magnetic field can do no net work on the charge. For the case of both Cartesian and cylindrical coordinates, we may, without loss of generality, consider H to be parallel to the z direction, so we then have:

$$\begin{aligned} (\dot{x})^2 + (\dot{y})^2 &= v^2, \\ (\dot{r})^2 + (r\dot{\theta})^2 &= v^2. \end{aligned} \quad (2)$$

Here v refers to the resultant velocity in a plane perpendicular to the z direction.

Written out in terms of Cartesian components, Eq. (1) becomes:

$$\begin{aligned} \ddot{x} &= -\frac{e}{mc} H \dot{y}, \\ \ddot{y} &= \frac{e}{mc} H \dot{x}, \end{aligned} \quad (3)$$

where H is the magnitude of the magnetic field, or:

$$\ddot{r} - r(\dot{\theta})^2 = -\frac{e}{mc} H r \dot{\theta}, \quad (4)$$

$$-\frac{1}{r} \frac{d}{dt} (r^2 \dot{\theta}) = \frac{e}{mc} H \dot{r},$$

in cylindrical coordinates. Equations (3) and (4) cannot in general be solved explicitly if H is a function of both coordinates, as the equations will not be linear.

If, however, H is a function of only one coordinate, the equations are solvable in a simple manner, as follows:

Referring to Eq. (3), we may assume, without loss of generality, for this case that $H = H(x)$, and define a function $f = f(x)$ as:

$$f = \frac{e}{vmc} \int H(x) dx. \quad (5)$$

Integrating the second of Eqs. (3), we get:

$$\dot{y} = \frac{e}{mc} \int H dx = vf. \quad (6)$$

Since $dy/dx = \dot{y}/\dot{x}$, we may combine Eqs. (6) and (7) to obtain:

$$\frac{dy}{dx} = \pm \frac{f}{(1 - f^2)^{\frac{1}{2}}}, \quad (8)$$

or:

$$y = \pm \int \frac{f dx}{(1 - f^2)^{\frac{1}{2}}}. \quad (9)$$

We see thus that when H is a function of only one Cartesian coordinate, the equations of the trajectory are reduced to the simple differential equation (8), which permits immediate integration. When the magnetic field is a function only of the cylindrical coordinate r , the treatment is similar. For this case we define a function $g(r)$ by:

$$g(r) = \frac{e}{vmc} \frac{1}{r} \int r H(r) dr. \quad (10)$$

Integrating the second of Eqs. (4), we find

$$r\dot{\theta} = \frac{e}{rmc} \int r H dr = vg. \quad (11)$$

Using Eqs. (2) and (11), we have:

$$\dot{r} = \pm v(1 - g^2)^{\frac{1}{2}}, \quad (12)$$

and since $r\dot{\theta}/\dot{r} = r(d\theta/dr)$, we have from Eqs. (11) and (12):

$$\frac{d\theta}{dr} = \pm \frac{1}{r} \frac{g}{(1 - g^2)^{\frac{1}{2}}}, \quad (13)$$

or:

$$\theta = \pm \int \frac{g dr}{r(1 - g^2)^{\frac{1}{2}}}. \quad (14)$$

We see, therefore, that the treatments for the Cartesian case and for the cylindrical case are similar, and involve essentially nothing more than two quadratures, either or both of which may be done numerically if not analytically.

Equations (5) and (10), which define f and g , will each contain a constant of integration. These constants may be used to specify the slope of the trajectory for any desired value of x or r by direct application of Eqs. (8) or (13). The

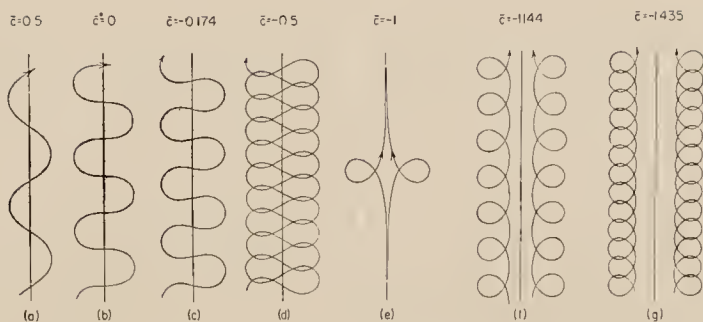


FIG. 1. Various types of orbits possible in a linearly varying magnetic field, determined by the parameter \bar{c} , defined by Eq. (17).

other initial condition, namely, the starting position in the x , y or θ , r plane is taken care of by the constant of integration in Eqs. (9) or (14).

The fact that the equations defining the trajectories involve the radical $(1-f^2)^{1/2}$ for the Cartesian case, and the radical $(1-g^2)^{1/2}$ for the cylindrical case, has a very simple and significant interpretation. Since these radicals must represent real magnitudes for any physically possible trajectory, we see immediately that the extension of the trajectory in the x or r coordinate will be given by $-1 \leq f \leq 1$, or $-1 \leq g \leq 1$, respectively.

If the equation

$$1-f^2=0 \quad (15)$$

has two real roots, the implication is that orbits will be bounded as regards extension in the x coordinate. This follows from the fact that dy/dx will be infinite for x equal to a real root of Eq. (15). If Eq. (15) has only one real root the orbit is one that comes in from and returns to plus or minus infinite values of x . For the case where Eq. (15) has two real roots the orbit will be either completely closed, or have an infinite extension in the y direction. The latter orbits will be of periodic behavior and will, in general, consist of an infinite number of loops of cycloidal appearance.

The same general considerations as just discussed for the case of Cartesian coordinates also hold for the cylindrical system and figures demonstrating them will follow in the detailed discussion of specific cases.

In the calculations for the paths in either coordinate system the quantity e/vmc enters as a fundamental constant of the motion. It is

convenient to define this quantity as a , i.e.:

$$a = e/vmc.$$

In the discussion of many cases of physical interest it is more expedient to refer to the potential of a charged particle as a measure of its energy rather than to its velocity. We may, therefore, write a as

$$a = \frac{1}{c} \left(\frac{150e}{mV} \right)^{1/2},$$

where V is the potential of the particle in volts or its energy in electron volts.

LINEARLY VARYING MAGNETIC FIELD

The linear magnetic field may be defined by:

$$H = bx, \quad (16)$$

the origin being placed where the field is zero. From Eq. (5) it follows that:

$$f = a \int H dx = \frac{abx^2}{2} + \bar{c}, \quad (17)$$

where \bar{c} is the constant integration and $a = e/vmc$, as previously indicated.

Introducing the change of variables:

$$\bar{y} = \left(\frac{ab}{2} \right)^{1/2} y; \quad \bar{x} = \left(\frac{ab}{2} \right)^{1/2} x, \quad (18)$$

so that \bar{y} and \bar{x} are dimensionless, we find Eq. (8) takes the form:

$$\frac{d\bar{y}}{d\bar{x}} = \pm \frac{\bar{c} + \bar{x}^2}{[(1 - \bar{c} - \bar{x}^2)(1 + \bar{c} + \bar{x}^2)]^{1/2}}. \quad (19)$$

By inspection of the right side of this equation it is clear that if it is to represent a real trajectory $\bar{c} < 1$. Moreover, the nature of the real trajectories will be determined by the magnitude of \bar{c} , as follows:

For $1 > \bar{c} > -1$, the trajectories will all cross the y axis, with a slope $= \bar{c}/[1 - \bar{c}^2]^{\frac{1}{2}}$. They will be symmetrical with respect to y , and the ion or electron will oscillate periodically between fixed values of x . If $1 > \bar{c} > 0$, the trajectory will simulate a sinusoidal oscillation with a monotonic increase or decrease in y , as illustrated in Fig. 1(a). When $\bar{c} = 0$, the trajectories will have an inflection when crossing the y axis, as shown in Fig. 1(b), so that the change in y is still monotonic as the path is traversed. For $0 > \bar{c} > -1$, the variation in y is no longer monotonic, and the trajectory tends to form loops as it oscillates between the fixed limits in x [cf. Fig. 1(c)]. At $\bar{c} = -0.46$, the loops of consecutive periods on either side of the x axis touch, and become interlaced [cf. Fig. 1(d)] as \bar{c} is still further decreased. Complete overlapping of the loops, so as to form a single figure-eight trajectory, develops for $\bar{c} = -0.6522$. For the range $-0.6522 > \bar{c} > -1$, they are again similar to a network of interlaced figure of eight oscillations, which spread out and ultimately degenerate into the single pair of split loops when $\bar{c} = -1$, as shown in Fig. 1(e).

In this whole range of \bar{c} the maximum extension of the oscillations, which may be obtained from the roots of Eq. (15), continually increases as \bar{c} decreases, according to the equation:

$$\bar{x}_{\max} = (1 - \bar{c})^{\frac{1}{2}}. \quad (20)$$

Moreover, from the roots of Eq. (15) the width of the oscillations is given by:

$$\bar{x}_{\max} - \bar{x}_{\min} = (1 - \bar{c})^{\frac{1}{2}} - (1 + \bar{c})^{\frac{1}{2}}. \quad (21)$$

The detailed calculation of the trajectories may be readily made by introducing the substitution: $\bar{x} = (1 - \bar{c})^{\frac{1}{2}} \cos \Phi$ and reducing the integral of Eq. (19) to standard elliptic integral form. It is thus found that:

$$\bar{y} = \frac{1}{\sqrt{2}} [2E(k) - K(k) - 2E(\Phi, k) + F(\Phi, k)], \quad (22)$$

where $E(\Phi, k)$, $F(\Phi, k)$ are the incomplete elliptic integrals corresponding to E , K . It is to be noted

that Eq. (21) applies directly only to the quarter-cycle of a single complete oscillation passing through the origin. Its continuation to both preceding and following elements of the trajectory is easily made by simple shifting of the initial point and appropriate changes in sign, as dictated by Eq. (19).

The wave-length, along y , of the oscillations is given by:

$$\lambda = 2\sqrt{2} |2E(k) - K(k)|, \quad (23)$$

where K and E are the complete elliptic integrals of the first and second kind, the modulus $k = [(1 - \bar{c})/2]^{\frac{1}{2}}$, and the absolute value is used to take care of the change in sign of the enclosed term at $\bar{c} = -0.6522$. λ is expressed in the same units as \bar{y} . It will be noted that $\lambda = 4\bar{y}(\bar{x}_{\max})$.

In the limiting case $\bar{c} = -1$, integration of Eq. (19) readily gives:

$$\pm \bar{y} = \frac{1}{\sqrt{2}} \log \frac{\sqrt{2} + (2 - \bar{x}^2)^{\frac{1}{2}}}{\bar{x}} - (2 - \bar{x}^2)^{\frac{1}{2}}, \quad \bar{x} > 0, \quad (24)$$

from which were plotted the trajectories of Fig. 1(e).

The trajectories of greatest practical interest are those for $\bar{c} < -1$. The general features of these can also be deduced by direct inspection of Eq. (19). These no longer cross the \bar{y} axis, but split up into two identically shaped individual trajectories, for each value of \bar{c} , placed symmetrically on the two sides of the \bar{y} axis. Each of these is composed of a series of interlaced or separated loops extending from

$$|\bar{x}_{\max}| = (-1 - \bar{c})^{\frac{1}{2}}, \quad \text{to} \quad |\bar{x}_{\min}| = (1 - \bar{c})^{\frac{1}{2}}, \quad (25)$$

and hence recede from the \bar{y} axis as \bar{c} is decreased. The overlapping of the loops increases as \bar{c} decreases [cf. Figs. 1(f) and 1(g)]. The wave-length is given by:

$$\lambda = 2(1 - \bar{c})^{\frac{1}{2}} \left[\left(1 - \frac{k^2}{2} \right) K - E \right] \quad (26)$$

where now the modulus $k = [2/(1 - \bar{c})]^{\frac{1}{2}}$. A plot of λ and $(\bar{x}_{\max} - \bar{x}_{\min})$ vs. \bar{x}_{\max} is given in Fig. 2. It will be seen that both λ and the lateral range of the oscillations decrease as \bar{x}_{\max} increases—i.e., as the trajectories are confined to regions of greater magnetic field. This is, of course, to be expected from elementary considerations.

For calculating the exact shape of the trajectories for this range of \bar{c} , the integral of Eq. (19) may again be transformed into standard elliptic integrals, by setting $\bar{x}^2 = \cos 2\Phi - \bar{c}$ with the result that:

$$\bar{y} = (1 - \bar{c})^{\frac{1}{2}} [E(\Phi, k) - (1 - \frac{1}{2}k^2)F(\Phi, k)]. \quad (27)$$

As remarked above, orbits of the type illustrated in Figs. 1(f) and 1(g) are of greatest interest. This is because of the practical difficulty of obtaining a field variation in which H is an odd linear function of x . Also, for any restricted region of an actual non-uniform field H may be

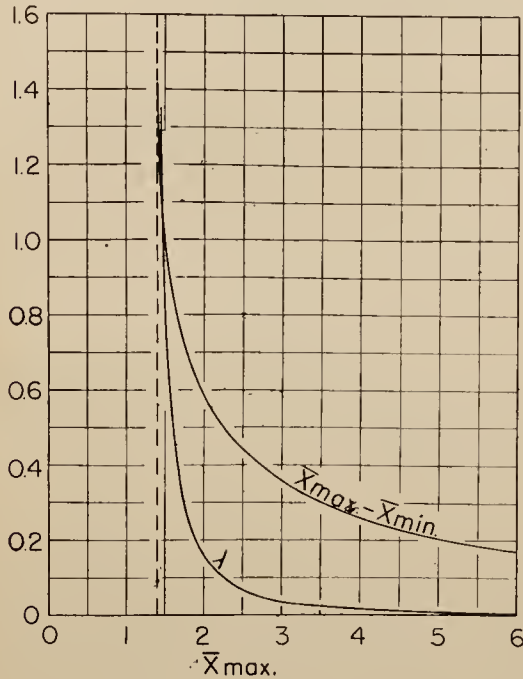


FIG. 2. The variation of the dimensionless wave-length λ and lateral range $\bar{x}_{\max} - \bar{x}_{\min}$, of periodic orbits in a linearly varying magnetic field, with the maximal extension \bar{x}_{\max} .

considered linear with distance to a first approximation. The orbits calculated from Eq. (19) will therefore represent the actual paths of the ions or electrons to at least a first approximation. Application of such orbits as in Figs. 1(g) and 1(f) to magnetic focusing instruments will be discussed below.

EXPONENTIALLY VARYING FIELD

For the case of an exponentially varying field in Cartesian coordinates we may write H as:

$$H = H_0 e^{bx},$$

where H_0 is the magnitude of the field strength at the value of x chosen as the origin of the coordinate system, and b is the constant determining the rate of change of H with x .

The function f then becomes:

$$f = \frac{aH_0}{b} e^{bx} + \bar{c}, \quad (28)$$

where \bar{c} is a constant of integration which may be adjusted to give the orbit the desired slope at any value of x . For this case Eq. (8) becomes:

$$\frac{dy}{dx} = \pm \frac{\frac{aH_0}{b} e^{bx} + \bar{c}}{\left\{ 1 - \left(\frac{aH_0}{b} e^{bx} + \bar{c} \right)^2 \right\}^{\frac{1}{2}}}. \quad (29)$$

By making the transformation:

$$v = \frac{aH_0}{b} e^{bx},$$

Eq. (29) may be readily integrated to give the general solution:

$$y = \pm \frac{1}{b} \left\{ \sin^{-1} (v + \bar{c}) - \frac{\bar{c}}{(1 - \bar{c}^2)^{\frac{1}{2}}} \times \log \left[\frac{\{1 - (v + \bar{c})^2\}^{\frac{1}{2}} + (1 - \bar{c}^2)^{\frac{1}{2}}}{v} - \frac{\bar{c}}{(1 - \bar{c}^2)^{\frac{1}{2}}} \right] \right\}, \quad (30)$$

when $|\bar{c}| < 1$, and

$$y = \pm \frac{1}{b} \left\{ \sin^{-1} (v + \bar{c}) + \frac{\bar{c}}{(\bar{c}^2 - 1)^{\frac{1}{2}}} \sin^{-1} \left[\frac{1 - \bar{c}^2 - \bar{c}v}{v} \right] \right\}, \quad (31)$$

when $\bar{c} < -1$.

For the special case, $\bar{c} = -1$,

$$y = \pm \frac{1}{b} \left\{ 2 \sin^{-1} \left(\frac{v}{2} \right) + \frac{(2v - v^2)^{\frac{1}{2}}}{v} \right\}.$$

Orbits defined by Eq. (30) are illustrated by (a), (b), and (c) in Fig. 3. In each case the particle enters the magnetic field from $x = -\infty$, or, physically speaking, from a region of very weak H . As must obviously be the case, each orbit is symmetrical about the x axis. Each path

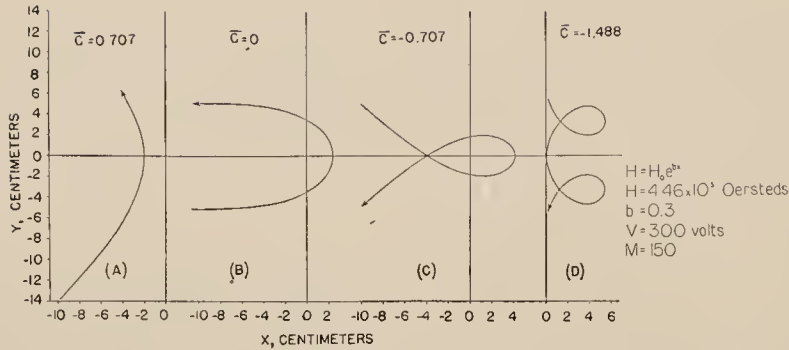


FIG. 3. Various types of orbits possible in an exponential magnetic field, determined by the parameter \bar{c} , defined by Eq. (28). All orbits are for singly-charged particles of 300-ev energy and 150 atomic mass units. Note: The second line of the explanation at the right of the cut should read $H_0 = 4.46 \times 10^3$ oersteds.

is shown in the neighborhood of $H = H_0$, which establishes the origin of the x coordinate. Orbits (a), (b), and (c) represent a particle of 150 atomic mass units and 300 electron volts energy coming from $x = -\infty$ with initial slope of 1, 0, and -1 , respectively. Orbit (d) is for a particle of the same mass and energy but so projected in the x, y plane that the path has infinite slope at $x = 0$.

Orbits of the type illustrated by (b) are of particular interest, as the total extension in the y direction depends only on the exponential coefficient b , and is independent of the values of the mass and velocity of the ion or electron. This fact is immediately seen upon setting $\bar{c} = 0$ in Eq. (30), which physically corresponds to the particles approaching regions of stronger magnetic field with an original direction parallel to the x direction. This situation affords an opportunity for perfect focusing, further discussion of which will be given later.

If the ion or electron is introduced into the magnetic field in such a manner that its subsequent orbit is bounded in the x direction, it will be of the type illustrated by (d), Fig. 3. This type of orbit is also of interest as regards application to focusing problems, and will be discussed in more detail below. For this type trajectory the total width in the x dimension is readily calculated from the separation of the roots of Eq. (15).

The behavior of orbits of type (d) as regards their total width in the x direction and their wave-length λ can be discussed in a manner

similar to that used for the linearly varying field. For a particular value of \bar{c} we have:

$$x_{\max} = \frac{1}{b} \log \frac{b}{aH_0} (1 - \bar{c}), \quad (32)$$

$$x_{\min} = \frac{1}{b} \log \frac{b}{aH_0} (-1 - \bar{c}).$$

As $\bar{c} < -1$ for all such orbits the arguments of the logarithms will be positive. We may express $x_{\max} - x_{\min}$ as a function of x_{\max} by eliminating \bar{c} in Eqs. (32) to give:

$$x_{\max} - x_{\min} = x_{\max} - \frac{1}{b} \log \left(e^{bx_{\max}} - \frac{2b}{aH_0} \right),$$

which behaves qualitatively like the similar quantity for the linear case which is plotted in Fig. 2.

From the nature of Eq. (31) it is seen that the orbits are periodic with a wave-length of λ given by:

$$\lambda = \frac{2\pi}{b} \left(1 + \frac{\bar{c}}{(\bar{c}^2 - 1)^{1/2}} \right), \quad (33)$$

or

$$\lambda = \frac{2\pi}{b} \left[1 + \frac{\frac{aH_0}{b} e^{bx_{\max}}}{\left[\left(1 - \frac{aH_0}{b} e^{bx_{\max}} \right)^2 - 1 \right]^{1/2}} \right].$$

RADIAL FIELDS

Although Eqs. (10) and (14) make it possible to determine the path of a charged particle in

any field of circular symmetry, the functional variation of H we shall discuss here is given by:

$$H = \frac{H_0}{r^{n+1}},$$

where $n > -1$, and H_0 is a constant. It will, of course, be physically impossible for H to obey this relation for values of r including the origin. However, it will suffice if the relation is obeyed within certain limits of r , or for values of r above a definite radius.

For this case (and $n \neq 1$) $g(r)$ becomes:

$$g = \frac{aH_0}{(1-n)r^n} + \frac{\bar{c}}{r}, \quad (34)$$

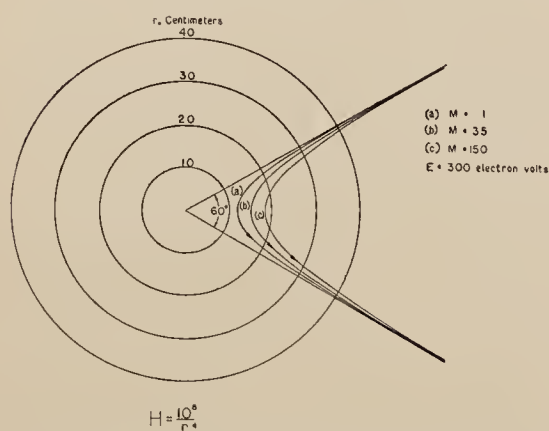


FIG. 4. Non-periodic orbits with common asymptotes in a radially varying magnetic field, with $n=3$, for singly-charged particles of 300 ev and various atomic masses M .

and we have:

$$\theta = \pm \int \left(\frac{aH_0}{(1-n)r^{n+1}} + \frac{\bar{c}}{r^2} \right) / \left[\left(1 - \left\{ \frac{aH_0}{(1-n)r^n} + \frac{\bar{c}}{r} \right\}^2 \right) \right]^{\frac{1}{2}} dr. \quad (35)$$

Equation (35) is in general more amenable to numerical than analytical treatment.

One case of important physical interest does, however, admit of simple analytical treatment. This is that of charged particles approaching regions of strong H from regions of weak H , and with an initial direction along a radius vector and toward the axis of symmetry.

Before discussing the solution for this particular case it will be of interest to examine the general features of the orbits defined by Eq. (35). It will be noted first, from Eq. (34), that if $n > 0$ ($\neq 1$), $g(r) \rightarrow 0$ as $r \rightarrow \infty$. Hence by Eq. (13), $r(d\theta/dr) \rightarrow 0$ as $r \rightarrow \infty$. This means that for $n > 0$ ($\neq 1$) all orbits entering the field from infinity must be asymptotically parallel to a radius vector. As all radii vectors are equivalent, these orbits may thus be considered as necessarily entering the field parallel to the polar axis ($\theta=0$). If, in particular, these orbits asymptotically degenerate into linear paths at a normal distance h from the polar axis, i.e., so that

$$r \sin \theta = h,$$

then it follows that in the limit as $r \rightarrow \infty$,

$$\frac{d\theta}{dr} \rightarrow -\frac{h}{r \cos \theta} \sim -\frac{h}{r} \sim g.$$

By Eq. (34), such an asymptotic behavior can be satisfied only if $n > 1$ and $\bar{c} = -h$. Accordingly, in inverse power radial fields for which $n > 1$, $-\bar{c}$ is simply the normal distance from the polar axis with which the particle enters the field. The restriction $n > 1$ evidently means that if $n < 1$ there can be no orbits which enter the field along linear paths parallel to a radius vector. If $0 < n < 1$ the value of \bar{c} can be determined by fixing $r(d\theta/dr)$ at a given radius, computing g from Eq. (13), and then \bar{c} by Eq. (34).

If $n=0$, the orbits entering or leaving the field at $r = \infty$ will asymptotically cut the radii vectors at an angle $\sin^{-1} aH_0$. For this case the integral for $\theta(r)$ can be readily evaluated to give expressions similar to Eqs. (30) and (31). If $-1 < n < 0$ the orbits will be restricted to finite regions of the (r, θ) plane, and be bounded by a maximum value of r .

Returning to the special case $n > 1$, and also assuming that the particle actually enters the field along the polar axis ($\bar{c}=0$), we may readily integrate Eq. (35) and obtain:

$$\theta = \pm \frac{1}{n} \sin^{-1} \frac{aH_0}{(1-n)r^n}. \quad (36)$$

Orbits of this type for $n=3$ are plotted in Fig. 4. It is interesting to note that these orbits

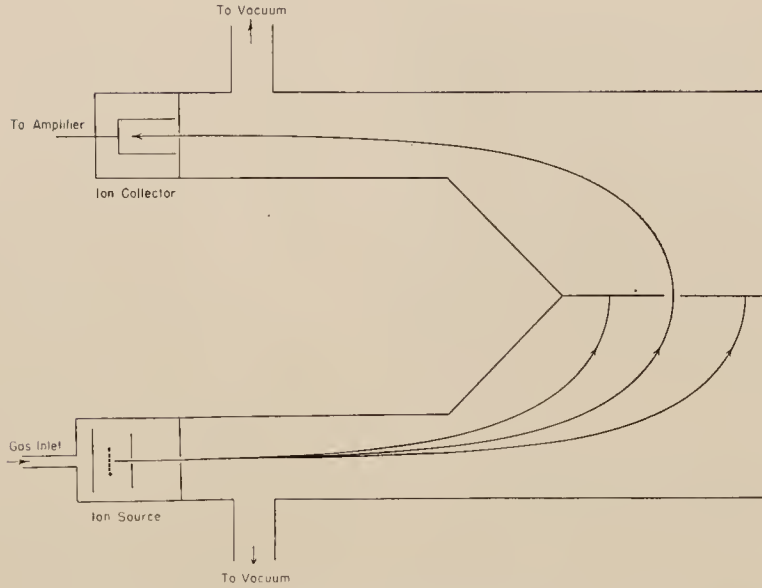


FIG. 8. Schematic diagram of a magnetic analyzer utilizing an exponentially varying magnetic field.

A schematic diagram of an instrument designed to employ this type of orbit is shown in Fig. 9. An idea of the dispersion obtainable may be seen from Fig. 4, and may be expressed analytically as:

$$\frac{\Delta r}{r} = \frac{1}{n} \frac{\Delta a}{a} = \frac{1}{n} \frac{\Delta(nv)}{nv},$$

where r and $r + \Delta r$ are the turning radii for particles of parameters a and $a + \Delta a$. Fields which decrease with radial distance with the same functional form have been successfully used in the betatron.²

To obtain the field variation just discussed the circularly symmetric pole faces must be so shaped that the following equations are satisfied:

$$\frac{\partial}{\partial r} \left(r^2 \frac{\partial M}{\partial r} \right) + \frac{1}{\sin \Phi} \frac{\partial}{\partial \Phi} \left(\sin \Phi \frac{\partial M}{\partial \Phi} \right) = 0, \quad (41)$$

$$\left. \begin{aligned} \frac{\partial M}{\partial r} &= 0, \\ \frac{1}{r} \left(\frac{\partial M}{\partial \Phi} \right) &= \frac{H_0}{r^{n+1}}, \end{aligned} \right\} \Phi = \pi/2, \quad (42)$$

where M is the magnetostatic potential, and Φ is the latitude angle.

Setting $\mu = \cos \Phi$, and $M = (H_0/r^n) F(\mu)$, we find $F(\mu)$ must satisfy the Legendre equation:

$$(\mu^2 - 1) \frac{d^2 F}{d\mu^2} + 2\mu \frac{dF}{d\mu} - n(n-1)F = 0.$$

To fix the specific solutions for $F(\mu)$ applying to the present problem, the equivalents of Eq. (42), namely: $F(0) = 0$; $F'(0) = -1$, are to be imposed on the functions $F(\mu)$.

If we let the opposite pole faces have magnetostatic potential $+M_0$ and $-M_0$, the contours will be given by:

$$r = \left\{ \frac{H_0 F(\theta)}{\pm M_0} \right\}^{1/n}, \quad (43)$$

the sign of $F(\theta)$ automatically changing in passing from one pole face to the other, so as to ensure a real value for r .

As the region over which it is desired that H have the specified functional form will not extend to the origin, the pole faces in this region need not follow the shape required by Eq. (43). This physical observation also obviates the apparent difficulty arising from the singularities at $\mu = \pm 1$ in the functions $F(\mu)$ when n is not an integer.

² D. W. Kerst, Phys. Rev. **60**, 47 (1941).

The periodic or cyclic orbits of the type in Figs. 1(f) and (g), and Fig. 3(d), also have properties of promise for focusing applications. One of the most important of these properties is illustrated in Fig. 2. This shows how the wave-length λ , or spatial periodicity of the orbit, decreases with increasing x_{\max} . This curve was drawn for H varying linearly with x , but its character will be essentially the same for other functional variations wherein H increases monotonically with increasing x .

An application of such orbits may be made to the design of a mass spectrometer or similar instrument, as indicated schematically in Fig. 10. In such an instrument the ions are so accelerated by a suitable source that they are projected into the magnetic field with the x_{\max} for each orbit lying within the exit slits.

In Fig. 11 may be seen a schematic diagram of the state of affairs at the exit slits S_1 and S_2 of such an ion source. We shall assume that the potential distribution in the source is such that all ions acquire essentially the same potential, and that the last two slits, i.e., S_1 and S_2 in Fig. 11, are at the same potential and are operative only in defining the emergent beam. Moreover, these slits will be assumed to be geometrically similar and located identically as regards the x coordinate.

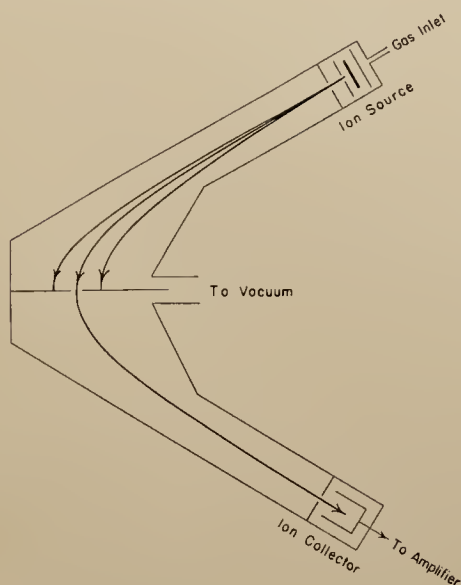


FIG. 9. Schematic diagram of a magnetic analyzer utilizing a radially varying magnetic field.

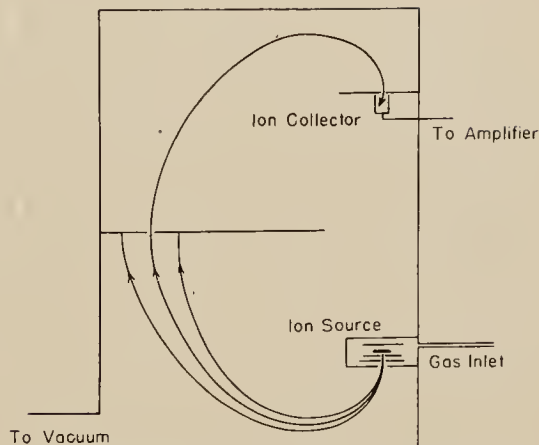


FIG. 10. Schematic diagram of a magnetic analyzer utilizing periodic orbits in an exponentially varying magnetic field.

With such an arrangement all ions leaving the exit slits will follow orbits having approximately the same radius of curvature at the slits, differing only in the angle of emergence.

In Fig. 11, (c) represents the orbit with the smallest value of x_{\max} that can emerge from the slits, (d) that with the largest value of x_{\max} , while (a) and (b) represent the paths of greatest divergence in angle of emergence. As S_1 and S_2 cover the same range along the x direction, the x_{\max} will be the same for orbits (a) and (b).

Consider now the orbits (a), (b), (c), and (d) when the particles have advanced by exactly one wave-length in their periodic paths. Since (a) and (b) have the same x_{\max} , they will have the same λ . Therefore a slit S_1' of the same width as S_1 and located at the same values of x , but displaced along y by a distance λ , will collect both (a) and (b). That is, (a) and (b) will pass through S_1' with exactly the same geometry as they passed through S_1 . As orbit (c) has a smaller value of x_{\max} , it will be displaced slightly upward, relative to (a) and (b). Conversely, as orbit (d) has a larger value of x_{\max} , its λ will be smaller than that of (a) and (b). Hence as it passes through S_1' it will be displaced slightly downward relative to (a) and (b).

This shifting of the orbits (c) and (d) relative to (a) and (b) means that the latter will limit the lateral spread in the ion beam when entering S_1' just as they defined the angular spread in

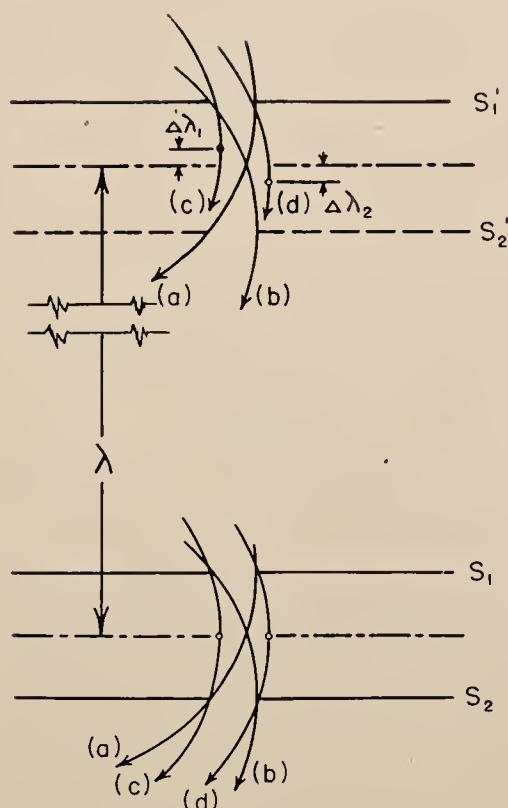


FIG. 11. Schematic diagram of the geometry of the orbits at the source and collector slits of an instrument of the type shown in Fig. 10.

the beam emerging from the source slits S_1 and S_2 . In the design of such an instrument, as schematically shown in Fig. 10, the final two exit slits will correspond to S_1 and S_2 , and the collector slit should be of the same dimensions as S_1 and located at the same distance along the x axis. The separation along the y axis between S_1 and S_1' will then define the wave-length λ for which the above-described focusing process applies. Any ion may be made to follow an orbit of any chosen λ by properly fixing the accelerating voltage in the ion source. It is to be noted that for the collector the one slit S_1' is sufficient. S_2' is shown in Fig. 11 only to indicate the geometry of the orbits at this point. If the instrument is to be used so that only ions of one mass or of small range of momentum are to pass the collector, an aperture or slit may be introduced, as shown in Fig. 10.

The calculation of the dispersion at the region of the selector slit or aperture is easily made by application of Eq. (29). For this purpose it is convenient to choose the origin at the exit slits of the ion source. Then, since $dy/dx = \infty$ at the ion source ($x=0$), \bar{e} must have the value

$$\bar{e} = 1 - \frac{aH_0}{b}.$$

At the turning point of the orbit, i.e., at the plane of the selecting slits, $dy/dx = \infty$ again, so that:

$$\bar{e} + \frac{aH_0}{b} e^{bx} = -1,$$

giving for the location of the turning point:

$$x = \frac{1}{b} \log \left\{ 1 - \frac{2b}{aH} \right\}.$$

For two ion beams of momentum parameters a_1 and a_2 the turning points will then be separated by a distance:

$$(x_1 - x_2) = \frac{1}{b} \log \left\{ \frac{1 - \frac{2b}{a_1 H}}{1 - \frac{2b}{a_2 H}} \right\}.$$

A similar type of instrument could be designed using the periodic orbits in a radial field, such as shown in Fig. 5. Similar considerations with respect to focusing and the use of selector slits will be applicable to such instruments. Finally, it should be noted that the above discussion has referred to particles moving in the median plane between the pole pieces generating the magnetic field. Hence in practical designs account will have to be taken of the perturbations in the orbits of particles off the median plane owing to the curvature of the magnetic flux lines.

The authors are indebted to Mr. N. F. Kerr for assistance in preparing the drawings and making the calculations, and to Dr. P. D. Foote, Executive Vice President of The Gulf Research and Development Company, for permission to publish this paper.

Gas Cell for Beckman Quartz Spectrophotometer

NORMAN D. COGGESHALL,
Gulf Research & Development Company, Pittsburgh, Pa.

Reprinted from Analytical Edition
INDUSTRIAL AND ENGINEERING CHEMISTRY
Vol. 17, Page 513, August 15, 1945

Gas Cell for Beckman Quartz Spectrophotometer

NORMAN D. COGGESHALL, Gulf Research & Development Company, Pittsburgh, Pa.

A double-compartment gas-absorption cell for use with the Beckman quartz spectrophotometer is described. The assembly consists of a machined brass block, quartz windows, and packless valves connected to standard ground-glass joints.

IN THE course of applying a Beckman quartz spectrophotometer to analytical work, it was found desirable to analyze for gaseous absorbers such as butadiene. Since most of the demands for analyses were for liquid samples and the need for the analyses of gas samples was not continuous, a gas cell that could be used in the same manner as the liquid cells without any special conversion was needed. The cell described below has been very successful for this type of need, and this description is being published that others may take advantage of the author's experience.

The complete cell assembly (Figure 1) consists of a brass block machined for two separate gas compartments, quartz plates cemented to the machined surfaces to form windows, and inner parts of ground-glass joints communicating to the gas compartments through two metal packless valves. These metal packless valves were designed for work with hydrocarbon gases and are described elsewhere (*1*). They are not much larger than glass stopcocks and are needle valves equipped with metal bellows for mechanical movement.

The distance between the centers of the two gas compartments is the same as the corresponding distance for two adjacent compartments of the liquid cell holder furnished with the Beckman instrument. The bottom dimensions of the brass block are almost identical with the bottom dimensions of the liquid cell holder and this allows it to be inserted and moved back and forth by means of the cell positioning knob. Relative to the bottom dimensions, the two gas compartments are located in the same positions as the two center liquid cell compartments and this allows light transmission to be obtained when the cell positioning rod is in position 2 or 3.

The packless valves are connected to the brass block by means of sections of 0.25-inch outside diameter metal tubing approxi-

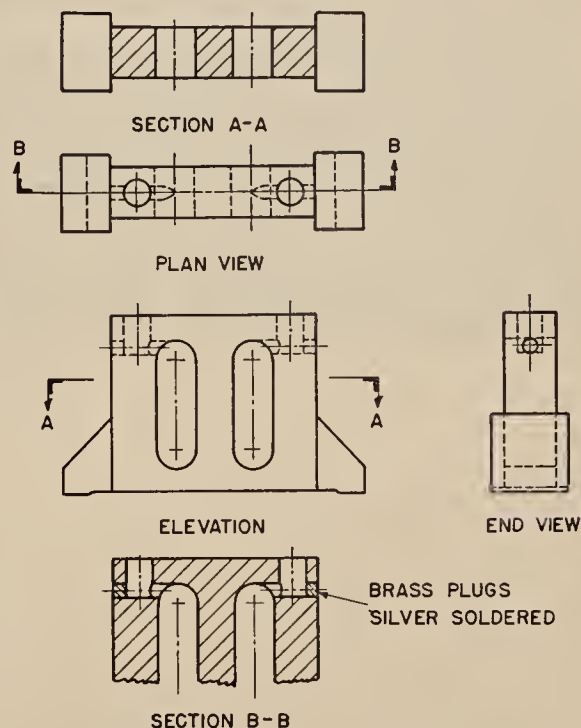


Figure 2. Structural Details of Brass Block Forming Main Body of Gas-Absorption Cell

mately 1 inch long. Attached to the ends of the valves opposite the metal cells are short sections of Kovar tubing onto each of which has been made a glass-to-metal seal. To this is sealed the inner part of a Pyrex ground-glass joint using a graded seal.

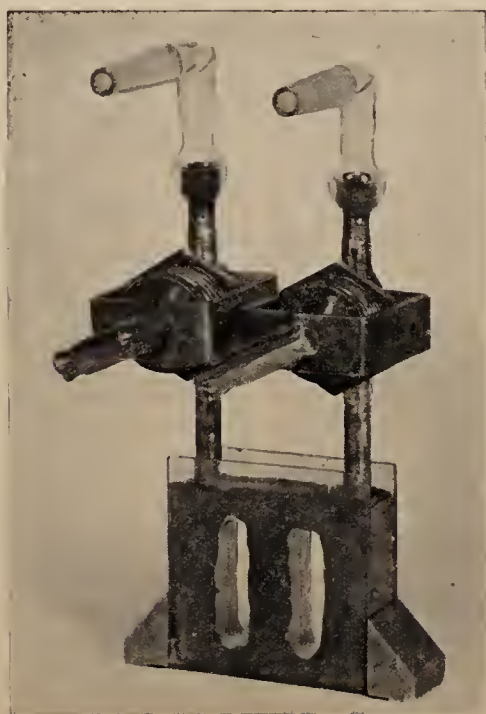


Figure 1. Double-Compartment Gas-Absorption Cell

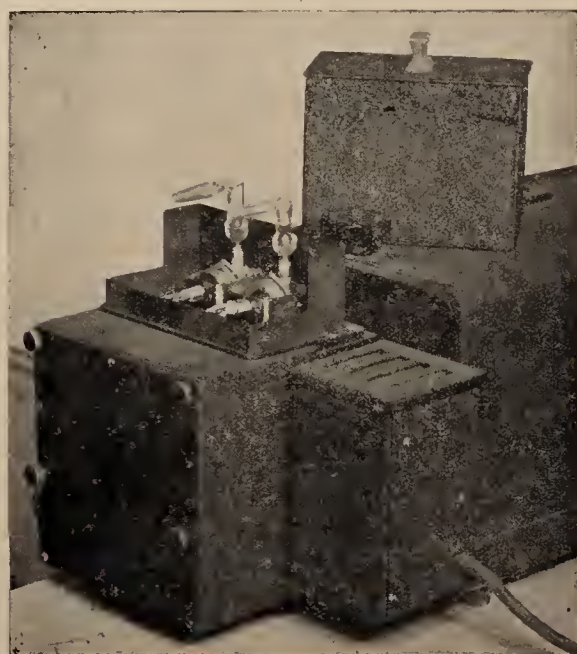


Figure 3. Gas-Absorption Cell in Working Position
Light-tight cover is behind slit-controlling knob

For evacuating a cell or filling it with a sample it is connected by means of the ground-glass joint to a vacuum and gas-handling system.

The windows on the two gas cells were made by cementing two quartz plates onto the machined faces of the brass. These quartz plates were obtained from The Thermal Syndicate, Ltd., 12 East 46th St., New York 17, N. Y., and were polished enough to give them good transparency. General Electric Glyptol No. 1201-red was used to cement them on.

In Figure 2 may be seen the construction details for the brass block, which is machined from a solid piece of metal by standard shop procedures. The metal tubes from the valves are soft-soldered into the holes entering the top of the block. The holes drilled from the ends to allow communication with the gas compartments are sealed by means of brass plugs set in silver solder.

The extended lightproof cover built onto the instrument to allow head room for the metal valves and the ground-glass joints can be seen in Figure 3. A metal flange is built around the sample compartment, and fastened down by screws to the metal parts that house the filter slide and sample mover. Onto this flange is slipped the rectangular cover seen resting on the instrument just beyond the slit-controlling knob. This arrangement provides a light-tight cover that allows adequate head room for

the movement of the complete gas cell assembly. The flange does not interfere with the placing of the liquid cell holder in the instrument, and the same cover is used for both gas and liquid work with no changes.

One compartment is used as comparison cell. Thus if the optical density of one cell is known, using the other as a standard, the optical density of the sample is corrected for the difference of cell transmission by a simple addition or subtraction. The cell correction can be found with the two cells either evacuated or filled with air. For the author's case, one cell had a transmission of about 98.5% of that of the other over the useful range of wave lengths.

The fact that this gas cell can be used at any time with no instrument modifications is a convenience, since gas and liquid samples may be run in sequence or an occasional gas sample may be run in the midst of a group of liquid analyses with no appreciable interruption of the analytical work.

LITERATURE CITED

- (1) Topanelian, E., Jr., and Coggeshall, N. D., *Rev. Sci. Instruments* in press.



INFRA-RED SPECTROSCOPY

by NORMAN D. COGGESHALL
Gulf Research & Development Co.
Pittsburgh, Pa.

INFRA-RED SPECTROSCOPY

Saves Time in Industrial Analysis and Research

by NORMAN D. COGGESHALL, Physicist
Gulf Research & Development Company
Pittsburgh, Pa.

ENOUGH HAS BEEN LEARNED ABOUT infra-red spectroscopy to permit its use in routine industrial analysis, as well as in research. Analyses, which by chemical methods require hours, can now be carried out in a few minutes by this technique. The initial cost—five thousand dollars, including all necessary accessories—is not prohibitive for the average equipment budget.

IN THE PAST few years there has been considerable excitement and publicity over the applications of infra-red spectroscopy to chemical problems. This has taken the form of a large number of articles, discussions, and technical publications¹ as well as advertisements issued by the instrument makers.² The principal applications which the chemical industry is making of this tool are analyses of chemical mixtures by techniques which are both speedier and more accurate than prior chemical means, and the solutions of research or control problems on such subjects as molecular structure, particle size, polymerization, etc.

For many years the fundamental aspects of infra-red spectroscopy have been delved into by physicists.³ During these studies the subject became sufficiently developed and the basic facts clearly enough understood so that widespread application naturally followed as soon as more rugged equipment was built. Now, by following directions from a manual or sheet of instructions carefully, it is possible for personnel without advanced academic training to use the equipment and techniques with a considerable saving of time and expense.

HOW IT WORKS

The region of the spectrum in which we are interested here, called the infra-red, lies between 1μ and 20μ ($1\mu = 10^{-4}\text{cm}$). These radiations have much longer wavelengths than the eye, photographic plates, or photoelectric cells can

detect. The manner of applying it is to utilize the differences in absorbing powers for different substances in this region. Since the optical instruments used (about which there will be some discussion below) can separate light of all wavelengths into beams of uniform wavelengths, it is possible to examine a substance at these individual wavelengths and in this way to "map" its absorption spectrum. For example, with the instrument set to allow measurements at a particular wavelength, we may determine the intensity of light falling upon a substance and the intensity of light which passes through it, thus allowing us to calculate the percent transmission. If we do this for successive wavelengths and plot the results, we obtain absorption spectra, such as those shown in Fig. 1.

In Fig. 2 is seen a schematic diagram of an infra-red spectrometer by means of which the data can be obtained. In this figure, A represents a source of infra-red radiation which may be a rod of carborundum through which electrical current is passing, causing it to operate at near white heat. Light from A is caught by the mirrors B' and B and focused on the slit D. Before reaching D, however, it passes through the sample cell C. After passing through the slit D the light goes on until it is reflected by the mirror E. This mirror gathers the light into a parallel beam and as such it falls upon the optical prism F. The prism is made of some material such as lithium fluoride, sodium chloride, or potassium bromide. Upon passing through the prism the different wavelengths are bent differently with the result that they emerge from the second face of the prism at slightly

different angles. The light is now reflected by the mirror G so that it again passes through the prism with additional angular separation of the wavelengths. Some of the light, after passing through F for the second time, is caught by E and reflected onto the mirror H which allows it to pass through the slit I onto the mirror J, which reflects it onto the final mirror K. From K the light goes to L, a vacuum thermocouple, from which electrical signals are obtained. With this arrangement of optical parts, the light passing through the slit I is practically all of the same wavelength. The wavelength of the light passing through I may be controlled by changing the angle of the mirror G. This is done by a mechanical arrangement so that readings may be taken manually, or the mirror may be rotated mechanically with automatic recording of the spectra. Specially built to be responsive to minute amounts of radiant energy, the thermocouples are operated in a vacuum to increase their sensitivity. In operation the sample cell C may be moved out of the light path to allow a determination of the light intensity of a certain wavelength which is incident upon the cell. When it is moved in place, the intensity of light of the same wavelength which is transmitted by the sample is determined. The windows as well as the prism must be of the materials mentioned above since glass or quartz will not transmit light of the wavelength used. In Fig. 3 may be seen a commercially made instrument, while Fig. 4 illustrates three different types of absorption cells in use. The one on the left is for gases, the center one is for materials in solution with a relatively transparent solvent such as CCl_4 , and the right hand one is for pure liquids. The instrument shown in Fig. 4 has gas cells in place in an adjustable carriage.

WHY IT WORKS

The manner in which a compound ab-

The author is indebted to Miss E. L. Saier for obtaining and tabulating some of the data used and to Dr. Paul D. Foote, executive vice-president of Gulf Research & Development Company, for permission to publish this material.

sorbs light in the infra-red region depends directly and intimately upon its molecular structure. The light energy absorbed excites vibrations between and among the atoms constituting the molecule. As a result the mechanical structure of the molecule, i.e. the geometrical disposition of the atoms and the forces between them, determines which wavelengths are strongly absorbed and which are not. Two basic facts emerge from this: different compounds with some similarities in structure will, in general, exhibit some similarities in their absorption spectra; and different types of molecules will have differences in molecular structure which are responsible for variations in the absorption spectra. As an example of the first fact, it is true that all compounds containing the C-H valence bond will have an absorption band near 3.4μ , while all molecules containing an O-H group will have a band near 2.75μ . Other types of bonds which will cause absorption at approximately the same wavelengths irrespective of the remainder of the molecule are N-H, Cl-H, C=O, C=C, etc.

If we look at Fig. 1, certain similarities and differences in the absorption spectra will be evident. For example, each compound shows heavy absorption at about 3.5μ . This absorption, as well as the doublet absorption at about 7μ , is due to the C-H valence groups in the molecules. This illustrates how compounds containing the same valence groups always have absorption bands at about the same wavelength. This phenomenon is of very great usefulness in research work, where problems of molecular structure are encountered. Valence groups which can readily be determined from the absorption spectra are O-H, C-H, N-H, C=O, C=C, and C=C as well as several others. In a particular problem an organic chemist may prepare a compound for which he knows the empirical formula, i.e. the relative numbers of the different elements present. However, he may not know the geometrical disposition of the atoms in the molecule, i.e. the structural formula. If the molecule contains an oxygen atom the compound may be an ether, an alcohol, or a ketone. If it is an alcohol an O-H absorption band will appear; if it is a ketone a C=O absorption band will appear; if it is an isomeric mixture of the keto and enol form both bands will be present; and if it is an ether neither of them will be evident. Thus, with such information as this and knowledge of its chemical nature supplied by the one preparing the compound, it is often possible to determine completely the molecular structure. Identification work of this sort is actually being done on an almost routine basis in many industrial laboratories today.

Returning again to Fig. 1 we see that there are a number of large and distinct differences between the spectra shown. These differences form the basis for the

use of infra-red absorption for quantitative analyses. The infra-red absorption at any particular wavelength for a mixture of compounds is the resultant of the absorption due to each individual one present. Thus, if the absorbing properties of the different compounds in the

pure state are known, the data obtained for a mixture can be used in calculations which will yield the individual concentrations. This process is really more complicated than has been indicated here and it is beyond the scope of this article to outline the details. It has been de-

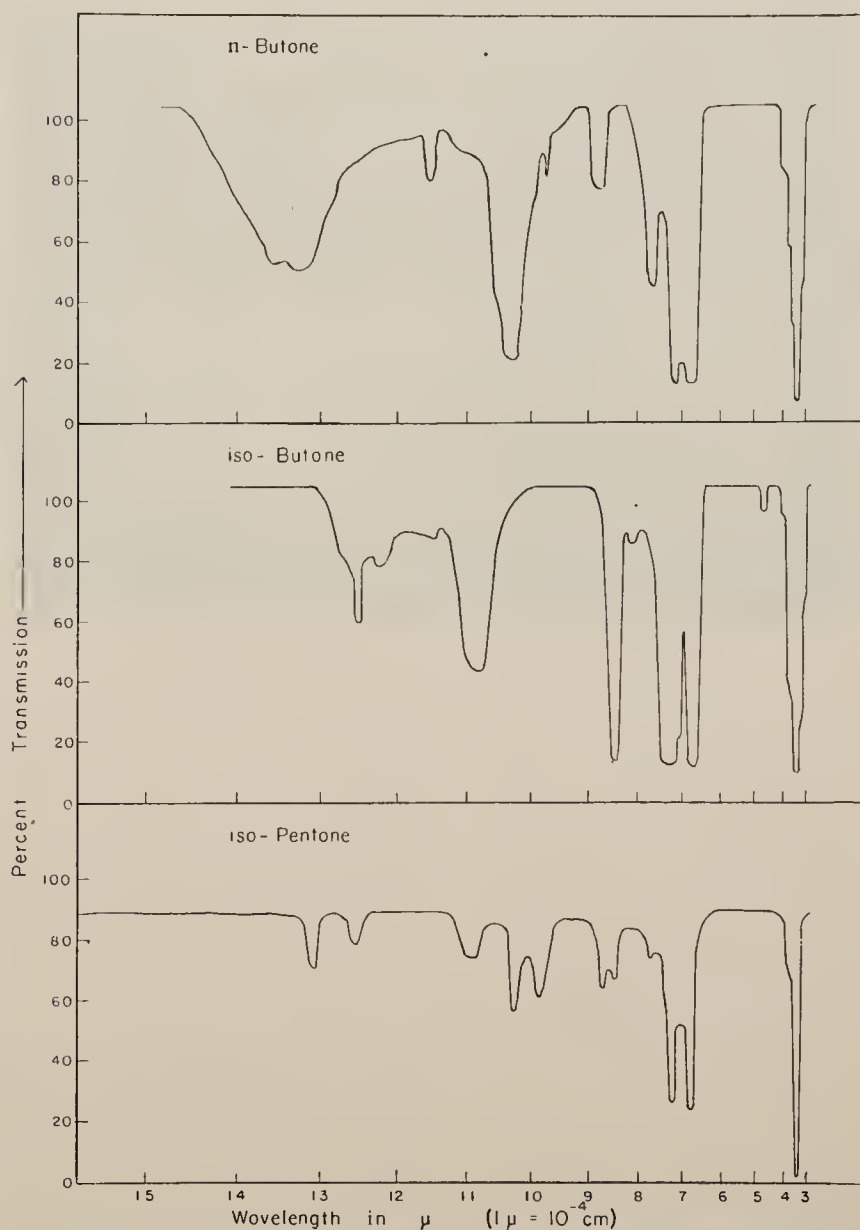
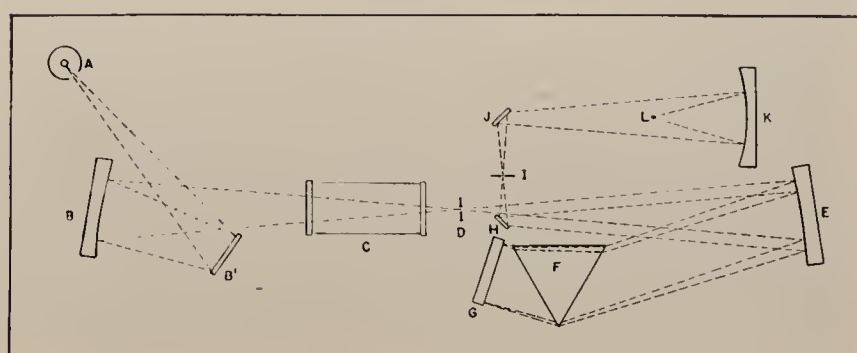


Fig. 1—Infra-red absorption spectra of n-butane, isobutane, and isopentane.



(Illustration Courtesy Perkin-Elmer Corporation)

Fig. 2—Optical diagram of versatile infra-red spectrometer.

scribed in the literature,⁴ however, and is in very wide use today.

USE IN ANALYSIS

An application of the quantitative method which has been of great value to the petroleum industry in the past few

of the instrument, and the mixture must be pretty nearly free of compounds not among the system for which the calibration is made. As an example of the latter, a mixture of the C₄ hydrocarbons named should not contain more than a few per cent of lighter or heavier

it can be obtained from Table II which gives a comparison between the compositions of the samples as blended and as found by infra-red.

A further application along the same line is the analysis of flue gases from a catalytic cracking unit. Periodic analyses of such flue gases for CO, CO₂, and SO₂ may be used for control purposes as well as for giving important information concerning the operation. Such analyses may be carried out in about twenty-five minutes total time, including calculations.⁵ Table III, which compares the results obtained for a series of synthetic blends with the compositions as blended, illustrates the accuracy obtainable using an ordinary monochromator and auxiliary apparatus.

In the analysis of mixtures of liquids all of which have nearly the same boiling points, fractional distillation is at a disadvantage if the concentrations of the individual compounds are desired. But since the individual compounds have differences in molecular structure, they will manifest differences in their infra-red absorption spectra which make the analyses by this method feasible. Even if the mixtures are of isomers which differ only in details of atomic groupings, their spectra will be distinctly different. Fig. 1 illustrates this, where it is obvious that *n*-butane and *i*-butane have quite different spectra. If the mixture is known or is found to contain a large number of separate compounds, it will in most cases be practical to fractionally distill it into cuts each containing a smaller number. These cuts may then be examined by infra-red to obtain the individual concentrations in each and the results for all

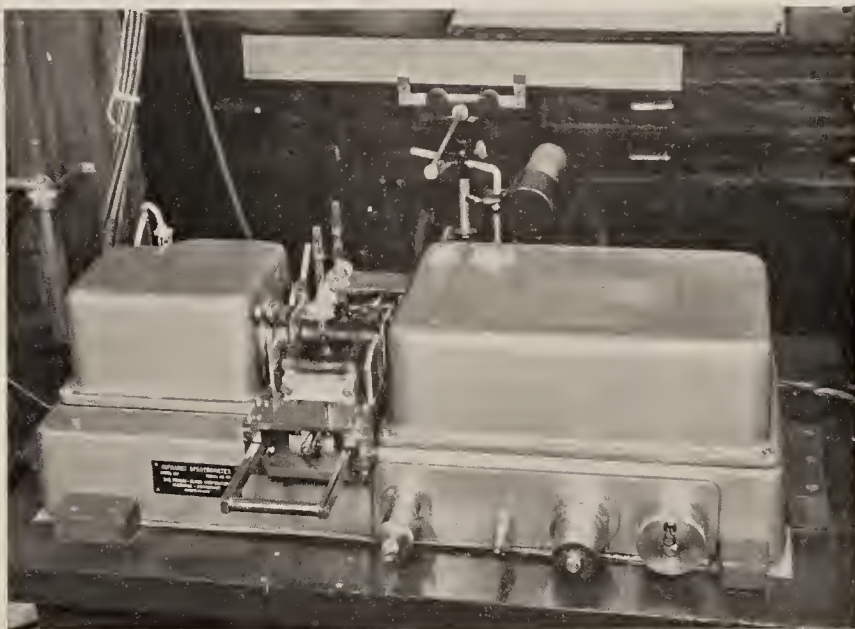


Fig. 3—Infra-red spectrometer set up for routine gas analysis.

years is the analysis of mixtures of the C₄ hydrocarbon, i.e. of *n*-butane, *i*-butane, butene-1, isobutylene, *cis*-butene-2, *trans*-butene-2, and butadiene. This analysis has been and continues to be of importance to steps in the manufacture of aviation gasoline and of synthetic rubber. These compounds boil between -11.7° C. and 1.5° C. and previously the mixtures had been analyzed by fractional distillation in rectifying columns. This method, however, has two disadvantages: it took several hours for each sample, and the separation of the olefin isomers was not very good.

Using the infra-red absorption method, however, an analysis may be made on a mixture of the seven compounds named with an expenditure of about one man-hour. If the number of samples warrants it, they can be handled by a team in such a manner that one is processed by the spectrometer every forty minutes or less. For analyses of this type certain requisites must be met: samples of each of the compounds to be determined must be available in pure form for calibration

hydrocarbons for highest accuracy. From Table I may be obtained an idea of the inherent accuracy of the method. In this table are given the compositions of several samples as they were actually blended, the calculated composition from the infra-red data, and the differences between the two. It is important to point out that the calibration data used for the calculations, as well as the data for the samples themselves, were obtained under the same conditions as used for routine analyses.

Another example of an analysis which is difficult to do by fractional distillation but which can be done very readily by infra-red absorption is the determination of methane content in hydrogen-rich gas mixtures such as those encountered in hydroforming.⁵ Since the other gases found in such samples are known not to have absorption bands that overlap with that of methane, a direct analysis for the latter alone can be made. This analysis can be carried out in a total time of about twenty minutes or less including calculations. The accuracy is quite adequate for the needs, and an appraisal of

TABLE II. Analysis for methane. Comparison between concentration of methane in synthetic samples and concentration as determined by infra-red absorption.

Sample No.	% methane Synthetic	% methane Calculated by I-R	% Difference
1	14.5	14.7	0.2
2	7.6	7.7	0.1
3	6.0	6.1	0.1
4	22.5	22.3	0.2
5	4.9	4.9	0.0
6	3.7	3.8	0.1
7	1.3	1.4	0.1
8	0.8	0.8	0.0

TABLE III. Comparison between blended synthetic samples and concentrations measured by infra-red absorption for flue gas analyses.

Sample No.	Compound	Synthetic	Observed	% Dev.
1	CO ₂	10.5	10.4	0.1
	SO ₂	2.1	2.3	0.2
	CO	4.2	3.9	0.3
	CO ₂	6.7	6.9	0.2
2	SO ₂	1.4	1.4	0.0
	CO	9.4	9.5	0.1
	CO ₂	6.2	6.2	0.0
	SO ₂	1.9	1.9	0.0
3	CO	4.0	4.1	0.1
	CO ₂	4.0	4.2	0.2
	SO ₂	1.3	1.3	0.0
	CO	2.6	2.5	0.1
4	CO ₂	2.7	2.8	0.1
	SO ₂	1.0	1.0	0.0
	CO	5.2	4.8	0.4
	CO ₂	1.7	1.9	0.2
5	SO ₂	0.6	0.6	0.0
	CO	3.4	3.1	0.3
	CO ₂	7.0	7.1	0.1
	SO ₂	1.9	1.9	0.0
6	CO	6.1	6.3	0.2
	CO ₂	4.4	4.6	0.2
	SO ₂	1.2	1.2	0.0
	CO	4.0	3.9	0.1

TABLE I. C₄ gas samples. Comparison between composition of blended synthetic samples and compositions determined by infra-red absorption (S = synthetic compositions and F = observed composition by infra-red means, Δ = per cent difference).

Sample No.	1			2			3			4			5			6		
	S%	F%	Δ%	S%	F%	Δ%	S%	F%	Δ%	S%	F%	Δ%	S%	F%	Δ%	S%	F%	Δ%
<i>n</i> -Butane	55.4	54.8	0.6	0.0	0.2	0.2	17.8	17.9	0.1	0.0	0.0	0.0	19.7	18.8	0.9	32.2	32.1	0.1
<i>i</i> -Butane	44.6	44.3	0.3	0.0	0.1	0.1	33.2	33.8	0.6	0.0	0.6	0.6	10.4	10.6	0.2	30.3	30.9	0.6
Butene-1	0.0	0.0	0.0	18.5	18.4	0.1	13.2	14.0	0.8	61.8	61.5	0.3	19.8	20.6	0.8	0.0	0.2	0.2
Isobutylene	0.0	0.3	0.3	14.0	14.4	0.4	11.6	11.1	0.5	0.0	0.0	0.0	16.8	16.9	0.1	20.1	19.8	0.3
<i>cis</i> -Butene-2	0.0	0.5	0.5	39.2	38.4	0.8	13.2	12.9	0.3	18.7	18.9	0.2	14.8	14.8	0.0	0.0	0.0	0.0
<i>trans</i> -Butene-2	0.0	0.1	0.1	28.3	28.5	0.2	11.0	10.3	0.7	19.5	19.0	0.5	18.5	18.3	0.2	17.4	17.0	0.4
Butadiene	0.0	0.0	0.0	0.0	0.0	0.0	0.0	0.0	0.0	0.0	0.0	0.0	0.0	0.0	0.0

cuts combined for the complete sample. The reason for the distillation into cuts is that it becomes rather difficult to obtain good quantitative results when too many compounds are present. It may be said that if the mixture contains of the order of 12 or more different compounds, such a procedure would be advisable. Table IV shows an analysis of a cut from the products formed by pyrolysis of a saturated naphtha and is representative of the type discussed above.

Along the line of isomer mixtures, Wright⁶ has described a method whereby

may refer to the study of hydrogen bonding, molecular association, formation of azeotropes, the vulcanization of rubber, studies of compounds of large molecular weight, studies in interatomic bond strengths, thermodynamical data, and pigment particle size.

WHAT IT COSTS

With the quality and versatility built into today's commercial infra-red spectrophotometers, it is possible very satisfactorily to use the same instrument for both routine analysis and research work. When

of vacuum systems, electrical apparatus, etc., will use up the remainder. But this allows the instrument only to be operated manually. If the program includes many research activities or work on liquids, automatic recording equipment is worth the additional cost which may range up to \$2,000. Usually extra, time-saving equipment is worth the cost, as the operators must be fairly skilled.

The basic components of this equipment do not wear out with use and do not need to be replaced periodically. When obsolescence does accrue it will be due to newer methods and apparatus which allow the same jobs to be done better and in less time. Also, the user of such equipment in the ordinary industrial laboratory need not have too much concern as to patents. Much of the equipment used is unpatentable, having been developed in academic institutions.

TABLE IV. Infra-Red Analysis of a distillation fraction from the products formed by pyrolysis of a saturated naphtha.

Compound	Concentration	Boiling Point
Methylheptanes	5%	117.4-119.2°C
3-Methyl-3-ethyl pentane	7%	118.4°C
3-Ethylhexane	11%	118.6°C
trans-1,4-Dimethylcyclohexane	4%	119.6°C
trans-1,2-Dimethylcyclohexane	6%	123.7°C
n-Octane	22%	125.4°C
cis-1,2-Dimethylcyclohexane	15%	130.1°C
Ethylcyclohexane	9%	130.4°C
1,1,3-Trimethylcyclohexane	14%	138.5°C
3,3-Diethylpentane	7%	139.2°C

he could determine the amount of 1,2-dibromopropane in 1,3-dibromopropane with an error of determination of about ± 0.05 per cent (total sample). This analysis can be done in five minutes, can detect a concentration as low as 0.3 per cent, and requires a sample of only about 0.1 cc. Recently Whiffen, Torkington and Thompson⁷ have published results on analyses of cresylic acid isomers. One of their tables illustrating the accuracy is reproduced as Table V and, as can be seen from it, the errors are small.

The analyses discussed above represents only a few of many that can and are being

such an instrument is purchased it is sometimes of advantage to formulate a policy concerning its use. Even though it may be intended that the instrument serve both purposes, the situation may develop, through greater priority being assigned some projects, that it is being monopolized for but one function. This may be the more expedient procedure at the time, but it may prove to be detrimental in realizing the fullest advantages of the equipment in the long run. The obvious solution—buying an additional instrument—may be impossible in the case of a small company with a limited budget for research.

TABLE V. Analyses for the isomers of cresylic acid showing comparison between synthetic composition and concentration found by infra-red (from Whiffen et. al. reference 7).

Mixture	g. per c.c.				Percentage.		
	ortho	meta	para.	total	ortho	meta	para
Taken	0.31	1.61	1.41	3.33	9.3	48.4	43.3
Found	0.30	1.60	1.45	3.35	8.9	47.8	43.3
Mixture 2							
Taken	0.60	1.61	1.27	3.48	17.2	46.2	36.6
Found	0.60	1.65	1.30	3.55	16.9	46.4	36.7

done today on a routine basis. As new analytical problems arise they are being solved by the various groups of investigators using this technique in the research organizations of many industrial concerns.

USE IN RESEARCH

As was mentioned earlier, certain atomic groups, such as O-H, C-H, N-H, C=O, C=C, etc., can be definitely proved to exist in a compound by virtue of their unique absorption properties in the infra-red. This is of great value in the research applications of the technique as it gives an additional powerful tool for the determination of molecular structure. Frequently knowledge gained by this approach coupled with chemical information concerning the preparation of a compound results in a complete description of the structure. Many other research applications of both academic and industrial interest are possible and the scope of the subject is being constantly enlarged. To mention a few of these applications, we

In setting up a program for infra-red work, for either routine analysis or control, about \$5,000 should be allowed for initial equipment cost. A good instrument may be purchased for a price near \$3,000. Auxiliary equipment in the form

BIBLIOGRAPHY

- ¹ See for example: Barnes, Gore, Liddel, and Williamis, "Infra-Red Spectroscopy," Reinhold Pub. Co., New York (1944); also April-May (1945) issue of *Transactions of the Faraday Society* devoted to "The Application of Infra-Red Spectra to Chemical Problems."
- ² The Perkin-Elmer Corp., Glenbrook, Conn.; National Technical Laboratories, Pasadena, Calif.; and the Gaertner Scientific Co., Chicago.
- ³ See for example: W. W. Coblentz, "Investigations of Infra-Red Spectra," Carnegie Institution of Washington (1905).
- ⁴ Brattain, Rasmussen and Cravath, *J. of App. Physics*, 14, 418 (1943).
- ⁵ Coggeshall and Saier, *Journal of Applied Physics*, in press.
- ⁶ N. Wright, *Ind. and Eng. Chem., Anal. Ed.*, 13, 1(1941).
- ⁷ Whiffen, Torkington and Thompson, *Trans. of Faraday Soc.*, 41, 200(1945).

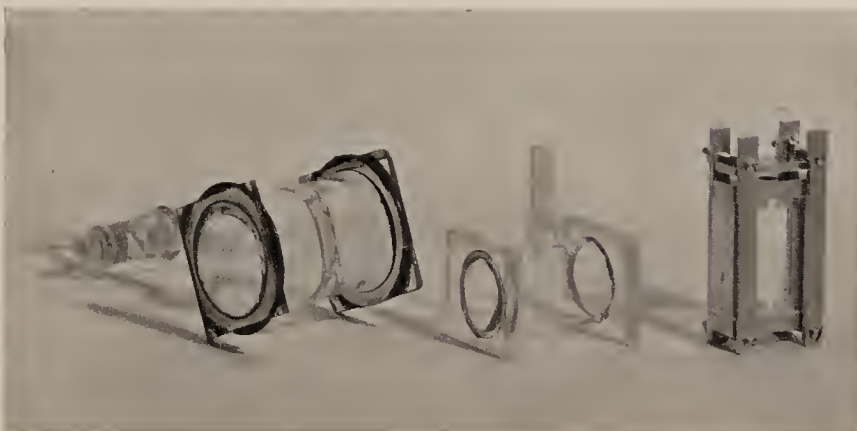


Fig. 4—Different types of absorption cells used for infra-red spectroscopy.



A Metal Packless Vacuum Valve

E. TOPANELIAN, JR. AND NORMAN D. COGGESHALL



Reprinted from *THE REVIEW OF SCIENTIFIC INSTRUMENTS*, Vol. 17, No. 1, pp. 38, January, 1946



A Metal Packless Vacuum Valve

E. TOPANELIAN, JR. AND NORMAN D. COGGESHALL
Gulf Research and Development Company, Pittsburgh, Pennsylvania
November 8, 1945

IN recent years the widespread and intensified application of infra-red spectrophotometry, ultraviolet spectrophotometry, Raman spectroscopy, mass spectrometry, and other physical methods to the analysis of mixtures of organic compounds, particularly hydrocarbons, has focused attention on the shortcomings of the usual laboratory glass stopcock. One generally objectionable feature is the presence of the stopcock grease. Most stopcock lubricants are hydrocarbon soluble to a certain extent and this raises the question of cross interference between samples and between calibration standards in analytical work. Other objections of perhaps lesser importance are: the need for periodic servicing, i.e., re-greasing; the lack of versatility in mounting; the fragility; and the inability of most greases to stand very large temperature changes.

With the idea in mind of making a vacuum valve which would be free of the above objections, the metal, packless valve described below was devised. In Fig. 1 are to be seen the structural details and in Fig. 2 can be seen the valve complete with glass connections and in such a manner as to emphasize its relative size.

The subject valve is of the needle type in which the adjusting movement of the needle shaft is a pure translatable back and forth motion. As can be seen in Fig. 1 the needle is coupled to the body of the valve by means of a bellows and this permits the extension and retraction of the needle.

Referring to Fig. 1, the body portion of the valve (1) is of a typical form. The hexagonal disk (4) is silver soldered to the body and onto it is soldered the bellows (5). To the other end of the bellows is soldered the base end of the needle (3). The threaded section of the shaft (9) engages in the interior threaded section of the needle and its movements, by virtue of the turning of the handle (8), transmit an advancing or receding movement to the needle. Assemblies (6) and (7) are anchored to the frame (2). The hexagonal nut directly above collar (6) constitutes a lock

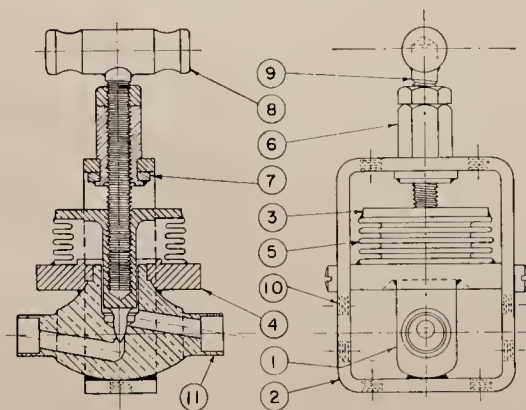


FIG. 1. Diagram of the packless valve showing the structural details.



FIG. 2. Photograph of the packless valve showing its external appearance and indicating its size.

unit when it is tightly screwed against (6) so that the shaft (9) and the assembly of (6) and (7) turn as one which allows (9) to rotate without advancing or receding. This rotating motion of (9) causes the needle (3) to move up or down to open or close the valve. In this valve the body is brass, the bellows of brass or other suitable alloy, and the needle of steel. The total movement of the needle due to the rotation of shaft (9) is about $\frac{5}{32}$ inch.

The frame (2) is soldered to the body (1) and also attached to the hexagonal disk (4) by means of machine screws. On each of the four sides of frame (2) are to be seen a pair of threaded holes such as (10). These are for mounting of the valves in frameworks, on panel racks, or in other assemblies, and they are a great advantage as they allow considerable choice of mounting position and the use of standard machine screws. For rear of panel mounting, handle (8) and shaft (9) can be removed by loosening the lock unit on collar (6). The unit can then be mounted like a rheostat or other radio device.

The female connections (11) are machined with an inside diameter to take $\frac{1}{4}$ " O.D. Kovar tubing. The walls of (11) are purposely cut thin, about $\frac{1}{32}$ ", so as to reduce the heat conductivity from the region where the Kovar tubing is soldered to the body of the valve. This is important not only in that it allows a good soldering job to be done without injuring the soldering on both ends of the bellows, but also in that with the small amount of heat required the Kovar does not become too hot in the region of the glass seal. As can be seen in Fig. 2, seals can readily be attached with quite short sections of Kovar tubing. We have soldered a considerable number of such connections and in no case has the glass-to-Kovar seal been injured.

These valves have been in use for some time in installations handling hydrocarbon gases and they have proven satisfactory. It is expected that the life of any one valve would be the fatigue life of the bellows. With a good seating needle they will hold a high vacuum for an apparently unlimited length of time.



LANCASTER PRESS, INC., LANCASTER, PA.

THE MASS SPECTROMETER

A Flexible Tool for Industrial Analysis and Research

by NORMAN D. COGGESHALL, Physicist
Gulf Research & Development Company
Pittsburgh, Pa.

USE OF the mass spectrometer is increasing rapidly in spite of its high initial cost. Because of its unique ability to sort out materials of differing molecular weights, the spectrometer is being used as a leak detector, for the analysis of mixtures of chemical compounds, and for the preparation of U-235 on the Manhattan Project.

THE MASS SPECTROMETER is an instrument that has made its entry into industrial laboratories only within the last few years. At the present time there are quite a number of such devices installed and operating. Other than its use on the Manhattan Project for the preparation of U-235, this instrument is used chiefly for analyses of mixtures of chemical compounds and for research and development work.

HOW IT WORKS

The mass spectrometer may be regarded as a large electronic tube furnishing certain information about the variable atmosphere which it holds. The sample which is usually in the vapor phase is introduced into the tube by means of a small gas leak, where the gas molecules are subjected to bombardment by electrons of controlled energies. These electrons, upon impact with the molecules, break them up into fragments and ionize some of these fragments, which are then sorted out according to the masses. Different compounds yield different intensities of the various ions, furnishing the differentiation necessary for analytical work.

One of the most important parts of the mass spectrometer is the ion source where the electrons traveling at high speed create the ions by impact. Fig. 1 is a schematic diagram of an ion source showing the principal parts and their

functional relationship. This consists of a vacuum tight envelope with a gas inlet connection and a vacuum pump connection. The filament F usually is of tungsten which, when incandescent, emits electrons. These electrons are drawn towards electrode A by virtue of a voltage difference between F and A. Some of them will pass through the hole in A into the region between B and A. The electrons passing through this region encounter the gas molecules present and create ions by impact which are drawn down to A due to a voltage difference between B and A. Some of them pass through the slit in A into the region between A and C. Here they are further accelerated by the voltage difference between A and C and some of them pass through the slit in C to form a ribbon of ions I. This ribbon-like stream of ions will contain all varieties created in the source and it passes on to the magnetic analyzer which will be described later. The electrons that continue through the region between B and A pass through a second hole in A and strike electrode D where they are trapped by a suitable applied voltage. External circuits incorporating some of the recent advances in the art of electronics, supply the necessary voltages. This electronic equipment is designed for great stability of electrical voltages and currents as this is of primary importance for successful use of the instrument. The interiors of the ion source and of the magnetic analyzer are maintained under a high vacuum. Usually a somewhat higher pressure in the ion source than

in the analyzer is achieved by the manner of introducing the gas and by the location of the vacuum connections.

The geometrical disposition of the ion source, the magnetic analyzer and the ion collector may be seen in Fig. 2. In this figure, which is somewhat exaggerated, a diverging beam of ions leaving the ion source may be seen progressing towards the magnetic field which is perpendicular to the plane of the figure. The effect of the magnetic analyzer is to allow only ions of one mass to pass through the entire field to the collector. Here S represents the ions that proceed to the collector; R, ions of a smaller mass; and T, those of a larger mass. The particular mass that is allowed to reach the collector may be controlled by means of the voltages in the ion source or the strength of the magnetic field. The ions that go to the

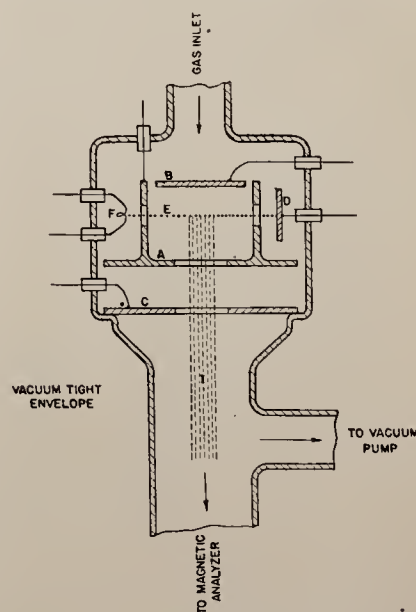


Fig. 1. Schematic diagram of mass spectrometer ion source.

The author is indebted to Mr. Nathan F. Kerr for obtaining and tabulating some of the data used and to Dr. Paul D. Foote, Executive Vice-president of Gulf Research and Development Co. for permission to publish this material.

vides further softening with lime and soda ash, after which the water is passed through rapid sand filters. Boiler feed water undergoes further purification to remove calcium, silicon, and magnesium.

The water used for washing the potatoes is recycled after removal of the soil and loose vegetation. The settled solids are suspended in water and pumped to the fields to enrich the soil and the only additional water added is that needed to replace what is pumped away.

Disposal of the "fruit-waters," i.e., the water separated from the pulp and starch in the potato, and the other watery wastes produced during the extracting operations is more involved. Such waters contain a large proportion of organic matter which must be rendered harmless to avoid pollution. These wastes are passed through 8-mesh screens and the solid material ground up for rescreening. The fluid is then heated to 85° F. and maintained at that temperature for four days while mesophilic digestion takes place. Nitrogen is added to support fermentation. The fermentation produces almost a million cubic feet of gas per day which is piped to the power plant where it fuels the boilers about a third of the time. The liquid is further clarified, chlorinated, and returned to the lake, and the settled solids are pumped to the fields for soil enrichment.

Other wastes are the potato vines and the pulp remaining after starch separation. It has been mentioned that the latter, amounting in weight to 50% of the recovered starch, is bagged and used as stock feed. The vines themselves, equal in weight to the potatoes, have high nutritive value as forage.

INNOVATIONS

The process is essentially the same as that used at the Laurel, Miss., plant except that improvements have been made in most of the procedures with equipment suited to high-speed continuous production. An outstanding difference is the use of high-speed continuous centrifugals at Clewiston for purification of the starch rather than settling tables used at Laurel and other older plants. At Laurel only rotary washers are used to clean the potatoes, and the potatoes are hammermilled rather than sliced and attrited.

Two other ways in which the Clewiston operations differ from those at Laurel is in the use of horizontal continuous centrifugals and continuous vacuum filters. The former are used, as has been described, to separate the fruit waters from the ground roots, and the latter to wash the starch after purification. At Laurel solid basket centrifuges are used for washing and regular centrifuges for drying. Also, at Laurel drying is done under vacuum; at Clewiston the Hershey rotary steam dryers are used at atmospheric pressure. Many of the techniques were evolved in cooperation with the



Drying, pulverizing, and blending follow the bleaching operation. Then it is conveyed to the scale house where it is automatically weighed and bagged and moved to the warehouse.

Laurel plant and the laboratories of the U. S. Department of Agriculture.

PLANS

After the 1946 crop is harvested and operations start in earnest, the corporation expects to produce about \$5,000,000 worth of products a year, the bulk of which will be represented by finished starch. The latter will be distributed

under the trade-name "Tubioca" through Morningstar, Nicol, Inc., exclusive sales agents for the starch products.

The starch project represents a substantial part of the corporation's \$20,000,000 diversification program, designed to take advantage of the agricultural richness of the Everglades in providing, as far as possible, year-round employment for the workers.

WOOD UTILIZATION IN GERMANY

UTILIZATION of the sugars in sulfite waste for alcohol production has been practiced in all German mills since World War I, although the economics are understood to be unfavorable. The development of the technology for yeast production when required by the use of beech is an important advance in recent years, and this industry may possibly survive under normal conditions. Further, the technology developed may find some application in American mills.

Except in the fermentation and growth of yeast on the wood sugar solutions, American development of the Scholler process for alcohol from wood is out in front.

Although the Scholler process was not greatly expanded in Germany during the war—contrary to widely published reports—plants producing alcohol by this method

and from sulfite liquor had capacities respectively totaling 10,000,000 and 25,000,000 liters per year. Total annual plant capacity for production of yeast from wood sugar was in excess of 25,000 metric tons. Additional plants for production of yeast from sulfite liquor were under construction at the end of the war.

There has been no significant progress in the technique of sugar production; but at the Holzminden plant a fermentation with *Torula* of wood sugar to alcohol is carried out by a rapid, continuous yeast re-use method requiring as little as five hours. The two Bergius wood sugar plants had not changed their prewar techniques.

Still bottoms from one Scholler plant in Germany, one in Switzerland, and from a Swiss sulfite liquor alcohol plant are processed to produce yeast, which is of interest in reducing stream pollution.

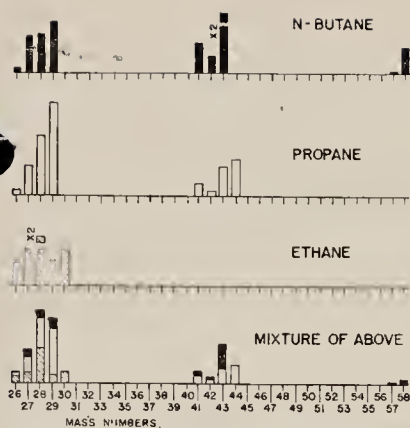


Fig. 3. Histogram representing relative ion yields from simple hydrocarbons and from a mixture of these hydrocarbons.

collector create a small electrical signal by virtue of their charge, which is amplified by suitable electronic circuits. Since the instrument can separate and measure the intensities of the ion beams for ions of different masses it is called a mass spectrometer. The magnetic focusing scheme shown in Fig. 2 is called the sector type. Other types of focusing exist although the overall function in each case is the same. For further details other papers should be consulted.

Although not indicated in Fig. 2, a vacuum tight envelope encompasses the ion source, the region of their travel in the magnetic analyzer, and the ion collector. The pressure in this must be of the order of 10^{-6} mm. of Hg. Such systems are continuously evacuated by diffusion pumps.

As previously noted, a molecule may be dissociated into a number of different types of ions when it collides with an electron. For example, n-butane, which has a molecular weight of 58 may yield ions of mass (in atomic mass units) 58, 57, 56, 55, 43, 42, etc. The first of these corresponds to the parent molecule losing an electron whereas, the others correspond to the parent atom losing one, two, or three hydrogen atoms, three hydrogen atoms plus a carbon atom, etc.

Fig. 3 is a histogram showing the yields of ions of various masses found for the three compounds n-butane, propane and ethane, and a mixture of the three. Due to the shape of the curve obtained when the signal representing ion current is plotted as a function of the voltages varied to bring the beam into focus, the terminology "ion peak" has become rather wide spread. The existence of an ion peak for a certain mass is equivalent to saying that ions of that mass are obtained. In Fig. 3, for example, we see that there are ion peaks for masses up to 58 for n-butane while propane does not yield ions of mass above 44 and ethane does not yield them above 30. There are additional small peaks due to isotopes which are not shown.

As different compounds vary in molecular structure their ion yields will be un-

like in mass and in intensity. When the mass spectra of two isomers such as n-butane and i-butane are compared the differences are in intensity alone. However, if two compounds are compared which do not have the same molecular weight the heavier will naturally yield certain ions that the lighter will not. This may be seen in Fig. 3 where propane does not have the higher mass peaks of n-butane. A similar result is noted for ethane. When a mixture of separate compounds is examined a mass spectrum is obtained which is a composite of the ion yields of the individual compounds present. The dissociation and ionization of one substance is not affected by the presence of another under the conditions used, making it possible to apply the instrument to problems of quantitative analysis. The mass spectrum of each compound in a pure state may be determined and this information used to calculate the percentages of the various constituents present when the spectrum for a mixture is obtained. For the details of this process the reader should consult other papers.^{3, 4}

USE IN ANALYSIS

Because of the nature of the data obtained the mass spectrometer is the ideal instrument for certain types of analyses. Because of speed, accuracy and range of components handled it is excellent for analyses for process control. For example, the three-carbon hydrocarbon content in the absorber gas of a polyforming unit used in petroleum refining may be used for control of the process. The analyses of the absorber gas for C_3 content, which at the same time yields both the propane and propylene, may be com-

pleted in a routine manner in a time of about 25 minutes, including calculations. The percent differences between the concentrations as blended and as found are about 0.2% of total sample and a group of results illustrating this analysis may be seen in Table I. This shows the C_3

Table I. Results for analyses of blends of C_3 hydrocarbons and lighter. $\Delta\%$ represents difference between actual and observed concentrations.

Blend No.	Component	Synthetic %	Observed %	$\Delta\%$
1	propane	3.93	4.01	+0.08
	propylene	2.89	3.06	+0.07
	total C_3 's	6.82	7.07	+0.25
2	propane	2.64	2.46	-0.18
	propylene	1.84	1.89	+0.05
	total C_3 's	4.48	4.35	-0.13
3	propane	1.92	2.12	+0.20
	propylene	1.03	1.14	+0.11
	total C_3 's	2.95	3.26	+0.31
4	propane	0.60	0.39	-0.21
	propylene	4.16	4.41	+0.25
	total C_3 's	4.76	4.80	+0.04
5	propane	1.64	1.58	-0.06
	propylene	0.54	0.71	+0.17
	total C_3 's	2.18	2.29	+0.11

content of a number of synthetic samples as blended and as determined by the mass spectrometer. These samples were analyzed and calculated under the routine conditions used for the control work.

An analysis very similar to the one just described and also for process control is the analysis of a gas recycle stream in a polyforming process such as above. This gas may contain four-carbon hydrocarbons as well as lighter gases and the amount of the former found is of use for the control. The analysis for the C_4 content yields i-butane, n-butane, the butenes and butadiene, if desired. The complete analysis, including calculations, can be done in approximately thirty minutes. In this determination the butenes may be lumped together as their properties in the mass spectrometer are not widely different. Table II shows the C_4 content

Table II. Results for analyses of blends of C_4 hydrocarbons and lighter. $\Delta\%$ represents difference between actual and observed concentrations.

Blend No.	Component	Synthetic %	Observed %	$\Delta\%$
1	i-butane	4.25	4.37	+0.12
	n-butane	0.00	0.00	0.00
	butenes	1.37	1.16	-0.21
	total C_4 's	5.62	5.53	-0.09
2	i-butane	0.89	0.95	+0.06
	n-butane	1.02	0.95	-0.07
	butenes	1.49	1.70	+0.21
	total C_4 's	3.40	3.60	+0.20
3	i-butane	3.20	2.36	+0.06
	n-butane	1.72	1.62	-0.10
	butenes	4.73	4.67	-0.06
	total C_4 's	9.65	9.55	-0.10
4	i-butane	0.00	0.07	+0.07
	n-butane	0.56	0.61	+0.05
	butenes	0.98	0.94	-0.04
	total C_4 's	1.54	1.62	+0.08
5	i-butane	2.81	2.94	+0.13
	n-butane	0.00	0.00	0.00
	butenes	2.52	2.34	-0.18
	total C_4 's	5.33	5.28	-0.05

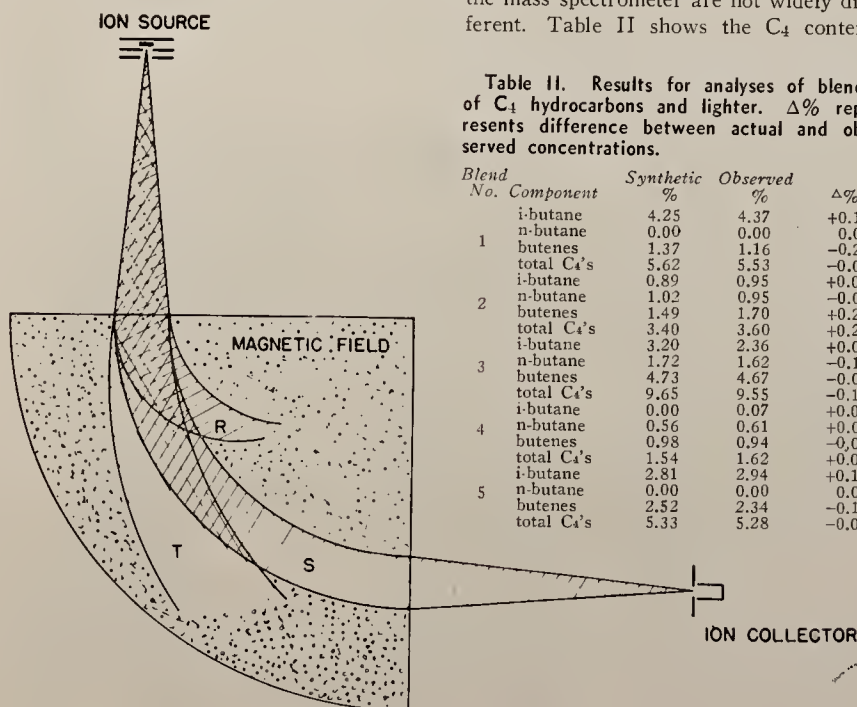


Fig. 2. Geometrical arrangement of ion source, magnetic field, and ion collector for sector type instrument.

of a number of synthetic samples as blended and as determined by routine analysis.

The two types of control analyses just described are examples of some of the simpler ones which can be done easily on night shifts. As the mass spectrometer is a quite complicated instrument, the period of training for any operator must necessarily be longer than for other types of equipment. Even with fully trained operators it is necessary to have a competent supervisor at hand to see that the routine of processing the samples is faithfully followed; that the calculations are carried out correctly; and to spot, diagnose and if possible correct any malfunctioning of the apparatus. Since the necessary data and calculations on the above two types of analyses are not as lengthy and involved as others to be described, they can be carried out in the absence of as much technical supervision. This is, of course, very desirable for night work.

In Table III, the data for a wet gas

Table III. Analysis of wet gas.⁵

Compound	Mass Spectrometer Mole %	Fractionating Column Mole %
Na	1.1	...
Methane	84.1	87.44
Ethane	4.9	4.60
Propane	4.7	4.30
Isobutane	1.1	0.72
n-Butane	1.7	1.47
Isopentane	0.7	0.55
n-Pentane	0.5	0.47
Co ⁺	0.2	0.45
C ₄ naphthenes	0.6	...
C ₅ naphthenes	0.3	...
C ₆ naphthenes	0.1	...

sample, which is from an article by Washburn, Wiley and Rock,⁵ illustrate the range of components for which routine analyses can be made, the comparison between these results and ones from a frac-

Table V. Two C₆ mixtures analyzed by the mass spectrometer method⁵ on two successive days. Composition from synthesis is given for comparison.

	Synthetic Mole	Mass Spectrometer 6-25 per cent	Mass Spectrometer 6-26	Synthetic Mole	Mass Spectrometer 6-25 per cent	Mass Spectrometer 6-26
2,2-Dimethylbutane	3.82	3.5	3.5	26.40	26.1	25.9
Cyclopentane	0	0	0	0	0	0
2,3-Dimethylbutane	0	0	0.3	0	0.5	0.2
2-Methylpentane	12.03	12.5	12.3	36.24	35.7	36.4
3-Methylpentane	6.16	6.8	1.3	20.26	20.8	20.6
n-Hexane	77.99	77.2	76.6	17.10	16.9	16.9

tionating column, and the total man hours needed. It is to be noted that this analysis covers compounds for molecular weights ranging from sixteen to over eighty-four. From Table IV it is also to be noted,

Table IV. Time Required for Analysis by Complete Direct Method.

	Minutes
Mass spectrometer (instrument time)	
Mixture	25
Prorated calibration	4
Taking data from record (technician's time)	
Mixture	20
Prorated calibration	4
Computing	80
Total man-hours	2.25

that, although the total man hours needed for this analysis is given as 2¼ hours, the instrument time is only 25 minutes. A team working to keep the instrument in constant use and the calculations going simultaneously can thus analyze many different samples.

data of this table are also taken from Washburn, Wiley and Rock.⁵ Any material that is to be examined mass spectrometrically in a routine manner must be in the vapor phase while in the ion source. This means then that such a sample as this must be vaporized. To avoid any errors due to differences in boiling point it is important that a small portion of the liquid sample, of the order of ½ ml. or less, be completely vaporized. Table V illustrates not only the comparison between the instrument analyses and the synthetic compositions, but also illustrates the day to day reproducibility. On both counts the error is only a few tenths per cent of total sample. From Table VI it is seen that the instrument

Table VI. Time Required for Analysis by Complete Direct Method

	Minutes
Mass spectrometer (instrument time)	
Mixture	25
Prorated calibration	12
Taking data from record (technician's time)	
Mixture	25
Prorated calibration	12
Computing	120
Total man-hours	3.25

time is quite small, i.e., 25 minutes, for such a complicated analysis.

The restrictions named above, that the material to be studied must be in the gas phase in the ion source, does not entirely rule out the examination of solids. It does, however, necessitate that the material be inserted in a furnace or on a heated disk within the source so that it may be vaporized. This procedure has been followed in research studies where the isotopic concentration of the elements was being studied.^{1, 6}

RESEARCH APPLICATIONS

By virtue of the peculiar type of data it supplies, namely the intensity and mass of the ion fragments, the mass spectrometer is particularly suited to certain research applications. One of growing importance is the studying of chemical reactions by means of isotopic tracers. Practically all of the elements in the periodic table consist of two or more isotopes which are merely atoms having the same chemical properties but different masses. Hydrogen consists of the ordinary isotope of atomic mass one and the rare one, deuterium of mass two. Carbon consists



Fig. 4. Westinghouse Electric Corp. mass spectrometer as set up for manual operation and as used by Gulf Research and Development Co.

of the ordinary isotope of mass twelve and another one of mass thirteen which is found to the extent of about 1% of the former. Modern methods now permit separation of appreciable quantities of the rare ones. Deuterium is perhaps the easiest to separate and is now available commercially.

If a molecule contains a heavy isotope, for example, an iso-butane molecule may contain three normal carbon atoms of mass twelve each and one carbon isotope of mass thirteen, its molecular weight will be one unit higher than normal. Actually these heavier molecules are detected for all hydrocarbons and other compounds and their intensities depend upon the abundance of the various isotopes involved. In Fig. 3 the peaks for molecular ions containing heavy isotopes were not shown as they are small. If a compound is synthesized from a sample of carbon in which the abundance of the isotope of mass thirteen has been increased over that found in nature, the distribution of ion peak intensities will be different than for the naturally occurring compound. This allows the compound to be tagged for tracer work. Considerable application of the technique has been made to biochemical problems.⁷ Rittenberg has used nitrogen enriched in the rare isotope of atomic weight 15 to synthesize amino acids. These tagged amino acids could then be followed through certain digestive and other biochemical changes. For exploring and attling certain problems of chemical reactions and catalysis this technique offers a powerful tool that is just beginning to be fully utilized.

For following or studying chemical reactions directly this instrument has been successfully used by Urey and his co-workers, Eltenton and others. In Eltenton's work he used the mass spectrometer to detect free radicals from a thermal reaction chamber in which were placed lead tetramethyl and different hydrocarbons.⁸ Leifer and Urey⁹ used the instrument to study the thermal decomposition of dimethyl ether and of acetaldehyde. In this work the intermediates and reaction products entered the ion source through a capillary leak which intruded into the reaction chamber. This is another type of application of this instrument which up to date has not been widely used but which, because of the singular type of data it can furnish, will play an increasingly important role in chemical research of a fundamental nature.

As was discussed above, when a molecule suffers impact by an electron any one of a number of ionized fragments is possible. By adjusting the energy of the electrons it is possible to create only certain classes of these ions. For example, it requires electrons of a definite minimum energy to tear a hydrogen atom off of a n-butane molecule and ionize the remainder. This minimum energy can be found experimentally with the mass spec-

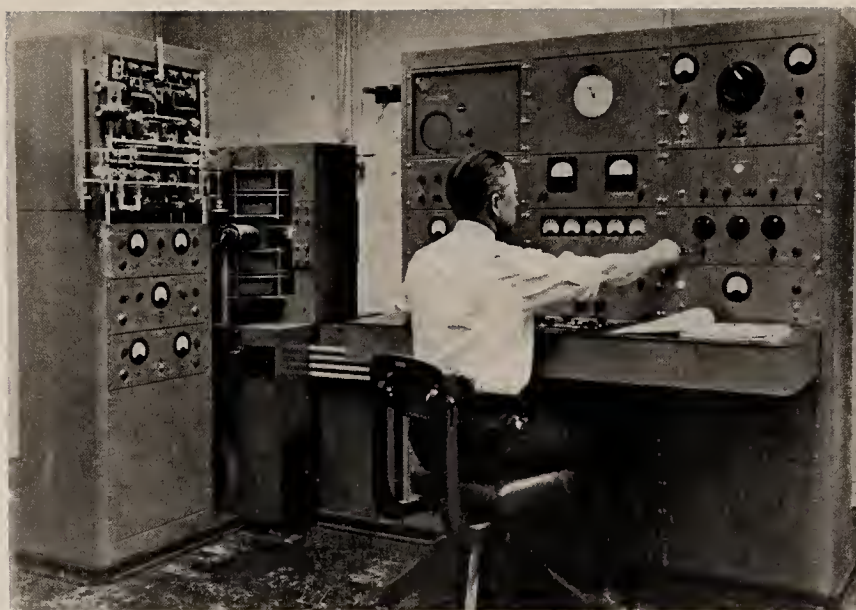


Fig. 5. Consolidated Engineering Corp. mass spectrometer complete with automatic recording equipment.

trimeter. To tear off a complete methyl radical from the same molecule and ionize the remainder requires a different minimum energy which can also be determined. The experimental determination of the energies and the correct correlation with the collision process giving rise to the ions allows a deduction of molecular bond strengths. Much work of an academic nature has been done along these lines and the results have furnished data of value for clarifying certain problems of molecular structure.¹⁰

According to Smyth¹¹ a mass spectrometric method of separation "... was the first to produce large amounts of the separated isotopes of uranium."¹² "The electromagnetic separation plant was in large scale operation during the winter of 1944-1945 and produced U-235 of sufficient purity for use in atomic bombs."¹³

COST

A number of large companies have hired physicists to build mass spectrometers for such uses as outlined above. At the present time this practice is not necessary in view of the commercial availability of suitable instruments.¹⁴ The instrument itself is quite complex and embodies a number of physical phenomena not as yet completely understood. Unless an instrument of special design is needed it is usually of greater utility for the available highly trained personnel to concentrate on the application and adaptation of the available instruments to the company's own problems. To establish a mass spectrometry laboratory with automatic recording, a company must be prepared to appropriate \$20,000-\$30,000.

(The development of a mass spectrometer capable of detecting a leak allowing passage of only one cubic centimeter of helium at atmospheric pressure in 16 years is announced on page 413 in this issue. EDITORS.)

BIBLIOGRAPHY

1. Coggeshall and Hipple, "The Mass Spectrometer and Its Applications," Vol. VI of Colloid Chemistry series, edited by Jerome Alexander, Reinhold Publishing Co., New York, 1946.
2. Jordan and Young, *J. of App. Phys.*, **13**, 526 (1942).
3. Hoover and Washburn, *Calif. Oil World*, **34**, No. 22, 21-2 (Nov. 1941).
4. John Hipple, *J. of App. Phys.*, **13**, 551 (1942).
5. Washburn, Wiley and Rock, *Anal. Ed., Ind. & Eng. Chem.*, **15**, 541 (1943).
6. K. L. Cook, *Phys. Rev.*, **64**, 278 (1943).
7. D. Rittenberg, *J. of App. Phys.*, **13**, 561 (1942).
8. Eltenton, *J. Chem. Phys.*, **10**, 403 (1942).
9. Leifer and Urey, *J.A.C.S.*, **64**, 994 (1942).
10. Smyth, *Rev. Mod. Physics*, **3**, 347 (1931).
11. Smyth, H. D. A General Account of the Development of Methods of Using Atomic Energy for Military Purposes under the Auspices of the United States Government 1940-1945.
12. *ibid.* Chapter 11, paragraph 48.
13. *ibid.* Chapter 11, paragraph 42.

HYDRAZINE HYDRATE

War Baby or New Chemical Intermediate?

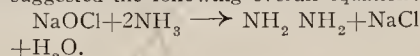
HYDRAZINE HYDRATE has been brought before the public eye because of its use in the second step in the launching of the German V-2 rocket. The following description of the first German plant for its production will aid in the proper evaluation of the place of this intermediate in the American economy.

HYDRAZINE HYDRATE, although deriving its prominence principally from the German proposal for its use in rocket propulsion, is now being prepared commercially in the United States with the same basic process that was utilized in Germany, namely, reaction of an alkali hypochlorite with excess ammonia. It is now being used by American industry for the synthesis of dyestuffs, pharmaceuticals and as a reducing agent for the deposition of metals on essentially non-conducting surfaces.

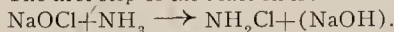
According to the Chemical Warfare Service¹ hydrazine hydrate was used in the second of three steps involved in rocket propulsion. First, permanganate reacted with hydrogen peroxide, giving superheated steam which drove a turbine connected to pumps. The pumps delivered hydrogen peroxide and a hydrazine hydrate in methanol solution to the combustion chamber, where an instantaneous, strongly exothermic reaction occurred. When the reaction chamber became hot enough, the permanganate and peroxide shut off automatically and the rocket drive was taken over by an oxygen-

hydrazine hydrate from alkali-hypochlorite and excess ammonia (an aqueous solution) in the presence of such materials as gelatin and glue, which raised the viscosity.

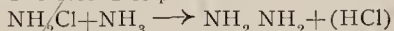
Raschig, who discovered the reaction, suggested the following overall equation:



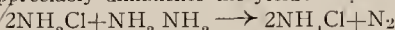
The first step of the reaction is:



The second step:



The following undesirable side reaction appreciably diminishes the yield:



It is possible to prepare hydrazine hydrate in good yield without the addition of glue if the chloramine solution, which is the product of the first step of the reaction, is heated with excess ammonia under pressure at a temperature of 150-200° C. and if the process is carried out as rapidly as possible. Pure chloramine solutions are not required but solutions containing sodium hypochlorite and ammonia (for the formation of chloramine) may be employed. The pressure tube in which the reaction is carried out may have very small dimensions as, under the indicated conditions, reaction is complete in a few seconds, if the reaction mix can be brought up to temperature fast enough. Following the reaction, a reduction in pressure of the solution allows the greater part of the excess ammonia to escape; the heat required to raise the temperature of the mixture to the boiling point being almost completely supplied by the heat of reaction. The remaining ammonia is driven off in another column, vaporization being so regulated that an ammonia solution results from a cooling of the effluent ammonia and water vapor and from the ammonia resulting from release of pressure on the solution, which can be directly used again in the reaction. This produces a crude hydrazine hydrate solution (concentration about 3 per cent). The yield (based on the active chlorine in the sodium hypochlorite solution) is 70-75 per cent.

The presence of heavy metal impurities has an especially bad effect on the yield; this is particularly true of copper and the ammonia solution must be continually tested for its copper content. In case the

sodium hypochlorite solution contains large amounts of iron, it is advisable to filter after dilution. The crude hydrazine hydrate solution contains 5-6 per cent sodium chloride and some sodium hydroxide and cannot be directly concentrated as these materials must first be removed. This is usually carried out in a salt evaporator from which the resulting 6-8 per cent hydrazine hydrate-water vapor mixture is driven over into a fractionating column.

The pure dilute hydrazine hydrate solution from the fractionating column is concentrated in two distillation columns. In the first column a concentration of 40-50 per cent is obtained; the second giving a concentration of 95-98 per cent. The second distillation must be carried out under a nitrogen atmosphere to avoid the possibility of explosion.

FLOW CHART

In the plant at Leverkusen the sodium hypochlorite solution, containing 12.7 per cent active chlorine, 0.4 g. alkali per liter, is adjusted to a concentration of about 70 g. of active chlorine per liter in container (0.1) by using water purified by ion exchange from another container (No. 2).

The ammonia solution is adjusted to a concentration of about 20-25 per cent (sp. gr. 0.910). Both solutions flow through measuring meters and then to a high pressure pump (No. 6), which is provided with mixing ducts. The inward flow of each solution is so adjusted that the ratio of sodium hypochlorite to ammonia is 1-2. The pump brings the reaction mixture to a pressure of 40-50 atmospheres and drives it into the reaction pressure tube (No. 7) which is heated to about 183° C. After the few seconds required in the reaction tube the pressure on the solution is reduced to atmospheric in the evaporation pot (No. 8). The resultant vapor and the residual liquid, in order to establish thermodynamic equilibrium, flow through a packed column (No. 9) which is connected from below to the evaporator pot (No. 8). The vapor, which is removed from below, is rectified in a second packed column (No. 10) by means of ammonia water, to avoid hydrazine losses. This solution plus the reflux in the second column (No. 10) then enters the separating column (No. 11), a circular tube evaporator (No. 12) being employed for the production of the vapors. A part of the heated vapor is obtained from the vaporization of the high-pressure condensate from the heater, the necessary amount of ammonia (as 100 per cent ammonia) being continuously introduced into the upper part of the separating column (No. 11), which is operated in such a way that the ammonia-water vapor mixture produced has the proper composition for use again in the process. This mixture is condensed in two tubular condensers (No. 13a and 13b) and flows back into the storage container (No. 5).

Reprint from Vol. VI of *Colloid Chemistry*
edited by Jerome Alexander, Reinhold Publishing
Co., N. Y., 1946.

The Mass Spectrometer and Its Applications

NORMAN D. COGGESHALL
Gulf Research & Development Co., Pittsburgh, Pa.

and

JOHN A. HIPPLE
Research Laboratory
Westinghouse Electric & Manufacturing Co., Pittsburgh, Pa.

Introduction

Unlike some instruments to be found today the present mass spectrometers are not the result of a few years of very intensive research by a fairly large number of technical men. The roots of this type of instrument may be said to be in the positive ray parabola experiments of Sir J. J. Thomson and in the first mass spectrographs of Aston.¹ A short history describing some of the various types of instru-

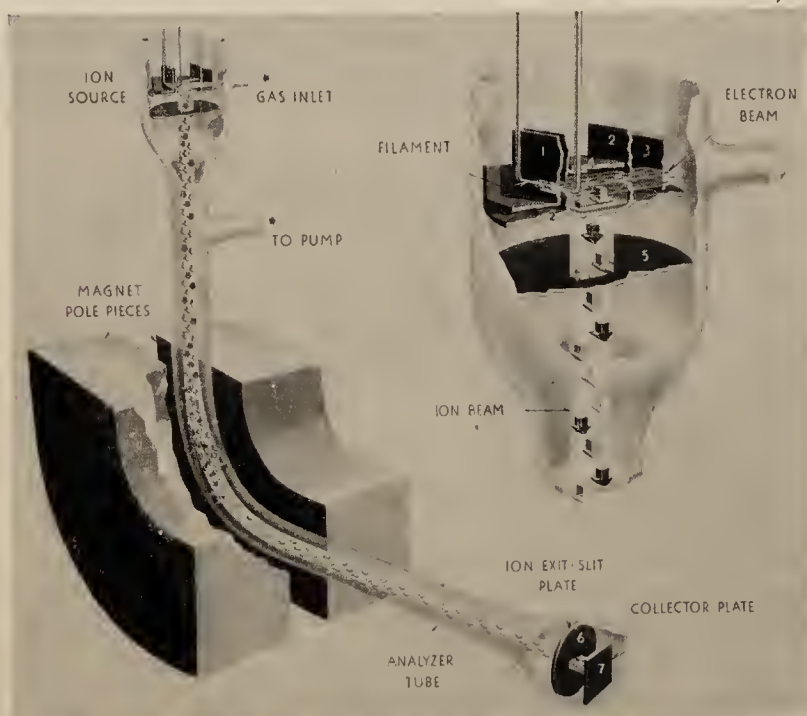


FIGURE 1. Pictorial representation of the mass spectrometer ion source, magnetic analyzer and ion collector.

ments developed over the last thirty-five years is to be found in an article by Jordan and Young.² For many years mass spectrometers were, with few exceptions, to be found only in the research departments of large universities, and the research done with them was of a fundamental nature. Now the research laboratories of many industrial companies are equipping themselves with this powerful research and analytical tool.

In the barest terms the primary processes involved in a mass spectrometer are: the creation of ions; the formation of these ions into a beam by electric fields; the sorting out by a magnetic field of the ions in the beam according to their momentum; and the measurement of the ion current in each momentum class. The perspective views in Fig. 1 show the spatial arrangement of parts and the manner of separation of the ion beams. The electron current from a hot filament is caused to pass between the system of electrodes 1, 2, 3, and 4. In this region there is a low pressure of the gas being investigated and the electrons create ions by impact on the gas atoms or molecules. The electric potentials on electrodes 2, 3, and 4 are so adjusted that the positive ions are drawn down through a slit in the bottom of electrode 2. A further difference of potential between electrodes 2 and 5 results in the ions being drawn down to 5 and the slit in 5, cut to match the one in 2, defines a ribbon-like beam of ions. In the figure, different ions are represented by differently shaded arrows. As all the ions formed in the ion source and drawn into the beam travel through the same electric fields, their kinetic energies will be essentially equal. Since the different types of ions have different masses, several momentum classes result. The magnetic field into which the ion beam passes sorts the ions according to their momentum, and the result is that the initial beam is split into as many separate beams as there are different ionic masses. The ion exit slit is located to catch the central ion beam; the ions pass onto a collector plate and the resulting minute current is measured by a special arrangement of a high resistance and suitably designed electronic amplification circuit.

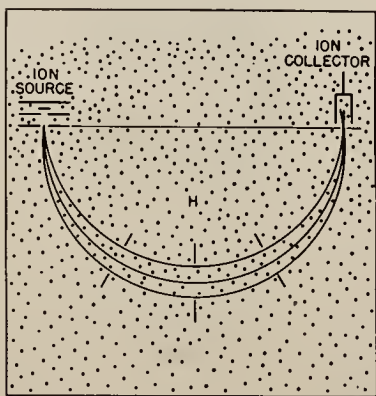


FIGURE 2. Schematic diagram of focussing in the 180° magnetic analyzer.

Fig. 2 shows schematically one focussing scheme in common use today. Here focussing is obtained when the ions are projected by an ion source in a region of uniform magnetic field and in a direction perpendicular to the lines of force. In such a case all ion paths will be portions of circles, and the ion source and collector are located at opposite ends of a diameter of one of the circular ion paths. The three dissimilar lines represent paths of ions of the same mass but slightly different angles of emergence from the ion source. Any type of ion desired may be caused to pass into the collector by varying either the accelerating voltages in the source or the magnetic field, H . Ions of masses different from that of the ions selected will travel

in arcs of different radii of curvature and will therefore not enter the collector slit. This type of instrument is sometimes called the 180° type.

Another type of focussing, sometimes called the sector type, is shown in Fig. 3. As is seen here, a diverging beam of ions leaving the ion source is focussed at the collector slit. The geometric relations governing this focussing are: that the ion source, ion collector and apex of the triangle, formed by the edges of the magnetic

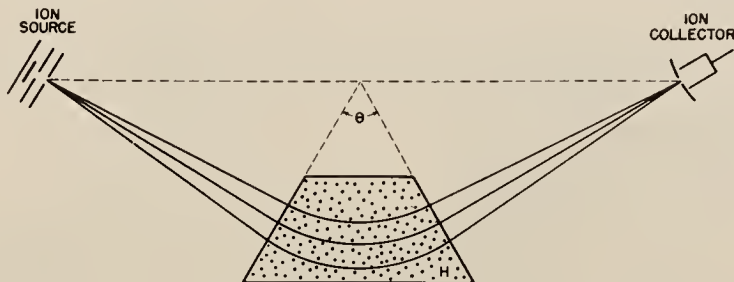


FIGURE 3. Schematic diagram of focussing in the sector type magnetic analyzer.

field, must lie on a line perpendicular to the bisector of the angle θ , which can be any desired angle. Focussing of any particular ion beam is achieved when its central ray enters the magnetic field perpendicular to the boundary and when the ion source voltages and the magnetic field strength are adjusted to give the ion path in the field a radius of curvature equal to the distance from the apex of the triangle to the point of entry of the central ray.

In both types of instruments described above it was stated that in a uniform magnetic field the ion paths are portions of circles. The equation relating this motion to the various physical parameters involved is easily obtainable from the two equations:

$$F = \frac{mv^2}{r}$$

which expresses the force F , necessary to keep a body of mass m moving in a circle of radius r , with velocity v , and

$$F' = \frac{Hev}{c}$$

which expresses the force F' acting on a charged particle of charge e moving with velocity v perpendicular to the magnetic field H . The quantity c is the velocity of light and enters as a units conversion factor. The force F' is perpendicular to both the velocity of the charged particle and the direction of the magnetic field. Combination of the two equations and simplification leads to the single equation:

$$\frac{c(mv)}{e} = rH.$$

If the velocity of the ion is expressed in terms of the accelerating potential V , the above equation becomes:

$$c\sqrt{\frac{2mV}{e}} = rH.$$

At this point we might indicate the functional difference between a mass spectrograph and a mass spectrometer. A mass spectrograph is an instrument operating on the same general principles, but carefully constructed to allow the research worker to correlate very accurately the positions of the ion beams with the ionic masses. It

is then an instrument designed primarily to measure, directly or indirectly, the atomic masses of the elements. The mass spectrometer, on the other hand, is designed for the measurement of the intensities of the ion beams. In the literature the designation "mass spectrograph" has often been used, although the investigator was really working with a spectrometer.

Operation

In Figs. 4 and 5 may be seen in more detail the geometrical and functional arrangement of the principal components of a mass spectrometer. Fig. 4 shows the

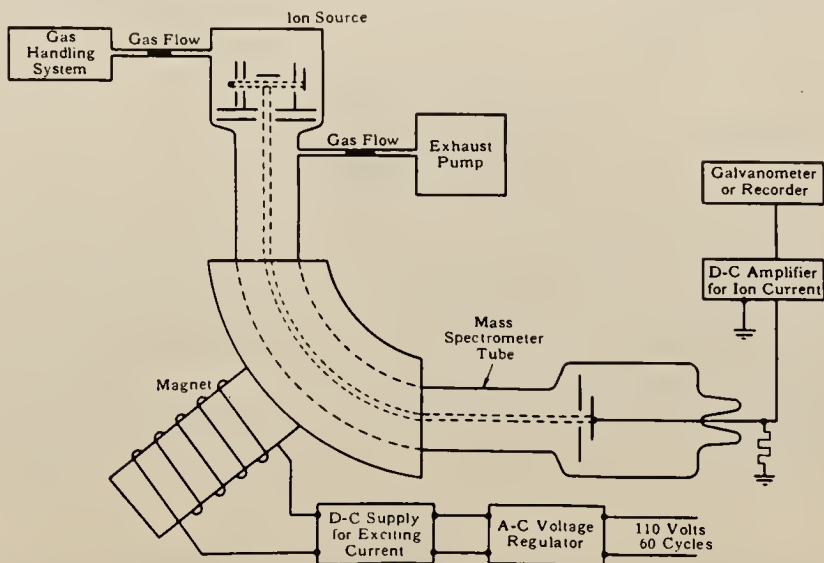


FIGURE 4. Schematic layout of main components involved in a mass spectrometer.

means provided for the entry of the gas being studied, etc. Fig. 5 gives a typical arrangement of electrical components and distribution of potentials needed in the operation of an ion source. Electrons emitted by the filament are accelerated by electrode 1, in which there is an aperture so that an electron stream passes through both 1 and 2, in which is also an aperture, into the ionization region. This ionization region is bounded by electrodes 2 and 4, between which there is a fairly weak electric field which draws the positive ions created by electron impact down toward a slit in electrode 2. After the ions pass through the slit in 2 they are further accelerated by the strong electric field between 2 and 5, and they emerge in a beam from the slit in 5. As may be seen, means are provided for maintaining all the electrodes at proper potentials. The function of electrode 3 is to collect the electrons that pass entirely through the ionization region.

When a monatomic gas is admitted into the ionization region the number of distinct ion peaks will be that of the number of isotopes of that element. When a polyatomic gas is being studied there results a multiplicity of peaks due mainly to the fact that a molecule may dissociate into various types of ionized fragments upon impact by an electron. The different ions may be brought into the collector by suitable adjustment of either or both the accelerating voltages in the ion source or the magnetic field strength. When the ion currents are plotted against either of these

two quantities there results a peak in the curve, called an ion peak, when the values are correct for focussing. Fig. 6 shows some of the ion peaks obtainable when *n*-butane is subjected to electron bombardment. Here the peaks are plotted against ionic mass. Such a curve is ordinarily referred to as a mass spectrum.

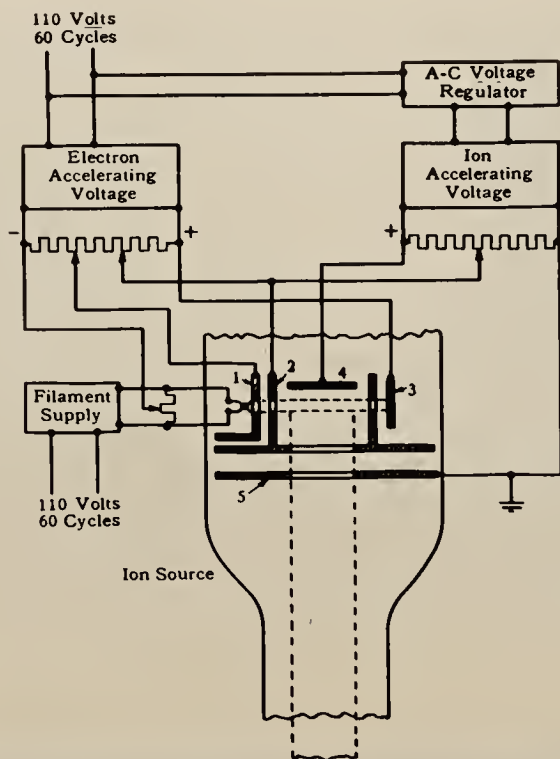


FIGURE 5. Schematic diagram of an ion source showing interrelation of electrical components.

In the utilization of this instrument for research and analytical problems the intensity of the ion beams, or the equivalent, the height of the ion peaks, is a problem of paramount importance, as will become clear later in the discussion of the applications. Consequently the operating parameters of the instrument which affect the ion intensities must be subject to close control so that they can be relied upon for constancy of operation.

Among these important variables are the filament current, the electron accelerating voltages, the positive ion accelerating voltages, the rate of inflow of gas to the ion source, and the temperature of the ion source. The magnetic field needs close control also, as fluctuations in it will cause the ion beam to fluctuate over the region of the collector slit. In recent years the great growth of the electronic art has benefitted the users of mass spectrometers enormously. Now amplifiers and voltage-stabilizing circuits are available which make it possible to dispense with some of the former equipment, which was both cumbersome and difficult to use.

In the ionization region a pressure of the order of 10^{-8} mm of Hg is often used. This allows ion beams of sufficient intensity to be obtained without the complications

of higher pressures. In the region of the magnetic analyzer, *i.e.*, between the ion source and the collector, it is important to have a considerably lower pressure. A vacuum of 10^{-5} mm of Hg or better is desirable to reduce scattering, which would weaken the ion beam intensities and harm the resolution. The pumping arrangement shown in Fig. 4 achieves the desired pressure differential.

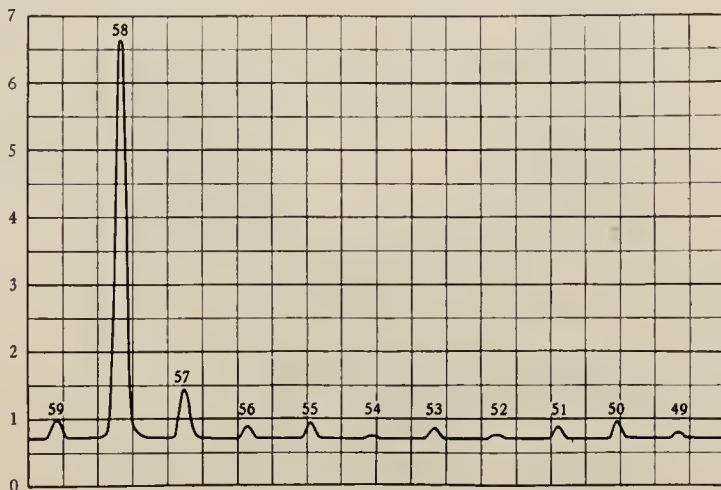


FIGURE 6. Mass spectrum of normal butane. The ordinate represents recorder deflection and the abscissa numbers refer to ionic masses.

At the present time the mass spectrometer has proven its value as a research and analytical tool to such an extent that such instruments are available commercially. Fig. 7 shows the spectrometer and its auxiliary equipment as built by the Consolidated Engineering Company.³ In Fig. 8 may be seen the Westinghouse Electric & Mfg. Company's mass spectrometer and part of the auxiliary equipment.⁴ Both these



FIGURE 7. Mass spectrometer and auxiliary equipment built by Consolidated Engineering Corporation.

instruments are highly engineered devices utilizing some of the latest advances in electronics, and both are equipped to provide automatic recording of the mass spectra of the materials being studied. They are built to measure mixtures or compounds that have appreciable vapor pressures at room temperature. The material is generally introduced into the ion source through a small leak.

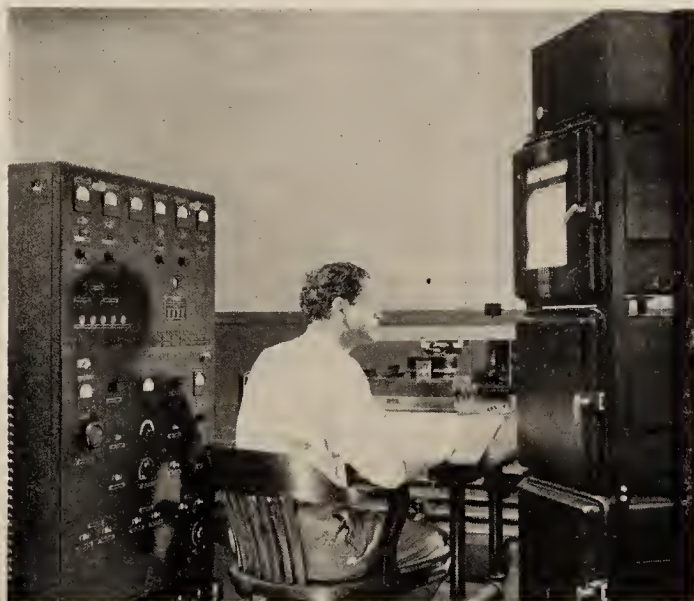


FIGURE 8. Mass spectrometer and part of the auxiliary equipment built by Westinghouse Electric and Manufacturing Co.

By virtue of the unique characteristics of the data obtainable with a mass spectrometer, it is very suitable for certain research and analytical problems. How the unique characteristics are utilized for specific problems will become more evident in the material which follows and which is devoted to a discussion of various applications. The applications are not discussed in any order of importance for either academic or industrial research.

Research and Analytical Applications

Natural Isotopic Abundances.* Ever since the concept of isotopes clarified itself to Rutherford, Soddy, and others about 1913, it has been a matter of vigorous interest to know definitely which of the elements are composed of isotopes, and in such cases, to know the isotopic weights and the relative abundances. It was for the job of studying isotopic abundances that many of the earlier instruments were built.

In the mass spectrographs of Aston and in those built by others the separate ion beams were focussed as thin lines on photographic plates. This resulted in a blackening at the lines of focussing, and the density of the blackening was used as a measure of the individual ion intensities. These studies resulted in some assignments of relative abundances being given to the isotopes of certain elements. However, the accuracy was none too good and more accurate figures have generally been obtained with mass spectrometers.

* A complete table of known isotopes of all elements, by Robley D. Evans, is printed as an Appendix to Vol. V of this series. J. A.

When neon, a monatomic gas, is introduced into a mass spectrometer it is possible to obtain ion peaks for the isotopes of mass numbers 20, 21, and 22. If it is assumed that no appreciable fractionation of the isotopes takes place at the small leak or orifice by which they are introduced into the ion source, the peak heights for the different isotopes will represent the relative abundances of the three isotopes.

For a diatomic molecule like N_2 , measurements can be taken of the peak heights of ions of atomic mass 28 and 29. These ions would be $N^{14}N^{14+}$ and $N^{14}N^{15+}$ respectively. Alternatively, the ions beams due to N^{14+} and N^{15+} could be measured, the latter arising from both dissociation and ionization of the molecules. In this manner, all the gases may be studied and the percentage distribution of the constituent isotopes evaluated.

In the case of materials which are solid at ordinary temperatures, various techniques have been used to produce vapors in the ion source. One method suitable for some elements and compounds has been to use a small furnace or oven near or integral with the ion source to project an atomic or molecular beam through the ionization region.⁵ For some elements, such as potassium, an ore or salt of the material may be deposited on a filament or heated disk.⁶ When the temperature of such mountings is sufficiently high, positive ions are given off which may be drawn directly into collimating slits to form the ion beam.

At the present time, there is fairly satisfactory information as to the isotopic constitution of most of the elements. Unfortunately, there still exists considerable doubt as to the accuracy of some of the determinations. This doubt is caused by the fact that different investigators using different instruments have not always checked one another's results to within the consistency of their individual studies. The complete reasons for the errors are not as yet fully known, but doubtless will clear up as the parameters affecting the performance of an ion source are better understood.⁷

The information as to the existence of the various isotopes and their relative abundances is of value for a variety of applications. Nuclear physicists are greatly interested in the theoretical implications of which combinations of neutrons and protons form stable nuclei. The relative abundances can be used with the mass values obtained with the mass spectrograph to establish a set of physical atomic weights based on O^{16} having an atomic weight of 16.000000, in contrast with the chemical system of atomic weights based on the natural mixture of oxygen isotopes having an atomic weight of the same. Also, as will be brought out later, it is possible to enrich certain isotopes in some of the elements and use them as chemical tracers. Obviously, the abundance ratios for the naturally occurring isotopes must be known. Tables giving the latest information of the relative abundances have been published by Livingood and Seaborg⁸ and by Seaborg.⁹

As a tool in following the progress and success of various methods of isotopic enrichment, the mass spectrometer has, of course, been an invaluable tool. A review of various methods of separating isotopes has been made by Urey.¹⁰

Isotopic Enrichment by Natural Processes. It is an intriguing question as to whether geological processes, organic processes, long-term chemical processes in the earth's crust, etc., can or have been effective in achieving any change in isotopic abundances in minerals, plants, etc.

Brewer⁶ made an early study of the potassium isotopes found in various minerals and plants. The specimens were pulverized or ashed, and the powder applied to a platinum disk which, when heated, gave off potassium ions. Brewer determined the K^{39}/K^{41} ratio and, after a large number of determinations, he concluded that there is small difference in this ratio for minerals; that plants sometimes show a marked variation, kelp giving the most pronounced; that the variations in plants depended upon such factors as age, soil, species, and section of the plant.

More recently Cook¹¹ made a quite extensive investigation of the K^{39}/K^{41} ratio as depending upon the source of material. His technique in generating positive po-

tassium ions was, in general, similar to that of Brewer, although he fused some of his material into a salt on the filament in some cases. He used a method whereby the samples were compared to a standard filament without appreciably affecting the operation of the instrument. Also, he used a double collector system in a 180° instrument so that the ratio was directly obtained from potentiometer readings. After examining some thirty-seven kelps, minerals, and rocks of varying geologic age, he formulated the following conclusions: (a) the K^{89}/K^{41} ratio for most Pacific kelps does not vary more than 1 per cent from that of rocks; (b) the ratio for the fossils examined does not vary definitely from that of rocks; (c) rocks of different geological age show no definite change in the ratio; (d) the observed fluctuations in the K^{89}/K^{41} ratio are apparently due to isotope effects in the ion source. That such conclusions are the result of the elaborate work done underlines the difficulty of obtaining completely definite data.

An investigation of the isotopes of oxygen from meteoric sources has been made by Manian, Urey and Bleakney.¹² Their results were negative in that no differences were found from terrestrial oxygen. Nier¹³ and his collaborators have made extensive studies of the variations in the carbon isotopes, and have found what appear to be significant differences. The results can be regarded as indicating a preference for C^{13} in limestones and for C^{12} in plants. In this work, the carbon was converted to carbon dioxide for admission to the ion source. Some of the results are shown in Table 1.

Table 1. C^{12}/C^{13} Ratio For Various Carbon Sources
(From Murphy and Nier¹³)

Source	No. of Samples	Average ratio for samples in group
Limestone	10	89.2
Coal (humic origin)	10	91.8
Wood	7	91.8
Petroleum	6	92.5
Bituminous shales	7	92.5
Torbinite and kerosene shales	3	91.7
Meteoritic carbon	7	91.3
Graphite	1	90.2
Zeolitic calcite	1	89.9
CO ₂ in air, Minneapolis, Minn. 3/1/41	1	91.5
Lycopodium spores	1	93.1
Balkashite algae	1	92.8
Marine shell	1	89.5
Sea water	1	89.3

Variations in the relative abundances of the lead isotope have been studied by Nier²⁸ and the results used to determine the geological age of various minerals. If lead is contaminated by naturally radioactive materials, the lead isotopic ratios will be changed, as some of them are the end products of particular radioactive decay processes.

Enriched Isotopes as Tracers. As we have seen, the natural isotopic ratios for the elements are fairly well known. If, then, it were possible to change the isotopic ratio artificially for a sample of some material, it would serve as a tracer in chemical studies. At the present, there has been considerable success in the separation of isotopes by electrolysis, exchange reactions, and thermal diffusion¹⁰ which has made possible the utilization of this new tracer technique. As the mass spectrometer can distinguish between ion peaks representing different isotopes, it is the desired instrument for the analytical work. Except for the case of the light elements, in which density measurements can be used, it is the only instrument capable of satisfactorily distinguishing the different isotope ratios.

A good review of the application of enriched isotopes as tracers has been given by Rittenberg,¹⁴ in which he describes some experiments of his own and others. Of chief interest here is the isotopic dilution method which is designed to make possible the quantitative analysis for organic compounds which are very difficult to determine by customary means. An example of such a compound is any one of the amino acids. Although it is virtually impossible to isolate all of one in a pure form from a protein hydrolyzate, it is possible to isolate a fraction of it which will be pure.

In the application of the isotope dilution method, a portion of the amino acid being studied is synthesized from nitrogen with N^{15} enriching it. A weighed amount of it is added to the protein hydrolyzate and then from this mixture is isolated a small amount of the same amino acid in pure form. The N^{14}/N^{15} ratio is determined for this sample; and from a knowledge of the same ratio for naturally occurring nitrogen, the same ratio in the enriched material, and the portion of synthesized material added, the amount of the amino acid existing in the original protein hydrolyzate can be calculated. This technique has been applied with considerable success by Rittenberg and others, and Table 2 shows a typical set of results obtained with it.

Table 2. Determination of Amino Acids in Fibrin
(From Rittenberg¹⁴)

Protein hydrolyzed (g)	Amino Acid Added Compound	Weight (g)	N^{15} Excess (atom %)	N^{15} excess in compound isolated at successive stages of recrystallization (atom %)	Amino Acid in protein found (%)
4.002	Glycerin	0.1315	2.00	0.781 0.784 0.782 0.782	5.12
4.995	<i>dl</i> -Glutamic acid	0.1266	2.10	0.182 0.186 0.185	13.2
5.382	<i>dl</i> -Glutamic acid	0.1152	2.10	0.162 0.161 0.157	13.0
5.034	<i>dl</i> -Glutamic acid	0.1222	2.10	0.185 0.176	12.9
	<i>dl</i> -Glutamic acid	0.4005	2.10	0.356 0.355	12.8
7.675	<i>dl</i> -Aspartic acid	0.4000	2.00	0.374 0.383	11.2

For biological studies the use of enriched isotopes also offers a powerful approach to problems of food assimilation. Animals which have been fed a diet one component of which consists of material with a changed isotopic ratio may be dissected and the same ratio determined for tissue from the various organs. This allows a determination of selective and time-dependent assimilation.

The application of C^{13} as a tracer in heterotrophic carbon dioxide assimilation processes has been made by Wood, Werkman, Hemingway, and Nier.¹⁵ The purpose of the investigation was to determine the distribution of fixed carbon dioxide in the products of bacterial fermentation. In this work, $NaHCO_3$ was enriched with C^{13} and added to a medium in which a substrate with a cell suspension was fermented. Their general conclusions were: Carbon dioxide fixed in the fermentation of galactose, pyruvic acid, and citric acid by *coli* occurs solely in the succinic and formic acids; in the fermentation of glycerol and glucose by *Propionibacterium*, the fixed carbon dioxide is in the succinic acid, propionic acid and propyl alcohol. Their results also had significant implications with respect to the specific intermediate reactions.

As new developments in the separation of isotopes become practical, it is to be

expected that great activity in the use of enriched isotopes as tracers in the biological field will follow.

Study of Chemical Reactions. The use of the mass spectrometer to study gaseous reactions is one field of application that has as yet not received a great deal of attention. The advantage of this instrument for such studies is its ability to measure the partial pressures of the constituent components as the reaction occurs. Hagstrum and Tate,¹⁶ for example, have studied the thermal activation of the oxygen molecule in this manner.

When a study of the dissociation of a particular molecule by electron impact is made, the instrument must be carefully designed to insure that there is no appreciable thermal dissociation by the hot filament. In their electron impact studies of the oxygen molecule, Hagstrum and Tate noticed that the abundances of the ions representing CO_2 , CO , and H_2O relative to O_2 depended on the temperature of the tungsten filament supplying the ionizing electrons. They then investigated this effect by inserting a platinum filament in the gas inlet line to the mass spectrometer and by replacing the tungsten filament by an oxide-coated one for the source of electrons in the ion source. When the platinum filament was run at 1600°K , the O_2 peak was found to decrease and the other peaks increased. After a 'short time with the filament at this temperature, the O_2 peak increased to its original value. It was suggested by the authors that the process involved activated adsorption of the oxygen molecules on the hot platinum surface. This would account for the bulb containing the platinum filament acting initially as a sink.

It was further suggested that the oxygen molecules were excited to a metastable state and evaporated, reacting with the very low vapor pressure material on the walls to produce CO_2 , CO , and H_2O . The disappearance of the effect may then be explained by this "clean up."

Eltenton¹⁷ has employed the mass spectrometer to detect free radicals and other intermediate products of chemical reactions. In his apparatus a thermal reaction chamber was placed adjacent to the ionization region in such a manner that a fraction of the products could escape through a small orifice in a thin diaphragm and be analyzed by the mass spectrometer. The electron voltage was set at a value below appearance potential of the free radicals arising from the dissociation by electron impact in C_2H_4 , C_2H_6 , and C_3H_6 , but above the ionization potential of the free radical itself. In one series of experiments the methyl radicals were produced from lead tetramethyl, and their interaction with the three carrier gases mentioned above was studied. It was found that the reaction was greatest between CH_3 and C_3H_6 . Methyl and ethyl radicals have been detected from ethane up to pressures as high as 120 mm.

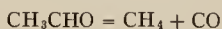
In a study of the kinetics of the thermal decomposition of dimethyl ether and acetaldehyde, Leifer and Urey¹⁸ used a mass spectrometer of the Bleakney type to detect intermediates and to measure their intensities. In this work the dimethyl ether or acetaldehyde was introduced into a hot reaction chamber into which intruded a capillary leak. This leak communicated to a line leading to the ion source of the mass spectrometer. Also, attached to the reaction chamber was a manometer by means of which they could measure the change of pressure with time and correlate this with the change of peak heights of the various ions measured. In Table 3 may be seen the ions resulting either from dissociation and ionization of the parent molecules or from ionization of the intermediates of the thermal decomposition. The voltages given here are the appearance potentials for these ions when produced from the parent molecules by electron impact. The electron voltages necessary to produce these ions from intermediates will be less. In this case the minimum energy required is that to produce ionization only, while the minimum energy mentioned above must be enough to produce both dissociation plus ionization as the ions are produced from parent molecules. Thus by using the proper voltage for the ionizing voltages, Leifer and Urey could be sure the ions they were producing were from the intermediates.

Table 3
(From Leifer and Urey ¹⁸)

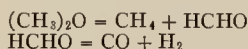
Dimethyl ether			Acetaldehyde		
Mass	Ion	Acc. voltage (volts)	Mass	Ion	Acc. voltage (volts)
30	HCHO ⁺	14.5	28	CO ⁺	16.0
28	CO ⁺	18.5	16	CH ₄ ⁺	14.5
16	CH ₄ ⁺	18.0			
2	H ₂ ⁺	20.0			

To determine the dependence of ion peak height on pressure behind the leak, preliminary tests were made which indicated the peak heights to be directly proportional to the pressure. This allowed the data for the ion peaks to be used at any time to determine the pressure in the reaction chamber.

The decomposition process was indicated from a consideration of the intermediates formed and their dependence on time to be:



for acetaldehyde, and:



for dimethyl ether. Also Leifer and Urey used the indicated pressures to determine rate coefficients for the processes. The rate coefficients were found to be dependent upon initial pressures and to fall off as decomposition proceeded. Also by using unpacked, partially packed and fully packed reaction vessels, the rate coefficient for dimethyl ether was found to be a function of the surface volume ratio. Other very interesting results were obtained from this work but space does not allow their discussion here. It is to be expected, as mass spectrometers become more common and as their ease and reliability of operation increase, that more fundamental studies of this sort will follow.

Dissociation of Molecules by Electron Impact. During the last twenty-five years, many research workers have employed the mass spectrometer in the study of the processes involved in the production of ions from molecules by electron impact. This was a natural outgrowth of the early Franck and Hertz experiments on the one hand, and the development of the techniques of the positive ray analysis on the other. A review of this field up to 1931 has been written by Smyth.¹⁹ The work up to this point was concerned primarily with the simpler molecules, composed of very few atoms. Since then, the experimental methods have been improved greatly, with the result that many of these molecules have been restudied and, in addition, some interesting interpretations have been made of the ionization processes of much more complex molecules. This advance has been largely made possible by the greatly increased sensitivity of the mass spectrometer due to instrument refinements, and more sensitive means of measuring the ion currents. The development of electrometer tubes has been a great impetus here. Now it is possible to operate the mass spectrometer at lower pressures and smaller electron currents, insuring that primary processes alone are being studied.

This instrument is able to obtain information not only on the appearance potential of the various fragments, but also on their relative abundances. The appearance potential for a particular ion formed by electron bombardment of gaseous molecules is the value of the ionizing electron voltage at which the ion may first be detected. It then serves as a lower limit for the energy sufficient to produce both the dissociation and ionization necessary for the ion to be formed from the parent molecule. In the study of appearance potentials, a particular mass is kept focussed on the exit slit and the current to the ion collector is studied as the electron energy is varied. The

same technique also furnishes ionization efficiency curves. The measurement of the relative abundances of ion fragments (or "cracking patterns") was usually considered of secondary interest until the recent application of the mass spectrometer as an analytical tool for routine analyses. The result of the application to this very practical problem has temporarily shifted the emphasis almost entirely to a study of the "cracking patterns." This will be discussed in a later section.

Methane was the first rather complicated molecule for which a serious attempt was made to interpret the process of ionization. A preliminary report of this was made by Bleakney, Condon, and Smith²⁰ and a more complete study was made by Smith.²¹ This molecule serves as a nice example to illustrate the type of data obtained with the mass spectrometer, since a general review of the field would be out of place in this paper. Table 4 is from Smith's article and is a resume of the data on methane and its interpretation in terms of the most probable processes involved.

The most abundant ions in methane are those of masses 16 (CH_4^+) and 15 (CH_3^+). However, practically all possible ions are found to occur. For example, at a single electron impact all the hydrogen atoms may be stripped from the methane molecule, leaving the C^+ ion to be detected when the instrument is set to collect ions of mass 12. Such a rich spectrum is rather typical of all the hydrocarbons. There is one important change exhibited by heavier hydrocarbons: that the ionized parent molecule is no longer the most abundant one. The mass 28 peak (C_2H_4^+) is the largest peak in the ethane spectrum; however in the isobutane spectrum,²² for example, the peak at mass 43 (C_4H_7^+) is more than ten times as abundant as the parent ($\text{C}_4\text{H}_{10}^+$) ion at mass 58. In some molecules such as tertiary butyl chloride, a parent peak cannot be detected. This may limit the complexity of the molecules that may be handled with the mass spectrometer. Thus far the chief reason why more complex molecules have not been studied is because of the difficulties of interpretation of the actual processes from the great number that one might assume for the production of the various fragments.

The interpretations shown in Table 4 were obtained by using thermochemical data in conjunction with the measured appearance potentials. In this way, additional information about the ionization and chemical bond energies may be inferred. The mass spectrometer cannot measure changes in the excitational energy of the molecule or kinetic energy of the neutral fragments. In many processes it has been found that these energies are small in the vicinity of the appearance potential. For instance, from the appearance potential of CH_3^+ Smith inferred that the ionization potential of CH_3 should be equal to or less than 9.9 volts. That is, this ion appears at 9.9 volts, and if the dissociation fragments possess no excitational or kinetic energy then it may be said that the ionization potential of the free radical CH_3 is 9.9 volts. If the more recent value $D(\text{CH}_3 - \text{H}) = 4.4$ volts (instead of 4.5 volts) is taken for the strength of the $\text{CH}_3 - \text{H}$ bond, then the deduced value for the ionization potential of CH_3 becomes 10.0 volts. Hipple and Stevenson²³ measured this ionization potential directly by thermally dissociating lead tetramethyl to produce the free methyl radicals in the ionization chamber of a mass spectrometer. This experiment yielded a value of 10.0 ± 0.1 volts, in excellent agreement with the value obtained with methane, assuming no excitational or kinetic energy.

Besides the question of the excess energy in the reaction which the mass spectrometer cannot detect, there is one other limitation in its application to the determination of the heats of dissociation of molecules. This is the inaccuracy due to the spread in velocity of the electron beam since the source of the electrons is a hot filament. The situation is improved somewhat by the use of an oxide-coated filament instead of one of tungsten, permitting the uncertainty to be cut down to 0.1 volt. However, from the viewpoint of the chemist, 0.1 volt is a large inaccuracy. There is a possibility of using a velocity filter on the electrons, but experimentally this is quite complicated and has not been attempted in this particular application.

In his paper on the study of butene-1 with the mass spectrometer, Stevenson²⁴ has summarized the heats of dissociation obtained from electron impact data. This summary is given in Table 5:

Table 5
Heats of Dissociation, $D(R' - R'')$, in E. V., for the
Reactions $R' - R'' = R' + R'' - D$
(From Stevenson²⁴)

R''	$R' = H$	CH_3	C_2H_5	C_2H_3	Cl
H	4.502
CH_3	4.40	3.62
C_2H_5	4.20	3.52	3.43
C_2H_3	3.95	3.43	3.30	3.32	...
Cl	4.46	3.50	3.45	3.1	2.50
$I^2 (R')$	13.5	10.07	8.67	9.9	12.9

Molecular Potential Energy Curves. In the discussion of the dissociation of molecules by electron impact, the fact that the kinetic energy of the fragments is unknown places a limitation on the method. No instrument has yet been designed that will provide information concerning the kinetic energy of the neutral fragments, but some fruitful investigations have been made on the kinetic energy of the ionic fragments. Information concerning the potential energy curves may be obtained in this way.

Bleakney²⁵ was able to demonstrate with his mass spectrometer the existence of the repulsion curves in hydrogen, predicted by quantum mechanics. The voltages in the ion source were so adjusted that only ions possessing greater than selected minimum kinetic energy could leave the ion source and enter the analyzer. Under these conditions no ions were observed when the electron accelerating voltage was below 26 volts. Above this voltage, however, atomic hydrogen ions possessing considerable kinetic energy were observed. These resulted from an electronic transition to a repulsion state in which the hydrogen atom and the ion fly apart with considerable kinetic energy. The Franck-Condon principle also predicts the formation by single electron impact of atomic hydrogen ions with little kinetic energy at an electron voltage of approximately 18 volts. These ions were observed. Lozier²⁶ investigated the velocity distribution of the high-speed ionic fragments in greater detail.

More recently a very interesting study of molecular potential energy curves as related to mass spectrometer peak shapes has been done by Hagstrum and Tate.²⁷ In this work they considered the collection efficiency of the usual ion source for ions of different initial kinetic energies. They obtained a curve of collection efficiency versus initial kinetic energy from a consideration of the manner in which the ions are collected by the first collimating slit and passed by the second. Also they considered the distribution of kinetic energy in the ions formed when certain diatomic molecules are dissociated and ionized by electron impact.

The theoretical distribution of initial kinetic energy of the ions was obtained by applying both the Franck-Condon principle and the quantum-mechanical wave functions for probability distributions as dependent upon internuclear separation. The Franck-Condon principle states that an electron impact with a molecule causes no significant change in internuclear separation because of the small mass and momentum carried by the electron. Excitation of a molecule to an ionized state may lead to dissociation if the minimum of the potential energy for the ground state is at a smaller internuclear distance than the minimum for the energy curve for the excited state. If the relative locations of the potential energy curves are known, the statistical distribution of ion velocities can be calculated by application of the square of the wave function representing the ground state. The product of the efficiency of collection function times the density distribution as a function of initial kinetic energy gives a curve representing the distribution of ions as a function of initial kinetic energy as they emerge from the slits of the ion source.

Depending upon the relative displacements of the potential energy curves of the ground and ionized states there may result any one of four distinct types of ion peaks. The difference is mainly in the shape, especially on the high mass side. They were able to explain the reason for satellite peaks and to demonstrate how the peak shapes can be used to deduce qualitative information concerning the potential energy curves for the excited ionized states giving rise to the ions.

This mode of attack is very interesting and has promise of more quantitative results if the conditions of ion collection can be more exactly controlled. A more precisely determined collection efficiency curve has been reported⁷ but the complete processes are not yet entirely understood.

Analysis of Mixtures with the Mass Spectrometer. A natural outgrowth of the studies of ionization and dissociation by electron impact was the application of the mass spectrometer to analytical problems. The early analyses were very simple ones, such as the determination of the purity of inert gases. The measurement of traces of impurities in gas samples remains a very important field of application today, but in the last few years the method has been extended successfully to the analysis of rather complex gas mixtures.²⁹

During the analysis the sample flows through the mass spectrometer tube at a constant rate. This is conventionally accomplished by bleeding the sample into the instrument through a flow-restricting device from a large reservoir at a rather high pressure (perhaps one millimeter of Hg). In maintaining a relatively constant flow rate in this manner, it is important that the "leak" have a linear flow characteristic, *i.e.*, the flow rate of each component must be a linear function of its partial pressure in the reservoir. There are a great many other problems to be solved in the successful application of the instrument, such as the design of a suitable pumping system, surface contamination of the electrodes, and thermal cracking of the molecules by the hot filament.

In obtaining the data for an analysis in routine operation a fast recording system is practically a necessity. This recorder should be able to record to an accuracy of 1 per cent ion currents differing in magnitude by a factor of several hundred because of the wide range of intensities in the spectra. This problem has been solved in the case of a photographic recorder by employing several galvanometers of different sensitivities.²⁹ Thus, the spot from the most sensitive galvanometers may be far off the scale, but under this circumstance a less sensitive galvanometer will be deflected sufficiently to provide an accurate reading. The required extended scale has been obtained with a pen and ink recorder by employing a logarithmic response coupled with an automatic change in sensitivity when the pen reaches the top of the scale.³⁰ By these methods a spectrum may be recorded accurately in about ten minutes.

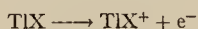
Before making an analysis the mass spectrometer must be calibrated. This involves the recording of the spectra of the pure components in the mixture as well as a determination of the relative sensitivity of the instrument to each component. The simplest method of calibration is that of simply employing a pressure standard. For each component, the spectrum is obtained for a known pressure in the reservoir behind the leak. With this information available the analysis of a mixture of these components may be made. Recalibrations are necessary from time to time as the spectra are sensitive to changes in the surface conditions of the electrodes and changes in geometry, voltages and temperature of the tube. By careful control the effect of these variables may be minimized. In spite of the difficulties involved, the mass spectrometer has an important role in gas analysis because of its speed, the wide range of masses that may be covered, and its ability to detect without ambiguity small traces of impurities. For complex mixtures, the calculations require much greater time than that consumed in obtaining the data with the instrument when automatic recording is employed. They involve the solution of a set of linear equations similar in form to those employed in the infrared method of analysis.

Application to Photochemistry. One research field for which it is potentially quite valuable but to which the mass spectrometer has not as yet been very widely applied is that of photochemistry. One limitation to its use, of course, is that only photochemical processes that give ions or radicals easily ionized can be studied.

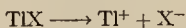
A direct application to the study of the products of the photo-dissociation of diatomic molecules into ions has been made by Terenin and Popov.³¹ In their studies they observed that it was possible to get quite large photo-currents when the vapors of certain salts such as TlI , TlBr , and TlCl were subjected to ultraviolet radiation. By a series of tests they were able to conclude that the effect was truly one of photo-ionization of the molecules in the gas phase. For example they found that the current was independent of the change of the polarity of the electrodes, that it reached a saturation value as the potential between the electrodes was increased, and that it was proportional to the amount of light falling in the ionization region.

The source of ultraviolet light was a spark which could be of any one of the three materials: Al , Cd , and Zn . Using a monochromator made of fluorite and quartz Terenin and Popov were able to separate out various spectral lines and to study the dependence of the photo-current upon still another parameter, the wave length of the radiation.

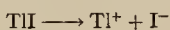
As the studies on mere photo-ionization of the Tl -halides did not indicate whether the process was:



or



a mass spectrometric study was made of the photo-ionization products. The ionization region was so constructed that an electric field would draw out the charged particles into a magnetic analyzer. By calculations as to the effective potential of these particles and by using a calibration of magnetic field as a function of their exciting current, Terenin and Popov were able to identify the ions and to demonstrate that the photo-ionization process was of the latter type, shown above. TlI , for example, was dissociated and ionized by the process:



Further fundamental information concerning the process was obtained by using the equation:

$$U = D + J - E$$

where U is the total energy necessary to produce dissociation and ionization, D is the dissociation energy of the molecule into neutral atoms, J is the ionization energy of Tl , and E is the electron affinity of the halogen atom. By correlating U with the energy of ultraviolet light in each case, which produced maximum ionization, and by using known values of D , J and E , they discovered that the kinetic energy of the dissociation products was of the order of 0.5 electron volt. Further work on photo-ionization confirming that of Terenin and Popov as well as investigating the process for other compounds was done by Wehrli and Halg.³²

There is another type of study which may yield to mass spectrometric techniques: that of identifying photo-dissociation products. Recent work^{17, 18} has demonstrated the feasibility of detecting radicals by using lowered ionizing electron voltages.

Ionization Studies. The reversal of ionization, *i.e.*, change of sign of the ion upon striking a metallic surface, has been studied by Arnot and his collaborators for several different types of ions.^{33, 34, 35, 36} In their investigations of the formation of diatomic Hg molecules they found negative ions of Hg in appreciable quantities. Using a mass spectrometer with special design of ion source they uncovered several significant facts about the production of Hg^- . In this ion source the filament was

located in line with the exit slits and, with the electric fields such as to draw negative ions from the region of the filament out of the source, the Hg^- ions were found. From their energies it was apparent that they were formed on or near the filament. The Hg^- ions were found to be proportional to the Hg^+ ions over a fair pressure range. The Hg^- ions have a quite large energy spread. Also it was found that ions of the same type appeared to be originating in the ion source at or near a metal gauze which served as an electrode for accelerating potentials. The recognition of the place of origin could be made by the electrostatic potential relations in the ion source and the correlation with the energy of the ions as determined using the magnetic analyzer.

From the above observations it was concluded that Hg^- ions are formed when a Hg^+ ion strikes the metal filament or electrode, that is, a certain fraction of the Hg^+ ions rebound in the form of Hg^- . Also, it was reasoned from the energy spread that the Hg^- ions have, on leaving the metal surface, some of the original energy which the Hg^+ ion carried. Further studies were made on a number of other gases showing atomic negative ions. As in the case of Hg^- , the investigations in each case indicated the negative ions to be the result of direct impact of the positive ion on a metal surface. Table 6 shows some of the results obtained.

Table 6. Probability of Conversion of 180-Volt Positive Ions into Negative Ions on a Nickel Surface (From Arnot ³⁴)

Negative Ion	Positive Ion From Which Formed	Probability of Formation on Units of 10 ⁻⁴
Hg^-	Hg^+	6.4
H^-	H_2^+	0.104
N^-	N^+	1.07
O^-	O_2^+	1.10
O_2^-	O_2^+	0.42
CO_2^-	CO_2^+	2.31
O_2^-	CO_2^+	2.51
CO^-	CO_2^+	10.8
O^-	CO^+	3.37
C^-		(0.1)
77.4% +22.6%		

The mass spectrometer has been used by Hogness and his collaborators in studying ions formed by collisions of the second kind.³⁹ In mixtures of NO and A and of NO and He, increase in the relative intensities of NO^+ with increase in pressure gave definite evidence of collisions of the second kind, that is:



and



A similar magnetic analyzer study has been made by Harnwell,³⁸ who studied the ratio of He^+/Ne^+ and of He^+/A^+ under various pressure conditions. The ionization of gases by collisions of their own accelerated molecules has been studied by Berry.³⁹ In this work, he accelerated ions which were then neutralized before producing the further ionization. His selection of velocities was by an electrostatic velocity selector.

A mass spectrometer arrangement has been used by Scott⁴⁰ to measure and identify the different ions produced in an ion source designed for high intensity ion currents. His ion source was one in which the ions were formed by bombarding a region of gas with a beam of focussed electrons. From this source he obtained hydrogen ion beams as high as 4 ma.

The complex processes involving multiple collisions at higher pressures have not received as much attention during recent years, although some interesting studies of ion sources of high current output employing the mass spectrometric measuring

method have been made by Schutze.⁴¹ In this work the intensity of H^+ was studied under different operating conditions of the ion sources.

References

1. Aston, "Mass Spectra and Isotopes," Edward Arnold & Co., London (1942).
2. Jordon and Young, J. App. Phys., 13, 526 (1942).
3. Consolidated Engineering Corp., Pasadena, Calif.
4. Westinghouse Electric & Manufacturing Co., Pittsburgh, Pa.
5. See for example: Bleakney, Blewett, Sherr and Smoluchowski, Phys. Rev., 50, 545 (1936).
6. See for example: A. K. Brewer, J. Am. Chem. Soc., 58, 365 (1936).
7. N. D. Coggeshall, J. Chem. Phys., 12, 19 (1944).
8. Livingood and Seaborg, Rev. Mod. Phys., 12, 30 (1940).
9. G. T. Seaborg, Rev. Mod. Phys., 16, 1 (1944).
10. H. C. Urey, Reports on Progress in Physics, VI, 48 (1939).
11. K. L. Cook, Phys. Rev., 64, 278 (1943).
12. Manian, Urey, and Bleakney, J. Am. Chem. Soc., 56, 2601 (1934).
13. See for example: Murphy and Nier, Phys. Rev., 59, 771 (1941).
14. D. Rittenberg, J. App. Phys., 13, 561 (1942).
15. Wood, Workman, Hemingway, and Nier, J. Biol. Chem., 139, 365 (1940).
16. Hagstrum and Tate, Phys. Rev., 59, 509 (1941).
17. Eltenton, J. Chem. Phys., 10, 403 (1942).
18. Leifer and Urey, J. A. C. S., 64, 994 (1942).
19. Smyth, Rev. Mod. Phys., 3, 347 (1931).
20. Bleakney, Condon, and Smith, J. Chem. Phys., 41 197 (1937).
21. Smith, Phys. Rev., 51, 263 (1937).
22. Stevenson and Hipple, J. A. C. S., 64, 1588 (1942).
23. Hipple and Stevenson, Phys. Rev., 63, 121 (1943).
24. Stevenson, J. A. C. S., 65, 209 (1943).
25. Bleakney, Phys. Rev., 35, 1180 (1930).
26. Lozier, Phys. Rev., 36, 1285 (1930).



bombarded by slow neutrons. This was confirmed by Kingdon, Pollock, Booth and Dunning.⁴⁸

In his War Department Report, Smythe discloses that a mass Spectrometric method was used in collecting appreciable quantities of U^{235} for use in the atomic bomb.⁴⁹ It may be that in the future the technical details of these separators will be made more known to the public.

42. Smythe, Rumbaugh and West, Phys. Rev., 45, 724 (1934).
43. Smythe, and Hemmendinger, Phys. Rev. 51, 178 (1937).
44. Hemmendinger and Smythe, Phys. Rev. 51, 1052 (1937).
45. Hahn, Strassman & Walling, Naturwiss., 25, 189 (1937).
46. J. Mattauach, Naturwiss., 25, 189 (1937).
47. Nier, Booth, Dunning and Grosse, Phys. Rev. 57, 546 (1940).
48. Kingdon, Pollock, Booth and Dunning, Phys. Rev. 57, 748 (1940).
49. War Department Report "A General Account of the Developments of Methods of Using Atomic Energy for Military Uses Under the Auspices of the United States Government," by H. D. Smythe. Publication authorized August, 1945.



SPECTROSCOPY

In the Ultra-Violet and Visible Bands

by RAYMOND G. RUSSELL* and NORMAN D. COGGESHALL**

Gulf Research & Development Company, Pittsburgh, Pa.

AFTER a somewhat slow beginning, the chemical industry is now utilizing more and more the technique and methods of spectroscopy for the solution of analytical and research problems. Here the applications of emission and absorption spectroscopy in the ultra-violet and visible region are discussed, consideration being given to methods of operation, accuracy and cost.

THE USE of a spectroscope for the separation of the various wavelengths of light has been known since the latter part of the 17th century, but it is only within the present century that it has been widely used as an analytical tool. In fact, it is only within the last decade that the improved source units and methods of recording and measuring spectra have caused it to be widely employed by industry.

EMISSION METHOD

There are complete books on the subject^{1, 2, 3} so this discussion will be purposely short. Any atom which is excited emits light of definite wavelengths. Theoretically, electrons surrounding an atom are driven out of their normal orbits by some form of excitation and as these electrons return to their normal states, they emit light corresponding to the energy gained by the excitation. Since each atom has a different number of electrons and a different electron configuration, the light emitted on the return to the normal state is different. Thus each element in the universe has a different spectrum.

INSTRUMENT

A spectrograph is an instrument which is able to take this assemblage of light of different wavelengths and spread them out in an orderly fashion, giving a visible representation on a photographic plate.

* Spectroscopist.

** Physicist.

The authors are indebted to Dr. Paul D. Foote, Executive Vice-President of the Gulf Research & Development Co. for permission to publish this material.

Fig. 1 gives the essential optics of a prism spectrograph used in the Gulf laboratory. The sample is excited at the position marked arc and the light is focussed on the slit and turned by the small prism toward the refracting prism. At the camera and collimating lens the light is made parallel and goes through the prism where the various wavelengths of light are each bent a different amount. The light, which returns from the prism due to reflection from a mirror on the back surface, passes through the camera and collimating lens and is focussed on the photographic plate. As the wavelengths of light were bent differently in the prism, they will appear at different positions on the photographic plate, the exact position being dependent on the wavelength of the beam of light. Fig. 2, which is a photograph of a portion of the spectrum, shows the appearance of the unlike wavelengths after focussing on the photographic plate.

Although each of the 92 elements has a distinct spectrum, our discussion will be limited to those elements whose spectra are excited by arc or spark currents in air, and whose spectra appear between wavelengths 2000A ($1\text{A} = 10^{-8}\text{ cm.}$) and 8000A. The wavelength range is limited by the emulsions in the photographic plates used to record the spectra and the light absorption due to air. Such limitations exclude from consideration the rare gases, all of the halides except fluorine, carbon, oxygen, nitrogen, sulfur, selenium, and hydrogen. These elements either do not give spectra in the range 2000A-8000A or are not excited by the arc or spark in air. Therefore, the discussion is limited chiefly to the inorganic elements and excludes the study of those compounds

which may be regarded as purely organic.

OPERATION

The dispersion of the spectrograph shown in Fig. 1 is such that approximately 30 inches of photographic plate are required to cover the complete range. This means that three separate samples must be weighed up in order to get the entire range on a ten inch plate. It takes approximately 2 minutes to completely burn an ordinary sample (i. e., an ash from an oil sample) in a 10 amp. arc so that it will take about 6 minutes to completely excite a sample over the wavelength range 2000A-8000A. Another 20 minutes are required for developing, washing, and drying the photographic plate, and 10 minutes for an experienced operator to interpret the spectra. Thus a complete qualitative analysis for about 75 elements is obtained within 45 minutes. In addition, other samples can be exposed on the same plate and an experienced operator can give an approximate concentration grouping to the elements found so that the time per sample is reduced even further and more nearly quantitative results are obtained. The various lines of the elements always occur at exactly the same place on a photographic plate with a reproduced setting of the spectrograph optics. The blackness of the element line is nearly proportional to its concentration in the sample. It is thus possible to compare line blacknesses with chemical analyses and to build up experience in grouping elements found present in a sample.

The time required for quantitative analyses is even shorter than that for qualitative analyses once a particular method is set up. Considerable time will be required to prepare a set of standards for quantitative analyses, to get exposure conditions correct and to pick the proper element lines for use, but once this is done, future quantitative analyses on samples of similar composition, as the standards, will be quite rapid. For in-

also twofold—to develop answers to the questions raised by industry and, if in the course of its current work the staff develops interesting market information, to pass such information on to the Industrial Sales Contacts Section for transmittal to interested industrial groups.

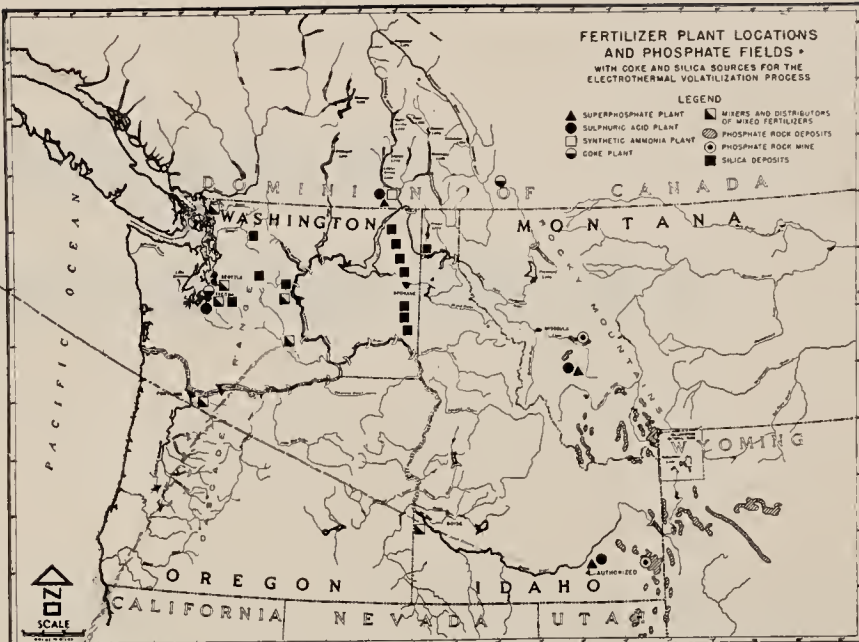
(3) The Industrial Analysis Section, under the direction of Mr. J. N. Carothers, is composed of technical men experienced in chemistry, metallurgy, forest products utilization, and mineral raw materials. It gathers, analyzes, and reports on the technological factors of industrial establishment in the Northwest and transmits its findings to the Industrial Sales Contacts Section for dissemination to industry.

The Division of Industrial and Resources Development cooperates closely with local civic organizations in the Northwest, and has the assistance of appropriate units of the Army Corps of Engineers, the U. S. Department of Agriculture, the Forest Service, and other agencies. The Division is desirous of maintaining constant contact with industrial organizations throughout the United States to build up a firm collaborative program.

The list of chemical industries which the Division is studying, with a view to drawing new establishments to the Northwest, includes aluminum, magnesium, iron, steel, ferrochromium, ferrosilicon, ferromanganese, ferrotungsten, ferromolybdenum, ferrotitanium, ferrovanadium, copper, lead, zinc, gold, silver, arsenic, sulfuric acid, manganese, chromium, ceramics, cement, glass, sodium silicate, silicon carbide, aluminous abrasives, hydrogen, oxygen, ammonia, liquid sulfur dioxide, acetylene, chlorine, caustic soda, hydrochloric acid, chlorates, perchlorates, carbon tetrachloride, carbide, tetrachloroethylene, trichloroethylene, acetic anhydride, glacial acetic acid, phosphates, silicon, carbon disulfide, phenolic resins, viscose rayon and cellophane, cellulose acetate, and ligno-plastics.

Studies which have been made by the Administration and published as documents available to the public are listed below, but these do not represent all of the material available to industry and located in the Division's files. For example, the Division has accumulated a file of coordinated mineral information which, it feels, is second to none in the Northwest. The files on economic information available in the Division are likewise extensive. They constitute an up-to-date and current collection of basic economic information, county by county, for the four Pacific Northwest states.

A valuable study issued in 1945 was "A Preliminary Report on the Plastics Industry as Related to Pacific Northwest Industry," for which the overwhelming demand had to be met with an immediate second printing. A new supplement in preparation deals with cellulose-base plastics, for which a great potential is be-



The above map is a portion of one of the brochures published by the Bonneville Power Administration to point out the commercial and industrial opportunities in the Pacific Northwest.

lieved to exist in the wood celluloid citadel of the Pacific Northwest.

An exhaustive report has been made on the zinc-lead mines of the Pacific Northwest and tributary areas.

The Columbia Basin Study, now under way, is perhaps indicative of the nature of future activities. For purposes of this study, a series of investigations are planned relative to above-listed industries and the possibility of attracting them to the Pacific Northwest as power consumers. Aspects of each industry to be studied include production technology, present producers, markets and market outlook, prices, raw materials, transportation and other pertinent factors.

PUBLICATIONS

Surveys are characterized by comprehensive scope and the splendid maps and charts with which a wealth of data are presented. Publications of interest to chemical market researchers include the following, which are available free of charge on request to the Bonneville Power Administration, Portland 8, Oregon.

- Pacific Northwest Opportunities (May 1944)
- Taxation of Industrial Corporations in Washington and Oregon (Sept. 1941)
- Pacific Northwest Mineral Occurrence (July 1947)
- Preliminary Report on the Plastics Industry as Related to Pacific Northwest Development (Nov. 1944)
- Upper and Mid-Columbia Basin Industrial Surveys (October 1942)
- Western Washington Industrial Surveys (September 1943)
- Western Oregon Industrial Surveys (October 1943)
- Columbia River Industrial Site Survey (September 1940; reissued April 1944)

A Series on "The Economic Base for Power Markets" separately covers each of about 20 counties.

A valuable survey "The External Trade of the Pacific Northwest" and a "Supplementary Analysis" were published in 1942 in cooperation with the National Resources Planning Board and the Northwest Regional Council. Based on rail and water freight movements these studies clearly showed the region's surplus of forest,

agricultural and animal products and its deficiency in manufactured products.

In cooperation with the National Resources Planning Board and Northwest Regional Council: The External Trade of the Pacific Northwest (1942) Supplementary Analysis of the External Trade of the Pacific Northwest (1943).

FISH AND WILDLIFE

The Fish and Wildlife Service provides a great deal of specialized information that is of value to process industries which are interested in the fur crop, fish for fertilizer, meal, glue, oil, food, vitamins, and rodent poisons. Established in 1940, this Service consolidates work formerly carried on by the Bureau of Fisheries and the Bureau of Biological Survey and brings the biological sciences to the aid of agriculture, stock raising, fisheries, forestry, and game animals.

The Fish and Wildlife Service has headquarters in the Merchandise Mart, Chicago, and regional offices in Portland, Ore., Albuquerque, Minneapolis, Atlanta, Boston, and Juneau. The Director is Dr. Ira N. Gabrielson.

PUBLICATIONS

The Fish and Wildlife Service publishes several excellent periodical statistical reports dealing with fisheries and fish products. This work is done under the direction of A. W. Anderson, Chief, Division of Commercial Fisheries, Fish and Wildlife Service. All publications listed may be obtained free by writing the Service.

An annotated list of these publications follows:

Current Fishery Trade. — A brief monthly summary of information on landings and receipts of fishery products; production and holdings of frozen and cured fish; production of canned fish, fish oils, fish meals; and production and

(Turn to page 597)

stance, it should be possible to make 50 separate determinations on steel rods in an hour.

Any type of sample can be handled for either qualitative or quantitative analysis. There are numerous factors to be considered before attempting to analyze a sample and some of these will be taken up under quantitative procedures. The following are some of the normal types of samples encountered: crude oils, used oils, oil additives, sucker rods or any metallic sample, corrosion products, geological samples, water samples, catalyst materials, flue dusts, plants, paints, and process solutions.

Samples sent to the spectroscopic laboratory must be representative of the material being analyzed. A dry sample is ground in a mortar and pestle, liquid or wet samples are evaporated to dryness and thoroughly mixed, oils or greases are heated until they ignite and are permitted to burn. The ash is then ignited at 500° C to burn off volatile and carbonaceous material remaining. Samples containing volatile inorganic compounds are converted to a non-volatile condition or are exposed directly.

Finally the samples are accurately weighed into deep cups drilled in the end of purified graphite rods. The electrode containing the sample is burned by means of a 10 amp., D. C. arc, the light being focussed on the slit of the spectrograph by means of a quartz lens.

The photographic plate is developed for 2 minutes in an agitated constant temperature (70° C) bath using D-19 developer. It is then hardened in a solution of dilute acetic acid and fixed with an acid fixer.

The dry developed plates are placed in a projector and an image of the plate is focussed on the wall. Fig. 2 is a photographic reproduction of a portion of an actual sample plate to give an idea of the appearance of spectra. Plates are read by reference to an iron spectrum placed on each plate and the elements are classified by the reader. Samples subsequently analyzed quantitatively in the chemical

laboratories give checks and help the reader in correctly interpreting the plates. Table I is a typical qualitative analysis.

TABLE I. Qualitative Analysis of an Oil Additive

Concentration Major Constituents	Element
1—10%	Ba, P
0.1—1%	Zn
0.01—0.1%	Si, Fe, Al
<0.01%	Ca, Cu, Na Pb, Sr
	Mg, Sn, Ti Ag, Cr

RESULTS

Many conditions should be satisfied before actually undertaking an analysis. Two of these are reproducibility and accuracy. Results may be quite reproducible without being near the true value. On a comparative basis within a given set of samples reproducibility is most important. Table II gives the reproducibility of a

TABLE II. Reproducibility of Na in Catalyst Materials

Chemical Analyses		Spectroscopic Analyses				
Sample No.		Run No. 1	2	3	4	5
106K	0.11	0.10	0.12	0.11	0.10	0.10
RN-23-25	0.33	0.32	0.35	0.32	0.34	0.35
RN-18-96A	0.14	0.14	0.16	0.13	0.16	0.15
RN-18-96B	0.18	0.19	0.16	0.16	0.20	0.17
RN-18-96C	...	0.20	0.23	0.21	0.22	0.23

few samples with a check against the chemical results (where known) which are assumed here to be the true values. In most instances the reproducibility is quite good. The accuracy seems equally good once standards are procured in which the elemental contents are known. Spectroscopic methods are in general decidedly superior in accuracy to regular routine chemical results in amounts less than 0.10%. They are of equal accuracy in amounts from 0.1 to 1.0% and somewhat less accurate in amounts above 1%. These groupings of accuracy are, however, quite general and should not be taken too seriously until an attempt has actually been made to analyze a sample. There is a trend towards increasing the accuracy in the higher percentage groups

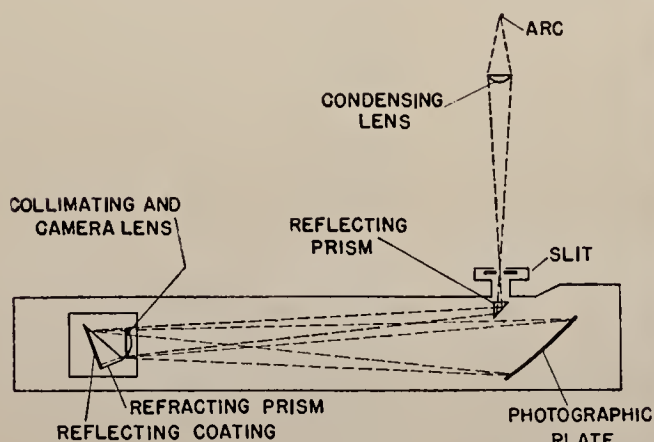
and so make analyses for elements present in higher percentages amenable to spectrographic methods.^{4,5}

There are many methods of making quantitative analyses spectrographically. DC arc excitation can be used, though it usually is not as reproducible as the AC spark. An example, the determination of Na in catalyst materials will make such methods clearer. A sample of catalyst is dried at 500° C and one gram of it thoroughly mixed with exactly 2.2 gms. of purified natural graphite (to act as a conductor, diluent, and briquetting medium), and 0.10 gm. of CuO (to act as an internal standard). The mixture is briquetted and the half inch briquets are excited by means of a 35,000 volt AC spark along with briquets of a set of standards of similar composition but in which the sodium content varies. The photographic plate on which the spectrum lines are recorded is developed, fixed and dried, and a sodium line and a copper line in each sample are measured for their

transmission values. These values are referred to an emulsion calibration curve and final intensity ratios of sodium line to copper line are plotted against percentage composition of the standards. The sodium values are as accurate as chemical analyses and are obtained in one-quarter the time.

ABSORPTION METHOD

In absorption spectroscopy use is made of the differences in light absorption by unlike compounds. One compound may absorb light very strongly in certain wavelength regions, while a second compound will have its regions of absorption which, in general, will not be the same. This, of course, is part of the phenomena



(Courtesy of Bausch & Lomb Co.)

SAMPLE 1

SAMPLE 2

SAMPLE 3

IRON

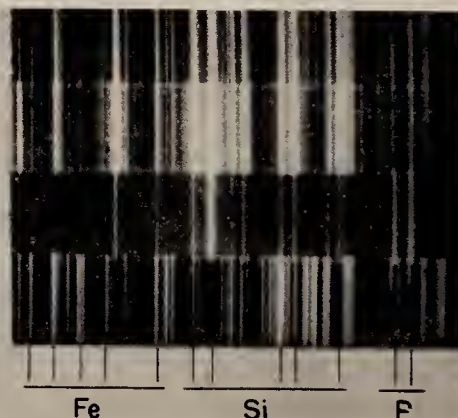


Fig. 1. Schematic diagram of a spectrograph used for emission work.

Fig. 2. Enlarged portion of spectra showing lines due to Fe, Si, and P.

of different compounds having different colors.

A molecule or an ion will, in general, absorb light of a particular wavelength if the energy carried by the individual photons is of a value nearly the same as that needed to excite the ion or molecule from its quantum ground state to a permissible quantum state. The factors which decide what wavelength regions in which a particular compound will absorb are inherent in the disposition of the electrons shared by the atoms and in the formation of the valence bonds. A complete understanding of these factors in terms of a manageable theory is not available at present and many of the applications have been worked out empirically.

In the investigation of the light absorbing properties of a material the gen-

chromium, is converted by a chemical reaction into a highly colored complex such as $\text{CrO}_4^{=}$ and its transmission read at definite wavelengths. Fig. 4 comprises two curves, one of K_2CrO_4 in alkaline solution, the other of $\text{Cu}(\text{NH}_3)_4^{++}$ in alkaline solution. Generally speaking ions are determined colorimetrically by being converted to highly colored ions in a solution of definite pH, their transmission at some previously determined wavelength being measured. This transmission value is then compared with the transmission values of a series of standards containing the ion in varying known concentrations. Numerous technical details must be investigated before such procedures are used. Interfering ions must be removed before making the readings, otherwise the readings obtained will not be truly rep-

were obtained for the compounds in solution using iso-octane as solvent and the dilutions used are shown in the figure. As the absorption cell that was used was only 1 cm. in thickness it is clear that these compounds are very strong absorbers in this region.

Referring to Fig. 5 it is seen that, whereas the curve for benzene has a number of unique features, those for toluene and m-xylene are quite similar. There are, however, enough differences in both intensity and position as regards wavelengths that such data form the basis for analytical work. The exact manner of utilizing the singularities in the absorption spectra of the individual compounds to analyze a mixture for the separate concentrations will not be described here. It is the same in principle as used for the infra-red analyses of multicomponent gas mixtures.^{8, 9}

In the petroleum industry one very useful application of the high ultra-violet absorption by benzene derivatives is the analysis of gasoline fractions for aromatic content. Since the paraffins, mono-olefins, and naphthenes do not absorb light in this region, the absorption found will be due to the aromatics present. If the instrument is properly calibrated the absorption data may be used in calculations which will yield the benzene, toluene, ethyl-benzene, o-xylene, m-xylene, and p-xylene concentrations directly. The accuracy of the method can be judged from Table III,



Fig. 3. National Technical Laboratories quartz spectrophotometer used for absorption spectroscopic studies.

eral procedure is to isolate light of a desired wavelength and to measure what percentage of the radiation the specimen will transmit. For this purpose an instrument such as shown in Fig. 1 may be used. However, in recent years the application of this branch of spectroscopy has increased to the point where it is of great value to have instruments designed especially for the purpose. Cary and Beckman⁶ have described such an instrument, which is now available commercially. One of these instruments with slight modifications is shown in Fig. 3. Here a photoelectric cell is used to measure the light intensity and it is located behind an exit slit, this assembly replacing the photographic plate as an energy registering device. A mechanical system allows the refracting prism to be rotated so that light of the desired wavelength passes through the exit slit. The sample is located between the exit slit and photoelectric cell and means are provided to move the sample in and out of the beam to measure the percentage transmission directly.

OPERATION

Such instruments are used both for the analysis of hydrocarbons and for the analysis of inorganic ions. In the case of the inorganic ions, the ion, such as

representative of the ion being determined. It is necessary to know whether Beer's law is obeyed. If this law is obeyed a plot of extinction against concentration results in a straight line.

RESULTS

Using the general techniques given above it is possible to determine all of the inorganic elements. In fact, books have been published giving details for most of the elements.⁷ Such colorimetric methods are valuable for odd samples for which the spectroscopic methods would not be justified.

The ultra-violet region of the spectrum, which may be roughly defined to lie between 2100Å and 4500Å, is a very fertile one for furnishing analytical methods in the investigation of certain classes of chemically unsaturated compounds. In this region neither paraffins, mono-olefins nor alcohols have any absorption. Aromatics are one class of compounds which do absorb in this region. The benzene ring nucleus is responsible for the absorption and gives rise to a minimum of transmission, the exact amount of transmission being dependent upon the specific derivative. Fig. 5 shows the absorption spectrum in this region of benzene, toluene and m-xylene. The data

TABLE III. Aromatic Analyses

Results for analyses of synthetic blends under routine conditions. S% = % in synthetic as blended, F% = % found in sample by ultra-violet absorption. Δ% = % difference in terms of total sample.

Blend No.	Compound	S%	F%	Δ%
1	benzene	1.0	0.9	-0.1
	toluene	19.0	19.3	+0.3
	total aromatics	20.0	20.2	+0.2
2	benzene	6.4	6.0	-0.4
	toluene	4.0	4.2	+0.2
	total aromatics	10.4	10.2	-0.2
3	benzene	0.5	0.6	+0.1
	toluene	2.0	2.1	+0.1
	ethyl-benzene	0.5	0.3	-0.2
4	total aromatics	3.0	3.0	0.0
	benzene	0.5	0.5	0.0
	toluene	1.5	1.4	-0.1
5	ethyl-benzene	0.2	0.0	-0.2
	total aromatics	2.2	1.9	-0.3
6	toluene	1.0	1.1	+0.1
	ethyl-benzene	8.0	8.1	+0.1
	p-xylene	1.0	1.0	0.0
7	total aromatics	10.0	10.2	+0.2
	ethyl benzene	1.0	1.0	0.0
	o-xylene	1.0	1.0	0.0
8	m-xylene	2.0	2.0	0.0
	p-xylene	6.0	6.1	+0.1
	total aromatics	10.0	10.1	+0.1
9	o-xylene	6.0	5.6	-0.4
	m-xylene	3.0	3.0	0.0
	p-xylene	1.0	1.0	0.0
10	total aromatics	10.0	9.6	-0.4
	o-xylene	4.0	3.6	-0.4
	m-xylene	3.0	3.1	+0.1
11	p-xylene	3.0	3.0	0.0
	total aromatics	10.0	9.7	-0.3

which shows the results between blended composition and observed concentrations on a series of samples examined in a routine manner.

As may be seen from Table III this method yields the concentrations of the individual aromatics with an average error of about 0.2% of total sample. This method has the advantages over the spe-

cific dispersion method of aromatic analyses in that it gives the concentrations of the individual aromatics, it is not necessary to determine bromine numbers or specific gravities and it allows analyses to be made on smaller samples. In general, there is an increase in accuracy, this being dependent upon the amount of care used in each technique. The complete routine analysis of a gasoline cut including preparation of sample, taking the data, making the calculations and reporting the results requires about 50 minutes.

The conjugated diolefin, butadiene, is a hydrocarbon that in the past few years assumed tremendous importance. Doubtlessly the use of this compound will continue in industry operating under peacetime conditions. For the detection and quantitative analysis of butadiene in the presence of mono-olefins and paraffins, ultra-violet absorption spectroscopy affords a very valuable and simple method. Due to the conjugation of its double bonds, this compound absorbs light very strongly in the ultra-violet region of 2300A. Since the mono-olefins and paraffins of similar molecular weight do not absorb in this region, an analysis for butadiene can be obtained directly, giving the concentration with errors of less than 0.1% of total sample. Such analyses can be done with an overall time expenditure of twenty minutes or less, including calculations. Beckman¹⁰ tells of the use of the method for automatic recording. He also tells of the utilization of the method for the automatic control of reflux ratio in plant installations producing butadiene. In this case equipment similar to that seen in Fig. 3 is shown with the addition of suitable electronic and mechanical devices for the utilization of the signals from the spectrophotometer.

Many examples could be listed of groups of chemically unsaturated compounds which are industrially important and for which the analytical problems are easily solved by means of ultra-violet absorption. General rules defining the combinations which can be analyzed by this method are not easily set up. This is because one compound may absorb light with much greater intensity than others occurring in the same process. Styrene, for example, has absorbing powers much greater than ethyl-benzene or the xylenes, although this absorption takes place at different wavelengths. When one compound absorbs so much more strongly than others, the analysis for the weaker ones is made difficult. This difference in absorption can in some cases be turned to good advantage as it makes possible direct analysis of a mixture for the strongly absorbing compound when data are taken at only one wavelength.

The ultra-violet absorption technique is a useful tool in many research problems. Usually when a compound has absorption in this region it may be ascribed to a certain part of the molecule. If the same molecular group occurs in a different com-

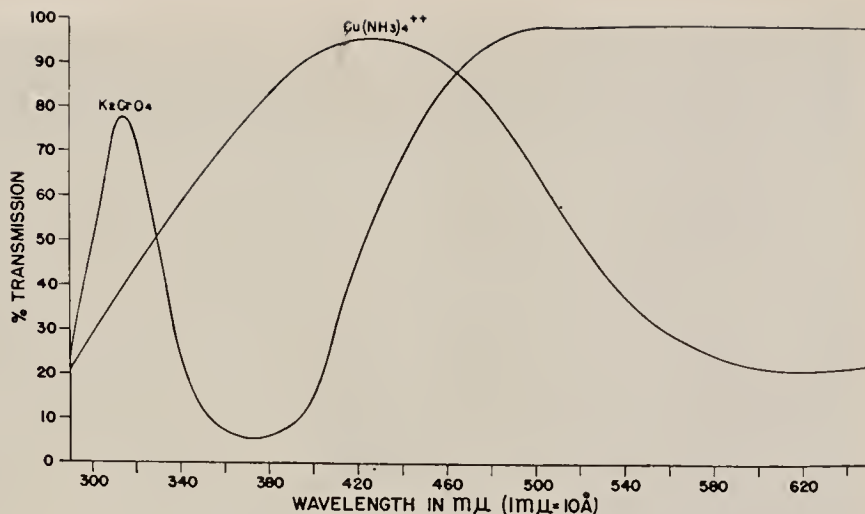


Fig. 4. Absorption spectra for two different species of inorganic ions.

pound, it, too, will have similar absorption properties. A simple example of this effect may be seen in Fig. 5. Here each of the aromatics shown has an absorption band lying between 240 and 280 $m\mu$ ($1 m\mu = 10^{-7}cm, = 10A$) which is due to absorbing powers of the benzene ring nucleus. Brode has tabulated some of the common groups responsible for absorption.¹¹ For example, the carbonyl group, $C=O$, has characteristic absorption around 280 $m\mu$, the mercapto group, $S-H$, around 230 $m\mu$, etc. Since these groups absorb in the same general wavelength region irrespective of the remainder of the molecule, it makes it possible to identify them in compounds whose structures are not completely known. When used in this manner the ultra-violet constitutes a tool of importance in the determination of molecular structure.

Many types of investigations and analyses, both exact and empirical, are possible by use of this technique. It is not exactly a new one in chemical industry, but recent needs associated with the war effort have accelerated the growth and perfections of new applications. Many fields are hardly touched as regards the proper interpretation of the results and many more applications are to be expected.

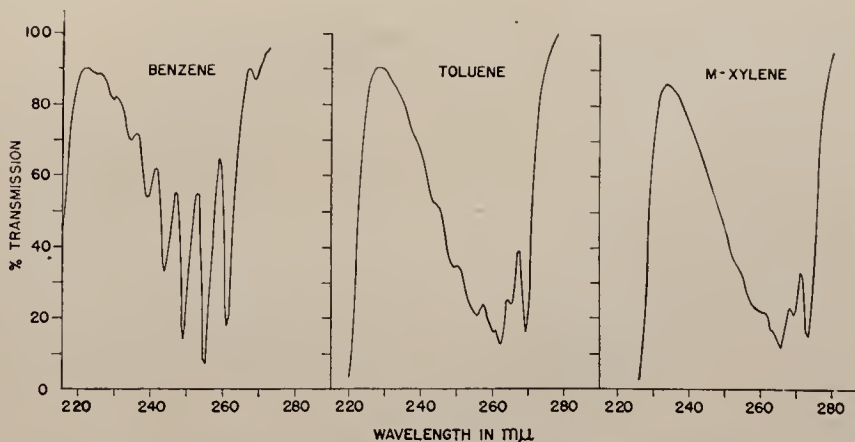


Fig. 5. Absorption spectra in ultra-violet region for three aromatics.

COST

If it is desired to set up an emission spectroscopic laboratory, a sum between \$7,000 and \$10,000 should be set aside for the buying of equipment. This includes the spectrograph, source units, briquetting press, densitometer, projector, developing equipment, etc. For the equipment necessary to do absorption work in the ultra-violet and visible, a minimum of about \$1,800 is needed for equipment. In either activity the hiring of competent technical personnel is very important if the apparatus is to be used on new problems.

BIBLIOGRAPHY

1. W. R. Brode, *Chemical Spectroscopy*, John Wiley & Sons, New York, N. Y., (1943).
2. R. A. Sawyer, *Experimental Spectroscopy*, Prentice-Hall Inc., New York, N. Y., (1944).
3. F. Twyman, *The Spectrochemical Analysis of Metals and Alloys*, Chemical Publishing Co. Inc., New York, N. Y., (1941).
4. J. R. Churchill & R. G. Russell, *Ind. & Eng. Chem., Anal. Ed.* 17, 24, (1945).
5. J. H. Coulliette, *Ibid.* 15, 732, (1943).
6. H. H. Cary & A. O. Beckman, *J. of Optical Society*, 31, 682, (1941).
7. E. B. Sandell, *Colorimetric Determination of Traces of Metals*, Interscience Publishers Inc., New York, N. Y., (1944).
8. Brattain, Rasmussen & Cravath, *J. of Applied Physics*, 14, 418, (1943).
9. N. D. Coggeshall, *Chemical Industries*, 58, 256, (1946).
10. A. O. Beckman, *Petroleum Engineer*, 16, 182, (1945).
11. W. R. Brode, *Op. Cit.*, Chap. VIII.



Agriculture is big business, and like any other business, it stands to benefit from the results of research on its particular problems.



NEW AGRICULTURAL CHEMICALS Combat Pests and Improve Crops

by E. D. WITMAN, Sherwin-Williams Research
Ohio State University Research Foundation
Columbus, Ohio

FOLLOWING IN THE WAKE OF DDT, a host of new chemicals have proved their usefulness in combatting insects and fungus growths, preventing premature drop of fruit crops, killing weeds, defoliation, and other applications where crops are saved or improved, or production expedited. In the face of a world-wide food shortage, these advances take on enhanced significance.

THE RECENT war, fought largely as it was in insect-infested, tropical areas like the South Pacific and North Africa, raised insecticides to a position of vital importance. Many of these insecticides, developed chiefly to combat lice and mosquitoes, are now finding use in agriculture. Awakened interest in agricultural chemicals in general has spurred development of other materials, too, which find special and important applications.

The subject matter in this discussion is divided into three general categories, (1) insecticides, (2) fungicides and (3) specialties. It is the intention of the author to cover only the recent findings and to describe their history, preparation, formulation and general properties.

INSECTICIDES

DDT.—The contraction DDT represents the product of the reaction of chloral and chlorobenzene in the presence of sulfuric acid. This product contains as major constituents two different chemicals, both called dichlorodiphenyltrichloroethane. The major constituent is the *p,p'*-isomer. Its chemical name is 1,1,1-trichloro-2,2-bis(*p*-chlorophenyl)ethane. It occurs in the product to the extent of about 70%. The other, the *o,p'*-isomer, makes up most of the 30% balance. The *p,p'*-isomer is much more insecticidal than the *o,p'*-isomer.

The product was first prepared in Germany about 80 years ago by Zeidler. He

subsequently isolated the pure *p,p'*-isomer and determined it as a pure chemical compound. Only recently, Mueller, of the Geigy Company, discovered and patented its insecticidal properties (U. S. patent 2,057,965).

DDT is manufactured today much the same as it was prepared 80 years ago by Zeidler—from chloral and chlorobenzene in the presence of sulfuric acid.

As mentioned before, the product of this reaction contains two isomers and is known as DDT. The product is generally used without further processing.

The formulation of DDT into insecticides presents quite a problem. DDT as it comes from the chemical process is nearly useless as an insecticide because of its physical properties—gumminess, large irregular particles, etc.

DDT is really our first outstanding synthetic organic insecticide with the necessary requirements of a high order of toxicity to insects, a low order of toxicity to plants and animals, long-lasting effectiveness and good compatibilities in general. Its position as a valuable addition to

Analyses of Mixtures of Light Gases by Infra-Red Absorption

NORMAN D. COGGESHALL AND ELEANOR L. SAIER

Reprinted from JOURNAL OF APPLIED PHYSICS, Vol. 17, No. 6, pp. 450-456, June, 1946



Analyses of Mixtures of Light Gases by Infra-Red Absorption

NORMAN D. COGGESHALL AND ELEANOR L. SAIER

Gulf Research and Development Company, Pittsburgh, Pennsylvania

(Received January 17, 1946)

A discussion is given of the application of infra-red absorption methods of analysis for light gases which do not obey Beer's law of absorption due to pressure broadening. Some of these gases do not obey Beer's law in the pure state or when contaminated by foreign gases. The method of analysis depends upon the nature and intensity of the pressure broadening effect of the different components in the sample upon each other. Data are presented showing the nature of some of these effects and illustrating the accuracy obtainable for certain types of analyses. The instrumentation used in routine gas analyses by infra-red in this laboratory is described.

IN the last few years there has been an intensified application of infra-red absorption spectrometry to problems of chemical analysis.¹⁻⁴ The technique is now being successfully applied to the analysis of mixtures in the gas and liquid phase and to identification and studies of molecular structure for materials in all phases. One application that has been of particular economic importance recently is gas analysis. Brattain, Rasmussen, and Cravath² published what was perhaps the first detailed procedure for multicomponent gas mixtures wherein they were interested in the four-carbon hydrocarbons. The same technique, which is based on the principle that the compounds present obey Beer's law of absorption, may be applied to other gas mixtures. These may be of C₅ hydrocarbons, i.e., pentanes and pentenes as well as many others.

Beer's law of absorption states that

$$I = I_0 e^{-\alpha l p}, \quad (1)$$

where I is the intensity of light of a particular wave-length transmitted by a sample of material, I_0 is the intensity of light of the same wave-length incident upon the sample, α is a constant which depends upon the material in the sample and the wave-length under investigation, l is the thickness of the sample, and p represents the concentration of the material in the sample which in case of gas would be the pressure. The constant α may assume different values depending upon what system of units is used for l and p .

For the successful application of the method of Brattain and others² to multicomponent mixtures, such that there is appreciable overlapping of the absorption bands of the different components, it is very important that each obey Beer's law of absorption. This is true for the mixtures named above as well as for others in both the gas and liquid phase. However, for some of the light gases such as CO, CO₂, SO₂, CH₄, N₂O, HCl, etc., Beer's law is not obeyed and a somewhat different technique must be used. For these gases, the light absorption depends upon the total pressure in the absorption cell as well as the partial pressures of the absorbing materials. For example, a cell, containing 10 cm of Hg pressure of methane alone, will not absorb the same as if the cell had in addition to the same pressure of methane a partial pressure of some gas such as H₂ which does not absorb in the infra-red. More will be said about this later.

This anomalous pressure dependence of the absorption of the light gases has been known for

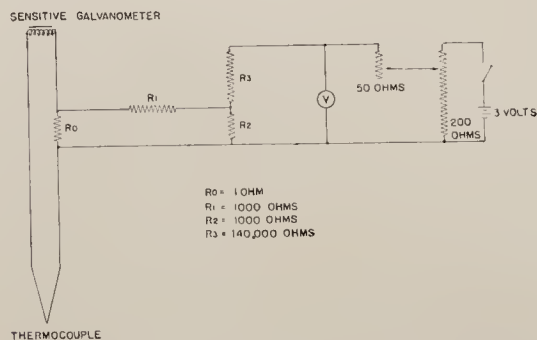


FIG. 1. Null circuit used to measure radiation intensities.

¹ Barnes, Gore, Liddel, and Williams, *Infra-Red Spectroscopy* (Reinhold Publishing Corporation, New York, 1944).

² Brattain, Rasmussen, and Cravath, *J. App. Phys.* **14**, 418 (1943).

³ Norman Wright, *Ind. Eng. Chem. Anal. Ed.* **13**, 1 (1941).

⁴ April-May, 1944 issue of *Transactions of the Faraday Society* devoted to "The Application of Infra-Red Spectra to Chemical Problems."

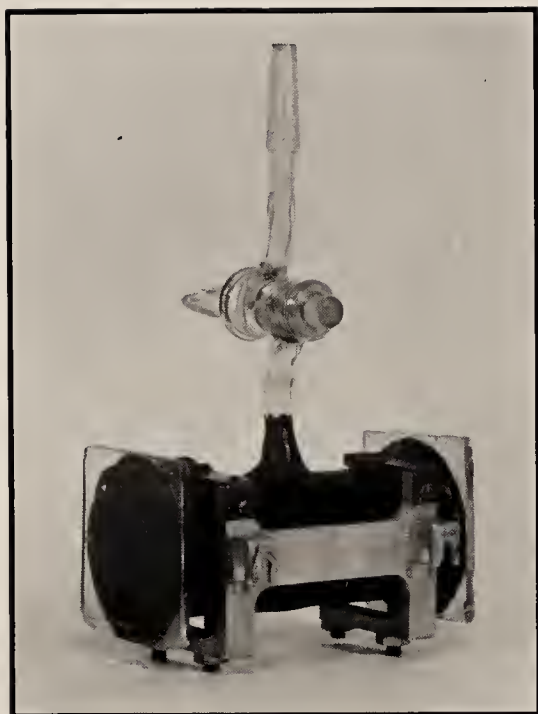


FIG. 2. Absorption cell assembly.

some time and various investigators have studied the effect in different materials.⁵⁻⁹ D. M. Dennison has made a theoretical study of the factors affecting the shape and intensities of infra-red absorption lines.¹⁰ His results are based on the assumption that the principal factor in the broadening of an absorption line is the limitation of the length of wave train a molecule may absorb due to its perturbation by thermal collisions. He found that the absorption depends upon the number of molecules per unit volume, the temperature of the gas, and the effective molecular diameters. Experimental work was done by Cross and Daniels on the absorption of nitrous oxide as influenced by foreign gases. In line with Dennison's results they analyzed their data to obtain "optical" collision diameters for the foreign gases.

⁵ Eva. v. Bahr, *Ann. d. Physik* **29**, 780 (1909); *Physik. Zeits.* **33**, 585 (1910); *Verh. d. D. Phys. Ges.* **15**, 710 (1913).

⁶ G. Hertz, *Verh. d. D. Phys. Ges.* **15**, 673 (1913).

⁷ C. Schafer and F. Matossi, *Das Ultra-Rote Spectrum* (Verlagsbuchhandlung Julius Springer, Berlin, 1930), §30.

⁸ P. C. Cross and F. Daniels, *J. Chem. Phys.* **2**, 6 (1934).

⁹ Other references can be found in article: Nielsen, Thornton, and Dale, *Rev. Mod. Phys.* **16**, 307 (1944).

¹⁰ D. M. Dennison, *Phys. Rev.* **31**, 503 (1928).

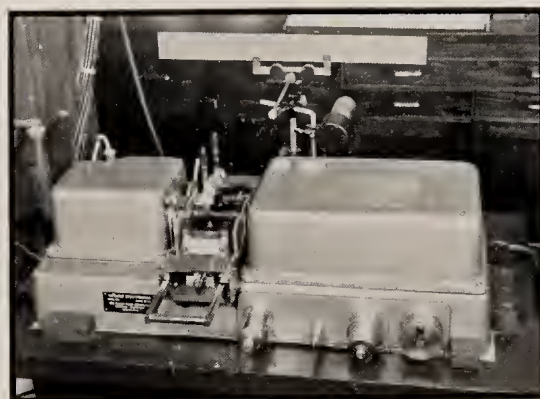


FIG. 3. Infra-red spectrometer used with added cell positioning equipment.

The data given below will illustrate the pressure broadening and how it is encountered in the making of actual analyses for some of the light gases. Several cases, for example, in the petroleum industry wherein it is desirable to make such analyses, are: hydrogen rich gases such as are encountered in hydroforming, flue gas from a catalytic cracking unit, and burn-off gases from catalyst regeneration. Others working in the application of infra-red spectroscopy have doubtlessly encountered the same problems and perhaps evolved essentially the same solution. In that case the material of this article will illustrate the method and apparatus as used by us, the particular procedure, the accuracy obtainable by this procedure, and data of general interest with regards to pressure broadening.

INSTRUMENTAL DETAILS

The infra-red spectrometer used in this work was a Perkin-Elmer Model 12A. The thermo-

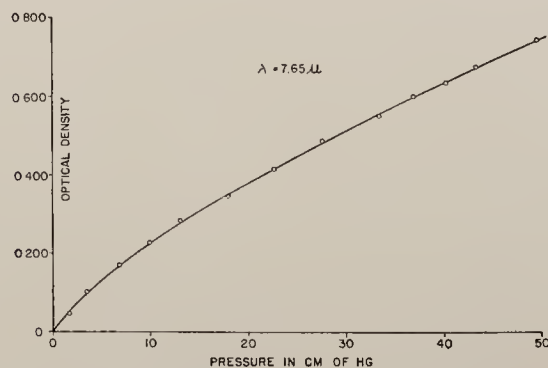


FIG. 4. Optical density vs. pressure for methane.

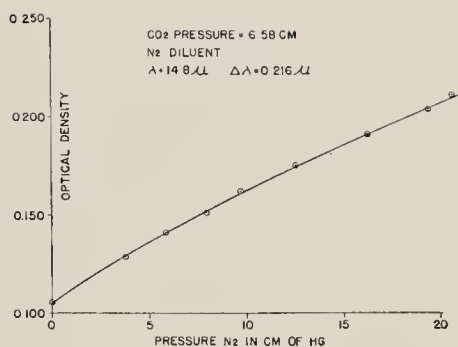


FIG. 5. Influence of N_2 on absorption of constant partial pressure of CO_2 .

couple signals were fed into a Leeds and Northrup, HS No. 2284-6, $0.05 \mu\text{v}/\text{mm}$ sensitivity galvanometer. A null method was used rather than a direct photometric method wherein the galvanometer deflections are read. For this a controlled voltage was fed into the circuit containing the thermocouple and galvanometer in a direction opposite to the voltage signals due to radiation falling on the thermocouple. The controlled voltage was not measured directly but by measuring a large voltage to which it was in constant proportion. The circuit for the null method is to be seen in Fig. 1. Here the bucking voltage originates from the 3-volt battery which is connected directly across a potentiometer which is of 200-ohm resistance. The moving contact on the 200-ohm potentiometer provides a fairly good control but an additional fine control is available through the moving contact on the 50-ohm potentiometer. The resulting voltage tapped off by this variable resistance system is read on the voltmeter which is a Weston, Model 45, and which has 3 volts full scale as one of its ranges.

It is to be noticed that the circuit integral with and to the left of the voltmeter in Fig. 1 is continuous in the sense of no moving or variable contacts. Therefore, the voltage across R_0 is always a constant fraction of that across the voltmeter. If V represents the voltage across the voltmeter and V_0 the impressed voltage across R_0 , we may deduce for the case of balance by simple applications of Ohm's law

$$V_0 = \frac{1}{2}(R_0/R_3)V, \quad (2)$$

when R_1 and R_2 are equal and $R_3 \gg R_1$. With the resistances as indicated on Fig. 1 it is possible

to introduce a bucking voltage across R_0 up to 3.6 microvolts. In operation, when a signal to the thermocouple is to be determined, the mechanical zero for the HS galvanometer is first observed on a ground glass scale with a shutter in the light path and with the potentiometers adjusted to give zero voltage across the voltmeter. When the shutter is removed the potentiometers are adjusted to bring the galvanometer deflection back to the starting point. The voltage appearing on the voltmeter is then read and recorded as representative of the signal to the thermocouple. The system is very reproducible, successive readings giving values which have variations not larger than 0.2 percent. The 3-volt battery is in reality a combination of two Burgess 4F2H batteries connected in parallel for longer life. The batteries, resistances, and potentiometers are all mounted in an iron-walled case. This is important to protect the circuit from magnetic disturbances, which in a network of these impedances can cause serious disturbances.

The infra-red absorption cells used in this work have glass walls, an inside length of 9.5 cm, and have rocksalt windows. They are equipped with a stopcock, an inner part of a ground glass joint, and an exterior aluminum mounting frame. The bodies of the cells were painted black to minimize the amount of radiation of visible wave-lengths which may enter the monochromator chamber. This assembly is shown in Fig. 2. The aluminum frame has adjusting screws which allow the cell to be positioned as desired relative to it. Also the frame is equipped with slotted positioning brackets so that it may be clamped securely in place in the spectrometer. Two absorption cells

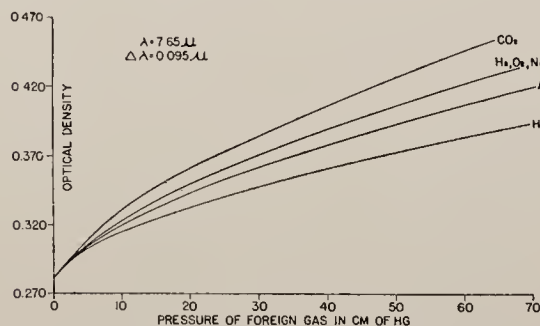


FIG. 6. Influence of gases: He, A, H_2 , O_2 , N_2 , and CO_2 on absorption of constant partial pressure of CH_4 .

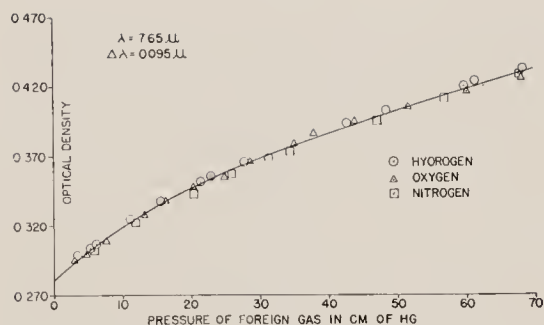


FIG. 7. Detail of influence of H_2 , O_2 , and N_2 on absorption of methane.

are used, one for the sample and one for comparison or incident energy readings. The two cells are mounted on a carriage mechanism which moves in such a manner that either cell may be moved into the optical path.

The instrument with the cell moving carriage with cells in place can be seen in Fig. 3. The carriage is equipped with a bar which the operator can use to position the cells. Adjustable stops insure that the cells always arrive in the same position in the light path. To remove the cells all that is necessary is to loosen two thumb-screws. The cells are evacuated and filled to measured pressures on a gas handling system separate from the instrument. Connected permanently to the thermocouple case in the instrument is a small mercury diffusion pump which is operated periodically to maintain a good vacuum in the presence of the radiation receiver. The apparatus here has been in use for some time for the analyses to be described as well as in the routine analysis of mixtures of the seven common C_4 hydrocarbons. For this, as well as for the present application, it has been very satisfactory and allows considerable speed of data taking. When it is desired to change the pressure in the absorption cell it is merely removed and engaged by means of its standard taper ground glass joint, into a gas handling system designed specifically for handling of routine samples.

In making blends and calibration mixtures for the analyses to be described as well as for other work of this type, it is important that the different components be thoroughly mixed. If the total pressure of the mixture in the absorption cell did not exceed 25 cm of Hg it was mixed in a separate, constant volume chamber.

This chamber was equipped with a thin steel diaphragm which is moved back and forth to mix the gases by means of exterior magnets. When the total pressure of the mixture in the cell exceeded 25 cm of Hg the mixing was done in the absorption cell itself. This was possible as the cell was equipped with a thin steel vane bent to fit the inside curvature of the cell. When the cell was in the operating position the vane lay flat against the bottom, out of the optical path. Mechanical motion of the cell such as shaking or rotating caused the vane to move back and forth, thoroughly mixing the gases.

DATA, CALIBRATION, AND PROCEDURE

For a gas obeying Beer's law a straight line curve is obtained when the observed optical density D ($D = \log I_0/I$) is plotted as a function of the pressure of the gas in the absorption cell. As stated above, some of the light gases do not obey Beer's law and data illustrating this may be seen in some of the following figures. In Fig. 4 is seen a graph of the optical density plotted against pressure for methane alone. As may be noticed, it is far from a straight line. It will be observed shortly that the general appearance of this plot is similar to those obtained when a constant pressure of methane is used and the partial pressure of a non-absorbing foreign gas is varied. In Fig. 5 may be seen a curve for the optical density for CO_2 plotted against partial pressure of added N_2 . It is observable that the effect of the N_2 is to increase the absorption very greatly. All the non-absorbing gases used were tested for absorption at the wave-lengths used. In each case they showed zero absorption.

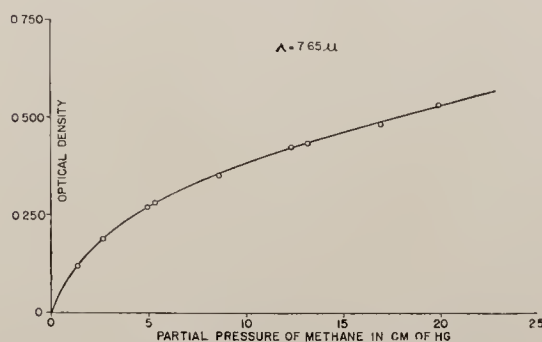


FIG. 8. Calibration curve constructed for analysis for methane.

Figure 6 shows the effect of various foreign gases on the absorption due to methane. The graphs shown in this figure were obtained by drawing smooth curves through the data obtained for each type of foreign gas. The amount of scattering of the data about the curve in each case is about the same as will be seen in Fig. 7. Here the ordinate represents the observed

TABLE I. Results for synthetic samples for methane analysis.

Sample No.	% CH ₄ (synthetic)	% CH ₄ (observed)	$\Delta\%$	Nature of remainder of sample
1	14.5	14.7	0.2	48% H ₂ ; 52% N ₂
2	7.6	7.7	0.1	N ₂
3	6.00	6.05	0.05	33% H ₂ ; 67% O ₂
4	22.5	22.3	0.2	O ₂
5	4.90	4.95	0.05	Air
6	3.71	3.76	0.05	H ₂
7	1.29	1.36	0.07	Air
8	0.83	0.85	0.02	3.9% Air; 96.1% H ₂

optical density and the abscissa represents the partial pressure of the foreign gas added. The data were all taken at the wave-length $\lambda = 7.65 \mu$ where methane has its strongest absorption. The slits were used at a setting which gave a spectral slit width of 0.095μ at this point. The partial pressure of methane was always constant, being 13.15 cm of Hg. The foreign gases added, namely, helium, argon, oxygen, nitrogen, hydrogen, and carbon dioxide, have no infra-red absorption at this wave-length and the large change in optical density produced is a manifestation of the pressure broadening effect mentioned earlier. It is to be noticed that the effects of the various gases are different, some of them being responsible for a greater increase in optical density than others. A study of these data in terms of the pressure broadening theory of Dennison and others has been made.¹¹ In Fig. 6 the effect due to nitrogen, hydrogen, or oxygen is shown as one curve; Fig. 7 shows in more detail the effects of these latter gases.

For the analyses in which we are interested here Fig. 7 is of primary importance. This shows that the effects of hydrogen, nitrogen, and oxygen as added gases are nearly the same. Thus it is possible to construct a single empirical calibration curve which will serve for the analysis of

¹¹ N. D. Coggeshall and E. L. Saier, *Bull. Am. Phys. Soc.* **21**, 17 (1946).

methane in the presence of any one or mixture of the three. This is important as the off gases for which the method is used vary with regards to the relative concentrations of H₂, N₂, and O₂.

Figure 8 shows the calibration curve constructed for this analysis. For every determination the total pressure in the absorption cell was the same, i.e., 80 cm of Hg. The points were obtained by blending known amounts of methane and hydrogen together, admitting to the cell, adjusting the pressure to 80 cm, and determining the optical density. Figure 8, therefore, represents the measured optical density *versus* partial pressure of methane, the total cell pressure being constant.

With this curve the actual analysis of sample consists only of the steps of: admitting the sample into the cell to the pressure of 80 cm, determining the optical density, and from the curve reading off the partial pressure. Table I gives some results for a series of synthetic samples analyzed by means of the previously constructed calibration curve. The table shows the percent of methane as blended, the percent as determined by the analysis, the nature of the remainder of the sample, and the percent difference in terms of total sample between the synthetic and observed concentrations. The table not only illustrates the obtainable accuracy but also shows it to be independent of the nature of the remainder of the sample. Hundreds of samples have been analyzed for methane by this method and the results at all times have been satisfactory. The time required for a complete analysis, including introducing the sample, taking the data, and making the calculations, is about 15 minutes under routine conditions.

An analysis somewhat similar to the one just

TABLE II. Composition of blends used to construct calibration curves for flue gas analyses.

Blend No.	% CO ₂	% SO ₂	% CO	% Air
1	9.5	2.0	3.4	85.1
2	12.7	2.0	6.6	78.7
3	3.9	1.7	8.7	85.7
4	2.5	1.1	10.8	85.6
5	1.6	0.7	10.9	86.8
6	7.6	1.3	4.7	86.4
7	7.0	0.4	1.4	91.2
8	4.9	1.2	2.9	91.0
9	6.5	0.6	1.3	91.6

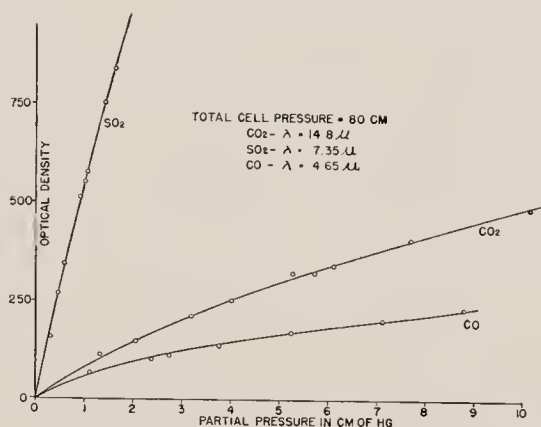


FIG. 9. Calibration curves for analysis of flue gas for CO_2 , SO_2 , and CO .

described, but involving more components, is the analysis of flue gases and burn-out gases from catalyst regeneration for CO_2 , CO , and SO_2 . In this case also the remainder of the samples varies, containing different amounts of O_2 , H_2 , and N_2 . Since for these samples the major part is generally a mixture of these three and since the concentration of any one of the three gases, CO , CO_2 , or SO_2 , is generally less than 10 percent it was decided to try the same method as used for the methane analysis.

A calibration curve for each of the three compounds CO , CO_2 , and SO_2 was constructed as was done for methane. In constructing these, blends of the three gases and of air were made and examined as before. The wave-length used for CO_2 was 14.8μ , for SO_2 it was 7.35μ , and for CO it was 4.65μ . Each gas has a maximum of absorption at about these wave-lengths and there is no overlapping between their absorption bands at these points. As before the blend was admitted to the absorption cell to the same pressure each time, this being 80 cm of Hg. In making the blends, care was taken to see that the concentrations of CO , CO_2 , and SO_2 were randomly distributed, that is to say: the concentration of any one of the three in any one of the blends was independent of the concentration of the other two. Table II gives the concentrations of the blends used for constructing the calibration curves.

The calibration curves are shown in Fig. 9. Here the uniformity and smoothness of the curves attests to the independence of the ab-


sorption of the three gases. In this figure the optical density observed at each wave-length was plotted against the partial pressure of the gas which absorbed at that point. The slits were set to a spectral slit width of 0.216μ for readings of 14.8μ ; 0.117μ for readings of 7.35μ ; and 0.085μ for readings of 4.65μ . Smaller slit widths could be used but the ones employed allowed the Globar element to be operated with about 150-watt supplied power. At this power level the life of each element is quite long. The shape of the curves indicates the deviations from Beer's law to be the same type as for methane.

Although the smoothness of the calibration curves is a manifestation of the internal consistency of the data, the usefulness and accuracy of the curves were tested by a further set of synthetic blends. The results are shown in Table III. Here it may be seen that the average error in terms of total sample is about 0.1 percent. The accuracy for CO is somewhat surprising in view of the flatness of the calibration curve for this compound.

As flue gas analyses may be used for process

TABLE III. Comparison between blended synthetic samples and concentrations measured by infra-red absorption for flue gas analyses.

Sample No.	Compound	Synthetic	Observed	% Dev.
1	CO_2	10.5	10.4	0.1
	SO_2	2.1	2.3	0.2
	CO	4.2	3.9	0.3
2	CO_2	6.7	6.9	0.2
	SO_2	1.4	1.4	0.0
	CO	9.4	9.5	0.1
3	CO_2	6.2	6.2	0.0
	SO_2	1.9	1.9	0.0
	CO	4.0	4.1	0.1
4	CO_2	4.0	4.2	0.2
	SO_2	1.3	1.3	0.0
	CO	2.6	2.5	0.1
5	CO_2	2.7	2.8	0.1
	SO_2	1.0	1.0	0.0
	CO	5.2	4.8	0.4
6	CO_2	1.7	1.9	0.2
	SO_2	0.6	0.6	0.0
	CO	3.4	3.1	0.3
7	CO_2	7.0	7.1	0.1
	SO_2	1.9	1.9	0.0
	CO	6.1	6.3	0.2
8	CO_2	4.4	4.6	0.2
	SO_2	1.2	1.2	0.0
	CO	4.0	3.9	0.1



control it is important that the complete procedure be as simple as possible. This is important since it allows them to be done on night shifts by relatively untrained personnel. The equipment and method as described above have been used for process control analysis for a fluid catalytic cracking unit for some time and hundreds of samples have been handled for this purpose. One operator is sufficient to carry out all steps and the complete analysis, including calculations, can

be done on a routine basis in about 35 minutes or less. This includes duplicate determinations of the optical densities at each wave-length value.

The authors are indebted to Mr. N. F. Kerr for aid in developing some of the equipment used, to Dr. Morris Muskat for various suggestions in the application of infra-red absorption methods, and to Dr. Paul D. Foote, Executive Vice-President of Gulf Research and Development Company for permission to publish this material.



LANCASTER PRESS, INC., LANCASTER, PA.

Infra-Red Absorption Cell for Liquids

NORMAN D. COGGESHALL

Reprinted from THE REVIEW OF SCIENTIFIC INSTRUMENTS, Vol. 17, No. 9, pp. 343-344, September, 1946

Infra-Red Absorption Cell for Liquids

NORMAN D. COGGESHALL
Gulf Research & Development Company,
Pittsburgh, Pennsylvania
 July 16, 1946

IN the past few years there have been described a number of absorption cells for the infra-red study and analysis of liquids.¹⁻⁴ Certain of these and variations of them have been used in this laboratory with varying degrees of success, depending upon the particular application. However, in each case certain shortcomings were observed and as a result the need was felt for a cell of greater general practicality. The characteristics desired for the cell were: ease and simplicity of construction, ruggedness, interchangeability of parts, complete tightness against loss of sample by evaporation, ease of cleaning, usefulness and facility of filling for both liquids of low and high viscosity, and ease of repairing and modification.

The design details of the cell may be seen in Fig. 1. Here 1 and 2 represent the two rocksalt plates which form the two windows. The amalgamated lead shim 3 separates the two salt plates by a pre-selected distance. This shim is continuous in its own plane, so that the liquid cannot escape in any direction between the plates. Units 4 and 7 together with bolts 8 provide pressure on the salt plates. This pressure is transmitted to the shim 3 to make a vapor tight seal at all points of contact with the salt plates. There are two each of the units 4 and 7 for each cell, these being located at opposite ends of the lead shim as shown in the upper view of Fig. 1. Liquid is introduced by means of the needle valve arrangement consisting of 4 and 5 of which the latter is the needle.

If it is intended to examine a liquid of high viscosity in a cell of a thickness of the order of 0.006", there may be difficulty in getting the material in the cell. This is not difficult if the two plates forming the cell windows can be separated and a drop of the fluid placed between them. In separating them, however, the seal between the shim and the face of the plate is broken, and this is undesirable if it is desired to later use the same cell for rather volatile liquids. In order to facilitate the introduction of such samples and also furnish a vapor tight seal, the needle valve arrangement was used. The needle 5 is machined so that there is a tolerance of only 0.0001" to 0.0004" between the shank of the needle and the hole in 4 leading directly to the valve seat. Thus when the sample is intro-

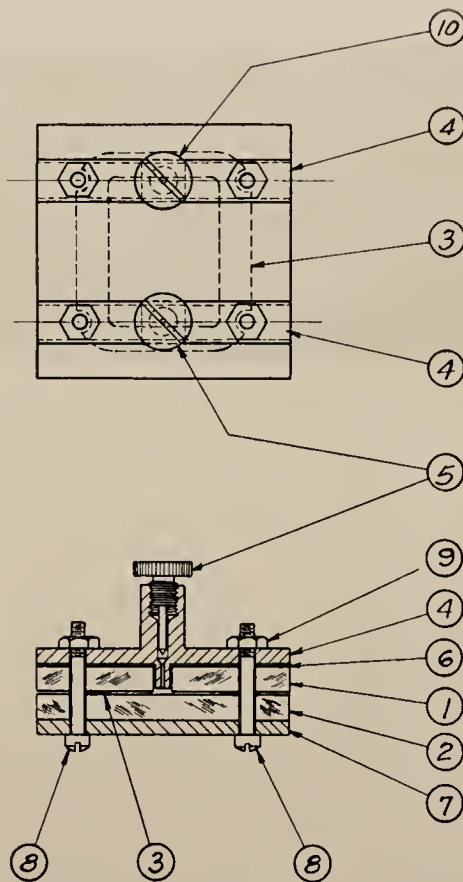


FIG. 1. Constructional details for infra-red absorption cell for liquids.

duced in the opening in 4 and the needle inserted, it acts as a fairly close fitting piston and pushes the fluid down into the region between the salt plates. The needle valve arrangement at the opposite end of the shim, namely 10 and 4 is different in that the corresponding tolerance in the

needle 10 is large enough that when it is screwed down it will not build up a back pressure which might break the cell windows. For easy identification the needles with small tolerances are stamped with a *T* (tight) on their top surface and the ones with larger tolerances are stamped with an *L* (loose). A photograph of the assembled cell can be seen in Fig. 2.

Amalgamated lead shims 6, of about 0.012" thickness, are used between the valve bodies 4 and the salt plate 1. These shims 6, the shim 3, and the needle valves make a vapor tight cell which will hold quite volatile liquids for long periods of time, of the order of weeks. The cell is easily flushed and cleaned by introducing solvent in one valve seat and applying a vacuum to the other. It is to be noted that no organic materials such as waxes, cement, or rubber are used in the construction.

The holes in the salt plates for the machine screws 8 and for the valve bodies 4 can be drilled using a drilling jig. When this is done, a series of cells constructed in this

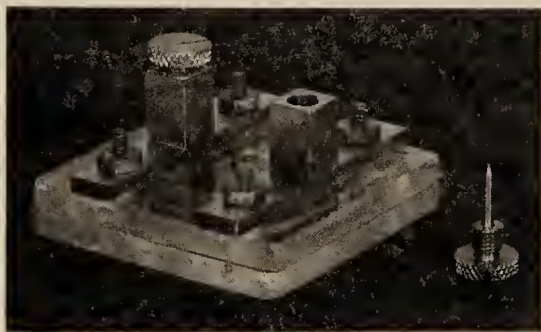


FIG. 2. Photograph of assembled cell.

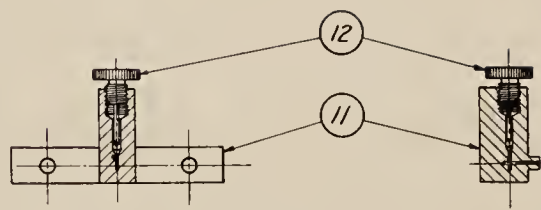


FIG. 3. Alternative type of valve body.

manner have completely interchangeable parts. This is of utility for making rapid repair jobs. The machine screws 8 can be utilized for anchoring the cells in a mechanically reproducible position in the instrument. The shims 3 are punched from rolled lead strips by means of a special punch built for the purpose. The valve bodies and needles can be made from a variety of materials. A number are in use here which are of stainless steel, the body parts being of type 303 and the needles of type 416.

An alternative type of valve body is also in use and the constructional details of this may be seen in Fig. 3. For this type the needle is parallel rather than perpendicular to the cell faces when in use. All shims, machine screws, and salt plates usable with one type can be used with the other.

This cell has been very satisfactory in work in which relatively untrained personnel have been extensively used. No special skills are needed to construct or repair the cell, and it is rugged and dependable. A number of them have been in service here for well over a year and are all in good condition.

¹ L. Gildart and N. Wright, *Rev. Sci. Inst.* **12**, 204 (1941).

² D. C. Smith and E. C. Miller, *J. Opt. Soc. Am.* **34**, 130 (1944).

³ R. R. Gordon and H. Powell, *J. Sci. Inst.* **22**, 12 (1945).

⁴ D. L. Fry, R. E. Nusbaum, and H. M. Randal, *J. App. Phys.* **17**, 150 (1946).

LANCASTER PRESS, INC., LANCASTER, PA.

The Paths of Ions and Electrons in Non-Uniform Crossed Electric
and Magnetic Fields

NORMAN D. COGGESHALL

Reprinted from THE PHYSICAL REVIEW, Vol. 70, Nos. 5 and 6, pp. 270-280, September 1 and 15, 1946

The Paths of Ions and Electrons in Non-Uniform Crossed Electric and Magnetic Fields*

NORMAN D. COGGESHALL

Gulf Research and Development Company, Pittsburgh, Pennsylvania

(Received December 8, 1945)

The integration of the force equations for a charged particle moving in the presence of particular types of crossed, non-uniform, electric, and magnetic fields is shown to be possible in a very simple manner. The cases which admit of the integration are those such that: the magnetic field is a function of only one coordinate (either Cartesian or the radius vector in a polar system); the electric field is a function of only one coordinate which for any particular case is the same coordinate with which the magnetic field varies; the electric field has a component only in the direction of the variable with which it varies; and the two fields are orthogonal. Since these conditions, in most cases, are only met on a median plane symmetrically situated relative to magnetic pole faces and electrostatic electrodes, the calculations refer to the motion in this plane. The equations are solved and discussions made of the orbits for several different field arrangements and for one a new type of perfect focusing. The method can be used with numerical integration when the analytical difficulties are too great or when the fields are only known empirically.

INTRODUCTION

THE integration of the Lorentz force equation for charged particles moving in the presence of certain types of non-uniform magnetic fields has been reported earlier.¹ The cases dealt with were those such that the magnetic field varied as a function of one coordinate only, either Cartesian or the radius in cylindrical or polar coordinates; the motion of the charged particles was in a plane perpendicular to the magnetic field (this in some cases restricts the motion to the median plane between the pole faces of a magnet or electromagnet); and there was no electric field present. This integration was of such a nature that it could be done analytically if the functions were simple enough

or, if not, it could always be done numerically to as fine an accuracy as desired. Furthermore, for cases where the magnetic field was known only experimentally, the integration could be done numerically to an accuracy equal to that of the data. Several cases of focusing were reported, some of which do not correspond to anything obtainable with uniform fields.

In the present paper the method of integration has been extended to cover certain cases of combined magnetic and electric fields which may or may not be uniform. The restrictions are: The magnetic field is constant or is a function of only one coordinate (either Cartesian or the radius vector in spherical or cylindrical coordinates); the electric field is constant or a function of only one coordinate which for any particular crossed field arrangement is the same coordinate with which the magnetic field varies; the electric and magnetic fields are perpendicular to each

* An abstract of a preliminary report is given in *Phys. Rev.* **68**, 98 (1945).

¹ N. D. Coggeshall and M. Muskat, *Phys. Rev.* **66**, 187 (1944).

other; and the electric field has a component only in the direction of the variable with which it varies. A simple example of a crossed field arrangement which meets the above requirements is afforded by a cylindrical condenser located in the center of a long solenoid and coaxial with it. Here the magnetic field is along the length of the solenoid and varies only with the cylindrical radius measured from the center; the electric field between the condenser electrodes is perpendicular to the magnetic field and varies only with the same radius. Orbits for this and other combinations will be discussed later. Some of these have appeared in the literature earlier but using different methods of calculations, usually based on approximations.

GENERAL THEORY

When a charged particle moves in the presence of both an electric and magnetic field the force it experiences is given by:

$$\mathbf{F} = e\mathbf{E} + e\mathbf{v} \times \mathbf{H}/c, \quad (1)$$

where e is the charge of the particle in e.s.u., c is the velocity of light in cm/sec., and v is the velocity of the particle in cm/sec.

If the electric field is a function of only one Cartesian coordinate, let us say x , and has only a component parallel to the x axis we have a kinetic energy equation:

$$\frac{1}{2}m(\dot{x}^2 + \dot{y}^2 + \dot{z}^2) = \frac{1}{2}mv_0^2 + e \int_{x_0}^x E(x) dx,$$

where v_0 is the initial velocity of the particle at a value of $x = x_0$. If the magnetic field is in the z direction, the component of the velocity in the z direction is constant and we may use instead of the above equation the following one:

$$\dot{x}^2 + \dot{y}^2 = \frac{2eV_0}{m} + \frac{2e}{m} \int_{x_0}^x E(x) dx, \quad (2)$$

where V_0 represents an initial kinetic energy expressed as potential.

In view of the special conditions named above Eq. (1) may be written as:

$$\ddot{y} = (e/mc)H\dot{x}, \quad (3)$$

$$\ddot{x} = eE/m - (e/mc)H\dot{y}. \quad (4)$$

If we define a function $f(x)$ as:

$$f(x) = \int_{x_0}^x H(x) dx + \bar{c}, \quad (5)$$

where \bar{c} is a constant of integration, we may integrate Eq. (3) to obtain:

$$\dot{y} = (e/mc)f(x). \quad (6)$$

Substituting Eq. (6) in Eq. (2) and solving for the ratio of the velocity components we obtain:

$$\frac{dy}{dx} = \pm \frac{f(x)}{[hV_0 + hV(x) - f^2(x)]^{1/2}}, \quad (7)$$

where

$$V(x) = \int_{x_0}^x E(x) dx$$

and

$$h = 2mc^2/e.$$

If the electric field is everywhere zero, Eq. (7) becomes just the equation obtained in the earlier paper¹ in which the paths of charged particles in non-uniform magnetic fields were considered.

It is to be noticed that Eq. (7) contains three constants which are effective in characterizing the orbits, i.e., \bar{c} , h , and V_0 . The constant \bar{c} is associated with the initial slope of the orbit as it may be seen that, for a group of orbits of charged particles of the same mass and of the same initial kinetic energy, the only difference in Eq. (6) for the different ones will be a variation in the value of \bar{c} . From their definitions, h and V_0 obviously specify the mass and initial energy of the charged particle.

The above named constants completely define an orbit and from them certain information as to its extension may be obtained without integrating Eq. (7). Since the terms in Eq. (7) must be real, we have the extension of the orbit limited by:

$$hV_0 + hV(x) - f^2(x) \geq 0.$$

If for a given set of constants the equation:

$$hV_0 + hV(x) - f^2(x) = 0, \quad (8)$$

has only one real root the orbit may extend to either positive or negative infinity in the x direction whereas if it contains two real roots the orbit may be limited in extension in the x direction. In the latter case the roots of Eq. (8)

may represent an x_{\max} and an x_{\min} as for these values $dy/dx = \pm \infty$.

Since the right-hand side of Eq. (7) is a function of x only, the integration of it to obtain the orbit in terms of y as a function of x is always possible, if not analytically, at least numerically. It is to be further noted that in case the magnetic field variation is known only experimentally or if the function defining $H(x)$ is too difficult, the integration involved in Eq. (5) may be done numerically with a subsequent numerical integration of Eq. (7).

If the electric field is such that it varies only with the radius vector r in cylindrical coordinates and has a component only in this direction, the kinetic energy equation may be written as:

$$\dot{r}^2 + (r\dot{\theta})^2 = \frac{2eV_0}{m} + \frac{2e}{m} \int_{r_0}^r E(r) dr. \quad (9)$$

If in addition the magnetic field has only a component in the z direction and if it varies only as a function of r , the force equations can be written as:

$$\ddot{r} - r\dot{\theta}^2 = eE - (e/mc)Hr\dot{\theta}, \quad (10)$$

$$\frac{1}{r} \frac{d}{dt}(r^2\dot{\theta}) = (e/mc)H\dot{r}. \quad (11)$$

If we at this time define a function $g(r)$ by:

$$g(r) = \frac{1}{r} \int_{r_0}^r H(r) r dr + \frac{\bar{c}}{r}, \quad (12)$$

\bar{c} again being a constant of integration, we may integrate Eq. (11) to get:

$$\dot{\theta} = -\frac{1}{r} \frac{e}{mc} g(r).$$

Substituting this result in Eq. (9) and solving for the ratio of the time derivatives we obtain:

$$\frac{d\dot{\theta}}{dr} = \pm \frac{g(r)}{r[hV_0 + hV(r) - g^2(r)]^{1/2}}, \quad (13)$$

where h has the same meaning as before and,

$$V(r) = \int_{r_0}^r E(r) dr.$$

Equation (13), for cylindrical coordinates, is analogous to Eq. (7) for Cartesian coordinates and here also information as to extension of the orbits is obtainable. The orbits may extend to $r = +\infty$ or lie between definite values of r depending upon whether the equation:

$$hV_0 + hV(r) - g^2(r) = 0 \quad (14)$$

has one or two real roots. Here again it is to be noticed that the integration necessary to obtain any orbit is always possible at least numerically if not analytically. This follows as the integration in Eq. (12) can be done numerically if necessary with a subsequent numerical integration of Eq. (13).

Since for free space

$$\text{div } H = 0 \quad \text{and} \quad \text{div } E = 0,$$

it is not possible, except for a few special cases, to obtain crossed fields that satisfy the conditions named above in a three-dimensional region. Usually the conditions of orthogonality and functional variation necessary for the above integrations exist only on a median plane which may be symmetrically located relative to magnetic pole faces and properly located relative to electrodes supplying an electrostatic field. In the development of Eqs. (7) and (13) it was assumed that the motion is in the median plane and that $\dot{z} = 0$. If $\dot{z} \neq 0$, Eqs. (7) and (13) will give the projection of the orbit on the same plane if the required field conditions exist in a three-dimensional region. If the field conditions are satisfied only on the median plane and $\dot{z} \neq 0$, Eqs. (7) and (13) will give an approximate representation of the projection of the orbit onto this plane in a region around the point at which the orbit crosses the plane.

As was seen in the earlier paper¹ and as will be seen later in this one, there are many cases of electron and ion orbits which are spatially periodic. This periodicity, or wave-length, is of great interest in focusing applications. The wave-length will depend upon the constants \bar{c} , h , and V_0 and sometimes upon others which are used in specifying the functional variation of E and H . In a mass spectrometer use may be made of the periodicity by placing the ion source and ion collector in the proper geometrical arrangement

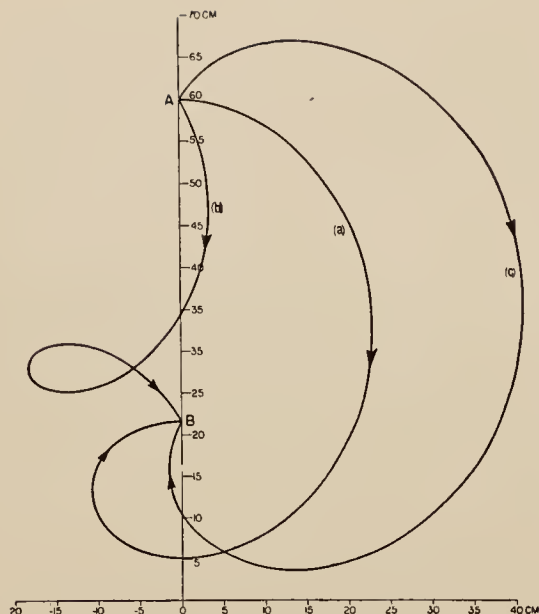


FIG. 1. Typical cycloidal orbits for case of E and H constant in Cartesian coordinates. $H_0 = 1500$ gauss, $E_0 = 30$ volts per cm, $V_0 = 600$ volts, $M = 44$, (a) $\bar{c} = 0$, (b) $\bar{c} = 2.03 \times 10^4$, (c) $\bar{c} = -2.03 \times 10^4$.

and with a certain distance of separation between them. If then the fields can be varied in intensity so as to give ions of a particular mass an orbit wave-length equal to this separation, they will enter the collector. The design of an ion source for a particular field arrangement may depend upon the manner in which the orbit wave-length depends upon the parameters associated with the ion source. If the spatial period or wave-length λ is independent of the parameter \bar{c} but is a function of the initial energy V_0 the ion source must be carefully designed to yield as nearly monoenergetic ions as possible. If the period is independent of the initial energy V_0 but depends upon the starting direction parameter \bar{c} the ion source must have a precise slit system to produce a parallel beam of ions. Examples of the different manners in which the wave-length depends upon the parameters will be seen below. Considerations of symmetry lead to the fact that if the orbits are periodic then the solution of Eq. (7) gives x implicitly as a periodic function of y or the solution of Eq. (13) gives r implicitly as a periodic function of θ . Since the integrand is either a function of x or r ,

the direct deduction of the type of periodicity and the functional dependence on the parameters poses a mathematical problem of some interest. If this were possible it would allow the focusing properties of certain field arrangements to be obtained without the integration of Eq. (7) or Eq. (13). This would be valuable as a number of arrangements of physical interest do not give integrals which are in the form of a finite number of terms. Also in cases such as this, numerical integration will not lead to complete conclusions as to the wave-lengths of the orbits and their dependence on the various parameters.

Let us suppose it is desired to find fields such that a pre-selected type of orbit is obtained. Theoretically this should be possible if for the chosen orbit dy/dx is a function of x alone or if $d\theta/dr$ is a function of r alone. If either the electric or the magnetic field is chosen then substitution in Eq. (7) or (13) will yield the other. Only in special cases would it be possible to calculate fields which would produce a pre-selected family of orbits. This is true as only in special cases will the parameter which defines the family of orbits enter into the equations in the same manner as one of the above named parameters, i.e., h , V_0 , E_0 , H_0 , \bar{c} .

SPECIFIC EXAMPLES

(A) Constant Electric and Magnetic Fields

The orbits and their properties for this case, deduced by other means, have been known for some time^{2,3} and an instrument has been built which utilized them.³ This treatment therefore produces no essentially new physical aspects but is included as it allows a more direct approach to calculations attendant to the orbits and it illustrates the application of the method. If we designate the constant electric and magnetic fields by E_0 and H_0 the differential equation for the orbit is:

$$\frac{dy}{dx} = \pm \frac{(H_0 x + \bar{c})}{[hV_0 + hE_0 x - (H_0 x + \bar{c})^2]^{\frac{1}{2}}}. \quad (15)$$

² Cf. Page and Adams, *Principles of Electricity* (D. Van Nostrand Company, Inc., New York), Chap. VIII.

³ W. Bleakney and J. A. Hipple, *Phys. Rev.* **53**, 521 (1938).

This may be readily integrated to yield:

$$y = \pm \frac{1}{H_0} \left\{ [(hV_0 - \tilde{c}^2) + (hE_0 - 2H_0\tilde{c})x - H_0^2x^2]^{\frac{1}{2}} - \frac{hE_0}{2H_0} \sin^{-1} \left(\frac{2H_0^2x + 2H_0\tilde{c} - hE_0}{[h^2E_0^2 + 4hH_0^2V_0 - 4hE_0H_0\tilde{c}]^{\frac{1}{2}}} \right) \right\} + F, \quad (16)$$

F =constant defining position in x, y plane. Equation (16) is that of a cycloid and the periodicity can be recognized from the arcsin function. From this the periodicity or wave-length λ of the orbits is easily found to be:

$$\lambda = 2\pi mc^2 E_0 / eH_0^2,$$

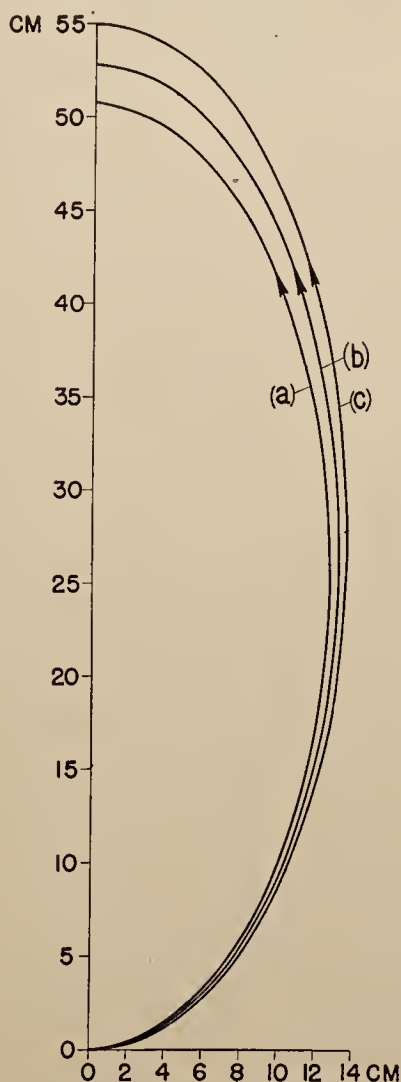


FIG. 2. Nearly elliptical orbits for case of H constant, $E = E_0x$, $H = H_0 = 2.5 \times 10^3$ gauss, $E_0 = 0.0333$ e.s.u., $M = 44$, $V_0 = 300$ volts, (a) $\tilde{c} = 2.88 \times 10^2$, (b) $\tilde{c} = 0$, (c) $\tilde{c} = -2.88 \times 10^2$.

the same result as obtained by Bleakney and Hipple. The dependence of λ upon the various parameters is ideal for focusing applications in a mass spectrometer or similar instrument. This is true since λ is independent of the initial energy and direction of the ions, which allows greater latitude in the design of the ion source and also permits ion currents of greater intensity. Furthermore the period λ is seen to be linearly dependent upon the mass. These facts were recognized by the previously named investigators and using them they built a mass spectrometer of improved focusing properties.³ In Fig. 1 may be seen the manner of utilizing the periodicity for focusing. Here all ions of the same mass which leave point A will follow different orbits, each of which, however, has the same period, i.e., the distance between A and B . Therefore, if the ion source is located at A and a collector at B we have an example of perfect focusing. In Fig. 1 the three curves are for ions of the same mass but different angles of departure from A , equivalently, different \tilde{c} 's.

(B) $E = E_0x$, $H = H_0$ =constant

The differential equation for this case is:

$$\frac{dy}{dx} = \pm \frac{(H_0x + \tilde{c})}{\left[hV_0 + \frac{hE_0}{2}x^2 - (H_0x + \tilde{c})^2 \right]^{\frac{1}{2}}}. \quad (17)$$

If we define the quantities A , B , and D as follows:

$$A = (hV_0 + hE_0\tilde{c}^2/2H_0^2),$$

$$B = -\tilde{c}hE_0/H^2,$$

$$D = (hE_0/2H_0^2 - 1),$$

F =constant defining position of orbit in x, y plane,

$$v = H_0x + \tilde{c}.$$

Eq. (17) may be integrated to yield:

$$y = \pm \frac{1}{H_0} \left\{ \frac{(A+Bv+Dv^2)^{\frac{1}{2}}}{D} - \frac{B}{2D\sqrt{D}} \log \left[(A+Bv+Dv^2)^{\frac{1}{2}} + v\sqrt{D} + \frac{B}{2\sqrt{D}} \right] \right\} + F \text{ for } D > 0, \quad (18)$$

and

$$y = \pm \frac{1}{H_0} \left\{ \frac{(A+Bv+Dv^2)^{\frac{1}{2}}}{D} - \frac{B}{2D(-D)^{\frac{1}{2}}} \sin^{-1} \left[\frac{-2Dv-B}{(B^2-4AD)^{\frac{1}{2}}} \right] \right\} + F \text{ for } D < 0. \quad (19)$$

It is to be noticed that the numerical sign of D is a criterion of the type of orbit since Eq. (18) gives open or aperiodic orbits and Eq. (19) gives closed or periodic orbits. Since E is an odd function of x , then for any admissible orbit or portion thereof on one side of the line $x=0$ there may be a corresponding orbit or portion thereof on the other side and they will be symmetrical with respect to the line $x=0$.

From the nature of the terms in Eq. (19) it can be seen that orbits passing through $x=0$ and with small values of dy/dx at $x=0$ will be nearly ellipses. It is therefore of interest to investigate this case to see if a type of focusing equivalent to that used in a 180° analyzer exists. In the 180° analyzer all ions leaving the ion source travel in circles and a beam of ions of one momentum value that diverges from the exit slit will converge to form a focus approximately at a point which is 180° removed from the exit slit and on the circle traveled by the principal ray.⁴ This focusing is characterized by the fact that the principal ray or orbit of the ion that leaves the exit slit in a direction perpendicular to the diameter of the circle, on which are located the ion source and the point of focus, will recross this diameter at a maximum distance from the source, i.e., ions of different starting directions will recross the diameter at points nearer the ion source. If we can demonstrate the existence of such an extremum for the principal ray in the present case, it will show if such focusing is possible.

The distance along the y axis which separates the point where an ion passing in the positive direction crosses the line $x=0$, from the point where it recrosses this line traveling in a negative direction, is given by:

$$\Delta y = 2 \{ y(x=x_{\max}) - y(x=0) \}.$$

⁴ Cf. E. B. Jordan and L. B. Young, J. App. Phys. 9, 526 (1942).

A necessary condition for the extremum discussed above is that the following equation be satisfied:

$$(\partial \Delta y / \partial \bar{c})_{\bar{c}=0} = 0. \quad (20)$$

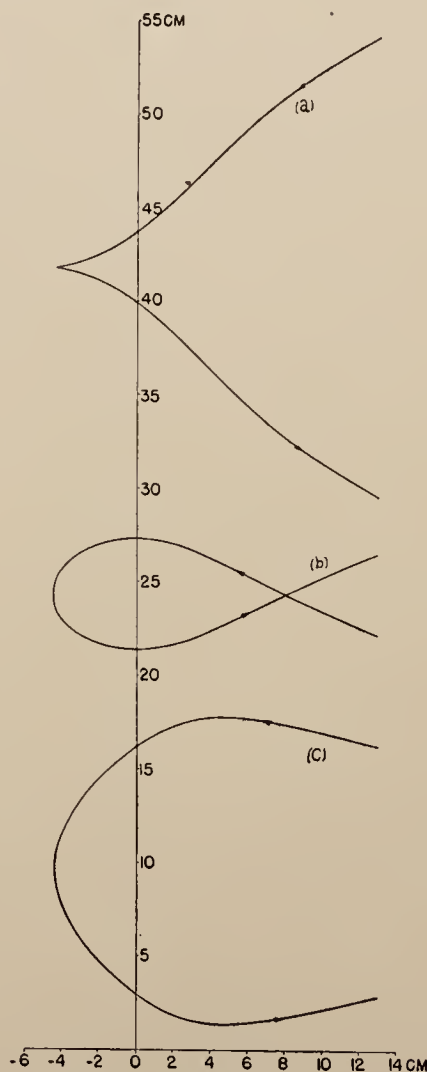


FIG. 3. Various orbits obtained for case of H constant, $E = E_0 x^2$, $V_0 = 300$ volts, $H_0 = 2.5 \times 10^3$ gauss, $E_0 = 0.0333$ e.s.u., $M = 44$, (a) $\bar{c} = 1.175 \times 10^4$, (b) $\bar{c} = 0$, (c) $\bar{c} = -1.175 \times 10^4$.

The validity of Eq. (20) can be easily tested by evaluating Δy in terms of the parameters involving \bar{c} . When the differentiation is carried out it is seen that Eq. (20) is not satisfied; hence we cannot expect the nearly elliptical orbits passing through $x=0$ to show focusing. This is further confirmed by an actual plot of three orbits which have only small differences in starting directions. These are seen in Fig. 2. Here (a), (b), and (c) are orbits with starting angles of $+1^\circ$, 0° , and -1° relative to the x axis.

(C) $E=E_0x^2$, $H=H_0=\text{constant}$

For this case the differential equation for the orbits is:

$$\frac{dy}{dx} = \pm \frac{H_0x + \bar{c}}{[hV_0 + (hE_0/3)x^3 - (h_0x + \bar{c})^2]^{\frac{1}{2}}}. \quad (21)$$

Equation (21) may be integrated in terms of elliptic functions but the trajectory of an ion or electron resulting from a given set of initial conditions is more conveniently obtained by numerical integration. In Fig. 3 may be seen three trajectories for an ion of mass 44 which crosses the line $x=0$ with energy equal to 300 electron volts and with a slope of $+1$, 0 , -1 . In curve (a) what appears to be a cusp in reality is a smooth turning point with an extremely small radius of curvature at that point. From the denominator of Eq. (21) it is clear that there can be either periodic or aperiodic orbits for a

given set of parameter values depending upon where the particle starts its trajectory relative to the three roots of the cubic in the radical. When Eq. (21) is set up in terms of standard elliptic integrals it is seen that the periods of the orbits depend upon \bar{c} and thus upon the starting slopes.

(D) $E=E_0e^{bx}$, $H=H_0e^{bx}$

In case the electric and magnetic fields vary in an exponential manner as above we have the following relationships:

$$f = \frac{H_0}{b}e^{bx} + \bar{c}, \quad V = V_0 + \frac{E_0}{b}e^{bx},$$

$$\frac{dy}{dx} = \pm \frac{(H_0/b)e^{bx} + \bar{c}}{\{hV_0 + (hE_0/b)e^{bx} - [(H_0/b)e^{bx} + \bar{c}]^2\}^{\frac{1}{2}}}. \quad (22)$$

If we make the transformation $v = e^{bx}/b$, Eq. (22) becomes:

$$\frac{dy}{dv} = \pm \frac{1}{b} \frac{(H_0v + \bar{c})}{v[hV_0 + hE_0v - (H_0v + \bar{c})^2]^{\frac{1}{2}}}. \quad (23)$$

Using the following definitions:

$$\begin{aligned} A &= (hV_0 - \bar{c}^2), \\ B &= (hE_0 - 2H_0\bar{c}), \\ D &= -H_0^2. \end{aligned}$$

We find Eq. (23) may be readily integrated to yield, upon substitution for v :

$$y = \pm \left[\frac{1}{b} \frac{H_0}{\sqrt{-D}} \sin^{-1} \left\{ \frac{-2De^{bx} - bB}{b(B^2 - 4AD)^{\frac{1}{2}}} \right\} - \frac{\bar{c}}{b\sqrt{A}} \log \left\{ \frac{(b^2A + bBe^{bx} + De^{2bx})^{\frac{1}{2}} + b\sqrt{A}}{e^{bx}} + \frac{B}{2\sqrt{A}} \right\} \right] + F \quad (24)$$

for $A > 0$, and

$$y = \pm \left[\frac{1}{b} \frac{H_0}{\sqrt{-D}} \sin^{-1} \left\{ \frac{-2De^{bx} - bB}{b(B^2 - 4AD)^{\frac{1}{2}}} \right\} - \frac{\bar{c}}{b\sqrt{-A}} \sin^{-1} \left\{ \frac{Be^{bx} + 2bA}{e^{bx}(B^2 - 4AD)^{\frac{1}{2}}} \right\} \right] + F \text{ for } A < 0. \quad (25)$$

An examination of the roots of the quadratic under the radical sign in Eq. (22) as well as an examination of the forms of Eqs. (24) and (25) shows that Eq. (24) represents aperiodic orbits which extend to $x = -\infty$, and that Eq. (25) represents periodic orbits bounded in the x dimension. Equation (25) represents periodic

orbits with the spatial period λ given by:

$$\lambda = 2\pi \left| \frac{H_0}{b\sqrt{-D}} - \frac{\bar{c}}{b\sqrt{-A}} \right|. \quad (26)$$

These orbits are clearly not suited for focusing of the type illustrated in Section A (cycloidal

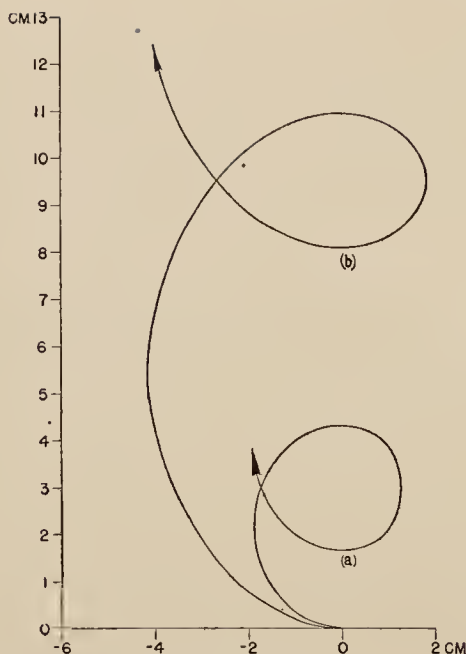


FIG. 4. Type of orbits obtainable for case of $H = H_0 e^{bz}$ and $E = E_0 e^{bz}$. $H_0 = 10^4$ gauss, $E_0 = 1/30$ e.s.u., $b = \frac{1}{2}$, $V_0 = 600$ volts, (a) $M = 16$, (b) $M = 44$.

orbits) as Eq. (26) shows the periodicity to depend upon two of the parameters of which it would be desirable to have the wave-length independent. These two parameters are V_0 and \tilde{c} which are related, respectively, to the initial energy and starting direction of each orbit. Figure 4 shows two such periodic orbits as represented by Eq. (25).

(F) $H = H_0 = \text{constant}$, $E = E_0/r$

The properties of orbits of charged particles in this arrangement of fields are particularly

interesting for several reasons. One reason is that such an arrangement may be achieved in electronic vacuum tubes of ordinary size. If a cylindrical condenser is placed inside a solenoid and with the axes of the condenser and the solenoid coincident we have the necessary conditions for this arrangement satisfied. There have been a number of theoretical papers written about the orbits for this set of conditions⁵⁻⁷ although in each case they have been concerned with orbits which are nearly circular. The properties of these nearly circular orbits may be obtained by approximations which do not eliminate the time t from Eqs. (10) and (11). These investigators have shown that, if these nearly circular orbits diverge from a point on the orbit of the principal ray, they will reunite to converge to a focus at a point which is on the same circle as the starting point but which is angularly displaced from it by an angle of $\pi/\sqrt{2}$. The circular orbit of the principal ray in this case is the equilibrium orbit wherein the combined effect of the electric and magnetic fields is to produce the angular acceleration necessary for uniform circular motion. A mass spectrograph utilizing this focusing principle has been built and operated.⁸

As will be seen, the present treatment does not conveniently give the same information about the nearly circular orbits but may on the other hand give information about orbits which are not nearly circular and for which the above mentioned approximations do not hold.

Making the proper substitutions in Eqs. (12) and (13) we arrive at the following differential equation for orbits with these field conditions:

$$\frac{d\theta}{dr} = \pm \frac{1}{r} \frac{(H_0 r/2) + (\tilde{c}/r)}{\{hV_0 + hE_0 \log r - [(H_0 r/2) + (\tilde{c}/r)]^2\}^{1/2}} \quad (27)$$

Unfortunately Eq. (27) cannot be integrated to give a closed system of simple functions. The integration by series is complicated by the nature of the poles where $d\theta/dr = \infty$. Numerical integration seems the best approach with particular care being taken as r approaches a point of

singularity. It is to be noticed that the squared term in the radical in the denominator will dominate the remainder of the radical for small values of r and also for large values of r . This means then that all orbits in this system are bounded in the r dimension. They are thus, then, either closed or periodic, in general, periodic

⁵ W. Bartky and A. J. Dempster, Phys. Rev. **33**, 1019 (1929).

⁶ R. Herzog, Zeits. f. Physik **19**, 335 (1934).

⁷ R. G. E. Hutter, Phys. Rev. **67**, 248 (1945).

⁸ H. Bondy, G. Johannsen, and K. Popper, Zeits. f. Physik **95**, 46 (1935).

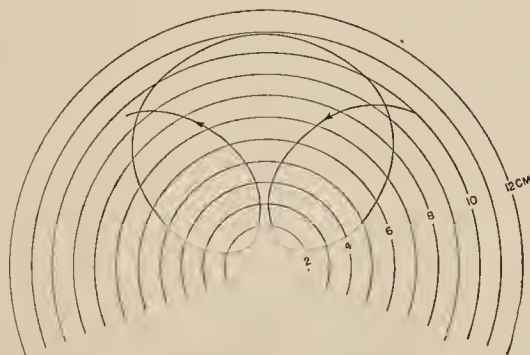


FIG. 5. Periodic type of orbit for case of H constant, $E=E_0/r$. $H_0=2.5 \times 10^3$ gauss, $E_0=0.175$ e.s.u., $V_0=100$ volts, $M=44$, $\bar{c}=-1.125 \times 10^4$.

with r as a periodic function of θ . The dependence of the periodicity upon the parameters, V_0 , h , H_0 , E_0 , and \bar{c} , would be highly interesting to know and perhaps of value for practical application but the nature of Eq. (27) makes this quite difficult if not impossible. It may be possible to deduce this dependence of the periodicity from the functional form of the right hand of Eq. (27) but the author has not been able to do so. A numerical integration approach is at best unsatisfactory.

Figure 5 shows more than a full cycle of a periodic orbit. This was obtained by numerical integration. Presumably orbits could be determined in this way for ions diverging from a point with a small angular spread and reconverging to form a focus, if such existed. This, however, must be done with considerable care as the integration for the orbit through points such that $d\theta/dr = \infty$ means numerically evaluating an improper integral. For Fig. 5 it is interesting to note the upper and lower limit for r in the orbits for the parameters used. These limits may, of course, be brought nearer each other by adjusting H_0 , E_0 , and V_0 .

For every cycle of such an orbit as seen in Fig. 5, it passes twice through a value of r such that $d\theta/dr = 0$, and from Eq. (27) we can see that there will be only one such value of r . Those portions of the orbit for greater values of r as well as those for smaller values may be regarded as analogous to the semi-circular paths in a 180° analyzer. Because of the difficulties of numerical integration the focusing effect cannot easily be determined although a knowledge of the disper-

sion of such a system can be easily obtained. Figure 6 shows a group of four orbits for ions of atomic masses 1, 2, 12, and 44. The orbits are shown for the values of r less than such that $d\theta/dr = 0$. The orbits shown correspond to those that would exist if a beam of ions were originated at a point 10 cm from the center, with an initial energy of the ions of 1000 electron volts, and with the ions all directed radially toward the center. It will be noticed that the separation on the $r=10$ cm circle between the points where the orbits for ions of one mass and those of a different mass again return to the condition $d\theta/dr = 0$ is very large for small values of M but becomes smaller rapidly for increasing values of M .

In Figs. 5 and 6 the orbits are for positively charged ions with a field applied radially outward from the center. In Fig. 7 are four orbits for the case of positive ions and a field applied radially in towards the origin. These are for ions of atomic mass 12, with a starting direction radially inwards, from a point 10 cm from the center and with initial energies of 300, 1000, 1800, and 3600 electron volts.

In conclusion regarding this arrangement of fields, it is highly desirable that an analytical means of integrating Eq. (27) become available as the numerical method is difficult because of the type of infinity of the integrand encountered and also an analytical treatment might give clearer information regarding periodicity and focusing.

(F) $H=H_0=\text{constant}$, $E=E_0/r$

This case, for which the electric field varies as the first power of the radial distance from the center, and is directed along this radius vector

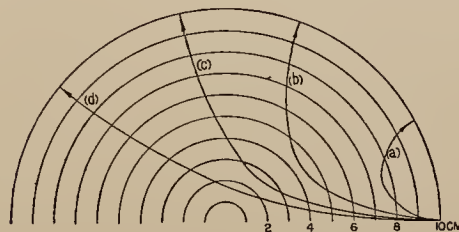


FIG. 6. Portions of orbits obtainable for case of H constant, $E=E_0/r$. $H_0=10^3$ gauss, $E_0=0.175$ e.s.u., $V_0=1000$ volts, $\bar{c}=-5 \times 10^4$, (a) $M=1$, (b) $M=2$, (c) $M=12$, (d) $M=44$.

is not a natural one in the sense of the field just previously treated, i.e., for a cylindrical condenser. The present field could be approximated by a double system of concentric guard rings or electrodes with the proper impressed voltages.

The differential equation of the orbits for this case is:

$$\frac{d\theta}{dr} = \pm \frac{(H_0 r/2) + (\tilde{c}/r)}{r \left[hV_0 + \frac{hE_0}{2} r^2 - \left(\frac{H_0 r}{2} + \frac{\tilde{c}}{r} \right)^2 \right]^{\frac{1}{2}}}. \quad (28)$$

If we make the following definitions:

$$\begin{aligned} A &= -\tilde{c}^2, \\ F &= (hV_0 - H_0 \tilde{c}), \\ D &= \left(\frac{1}{2} hE_0 - \frac{1}{4} H_0^2 \right). \end{aligned}$$

Equation (28) may by simple substitutions be integrated to give:

$$\begin{aligned} \theta = \frac{H_0}{4D} \log \left\{ [A + Br^2 + Dr^4]^{\frac{1}{2}} + r^2 \sqrt{D} + \frac{B}{2D} \right\} \\ + \frac{1}{2} \sin^{-1} \left\{ \frac{Br^2 + 2A}{r^2(B^2 - 4AD)^{\frac{1}{2}}} \right\} \text{ for } D > 0, \quad (29) \end{aligned}$$

and

$$\begin{aligned} \theta = \frac{H_0}{4} \frac{1}{\sqrt{-D}} \sin^{-1} \left\{ \frac{-2Dr^2 - B}{(B^2 - 4AD)^{\frac{1}{2}}} \right\} \\ + \frac{1}{2} \sin^{-1} \left\{ \frac{Br^2 + 2A}{r^2(B^2 - 4AD)^{\frac{1}{2}}} \right\} \text{ for } D < 0. \quad (30) \end{aligned}$$

As Eq. (29) is for aperiodic orbits and Eq. (30) for periodic ones we have $\frac{1}{2}hE_0 > \frac{1}{4}H_0^2$ or $\frac{1}{2}hE_0 < \frac{1}{4}H_0^2$ as the criterion for such. Here we are interested principally in the case of periodic orbits. We note that Eq. (30) is for orbits where in r is a periodic function of θ . When Eq. (30) is evaluated for a specific case it becomes evident that the period is given by:

$$\lambda_\theta = \pi - (\pi H_0/2(-D)^{\frac{1}{2}}). \quad (31)$$

Since the term D in Eq. (31) involves only m , E_0 , and H_0 and not V_0 or \tilde{c} we see that here again we have the perfect focusing of the type found for the cycloidal orbits. This means that for any orbit the angular period λ_0 as given by

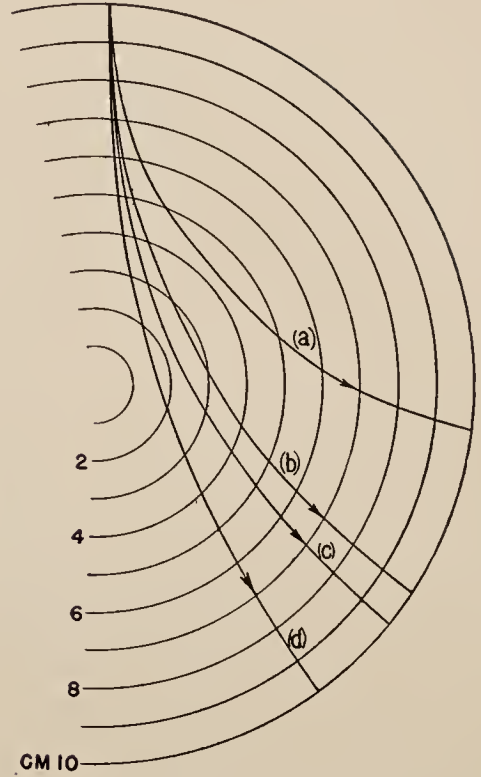


FIG. 7. Other variations in orbits obtainable for H constant, $E = E_0/r$, $H = H_0 = 10^3$ gauss, $E_0 = -0.175$ e.s.u., $M = 12$, $\tilde{c} = -5 \times 10^4$, (a) $V_0 = 300$ volts, (b) $V_0 = 1000$ volts, (c) $V_0 = 1800$ volts, (d) $V_0 = 3600$ volts.

Eq. (31) is independent of the starting energy V_0 and of the starting velocity vector which is characterized by \tilde{c} . Thus an instrument using such fields could afford considerable latitude in the design of the ion source or electron source. This would make it possible to achieve more intense ion currents as wide slits and a strong ion or electron collecting voltage may be used. In an ordinary mass spectrometer, for instance, the slit widths and ion collecting voltage must both be small in order to insure good focusing and resolution. However, these conditions for good focusing result in weak ion currents with the resultant need of electrometer amplifiers which by their nature are difficult to use.

In Fig. 8 can be seen a family of this type of orbits for ions of the same mass and charge. Here (a), (b), and (c) are orbits with considerably different starting directions from the point A . As is seen these orbits converge at the point B which is one angular wave-length displaced from

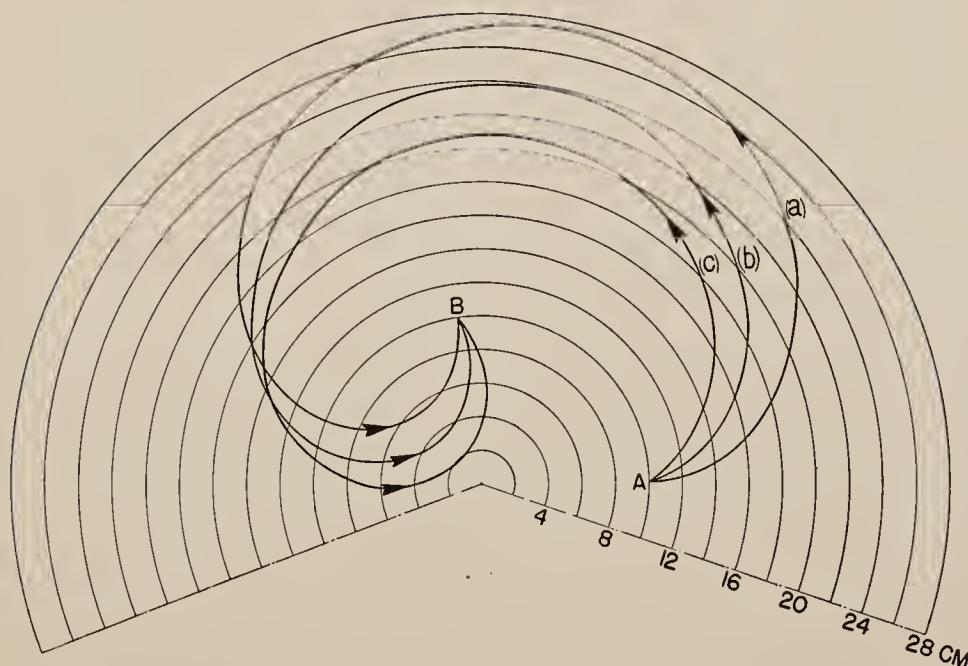


FIG. 8. Periodic orbits with preferred focusing properties for case of H constant, $E = E_0 r$, $H_0 = 4 \times 10^3$ gauss, $E_0 = 5$ volts per cm, $M = 44$, $V_0 = 600$ volts, (a) $c = -2 \times 10^5$, (b) $c = -1.13 \times 10^5$, (c) $c = -5 \times 10^4$.

A and on the same circle. In an instrument utilizing this focusing the ion source could be located at A and the ion collector at B . Since the focusing is independent of the starting voltage, relatively small voltages could be used in the ion source thus reducing the troubles due to stray fields from within the ion source interfering with the field outside the source. Also from the nature of the periodicity it is not necessary that the slits be aligned as carefully as in other types of instruments. Furthermore the angular separation need not be adjusted with particular care as the periodicity can be adjusted using either E_0 or H_0 . Since the con-

stant h is proportional to the mass of the ion and since h and E_0 enter in the definition of D as:

$$D = \frac{1}{2} h E_0 - \frac{1}{2} H_0^2$$

we see that if H_0 is held constant it is necessary to vary E_0 alone to bring in different ion masses to the collector. The relation, $h E_0 = \text{constant}$, is convenient for this procedure.

The author is indebted to Miss M. O. Taylor for some of the numerical integrations used, to Dr. M. Muskat for some stimulating discussions of the subject, and to Dr. P. D. Foote, Executive Vice President of Gulf Research and Development Company, for permission to publish this material.



LANCASTER PRESS, INC., LANCASTER, PA.

Pressure Broadening in the Infra-Red and Optical Collision Diameters

NORMAN D. COGGESHALL AND ELEANOR L. SAIER

Reprinted from THE JOURNAL OF CHEMICAL PHYSICS, Vol. 15, No. 1, pp. 65-71, January, 1947

Pressure Broadening in the Infra-Red and Optical Collision Diameters*

NORMAN D. COGGESHALL AND ELEANOR L. SAIER

Gulf Research and Development Company, Pittsburgh, Pennsylvania

(Received October 29, 1946)

The pressure broadening effects of a number of foreign gases on the infra-red absorption of methane at 7.65μ have been determined. Also the pressure broadening effects of a number of foreign gases on the absorption of carbon dioxide at 4.3μ and 14.8μ have been investigated. The data have been analyzed to obtain optical collision diameters for the various gases and the absorbers. By optical collision is meant any collision which is effective in interrupting the processes of radiation absorption. The data are discussed in terms of the Lorentz theory of pressure broadening and are shown to confirm it. From the results obtained, it is clear that the pressure broadening effects of certain gases on one absorber cannot be reliably extrapolated to predict the effects on another absorber. Also the effects at one wave-length are not in general the same at another wave-length for the same absorber. The optical collision diameter effective for a foreign gas and an absorbing gas at a particular wave-length is a specific function of the two gases and the wave-length. Empirical results on the shape of the curves obtained are presented. The deviation from Beer's law of absorption evidenced by isobutylene at 11.23μ is shown to be not due to pressure broadening.

A NUMBER of gases are known to deviate from Beer's law of absorption when examined in the infra-red region. For example, the optical density of a given gas at a particular wave-length will depend upon the partial pressure but not be directly proportional to it. Also for these gases the optical density will, in general, depend upon the total gas pressure in the sample. For those gases whose molecules possess small moments of inertia and appreciable spacing between the rotational fine structure, these deviations from Beer's law are explained in terms of the Lorentz pressure broadening theory. This subject has been theoretically studied by a number of investigators,¹⁻³ and their results show that the shape of a rotational line is dependent upon the frequency of molecular collisions. Dennison² showed that this change of shape together with a consideration of the energy transmittance of a spectrometer would explain some of the characteristics of the infra-red spectrum of HCl.

A complete application of the theories of Dennison and others to the treatment of experi-

mental data for any particular gas is very difficult unless the data have been obtained with a spectrometer of quite high resolution. However, with instruments of medium resolution, data may be obtained which can be interpreted to give information about the optical collision diameters of the gases studied. The optical collision diameters are the diameters which govern the frequency of effective collisions between molecules of absorbing gas or of absorbing and foreign gas. By effective collisions are meant collisions which are effective in interrupting the processes of radiation absorption.

The present work is an experimental study of the effects of various foreign gases on the infra-red absorption of methane, carbon dioxide, and isobutylene. Optical collision diameters between various pairs of molecules are obtained and discussed. The data show that results for one absorbing gas can only be applied in a general way in predicting the behavior of another.

EXPERIMENTAL DETAILS

The spectrometer used in this work was an NaCl prism type.⁴ The method of obtaining optical densities for the gas mixtures was the same as described by us elsewhere.⁵ In it, the

* Some of this material was presented at the Symposium on Molecular Spectroscopy and Molecular Structure, Ohio State University, June, 1946.

¹ H. A. Lorentz, *The Theory of Electrons* (Stechert & Company, New York, 1909), note 57.

² D. M. Dennison, *Phys. Rev.* **31**, 503 (1928).

³ J. H. Van Vleck and V. F. Weisskopf, *Rev. Mod. Phys.* **17**, 227 (1945).

⁴ Model 12-A manufactured by the Perkin-Elmer Corporation, Glenbrook, Connecticut.

⁵ N. D. Coggeshall and E. L. Saier, *J. App. Phys.* **17**, 450 (1946).

radiation intensities are measured by a null method, which allows greater accuracy and convenience than the method of measuring galvanometer deflections. The optical densities were obtained by using a pair of cells. One of these cells was the gas cell and the other an evacuated comparison cell. The gas cell was evacuated, and the ratio of its transmission to that of the comparison cell was obtained for each wavelength being investigated. These ratios were then combined with the corresponding ones obtained for the sample in the gas cell to get the true optical densities.

Two absorption cells were used, one of 9.50 cm length and one of 3.15 cm length. Both had NaCl windows and were mounted in the manner described in reference 5. The spectrometer and gas blending equipment were located in an air conditioned room in which the temperature was kept within 1°C of a mean value. This was significant as the temperature is an important parameter in pressure broadening, and our method of analyzing the data required that it be constant. The blending and mixing of the gases was achieved in either of two ways, depending upon the relative concentrations of the components. One of these involved a special blending system in which mixing was achieved in a reservoir by moving an iron vane by means of exterior magnets. The other method was to introduce both gases into the absorption cell and mix them there by mechanical motion. This was possible as the cell contained a metal vane which lay out of the optical path when the cell was in an operating position, but which could otherwise be moved throughout the interior to mix the gases. A thorough mixing of the components is very important in obtaining data of this sort. The gases used were the purest obtainable commercially,⁶ and in each case the impurities present were of such small concentration as not to affect the results.

DATA AND DISCUSSION

According to the Lorentz theory, the absorption for the individual line as a function of

⁶ The companies from whom the gases were obtained were: The Linde Air Products Co., Buffalo, N. Y.; The Matheson Co., East Rutherford, N. J.; Phillips Petroleum Co., Special Products Division, Bartlesville, Oklahoma; The Ohio Chemical & Mfg. Co., Cleveland, Ohio.

frequency has the form,

$$K(\gamma) = \frac{a_i n l (1/\tau)}{4\pi^2(\gamma - \gamma_i)^2 + (1/\tau)^2}, \quad (1)$$

where a_i is a constant characteristic of the individual line; n is the number of absorbing gas molecules per unit volume; l is the length of the absorption cell; τ is the mean time between collisions; and γ_i is the frequency of maximum absorption for the line. In correlating the information included in (1) with actual experimental data the limitations on resolution of the spectrometer used must be considered. For this we use the energy transmittance function $f(\gamma, \gamma_0)$ which gives the energy as a function of frequency in the spectral band width transmitted by the instrument when set to pass radiation of frequency γ_0 .⁷ The transmission for a sample of gas is given by

$$T = A \int_{-\infty}^{\infty} \exp \left\{ -nl \sum_i \left(\frac{a_i (1/\tau)}{4\pi^2(\gamma - \gamma_i)^2 + (1/\tau)^2} \right) \right\} \times f(\gamma, \gamma_0) d\gamma, \quad (2)$$

where A is a constant which takes into account the integral of the transmittance function over the same spectral region. Although the limits of the integral in Eq. (2) are $-\infty$ and $+\infty$, this does not imply significant contributions from frequencies very far removed from γ_0 . Actually the transmittance function $f(\gamma, \gamma_0)$ will be such that it goes to zero very rapidly for values of γ further removed from γ_0 than one-half the spectral slit width. Dennison² has found that for the transmittance function both a Gaussian and triangular form are about equally effective in calculating transmissions. The summation in the exponential under the integral in Eq. (2) must be taken over all frequencies which are included in the spectral slit widths. For this reason the analytical evaluation of (2) is very difficult unless a spectral slit width characteristic of an instrument of high resolution is used.

Despite the difficulties of directly using Eq. (2) to correlate theory and experiment or to obtain values of the characteristic constants, use may be made of it to obtain information

⁷ See for example: J. R. Nielson, V. Thornton, and E. B. Dale, *Rev. Mod. Phys.* **16**, 307 (1944).

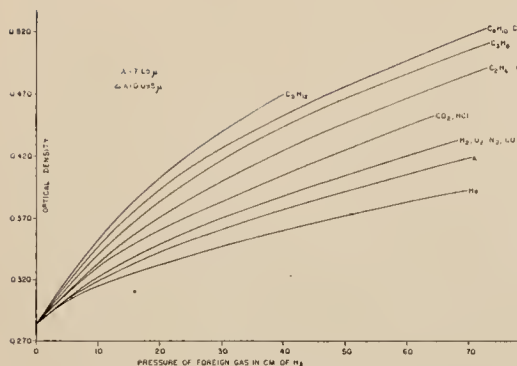


FIG. 1. Effects of various foreign gases on the infra-red absorption of methane at 7.65μ .

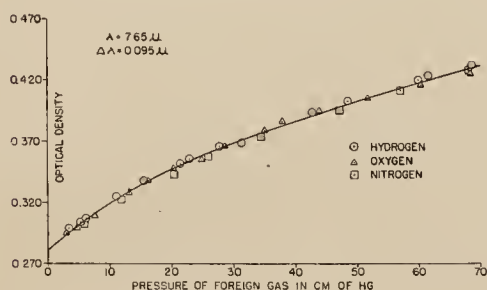


FIG. 2. Detail of similar effects of H_2 , O_2 , and N_2 on methane absorption at 7.65μ .

concerning the optical collision diameters of various molecules. A consideration of the terms in (2) shows that if the concentration of the absorbing gas, the wave-length, and the slit settings are kept constant, while various foreign, non-absorbing gases are used, the only varying parameter between separate evaluations of (2) will be τ , the mean time between collisions. Figure 1 shows some experimental data taken under the conditions set forth above. Here is plotted the optical density D , $D = \log(1/T)$ for 13.5 cm of Hg pressure of CH_4 in the presence of the different foreign gases indicated. This data was taken with the 9.50 cm cell.

Figure 1 indicates that the effect of foreign gases varies widely and depends upon the individual gases showing a general trend of increasing effect with molecules of increasing multiplicity of atoms. It is to be noticed that for a number of cases more than one foreign gas is represented by one curve. For these cases the effects were so similar that only a single curve was drawn. In Fig. 2 may be seen a more detailed curve for one

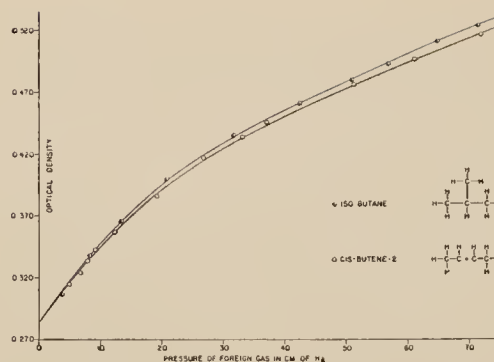


FIG. 3. Detail effects of isobutane and cis-butene-2 on methane absorption at 7.65μ .

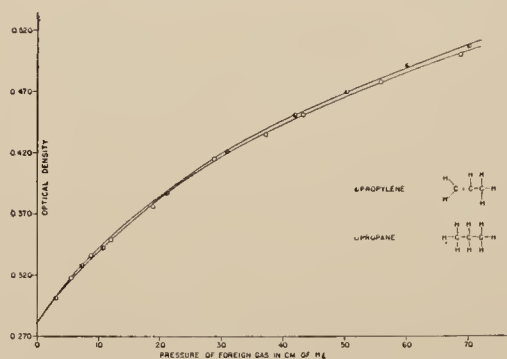


FIG. 4. Detail of effects of propylene and propane on methane absorption at 7.65μ .

of these cases. Here it is seen that the foreign gases H_2 , O_2 , and N_2 have the same effects to within the scattering of the data. It might be inferred that the similar effects were caused by some common characteristic of these gases, but, as will be discussed later, we believe it to be merely fortuitous. In a similar study of the effects of foreign gases on the infra-red absorption of N_2O , Cross and Daniels⁸ found the order of gases with increasing effects on the optical density to be as follows: A , O_2 , N_2 , C_2H_6 , CO_2 , and H_2 . From our data when compared with this it is obvious that the order of increasing effect cannot be extrapolated from one absorbing gas to another, and this will be further confirmed by additional data below.

Figure 3 shows a detail graph of the effects of isobutane and cis-butene-2. This was of interest in view of the much greater chemical reactivity of the olefin and the possible relation of this

⁸ P. C. Cross and F. Daniels, J. Chem. Phys. 2, 6 (1934).

difference of chemical reactivity to the pressure broadening effects. A similar graph for propane and propylene may be seen in Fig. 4. From Figs. 3 and 4 it is seen that apparently the chemical reactivity has no direct connection with the pressure broadening, as in one case the more reactive compound of two of about the same molecular weight has a slightly greater effect and in the other case the situation is reversed. It should be mentioned at this point that at the wave-length investigated some of the hydrocarbons used had absorption coefficients which were quite small but not zero. To correct the results for their absorption, Beer's law was assumed to be obeyed by them at this wave-length, and the observed optical density was accordingly corrected. From the general consistency of results discussed below, it is believed that this procedure is correct.

The manner of obtaining data used here wherein only the partial pressure of the foreign gas is varied is equivalent to varying the parameter τ in Eq. (2). Cross and Daniels⁸ showed that this procedure may be used to obtain information about the optical collision diameters of the absorbing and foreign gas molecules. Their postulate that the mean free path of the absorbing molecules is the same in all gas mixtures which exhibit the same relative absorption coefficient is equivalent in this case to assuming that Eq. (2) is correct. They showed that if the partial pressures of different foreign gases which produced the same increase of optical density under the conditions above could be experimentally determined, the ratios of their optical collision diameters could be deduced. This is done by straightforward application of the kinetic

theory of gases and the result is:

$$D_{AX}/D_{AY} = (p_Y/p_X)^{\frac{1}{2}} \times [M_X(M_A + M_Y)/M_Y(M_A + M_X)]^{\frac{1}{2}}, \quad (3)$$

where D_{AX} is the distance between the centers of absorbing molecule A and the foreign gas molecule X , at which the process of absorption of radiation by A is interrupted. It is then the sum of the optical collision radii of each of the two molecules. D_{AY} is the corresponding quantity for the case of foreign gas Y in the presence of A . P_Y and P_X are partial pressures of gases Y and X which produce the same optical density. M_A , M_X , and M_Y are the molecular weights. For the derivation of (3) from the principle that equal values of τ used in (2) will produce equal optical densities, it is necessary that the temperature of the gas be the same for the different observations. This was achieved in our experiments by allowing equilibrium to be reached between the gas and the room temperature which was controlled.

In the determination of molecular diameters from viscosity or other gas kinetic data, values are obtained which are representative of the distance between molecular centers such that momentum may be transferred. Or, in other words, only those collisions wherein there is a transfer of momentum affect the experimental results. Certainly each such collision would be expected to interrupt the process of radiation absorption by an absorbing molecule. In addition the perturbation of vibrational and rotational states by Van der Waals interactions would be expected to alter the absorption processes in many encounters not close enough to affect momentum transfer. For this reason, a determination of molecular diameters by an application of Lorentz pressure broadening theory gives values called optical collision diameters which are larger than the molecular diameters obtained from kinetic data. The present work gives only ratios between diameters for reasons which will be discussed below. Recently Bleaney and Penrose,⁹ in a study of the ammonia bands in the 1-cm region using the microwave technique, have found that the optical diameter effective in

TABLE I. Values of p_Y/p_X for different values of D .

D	$p_{\text{He}}/p_{\text{CO}_2}$	$p_{\text{A}}/p_{\text{CO}_2}$	$p_{\text{H}_2}/p_{\text{CO}_2}$
0.330	1.86	—	1.33
0.340	1.95	1.43	1.33
0.350	1.99	1.44	1.31
0.360	2.00	1.46	1.29
0.370	1.99	1.44	1.28
0.380	2.00	1.45	1.28
0.390	2.02	1.46	1.28
0.400	—	1.47	1.29
0.410	—	1.47	1.29
0.420	—	1.49	1.31

⁹ B. Bleaney and R. P. Penrose, *Nature* **157**, 339 (1946).

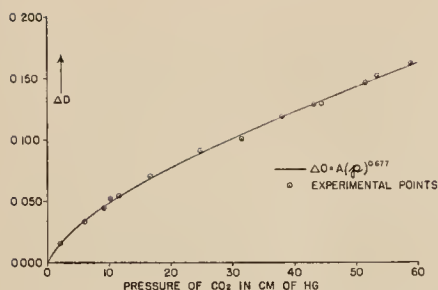


FIG. 5. Increase in optical density of constant pressure of methane as a function of foreign gas pressure.

broadening these bands to be about four times the normal diameter.

Since the optical collision diameters should be independent of gas pressure, Eq. (3) may be used to confirm the physical basis and reasoning used in deriving it. For if these are correct, Eq. (3) may be applied to any pair of partial pressures giving the same optical densities. Therefore the ratio p_Y/p_X should be constant for all values of optical density for which it is determined. Table I gives the values of this ratio for several different pairs of foreign gases at different values of optical density D using the data of Fig. 1.

In this table we may see that the ratios of the pairs of pressure determinations do not vary more than a few percent over the range of optical density used. The greatest variation occurred for the smaller values of optical density, and this could have been caused by experimental difficulties in obtaining the lower end of the curves in Fig. 1. Certainly the values of p_Y/p_X are constant enough to give confirmation to the correctness of Eq. (3).

Returning for the moment to Eq. (2), we note that n , the number of absorbing centers per unit volume, and l , the cell length, enter the integral as a product. Thus, if the product nl is kept constant and the mean time between collisions is kept constant it is possible to achieve the same value of the integral under various experimental conditions. For example, if one has the absorbing gas at a high pressure p_1 , in a short cell of length l_1 , with no foreign gas present, a certain optical density is obtained. If a second pressure p_2 is used in a cell of greater length l_2 , yet adjusted so that $p_1 l_1 = p_2 l_2$, foreign gas must be added to the longer cell to get the same optical density as obtained with the shorter one.

This is because the τ due to the absorbing gas alone will change with change of pressure. Using these two different arrangements allows a determination of D_{AA}/D_{AX} . This is given by Eq. (4) which is derived by the same arguments as Eq. (3).

$$D_{AA}/D_{AX} = [p_X/(p_1 - p_2)]^{1/2} \times [(M_A + M_X)/2M_X]^{1/2}. \quad (4)$$

Here p_X is the pressure of foreign gas X that must be added to get an optical density using the longer cell equal to that obtained with the shorter one. In our work, the short cell was 3.15 cm in length, and the pressure of methane used in it was 39.70 cm of Hg. The values of p_X used to evaluate Eq. (4) were obtained by reading off from the curves in Fig. 1. The results of using Eq. (4) on the data obtained with the short cell and the data of Fig. 1 are given in Table II.

We note here that, in general, the ratio D_{AA}/D_{AX} decreases with increasing complexity of the X molecules, or in other words the optical diameters of the X molecules increase with increasing size. HCl is somewhat out of place in this respect, but its large optical diameter is believed to be owing to its large dipole moment.

An interesting empirical result is illustrated in Fig. 5. Here ΔD which is the difference between the observed optical density when a foreign gas is used and the optical density obtained for the methane in the cell alone is plotted *versus* the partial pressure of foreign gas, in this case CO_2 . Here it is seen that ΔD is given by the equation:

$$\Delta D = A p^s, \quad (5)$$

where A and s are empirically determined constants. As may be seen the agreement between the points and the curve fitted to two of them is

TABLE II. Values of D_{AA}/D_{AX} for various foreign gases. (A = methane; X = foreign gas used; $\lambda = 7.65\mu$.)

X	D_{AA}/D_{AX}	X	D_{AA}/D_{AX}
He	1.72	C_2H_4	0.82
A	1.07	C_2H_6	0.82
H_2	1.59	C_3H_6	0.72
N_2	1.03	C_3H_8	0.73
O_2	1.01	C_4H_8	0.68
CO	1.03	C_4H_{10}	0.66
CO_2	0.87	C_6H_{12}	0.63
HCl	0.88		

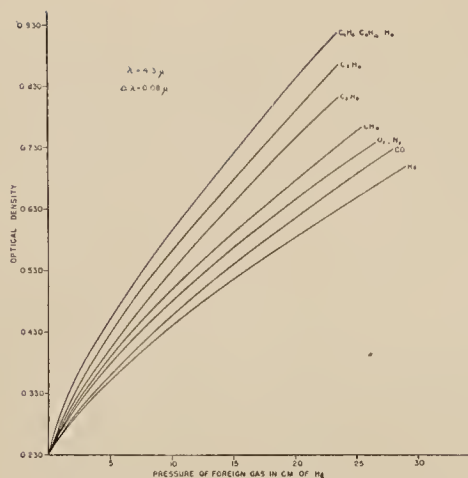


FIG. 6. Effects of various foreign gases on the infra-red absorption of carbon dioxide at 4.3μ .

quite good. From the agreement of the data with Eq. (5) for the case of CO_2 and from constancy of the ratios in Table I we may conclude that agreement may be had for the other foreign gases and that the value of the exponent will be 0.677 for each. A curve of optical density *vs.* pressure for various pressures of methane alone in the 9.50 cm cell gave good agreement with the empirical equation $D = Ap^s$ which is very similar to Eq. (5). The value of the exponent in this case was 0.743.

In addition to the work done on methane the effect of various foreign gases on the absorption of CO_2 was investigated at two different wavelengths 4.3μ and 14.8μ at which absorption takes place due to stretching and bending vibrations respectively. The results for the 4.3μ investigation are seen in Fig. 6, and the results for the 14.8μ work are seen in Fig. 7. Here again the 9.50-cm cell was used, and the partial pressure of CO_2 used at 4.3μ was 3.50 cm of Hg, and at 14.8μ a partial pressure of 9.86 cm of Hg was used. Since with the instrument used the optical path at one place passed through an open space this created some experimental difficulty. This was owing to the fact that if the carbon dioxide content in the room was not constant then the transmittance function $f(\gamma, \gamma_0)$ used in Eq. (2) would not be the same in each case. For this reason data for CO_2 studies were only taken after a CO_2 equilibrium was reached in the room.

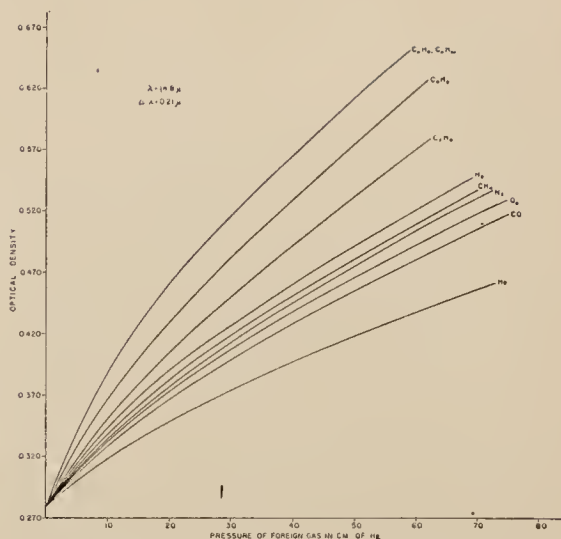


FIG. 7. Effects of various foreign gases on the infra-red absorption of carbon dioxide at 14.8μ .

Reproducibility tests indicated the equilibrium concentration to be nearly the same each day.

An inspection of Figs. 6 and 7 shows that in general the order of increasing effect of the foreign gases is the same for the two different spectral regions. Two exceptions to this are that O_2 and N_2 have the same effect at 4.3μ but distinctly different effects for 14.8μ . Another and more striking exception is that of H_2 which has an effect similar to that of methane for 14.8μ absorption but has a relatively much greater effect at 4.8μ , being of the same magnitude as for isobutane and butadiene. In connection with the latter point, it is interesting to note that the two compounds, isobutane and butadiene, which differ radically in chemical reactivity, have the same pressure broadening effect for CO_2 for both the 4.3μ and 14.8μ bands. From this and the observations on methane it seems safe to conclude that chemical reactivity is not to be directly correlated with optical collision diameters.

The ratios of D_{AA}/D_{AX} were obtained in the same manner as for methane, using the 3.50 cm cell, and the results are given in Tables III and IV.

An examination of the values of D_{AA}/D_{AX} in Tables III and IV shows that for each different gas X considered the values for the two wavelengths are equal to within about 8 percent.

except for the gases H_2 , C_3H_8 , C_4H_{10} , and C_4H_6 . These differences, however, plus the variations in order of increasing effect shown for the different absorbing gases confirm our belief that the optical collision diameter ratio is a specific function of the pair of gases under consideration and of definite absorption frequencies. That is, the pressure broadening effect of a gas on one absorber cannot reliably be extrapolated to predict the effect on another. Nor can the results for one particular wave-length be reliably extrapolated to another for the same pair of gases. Thus, optical collision radii have definite quantitative meaning only for specific cases. These conclusions are in line with the recently published work of Foley¹⁰ which indicates the complicated nature of the dependence of the pressure broadening on the molecular interactions. As would be expected, the optical collision diameters depend upon the nature of the Van der Waals interactions and upon the excited states of the gas molecules.

Although data of the type discussed above can give only relative results, i.e., ratios between various optical collision diameters, recent work

TABLE III. Values of D_{AX}/D_{AA} for various foreign gases. (A = carbon dioxide; X = foreign gas used; $\tau = 4.3\mu$.)

X	D_{AA}/D_{AX}	X	D_{AA}/D_{AX}
H_2	2.18	CH_4	1.26
O_2	1.20	C_2H_6	1.00
N_2	1.19	C_3H_8	0.85
H_2	1.90	C_4H_{10}	0.72
CO	1.29	C_4H_6	0.72

TABLE IV. Values of D_{AA}/D_{AX} for various foreign gases. (A = carbon dioxide; X = foreign gas used; $\lambda = 14.8\mu$.)

X	D_{AA}/D_{AX}	X	D_{AA}/D_{AX}
H_2	1.98	CH_4	1.25
O_2	1.17	C_2H_6	1.07
N_2	1.19	C_3H_8	0.97
H_2	1.64	C_4H_{10}	0.86
CO	1.27	C_4H_6	0.87

¹⁰ H. M. Foley, Phys. Rev. 69, 616 (1946).

in microwave technique has demonstrated its possibilities for obtaining absolute values for those wave-length regions.^{9, 11, 12}

Another gas given some investigation was isobutylene. If the optical density is plotted *vs.* pressure of isobutylene at the wave-length of 11.23μ (the center of the Q branch) there results a curved line similar in appearance to Fig. 5. This deviation from Beer's law would not seem likely to be caused by pressure broadening due to the large moments of inertia and consequent small spacing between rotational levels for the isobutylene molecule. However, the pressure broadening possibility was checked by comparing the optical density of a particular pressure of isobutylene with the optical density obtained when various pressures of foreign gases were added. In this work a constant pressure of 2.35 cm of isobutylene was used in the 9.50-cm cell. To this were added various pressures of H_2 , N_2 , and CO_2 ranging from 20 to 75 cm. For each observation regardless of type or pressure of foreign gas the optical density was equal, within experimental error, of the optical density obtained for the isobutylene by itself. This we believe is conclusive evidence that this particular deviation from Beer's law is not due to pressure broadening. It seems likely that it may be owing only to the combined effect of line shape and finite slit widths.

The above data are of interest for applications of infra-red absorption spectroscopy for analytical uses. Gases subject to pressure broadening may be quantitatively measured in mixtures, but allowance must be made for the pressure broadening effects.⁵

The authors are grateful to Dr. M. Muskat for discussions of this work and to Dr. P. D. Foote, Executive Vice President of this Company, for permission to publish this material.

¹¹ R. Beringer, Phys. Rev. 70, 53 (1946).

¹² W. E. Good, Phys. Rev. 70, 213 (1946).



LANCASTER PRESS, INC., LANCASTER, PA.

[Reprinted from the Journal of the American Chemical Society, **69**, 1620 (1947).]

Infrared Spectroscopic Investigations of Hydrogen Bonding in Hindered and Unhindered Phenols

By Norman D. Coggeshall

[CONTRIBUTION FROM THE GULF RESEARCH & DEVELOPMENT COMPANY]

Infrared Spectroscopic Investigations of Hydrogen Bonding in Hindered and Unhindered Phenols¹

By NORMAN D. COGGESHALL

The hindered phenols which are formed when large alkyl substituents such as *t*-butyl, *s*-butyl or *t*-amyl are added to the two positions *ortho* to the hydroxyl group have markedly different chemical properties compared to the simpler phenols.² The present investigation was made with two objectives: (1) to determine the effect of the large *ortho* substituted alkyl groups on the hydrogen bonding of phenols, and (2) to correlate the chemical and physical properties of the various phenols with their hydrogen bonding behavior.

Infrared absorption spectroscopy offers a very powerful tool for the direct investigation of hydrogen bonding through the study of the radiation absorbing properties of the hydroxyl groups themselves. When a hydroxy compound is in the vapor state or in dilute solution there is little chance for hydrogen bonding complexes to form or to be maintained. Consequently there will be obtained an infrared absorption band at about 2.7 μ which is characteristic of the unperturbed hydroxyl group. However, in solutions of sufficient concentration that hydrogen bonding occurs there is found an absorption band at 3.0 μ characteristic of hydroxyl groups in such complexes. Figure 1 illustrates this phenomenon. In the curves of Fig. 1 and of the other figures in this paper the transmitted energy is plotted *versus* wave length so that absorption maxima are represented by minima in the curves. Here the top curve is for a dilute solution of ethyl alcohol in carbon tetrachloride and there is seen an absorption band at about 2.7 μ . Also seen in this and the other curves is an absorption band at 3.4 μ which is due to carbon-hydrogen valence bond vibrations. This is included in each curve to furnish a visual reference point. In the middle curve is seen the spectrum for an intermediate solution. There is seen to be a weakened band at 2.7 μ and a new band at 3.0 μ . In the lower curve is seen the spectra for a more concentrated solution and here it is seen that 2.7 μ band has completely disappeared, indicating that all the alcohol molecules are involved in complexes. The wave length shift between the absorption of unperturbed hydroxyl groups and bound hydroxyl groups is indicated as $\Delta\lambda$ and may be used as a measure of the strength of the hydrogen bonds formed.^{3,4} A number of substituted phenols have been examined in dilute and concentrated solu-

tions and $\Delta\lambda$ tabulated for each. The consideration of $\Delta\lambda$ in view of the type and position of substituents allows conclusions to be drawn regarding steric hindrance to hydrogen bonding and the chemical properties as dependent upon the substituents.

Experimental Details

The infrared spectrometer was a small sodium chloride prism type. It was supplied with automatic recording equipment which gives records of total energy transmitted as a function of wave length.⁵

In all solutions used the compounds were dissolved in carbon tetrachloride. For solutions of strength of the order of 0.03 mole per liter an absorption cell of 14 mm. length was used. For solutions of about 0.2 mole per liter a cell of 0.91 mm. length was used and for those of about 1 mole per liter a cell of 0.15 mm. length was used. The shorter cells were constructed with amalgamated lead spacers and stainless steel needle valves for filling and sealing.⁶ For the compounds examined in the crystalline state the samples were prepared in the form of thin films. This was done by melting some of the material on a rock salt plate in an oven and pressing another rock salt plate, also oven heated, onto it and allowing them to cool slowly.

The compounds used in this work were supplied by Dr. D. R. Stevens⁷ and Dr. G. H. Stillson² and were believed to be 99% pure with two exceptions which will be discussed later. The carbon tetrachloride was C. P. and was tested in each case for transmission in the hydroxyl region before using. As will be seen from the curves presented the instrument did not have really high resolution in the wave length region. For this reason and also because of a slight uncertainty in exact wave length calibration the absolute wave length values of the unperturbed and shifted hydroxyl bands are not given. In the figures presented the curves are purposely shifted relative to each other in the vertical direction for purposes of clarity.

Data and Discussion

In Fig. 1 is seen the wave length shift $\Delta\lambda$ which occurs for ethyl alcohol in going from a dilute to a concentrated solution. In Fig. 2 may be seen the comparable data for 2,6-dimethyl-4-*t*-butylphenol. Here it is seen that the methyl groups on the *ortho* positions apparently are not

(1) Presented in part before the Division of Physical and Inorganic Chemistry at the Chicago meeting of the American Chemical Society, September, 1946.

(2) G. H. Stillson, D. W. Sawyer and C. K. Hunt, *THIS JOURNAL*, **67**, 303 (1945).

(3) L. Pauling, *ibid.*, **58**, 94 (1936).

(4) J. J. Fox and A. E. Martin, *Proc. Roy. Soc. (London)*, **162**, 419 (1937).

(5) The optics and recording system for this instrument were supplied by the Perkin-Elmer Corp., Glenbrook, Conn. The instrument itself is not, however, one of their current commercial models.

(6) N. D. Coggeshall, *Rev. Sci. Instruments*, **17**, 343 (1946).

(7) D. R. Stevens, *Ind. Eng. Chem.*, **35**, 655 (1943).

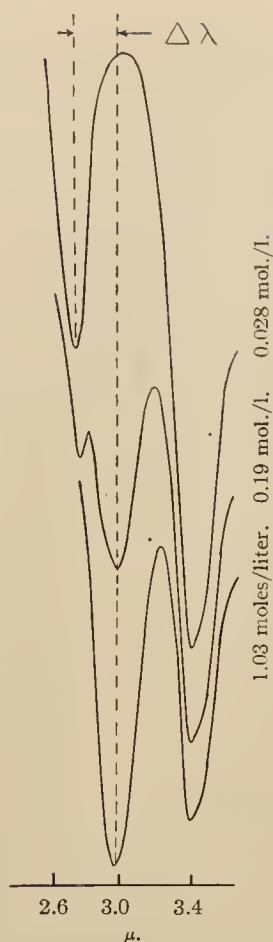


Fig. 1.—Infrared absorption spectra in the hydroxyl region for various concentrations of ethyl alcohol.

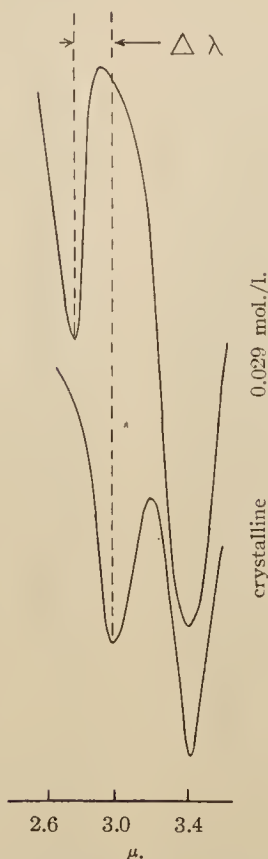


Fig. 2.—Infrared absorption spectra in the hydroxyl region for different concentrations of 2,6-dimethyl-4-*t*-butylphenol.

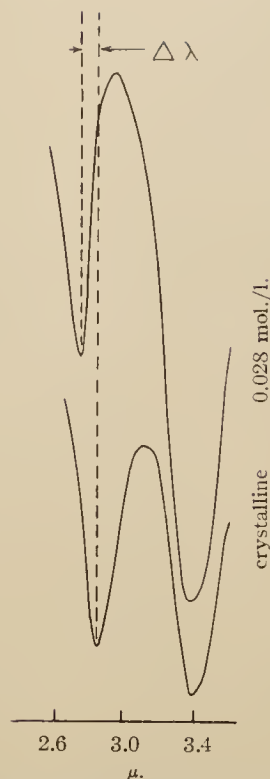


Fig. 3.—Infrared absorption spectra in the hydroxyl region for different concentrations of 2,4-di-*t*-butylphenol.

very effective in hindering molecular association. Other phenols exhibiting wave length shifts comparable to that found for ethyl alcohol are listed in Table I.

TABLE I

WAVE LENGTH SHIFTS FOR UNHINDERED PHENOLS	
Compound	$\Delta \lambda$ in μ
<i>p</i> -Cresol	0.25
<i>p</i> - <i>t</i> -Butylphenol	.45
<i>p</i> - <i>t</i> -Amylphenol	.40
2,6-Dimethyl-4- <i>t</i> -butylphenol	.30

In Fig. 3 may be seen the wave length shift $\Delta \lambda$ which occurs for 2,4-di-*t*-butylphenol in going from a dilute solution to the crystalline state. Here it can be easily seen that the wave length shift is considerably smaller than for the phenol illustrated in Fig. 2. The wave length shift for the present case is 0.12 μ . The large decrease of this shift is believed to be due to weaker hydrogen bonds for this material. The weaker bonds in turn are believed to be due to the hindering effect the

t-butyl group on the *ortho* position has on the approach of the hydroxyl groups to each other when a complex is formed. A case of even smaller wave length shift is seen in Fig. 4 which is for 2-methyl-4,6-di-*t*-butylphenol where $\Delta \lambda = 0.06 \mu$. The decreased shift of this case over the one in Fig. 3 may be ascribed to the increase in hindrance produced by the addition of a methyl group on the other *ortho* position. These two compounds plus others which we have classed in the same group are tabulated in Table II.

TABLE II

WAVE LENGTH SHIFTS FOR PARTIALLY HINDERED PHENOLS	
Compound	$\Delta \lambda$ in μ
2- <i>t</i> -Amyl-4-methylphenol	0.05
3-Methyl-6- <i>t</i> -butylphenol	.08
2-Methyl-4,6-di- <i>t</i> -butylphenol	.06
2,4-Di- <i>t</i> -butylphenol	.12
2- <i>t</i> -Butyl-4-methylphenol	.12

From Tables I and II can be seen the wave length shifts that occur when both *ortho* positions

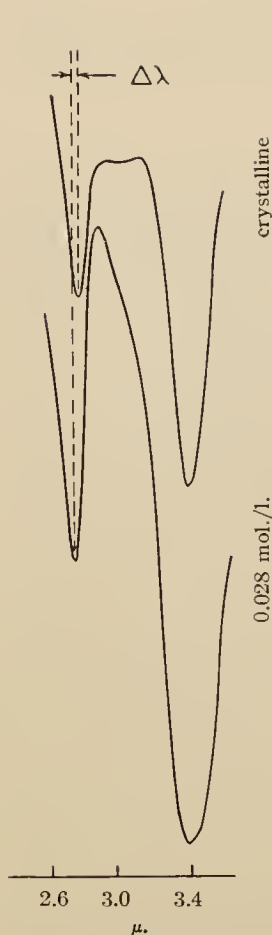


Fig. 4.—Infrared absorption characteristics in the hydroxyl region for unlike concentrations of 2-methyl-4,6-di-*t*-butylphenol.

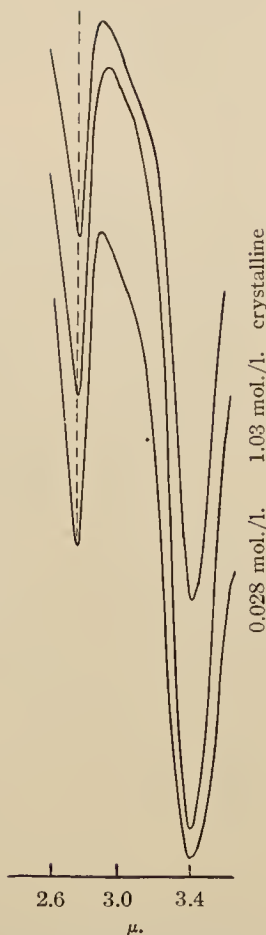


Fig. 5.—Infrared absorption behavior in the hydroxyl region of unlike concentrations of 2,6-di-*t*-butyl-4-methylphenol.

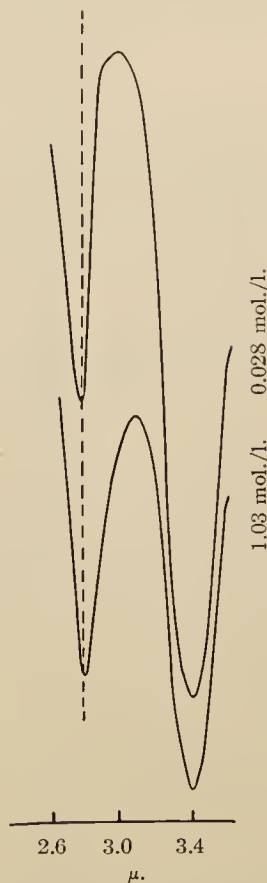


Fig. 6.—Infrared absorption behavior in the hydroxyl region of different concentrations of 2,6-di-*t*-butyl-4-phenylphenol.

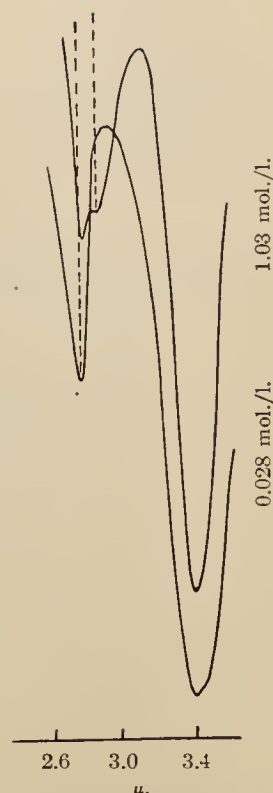


Fig. 7.—Infrared absorption spectra in the hydroxyl region of various concentrations of 2,6-di-*t*-amyl-4-*t*-butylphenol.

are vacant, have only methyl groups on them or have a large group on one such as *t*-butyl. In Fig. 5 may be seen the behavior when large groups are attached to both *ortho* positions. Here are shown the results for a dilute solution, a concentrated solution and a crystalline sample. The reason for testing both the heavy solution and the crystalline sample was to see if the change of phase had any effect on the hydrogen bonding. The indications are that it does not. There was observed for the compound illustrated in Fig. 5 a very small wave length shift which, however, was too small to be demonstrated in the manner used in the other figures. Another example of the behavior of a phenol with both *ortho* positions occupied by large groups may be seen in Fig. 6 which is for 2,6-di-*t*-butyl-4-phenylphenol. The wave length shifts for these compounds and others with similar *ortho* substitutions are given in Table III.

After the data were obtained for the phenols named in the above tables, they were classified ac-

cording to wave length shift, $\Delta\lambda$. For $\Delta\lambda > 0.15 \mu$ the compounds were put in Table I and were termed the unhindered phenols. For $0.04 \mu < \Delta\lambda < 0.15 \mu$ the compounds were put in Table II and were termed the partially hindered phenols. If $\Delta\lambda < 0.04 \mu$ the compounds were put in Table III which represents those compounds termed as hindered phenols. It is very significant that the above classification according to wave length shift also produces a classification characterized by the *ortho* substituents. Those phenols

TABLE III
WAVE LENGTH SHIFTS FOR HINDERED PHENOLS

Compound	$\Delta\lambda$ in μ
2,6-Di- <i>t</i> -butyl-4-methylphenol	0.02
2,6-Di- <i>t</i> -butyl-4-ethylphenol	.02
2,4,6-Tri- <i>t</i> -butylphenol	.01
2,4-Di- <i>t</i> -butyl-4-diisobutylphenol	.02
2,6-Di- <i>t</i> -butyl-4-phenylphenol	.03
2,6-Di- <i>s</i> -butyl-4-methylphenol	.01

in Table I have no substituents on the *ortho* positions larger than methyl groups. The phenols in Table II have one *ortho* position occupied by a large group and the other position either vacant or occupied by a small group. The phenols in Table III have both *ortho* positions occupied by large groups. From these results we may definitely conclude that hydrogen bonding in phenols is sterically hindered by large groups on the *ortho* positions. This is important when a model of the hydrogen bond is considered and this will be discussed further below.

The compounds listed in Table III are seen to be of the same class as those designated by Stillson, Sawyer and Hunt as hindered phenols because of their chemical properties.² The hindered phenols have certain chemical properties quite in contrast to the simple phenols and they are listed below⁸ (a) insoluble in water, aqueous alkali of any strength and sparingly soluble in alcoholic alkali similar to Claisen's solution. (b) Failure to give the customary phenol coloration with aqueous or alcoholic ferric chloride solution. (c) Will not react with metallic sodium in anhydrous petroleum ether or diethyl ether solutions, even at reflux temperatures. (d) Will not form derivatives such as acetates or benzoates by the methods usually applicable to phenols in preparing such derivatives.

In designating these phenols as hindered phenols the above mentioned investigators assumed that the addition of the large groups on the *ortho* positions might interfere with the normal functions of the hydroxyl group by steric hindrance and thus be responsible for their peculiar chemical properties. The present work confirms this assumption insofar as it shows in a direct manner that the large *ortho* substituents are responsible for steric hindrance to hydrogen bonding. The fact that in the hindered phenols with their particular chemical properties the functions of the hydroxyl group are masked or hindered by the large *ortho* substituents emphasizes strongly the importance of the hydroxyl groups for the contrasting chemical behavior of the simpler phenols.

The phenols included in Table II and classified here as partially hindered fall into the so-called cryptophenol class.^{2,9} These phenols are insoluble in water and sparingly soluble in aqueous alkali although soluble in alcoholic alkali solutions of the Claisen solution type. Their solubility characteristics are intermediate between those of the simple phenols and those of the hindered phenols. This is additional evidence that the degree of masking or inactivation of the hydroxyl group by steric hindrance is instrumental in controlling the solubility characteristics.

Since the hydrogen bond represents an attractive force which must be overcome when the substance is to be vaporized it is to be expected that

in a series of *ortho*, *meta* and *para* isomers, the one with the weakest hydrogen bond would in general have the lowest boiling point. The infrared absorption data presented here indicate that the one with the weakest hydrogen bond would be the *ortho* isomer and this is in general agreement with actual experimental boiling point determinations. These latter show that the addition of a *t*-butyl or other large alkyl group to the *ortho* position in a phenol produces a smaller increase in boiling point than when added to a *meta* or *para* position.¹⁰

A scrutiny of Tables I, II and III indicates that the type and order of substitution on the 3, 4 and 5 positions have at best only a small second order effect on the hydrogen bonding characteristics.

In their studies of hydrogen bonding in various hydroxy compounds in which they obtained quantitative data for different solutions Fox and Martin⁴ considered three possible types of hydrogen bond complexes: (a) A dimer type of complex in which the hydrogen atom of one of the hydroxyl groups is held between the two oxygen atoms while the other hydrogen atom is "free." This corresponds to the absorption characteristics of one hydroxyl group being changed and one being unchanged. (b) A polymerized type of complex wherein the hydroxy compounds are held in a long chain by hydrogen bonding forces. In this model the hydrogen atom of the hydroxyl group of any one of the molecules is held between the oxygen atom of that molecule and the oxygen atom of the successive molecule in the chain. This model corresponds to all except the terminal hydroxyl groups being perturbed. (c) A dimer type of complex wherein both hydroxyl groups are involved. They compared the theoretical and experimental results assuming the different types of complexes and concluded that type (c) is correct. This type (c) complex corresponds to the hydrogen bond forces being due to van der Waals dipole-dipole interactions. Since for such an interaction the potential energy varies inversely with the sixth power of the distance of separation,¹¹ any change in the separation distance will greatly affect the strength of the bond. The present results may be interpreted as consistent with this model as the groups in the *ortho* positions increase the minimum distance of separation and greatly reduced hydrogen bonds result as evidenced by the very small wave length shifts.

From Tables I, II and III it is seen that for all phenols examined there is agreement between the classification according to wave length shift and classification according to substitution on the *ortho* positions. Although exceptions may be found the results in the tables seem conclusive enough to formulate tentative general rules for the study of phenols of unknown structure. Thus if a phenol exhibits a wave length shift which fits any one of the three classifications, reliable conclu-

(8) The author is indebted to Dr. G. H. Stillson of this Company for preparing this listing of properties.

(9) J. B. Niederl, *Ind. Eng. Chem.*, **30**, 1269 (1938).

(10) Robert S. Bowman, Mellon Institute, Pittsburgh, Pa., unpublished material.

(11) H. Margenau, *Rev. Modern Phys.*, **11**, 1 (1939).

sions concerning its *ortho* substitutions may be possible.

It was mentioned earlier that two compounds examined were not of the 99% purity believed true of the others. These two compounds were 2,6-di-*t*-amyl-4-*t*-butylphenol and 2,6-di-*t*-amyl-4-methylphenol. Those compounds (liquid at room temperature) were somewhat discolored and were not believed to be of high purity from their history. Their infrared spectra gave interesting results in suggesting the presence of mono-substituted phenols as impurities. Figure 7 shows the results for 2,6-*t*-amyl-4-*t*-butylphenol. As can be seen there is an extra absorption band which shows up for the heavy concentration. This band is indicated by the dashed line to the right and is so close to the main OH absorption band that the two are not resolved. This second band is believed to be due to mono-substituted phenols, *i. e.*, molecules with only one large alkyl group on an *ortho* position. This explanation is confirmed by the fact that no such band appears in the spectrum of the dilute solution. A similar doublet was observed for 2,6-di-*t*-amyl-4-methylphenol and its cause also is believed to be the same. The behavior of the spectra of the concentrated solutions for these cases suggests a method for checking the purity of phenol samples. To test this a number of synthetic mixtures were prepared from mono and di-substituted phenols of high purity. The spectra of these mixtures confirmed the feasibility of checking the purity in this manner.

Acknowledgment.—The author is indebted to Dr. D. R. Stevens and Dr. G. H. Stillson for kindly supplying the compounds studied, also to Dr. M. Muskat for supporting this work and

to Dr. P. D. Foote, Executive Vice-President of Gulf Research and Development Company, for permission to publish this material.

Summary

An infrared absorption spectroscopic investigation has been made of the hydrogen bonding in various phenols. The wave length shift of the hydroxyl absorption band attendant to the formation of the hydrogen bond was measured for each phenol. The results allow a classification of the phenols according to the magnitude of this shift. For the wave length shift $\Delta\lambda > 0.15 \mu$ the compounds are classed as unhindered phenols, for $0.04 \mu < \Delta\lambda < 0.15 \mu$ they are classed as partially hindered phenols, and for $\Delta\lambda < 0.04 \mu$ they are classed as hindered phenols. The unhindered phenols were those with either no or small substituent groups on the *ortho* positions; the partially hindered phenols were those with either one *ortho* position vacant and the other having a large alkyl group, or one small *ortho* substituent and one large one; the hindered phenols were those with large alkyl groups on both *ortho* positions. These results directly indicate that the *ortho* groups offer steric hindrance to hydrogen bonding. This confirms postulated reasons for the peculiar chemical behavior of the hindered phenols. Evidence is obtained that the substituents on the 3, 4 and 5 positions are not important in affecting hydrogen bonding. A method is provided for aid in determining position of substitution in phenols of unknown structure. A method is indicated for the study of purity of di-substituted phenols.

PITTSBURGH, PENNSYLVANIA

RECEIVED DECEMBER 28, 1946

Fringing Flux Corrections for Magnetic Focusing Devices

NORMAN D. COGGESHALL

Reprinted from JOURNAL OF APPLIED PHYSICS, Vol. 18, No. 10, pp. 855-861, October, 1947

Fringing Flux Corrections for Magnetic Focusing Devices

NORMAN D. COGGESHALL

Gulf Research and Development Company, Pittsburgh, Pennsylvania

(Received March 27, 1947)

When a charged particle approaches a region of uniform magnetic field its trajectory is affected by the fringing field. Compensation for the effect of the fringing field may in some cases be achieved by the use of virtual field boundaries which are outwardly displaced from the actual boundaries. A definition of the virtual boundary in terms of the effect of the fringing field upon the trajectories is formulated. A procedure for calculating the displacement d of the virtual from the actual field boundary is given using the methods previously developed for calculating ion trajectories in non-uniform magnetic fields. Using this procedure several values of the displacement for various magnet dimensions and conditions have been calculated. A method of altering the geometry of sector-type mass spectrometers to correct for the effects of the fringing fields is proposed. It is shown that the angular and spatial separations of the individual ion trajectories in an ion beam of small angular spread as it approaches a uniform field region through a fringing field are approximately the same as for the ideal case wherein the magnet field changes discontinuously at the boundary.

IT is well known that the magnetic field of a magnet does not discontinuously go from its maximum value to zero as the boundary of the region between the pole faces is passed. Rather the field falls off gradually in conformation with the laws of potential theory, and the result is an appreciable amount of fringing flux for some distance away from the pole-face boundaries.

In the sector-type mass spectrometer, schematically illustrated in Fig. 1, the ions proceed from the ion source through a magnetic-field-free region to the magnetic analyzer. The magnetic analyzer consists of a uniform magnetic field perpendicular to the plane of the figure and with the shape of a truncated sector. After passing through the magnetic analyzer the ions again pass through a magnetic-field-free region on their

way to the ion collector. In the derivation¹ of the focusing properties of this system, it is assumed that the magnetic field region has sharp boundaries such as delineated in Fig. 1. Actually no magnet provides sharp boundaries to the magnetic field region, and in calculating the geometrical arrangement of ion source, magnetic analyzer, and ion collector, the effects of fringing magnetic field must be taken into account. One means of doing this is to use virtual boundaries of the sector-shaped field region which are displaced outwards from the actual boundaries. In this method it is assumed that fringing flux corrections can be effectively made by such a simple displacement of field boundaries. It is the purpose of this article to provide an analytical method for the determination of d , the displacement of the

¹W. E. Stephens, Phys. Rev. 45, 513 (1934).

virtual field boundaries from the actual field boundaries. This displacement is considered under various conditions and several numerical cases evaluated. It is a further purpose of this article to consider the effectiveness of such a procedure as the use of virtual field boundaries for fringing flux corrections and to provide an alternative procedure which is believed to be more effective.

If we consider the magnetic field on the median plane, i.e., the plane parallel to and midway between the pole faces, the flux on it may to a reasonable approximation be regarded as a function of only one variable, the perpendicular distance from the boundary of the uniform field region. Thus the methods previously developed² for the calculation of ion paths in non-uniform magnetic fields may be used to determine analytically the trajectories of the central ray and others between the ion source and their penetration into the uniform field region.

In the past there have been indicated approximate methods of correcting for stray fields,³⁻⁵ but they do not allow the exact calculations of the trajectories as will be described below.

In reference 2 it was shown that the exact determination of ion paths could be readily achieved for such cases where the ions move in a plane through a non-uniform magnetic field which is a function of only one coordinate and is everywhere perpendicular to this coordinate and to the orthogonal coordinate in the same plane. This was shown to be true for both Cartesian and polar coordinate systems, the magnetic field being a function of the radial distance in the

latter. For the case at hand we may use the distance from the uniform field region and on a line normal to its boundary as the x coordinate in a Cartesian system and apply these methods.

In reference 2 it was shown that the ion trajectory is determined from the differential equation:

$$dy/dx = \pm f/(1-f^2)^{1/2}, \quad (1)$$

where $f=f(x)$ and is defined as:

$$f = (e/vmc) \int H(x) dx,$$

and v =velocity of ion in cm/sec., c =velocity of light, e =electrical charge of the ion in e.s.u., and m the mass of the ion in grams. For convenience in the present applications we define a function $h(x)$ as follows:

$$H(x) = H_0 h(x).$$

The function $h(x)$ then specifies the ratio of the magnetic field at any point to the maximum field H_0 in the uniform field region. With this we may rewrite (1) as:

$$dy/dx = \pm \tilde{f}/(r^2 - \tilde{f}^2)^{1/2}, \quad (2)$$

where

$$f = \tilde{f}(x) = \int h(x) dx \quad \text{and} \quad r = (vmc/H_0 e).$$

The quantity r is the radius of curvature of the ion path in the uniform field H_0 .

It is to be noticed that the right-hand portion of Eq. (2) is a function of x only. Therefore, an integration, either numerical or analytical, may be made to determine y as a function of x and thus obtain the trajectory. If the function $h(x)$ is known only experimentally then $\tilde{f}(x)$ may be determined by numerical integration and the resulting values used in a numerical integration of Eq. (2).

The application of the foregoing equations may be seen in Fig. 2. Here is plotted the trajectory of an ion as it passes from the ion source to and through a uniform magnetic field. Although the ion source is so oriented that its axis is perpendicular to the boundary of the magnetic field region, the fringing flux causes the central ray to actually enter the uniform field region with an angle other than 90° and at a

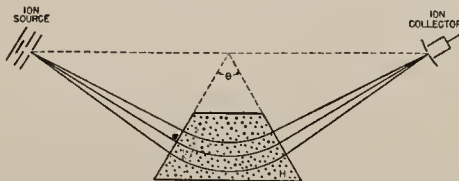


FIG. 1. Focusing scheme used in sector-type spectrometer.

² N. D. Coggeshall and M. Muskat, Phys. Rev. 66, 187 (1944).

³ A. J. Dempster, Phys. Rev. 11, 316 (1918).

⁴ R. Herzog, Zeits. f. Physik 89, 447 (1934).

⁵ J. Mattauich and R. Herzog, Zeits. f. Physik 89, 786 (1934).

point considerably displaced from the entrance point of the axis. The net effect of the fringing field is to so determine the trajectory that as the ion passes through the uniform field region the center of curvature is a distance d normal to the pole-face boundary. This is in contrast to the ideal case wherein the magnetic field would be discontinuous at the boundary and the center of curvature would be on the boundary. We may therefore define a virtual boundary as one parallel to the actual boundary and displaced from it so as to include as a point the center of curvature for that part of the trajectory in the uniform field region. We shall consider d at present only for the case wherein the axis of the ion source is perpendicular to the pole-face boundaries. As will be discussed in more detail later, d depends upon the distance of the ion source from the uniform field region and upon the angle of emergence of the ions from the source. In Fig. 2 the virtual boundary is represented by the dashed line which contains the center of curvature as a point. It is useful to know the displacement d , although as we shall see later these virtual boundaries do not allow the use of the ideal geometrical arrangements considered in reference 1.

The determination of the displacement d is readily made from Eq. (2). We note that $dy/dx = \infty$ for a value \bar{x} such that $\bar{f}(\bar{x}) = \pm r$. Suppose the actual pole-face boundary is taken as the line $x=0$, then since in the x -coordinate system the center of curvature will be located r units from \bar{x} , it follows that:

$$d = (r - |\bar{x}|). \quad (3)$$

The absolute value is used here since \bar{x} may have a negative value, depending on manner of using the coordinate system. To obtain \bar{x} we must use the relationship

$$\int_{x_0}^{\bar{x}} h(x) dx = \pm r, \quad (4)$$

where x_0 is the value of the x coordinate at the ion source exit slit.

Thus the problem of determining d reduces to obtaining the function $h(x)$ and to carrying out the integration of Eq. (4). Actually for any particular magnet $h(x)$ should be determined experi-

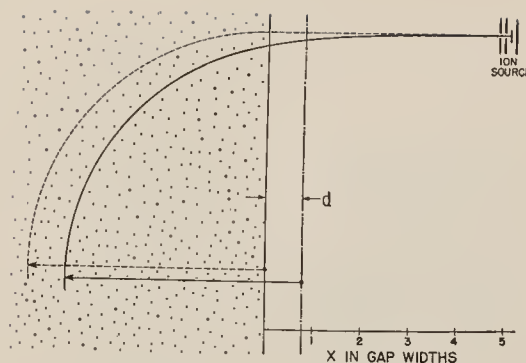


FIG. 2. Comparison between ion trajectories for the ideal case and for the actual case wherein the fringing flux is effective.

mentally. We may, however, get some idea of the order of magnitude of d and its change with variations of magnets by using the Schwarz-Christoffel transformation⁶ to obtain $h(x)$. Figure 3 shows the type of magnet pole considered and the differential equation used for the conformal transformation. Here the magnet poles are considered to extend to ∞ in both directions perpendicular to the paper. They are in the form of jaws with the outer surface of each jaw being n times further from the median plane than the inner surface. For simplicity the transformation is made for the case shown by the cross-hatching in Fig. 3, i.e., one magnet pole as one surface of constant magnetic potential and the median plane as the other. The differential equation shown transforms the edge of the upper magnet pole onto the left-hand half of the real axis in the ω plane and transforms the edge of the other region of constant magnetic potential onto the right-hand half of the real axis. In the differential equation T is the usual orientation factor necessary for the transformation. The constants in the equation shown in Fig. 3, which expresses z in terms of ω , are given by:

$$\begin{aligned} a &= (n + (n^2 - 1)^{1/2})/\pi, \\ b &= (n - (n^2 - 1)^{1/2})/\pi, \\ c &= -((a+b)/2) \log(a-b) - (ab)^{1/2} \log(a-b). \end{aligned}$$

The transformation given in Fig. 3 allows the flux on the median plane to be calculated for various values of n . Changing the value of n

⁶ See for example: W. R. Smythe, *Static and Dynamic Electricity* (McGraw-Hill Book Company Inc., New York, 1939), Chapter IV.

n VARIABLE

$$\frac{dZ}{d\omega} = T \frac{\sqrt{\omega+a} \sqrt{\omega+b}}{\omega}$$

$$Z = A + \frac{a+b}{2} \log(2A+2\omega+a+b) - \sqrt{ab} \log(2\sqrt{ab}A+2ab+a\omega+b\omega) + \sqrt{ab} \log \omega + C$$

$$A = \sqrt{\omega+a} \sqrt{\omega+b}$$

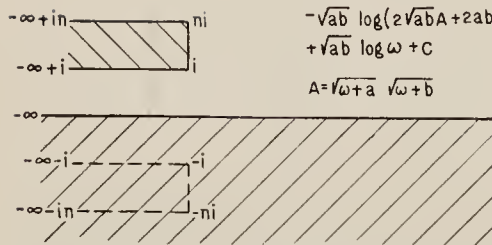


FIG. 3. Type of magnet pole construction considered and conformal transformation used.

corresponds to changing the thickness of the pole pieces relative to the gap width. The function $h(x)$ has been evaluated for several values of n , and the results are shown in Fig. 6.

In addition to the evaluation of $h(x)$ for several values of n the two extreme cases of $n=1$ and $n=\infty$ have been treated. Figure 4 shows the boundaries to be transformed and the differential equation for the extreme case of $n=1$. This case which is physically impossible corresponds to the pole pieces being thin sheets of magnetic material. The other extreme case of $n=\infty$, illustrated in Fig. 5, is also physically impossible but may be representative of magnets which have a large ratio of thickness to gap width. The results of the evaluation of $h(x)$ for these two extreme cases are also shown in Fig. 6.

It is somewhat surprising in inspecting Fig. 6 to see how little effect the variation of pole piece thickness has on the fringing flux. In this figure $h(x)$ is plotted against distance from pole-face boundary with the unit of distance as one gap width. Values of d obtained from using these evaluations of $h(x)$ cannot be expected to give true values of d for actual magnets. This is because an actual magnet will have finite dimensions in all directions and for it $h(x)$ will fall to zero more rapidly for large values of distance from pole-face boundary than shown in Fig. 6.

TABLE I. Variation of d with various values of n and r .

rn	1	2	5	10	∞
5	0.69	0.84	0.92	0.95	0.98
10	0.81	0.97	1.07	1.14	1.20

If the dimensions are, however, reasonably large compared to the gap width, then the obtained values of $h(x)$ may be expected to be fairly accurate throughout the region wherein its greatest reduction in value occurs, i.e., up to about 2 gap widths.

In order to appraise the value of d obtainable for the two-dimensional cases discussed above the necessary integrations as in Eq. (4) were carried out. The results are given in Table I. Here d is given in gap widths as a function of the two variables n and r . In each case it applies to the central ray. Actually d is not directly dependent on r but rather on the distance of the ion source from the uniform field region. For the cases evaluated in Table I this distance was taken as equal to r , a situation which exists in a sector-type spectrometer when the sector angle is 90° . The values considered were: $r=5$ gap widths and $r=10$ gap widths.

As is evident from Table I, a large change in ion source distance will cause considerable change in d . Although the magnetic field strength is small at large distances it has a large cumulative effect. In determining $h(x)$ experimentally for a determination of d by numerical integration it is important to take the measurements under as near operating conditions as possible. For example, if an auxiliary magnet is used with the ion source to align the beam of ionizing electrons the experimental determination of $h(x)$ must include its effects.

It has sometimes been assumed that effective corrections for the influence of the fringing flux could be made by the simple use of the virtual field boundaries. Thus in locating the ion source and ion collector relative to the magnetic field the apex formed by the virtual field boundary is

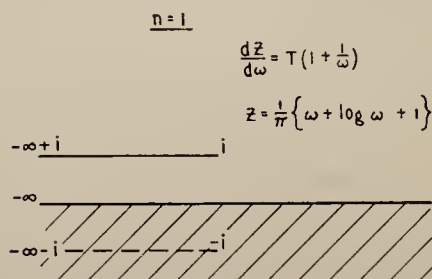


FIG. 4. Extreme case of magnet pole construction wherein $n=1$.

obtained by some approximate or graphical method. Such a method of correction assumes that the central ray will have its center of curvature located on the virtual sector apex.

We now wish to show that this method is not exact and that not only must the displacement of virtual field boundaries be taken into account but also the deviation of the trajectory from a straight line in the region between the ion source and the magnetic analyzer.

Figure 7 represents the geometry such as found in a 90° sector-type spectrometer with symmetrical location of ion source and collector. Here A represents the position of an ion source with its axis coincident with line AB . The effect of the fringing field is to cause the ions emerging from the source on the line AB to move away from it as they approach the magnetic analyzer. In the scale of dimensions used in constructing this figure AB is 5 gap widths which would be proper for a 90° instrument utilizing trajectories with radii of curvature also of 5 gap widths. The center of curvature for that portion of the central ray within the uniform field region is at D , the intersection of the virtual field boundaries DH and DI . Now if one were to use DH and DI as the new boundaries of an ideal magnetic field region, the ion source would be located at F which will be 5 gap widths from DH and which lies on the line perpendicular to ED , the bisector of the sector angle. However, it is clear that the location of the ion source at F will give a central ray with a center of curvature below and slightly to the right of D as the fringing field will still be operative. Thus the assumption that the use of virtual field boundaries would allow the use of

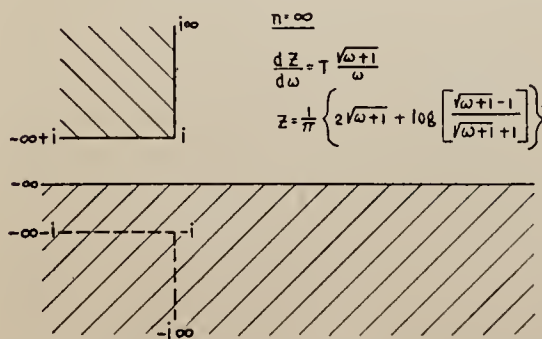


FIG. 5. Extreme case of magnet pole construction wherein $n = \infty$.

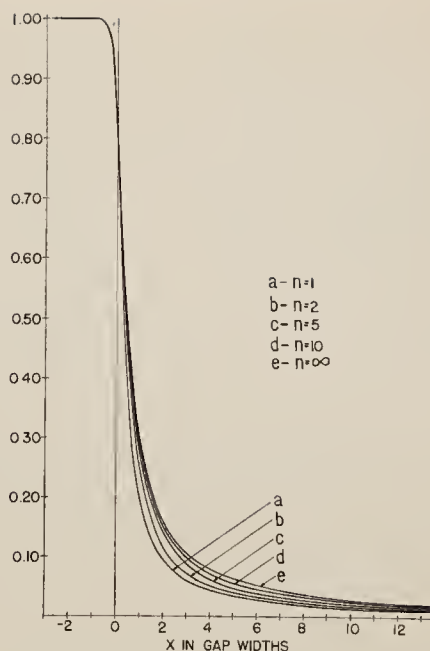


FIG. 6. Fringing magnetic field plotted as a function of distance from magnet pole faces for various values of n .

the exact geometrical relations prescribed for this type of instrument (reference 1) is seen not to be true. It is to be noticed that this result does not depend on the numerical value of d or of the sector angle, i.e., the use of virtual field boundaries and the exact geometrical relationships described above will always yield a center of curvature of the central ray offset from the virtual field boundary apex.

A method of correcting for fringing flux which depends upon an assumption concerning optimum focusing is now suggested. It is assumed that optimum focusing conditions are achieved when the ion source and ion collector are located the same distance from the actual field boundaries as would be used for the ideal case wherein there were no fringing flux and are so located relative to the sector apex that the central ray leaves the ion source in a direction normal to one pole-face boundary and enters the ion collector in a direction normal to the other pole-face boundary. Such a condition is illustrated in Fig. 7. There the distances AB and CG are equal to the radius of curvature for the uniform field region which is a condition necessary for the ideal 90° sector-type analyzer. One basis for the above

assumption about optimum focusing conditions is the close correspondence between the geometry stated and the geometry of the ideal case which was used in the derivation of the focusing properties of this type of analyzer. Another basis for the assumption is that as an ion beam of small angular spread reaches the actual pole-face boundary, after passing from the ion source through the fringing flux, the angular and spatial separations of the individual trajectories are approximately the same as would be obtained in the ideal case wherein there were no fringing field. Also the centers of curvature of the trajectories as they pass through the uniform field region will be separated by approximately the same distances as for the ideal case. These latter statements will be seen to be true later when we consider the changes in Eqs. (2) and (3) for ion trajectories of different angles of emergence from the source.

By way of demonstrating the above assumption concerning optimum fringing flux corrections let us suppose it is desired to make the corrections for a 90° sector-type instrument with symmetrical location of ion source and collector. Referring to Fig. 7, AB will be the distance of the ion source from the actual field boundary and will be equal to the radius of curvature chosen for operation. Supposing $h(x)$ to be available it will be possible to obtain $\hat{f}(x)$ and to

use it in the integration of Eq. (2), which will give the deviation of the central ray trajectory from the line AB and will trace its entry into the uniform field region. When the trajectory reaches a point deep enough in the uniform field region that $h(x)=1$, the slope dy/dx may be evaluated and the location of point D , the center of curvature, determined. Now it is clear that we may expect the ion to leave the field in a trajectory exactly similar to the entry one if symmetrical conditions are provided. To do so a line which is at 45°, half the sector angle, with DH , the virtual field boundary, is projected to the actual field boundary. This locates E , the actual sector apex. Now it is seen that exactly symmetrical conditions are provided. The dimension of significance now is EB which locates the distances of the ion source and ion-collector axes from the actual sector apex. This is readily obtained in simple steps, using the location of point D relative to points A and E and to the point of entry of line AB into the uniform field region.

If it is desired to determine the flux corrections for an unsymmetrical system such that the angles θ and γ , as defined in reference 1, are unequal it may be done using the methods of above. In this case it would be necessary to determine the trajectories for two fringing field conditions, i.e., for the ion source and ion-collector sides, and match them in the uniform field region.

For the trajectories and geometry considered so far

$$f(x) = \int_{x_0}^x h(x) dx,$$

that is $\hat{f}(x_0)=0$ so that $(dy/dx)_{x_0}=0$. This is the condition imposed on the central ray, i.e., that it leave the ion source normal to the slits (using such a case as in Fig. 7 where the ion source axis is parallel to the x axis and the pole-face boundary is parallel to the y axis). However, for ions emerging from the ion source at a small angle α with the normal to the slits we will have:

$$f(x) = \int_{x_0}^x h(x) dx + \bar{c},$$

where \bar{c} is a constant to be correlated with the initial slope.²

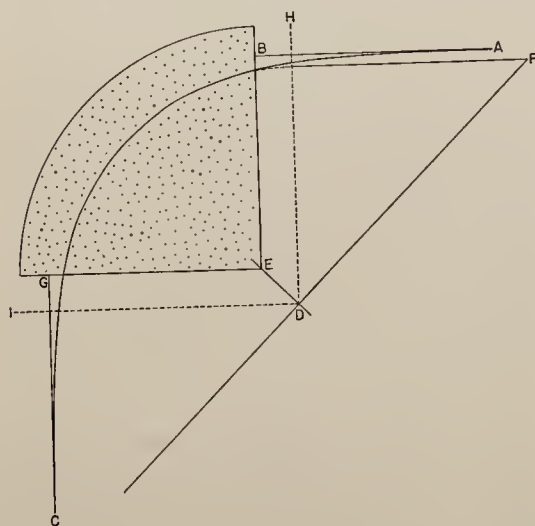


FIG. 7. Geometry of fringing flux corrections for sector-type instrument.

From Eq. (1) we have then:

$$(dy/dx)x_0 = \tan\alpha = \bar{c}/(r^2 - \bar{c}^2)^{1/2}.$$

Since for small α (as would be true for an actual ion beam) $r \gg \bar{c}$ we obtain $\bar{c} = r \tan\alpha$.

The virtual boundary displacement for such a trajectory will be obtained from:

$$r = \pm \int_{x_0}^{\bar{x}} h(x) dx + r \tan\alpha.$$

Since $h(x)$ is equal to unity in the uniform field region we have for the virtual boundary displacement $d(\alpha)$ for a trajectory of starting angle α

$$d(\alpha) = d(0) + r \tan\alpha.$$

The separation then between the virtual boundary effective for a trajectory of starting angle α and the virtual boundary effective for the principal ray is seen to be $r \tan\alpha$ which is the same as is obtained for the ideal case. This result is part of the basis for the assumption above concerning optimum focusing conditions.

The separation in the y direction at the pole-face boundary between the central ray and one emerging from the ion source with angle α may be seen to be approximately the same as for the ideal case. To calculate this difference we integrate Eq. (2) for the two cases. We get then for the separation

$$\Delta y = \bar{c} \int_{x_0}^0 \frac{dx}{(r^2 - (\bar{f} + \bar{c})^2)^{1/2}}.$$

However, since $r \gg \bar{c}$ and since $\bar{f}(x)$ is always found to be small enough so that $(r^2 - (\bar{f} + \bar{c})^2)^{1/2} = r$ to within about 2 percent or better for all of

$0 < x < x_0$ we have $\Delta y = \bar{c}x_0/r$ which is equal to $x_0 \tan\alpha$, the same value as for the ideal case.

By use of Eq. (2) and the approximations above we may show that the angular spread of the trajectories as they enter the uniform magnetic field region is approximately the same for the actual case as for the ideal one. We shall denote the slope angle at $x=0$ as β . Then from Eq. (2) we have:

$$\tan\beta = (\bar{f}(0) + \bar{c}) / (r^2 - (\bar{f}(0) + \bar{c})^2)^{1/2}. \quad (5)$$

By differentiation we get

$$(1 + \tan^2\beta)\Delta\beta = r^2\Delta\bar{c} / (r^2 - (\bar{f}(0) + \bar{c})^2)^{1/2}.$$

Using Eq. (5) and the approximation of above this reduces to $\Delta\beta = \Delta\bar{c}/r$. For the central ray and one emerging from the source at a small angle α we have $\Delta\bar{c} = \bar{c} = r \tan\alpha = r\alpha$ so that $\Delta\beta = \alpha$; i.e., the trajectories will have approximately the same angular divergence at $x=0$ as at the ion source. An actual calculation of the angular spread at $x=0$ for one of the cases for which d was evaluated above is illuminating. The conditions used were: $n=10$, $r=5$, and $\alpha=3^\circ40'$. For this case $\bar{f}(x)$ was calculated for the region between the ion source and the actual field boundary using the values of $h(x)$ shown in Fig. 6. From this and from Eq. (5) it was determined that the angle at $x=0$ between the tangents of the two trajectories, was $3^\circ44'$, i.e., the same as the starting angle to within less than 2 percent discrepancy.

The author is indebted to Dr. M. Muskat for several discussions of this problem and to Dr. P. D. Foote, Executive Vice-President of Gulf Research and Development Company, for permission to publish this material.

LANCASTER PRESS, INC., LANCASTER, PA.

Oct. 19, 1948.

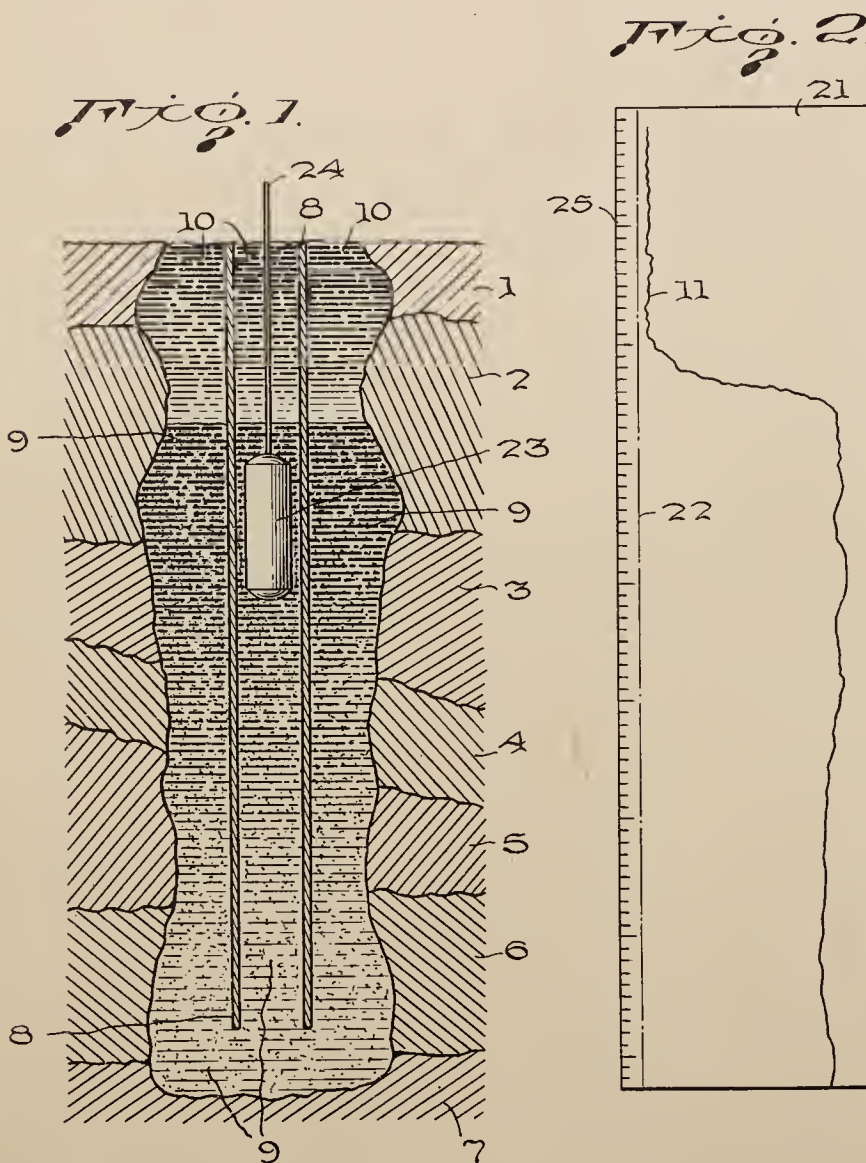
N. D. COGGESHALL

2,451,472

METHOD OF CEMENTING WELLS

Filed April 16, 1945

2 Sheets-Sheet 1



Inventor
NORMAN D. COGGESHALL

By *G. M. Houghton*
his Attorney

Oct. 19, 1948.

N. D. COGGESHALL

2,451,472

METHOD OF CEMENTING WELLS

Filed April 16, 1945

2 Sheets-Sheet 2

Fig. 3.

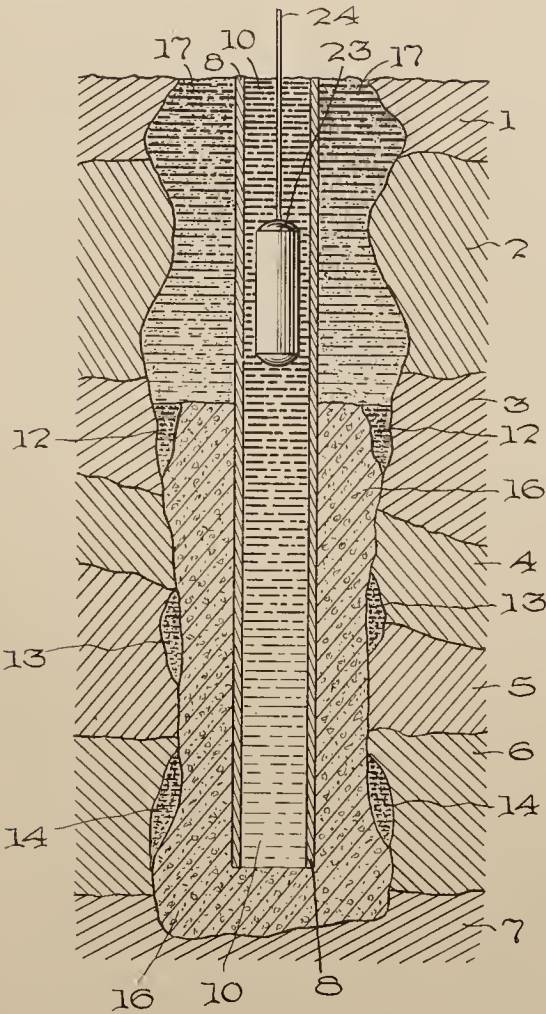
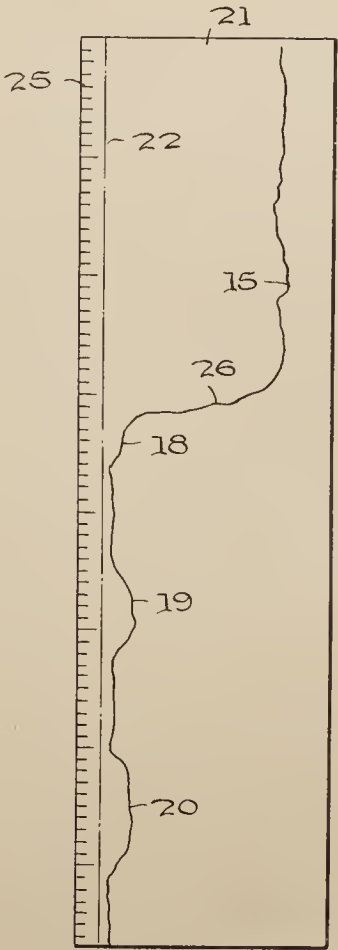


Fig. 4.



Inventor
NORMAN D. COGGESHALL

By G. M. Houghton
Attorney

UNITED STATES PATENT OFFICE

2,451,472

METHOD OF CEMENTING WELLS

Norman D. Coggeshall, O'Hara Township, Allegheny County, Pa., assignor to Gulf Research & Development Company, Pittsburgh, Pa., a corporation of Delaware

Application April 16, 1945, Serial No. 538,440

1 Claim. (Cl. 166—22)

1

This invention concerns a method of procedure for use in the cementing of oil wells, and in particular it relates to a cementing method by which it is possible to subsequently determine the completeness of the cement job by the application of gamma ray logging.

Present day oil well completion practice consists in drilling the well to final depth through the producing formation, lowering a casing of smaller diameter than the borehole, and cementing the casing in the hole by forcing cement down through it and up into the annular space between the casing and the wall of the hole. The process of cementing the casing results in a sheath of cement around the outside of the casing extending from the bottom of the hole some distance up beyond the producing strata. The cemented casing is then perforated at the proper level by means of a gun perforator which produces holes through both the casing and the cement sheath, and it is through these holes that the oil and gas are produced. The cement sheath thus serves the extremely important function of blocking off the strata adjacent to the oil bearing zones. This is necessary because these adjacent strata often contain water or gas in such quantities that if such blocking were not effected the oil production would be seriously impeded.

Often the cementing operation discussed above is unsuccessful in that it does not completely block off the strata in the critical region. This failure is generally due to the fact that the cement, as it comes up around the casing, pushing the mud before it, does not completely clean out the mud as it goes along. This results in streaks or sheaths of mud which subsequently provide a means of communication between the oil bearing strata and others that contain water or gas. Heretofore it has been possible to determine if the cementing has been successful only after the casing is perforated and a production test made.

The object of this invention is to provide a method of determining the completeness of a well cementing operation.

A secondary object of this invention is to provide a method of locating any channels which may be left in the section of a well which has been cemented.

A further object of this invention is to provide a method of determining the completeness of a well cementing operation in the region to be perforated and before such perforating is attempted.

These objects are accomplished by the practice of this invention in the following manner. The first step in the procedure is to replace the drill-

2

ing mud in the open hole, in the region to be cemented, by a mud of similar physical properties, such as viscosity and density, but having added to it a radioactive material, such as finely ground carnotite in suspended form or a salt of radium or other radioactive element in a dissolved form. This may be done either by spotting the radioactive mud through the drill pipe just before removing the latter, or by forcing the radioactive mud down through the casing after it is lowered into the hole. The first procedure is to be preferred because it results in obtaining a larger quantity of radioactive material in the mud cake. The cementing operation is then performed and it is expected that the cement will force all the radioactive mud on up the annular space ahead of it. If any uncemented pockets remain, they may subsequently be detected by running a radioactivity log, e. g., a gamma ray log.

A further understanding of the invention may be obtained by reference to the drawings in which

Figure 1 shows a cross section of the borehole before the cementing operation is performed;

Figure 2 is an illustrative gamma ray log curve obtained before cementing;

Figure 3 is a cross section of the borehole after cementing; and

Figure 4 is a gamma ray log obtained after cementing and illustrates how channels in the cement are indicated.

Figure 1 illustrates the situation which would exist at the bottom of a well after the step of adding the radioactive mud. Here numerals 1, 2, 3, 4, 5, 6 and 7 represent the different strata traversed by the lower end of the borehole and 8 represents the casing suspended in the hole with its end near the bottom. For simplicity, the upper part of the well and the usual surface equipment are not shown, since these are conventional and do not form a part of this invention. The radioactive mud 9 is shown as having been spotted at the bottom of the hole, either through the casing 8 or through the drill pipe prior to the latter's removal. The level of radioactive mud 9 inside and outside the casing are shown as being the same, but they need not necessarily be so, and these levels depend on the manner of introducing the radioactive mud 9. The inert mud forced upward by the radioactive mud is designated by numeral 10.

With the radioactive mud in the bottom of the hole as shown in Figure 1, a gamma ray detector 23 lowered into the borehole on cable 24 would give an intensity response such as illustrated in Figure 2, which is a chart obtained from a con-

ventional gamma ray logging apparatus. Numeral 11 represents a gamma ray intensity curve drawn by the apparatus on chart 21 in the customary manner. The zero line of the curve is indicated by line 22, and along the left hand edge of the chart a record of depth 25 tells the position of the detector at which the indicated intensities are observed. Here it is seen that the intensity increases to a very high value at the level where the bulk of the active mud begins, and it continues at a high intensity down the hole. The presence of the casing in the hole will not appreciably interfere, as the gamma rays of carnotite and radium, as well as other materials which would be used, are of sufficient hardness to penetrate the iron easily.

The next step in the procedure is to carry out the cementing as in any other well. The cement is forced down through the casing, and as it comes up the annular space, it forces the mud in the borehole ahead of it. If the cementing operation is "perfect," all the mud in the lower region of the hole will be forced ahead of the cement. If, however, the operations are imperfect, some mud will remain in the bottom part of the hole in the form of streaks or massive accumulations. Such a situation is shown in Figure 3.

In Figure 3 numeral 16 represents the cement which has been forced down the casing 8, while 17 represents the radioactive mud which has been forced along ahead of the cement. Accumulations or bodies of the radioactive mud which have not been displaced by the cement are illustrated at 12, 13 and 14. Such regions of mud as 12, 13 and 14 are undesirable as they later form channels which may admit excessive gas or water. By establishing the presence of imperfections 12, 13 and 14 and determining their location, the necessary squeeze cementing may be done in these regions of poor cementing prior to the perforation for production, thus saving time and the cost of poor completions.

The method of detecting such regions of poor cementing as 12, 13 and 14 is to again lower a gamma ray detector 23 into the casing 8 (shown in Figure 3 to be cleaned of cement) and to obtain a log of the gamma ray intensity versus depth as before. Such a curve is indicated by numeral 15 in Figure 4. The large intensity indicated at region 15 corresponds to the radioactive mud which has been forced ahead of the cement. A marked decrease is observed on the curve at point 26 opposite the cement, since the cement is not radioactive. Further down on the graph, the regions of anomalous intensity 18, 19, 20 are due to the radioactive mud in regions 12, 13 and 14, respectively. The regions of defective cementing 12, 13 and 14 may thus be located and corrective measures taken before the well is put in production.

In carrying out my invention, it is not only possible to locate regions of defective cementing but it is obvious that the method at the same time also tells the level to which the cement has been forced in the annular space around the casing. This is indicated by the decrease in curve 15 observed at point 26 opposite the top of the cement. This information is of considerable importance in all cementing operations.

The method of my invention may also be used advantageously in carrying out cementing operations further up the borehole. Thus, if a well has been producing from an upper horizon and begins to produce excessive water, it may be advisable to shut it off with cement. In perform-

ing such a cement job, I would first spot the radioactive mud opposite the perforations leading to this horizon and apply pressure to force the radioactive mud through the casing into the annular space behind it. Any excess is then removed from inside the casing and the usual cement spotted at the proper level with a conventional squeeze tool and forced through the casing into the annular space. The radioactive mud will be pushed ahead of the cement both above and below the cement plug. The top and bottom levels of the cement in the annular space may afterward be located by running a gamma ray log, and any intermediate improperly sealed regions will also show on the log due to the radioactive mud remaining in such imperfections.

This method of studying cementing may be contrasted with the procedure hitherto used of making the cement radioactive and attempting to interpret the resulting gamma ray curve regarding the success of the cementing operation. The latter method does not definitely establish the presence of incompletely cemented regions. However, the method of my invention does make it possible to determine whether the cementing is incomplete by indicating the presence of mud when the latter is not completely displaced.

The scope of this invention is not to be limited to the use of radioactive muds merely as replacement for the original drilling mud prior to cementing. It is also to include the use of radioactive tracers in the drilling mud with subsequent logging to determine the degree to which it has been displaced by the cement.

My invention may furthermore be advantageously used as a step in the completion of a cased well, said step insuring that a successful completion will result. By employing my invention channels and crevices in the cement may be avoided by perforating and recementing those regions where radioactive mud is found to remain undisplaced by the cement. This may be repeated until all such radioactive mud is effectively displaced whereupon no channels will remain. Subsequent perforations of the producing horizon will allow uncontaminated fluid to enter the well.

What I claim as my invention is:

A method of cementing a well so that the degree of completion of the cementing operation may be determined which comprises replacing the normally used drilling mud in the region to be cemented with a radioactive drilling mud introduced through the drill stem, removing the drill stem, inserting the casing into the well, measuring the variation with depth of the radioactivity in the well, forcing cement into place around the casing so as to displace the radioactive drilling mud in the annular space around the casing and again measuring the variation with depth of the radioactivity in the well, whereby by comparison with the first said measurement the location of undisplaced radioactive drilling mud may be determined.

NORMAN D. COGGESHALL.

REFERENCES CITED

The following references are of record in the file of this patent:

UNITED STATES PATENTS

Number	Name	Date
1,563,520	Owen	Dec. 1, 1925
2,320,892	Scherbatskoy et al.	June 11, 1943
2,339,129	Albertson	Jan. 11, 1944

Infrared Analysis of Organic Mixtures

Using C—H Band Structure Resolved by a
Lithium Fluoride Prism

ELEANOR L. SAIER AND NORMAN D. COGGESHALL
Gulf Research & Development Company, Pittsburgh, Pa.

Reprinted from
ANALYTICAL CHEMISTRY
Vol. 20, Page 812, September 1948

Infrared Analysis of Organic Mixtures

Using C—H Band Structure Resolved by a
Lithium Fluoride Prism

ELEANOR L. SAIER AND NORMAN D. COGGESHALL
Gulf Research & Development Company, Pittsburgh, Pa.

Reprinted from

ANALYTICAL CHEMISTRY

Vol. 20, Page 812, September 1948

Reprinted from ANALYTICAL CHEMISTRY, Volume 20, Page 812, September 1948
Copyright 1948 by the American Chemical Society and reprinted by permission of the copyright owner

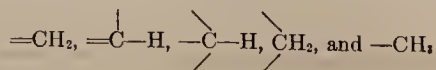
Infrared Analysis of Organic Mixtures

Using C—H Band Structure Resolved by a Lithium Fluoride Prism

ELEANOR L. SAIER AND NORMAN D. COGGESHALL
Gulf Research & Development Company, Pittsburgh, Pa.

THE present-day availability of lithium fluoride prisms for the various commercially available infrared spectrometers extends the usefulness of infrared spectroscopy very greatly. It is well known (1, 9) that lithium fluoride provides a large increase in dispersion over sodium chloride in the 2 to 5.5 μ (5000 to 1820 cm^{-1}) region. This brings out structure characteristics, particularly in the spectra due to the stretching vibrations of the C—H valence bonds. Fox and Martin (6) and Rose (8) have shown that different types of substitutions in hydrocarbons

produce different, recognizable C—H absorption bands. Fox and Martin considered the following groups:



The bands due to these groups all lie near 3.4 μ and are so closely spaced that they are not satisfactorily resolved in the ordinary instrument that employs a sodium chloride prism.

With a prism of sodium chloride the usual infrared spectrometer does not resolve the structure of the absorption bands due to C—H groups. A lithium fluoride prism which possesses high dispersion in this spectral region resolves these bands very satisfactorily and makes them available for analytical determinations. Such a use of a lithium fluoride prism has been explored and a number of specific analyses have been developed. This method of analysis allows the examination of compounds and mixtures in dilute solutions of carbon tetrachloride as well as the analysis of compounds subject to complex formation such as hydrogen bonding and the analysis of mixtures possessing large differences of intensity of absorption in the sodium chloride region. It makes possible a new approach to systems of very similar isomers; and it extends the usefulness of instruments equipped with such a prism for molecular structure determination work.

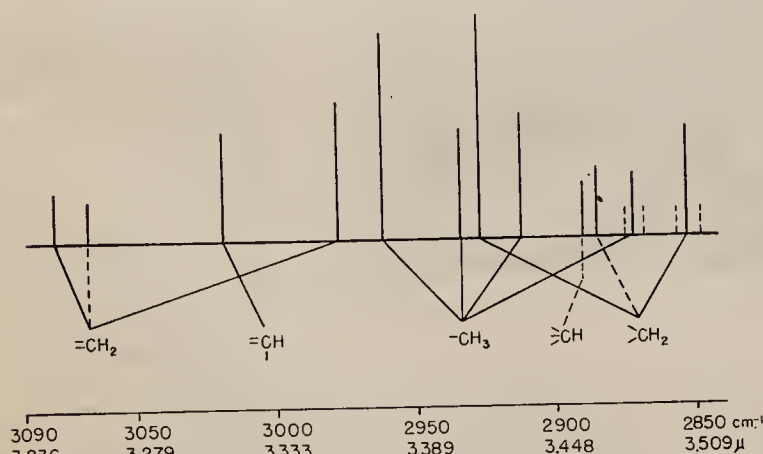


Figure 1. Absorption Frequencies Observable for Different Classes of C—H Groups in Hydrocarbons When Sufficient Resolution Is Achieved with Lithium Fluoride Prism

Data from Fox and Martin (6)

The use of a lithium fluoride prism, however, makes possible the utilization of the C—H structural bands for analytical applications. The present paper reports some of the results obtained in these applications.

Figure 1 presents an absorption band diagram synthesized from the empirical data of Fox and Martin (6) for hydrocarbons. This shows the positions and multiplicity of the absorption bands due to the various types of carbon-hydrogen groupings. The relative heights of the lines are some indication of the intensities of the observed absorption bands. However, neither these nor the wave-length positions may be regarded as exact, as variations occur in going from compound to compound. The dashed lines below the base line represent absorption bands observed only in some of the cases studied. The dashed lines above the base line are for the cases where a single band splits into a doublet. Despite these limitations it is evident from the figure that with the satisfactory resolution of these bands, which is possible using a lithium fluoride prism, the scope of applications of infrared spectroscopy may be greatly enlarged. As more data become available in the future it will be possible to determine the specific limitations and generalities of such data as those presented in Figure 1.

It is to be observed in Figure 1 that the absorption bands for the saturated carbon-hydrogen groupings occur at longer wave lengths than do those for the unsaturated groupings. This immediately suggests the use of the C—H bands for the quantitative analysis of mixtures of olefins and paraffins. These systems may be handled, as well as ones containing aromatics and oxygenated compounds. Because of the relatively narrow spectral

region and the limited number of bands available, the number of components per sample cannot be as large as can be handled when a sodium chloride prism is used in the longer wave-length region. However, the advantages of the present method lie in the handling of special types of mixtures which often have only a small number of components.

One advantage in the use of the C—H absorption band structure lies in the availability of an excellent solvent for this region. Carbon tetrachloride is very transparent throughout this region and many compounds and systems of compounds are soluble in it. It is so transparent that cells up to several centimeters in length can be used. This makes it possible to examine compounds and mixtures in dilute solutions. Under these conditions the inherent difficulties due to molecular association such as hydrogen bonding may be avoided. Also it makes possible the simultaneous analysis in the same mixture of compounds that may have large differences of intensity of absorption in the longer wave-length regions such as paraffins and some of the polar or unsaturated materials. In some cases, mixtures of homologous compounds which do not have appreciably different spectra in the long wave-length region can be satisfactorily analyzed by this method. A further advantage of the method is a spectrometric one. Because the spectral region used is near the maximum for the radiation curve, the scattered light is very weak. In fact, it is so weak that the authors have detected none at all. This eliminates a correction procedure that must be applied at the longer wave lengths for best results. A further advantage lies in the extension of usage to analytical problems of an instrument equipped with a lithium fluoride prism and otherwise primarily used for molecular structure determination work. The use of the samples in solution also gives greater accuracy, in that it allows a true correction for the absorption, reflection, and scattering of the radiation beam by the cell itself. This is done by comparing the transmittance of the sample in solution with the transmittance of the solvent alone.

The accuracy attainable for a specific mixture depends upon the differences in intensity of absorption that can be utilized. In some cases where unique absorption bands can be found, the average errors are of the order of 0.1 to 0.2% of total sample. Where the wave length and intensity discrimination are not very good, the average errors may be of the order of 1.0% of total sample. High accuracy was not an all-important aim of the present work. Rather, a compromise in reasonable accuracy, rapidity of analyses, and ease of analyses by nontechnically trained personnel was desired. All calibration data and synthetic samples were processed under routine conditions.

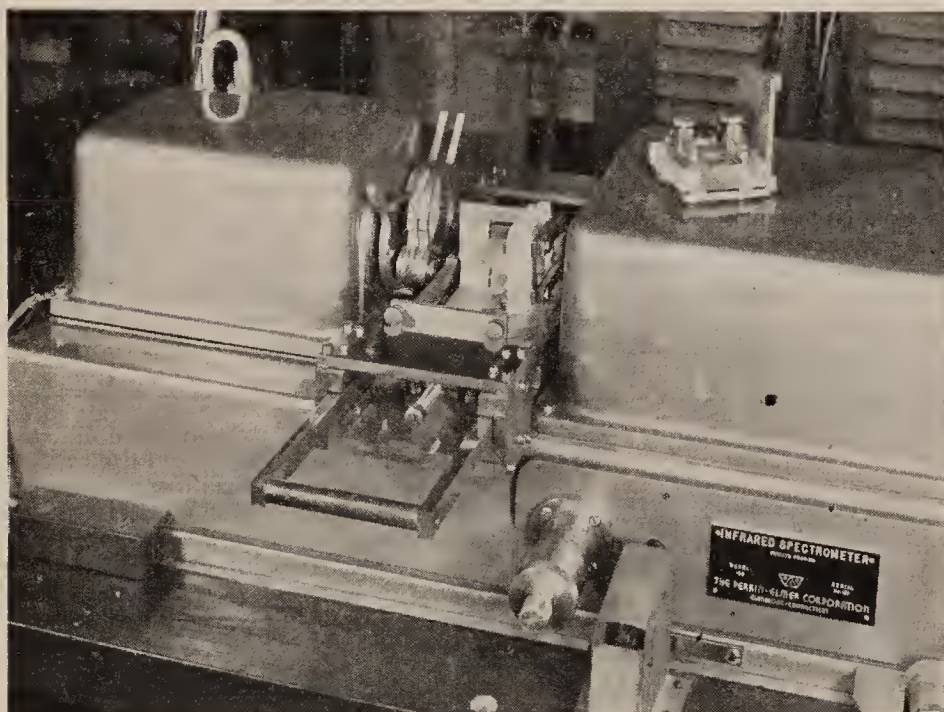


Figure 2. Liquid Absorption Cells and Mounting Arrangements Used in Analytical Work

An assay of the accuracy of the method under routine conditions may be made from the results reported for the synthetic samples below.

EXPERIMENTAL METHODS AND TECHNIQUES

The instrument on which the present work was done was a Perkin-Elmer Model 12B infrared spectrometer. Sodium chloride and lithium fluoride prisms are used in it interchangeably. A cell-in-cell-out arrangement is used wherein the absorption cells are securely clamped to a movable carriage. In Figure 2 may be seen one of the cells clamped in place and another one resting on top of the instrument. The type of cell used has been described (3). The carriage arrangement is the same as used in routine gas analysis (4). The liquid cells are equipped with a mounting frame which allows them to be held in the movable carriage by means of thumbscrews. The cell employs two needle valves, one fabricated to act as a filling piston when loading the cell. These cells have interchangeable parts and are easily fabricated and repaired. The thickness used most commonly in the present work was 0.006 inch.

For quantitatively measuring the radiation intensities at the various wave lengths, the same system of null measurements (4) was used. A high sensitivity galvanometer is used merely as an indicator and the thermocouple signals are balanced out by means of a low voltage obtained from a resistor and potentiometer network. Difficulties due to nonlinearity or change of sensitivity of the high sensitivity galvanometer are thereby eliminated. The instrument is equipped with an Amphenol connector for the thermocouple outlet. With this arrangement either the galvanometer and null system equipment or the automatic recorder may be connected at will. It has been found very convenient to use the automatic recorder to obtain a spectrum of the sample throughout the wave-length region used. This may then be examined to determine what compounds are present or, if the sample is a calibration standard, to determine the most desirable wave lengths to use in the analytical procedure. However, for quantitative measurements of transmittance at specific wave lengths consistently more accurate data are obtained manually, using the null method. The same equipment and general methods have been in use here for several

years for the quantitative analysis of multicomponent mixtures of hydrocarbons, using a sodium chloride prism and the longer wave-length region.

Tests for the scattered radiation intensity were made by the total absorber method (2). For some of these an absorption cell of 0.036-inch thickness was used. Almost any material containing C-H groups is suitable as solute for such tests in the 3.4μ region, provided a strong enough concentration is used.

In the present work all dilutions were made volumetrically in graduated pipets and burets. In certain cases care must be taken to follow a definite procedure in making the calibration blends, diluting the samples, and obtaining the data, in order to avoid trouble caused by differences in evaporation rates. It is well known (7) that the high boiling points of the simple alcohols, in comparison with other compounds of similar molecular weights,

are due to the hydrogen bonding forces between the molecules. These hydrogen bonding forces, due to the hydroxyl groups, are responsible for molecular association between the molecules and the attendant reduction in vapor pressure. However, in dilute solutions in a solvent such as carbon tetrachloride the relative degree of hydrogen bonding is reduced because of the greater average distance between hydroxylated molecules. Consequently, the alcohol molecules in such a solution will escape much more rapidly, on a relative basis, than from a concentrated solution. This effect is so strong that the same procedure as regards time intervals must be used on the samples to be analyzed and on the calibration blends. Otherwise errors will arise due to loss of some of the material by evaporation. In Figure 3 may be seen the optical density plotted as a function of the number of times analyzed for a 2.5% by volume solution of ethyl alcohol in carbon tetrachloride. This sample was kept in a glass-stoppered bottle and analyzed on successive days. During these tests the concentration of ethyl alcohol changed radically. The

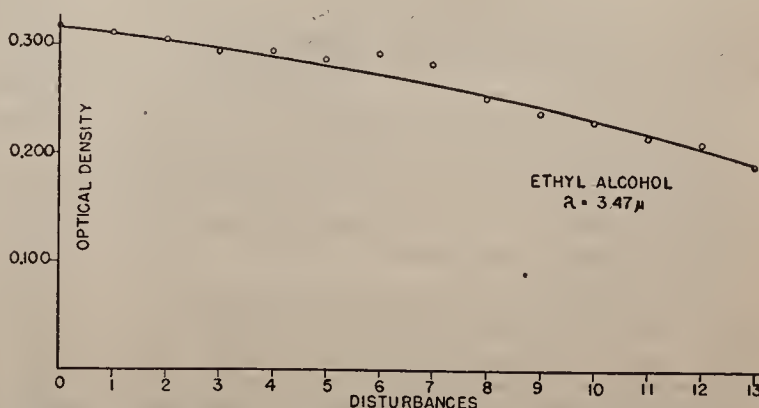


Figure 3. Optical Density of Dilute Solution of Ethyl Alcohol in Carbon Tetrachloride Solution as a Function of Number of Times Analyzed (Disturbances)

authors have found it most advisable to obtain the data for such a solution on the same day as it was prepared.

As Beer's law of absorption is obeyed by the compounds under investigation the calculations and handling of data are straightforward. The absorption, reflection, and scattering effects due to the cell may be eliminated by comparing the transmittance of the sample in solution with the transmittance of the solution alone. Actually this is accomplished by a suitable subtraction of optical densities.

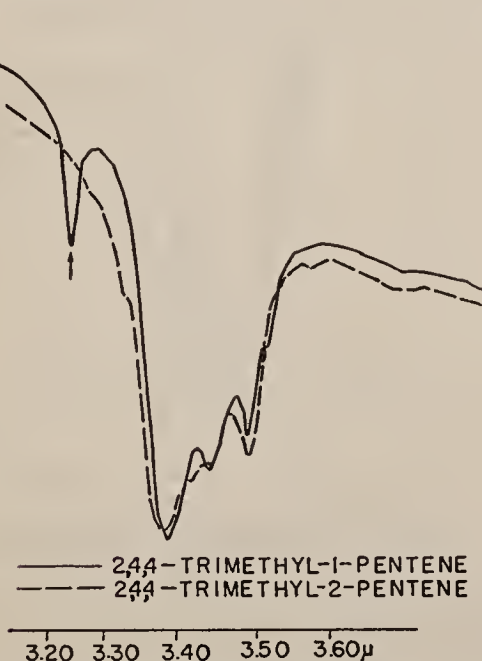


Figure 4. Infrared Absorption Spectra in C—H Region of Isomeric Trimethylpentenes

To see this let us consider the transmittance of a solution of pure compound at wave length λ_i . We have for the solution:

$$D_i = \log (I_0/I) = A_i C + K_i \quad (1)$$

where D_i is the optical density, I_0 is the incident radiation intensity, I is the transmitted radiation intensity, A_i is the calibration coefficient for the pure compound at wave length λ_i , C is the concentration of the solute, and K_i is an attenuation factor due to the absorption, reflection, and scattering by the cell and absorption by the solvent. Since the concentrations of solute used are small, between 1 and 6% for the present work, the K_i in Equation 1 may be evaluated by obtaining the optical density for the cell filled with solvent only. A subtraction of this value from the D_i of Equation 1 then gives the component of optical density due to the compound. With this method of obtaining the optical density, Beer's law was tested for a number of the compounds in the examples below and found to hold in each case.

With the above method of obtaining true optical densities and with the additivity of optical densities that occurs when Beer's law is obeyed, simple equations of the type below are obtained. Here a three-component system is assumed.

$$\begin{aligned} D_1 &= A_{11}C_1 + A_{12}C_2 + A_{13}C_3 \\ D_2 &= A_{21}C_1 + A_{22}C_2 + A_{23}C_3 \\ D_3 &= A_{31}C_1 + A_{32}C_2 + A_{33}C_3 \end{aligned} \quad (2)$$

Here D_1, D_2, D_3 refer to the true optical densities of the mixture at the three wave lengths chosen for operation; A_{11} is the calibration coefficient of the first compound at the first wave length, A_{22} is the calibration coefficient of the third compound at the second wave length, etc.; and C_1, C_2 , and C_3 are the concentrations of the three compounds. These equations may be readily solved for the concentrations by matrix methods (2) or by successive

approximations. In the method of successive approximations concentrations C_2 and C_3 are assumed to be zero in the first equation and it is solved directly for C_1 . This value is used in the second equation with the assumption that C_3 is zero and a value for C_2 is determined. Next the values of C_1 and C_2 obtained in the first two steps are used in the third equation and it is solved for C_3 . The cycle is repeated with the values of C_2 and C_3 from the latter two steps substituted in the first equation and a new value of C_1 is determined. The second equation is then solved for C_2 using the most recent values of C_1 and C_3 , etc. Several cycles can be quickly run with a semi-automatic or automatic calculating machine in a few minutes.

A wave-length calibration of the C—H region was prepared from the data of Fox and Martin (5, 6). No attempt was made to make a highly precise calibration. In practice the wave lengths for specific analyses are specified in terms of the instrument vernier readings. For that reason specific wave lengths are not given below. For some of the examples the wave-length values may be appraised from the figures. It is believed that these may be relied on to within about 0.005μ or better.

APPLICATION TO SPECIFIC ANALYSES

From the information given in Figure 1 a prediction may often be made as to whether or not a specific mixture can be analyzed. For example, a binary mixture containing two compounds with differences in types of unsaturated groups may generally be analyzed with ease.

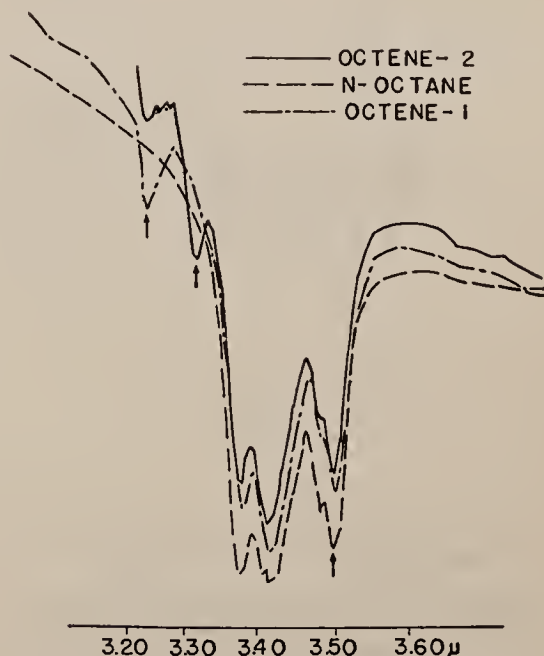


Figure 5. C—H Structure Absorption Bands for 2-Octene, *n*-Octane, and 1-Octene

A specific example of this is a mixture of similarly branched trimethylpentenes. In Figure 4 may be seen the spectra of 2,4,4-trimethyl-1-pentene and 2,4,4-trimethyl-2-pentene. In these curves, which are reproductions of the automatically recorded spectra, the transmitted energy is plotted as a function of wave length. Here, as indicated by the arrow, may be seen the absorption band due to the terminal $=CH_2$ group in one of the compounds. Actually, the difference in absorption is great enough here to permit taking data at this point only. Then instead of having two equations of the type of Equations 2 we have but one plus the equation:

$$C_1 + C_2 = C \quad (3)$$

where C is the concentration of sample in solution. The results of analyses of two synthetic samples may be seen in Table I.

Table I. Analyses of Synthetic Mixtures of Binary Mixture of Trimethylpentenes

Compound	Synthetic, %	Calculated, %	Difference, %
2,4,4-Trimethyl-1-pentene	50.0	50.4	0.4
2,4,4-Trimethyl-2-pentene	50.0	49.6	-0.4
2,4,4-Trimethyl-1-pentene	30.0	30.6	0.6
2,4,4-Trimethyl-2-pentene	70.0	69.4	-0.6

Table II. Analyses of Synthetic Mixture of Hydrocarbons Containing Paraffins and Unsaturates

Compound	Synthetic, %	Calculated, %	Difference, %
<i>n</i> -Octane	20.0	18.9	-1.1
2-Octene	30.0	31.0	1.0
1-Octene	50.0	50.1	0.1
<i>n</i> -Heptane	50.0	49.9	-0.1
Benzene	50.0	50.1	0.1
<i>n</i> -Heptane	75.0	75.1	0.1
Benzene	25.0	24.9	-0.1



Figure 6. Infrared Absorption Structure in C-H Region for Benzyl Alcohol, *n*-Octanol, and Methyl Ethyl Ketone

Continuing with hydrocarbon systems we see in Figure 5 that satisfactory wave-length discrimination is obtainable for the ternary system of *n*-octane, 2-octene, and 1-octene. The wave lengths used for analysis are indicated by the arrows. At about 3.26μ may be seen the band characteristic of the terminal $=CH_2$ group of 1-octene, at about 3.32μ the band characteristic of the $=CH$ group of 2-octene, and at about 3.50μ the band characteristic of the CH_2 groups, which is stronger for *n*-octane than for the others. The 2-octene shows some of the bands characteristic of the other compounds, because the sample used for recording was not pure.

Although definite differences in spectra are found, the differences in intensity of absorption are not great (Figure 5). Despite this, fair accuracy is obtainable, as may be seen in Table II.

Table II also gives the results for two synthetic samples of the binary system of *n*-heptane and benzene, for which considerably better accuracy is possible.

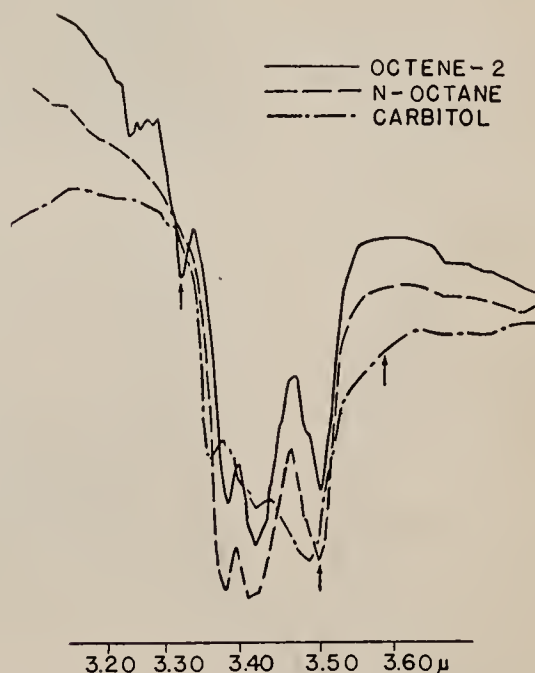


Figure 7. C-H Structure of Absorption Bands for 2-Octene, *n*-Octane, and Carbitol

In the preceding type of examples predictions could be made in advance concerning the success of the method. In other cases, such as the examples discussed below, an idea of the feasibility cannot be reliably formulated until the spectra of the pure compounds are obtained. A number of ternary mixtures of particular interest in the study of azeotropes may be easily analyzed. In general, these systems contain a paraffin, an aromatic or olefin, and an oxygenated compound. Other systems containing all oxygenated compounds may in some cases be analyzed with good accuracy.

In Figure 6 may be seen the spectra in the 3.4μ region of benzyl alcohol, *n*-octanol, and methyl ethyl ketone. Here it is observed that three distinct and unique wave lengths, indicated by arrows, may be chosen for analysis. Table III gives the results on synthetic samples made up to test the accuracy on such a system.

Table III. Analyses of Synthetic Mixtures of the System: *n*-Octanol-Methyl Ethyl Ketone-Benzyl Alcohol

Compound	Synthetic, %	Calculated, %	Difference, %
<i>n</i> -Octanol	30.0	30.3	0.3
Methyl ethyl ketone	30.0	29.4	-0.6
Benzyl alcohol	40.0	40.3	0.3
<i>n</i> -Octanol	25.0	24.5	-0.5
Methyl ethyl ketone	50.0	50.5	0.5
Benzyl alcohol	25.0	25.0	0.0

In some cases the spectra of the compounds in the mixtures to be analyzed have such similar spectra that distinctive wave lengths may not be found, but sometimes it is possible to utilize the difference of intensity on the shoulders of the bands for analytical application.

An example of such a case is seen in Figure 7, which is for the system 2-octene-*n*-octane-Carbitol (diethylene glycol monoethyl ether). Here the arrows again illustrate the wave lengths used for analysis. For the Carbitol, utilization is made of its increased absorption in the long wave-length shoulder of its

Table IV. Analyses of Synthetic Samples of Ternaries of *n*-Octane, 2-Octene, Carbitol, and Ethylbenzene

Compound	Synthetic, %	Calculated, %	Difference, %
Carbitol	47.4	47.1	-0.3
<i>n</i> -Octane	18.0	17.6	-0.4
2-Octene	34.6	35.3	0.7
Carbitol	37.5	37.2	-0.3
<i>n</i> -Octane	25.0	25.3	0.3
Ethylbenzene	37.5	37.5	0.0

Table V. Analyses of Synthetic Samples of Ternaries Containing a Paraffin, an Unsaturate, and an Oxygenated Compound

Compound	Synthetic, %	Calculated, %	Difference, %
Methylcyclohexane	25.0	24.6	-0.4
Methyl ethyl ketone	35.0	34.7	-0.3
Toluene	40.0	40.7	0.7
Dichloroethyl ether	70.0	68.7	-1.3
<i>n</i> -Octane	10.0	10.9	0.9
Ethylbenzene	20.0	20.4	0.4
Cyclohexane	30.0	30.7	0.7
Ethyl alcohol	40.0	39.4	-0.6
Benzene	30.0	29.9	-0.1
Hexanol	40.0	40.3	0.3
<i>n</i> -Heptane	20.0	21.0	1.0
Heptenes (mixture)	40.0	38.7	-1.3

Table VI. Analyses of Synthetic Samples of Binary Mixtures of Methyl and Ethyl Alcohol

Compound	Synthetic, %	Calculated, %	Difference, %
Methyl alcohol	51.6	52.0	0.4
Ethyl alcohol	48.4	48.0	-0.4
Methyl alcohol	91.4	92.1	0.7
Ethyl alcohol	8.6	7.9	-0.7

C—H absorption region. Distinct bands near 3.40μ for *n*-octane are available but are not used, because the absorption there is too strong at the concentrations necessary to bring out adequate absorptions at the other wave lengths. The results for this system as well as those for a closely similar system in which the 2-octene is replaced by ethyl benzene may be seen in Table IV. In this latter system the difference of absorption intensity on the long wave-length shoulder was again utilized.

In the preceding discussion a few specific types of analyses found to be practical have been enumerated and the results given on some synthetic mixtures. The practicality of the method for such systems can best be determined after the absorption bands are automatically recorded. In Table V are given a few more results on other systems for which the spectra will not be shown. In Table VI are given the results of tests on synthetic samples of binary mixtures of methyl and ethyl alcohol.

The attainable accuracy depends upon the particular system being analyzed. The method has been found to give satisfactory results for almost all binary and ternary systems investigated. It is also suitable for the analysis of gas mixtures. It considerably augments the usefulness of the absorption spectroscopic techniques in use at this laboratory and is now used as a routine procedure. The time required per sample is approximately the same, except for the dilutions, as for analyses by infrared when a sodium chloride prism and the longer wave lengths are used.

ACKNOWLEDGMENT

The authors wish to express acknowledgment to Paul D. Foote, executive vice president of Gulf Research and Development Company, for permission to publish this material.

LITERATURE CITED

- (1) Barnes, R. B., McDonald, R. S., Williams, V. F., and Kinnaird, R. F., *J. Applied Phys.*, **16**, 77 (1947).
- (2) Brattain, R. R., Rasmussen, R. S., and Cravath, A. M., *Ibid.*, **14**, 418 (1943).
- (3) Coggeshall, N. D., *Rev. Sci. Instruments*, **17**, 343 (1946).
- (4) Coggeshall, N. D., and Saier, E. L., *J. Applied Phys.*, **17**, 450 (1946).
- (5) Fox, J. J., and Martin, A. E., *Proc. Roy. Soc. (London)*, **162**, 419 (1937).
- (6) *Ibid.*, **175**, 208 (1940).
- (7) Pauling, L., "Nature of the Chemical Bond," Chap. IX, Ithaca, N. Y., Cornell University Press, 1944.
- (8) Rose, F. W., *Bur. Standards J. Research*, **20**, 129 (1938).
- (9) Wright, N., *Rev. Sci. Instruments*, **15**, 22 (1947).

RECEIVED JANUARY 28, 1948.

PRINTED IN U. S. A.

Dec. 14, 1948.

M. MUSKAT ET AL

2,455,940

METHOD OF GEOPHYSICAL EXPLORATION BY MICROWAVES

Filed Nov. 28, 1944

2 Sheets-Sheet 1

FIG. 1

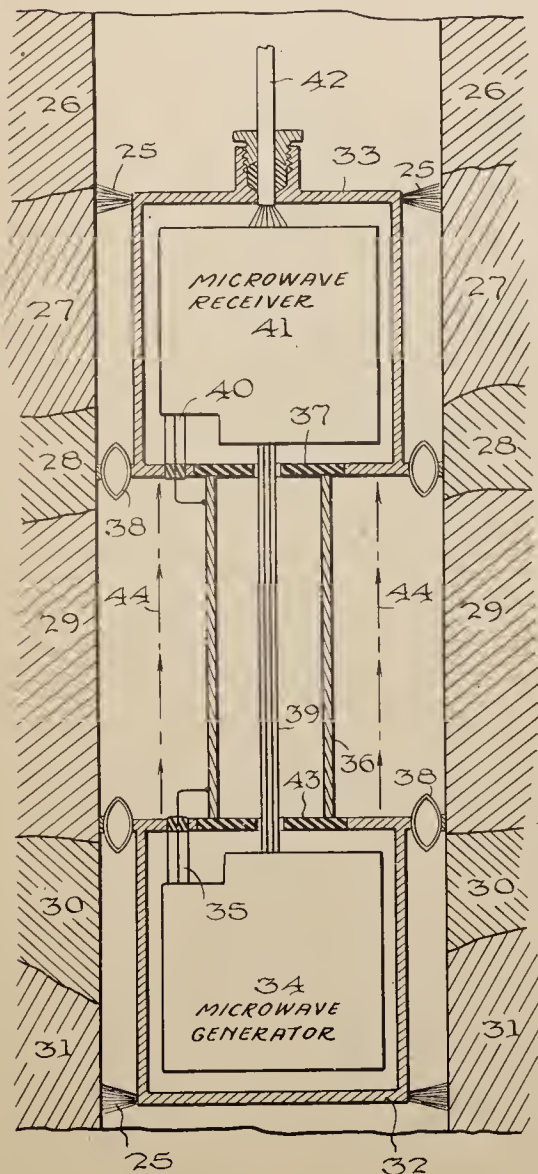
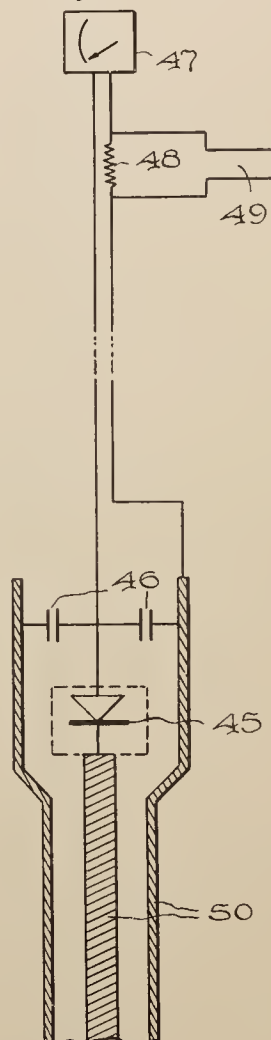


FIG. 2



Inventor

MORRIS MUSKAT
NORMAN D. COGGESHALL

By *G. M. Houghton*
their Attorney

Dec. 14, 1948.

M. MUSKAT ET AL

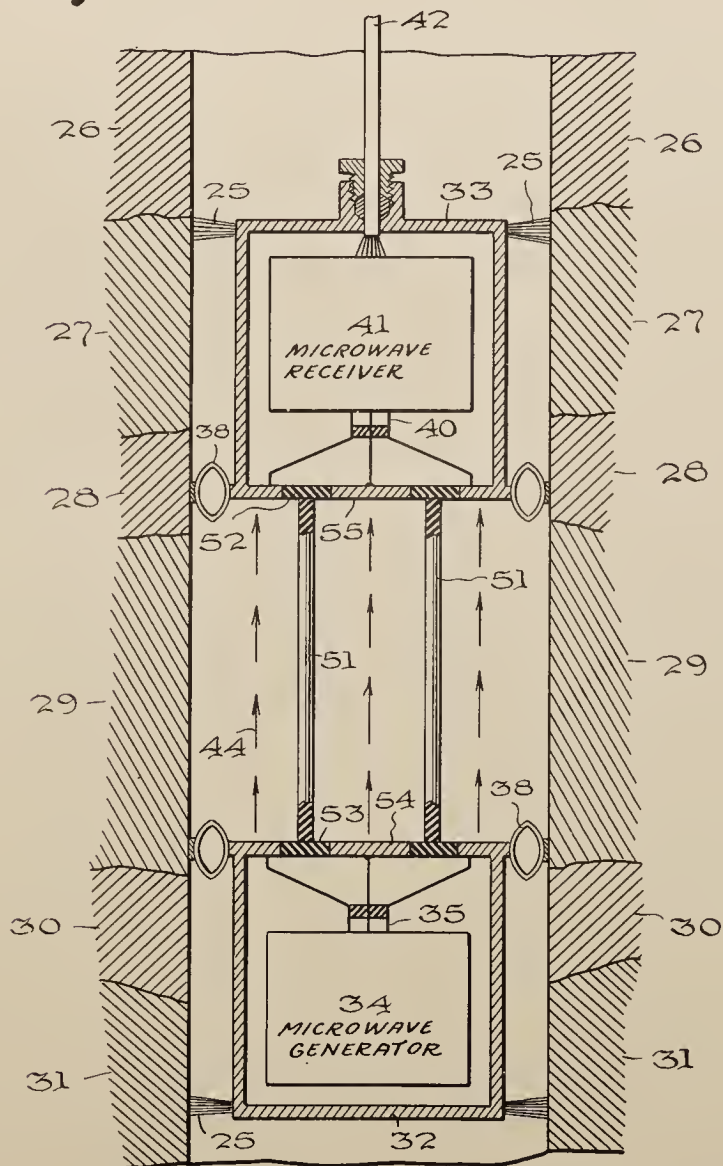
2,455,940

METHOD OF GEOPHYSICAL EXPLORATION BY MICROWAVES

Filed Nov. 28, 1944

2 Sheets-Sheet 2

Fig. 3.



Inventors

MORRIS MUSKAT
NORMAN D. COGGESHALL

By *A. M. Houghton*
Hein Attorney

UNITED STATES PATENT OFFICE

2,455,940

METHOD OF GEOPHYSICAL EXPLORATION
BY MICROWAVES

Morris Muskat, Oakmont, and Norman D. Coggeshall, O'Hara Township, Allegheny County, Pa., assignors to Gulf Research & Development Company, Pittsburgh, Pa., a corporation of Delaware

Application November 28, 1944, Serial No. 565,514

1 Claim. (Cl. 175—182)

1

This invention concerns a method of geophysical exploration, more particularly a geophysical method of logging uncased boreholes. This invention depends for its novelty on the use of microwaves for determining the characteristics of formations encountered in a borehole. In the drilling of wells, particularly oil wells, the problem of determining the nature of the formation traversed is an important one. The driller's log of the formation as reflecting the reaction of the formation to the drill is not always reliable. Coring when resorted to, is slow and expensive and oftentimes unreliable. Electrical logging and other logging methods have been used with considerable success but fail in many cases to locate strata of particular interest, or have insufficient resolving power to indicate very thin beds, or to differentiate between beds having very similar characteristics.

In the method of this invention, a new principle is applied for obtaining information regarding subsurface strata. It involves the transmission of microwave radiation down the well bore and the determination of its propagation and attenuation characteristics at various depths. By microwave radiation is meant electromagnetic energy whose frequency is higher than that used for conventional broadcasting, and lying in the region of wave length from several meters to fractions of a millimeter.

Microwaves may be transmitted with very little attenuation in so-called wave guides. These guides are tubular conductors which may either be empty or filled with a dielectric material. The radiation travels along the interior of these guides and penetrates the guiding conduit only slightly. The efficiency of transmission or the degree of attenuation of the microwave energy along the guide is quantitatively related to the conductivity and other electrical properties of the conduit material. Metallic bodies easily reflect or, if properly arranged transmit along their surface, these high frequency microwave radiations, while dielectric or insulating materials are essentially transparent. The nature of the wall of the borehole may thus be determined by causing it to be the guiding conduit for a microwave system.

There are two advantages to be gained by the use of microwave instead of longer wave length electromagnetic energy. Because of the very short wave length of microwaves the resolving power in detecting changes in the characteristics of the wave guide, namely, the formations adjacent the borehole, will be greater. In general, a wave system can experience characteristic changes which have the same order of dimension as the wave length. Since microwaves have wave lengths generally less than one meter, they are ideal for electrically detecting the fine structure of stratified formations.

2

Many formations have electrical properties which are so similar that heretofore known methods have not been able to discriminate between them. By the use of microwaves the contrast in propagation properties will be greater, and hence a conjunction between conducting and insulating material will be more easily detected. The use of microwaves will also to some extent reveal the surface nature of the formations encountered and this property is useful in further differentiating various layers.

It is accordingly an object of this invention to provide a borehole logging method which will have improved resolving power in the detecting of thin beds.

It is another object of this invention to provide a logging method which will have improved contrast between formations.

Another object of this invention is to provide means for logging boreholes by the application of microwaves to the surface presented by the formation in the borehole traversing it.

Another object of this invention is to provide a method of measuring the electrical properties of the surface of the formations encountered in a borehole.

Details of the invention will be more apparent from a study of the accompanying drawings, in which

Fig. 1 shows one apparatus for the application of this invention,

Fig. 2 shows a detector for detecting and measuring microwave energy in a borehole and

Fig. 3 shows an embodiment of our invention in which the microwave generator has self-contained power supply.

Referring to Fig. 1, which is a cross section of the earth and the borehole penetrating earth formations 26, 27, 28, 29, 30, 31, the apparatus of this invention is shown supported on electric conductor cable 42. Cable 42 is wound on a reel at the surface and there are provided conventional means for measuring the length of cable fed down into the hole. Also on the surface there may be conventional recording devices or control apparatus for other investigations simultaneously made in the well according to well known procedures.

The apparatus in the well consists of a microwave generator and a microwave receiver spaced a short distance apart. These are respectively housed in metal cases 32 and 33, Fig. 1, and connected by metal tube 36 which is insulated from the cases. Numeral 32 indicates a watertight case containing a conventional microwave generator 34. The unit 34 may conveniently be a Klystron or other velocity modulated electron oscillator well known in the art as means for generating microwave energy. Such a microwave generator is described for instance in the book

"Ultra-High Frequency Techniques," by Brainard et al., p. 338 (1942), Van Nostrand & Co., New York. Power is supplied to it through cable 42 and wires 39. The microwave energy generated is fed out of case 32 through coaxial cable 35. The sheath of this cable connects to the conducting case 32, while the central wire connects to conducting tube 36. Insulated section 43 of the case serves to insulate tube 36 from case 32. Electrical contact is made between case 32 and the formations in the borehole by means of springs 38. These springs may alternatively also have the form of wipers or scrapers as indicated by 25 for removing mud from the sides of the hole, and thus ensure encountering a clean surface. Microwaves are generated by this system and these waves travel up the annular space between the walls of the borehole and the tube 36. Since tube 36 is a good conductor, any attenuation which the microwaves suffer is a function of the characteristics of adjacent formations. After passing along the borehole a short distance, generally of the order of several diameters of the borehole, they are picked up by unit 41 to be described in detail later in connection with Figure 2 housed in conducting case 33. The microwave energy is fed in through coaxial cable 40. Insulator 37 serves to insulate conducting tube 36 from conducting case 33. An indication of the energy picked up by unit 41 is fed to the surface through cable 42.

Fig. 2 shows details of a detector which may be used to pick up microwave energy such as may be used in unit 41 of Fig. 1. Numeral 50 represents a coaxial cable carrying the energy into the receiver case. In series with a central conductor of this cable is a crystal rectifier 45. Numeral 46 represents a capacity which bypasses any high frequency unrectified energy and across this condenser an easily measurable D.-C. potential is developed. This potential may be measured by means of current meter 47, or, if desired, the potential across resistor 48 may be amplified by a conventional amplifier connected to wires 49 and recorded by conventional means at the surface.

Because of the symmetry of units 41 and 34 in Fig. 1 they may be interchanged in position without affecting the operation of the invention. Alternatively, also, the generator unit 34 may be made to have self-contained power supply, thus eliminating the need for cables 39. Elimination of cables 39 also eliminates need for conducting tube 36 and permits use of the borehole alone as a wave guide. Such an embodiment is shown in Fig. 3.

In Fig. 3 the transmitter case 32 is suspended below the receiving unit case 33 by means of insulating supports 51 having the form of one or more insulating rods which do not interfere with the microwave transmission. Generator 34 may be connected to antenna 54 by means of coaxial cable 35, the sheath of this cable being fanned out to the conducting case 32 and the central conductor connected to antenna 54. Microwaves will be radiated into the borehole, the latter acting as a wave guide, so that the energy follows up the borehole as indicated by the arrows 44. The energy is picked up by receiving antenna 55 which is insulated from case 33 by means of insulation 52. Coaxial cable 40 leads the energy into receiver 41 where it is detected or recorded or appropriate signals sent to the surface over cable 42. Other numerals on Fig. 3 indicate parts having the same function as in Fig. 1.

We have thus indicated an apparatus for mak-

ing measurements according to the method of this invention. In practice the generator may be operated to supply constant microwave energy and the energy picked up by receiver (Fig. 2) recorded as a function of depth. Still another way of practicing the invention consists in using a generator whose microwave frequency is varied over appropriate limits, as for instance by driving the Klystron adjusting screws by means of a reciprocating motor. This device being housed in case 32. A record of the energy picked up from such a variable frequency generator will indicate strata having unusual dispersion characteristics or anomalous absorption. These effects are closely associated with surface structure of the wave guide material, namely, the walls of the borehole.

In order to successfully apply the method of borehole logging by means of microwaves, it is necessary to remove from the borehole any conducting material, such as drilling mud or salt water. Holes drilled by cable tool methods and which are dry are advantageously logged by our invention. Rotary drill holes may first be flushed or conditioned with fresh water or, more preferable, an oil base or insulating drilling fluid may be used. Since the microwaves travel on the surface of conductors, any conducting mud cake must be removed from the walls of the hole as by means of scrapers 25 as indicated in Fig. 1.

The invention is not to be construed as limited to the apparatus herein set forth, as this is merely illustrative of one means of carrying out our method. Other types of microwave generators or detectors known in the art may be used within the scope of our invention. The distance between the microwave generator and receiver may be varied to suit the geological conditions to be logged, as may also the frequency of the microwaves employed. Higher frequencies permit the generator and receiver to be placed closer together and this improves the resolution of detailed geological bedding.

What we claim is:

A method of earth testing for use in logging a bore-hole comprising replacing the borehole fluid by an insulating medium, scraping the walls of the borehole substantially free of extraneous conducting material, generating microwave energy, transmitting microwave energy via the wall of a selected portion of the borehole, receiving said microwave energy and measuring a characteristic value of the received energy.

MORRIS MUSKAT.

NORMAN D. COGGESHALL.

REFERENCES CITED

The following references are of record in the file of this patent:

UNITED STATES PATENTS

Number	Name	Date
1,838,371	Deardorff	Dec. 29, 1931
2,075,808	Fliess	Apr. 6, 1937
2,139,460	Potapenko	Dec. 6, 1938
2,230,502	Pearson	Feb. 4, 1941
2,271,951	Pearson	Feb. 3, 1942
2,334,475	Claudet	Nov. 16, 1948
2,400,678	Archie	May 21, 1946

OTHER REFERENCES

Proceedings of the Physical Society, vol. 56, part 1, January 1, 1944, pp. 1-3, article by D. Rogers.

Dec. 14, 1948.

M. MUSKAT ET AL

2,455,941

GEOPHYSICAL PROSPECTING IN BORE HOLES BY MICROWAVES

Filed Dec. 13, 1944

2 Sheets-Sheet 1

Fig. 2.

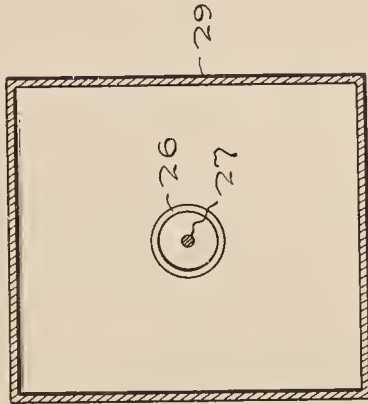


Fig. 3.

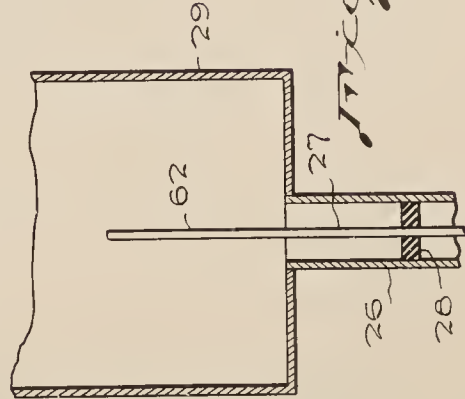
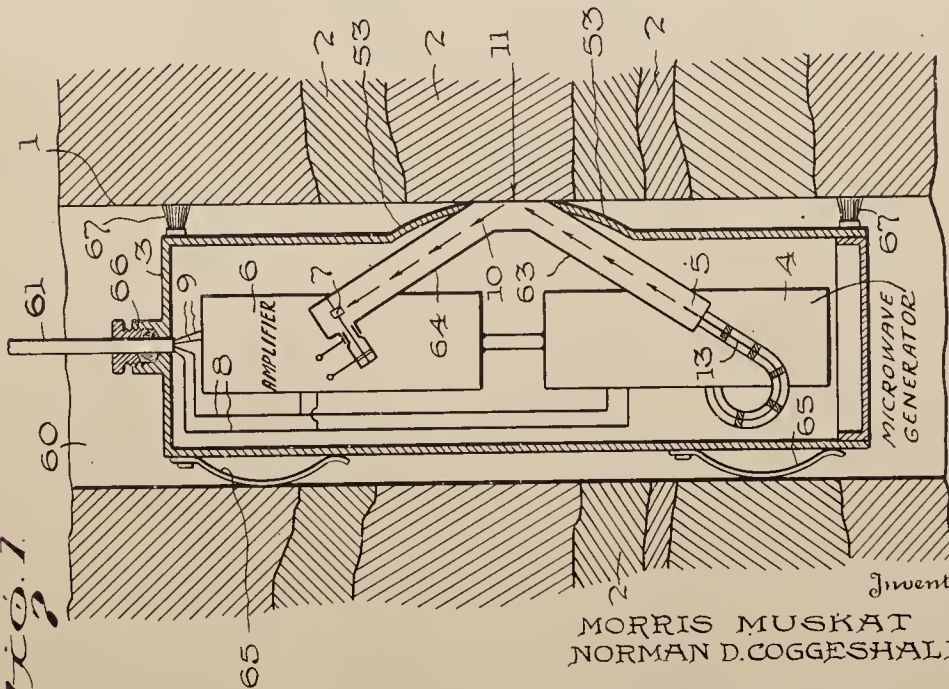


Fig. 1.



MORRIS MUSKAT
NORMAN D. COGGESHALL

Inventors

By A. McFoughton
Attorney

Dec. 14, 1948.

M. MUSKAT ET AL .

2,455,941

GEOPHYSICAL PROSPECTING IN BORE HOLES BY MICROWAVES

Filed Dec. 13, 1944

2 Sheets-Sheet 2

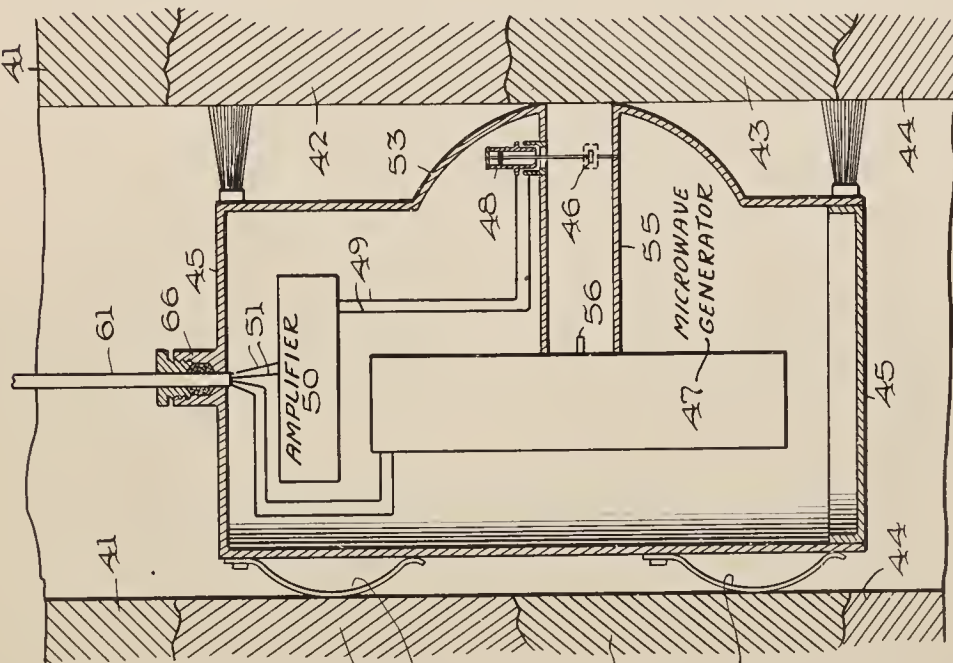


Fig. 5.

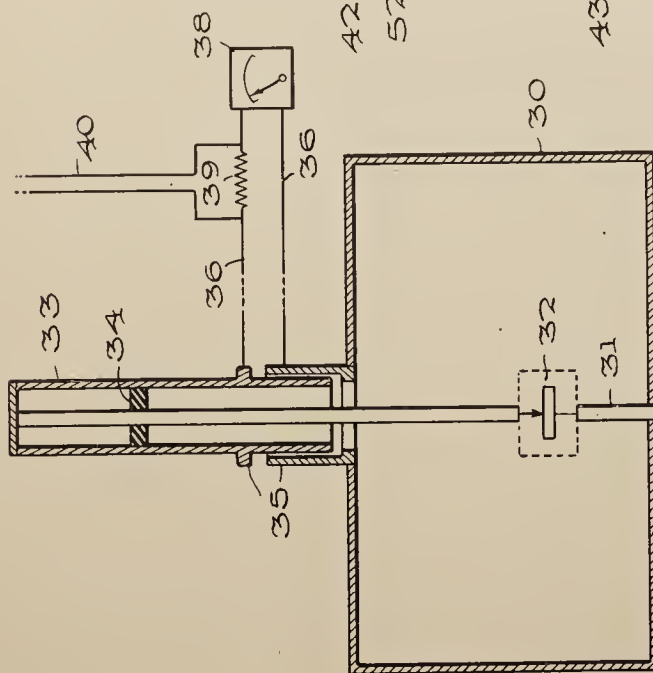


Fig. 4.

Inventors
MORRIS MUSKAT
NORMAN D. COGGESHALL

By *E. M. Hough*
their Attorney

UNITED STATES PATENT OFFICE

2,455,941

GEOPHYSICAL PROSPECTING IN BORE-
HOLES BY MICROWAVES

Morris Muskat, Oakmont, and Norman D. Coggeshall, O'Hara Township, Allegheny County, Pa., assignors to Gulf Research & Development Company, Pittsburgh, Pa., a corporation of Delaware

Application December 13, 1944, Serial No. 568,059

2 Claims. (Cl. 175—182)

1

This invention concerns a new and improved geophysical method and apparatus for borehole logging and more especially one involving the use of microwaves. More particularly it is a method and apparatus by means of which geological formations adjacent to the borehole may be logged with regard to their microwave reflection properties.

In the art of geophysical prospecting, when applied to boreholes, the methods thus far developed have consisted of two classes of measurement. In the first, the rock strata traversed by the borehole have been subjected to various types of energy excitation, and diffusion or propagation of such excitation has been measured and recorded at points distant from the source. From these measurements inferences are drawn regarding the intervening medium. In the second class, streams of particles or radiation have been directed at the face of the borehole and the reaction of the strata has been taken as an indication of the nature of the strata at the location where the stream has impinged upon them.

In the former class, the methods of excitation have been mainly either of the electrical or acoustic type. That is, electrical fields of zero or low frequency have been imposed on the rock strata, while the diffusion and transmission of these fields have been measured at distant points. The absolute magnitudes or differential magnitudes of the fields at these points have been taken as an indication of the intervening medium. In a similar way, elastic or acoustic measurements of the exposed strata have been used to correlate or identify rock formations. Because of the relatively low frequency or long wave lengths of the excitation fields, the values observed at distant points have represented averages over large masses of intervening strata, thereby giving a rather low resolving power in the differentiation of such strata. Moreover, the problems of the coupling of the exciting sources to the rock strata, as well as of the detecting instruments, have created considerable uncertainty regarding the significance of the absolute values of the measurements.

In the second class of borehole investigation methods, particle streams, such as those of neutrons, or extremely hard and short wave length electromagnetic radiations as γ -rays, have provided the means for determining the characteristics of the exposed faces of rock strata. Such methods enjoy the advantage of providing measurements of the characteristics of rock strata at the region of incidence of the particle or radiation

2

stream of small areal extent. The disadvantage of this type of measurement, however, is that it may be difficult to provide a sufficiently high intensity source of the particle stream, such as neutrons. The same is true with respect to wave streams such as those of γ -rays. Moreover, the physical interpretation and meaning of the reactions of the rock strata to these particles or wave streams is rather obscure, and the correlation has to be largely empirical.

In the invention herein disclosed, a new method has been devised which obviates the disadvantages of the previously devised techniques. It is of the type related to the second class described above, and comprises essentially the method of directing beams of microwaves against the rock strata, and measuring or recording the intensity of the reflected or scattered beam. Microwaves comprise that class of electromagnetic waves whose wave length lies approximately between one meter and a fraction of a mm. From a physical point of view these possess many advantages over lower frequency electromagnetic waves, such as the radio-waves. Because of their extremely short wave length, they can be excited and transmitted as directed beams. The receiving apparatus can also be made of small dimensions. This question of apparatus dimensions is of significance, in that it permits their application in the limited confines of well bores. While electromagnetic waves, as radio waves, or even those in the low frequency region can also be generated within well bores, they cannot be transmitted or directed in beams without the use of transmitting antennas or equipment having dimensions comparable to the wave length. On the other hand, microwaves have similar attributes and their interaction with matter is of the same type as of radiowaves. This feature does not obtain, in the case of γ -rays. The similarity of microwaves to lower frequency electromagnetic radiation is of major importance with respect to the interpretation of the reaction of microwaves with the rock strata being explored. Thus, for example, both radio and microwaves are highly reflected by metallic or other conducting media. However, insulators provide easy transmission of microwaves and have low reflecting power for them.

It is accordingly an object of this invention to show a method and apparatus for borehole logging which is sensitive to electrical properties of the formations encountered.

Another object is to describe a method and apparatus for borehole logging which is responsive to the surface characteristics of the formations,

Still another object is to describe a method and apparatus for borehole logging which makes use of microwaves in investigating the properties of the formations.

A still further object is to describe a method and apparatus for borehole logging which measures the microwave reflection properties of the formations.

Our invention is described in detail and will be best understood by reference to the accompanying drawings in which,

Fig. 1 shows one assembly of the borehole logging apparatus suspended in a well;

Figs. 2 and 3 show one form of microwave radiator which may be used;

Fig. 4 shows in transverse cross-section one form of microwave detector which may be used; and

Fig. 5 shows another particular embodiment of our invention.

In Figure 1 we have shown a cross section of the earth, with borehole 60 and exposed face 1 of rock formations stratified as indicated by 2. Numeral 3 represents the external case of the microwave apparatus supported by cable 61 entering the apparatus by stuffing box and clamp 66. Cable 61 also supplies power to the apparatus through wires 8. Wires 9 are also carried through cable 61 and serve to transmit signals to the surface for observation and recording. Cable 61 is wound on a reel at the surface and there is provided conventional means for measuring the length of cable fed down into the hole or other means of determining the depth of unit 3. Also on the surface there may be conventional recording devices or control apparatus for other investigations simultaneously made in the well according to well known procedures.

The transmitting unit is housed in 4, and the microwaves generated in 4 and emanating from the radiator 5 follow the arrows along the wave guide 63 and after reflecting from the wall of the borehole at 11 proceed along wave guide 64 as arrow 10 to the detector 7 contained in receiving unit 6. Conductor cables 8 bring the power from the surface into the transmitting unit, and cables 9 transmit the received signals back to the surface. The reflected signals received at 7 may be subjected to amplification and transformation before being sent to the surface.

In order to remove from the walls of the borehole any mud cake which may cover the formations, the case 3 is provided with scrapers 67. A bumper or guide 53 is provided with an opening at 11 to permit the microwave radiation to impinge on the clean formation. Springs 65 are provided on the opposite side of unit 3 in order to maintain guide 53 in contact with the formation wall. The well fluid may enter wave guides 63 and 64 and in order to prevent interference with the microwave transmission the fluid must be electrically non-conducting. The well may be flushed or conditioned with fresh water or with an oil base drilling fluid having low electrical conductivity.

Unit 4 represents any known type of microwave generator, such as a Klystron. These generators are of the velocity modulated electron stream type and supply microwave energy through a coaxial cable designated as 13. The energy is emitted from radiator 5 which is shown in more detail in Figs. 2 and 3, Fig. 2 being in section and Fig. 3 in elevation.

In Figs. 2 and 3, the sheath of the coaxial cable supplying microwave energy is shown at 26 and

the central conductor at 27. These are kept separated by insulator 28 in the conventional way. The cable is joined to a wave guide 29 and the central wire has an extension 62 which extends into the cavity of the wave guide 29. The wave guide 29, Figs. 2 and 3, or 63, Fig. 1, may be either circular or rectangular in cross section and of dimensions in keeping with the frequency used in a well known relationship.

Referring again to Fig. 1, after the microwaves leave radiator 5 and proceed along wave guide 63 they impinge on the rock strata in the region 11. Here they may be reflected, the fraction of energy reflected being a characteristic property of the formation encountered. Some reflection takes place in the direction of wave guide 64 which is similar in construction to 63. The reflected energy is picked up by detector 7 which may be of a known form.

A suitable type of radiation detector would be one having the transverse cross-section illustrated in Fig. 4. This consists of a probe 31 extending through the wall 30 of the wave guide, a rectifying crystal 32 included in the length of the probe, a by-pass condenser 35, a tuning cylinder 33 and tuning piston 34, leads 36 taking the rectified component of the current to a resistance 39 and a current meter 38. As the probe extends through the wave guide 30 and makes electrical contact with it, it tends to absorb a considerable amount of electromagnetic energy. To make it measurable the crystal 32 gives rectification and the by-pass condenser 35 serves as a shunt for the unrectified component. The tuning cylinder and piston 33 and 34, respectively, allow one to change the inherent impedance of the wave guide so as to select conditions best suited for maximum sensitivity. The rectified currents can be read directly on the meter 38 or the voltage drop across 39 may be fed into an electronic amplifier by means of leads 40. From there it may be fed into a recording device. Alternatively, 38 could be made a recording meter, so as to record the received signals.

In Fig. 5 is drawn the general arrangement of the component parts assembled in a manner to practice the invention in the special case of normal incidence of the microwaves on the strata being logged. Numerals 41, 42, 43 and 44 illustrate strata adjacent to the borehole, while 45 represents the outside case for the logging unit suspended by conductor cable 61 passing through stuffing box 66. Numeral 56 denotes a radiating antenna for emitting energy in microwave form into the wave guide 55. The microwaves are guided down the wave guide to the opposite end which is in contact with the adjacent strata. Here some of the energy is transmitted into the strata and some is reflected, the relative proportions depending upon the nature of the strata at that point. The relative proportions can be determined by a knowledge of the energy output of the microwave generator 47 and the amount of energy picked up by the detector probe 46. The energy detected by 46 is proportional to the sum of the amount transmitted from the antenna 56 to that point plus the amount reflected from the strata. The energy output of the microwave generator can be determined from a knowledge of its efficiency and its operating parameters, such as currents and voltages, which may be measured or kept constant. Numeral 48 represents the tuning piston part of the detector, such as shown in detail in Fig. 4, and in 46 is located the conventional crystal rectifier, and 49 are leads

which take the rectified signal to an amplifier 50 which sends its signals to the surface of the ground through wires 51. In order to allow the unit to adjust itself to irregularities of the borehole a bumper or guide 53 is provided. Fig. 5 also indicates an arrangement of springs 52 whereby the wave guide is held in contact with the walls of the borehole.

Any characteristic of the reflected microwave beam, such as magnitude, phase or wave form may be observed in the receiver 6. For a measurement of the reflection coefficient of the rock strata between the transmitting and receiving units, the ratio of intensity of the reflected beam to that of the incident beam constitutes the identifying characteristic. If the incident energy is kept constant by using at 4 a constant output microwave generator, then the reflected intensity itself will serve as a measure of the reflection coefficient. Broadly speaking, conducting beds, such as salt water strata, will give high reflected intensities, whereas non-conducting formations such as free gas zones, or strata saturated with oil, will give reflected beams of low intensity. Thus, a record of the variation of the reflected beams will provide not only a means of identifying rocks, but will also give an indication of the fluid content.

The invention and method herein disclosed may be operated at a frequency chosen so as to be appropriate to the average strata traversed by the well bore, or the measurement may be conducted in such a way as to study the variation of the reflected beams with frequency. In particular, the frequency dispersion behavior of the rock formations may be used to indicate the nature of the strata. When granular media, such as rock strata, are irradiated by microwaves of wave lengths comparable to the particle dimensions, pronounced resonance, absorption and scattering effects will take place. By observing the frequency of the incident radiation which gives rise to such resonance effects, the detailed structure and characteristics of the medium may be obtained. This type of exploration is to be included in the scope of this invention. For this application unit 4 in Fig. 1 may contain a variable frequency transmitter and the receiving unit 6 may be a variable frequency or tuned receiver or other equivalent microwave detector. In general, 4 and 6 will be of the cavity resonator type, although this invention is not to be limited to the use of such particular microwave equipment.

The angles of incidence and reflection are not limited to those shown in Figures 1 and 5, but may be any angle. While in Figure 1 we have shown the observation angle of wave guide 64 to be the same as the incident angle of wave guide 63 such as would result from a specular type of reflection, the invention is not to be limited to this condition. The observation angle may be different from the incident angle, in which

case the intensity of scattered reflection may be measured.

In order to successfully apply the method of this invention it is necessary to remove from the borehole any electrically conducting material such as drilling mud or salt water. Holes drilled by cable tool methods and which are dry are advantageously logged by our invention. Rotary drill holes may first be flushed or conditioned with fresh water or more preferably, an electrically insulating oil base drilling fluid may be used. Furthermore any conducting sheath on the borehole wall will shield the formation, and such sheath or so-called mud cake must be removed either by scrapers or by other methods known in the art.

What we claim is:

1. A method of earth testing for use in logging a borehole which comprises exciting a tubular open-ended wave guide with microwave energy, terminating said wave guide by peripheral contact with the side wall of the borehole so that the axis of the wave guide makes an acute angle with the plane tangent to the borehole wall, exciting from substantially the same microwave-terminating portion of the borehole wall a second tubular open-ended wave guide directed to receive microwaves reflected from said termination and measuring the microwave excitation of the second wave guide.

2. Borehole logging apparatus adapted for use against a borehole wall to determine a characteristic thereof comprising two intersecting open-ended wave guides having a common end opening at their intersection, said opening constituting an output end of the first wave guide and an input end of the second wave guide, the opening being shaped so as to engage the borehole wall substantially throughout the periphery of the opening, whereby said wave guides are terminated by the borehole wall when put into engagement therewith, a microwave generator connected to the input end of the first wave guide, microwave excitation measuring means connected to the output end of the second wave guide and means for urging the periphery of said opening substantially into contact with the borehole wall.

MORRIS MUSKAT.
NORMAN D. COGGESHALL.

REFERENCES CITED

The following references are of record in the file of this patent:

UNITED STATES PATENTS

Number	Name	Date
1,838,371	Deardorff	Dec. 29, 1931
2,075,808	Fliess	Apr. 6, 1937
2,139,460	Potapenko	Dec. 6, 1938
2,334,475	Claudet	Nov. 16, 1943
2,346,481	Garrison	Apr. 11, 1944

੮੪

21

2

418

41

1

..

1

(12)

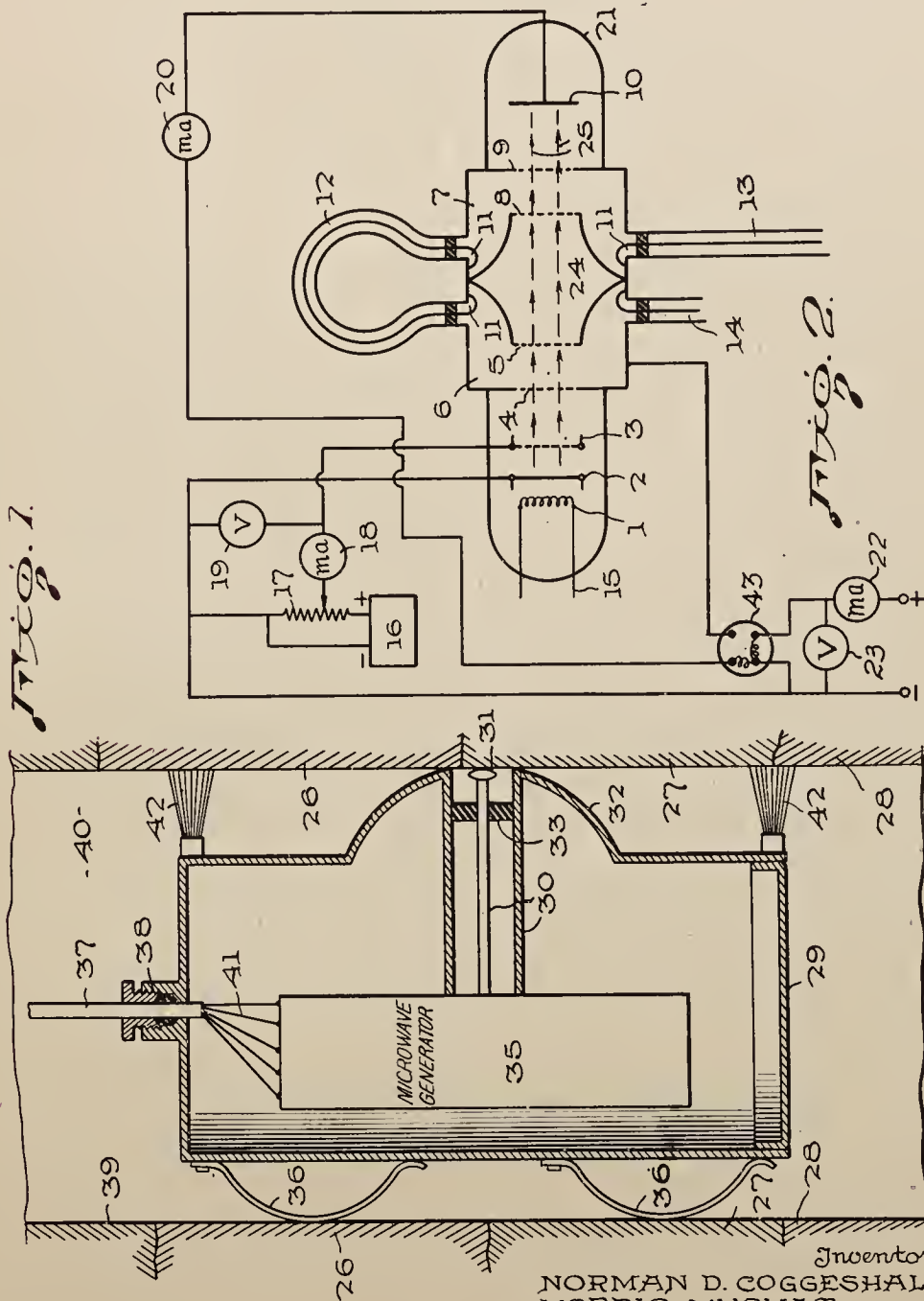
Dec. 14, 1948.

N. D. COGGESHALL ET AL

2,455,942

GEOPHYSICAL EXPLORATION OF BORE HOLES BY MICROWAVES

Filed Dec. 13, 1944



Inventors
NORMAN D. COGGESHALL
MORRIS MUSKAT

By E. M. Foughton
their Attorneys

UNITED STATES PATENT OFFICE

2,455,942

GEOPHYSICAL EXPLORATION OF BORE-
HOLES BY MICROWAVES

Norman D. Coggeshall, O'Hara Township, Allegheny County, and Morris Muskat, Oakmont, Pa., assignors to Gulf Research & Development Company, Pittsburgh, Pa., a corporation of Delaware

Application December 13, 1944, Serial No. 568,060

2 Claims. (Cl. 175-182)

1

This invention concerns a new and improved geophysical method of borehole logging and apparatus therefor and involving the use of microwaves. More particularly it is a method and apparatus by means of which geological formations adjacent to the borehole may be logged with regard to their microwave absorption properties.

In the art of geophysical prospecting, when applied to boreholes, the methods thus far developed have consisted of two classes of measurement. In the first, the rock strata traversed by the borehole have been subjected to various types of energy excitation, and diffusion or propagation of such excitation has been measured and recorded at points distant from the source. From these measurements, inferences are drawn, regarding the intervening medium. In the second class, streams of particles or radiation have been directed at the face of the borehole and the reaction of the strata has been taken as an indication of the nature of the strata at the location where the stream has impinged upon them.

In the former class, the methods of excitation have been mainly either of the electrical or acoustic type. That is, electrical fields of zero or low frequency have been imposed on the rock strata, while the diffusion and transmission of these fields have been measured at distant points. The absolute magnitudes or differential magnitudes of the fields at these points have been taken as an indication of the intervening medium. In a similar way, elastic or acoustic measurements of the exposed strata have been used to correlate or identify rock formations. Because of the relatively low frequency or long wave lengths of the excitation fields, the values observed at distant points have represented averages over large masses of intervening strata, thereby giving a rather low resolving power in the differentiation of such strata. Moreover, the problems of the coupling of the exciting sources to the rock strata, as well as of the detecting instruments, have created considerable uncertainty regarding the significance of the absolute values of the measurements.

In the second class of borehole investigation methods, the particle streams, such as those of neutrons, or extremely hard and short wave length electromagnetic radiations as γ rays, have provided the means for determining the characteristics of the exposed faces of rock strata. Such methods enjoy the advantage of providing measurements of the characteristics of rock strata at the region of incidence of the particle or radiation stream of small areal extent. The disad-

2

vantage of this type of measurement, however, is that it may be difficult to provide a sufficiently high intensity source of the particle stream, such as neutrons. The same is true with respect to wave streams such as those of γ rays. Moreover, the physical interpretation and meaning of the reactions of the rock strata to these particles or wave streams is rather obscure, and the correlation has to be largely empirical.

In the invention herein disclosed, a new method has been devised which obviates the disadvantages of the previously used techniques. It is of the type related to the second class described above, and comprises essentially the method of directing beams of microwaves against the rock strata and measuring or recording the degree of absorption of the incident beam. Microwaves comprise that class of electromagnetic waves whose wave length lies approximately between one meter and a fraction of a mm. From a physical point of view these possess many advantages over lower frequency electromagnetic waves, such as the radiowaves. While electromagnetic waves, as radio waves, or even those in the low frequency region can also be generated within well bores, they cannot be transmitted or directed in beams without the use of transmitting antennas having dimensions comparable to the wave length, and such dimensions are impossible to attain in a borehole. Because of their extremely short wave length microwaves can be excited and transmitted as directed beams, and the generating apparatus can be made of small dimensions. This question of apparatus dimensions is of significance, in that it permits their application in limited confines of well bores. On the other hand, microwaves have the same attributes and their interaction with matter is of the same type as of radiowaves. This feature does not obtain, in the case of γ rays. The similarity of microwaves to lower frequency electromagnetic radiation is of major importance with respect to the interpretation of the reaction of microwaves with the rock strata being explored. Thus, for example, both radio and microwaves are highly reflected by metallic or other conducting media. However, insulators provide easy transmission of microwaves and a beam directed into them will be absorbed or dissipated.

It is accordingly an object of this invention to provide a method and apparatus for borehole logging which is sensitive to electrical properties of the formations encountered.

Another object is to provide a method and apparatus for borehole logging which is sensitive

to the surface or near surface characteristics of the formations.

Still another object is to provide a method and apparatus for borehole logging which makes use of microwaves in investigating the properties of the formations.

A still further object is to provide a method and apparatus for borehole logging which measures the microwave absorption properties of the formations.

Our invention is described in detail and will be best understood by reference to the accompanying drawings in which,

Fig. 1 shows one assembly of the borehole logging apparatus suspended in a well; and

Fig. 2 is a diagrammatic representation of one form of microwave generator which may be used.

In Fig. 1 we have shown a cross section of the earth, with borehole 40 and exposed face 39 of rock formations stratified as shown by 26, 27 and 28. Numeral 29 represents the external case of the microwave apparatus supported by cable 37 entering the apparatus by stuffing box and clamp 38. Cable 37 also supplies power to the apparatus through wires 41. Cable 37 is wound on a reel at the surface and there is provided conventional means for measuring the length of cable fed down into the hole or other means of determining the depth of unit 29. Also on the surface there may be conventional recording devices or control apparatus for other investigations simultaneously made in the well according to well known procedures.

The microwave generator is housed in 35 and the microwaves emanating from it follow wave guide 30 to the formation wall. Unit 30 may be either of coaxial cable extending from the microwave generator itself to the formation, or it may have the dimensions of a wave guide. The mode of excitation of unit 30 is such that it functions to feed microwave energy into the strata, that is, it electrically couples the formation medium tightly to the microwave generator 35.

If the formation has the properties of an electrical conductor it will act as a microwave reflector and no energy will enter the formation from wave guide 30. This will result in negligible loss of energy from the generator 35. On the other hand if the formation has the properties of an electrical insulator it will be transparent to microwaves and wave guide 30 will feed or radiate energy into the formation with resulting loss of energy from the generator 35. The generator 35 is so constructed that the power load equivalent of the rock strata reacts upon the generator in a measurable way. Such power load may be measured by measuring the net power output of the generator. Alternatively, the generator may be constructed so that variations in the power load will change its frequency of oscillation. By measuring the change in frequency the nature of the rock strata opposite the generator may be inferred. Unit 35 contains a microwave generator of a load sensitive type, plus other electrical equipment to permit obtaining an indication of the load.

One type of microwave generator which may be used in the above invention is called a Klystron. Its principal parts are shown diagrammatically in Fig. 2. Its principle of operation is discussed in a book by Brainerd et al. titled Ultra-High Frequency Techniques, page 330, et seq. This generator depends upon the electrodynamic resonance properties of closed or nearly closed metallic vessels. In Fig. 2, numeral 1 represents a heating filament which furnishes heat for a cathode 2

which emits electrons. Between the cathode 2 and grid 3 there is applied an accelerating voltage for the electrons. Thereupon the electrons travel to the grid 4 and practically all of them pass into 5 and through the resonator space 6. It will be assumed that the generator is in operation, so that the electromagnetic oscillations exist in the resonator space 6. Depending upon the instantaneous phase of the oscillations there will be an electric field from 4 to 5 or from 5 to 4. Its action upon the electrons passing between grids 4 and 5 will be to speed them up or slow them down. This will result in their being bunched as they pass through the field free space 24.

The cavity space 7 is geometrically the same as 6, and therefore the resonant frequency of 7 will be same as for 6. Moreover, the electromagnetic resonators 6 and 7 are energetically coupled by the coaxial cable arrangement 12 which has an antenna 11 on each end. This allows either 6 to feed energy into 7 or vice versa. Therefore cavities 6 and 7 will both be in oscillation at once and at the same frequency. Consequently if the phase of the oscillations of resonator 7 is in proper relation to the phase of the bunches of electrons coming on paths 25, these electrons, by virtue of their kinetic energy, can either feed energy into 7 or absorb it from it. If they feed energy into 7 they will be slowed down; if not, they will be speeded up. Proper operating conditions, of course, are when they are slowed down to allow maximum energy transfer to the cavity resonator 7. The coaxial cable arrangement 13 allows energy in the form of microwaves to be drained off and utilized for whatever purpose is desired. In this case they are radiated onto the formation wall.

The coaxial cable arrangement 14 serves to preserve the symmetry of the two resonant cavities. After passing through grids 8 and 9, which are part of the resonator 7, the electrons pass into the anode 10 where they are collected. Numeral 21 represents the overall metal case of the generator and the leads to the various elements such as 1, 2, 3 and 10 enter the case through well-known insulating vacuum-tight bushings or glass seals not shown. The case 21 is customarily kept at ground potential while the cathode 2 and the anode 10 are at a high negative potential. Meter 20 measures the flow of electrons from the cathode 2 to the anode 10 and this current depends on the adjustment and state of oscillation of the tube and its load. Battery 16 is the voltage source for the first acceleration of electrons, and variable resistance 17 allows it to be controlled. Meter 18 measures that part of the emission from the cathode which is caught on grid 3, and 19 measures the voltage between 2 and 3. Voltmeter 23 measures the voltage applied to the electrons while between cathode 2 and grid 4, and meter 22 measures the flow of electrons from cathode 2 to the external case 21. Customary adjustment of a Klystron oscillator is such that some electrons leaving cathode 2 reach the anode 10. Even though the elements 2 and 10 are at substantially the same D.-C. potential, the instantaneous potentials acting on the electrons moving between the various elements when under conditions of oscillation as described above are such as to cause a current through meter 20, and for a particular adjustment this current is a maximum with no load on the oscillator. When microwave power is taken from the oscillator through coaxial cable 13, the reading of meter

20 will decrease and the reading of meter 22 will increase.

Referring again to Fig. 1, the case 29 is formed with a bumper flange 32 to keep the projecting wave guide 30 from getting caught in the well due to unevenness of the walls. The central conductor of 30 has a circular spring 31 attached to its end to maintain electrical contact with the strata regardless of their irregularities. An insulating bushing 33 serves to center the central conductor and its spring contact 31. Continuous contact between the guide 32 and the walls of the borehole is maintained by means of springs 36 which also permit the unit to adapt itself to variations in borehole diameter. Scrapers 42 clean off any mud cake which may have formed on the wall of the hole so that contacts 31 and 32 may contact the clean formation.

One method of practicing this invention consists of recording, as a correlation against depth, the amount of power transmitted into the strata by conductors 31 and 32, Fig. 1. A knowledge of this power output can be gained from the previously determined operating efficiency of the unit and from the instantaneous values of the operating parameters, such as the voltages and currents which may be measured by the meters shown in Fig. 2. For example, the power may be determined by readings of the voltmeter 23 and the current measuring meter 20. More conveniently these can be replaced by a single power measuring unit, such as a wattmeter 43. An example of such a wattmeter is a galvanometer of the well known dynamometer type in which the field coils are actuated by current set up by the voltage shown measured by 23 and the armature carries the current shown measured by 20. Such a galvanometer then has a resultant swing which is proportional to the product of the current and the voltage and which is a measure of power. As stated above, when microwave power is absorbed from the Klystron oscillator by the adjacent formation coupled thereto the current in meter 20 decreases thereby decreasing the deflection of wattmeter 43. The wattmeter 43 may be made to reflect a beam of light upon a moving photographic film in well known manner and arranged so that different amplitudes of swings would be correlated with position of the logging unit in the well by the method used by Fearon in Patent 2,309,835.

Broadly speaking, conducting beds, such as salt water strata, will have low absorption characteristics whereas non-conducting formations such as free gas zones, or strata saturated with oil, will allow the microwave energy to penetrate with resulting power absorption. Thus, a record of the variation of the absorption will provide not only a means of identifying rocks, but will also give an indication of the fluid content.

The invention and method herein disclosed may be operated at a frequency chosen so as to be appropriate to the average strata traversed by the well bore, or the measurement may be conducted in such a way as to study the variation of the absorbed energy with frequency. In particular, the frequency dispersion behavior of the rock formations may be used to indicate the nature of the strata. When granular media, such as rock strata, are irradiated by electromagnetic radiations of wave lengths comparable to the particle dimensions, pronounced anomalous absorption effects will take place. By observing the frequency of the incident radiation

which gives rise to such resonance effects, the detailed structure and characteristics of the medium may be obtained. This type of exploration is to be included in the scope of invention.

For such operation unit 35 in Fig. 1 may be conceived as a variable frequency generator. In general this generator will be of the cavity resonator type, although this invention is not to be limited to the use of such microwave equipment.

For the successful application of our invention any electrically conducting well drilling fluid must be removed from the borehole. Holes drilled by cable tool methods and which are dry are advantageously logged by our invention. Rotary drill holes may first be flushed or conditioned with fresh water or, more preferably, flushed with an electrically insulating oil base drilling fluid. The well fluid may enter the wave guide 30 since being non-conducting it will not interfere with its operation. Any conducting mud cake which would shield the formations must be removed from the walls of the hole as indicated by scrapers 42 in Fig. 1.

The invention is not to be construed as limited to the type of microwave generator herein set forth as this is merely illustrative. The frequency may be varied to suit geological conditions and the dimensions of the borehole.

What we claim is:

1. Borehole logging apparatus comprising a microwave generator, a tubular open-ended microwave guide coupled thereto, means for supporting said microwave guide so that its open end is directed substantially perpendicular to the axis of the borehole, means for urging an open end of said microwave guide substantially throughout its periphery against the wall of the borehole and means for measuring the power absorbed by the microwave generator.

2. Borehole logging apparatus comprising a microwave generator, a tubular open-ended microwave guide coupled thereto, said tubular microwave guide being of diameter less than half the diameter of the bore hole, means for supporting said microwave guide so that its open end is directed substantially perpendicular to the axis of the borehole, means for urging an open end of said microwave guide substantially throughout its periphery against the wall of the borehole and means for measuring the power absorbed by the microwave generator.

NORMAN D. COGGESHALL.
MORRIS MUSKAT.

REFERENCES CITED

The following references are of record in the file of this patent:

UNITED STATES PATENTS

Number	Name	Date
2,075,808	Fliess	Apr. 6, 1937
2,129,711	Southworth	Sept. 13, 1938
2,129,712	Southworth	Sept. 13, 1938
2,139,460	Potapenko	Dec. 6, 1938
2,167,630	Bazzoni	Aug. 1, 1939
2,253,589	Southworth	Aug. 26, 1941
2,334,475	Claudet	Nov. 16, 1943
2,343,531	Buchholz	Mar. 7, 1944
2,346,481	Garrison	Apr. 11, 1944

OTHER REFERENCES

"Geophysical Exploration," Hieland, page 627, pub. 1940 by Prentice Hall, Inc., New York city.

1000

1000

1000

1000

1000

1000

1000

1000

1000

1000

1000

1000

1000

1000

1000

1000

1000

1000

1000

1000

1000

Dec. 14, 1948.

M. MUSKAT ET AL

2,456,012

METHOD OF AND APPARATUS FOR MEASURING THE ELECTRICAL
PROPERTIES AND SURFACE CHARACTERISTICS OF MATERIALS

Filed Dec. 21, 1944

3 Sheets-Sheet 1

Fig. 1.

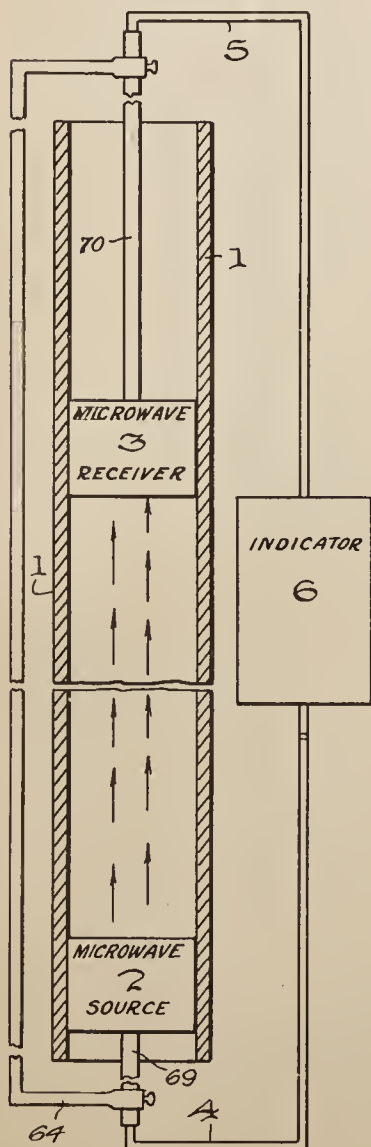
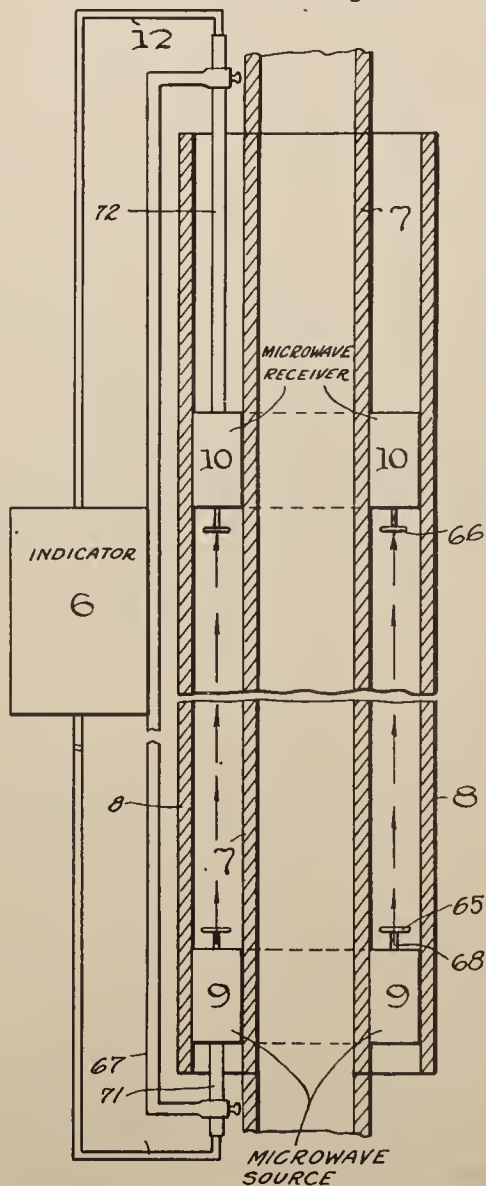


Fig. 2.



Inventors

MORRIS MUSKAT
NORMAN D. COGGESHALL

By *C. M. Gough*

their Attorney

Dec. 14, 1948.

M. MUSKAT ET AL

2,456,012

METHOD OF AND APPARATUS FOR MEASURING THE ELECTRICAL
PROPERTIES AND SURFACE CHARACTERISTICS OF MATERIALS

Filed Dec. 21, 1944

3 Sheets-Sheet 2

Fig. 3.

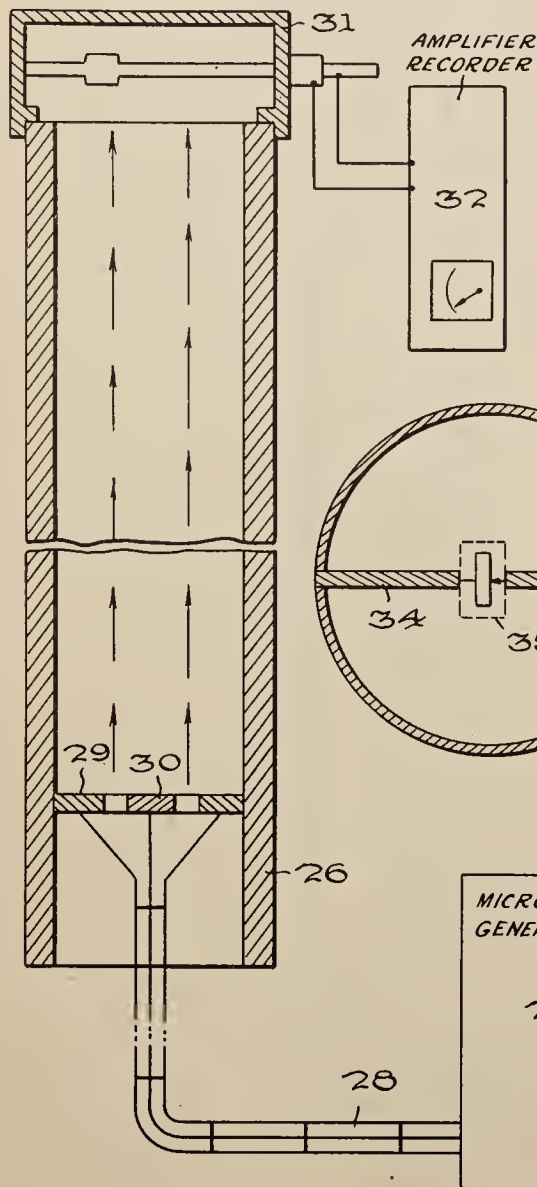


Fig. 4.

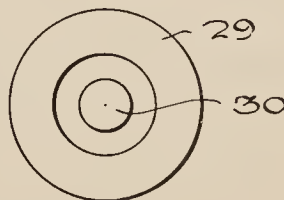
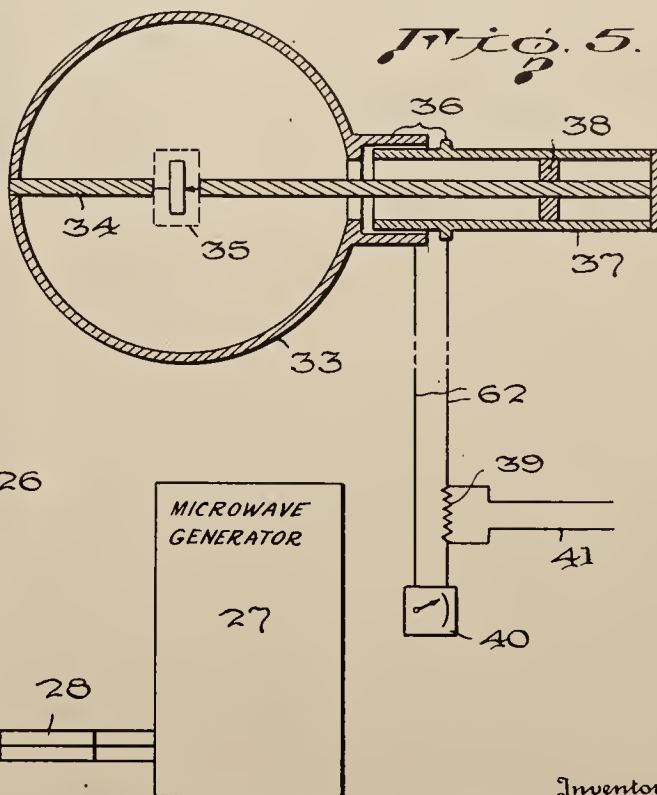


Fig. 5.



Inventors

MORRIS MUSKAT
NORMAN D. COGGESHALL

By *G. M. Houghton*
their Attorney

Dec. 14, 1948.

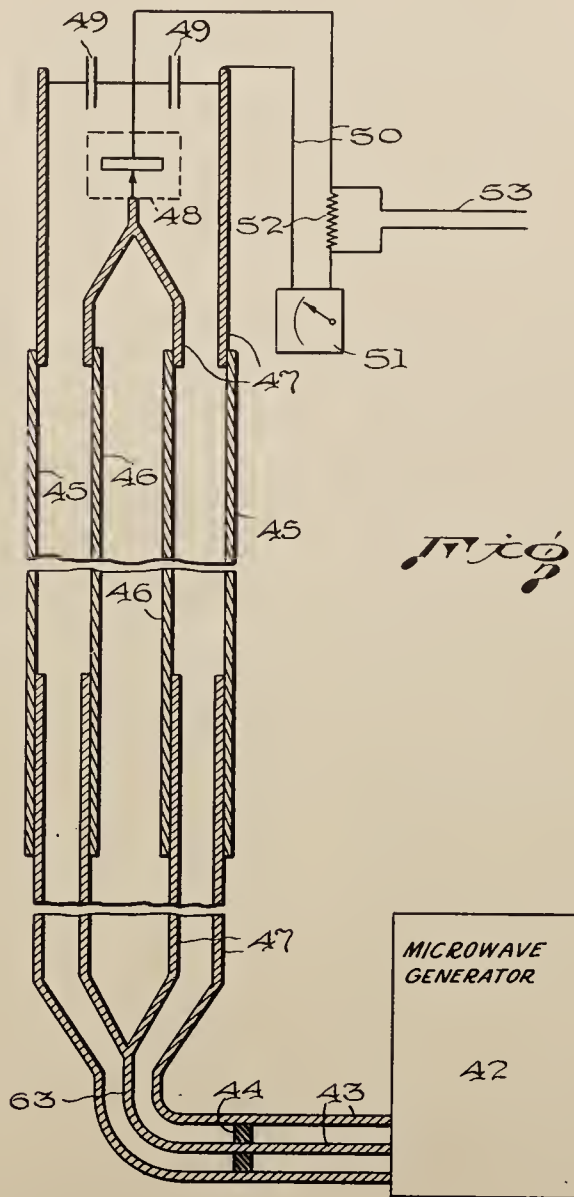
M. MUSKAT ET AL

2,456,012

METHOD OF AND APPARATUS FOR MEASURING THE ELECTRICAL
PROPERTIES AND SURFACE CHARACTERISTICS OF MATERIALS

Filed Dec. 21, 1944

3 Sheets-Sheet 3



Inventors
MORRIS MUSKAT
NORMAN D. COGGESHALL

By *E. M. Houghton*
their Attorney

UNITED STATES PATENT OFFICE

2,456,012

METHOD OF AND APPARATUS FOR MEASURING THE ELECTRICAL PROPERTIES AND SURFACE CHARACTERISTICS OF MATERIALS

Morris Muskat, Oakmont, and Norman D. Coggeshall, O'Hara Township, Allegheny County, Pa., assignors to Gulf Research & Development Company, Pittsburgh, Pa., a corporation of Delaware

Application December 21, 1944, Serial No. 569,224

2 Claims. (Cl. 175-183)

1

2

This invention concerns a new method of testing materials, in particular it concerns a method of testing tubular materials for surface cracks either on the inside or outside surface by means of very high frequency electromagnetic waves commonly called microwaves.

In the testing and inspecting of materials various methods have been devised for locating flaws. In the inspection of pipe it is comparatively simple to locate large leaks. Smaller flaws or cracks which go deep or all the way through the material wall may be found by various magnetic inspection or testing methods also well known in the art. However, it is known that even in an otherwise apparently perfect piece of metal, failure may eventually occur due to the presence of minute surface cracks which escape ordinary detecting methods. These cracks cause stress concentrations which tend to gradually enlarge the crack and failure ultimately takes place. Cracks may also occur in the case hardening or the carburized surface of treated materials. Minute surface cracks are also thought to be associated with the cause of "fatigue" failures, that is, "fatigue" is the gradual weakening of the material through growth of minute surface cracks. Heretofore no testing or inspection method has been able to locate these cracks.

A purpose of this invention is to provide a method for the inspection and testing of tubular materials for locating surface cracks which may be the incipient cause of future failure.

Another object is to provide a method of locating surface cracks on either the inside or outside surface of metal tubes or the outside surface of metal rods.

Another object is to provide a method for determining the surface characteristics of metal tubes or rods to locate any variation in surface material caused by irregular surface treatment.

A still further object is to provide a method of testing tubular insulating material to determine its surface characteristics.

The invention makes use of electromagnetic waves having wave lengths shorter than those used in normal long wave length radio broadcasting and on down through the microwave region, namely wave lengths of from a few meters to a fraction of a mm. The art of ultra high frequency communication and power transmission has shown that ultra high frequency electromagnetic waves can be efficiently transmitted in metallic conduits. Such conduits are called wave guides. The attenuation in these metallic wave guides is low and the wave system penetrates only

slightly into the surface of the confining walls. This is the basic fact underlying the use of coaxial cables for the transmission of ultra high frequency electromagnetic waves.

Whereas the efficiency of wave guide transmission depends on the highly conducting character of the confining walls, it is true, conversely, that variations from the condition of high electrical conductivity will lead to loss in transmission efficiency and greater attenuation. Poorly conducting or insulating media are relatively transparent to ultra high frequency waves, and when the latter come in contact with them they will leak through them and leave the wave system. The change in metallic high conductivity may be due either to the interposition of dielectric material or faults or cracks in the metal surface such as may increase its effective electrical resistivity. In fact, the magnitude of the rate of attenuation and change in character of an ultra high frequency wave system, as it passes down a tubular body, is quantitatively related to the electrical properties of the wave guide material.

The tubular material may have any value of electrical characteristic, ranging from those for very good conductors to those for very poor conductors. If the tubular material is a good conductor, the attenuation of the received signal will be low, and an abnormally high attenuation will indicate the presence of faults or cracks in the surface or the presence of high resistance coatings. If the tubular material is a poor conductor, the attenuation will be high, and an abnormally low attenuation will indicate the presence of conducting defects such as the condensation of moisture on the surface or moisture entrained in surface pores or even surface decomposition.

In the event that coatings have been deliberately put on the surface of the tubular material, the method of this invention will serve to determine its thickness, as well as flaws or cracks therein. In the case of conducting surfaces on conductors such as obtained by metal plating or surface chemical processes, it becomes possible to detect cracks or thin spots. It is similarly possible to detect cracks or thin spots in insulating coatings put on the surface of metal pipe, etc. Furthermore, in the case of metallic surface coatings on insulating materials it becomes possible to detect breaks or thin spots in the metallic coating.

In describing the method of practicing the invention reference will be made to the accompanying drawings, wherein

Fig. 11 shows the arrangement of apparatus

Dec. 28, 1948.

N. D. COGGESHALL ET AL

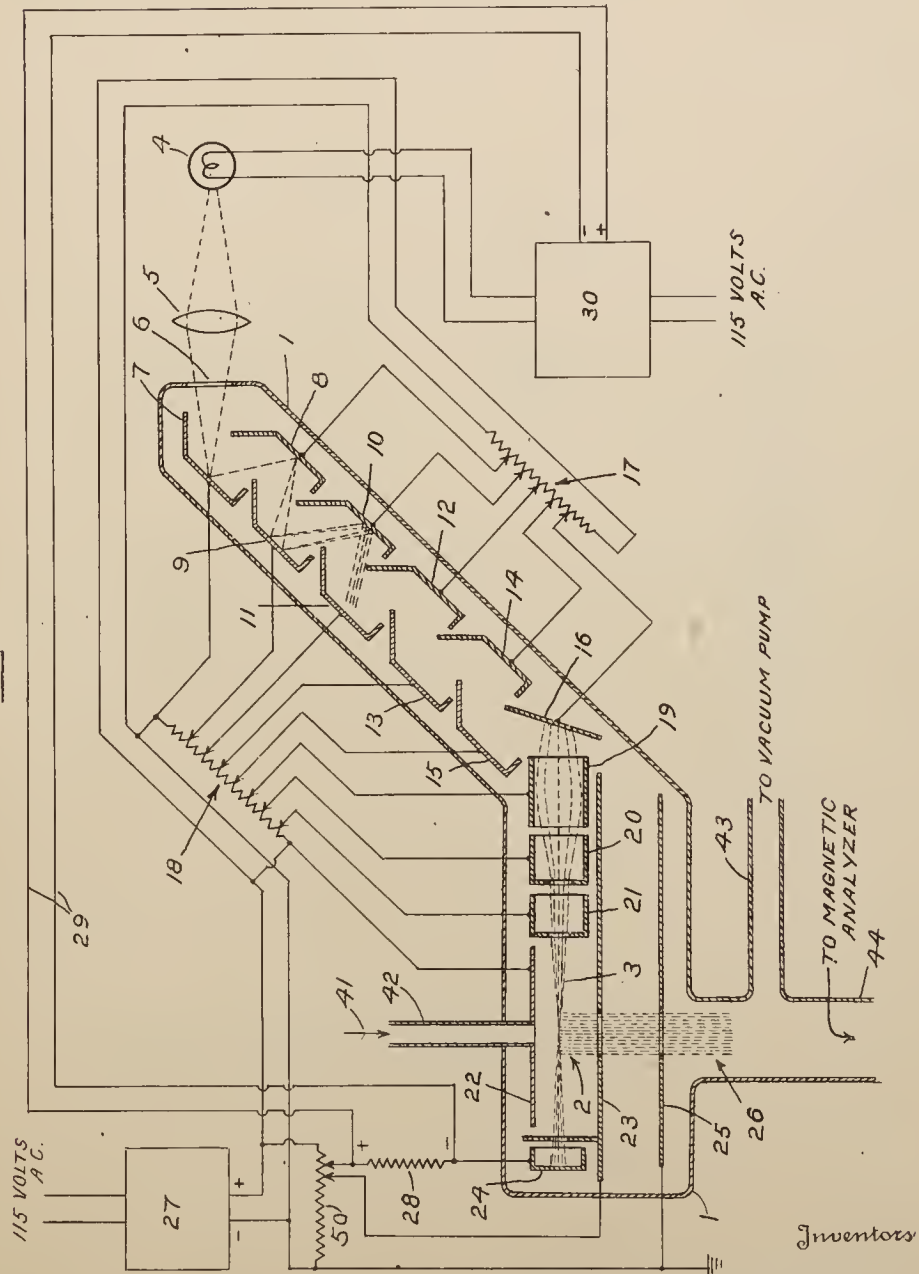
2,457,530

ELECTRON GUN FOR MASS SPECTROMETERS

Filed Aug. 6, 1946

2 Sheets-Sheet 1

Fig. 1-

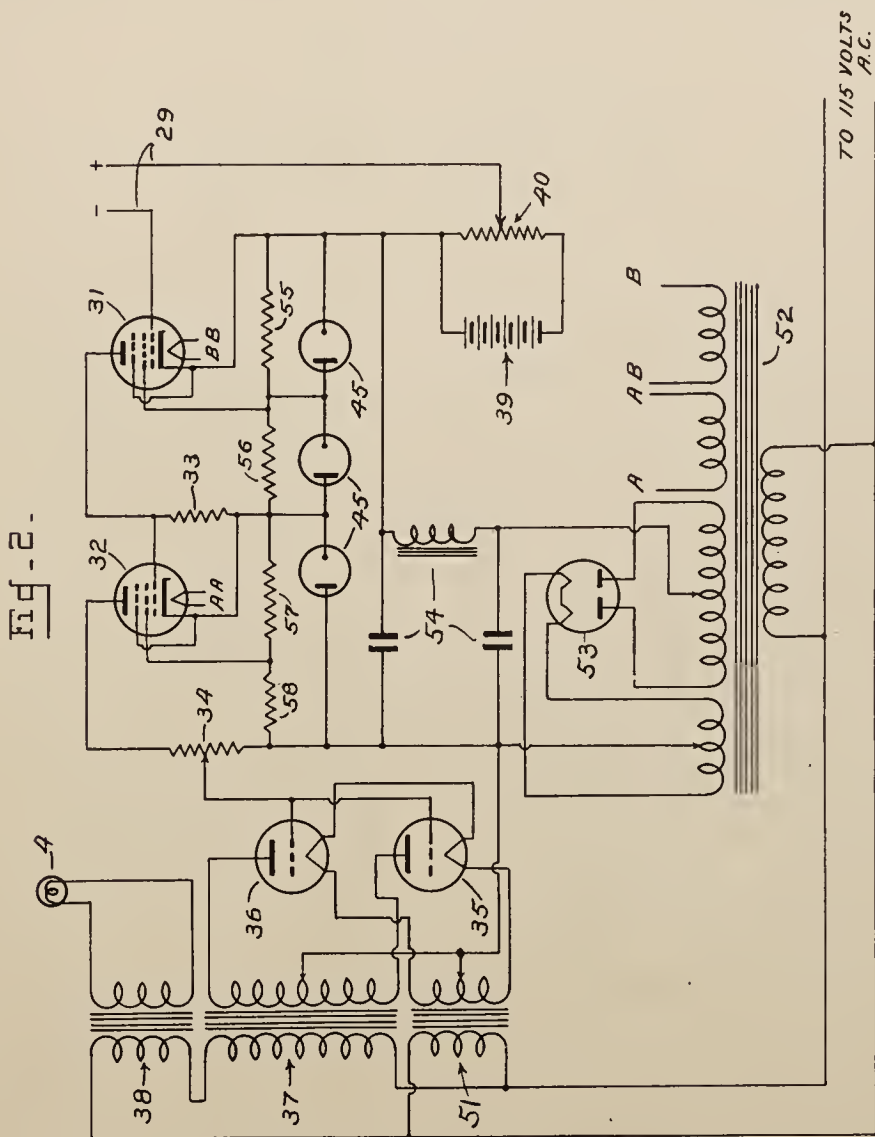


Norman D. Coggeshall
Nathan F. Kerr

By *A. M. Houghton*
their Attorney

2,457,530

2 Sheets-Sheet 2



By A. M. Houghton
their Attorney

UNITED STATES PATENT OFFICE

2,457,530

ELECTRON GUN FOR MASS
SPECTROMETERS

Norman D. Coggeshall, Verona, and Nathan F.
Kerr, Pittsburgh, Pa., assignors to Gulf Re-
search & Development Company, Pittsburgh,
Pa., a corporation of Delaware

Application August 6, 1946, Serial No. 688,736

5 Claims. (Cl. 250-41.9)

1

This invention relates to devices for furnishing a plurality of electrons in motion and for employing the said electrons.

The mass spectrometer is today an analytical and research instrument of great economic importance. It is used for routine analysis of gas and liquid samples, hydrocarbon analyses adjunct to refinery control, for following isotopic tracers, for studying molecular energy levels, and for other purposes. In the mass spectrometers in use today the ion beam is formed by that component of the apparatus known as the ion source. Basically, this consists of an arrangement of electrodes across which there are impressed direct current voltages. In the free space between the electrodes an electron beam is made to pass. In traversing this region the electrons create positive ions from the gas molecules or atoms present. These ions are drawn in one direction by the impressed voltages, and by means of two slit apertures a beam of ions is defined. The electron beam has heretofore been formed by a filament and electrode arrangement known as an electron gun. It may consist merely of a filament which emits electrons and one or more electrodes with apertures which are at a positive potential relative to the filament. This results in electrons being drawn towards the electrodes and passing through the apertures to form a beam. A relatively weak magnetic field in the direction of electron travel may be employed to aid in the forming and maintaining of a beam.

The filament used by the electron gun may be tungsten, thoriated tungsten or the source of electrons may be an indirectly heated oxide coated cathode. In any case, the electron beam originates from a source of thermionic emission. A thermionic emission source of electrons, although practically the only type heretofore usable in mass spectrometers, has several very serious disadvantages. These disadvantages, which will be explained below, result in considerable expenditure of time and money to keep the instrument in operating order.

The enumeration and description of the disadvantages of the thermionic emission type of cathode may be limited to a discussion of ordinary tungsten filaments, inasmuch as they are easier to use than oxide coated cathodes or thoriated tungsten filaments. The latter two are very susceptible to "poisoning" of the emitting surfaces by improper vacuum conditions and are not considered practical to use in a routine instrument. Furthermore, most of the disadvan-

2

tages named for the tungsten filament will be common to these other two types of sources.

In the application of the mass spectrometer to the problem of quantitative analysis of multicomponent mixtures of hydrocarbons the cracking patterns of the individual components are used. When a single compound is examined in the instrument it is found that in the ion beam there are ions of many different masses. That is, there may be the molecule ionized by losing an electron, but it may also dissociate by electron impact to form neutral and ionized fragments. For example, n-butane will give rise to ions of masses 58, 56, 43, 42, and so forth. Iso-butane will give rise to ions of the same masses but their relative intensities will be considerably different. The pattern of ionic masses and their relative intensities for any compound is referred to as its "cracking" pattern and it is the differences in these patterns that make the analysis of multicomponent mixtures possible. The instrument is calibrated for any particular mixture by examining in a pure form each of the components contained in the mixture. This data, that is, the relative intensities of the various ions formed, must be known accurately in order to perform accurate quantitative analyses. Furthermore, the instrument must be so designed and operated as to render the cracking patterns as independent as possible of such parameters within the ion source as may change with time. This condition is very important for if not satisfied it may be necessary to recalibrate the instrument quite often, perhaps once a week or every few days, and this is an expensive and time consuming operation. As will be explained, the filament type of electron source is very troublesome in causing changes in the cracking patterns.

Although the major part of the ions coming from the ion source are due directly to electron impact on the gas molecules there are a substantial number that owe their origin partly or wholly to the filament. One reason for this is that the filament which operates in the neighborhood of 2000° Kelvin causes the dissociation of some of the molecules that impinge on it. The neutral fragments may then by diffusion enter the ionization region where they may be converted into ions. Also the process may take place wherein some of the parent molecules or their fragments may be ionized on the surface of the filament and subsequently diffuse into the ion beam. The two above effects, although not responsible for the major number of ions in the ion beam, can contribute a substantial number. Furthermore,

the contribution from these two effects depends greatly upon the filament temperature and surface condition which change with time and mode of operation. This causes the cracking patterns of the pure compounds to change with time and mode of operation, a highly undesirable situation.

Attempts have been made to remedy the above effects by placing a separate vacuum pumping connection on the filament assembly so that there is a pressure differential across the apertures through which the electrons pass from the filament into the ionization region. This is not very successful, due to the high mobility of the molecules and ions at the temperatures encountered and due to long mean free paths at the pressures used.

Another disadvantage somewhat akin to the ones explained above comes about from the heat output from the filament. As the filament is surrounded on all sides by electrodes or shielding, and as the gas pressure surrounding it is low, being of the order of 10^{-4} mm. of mercury, most of its heat output is absorbed as radiant energy by the metal parts of the electron gun and ion source. This results in a temperature of these parts higher than the ambient one. Molecules impinging on the walls of the ion source will assume a nearly equivalent temperature and this affects their mobility or average velocity. This latter quantity is an important one in controlling the speed of pumping of the gas through the ion source. This means then that the temperature of the ion source affects the molecular density within it and this in turn affects the intensity of the ion beam which it is desirable to maintain very constant. If the temperature of the ion source could be maintained very constant, the above effect would not be very important. However, due to the relatively poor vacuum in which the filament must operate and to the variety of compounds with which it has contact, the surface conditions on it change in such a manner that it operates at different temperatures at different times. This gives rise to the effects just explained and it constitutes a serious disadvantage in using this type of electron source. For example, we have experimentally found that the sensitivity of the mass spectrometer may vary as much as 0.3 per cent per degree Centigrade change of ion source temperature. Sensitivity as here used means the ion intensities per unit pressure of admitted gas.

As we have seen above, there are strong disadvantages of a filament or heated cathode type of electron source when it is desired to operate a mass spectrometer under very constant conditions. There are in addition certain other disadvantages due to the frequent maintenance this type of electron source requires. Since the gas atmosphere in a mass spectrometer is of the order of 10^{-4} mm. of mercury, which is a much higher pressure than in a sealed vacuum tube, the filament is subjected to the emission inhibiting effects of the different gases. As a result the operating temperature must be raised above that for a filament in a vacuum tube of the conventional type, in order to get sufficient emission. At this temperature, an appreciable amount of tungsten evaporates, weakening the filament and eventually necessitating a change of filaments, a costly job and one which puts the instrument out of operation for at least several hours.

Often, the gas being examined by a mass spectrometer has oxygen as one of its constituents. It

is well known that oxygen can poison certain electron emitting surfaces and that it can cause oxidation of tungsten filaments, thus shortening their lives. Another disadvantage of the tungsten filament is its fragility. For example, a filament that has been operated for some time becomes very brittle and a slight disturbance will break it. This means that practically each time the filament assembly is removed from the ion source for inspection or repair, the filament must be replaced before re-assembly. This is very undesirable, as it increases the time during which the instrument is out of operation.

It is an object of this invention to provide an electron gun for mass spectrometers, cathode ray oscillographs, television equipment, electron microscopes and other devices, that does not have the disadvantages named above which are attendant to a thermionic emission type of electron source.

It is a further object of this invention to provide an electron gun for the above named instruments which has certain positive advantages, as will be apparent from the following explanation, over conventional types of electron guns which employ thermionic emission as the source of electrons.

It is another object of this invention to provide apparatus and several alternative means for the close and accurate control of an electron stream emerging from the new type of electron gun described below.

A further object of this invention is to provide means of using the ion accelerating voltage supply of a mass spectrometer to operate our new type electron gun, when it is used on a mass spectrometer, thus eliminating the need of extra equipment.

Still another object of this invention is to provide a mass spectrometer having an external light source casting light through a window in an envelope containing a photocathode, electron multiplier and electron lens for forming a stream of electrons for ionizing gaseous and gaslike matter in said envelope.

Other objects and advantages, together with certain details of construction and mode of operation, will be apparent from the following description of a preferred embodiment of the invention as illustrated in the accompanying drawings, and in which,

Figure 1 is a diagram illustrating the application of our invention as a source of electrons in a mass spectrometer, and

Figure 2 shows one type of control circuit that may be used to regulate the current output from the electron gun.

In Figure 1, the vacuum tight envelope housing the ion source and electron gun is represented by 1. Inside the envelope, numeral 2 represents the region of ionization through which passes the stream of electrons 3. In one mode of practicing this invention there is a light source 4 which may be a tungsten filament incandescent lamp. Light from 4 is focussed by the lens 5 onto a photosensitive cathode 7, passing into the evacuated envelope through the transparent window 6. Electrodes 8, 9, 10, 11, 12, 13, 14, 15, 16 are arranged inside the evacuated envelope in juxtaposition somewhat as shown and maintained at successively increasing positive potentials in the known manner of electron multipliers. Light from the lamp 4 falling on the cathode 7 causes photoelectrons to be emitted from the cathode 7. These photoelectrons are drawn towards electrode

8 by the potential difference between the cathode 7 and the electrode 8. These electrons strike electrode 8 with considerable velocity and cause secondary electrons to be emitted. The secondary electrons are emitted with a small initial energy, of the order of a few volts, and as a result are drawn to electrode 9 by the potential difference between electrodes 8 and 9. At the surface of electrode 9, these electrons in turn cause the emission of more secondary electrons. As the surfaces chosen for the electrodes 8, 9, and so on, are such that the secondary electron emission coefficient is greater than unity, being preferably from 4 to 8, there is a multiplication at each successive electrode. As a result the electron emission from electrode 16 is very much larger than that from electrode 7. There are a number of factors that control the final current from electrode 16 and they will be discussed below when automatic controlling methods of the unit are described.

The operating voltages for the electrodes of the electron multiplier are obtained by tapping off suitable fractions of the resistances 17 and 18. The tapping off contacts are made so that each successive electrode is at a higher potential, that is, 8 is higher than 7, 9 is higher than 8, and so forth. These voltages may alternatively be obtained by suitably tapping off from a single resistor.

Electrons leaving the last secondary emission electrode 16 are focussed by means of an electron lens. One way in which this may be done is to accelerate them towards the cylindrical electrode 19 and towards the electrodes 20 and 21. The three electrodes 19, 20 and 21 may be so arranged and have such potential distribution as to form a beam of electrons from those originating from electrode 16. This illustrates only one of several types of electrostatic and/or magnetostatic electron lenses which may be employed.

The beam of electrons is made to pass between electrodes 22 and 23 and through an aperture in 23, to the electron collector electrode 24. A potential is maintained between electrodes 23 and 24 so that 24 functions essentially as a trap and secondary electrons from electrode 24 are drawn back to it. The voltages for the focussing electrodes 19, 20 and 21 may be obtained by taps from the resistor 18 and the potential between electrodes 23 and 24 may be obtained from taps on resistor 50.

In operation, the electron beam traversing the region between electrodes 22 and 23 creates ions by impact of the individual electrons on the gas molecules or atoms present. These ions, which are mainly positive, are drawn by the existing potential differences towards electrode 23. A slit in electrode 23 allows some of the ions to emerge into the region between electrodes 23 and 25. A large potential difference, of the order of a thousand volts is maintained between electrodes 23 and 25. The ions are thereby further accelerated and as a result pass through a slit in electrode 25 in a spatially well defined beam of ions 26 having the form of a ribbon. This beam of ions 26 goes to the magnetic analyzer through tube 44 and is separated into individual beams of different mass characteristics in the usual manner of a mass spectrometer. The gas to be analyzed enters the envelope 1 along the path indicated by arrow 41 through inlet tube 42 which is normally small in cross section, a vacuum pump being connected to tube 43.

As seen in Figure 1, all the voltages required to operate the ion source and the associated elec-

tron multiplier electron gun are obtained from one voltage supply shown as 27. It is of great advantage to be able to use the same high voltage supply for both the acceleration of the ions and also for operation of the electron gun.

In one mode of operation, the different ion masses to be found in the ion beam 26 are successively brought to the mass spectrometer collector by varying the magnetic field of the magnetic analyzer in a manner well known in mass spectrometry. Another mode of operation is to bring the different ion masses to the collector by varying the total ion accelerating voltage. The former mode is to be preferred, however, as it lends itself to overall simpler operation.

It is very important to keep the electron gun current quite constant as the intensity of the ion beams will depend upon it. As mentioned above, there are a number of ways in which the current output of the electron gun may be controlled and in Figure 1 is to be seen one preferred manner. In this case, the electron collector 24 collects a certain fraction of the total electron emission from electrode 16. The electron current collected by 24 is that which traverses the entire length of the ionization region. Current collected by electrode 24 returns to electrode 16 after passing through the high resistance 28. Variations in the current from electrode 24 will cause voltage variations across resistance 28 and these variations are conducted by lead wires 29 to the low voltage power supply 30.

The power supply 30, which is shown in more detail in Figure 2, responds to voltage variations in leads 29 in such a way as to maintain constant the electron current that passes through the ionization region and which is collected by electrode 24. The control is through the temperature of the filament of lamp 4, that is, an increase of voltage across resistor 28, due to an increase in electron current, will cause a drop in the filament temperature and conversely a decrease in voltage across resistor 28 will cause an increase in filament temperature of lamp 4. These temperature changes may be made in the direction to maintain a constant electron flow, since the number of photoelectrons initially leaving electrode 7 depends upon the light output of lamp 4.

Figure 2 shows the controlling circuit which utilizes and amplifies the signal on leads 29 in such manner as to control the heating current in lamp 4. Here 31 represents a first amplifier tube and 32 a second. When the electron current falling on collector 24 (Figure 1) exceeds its normal value it causes an increase of potential drop in resistance 28 (Figure 1) which causes an increase of negative grid bias in tube 31 of Figure 2. Grid bias battery 39 and potentiometer 40 provide grid voltage and adjustment thereof in tube 31 in conjunction with resistor 28 of Figure 1. The change in control grid bias of tube 31, due to the increase of potential drop in resistor 28 decreases the plate current of tube 31, with the result that the potential drop across resistor 33 is decreased. As this drop controls the bias of the control grid of tube 32, the result of the above changes is an effective positive increase of the control grid bias in tube 32 with a consequent increase in its plate current. This increase of plate current will cause an increased potential drop across resistance 34. Resistance 34 controls the bias of the grids in both tubes 35 and 36, the net result being a decrease in the plate currents of both. The triodes 35 and 36, together with the secondary windings of trans-

formers 37 and 51, which supply the plate and heater voltages, form a dissipative circuit controlled only by the grid voltage which is the voltage drop across resistor 34.

It is to be noticed that the transformer 37 which supplies the plate voltage for tubes 35 and 36 has its primary in series with the primary of transformer 38 which supplies the current for lamp 4. Thus, if the current flow through tubes 35 and 36 is reduced, it is equivalent to increasing the impedance of the secondary of transformer 37. This in turn increases the impedance of the primary of transformer 37, with the result that the primary current of both 37 and 38 is reduced. A reduction of primary current of transformer 38 reduces the secondary current with the result that the light intensity of lamp 4 is reduced. This is the desired end effect, as it will reduce the number of photoelectrons emitted by electrode 7 of Figure 1.

If one assumes the opposite condition, that is, a decrease of electron current reaching electrode 24 and follows out the resulting changes of operation of the components of Figure 2, one finds that the end result is an increase of light from lamp 4 which would cause more initial photoelectrons to be emitted. Thus, we have the conditions satisfied for self regulation, that is, the electron current or stream of electrons creates a signal which is utilized to maintain the current constant. In Figure 2, power is supplied to tubes 31 and 32 through power transformer 52 with rectifier 53 and filter components 54 in conventional manner. Screen voltages are obtained through resistors 55, 56, 57, 58 whose voltages are regulated by regulator tubes 45.

The above circuit represents one method of achieving self control but it is not by any means to be construed to be the only method by which the result may be achieved, since it is intended to represent only one operable method of many. Other well known types of regulating circuits may be used, and it is intended that their use fall within the scope of this invention.

Although we have shown the control signal coming from the current to the collector electrode 24 of Figure 1, there are other means of obtaining a control signal and it is intended that they all fall within the scope of this invention. For example, that portion of the electron current which is collected by electrode 21, Figure 1, may be used for a control signal and similarly for the currents collected by electrodes 23, 20 or 19. Furthermore, the final means of control, which is the temperature of the filament of the lamp 4 in the mode of operation explained above, can be any of several possibilities each of which falls within the intended scope of this invention. For example, the control signal may be utilized to control a power supply so that a decrease of electron current would cause an increase of voltage between the electrodes of the electron multiplier and, conversely, an increase would cause a decrease of voltage. The circuit for such a control would be familiar to those versed in the art.

Although we have illustrated our invention with one arrangement of electrodes, it is not to be limited to this arrangement but rather applies to all such configurations as admit multiplication of an electron current by secondary electron emission. Also, we have shown our new type electron gun as applied to a mass spectrometer; however, it is not to be construed that this places a limitation on its use, as other applications, as in electron microscopes, cathode ray oscillographs,

television equipment and other uses, are intended.

Our illustration also shows an electron multiplier, the initial electrons of which are those due to photo-emission. It is not intended that this invention be limited to electron multipliers of this type but should embrace all types including those where the initial electrons are due to thermionic emission, electrons from radioactive transformations, and so forth.

Some positive advantages of our new type of electron gun may be mentioned. Our improved new electron gun has unlimited lifetime and does not need to be periodically replaced as does a tungsten or other type of filament. Our new type of electron gun may run cold, thus eliminating two undesirable features of the filament type gun, namely, the change of cracking pattern due to pyrolysis on the filament surface and the overall rise of temperature of the ion source which affects instrument sensitivity. Our new type of electron gun is sturdier. If it is desired to remove it for alteration of the instrument, it contains no sensitive, brittle filament that is easily broken. Our new type of electron gun can be put into operation immediately after applying the light signal and the necessary voltages; it requires no warm-up time for proper emission, as do some thermionic emitters; also, it does not necessitate a lengthy wait for overall temperature equilibrium, as do some thermionic emitters.

In our Figure 1, we have shown an electron gun as applied to a mass spectrometer. While we have shown no separate vacuum pumping line direct to the electron gun, it may, under certain conditions, be advisable and it is intended that our invention cover such modification. Also, it is intended that the scope of this invention encompass the situation wherein the electrodes of the new type electron run hot, that is, at whatever elevated temperature is desired. Often it is desired to operate a mass spectrometer with the ion source hot and in such a case the electron gun must be at the same temperature. The heating in this instance could be attained either using suitable insulated internal heaters or by using an external heater of high resistance wire suitably applied to the vacuum jacket.

Although we have described a preferred embodiment of our invention in specific terms, it is to be understood that various changes may be made in the size, shape, materials and arrangement without departing from the spirit and scope of the invention as claimed.

What we claim as our invention is:

1. A mass spectrometer comprising an envelope having a light permeable window, a photo-sensitive cathode in said envelope for receiving light entering through said window, a plurality of multiplying electrodes in said envelope, means comprising at least one electron lens element for focusing electrons from said multiplying electrodes into an electron stream, a collector electrode disposed in the path of said stream for collecting electrons therefrom, means for admitting molecules into said envelope into the path of said electron stream for ionizing said molecules, and analyzer means including a magnet for analyzing said molecules.

2. A mass spectrometer comprising an envelope, light permeable means for permitting light to enter said envelope, a photocathode disposed in said envelope in the path of said entering light, a plurality of electron multiplying electrodes in said envelope in cooperative relationship to said photocathode, means comprising at least one electron

lens element for focusing electrons from said multiplying electrodes into an electron stream, a collector electrode disposed in said envelope for collecting electrons from said stream, means for admitting gaseous and gas-like matter into said envelope, means for moving said matter through said electron stream whereby at least a portion of said matter becomes ionized, analyzing means operating upon at least a portion of said ionized matter for analyzing said matter, and self regulating means constructed and arranged for maintaining the magnitude of said electron stream at a predetermined level by regulating the light entering said envelope.

3. In a mass spectrometer, the improvement which comprises an external light source, a light permeable window in the envelope of the mass spectrometer, a photocathode within said envelope for receiving light from said external source, electrodes for forming an electron stream, self regulating means constructed and arranged for maintaining the magnitude of said electron stream at a predetermined level by automatically regulating the light entering said envelope.

4. A mass spectrometer comprising an envelope, means for admitting molecules to be ionized into said envelope, means for producing and forming an electron stream in said envelope for ionizing said molecules, said means including a photocathode actuated responsive to light entering said envelope from an external source, an electron collecting electrode upon which said electron stream impinges self regulating means actuated responsive to the current from said collecting electrode and constructed and arranged for maintaining the flow of electrons in said stream at a predetermined level by regulating the said light that enters the envelope, means including a magnet for analytically operating upon said ionized molecules, and means for moving at least a por-

tion of said ionized molecules into cooperative relationship with said last named means.

5. A mass spectrometer comprising an envelope, means for admitting molecules to be ionized into said envelope, an external source of light, means for producing and forming an electron stream in said envelope for ionizing said molecules, said means including a photocathode actuated responsive to light entering said envelope from said external source, a plurality of electron multiplier electrodes in the path of electrons emitted by said photocathode, electron lens means cooperating with said multiplier electrodes for forming a fast moving, relatively concentrated electron stream in the path of said molecules being admitted whereby ions are produced, an electron collecting electrode upon which said electron stream impinges, means including a magnet for operating upon and analyzing at least a portion of said ions, and regulating means actuated responsive to the current from said collecting electrode for maintaining the magnitude of said electron stream at a predetermined level by regulating the intensity of said external light source.

NORMAN D. COGGESHALL.
NATHAN F. KERR.

REFERENCES CITED

The following references are of record in the file of this patent:

UNITED STATES PATENTS

Number	Name	Date
Re. 21,907	Balsley -----	Sept. 30, 1941
1,961,703	Morrison -----	June 5, 1934
2,149,080	Wolff -----	Feb. 28, 1939
2,181,720	Barthelmy -----	Nov. 28, 1939
2,240,713	Orthuber et al. -----	May 6, 1941
2,373,151	Taylor -----	Apr. 10, 1945

[Reprinted from the *Journal of the American Chemical Society*, **70**, 3283 (1948).]

Influence of Solvent, Hydrogen Bonding, Temperature and Conjugation on the Ultraviolet Spectra of Phenols and Aromatic Hydrocarbons

By Norman D. Coggeshall and Eleanor M. Lang

[CONTRIBUTION FROM GULF RESEARCH & DEVELOPMENT COMPANY]

Influence of Solvent, Hydrogen Bonding, Temperature and Conjugation on the Ultraviolet Spectra of Phenols and Aromatic Hydrocarbons¹

BY NORMAN D. COGGESHALL AND ELEANOR M. LANG^{1a}

It is well known that for some ultraviolet absorbing compounds the absorption spectra are dependent on the nature of the solvents used. For example, the spectrum obtained from a simple phenol in a paraffin solvent will be considerably different for that obtained with ethyl alcohol as the solvent. For the latter the spectrum is changed in shape from the former and shifted to the red. This phenomenon is quite general among the polar substituted aromatics.

It has been assumed that highly polar structures make a greater contribution to the excited than to the ground states of such compounds as polar substituted aromatics.² From this it follows that any factors which stabilize these structures will decrease the energy of transition and shift the absorption bands to longer wave lengths. The shifts to longer wave lengths that occur for such compounds when examined in a polar solvent as compared to similar data obtained for a neutral solvent may then be explained on this basis.

The present investigation was concerned with some of the factors expected to be effective in stabilizing the excited polar structures. Such stabilization would result from electrostatic or dipole

interaction of the hydrogen bonding type, between the ionic structure of the excited state of the solute molecule and the polar component of the solvent molecule. Recent studies, by infrared absorption, of steric hindrance to hydrogen bonding in substituted phenols³ furnish useful information for the correlation of these spectral shifts with the known hydrogen bonding characteristics of the phenols. It was shown from the infrared data that large alkyl groups such as *t*-butyl on one or both the ortho positions of a phenol are effective in hindering inter-molecular hydrogen bonding. These studies gave a classification of phenols into three classes: hindered, partially hindered, and unhindered. The same series of phenols were studied in this investigation.

Errera and Sack⁴ found that the population of intermolecular complexes between ethyl alcohol and dioxane in a carbon tetrachloride solution is very strongly reduced by a change in temperature from 20 to 55°. From the infrared spectral changes it is believed that the energy per complex for association between a phenol and an alcohol solvent will be of the same order of magnitude as for the type of complex studied by Errera and Sack. Consequently, the ultraviolet spectra of the phenols in alcohol solution as a function of temperature should clarify the role of stable com-

(1) Presented in part before the Division of Physical Chemistry at the 112th American Chemical Society meeting, New York, September, 1947.

(1a) Now at Camp Detrick, Frederick, Maryland.

(2) C. Curran, Paper P6, American Chemical Society meeting, Chicago, September, 1946.

(3) N. D. Coggeshall, *THIS JOURNAL*, **69**, 1620 (1947).

(4) J. Errera and H. Sack, *Trans. Faraday Soc.*, **34**, 728 (1938).

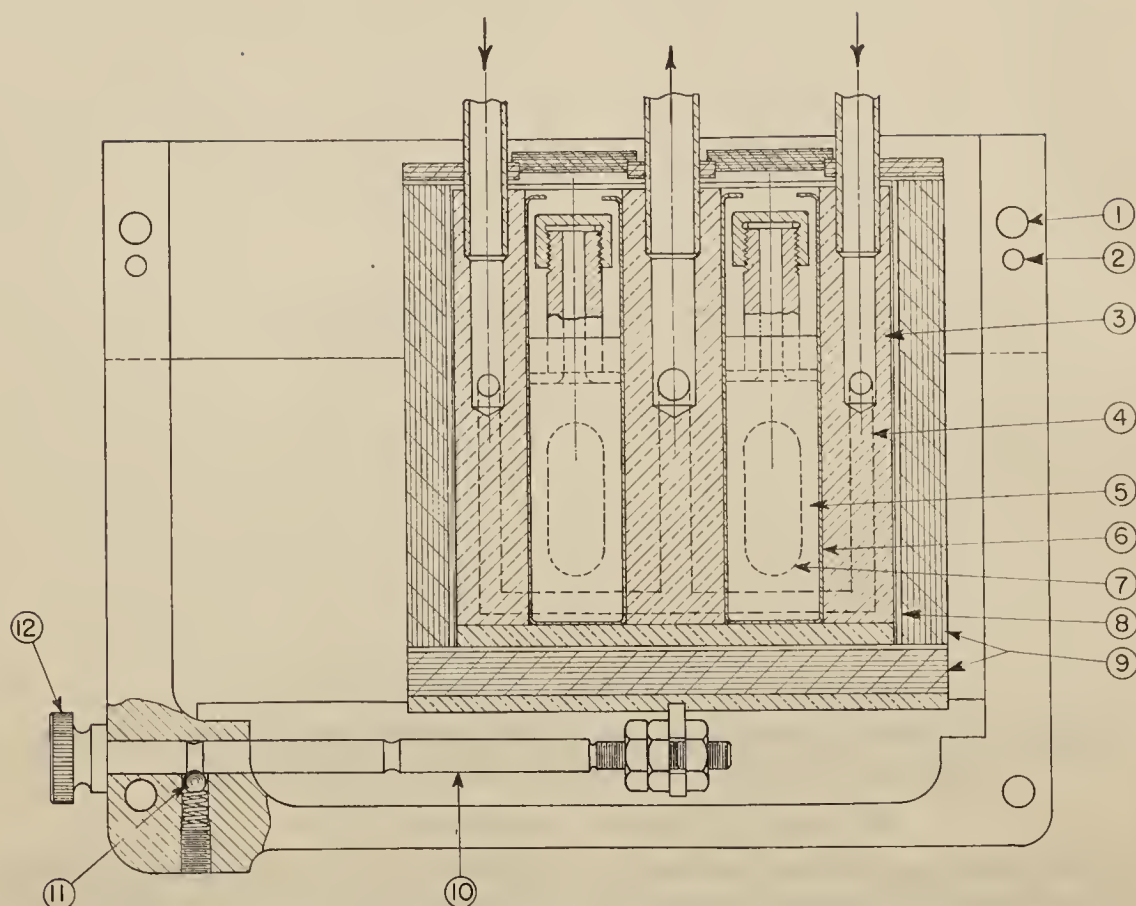


Fig. 1.—Schematic diagram of temperature controlled absorption cell compartment.

plexes in the processes responsible for the spectral changes. For this reason a temperature controlled cell compartment was constructed and utilized.

Since the instantaneous dipole moment of the polar form of an excited molecule will depend upon its geometrical extension, a number of aromatic compounds of varying degrees of conjugation and extension were studied. An effect was found for the diphenylbenzene isomers which confirms the above assumptions concerning the alteration of the spectra. Consideration has been given to the change of shape of the spectra as well as to the shifting of bands to the red. Tentative explanations, based on considerations of the intermolecular interactions, have been formulated for the observed results.

Experimental

All the absorption spectroscopic data were obtained with a standard Beckman Quartz Spectrophotometer. The substituted phenols were prepared in this Laboratory^{5,6} and each was believed to be at least 99% pure. The other compounds were the best obtainable commercially and, when necessary, were further purified by recrystallization.

(5) D. R. Stevens, *Ind. Eng. Chem.*, **35**, 655 (1943).

(6) G. H. Stillson, D. W. Sawyer and C. K. Hunt, *THIS JOURNAL*, **67**, 303 (1945).

The solvents used were isoöctane (2,2,4-trimethylpentane), absolute ethanol and distilled water. Effects due to benzene in the ethanol were eliminated by using the solvent for the sample and for the comparison cell from the same bottle.

In order to study the temperature dependence of the various spectra a constant temperature cell compartment suitable for use with the Beckman Spectrophotometer was designed. In the design of this, which is in some ways similar to the one recently described by Bell and Stryker,⁷ a number of specific objectives were kept in mind: the assembly would be kept at constant temperature by the circulation of water from a commercial constant temperature bath, all essential components would be integral in a removable assembly, and this assembly would occupy the place of the regular cell compartment.

The essential elements of this assembly are seen in Fig. 1. Here 1 represents one of the four holes through which the retaining screws pass. The small hole 2 is one of two dowel holes which serve to position the unit relative to the body of the spectrometer. The heart of the device is represented by 3. It is a machined brass block through which the water circulates. There are two inlet and one outlet ports for the water, as indicated by the arrows. The channels for these are drilled about halfway through the block. Each then divides into two smaller channels, one of which is represented by 4. These smaller channels are located symmetrically relative to the center plane of the block which is represented by the figure. Also, in the block are milled two square holes which accommodate the cells, one of which is represented by 5. These cells are

(7) P. H. Bell and C. R. Stryker, *Science*, **105**, 414 (1947).

enclosed on three sides by metal strips 6, which are used for insertion and removal.

Two windows, indicated by 7, are cut through the brass block to communicate with each hole containing a cell. The light passes through these in a direction perpendicular to the plane of the figure.

The brass block is surrounded by a Bakelite housing 9.

Between the Bakelite and the block are strips of felt 8. This combination has proven to be quite effective insulation. Openings are cut in front and back sides to match the windows in the block. Onto the Bakelite and over these openings are sealed thin quartz windows (about $\frac{3}{32}$ " thick). The assembly is moved back and forth by the rod 10, to which is attached the knurled knob 12. It is held in either one of two pre-determined positions by a ball-lock 11.

Since the samples under examination are varied in temperature, it is necessary that the cells be vapor tight. A cross section of such a cell is seen in Fig. 2. Here the cell body is represented by 17. The unit 16 is a filling port. Units 16 and 17 are sealed together by means of Sauer-eisen⁸ cement 13. Units 16 and 15

Fig. 2.—Schematic diagram of vapor-tight absorption cell.

are of Invar metal. A solid lead washer 14 is used to make a seal when the cap is tightened on 16.

Data and Discussion

A. Behavior of the Substituted Phenols; Spectral Changes and Steric Hindrance to Hydrogen Bonding.—Since the phenols as a class exhibit strong dependence of spectra on the type of solvent used, and since definite information concerning their hydrogen bonding characteristics is now available,³ a large part of this investigation deals with them. In Fig. 3 may be seen the data for the unhindered phenol *p*-*t*-butylphenol. Two major differences between the spectra are observable. The spectrum for the ethanol solvent is shifted considerably to the longer wave lengths, or red portion of the spectrum. The other difference is in the shape and intensity of the bands. We note that the detailed structure of the band near 280 $m\mu$ as obtained in the iso-octane is almost completely blurred out when the alcohol is used. These two effects are characteristic, in varying degrees, of all the phenols. The results for another unhindered phenol may be seen in Fig. 4, which refers to *p*-cresol. The same two effects of wave length shift to the red and blurring of band structure are rather prominently displayed here.

An example of one of the partially hindered phenols may be seen in Fig. 5, for 2,4-di-*t*-butylphenol. Here again the same two effects may be seen. It is also to be noticed that the degree of detailed structure for the fundamental band centering near 275 $m\mu$ in iso-octane is less than observed for the simpler phenols. The behavior of this phenol is essentially representative of the other partially hindered phenols examined.

The results for one of the hindered phenols may

(8) Mfd. by Sauereisen Cements Co., Pittsburgh, Pa.

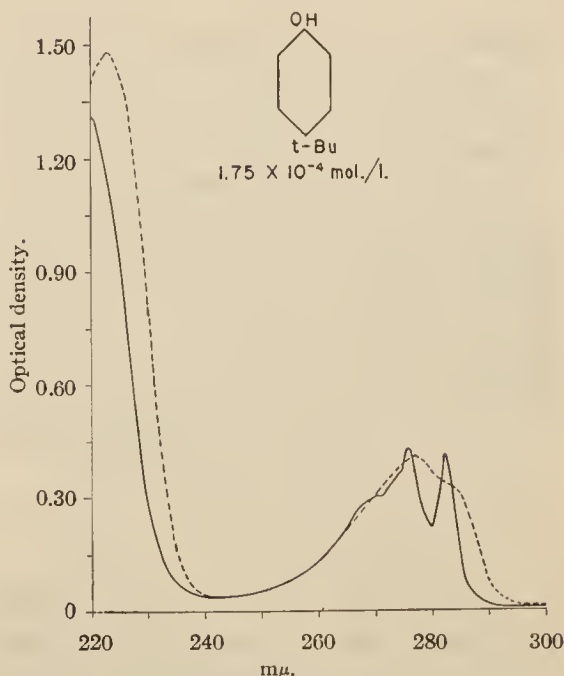


Fig. 3.—Ultraviolet absorption spectra of *p*-*t*-butylphenol, solid curve for iso-octane solution, dashed curve for alcohol solution.

be seen in Fig. 6, which is for 2,6-di-*t*-butyl-4-cyclohexylphenol. We note here that the shift to the red of the fundamental absorption band is greatly reduced, in comparison to the above com-

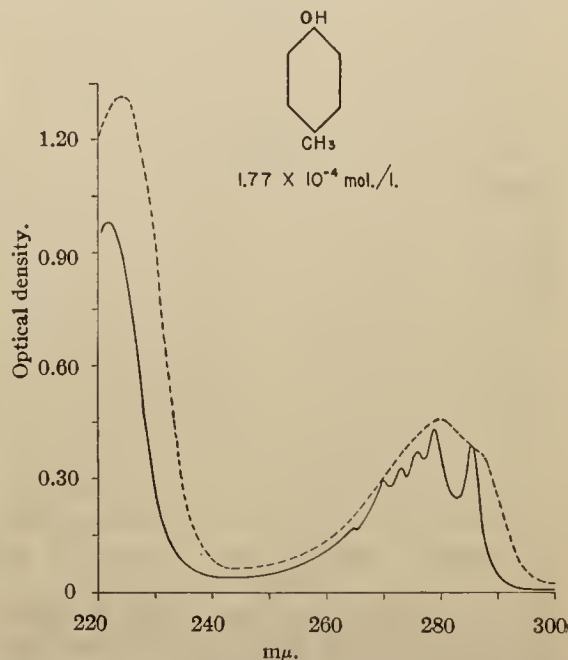


Fig. 4.—Ultraviolet absorption spectra of *p*-cresol, solid curve for iso-octane solution, dashed curve for alcohol solution.

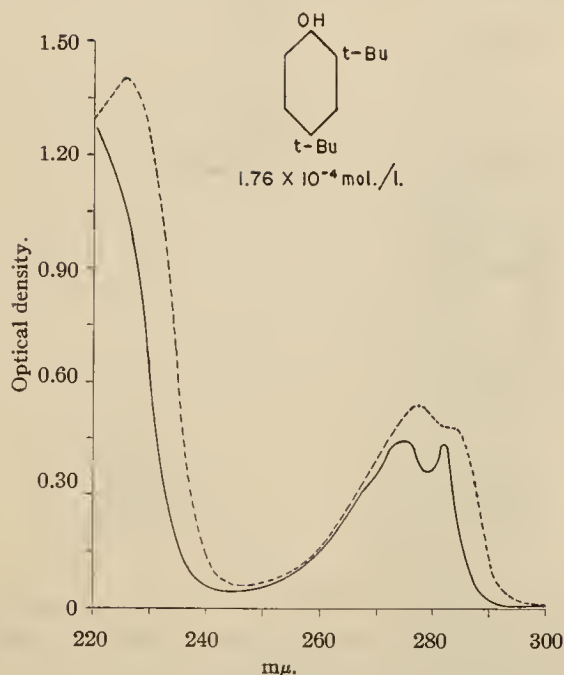


Fig. 5.—Ultraviolet absorption spectra of 2,4-di-*t*-butylphenol, solid curve for isoöctane solution, dashed curve for alcohol solution.

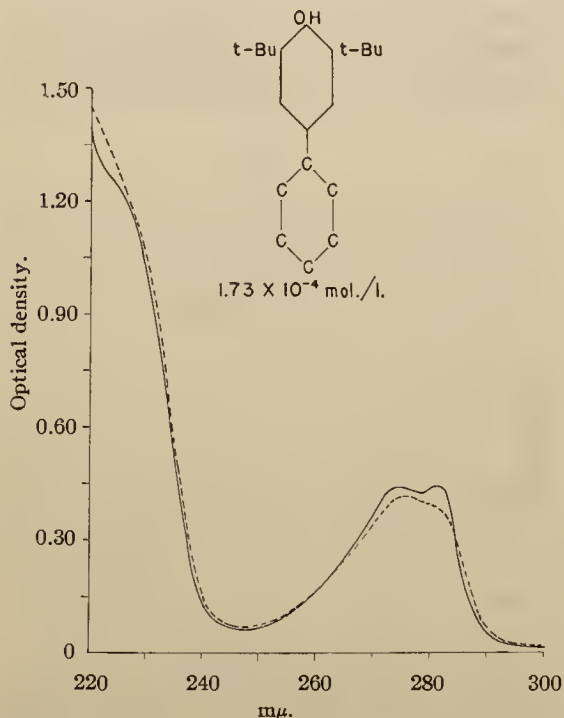


Fig. 6.—Ultraviolet absorption spectra of 2,6-di-*t*-butyl-4-cyclohexylphenol, solid curve for isoöctane solution, dashed curve for alcohol solution.

pounds. Another hindered phenol, exhibiting a very small shift to the red, is seen in Fig. 7 which

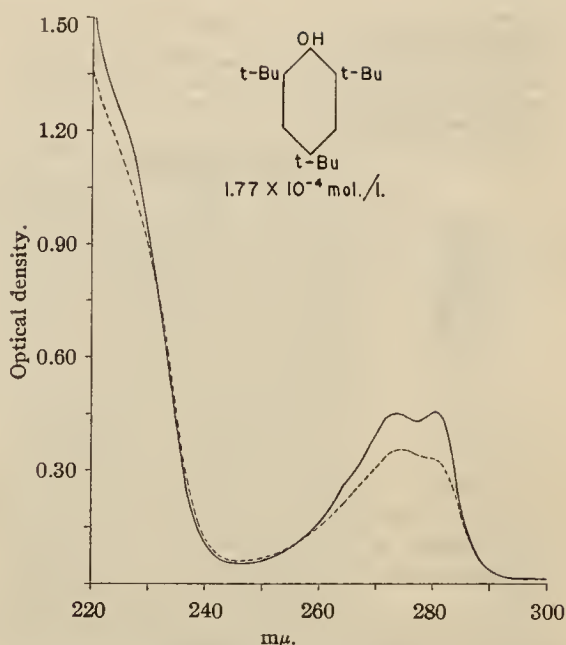


Fig. 7.—Ultraviolet absorption spectra of 2,4,6-tri-*t*-butylphenol, solid curve for isoöctane solution, dashed curve for alcohol solution.

represents 2,4,6-tri-*t*-butylphenol. Note that there is practically no detailed structure in the 280 $m\mu$ absorption for either solvent. This is to be expected from the more complex nature of the molecules, *i. e.*, more allowable vibrational states due to the larger substituent groups.

Although the data are shown for only a few of the phenols examined, further curves would be superfluous as the examples chosen are representative of their classes. An examination of the absorption spectra leads one to conclude that the unhindered and partially hindered phenols behave essentially as a single class with respect to the solvent dependence of their spectra. In contrast to this behavior the hindered phenols behave as a distinct class, since the red shift for them is so slight.

These results are based on visual observations of the spectra and it is desirable to verify them from quantitative data. For that reason a "center of gravity" of the spectral bands is defined and used. If we regard optical density as corresponding to mass and the wave length values as corresponding to distance then our spectral "center of gravity" is analogous to the mechanical concept. The spectral center of gravity will lie on a wave length $\bar{\lambda}$ determined by

$$\bar{\lambda} = \frac{\int_{\lambda_1}^{\lambda_2} \lambda D(\lambda) d\lambda}{\int_{\lambda_1}^{\lambda_2} D(\lambda) d\lambda} \quad (1)$$

where the effective wave length limits for the absorption band under consideration are λ_1 and λ_2 , and $D(\lambda)$ is the optical density for wave length λ .

It is clear from the figures that a change in

solvent from isoöctane to ethyl alcohol shifts the center of gravity of the fundamental band to the red for each of the above compounds. The use of the center of gravity concept allows a quantitative calculation of these shifts. For this Eq. 1 was evaluated for each compound by numerical integration by using the equation

$$\bar{\lambda} = \sum \lambda_i D(\lambda_i) / \sum D(\lambda_i) \quad (2)$$

where $\lambda_{i+1} - \lambda_i = 1 \text{ m}\mu$. The wave length shift $\Delta\bar{\lambda}$ occurring in going from one solvent to another was obtained for each phenol by determining the difference in $\bar{\lambda}$ calculated for the two solvents. In Table I may be seen these values for the unhindered phenols.

TABLE I

VALUES OF $\bar{\lambda}$ AND $\Delta\bar{\lambda}$ IN $\text{m}\mu$ FOR THE UNHINDERED PHENOLS FOR ISOÖCTANE AND ETHYL ALCOHOL SOLVENTS

Compound	$\bar{\lambda}$ (iso-octane)	$\bar{\lambda}$ (alcohol)	$\Delta\bar{\lambda}$
Phenol	268.3	270.5	2.2
<i>o</i> -Cresol	269.4	271.6	2.2
<i>m</i> -Cresol	270.6	275.7	5.1
<i>p</i> -Cresol	273.9	275.8	1.9
<i>p</i> - <i>t</i> -Amylphenol	271.6	273.5	1.9
<i>p</i> - <i>t</i> -Butylphenol	271.9	274.0	2.1
2,6-Dimethyl-4- <i>t</i> -butylphenol	272.5	273.3	0.8
Average $\Delta\bar{\lambda} = 2.3 \text{ m}\mu$.			

For each of the compounds in Table I and for the other substituted phenols examined the band over which the $\bar{\lambda}$'s and the $\Delta\bar{\lambda}$ were calculated was taken as extending from 245 $\text{m}\mu$ to 310 $\text{m}\mu$. Calculations were not made for the lower wave length band as complete data were not available for it. Results for the partially hindered phenols are given in Table II.

TABLE II

VALUES OF $\bar{\lambda}$ AND $\Delta\bar{\lambda}$ FOR THE PARTIALLY HINDERED PHENOLS

Compound	$\bar{\lambda}$ (iso-octane)	$\bar{\lambda}$ (alcohol)	$\Delta\bar{\lambda}$
2-Methyl-4,6-di- <i>t</i> -butylphenol	272.1	273.2	1.1
2,4-Di- <i>t</i> -butylphenol	272.3	274.4	2.1
2- <i>t</i> -Butyl-4-methylphenol	274.5	276.9	2.4
3-Methyl-6- <i>t</i> -butylphenol	270.7	272.7	2.0
2- <i>t</i> -Amyl-4-methylphenol	275.3	277.5	2.2
4-Ethyl-6- <i>t</i> -butylphenol	273.6	276.0	2.4
Average $\Delta\bar{\lambda} = 2.1 \text{ m}\mu$.			

The results for the hindered phenols are seen in Table III. Inspection of these shows that some of the $\Delta\bar{\lambda}$'s and the average $\Delta\bar{\lambda}$ for the hindered phenols are negative. It is not true, however, that the spectra for those cases have been shifted to the blue, *i. e.*, to shorter wave lengths. These negative values result from the change of shape of the spectral bands together with the manner of computing $\bar{\lambda}$. In Fig. 7 may be seen an example of this. Here the fundamental band, centering near 280 $\text{m}\mu$, has two poorly resolved branches for the

isoöctane solution. It is clear that the longer wave length one will contribute more to the calculated value of $\bar{\lambda}$. The same band for ethyl alcohol solution shows two even more poorly resolved branches, the one at shorter wave length now predominating. This weights the calculation in such a manner as to induce an "apparent" blue shift. From the shoulders and sides of the band it is apparent, however, that there is a slight red shift. The same type of band-shape change also occurs for the other compounds in the table exhibiting negative $\Delta\bar{\lambda}$'s. With this in mind we see from a comparison of the tables that the red shifts for the hindered phenols are much smaller than for the unhindered and partially hindered phenols. Also, we see that these latter two classes are essentially the same with regard to this shift.

TABLE III

VALUES OF $\bar{\lambda}$ AND $\Delta\bar{\lambda}$ IN $\text{m}\mu$ FOR THE HINDERED PHENOLS

Compound	$\bar{\lambda}$ (iso-octane)	$\bar{\lambda}$ (alcohol)	$\Delta\bar{\lambda}$
2,6-Di- <i>t</i> -butyl-4-cyclohexylphenol	273.0	273.1	0.1
2,4,6-Tri- <i>t</i> -butylphenol	273.0	272.0	-1.0
2,6-Di- <i>t</i> -butyl-4-methylphenol	274.8	274.2	-0.6
2,6-Di- <i>t</i> -butyl-4-ethylphenol	273.3	273.6	0.3
2,6-Di- <i>s</i> -butyl-4-methylphenol	275.0	274.1	-0.9
2- <i>t</i> -Butyl-6- <i>t</i> -amyl-4-methylphenol	273.8	273.8	0.0
2,6-Di- <i>t</i> -butyl-4-diisobutylphenol	271.6	272.0	0.4

Average $\Delta\bar{\lambda} = -0.2 \text{ m}\mu$.

One hindered phenol, 2,6-di-*t*-butyl-4-phenylphenol, exhibited anomalous behavior in comparison to the others. This behavior, to be seen in Fig. 11, is believed to be due in part to the conjugation between the two phenyl rings. For that reason it is not included in the above tables nor considered in drawing conclusions from these tables.

On the assumption that hydrogen bonding between solute and solvent molecules is important to the processes responsible for the alteration of spectra, the fact that the unhindered and partially hindered phenols behave as a single class would seem in variance with the infrared results. It must be remembered, however, that the classification from infrared studies is based on the steric hindrance to hydrogen bonding between like molecules. Two unhindered phenol molecules may associate very strongly. Two partially hindered phenols will be partially hindered in their association by the large alkyl groups on the ortho positions. However, due to the relatively small dimensions of the ethanol molecule it may associate easily with either unhindered or partially hindered phenol molecules. This may be easily seen by the use of atom models. This equal ease of association explains the similar behavior of these two classes of phenols. The reduced alteration of spectra observed for the hindered phenols is ascribed to the hindrance the large alkyl groups on the ortho positions offer to the approach of the ethanol molecules to the phenol hydroxyl groups.

It would thus seem that a direct correlation

might be made between the observed degree of spectral change and the strength of intermolecular hydrogen bonding. However, we cannot conclude that it is hydrogen bonding itself which is to be correlated with the spectral changes but rather the distance of approach of the ethanol molecule to the hydroxyl group of the phenol.

B. Temperature Effects.—As was stated earlier, it was decided to study the spectra as a function of temperature to determine the importance of hydrogen bonded complexes. If it were true that such complexes were necessary to produce the spectral changes then a progressive rise in temperature should progressively modify the alcohol solution spectrum to resemble the iso-octane solution spectrum. This would be true as the population of complexes would be progressively reduced by the increase of temperature.

Phenol was chosen as the compound to examine and its spectra in iso-octane and alcohol solution at room temperature may be seen in Fig. 8.

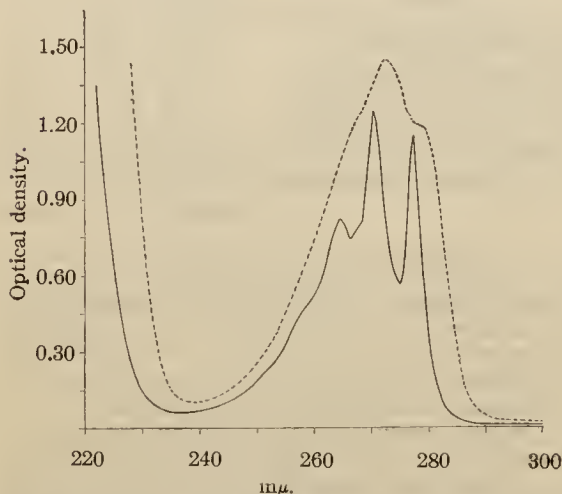


Fig. 8.—Ultraviolet absorption spectra of phenol, solid curve for iso-octane solution, dashed curve for alcohol solution.

In Fig. 9 may be seen a series of temperature runs made with the temperature-controlled cell compartment described above. Here the successive spectra are shifted vertically for clarity. There are no discernible changes in the spectra even though the temperature change is quite adequate to destroy the hydrogen bonded complexes. Similar tests were made with other compounds. Aniline shows large spectral changes between the spectra obtained in iso-octane and water solutions. However, when a water solution of aniline was examined through a series of increasing temperatures as for phenol no changes of spectra were found. Acetylacetone shows a large red shift between the spectra for iso-octane and ethyl alcohol solutions. No changes of spectra were found for it when an alcohol solution was examined through a similar series of temperature.

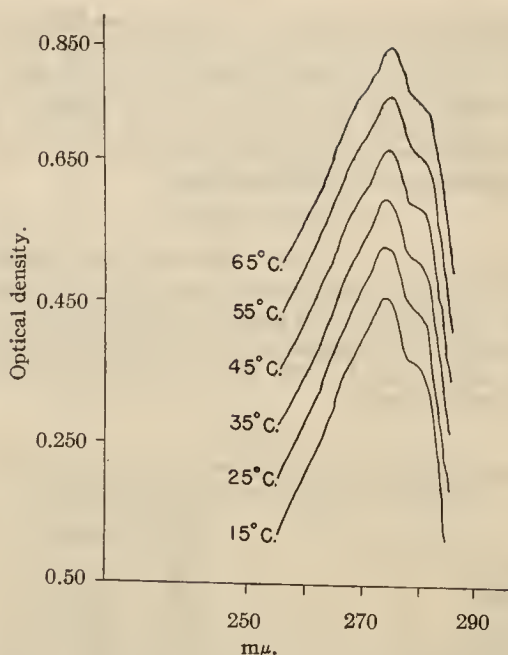


Fig. 9.—Spectra of phenol in ethanol solution at various temperatures.

Since these tests show no dependence of spectra on temperature, we may conclude that stable hydrogen bonded complexes are not necessary for the change of spectra observed for ethyl alcohol solutions. These observations together with those on the substituted phenols indicate that the spectral changes are due to the close proximity between the hydroxyl groups of the ethanol and phenol molecules. The stabilization of the polar excited states may be assumed to be due to electronic interaction between the dipole moment of the alcohol and the ionic form of the excited state. This interaction is evidently non-specific in the sense of not depending upon stable complexes.

As a further test of the temperature dependence of the spectra a series of runs was made of a solution of phenol in a solvent consisting of 0.2 mole per liter of ethanol in iso-octane. These results are seen in Fig. 10. Again the spectra are vertically displaced for clarity. At the end of the series the sample was returned to approximately room temperature to ascertain if any permanent changes had been produced in the solution. This spectrum is the top one in the figure. It shows no significant differences from the initial one. It is to be observed in this series of curves that the spectra at increasing temperatures approach nearer and nearer the spectrum for phenol in iso-octane. The trend of these spectra is the same as achieved when a series of similar solutions containing progressively smaller concentrations of alcohol are examined. In view of the results and the above temperature studies, it is believed that the phenomenon of spectral change with temperature seen in Fig. 10 is due to changes in the im-

mediate surroundings of the solute molecules. Due to dipole-dipole interactions between the phenol molecules and the alcohol molecules there will be a tendency for the former to be in close proximity with one or more of the latter. An increase in temperature, however, will tend to disperse such clusters due to thermal agitations. Thus an increase in temperature will create the observed effect which is the same as reducing the concentration of the alcohol in the solvent.

C. Smoothing and Asymmetrical Broadening of the Absorption Bands.—It is well known that the band structure observed in the ultraviolet is the result of transitions from the vibrational energy levels of one electronic configuration to the vibrational energy levels of another.⁹ With an increase of atomic groupings in the molecule there will be more allowable vibrational levels and the detailed band structure will be less distinct. This may be observed from Figs. 3, 4, 5, 6, 7 and 8. It is noted that the partially hindered phenols possessing more alkyl substitution than the unhindered phenols have less detailed band structure. In turn the hindered phenols have even less structure. These observations are true of all the phenols examined.

In examining the same set of figures as above, it may be observed that in each case the band structure is almost lost in the ethanol solutions. Before proposing an explanation for this, let us consider another effect. It is to be observed, particularly in Figs. 3, 4 and 5, that, in passing from iso-octane to ethanol solution, the fundamental band centering near 280 $m\mu$ is asymmetrically broadened. It is extended into the red with very little change in behavior on the short wave length side. This phenomenon is characteristic of all the phenols examined, especially the unhindered and partially hindered ones. This asymmetrical broadening is not observed for the aromatic hydrocarbons even though they may exhibit appreciable values of $\Delta\lambda$. This latter fact together with the effects of temperature variation lead us to explanations for the present phenomena based on the proximity of the hydroxyl groups of alcohol and phenol molecules.

Due to the dipole-dipole interaction between the hydroxyl groups there will be a tendency for the alcohol and phenol molecules to approach very closely to each other and at room temperature and somewhat above to form complexes. However, due to thermal agitations, all phenol molecules in the solution will not be members of complexes. Rather, at any instant, there will be a weighted statistical distribution over the dipole-(phenol)-dipole(alcohol) distance. It is known from the above data that this distance influences the degree of spectral shift. The spectra for an alcohol solution will be the superposition of the spectra for all values of the dipole-dipole distance. Those phenol molecules with their hy-

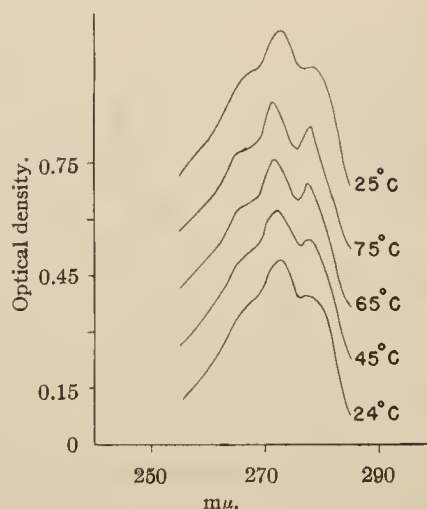


Fig. 10.—Spectra of phenol at various temperatures for a concentration of 2.88×10^{-4} mol./l. in a solvent comprising 0.2 mol./l. of ethanol in iso-octane.

droxyl groups in close proximity to the hydroxyl groups of alcohol molecules would be expected to contribute heavily to the red side of the band. Those with large or normal distances would be expected to absorb approximately as if they were in an iso-octane solution. This latter statement is based on results obtained for benzene and toluene, to be discussed later. It is clear then that such a superposition would lead to an asymmetrical broadening as observed. It would also lead to a blurring of the band structure.

In addition to the blurring due to a spread in dipole-dipole distances there are two other effects expected to contribute to it. One is the effect of the electric fields due to the dipoles of the hydroxyl groups in the alcohol molecules. At short distances the intensity of the electric fields of such a dipole is very large. Therefore, for the phenol molecules in close proximity to ethanol molecules we would expect a smoothing or displacement of band structure due to the perturbing effects of the large electric fields. The other effect expected to contribute to the smoothing of the band structure is inherent in the strong dipole-dipole attractions between the phenol and alcohol molecules. Because of these strong forces, a phenol molecule may be regarded as mechanically coupled in a non-rigid manner to one or more neighboring alcohol molecules. Since this is somewhat equivalent to adding further substituent groups we would expect a reduction of band structure for the same reasons that the addition of further groups on a simple phenol reduces the structure.

D. Effects Obtained with Conjugated Aromatics.—As was mentioned above, 2,6-di-*t*-butyl-4-phenylphenol behaves anomalously compared to the other phenols. Its spectra may be seen in Fig. 11. We note that it not only exhibits a quite large wave length shift, but it does not show

(9) See, for example, G. N. Lewis and M. Calvin, *Chem. Rev.*, **25**, 273 (1939).

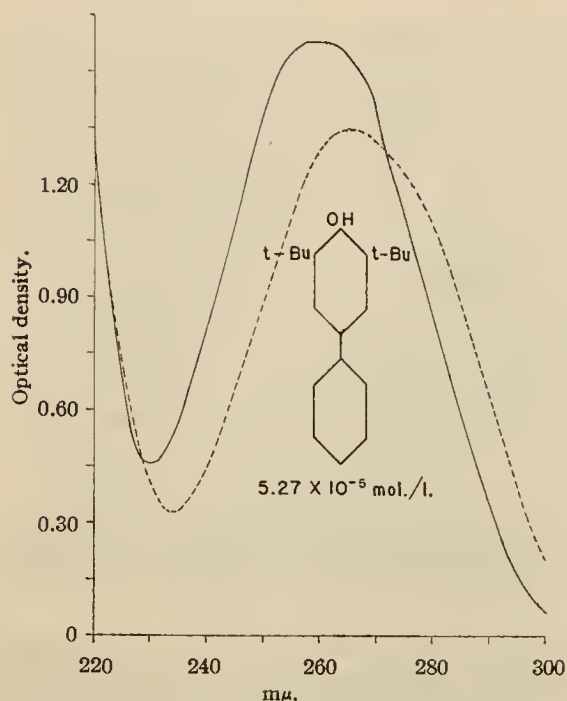


Fig. 11.—Ultraviolet absorption spectra of 2,6-di-*t*-butyl-4-phenylphenol, solid curve for isoöctane solution, dashed curve for alcohol solution.

the asymmetrical band broadening. The calculated values for this compound are: $\bar{\lambda}$ (isoöctane) = 265.1 mμ, $\bar{\lambda}$ (alcohol) = 269.8 mμ, and $\Delta\bar{\lambda}$ = 4.7 mμ. We have assumed that this anomalous behavior is due to the conjugation of the phenyl and phenol groups. Confirming evidence for this may be seen below wherein wave length shifts are observed for conjugated aromatic systems.

In order to appraise the degree of spectral shift

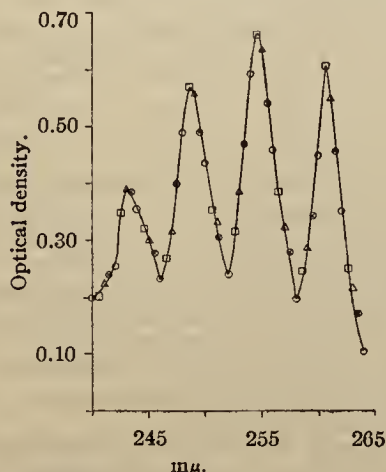


Fig. 12.—Absorption spectra of benzene under various solvent conditions: O, isoöctane; Δ, ethyl alcohol; □, ethyl alcohol + sodium chloride; ⊗, ethyl alcohol + water.

for conjugated hydrocarbon systems a number of aromatic hydrocarbons were examined. In Fig. 12 may be seen the results for benzene examined under four different conditions. The solvents for these were isoöctane, ethanol, ethanol containing water in equal concentrations to the solute an ethanol saturated with sodium chloride. No significant spectral changes nor wave length shifts are observable. Toluene was also examined in isoöctane and alcohol with no observable shift. In Fig. 13 may be seen the spectra in isoöctane and ethanol of naphthalene. Here a definite shift to

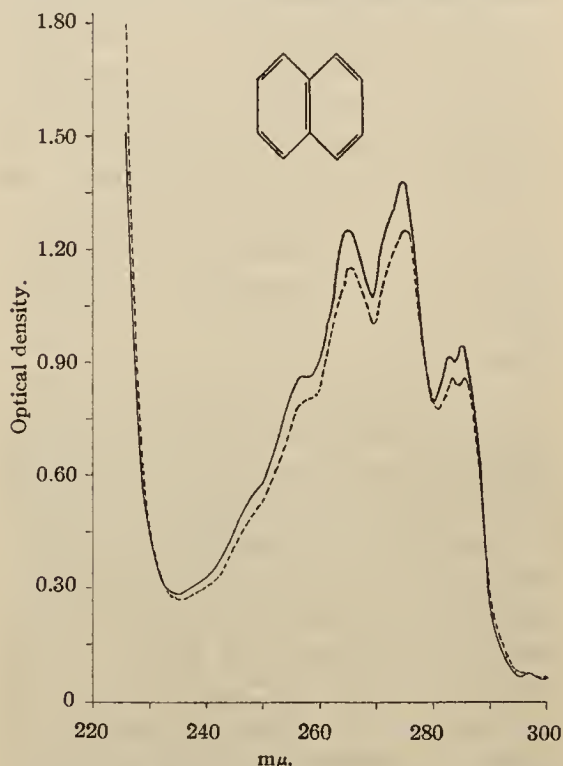


Fig. 13.—Ultraviolet absorption spectra of naphthalene, solid curve for isoöctane solution, dashed curve for alcohol solution.

the red is observable. It would be even more so were it not that two slightly different concentrations were used. A number of other hydrocarbons possessing a degree of conjugation greater than benzene were examined and the results for these are tabulated in Table IV. As the wave length regions considered are different for the various compounds they are also included.

In Fig. 14 may be seen the results for another of the aromatic hydrocarbons, *p*-diphenylbenzene. In this figure it may be seen that the complete fundamental band in the 280 mμ region is shifted to the red rather than asymmetrally broadened as for the phenols. This effect of complete band shift rather than asymmetrical broadening was observed for all the aromatic hydrocarbons examined. It suggests a definite difference, between

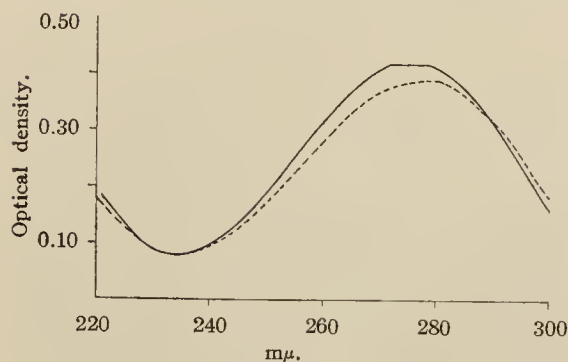


Fig. 14.—Ultraviolet absorption spectra of *p*-diphenylbenzene, solid curve for iso-octane solution, dashed curve for alcohol solution.

the phenols and aromatic hydrocarbons, in the processes responsible for the alteration of spectra.

TABLE IV

VALUES OF $\bar{\lambda}$ AND $\Delta\bar{\lambda}$ IN $m\mu$ FOR VARIOUS AROMATIC HYDROCARBONS

Compound	Wave length region, $m\mu$	μ (iso-octane)	$\bar{\lambda}$ (alcohol)	$\Delta\bar{\lambda}$
Styrene	220-265	242.9	243.3	0.4
Naphthalene	235-305	257.4	257.8	.4
Diphenyl	220-290	247.8	248.6	.8
<i>o</i> -Diphenylbenzene	224-255	237.4	237.5	.1
<i>m</i> -Diphenylbenzene	222-290	250.6	250.9	.3
<i>p</i> -Diphenylbenzene	239-320	272.9	273.7	.8

Since the aromatics of Table IV all have more conjugation than benzene and toluene we may assume that the dipole moments of their polar excited states will be correspondingly larger. We may further assume that it is the interaction of these larger dipole moments with the surrounding ethanol molecules that accounts for the red shift. Since these aromatic hydrocarbons in the ground state are not possessed of strong dipole moments there will not be the same tendency for preferential alignment and complex formation between them and the alcohol molecules as for the phenols. Therefore, when an aromatic hydrocarbon is raised to an excited state it should find an "average" state of affairs as regards the neighboring alcohol molecules. This would account for the complete shift of the band rather than an asymmetrical broadening.

When a dipole is imbedded in a dielectric the interaction energy will be a function of the dipole strength. We would, therefore, expect larger wave length shifts for molecules possessed of larger dipole moments of the excited states. It is interesting to observe the behavior of the diphenylbenzene isomers. Due to spatial extension it is to be expected that the dipole moment of the excited state of the para isomer will be larger than that of the meta isomer which in turn will be greater than that of the ortho isomer. The wave length shifts would then be expected to have the

same order. An examination of Table IV shows this to be true.

E. Behavior of the bis-Phenols.—Interesting results were obtained on several bis-phenols kindly supplied us by Dr. D. Stevens and Mr. A. C. Dubbs of this Laboratory. The data for one of these may be seen in Fig. 15. The dashed

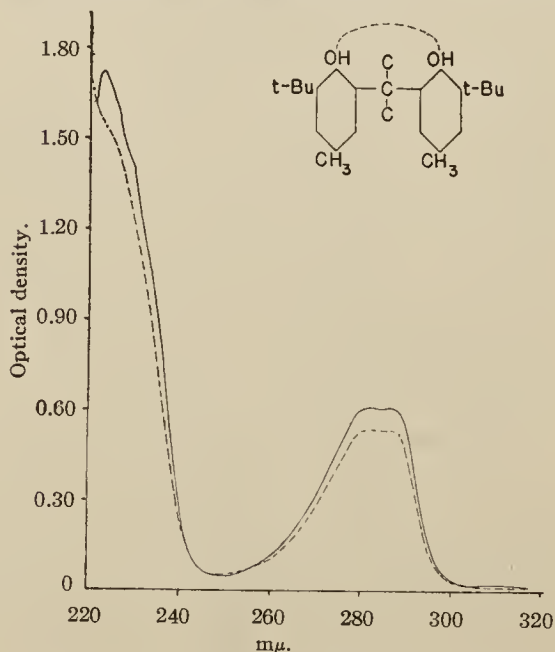


Fig. 15.—Ultraviolet absorption spectra of 2,2-bis-(2-hydroxy-3-*t*-butyl-5-methylphenyl)-propane, solid curve for iso-octane solution, dashed curve for alcohol solution.

line joining the hydroxyl groups in the figure is meant to represent the existence of an intramolecular hydrogen bond. It was found by infrared absorption studies that in each of these compounds studied there was very good evidence of such internal hydrogen bonds.¹⁰ The manner of representing the structure used in Fig. 15 does not indicate that the hydroxyls can achieve enough proximity to hydrogen bond. However, an examination using atom models shows that such proximity is possible. The values of the $\bar{\lambda}$'s and $\Delta\bar{\lambda}$'s found for these compounds may be seen in Table V.

TABLE V

VALUES OF $\bar{\lambda}$ AND $\Delta\bar{\lambda}$ IN $m\mu$ FOR THE BIS-PHENOLS

Compound	$\bar{\lambda}$ (iso-octane)	$\bar{\lambda}$ (alcohol)	$\Delta\bar{\lambda}$
bis-(2-Hydroxy-3- <i>t</i> -butyl-5-methylphenyl)-methane	280.1	279.7	-0.4
2,2-bis-(2-Hydroxy-3- <i>t</i> -butyl-5-methylphenyl)-propane	280.5	280.6	.1
2,2-bis-(2-Hydroxy-3- <i>t</i> -butyl-5-methylphenyl)-butane	280.9	280.9	.0
1,1-bis-(2-Hydroxy-3- <i>t</i> -butyl-5-methylphenyl)-isobutane	281.4	281.6	.2

(10) Unpublished results.

The values of $\Delta\bar{\lambda}$ are approximately the same as for the hindered phenols. This is to be expected in view of the steric hindrance the *t*-butyl groups on the ortho positions will offer to the approach of ethanol molecules and to the fact that in the intramolecular hydrogen bond the dipole moments of the hydroxyls will partially cancel each other, thus reducing the attraction of such a molecule for the alcohol molecules.

It is interesting to note that the center of the fundamental band for each of these compounds is about 280 $m\mu$. This is further to the red than the centers of the corresponding band for the simpler phenols. Part of this displacement may be thought to be due to the hydrogen bonding or close proximity effects of the two phenol rings on each other. The positioning of one phenol group in close proximity to another should be expected to produce a red shift just as ethyl alcohol solvent does for a simpler phenol. Therefore, the spectra of a bis-phenol in isoöctane solution would be expected to show the center of its fundamental band at longer wave lengths than a simple phenol.

Acknowledgment.—Acknowledgment is gratefully made to Dr. D. Stevens, Dr. G. Stillson and Mr. A. C. Dubbs for furnishing some of the compounds studied. We also wish to express acknowledgment to Brother C. Curran of Notre Dame University for discussions of the subject, to Mr. A. Glessner for aid in taking some of the data, and to Paul D. Foote, Executive Vice-President of Gulf Research & Development Company, for permission to publish this material.

Summary

A study has been made of the changes in ultraviolet absorption spectra for twenty-one phenols that occur when the solvent is changed from a paraffin to an alcohol. Three different effects are observed: a shift of the spectral center of gravity to longer wave lengths, a smoothing of the band structure, and an asymmetrical broadening of the fundamental absorption band. It is found that that the spectral change depends upon the degree of steric hindrance offered to the approach of the alcohol molecules to the hydroxyl group of the phenol. In alcohol solutions the spectra of the phenols and other compounds do not change with increasing temperature, indicating that the processes primary to the spectral changes do not depend on stable hydrogen bonded complexes. Data are given for the unhindered, partially hindered and hindered phenols.

Tentative explanations are provided for some of the temperature effects, the smoothing of the band structure, and the asymmetrical broadening of the bands. These are based on considerations of the intermolecular interactions. No significant spectral changes were observed for benzene or toluene whereas a shift to the red was observed for aromatic hydrocarbons of higher conjugation. This is discussed in terms of the stabilization of the excited polar states through interactions with the alcohol molecules. Data and discussion are provided for four bis-phenols.

PITTSBURGH, PA.

RECEIVED JANUARY 19, 1948

Jan. 4, 1949.

M. MUSKAT ET AL

2,458,093

METHOD OF DETERMINING THE FLUID CONTENT OF WELL CORES

Filed Feb. 19, 1945

FIG. 1.

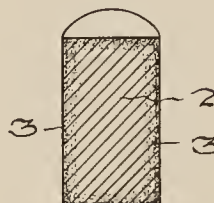


FIG. 2.

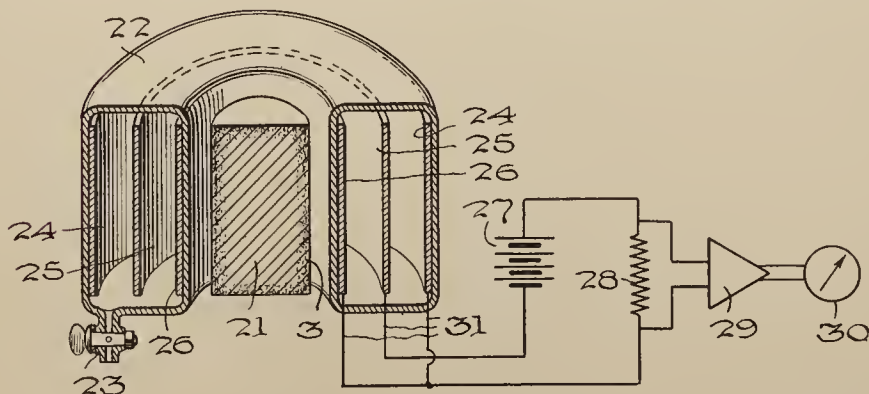
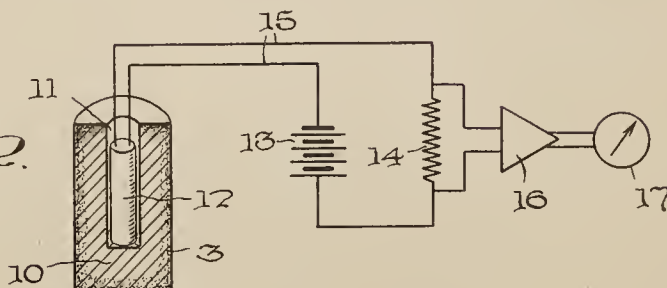


FIG. 3.

Inventors
MORRIS MUSKAT
NORMAN D. COGGESHALL

By *W. McLaughlin*
Attorney

UNITED STATES PATENT OFFICE

2,458,093

METHOD OF DETERMINING THE FLUID
CONTENT OF WELL CORES

Morris Muskat, Oakmont, and Norman D. Coggeshall, O'Hara Township, Allegheny County, Pa., assignors to Gulf Research & Development Company, Pittsburgh, Pa., a corporation of Delaware

Application February 19, 1945, Serial No. 578,748

1 Claim. (Cl. 250—83)

1

This invention concerns an improved method of determining the amount of fluid in a core obtained from a certain level in a well bore. More particularly, it involves a method of determining by means of a radioactive technique the drilling fluid content of a well core, so that this information may be used as a method of logging or applied as a correction to connate fluid determinations.

In the drilling and producing of oil wells, it is customary to cut cores of the formations penetrated. These cores are useful for identifying formations which might be oil bearing, and they are particularly useful in determining the productivity which might be expected of the various formation horizons encountered in the well.

In the determination of the productivity of an oil bearing horizon, a core sample is subjected to certain well known tests. These tests involve determination of porosity and permeability by known methods. It is also necessary to know the pore content of the producing formation. This is done by taking bottom hole samples under pressure, bringing them to the surface and analyzing them. The samples may contain gas or oil or connate water.

A serious difficulty in the above determinations arises from the fact that wells are drilled with the use of a fluid of some type to cool the drill and remove drill cuttings and carry them to the surface. This drilling fluid is commonly maintained with a bottom hole pressure slightly greater than that of the formation being drilled, in order that the well may at all times be kept under control. Any formation which is porous enough to produce oil will obviously have forced into it a certain amount of the drilling fluid during the drilling process and this fluid contaminates the connate fluid in the formation to such an extent that a subsequent test on a sample brought to the surface may not give reliable results. In case an oil base drilling fluid is used, the oil content analysis may obviously be in error. If an aqueous drilling fluid is used, the connate water analysis may be in error.

A further limitation arises from the fact that the determination of connate fluids is a time consuming and expensive laboratory procedure and is therefore ordinarily not used except for relatively widely spaced samples. A more continuous log of the borehole with respect to the amount of drilling fluid entrained in the core has heretofore not been commercially practicable because of the difficulty and uncertainty heretofore incident to the measurements. The method of our invention when applied to cores would per-

2

mit such measurements to be made very simply and quickly so that one may log the cores with respect to the amount of drilling fluid invasion as a basis of correlation and indexing the type of strata which the drill has traversed. Such a log will reflect the variations in permeability and porosity of the strata. An especially advantageous feature of our invention is that quantitative measurements of the drilling fluid invasion may be made before and without the tedious process of extraction, whereas in other methods extraction is necessary.

One of the objects of this invention is the evaluation of a correction in a core fluid determination for the amount of drilling fluid foreign to the core which was forced into the core during the drilling process before or during the cutting of the core.

Another object of this invention is to provide a simple and accurate method of correcting a core fluid determination for the amount of fluid absorbed by the core from the drilling fluid.

A still further object of this invention is to determine the amount of drilling fluid absorbed by the core by means of introducing a radioactive tracer into the fluid.

An ancillary object of this invention is to provide a simple, quick and accurate method of logging the cores of a borehole with respect to drilling fluid invasion.

These and other useful objects of the invention are accomplished in the manner described in the following specification.

A fuller understanding of our invention may be obtained by reference to the drawing, in which:

Figure 1 shows in section a core sample taken from a well bore in the manner of our invention;

Figure 2 shows an arrangement of measuring device for determining the amount of drilling fluid penetrating such a core sample; and

Figure 3 shows another arrangement of measuring device for determining the amount of drilling fluid in such a core sample.

The invention comprises in its simplest form adding to the drilling mud in known and controlled proportions a radioactive material which becomes homogeneously mixed in the mud. The core is cut with the use of this radioactive mud, and then later the radioactivity in the core sample is measured. The measured radioactivity will allow a determination of the amount of drilling fluid which actually penetrated into the core. This information may then be plotted in the form of a well log. If the core is extracted to determine connate fluid, the information obtained by our

invention may be used to identify that part of the extracted fluid which is entrained drilling fluid.

Several types of radioactive materials are advantageously added to the drilling fluid. Naturally radioactive material in the form of a salt of uranium, thorium or radium may be used. If the drilling fluid is of the aqueous type, the radioactive salts should be water soluble. In the case of oil base drilling fluids, they should be oil soluble such as, for instance, soaps of radioactive elements. Radium naphthenate or barium-radium-petronate are satisfactory oil soluble tracers. It is also possible to use artificially radioactivated substances. Examples of such artificial radioactive tracer materials are the isotopes of ordinary sodium, namely Na^{22} or Na^{24} which may be formed by various well known means. Salts of these isotopes are water soluble and emit energetic gamma rays and have suitable decay periods. Sodium naphthenate or sodium petronate are satisfactory as oil soluble artificially radioactive tracers. Artificial radioactive materials may be chosen with lifetime sufficiently long to carry out the methods of this invention and yet short enough so that later radioactivity logs of the well would not be appreciably affected by any mud which might remain attached to the rock strata.

In Figure 1 we have shown in cross section a sample of core 2 cut from a well using mud containing a dissolved radioactive material. The core is somewhat porous and a certain amount of radioactive drilling fluid penetrates the core as indicated in the figures by numeral 3. While the entire core 2 contains connate fluid an extraction would also include the extraneous fluid 3. The amount of fluid 3 is some function of the permeability and porosity of core 2. By means of this invention one may determine the amount of fluid 3. This may then be subtracted from the total amount of extracted fluid in the core to arrive at the correct amount of connate fluid.

After the core has been cut and removed to the surface, its radioactivity may be determined by means of the apparatus shown in Figure 2. Numeral 10 represents a section of core removed from the core barrel, the entrained radioactive drilling fluid being indicated by numeral 3. A small hole 11 may be drilled into the face of the core and into this hole is inserted a detector of radioactivity, such as an ionization chamber or Geiger counter indicated by numeral 12. The counter 12 is supplied high potential by the battery 13 through resistance 14 and leads 15. The potential across resistor 14 may be amplified by amplifier 16 whose output is indicated on meter 17. The meter 17 may be calibrated to read directly the amount of entrained radioactive drilling fluid 3 indicated in the core sample 10.

Another method of determining the radioactivity of the core is by the use of a specially shaped ionization chamber shown in Figure 3. Numeral 21 represents the core being studied having entrained radioactive drilling fluid 3. Numeral 22 represents a vessel which contains an ionization chamber. Stopcock 23 is a connection to the air or to a suitable gas reservoir. The vessel 22 contains three cylindrical conductors, 24 being the outermost, 25 being the intermediate one and 26 the innermost one. All are concentric and inside the annular vessel 22. Leads are brought out as indicated at points 31 and con-

nected as shown to battery 27 and resistor 28. When the core sample is placed inside this annular vessel, the gamma rays emitted from the core pass through the vessel and electrodes and ionize the gas contained in the vessel. As a result of the potential applied by the battery 27, all the ions formed in the region between 24 and 25 and between 25 and 26 are collected. The resulting current traverses resistance 28 and the consequent voltage drop across resistance 28 is a measure of the radioactivity of the core. The potential drop across 28 is amplified by the amplifier 29 and the output fed to meter 30. The indicating meter 30 therefore gives a reading proportional to the ionization current which in turn is a measure of the drilling fluid absorbed by the core. This device is easily calibrated by merely inserting, instead of core 21, a thin walled container filled with a measured sample of drilling fluid. The apparatus of Figure 3 is particularly adapted to logging of long cores in which case the annular vessel 22 may simply be slipped over the core and measurement made along the length of the core.

The concentration of the radioactive material used in the drilling fluid need not be very large because the natural radioactivity of the rocks normally encountered in oil producing formations is very small. The determination may in any case be improved by subtracting from the reading of meters 17 or 30 any indication obtained from a core not drilled with radioactive mud. Such core samples are readily available, so that the reading obtained with a blank core would be known.

In the practice of the invention, the radioactive material is preferably contained in the fluid in a dissolved state, so that it will not be filtered by small pores in the core sample. It should, furthermore, be of such chemical composition that it will not react with or be precipitated by the rocks or the fluids encountered in drilling. We have mentioned several radioactive compounds which may be used in our invention and these are by way of illustration only, many other similar compounds being available for accomplishing the objects of our invention.

What we claim as our invention is:

A method of determining the connate fluid content of a well core sample comprising adding to the drilling fluid a known concentration of artificially radioactivated material soluble in the drilling fluid, cutting and removing the core sample from the well, measuring the radioactivity of a known quantity of core sample to determine the amount of drilling fluid absorbed in the sample, determining the nature and quantity of total fluids in the core sample and subtracting therefrom the said determined amount of drilling fluid absorbed.

MORRIS MUSKAT.
NORMAN D. COGGESHALL.

REFERENCES CITED

The following references are of record in the file of this patent:

UNITED STATES PATENTS

Number	Name	Date
2,330,829	Lundberg	Oct. 5, 1943
2,349,712	Fearon	May 23, 1944
2,352,993	Albertson	July 4, 1944
2,364,975	Heigl	Dec. 12, 1944

March 1, 1949.

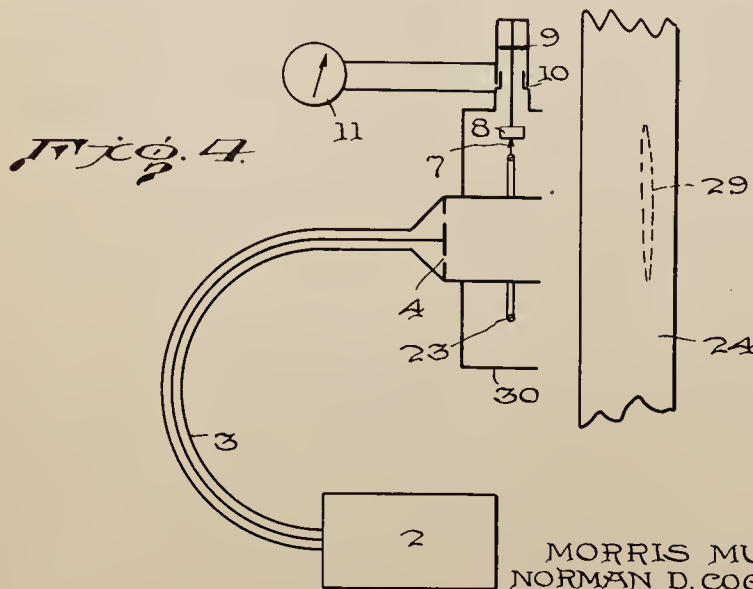
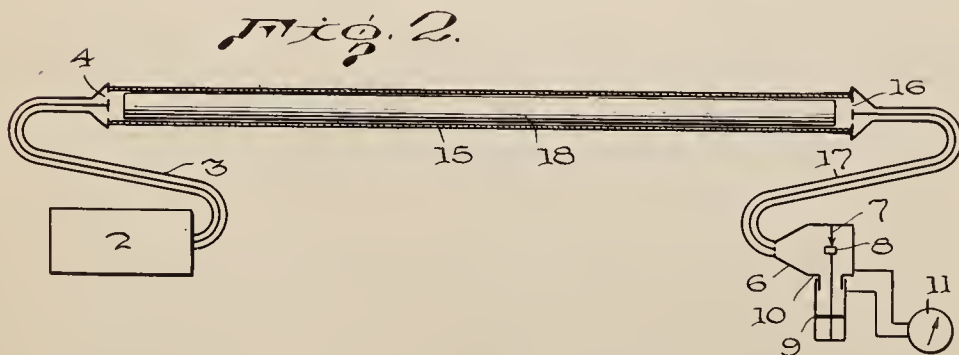
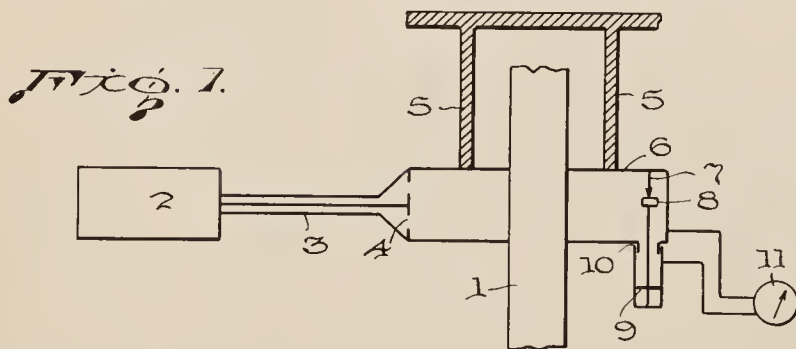
M. MUSKAT ET AL

2,463,297

APPARATUS FOR TESTING INSULATING MATERIALS

Filed Dec. 21, 1944

2 Sheets-Sheet 1



Inventors
MORRIS MUSKAT
NORMAN D. COGGESHALL

By *G. M. Houghton*
their Attorney

March 1, 1949.

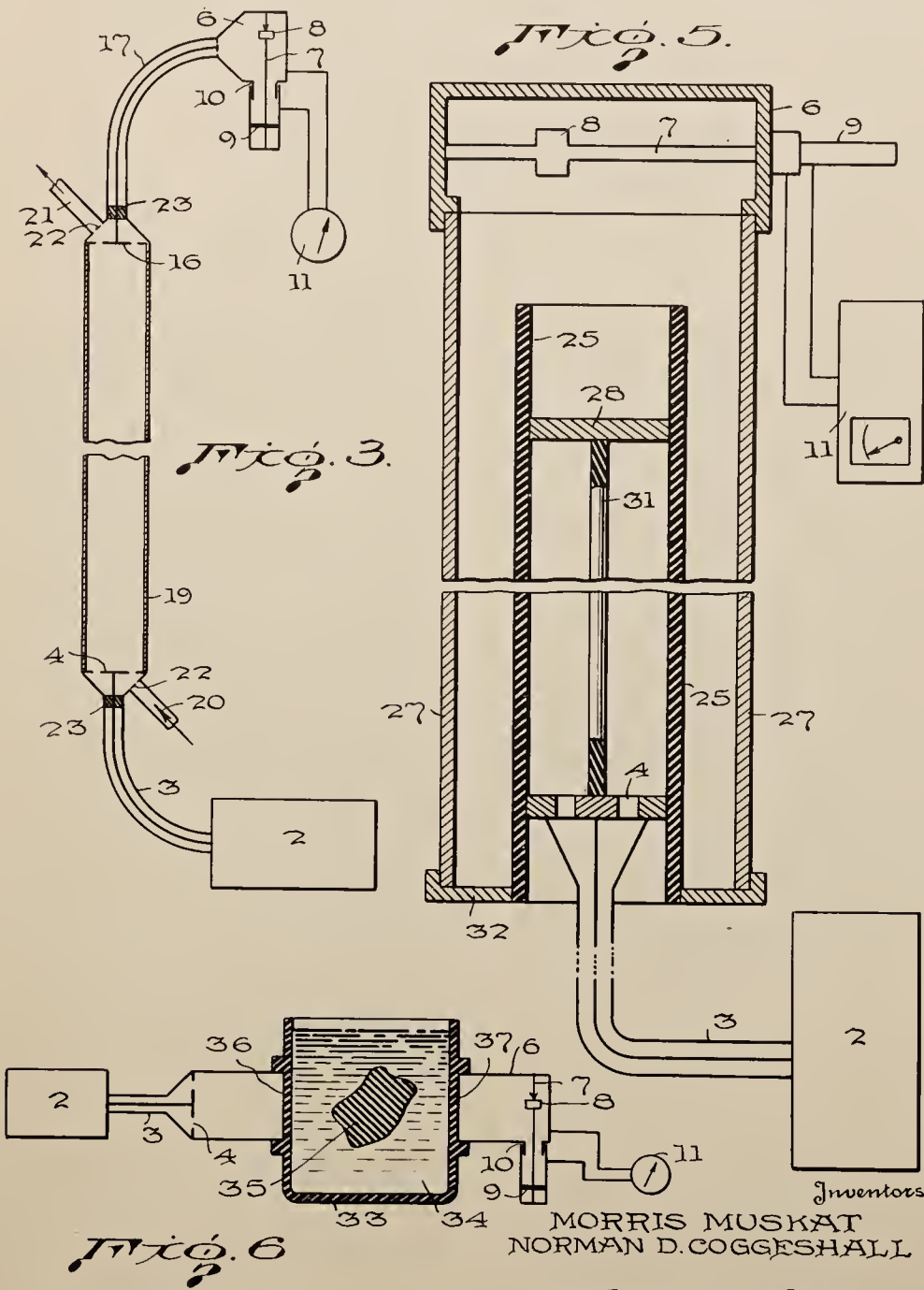
M. MUSKAT ET AL

2,463,297

APPARATUS FOR TESTING INSULATING MATERIALS

Filed Dec. 21, 1944

2 Sheets-Sheet 2



Inventors
MORRIS MUSKAT
NORMAN D. COGGESHALL
By *A. M. Foughton*
Attorney

UNITED STATES PATENT OFFICE

2,463,297

APPARATUS FOR TESTING INSULATING MATERIALS

Morris Muskat, Oakmont, and Norman D. Coggeshall, O'Hara Township, Allegheny County, Pa., assignors to Gulf Research & Development Company, Pittsburgh, Pa., a corporation of Delaware

Application December 21, 1944, Serial No. 569,225

1 Claim. (Cl. 175-183)

1

This invention concerns apparatus for testing insulating materials, in particular it concerns apparatus for testing the transparency of such materials to the type of energy commonly known as microwaves.

In the testing and inspection of electrical insulating materials which are to be used in very high frequency electrical apparatus, it is necessary to measure the properties of the material at the frequencies at which the apparatus is designed to operate. This is due to the fact that the ordinary electrical properties of insulating materials do not reflect the properties which these materials have at the very high electromagnetic frequencies. This is particularly true for microwave frequencies. Energy losses in microwave apparatus may occur in the insulating materials used in its construction. This results in the production of heat and a reduction in operating efficiency. Many ordinarily good insulators are poor or dissipative insulators at microwave frequencies.

The manufacture of efficient microwave apparatus requires the use of non-dissipative insulating material. Such materials are used to support various internal structures in microwave generators and receivers. They are used for supports in microwave antennae or radiators. Considerable quantity is also used in the manufacture of coaxial cable for transmitting microwave energy from the generator to the radiator, the central conductor of such a coaxial cable being held in place by insulating spacers. In all of these uses the insulators should absorb no energy, and a test is required to determine this before fabrication.

This invention uses for a criterion of the non-dissipative quality of the insulating material its transparency to a microwave beam. If a beam of energy strikes a new medium the energy may be either reflected or transmitted. If it is transmitted, the transmission may take place with loss of energy or without such loss. In the latter case the material is said to be transparent. If during the transmission, energy is transformed to some other form, the material is said to absorb energy, and particularly if the energy beam is converted into heat, the medium is said to dissipate the energy. Obviously a uniform medium which is non-dissipative is transparent to the beam. Electrical insulators fall in the class of transparent or partially transparent microwave media. Good electrical conductors act as good microwave reflectors; they do not transmit micro-

2

wave energy into their interior. We may therefore use the microwave transparency of an insulating material as a measure of its microwave nondissipative quality.

In addition to the possibility of insulating material having undesirable microwave transmission characteristics, there is also the possibility of such material occasionally having metallic or conducting inclusions which may act as reflectors of microwave energy. Such inclusions may be due to manufacturing defects or may be due to internal decomposition or ageing. Such conductive defects may not be dissipative in themselves but may be reflectors of microwave energy, and interfere with the regular transmission or propagation of microwave energy through the insulating material, thus causing the apparatus to behave in an abnormal and unpredictable manner. It is accordingly an object of this invention to provide apparatus for testing insulating materials for their efficiency in transmitting microwave beams.

A further object of this invention is to provide apparatus for testing insulating materials for their dissipative action when subject to microwave energy.

Still another object of this invention is to provide apparatus for testing insulating materials for internal defects of a character non-transparent to microwaves.

Still another object of this invention is to provide apparatus for testing insulating materials for internal defects of a character reflecting microwaves.

This invention will be more fully understood in detail by reference to the accompanying drawings, in which

Fig. 1 shows an embodiment for testing the microwave transparency of materials.

Fig. 2 shows an embodiment for testing the microwave transparency of insulating material having the form of a bar or rod.

Fig. 3 shows an embodiment for testing the microwave transparency of insulation liquids.

Fig. 4 shows an embodiment for testing insulating materials for microwave reflecting inclusions.

Fig. 5 shows an embodiment which is particularly adapted to testing the microwave transparency of insulating material having the form of a tube.

Fig. 6 shows a form which is useful in testing the microwave transparency of irregularly shaped bodies.

In each of the figures equivalent parts are indicated by the same numeral.

Referring to Fig. 1, the numeral 1 represents the insulating material whose microwave transparency is being tested, 2 represents a generator of microwave energy, such as a Klystron, connected by a coaxial cable 3 to a beam-forming radiator such as an electromagnetic horn 4 mounted on support 5. These devices are known in the microwave art. Also fastened to the support is a known type of microwave receiver 6 having a conducting probe 7, crystal rectifier 8 and tuning pinion 9. Upon receiving microwave energy this system gives rise to a D.-C. potential across condenser 10. This potential is a measure of the intensity of the microwave beam and may be measured by means of D.-C. meter 11. Thus one may "shine" a beam of microwave energy through the insulating material, and compare the intensity which is transmitted by the material with that observed when the material is absent, and thus determine the microwave transparency of the material. By moving the material about with respect to the beam, one may locate regions of absorption or other microwave defects. Complete microwave opacity would be indicated by zero reading on meter 11. The microwave produced by 4 need not be a parallel beam, but may be a divergent or convergent one, or may have rays in many directions only some of which enter receiver 6.

Fig. 1 is primarily adapted for testing insulating material in the form of sheets or other shapes having parallel sides. Irregular shapes may be immersed in a microwave transparent medium contained in a parallel sided tank as shown in Fig. 6. Here 33 is a container made of insulating, microwave transparent material having parallel sides 36 and 37, and containing an insulating liquid such as oil having microwave properties similar to those of the material 35 being tested. The material 35 being tested is in the microwave beam and is immersed in the liquid 34 in order to avoid erroneous readings resulting from surface or interfacial reflections. The tank 33 may be long in the direction normal to the microwave beam so that round or irregularly shaped rods may be inspected. Alternatively also the microwave radiator 4 and receiver 6 may be themselves immersed in the medium 34 inside the tank.

Fig. 2 shows apparatus for testing insulating bars or rods. Here 2 is a microwave generator connected by coaxial cable 3 to radiator 4. Radiator 4 is placed at one end of an internally polished tube 15 made of a good electrical conductor, preferably metal. The microwave radiation from 4 will travel inside the tube 15 without attenuation and excite receiver 16 connected by coaxial cable 17 to detector 6 which is similar in construction to that used in Fig. 1. A reading of intensity is obtained on D.-C. meter 11. Upon introducing into tube 15 a bar of insulating material 18 to be tested, any attenuation which is observed will be indicative of a dissipative inclusion in the insulating bar 18 being tested. Such inclusions may be further localized by examining the rod transversely in a microwave beam as indicated in Fig. 6.

In Fig. 3 we have indicated a way of examining insulating liquids for their microwave transparency. Such liquids as various types of oils may be used for cooling as well as insulating media in microwave generators. In Fig. 3 like numbered parts have the same form and function as in Fig.

2. The liquid under test may be passed into the conducting tube 19 at one end through opening 20 and removed at the other end through opening 21. In order for the openings to produce a minimum disturbance to the microwave system they are supplied with covers 22 having fine perforations through which the liquid may pass. Insulating bushings 23 prevent the oil from entering the coaxial cable. The dimensions of tube 19 may be adjusted to the rate of fluid flow to be handled and the frequency of microwaves to be used.

In Fig. 4 we have shown an application of our invention to the testing of insulating materials which are suspected of having reflecting, e. g. partially conducting, inclusions. Such conducting inclusions may result from impurities or from defects in manufacture of the insulators. Here 2 is a Klystron generator whose energy is fed by cable 3 to a microwave beam-forming radiator 4. The material 24 being tested is held in the beam of microwave energy radiated from 4 and a short distance away so that any conducting inclusions 29 if present will reflect some of the primary energy to an adjacent receiver. Receiver 23 forms the central conductor of a wave guide 30 which has an annular form around radiator 4. The conductor 23 is connected to probe 7, rectifier 8, and tuning piston 9, the potential across condenser 10 being read on D.-C. meter 11. Thus if the material 29 has no conducting inclusions, meter 11 will show a minimum indication. However, if conducting inclusions are present, microwave energy will be reflected to the receiver 23 and indicated on meter 11. If material 24 is a perfect reflector a maximum indication is obtained on meter 11. Other relative arrangements of primary radiator and reflection detector may be used.

Fig. 5 illustrates apparatus testing tubular insulating materials. In this case it is desired to measure the transparency of the wall of the tube indicated by 25. The microwave generator 2 feeds energy through coaxial cable 3 to radiator assembly 4. A metal plate 28 is placed some distance away from radiator 4 to keep the microwave radiation in tube 25 localized to the region being examined. The metal plate 28 is spaced from radiator 4 by an insulating rod 31. The assembly consisting of parts 4, 28 and 31 may then be moved inside the tube 25 to inspect its entirety. Tube 25 is coaxially surrounded by a larger conducting tube 27 which picks up the energy coming through the walls of the tube 25 under test. One end of the annular space between the two tubes is closed by metal shield 32. Tube 27 guides the microwaves to detector 6 of a known type previously described. Thus any lack of transparency of the walls of tube 25 may be detected by a decreased reading of meter 11. On the other hand complete opacity would result in a zero reading on meter 11.

The meter indicated in the figures by 11 may take the form of a recording device. For continuous testing an amplifier may be used here together with a relay and appropriate mechanisms for throwing out sections of material found to be defective. Furthermore, other known types of microwave generators or detectors may be used for the practice of this invention. The microwave energy employed may have any wave length in the microwave region of electromagnetic radiation, namely from one meter to a fraction of a millimeter. Tests may be made at any frequency, but are advantageously made at the

frequency or frequencies to be handled by the apparatus in which the insulating material is to be used.

What we claim as our invention is:

Apparatus for measuring the microwave characteristics of an insulating cylinder comprising, a source of microwave energy, means attached thereto for transmitting the microwave energy into said cylinder, a conducting reflector inside said cylinder to limit the axial flow of microwave energy to a selected portion of said cylinder, a larger conducting cylinder surrounding said insulating cylinder, a receiver of microwave energy in the conducting cylinder, and means for indicating at least one parameter of the microwave energy received and the manner in which such parameter changes from place to place along the insulating cylinder.

MORRIS MUSKAT.
NORMAN D. COGGESHALL.

REFERENCES CITED

The following references are of record in the file of this patent:

UNITED STATES PATENTS

Number	Name	Date
2,075,808	Fliess -----	Apr. 6, 1937
2,085,798	Gerhard -----	July 6, 1937
2,109,843	Kossner -----	Mar. 1, 1938
2,142,648	Linder -----	Jan. 3, 1939
2,197,122	Bowen -----	Apr. 16, 1940
2,197,123	King -----	Apr. 16, 1940
2,222,450	Trost -----	Nov. 19, 1940
2,301,251	Capen -----	Nov. 10, 1942
2,403,289	Korman -----	July 2, 1946
2,423,383	Hershberger -----	July 1, 1947

OTHER REFERENCES

Short Wave and Television, April 1938, pages 20 669, 706 and 707.

March 1, 1949.

N. D. COGGESHALL ET AL
AUTOMATIC SYSTEM OF PROCESS CONTROL
BY INFRARED SPECTROMETRY

2,462,946

Filed April 11, 1947

5 Sheets-Sheet 1

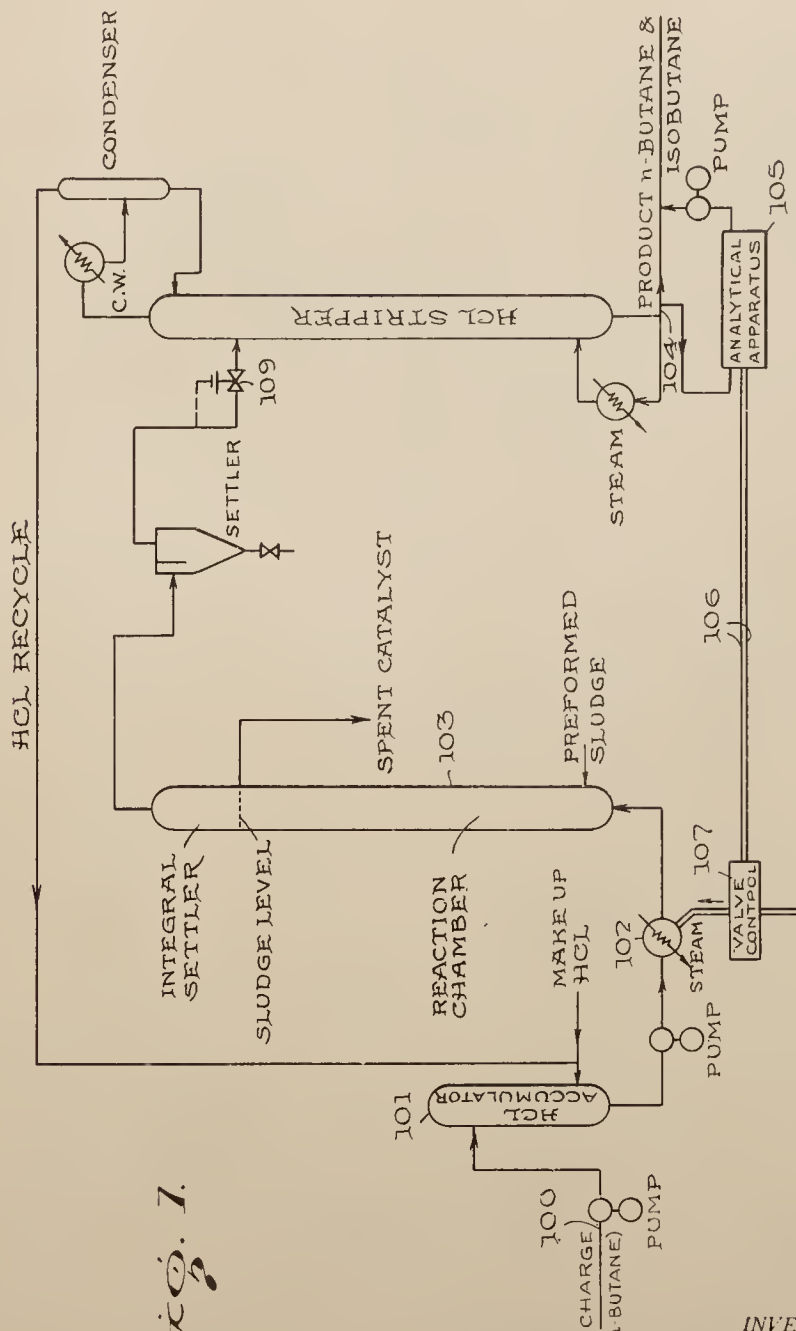


Fig. 1.

INVENTORS
NORMAN D. COGGESHALL
MORRIS MUSKAT

BY

A. M. Houghton
their ATTORNEY

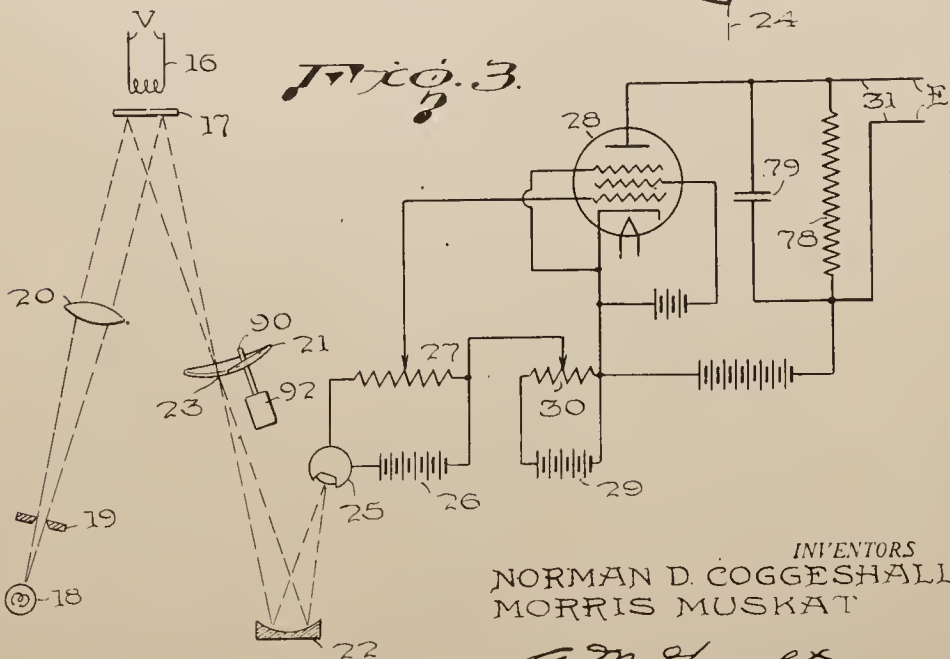
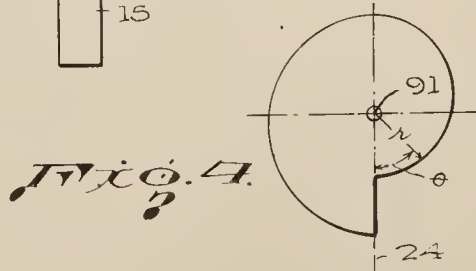
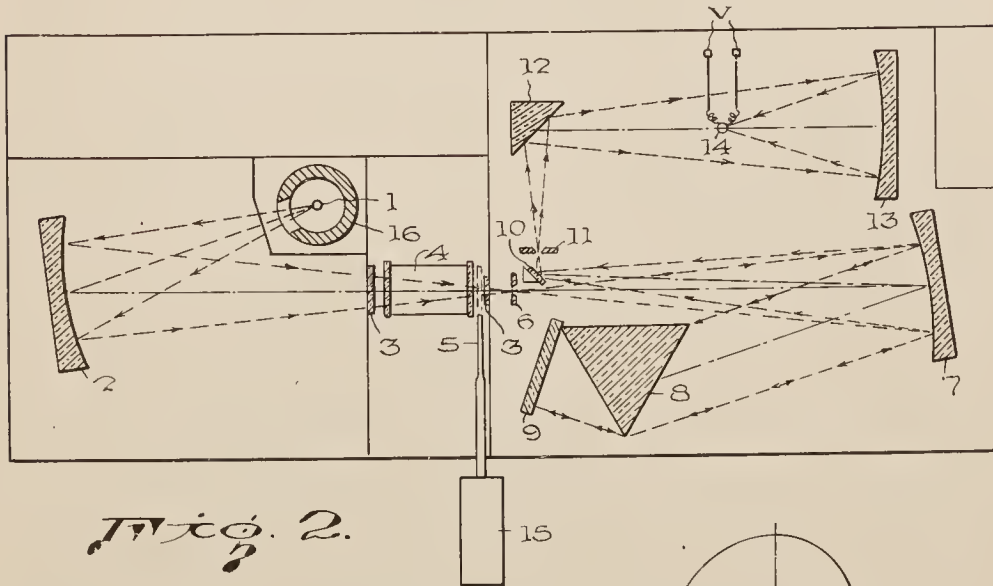
March 1, 1949.

N. D. COGGESHALL ET AL.
AUTOMATIC SYSTEM OF PROCESS CONTROL
BY INFRARED SPECTROMETRY

2,462,946

Filed April 11, 1947

5 Sheets-Sheet 2



INVENTORS
NORMAN D. COGGESHALL
MORRIS MUSKAT
BY *A. M. Houghton*
ATTORNEY

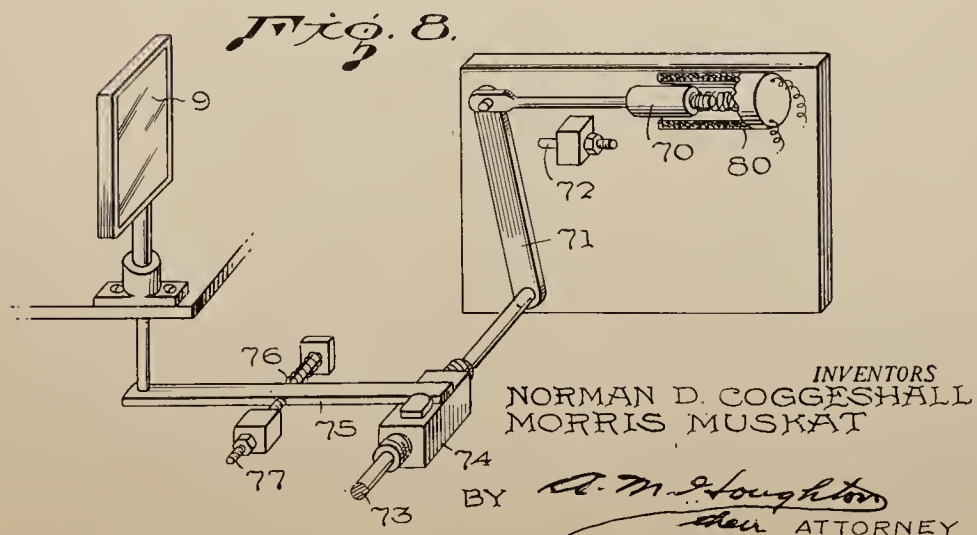
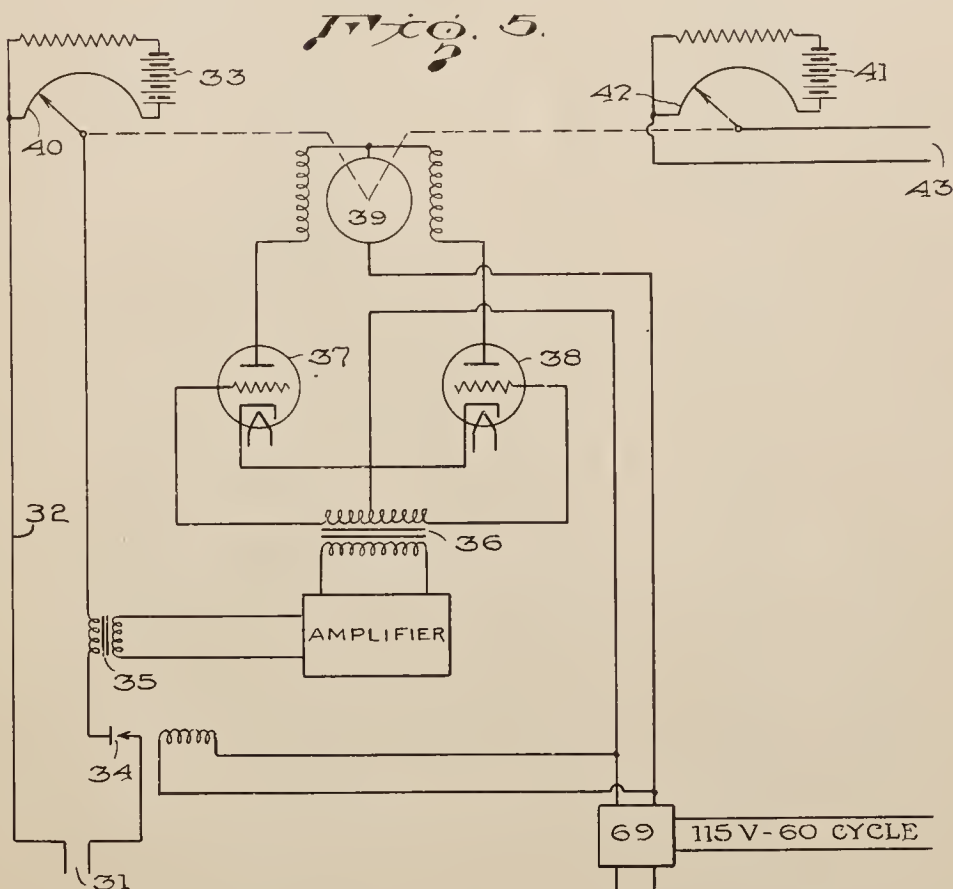
March 1, 1949.

N. D. COGGESHALL ET AL
AUTOMATIC SYSTEM OF PROCESS CONTROL
BY INFRARED SPECTROMETRY

2,462,946

Filed April 11, 1947

5 Sheets-Sheet 3



March 1, 1949.

N. D. COGGESHALL ET AL
AUTOMATIC SYSTEM OF PROCESS CONTROL
BY INFRARED SPECTROMETRY

2,462,946

Filed April 11, 1947

5 Sheets-Sheet 4

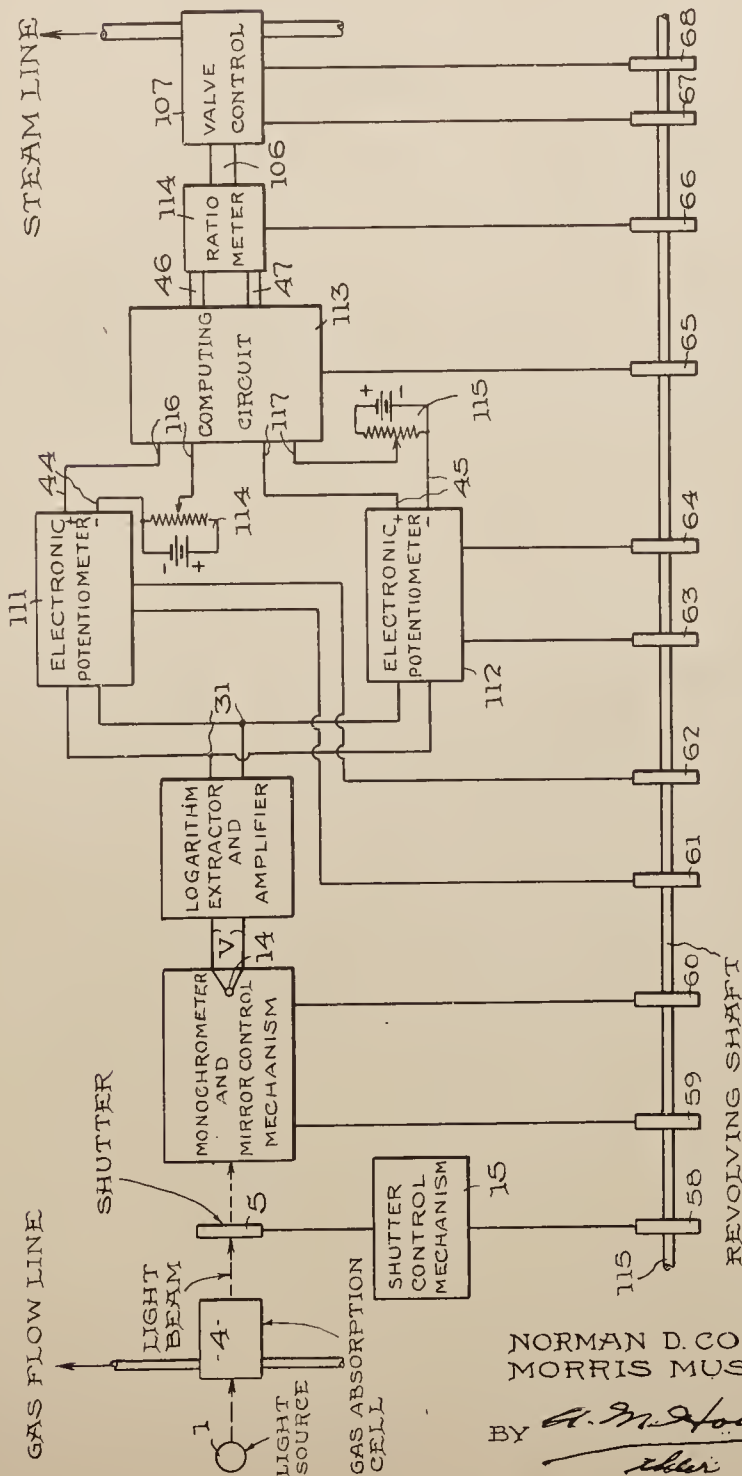


Fig. 6.

INVENTORS
NORMAN D. COGGESHALL
MORRIS MUSKAT

BY *G. M. Houghton*
ATTORNEY

March 1, 1949.

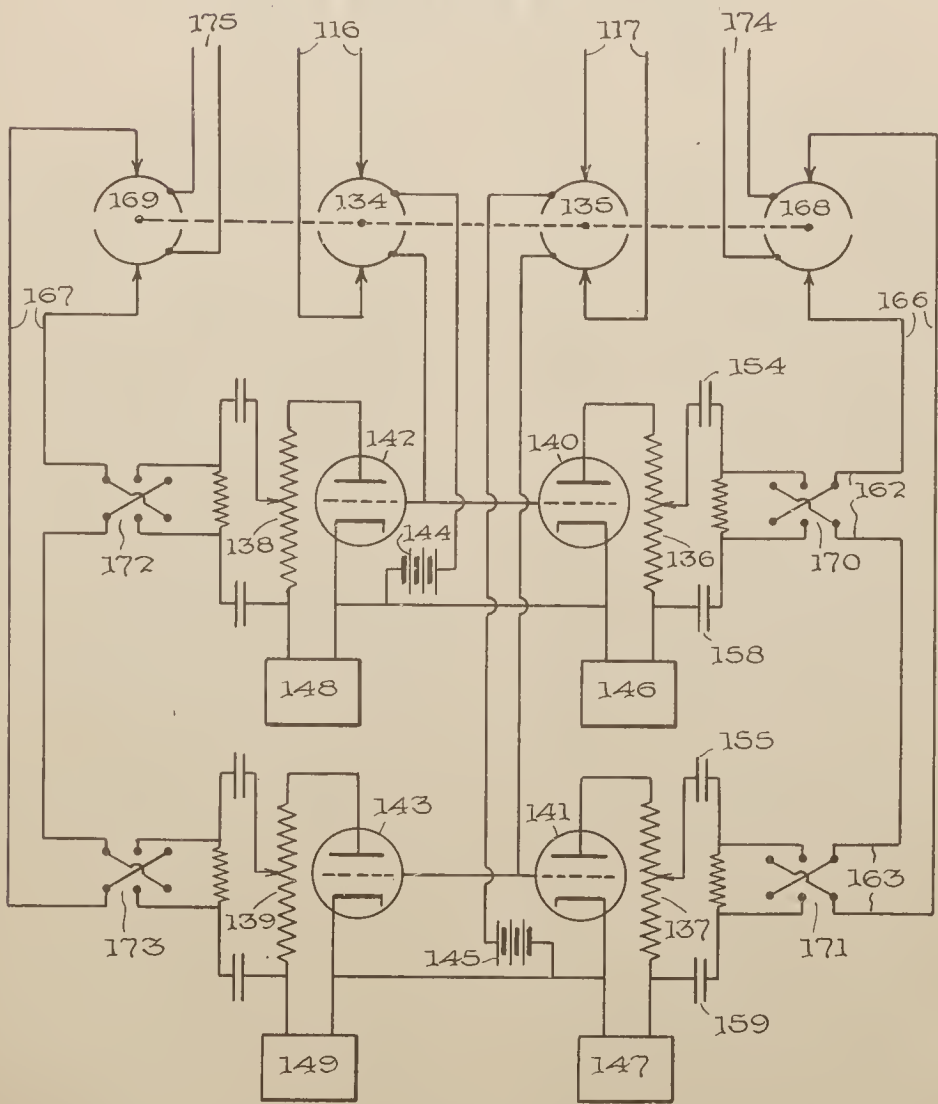
N. D. COGGESHALL ET AL
AUTOMATIC SYSTEM OF PROCESS CONTROL
BY INFRARED SPECTROMETRY

2,462,946

Filed April 11, 1947

5 Sheets-Sheet 5

Fig. 2



INVENTORS
NORMAN D. COGGESHALL
MORRIS MUSKAT

BY *N. M. Houghton*
their ATTORNEY

UNITED STATES PATENT OFFICE

2,462,946

AUTOMATIC SYSTEM OF PROCESS CONTROL
BY INFRARED SPECTROMETRY

Norman D. Coggeshall, Verona, and Morris
Muskat, Oakmont, Pa., assignors to Gulf Re-
search & Development Company, Pittsburgh,
Pa., a corporation of Delaware

Application April 11, 1947, Serial No. 740,828

6 Claims. (Cl. 250—43)

1

This invention concerns indicating, recording and control apparatus for manufacturing processes. More particularly it involves the use of an infra-red spectrometer as a control apparatus for a chemical process.

In conducting chemical reactions or physico-chemical processes, in the manufacture of chemicals or other products, it is customary to run one or more source materials or primary chemicals into a reaction chamber. This chamber may consist of a single vessel, such as a retort, or in more complicated processes, it may be an elaborate assembly of chemical process equipment. In many reactions, the primary chemicals do not react so as to completely combine, but instead reach an equilibrium condition in which the primary chemicals and products formed are in a state of dissociation and recombination so that the desired product is contaminated by either primary chemicals or intermediate compounds. On the other hand there may be practical limitations of conditions, such as temperature and pressure, which arise for instance because of the physical properties of materials of which the reaction chamber is made or because of decomposition reactions which may set in. As a result it is usually desirable to operate a reaction or process at some known optimum set of conditions which give high output together with operating efficiency. In order to maintain the reaction under these optimum conditions, various elements or conditions are brought under control. One may, for instance, control the temperature of a reaction or the pressure, or the amount or character of catalyst, or the relative concentrations of primary chemicals which are used, etc. All of these things will affect the product obtained.

The problem of determining the composition of gaseous products in order to control the producing process is one of major importance in the chemical industry. An analytical determination must be made each time a control adjustment is to be determined. Moreover, such determinations need to be made often upon the products of continuous processes such as isomerization units, alkylation units, and petroleum cracking and distillation units, to determine whether or not they are operating as desired.

Heretofore, for oil refinery processes there has been achieved a certain measure of control by extracting from some point in the process a sample of hydrocarbon gas, transferring this sample in its container to a routine spectrophotometer, measuring the infra-red light absorption at certain preselected wave lengths, calculating the

2

composition of the gas sample from these measurements, and making such changes in the operating conditions of the process as indicated by the composition of the sample. These operations might take of the order of one or two hours and, although somewhat lengthy, they still represent an advantage over previous methods based on analyses by fractional distillation which might require as long as six hours for completion.

The apparatus of this invention makes it possible to carry out the general steps outlined above in a fully automatic and essentially continuous manner. It thus has the advantage that it maintains much closer control of the reaction. The time lapse between the sample withdrawal and the signal analysis and the application of the necessary adjustments to the process operating parameters is only of the order of 30 seconds. A further advantage is that this invention is wholly automatic in that it will function for long periods of time without attention. This has the advantage of eliminating personal errors and in reducing operating costs, as the operators of even routine spectrophotometers must be skilled and experienced.

The apparatus of this invention automatically accomplishes the following sequence of operations: (1) withdrawing a sample of gas from a selected point in the process equipment; (2) automatically taking light transmission values at definite wave lengths; (3) transducing and mixing the transmission values in such a way as to obtain signals representing the various concentrations of the components of the sample; and (4) applying these signals directly or by means of their ratio to govern such operating devices as valves, heater coils, etc. which in turn are effective in controlling the course of the chemical reaction which produced the samples.

It is accordingly an object of this invention to provide apparatus for automatically analyzing the products of a chemical reaction, together with the necessary devices for automatically interpreting these analyses in terms of reaction parameters which may, in turn, be controlled so as to keep the reaction in the optimum condition of operation.

It is another object of this invention to provide means for achieving a substantially continuous analysis in the form of electrical signals which, in turn, may be directed so as to activate and influence control mechanisms affecting the chemical reaction or physical operations giving rise to the gas stream being analyzed.

It is a further object of this invention to pro-

vide an apparatus for automatically taking spectroscopic measurements on gaseous products of large scale chemical reactions, and using these measurements to automatically make the desired changes in the operating parameters of the reaction.

It is a still further object of this invention to provide apparatus comprising an infra-red spectrometer in conjunction with an automatic calculating device and a regulating mechanism which responds to signals from the calculating device, to continuously sample the gaseous products from a large scale chemical process, and to utilize the signals representing the concentration ratio of two or more components to control operating parameters of the process.

An explanation of how these objects are attained by this invention may be more clearly understood by referring to the drawings forming a part of this specification, and in which

Figure 1 shows the major component parts of a butane isomerization process which we may use as an example of a chemical process into which the apparatus of this invention may be fitted so as to control the reaction;

Figure 2 shows the optical diagram of an infra-red spectrophotometer which may be used in this invention, also an associated absorption cell and light shutter used to control the passage of radiation through the monochromator;

Figure 3 shows a combined optical-electronic device which may be employed to amplify the signals from the monochromator and to extract the logarithm of the resulting signals;

Figure 4 is a plan view of the logarithmic sector disk which may be used in the apparatus of Figure 3;

Figure 5 is a schematic diagram of a type of electronic potentiometer which may be used in our invention;

Figure 6 is a block diagram showing the main operating components of our invention;

Figure 7 is a schematic diagram of one type of computing circuit which may be used to resolve signals which determine the concentration of the various components of the process product; and

Figure 8 shows a type of mechanism which may be used to position the wave length controlling mirror in the monochromator.

This invention contemplates the use of infra-red absorption measurements for the purpose of analyzing the gaseous products of a reaction. The infra-red absorption of a gas depends on its molecular structure and therefore often gives information difficult to obtain by other methods, especially when the gaseous components are isomers and therefore chemically very similar.

When light of monochromatic radiation falls upon a substance some of the light is absorbed. The per cent of light absorbed depends upon the compound and upon the wave length of the light. If the light passes through a thickness d of the material, and if the density is such as to provide a concentration C , then the relation between the light intensity I_0 incident on the layer of material and the intensity I which is transmitted through it is:

$$\text{Log } (I_0/I) = \bar{a}Cd$$

where \bar{a} is a physical constant called the "extinction coefficient" and which is known to depend only upon the compound and upon the wave length. This relationship is known as Beer's law, and it is generally followed by most compounds.

For a given wave length the absorbing powers of different pure materials are characterized by numerical differences in the individual extinction coefficients. The extinction coefficients for a particular compound depend upon wave length, and in the infra-red region there will be wave length values for which the extinction coefficient is known to be large compared to other regions. These correspond to the well known infra-red absorption bands.

The quantity $\log (I_0/I)$ is designated as the optical density, and may be denoted by D . For a mixture of materials the resulting optical density is known to be an additive function of the contributions of the individual compounds. That is, the optical density for a mixture consisting of a concentration C_1 of compound 1 and a concentration C_2 of compound 2 will at a definite wave length be given by:

$$D = \bar{a}_1 C_1 d + \bar{a}_2 C_2 d$$

or, if the length d of the adsorption cell is always constant one may combine the extinction coefficients and the length into single constants to get:

$$D = a_1 C_1 + a_2 C_2 \quad (1)$$

The presence of other compounds will only serve to add additional products of extinction coefficients by concentration on the right-hand side of Equation 1. This equation may serve as a basis for analysis of a mixture of compounds having different values of a , provided D is determined for at least as many wave lengths as there are compounds in the mixture.

Thus, for example, in making infra-red analyses of n-butane and isobutane mixtures it is sufficient to determine the optical densities at two wave lengths. The wave lengths which may advantageously be used for this case are: 10.2μ and 8.45μ ($\mu = 10^{-4}$ cm.). At 10.2μ n-butane absorbs strongly and isobutane weakly; at 8.45μ isobutane absorbs strongly. The optical densities, D_1 and D_2 at these two wave lengths will therefore be:

$$\begin{cases} D_1 = a_{11}C_1 + a_{12}C_2 \\ D_2 = a_{21}C_1 + a_{22}C_2 \end{cases} \quad (2)$$

where a_{11} and a_{21} refer to the extinction coefficients of n-butane for wave lengths 1 and 2 respectively, while a_{12} and a_{22} refer to the extinction coefficients of isobutane for wave lengths 1 and 2 respectively; C_1 and C_2 being the concentrations of n-butane and isobutane in the sample of gas.

Equations 2 will hold for any concentrations C_1 and C_2 . Also, since the extinction coefficients are numerical constants these equations may be solved to yield:

$$\begin{cases} C_1 = A_1 D_1 + B_1 D_2 \\ C_2 = A_2 D_1 + B_2 D_2 \end{cases} \quad (3)$$

where the A_1 , A_2 , B_1 and B_2 are functions of the extinction coefficients and can be computed by simple algebra.

In essence this invention applies the principles of infra-red spectroscopy to the automatic control of a butane isomerization unit by admitting a sample of the output mixture into an absorption cell, measuring the above-mentioned values of D_1 and D_2 , automatically using these signals in electric circuits which give signals representing C_1 and C_2 , automatically obtaining a ratio between them, and using the resultant signal to control one of the process operating pa-

5

rameters, such as the temperature of the reaction vessel. Application to a butane isomerization process is by way of example only and is not a limitation of our invention, as it may be applied to any process whose products are susceptible of analysis by infra-red absorption measurements.

Figure 1 shows a diagram of a well known butane isomerization unit in which n-butane may be isomerized to isobutane and to which our invention has been applied. Here the n-butane entering the system at 100, is pumped into an HCl accumulator 101 from which the mixture of n-butane and HCl is pumped through a heater 102, and into the reaction vessel 103, where it comes in contact with the catalyst, which may be AlCl_3 . In the reaction vessel 103 the n-butane is largely isomerized to isobutane, and the resultant gas goes through a series of stripping operations to remove the catalyst and the HCl before being delivered as a final product. At the point 104 where the product gas, mainly isobutane, leaves the flow system, is installed the analytical apparatus 105 described in this invention. The measurements made by apparatus 105 and the transformation of the resulting signals finally yields an electrical signal in wires 106 which is proportional to the ratio p_n/p_i , where p_n is the partial pressure of n-butane in the product stream and p_i is the partial pressure of isobutane. This signal, applied to electric control valve 107, is used to control the steam flow in heater 102 which heats the n-butane as it goes into the reaction vessel. This, in turn, controls the effectiveness of the reaction, so that it is possible to keep the ratio p_n/p_i less than a pre-selected value or within a pre-selected narrow range of values. The analytical apparatus 105 comprises an infra-red absorption spectrometer whose monochromator is alternately adjusted to two predetermined wave lengths, and automatic computing devices which finally deliver to the wires 106 an electrical signal which is indicative of the chemical analysis of the products obtained at point 104. The various components of the apparatus 105 will be described in detail.

In Figure 2 is a diagram showing the essential parts of the optical system of a known type of infra-red absorption spectrometer arranged according to the functional relationship of the parts. Numeral 1 designates the light source which may be an electrically operated Globar heater, 16 is a water jacket to keep the light source from heating up the rest of the apparatus. Numeral 2 is a condenser mirror which focuses the radiation onto entrance slit 6, numeral 3 represents rock salt windows, 4 represents a gas absorption cell with rock salt end plates, and 5 is a shutter which intermittently allows the radiation to pass, as will be explained in more detail later. The windows are of rock salt so as to transmit the infra-red radiation used in the optical system. The shutter 5 is operated by electrical device 15, which may be a solenoid or electric motor.

Slit 6, Figure 2, defines a divergent beam of light (as indicated by arrows) which passes to the collimating mirror 7. This in turn reflects the light as a beam of parallel rays to the rock salt prism 8. The light passes through the prism and is reflected by the mirror 9. All the mirrors are first surface mirrors to eliminate absorption of the radiation. As the different wave lengths of light will be refracted through different angles as the beam passes through the prism 8 and from mirror 9, there will be a different wave

6

length for every different angle of return from the prism 8. The collimating mirror 7 will intercept only a small angle of the returning light and will focus this nearly monochromatic light onto the mirror 10 in such a way that an image of the slit 6 falls on the plane of the exit slit 11. The wave length of the light falling on the exit slit 11 depends upon the angular position of the mirror 9. In the present application to a n-butane/i-butane isomerization unit the mirror 9 is limited to two positions to allow light of 10.2μ and 8.45μ to pass alternately by a means which will be explained later.

The light passing through slit 11 passes to the mirror 12, from which it passes to the concave mirror 13. This mirror 13 is so located and is of such optical dimensions as to focus the radiation onto 14, which is a well known radiation detector such as a vacuum thermocouple or bolometer or any other suitable radiation measuring device.

Figure 3 illustrates an apparatus which may be used to derive an electrical signal proportioned to the logarithm of the intensity I of the radiation transmitted to device 14 of Figure 2. It is customary in the art to connect a galvanometer to radiation measuring device 14, the characteristics of these two devices being such that the angular galvanometer deflection is a linear function of the intensity I. Any known combination of radiation detector and galvanometer may be used. Thus, by way of example one may use for device 14 a vacuum thermopile which delivers an electrical voltage V proportional to the intensity I of transmitted radiation, i. e., $I=jV$, j being the proportionality constant. The thermopile 14, Figure 2, is connected to a galvanometer 16, Figure 3, on which it impresses its voltage V. Thus 16 may represent the moving coil of a high sensitivity galvanometer of low internal resistance designed especially for use with thermocouples such that its angular deflection is proportional to the intensity of radiation I striking the device 14 of Figure 2.

The mirror which moves with the galvanometer coil is represented by numeral 17. A small lamp 18 furnishes light passing through the lens 20 and reflected from the galvanometer mirror 17 to form an image of the aperture 19 at a point indicated by 23. This point will move as the galvanometer mirror 17 moves, and it will move on the arc of a circle the center of which is at the axis of rotation of the mirror 17. A logarithmic sector disk 21, shown in a plan in Figure 4, is located on the locus of point 23 and is rotated on a shaft 90. This disk is so constructed that the radius on any point of its periphery has the following relation between the radial distance r from the axis 91, Figure 4, and the angular distance θ as measured from the base line 24:

$$r = e^{\theta} \quad \text{or} \quad \theta = \log r \quad (4)$$

The surface of disk 21 is made slightly concave with its center of curvature at the center of rotation of mirror 17. Therefore, the radial distance used in the Equation 4 is the distance from the center of the disk to a point on the periphery as measured along the concave surface of the disk rather than perpendicular to the axis of rotation of the disk. The smaller radius on the base line 24 is taken as unit distance.

Lamp 18, aperture 19 and lens 20 are mounted rigidly with respect to each other and located so as to obtain a very small, intense spot of light at the point 23. When there is no input signal to

the galvanometer, the optical system is so adjusted that the image 23 falls on the disk at a point coincident with the axis of the shaft rotating it. Either the slit widths used, the cell length, the working gas pressure, or the sensitivity of the galvanometer are easily adjusted so that the maximum signal encountered in practice will cause the point of focus 23 to move on the disk to a point which does not exceed its peripheral radius. Also these same parameters are adjusted so that the minimum signal will cause the point 23 to move to a point which always exceeds the minimum radius of the disk. With these conditions Eq. 4 above will be satisfied.

From point 23 the light beam diverges and falls on the surface of the concave mirror 22 from which it is reflected into the photocell 25. The geometry and optics are so arranged that for any position which point 23 may occupy along the curved surface of the disk, a second image will fall on the photosensitive surface of the photocell 25.

Disk 21 is mounted on a shaft 50 through its center point 91 (Figure 4) this being the origin of the spiral $r=e^t$, and is driven by motor 92 at a relatively constant speed, say 30 revolutions per second. The interruptions of the light beam caused by rotating disk 21 define a series of illumination pulses in the phototube 25. If the galvanometer 16 receives a signal such as to deflect the point 23 to a radius r as measured along the disk from its axis of rotation, the light will be allowed to pass only for a fraction of the time of the disk's rotation. The fraction of the time during which the beam may pass is $\theta/2\pi$ and during the rest of the time it is cut off by the disk. Thus, the fraction of time during which the photocell 25 is activated depends on the position of the image point 23, which in turn depends on the signal from thermocouple 14, Figure 2. Therefore, since the coordinate r which specifies the deflection of point 23 is proportional to the signal V to the galvanometer:

$$\theta/2\pi = (\frac{1}{2}\pi) \log r = (\frac{1}{2}\pi) \log V = f \quad (5)$$

where f represents the fractional time that the signal actuates the photocell. Thus, as the disk rotates at a constant speed, there results a succession of light pulses falling on the phototube, the duration time of each being proportional to the logarithm of the voltage V developed by the thermocouple 14, Figure 2.

The photocell 25, Figure 3, which is supplied voltage by battery 26, causes current pulses to flow in resistance 27 which correspond in time duration to the light pulses it receives. The current pulses in resistance 27 create voltage pulses on the grid of the pentode vacuum tube 28. When no current is flowing in 27, the bias voltage of the tube, coming from the battery and resistance combination 30 is such as to allow no plate current to flow. The battery and resistance combination 26 and 27 are such, however, that when the phototube 25 is activated and current flows in 27 the tube 28 is biased to allow plate current to flow. As a result there will be a series of current pulses to the plate of tube 28 which correspond in frequency and time of duration to the illumination pulses falling on 25. Values for the resistance 78 and the condenser 73 are chosen so that the time constant of the combination is long compared to the period of rotation of disk 21. The resulting steady voltage E which is developed across leads 31 is proportional to the fractional time of duration of the illumination pulses, and the voltage E across leads 31 is therefore propor-

tional to the logarithm of the voltage V applied to the galvanometer by the thermocouple, i. e.,

$$E = K \log V \quad (6)$$

where K is a constant of proportionality.

The signal E is conducted to the leads 31 of the electronic potentiometer shown in Figure 5. The latter is of a type well known in the art, and employs a voltage from battery 33 to buck out or oppose the D.-C. voltage on leads 31. A vibrator or interrupter 34 creates an A.-C. signal in the transformer 35 when current flows in leads 32 due to lack of balance of the voltages. The A.-C. signal from the secondary of transformer 35 is amplified and goes into the primary of transformer 36. The center tapped secondary of 36 feeds the grids of two thyratrons 37 and 38. The plate voltage on these tubes is supplied from the same A.-C. source as drives the vibrator, and since the grid signals will be out of phase with each other one tube or the other will pass current depending upon the direction of the current in the primary of 35. As one tube conducts while the other does not, this results in current flowing in only one side of the split field balancing motor 39. Mechanically coupled to the armature of 39 is the moving contact of the variable potentiometer 40. The movement of the armature 39 is such that it causes movement of the contact on 40 in a direction required to restore equilibrium. The signal coming in on leads 31 is opposed by the voltage picked off on potentiometer 40, and when the two voltages are balanced there is no signal to the thyatron grids and the motor does not turn.

An additional battery and variable resistance arrangement 41 and 42 are mounted with the movable contact mechanically coupled to the motor 39 in the same manner as 40. This added circuit gives a voltage signal on leads 43 which is equal to the voltage signal coming in on leads 31. The circuit of leads 43 is electrically isolated from the input circuit of leads 31. Also, as will be seen later, the current to the motor 39 is only turned on for a certain portion of a definite time cycle during which a balance is obtained. After the balance is obtained the current to the field coils of the motor is shut off for the remainder of the time cycle. However, during this idle period the signal remains unchanged on leads 43 and it is during this time that the signal is utilized, as will be explained below.

One may now refer to Figure 6, which is a schematic block diagram indicating the principal components of the analytical apparatus designated on Figure 1 by numeral 105. Numerals on Figure 6 which are common to those used on the more detailed figures designate corresponding components. A source of radiation 1 causes a beam of infra-red light to pass through the gas absorption cell 4 at which point it may or may not be intercepted by the shutter 5. If not intercepted, it goes into the monochromator part of the spectrophotometer and generates a voltage signal V on the thermocouple 14, the intensity of which is proportional to the amount of light getting through the cell. This signal V is transmitted via wires to the logarithm extractor and amplifier previously described as Figure 4. From wires 31, a signal E , which is proportional to the logarithm of the transmitted light intensity, goes to one of two electronic potentiometers 111 and 112 each similar to that shown in Figure 5.

Now with the wave length controlling mirror 9, of Figure 2, set to admit light of wave length

λ_1 ($=10.2\mu$) the signal is sent to the electronic potentiometer 111 of Figure 6. This device receives its signal on leads 81, corresponding to leads 31 of Figures 3 and 5. The sequence of automatic operations is so arranged that the current driving the motor 39, Figure 5, is cut off before the input signal on leads 31 is cut off and this leaves the signal on output leads 43 of Figure 5 or 44 of Figure 6. This effectively amounts to the device 111 maintaining the signal obtained for λ_1 . The apparatus then goes through a sequence which positions the mirror 9 to admit light of wave length λ_2 ($=8.45\mu$) to the thermocouple, with a resulting signal to the logarithm extractor and amplifier. This latter signal from the amplifier is fed to the electronic potentiometer 112 of Figure 6, which is the same in every respect as 111. It also operates in the same manner, and after a certain point in the sequence of events, potentiometers 111 and 112 will in effect each be delivering signals which are representative of the logarithms of the original signals to the thermocouple. These signals are delivered through the leads 44 and 45 of Figure 6, to potentiometers 114 and 115 respectively and into a computing circuit 113.

To aid in understanding the function of the computing circuit 113 of Figure 6, it is convenient to return to some of the original equations, namely:

$$\begin{aligned} C_1 &= A_1 D_1 + B_1 D_2 \\ C_2 &= A_2 D_1 + B_2 D_2 \end{aligned} \quad (3)$$

and

$$E = K \log V \quad (6)$$

where V is proportional to the intensity of light falling on the thermocouple.

Let I_1 be the intensity of light falling on the thermocouple when light of wave length λ_1 is admitted to it, and I_2 that for light of wave length λ_2 . These two quantities will be the light intensities when there is an actual sample in the absorption cell. If the cell is evacuated the signals for the two wave lengths will represent the intensities of the light source, which may be denoted by I_{01} and I_{02} .

From the definition of the optical density:

$$D_1 = \log (I_{01}/I_1) = \log I_{01} - \log I_1$$

and

$$D_2 = \log (I_{02}/I_2) = \log I_{02} - \log I_2$$

Also since $I = jV$, and using Equation 6 we may write:

$$D_1 = M_1 - \log V_1 \text{ or } D_1 = M_1 - E_1/K$$

wherein M_1 is a constant depending upon the magnitude of I_{01} and upon other proportionality constants, and E_1 is the voltage signal for λ_1 delivered by electronic potentiometer 111, Figure 6, on wires 44.

By a similar derivation, one may show that:

$$D_2 = M_2 - E_2/K$$

where E_2 is the voltage signal for λ_2 delivered by electronic potentiometer 112, Figure 6, on wires 45. We therefore have the equation:

$$\begin{aligned} KD_1 &= KM_1 - E_1 \\ KD_2 &= KM_2 - E_2 \end{aligned} \quad (7)$$

In order to obtain signals KD_1 and KD_2 it is necessary to properly combine E_1 and E_2 with constant voltages KM_1 and KM_2 . The latter may be obtained through the use of simple voltage divider circuits, such as 114 and 115, Figure 6, each

connected in series with the voltages from 44 and 45, so that the voltages on lines 116 and 117 represent the right hand side of Equations 7, equivalent to KD_1 and KD_2 , respectively. The constant voltages KM_1 and KM_2 , which depend on I_{01} and I_{02} as well as other apparatus parameters may be determined beforehand and potentiometers 114 and 115 may be set before the system is put in operation.

Having thus obtained voltages proportional to D_1 and D_2 , the interpretation of these electrical signals obtained in wires 116 and 117 involves the solution of a system of linear, simultaneous, algebraic equations such as the Equations 3 in the present example. Several such devices are known, one being described by R. R. M. Mallock, Proc. Royal Soc. A 140, 457 (1933). Another has been described by J. R. Bowman in U. S. patent application Serial No. 479,790. Circuit 113, Figure 6, may be such a device.

For the simple case described here by way of example, wherein only two electrical signals are obtained from the infra-red absorption spectrometer, a means of solving the two simultaneous equations by combining the electrical quantities so as to obtain the concentrations of n-butane and i-butane is shown in Figure 7. Here 116 and 117 represent the leads bringing in the D.-C. voltage signals representing KD_1 and KD_2 respectively. Split ring commutators 134 and 135 run synchronously at about 3000 R. P. M. and convert these voltage signals into two A.-C. voltage signals which are in phase with each other. These A.-C. voltage signals will also be proportional to the quantities D_1 and D_2 . Denoting the voltage from wires 116 by V_{g1} and that from wires 117 by V_{g2} , we may write $V_{g1} = hD_1$ and $V_{g2} = hD_2$ where h is the proportionality constant. These voltages are each fed into two tubes whose outputs are made proportional to the A_1 , B_1 , A_2 , B_2 and combined in accordance with Equations 3 to yield the solutions of these equations.

In Figure 7 the filament circuits are conventional and not shown, while 146, 147, 148, 149 represent plate supply devices isolated from each other. The signal from commutator 134 is added to the steady grid bias from battery 144 and applied to the grid of tubes 140 and 142. The plate current of tube 140 will depend on the voltage of battery 144 and of the voltage supply 146, and there will be an A.-C. component which depends on the magnitude of V_{g1} . By means of condensers 154 and 158 the D.-C. component of plate voltage is blocked out. The A.-C. component may be adjusted to the appropriate value proportional to A_1 by means of the sliding contact on resistance 136. Thus leads 162 will carry an A.-C. voltage which may be adjusted to be equal to the quantity $(A_1 D_1)$. Similarly the A.-C. voltage on the grid of tube 141 coming from commutator 135 will be $V_{g2} = hD_2$ and the plate output of tube 141 may be adjusted equal to the quantity $(B_1 D_2)$. The D.-C. component of the output from tube 141 is blocked out by means of condensers 155 and 159. Thus the A.-C. voltages in leads 162 and 163 are seen to represent the two quantities on the right-hand side of Equation 3 and furthermore they are in phase. The addition may be made by simply connecting them in series so that wires 166 carry an A.-C. voltage equal to $A_1 D_1 + B_1 D_2$ and therefore equal to C_1 . Thus the electrical signal in wires 166 is indicative of the concentration C_2 of n-butane in the product stream and therefore equal to $h p_n$ where h is a proportionality constant and p_n

is the partial pressure of n-butane. Similarly, the signals coming from commutators 134 and 135 are impressed on tubes 142 and 143 respectively. Output from these tubes is made proportional to A_2 and B_2 by an adjustment of potentiometers 138 and 139 respectively. Wires 167 are in this way made to deliver an A.-C. signal equal to $A_2D_1+B_2D_2$ and therefore indicative of C_2 and equal to hp_1 . From the wires 166 and 167 the values of p_n and p_i are easily obtained directly if desired. Reversing switches 170, 171, 172 and 173 are provided to take care of the algebraic sign of the quantities A_1, B_1, A_2, B_2 .

If the voltage representing p_n and p_i are desired to be D.-C. instead of A.-C. they may be rectified by means of synchronous commutators 168 and 169. Thus wires 116 and 117 carry into the device of Figure 7 respectively D.-C. voltages proportional to the logarithm of the spectrometer signal at wave length λ_1 and at wave length λ_2 , while wires 174 and 175 deliver D.-C. voltages proportional to the components n-butane and i-butane present in the gas stream being analyzed. These currents are essentially continuous signals which may be recorded or used for desirable control purposes as indicated generally in Figure 1.

While we have shown in Figure 7 a circuit for obtaining an analysis of a two-component mixture, this circuit may be expanded to analyze systems of more than two components. Thus for three components the input signals (wires 116 and 117) would each be fed into three tubes. For three components, measurement would be made at three wave lengths and there would be three signals. Thus a total of nine tubes would be required. The output of each tube may be adjusted to a value proportional to the appropriate one of the coefficients of Equations 3. These coefficients may be computed algebraically beforehand.

Another device which may be used instead of Figure 7 to perform the mathematical computation in the analysis of a complex mixture is the computing device disclosed by John R. Bowman in U. S. patent application Serial No. 479,790. Inasmuch as this machine operates on D.-C., no commutators such as are indicated by 134, 135, 168 and 169 in Figure 7 would be required.

For some processes the ratio or other function of the concentration of certain components is more desirable than the concentration values themselves. If the product of the concentrations is desired the voltages from wires 174 and 175 may be multiplied and indicated, for example, by means of a wattmeter. A device suitable for obtaining the quotient of the voltages in wires 174 and 175 is one such as described in U. S. Patent 2,129,880 granted to S. A. Sherbatskoy and J. Neufeld. Another device for obtaining the ratio of these voltages is the "Megger." This device indicates the ratio directly and may be used as a relay. Still another type is one very similar to the electronic potentiometer shown in Figure 5. In the modification of the apparatus of Figure 5 for purposes of a ratio meter the signal hp_1 would come in on leads 31 and the battery 33 would be replaced by the leads conducting voltage signal hp_2 . The function of the rest of the apparatus would be the same, and the signal across leads 43 would be proportional to the ratio p_1/p_2 .

Returning to Figure 6 and our present example of a butane isomerization unit, the ratio p_n/p_i or p_i/p_n may be used to keep the process operating

within a pre-chosen range of values of the i-butane and n-butane percentages. Therefore electrical voltages equal to hp_1 and hp_2 are delivered from the computing circuit 113 on leads 46 and 47 to a ratio meter 114. From the ratio meter the signal representing p_n/p_i may be transmitted on leads 106, Figures 1 and 6, to the valve control 107 on the steam line of the isomerization process.

The proper functioning of our invention depends upon the operation of the various components of the apparatus described above in a predetermined sequence with controlled time intervals. The timing is controlled by the constant speed revolving shaft 115 shown in Figure 6. On this shaft may be mounted a number of contactors 52-58 which make and break electrical circuits at the required phases in the time cycle. Instead of shaft 115 with contact disks one may use a program motor in which cams operate electrical contacts. These devices are well known in the art, and the shaft 115 with contactor 52-58 is merely a diagrammatic representation of such a device. The arrangement of the conducting portions of the contactors is such as to make operable the sequence described. A contactor may make two or more contacts per cycle, so that its solenoid for example may be activated during more than one portion of the cycle. Contactor 58 controls the movement of the shutter shown as 5 in Figure 2. Contactor 59 controls the operations of the slits 6 and 11. Contactor 60 controls the positioning mirror 9 as will be shown later. Contactor 61 controls contact switches which admit or shut off the signals to the electronic potentiometer 111. The power supply to the follow-up motor 39 is controlled by the contactor 62 which acts to turn it off or on by means of the relay 69, Figure 5. Contactor 63 controls the signals to electronic potentiometer 112 and 64 controls its motor supply current. The contactor 65 controls the entry of signals into the computing circuit. The portion of the time cycle during which signals from the mixing circuit are admitted to the ratio meter is controlled by 66, while 67 controls the input of signals from the ratio meter to the valve control, and 68 controls the valve positioning motor.

Figure 8 shows an apparatus which may be used to position the wave length controlling mirror 9. The angular position of mirror 9 determines the wave length at which measurements are being made, and a means of precise setting is required. Here 80 is a solenoid, the flow of current through which is controlled by disk 60. When current flows in it, the iron cylinder 70 is pulled to the right. The movement to the right is terminated when the bar 71 contacts the positioning screw 72. The movement of 71 turns the shaft 73 which has a threaded section engaging the threaded interior of block 74. The direction of the threads are such as to move the block forward, i. e. toward the bar 71 when the cylinder 70 moves to the right. When bar 74 moves forward to its final position the mirror 9 is positioned properly to admit light of wave length λ_1 to the thermocouple. When the solenoid 80 is deactivated block 74 moves back until it no longer contacts bar 75. The spring 76 pushes bar 75 back until it encounters the positioning screw 77. The angular position of the mirror is then such as to admit light of wave length λ_2 to the thermocouple.

To describe the complete sequence of operations, one may begin with the initial state in which gas is in the cell, the shutter is withdrawn

to allow light to pass into the monochromator, the slits are set for light of λ_1 , the mirror is positioned for light of λ_1 , the signal from the logarithm extractor is feeding into electronic potentiometer 111, and the motor in it is activated, other switches being open. This state is maintained for several seconds to insure equilibrium so that the signal on leads 31 represents the logarithm of the intensity of the signal to the thermocouple.

Next the power to the motor of electronic potentiometer 111 is cut off, which isolates and holds the signal on leads 44. The shutter is then allowed to intercept the light beam and the slits change to the position for light of wave length λ_2 , and the mirror 9 takes the position to allow light of wave length λ_2 to reach the thermocouple. The signal from the logarithm extractor is then switched to electronic potentiometer 112 and its motor is activated. The shutter is withdrawn and a state analogous to the first is developed. This continues for several seconds to allow equilibrium to be reached and for leads 45 to carry the proper voltage representing the logarithm of the light intensity to λ_2 . The motor of electronic potentiometer 112 is then shut off isolating this voltage.

Next the signals on leads 44 and 45 are switched into the computing circuit 113 and a time of the order of a fraction of a second is allowed to elapse for equilibrium to be established, and then the output signals representing p_n and p_i and switched into the ratio meter. After a period of the order of two or three seconds or less, during which the ratio meter can balance itself, the resulting signal representing p_n/p_i is switched into the valve control mechanism. This may be of any of the standard types well known in the art. A control to hold the valve position in one setting until the entire apparatus goes through its sequence of events is provided by the control contactor 68. Such step by step operation of the control valve will also tend to prevent hunting of the control system.

During the operation of the components 113, 114 and 107 the slits and positioning mirror in the monochromator resume the positions for λ_1 , and the necessary electrical contacts are made so that when the current is cut off in the valve control mechanism 107, the system is in the original state, i. e. ready to determine signals for λ_1 again.

The valve control may be any one of several known in the art. It may be a solenoid valve or a motor driven valve, or in the case of more complicated control it may be a program motor (cf.; "Industrial Instruments for Measurements and Control" by T. J. Rhodes; McGraw-Hill). The valve control mechanism may be adjusted so that when the p_n/p_i ratio as expressed by the signal from the computer rises above a certain predetermined value the rate of flow of steam into the heat exchanger is increased. This will raise the temperature in the reaction vessel 103 with a subsequent drop in the p_n/p_i ratio. If it is desired to keep the value of p_n/p_i within certain limits, the valve control mechanism may be so adjusted that the rate of flow of steam will be lowered when p_n/p_i goes below a certain predetermined value. In this manner the automatic control valve will function within a predetermined range of values of p_n/p_i in the output.

The valve 105, Figure 1, shown as a pressure regulated valve, may alternatively also be of a controlled type appropriately connected to the

control mechanism so as to hold the pressure at a value best suited to the range of p_n/p_i desired and compatible with the safe operating pressure of the system.

The gas in the absorption cell 4, Figure 2, may be kept flowing continuously or a changing mechanism may be used which will change the gas in the cell for each new repetition of the operation sequence. This changing mechanism may be controlled by an additional contactor added to the revolving shaft 115, and may be comprised of inlet and outlet valves which are open for a sufficiently long time during each cycle to allow a complete flushing and replacement of the gas in the cell.

The complete sequence of control operation takes less than one minute. With the steam controlling valve thus being reset or at least checked in position once every minute, the result is effectively equivalent to continuous sampling and control of the process.

The width of the slits 6 and 11 in Figure 2 may be changed with each wave length or may alternatively be kept constant. If it is desired to change the slit width for each wave length a controlling device similar to that shown in Figure 8 may be used. Other known alternatives in the construction and operation of various components of the apparatus may be used without departing from the scope of our invention. For example, a Nernst glower may be used instead of a Globar heater as the radiation source.

We have described in detail the apparatus of our invention as applied to systems of two components but it is not thereby to be restricted to such simple systems. An obvious extension in the number of component working parts will make the apparatus suitable for mixtures of more than two compounds. For such a system the number of positions of the wave length controlling mirror would be increased, the number of electronic potentiometers would be increased and the scope of the computing circuit would be increased.

While we have further described our invention as applied to a particular chemical process, this is for illustrative and descriptive purposes only and our invention is not limited thereto. An infra-red spectrometer and computing device as automatic controlling means for any chemical or physical process is contemplated within the scope of this invention. An infra-red spectrometer and such associated devices as described herein may also be used for partial control as supplementary to other known control means, and such supplementary apparatus is regarded as also within the scope of this invention. Moreover, this invention is not to be construed as applying only to the type of infra-red spectrometer shown but to any kind which operates at a multiplicity of wavelengths. The apparatus is not limited to obtaining a single ratio of two components, but may be applied where it is desired to obtain and control several concentration ratios or individual concentrations in the product, and with knowledge available about how the operating conditions affect these ratios, the signals representing these ratios or concentrations may be utilized to control the operating conditions of any process or any part thereof. The concentration ratios or individual component concentrations may be recorded if desired by the addition of well known electric recorders to the output of the computing circuit, Figure 7, or its equivalent. Such a recorded record will serve to monitor the operation of the automatic control comprising

our invention and will give a permanent record of its action.

What we claim as our invention is:

1. A device for controlling an oil refinery process in which a product containing a plurality of final compounds are produced, comprising a source of infra-red radiation, a gas absorption cell disposed in the path of said radiation and adapted to receive a sample of the product, electrically actuated means for controlling at least one of the process operating parameters, monochromator means disposed in the path of radiation transmitted through said absorption cell and adapted to alternately separate from said transmitted radiation and direct upon said radiation detector rays of two wavelengths, each representative of one of said final compounds as present in the product, whereby successive pulses of electric energy proportional to the intensities of said wavelengths of transmitted radiation are produced, means for transforming said pulses of electrical energy into successive first electrical signals the magnitudes of which are proportional to the logarithms of their respective pulses produced by said radiation detector, and thus to the logarithm of the transmitted radiation intensity, a plurality of electronic potentiometers for receiving each of said electrical signals and including automatic isolated follow-up means for retaining the indicated magnitudes of said electrical signals for a predetermined time interval, computing circuit means for receiving simultaneously the indicated magnitudes of said electrical signals from said potentiometers and for solving a system of linear, simultaneous algebraic equations relating said magnitudes to the concentrations of compounds in the product, in such manner as to obtain electrical signals proportional to the respective concentrations of the said compounds in the said product, and means responsive to at least one of said concentration signals for actuating said operating parameter control means.

2. A device for controlling an oil refinery process in which a product containing a plurality of final compounds is produced, comprising a source of infra-red radiation, a gas absorption cell disposed in the path of said radiation and adapted to receive a sample of the product, electrically actuated means for controlling at least one of the process operating parameters, monochromator means disposed in the path of radiation transmitted through said absorption cell and adapted to successively separate from said transmitted radiation and direct upon said radiation detector rays of a plurality of wavelengths, each representative of a component of said product, whereby successive pulses of electric energy proportional to the intensities of said wavelengths of transmitted radiation are produced, means for transforming said pulses of electrical energy into successive first electrical signals the magnitudes of which are proportional to the logarithms of their respective pulses produced by the said radiation detector and thus to the logarithms of the transmitted radiation intensity, a plurality of electronic potentiometers each adapted to receive one of said electrical signals and including automatic isolated follow-up means for retaining the indicated magnitudes of said electrical signals during a predetermined time interval, computing circuit means for receiving simultaneously the indicated magnitudes of said electrical signals from said follow-up means and for solving a system of linear, simultaneous, algebraic equations relating said magnitudes to the concentration of said

components in said product in such manner as to obtain electrical signals proportional to the respective concentrations of the said components in said product, means for obtaining electrical signals proportional to the ratio of the concentrations of at least two selected components, and means responsive to said ratio signals for actuating said operating parameter control means.

3. A device for controlling an oil refinery process in which a product is produced which contains a plurality of final compounds, comprising a source of infra-red radiation, an absorption cell disposed in the path of said radiation and adapted to receive a sample of said product, means for measuring the optical density of the sample to said radiation for a plurality of wavelengths corresponding in number to the number of final compounds in the product, and corresponding in their respective wavelengths to values for which the extinction coefficient for each individual final compound is large compared to other regions, means for automatically transforming said optical density measurements into first electrical signals representative thereof, means for automatically using these first electrical signals in electric circuits which give second signals representative of the concentrations of each of said final compounds in the product, means for automatically obtaining in the form of a third signal a ratio between any selected second signals, and means for using the resultant third signal to control one of the process operating parameters.

4. A device for controlling an oil refinery process in which a product is produced which contains a plurality of compounds, comprising a source of infra-red radiation, an absorption cell disposed in the path of said radiation and adapted to receive a sample of said product, means for measuring the optical density of the sample to said radiation for each of a plurality of wavelengths corresponding in number to the number of compounds in the product, and corresponding in their respective wavelengths to values for which the extinction coefficient for each individual compound is large compared to other regions, means for automatically transforming said optical density measurements into first electrical signals representative thereof, means for automatically using these first electrical signals in electric circuits which give second signals representative of the partial pressures of each of said compounds in the product, means for automatically obtaining in the form of a third signal a ratio between any selected second signals, and means for using the resultant third signal to control at least one of the process operating parameters.

5. The combination of a source of infra-red radiation, a monochromator disposed in the path of said radiation, a radiation detector adapted to receive radiation from said monochromator and to transform said radiation into electrical currents, means for amplifying the currents, means for conducting a sample of a refinery product into the path of the radiation between the infra-red source and the monochromator, whereby only the radiation transmitted through the product is received by the monochromator, said monochromator having means for causing first and second monochromated bands of transmitted radiation to strike said radiation detector successively, whereby they are transformed into successive first and second electrical currents proportional to the intensity of the transmitted radiation bands from which they are derived, means for trans-

forming said first and second currents into successive beams of visible light the time duration of which is proportional to the logarithm of the intensity of the transmitted radiation bands from which they are derived, an electric circuit including a photocell disposed in the path of said beams of visible light and an electronic amplifier whereby said beams of light are transformed into an electrical signal proportioned to the logarithm of the intensity of the said transmitted radiation bands, a plurality of electronic potentiometers each adapted to receive one of said last-mentioned electrical signal and including automatic isolated follow-up means for retaining the indicated magnitudes of said electrical signals during a predetermined time interval, computing circuit means receiving simultaneously said electrical signals from said follow-up means and electrically transducing said signals in accordance with a system of linear, simultaneous algebraic equations relating the logarithm of the intensity of the transmitted radiation bands represented by said last-named signals with the concentrations of components in the product sample, in such manner as to deliver electrical signals proportional to the respective concentrations of the components in said product, means for obtaining in the form of final electrical signals the ratios of the signals representing the concentrations of any selected components of the product, and means responsive to the magnitudes of said final signals for actuating means for controlling at least one of the operating parameters of a process for producing the said refinery product sample.

6. In a spectrograph of the type in which infrared radiation from a source is passed through an absorption cell containing a product including a plurality of compounds and then through a monochromator having an exit slit and containing a

prism and a pivotable mirror for directing through said exit slit any pre-selected band of infra-red radiation and upon a radiation detector, the combination with said mirror of a shaft for supporting said mirror for rotation about an axis lying intermediate its ends, a pivotal support for said shaft, a crank secured at its proximal end to said shaft, a block engaging said crank at a point removed from its proximal end, and having a threaded bore, a rod threadedly engaging said bore, a second crank secured upon said rod for turning the same, a solenoid having a plunger for turning said second crank, whereby the mirror is moved through an arc to a final position, and spring means operative upon de-energization of the said solenoid, for returning said second crank to initial position, whereby said mirror is moved through an arc to its initial position, and whereby transmitted radiation of a plurality of wavelengths may be successively directed upon said radiation detector upon appropriate movement of the mirror.

NORMAN D. COGGESHALL.
MORRIS MUSKAT.

REFERENCES CITED

The following references are of record in the file of this patent:

UNITED STATES PATENTS

Number	Name	Date
1,746,525	Darrah -----	Feb. 11, 1930
2,063,140	Allison -----	Dec. 8, 1936
2,176,013	Pineo -----	Oct. 10, 1939
2,314,800	Pineo -----	Mar. 23, 1943
2,376,311	Hood -----	May 15, 1945
2,386,831	Wright -----	Oct. 16, 1945
2,404,064	Heigl et al. -----	July 16, 1946

NC

Certificate of Correction

Patent No. 2,471,935.

May 31, 1949.

NORMAN D. COGGESHALL ET AL.

It is hereby certified that errors appear in the printed specification of the above numbered patent requiring correction as follows:

Column 2, line 13, for the words "of an" read *of any*; lines 51 and 52, for "obtained" read *obtained*; column 4, line 34, strike out "different momentum in the beam to travel in dif-"; line 36, for "diffrent" read *different*; column 6, line 60, for that portion of the equation reading " $(+v\bar{c})$ " read $(v+\bar{c})$; column 9, line 42, for "sme" read *same*; column 13, line 11, for "unifority" read *uniformity*;

and that the said Letters Patent should be read with these corrections therein that the same may conform to the record of the case in the Patent Office.

Signed and sealed this 18th day of October, A. D. 1949.

[SEAL]

THOMAS F. MURPHY,
Assistant Commissioner of Patents.

NDC

May 31, 1949.

N. D. COGGESHALL ET AL
METHOD AND APPARATUS FOR SEPARATING CHARGED
PARTICLES OF DIFFERENT MASSES

2,471,935

Filed March 19, 1945

10 Sheets-Sheet 1

FIG. 1

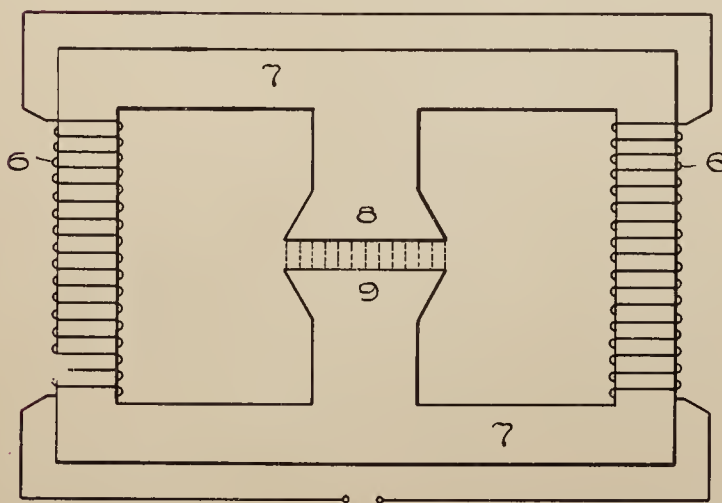
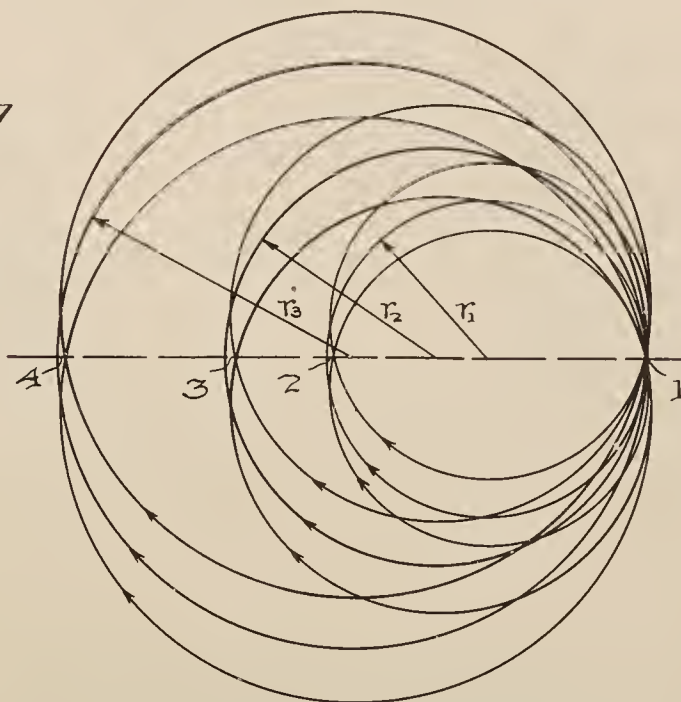


FIG. 2

Inventors
NORMAN D. COGGESHALL
MORRIS MUSKAT

By *G. M. Houghton*
their Attorney

May 31, 1949.

N. D. COGGESHALL ET AL
METHOD AND APPARATUS FOR SEPARATING CHARGED
PARTICLES OF DIFFERENT MASSES

2,471,935

Filed March 19, 1945

10 Sheets-Sheet 2

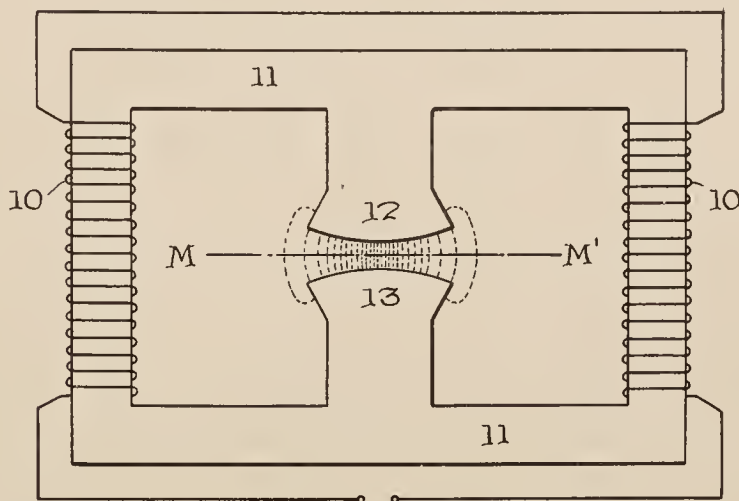


Fig. 3.

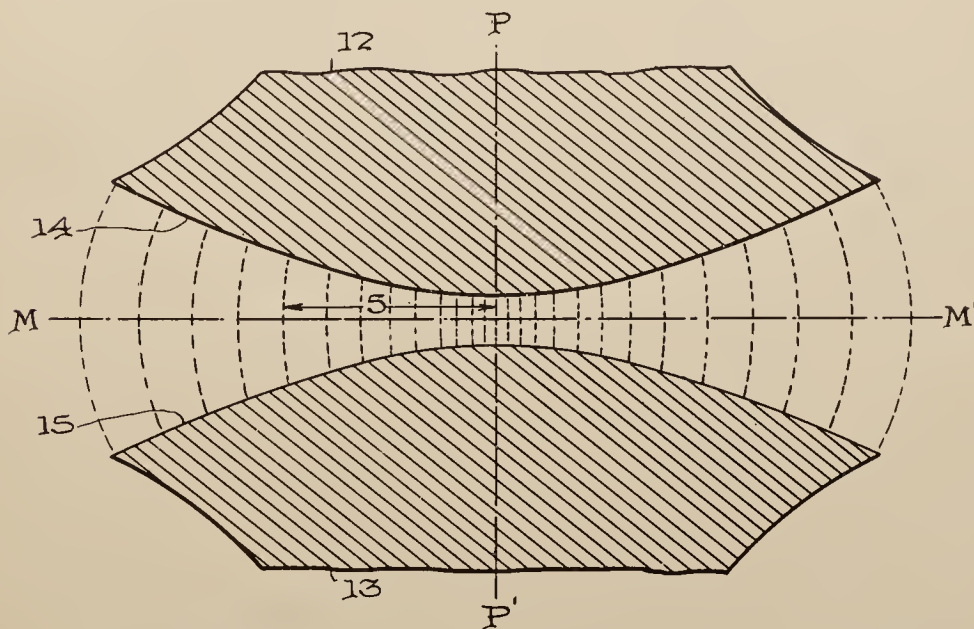


Fig. 4.

Inventors
NORMAN D. COGGESHALL
MORRIS MUSKAT

By G. M. Houghton
their Attorney

May 31, 1949.

N. D. COGGESHALL ET AL
METHOD AND APPARATUS FOR SEPARATING CHARGED
PARTICLES OF DIFFERENT MASSES

2,471,935

Filed March 19, 1945

10 Sheets-Sheet 3

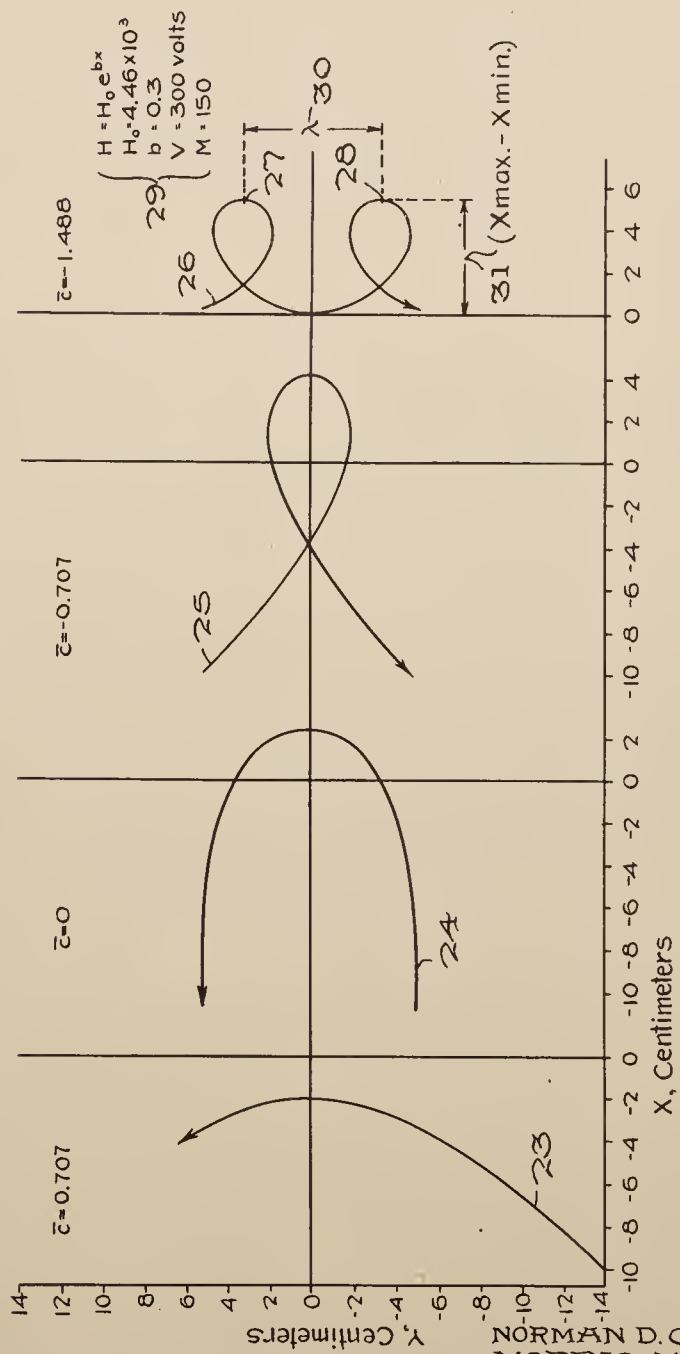


Fig. 5.

Inventors

NORMAN D. COGGESHALL
MORRIS MUSKAT

By A. M. Foughton
their Attorney

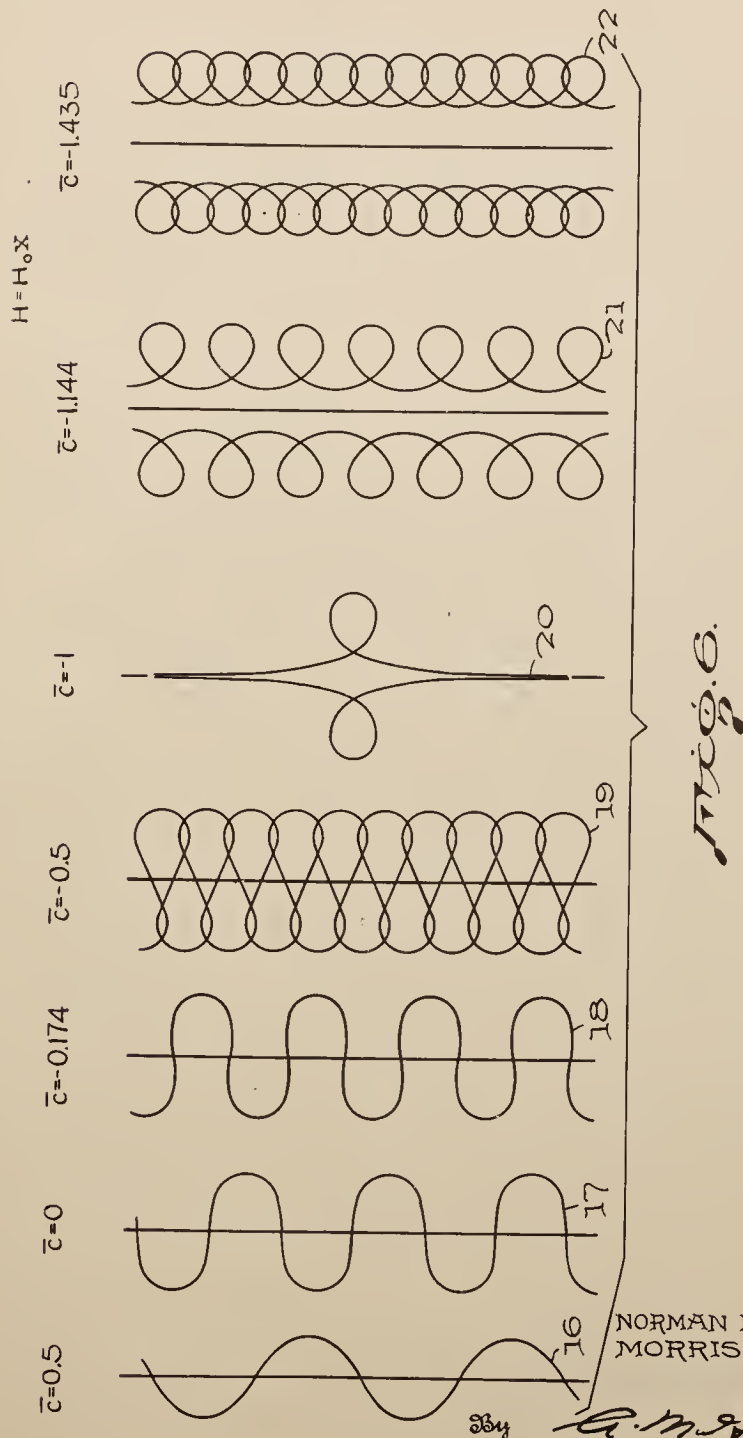
May 31, 1949.

N. D. COGGESHALL ET AL
METHOD AND APPARATUS FOR SEPARATING CHARGED
PARTICLES OF DIFFERENT MASSES

2,471,935

Filed March 19, 1945

10 Sheets-Sheet 4



Inventors
NORMAN D. COGGESHALL
MORRIS MUSKAT

G. M. Vaughan
their Attorney

May 31, 1949.

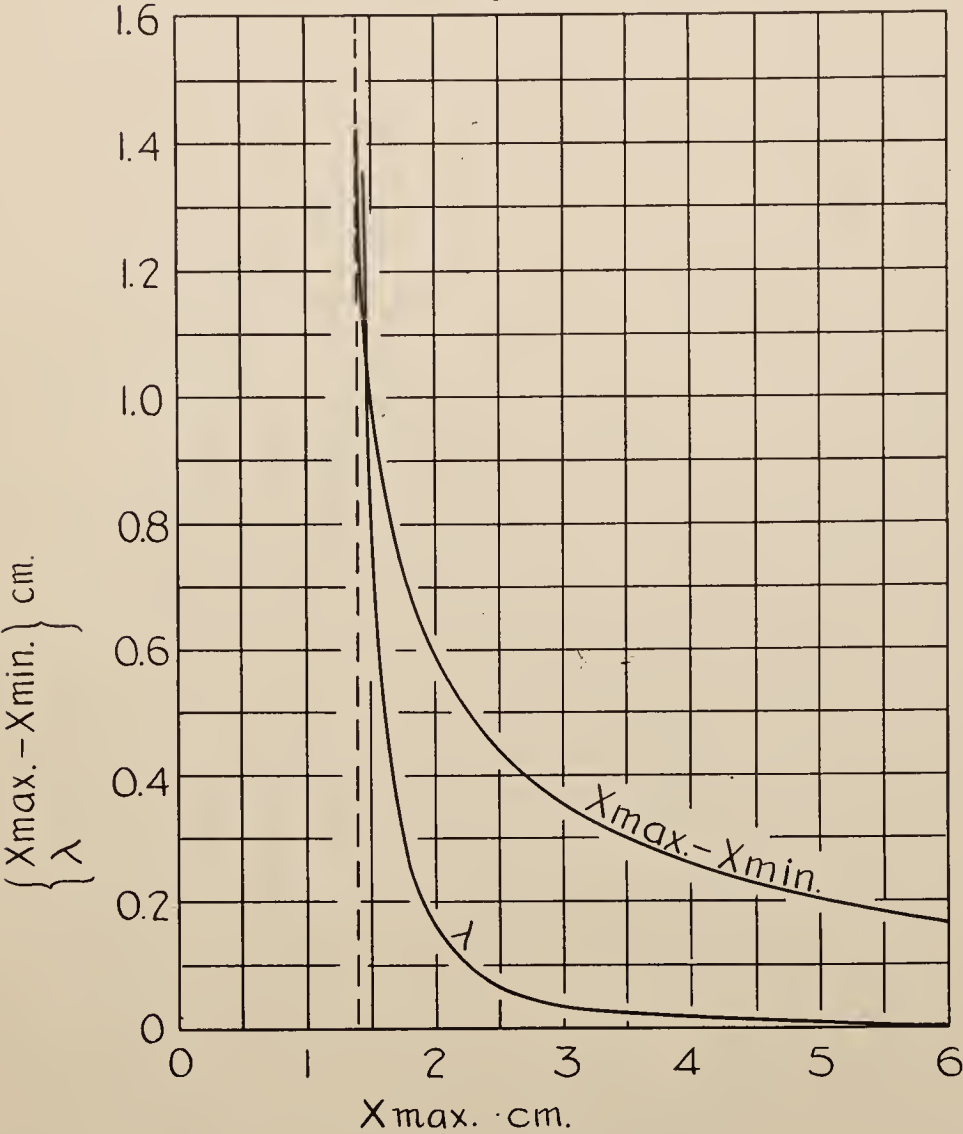
N. D. COGGESHALL ET AL
METHOD AND APPARATUS FOR SEPARATING CHARGED
PARTICLES OF DIFFERENT MASSES

2,471,935

Filed March 19, 1945

10 Sheets-Sheet 5

Fig. 7.



Inventors

NORMAN D. COGGESHALL
MORRIS MUSKAT

By A. M. Houghton
their Attorney

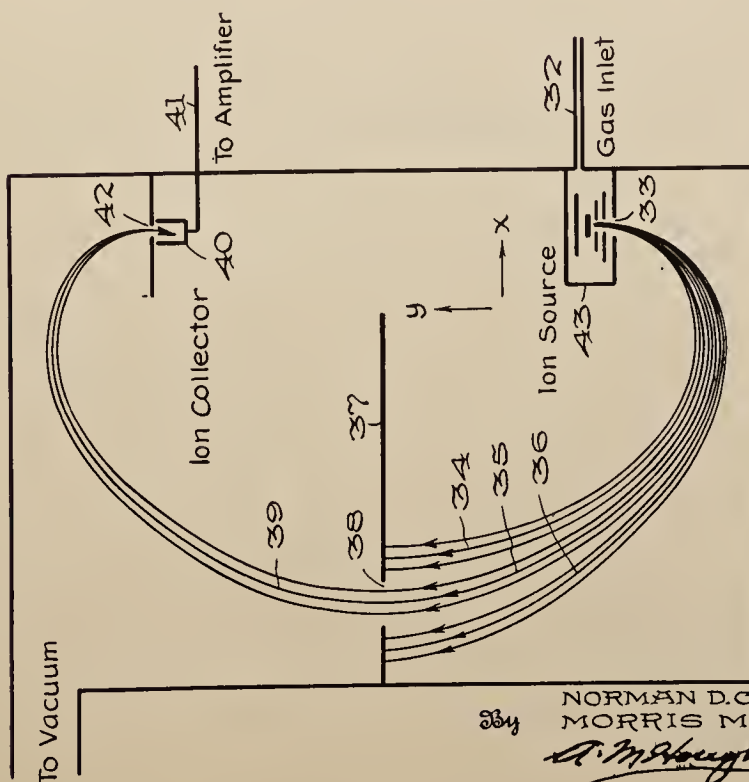
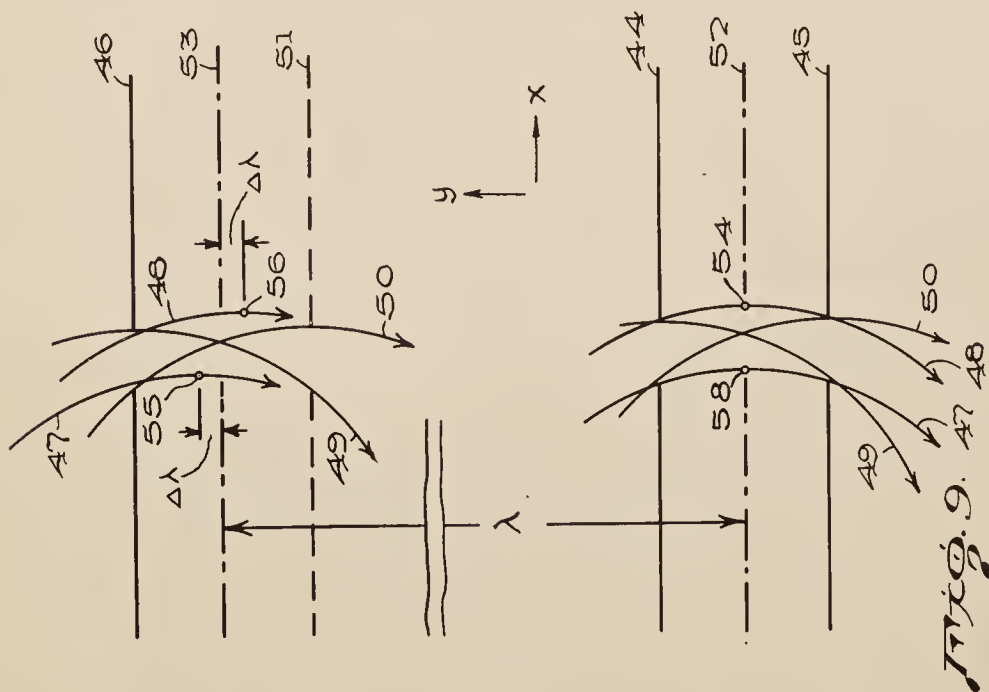
May 31, 1949.

N. D. COGGESHALL ET AL
METHOD AND APPARATUS FOR SEPARATING CHARGED
PARTICLES OF DIFFERENT MASSES

2,471,935

Filed March 19, 1945

10 Sheets-Sheet 6



NORMAN D. COGGESHALL
MORRIS MUSKAT

A. M. Houghton his Attorney

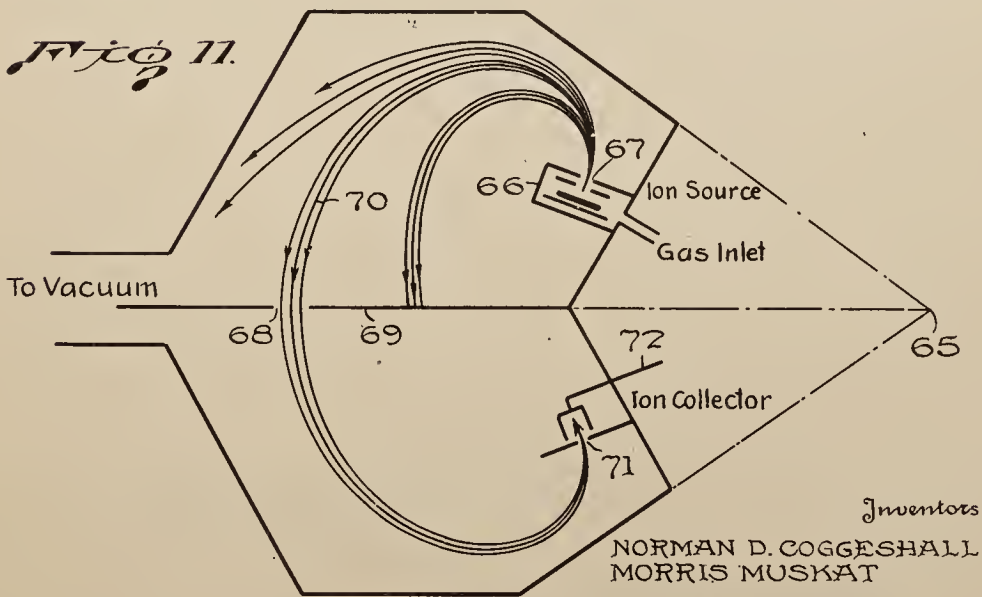
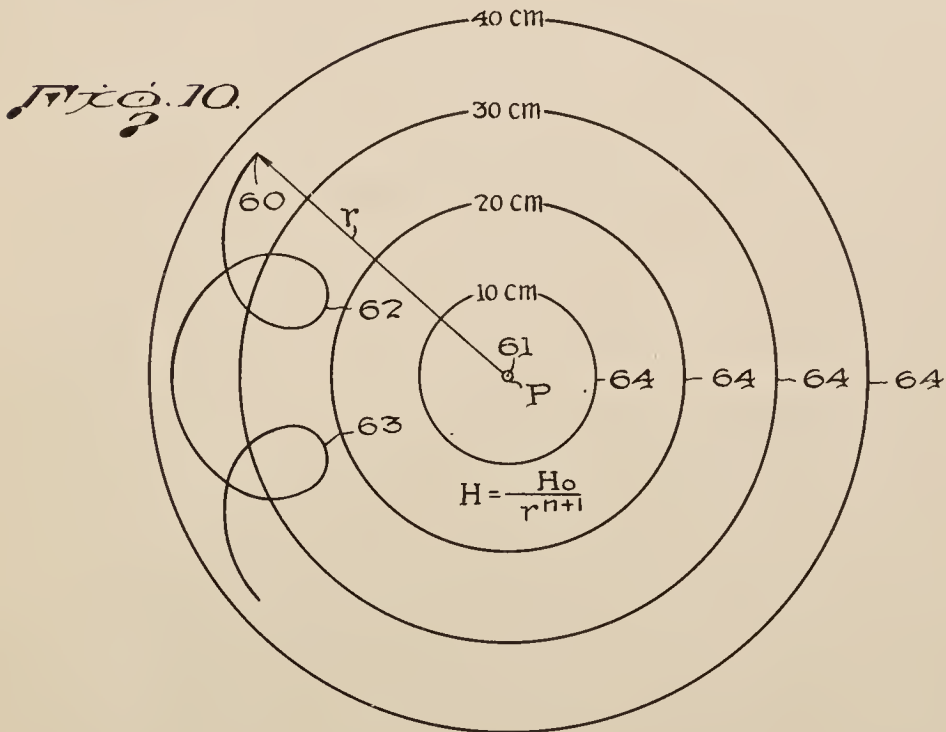
May 31, 1949.

N. D. COGGESHALL ET AL
METHOD AND APPARATUS FOR SEPARATING CHARGED
PARTICLES OF DIFFERENT MASSES

2,471,935

Filed March 19, 1945

10 Sheets-Sheet 7



By A. M. Houghton their Attorney

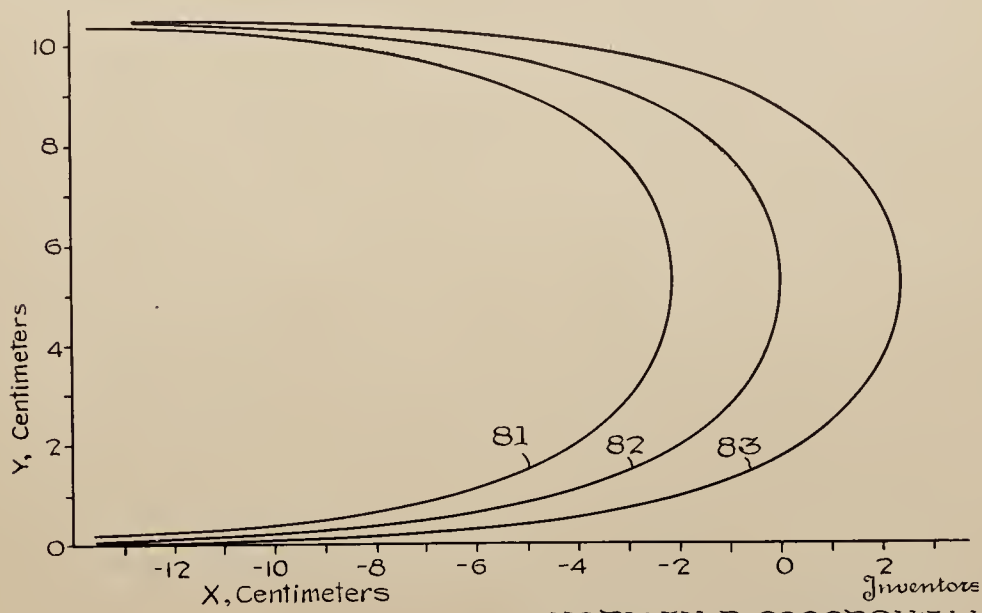
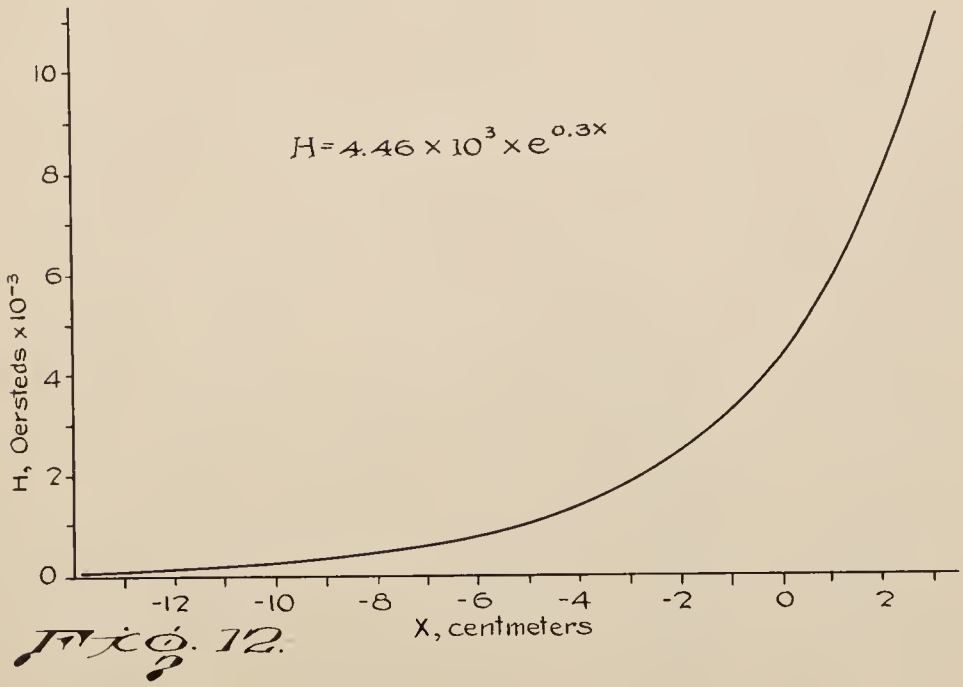
May 31, 1949.

N. D. COGGESHALL ET AL
METHOD AND APPARATUS FOR SEPARATING CHARGED
PARTICLES OF DIFFERENT MASSES

2,471,935

Filed March 19, 1945

10 Sheets-Sheet 8



NORMAN D. COGGESHALL
MORRIS MUSKAT.

By *A. M. Houghton*
their Attorney

May 31, 1949.

N. D. COGGESHALL ET AL
METHOD AND APPARATUS FOR SEPARATING CHARGED
PARTICLES OF DIFFERENT MASSES

2,471,935

Filed March 19, 1945

10 Sheets-Sheet 9

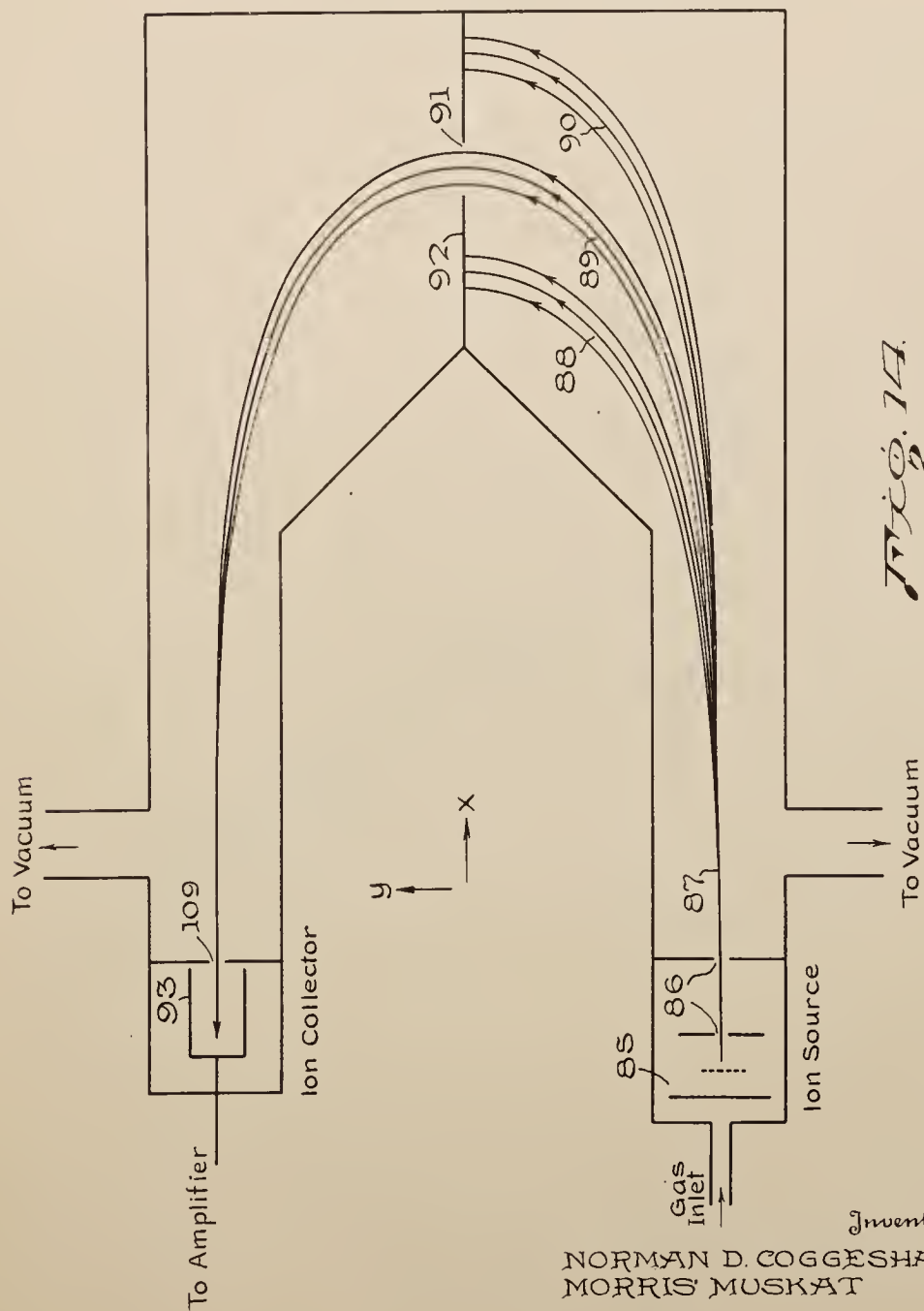


Fig. 14.

Inventors
NORMAN D. COGGESHALL
MORRIS MUSKAT

By

A. M. Houghton

their Attorney

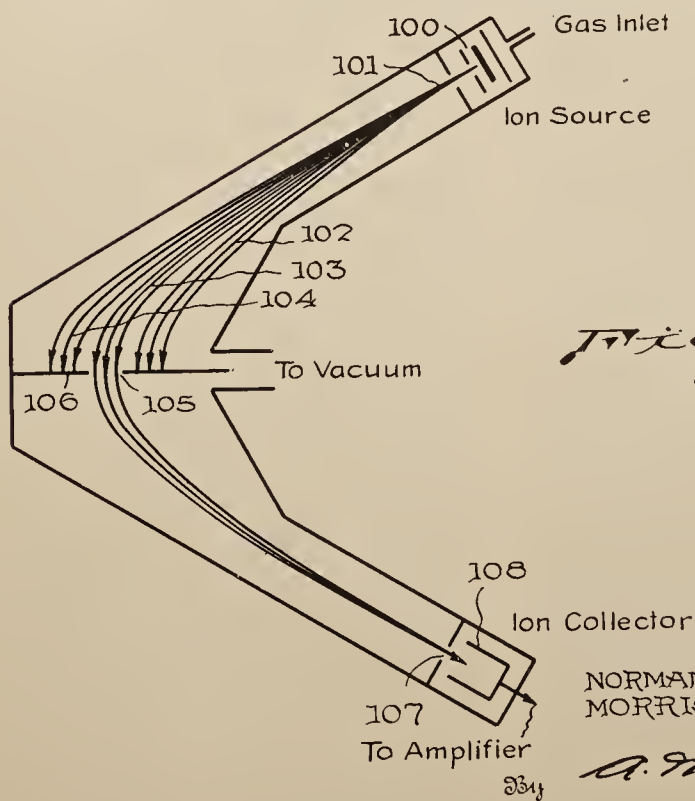
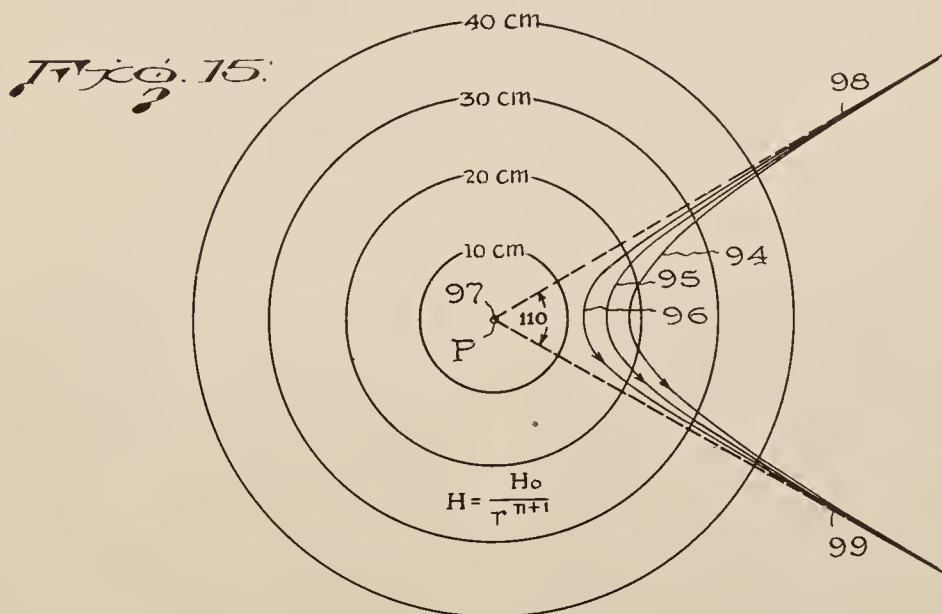
May 31, 1949.

N. D. COGGESHALL ET AL
METHOD AND APPARATUS FOR SEPARATING CHARGED
PARTICLES OF DIFFERENT MASSES

2,471,935

Filed March 19, 1945

10 Sheets-Sheet 10



Inventors

NORMAN D. COGGESHALL
MORRIS MUSKAT

A. M. Houghton

these Attorney

UNITED STATES PATENT OFFICE

2,471,935

METHOD AND APPARATUS FOR SEPARATING CHARGED PARTICLES OF DIFFERENT MASSES

Norman D. Coggeshall, O'Hara Township, Allegheny County, and Morris Muskat, Oakmont, Pa., assignors to Gulf Research & Development Company, Pittsburgh, Pa., a corporation of Delaware

Application March 19, 1945, Serial No. 583,432

26 Claims. (Cl. 250—41.9)

1

This invention concerns a new and improved method of focusing electrically charged particles and more particularly a method and apparatus for ion focusing in a mass spectrometer. The invention may be utilized either for space focusing or for momentum focusing, and depends for its operation on the motion of an electrically charged particle in a non-homogeneous field of a special type.

In the last two decades there have been great advancements in the application of magnetic fields for the focusing of electrons and ions. Among instruments using magnetic lenses are: mass spectrographs, mass spectrometers, beta-ray spectrometers, isotope separators, electron microscopes, electron diffraction apparatus, electron scattering apparatus, and television equipment. A discussion of the history of the application of magnetic lenses for the study of isotopes may be found in an article, "A short history of isotopes and their measurement," by E. B. Jordan and L. B. Young (Journal of Applied Physics, vol. 13, p. 526, Sept. 1942). In these applications the action of the magnetic field is to so deflect a diverging beam of electrons or ions as to cause it to converge or come to a focus.

The mass spectrometer has been used extensively for the separation of gaseous ions. As an analytical tool; it is able to separately determine constituents not separable by ordinary chemical means. It may be used to determine isotopic concentrations or to determine the concentrations of isomers in complicated chemical materials. Essentially, it separates ions according to their mass/charge ratio and permits measuring the amount of each type of ion present. The material to be analyzed is ionized in the instrument and the ions are separated by the action of electric or magnetic fields or both either successively or simultaneously. Ordinarily the material is introduced into the ion source as a gas at low pressure, and the rest of the apparatus is maintained under high vacuum so that the ions meet no obstacles in their path. In most recent instruments the ions are produced by electron impact and accelerated by electric fields in an "ion gun," from which they are projected into a region of magnetic field in a direction at right angles to the lines of force. Ions having different momenta execute different orbits in the magnetic field and the groups of ions are caught at appropriate places.

It is well known that ions moving in a uniform homogeneous magnetic field at right angles to the lines of force will move in circular arcs. Homogeneous and uniform magnetic fields have

2

been employed in various arrangements designed for mass spectrometers to be used for various purposes. The function of the magnetic field in each case is to reunite or focus particles of a divergent ion beam and at the same time permit sorting them according to their mass/charge ratio.

It is the purpose of this invention to provide several new focusing arrangements with distinct advantages over the ones heretofore in use. In the practice of the heretofore known art, it is customary to use the focusing properties of uniform and homogeneous magnetic fields, and the presence of an inhomogeneity is undesirable and usually harmful. In the focusing arrangements provided by this invention, the magnetic field is deliberately made non-homogeneous, and advantage is taken of paths of ions or electrons in such a non-homogeneous field to achieve proper focusing.

It is accordingly an object of this invention to provide a method and apparatus for more perfect space focusing of charged particles.

Another object of this invention is to provide a method and apparatus for space focusing of charged particles by means of a non-homogeneous magnetic field.

Another object of this invention is to provide a method and apparatus for momentum focusing of charged particles.

Another object of this invention is to provide a method and apparatus for momentum focusing of charged particles by means of a non-homogeneous magnetic field.

A further object of this invention is to provide a method and apparatus whereby improved ion sorting is achieved in a mass spectrometer.

The manner of accomplishing these and other objects are made apparent in the following specification, of which the drawings also form a part, and in which:

Figure 1 is a diagram of the ion paths in a mass spectrometer having a homogeneous field as heretofore used.

Figure 2 is a diagram of a magnet which produces the type of homogeneous field heretofore used in mass spectrometers.

Figure 3 is a diagram of a magnet which may be used for producing a non-homogeneous field.

Figure 4 is an enlarged view of the magnet pole pieces which may be used.

Figure 5 shows ion paths which may be obtained in a magnetic field having one-dimensional (Cartesian) inhomogeneity of an exponential type.

Figure 6 shows ion paths which may be ob-

tained in a magnetic field having one-dimensional (Cartesian) inhomogeneity and having linear variation.

Figure 7 is a graph showing the relation between certain parameters of a orbit executed by a charged particle in an inhomogeneous field as used in our invention.

Figure 8 is a diagram of a mass spectrometer utilizing a magnetic field of one-dimensional (Cartesian) inhomogeneity.

Figure 9 is an enlarged view of the source and collector slits of Figure 8 showing how space focusing takes place.

Figure 10 shows a type of ion path which may be obtained in a magnetic field having axial symmetry.

Figure 11 is a diagram of a mass spectrometer utilizing a magnetic field having axial symmetry.

Figure 12 is a graph showing the intensity of a magnetic field having one-dimensional (Cartesian) inhomogeneity of an exponential type.

Figure 13 shows ion paths of a special type which may be obtained in the exponential field of Figure 12.

Figure 14 is a diagram of a mass spectrometer utilizing the special type of ion path shown in Figure 13.

Figure 15 shows another special type of ion path which may be obtained in a magnetic field having axial symmetry.

Figure 16 is a diagram of a mass spectrometer utilizing the special type of ion path shown in Figure 15.

When a charged particle moves in the presence of and perpendicular to a magnetic field and in the absence of an electric field it will move along the arc of a circle. The radius of curvature of the arc depends upon the mass of the particle, its kinetic energy, and upon the strength of the magnetic field. If the magnetic field is constant and if a number of ions of the same kinetic energy but different masses (i. e. different momenta) move in the field they will move along circles of different radii. One method in which this fact is used to achieve focusing of electrons or ions is illustrated in Figure 1 of the drawings. Here point 1 represents the location of a source of ions. A uniform magnetic field is directed normal to the plane of Figure 1. Such a field may be obtained by means of an electromagnet shown in Figure 2. A direct current is passed through coils 6 magnetizing yoke 7 so that a uniform and homogeneous flux is set up in the air gap between pole pieces 8 and 9. The mass spectrometer apparatus is placed in the air gap in such a way that ions will move in a plane normal to the uniformly distributed lines of force. An attempt is made to project the ion beams from point 1 (Figure 1) with practically the same kinetic energy. If there are three different types of ions issuing from the source at point 1 (Figure 1), i. e., having three different masses, they will execute paths of three different radii, shown as r_1 , r_2 and r_3 . There will be an angular spread of the paths because of the space divergence of the ion beam. As may be seen from the figure, there is a "semi-focusing" of the separate groups of ions at points 2, 3 and 4. Although the ion beams are perfectly focused in returning to 1, it is not feasible to exploit this fact in an actual instrument because of the practical difficulty of locating both a source and collector of ions at the same point 1. A quite common application of the focusing illustrated in Figure 1 is to utilize the "semi-focusing" points 2, 3 or 4. That is, an ion source is located

at 1 and a collector at one or more such points as 2, 3 or 4. As may be seen, this is far from ideal, because the collector for the ions is not at the point of best focusing. This leads to difficulty in getting the desired resolution between ion beams. High resolution is required to separate ion beams of large masses.

Other applications of uniform magnetic fields for the focusing of ion beams may be found in the article by Jordan et al. mentioned above. In none of them is it possible to use such a point of perfect focusing as the point 1 in Figure 1 and an imperfect semi-focusing is used instead. In this invention we shall describe how it is possible to obtain points of perfect focusing for application in focusing instruments by using non-homogeneous magnetic fields.

In the mass spectrometers in general use today a beam of ions is created by drawing out from the ionization region the ions formed by electron impact. This is accomplished by the application of electric fields, and the ions emerge from the final slit of the ion source in the form of a ribbon. The ribbon surface of the emerging ribbon-like beam is always parallel to the direction of the magnetic field used for focusing so that the ions travel normal to the field. It is impossible, however, to obtain a ribbon of emerging ions in which their directions of travel are strictly parallel. Instead, there will be an angular spread such that some ions will be diverging or travelling away on both sides from the central part of the ribbon. It is the purpose of the focusing element of the spectrometer, usually a magnetic lens, to cause ions of different momentum in the beam to travel in different paths, and, at the same time, to cause the diverging ions of any one momentum later to converge at a "focal point." This is termed space focusing or angular focusing.

In actual ion beams there will be several momentum classes, each corresponding to a fixed ion mass, but there will also be a momentum spread due to the ions created at different points of electrostatic potential in the ionization region. When the ions being studied are caused by dissociation and ionization of polyatomic molecules, there results a rather large momentum spread from this cause. This is due to the fact that in such processes there is a considerable variation in the kinetic energy with which the ions may be formed. In cases where the ions are formed with little or no kinetic energy, almost all of the ions of a particular mass can be collected with one setting of the accelerating voltage. That is, the focusing at the collector slit is sufficient to collect practically all of the ions, with the rather large collector slit opening used (as compared with the source slit opening). However, when the ions are formed with considerable variation in kinetic energy, there results a considerable spread in momentum, and the ions in the beam do not converge enough to fall entirely within the dimensions of the collector slit. This results in a broadening and change of shape of the peak when the ion current is plotted against accelerating voltage, and introduces an uncertainty in the measured intensity of the beam. In analytical uses of a mass spectrometer the intensity of any particular ion beam is a quantity of paramount importance, and must be subject to determination with high precision.

Up to the present, all of the focusing schemes now in use depend upon a semi-perfect focusing of diverging ion beams, and in all of them a spread

of momentum causes a superposed blurring of the focusing. In one form of this invention perfect angular focusing is obtained. In another form of this invention the momentum blurring is avoided and the effect produced is termed momentum focusing.

To illustrate our invention we shall describe several new and different focusing schemes. In two of them, utilizing periodic ion orbits, the momentum blurring is not removed, but the angular focusing is more nearly perfect than in existing instruments. In these instruments, therefore, the collector slit can be made smaller, with greater resultant resolution. In the other two schemes, utilizing aperiodic orbits, there is no angular focusing, but a new focusing principle is applied. This is momentum focusing. In the instruments in which such momentum focusing is achieved, the angular spread is closely controlled by using a narrower slit system in the ion source. However, ions of different momentum values passing out of the exit slits are focused into a single collector slit.

The difference between the application of angular and momentum focusing may be stated as follows: In the former (angular focusing) ions of the same momentum value, but different angles of emergence from the source slit, are focused into a single collector slit; in the latter (momentum focusing) ions with the same direction of emergence but with different momentum values are focused into a single collector slit.

An important advantage of our described instruments using periodic orbits and providing angular focusing is increased resolution. At present, mass spectrometers in use for analytical work are usually limited to ions of atomic mass of 150 or less. In analyzing organic mixtures, ions of greater atomic mass are often encountered, and for analytical work on these greater resolution is necessary.

In considering the actual non-uniform magnetic field used in our invention, reference is made to the magnetic field due to the magnet shown schematically in Figure 3. This is similar to Figure 2 except in the shape of the pole pieces. An electric potential difference applied between the terminals gives rise to a current flowing through the wire coils 10 of the electromagnet. The iron yoke 11 is magnetized so that there is a magnetic field between the two pole pieces 12 and 13. The pole pieces are geometrically symmetrical with reference to the median plane MM' so that the magnetic flux lines (shown as dashed curves) will also be symmetrical with respect to it. As a consequence, the vector representing the magnetic field intensity at any point on the plane MM' will be perpendicular to it. This means that all the magnetic flux lines are parallel as they intersect the plane MM' so that the magnetic field is uniform in direction and its magnitude at any point on the plane can be expressed as a function of the position of the point on plane MM'. For pole pieces of axial symmetry we will thus have magnetic fields which are expressible as $H=H_0(r)$ on the median plane, where r is the radial distance from the axis of symmetry. For pole pieces having a rectangular cross section with a relatively long dimension in the direction perpendicular to the plane of Figure 3 the fields may be described on the median plane in Cartesian coordinates as $H=H_0(x)$ where x is the coordinate measuring the distance right and left on the plane MM' in Figure 3; the field in this case

being invariant in the direction y which is normal to the plane of Figure 3.

In Figure 4 we have shown an enlarged view of the pole pieces 12 and 13. There is symmetry about the plane MM', and the field is everywhere normal to this plane. To obtain a field having axial symmetry, the figure is rotated about an axis PP', and the resulting field may be expressed by $H=H_0(r)$ where r is the distance from axis PP'. To obtain a field having one-dimensional (Cartesian) inhomogeneity, the figure is extended parallel to itself in a direction normal to the figure, and the resulting field may be expressed by $H=H_0(x)$ where x is the distance right or left from a plane PP'. The coordinate 5 in Figure 4 will be r or x respectively in these two cases.

The manner in which the field H varies with r or x respectively in the above two cases may be controlled by the shape of the pole surfaces 14 and 15 of the pole pieces 12 and 13. The required shape of these surfaces may be computed or determined empirically to obtain the desired variation of H in the plane MM'. The mass spectrometer apparatus is then placed in the gap between the pole faces 14 and 15 in such a way that the ion beams emerging from the ion source will be in or parallel to the plane MM'. The ions will execute paths or orbits in or parallel to the plane MM' as a result of the magnetic field, and the trajectories may be best pictured by a plot in the plane MM' itself.

The full mathematical theory of the motion of charged particles in magnetic fields of the type used in our invention is given in an article titled "The paths of ions and electrons in non-uniform magnetic fields" by N. D. Coggeshall and M. Muskat in The Physical Review, vol. 66, Nos. 7 and 8, 187-198, October 1 and 15, 1944. Summarizing the results of this article, if the magnetic field varies smoothly with the coordinate x (indicated by numeral 5 in Figure 4), for example either as a linear function $H=H_0x$, or as an exponential function $H=H_0e^{bx}$, then the orbit of a charged particle is formally given by the integral.

$$y = \pm \int \frac{f dx}{(1-f^2)^{1/2}} \text{ where } f = a \int H_0(x) dx \quad (1)$$

The integral for y may be evaluated for special forms of the function H , and we have done this for the linear and exponential forms mentioned above. Two types of orbits are in general obtained, one type being periodic in nature and one type being aperiodic.

In the case of a field having such one-dimensional (Cartesian) inhomogeneity of an exponential type as $H=H_0e^{bx}$, the general equation for the periodic orbit is:

$$y = \pm \frac{1}{b} \left\{ \sin^{-1} \left(\frac{A}{y} \right) + \frac{\bar{c}}{(\bar{c}^2 - 1)^{1/2}} \sin^{-1} \left[\frac{1 - \bar{c}^2 - \bar{c}v}{v} \right] \right\} \quad (2)$$

where

$$v = \frac{aH_0e^{bx}}{b}, \quad a = \frac{1}{c} \left\{ \frac{150e}{mV} \right\}$$

 \bar{c} is a constant to be adjusted to fit the solution to the proper starting conditions, e is the charge of the ion in E. S. U., c is the velocity of light in cm./sec., m is the mass of the ion in grams, and V is the energy of the ion in electron-volts.

In Figure 5 we have plotted trajectories obtained by solutions of Equation 1. Orbit 26 is of the type given by Equation 2 above. When this orbit is applied to a mass spectrometer, the charged particle may be projected from point

27 in a direction parallel to the Y axis. The magnetic field is perpendicular to the figure, is invariant in the y direction and varies as $H=H_0e^{bx}$ in the x direction. Other constants of the orbit are given in the legend under numeral 29. A collector is placed at point 28 to catch the ions.

In Figure 6 we have illustrated various types of orbits obtainable when the magnetic field has the simple linear form $H=H_0x$. The orbits 16, 17, 18, 19, 20, 21 and 22 differ according to the integration constant \bar{c} which depends on the starting conditions and which is stated above each orbit. The same is true of other orbits 23, 24, 25 and 26 obtainable in an exponential field as shown in Figure 5.

The orbits shown at 21 and 22 in Figure 6 are of a similar type as 26 in Figure 5, in that they have certain properties useful in space focusing of ion beams. As these orbits consist of repeated cycles of the same type of motion, we may ascribe to them a "wave length" λ which we may define as the distance between geometrically similar points. Two such points are 27 and 28 of Figure 5, the λ being indicated at 30. Another characteristic parameter of such an orbit is the total width in the x direction, which we may call $(x_{\max}-x_{\min})$ and is indicated at 31. We have found that for such orbits λ and $(x_{\max}-x_{\min})$ decrease with increasing x . A plot showing how λ and $(x_{\max}-x_{\min})$ vary with x_{\max} in a particular instance is shown in Figure 7. The points of x_{\max} are the positions of smallest curvature of the orbits and the place where the orbits are also perpendicular to the X-axis. It is a result of the mathematical derivation leading to these orbits that λ decreases as x_{\max} increases.

It is to be emphasized that it is always possible to obtain the periodic type of orbit similar to 26 (Figure 5) when the field H is a function of x only and increases with increasing x . The fact that λ for such orbits decreases for those orbits located in regions of stronger H is fundamental for the space focusing principle used in our invention.

Figure 8 is a schematic diagram of a mass spectrometer utilizing periodic orbits similar to 26 in Figure 5. In Figure 8 numeral 43 represents a conventional ion source in which gas molecules entering through inlet 32 are ionized by electron impact. Strong electric fields maintained between the slits inside the ion gun project the ions out through the exit slit 33. There is a considerable angular spread in the ion stream issuing from slit 33. The ion stream is further composed of ions having different mass/charge ratio, the relative numbers of which the analysis is to determine. A magnetic field is set up perpendicular to the plane of Figure 8 by means of a magnet (similar to Figure 3) such that the field increases in magnitude in the direction indicated by x in Figure 8 in an exponential manner as $H=H_0e^{bx}$, and is invariant in the direction indicated by y in Figure 8. Under the action of such a field the ion streams will be bent into the curved paths shown. Numerals 34, 35 and 36 each represent diverging beams of ions having different masses. A diaphragm 37 has a slit 38 narrow enough to allow only one beam of a single mass value to pass through and reach the ion collector. Thus all the ions in beam 39 after passing through slit 38 have the same mass. These are brought into convergence by the magnetic field and pass through a slit 42 and collected at 40 by an insulated ion collector or Faraday pail having a lead 41 to an amplifier and indi-

cating apparatus in the conventional way. The various beams having different ion-mass are brought into the ion collector slit 42 either by adjusting the accelerating potentials in the ion gun or by adjusting the strength of the magnetic field. It is customary to measure the ion current collected by ion collector 40 as a function of one of the above parameters and the peaks on the resulting plot are proportional to the concentration of the various ions present in the ionized material in the ion source.

The arrangement of component parts in Figure 8 is such that the ion-source exit slit 33 corresponds to point 29 in Figure 5 and the collector entrance slit 42 corresponds to point 27 in Figure 5. The direction of movement of the particles is different in the two cases but this difference merely corresponds to a reversal of the direction of magnetic field. We have found that perfect focusing is obtained at 42 (Figure 8) in the sense that all the ions of a given mass and energy will enter a collector slit 42 no larger than the ion-source slit 33. This is because the ion-source opening 33 and the collector opening 42 are placed at points in the orbits corresponding to points 27 and 28 of Figure 5. Ions of the same mass and kinetic energy leaving either points 27 or 28 will arrive at either 28 or 27 in perfect focus in the above sense as a consequence of the fact that $(x_{\max}-x_{\min})$ decreases with increasing values of x .

Figure 9 illustrates in more detail the manner in which this angular focusing is achieved. Figure 9 is a schematic diagram of the geometrical configurations at the exit slits 44 and 45 of the ion source of an instrument such as shown in Figure 8, and also at the entrance slit 46 of the ion collector. In Figure 8 numeral 33 shows only one ion-source slit but two are commonly used in order to obtain some collimation of the ion beam. By proper distribution of potentials in the ion source, using well-known methods, the ions are caused to acquire essentially the same potential. The slits 44 and 45 (Figure 9) are at the same potential and are operative only in defining the emergent beam. Moreover, these slits are geometrically similar and located identically as regards the x coordinate. With such an arrangement all ions leaving the exit slit will follow orbits having approximately the same radius of curvature at the exit slits, the orbits differing only in the angle of emergence. In Figure 9 the arrow 47 represents the orbit with the smallest value of x_{\max} that can emerge, 48 that with the largest value of x_{\max} . The respective positions of x_{\max} for these orbits are indicated by points 58 and 54. These points will lie on a center line 52 midway between slits 44 and 45. Arrows 49 and 50 represent the paths of greatest divergence in angle of emergence. Since slits 44 and 45 cover the same range along the x direction, orbits 49 and 50 will have the same x_{\max} .

Consider now the orbits 47, 48, 49 and 50 when the ions have advanced by exactly one wave length in their periodic paths. The collector slit 46 is displaced from source slit 44 by one wave length λ . To clarify the geometry we may introduce a phantom collector slit 51 displaced from 45 by λ . A center line 53 is also shown displaced from center line 52 by λ . Since orbits 49 and 50 have the same x_{\max} , they will have the same λ . Therefore, a slit 46 of the same width as 44 and located at the same value of x , but displaced along y by a pre-chosen value λ , will collect both 49 and 50. That is, orbits 49 and 50

will pass through slit 46 with exactly the same geometry as they pass through slit 44. Thus this arrangement of orbits and slits will provide perfect angular focusing in that diverging rays leaving the ion source will converge within collector slits no wider than the source slits. Furthermore since orbit 47 has a smaller value of x_{\max} , and hence slightly larger λ , it will be displaced slightly upwards relative to 49 and 50 in the region of slit 46. Thus its new x_{\max} at point 55 is displaced upward from the center line 53 a small amount as $\Delta\lambda$ and this permits it to easily clear the edge of slit 46. Conversely, as orbit 48 has a larger value of x_{\max} , its λ will be smaller than that of 49 and 50. Hence as it passes through slit 46 its new position of x_{\max} at point 56 will be displaced slightly downward from the center line 53 a small amount shown as $\Delta\lambda$ and this permits this orbit also to clear the edge of slit 46.

This shifting of the orbits 47 and 48 relative to 49 and 50 means that the latter will limit the lateral spread in the ion beam when entering collector slit 46 just as they define the angular spread in the beam emerging from the source slits 44 and 45. We thus have the condition for perfect space focusing satisfied, in the sense that if we control the momentum spread closely enough all the ions of a certain momentum leaving the exit slits will be collected by the collector slits. The phantom slit 51 shown in the Figure 9 bears the same relationship to 46 as 45 does to 44. It is shown in Figure 9 only for the sake of clarity, and there will be no such slit in the actual collector.

The λ chosen for operation is entirely arbitrary, and ions of any mass can be collected as desired by varying either the magnetic field or the accelerating potential, or both. Since the voltage spread in the ion source can be closely controlled, there will emerge from the ion source only definite classes of ion beams, each class characterized by a definite mass. These different classes cannot have the same orbits, and there will be an increasing divergence between the different orbits as they proceed into regions of smaller x . This spread will be at a maximum at the position of the diaphragm 37 shown in Figure 8. The slit 38 (Figure 8) serves to separate the ions as regards mass. The three orbits shown for each class illustrate a typical spread caused by divergence at the exit slit, plus some spread in momentum.

While we have described in Figures 8 and 9 how our method of angular focusing operates when a magnetic field is used having one-dimensional (Cartesian) inhomogeneity of an exponential form as $H=H_0e^{bx}$, the same effect takes place for a one-dimensional (Cartesian) inhomogeneity of a linear form. This focusing effect takes place in any form of field variation in which a periodic orbit is obtained.

It is further possible to obtain such focusing by employing periodic orbits in a field having axial symmetry. In such cases the field H is a function of the radial distance r from the axis of symmetry, such a function being

$$H = \frac{H_0}{r^{n+1}}$$

for example, where n is a positive number. The orbit in polar coordinates is formally given by the integral:

$$\theta = \pm \int \left\{ \frac{aH_0}{(1-n)r^{n+1}} + \frac{\bar{c}}{r^2} \right\} \left[1 - \left\{ \frac{aH_0}{(1-n)r^n} + \frac{\bar{c}}{r} \right\}^2 \right]^{-\frac{1}{2}} \cdot dr \quad (3)$$

We have determined some of these orbits by

numerical integration of Equation 3. A periodic orbit of this type is illustrated in Figure 10. The magnetic field is directed normal to Figure 10 and is axially symmetrical about the center point P at 61. The radial scale is indicated by the circles 64. Under proper conditions a charged particle projected at a point 60 in the plane of Figure 10, and normal to a radius from P will execute the periodic orbit shown. On such an orbit, points 62 and 63 are points of nearest approach to the axis and the path at these points is again normal to a radius.

Figure 11 shows how periodic orbits in an axially symmetrical field may be used for angular focusing in a mass spectrometer. The magnetic field is normal to Figure 11 and has its axis of symmetry at point 65. The ion gun at 66 with its exit slit 67 is located so as to project the ions approximately normal to the radius vector whereupon they execute the orbits shown. The divergent beams are sorted by the magnetic field, and only the beam 70 having a desired mass passes through the slit 68 in diaphragm 69. Due to geometrical conditions similar to those described with respect to Figure 9, the divergent beam 70 will again be brought to a focus at the collector slit 71 and the intensity of the beam having this particular mass value may be measured by the ion current in lead 72.

Momentum focusing previously referred to is produced by the use of aperiodic orbits similar to 24 of Figure 5. These are of a special type obtained, for instance, when the magnetic field varies exponentially with x , that is $H=H_0e^{bx}$. The general equation of this type of orbit is found to be:

$$y = \pm \frac{1}{b} \sin^{-1} \left\{ \frac{aH_0}{b} e^{bx} \right\} \quad (4)$$

Physically this type of orbit may be described as one traced out by an ion which is projected parallel to the X-axis and from a point of weak H. Mathematically, it corresponds to an ion or electron starting from $x=-\infty$. Physically, this is not necessary, and it suffices if the orbits begin at values of x such that the magnetic field is negligibly weak. These orbits all start out in a direction parallel to the X-axis, make one half-turn, and return to the region of weak H along a path that is asymptotic to a line parallel to the X-axis. Physically, this means that after the ion has returned from regions of higher H, its direction is essentially parallel to the X-axis. The unique result which we utilize is predicted by the above Equation 4 defining these orbits, namely that the separation in the y direction between the line of approach and the line of departure depends only on the constant b , which determines the rapidity of growth of H in the equation: $H=H_0e^{bx}$.

Hence, all ions that are projected into regions of increasing H from a region of very weak H, and in a direction parallel to the X-axis, will turn and recede, all passing through essentially the same point, which is displaced in the y direction by a distance of π/b . The depth of penetration of the ion into the region of increasing values of x will depend upon its momentum. This is illustrated by Figure 13 in which we have drawn the calculated paths for ions of atomic mass 1, 35, and 150, all with 300 electron volt energy, in a field defined by: $H=4.46 \times 10^3 \times e^{0.3x}$.

Figure 12 shows a graph of the intensity of a magnetic field of the above form, specifically $H=4.46 \times 10^3 \times e^{0.3x}$. The field is invariant in the

y direction. Figure 13 shows the calculated aperiodic orbits in such a field, the three orbits 81 and 82 and 83 being for ions of mass 1, 35 and 150 respectively, each having an energy of 300 electron-volts. These orbits have the property of separating and reuniting beams of ions originally starting from the same point in essentially the same direction but with different momenta. This is what we have termed momentum focusing. The manner in which the ions of greater mass penetrate to higher values of field strength is seen by comparing Figures 12 and 13.

Figure 14 shows an instrument employing such aperiodic orbits and achieving momentum focusing. An instrument employing these aperiodic orbits will evidently provide momentum focusing. The magnetic field is directed perpendicular to the plane of Figure 14, increases exponentially in the manner of Figure 12 in the direction indicated as x (i. e. toward the right) and is invariant in the direction indicated as y . The ion source 85 will employ a fine slit system 86 which will project the ions in the x direction of increasing H . The emerging beam 87 will have a negligible angular spread. The spread of the ion bundles as they approach their points of greatest penetration in the x -direction is due to the spread of momentum. We have shown in Figure 14 ion beams 88, 89 and 90 of three different masses. The spread or broadening of beam 89 for instance is due to slight momentum variations among ions having the same mass. The desired beam is allowed to pass through a slit 91 in diaphragm 92. As a consequence of the form of the aperiodic orbits the particles constituting beam 89 subsequently again converge and enter the collector slit 109 where they are caught on the ion collector 93 and measured in the conventional manner.

Such a mass spectrometer or beta-ray spectrometer as Figure 14 is especially valuable in an application where it is difficult to keep the energy of the emerging ions within small tolerances. These cases arise where it is desired to collect ions or electrons over a wide region between accelerating electrodes or when the ions are created with large differences in kinetic energy. As the charged particles may originate from different places between the electrodes, their total potential will vary. Such an instrument is particularly valuable when used to study photo-ionization, in which application it is desirable to collect the ions over an extended region to gain greater intensity in the ion beam.

A similar type of aperiodic orbit useful for momentum focusing may be obtained in the axially symmetrical field previously referred to in connection with Figure 10. The general equation of the aperiodic orbit in such a field where

$$H = \frac{H_0}{r^{n+1}}$$

and n is a positive number greater than unity, is:

$$\theta = \pm \frac{1}{n} \sin^{-1} \left\{ \frac{aH_0}{(1-n)r^n} \right\}$$

Figure 15 illustrates three such orbits 94, 95 and 96 which result when ions are initially projected radially into a field directed normal to the plane of Figure 15 and whose value is

$$H = \frac{H_0}{r^{n+1}}$$

where r is the distance from the axis of symmetry P at point 97. The ions reach a point of minimum r and finally return in a direction

which is asymptotic to a radius vector displaced by an angle θ from the radius vector of approach. The angular separation 110 will be π/n and is independent of the momentum of the individual ions. Ions having different momenta penetrate the field to different distances, but all entering the field along a common radius as 98 also leave along another common radius as 99.

In Figure 16 we have shown diagrammatically an instrument utilizing the aperiodic orbits of Figure 15 to produce momentum focusing. The magnetic field used is directed perpendicular to the plane of Figure 16 and its intensity has axial symmetry similar to that of Figure 15. The ion source 100 produces a very narrow beam 101 directed at the axis of symmetry of the magnetic field. The spreading of the beam 101 results from momentum variations. Three mass groups 102, 103 and 104 are shown, each spread slightly due to momentum inhomogeneity. The desired beam is obtained through slit 105 in the diaphragm 106 and the ions which pass are reunited as a consequence of the form of the orbits at the collector slits 107 and enter the collector 108 whose ion current may be measured or recorded in a conventional manner. Momentum focusing is thus achieved in this instrument.

In the instruments illustrated by Figures 14 and 16, the ion sorting or choice of the desired mass ion to be collected is made by the diaphragm slits 91 and 105 respectively. The desired beam may be brought to traverse the slit by changing either the accelerating potential in the ion-source, or the strength of the magnetic field, or the position of the sorting slit. The ability to sort the ions by simply moving the slit 91 or 105 without moving either the source or collector is peculiar to the instruments of Figures 14 and 16 and is of great advantage. It is difficult to vary the magnetic field and still maintain its exact form. It is also difficult to apply a series of accelerating voltages to the ion-source without causing distortion which changes the angular spread of the beam and also without introducing electrical interference in associated apparatus. By the use of our invention the sorting may be done by placing mechanically controlled shutters on one or more sorting slits such as 91 and 105 of instruments Figures 14 and 16. This makes it possible to measure all ions in beams which fall within any desired momentum range by widening the slits 91 and 105. It is also possible to select two distinct momentum ranges and measure the total number of ions in either one in sequence or in both at once. By placing a series of mechanically controlled shutters on the diaphragm 92 (Figure 14) or on the diaphragm 106 (Figure 16) it is possible to obtain a sequence of signals on the collector of any desired frequency or order of succession. The ability to obtain such a sequence by mechanical operations only is of great value in analytical application of the mass spectrometer.

While we have diagrammatically shown the instrument with a gas inlet, our invention is not restricted to the examination of gaseous materials. The invention encompasses all types of mass spectrometers, including those in which the material to be studied may be volatilized in the ion source itself, for instance by means of a furnace.

We have described our invention as applied to focusing of ion beams but the invention includes also similar application to other charged particles such as electrons, positrons, etc.

The method of obtaining the uniformly directed non-homogeneous magnetic field employed in our invention is further not to be restricted to the type of pole pieces shown in Figures 3 and 4 but these are for illustration only. Any known method of obtaining a magnetic field of the desired form may be used, including permanent magnets or current-carrying coils having non-ferrous cores.

The term "uniform," as applied to a magnetic field, is herein meant to imply uniformity in direction, while the term "homogeneous" is meant to imply homogeneity in intensity. Inasmuch as a magnetic field is a vector quantity, both direction and magnitude characteristics are specified. The magnetic fields utilized by our invention are described as uniform in direction and by this is meant uniformity within practical limitations. We have defined the magnetic field intensity perpendicular to the plane MM' (Fig. 4) and for purposes of clarity have illustrated in the plane MM' the trajectories of orbits used, but this is not to be construed as a limitation. Extension of the apparatus so as to have practical thickness above and below the plane MM' with maintenance of the appropriate parameters within practical limitations is to be included in the scope of our invention. We have furthermore herein referred to planar orbits but this also is not to be limited to the strict mathematical interpretation, but is to be interpreted within practical limitations and attainments.

What we claim as our invention is:

1. A mass spectrometer or the like comprising means for producing a region having a substantially uniformly directed magnetic field whose intensity varies in a manner to impart to a moving charged particle therein an open orbit having spatial periodicity, a source of moving charged particles, a collector of charged particles and a perforated diaphragm, said source and said collector being located in said field at successive points of maximum field strength along a spatially periodic planar open orbit for the desired particles, and said diaphragm being located transverse to the orbit of the charged particles moving between said source and said collector and with its opening positioned on the orbit of the desired particles.

2. A mass spectrometer or the like comprising means for producing a region having a substantially uniformly directed magnetic field whose intensity perpendicular to a normal plane is invariant with one Cartesian coordinate in said plane and varies in a monotonic manner with the other coordinate in said plane, a source of moving charged particles, a collector of charged particles and a perforated diaphragm, said source and said collector being located in said field at successive points of maximum field strength along a spatially periodic planar orbit for the desired particles, and said diaphragm being located transverse to the orbit of the charged particles moving between said source and said collector and with its opening positioned on the orbit of the desired particles.

3. A mass spectrometer or the like comprising means for producing a region having a substantially uniformly directed magnetic field whose intensity perpendicular to a normal plane is invariant with one Cartesian coordinate in said plane and varies linearly with the other coordinate in said plane, a source of moving charged particles, a collector of charged particles and a perforated diaphragm, said source and said

collector being located in said field at successive points of maximum field strength along a spatially periodic planar orbit for the desired particles, and said diaphragm being located transverse to the orbit of the charged particles moving between said source and said collector and with its opening positioned on the orbit of the desired particles.

4. A mass spectrometer or the like comprising means for producing a region having a substantially uniformly directed magnetic field whose intensity perpendicular to a normal plane is invariant with one Cartesian coordinate in said plane and varies exponentially with the other coordinate in said plane, a source of moving charged particles, a collector of charged particles and a perforated diaphragm, said source and said collector being located in said field at successive points of maximum field strength along a spatially periodic planar orbit for the desired particles, and said diaphragm being located transverse to the orbit of the charged particles moving between said source and said collector and with its opening positioned on the orbit of the desired particles.

5. A mass spectrometer or the like comprising means for producing a region having a substantially uniformly directed magnetic field whose intensity perpendicular to a normal plane decreases monotonically with the radial distance from an axis of symmetry, a source of moving charged particles, a collector of charged particles, and a perforated diaphragm, said source and said collector being located in said field at successive points of maximum field strength along a planar orbit which for the desired particles is spatially periodic with respect to polar coordinates, and said diaphragm being located transverse to the orbit of the charged particles moving between said source and said collector and with its opening positioned on the orbit of the desired particles.

6. A mass spectrometer or the like comprising means for producing a region having a substantially uniformly directed magnetic field which varies spatially in a monotonic manner, a source of substantially uniformly directed charged particles, a collector of charged particles and a perforated diaphragm, said source projecting charged particles into said field in the direction of maximum positive field strength gradient, said collector facing in the direction of maximum positive field strength gradient and laterally displaced from said source by the amount of lateral orbital deflection undergone by the charged particles from said source, and said diaphragm being located transverse to the orbit of the charged particles moving between said source and said collector and with its opening positioned on the orbit of particles to be collected.

7. A mass spectrometer or the like comprising means for producing a region having a substantially uniformly directed magnetic field whose intensity perpendicular to a normal plane is invariant with one Cartesian coordinate in said plane and varies in a monotonic manner with the other coordinate in said plane, a source of substantially uniformly directed charged particles, a collector of charged particles and a perforated diaphragm, said source projecting charged particles into said field in the direction of maximum positive field strength gradient, said collector facing in the direction of maximum positive field strength gradient and laterally displaced from said source by the amount of lateral orbital

deflection undergone by the charged particles from said source, and said diaphragm being located transverse to the orbit of the charged particles moving between said source and said collector and with its opening positioned on the orbit of particles to be collected.

8. A mass spectrometer or the like comprising means for producing a region having a substantially uniformly directed magnetic field whose intensity perpendicular to a normal plane is invariant with one Cartesian coordinate in said plane and varies exponentially with the other coordinate in said plane, a source of substantially uniformly directed charged particles, a collector of charged particles and a perforated diaphragm, said source projecting charged particles into said field in the direction of maximum positive field strength gradient, said collector facing in the direction of maximum positive field strength gradient and laterally displaced from said source by the amount of lateral orbital deflection undergone by the charged particles from said source, and said diaphragm being located transverse to the orbit of the charged particles moving between said source and said collector and with its opening positioned on the orbit of particles to be collected.

9. A mass spectrometer or the like comprising means for producing a region having a substantially uniformly directed magnetic field whose intensity perpendicular to a normal plane decreases monotonically with the radial distance from an axis of symmetry, a source of substantially uniformly directed charged particles, a collector of charged particles and a perforated diaphragm, said source projecting charged particles into said field in the direction of maximum positive field strength gradient, said collector facing in the direction of maximum positive field strength gradient and displaced from said source angularly about said axis of symmetry by the amount of angular orbital deflection undergone by the charged particles from said source, and said diaphragm being located transverse to the orbit of the charged particles moving between said source and said collector and with its opening positioned on the orbit of particles to be collected.

10. A mass spectrometer or the like comprising means for producing a region having a substantially uniformly directed magnetic field which varies spatially in a monotonic manner, a source of substantially uniformly directed charged particles, a collector of charged particles and a diaphragm having a movable opening therein, said source projecting charged particles into said field in the direction of maximum positive field strength gradient, said collector facing in the direction of maximum positive field strength gradient and laterally displaced from said source by the amount of orbital deflection undergone by the charged particles from said source whereby said collector may collect particles of different momenta, and said diaphragm being located transverse to the orbit of the charged particles moving between said source and said collector and with its opening positioned on the orbit of particles of desired momentum and means for adjusting the location of said opening in said diaphragm.

11. A mass spectrometer or the like comprising means for producing a region having a substantially uniformly directed magnetic field whose intensity perpendicular to a normal plane is invariant with one Cartesian coordinate in said

plane and varies in a monotonic manner with the other coordinate in said plane, a source of substantially uniformly directed charged particles, a collector of charged particles and a diaphragm having a movable opening therein, said source projecting charged particles into said field in the direction of maximum positive field strength gradient, said collector facing in the direction of maximum positive field strength gradient and laterally displaced from said source by the amount of orbital deflection undergone by the charged particles from said source whereby said collector may collect particles of different momenta, and said diaphragm being located transverse to the orbit of the charged particles moving between said source and said collector and with its opening positioned on the orbit of particles of desired momentum, and means for adjusting the location of said opening in said diaphragm.

12. A mass spectrometer or the like comprising means for producing a region having a substantially uniformly directed magnetic field whose intensity perpendicular to a normal plane is invariant with one Cartesian coordinate in said plane and varies exponentially with the other coordinate in said plane, a source of substantially uniformly directed charged particles, a collector of charged particles and a diaphragm having a movable opening therein, said source projecting charged particles into said field in the direction of maximum positive field strength gradient, said collector facing in the direction of maximum positive field strength gradient and laterally displaced from said source by the amount of orbital deflection undergone by the charged particles from said source whereby said collector may collect particles of different momenta, and said diaphragm being located transverse to the orbit of the charged particles moving between said source and said collector and with its opening positioned on the orbit of particles of desired momentum and means for adjusting the location of said opening in said diaphragm.

13. A mass spectrometer or the like comprising means for producing a region having a substantially uniformly directed magnetic field whose intensity perpendicular to a normal plane decreases monotonically with the radial distance from an axis of symmetry, a source of substantially uniformly directed charged particles, a collector of charged particles and a diaphragm having a movable opening therein, said source projecting charged particles into said field in a radial direction toward the axis of symmetry, said collector facing said axis of symmetry and displaced from said source angularly about said axis of symmetry by the amount of orbital deflection undergone by the charged particles from said source whereby said collector may collect particles of different momenta, said diaphragm being located transverse to the orbit of the charged particles moving between said source and said collector and with its opening positioned on the orbit of particles of desired momenta, and means for adjusting the location of said opening in said diaphragm.

14. A method of focusing moving charged particles in a mass spectrometer or the like which comprises projecting the moving charged particles in the direction of maximum positive field strength gradient into a substantially uniformly directed magnetic field which varies spatially in a monotonic manner and collecting the parti-

cles at a point common to orbits of charged particles having different momenta.

15. A method of focusing moving charged particles in a mass spectrometer or the like which comprises projecting the moving charged particles in the direction of maximum positive field strength gradient into a substantially uniformly directed magnetic field whose intensity perpendicular to a normal plane is invariant in one Cartesian coordinate in said plane and varies in a monotonic manner with the other coordinate in said plane and collecting the particles at a point common to orbits of charged particles having different momenta.

16. A method of focusing moving charged particles in a mass spectrometer or the like which comprises projecting the moving charged particles in the direction of maximum positive field strength gradient into a substantially uniformly directed magnetic field whose intensity perpendicular to a normal plane is invariant in one Cartesian coordinate in said plane and varies exponentially with the other coordinate in said plane and collecting the particles at a point common to orbits of charged particles having different momenta.

17. A method of focusing moving charged particles in a mass spectrometer or the like which comprises projecting the moving charged particles in the direction of maximum positive field strength gradient into a substantially uniformly directed magnetic field whose intensity perpendicular to a normal plane decreases monotonically with the radial distance from an axis of symmetry and collecting the particles at a point common to orbits of charged particles having different momenta.

18. A method of sorting moving charged particles in a mass spectrometer or the like which comprises projecting the moving charged particles in the direction of maximum positive field strength gradient into a substantially uniformly directed magnetic field which varies spatially in a monotonic manner, collecting the desired particles at a point common to orbits of charged particles having different momenta and obstructing the motion of undesired particles.

19. A method of sorting moving charged particles in a mass spectrometer or the like which comprises projecting the moving charged particles in the direction of maximum positive field strength gradient into a substantially uniformly directed magnetic field whose intensity perpendicular to a normal plane is invariant with one Cartesian coordinate in said plane and varies in a monotonic manner with the other coordinate in said plane, collecting the desired particles at a point common to the orbits of charged particles having different momenta and obstructing the motion of undesired particles.

20. A method of sorting moving charged particles in a mass spectrometer or the like which comprises projecting the moving charged particles in the direction of maximum positive field strength gradient into a substantially uniformly directed magnetic field whose intensity perpendicular to a normal plane is invariant with one Cartesian coordinate in said plane and varies exponentially with the other coordinate in said plane, collecting the desired particles at a point common to the orbits of charged particles having different momenta and obstructing the motion of undesired particles.

21. A method of sorting moving charged particles in a mass spectrometer or the like which

comprises projecting the moving charged particles in the direction of maximum positive field strength gradient into a substantially uniformly directed magnetic field whose intensity perpendicular to a normal plane varies monotonically with the radial distance from an axis of symmetry, collecting the desired particles at a point common to orbits of charged particles having different momenta and obstructing the motion of undesired particles.

22. A method of focusing moving charged particles by means of a magnetic field in a mass spectrometer or the like which comprises generating a substantially uniformly directed magnetic field whose intensity varies in such manner that the charged particles execute trochoid-like open orbits having spatial periodicity, launching the moving charged particles in the field in a direction substantially perpendicular to the field at a point of farthest penetration into the field along the orbit and collecting the particles at a point on the orbit which is an integral spatial period from the source.

23. A method of focusing moving charged particles by means of a magnetic field in a mass spectrometer or the like which comprises generating a substantially uniformly directed magnetic field whose intensity perpendicular to the normal plane is invariant with one Cartesian coordinate in said plane and varies in a monotonic manner with the other coordinate in said plane whereby the charged particles will execute trochoid-like open orbits having spatial periodicity, launching the moving charged particles in the field in a direction substantially perpendicular to the field at a point of farthest penetration into the field along the orbit and collecting the particles at a point on the orbit which is an integral spatial period from the source.

24. A method of focusing moving charged particles by means of a magnetic field in a mass spectrometer or the like which comprises generating a substantially uniformly directed magnetic field whose intensity perpendicular to the normal plane is invariant with one Cartesian coordinate in said plane and varies linearly with the other coordinate in said plane whereby the charged particles will execute trochoid-like open orbits having spatial periodicity, launching the moving charged particles in the field in a direction substantially perpendicular to the field at a point of farthest penetration into the field along the orbit and collecting the particles at a point on the orbit which is an integral spatial period from the source.

25. A method of focusing moving charged particles by means of a magnetic field in a mass spectrometer or the like which comprises generating a substantially uniformly directed magnetic field whose intensity perpendicular to the normal plane is invariant with one Cartesian coordinate in said plane and varies exponentially with the other coordinate in said plane whereby the charged particles will execute trochoid-like open orbits having spatial periodicity, launching the moving charged particles in the field in a direction substantially perpendicular to the field at a point of farthest penetration into the field along the orbit and collecting the particles at a point on the orbit which is an integral spatial period from the source.

26. A method of focusing moving charged particles by means of a magnetic field in a mass spectrometer or the like which comprises generating a substantially uniformly directed mag-

netic field whose intensity perpendicular to a normal plane decreases monotonically with the radial distance from an axis of symmetry whereby the charged particles will execute trochoid-like open orbits which are spatially periodic with respect to polar coordinates, launching the moving charged particles in the field in a direction substantially perpendicular to the field at a point of farthest penetration into the field along the orbit and collecting the particles at a point on the orbit which is an integral spatial period from the source.

NORMAN D. COGGESHALL.
MORRIS MUSKAT.

REFERENCES CITED

The following references are of record in the file of this patent:

UNITED STATES PATENTS

Number	Name	Date
2,221,467	Bleakney -----	Nov. 12, 1940
5 2,297,305	Kerst -----	Sept. 29, 1942

OTHER REFERENCES

Tech. pub. entitled Positive-ray analysis of potassium, calcium and zinc, by A. J. Dempster, in Physical Review, 2d series, vol. 20, 1922, pages 631-638.

Tech. pub. entitled The mass-spectrograph and its uses, by Walter Bleakney, in American Physics Teacher, Feb. 1936, vol. 4, pp. 12-23.

15 Tech. pub. entitled Mass spectrum analysis, in Physical Review, Aug. 15, 1936, vol. 50, pages 282-296.

Ultraviolet Absorption Analysis for Naphthalenes

NORMAN D. COGGESHALL AND ALVIN S. GLESSNER, JR.
Gulf Research & Development Company, Pittsburgh, Pa.

Reprinted from
ANALYTICAL CHEMISTRY
Vol. 21, Page 550, May 1949

Reprinted from ANALYTICAL CHEMISTRY, Volume 21, Page 550, May 1949
Copyright 1949 by the American Chemical Society and reprinted by permission of the copyright owner

Ultraviolet Absorption Analysis for Naphthalenes

NORMAN D. COGGESHALL AND ALVIN S. GLESSNER, JR.
Gulf Research & Development Company, Pittsburgh, Pa.

THE present report describes analytical methods based on ultraviolet absorption spectra, developed for the determination of naphthalene, α -methylnaphthalene, and β -methylnaphthalene in hydrocarbon mixtures boiling in the kerosene range. Despite the rather close similarity and proximity of the absorption bands of these compounds, it has been found practical to utilize them for quantitative analysis work. Such a method is feasible because of the nature of the ultraviolet absorption of the other types of compounds found in such samples. The semiempirical theory of electronic oscillations ($2,3$), together with the rather wide range of data now available for various classes of hydrocarbons, allows a reliable prediction to be made of the ultraviolet absorption of definite classes of hydrocarbons in the different spectral regions.

Paraffins, naphthenes, mono-olefins, and nonconjugated diolefins are known to possess no appreciable absorption at wave lengths longer than $200\text{ m}\mu$ (3). The onset of absorption for conjugated diolefins is near $230\text{ m}\mu$ and is continuous for shorter wave lengths. Alkyl benzenes and polycyclic aromatics possessing only one benzene ring—Tetralin, for example—have strong absorption in the characteristic benzene ring region, 250 to $280\text{ m}\mu$. Mononuclear aromatics with unsaturated side chains—styrene, for example—may possess additional bands around $290\text{ m}\mu$ if the benzene ring and an olefin group are conjugated. For all these classes, the intensity of absorption is generally decreasing very rapidly with increasing wave lengths in the vicinity of $300\text{ m}\mu$. Thus they may contribute relatively little to the absorption in the region of the characteristic naphthalene

A method, based on the ultraviolet absorption of the naphthalenes, is described for the analysis of hydrocarbon mixtures boiling in the kerosene range for naphthalene, α -methylnaphthalene, and β -methylnaphthalene. For the lower boiling cuts a method of analyzing for naphthalene alone is described. This utilizes a system of correcting for the background absorption due to other unsaturated compounds present. For the higher boiling cuts containing all three naphthalenes the method is based on data taken at three separate wave lengths. The accuracy obtainable under routine conditions is satisfactory; the average errors are less than 0.3% of total sample. For proper utilization the cuts must be made between definite temperature limits. Results of accuracy tests and tests made on synthetic samples are given.

bands, 300 to 330 $m\mu$. Certain polycyclic compounds such as acenaphthene and fluorene possess appreciable absorption in this region but fortunately have boiling points outside the range of the samples considered here.

The method is a straightforward one based on Beer's law of absorption given in Equations 1 and 2:

$$I = I_0 \times 10^{-ac} \quad (1)$$

$$D = \log (I_0/I) = ac \quad (2)$$

where a is a constant depending upon the absorbing material, the wave length at which data are being taken, and the thickness of the cell; and c is the concentration of the absorbing material in the cell. a is known as the calibration coefficient. When several absorbing compounds are present in the sample, all of which obey Beer's law, it is known that the resulting optical density is linearly dependent on each (1)

$$D = a_1c_1 + a_2c_2 + a_3c_3 \quad (3)$$

where a_1 is the calibration coefficient for the first compound, c_1 is the concentration of the first compound, etc. This allows different wave lengths to be used when several different components are being sought; the individual concentrations are then obtained as solutions of simultaneous equations of the type illustrated by Equation 3.

EXPERIMENTAL DETAILS

The instrument used throughout was the quartz spectrophotometer equipped for ultraviolet work as manufactured by the National Technical Laboratories, South Pasadena, Calif. The naphthalene and β -methylnaphthalene were obtained from Eastman Kodak Company and the α -methylnaphthalene was obtained from J. E. Nickels of Mellon Institute. The solvent used throughout was iso-octane (2,2,4-trimethylpentane) obtained from Rohm & Haas Company, Philadelphia, Pa. All dilutions in both the calibration and analytical work were by weight, using an analytical balance. Glass-stoppered bottles were used throughout. Between uses both bottles and stoppers were thoroughly washed in a Drene solution and given a subsequent oven drying.

In some cases the solutions containing the calibration and unknown samples were given an alkaline permanganate treatment to remove olefinic mate-

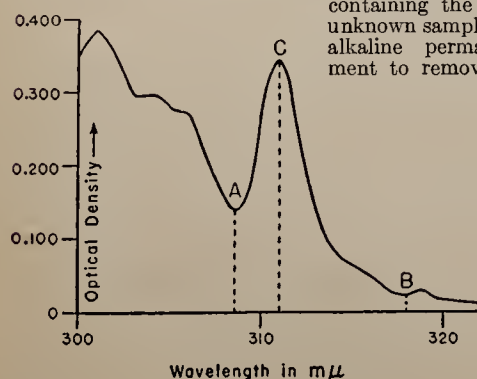


Figure 1. Ultraviolet Absorption Spectrum of Naphthalene

rials. This treatment is widely used for the treatment of samples prior to an ultraviolet analysis for the C_8 and lighter aromatics. It consists of agitating the solution of sample in iso-octane in a strong aqueous solution of potassium permanganate and potassium hydroxide for some 10 to 20 minutes at room temperature.

NAPHTHALENE ANALYSIS

It is often desired to determine the naphthalene content of hydrocarbon fractions that have boiling point ranges sufficiently below those of the α - and β -methylnaphthalenes that they do not contain these latter compounds in appreciable quantities. Low concentrations of the latter may be appraised from the appearance of the absorption bands. On the other hand, kerosene fractions having low initial boiling points may include high percentages of mononuclear aromatics. Although the region of principal absorption of this latter class of compounds is around 260 $m\mu$, they may produce an appreciable background absorption in the 300- to 320- $m\mu$ range due to their heavy concentrations. A method of correcting for this must therefore be used.

In Figure 1 may be seen the absorption spectrum for naphthalene in the 300- to 320- $m\mu$ region. The wave length designated as C , where naphthalene possesses a maximum of absorption, is chosen for the calculation of the naphthalene concentration. In a sample containing a heavy concentration of compounds that give rise to background absorption in this region, the appearance of the curve will be altered. The left-hand portion will generally be elevated relative to the right-hand portion as the absorption of the interfering materials will be decreasing with increasing wave length. To achieve a background correction wave lengths A and B were chosen to be used with C .

Method of Correction. For pure naphthalene, the following ratios were determined:

$$R_1 = D_c/D_a \text{ and } R_2 = D_c/D_b$$

where D_a , D_c , and D_b are the optical densities at wave lengths A , C , and B , which are 308.5, 311, and 318 $m\mu$, respectively. The corresponding optical densities, $D_{a,s}$, $D_{c,s}$, and $D_{b,s}$, are then determined for the sample. Assuming an average correction, d_1 , to apply between the 308.5- and 311- $m\mu$ points and d_2 to apply between the 311- and 318- $m\mu$ points, we may solve for these quantities by means of the following equations:

$$R_1 = (D_{c,s} - d_1)/(D_{a,s} - d_1) \quad (4)$$

$$R_2 = (D_{c,s} - d_2)/(D_{b,s} - d_2) \quad (5)$$

Next a mean value between d_1 and d_2 , which is designated as d , is determined. This is used for wave length C . The true optical density at C , due to the naphthalene alone, is then $(D_{c,s} - d)$. To obtain the weight percentage of naphthalene in the solution, C_1 , we merely use

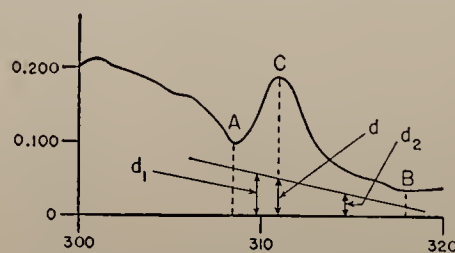


Figure 2. Ultraviolet Absorption Spectrum of Naphthalene
Sample possesses large background correction near 310 $m\mu$

Table I. Comparison between Known and Analyzed Concentrations of Naphthalenes in Synthetic Samples

Sample No.	Known % of Naphthalene	Calculated % of Naphthalene	% Difference
1	8.28	8.07	-0.21
2	6.16	6.05	-0.11
3	3.22	3.33	0.11
4	2.40	2.33	-0.07
5	3.27	3.30	0.03
6	1.02	1.03	0.01
Average error = 0.09%			

Table II. Comparisons between Known Increases of Naphthalene Concentrations in an Actual Sample and Calculated Increases

Sample No.	Increased % of Naphthalene	Calculated Increase of Naphthalene, %	% Difference
1	0.81	0.77	-0.04
2	1.92	1.90	-0.02
3	3.24	3.25	0.01
4	4.31	4.26	-0.05
5	5.26	5.32	0.06
6	6.80	6.53	-0.27
Average error = 0.08%			

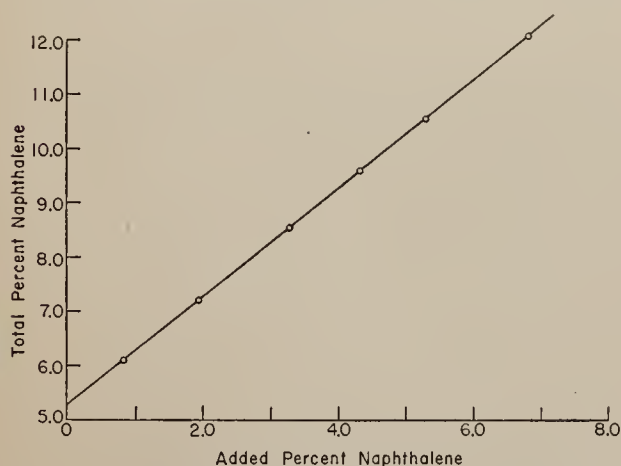


Figure 3. Observed, Total Naphthalene Concentration in Sample

Plotted against known amounts of naphthalene added to sample

$$C_1 = (D_{c.s} - d)/a_1 \quad (6)$$

where a_1 is the calibration coefficient for naphthalene at wave length C determined by using the pure material. In Figure 2 may be seen a schematic plot of the data for an actual unknown sample. This illustrates the general relationship of d_1 , d_2 , and d .

To test the effectiveness and accuracy of this method, three types of tests were made: Synthetic samples containing large amounts of interfering compounds were analyzed, known amounts of naphthalene were added to submitted samples possessing appreciable background corrections with subsequent re-examinations, and an extrapolation procedure was used. In Table I may be seen the results obtained when synthetic samples were prepared. These samples were made to contain varying amounts of interfering compounds (up to 30% by volume) and were analyzed by the above procedure. The average error in terms of total sample is only 0.09%.

Further tests of the accuracy were made by adding known amounts of naphthalene to actual submitted samples which were then re-examined. If the calculated naphthalene concentrations in the original unknown samples were in error because of improper corrections for background, the calculated increase in concentration would also be expected to be in error. The agreement between added and calculated naphthalene concentrations seen in Table II gives further assurance as to the effectiveness of the method. The average error is of the same order of magnitude as given in Table I.

A further test of the method is to make such a series of increases of naphthalene concentrations to a single sample, plot total observed naphthalene concentration against added concentration, and extrapolate back to zero added material. If the method is correct, the extrapolated concentration should be close to the concentration observed for the original material. This has been found true for all samples thus tested. In Figure 3 may be seen a plot for such an example. Here are plotted the observed, total naphthalene concentrations against the known, added concentrations. The extrapolation of the curve to zero added material yields 5.25% naphthalene for the original sample. The analysis of the original sample, using wave lengths A , B , and C by the procedure described above, yields a naphthalene concentration of 5.28%. This agreement for the naphthalene concentration obtained by the two procedures adds further validity to the methods used on routine samples.

A routine analysis of a submitted sample may be carried out in about 1 hour, including the necessary time for dilutions and calculations. The complete spectrum between 300 and 320 $m\mu$ is always obtained and inspected to determine whether either of the monomethylnaphthalenes is present. They may be detected by the resultant alteration in the shape of the spectrum. When the sample is given an alkaline permanganate treatment to remove some of the interfering compounds, the naphthalene concentrations are always the same as the untreated sample to within a few hundredths per cent. Tests have shown that this treatment leaves the naphthalene concentration essentially unchanged.

Of the many unknown samples examined, the background correction was frequently low. It could actually have been neglected in some cases with a maximum resultant error of only a few tenths per cent (based on total sample) of naphthalene. However, for the most reliable accuracy it should be corrected for in all cases.

Two alternative methods of calculating the background correction, d , were tested.

In one of these a correction, d , was assumed for wave length C , a correction, $d + \Delta d$, was assumed for wave length A , and a correction, $d - \Delta d$, was assumed for wave length B . Using equations similar to 4 and 5 it is possible to eliminate Δd and to solve for d in terms of R_1 , R_2 , $D_{a.s.}$, $D_{c.s.}$, and $D_{b.s.}$. In the other method it was assumed that the change of background optical density is linear through this region. Then with the assumption of a correction, d , for wave length C , the correction for wave length A would be $d + 2.5\Delta d$ and the correction for B would be $d - 7\Delta d$ where Δd is now the change in background optical density per $m\mu$. Using similar equations a solution for d may also be obtained in terms of the above quantities.

Neither of these two methods gave as good agreement for the synthetic samples as the one used and both were more involved in application.

ANALYSIS FOR NAPHTHALENE, α -METHYLNAPHTHALENE, AND β -METHYLNAPHTHALENE

When the absorption spectra for naphthalene, α -methylnaphthalene, and β -methylnaphthalene are viewed individually they are seen to possess some close similarities which at first would seem to rule out the possibility of a simultaneous analysis. However, when they are plotted together as in Figure 4, there are enough distinct differences to allow such an analysis. The absorption peaks chosen for analysis are those designated by arrows in the figure and they lie at 311, 314, and 319 $m\mu$. They are representative of naphthalene, α -methylnaphthalene, and β -methylnaphthalene, respectively. The α -methylnaphthalene used for the data of Figure 4 was not so pure as that used for calibration and shows a small concentration of β -methylnaphthalene.

If we designate by D_1 , D_2 , and D_3 the observed optical densities at wave lengths 311, 314, and 319 $m\mu$, respectively, and let C_1 , C_2 , and C_3 represent the weight percentages of naphthalene, α -meth-

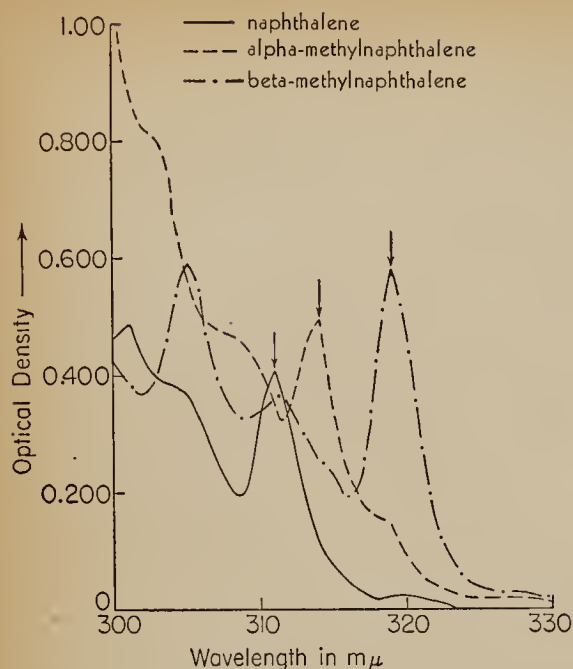


Figure 4. Ultraviolet Absorption Spectra

Arrows indicate wave lengths used for analysis

ynaphthalene, and β -methylnaphthalene in the solution as examined, we have:

$$\begin{aligned} D_1 &= 1.338 C_1 + 1.138 C_2 + 1.326 C_3 \\ D_2 &= 0.335 C_1 + 1.580 C_2 + 0.990 C_3 \\ D_3 &= 0.107 C_1 + 0.446 C_2 + 2.152 C_3 \end{aligned} \quad (6)$$

where the calibration coefficients obtained with the pure compounds have been used. These calibration coefficients are unique to the absorption cells and slit widths used and are representative of concentrations expressed in grams per kilogram of solution in the absorption cells. For optimum accuracy in an absorption spectroscopic method, it is important that the optical density at each wave length be dominated by one compound and that each compound be represented by such a wave length. These conditions are not exactly fulfilled in Equations 6. The largest coefficient for D_1 comes from naphthalene, the largest for D_2 comes from α -methylnaphthalene, and the largest for D_3 comes from β -methylnaphthalene. However, the calibration coefficient for β -methylnaphthalene at 311 $m\mu$ is almost as large as that for naphthalene. Although this is a departure from the ideal conditions suitable for best accuracy, the equations can be solved with very satisfactory results.

In the simultaneous analysis for the three naphthalenes no correction was made for background, for several reasons. In the work on samples containing only naphthalene and using the method of the previous section the background correction was often small enough to be neglected with relatively small error. In the samples containing naphthalene plus the α and β isomers, the total naphthalene was generally high, making the errors caused by neglecting the background small. The distillation cuts were sharper; this actually eliminated many of the lower boiling point materials that contribute to the background. Those that remained were in some cases eliminated by the alkaline permanganate treatment. A consideration of the source of the samples also indicated that few if any interfering compounds would be present.

In Table III may be seen the results of analyses of a series of synthetic samples of mixtures containing up to about 30% naphthalenes by weight. As the accuracy is in general less than that for the analysis for naphthalene alone, the concentrations are reported only to the nearest 0.1%. The same degree of absolute accuracy is obtainable for higher concentrations.

An application of the analysis may be seen in Table IV, which gives the calculated concentrations for several of a series of sharp distillation cuts from an aromatic-rich hydrocarbon sample. When such a series is analyzed, the various naphthalene concentrations are readily obtained and a complete naphthalene analysis for the material boiling below about 248° C. is possible. Cuts boiling in this region and above cannot in general be accurately analyzed because of the presence of interfering compounds of higher boiling points. The time per analysis is about 1.25 hours. This includes the dilutions, reading the data, making the calculations, and plotting the curves. The spectra through the naphthalene range are plotted for all samples, to determine the presence of any possible interfering compounds.

In addition to the tests of the analysis displayed by the results on the synthetic samples, material balance calculations have been carried out for several complete distillation and concentration processes. For the necessary data the initial material, the intermediate products, and the final products were all analyzed for the three naphthalenes. The results were combined with the yield data for the process in the material balance calculations. The results were consistent to a few tenths per cent of total sample.

Table III. Comparison between Known and Calculated Concentrations for Naphthalene, α -Methylnaphthalene, and β -Methylnaphthalene in Synthetic Samples

Compound	Known, %	Calculated, %	% Error
Naphthalene	4.7	4.7	0.0
α -Methylnaphthalene	9.5	9.5	0.0
β -Methylnaphthalene	2.4	2.3	-0.1
Naphthalene	0.6	0.6	0.0
α -Methylnaphthalene	4.0	4.0	0.0
β -Methylnaphthalene	7.4	7.3	-0.1
Naphthalene	1.4	1.0	-0.4
α -Methylnaphthalene	24.0	24.0	0.0
β -Methylnaphthalene	2.8	2.6	-0.2
Naphthalene	6.2	6.0	-0.2
α -Methylnaphthalene	4.7	4.5	-0.2
β -Methylnaphthalene	10.7	10.4	-0.3
Naphthalene	5.7	6.1	0.4
α -Methylnaphthalene	0.0	0.0	0.0
β -Methylnaphthalene	10.0	9.6	-0.4
Naphthalene	3.6	3.9	0.3
α -Methylnaphthalene	3.9	3.9	0.0
β -Methylnaphthalene	4.4	4.3	-0.1
Average error = 0.2%			

Table IV. Naphthalenes in Distillation Cuts from an Aromatic-Rich Hydrocarbon Sample

Boiling Point Range, ° C.	Naphthalene, %	α -Methylnaphthalene, %	β -Methylnaphthalene, %
210-215	9.4	0.0	0.0
215-220	17.1	0.0	0.0
220-225	18.2	0.0	0.0
225-230	8.2	0.3	2.1
230-235	0.3	0.9	8.9
235-240	0.0	4.2	27.3
240-245	0.0	13.5	45.0

ACKNOWLEDGMENTS

The authors wish to express their gratitude to James Harrison for supplying the data on the concentration processes and the material balance calculations, to J. E. Nickels of the Mellon Institute for supplying the pure α -methylnaphthalene, and to Paul D. Foote, executive vice president of Gulf Research & Development Company, for permission to publish this material.

LITERATURE CITED

- (1) Brattain, R., Rassmussen, R. S., and Cravath, A. M., *J. Applied Phys.*, **14**, 418 (1943).
- (2) Brode, W. R., "Chemical Spectroscopy," Chap. VIII, New York. John Wiley & Sons, 1943.
- (3) Lewis, G. N., and Calvin, M., *Chem. Revs.*, **25**, 273 (1939).

RECEIVED June 9, 1948.

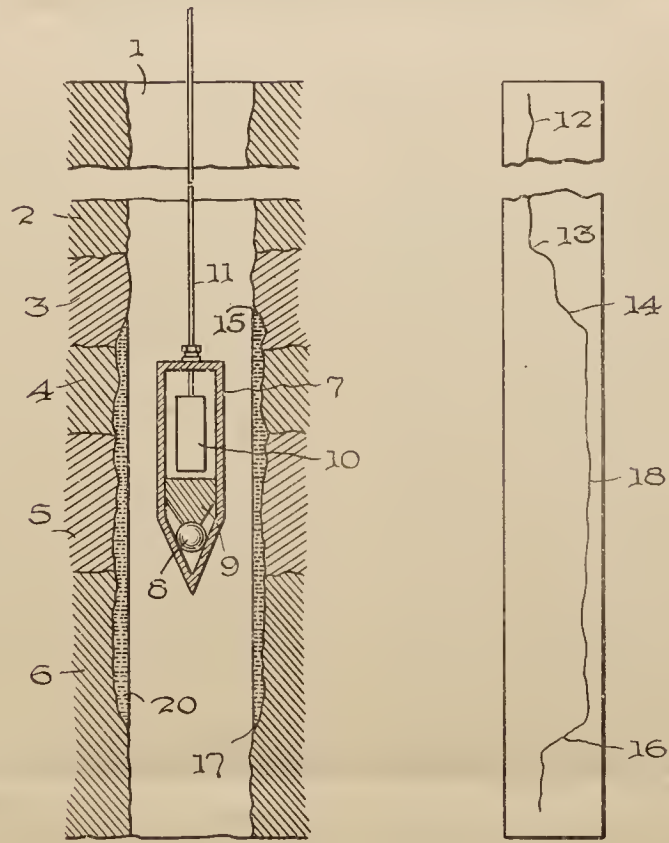
Oct. 11, 1949.

M. MUSKAT ET AL
METHOD OF DETECTING MUD FILMS
ON EXPOSED ROCK STRATA
Filed Jan. 11, 1945

2,484,422

Fig. 1.

Fig. 2.



Inventors
MORRIS MUSKAT
NORMAN D. COGGESHALL

By *G. M. Houghton*
his Attorney

UNITED STATES PATENT OFFICE

2,484,422

METHOD OF DETECTING MUD FILMS ON
EXPOSED ROCK STRATA

Morris Muskat, Oakmont, and Norman D. Coggeshall, O'Hara Township, Allegheny County, Pa., assignors to Gulf Research & Development Company, Pittsburgh, Pa., a corporation of Delaware

Application January 11, 1945, Serial No. 572,304

4 Claims. (Cl. 250—83.6)

1

This invention concerns a method of detecting the presence of mud films on the walls of a borehole.

One of the most important problems involved in well completions is the removal of the mud film from the exposed faces of producing formations. This mud film, also called mud cake or filter cake, is formed during the course of drilling through the use of mud laden drilling fluids. When the well is put on production, the presence of the mud cake interferes with the flow of oil from the formation into the well. Washing the face of the rock strata is very effective in removing the mud cake in many cases. Chemical cleaners and abrasive methods have also been used to remove mud film. However, in spite of these procedures, the mud film often remains attached to the rock strata. Evidence for this is the fact that the productivity of the well when it is put on production test is often considerably less than that predicted from the permeability analysis of cores taken from the producing formation.

In attempting to remove the mud cake it is sometimes difficult to determine to what extent the mud has been removed. Due to porosity of formations, plastering properties of the mud, and chemical reactions which may take place between connate waters and the mud, it is often found that a hard, thick mud cake has resulted and which is not easily removed. It has been proposed (in U. S. Patent No. 2,339,129) to add radioactive materials to the mud flush before it is used in the drilling operation. The presence of the mud film may then be detected by the gamma ray activity of the radioactive material contained in the mud. Ordinary radioactive minerals, when used for this purpose, seriously interfere with subsequent gamma ray logs made in the well for formation correlation purposes. Artificially radioactivated materials may be used but these have the disadvantage of losing their activation so that they cannot be detected very long after the mud cake has formed and drilling has passed a given level in the well. Furthermore, the preparation of these artificial radioactive materials is one requiring additional equipment and when activated these materials are a danger to personnel handling them and to the personnel engaged in drilling the well.

2

This invention consists in adding to the mud a material which may be activated in the mud cake should any such mud cake remain in place after cleaning operations have been attempted. The method of activation is by bombardment with neutrons and detection is by means of a gamma ray detector, the combination of these two steps being generally known as neutron logging.

It is a primary object of this invention to provide a simple, inexpensive and convenient method of locating any mud film remaining on a formation adjacent to a borehole.

Another object is to provide a method of locating mud film which may be applied to the well at any time.

Another object is to provide a method of locating mud film by the application of neutron logging.

Another object is to determine the thickness of mud cakes formed during the drilling of wells.

Details of the invention and the manner in which these objects are accomplished will be more fully understood by reference to the accompanying drawings in which:

Fig. 1 represents a cross-section of a borehole and apparatus for practicing the invention;

Fig. 2 shows a neutron log curve obtained when using this invention.

Methods and apparatus for neutron logging of wells have been proposed in the literature and in several U. S. patents. These methods generally expose the formations to a bombardment by neutrons and recording either the scattered or reflected neutrons or the gamma rays emitted by the excited nuclei. Certain elements are particularly effective for neutron log identification because of the nature of their nuclear structure. The gamma ray activity is commonly induced in aluminum, chlorine and arsenic by neutron bombardment.

Referring to Fig. 1, numeral 1 indicates a borehole passing through earth formations 2, 3, 4, 5, and 6. Equipment for drilling the well and pumping the mud used in the drilling operation are not shown since they do not constitute a part of this invention. Suspended inside the casing is a neutron logging apparatus contained in outer casing 7. This apparatus contains a source of neutrons 8 which may be a mixture of radium and beryllium. Directly above it is a shield 9 which is

composed of a neutron absorbing material such as cadmium or boron which prevents the neutrons from directly reaching detecting element 10. Device 10 consists of a gamma ray indicator and the necessary apparatus for conveying indication of the gamma ray activity to the surface by means of cable 11. When this apparatus is run into the well the neutrons produced by source 8 easily pass through the casing 7 and into the formations. Upon capture by the nuclei of certain elements such as aluminum, chlorine or arsenic, gamma rays are produced which radiate back through the casing into the borehole and are detected by unit 10. Indications of the intensity of the gamma radiation is conducted over cable 11 to the surface where it is recorded by known devices.

In drilling the well the drilling fluid is weighted with a mud whose purpose is to control pressures encountered in the formations, hold the formation face in place to keep it from falling into the hole, and to prevent interchange of fluids. This mud film or mud cake is indicated in Fig. 1 by numeral 20.

In this invention a method is provided for detecting the presence and estimating the amount of mud cake plastered on the walls of the borehole. If the mud film is to be removed the method will serve as an indicator of the effectiveness of such removal and thus serve as a guide for further cleaning processes. In the practice of this invention a material is added to the mud which may be easily activated in the well to gamma ray activity by neutron bombardment. Such materials are aluminum or chlorine or arsenic or compounds of them or mixtures of such compounds. Mud containing these elements in sufficiently large concentration will register as a high value on a neutron log obtained by means of the apparatus of Fig. 1. Each of these elements will give sufficient gamma rays of more than 2 m. e. v. energy when bombarded with neutrons. If the mud already possesses one or more of these agents in sufficient concentration to show up stronger on the neutron log against the effect of the logged strata themselves, no more need be added. An analysis of the composition of the natural mud material and of the type of rock strata anticipated in the drilling will indicate the type of element to be added. Different materials require more or less time to reach an equilibrium value of gamma ray activity in the presence of an inducing neutron radiation. The nature of the adjacent strata and their connate fluids will indicate the choice and amount of material to be added to the mud. Since the concentration of aluminum, chlorine or arsenic in the formations is usually approximately known in advance of drilling, one may add to the mud either a higher concentration of one or more of these same elements or use different ones to distinguish the mud from its surrounding formation.

Fig. 2 shows a neutron log obtained after a well has been drilled using a mud of the type here indicated. Curve 12 shows how the induced gamma ray activity varies down the hole. Assuming that the zero of the chart is on the left-hand edge, it is seen that formation 3 produces a larger effect than formation 2. At the point 15 where the neutrons meet the additive in the mud, a large increase in activity is obtained and is indicated on the log at point 14. This increase to the large value 18 is due to the induced activity of the tracer material which has been added to the mud, and by this increase in gamma ray

activity any residual mud film may be detected. At the point 17 below which the mud cake is absent there is a return to the normal neutron log indication of the formations as indicated by the decrease 16 on Fig. 2.

The compounds of elements aluminum, chlorine or arsenic used may be any of a great variety. Other elements may also be used, it being merely necessary that the element should on neutron bombardment emit gamma rays of sufficiently short wave length to pass through the mud and enter the detecting apparatus. Preferably they are added to the mud in suspension form so that they will remain in the mud and not be leached out by washing operations. Chemical compositions between constituents of the mud and the added aluminum, chlorine or arsenic would in no means interfere with the practice of this invention.

What we claim is:

1. The method of locating the level of mud film on the walls of a borehole which comprises adding to the drilling mud before drilling a tracer constituent in sufficient concentration to produce when bombarded with neutrons an identifiable gamma ray intensity higher than that of the formations to be penetrated, said tracer constituent comprising the chemical element aluminum, bombarding a portion of the wall of the borehole with neutrons, simultaneously measuring at said portion the gamma ray intensity inside the borehole and measuring the depth of said portion of the borehole.

2. The method of locating the level of mud film on the walls of a borehole which comprises adding to the drilling mud before drilling an insoluble tracer constituent in sufficient concentration to produce when bombarded with neutrons an identifiable gamma ray intensity higher than that of the formations to be penetrated, said tracer constituent comprising the chemical element chlorine, bombarding a portion of the wall of the borehole with neutrons, simultaneously measuring at said portion the gamma ray intensity inside the borehole and measuring the depth of said portion of the borehole.

3. The method of locating the level of mud film on the walls of a borehole which comprises adding to the drilling mud before drilling a tracer constituent in sufficient concentration to produce when bombarded with neutrons an identifiable gamma ray intensity higher than that of the formations to be penetrated, said tracer constituent comprising the chemical element arsenic, bombarding a portion of the wall of the borehole with neutrons, simultaneously measuring at said portion the gamma ray intensity inside the borehole and measuring the depth of said portion of the borehole.

4. The method of locating the level of mud film on the walls of a borehole which comprises adding to the drilling fluid before drilling an insoluble tracer constituent in sufficient concentration to produce when bombarded with neutrons an identifiable gamma ray intensity higher than that of the formations to be penetrated, bombarding the wall of the borehole with neutrons at a known level, simultaneously measuring at said level the gamma ray intensity inside the borehole and measuring the depth of said level of measurement.

MORRIS MUSKAT.
NORMAN D. COGGESHALL.

(References on following page)

5

REFERENCES CITED

The following references are of record in the file of this patent:

UNITED STATES PATENTS

Number	Name	Date
2,231,577	Hare -----	Feb. 11, 1941
2,303,688	Fearon -----	Dec. 1, 1942
2,339,129	Albertson -----	Jan. 11, 1944

5

6

Number	Name	Date
2,349,712	Fearon -----	May 23, 1944
2,364,975	Heigl -----	Dec. 12, 1944
2,443,680	Herzog -----	June 22, 1948

OTHER REFERENCES

Livingood and Seaborg, Reviews of Modern Physics, January, 1940, vol. 12, pp. 30-43.

[Reprinted from the Journal of the American Chemical Society, **71**, 3150 (1949).]
Copyright 1949 by the American Chemical Society and reprinted by permission of the copyright owner.

[CONTRIBUTION FROM GULF RESEARCH & DEVELOPMENT COMPANY, PITTSBURGH, PENNSYLVANIA]

Ultraviolet Absorption Study of the Ionization of Substituted Phenols in Ethanol

BY NORMAN D. COGGESHALL AND ALVIN S. GLESSNER, JR.

It is well known that the ultraviolet absorption spectra for the anions or cations of many polar substituted aromatic materials are markedly different from the spectra obtained for the compounds themselves. The spectra of the ions generally exhibit a large bathochromic shift of the absorption ascribed to the phenyl ring chromophore. In addition the intensity of absorption is increased. Since the spectral shift is large, often of the order of 20 m μ or larger, it provides a method whereby dissociation constants may be determined. Ordinarily these cannot be calculated from the spectrophotometric data alone but depend also on separately determined values of *pH* or on previously determined equilibrium constants which are pertinent to the processes involved.

In this manner Stendstrom and co-workers^{1,2} demonstrated that the shift of the phenol spec-

trum induced by the addition of sodium hydroxide is due to the creation of the phenolate ions. From their data they obtained a value of the dissociation constant for phenol. Using the same procedure, Flexser, Hammett and Dingwall³ calculated the ionization constants for benzoic acid, 2,4-dinitrophenol and acetophenone. More recently Ewing and Steck⁴ have utilized this phenomenon in studies of the acidic and basic properties of quinolins and isoquinolins. Similar studies were made of various 4-aminoquinolines by Irvin and Irvin.⁵

The present studies are of the substituted phenols. The substituted phenols may be divided into three classes according to their steric hindrance to inter-molecular hydrogen bonding.⁶ Phenols with the ortho positions either unsubsti-

(3) L. A. Flexser, L. P. Hammett and A. Dingwall, *THIS JOURNAL*, **57**, 2103 (1935).

(4) G. W. Ewing and E. A. Steck, *ibid.*, **68**, 2181 (1946).

(5) J. L. Irvin and E. M. Irvin, *ibid.*, **69**, 1091 (1947).

(6) N. D. Coggeshall, *ibid.*, **69**, 1620 (1947).

(1) W. Stendstrom and M. Reinhard, *J. Phys. Chem.*, **29**, 1477 (1925).

(2) W. Stendstrom and N. Goldsmith, *ibid.*, **30**, 1683 (1926).

tuted or occupied by a small group such as a methyl are known as unhindered phenols. Those with one ortho position occupied by a large group such as a *t*-butyl and the other either unsubstituted or occupied by a small group are known as partially hindered phenols. Those with both ortho positions occupied by large groups are known as the hindered phenols. It is well known that the same type of hindrance that influences intermolecular hydrogen bonding is effective in hindering intermolecular association effects which influence the ultraviolet absorption spectra of the phenols.⁷ The hindered phenols, for example, exhibit quite small spectral changes between examination in paraffin and in polar solvents such as ethanol whereas large changes are observed for the unhindered and partially hindered phenols. The differences have been interpreted as due to the different degrees of proximity possible between the hydroxyl groups of the phenols and the polar groups of the solvent.

In view of the above results it is to be expected that the behavior of the various phenols in a solvent containing a strong base such as sodium hydroxide will vary in accordance with the steric hindrance of the above type. Since the formation of a phenolate ion involves the removal of the hydrogen nucleus from the hydroxyl group any shielding such as offered by large groups on the ortho positions would be expected to be effective in reducing the ionization. It is important to evaluate such effects not only as a method of determining the relative acidity of the various phenols, but also in order to provide information pertinent to a detailed consideration of the ionization processes in the liquid phase. The present report is of a study of the ultraviolet absorption spectra of a series of substituted phenols in ethanol and in ethanol containing sodium hydroxide. The data are interpreted in terms of the influence of steric hindrance on the ionization.

Experimental

All of the absorption spectra were obtained with the use of a Beckman Quartz Spectrophotometer equipped for work in the ultraviolet. In some of the preliminary investigations a study was made of the dependence of spectral changes on temperature. For this the temperature controlled absorption cell compartment previously described⁷ was used. A Precision Scientific Company constant temperature bath was employed to provide the water used to regulate the temperature of this compartment.

With the exception of the simpler ones, the substituted phenols studied were prepared in this Laboratory.^{8,9} There was evidence that each compound used was at least 99% pure. Such other chemicals as were used were the best available commercially and were, when necessary, further

purified by recrystallization. Absolute ethanol was used as the solvent in all cases. Effects due to benzene in the ethanol were eliminated by using the same solvent in the comparison cell as used in the sample cell.

In these studies the ethanol solutions containing hydroxyl ions were prepared by the use of aqueous solutions containing one mole/liter or more of sodium hydroxide or of other bases. Solutions containing other inorganic materials were prepared in the same general manner. In every case the reference cell was filled with the same combination solvent as used for the particular phenol being investigated. In this manner any errors or discrepancies which might have been introduced through impurities in the sodium hydroxide or other inorganic material were avoided.

Data and Discussion

Preliminary Experiments.—In examining the literature on the subject of changes of ultraviolet absorption spectra of polar substituted aromatics induced by addition of specific types of ions in the solvent, it was apparent that sufficient proof that the shifted spectra are due to ionized solute was lacking. It was desirable to obtain further data to verify that this explanation is correct and the effect is not due to intermolecular effects such as hydrogen bonding or the formation of transient complexes between neutral molecules and ions. For that reason a number of experiments were performed on phenols in ethanol containing various inorganic materials. The fact that the present work was done with ethanol as the solvent instead of water, as was the case for most of the previous work, made it further desirable that such experiments be done. This was to verify that the processes were the same for the two solvents.

p-Cresol was examined in solutions containing the bases sodium hydroxide, lithium hydroxide, potassium hydroxide, calcium hydroxide, barium hydroxide, and ammonium hydroxide. The same spectral shift was observed in every case although with differences in degree of ionization. For a concentration of 3×10^{-4} mole/liter of *p*-cresol in solution a concentration of about 12 moles/liter of the weak base ammonium hydroxide was required for complete ionization whereas for lithium, sodium and potassium hydroxides, concentrations of less than one tenth mole/liter were sufficient. These data confirm previous work, but do not rule out the possibilities of complexes being responsible for the shift. Hence to determine if the phenomenon depended specifically upon the addition of hydroxyl ions data were obtained for *p*-cresol in solutions containing sodium chloride and hydrogen chloride. The resulting spectra were virtually indistinguishable from the spectrum obtained with pure ethanol as the solvent. Next a reversal procedure was tested on several phenols. In this the spectra were shifted by the addition of sodium hydroxide and then brought back to that observed

(7) N. D. Coggeshall and E. M. Lang, *ibid.*, **70**, 3283 (1948).

(8) D. R. Stevens, *Ind. Eng. Chem.*, **35**, 655 (1943).

(9) G. H. Stillson, D. W. Sawyer and C. K. Hunt, *THIS JOURNAL*, **67**, 303 (1945).

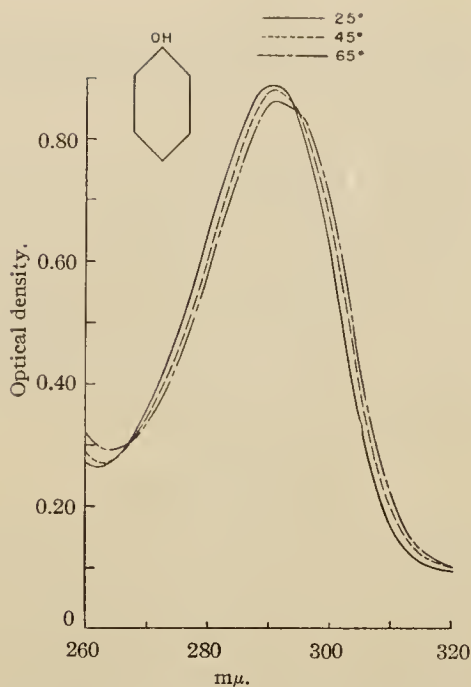


Fig. 1.—Ultraviolet absorption spectra of 2.8×10^{-4} mole/liter of phenol at various temperatures in ethanol containing 1.0×10^{-1} mole/liter of sodium hydroxide.

for pure ethanol solvent by the addition of hydrogen chloride to the same solutions. A complete reversal was achieved for each of the phenols tested, namely, *p*-cresol, 2-methyl-4,6-di-*t*-butylphenol and 2,4,6-tri-*t*-butylphenol.

nol and dioxane in a carbon tetrachloride solution is very strongly reduced by an increase of temperature from 20 to 55°. It would be expected that the energy per intermolecular hydrogen bond or complex between a phenol molecule and an ion would be of the same order of magnitude as for the complexes studied by Errera and Sack. Therefore, if the spectral shift considered here were due to such effects we would get at least a partial reversion to that observed for the ethanol solution when the temperature was elevated. In Fig. 1 may be seen the results for such a test on 2.8×10^{-4} mole/liter of phenol in an ethanol solution containing one-tenth mole/liter of sodium hydroxide. Here the optical density is plotted *versus* wave length. The optical density D is defined by $D = \log I_0/I$, where I_0 and I are the incident and transmitted energies, respectively. It may be seen that the rise in temperature to 65° produces only a very minor change and it is in the opposite direction to that which would be expected if the spectral changes were due to intermolecular effects. The same results were also obtained for 2-methyl-4,6-di-*t*-butylphenol and for 2,6-di-*t*-butyl-4-ethylphenol. The preliminary experiments therefore all definitely confirm the ionization explanation for the spectral shift observed for the phenols.

Unhindered Phenols.—In Fig. 2 may be seen the data for three of the unhindered phenols examined. Here are given the spectra for the materials in pure ethanol and in ethanol containing one-tenth mole/liter of sodium hydroxide. The concentration of absorbing material is about the same in each case being 2.5×10^{-4} mole/liter for the *p*-*t*-butylphenol, 2.0×10^{-4} mole/liter for

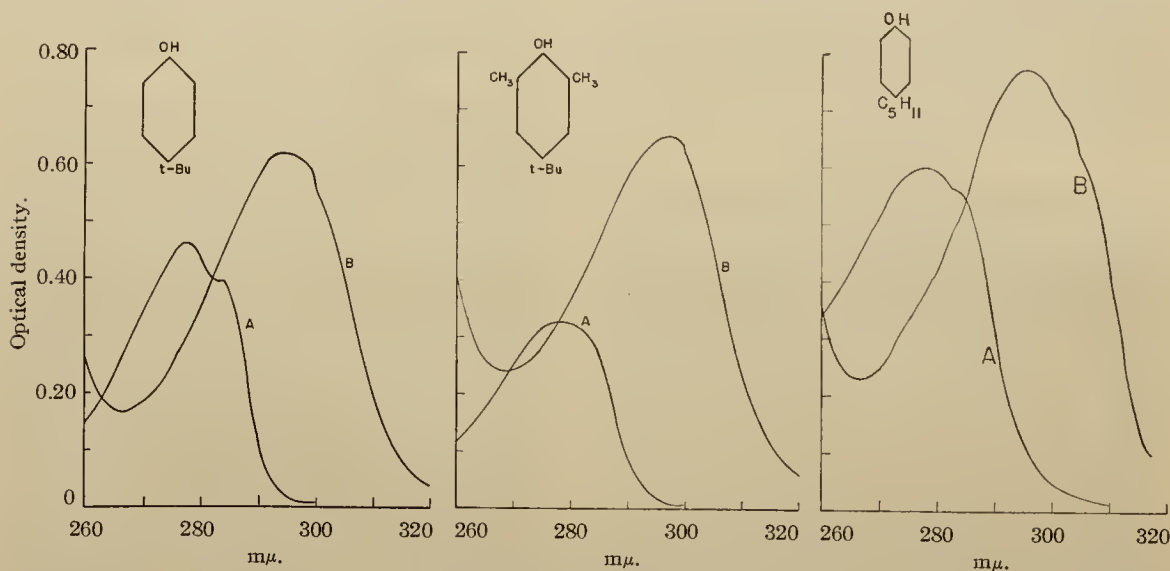


Fig. 2.—Ultraviolet absorption spectra of three unhindered phenols in: A, pure ethanol; B, ethanol containing 1.0×10^{-1} mole/liter of sodium hydroxide.

Errera and Sack¹⁰ have shown that the population of intermolecular complexes between etha-

(10) J. Errera and H. Sack, *Trans. Faraday Soc.*, **34**, 725 (1938).

the 2,6-dimethyl-4-*t*-butylphenol, and 2.0×10^{-4} mole/liter for the *p*-*t*-amylphenol. It is to be noted that in each case there is a complete spectral

shift. By this is meant that the spectra observed for the solutions containing sodium hydroxide show no evidence for any un-ionized phenol molecules, *i. e.*, no maxima at the wave lengths at which the maxima occur for the compounds in pure ethanol solutions.

For solutions containing lower concentrations of sodium hydroxide two absorption maxima are observed, one representing the un-ionized phenol molecules, and one representing the phenolate ions. For the unhindered phenols a sodium hydroxide concentration of less than 1.0×10^{-1} mole/liter is sufficient to produce the complete spectral shift. However, as will be discussed below, the concentrations of sodium hydroxide at which the shifts become apparently complete were not determined as there are difficulties in utilizing these data in a quantitative manner. The sodium hydroxide concentration of 1.0×10^{-1} mole/liter was chosen as a convenient reference for comparison between the different classes of phenols. In Table I may be seen the wave lengths of maximum absorption for the various unhindered phenols in

pure ethanol and in ethanol plus 1.0×10^{-1} mole/liter of sodium hydroxide. The spectral shift $\Delta(1/\lambda)$, calculated from these wave lengths, is also given. As the absorption bands are broad the maxima are only given to the nearest $m\mu$. The values of $\Delta(1/\lambda)$ are therefore only reliable to two significant figures.

Partially Hindered Phenols.—In Fig. 3 may be seen the behavior of three partially hindered phenols. The concentrations were: 1.5×10^{-4} mole/liter of 2-methyl-4,6-di-*t*-butylphenol, 1.7×10^{-4} mole/liter of 2,4-di-*t*-butylphenol, and 2.0×10^{-4} mole/liter of 2-*t*-butyl-4-methylphenol. It is immediately evident that a concentration of 1.0×10^{-1} mole/liter of sodium hydroxide which produced a complete spectral shift for the unhindered phenols, produces only a partial shift in the present cases. This is evident from the fact that the B curves all show maxima representative of the un-ionized material. In each case it is seen that these maxima are shifted to the red as compared to the maxima for the A curves. This is believed to be the result of an actual change in the absorption frequencies of the un-ionized material and of the geometrical superposition of the independent effects of the ionized and un-ionized materials. The latter effect was confirmed in a number of cases by the numerical construction of such intermediate curves. This was done by making suitable combinations of the data for the case of ethanol alone and the data for the 5.0×10^{-1} mole/liter of sodium hydroxide solutions wherein complete shifts were exhibited. The concentration of 5.0×10^{-1} mole/liter was somewhat more than necessary to produce the complete spectral shift, but was chosen as a convenient reference for comparisons between the various classes of phenols. In Table II are the values of the absorption maxima and of the $\Delta(1/\lambda)$'s.

TABLE I
WAVE LENGTHS OF MAXIMUM ABSORPTION FOR UNHINDERED PHENOLS IN ETHANOL AND ETHANOL PLUS SODIUM HYDROXIDE AND $\Delta(1/\lambda)$ VALUES

Compound	λ max. ($m\mu$) (ethanol)	λ max. ($m\mu$) plus NaOH	$\Delta(1/\lambda)$ $cm.^{-1}$
<i>p</i> -Cresol	280	299	2200
<i>p</i> - <i>t</i> -Butylphenol	278	294	2000
<i>p</i> - <i>t</i> -Amylphenol	278	295	2100
<i>m</i> -Cresol	274	291	2100
<i>o</i> -Cresol	274	291	2100
2,6-Di-methyl-4- <i>t</i> -butylphenol	278	297	2300

Average value of $\Delta(1/\lambda) = 2100$

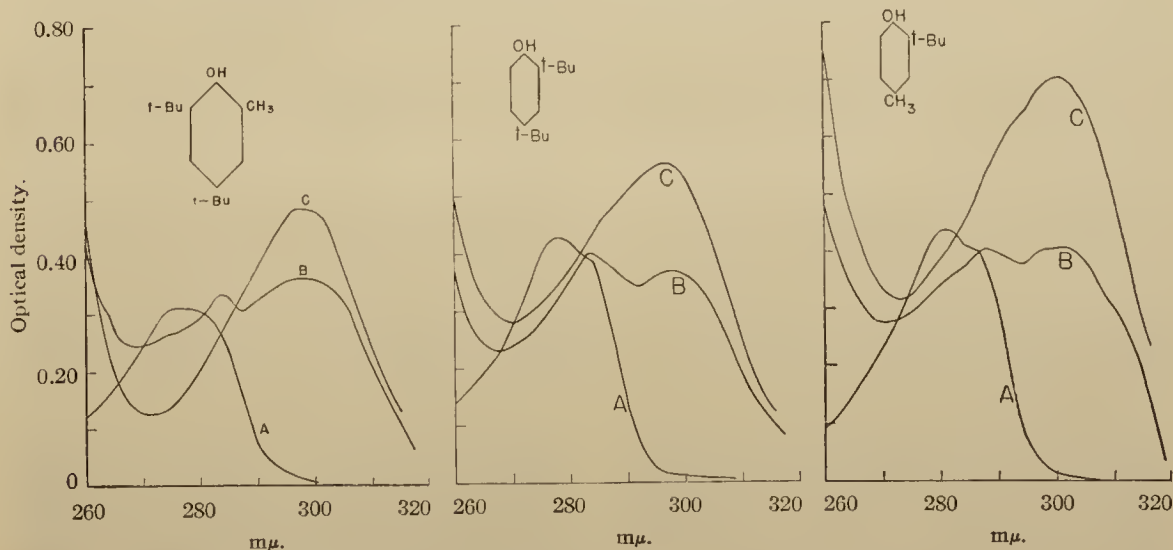


Fig. 3.—Ultraviolet absorption spectra of three partially hindered phenols in: A, pure ethanol; B, ethanol plus 1.0×10^{-1} mole/liter of sodium hydroxide, and C, ethanol plus 5.0×10^{-1} mole/liter of sodium hydroxide.

TABLE II

WAVE LENGTHS OF MAXIMUM ABSORPTION FOR PARTIALLY HINDERED PHENOLS IN ETHANOL AND ETHANOL PLUS SODIUM HYDROXIDE AND $\Delta(1/\lambda)$ VALUES

Compound	λ max. ($m\mu$) (ethanol)	λ max. ($m\mu$) + NaOH	$\Delta(1/\lambda)$ $cm.^{-1}$
2-Methyl-4,6-di- <i>t</i> -butylphenol	277	298	2500
2- <i>t</i> -Butyl-4-methylphenol	281	301	2300
2,4-Di- <i>t</i> -butylphenol	278	297	2300
3-Methyl-6- <i>t</i> -butylphenol	276	294	2200

Average value of $\Delta(1/\lambda) = 2300$

Hindered Phenols.—In Fig. 4 may be seen the data for three hindered phenols. In each case the concentration of the phenol is approximately 1.7×10^{-4} mole/liter. It may be seen that a sodium hydroxide concentration of 1.0×10^{-1} mole/liter produces only minor spectral changes and that a concentration of 5.0×10^{-1} mole/liter which produces a complete shift for the partially hindered phenols is responsible here for only a partial shift. In the D curves are given the spectra for the phenols in the presence of 5.0 mole/liter of sodium hydroxide. Even this concentration does not produce a complete ionization.

TABLE III

WAVE LENGTHS OF MAXIMUM ABSORPTION FOR HINDERED PHENOLS IN ETHANOL AND ETHANOL PLUS SODIUM HYDROXIDE AND $\Delta(1/\lambda)$ VALUES

Compound	λ max. ($m\mu$) (ethanol)	λ max. ($m\mu$) + NaOH	$\Delta(1/\lambda)$ $cm.^{-1}$
2,6-Di- <i>t</i> -butyl-4-methylphenol	277	303	3100
2,6-Di- <i>t</i> -butyl-4-cyclohexylphenol	275	300	3100
2,4,6-Tri- <i>t</i> -butylphenol	275	302	3300
2,6-Di- <i>t</i> -butyl-4-ethylphenol	276	303	3200
2,6-Di- <i>t</i> -butyl-4-phenylphenol	266	302	4500

Average value of $\Delta(1/\lambda) = 3400$

Discussion.—It is obvious from the data given in the figures that great differences exist between the three classes of phenols as regards their ease of ionization in ethanol solution. These differences are ascribed to the steric hindering effects of the large ortho substituents. Although one-tenth mole/liter of sodium hydroxide was sufficient to achieve complete ionization for the unhindered phenols it resulted in only partial ionization of the partially hindered phenols. A sodium hydroxide concentration of 5.0×10^{-1} mole/liter was sufficient to produce complete

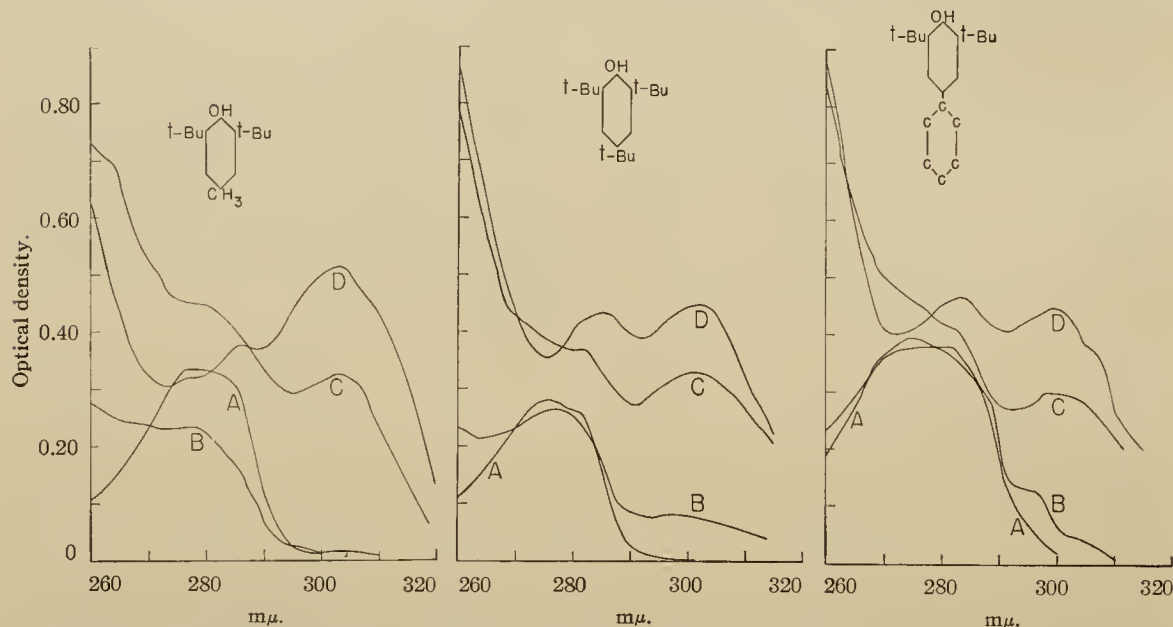


Fig. 4.—Ultraviolet absorption spectra of three hindered phenols in: A, pure ethanol; B, ethanol plus 1.0×10^{-1} mole/liter of sodium hydroxide; C, ethanol plus 5.0×10^{-1} mole/liter of sodium hydroxide, and D, ethanol plus 5.0 mole/liter of sodium hydroxide.

With the dilution scheme used it was impossible to go over about 5.0 mole/liter of sodium hydroxide due to the precipitation of sodium hydroxide. Hence the complete ionization of the unhindered phenols cannot be achieved in this manner. In Table III may be seen the wave lengths of maximum absorption and the $\Delta(1/\lambda)$ values.

ionization for the latter compounds but definitely only produced a partial ionization of the hindered phenols. In addition the hindered phenols were not completely ionized by as much as 5.0 mole/liter of sodium hydroxide. This positively establishes the role of the large ortho groups in hindering the ionization.

There is a very interesting implication in the above data regarding the processes of ionization. The data show that the large groups on the ortho position sterically hinder the ionization. They are large in spatial extension and therefore shield the phenolic hydroxyl group from close approach by other molecules or ions. Since they also hinder the ionization, we may therefore assume that the ionization process is a result of a close approach or collision between a phenolic hydroxyl group and other molecules or ions. With this assumption the primary factors affecting ionization are the details of geometry and electric fields of the molecules and ions involved rather than gross dielectric properties.

It is evident from the data in the tables that there is a further difference between the spectral behavior of the phenols. The difference in frequency of maximum absorption $\Delta(1/\lambda)$ between the molecules and the phenolate ion is in each case expressed in wave numbers. This provides a measure of the differences of transition energies between the ground and first excited electronic states. As was stated above the wave lengths of maximum absorption are only reliable to about 1 μ . Hence the $\Delta(1/\lambda)$ values are reliable to only two significant figures. Despite this limitation it is clear that a definite difference exists between the unhindered and partially hindered phenols. For the former the average value of $\Delta(1/\lambda)$ was 2100 cm^{-1} , whereas it was 2300 cm^{-1} for the latter. This implies that the size of the ortho substituent affects the transition energy for the phenolate ion. This implication is further confirmed by a comparison between the partially hindered and the hindered phenols. The average value of $\Delta(1/\lambda)$ for the latter was 3200 cm^{-1} , excluding a consideration of 2,6-di-*t*-butyl-4-phenylphenol. This compound has an anomalously high $\Delta(1/\lambda)$ value presumably due to some effect of the conjugation of the phenyl rings.

The data then show that the large groups on the ortho positions affect the energy of transition between the ground and the first excited electronic states of the phenolate ions. This may be explained as the result of the energy of polarization of the *t*-butyl groups by the electric fields resulting from the polar resonance forms of the first excited state. This carries a further implication that in the polar resonance forms which contribute the most to the first excited state there is an accumulation of electric charge on the number one position of the phenyl ring. This is necessary since it is the ortho substituents that affect the energy. Such an accumulation of charge would create large fields which would polarize the ortho substituents.

The above results make another tool available for the determination of molecular structure of phenols of unknown composition. Since the behavior of the three classes is different for each, a phenol of unknown composition may be examined under the various conditions and thereby assigned

to one of the classes. Another application has been made to analytical problems. Ordinarily it is impossible to quantitatively analyze a mixture of mononuclear aromatic hydrocarbons and phenols by ultraviolet absorption. This is because the absorption is approximately the same for each class, being due to the phenyl ring chromophore. The addition of sodium hydroxide however results in the ionization of the phenols with the resultant spectral shift. This allows data to be obtained independently for the aromatics and for the phenols. Similar considerations apply to other polar substituted aromatics. If the material in question is basic the addition of an acid will result in ionization and the same type of spectral shift.

Acknowledgment is gratefully made to Dr. Donald R. Stevens and Dr. G. Stillson for furnishing some of the substituted phenols examined. Appreciation is also due Dr. Paul D. Foote, Executive Vice-President of Gulf Research & Development Company, for permission to publish this material.

Summary

A study has been made of the ultraviolet absorption spectra of substituted phenols in ethanol solutions containing sodium hydroxide. Preliminary work was done to verify that the spectral shift which occurs when sodium hydroxide is added is due to the formation of phenolate ions. This comprised tests with different bases, acids and salts; the reversal of the effect by the addition of acid to a basic solution; and a study of the temperature dependence of the spectral shift. The unhindered phenols gave evidence of complete ionization in solutions containing 1.0×10^{-1} mole/liter of sodium hydroxide. The partially hindered phenols were only partially ionized at this concentration of sodium hydroxide, but demonstrated complete ionization for a concentration of 5.0×10^{-1} mole/liter of sodium hydroxide. The hindered phenols were neither completely ionized with the latter concentration of sodium hydroxide nor for the much larger concentration of 5.0 mole/liter. These results demonstrate the great differences in acidity between the different classes of phenols and show that ionization is hindered by the presence of large ortho substituents. This leads to the conclusion that the process of ionization is the result of a collision or of a small distance of approach between the phenolic hydroxyl and other molecules or ions. The difference of energy of transition between the ground and first excited state for the neutral molecule and for the phenolate ion depends upon the type of phenol. An explanation is given which is based on the energy of polarization of the large ortho groups. Applications of the phenomenon to analytical and molecular structure problems are given.

Mass Spectrometer Studies of Thermal Decomposition Products from Hydrocarbons

NORMAN D. COGGESHALL AND NATHAN F. KERR*

Gulf Research & Development Company, Pittsburgh, Pennsylvania

(Received January 14, 1949)

A study, by means of a mass spectrometer, has been made of the thermal decomposition products of hydrocarbons. The materials were pyrolyzed in closed ampoules which were subsequently opened to allow the products to be analyzed. A series of runs were made for cetane, *n*-tetradecane and tetradecene-1 in which the pyrolysis time and temperature were independently varied. Data were obtained giving the compositions of the product gases as a function of the pyrolysis parameters. In examining a series of aromatic hydrocarbons it was found that the amount of yield depends primarily upon the number of substituted carbon atoms. A molar yield was defined and found to be a regular function of A/N where A is the number of substituted carbon atoms and N is the total number of carbon atoms per molecule. The pyrolysis residues were washed with iso-octane which was then examined by ultraviolet absorption spectroscopy. It was found that the aromatic skeletons often remained intact throughout the cracking. In addition, it was found that these structures often polymerized or condensed, giving longer wave-length absorption bands.

BY virtue of the range of gaseous products which it can analyze, the minute samples necessary for investigation, its accuracy, and the type of detailed information available, the mass spectrometer is becoming of increasing importance in investigating the thermal decomposition products of organic materials. Brewer¹ and Madorsky and Strauss² have studied the decomposition products from polymeric substances. Leifer and Urey³ have used the instrument to follow the thermal decomposition of dimethyl ether and acetaldehyde. Hipple and Stevenson⁴ made a study of the CH_3 radicals produced by thermal decomposition of lead tetramethyl and Eltenton⁵ has studied the intermediates occurring during the decomposition of various hydrocarbons ranging from methane to the butylenes. In some of the above investigations specific information in terms of intermediate products and radicals was obtained.

The present report is of some preliminary work wherein no attempt was made to study the inter-

mediate radicals or products. Rather the aim was to obtain information on final decomposition products, obtained under controlled conditions, and to correlate and interpret this in terms of starting materials and decomposition parameters. The method was an empirical one wherein the gaseous products were analyzed after decomposition had ceased. The sample of starting material was in each case charged into a pre-cleaned ampoule. The air was then removed and the ampoule sealed-off. After the pyrolysis a glass tip on the ampoule was broken and the gaseous products removed and analyzed in the mass spectrometer.

EXPERIMENTAL DETAILS

In Fig. 1 may be seen a cross-sectional view of the type of ampoule used. These were fabricated from Pyrex and with the approximate dimensions shown. In cleaning the ampoule prior to a pyrolysis run the interior of the ampoule was thoroughly washed with carbon tetrachloride and then with dry acetone. A vacuum line was then attached to the 9-mm O.D. tubing and the vapors removed. At the same time a soft flame was applied to the region between the break-off tip and the section line BB' to bake out the interior surface. Immediately after cleaning the ampoule was charged with the material being investigated. If the sample was liquid and of a sufficiently low viscosity it was introduced by means of a 0.1-ml pipette. If the material was solid or of high viscosity the ampoule was charged by a weight measure. In charging the ampoules it is important that no material cling to the sides near section line BB' , as this region gets hot when the ampoule is sealed off and preliminary decomposition may occur in such an event.

With samples of low vapor pressure a vacuum line was attached to the 9-mm O.D. tubing after the charging and the interior pumped down to 10^{-3} mm of Hg or lower. With the vacuum still applied the ampoule was closed off by applying a flame at section line BB' . In the case of volatile materials the ampoule was positioned to the necessary depth in a flask of liquid nitrogen

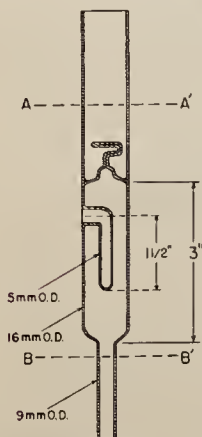


FIG. 1. Schematic view of the decomposition ampoule.

* A. K. Brewer, A. S. T. M. Bulletin, 140 (May, 1946).

² S. L. Madorsky and S. Strauss, Ind. Eng. Chem. 40, 848 (1948).

³ E. Leifer and H. C. Urey, J. Am. Chem. Soc. 64, 994 (1942).

⁴ J. A. Hipple and D. P. Stevenson, Phys. Rev. 63, 121 (1943).

⁵ G. C. Eltenton, J. Chem. Phys. 15, 455 (1947).

TABLE I. Composition of decomposition products of refined oil of 375 SUV (210°F)

Compound	Run No. 2	Run No. 13	Run No. 28	Run No. 25
methane	69.9 percent	25.9 percent	23.2 percent	30.5 percent
ethane	25.2 percent	16.1 percent	14.6 percent	22.3 percent
ethylene	1.3 percent	18.8 percent	22.3 percent	7.7 percent
propane	1.7 percent	5.4 percent	4.3 percent	10.5 percent
propylene	0.6 percent	18.8 percent	22.6 percent	13.2 percent
<i>n</i> -butane	—	0.4 percent	0.3 percent	2.0 percent
<i>i</i> -butane	—	1.8 percent	1.7 percent	2.2 percent
butenes	—	8.9 percent	7.6 percent	7.7 percent
C ₅ 's	—	3.6 percent	3.4 percent	3.9 percent
benzene	1.3 percent	0.3 percent	—	—
Run No. 2— 75 minutes at 564°C				
Run No. 13— 75 minutes at 473°C				
Run No. 28— 45 minutes at 470°C				
Run No. 25—120 minutes at 470°C				

just prior to the evacuation and during the sealing. The re-entrant 5-mm, O.D. tubing allowed a thermocouple to be inserted to the geometrical center of the ampoule and thus to a position at which the mean temperature would be expected.

The windings of the furnace were of Nichrome wire and the overall length of the heated region was 12 inches. The ampoule was positioned at the center of this for the pyrolysis and the cross-section of the furnace was so designed so that the ampoule and the controlling element of the thermostat were side-by-side. The furnace was controlled with a Partlow Chromalox Thermostat.* The actual temperatures reported in the data were those determined with the thermocouple mentioned above. After pyrolysis the upper tubing of the ampoule was cut along section line *AA'* and a stopcock and an iron slug for the magnetic break-off were sealed on.

The materials examined were obtained from Phillips Petroleum Company, Eastman, Dupont, Sharples, and Connecticut Hard Rubber Company. In each case they were of the highest purity obtainable. In some cases there was doubt as to the high purity of the material. However, these were not further purified in view of the preliminary nature of the work.

The volume of each ampoule was approximately the same. When the gas was extracted from the ampoule it was expanded into a constant, evacuated volume in each case. The gas in a definite and constant portion of this volume was then further expanded into an expan-

sion reservoir which connected directly with the leak which admitted the gas to the ionization region of the mass spectrometer. Since constant volume relationships existed in each case it was possible to analyze, by well-known methods,^{6,7} the mass spectra for the mixtures and to calculate the concentrations of the individual components. These were calculated in terms of convenient arbitrary pressure units which are adequate to allow absolute comparisons between separate samples. Absolute pressure values for individual samples may be obtained by the proper calibration technique. The concentration of molecular hydrogen could not be determined due to a defect in the ion source which would not allow the use of the necessary high accelerating voltages.

In a number of cases the iso-octane soluble components of the residue in the ampoule were examined by ultraviolet absorption spectroscopy. This was done by washing the interior of the ampoule with pure iso-octane which was subsequently examined in a Beckman Quartz Spectrophotometer.

DATA AND DISCUSSION

The initial experiments were carried out on a sample of refined oil of 375 Saybolt Universal Viscosity (210°F).

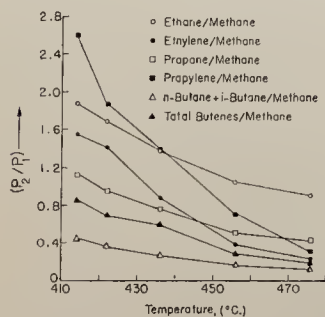


FIG. 2. Plot of (p_2/p_1) ratios for *n*-tetradecane decomposition at various temperatures with a pyrolysis time of 75 minutes.

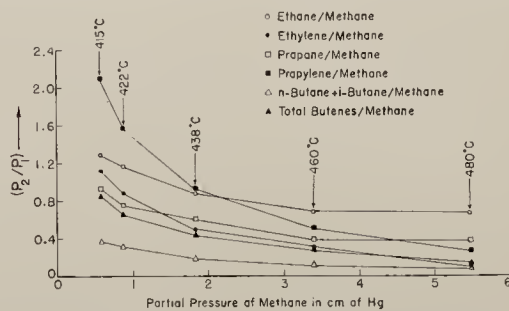


FIG. 3. Plot of (p_2/p_1) ratios versus methane content for tetradecene-1. Constant time of 75 minutes, temperature varied.

⁶ Washburn, Wiley, and Rock, Ind. Eng. Chem., Anal. Chem. 15, 541 (1943).

⁷ N. D. Coggeshall and J. A. Hipple, Colloid Chemistry, Vol. VI, edited by Jerome Alexander (Reinhold Publishing Corporation, N. Y., 1946), p. 89.

* Obtainable from Edwin L. Wiegand Co., Pittsburgh, Pa.

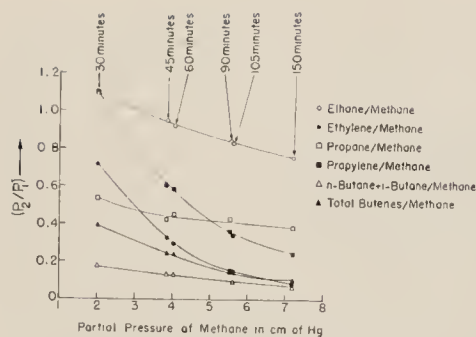


FIG. 4. Plot of (p_2/p_1) ratios versus methane content for cetane. Constant temperature of 475°C , pyrolysis time varied.

This particular oil was of no specific interest but was merely chosen as a convenient material for exploratory work in establishing methods, technique, testing of reproducibility, etc. In Table I may be seen some typical data from the runs made on this material. In each case the concentrations are given as percentages of total gaseous hydrocarbon product. Except as a means of establishing the technique used for later samples the results from these runs were of relatively little value. They did demonstrate that for a constant pyrolysis time an increase of temperature increases the methane and other light material content at the expense of the heavier hydrocarbons. Also they showed that the same thing happened for a series of runs wherein the temperature was maintained constant and the pyrolysis time was increased. In the latter case the rate of change of concentrations was relatively slow. It was found to be difficult to obtain reproducible results for a material of this sort. Part of the trouble was believed to be due to the detailed manner in which the ampoule was charged, i.e., whether the oil was smeared over a sizeable surface or concentrated in a globule.

In order to obtain reproducible data and at the same time to investigate the effects of small differences of molecular structure on the decomposition products a series of runs were made on cetane, *n*-tetradecane, and tetradecene-1. Two sets of data were taken for each compound. In one, the time of pyrolysis was 75 minutes in each case, and the temperature was varied. In the other, the pyrolysis temperature was held constant and the time varied. It was standard practice to charge the ampoule with 0.1 ml of material.

It was found upon scrutinizing the data that the partial pressures of the gaseous products did not always correlate with the pyrolysis parameter, i.e., time or temperature, with the expected consistency. However, the changes of composition were quite regular and it is believed that the inconsistencies are primarily due to an inability to control the degree of thermal cracking by this technique. Therefore, the changes of composition rather than absolute yield values were determined for each pyrolysis. It was found convenient to use the ratios of concentrations of the various products to that of methane as the dependent variables for following the decomposition. This served to demonstrate the composition changes in a manner that allows exact comparisons to be made between samples without determining the absolute yield values. In Fig. 2 may be seen some of the data for *n*-tetradecane. Here may be seen the ratios (p_2/p_1) plotted versus the pyrolysis temperature where p_1 refers to the methane partial pressure in our arbitrary scale of units and p_2 refers to the partial pressure of any of the other components in the same set of units.

We note in Fig. 2 that no data are given for temperatures below 415°C . This is due to the fact that at lower temperatures, using a pyrolysis time of 75 minutes, there is a very small amount of cracking and it becomes difficult to reliably analyze the minute amount of gase-

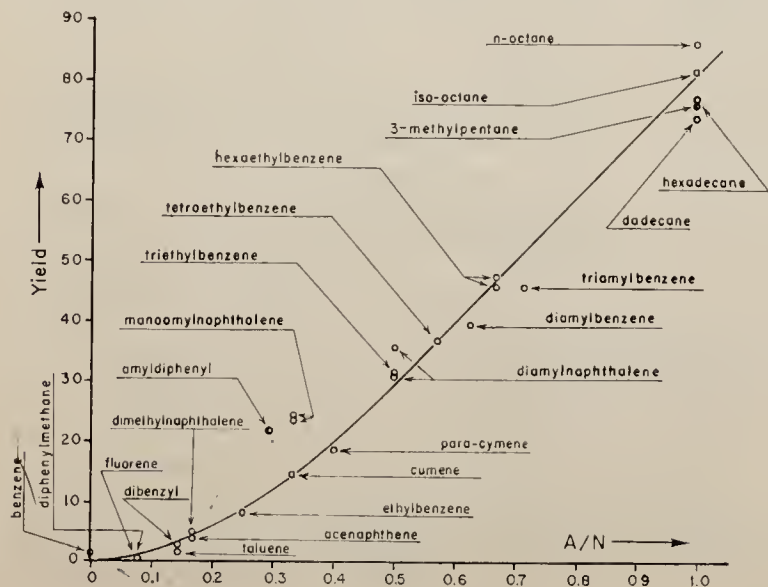


FIG. 5. Molar yield as a function of the A/N ratio for twenty-three hydrocarbons.

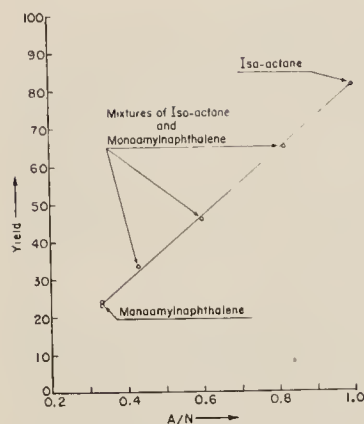


FIG. 6. Molar yield as a function of the A/N ratio for a series of synthetically prepared samples.

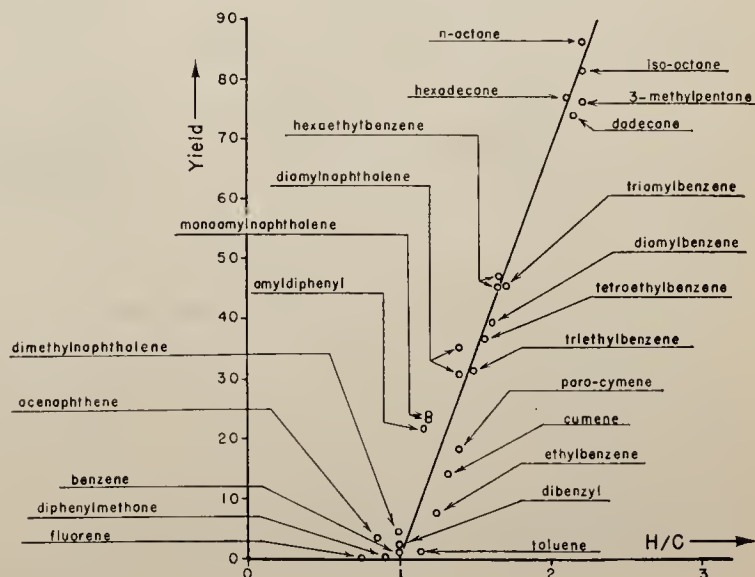
ous material formed. This limitation applies to all of the data shown at the low end of the independent variable. In some cases it was found that the composition changes were not regular with changes of cracking temperature or time, but depended rather on the amount of gaseous product formed. This again is due to the inability of the technique to accurately control the degree of cracking. However, if the partial pressure of methane in the product is used as a measure of degree of cracking the data become quite consistent. This may be seen in Fig. 3 where (p_2/p_1) is plotted *versus* the methane concentration for the products from the pyrolysis of tetradecene-1. Here it may be seen that there are regular trends of the composition with increasing methane yield. The cracking time for these runs was 75 minutes. Another set of data, this time for cetane with a constant pyrolysis temperature of 475°C, may be seen in Fig. 4. Here again we have (p_2/p_1) plotted *versus* methane concentration, and it is seen that the data are consistent even though the pyrolysis times are not regularly distributed along the curve.

Complete data, i.e., (p_2/p_1) *versus* temperature,

versus methane concentration with constant pyrolysis temperature, and *versus* methane concentration with constant pyrolysis time, were obtained and plotted for cetane, *n*-tetradecane, and tetradecene-1. No significant differences in the data which could be correlated with differences in molecular structure were evident. This is really to be expected in view of the close similarities of structure and the fact that after the cracking is well started it is essentially a thermodynamic process. It is significant that in the data shown in Figs. 2, 3, and 4 the concentrations of the olefins changed much more rapidly with temperature and with degree of cracking than did the paraffin concentrations. This shows that the olefins are much more predominant in the early stages of decomposition. Presumably this is because an aliphatic radical may be split off which may, after some re-arrangement and in some cases a loss of a hydrogen atom, become an olefin whereas the formation of a paraffin would require some recombination. As a means of differentiating between compounds which are quite similar in structure this technique appears to hold little promise although the above data demonstrate that consistent data may thereby be obtained for following the change of composition with pyrolysis temperature and with the degree of cracking.

In scrutinizing the data obtained in this manner for a large number of aromatic hydrocarbons it was evident that the amount of product formed depended primarily upon the aliphatic substituents. It is well known that aromatic ring structures are very stable against thermal decomposition and hence this result is not surprising. However, as there appeared to be a regular trend for the amount of product as a function of the number of substituted aliphatic carbons, a procedure for quantitatively evaluating it was tested. In order to do this it was necessary to obtain a total yield figure for each pyrolysis. It was necessary that this

FIG. 7. Molar yield as a function of the H/C ratio for twenty-three hydrocarbons.



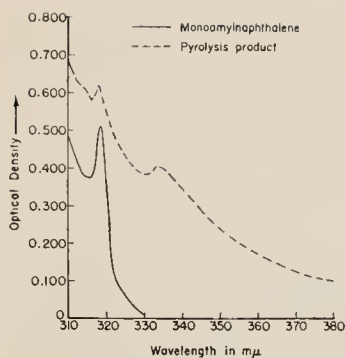


FIG. 8. Ultraviolet absorption spectra of monoamyl naphthalene and of its iso-octane soluble pyrolysis products.

figure account for the total number of carbon atoms in the gaseous products formed by the decomposition. The total yield is defined as:

$$\text{total yield} = \sum n_i p_i$$

where p_i represents the partial pressure of the i th component and n_i is the number of carbon atoms per molecule of this component. Since the partial pressure values are in arbitrary units, the total yield will be in arbitrary units. However, it will allow absolute comparisons to be made between various compounds and pyrolysis conditions.

Since the densities of the various liquid materials varied and since some of the samples were charged as solids it was necessary to put the results on a common basis which would account for variations in amount of material charged. For this purpose a molar yield was defined. This was defined as the total yield per mole of carbon atoms charged. The moles of carbon atoms charged is merely the fractional mole of material charged multiplied by the total number of carbon atoms per molecule. The molar yield hence gave a value for the pyrolysis products from a sample which could be correlated with the degree of aromaticity. The degree of aromaticity, or conversely of paraffinicity, was defined as the ratio A/N where A is the number of aliphatic carbon atoms and N is the total number of carbon atoms per molecule. With this definition $A/N=0$ for all completely aromatic compounds and $A/N=1$ for all completely paraffin compounds. Aromatic hydrocarbons with unsaturated substituents were not included in the data to be shown as they apparently have different decomposition properties. It was impossible to obtain a sufficient number of these compounds to definitely establish this.

In Fig. 5 may be seen the results when the molar yield is plotted *versus* A/N for twenty-three different compounds. These data are all from 75 minute runs at 520°C. It is to be observed that a definite relationship exists. It is difficult to determine to what extent the scattering of the data depends upon the differences in molecular structure or on the impurity of some of the materials. There was no way in which the purity of the materials exhibiting the greatest deviations from the smooth curve could be reliably assayed. If the experi-

mental data were not quite reproducible it would of course lead to such a scattering. In order to determine the inherent reproducibility of these data repeat runs were made for the three compounds: monoamyl naphthalene, hexaethylbenzene, and diamyl naphthalene. As may be seen from the figure the first two gave quite reproducible values. The data for the latter material did not check so well, although the agreement is still within the scattering exhibited elsewhere along the curve. In view of these results it is believed that the scattering is largely due to impure materials. It is quite significant that the observed correlation exists throughout the various classes of compounds examined. This establishes that the yield of decomposition products depends upon the number of carbon atoms in the substituted groups.

The relationship shown in Fig. 5 immediately suggests the usefulness of such data for assaying the A/N ratio, which may be interpreted in terms of the aromaticity, for a sample of unknown constitution or for a mixture whose proportions are unknown. In order to test such a procedure a series of synthetic samples were made and examined. In one case these samples were made as mixtures of monoamyl naphthalene and iso-octane. The results for them may be seen in Fig. 6. Here it is to be observed that the data for the mixture lie on a straight line drawn between the points for monoamyl naphthalene and iso-octane. Another series of mixtures composed of ethylbenzene and iso-octane were also examined. In this latter case the data also defined a straight line relationship. This is consistent with the data of Fig. 5 as the range of the A/N ratio for the mixtures was over that part of the region wherein the curve of Fig. 5 is essentially a straight line.

The H/C ratio, i.e., ratio of number of hydrogen atoms to the number of carbon atoms per molecule, was calculated for each compound. The molar yield was then plotted *versus* H/C for the same series of material to test for any correlation. The data for this are shown in Fig. 7. Although a definite trend is demonstrated it is clear that no such definite relationship as seen in Fig. 5 exists. This indirectly confirms the conclusion of above which stated that the molar yield of gaseous products depended primarily upon the number of substituted carbon atoms.

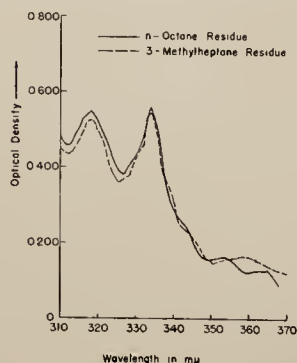


FIG. 9. Ultraviolet absorption spectra of the iso-octane soluble pyrolysis products from *n*-octane and 3-methylheptane.

It is well known that the phenyl ring and other condensed ring aromatic structures are very stable against thermal decomposition. In view of this and of the above results it would be expected that a number of condensation and polymerization products would be found in the pyrolysis residue. As parts of the substituent groups were cracked off it would be expected that there would be considerable condensation taking place among the remaining aromatic radicals. It is fortunate that this may be tested.

It is well known that the absorption in the ultraviolet for aromatic hydrocarbons is due to a resonance phenomenon involving the phenyl rings.⁸ It is further known that the conjugation of two such resonating structures or the conjugation of an olefin group with such a resonating structure will give rise to an absorption band occurring at a longer wave-length than the absorption bands possessed by the original components. Hence in comparing the ultraviolet spectra of the pyrolysis residues with the spectra of the original materials we would expect to find two things. One would be the spectra indicative of the original aromatic structure and the other would be absorption bands at longer wave-lengths indicating the conjugation of such structures, either with themselves or with olefin groups which could arise from the cracking of the substituent groups. Such results may be seen in Fig. 8 which shows the spectra between 310 and 380 $m\mu$ for monoamyl-naphthalene and its pyrolysis product. In this figure the optical density, defined by: optical density = $\log(I_0/I)$, where I_0 is the intensity of the light incident on the sample and I is the intensity of the transmitted light, is plotted versus wave-length. The absorption maximum appearing at about 320 $m\mu$ is characteristic of the naphthalene structure. It is to be seen that this same maximum appears in the spectrum of the pyrolysis product. In addition there is another absorption maximum appearing at about 335 $m\mu$ which is seen to be absent in the naphthalene spectrum. This longer wave-length band is ascribed to the conjugation of the types described above.

⁸ G. N. Lewis and M. Calvin, Chem. Rev. 25, 273 (1939).

Further results of this type in which conjugation is evidenced by longer wave-length absorption were observed for several other materials. Diamylnaphthalene gave a result essentially the same as seen in Fig. 8. The pyrolysis product from diphenylmethane gave spectra indicative of an olefinic group conjugated with a benzene ring and also of a fluorene type structure. The latter is believed to be due to a partial dehydrogenation of the benzene rings with consequent bridging between them. An interesting result was provided by phenanthrene which possesses no substituted aliphatic groups. The spectrum of its pyrolysis products exhibited the same absorption bands as did the original material. However, the relative intensities were varied with the result that the longer wave-length bands were relatively increased in intensity while the shorter wave-length bands were decreased in intensity. It is not known what this indicates unless it is a polymerization of the structures resulting from partial dehydrogenation. An interesting result of a case wherein the thermal cracking apparently produced some aromatic or other unsaturated material may be seen in Fig. 9. This shows the spectra for the pyrolysis residue for *n*-octane and for 3-methylheptane. Both of these compounds are transparent in this region. The bands exhibited in both cases fall in the region characteristic of naphthalene structures. It is remarkable that the residues from both of these hydrocarbons gave approximately the same spectrum. When the residue from the pyrolysis of dibenzyl (1,2-diphenylethane) was examined it was found to possess a spectrum believed to be due to a higher degree of unsaturation and conjugation. This could result from the partial dehydrogenation of the C_2H_4 group joining the phenyl ring and from bridging between partially dehydrogenated phenyl rings.

Acknowledgment is gratefully made to Dr. C. W. Montgomery for discussions of the subject, to Mr. A. S. Glessner for obtaining some of the ultraviolet absorption data, and to Dr. P. D. Foote, executive Vice-President of Gulf Research and Development Company for permission to publish this work.



NPC

Feb. 14, 1950

N. D. COGGESHALL

2,497,208

ELECTRICAL LOGARITHM COMPUTER

Filed Aug. 27, 1948

2 Sheets-Sheet 1

FIG. 1.

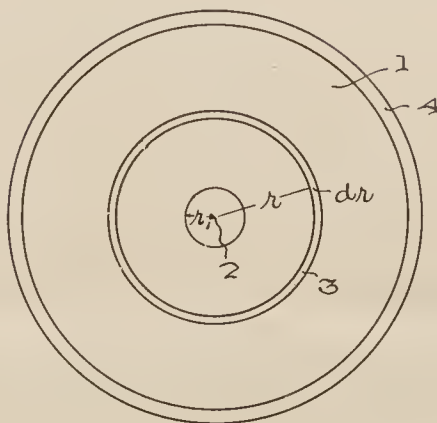


FIG. 4.

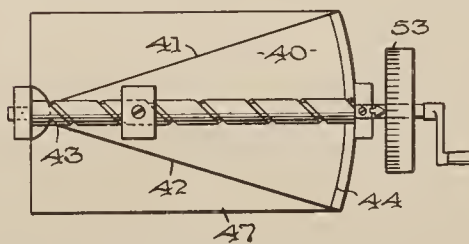
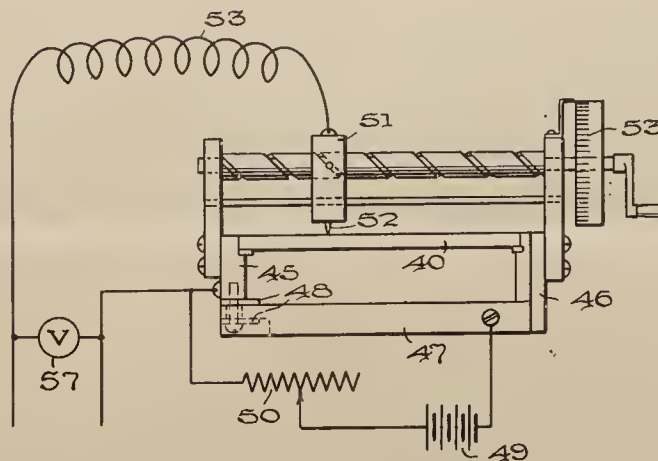


FIG. 5.



INVENTOR.
NORMAN D. COGGESHALL

BY *A. M. Houghton*

his ATTORNEY

Feb. 14, 1950

N. D. COGGESHALL
ELECTRICAL LOGARITHM COMPUTER

2,497,208

Filed Aug. 27, 1948

2 Sheets-Sheet 2

Fig. 2.

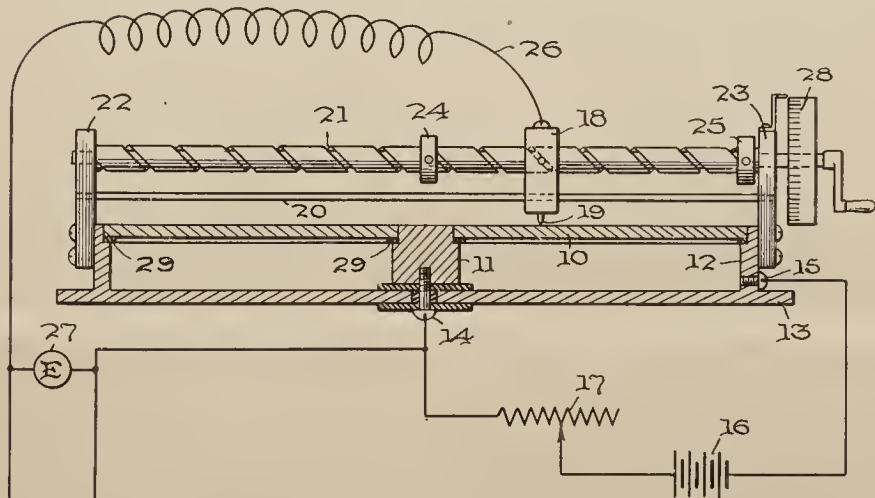
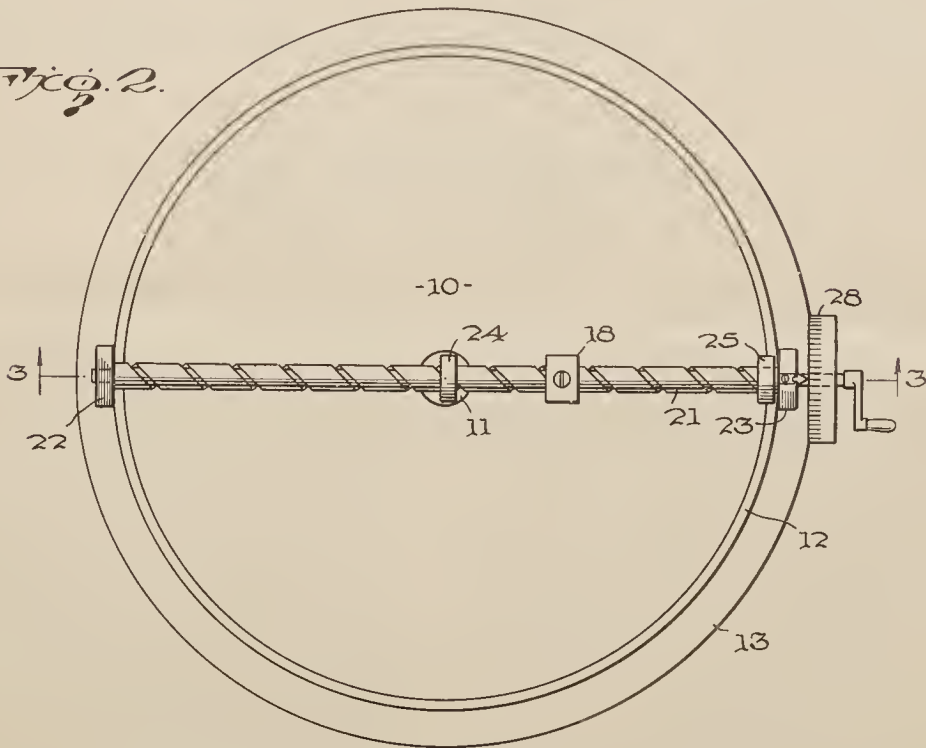


Fig. 3.

INVENTOR.
NORMAN D. COGGESHALL

BY *A. M. Hough*
his ATTORNEY

UNITED STATES PATENT OFFICE

2,497,208

ELECTRICAL LOGARITHM COMPUTER

Norman D. Coggeshall, Verona, Pa., assignor to
Gulf Research & Development Company, Pitts-
burgh, Pa., a corporation of Delaware

Application August 27, 1948, Serial No. 46,899

4 Claims. (Cl. 235—61)

1

This invention concerns an electrical apparatus for computing the logarithm of numbers and more particularly concerns a logarithmic potentiometer having a high degree of precision.

In many mathematical computations it is often necessary to determine logarithms to some predetermined or preassigned base. Such computations occur in various general computing systems and are also often encountered in various types of control and recording apparatus. While various empirical means have been devised for electrically obtaining a logarithmic signal, these devices have generally been subject to errors of calibration and errors in their empirical design which are eliminated by the present invention. The present invention is useful as an element of an electric computing machine, and is particularly useful in that the logarithmic function is inherent in a very simple geometrical design of the electric current-conducting medium.

It is accordingly an object of this invention to provide means for generating an electrical signal proportional to the logarithm of a number to which the machine is set.

It is a further object of this invention to provide apparatus for obtaining a logarithm signal of high precision.

It is a still further object of this invention to provide a potentiometer by means of which a logarithmic variation of potential may be obtained with a high degree of precision.

It is a still further object of this invention to provide a logarithm computer by means of which logarithms may be computed to any desired base.

It is a further object of this invention to provide a logarithm computing apparatus which is extremely simple in its construction and which is inherently precise.

These and other objects of this invention are attained as described in the following specification, of which the accompanying figures form a part, and in which

Figure 1 is a mathematical diagram used for explaining the principles of my invention;

Figures 2 and 3 show respectively a top and side view (partly in section) of an embodiment of my invention wherein a circular concentric annular disc is used as the electrical current-carrying or resistance medium; and

Figures 4 and 5 show respectively a top and side view of a preferred embodiment of my invention wherein a sector of a circular annular disc is used as the current-carrying medium.

This invention makes use of the fact that when an electric current flows radially outward in a

2

thin disc there results a radial distribution of potential which is logarithmic. This may be explained by reference to Figure 1, in which numeral 1 indicates a circular disc of uniform resistivity ρ and uniform thickness t . Assume that an electric current is introduced at the center point 2 and collected uniformly around the periphery of 1 by an outer ring 4 having a low resistance. Since the resistance of the disc along any radius from 2 to 4 is the same, there will be a uniform circumferential distribution of the current as it flows radially outward. Let an annular ring of the disc, such as 3, have a radius r and a radial width dr . Then the resistance across this ring will be expressed by

$$dR = \frac{\rho dr}{2t\pi r}$$

The total resistance of the disc from any inner radius r_1 out to the radius r may be obtained by integrating as follows:

$$R = \frac{\rho}{2t\pi} \int_{r_1}^r \frac{dr}{r} = \frac{\rho}{2t\pi} [\log r]_{r_1}^r$$

$$R = \frac{\rho}{2t\pi} (\log r - \log r_1)$$

$$R = \frac{\rho}{2t\pi} \log \frac{r}{r_1}$$

If the current which flows from 2 to 4 is i then the potential drop iR will be given by

$$e = i \frac{\rho}{2t\pi} \log \frac{r}{r_1}$$

If we let $i\rho/2t\pi = k$ and make $r_1 = 1$ then we have simply $e = k \log r$.

In this invention such a disc may be of suitable electrically uniform conducting (but nevertheless resistive) material and arranged so that the current enters at a radius (r_1) which may conveniently be one scale unit. The constant k is then set by adjusting the current through the disc as explained later.

The foregoing principles are employed in my invention as shown in Figures 2 and 3. Circular concentric annular disc 10, may be of metal foil, or graphite, or any well known resistance material molded in the form of a disc of uniform thickness and resistivity; or such a disc may comprise a coating of foil or graphite on the surface of a supporting insulating disc, or may be of other well known resistance material. It is merely necessary that the conducting portion be in the shape of a relatively thin, uniform, concentric, circular, annular disc.

The disc may be supported at the center by a low resistance metal bushing 11 which makes uniform electrical contact to the inner edge of the disc. It is supported on the outside by a low resistance metal ring 12 which makes electrical contact uniformly around the periphery of the disc. The disc 10 may rest on insulation 25 which in turn rests against a shoulder on the supporting elements 11 and 12. The ring 12 may be mounted on a base plate 13 of any convenient form and the bushing 11 is also supported on the base plate 13 and insulating therefrom. Electrical connection may be made to bushing 11 by means of a screw such as 14 insulated from the base plate and electrical connection is made to the ring 12 by means of screw 15. A battery 16 and adjustable series resistor 17 are placed in the circuit to supply electric current to the disc 10.

Mounted above the disc 10 is a movable slider or carrier 18 having a spring pressed contact 19 which bears against the surface of the disc 10. The carrier 18 is guided on rod 20 and screw 21 with which it engages, the screw serving thereby as a means for moving the slider along the radius of the disc 10. Rod 20 and screw 21 are supported diametrically across the disc 10 by means of end bearings 22 and 23, which are of insulating material and conveniently supported on ring 12. The screw 21 may be extended through bearing 23 and carry a crank or adjusting wheel and an indicator dial 28 which indicates the radial position of the contact 19. Screw 21 may be equipped with an inner stop 24 which is set at a point so that the contactor 19 just begins to contact disc 10 and an outer stop 25 set at some convenient outer limit of the scale. The latter is not necessarily the outer boundary of the disc, i. e. the disc may extend beyond this point. A flexible lead 26 connects to contactor 19 and serves to tap off the logarithmic voltage desired, the potential being measured between contactor 19 and center post 11 and read on a meter 27, which is preferably of a high resistance or potentiometer type.

The dial 28 and the screw 21 are together arranged so that this dial reads 1.000 when the carriage 18 is against the inner stop 24 and the contactor 19 just begins to contact the disc 10. There will at this point be zero potential indicated at 27. The screw 21 and the indicator dial may then be turned to move the carriage 18 outward to some convenient standard point, say the outer periphery of the disc, which may be conveniently made ten times the radius of the inner bushing 11. A potential will at this point be indicated at 27 and this potential may be adjusted by means of the resistor 17 to indicate the value of the logarithm to any preassigned base, for the radius indicated on dial 28.

Thus, if it is desired to use the device to compute logarithms to the base ten, resistor 17 is adjusted so that meter 27 reads 1.000 volts when the dial 28 is set at radius 10.000. Then for all intermediate numbers between 1.000 and 10.000 as set on dial 28, the meter 27 will indicate the logarithm to the base ten.

If it is desired to determine the logarithm of numbers to the base e the resistor 17 is adjusted so that meter 27 reads 2.302 volts when the dial 28 is set at radius 10.000. Intermediate settings of dial 28 then result in the meter reading 27 being the natural logarithm of the dial setting. It is apparent that any other convenient base may be chosen for a particular problem or ap-

plication, it being only necessary to know the logarithm of one point on the dial scale to the base desired. This evaluates the constant k in the equation $e = k \log r$.

It is apparent that since the distribution of current in the disc is uniform and the current lines of flow are radial one may use instead of a disc, a sector of an annulus as shown in Figures 3 and 4 as 40. Such a sector of an annulus may be cut with straight radial edges 41 and 42 and concentric circular inner and outer boundaries 43 and 44, respectively, uniform electrical contact being made to circular inner edge 43 by means of low resistance metal post 45 and uniform contact to the outer circular edge being by means of outer low resistance metal support 46, the latter conveniently being made integral with the base 47. Base 47 supports at its opposite end the post 45 insulated therefrom by means of washers 48. Current flow is set up by passing a current from 45 to 46 through battery 49 and rheostat 50. Carriage 51, insulated from the base and carrying contactor 52, is arranged in a manner similar to that shown in Figures 2 and 3, dial 53 being arranged to read 1.000 when the contactor 52 is just beginning to make contact with the inner radius of sector 40 and reads 10.000 at some convenient outer radius ten times as large. The latter is not necessarily the outer boundary of the annular sector and the sector may extend beyond this point. Logarithmic voltage is then obtained from a flexible lead 53 attached to the carrier 51 and connected to the contactor 52. The potential difference is measured by meter 57 connected between the lead 53 and the inner post 45. It can be shown mathematically that this variation of potential is also logarithmic exactly as in the case of a disc. Adjustment of the current through the potentiometer element 40 is made in the same manner as that described in connection with Figures 2 and 3 and is accomplished by adjusting rheostat 50.

It is to be noted that it is not necessary to calibrate the resistor 10, Figure 2, or 40, Figure 4. If the disc or the disc sector is accurately machined and uniform in thickness and resistivity, this being relatively simple of attainment, then only one point of calibration, as above indicated, is required to adjust the base to which logarithmic variation applies. This one setting calibrates the entire unit with a high degree of precision. This results because the logarithmic variation in potential is not introduced by any empirical form of the resistor, but rather results as an inherent property of the radial current flow in the thin conducting medium employed.

In order to preserve the precision of my invention, the terminal elements 11 and 12 of Figures 2 and 3 and 45 and 46 of Figures 4 and 5 should be of much lower resistivity than the disc 10 or sector 40. The terminal elements are preferably made of copper or silver. Further, mechanical refinements in the slider-moving screw may be made in a manner well known in the art, and lost motion in the contactor 19 or 52 is to be avoided. Also the indicator dial and the adjusting screw may be made so that the number of revolutions is indicated and the dial may have a vernier as is customary in devices of this type.

My invention may also be used for obtaining antilogs in well known manner and in fact may be used for any computation involving the logarithm according to the well known properties of the logarithm function.

5

The term "sector-like member," as used in the claims is defined as a sector having any finite angle from 0 to 360° included between its radial boundaries. When the included angle is 360°, such sector-like member takes the form of a disc.

What I claim as my invention is:

1. Apparatus for obtaining an electric signal which varies in a logarithmic manner with a linearly varying adjustment comprising a uniform concentric circular annular disc of electrically conducting material, means for flowing an electric current uniformly between the inner circular edge of said disc and the outer circular edge of said disc, means for electrically contacting a point on the surface of said disc, means for radially adjusting said contact point, and an output circuit connected between said contact point and an edge of said disc.

2. Apparatus for obtaining an electric signal which varies in a logarithmic manner with a linearly varying adjustment comprising a uniform concentric circular annular sector-like member of electrically conducting material, means for flowing an electric current uniformly between the inner circular edge of said sector-like member and the outer circular edge of said sector-like member, means for electrically contacting a point on the surface of said sector-like member, means for radially adjusting said contact point, and an output circuit connected between said contact point and a circular edge of said sector-like member.

3. Apparatus for computing logarithms comprising a uniform concentric circular annular disc of electrical conducting material, means for

6

introducing an electric current at the inner edge of said disc, means for gathering the electric current uniformly around the outer periphery of said disc, a radially adjustable contactor contacting the surface of said disc, means for moving said contactor radially along said disc, means for positioning said contactor at a known radius, means for adjusting the electric current flowing through said disc, and means for measuring the electric voltage between said contactor and an edge of said disc.

4. Apparatus for computing logarithms comprising a uniform concentric circular annular sector-like member of electrical conducting material, means for introducing an electric current at an inner circular edge of said sector-like member, means for gathering the electric current uniformly around the outer circular edge of said sector-like member, means for moving the contactor radially along the surface of said sector-like member, means for positioning said contactor at a known radius, means for adjusting the electric current flowing through said sector-like member, and means for measuring the electric voltage between said contactor and a circular edge of said sector-like member.

NORMAN D. COGGESHALL.

REFERENCES CITED

The following references are of record in the file of this patent:

UNITED STATES PATENTS

Number	Name	Date
1,918,001	Stone	July 11, 1933
2,452,664	Koenig, Jr.	Nov. 2, 1948



Reprinted from ANALYTICAL CHEMISTRY, Volume 22, Page 381, March 1950
Copyright 1950 by the American Chemical Society and reprinted by permission of the copyright owner

Determination of Organic Functionality by Molecular Spectroscopy

NORMAN D. COGGESHALL, *Gulf Research & Development Company, Pittsburgh, Pa.*

IN RECENT years analytical chemistry has experienced, with great impact, the inclusion of methods and techniques that utilize molecular spectroscopy. Certain classical analyses and tests have been essentially replaced with an increase in efficiency, accuracy, and information obtainable. Inherent and basic in this process is the fact that by the techniques of molecular spectroscopy information of a very fundamental and characteristic nature is obtained. Because of these successes, there has arisen a rather widespread notion that such techniques will with time become omnipotent with regard to analytical problems. This is not the case, and hence it is important, at this time, to discuss the limitations as well as the scope and generality of the methods now

available and those that may be reasonably anticipated. Many of those who are not directly engaged in absorption spectroscopy believe that infrared, Raman, ultraviolet, and mass spectroscopy are competitive in the sense that the same problems may be solved with their use. Although this is largely true for the first two, the latter two furnish information of a completely different nature and there is relatively little overlapping of application.

INFRARED AND RAMAN SPECTROSCOPIC METHODS

A molecule is not a rigid structure. It comprises an assembly of atoms that are constrained by their mutual interactions to define

equilibrium positions. The valence bonds are elastic in nature and hence the geometrical structure that is the molecule can vibrate and rotate in a manner analogous to bodies of macroscopic experience. Excepting collisions between molecules, the principal means whereby the vibrations of this geometrical structure may absorb or give up energy is by the absorption or emission of radiant energy.

A molecule will possess definite modes of vibration and hence will show strong absorption only to those wave lengths that will excite these modes. In the classical theory the molecule is regarded as absorbing electromagnetic frequencies that are identical with its own vibrational frequencies. From quantum mechanics we know that this is not the most correct interpretation. However, for the analytical applications and for work in determination of molecular structure this interpretation is adequate.

In the simplest type of molecule, the diatomic, the frequency of the vibration wherein the two atoms move back and forth toward each other along the valence bond is given by:

$$\nu = \frac{1}{2\pi} \sqrt{\frac{k}{\mu}} \quad (1)$$

where k is the force constant for the valence bond and μ is the reduced mass, being given by $\mu = m_1 m_2 / (m_1 + m_2)$ where m_1 and m_2 are the masses of the atoms involved. It should be noted from Equation 1 that as the valence bond strength increases, k will increase, with an increase in the vibrational frequency. As the masses of the constituent atoms increase, it will result in a decrease of the frequency.

As the complexity of the molecule increases, so also do the number and complexity of the possible vibrational modes. In Figure 1 may be seen the three modes for the triangular triatomic molecule, YX_2 . In principle, it is possible to calculate the frequencies and determine the modes for any molecule. Except for the simpler ones, this meets with the most formidable mathematical difficulties and such results have been obtained on only a very few of the total number of known molecular species. The practical application of vibrational spectroscopy to the determination of structure of complex molecules must therefore be pursued by essentially empirical methods. These utilize the results extrapolated from the study of simpler molecules as well as correlations obtained by examination of series of homologous and similar compounds.

In infrared absorption spectroscopy, the fraction of light energy absorbed by the sample as a function of wave length is determined. Such data show regions or bands of intense absorption, each of which may be correlated with a particular vibrational mode. In general, the bands may be regarded as falling into either of two classes, bands characteristic of group-type (such as O—H, C=O, N—H, C—C; etc.) vibrations and bands due to over-all or skeletal vibrations. The former vibrational frequencies are essentially constant, independent of the remainder of the molecule, and hence furnish a most valuable tool for determination



Figure 1. Vibrational Modes for Nonlinear YX_2 Molecule

of molecular structure. As the latter depend specifically upon the geometry, constituent atoms, and valence forces of the molecule, they furnish a unique pattern or "fingerprint" for each molecule species. This allows the use of the spectra for identification (through comparison with spectra of known materials) of unknown materials and furnishes the basis for the analytical applications of spectra wherein unique bands are utilized for quantitative determinations.

In Raman spectroscopy the sample is irradiated with monochromatic ultraviolet or visible light. When the light scattered at right angles by the sample is spectrally examined, it is found that it is not all of the same frequency as the incident light. Some of the radiation is displaced in small but definite amounts from the frequency of the incident light. These displacements are called Raman shifts. Through a process of absorption and re-emission of the incident light, energy is either added to or subtracted from the molecular vibrational mode, just as an infrared absorption band is found for each infrared active vibrational mode. Hence the same fundamental information is furnished by the two techniques. There are some exceptions to this, based on symmetry elements in the molecules, but for the requirements of analytical chemistry they are relatively minor.

The experimental details of instrumentation and operation in infrared and Raman spectroscopy have been abundantly published (3, 57). At the present time infrared absorption is much more intensively applied than are Raman spectra. Infrared equipment has been more generally available and the techniques are simpler. The material in this paper is discussed largely in terms of infrared absorption. In a general way, the scope and limitations that apply to infrared absorption also apply to the Raman methods.

When the capacity of each molecule in a sample to absorb radiation is independent of its environment, Beer's law of absorption applies. This is given by:

$$D = \log (I_0/I) = ac l \quad (2)$$

where D is known as the optical density, I_0 and I are the intensities of the incident and transmitted energies, respectively, a is a constant depending upon the material and upon the wave length, c is the concentration of the material, and l is the thickness of the sample. If a constant absorption cell thickness is used, it is common practice to denote product al as the calibration coefficient, b . If several materials are present—three, for example—Beer's law becomes:

$$D_1 = b_{11}C_1 + b_{12}C_2 + b_{13}C_3 \quad (3)$$

where D_1 refers to a particular wave length λ_1 , b_{11} is the calibration coefficient for the first compound at that wave length, b_{12} and b_{13} apply similarly to the second and third compounds at the same wave length, and C_1 , C_2 , and C_3 refer to the concentrations of the first, second, and third compounds, respectively. If such data are taken at three separate wave lengths, three simple linear equations are obtained which may be solved for the concentrations, thus yielding the analysis.

For a successful analysis of this type, two conditions must in general be fulfilled. In order to obtain the calibration coefficients, it is necessary that pure compounds be available. In order to solve the sets of linear equations with satisfactory accuracy, it is important that optical discrimination be achieved. By optical discrimination is meant that at each wave length used, one compound absorbs more strongly than the others and that each compound is represented by one such wave length.

Gas Analysis. The analysis of C_4 hydrocarbon mixtures containing *n*-butane, isobutane, 1-butene, isobutylene, *cis*-2-butene, *trans*-2-butene, and 1,3-butadiene has probably been the most outstanding application of infrared absorption to gas analysis (8). Figure 2 shows the absorption spectra of three of the gases mentioned. This demonstrates how the data may be plotted in such a way as to simplify the choice of wave lengths to

In recent years methods and techniques that utilize molecular spectroscopy have replaced many classical analyses and tests with an increase in efficiency and accuracy. Information of a very fundamental and characteristic nature is obtained. Although infrared and Raman spectroscopic methods may often be used to solve the same problems, ultraviolet and mass spectroscopy furnish information of a completely different nature and there is relatively little overlapping of application. The limitations as well as the scope and applicability of molecular spectroscopy methods are discussed.

use in the analysis. At each wave length designated by an arrow in the figure, one compound always absorbs much more strongly than the others.

Suitable wave lengths may be found for all the above C_4 's and it is possible to set up the equations and organize a very efficient and effective analysis procedure. The accuracy is very good, the average errors being of the order of 0.5% total sample or less. A typical analysis on a synthetically blended sample may be seen in Table I. These data were taken under completely routine conditions and represent the accuracy attainable in day-to-day operations. It is important that the sample be fairly free of C_3 and C_5 components, as a few per cent of either can cause serious errors. This is usually achieved by making a C_4 cut on low temperature distillation equipment.

Methane, acetylene, carbon monoxide, sulfur dioxide, and other gases of low molecular weight cannot be analyzed by this method, owing to an effect known as pressure broadening. Because of this effect, the absorption due to any one of these gases depends not

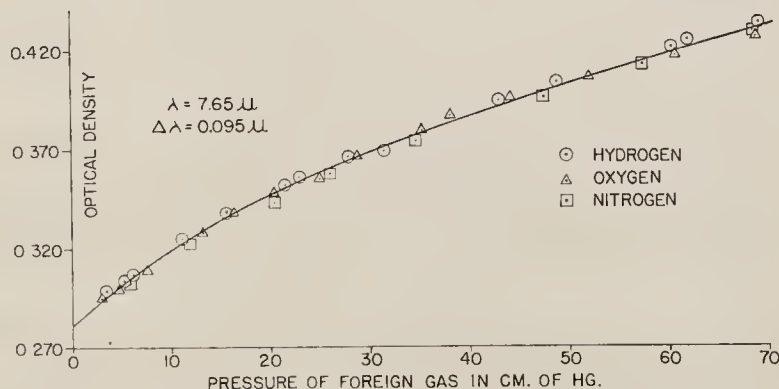


Figure 3. Optical Density of Constant Pressure of Methane Plotted against Pressure of Foreign Gas (20)

only on its concentration, but also upon the total pressure in the cell, and Beer's law is not obeyed. Methods suitable for such systems are discussed below. Other gaseous hydrocarbons in the C_3 and C_5 range may readily be analyzed in the gas phase by the above method. An interesting application of the use of this technique for the control of plant operations by the analysis of multi-component C_5 mixtures has recently been described (60).

Symmetrical diatomic gases such as oxygen, hydrogen, and nitrogen, and the monatomic gases possess no absorption in the infrared. However, except that the gases must obey Beer's law, there are no particular restrictions on what mixtures of gases will yield to the above procedure. Raman spectroscopy is not very well suited to gas analysis because of the low scattering power of the gas, which is a result of the relatively low molecular density.

Trace analysis may sometimes be done by the above procedure. However, for high sensitivity in trace analysis, the gas that one is seeking must possess a very much larger absorption coefficient at a particular wave length than any of the major constituents; otherwise the absorption of the latter will obscure the absorption of the trace gas at low concentrations. If suitable wave lengths can be found, it is sometimes possible to increase sensitivity by the use of very long path lengths or of high pressure gas cells; concentrations of water as low as 1 p.p.m. may be determined in a number of commercial refrigerants (7).

Significant future developments in infrared gas analysis will probably be in improved apparatus and technique, allowing greater accuracy of optical density determinations in shorter times.

Analysis of Gases Not Obeying Beer's Law. The gases of low molecular weight do not obey Beer's law and manifest the phenomenon of pressure broadening. Their absorption depends not only upon the molecular density but also on the total pressure. This is a consequence of broadening of the individual rotational lines as a function of the time between collisions (63).

Table I. Typical Infrared Analysis of Synthetic Blend of C_4 Hydrocarbons (15)

Compound	Synthetic, %	Calculated, %	Difference, %
n-Butane	19.7	19.1	-0.6
Isobutane	10.4	10.6	+0.2
1-Butene	19.8	20.4	+0.6
Isobutylene	16.8	16.9	+0.1
cis-2-Butene	14.8	14.6	-0.2
trans-2-Butene	18.5	18.3	-0.2
Butadiene	0.0	0.1	+0.1

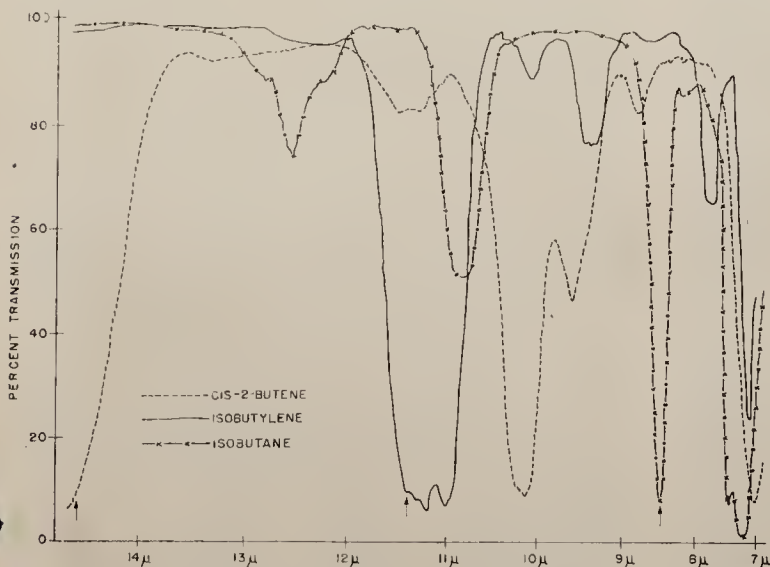


Figure 2. Infrared Absorption Spectra of Three C_4 Hydrocarbon Gases between 7 and 14μ (15)

Data illustrating the pressure-broadening effect may be seen in Figure 3, where the optical density of a constant partial pressure of methane is plotted as a function of the pressure of nonabsorbing or foreign gas present. If Beer's law were obeyed by the methane, all pressures of foreign gas would result in the same optical density value. It is merely fortuitous that the effects of hydrogen, oxygen, and nitrogen are essentially identical for the case demonstrated. In general, it has been shown that different foreign gases will have different effects and that the order of effects cannot always be extrapolated from one absorption band of the absorbing gas to another (21).

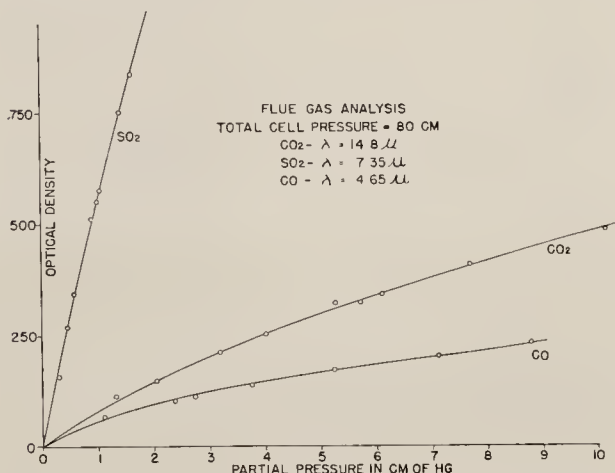


Figure 4. Calibration Curve for Determination of Carbon Dioxide, Sulfur Dioxide, and Carbon Monoxide in Gaseous Mixtures (20)

Constant cell pressure maintained for all samples

If the pressure-broadening effects of the foreign gases are known, it is possible in some cases to set up empirical calibration curves for the desired gases. In such a case, it has proved convenient to render the pressure-broadening effect of the foreign gases constant by using a constant total pressure for the sample while constructing the calibration curves and obtaining the data for unknown samples. Using this procedure, very satisfactory determinations may be made of methane, sulfur dioxide, carbon dioxide, and carbon monoxide (20). The calibration curves for the latter three may be seen in Figure 4. Similar methods for these and other gases subject to pressure broadening have been published (41, 56).

Analysis of Unassociated Materials in the Liquid Phase. Mixtures of unassociated liquids may be analyzed in the same straightforward manner utilizing simultaneous equations as used for gas analysis. The term "unassociated liquids" is used to specify materials that are not subject to intense, short-range forces which give rise to the formation of complexes such as those found for hydrogen bonding. In this respect the hydrocarbons are very inert and very easily handled. In practice, when I and I_0 of Equation 2 are determined by a cell-in-cell-out procedure we have:

$$D = \log I_0/I = bc + k \quad (4)$$

where k , the cell attenuation factor, has its origin in the absorption and reflection of the light by the cell windows. In gas analysis it is easy to eliminate k from the equations by obtaining D for the evacuated cell. However, this cannot be done for a liquid cell because of the large changes in reflectivity between an empty and filled cell. If the analyses are made with the desired compounds in a transparent solvent, k can be evaluated by examining the cell filled with solvent. However, the use of solvents is often not practical when certain mixtures such as paraffins are analyzed. Here the calibration is done with the pure materials in the cell and

data are obtained on the mixtures with the same cell. The use of the same cell allows an algebraic elimination of the k values.

Let us consider the optical density at λ_1 for the first of three compounds for which calibration data are being obtained for a ternary mixture. With the pure material in the cell we have:

$$\bar{D}_{11} = b_{11}C_1 + k \quad (5)$$

where \bar{D}_{11} is the measured optical density and b_{11} is the true calibration coefficient. Because $C_1 = 1.00$ for the calibration we have:

$$b_{11} = \bar{D}_{11} - k \quad (6)$$

When the optical density, D_1 , for the ternary mixture is measured at the same wave length we have:

$$D_1 = b_{11}C_1 + b_{12}C_2 + b_{13}C_3 + k \quad (7)$$

If we substitute the results of Equation 6 and similar ones, we obtain:

$$D_1 = \bar{D}_{11}C_1 + \bar{D}_{12}C_2 + \bar{D}_{13}C_3 - (C_1 + C_2 + C_3)k - k \quad (8)$$

However, because $C_1 + C_2 + C_3 = 1.00$ we have:

$$D_1 = \bar{D}_{11}C_1 + \bar{D}_{12}C_2 + \bar{D}_{13}C_3 \quad (9)$$

Thus it is possible to get sets of linear equations which may be solved for the C_i 's without actual evaluation of the attenuation factors.

This method has been used with considerable success for the analysis of mixtures of paraffins boiling in the gasoline range. Unless the sample is from a rather special process which involves only a few materials, it will contain many compounds over an extended boiling point range. Direct infrared examination of such a sample is not practical. Rather the material should be fractionated into a series of cuts containing on the order of five or less compounds each. The choice of wave lengths then follows the procedure used in gas analysis. In Figure 5 may be seen the recorded spectra and three suitable absorption bands for a ternary

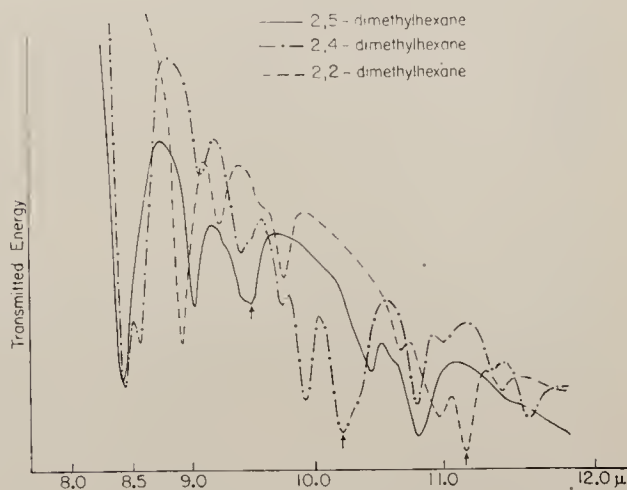


Figure 5. Spectra of Three Dimethylhexane Isomers (15)

Curves are tracings of automatically recorded spectra

Table II. Comparison between Blended and Analyzed Composition of Paraffin Mixtures

Compound	Synthetic, %	Calculated, %	Difference, %
n-Heptane	22.2	21.8	-0.4
Methylcyclohexane	27.8	27.8	0.0
Methylcyclopentane	50.0	50.4	+0.4
2,5-Dimethylhexane	22.2	21.5	-0.7
2,4-Dimethylhexane	22.2	22.5	+0.3
2,3,4-Trimethylpentane	22.2	22.8	+0.6
2,3,3-Trimethylpentane	11.2	11.3	+0.1
2,2,3-Trimethylpentane	22.2	21.9	-0.3

mixture of dimethylhexane isomers. As the spectra for such materials are generally rich in bands, it is usually easy to satisfy the condition of optical discrimination. Table II shows some typical results when synthetically blended mixtures have been analyzed by this technique.

Although paraffins may be readily analyzed by the above technique in a cell on the order of 0.006 inch thick, it is not so easy to handle olefins and many polar compounds by the same method, because of the much greater intensity of absorption displayed by the latter materials. In order to get reliable quantitative data, it is often necessary to work with the material in solution. Although this simplifies the cell attenuation factor problem, it introduces new steps into the procedures and also new problems associated with the solvent. Because all solvents are themselves chemical compounds, each will display its own infrared spectrum. The absorption bands of the solvent will interfere with the absorption bands of the solute unless the solvent is transparent in the special region of interest. Although it is not possible to choose a solvent that is transparent throughout the entire infrared region, it is possible to choose a series of solvents with overlapping regions of transparencies, so that investigations over the whole region can be made (61). Cyclohexane and carbon disulfide are favorite solvents for analytical work, as they are both transparent in the region wherein is found the greatest abundance of bands suitable for analytical work.

Although the applications of infrared and Raman spectra for the analysis of nonassociating liquids are parallel, there are some advantages unique to each by virtue of the fundamental processes involved. Whereas the optical density of an infrared absorption band varies exponentially with the concentration of the absorbing component, the intensity of a Raman line varies linearly with the concentration. This makes the infrared method more suitable for measuring low concentrations and the Raman method more suitable for measuring concentrations near 100%. Although a recent publication describes the use of Raman spectra for the determination of olefins (34), the technique has probably been utilized most, to date, for the analysis of aromatics (28, 55).

As long as the materials involved do not associate and there are not too many components in each sample, there is no fundamental limitation to the infrared analysis. If weak and strong absorbers are present together, it may not be possible to measure the former with an accuracy comparable to that possible for the latter. Usually some auxiliary technique like bromination may be called upon to alleviate the situation. In many cases it is not possible to predict reliably whether or not a system is subject to association, chemical interaction, or other interatomic effects whereby Beer's law is violated. In such cases, it is necessary to make detailed

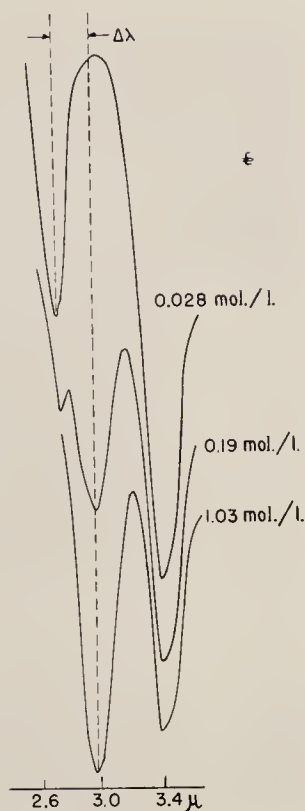


Figure 6. Infrared Spectra in Hydroxyl Absorption Region of Various Concentrations of Ethyl Alcohol in Carbon Tetrachloride Solution (14)

tests in order to determine the behavior. As a general rule, trouble of this type may be expected to occur for any system which is known to contain compounds that will form complexes such as hydrogen bonding. Dilute solutions, whereby the average intermolecular distance negates the association effects, may sometimes be used (55). This, unfortunately, often introduces problems of solvent transparency.

Analysis of Liquid Materials Subject to Association. The term "association" in the liquid phase is used here in a very general sense, to specify any phenomenon which is responsible for severe deviations from Beer's law. A common cause of such deviations in the liquid phase is the perturbation effects due to strong electric fields. When two molecules hydrogen-bond, for example, there is a very strong attraction between the dipoles resident in the hydroxyl groups. The effect of the dipole field of one hydroxyl group on the other is such as to shift the resonant frequency and to enhance the intensity of absorption (28). Actually, some of the phenomena responsible for the deviations from Beer's law are neither understood nor have as yet been thoroughly investigated. On one hand, this is a discouragement to the use of infrared and Raman methods for the treatment of such systems, while on the other the very fact that the phenomena manifest themselves in photometric anomalies makes it possible for spectroscopic methods to aid abundantly in their clarification. Thus the research necessary to apply these methods is yielding a rich return in fundamental understanding of some of the chemical and physical interactions that occur between molecules in the liquid state.

Hydrogen bonding is one of the most commonly known forms of association. When it occurs, the absorption due to the hydroxyl group is drastically altered. This may be seen in Figure 6. Here are given the spectra in the hydroxyl region of three different concentrations of ethyl alcohol in carbon tetrachloride solution.

In the 0.028 mole per liter solution may be observed a band at about 2.76μ which is due to the free or unassociated hydroxyl group. At such concentrations the free band is observed, as the average intermolecular distance does not permit hydrogen bonding. In each curve the absorption band at 3.4μ is due to C—H stretching vibrations. For 0.19 mole per liter it is observed that the intensity of the free hydroxyl absorption band has decreased and that a new band at about 3.0μ has appeared. For 1.03 moles per liter the free hydroxyl band has disappeared and the 3.0μ band has become very strong.

The interpretation is that as a molecule becomes hydrogen-bonded the effective force constant for the hydroxyl valence bond is weakened. This weakening results in a shift of the resonant frequency to a lower value; hence the absorption band shifts to a longer wave length. In addition to this change there is also a great enhancement of intensity of absorption. It is clear that in the face of such changes as these, the straightforward application of Beer's law on the hydroxyl absorption band for analytical purposes would be useless. Such difficulties may, however, be circumvented by the use of a solvent such as carbon tetrachloride and a thick cell wherein the material is examined in such low concentration that association does not occur. Very accurate determinations may thus be made of individual phenols and alcohols in the presence of nonhydroxylated materials and of total hydroxyl content in group-type analyses.

An example of another effect, not so clearly understood, is the interaction that occurs between alcohols and ketones with an alteration of the spectra of the latter (54). In Figure 7 is plotted the optical density of methyl ethyl ketone at two different wave lengths as a function of ethyl alcohol content. The concentration of methyl ethyl ketone is constant throughout and a correction is made at each point for the absorption due to the ethyl alcohol. It is clear that Beer's law is not followed, for a constant concentration of the ketone would then yield constant optical density values. At one wave length the ethyl alcohol enhances the optical density, whereas it decreases it at another. The 5.82μ wave length is the carbonyl stretching band. This band might be expected to be affected by association between the carbonyl groups and the

Table III. Comparison between Analyses of a System of Oxygenated Compounds with and without Sodium Carbonate Treatment

	Untreated Sample			Treated Sample		
	Known, %	Observed, %	Diff., %	Known, %	Observed, %	Diff., %
Propionaldehyde	40	31.0	-9.0	40	37.8	-2.2
Methanol	30	33.7	+3.7	20	19.0	-1.0
Acetone	30	35.3	+5.3	40	43.2	+3.2
Average difference			6.0			2.1

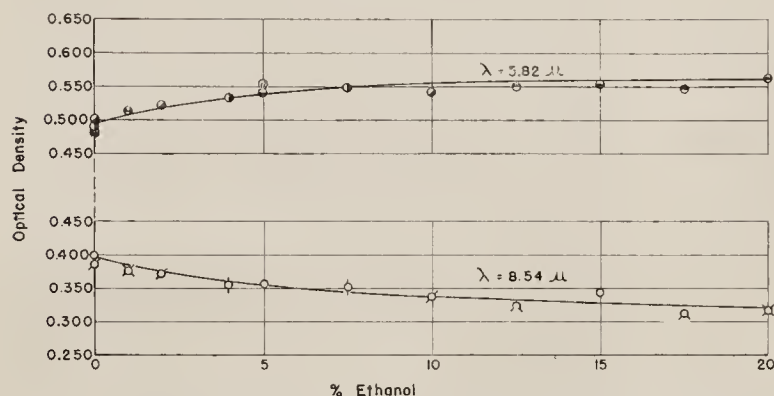


Figure 7. Effect of Concentration of Ethyl Alcohol on Optical Density of Constant Concentration of Acetone at Two Wave Lengths of Maximum Absorption

Methyl ethyl ketone. Solvent, carbon disulfide. 0.006-inch cell

hydroxyl groups of the ethyl alcohol. Such interactions have been reported and studied (30, 31). However, in the present case two factors indicate that the effects are not due to such association. One is that the wave length of maximum absorption for the carbonyl band does not change. Any association phenomenon strong enough to affect the intensity of absorption of a group vibration would be expected to change the resonant frequency. Another factor is that the 8.54μ band absorption decreases as the ethyl alcohol concentration increases, which is contrary to the expected behavior for a frequency perturbed by a hydrogen-bonded complex. The results shown in Figure 7 are typical of those obtainable for a number of combinations of ketones and alcohols.

In view of the slight acidity of alcohols it was postulated that the effect was of the nature of a ketone-alcohol equilibrium disturbance due to a change in ionic balance. Specific experiments have borne out the dependence of the effect upon the types of ions present. Accordingly, the calibration and sample systems were all made basic with an inorganic material. The effects of such treatment may be seen in Table III. Here are given the results of the analysis of a synthetic blend containing propionaldehyde, methanol, and acetone which was handled by the method described above for unassociated liquids. In addition are given the results for the analysis of the sample wherein the solutions were rendered basic in each case. It is seen that there is a great reduction of the differences between observed and calculated concentrations. Even with the treatment these differences are large. Nevertheless, they are satisfactory for some purposes and in view of the other undesirable phenomena that occur in such a mixture it is perhaps remarkable that an analysis is feasible. Other known phenomena occurring are: the formation of acetals by

reaction between the alcohol and aldehyde, hydrogen bonding, and differential evaporation rates.

The latter phenomenon can be troublesome in systems containing the low molecular weight alcohols in small concentrations. It is well known that the high boiling points of the simpler alcohols are due to the intermolecular attraction hydrogen-bonding forces (48). When the alcohols are present in small enough concentrations, these forces are inoperative and the relative rate of escape through evaporation is hastened. Hence, it is difficult to maintain a fixed level of concentration and special techniques are called for in the calibration and handling of such systems. A manifestation of this effect may be seen in Figure 8, in which are plotted the optical densities at 9.7μ , a characteristic band for methanol, for three different series of samples.

In each case the methanol concentration was constant and the percentage of acetone varied. In the top curve it is to be seen that the points scatter very much. These samples were prepared under ordinary conditions, with the materials being mixed by shaking in glass-stoppered bottles. As the scattering was ascribed to uncontrolled evaporation losses, the data for the middle curve were obtained by mixing the samples in cork-stoppered bottles. A definite improvement is observed. As a means of decreasing the scattering, the samples were next mixed in cork-stoppered bottles which were filled to the top and had glass beads added to provide agitation. This gave the data seen in the bottom curve. Two things are clear from this: the importance of a very careful handling technique and the fact that acetone has no association effects on the optical density of methanol at 9.7μ .

As further applications of molecular spectroscopy are made, the study of the more difficult systems and the development of methods for handling them will add much to the physical chemistry of liquid mixtures, particularly organic mixtures. In fact, a full understanding of some of the phenomena will be necessary before generalized analytical techniques can be outlined.

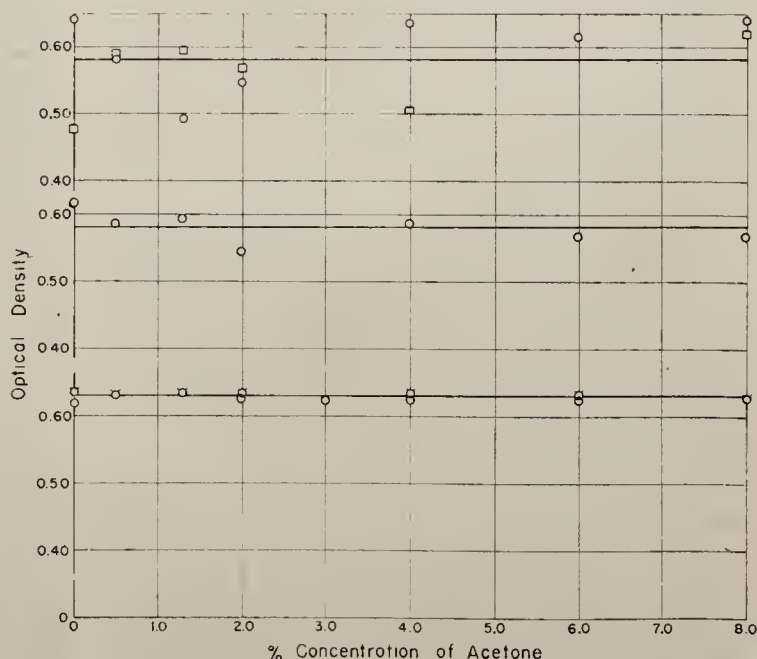


Figure 8. Optical Density of Constant Concentration of Methanol Plotted against Concentration of Acetone Present

Three experimental techniques of mixing

Group-Type Analyses. In group-type analyses the aim is to determine by a minimum number of observations the molal concentration of a particular atomic grouping such as hydroxyl, carbonyl, carboxyl, etc., in a sample. Two factors combine to make such analyses possible by infrared and Raman spectroscopy. One is the fact that, in the absence of molecular association, the absorption frequency of a particular group is essentially independent of the remainder of the molecule. This makes it possible to take data in a small wave-length span and to know that there will be a contribution to the absorption or to the Raman scattering from the same group in each molecular species present. The other factor is that the absorption per atomic group is approximately constant for all molecules containing the group.

Table IV. Determination of CH₃, CH₂, and Aromatic CH in Blends of Single-Ring Aromatics (35)

Aromatic Blend No.	No. of CH ₃ Groups			No. of CH ₂ Groups			No. of Aromatic CH Groups		
	Found	True	Diff.	Found	True	Diff.	Found	True	Diff.
A-1	1.02	0.99	0.03	0.35	0.33	0.02	5.09	5.16	-0.07
A-2	1.29	1.25	0.04	0.58	0.65	-0.07	4.99	4.85	0.14
A-3	1.64	1.46	0.18	0.88	0.98	-0.10	4.76	4.70	0.06
A-4	2.12	2.00	0.12	0.51	0.69	-0.18	4.23	4.29	-0.06
A-5	1.66	1.58	0.08	0.83	0.89	-0.06	4.61	4.51	0.10
Av. error in number of groups			0.09			0.09			0.09

This application may be said to have had its start in the early work of Rose at the National Bureau of Standards (51, 52). Working in the overtone region between 1.2 and 1.8 μ , he showed that the contributions to the optical density of the various functional groups on a molal basis are nearly constant in different hydrocarbons. Work in the overtone region has recently been extended by Hibbard and Cleaves (35), who have developed a method whereby the CH₃, CH₂, and aromatic CH concentrations may be determined in hydrocarbon samples. In this, they located characteristic bands in the 1.10 to 1.25 μ region at which molal absorption coefficients were determined for each of the groups. In Table IV may be seen the results of applying their method to a series of known blends containing single-ring aromatics. The results are in terms of average number of groups per molecule and the agreement between calculated and observed values is remarkably good.

The invariance of the absorption coefficient of a particular atomic group throughout a series of compounds may be seen from Table V, which gives the hydroxyl absorption coefficient for a series of alcohols and of phenols. The units in each case are arbitrary, as they depend upon cell thickness. For the alcohols the coefficients have been determined for concentrations in terms of moles per liter and for the phenols in terms of moles per gram.

Table V. Absorption Coefficients for Free Hydroxyl Band for Alcohols and Phenols

Alcohol	Coefficient	Phenol	Coefficient
Ethyl	62.4	Phenol	3.10×10^6
n-Propyl	65.9	o-Cresol	2.94×10^6
n-Butyl	64.8	p-Cresol	3.19×10^6
n-Amyl	62.8	2,4-Di-tert-butylphenol	3.02×10^6
n-Octyl	68.6	2,4,6-Tri-tert-butylphenol	2.89×10^6

Table VI. Comparison between Known Hydroxyl Content of Blended Samples and Observed Concentrations

Alcohol	Sample 1	Sample 2	Sample 3
	Moles per Liter		
Ethyl	5.7		3.4
n-Propyl	4.5	2.7	2.7
n-Butyl	3.6	2.2	2.2
n-Amyl	...	3.7	1.8
n-Octyl	...	1.2	1.3
Known hydroxyl	13.8	9.8	11.4
Observed hydroxyl	13.4	9.6	11.1
Error	0.4	0.2	0.3

These data were obtained at the 2.76 μ band (the free hydroxyl) in carbon tetrachloride solution and at concentrations below that necessary for hydrogen bonding.

The accuracy whereby such data may be applied to a determination of actual molal concentrations may be seen in Table VI, which gives the composition of blends containing alcohols and the concentrations calculated from infrared data.

Anderson and Seyfried (2) have recently reported extensive application of group-type analysis to the determination of alcohols, esters, carboxylic acids, ketones, and five different olefin types in hydrocarbon synthesis naphthas. The wave lengths (with the exception of the one for hydroxyl groups) they used are given in Table VII. Investigations of group-type analyses are being pursued concurrently in a number of places and future developments may be expected to yield increased precision of methods, more extensive applications, and a fuller understanding of the dependence of the second-order variations of the absorption coefficients on the remainder of the molecules. The Raman scattering coefficients are also invariant and an application of them for the determination of total olefin and aromatic content has recently been reported (34).

Molecular Structure Determination. It is possible in principle to derive mathematically the vibrational modes and frequencies of one molecule wherein the interatomic distances, bond angles, and force constants are known. However, this process is much too difficult and laborious for all but the simplest of molecules, and hence, spectra and known structure of most molecules must be correlated on a semiempirical basis. The converse of this correlation is of interest in molecular structure determination—i.e., to determine from an observed spectrum the structure of the material examined. In the application of infrared and Raman spectra this is done almost entirely by the use of diatomic and group-type frequencies.

Table VII. Characteristic Band Positions for Various Functional Groups (2)

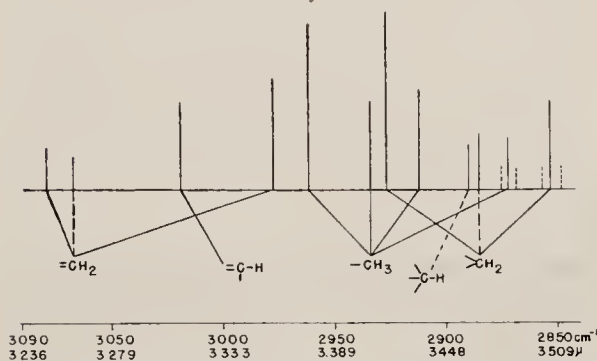
Functional Group	Wave Length, μ
CHO (aldehydes)	3.63 ± 0.01
COOH (acids)	3.82 (broad band)
COO (esters)	$5.71 \pm (0.01)^a$
CO (ketones)	$5.78 \pm (0.01)^a$
—O— (acetals and ethers)	8.8
Olefinic Group	
RCH=CH ₂	10.05, 10.98 \pm (0.02)
$\begin{array}{c} R_1 \\ \diagdown \\ C=CH_2 \\ \diagup \\ R_2 \end{array}$	11.24 \pm (0.02)
$\begin{array}{c} R_2 \\ \diagdown \\ C=CHR_1 \\ \diagup \\ R_1 \end{array}$	10.36 \pm 0.02
trans-R ₁ CH=CHR ₂	14.0–14.6 (variable)
cis-R ₁ CH=CHR ₂	
$\begin{array}{c} R_1 \\ \diagdown \\ C=CHR_2 \\ \diagup \\ R_2 \end{array}$	11.9–12.7 (variable)

^a Except for first few members of series.

In Equation 1 was given the vibrational frequency of a diatomic molecule in terms of the force constant and the reduced mass. This is applicable as a first approximation to the valence bond vibrations of diatomic groups in more complicated molecules. This rests upon the fact that such vibrations are roughly independent of the remainder of the molecule. Hence, all molecules containing CH groups will absorb in the neighborhood of 3.4 μ , all molecules containing C=O groups will absorb in the neighborhood of 5.7 μ , etc. This, of course, allows the empirical assignment of absorption bands to various groups on the basis of the spectra of homologous series. Once these assignments are established, they may be used in the examination of materials of unknown structure to determine the presence or absence of specific groups. In Table VIII may be seen a number of groups and the frequencies or wave lengths at which Raman scattering or infrared absorption is observed.

Table VIII. Fundamental Stretching Vibration Frequencies of Diatomic Groups

Group	Frequency, Cm. ⁻¹	Wave Length, μ	Group	Frequency, Cm. ⁻¹	Wave Length, μ
O—H	3680	2.7	C=O	1740	5.7
C—H	2920	3.4	C—O	1030	9.7
N—H	3350	3.0	C≡N	2090	4.8
C≡C	1970	5.1	C=N	1650	6.0
C=C	1620	6.2	C—N	1050	9.5
C—C	990	10.1	S—H	2600	3.6

**Figure 9. Infrared Absorption Frequencies Observed for Various Types of Carbon Hydrogen Groups in 3.4 μ Region (55)**

Based on data from (29)

In addition to these values the ones given in Table VII and as used for quantitative group-type analysis may be used, particularly for the determination of olefin substitution. The wave lengths of Table VIII are meant to represent the approximate centers of the spectral regions in which the different groups are observed. There may be considerable variation in how a particular group type absorbs. Although this may be a disadvantage in some cases, owing to overlapping of regions, it is an advantage in others in that it allows a further classification. For example, Barnes *et al.* (3) have shown absorption frequencies for five different types of compounds containing carbonyl groups—i.e., anhydrides, esters, acids, ketones, and aldehydes. Regularities, according to class, are observed which allow in some cases an assignment of a compound observed to contain a carbonyl group into one of the five classes. They have similarly discussed the aliphatic C=C and the aromatic ring frequencies. From the same laboratory has come one of the most complete assignment charts published (4). It gives not only the frequency values for almost all groups that may be reliably recognized by this technique, but the ranges of variation as well. Among the groups that may be identified by their data are those of Table VIII, and various types of aliphatic C—H groups, of phenyl ring substitution, of olefin substitution, etc.

An example of the variation observed for a particular diatomic group type may be seen in the work of Fox and Martin (29). They found in a study of hydrocarbons in the neighborhood of 3.4 μ that the spectra could be classified according to whether the C—H group was one of the following types: =CH₂, =C—H,

—CH₃, —C—H, and >CH₂. A diagram constructed from their

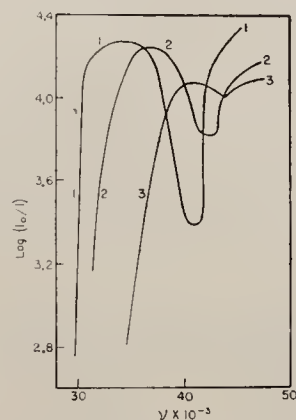
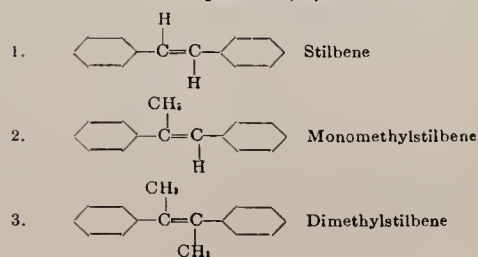
data may be seen in Figure 9. Here the dashed lines indicate frequencies that are not always observed. Such details of structure are of tremendous importance in some structure problems, in that by the use of them alone it is sometimes possible to choose between several alternative structures. The detail of structure illustrated by Figure 9 is not resolved by the ordinary rock salt infrared spectrometer, but required either a grating instrument or the

use of a prism of highly dispersing material such as lithium fluoride. It is expected that the further study of CH structure detail in molecules other than hydrocarbons will yield rules of very extensive use in the examination of other classes of organic materials.

Probably the most important single factor in the application of molecular spectra to problems of structure is experience. Fortunately, this may often be obtained by a gradual process, whereby the worker is able to learn and gain confidence by the recognition of the more easily established groupings. As his proficiency advances he must draw upon other sources of information than the mere location of absorption bands. He must know the selection rules whereby certain vibrations are forbidden in infrared spectra and others in Raman spectra. With the use of judgment, gained through experience, the investigator can often utilize to good advantage the shapes and intensities of the observed bands. The invariance of the intensities as used above in group-type analysis is often an aid in deciding whether a molecule may be singly or doubly substituted with a particular group. The information that may be supplied by the chemist as to the most probable structure from the chemistry involved is often invaluable, as it provides the initial direction of thought. The use of auxiliary chemical treatments whereby specific groups are either removed or added in preferred positions is often extremely useful. At the present time, infrared dichroism is very promising as another auxiliary technique (25). The use of recently developed selenium polarizers, either transmission or reflecting, makes the examination of materials with polarized infrared radiation practical. Differences of intensities of specific bands as a function of the angle of the electric vector of the incident radiation relative to the sample allow the determination of the orientation of the absorbing groups.

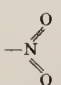



ULTRAVIOLET ABSORPTION SPECTROSCOPY

When radiant energy in the ultraviolet part of the spectrum, roughly 2000 to 4000 Å., is absorbed by a material, the energy is utilized for the excitation of the electronic energy levels. These involve the displacement of the valence bonding electrons and

**Figure 10. Steric Hindrance to Resonance between Conjugated Chromophores (42)**

the energies, of the order of 100 kg.-cal. per mole, are very much higher than those involved in the excitation of molecular vibration and rotational frequencies. The exact theoretical description of the electronic energy levels and associated phenomena is necessarily in the language and methods of quantum mechanics (43, 46), but for practical applications this approach is too difficult and complex for the usual analytical chemist. It is, therefore, very fortunate that there exists an empirical and descriptive theory which deals with the ultraviolet absorption in terms of absorption ascribable to specific atomic groupings. This theory, which might be called the chromophore theory, has been excellently described by Lewis and Calvin (42) and recently reviewed by Ferguson (27) and others (15).

Table IX. Chromophoric Groups and Characteristic Wave Lengths

Group	Wave Length, $m\mu$
C=O	280
—S—H	228
—N=N—	350
	366
	265
	311
	475

In this theory, the electric vector of the electromagnetic radiation induces oscillations of the valence electrons. Hence the more mobile or loosely bound are the electrons, the lower the frequency of absorption. This relates the absorption very closely to resonance, as resonating structures allow a greater mobility of the binding electrons than do saturated systems. Indeed, it is found that, in general, those materials known to possess resonance will absorb in the ultraviolet and visible spectral regions, whereas the nonresonating compounds are essentially transparent. An example of such a comparison is between the aromatics and the paraffins. The aromatics which possess the well-known resonance characteristics of the benzene ring possess characteristic ultraviolet absorption, whereas the paraffins are transparent throughout the visible and the ultraviolet down into the vacuum ultraviolet region below 2000 Å.

Empirical studies have shown that the ultraviolet absorption may be ascribed to certain atomic groupings called chromophores. An example is the benzene ring. All compounds containing it will possess absorption somewhere in the vicinity of 250 to 280 $m\mu$. Furthermore, in a homologous series such as the alkylbenzenes, for example, the spectra will all be very similar in spectral location, shape, and intensity. Such data show that the absorption is due to the unsaturation and resonance effects inherent in the benzene ring and is essentially independent of the alkyl substituents. Several common chromophores and the wave lengths characteristic of their absorption bands may be seen in Table IX. These wave lengths are not exact, but rather serve to locate the region of absorption.

The fact that the absorption is governed by the chromophores within the molecule results in ultraviolet spectra having distinct general properties in comparison to infrared and Raman spectra. For the latter two, a unique spectrum is found for each different

compound, whereas for the former the materials absorb according to class, which in this case is determined by the chromophoric constitution. This is both an advantage and a disadvantage. In analytical applications it means that the multicomponent analysis of systems of similar materials on the basis of their ultraviolet spectra is often not feasible. However, it is often possible to examine a mixture of several compounds and readily determine the concentration of a particular class.

When two chromophores are conjugated, the over-all resonance of the molecule is increased. The combination exhibits not only the absorption frequencies characteristic of the individual chromophores, but also a new and lower frequency. The situation is somewhat analogous to the joining of two segments of vibrating string. The new segment comprising the original two will possess a lower fundamental vibration frequency. Needless to say, this phenomenon of decrease of frequency with conjugation is a most valuable tool in determination of molecular structure. If there exists a condition which will tend to inhibit the resonance of the two chromophores together, the spectrum will revert toward that which is a mere superposition of the spectra of the individual chromophoric groups. An example of this may be seen in Figure 10.

In curve 1 is given the spectrum of stilbene. The low frequency band is due to the conjugation of the phenyl rings through the olefin group. In curve 2 is given the spectrum for monomethylstilbene. It is seen that the corresponding band has shifted to a higher frequency, as a result of the steric hindrance of methyl group to the coplanarity of the two phenyl rings. Curve 3 gives the spectrum for dimethylstilbene, and the effect is demonstrated to a greater degree—i.e., the two methyl groups inhibit the coplanarity of the two structures with a large resultant shift to higher frequencies. Such observations are at times very significant in locating the positions of substitutions relative to resonating structures.

Analytical Applications.

Most quantitative analytical applications of ultraviolet absorption are based on Beer's law of absorption as given in Equation 2. Deviations from Beer's law are not so frequently encountered in ultraviolet absorption as in infrared absorption. One reason for this is that the energies involved in electronic transitions are much greater than those involved in vibrational transitions and, hence, are less affected by low energy intermolecular interactions. Several notable exceptions do occur, however. Because materials of a given class possess very similar spectra, ultraviolet absorption is not a tool of wide applicability for the analysis of multicomponent mixtures of similar compounds.

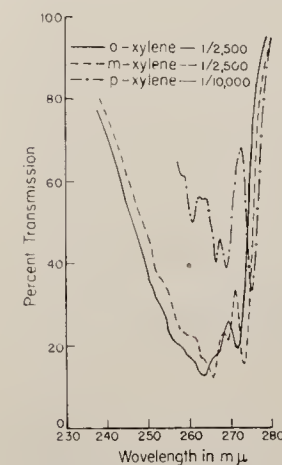


Figure 11. Ultraviolet Absorption of *o*-, *m*-, and *p*-Xylenes

Figures give dilution factors for materials in iso-octane solution (15)

Exceptions to this occur, of course, and one of particular importance is the analyses of mixtures for the light aromatics: benzene, toluene, ethylbenzene, *o*-xylene, *m*-xylene, and *p*-xylene. Although these all possess the phenyl ring chromophore absorption, there are second-order differences due to the different substitutions. These are sufficient to allow choice of wave length for each compound and the use of simultaneous equations as described above. An idea of the similarity of spectra may be attained from Figure 11, which gives the per cent transmission plotted against wave length for the xylene isomers. The numbers give the dilution ratios, and it is noted that the *p*-xylene

Table X. Comparison between Blended and Observed Aromatic Concentrations (15)

Compound	Blended, %	Observed, %	Difference, %
Benzene	7.7	7.4	-0.3
Toluene	15.4	15.1	-0.3
Total aromatics	23.1	22.5	-0.6
Benzene	0.5	0.6	+0.1
Toluene	2.0	2.1	+0.1
Ethylbenzene	0.5	0.3	-0.2
Total aromatics	3.0	3.0	0.0
Ethylbenzene	0.5	0.6	+0.1
<i>o</i> -Xylene	1.5	1.3	-0.2
<i>m</i> -Xylene	4.0	4.5	+0.5
<i>p</i> -Xylene	4.0	4.2	+0.2
Total aromatics	10.0	10.6	+0.6

absorbs with approximately twice the intensity of the others. This is a general characteristic of para substitution. Because of the very intense absorption displayed by most absorbing materials it is necessary to use rather dilute solutions in such nonabsorbing solvents as iso-octane or other paraffins when working with absorption cells with thicknesses of the order of 1 cm. This is the standard cell thickness for the Beckman quartz spectrophotometer (12), which is without doubt the most widely used instrument of this type today. Working in such dilution ranges calls for careful operation and cleanliness of glassware, cells, etc.

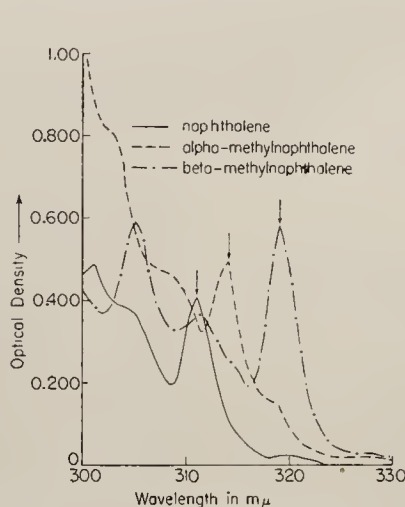


Figure 12. Ultraviolet Absorption Spectra (16)

Although wave lengths may be chosen for each of the six aromatics named, the differences are not great enough to give good optical discrimination. As a result, it is necessary that a sample be subjected to distillation to reduce the number of aromatics in any one sample. This can be done by making a benzene cut, a toluene cut, and a xylene cut, each of which is analyzed for the compounds named plus those boiling nearby. In this manner, satisfactory accuracy is achieved. Typical results may be seen in Table X, which compares the blended and observed concentrations for several synthetic samples.

Individual concentrations of the heavier alkylbenzenes cannot be determined without severe fractionation, because of the multiplicity of the higher aromatics and their closely grouped boiling points. It is possible to make several cuts through the C_9 aromatic range and by suitable groupings to get satisfactory total aromatic content. Satisfactory determinations of naphthalene in mixtures boiling in the kerosene range may be made by use of the characteristic absorption of the naphthalene chromophore (1, 13, 16). This absorption occurs in the 300 to 320 $m\mu$ range, in which the mononuclear aromatics possess no characteristic

bands. In samples containing high concentrations of the mononuclear aromatics, there will be a certain amount of background absorption. Suitable correction may be made for this by the use of the shapes of the absorption bands. In somewhat higher boiling cuts naphthalene, 1-methylnaphthalene, and 2-methylnaphthalene may be determined simultaneously. The spectra for these three compounds may be seen in Figure 12. Here again we have the situation of the absorption in each case being due to a common chromophore and yet there being enough differences to allow a multicomponent analysis. The arrows in Figure 12 indicate the wave lengths used for calculation, and the concentrations are determined by a set of simultaneous equations based on Beer's law of absorption as described above. Ultraviolet absorption is readily extended for the calculation of the anthracene and phenanthrene concentrations. In each case, the absorption is due to a chromophore formed by several condensed ring aromatics. Total concentrations of dimethyl and ethylnaphthalenes may be reliably estimated, but the calculation of the individual components is not practical without severe fractionation.

The localization of the absorption in specific chromophores is responsible for one of the most distinguishing features of analysis by ultraviolet absorption, especially in contrast to infrared and Raman spectroscopy. It often allows the determination of one or a class of compounds in a mixture independent of the remainder. During the war it was used extensively for the determination of butadiene (6, 53) in C_4 hydrocarbon fractions. This is possible because of the conjugated diolefin chromophore, which has an onset of absorption at about 235 $m\mu$. The same chromophore makes possible the determination of pentadienes (47), hexadienes, etc. Many other examples could be cited wherein the absorption due to a chromophoric group is utilized to determine one compound or class of compounds in a mixture. The carbonyl chromophore allows the determination of ketones in the presence of other organic materials. Distilled water is very transparent throughout the ultraviolet region and makes an excellent solvent when it can be used. The simple alcohols are also transparent and suitable for solvents. In going to the higher alcohols, one may encounter impurities in the form of organic acids which render the material unsuitable, owing to the heavy absorption by the carboxyl group in the shorter wave lengths.

Other examples include the determination of styrene in hydrocarbon mixtures. Because of the conjugation of an olefin group, which as a true chromophore possesses absorption at about 190 $m\mu$, with the benzene ring a new band near 290 $m\mu$ appears. This allows a precise determination of styrene in the presence of alkylbenzenes. Furfural may be determined in gas oils, although in such a case there may be considerable absorption due to the oil itself. To correct for it suitably may necessitate an examination of the furfural-free oil. By virtue of the phenyl ring absorption and the variations due to substituent changes, it is possible to determine phenol and the isomeric cresols (50) and aniline, *N*-methylaniline, and *N,N*-dimethylaniline (62).

In the chemistry of materials from natural sources the technique of ultraviolet absorption has been very valuable, particularly in the study of the fatty acids. Brode and co-workers (10) have described a method of determining the amount of two, three, and four double bond conjugation in the presence of nonconjugated unsaturated fatty acids. Other workers have reported an ultraviolet absorption method for the determination of polyunsaturated constituents in fatty materials (9), a relationship between unsaturation and ultraviolet absorption spectra of various fats and fatty acids (5), and data for isomerized arachidonic and linolenic soaps in fatty materials. Ultraviolet absorption has also been used for the determination of vitamin A in margarine (44), and in the study of the changes during oxidation of vitamin A oils (33). A spectrophotometric method for the determination of α -eleostearic acid in tung oil has been described (46).

Molecular Structure Determination. Because compounds absorb in the ultraviolet according to chromophores, the technique

of ultraviolet absorption is particularly useful in the classification of materials of unknown structure. The spectrum of the unknown material is obtained and regions of maximum absorption are ascertained for comparison with tables of results for known chromophores such as those given in Table IX.¹ This may be sufficient, for example, to determine whether the compound is a mono-, di-, trinuclear, etc., aromatic; whether it may contain the conjugated diolefin structure, a mercaptan group, a nitro group, etc.; or whether it may possess two chromophores arranged in conjugation. It is well known that the conjugation of two chromophores results in the appearance of new bands at longer wave lengths. Ordinarily, the interpretation of the ultraviolet spectra is greatly aided by information available from other sources, such as predictions based on the synthesis of the materials, the history of any treatments, and the results of auxiliary chemical tests. Such information is usually adequate to remove the ambiguity which may result if a material exhibits absorption that may be ascribed to either of two chromophores. This latter is not an unusual situation, because the bands for the more highly substituted materials are generally very broad.

Once the material is classified according to chromophore, further information may be deduced from the shape, intensity, and detailed location of the bands. For example, para substituted aromatics are known to be very strong absorbers in comparison to ortho and meta substituted ones. As the complexity of the substituents increases, the detailed structure of the bands for alkyl-benzenes and polar substituted aromatics disappears. The structure of a band—i.e., the appearance of a number of maxima—results from the multiplicity of vibrational transitions that may accompany an electronic transition. An increase of complexity of substitution effectively increases the number of allowable vibrational transitions which may overlap at the expense of the detailed structure. A rather voluminous literature exists on the empirical interpretation of ultraviolet spectra; review articles by Lewis and Calvin (42) and by Ferguson (27) and the detailed studies of aromatic systems by Jones (40) are recommended. As in the case of infrared and Raman spectroscopic studies, the experience of the investigator is of great importance, for he will be able to deduce valuable information from other characteristics, such as shape and size, than the wave lengths of maximum absorption.

The use of various solvent effects is valuable for augmenting the information available from the spectra. By solvent effects are meant the changes in spectra that occur when the material is examined in various solvents. Three of these can be mentioned: ionization, wave-length shifts depending upon localized interaction between the solute molecules and the solvent, and wave-length shifts that are nonspecific in the sense of not depending

upon definite, localized atomic groupings in the solute molecules. Many polar substituted aromatics exhibit very large shifts to the red of their absorption maxima when examined in basic or acidic solution. The shifted spectra are really not due to a perturbation of the energy levels of the solute molecules, but are rather the spectra of the ionized materials. In this manner, it may be readily determined whether a substance of unknown or questionable structure is itself acidic or basic in nature by observing which type of solvent produces a large shift of the spectrum. For this type of investigation distilled water to which has been added either an inorganic acid or base is a satisfactory solvent in many cases. As examples of such applications, Ewing and Steck (26) have recently utilized the technique in their studies of the acidic and basic properties of quinolinols and isoquinolinols and Irvin and Irvin (39) have made similar studies of various 4-amino-quinolines. In addition to indicating whether the solute material is acidic or basic, the behavior of the ion spectra may be utilized to determine substitution.

It has recently been determined (17) that the classes of substituted phenols vary a great deal in their activity. The unhindered phenols—i.e., those with small or no substituents on the ortho positions—are relatively acidic. The partially hindered phenols—i.e., those with a bulky substituent such as a *tert*-butyl on one ortho position—are much less acidic, whereas the hindered phenols—i.e., those with both ortho positions occupied by large substituents—are very much less acidic. These behaviors are demonstrated in Figure 13. Here are seen the spectra for one of each type of phenol under various solvent conditions. The concentration of sodium hydroxide which produces a complete shift of spectrum for the unhindered phenol produces an incomplete shift for the partially hindered phenol, and the concentration which produces a complete shift for the latter produces only a partial shift for the hindered phenol. Such results demonstrate the very strong hindering effects of the ortho positions and show how the ionization behavior may be used to gain information concerning the ortho substituents. This ionization behavior allows the same sample to be analyzed for both phenols and aromatics, inasmuch as the spectra for the two are separated by the use of the sodium hydroxide solution.

Another phenomenon whereby the ortho substitution may be assayed is the wave-length shifts attendant to short-range intermolecular interactions. If a simple phenol is examined in ethyl alcohol solution, its spectrum is shifted to the red in comparison to its behavior in a nonpolar solvent such as a paraffin. This shift is known to be due to an interaction between the hydroxyl groups of the solute molecules and the solvent molecules (19). When the positions ortho to the hydroxyl group are occupied by large groups such as *tert*-butyl the shift is practically eliminated,

because the hydroxyl group of the phenol is hindered from attaining close proximity with the polar solvent molecules. This effect is demonstrated in Figure 14. It is obvious that such data can be used to determine the presence or absence of large ortho substituents in materials of unknown composition.

The other solvent effect mentioned is nonspecific, in so far as it does not depend upon the presence of a particular acidic, basic, or polar group in the solute molecule. It is the result of electronic polarization interactions between the resonant system of the absorbing molecule and the solvent

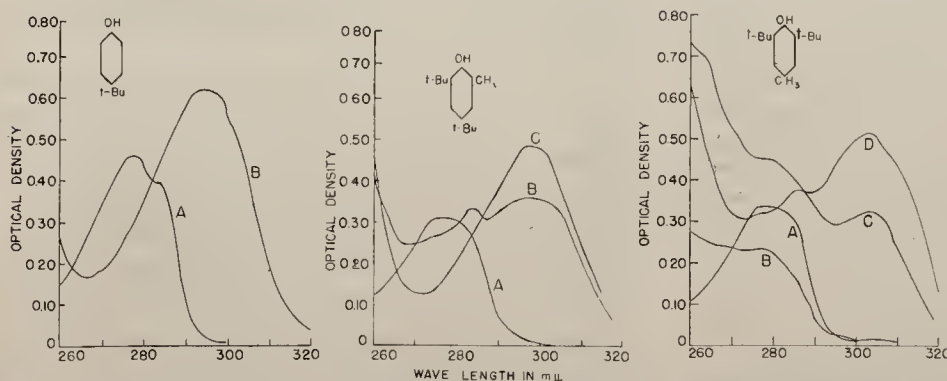


Figure 13. Ultraviolet Absorption Spectra of *p*-*tert*-Butylphenol, 2-Methyl-4,6-di-*tert*-butylphenol, and 2,6-Di-*tert*-butyl-4-methylphenol (17)

- A. Ethyl alcohol
- B. Ethyl alcohol plus 1.0×10^{-1} mole per liter of sodium hydroxide
- C. Ethyl alcohol plus 5.0×10^{-1} mole per liter of sodium hydroxide
- D. Ethyl alcohol plus 5 moles per liter of sodium hydroxide

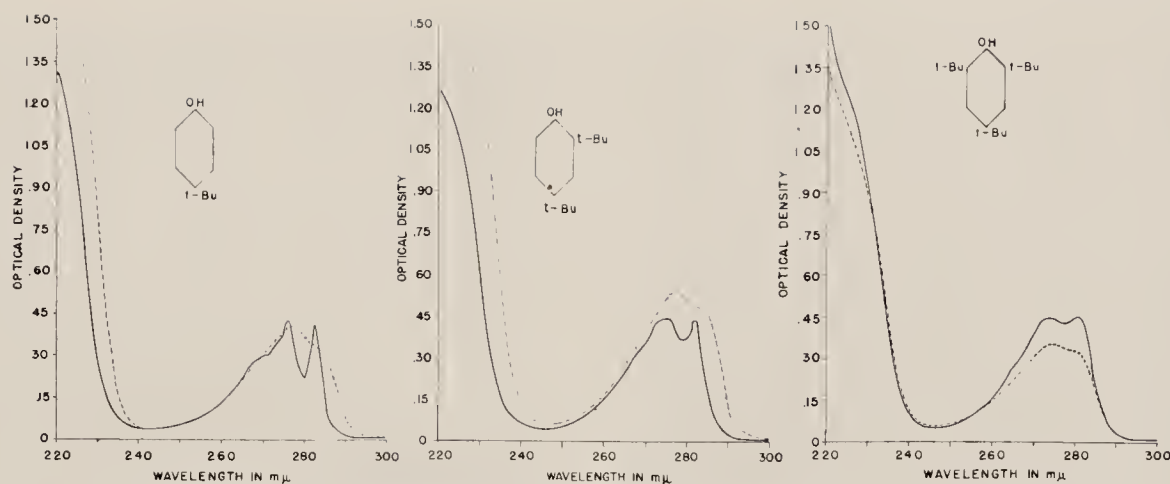


Figure 14. Ultraviolet Absorption Spectra of *p*-*tert*-Butylphenol, 2,4-Di-*tert*-butylphenol, and 2,4,6-Tri-*tert*-butylphenol (19)

Solid curve, iso-octane solution; dashed curve, ethyl alcohol solution

molecules. It is strong for the polynuclear aromatics. The effect may be seen in Figure 15, which shows the large wavelength changes observed for naphthacene when examined in benzene as contrasted with the spectrum obtained in iso-octane solution. When precise values for wave lengths of maximum absorption are being obtained, it is therefore necessary to consider the solvent in which the material is being examined.

In the over-all picture, ultraviolet absorption, despite its particular advantages, must be regarded as a somewhat less powerful tool for structure determination than infrared absorption or Raman spectra. One major reason for this is that many compounds possess no ultraviolet absorption at all and the technique is, therefore, powerless for them. The number of known and well established chromophores is fairly small and there is considerable overlapping of the bands observed for them. Of course, the fact that the absorption depends essentially upon the chromophore and not upon the remainder of the molecule imposes limitations on the deduction of detailed information. For best results, the ultraviolet technique should be used in conjunction with infrared or Raman spectroscopy. In this manner, they complement each other and the solution of many problems is greatly simplified.

MICROWAVE SPECTROSCOPY

In the gas phase, molecules possess discrete rotational energies. This was first observed in the fine structure of infrared absorption bands wherein transitions occur simultaneously between vibrational and rotational levels. The energies involved in the rotational states are small and the energy differences between states are so minute that they generally cannot be directly observed with any standard optical equipment. Until the development of radar in World War II, the spectral region in the neighborhood of 1-cm. waves was inaccessible for precise experimental investigations. Therefore, many rotational bands were not discovered and measured until very recently. Since the war, there has been a great burst of activity in microwave spectroscopy in both industrial and academic institutions and there has been continuous progress both in the number of compounds investigated and in improvements of equipment and technique.

In simplest terms, the method consists of passing electromagnetic waves in the microwave region through a sample of material and observing the frequencies at which absorption occurs and the intensities of absorption. The material must be examined in the gas phase because of very severe pressure broadening. This is a

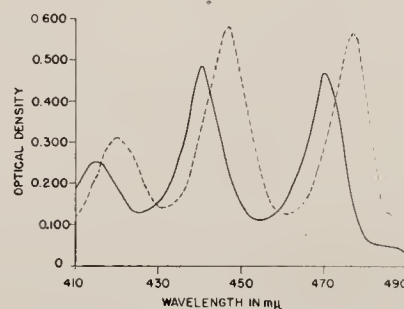


Figure 15. Ultraviolet Absorption Spectra of Naphthacene

Solid curve, iso-octane solution; dashed curve, benzene solution

result of the fact that satisfactorily to observe transitions involving such small energies, relatively long intervals between collisions are necessary. The source of radiation is a microwave generator which produces monochromatic radiation. The wave length is changed either by changing generators or by changing operating conditions. This is simpler than most molecular spectroscopy work wherein the source generates a spread of wave lengths from which a monochromator isolates a narrow region. The sample being investigated is contained in a wave guide which may be several meters in length and at a pressure of the order of 1 mm. of mercury or less.

The rotational absorption frequencies depend only upon the moments of inertia of the molecule. Each absorbing molecule displays a set of lines that is similar to the emission lines from the elements. As the microwave region is broad and excellent resolution is obtainable, the technique looks very favorable for the identification and measurement of specific compounds in mixtures on the basis of individual absorption lines. This has been pointed out by Dailey (23), who estimated that, in principle, 1000 different organic compounds could be quantitatively determined from a sample smaller than 1 microgram. That is a very exciting picture, but it must be tempered with a realization of the limitations of the method. In the first place, only molecules possessing permanent dipole moments will have pure rotational spectra. This immediately eliminates many desirable applications. Furthermore, many compounds of high molecular weight cannot be observed because of low vapor pressures or very low absorptions resulting from their large diameters. The use of

wave guides with metal surfaces also introduces difficulties due to corrosion and to the adsorption of the material on the wall surface.

Microwave spectroscopy is particularly suited to the special analytical problem of determining relative abundances of isotopic species. With a change of mass of one of the constituent atoms there is often a large change in observed rotational frequencies. Because the individual lines may be correlated with molecules containing the individual isotopic species, there results an excellent technique for determining the abundance of each. It is probable that this method may supplant the use of the mass spectrometer for this purpose in many cases.

MASS SPECTROMETRY

In the mass spectrometer, a completely different phenomenon from those discussed above is utilized. In it the material under investigation is subjected to electron bombardment in the gas phase. As the kinetic energies of the electrons are larger than the sum of individual bond and ionization energies, the molecules are disintegrated into ionized fragments by impact. By a system of electrodes the ions are formed into a beam which then passes through a magnetic lens. This accomplishes a separation of the ionic species according to mass. This allows a mass spectrum, a plot relating the number of ions as a function of mass, to be obtained. Unlike compounds provide different mass spectra, and the differences in the spectra provide the basis of the analytical applications. It is probable that in no other tool of molecular spectroscopy are so many diverse devices of modern technology utilized. As a number of review articles (18, 38, 64) have adequately discussed the details of theory, construction, and operation of this instrument, no account of them is given here. An outline of the over-all processes may be seen in the flow diagram of Figure 16.

The ion current obtained for a particular mass is linearly dependent upon the partial pressures of all compounds present in the sample which may contribute to it. This makes it possible to obtain data for a set of ion peaks and to set up linear algebraic equations of the type given in Equation 3 relating the ion currents to the concentrations of the constituent compounds. The coefficients, which give the dependence of the ion currents on the concentrations of the individual compounds, are obtained by examination of the latter in pure state. When these are obtainable, the equations may be solved, thus yielding the analysis.

The gas is admitted to the ionization region where the pressure is of the order of 10^{-6} mm. of mercury through a leak from a chamber wherein the pressure is of the order of 0.3 mm. of mer-

cury. In the ionization region the material must be in the gas phase. This places a limitation on the use of the device for the less volatile materials. Although it is possible to place a sample in a furnace within the ion source in order to produce a gas that may be ionized, this is a very special procedure and requires an instrument modified for the purpose. In this way, Hickam (36) has detected the impurities in copper with a sensitivity of 1 p.p.m. with 2-mg. samples.

The mass spectrometers that are used for extensive analytical work are equipped with automatic recording equipment. This suitably varies the electric or magnetic field so that the material is "scanned"—i.e., all the ionic species are successively brought to the detector, so that the mass spectrum, a plot of ion current as a function of mass, is automatically obtained. In view of the complex nature of some of the gas samples examined, this is done in a very short time. Complete sample time in the instrument including introduction, scanning, and removal may vary from 10 to 20 minutes. This rapidity of sample processing has been a most important factor in establishing this instrument in its present eminent place. It allows a mass spectrometer group using one instrument on one or several shifts per day to analyze several hundred gas samples per week.

The ionizing electrons are given an energy sufficient to ionize all types of molecules. Hence, if a compound is present in the sample in adequate concentration, data for it will be included in the recorded spectrum. If other materials contribute ions at the same masses, its presence may be evident only after calculation. However, multitudinous examples exist wherein the presence of a particular compound may be established from a single ion peak. In the case of polar materials, there is often difficulty in obtaining correct quantitative results due to adsorption of the material on the internal surfaces. However, indications are almost always recorded and there results a completeness of record, in the sense of acquiring data for all compounds present, that is hardly matched by any other gas analysis tool.

Gas Analysis. The analysis of gaseous mixtures is, in general procedure, very similar to the analysis by infrared absorption. The pure materials known to be present in the sample are scanned, masses chosen at which analytical data will be taken, and the corresponding calibration values determined. These are then applied to the data obtained for the mixtures through the system of linear equations mentioned and the individual concentrations are calculated. It is in gas analysis that the mass spectrometer has been economically the most important. It allows a considerably larger load of samples to be handled with a

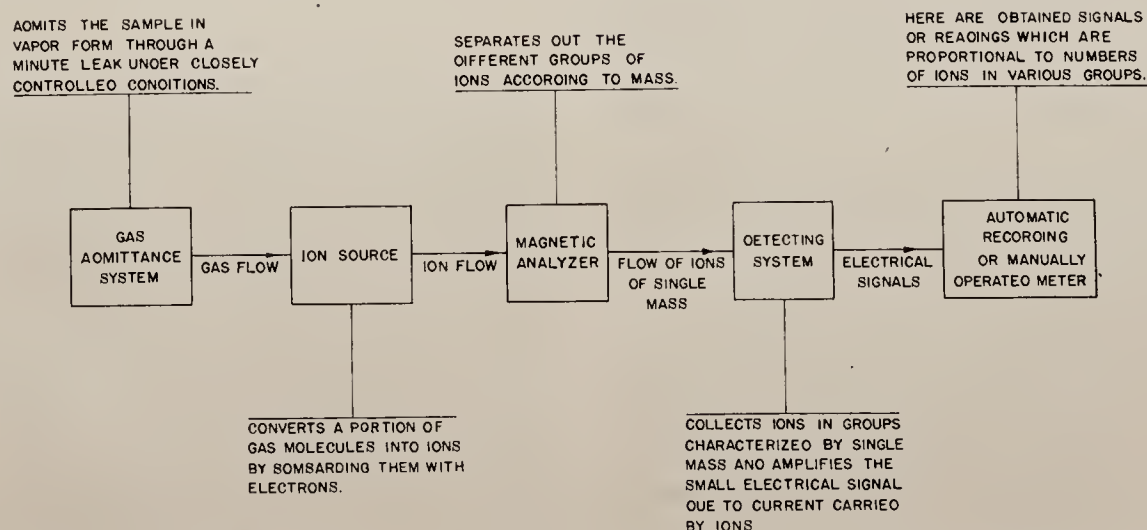


Figure 16. Block Diagram Demonstrating Steps and Process Utilized in a Recording Mass Spectrometer

Table XI. Comparison between Blended and Calculated Concentrations for Paraffin-Olefin Mixtures (64)

	C ₁ -C ₅ , %			C ₂ -C ₆ , %			C ₃ -C ₇ , %		
	Syn.	Calcd.	Diff.	Syn.	Calcd.	Diff.	Syn.	Calcd.	Diff.
H ₂	3.0	3.2	+0.2
Methane	10.8	10.3	-0.5
Ethylene	6.0	5.9	-0.1
Ethane	6.0	5.8	-0.2
Propene	11.1	11.1	0.0	12.5	13.1	+0.6	13.2	13.4	+0.2
Propane	19.2	19.5	+0.3	24.8	24.9	+0.1	25.9	26.4	+0.5
Isobutane	20.1	20.0	-0.1	25.0	25.0	0.0	25.6	25.6	0.0
Isobutene	2.8	1.6	-1.2	3.8	3.6	-0.2	4.1	3.0	-1.1
n-Butene	2.9	4.1	+1.2	5.4	5.3	-0.1	5.4	6.5	+1.1
n-Butane	5.0	5.2	+0.2	7.5	7.7	+0.2	7.6	7.8	+0.2
Isopentane	10.1	10.2	+0.1	6.4	6.4	0.0	6.7	6.5	-0.2
Pentenes	3.0	3.1	+0.1	8.2	7.5	-0.7	4.9	4.6	-0.3
n-Pentene	6.4	6.5	+0.1	6.6	6.2	-0.4

smaller personnel than previously and the analyses are usually more complete and accurate. The petroleum industry uses this device more extensively than others. An example of the type of gas sample for which it is particularly valuable is one containing C₆ and lighter paraffins and olefins. In addition, it may contain hydrogen, oxygen, nitrogen, and carbon dioxide. Such a sample may be completely processed with a total operator time of the order of 1.25 hours, including the calculations. In Table XI may be seen a comparison between blended and calculated compositions for several samples.

It is to be noticed that in Table XI the pentenes are lumped together and the poorest accuracy was for the butenes. This is due to the close similarities of the mass spectra of the butenes as a class and of the pentenes as a class. It is, therefore, oftentimes common practice to lump the butenes in routine samples as well as the pentenes.

There is more difficulty in the analysis of polar gas due to adsorption effects. Such effects occur for sulfur dioxide, hydrogen sulfide, water, methanol, etc. In a few cases there is difficulty in attaining high accuracy, because the material has a low ionization efficiency, coupled with the fact that other compounds contribute ions of the same mass. Carbon monoxide is such an example. At its parent mass of 28, ion current contributions are given by nitrogen and by all hydrocarbons above acetylene in molecular weight. At mass 16 methane interferes and at mass 12 all the hydrocarbons plus carbon dioxide interfere. At apparent mass 14, at which the doubly charged ion of mass 28 appears, contributions come from nitrogen and all the hydrocarbons. Improvement in accuracy in such a case can come only by increased precision of measurements. However, for the polar gases, great improvement is being made by conditioning the instrument for a sample, introducing the sample almost directly into ion source, and heating the inlet systems. A number of gas analysis applications are described below in connection with elemental and isotope distribution measurements. An interesting analysis of the volatile products of metabolism, wherein several oxygenated compounds were found, has recently been reported (24).

Liquid Analysis. Any liquid sample that is examined by the mass spectrometer must be vaporized before passing through the leak into the ionization chamber. This limits the application to liquids possessing a vapor pressure of the order of 0.2 mm. of mercury or higher at room temperature. Raising the temperature of the inlet system allows less volatile liquids to be examined, but is to be avoided as a general practice. The general procedure for multicomponent analysis—the scanning of pure compounds, selection of masses, determination of calibration values—follows the same lines as for gases. The introduction problem is considerably more difficult for liquids than for gases. If the materials have vapor pressures of the order of 1 cm., reasonably accurate results may be obtained by vaporizing a sample into a standard volume and measuring the pressure with a manometer. For the lower pressures, the accuracy drops off and it is desirable to

vaporize totally a known volume or mass of material. This is very satisfactorily done by means of sintered-glass valves (11, 58, 59). In this technique a sintered-glass disk is covered with mercury. As the mercury cannot pass through the disk, a vacuum may be maintained on the opposite side. If a small-bore pipet is brought through the mercury and into contact with the sintered disk, the fluid contained therein may pass through the disk and be vaporized into the evacuated space. This makes it possible to inject known amounts of fluid simply and to avoid the absorption of the heavy molecular weight materials by the stop-cock greases.

As in the case of gas analysis, the petroleum industry probably makes the most extensive application of the mass spectrometer to liquid analysis problems. Surprising accuracy is attainable for hydrocarbon analysis, and the technique adds a tool of great power in the detailed analyses of mixtures in the gasoline range. In working with oxygenated and other polar compounds, the difficulties may, of course, be even more serious than for the polar gases, owing to the higher molecular weights. However, very promising results are now being obtained on mixtures of such materials by the use of special introduction systems and techniques (22). An idea of both the scope and precision of the method for liquid hydrocarbon analyses may be obtained from Table XII, which gives a comparison between blended and calculated concentrations for a mixture of C₇ paraffins. Considered in terms of the number of compounds handled, the fact that they are all isomers, and the relative newness of the method, the results are rather astonishing.

Table XII. Comparison between Blended and Calculated Composition of a Mixture of C₇ Paraffins (11)

Component	Known Composition	Determined Composition		Mean Difference	
		<i>Mole per cent</i>			
2,2-Dimethylpentane	3.5	} 5.7	5.8	5.7	0.1
2,2,3-Trimethylpentane	2.2				
2,4-Dimethylpentane	50.7	48.9	49.3	1.6	
3,3-Dimethylpentane	1.9	1.9	1.8	0.1	
2,3-Dimethylpentane	31.7	33.0	33.6	1.6	
2-Methylhexane	1.7	1.3	0.9	0.6	
3-Methylhexane	3.8	4.6	3.0	0.8	
3-Ethylpentane	1.8	1.6	2.5	0.5	
n-Heptane	1.3	1.6	2.0	0.5	
2,2,4-Trimethylpentane	1.4	1.3	1.2	0.2	
Total	100.0	100.0	100.0		

Elemental and Isotope Dilution Analyses. The availability of the enriched stable isotopes in recent years has given the research worker a new tool for the tagging of molecules through synthesis. What is perhaps less commonly known is that it has made possible new analytical techniques for some very difficult analyses. Rittenberg (49) has described his isotope dilution method as applied to the determination of amino acids in proteins. It has been found that the determination of a particular protein, by standard chemical means, depends upon its isolation in the pure state and in quantitative yield from the protein hydrolyzate. Unfortunately, these two requirements are mutually contradictory. In the isotope dilution method, only one requirement—namely, isolation in the pure state—need be met. In this method a small amount of the amino acid sought, which has been synthesized with an excess of the heavy isotope N¹⁵, is added to the hydrolyzate. In all subsequent operations the added amino acid and the same amino acid originally in the hydrolyzate are chemically inseparable. A small sample is isolated and degraded and the N¹⁵/N¹⁴ ratio is determined. This ratio, together with

the ratio for the naturally occurring material, the ratio for the added amino acid, the weight of the added amino acid, and the weight of original hydrolyzate, may be used to calculate the amount of the amino acid in the latter.

Grosse and his associates (32) have utilized this method in some very promising elemental analysis for carbon, oxygen, and nitrogen in organic compounds. For the oxygen determinations they utilized material enriched in O^{18} , for carbon they used material enriched in C^{13} , and for nitrogen they used material enriched in N^{15} . Instead of isolating some of the same type of material as was added, they subjected the material to temperatures above red heat and examined the pyrolysis products. They were able to show that equilibrium distribution among the isotopes was achieved even in the absence of complete combustion. Thus, in the determination of oxygen, it was only necessary to obtain data for some of the carbon dioxide obtained. Examples of the agreement between known and observed concentrations of oxygen in several compounds may be seen in Table XIII.

A somewhat similar method for the analysis for nitrogen, but without the use of enriched isotopes, has been reported by the same group (37). In this procedure nitrogen was formed by copper oxide reduction of the sample with subsequent reduction of the oxides by metallic copper. The nitrogen was then determined relative to the concentration of neon which had been added as an internal standard. This method obviates the use of the rather expensive enriched isotopes. A quantitative recovery of the gases is not necessary, as the ratio of nitrogen to neon is constant. With this procedure they achieved satisfactory agreement with known materials, among which were such compounds as pyridine, quinoline, indole, carbazole, and nitrobenzene.

Table XIII. Determination of Oxygen by the Isotope Dilution Method (32)

Analysis No.	1	2	3	4	5
Substance analyzed	Formic acid	Formic acid	Acetic acid	1-Nitroethane	Ethyl ether
Observed % oxygen	70.8	69.8	53.4	40.3	19.8
Known % oxygen	69.5	69.5	53.3	42.6	21.6

ACKNOWLEDGMENT

Acknowledgment is gratefully made to Miss E. L. Saier and A. S. Glessner, Jr., for aid in obtaining part of the data used, to M. Muskat for discussion of various subjects, and to Paul D. Foote, executive vice president of Gulf Research & Development Company, for permission to publish this material.

LITERATURE CITED

- Anderson, J. A., *Oil Gas J.*, 47, No. 28, 264 (1948).
- Anderson, J. A., and Seyfried, W. D., *ANAL. CHEM.*, 20, 998 (1948).
- Barnes, R. B., Gore, R. C., Liddel, Urner, and Williams, V. Z., "Infrared Spectroscopy," New York, Reinhold Publishing Corp., 1944.
- Barnes, R. B., Gore, R. C., Stafford, R. W., and Williams, V. Z., *ANAL. CHEM.*, 20, 402 (1948).
- Barnes, R. H., Rusoff, I. I., Miller, E. S., and Burr, G. O., *IND. ENG. CHEM., ANAL. ED.*, 16, 385 (1944).
- Beckman, A. O., *Petroleum Engr.*, 16, No. 4, 173 (1945).
- Benning, A. F., Ebert, A. A., and Erwin, C. F., *ANAL. CHEM.*, 19, 867 (1947).
- Brattain, R. R., Rasmussen, R. S., and Cravath, A. M., *J. Applied Phys.*, 14, 418 (1943).
- Brice, B. A., and Swain, M. L., *J. Optical Soc. Am.*, 35, 532 (1945).
- Brode, W. R., Patterson, J. W., Brown, J. B., and Frankel, J., *IND. ENG. CHEM., ANAL. ED.*, 16, 77 (1944).
- Brown, R. A., Taylor, R. C., Melpolder, F. W., and Young, W. S., *ANAL. CHEM.*, 20, 5 (1948).
- Cary, H. H., and Beckman, A. O., *J. Optical Soc. Am.*, 31, 682 (1941).
- Cleaves, A. P., Carver, M. S., and Hibbard, R. R., *Natl. Advisory Com. Aeronaut., Rept. TN 1608* (1948).
- Coggeshall, N. D., *J. Am. Chem. Soc.*, 69, 1620 (1947).
- Coggeshall, N. D., "Physical Chemistry of Hydrocarbons," ed. by A. Farkis, Chaps. 4 and 5, New York, Academic Press, 1950.
- Coggeshall, N. D., and Glessner, A. G., Jr., *ANAL. CHEM.*, 21, 550 (1949).
- Coggeshall, N. D., and Glessner, A. G., Jr., *J. Am. Chem. Soc.*, 71, 3150 (1949).
- Coggeshall, N. D., and Hipple, J. A., "Colloid Chemistry," ed. by Jerome Alexander, Vol. VI, p. 89, New York, Reinhold Publishing Corp., 1946.
- Coggeshall, N. D., and Lang, E. M., *J. Am. Chem. Soc.*, 70, 3283 (1948).
- Coggeshall, N. D., and Saier, E. L., *J. Applied Phys.*, 17, 450 (1946).
- Coggeshall, N. D., and Saier, E. L., *J. Chem. Phys.*, 15, 65 (1947).
- Consolidated Engineering Corp., "Analysis of Alcohols by the Mass Spectrophotometer," *Group Rept. 52*.
- Dailey, B. P., *ANAL. CHEM.*, 21, 540 (1949).
- Dempster, A. J., Inghram, M. G., and Hess, D. C., U. S. Atomic Energy Commission, *Rept. AECD 2027*.
- Elliot, A., Ambrose, E. J., and Temple, R. B., *J. Chem. Phys.*, 16, 877 (1948).
- Ewing, G. W., and Steck, E. A., *J. Am. Chem. Soc.*, 68, 6181 (1946).
- Ferguson, L. N., *Chem. Revs.*, 43, 385 (1948).
- Fox, J. J., and Martin, A. E., *Proc. Roy Soc. (London)*, 162, 419 (1937).
- Ibid.*, 175, 208 (1940).
- Gordy, W., *J. Chem. Phys.*, 8, 516 (1940).
- Gordy, W., and Stanford, S. C., *Ibid.*, 9, 204 (1941).
- Grosse, A. V., Hindin, S. G., and Kirshenbaum, A. D., *ANAL. CHEM.*, 21, 386 (1949).
- Halpern, G. H., *IND. ENG. CHEM., ANAL. ED.*, 18, 621 (1946).
- Heigl, J. J., Black, J. F., and Dudenbostel, B. F., *ANAL. CHEM.*, 21, 555 (1949).
- Hibbard, R. R., and Cleaves, A. P., *Ibid.*, 21, 486 (1949).
- Hickam, W. M., *Phys. Rev.*, 74, 1222A (1948).
- Hindin, S. G., and Grosse, A. V., *ANAL. CHEM.*, 20, 1019 (1948).
- Hipple, J. A., and Shepherd, M., *Ibid.*, 21, 32 (1949).
- Irvu, J. L., and Irvin, E. M., *J. Am. Chem. Soc.*, 69, 1091 (1947).
- Jones, R. N., *Chem. Revs.*, 32, 1 (1943).
- Lee, J. H., *IND. ENG. CHEM., ANAL. ED.*, 18, 659 (1946).
- Lewis, G. N., and Calvin, M., *Chem. Revs.*, 25, 273 (1939).
- Mulliken, R. S., *J. Chem. Phys.*, 7, 14, 20, 121, 339, 353, 356, 364, 570 (1939).
- Neal, R. H., and Luckmann, F. H., *IND. ENG. CHEM., ANAL. ED.*, 16, 358 (1944).
- Noyes, W. A., Jr., and Leighton, P. A., "Photochemistry of Gases," Chap. III, New York, Reinhold Publishing Corp., 1941.
- O'Connor, R. T., Heinzelman, D. C., Freeman, A. F., and Pack, F. C., *IND. ENG. CHEM., ANAL. ED.*, 17, 467 (1945).
- Powell, J. S., and Edson, K. C., *ANAL. CHEM.*, 20, 510 (1948).
- Pauling, Linus, "Nature of the Chemical Bond," Chap. IX, Ithaca, N. Y., Cornell University Press, 1944.
- Rittenberg, D., *J. Applied Phys.*, 13, 561 (1942).
- Robertson, W. W., Ginsburg, N., and Matsen, F., *IND. ENG. CHEM., ANAL. ED.*, 18, 746 (1946).
- Rose, F. W., *J. Research Natl. Bur. Standards*, 19, 143 (1937).
- Ibid.*, 20, 129 (1938).
- Rosenbaum, E. J., and Stanton, L., *ANAL. CHEM.*, 19, 794 (1947).
- Saier, E. L., unpublished material.
- Saier, E. L., and Coggeshall, N. D., *ANAL. CHEM.*, 20, 812 (1948).
- Seyfried, W. O., and Hastings, S. H., *Ibid.*, 19, 298 (1947).
- Stamm, R. F., *IND. ENG. CHEM., ANAL. ED.*, 17, 318 (1945).
- Taylor, R. C., Brown, R. A., Young, W. S., and Headington, C. E., *ANAL. CHEM.*, 20, 396 (1948).
- Taylor, R. C., and Young, W. S., *IND. ENG. CHEM., ANAL. ED.*, 17, 811 (1945).
- Thornton, V., and Herald, A. E., *ANAL. CHEM.*, 20, 9 (1948).
- Torkington, P., and Thompson, H. W., *Trans. Faraday Soc.*, XLI, 184 (1945).
- Tunncliffe, D. D., *ANAL. CHEM.*, 20, 828 (1948).
- Van Vleck, J. H., and Weisskopf, V. F., *Rev. Modern Phys.*, 17, 227 (1945).
- Washburn, H. W., Wiley, H. F., Rock, S. M., and Berry, C. E., *IND. ENG. CHEM., ANAL. ED.*, 17, 74 (1945).

RECEIVED November 22, 1949.

Instrumentation and Auxiliary Equipment for Automatic Infrared Gas Analyzers

By WILLIAM J. HAPPEL and NORMAN D. COGGESHALL,
Gulf Research & Development Co., Pittsburgh, Penna.

IN the development of petroleum processes from their pilot unit operation the continuous-flow infrared gas analyzer^{1,4,5} offers a new and powerful tool. When correctly adjusted to a pilot process gas stream, the continuous record of such an instrument effectively creates a window into the process reaction by giving an instantaneous visual indication of the control gas concentration. Sudden variations or sharp peaks in stream concentrations, normally missed by most spot sampling techniques, are immediately indicated and, as is important in such cases, located in a time record with the variation in the process temperatures, pressures or other variables. Normally, the value of such a visual presentation is further enhanced by a greater instrument sensitivity (to extremely low control gas concentrations) than can be obtained in the standard analysis of spot samples. Therefore, the use of the instrument calibration with the continuous concentration record permits

a far greater over-all accuracy in material balance calculations than previously possible.

In addition to these advantages in the preliminary investigation of a process operation, the analyzer may be operated also as a monitor or automatic controller to maintain a desired level of gas concentration once a set of operating conditions has been chosen. This may be readily done either through an alarm system to the unit operators or in a completely automatic manner by direct control of the appropriate process valves or other operating parameters.

Some typical applications of this type of instrument are: the continuous determination of carbon monoxide and carbon dioxide in flue gases³; the monitoring of the sulphur dioxide concentration in a stream also containing nitrogen, hydrogen, and hydrocarbon gases; the determination of the methane concentration in a stream containing other hydrocarbon gases; and the determination of ethylene oxide in the catalytic oxidation of ethylene gas.²

These examples are just a few of the many problems that can be and have been solved by the continuous-flow infrared gas analyzer.

A primary limitation of the instrument is that it cannot analyze for infrared inactive gases such as the monatomic and symmetrical diatomic ones. However, for mixtures of infrared-active gases, a satisfactory operation may be achieved in many cases suffering optical interference by the judicious use of gas blends in the compensator and interference cells.

In such applications of the instrument, it has been found that to be of optimum advantage the analyzer should maintain its sensitivity and accuracy while having a simplicity of operation and a ruggedness that gives a freedom from all but minor maintenance. This article concerns the construction of a continuous-flow analyzer for pilot plant operation with the above principles as primary requirements.

GENERAL CONSTRUCTION

Fig. 1 shows the front view and general construction of the complete instrument. All components of the analyzer—including the gas handling equipment—are assembled in a standard closed relay rack which is mounted on a rubber-tired dolly to permit ease in moving the instrument. The infrared analysis of the stream originates in the thermostated optical compartment occupying the lower section of the relay

rack. The chief component in this compartment is the optical tank which was purchased from Baird Associates Co., of Cambridge, Mass., and contains the infrared source, absorption cells and bolometer detectors. The thermostated compartment is sealed by rubber gaskets on the doors (as are the bridge control chassis and recorder case) so that a low positive pressure of instrument air may be maintained within it to prevent formation of gas pockets and reduce explosion hazards. The compartment is also insulated so that it may be maintained at about 120 F. to eliminate the effect of ambient temperature drifts. This is very important for the successful operation of the instrument.

The temperature regulation is effected by a mercury thermometer type electrical thermoregulator mounted alongside the optical tank. A change in temperature of 0.1 F. at the thermoregulator will actuate a mercury relay located at the rear of the gas control



Fig. 1



Fig. 2

Electric Power Re-enters Servo Race Gets an Assist from Good Old Mechanics

ONE of the reasons why instrumentation fascinates all of us may be found in the big-league and minor-league contests that go on incessantly. Some are relatively slow-like marathons, or tugs-of-war. Years elapse before the advantage passes from one team to another. (Example, the race for "Most Stable Amplifier"

"cost," "weight," "maintenance," "liveliness," "cleanliness," "safety," etc.

Until recently, electric power held last place in the "liveliness" race, which many persons consider the most important. "Liveliness" can be described as the speed with which the "slave" is able to carry out the commands of the "master" (see Fig. 1). One technical definition is the time for the power unit to reverse from full speed in one direction to full speed in the other. A more precise definition is the *characteristic time* (or "time constant") which is the time for the power unit to come up to 63.2 percent of full speed.

Until recently, hydraulic servomotors were reported to be a little more lively than pneumatic servomotors and about

baum's disclosure. (For full details see the full text of his paper in the 1949 *Transactions AIEE*.)

Hydraulics and pneumatics were still ahead when, a few weeks ago, the National Bureau of Standards disclosed a radically new method which closes the gap between the electric and pneumatic runners and perhaps will put electric power ahead of the other two contestants. Figs. 3 and 4 show an experimental embodiment of the NBS method; Fig. 5 has been drawn from NBS data (which were *not* in terms of rpm., so that we assume responsibility in case it's not 100 percent accurate) and it shows conclusively that the liveliness of the secret motors (if they ever existed!) has been outdone. For this remarkable development, instrument users can thank Dr. Jacob Rabinow—the same NBS scientist who invented the magnetic-fluid clutch announced by the NBS two years ago (and fully described, with 14 illustrations, in our August 1948 issue, pages 756-764). For a complete description of the new high-speed reversal method see the NBS *Technical News Bulletin*, May 1950, page 63.

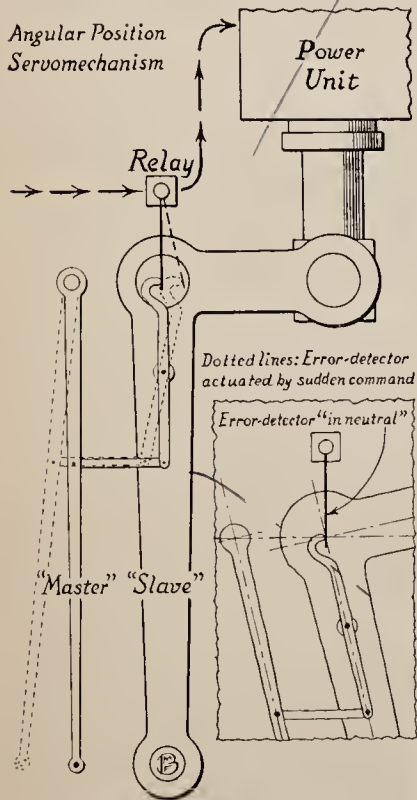


Fig. 1.

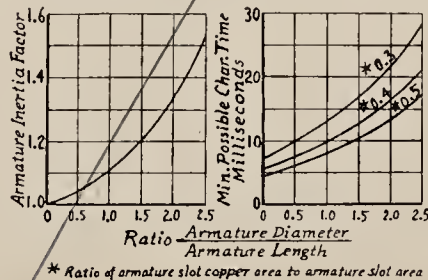


Fig. 2.

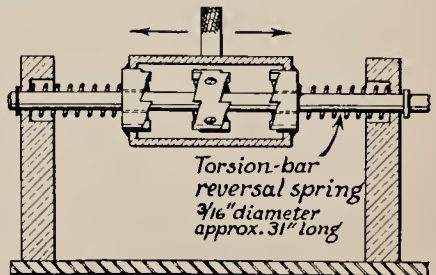


Fig. 3.



Fig. 4. NBS quick-reversal "breadboard." With the motor operating in either direction at 3200 rpm., the second of the two positive unidirectional clutches at the left end of the 31-inch steel torsion bar is engaged, thus stopping the rotation of the adjacent end of the bar. The kinetic energy of the motor is converted into potential energy in the torsion bar by approximately 20-degree additional rotation of the motor, and used to accelerate the motor rapidly in the opposite direction.

ten times as lively as electric servomotors. However, rumors were being whispered about military d-c. motors the size and shape of fountain pens, capable of reversing from thousands of rpm. clockwise to an equal speed counterclockwise in a small fraction of a second.

Last October the electric entry made a big spurt in the liveliness race when Paul Lebenbaum, Jr., of G-E, presented his paper on "D-c. Motors for Automatic-control Systems" at the AIEE Fall Meeting. Maybe it was the unwrapping of the wartime secret at long last; maybe not; but Fig. 2 shows what we believe to be the heart of Leben-

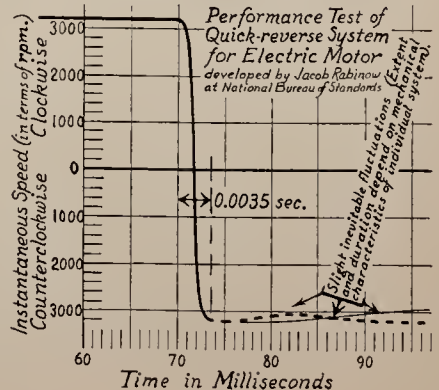
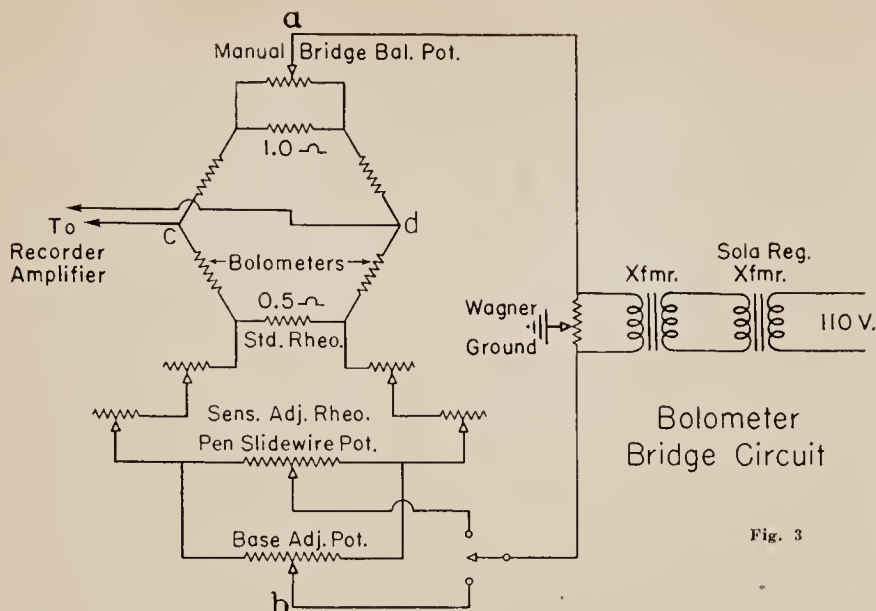


Fig. 5.

where most entrants have been neck-and-neck for nearly two decades.) Some contests are relatively fast—like squash or jai-alai. You have to read your favorite magazine every month to know what teams are ahead. And you've got to read it attentively, because the big news of important sports events may be hidden in brief items from instrument firms or research labs. One of the reasons is the characteristic modesty of Instrumentation competitors; another reason is that, in many cases, the fellow that suddenly forges ahead in one race doesn't know he's in line for several other trophies.

Of all the races being run, you'll probably agree that the most exciting is the one where the contestants are the various forms of auxiliary power. This is not merely one race but a big track meet, some of the races being



panel, turning on or off a set of heaters mounted in front of a small continuously-running circulating fan. The internal temperature of the compartment is indicated by a dial thermometer on the front door just below the heater pilot light indication.

The thermostated compartment is readily accessible from the front and rear through hinged doors. This facilitates the maintenance and adjustment of the components housed in the compartment. Fig. 2 shows the mounting of the recessed gas control panel and

some of the cabling and stainless-steel tubing used throughout the instrument. This style of cabling permits the removal of any or all of the individual units for bench testing; the stainless-steel tubing permits application of the instrument to corrosive gas streams.

All input power is through a single Amphenol connector. Power for the Brown recorder amplifier, the source and the bridge circuits, is supplied from a Sola voltage-regulating transformer mounted at the rear of the recorder. The main power switch and the

auxiliary electrical gas-handling equipment controls are located on the recessed gas control panel just above the thermostated compartment. The auxiliary gas handling equipment also mounted on this panel includes the stream flowmeter, stream-pressure mercury safety valve, and the instrument air and process stream regulators.

To maintain simplicity of operation, the bridge control chassis, mounted just above the recessed gas control panel, was designed so that the only adjustments available for normal operator use are the bridge base line control and the sensitivity adjustment or scale expander rheostats. The gasketed Bakelite instrument label located at the center of the chassis may be removed in instrument servicing for access to the source and test signal switches. This latter switch creates a predetermined bridge unbalance with a consequent error signal that is independent of the infrared beam absorption for the examination of the instrument signal circuits. The adjustable Wagner ground, used to minimize stray pickup in the bridge circuit and associated cabling, is mounted on the rear of this chassis and protected after adjustment by a knurled cap covering the shaft.

ELECTRICAL SYSTEM

A Brown "Electronik" strip-chart recorder with a $4\frac{1}{2}$ -second full-scale pen speed and a high-gain high-impedance amplifier was modified for operation with the bolometer bridge circuit. The input converter to the recorder



Fig. 4

amplifier was by-passed and the a-c. bridge error signal fed directly to the first stage of the amplifier through an input transformer. The standard cell and the associated Brown d-c. standardizing circuits were removed from the recorder to permit the rewiring of the pen slidewire with the Brown standardizing battery rheostats and switch into the bolometer bridge circuit as shown by Fig. 3.

In this circuit the pen slidewire is a shunt on the small 0.5-ohm bridge resistor. As the pen is moved, the slidewire potential-dividing resistor is rotated and effectively transfers part of the 0.5-ohm shunt from one bolometer arm to the other in such a manner as to maintain bridge balance. The system of variable rheostats connected in series with this slidewire is for automatic standardization and for instrument sensitivity control.

The automatic standardizing circuit used here is well-known and has merely been adapted to operation with the Brown Recorder. The standardizing rheostats are tandem-mounted so that the sum of their resistances will be maintained at 30 ohms. As one rheostat has more of its resistance cut into the circuit, the resistance of the other rheostat is equally reduced. The effect of rotating their shaft is to shift the curve which the pen traces either to the right or left since the pen slidewire will now have to be moved to maintain the original bridge balance conditions. Such a correction as this is required if there has been a small drift in the

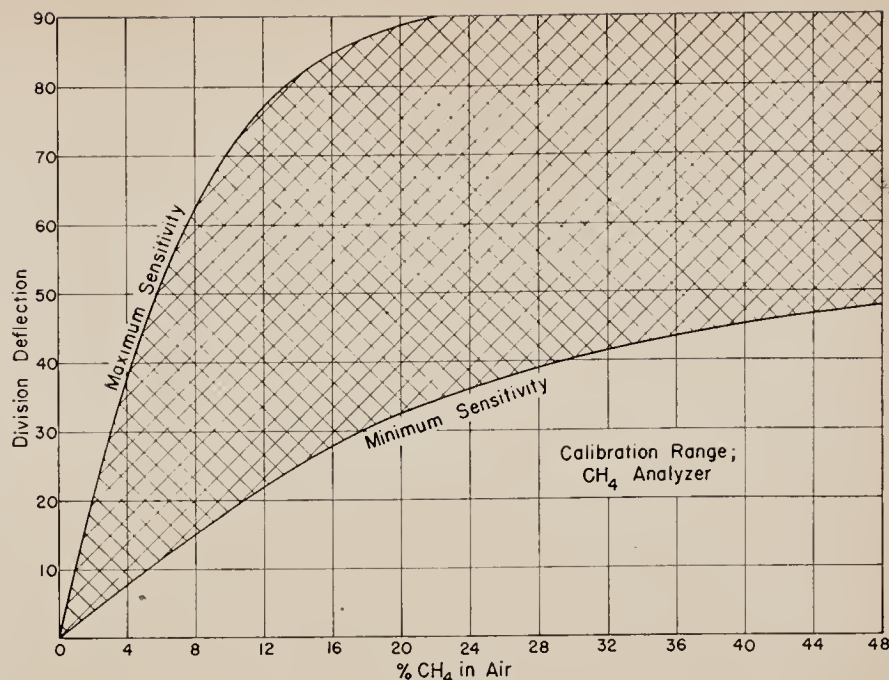


Fig. 5

The base line is subject to a drift which is corrected automatically once every hour by the injection of nitrogen or instrument air to obtain zero stream concentration and followed by the subsequent adjustment of the standardizing rheostats to maintain the original base line setting. To obtain this operation, a 1-rph. clock motor drives a set

from the chart-drive motor or manually from a push-rod on the front of the recorder. In this particular application the triggering spur on the gear train was removed and a small relay was mounted so that on closure its armature would operate the manual push-rod. When this relay is energized, the clutch is released on the standardizing battery rheostats, permitting them to be driven by the balancing motor. At the same time, the movement of the clutch will throw a switch which removes the recorder slidewire from the circuit and substitutes another potential-dividing resistor (the base selector resistor located at the top of the recorder) that has been previously adjusted manually. If, because of some drift, the base-line to which the pen return is not the correct one, there will be an error signal when the clutch is thrown which will drive the standardizing rheostats in such a direction and through a sufficient distance to restore the original base-line position of the pen.

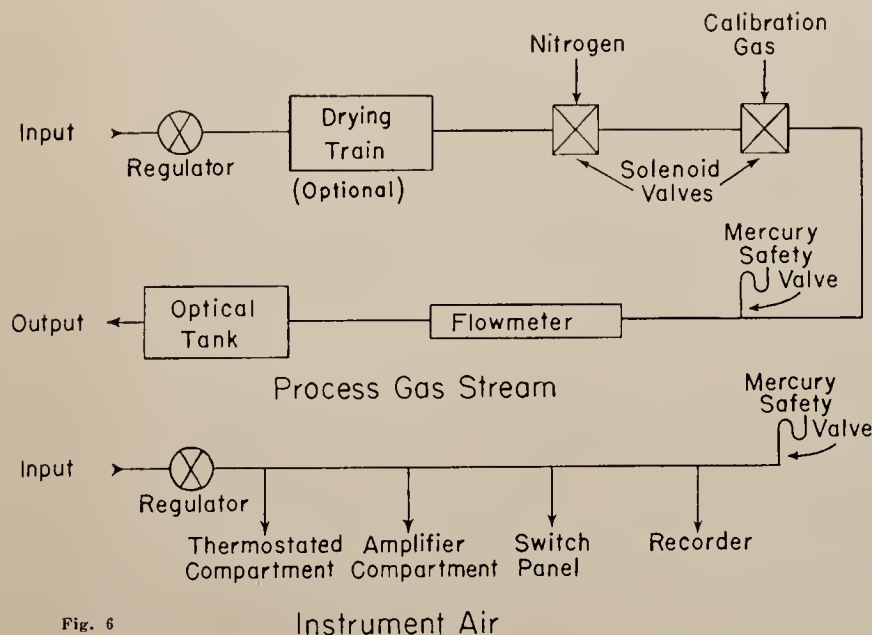


Fig. 6

operating points of the bridge bolometers or any other change which temporarily unbalances the system without changing its calibration significantly.

A point on the recorder chart, near the left edge, corresponds to zero concentration in the stream. The pen left at this point will trace out a base line which may be changed arbitrarily by adjusting the bridge balance control, Fig. 3, fixing the initial bridge balance.

of cams (see Fig. 4.) one of which triggers a Microswitch operating the relay cutting off the stream flow and turning on the nitrogen. The nitrogen flows through the sample cell for about two minutes. Then a second cam triggers its Microswitch to operate a small relay energizing the standardizing mechanism. The original recorder standardizing mechanism could be triggered automatically by a gear train

The sensitivity adjustment resistances are also matched tandem-mounted rheostats. They are, however, manually operated and so connected that each rheostat will turn in the same amount of resistance per unit angle shaft rotation. When this shaft is turned so that the resistance of the sensitivity adjustment rheostats is zero, the maximum variation of the pen slidewire would mean a fractional change, to first approximation, of 0.005 of a bolometer arm resistance, omitting, for simplicity, the resistances of the standardizing rheostats. On the other hand, with the maximum resistance of the sensitivity adjustment rheostats turned completely in, the same variation of the pen slidewire would now give only a fractional change of approximately

$$(0.5/1000) \times [R_3 / (R_1 + R_2 + R_3)]$$

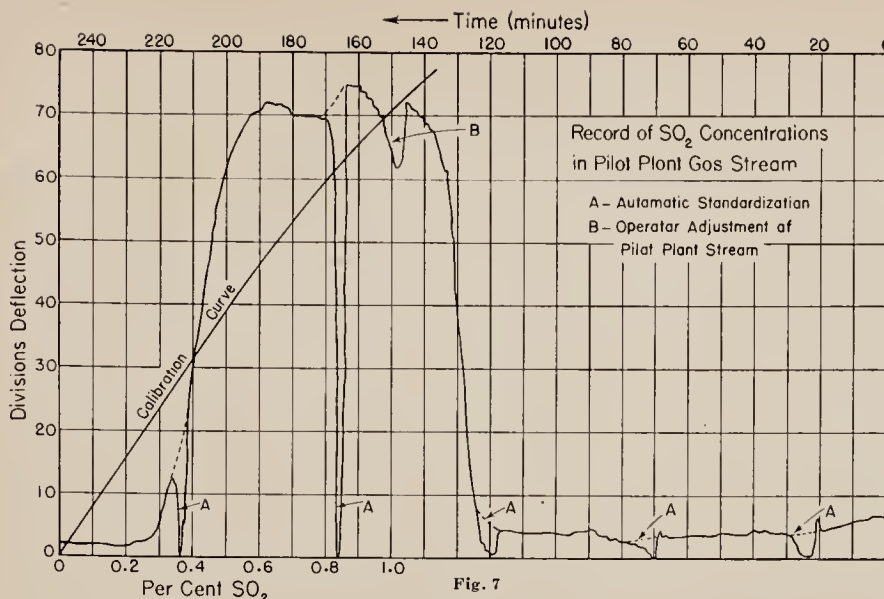


Fig. 7

where R_3 is total resistance of the pen slidewire and R_1 and R_2 are the resistances of the sensitivity adjustment rheostats. Hence, for a given bridge unbalance signal, the amount of movement (pen deflection from base line) in the pen slidewire required to bring the bridge back to balance will be $(R_1 + R_2 + R_3)/R_3$ greater for the latter case where $R_1 = R_2 = \text{maximum}$ than for $R_1 = R_2 = 0$. For sensitivity scale changes, this control was made to give a range of about 3 to 1 in a continuous

manner. Taking into consideration the value of the standardizing resistances and the base-line adjustment potential dividers, this amounted to a transfer of 0.24 ohm to 0.09 ohm for a minimum to maximum variation of the sensitivity adjustment control on a full-scale pen deflection.

Such a control is of great use to the pilot-plant operator in the correction of the slow decay of instrument sensitivity and the elimination of instrument recalibration. If, for example,

adjust the control to obtain a three-inch deflection for the same concentration in order to magnify any minor changes in the process stream. This control has been found quite useful also where different unit streams on the same problem have different levels of the desired component concentration. Fig. 5 shows the possible sensitivity range obtainable by the sensitivity adjustment control.

The bolometer detectors are located in a standard Wheatstone bridge circuit energized from a step-down transformer across points a-b, Fig. 3. The bridge may be balanced manually by the bridge balance control located on the bridge control chassis. The error signal caused by variations in the product stream concentrations is applied to the amplifier input transformer in the recorder through a short length of shielded two conductor cable to drive the balancing motor and coupled pen slidewire in such a direction as to return the bridge to balance. A Wagner ground was used across the bridge source to minimize the stray pickup in the bridge circuit and associated cabling.

GAS-HANDLING SYSTEM

Fig. 6 shows the schematic diagram of the analyzer gas-handling system including both process stream circuit and instrument air pressurization lines. Stainless steel quarter-inch O.D., $\frac{3}{16}$ -inch I.D. tubing with Ermetto type fittings was used throughout the instru-

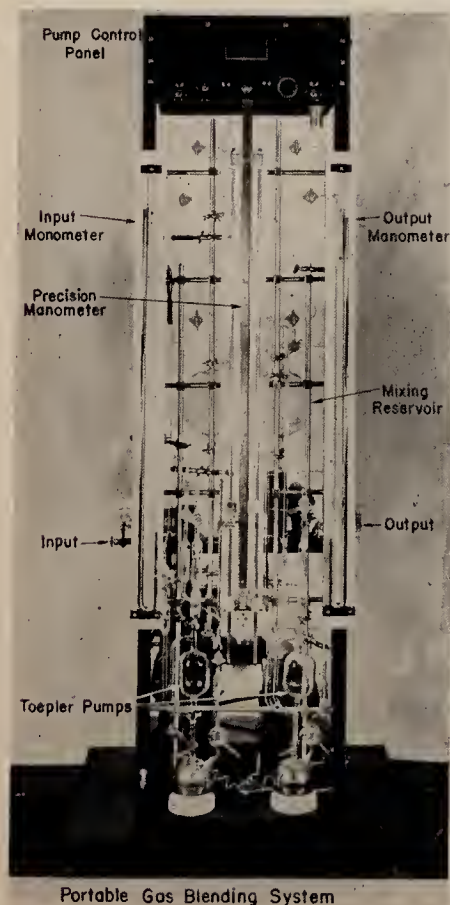


Fig. 8

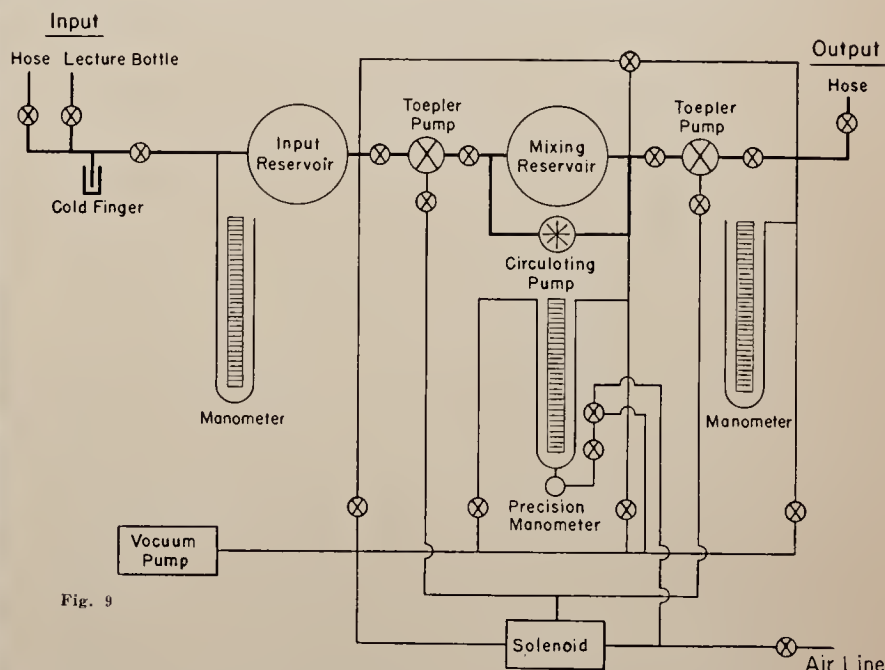


Fig. 9

the operating concentration of the component in the process stream should give a one-inch deflection for the condition of minimum sensitivity adjustment resistance, and if a fogging of the sample cell lenses or slight gas leak should occur (which would result in a sensitivity loss) it is now possible to maintain the original calibration without instrument shut-down or recalibration. In addition, it is possible to

ment to eliminate corrosion. The base line register solenoid, which cuts off the stream flow and flushes the system with nitrogen, is operated by the cam-tripped Microswitch driven by the 1-rph. clock motor. This solenoid may also be tripped by a manually-operated mercury switch on the gas-control panel below the recorder permitting a nitrogen flush of the sample cell at the will of the operator to register the base

line. The adjacent switch permits the injection of a standard gas blend to calibrate the instrument. A second solenoid valve, but no relay, is employed in the sample line to accomplish this. The solenoid valves (Automatic Switch Co. P32X) are of the three-way type, connected with the stream passing through to the sample cell in the optical tank when they are in the unenergized position. When either valve is energized, the stream is turned off and the appropriate gas, either nitrogen or the known blend, passes through a regulator from its storage tank to the sample cell.

The normal calibration check procedure requires: first, throwing the base-line register switch to establish the base line, with the nitrogen flush, and then the calibrate switch for the injection of a known blend. After the pen has indicated the final deflection, both switches may be turned off and the instrument returned to the stream gas.

A flowmeter (Fischer & Porter No. 180) is inserted between the valves and the sample cell, when the float is at about 4 on the scale of the flowmeter, the flow rate is about 1 cfh. At the stream input to the instrument, there is a Conoflow diaphragm regulator to reduce the line pressure to a few inches of water pressure. Between the flowmeter and the optical tank, a mercury safety valve diverts the stream to the room in the event of regulator maladjustment or failure and thus prevents excess pressures in the optical cells. All of these components on the stream are located on the gas-control panel in full view of the operator.

The instrument air stream, used to prevent combustible gas pocketing in the compartments, is regulated by a Conoflow diaphragm regulator. As in the process stream, a mercury safety valve is used after the regulator to prevent excessive pressure in the instrument compartments in case of an accident. Normal instrument air pressure is about a quarter-inch mercury column.

OPERATION

The continuous-flow infrared gas analysis of process streams is satisfactorily achieved by the type of instrument described. Fig. 7 demonstrates a typical recorder-chart record obtained when the instrument was applied to the determination of the SO_2 concentration in a process stream. The instrument calibration curve has been superimposed on the tracing of the recorder chart, showing that for this run the peak SO_2 concentration was of the order of one percent. Knowing the flow-rate of the process stream, the total SO_2 generated by the unit can be determined from the area under the curve. For this use, it would be necessary to extrapolate the curve as shown by the dashed lines at the standardizing points A. It is necessary, however, that all the components of the analyzed stream be known and the possibility of interference effects investigated and eliminated. This can only be satisfac-

torily done by the use of mixtures of known composition. In order to readily investigate the range and sensitivity of the instrument described above, a portable gas-blending system was constructed as shown in Fig. 8.

GAS-BLENDING SYSTEM

This system permits the precise blending of synthetic gas mixture up to two liters at atmospheric pressure. This is done by successively inserting individual components into the same volume and then computing the concentration from the corresponding pressure changes in the constant volume.

The gas-blending system as shown is constructed of glass. A schematic diagram of the system appears in Fig. 9. In operation, the general procedure is to evacuate the system and admit a pure gas from the tank manifold (upper left in the schematic) to the input reservoir. The gas is transferred by the Toepler pump to the mixing reservoir. The input reservoir is then evacuated and the next component gas admitted. After all the desired components have been introduced into the mixing reservoirs and their partial pressures determined, the gases are thoroughly mixed by the action of a circulating pump which moves the gases in and through the reservoir. The blend may then be transferred to a sample receiver by the second Toepler pump. The Toepler pumps are automatically cycled by delay circuits so that no sparks occur within that part of the pump containing the gas blend—to eliminate the danger of explosions with flammable mixtures.

A Welch "Duo-Seal" rotary vacuum pump serves to evacuate the system and sample receiver before a blend is made. During the blending process, this same vacuum pump operates the mercury displacement arrangements used to transfer gases into and out of the blending reservoir and also to con-

trol the mercury content of the precision manometer on which the blend pressure is read.

The mixing of the blend, which is necessary to obtain homogeneous mixtures and reproducible calibration data, is obtained by a sealed centrifugal type pump. The pump was constructed by increasing the air gap of a 4-pole 1/80-hp. Alliance induction motor to permit mounting of the motor armature in Oilite type bearings within a thin-walled brass housing sealed at one end. The field from the pole shoes penetrates the brass to obtain armature torque, driving the armature at about 25 percent slip. A three-inch centrifugal type impeller supplies the necessary pressure differential to give circulation within the mixing reservoir. Kovar glass seals are used for the bond between the glassware of the system and the metal of the impeller housing and, by using a ring seal, a good vacuum can be maintained.

Acknowledgment.—Acknowledgment is gratefully made to Dr. Paul D. Foote, Executive Vice-President of Gulf Research and Development Company for permission to publish this material.

REFERENCES

1. W. G. Fastie and A. H. Pfund. "Selective Infrared Gas Analyzer." *Journal of the Optical Society of America*, Vol. 37, No. 10, October 1947, pages 762-768.
2. H. G. Hasegawa and R. G. Simard. "Continuous Infrared Determination of Ethylene Oxide in Pilot Plant Facilities Process Development." *Oil and Gas Journal*, Vol. 47, No. 28, November 1948, pages 280-283.
3. H. Sobcoff and E. P. Hochgesang. "Continuous Determination of CO and CO₂ in Pilot Plant and Refinery Operation Using an Infrared Gas Analyzer." *Oil and Gas Journal*, Vol. 47, No. 28, November 1948, pages 274-276.
4. N. Wright and L. W. Herscher. "Recording Infrared Analyzers for Butadiene and Styrene Plant Streams." *Journal of the Optical Society of America*, Vol. 36, No. 4, April 1946, pages 195-202.
5. G. A. Martin. "Control of Product Quality by Plant Type Infrared Analyzers." *Instruments*, Vol. 22, December 1949, pages 1102-1105.

Instruments' Publisher in England



Richard Rimbach, President of The Instruments Publishing Co., returned from his six-week Western Europe trip shortly before this issue went to press. His articles will start in our July issue. This photograph shows him (gray suit, center) at a reception for publishers given by the Council of the Radio & Electronic Component Manufacturers' Federation at Grosvenor House, London, on April 17.

Electrostatic Interaction in Hydrogen Bonding

NORMAN D. COGGESHALL

Gulf Research and Development Company, Pittsburgh, Pennsylvania

(Received March 20, 1950)

An attempt has been made to calculate the frequency shift, the intensity of absorption, and the energy of association of a hydroxyl group which is a participant in a hydrogen-bonded complex. When a term expressing the polarization energy of a hydroxyl group due to electrostatic interaction is added to the Morse function, the Schrödinger equation may be solved. The calculated wave-length of maximum absorption agrees with the experimental value fairly well for benzyl alcohol and exactly for catechol. Agreement between calculated and observed absorption intensity is satisfactory. The association energy, calculated on the linear polymer model, agrees quite well with the experimental results reported by Mecke.

SINCE the hydrogen bond was first recognized some thirty years ago there has been an increasing interest in it due to its great importance in the physical and chemical behavior of many polar materials. A voluminous literature dealing with the qualitative aspects has accumulated whereas the quantitative aspects have received much less attention. However, at the present time it is necessary to obtain a fuller understanding of the quantitative aspects of the phenomenon in order to further utilize the data. The present material reports upon some calculations of the fundamental stretching frequency of a hydroxyl group attendant to participation in a hydrogen bond.

THE NATURE OF THE BOND

From the x-ray studies of strongly bonded crystalline materials¹ it is known that the hydrogen bonds are of

the general type shown in Fig. 1. Here the proton of one hydroxyl group is electrostatically attracted to the oxygen of another. This model is consistent with the statistical analysis of Kempter and Mecke² who showed that the dependence of degree of association of phenol on concentration cannot be explained by the dimer model wherein hydroxyl groups are bonded together through dipole-dipole attraction. It is clear that in an attempt to calculate the stretching frequency due to a hydrogen-bonded hydroxyl group the exact force conditions would be difficult to describe. In addition to the electrostatic effects of the nearest oxygen and proton atoms there are the van der Waals interactions between various members. Furthermore, by virtue of the relatively loose coupling of the hydrogen bonds, the

¹ L. Pauling, *The Nature of the Chemical Bond* (Cornell University Press, Ithaca, New York, 1944), Chapter IX.

² H. Kempter and R. Mecke, *Zeits. f. physik. Chemie* **46B**, 229 (1941).

molecules cannot be regarded as independent of one another.

In order to make the problem tractable we shall use a simplified force field situation. The hydroxyl frequencies are independent of the remainder of the molecule to a first approximation. Further, let us consider a diatomic group possessing a dipole moment immersed in a constant electric field. There will be an interaction energy depending upon the dipole moment, the angle of orientation, and the electric field. This will not be evidenced in the transition energies for the vibrational states of the group as they will all be shifted the same amount. There will be, however, a change of potential energy of the diatomic group due to polarization. This will be $-qE_p z$, where q is the charge unbalance for the group, E_p is the electric field component parallel to the direction of the valence bond, and z is the internuclear displacement from equilibrium. This change of potential energy will be evidenced in changes in the transition energies.

THE HARMONIC OSCILLATOR MODEL

When we apply the new energy term $-qE_p z$ to the Schrödinger equation there results a shift of all the energy levels for this model but no changes in the transition energies. This is readily seen from Eq. (1) which is the Schrödinger equation applied to the harmonic oscillator with the added energy term.

$$\frac{d^2\Psi}{dz^2} + \frac{8\pi^2\mu}{h^2} \left\{ W - \frac{kz^2}{2} + qE_p z \right\} \Psi = 0. \quad (1)$$

Here μ is the reduced mass for the oscillator and k is the force constant. It is obvious that a linear transformation of the displacement variable will restore the equation to its original form, i.e., without the new energy term, and with the only change being in the constant term W . This results in an equal shift of all the levels.

DIATOMIC GROUP WITH MORSE FUNCTION

The Schrödinger equation for the diatomic group with a Morse potential energy function and with the new term will be:

$$\frac{d^2\Psi}{dz^2} + \frac{8\pi^2\mu}{h^2} \{ W - D(1 - e^{-az})^2 + qE_p z \} \Psi = 0. \quad (2)$$

If we let $x = e^{-az}$ and expand $\log x$ in terms of $x-1$, dropping cubic and higher order terms, Eq. (2) becomes:

$$\frac{d^2\Psi}{dx^2} + \frac{d\Psi}{xdx} + \frac{8\pi^2\mu}{a^2h^2} \times \left\{ \frac{W-D-C_0}{x^2} + \frac{2D-C_1}{x} - D-C_2 \right\} \Psi = 0, \quad (3)$$

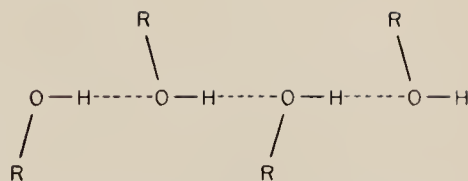


FIG. 1. Schematic linear model of hydrogen bonding; electrostatic interaction is along dashed lines.

where:

$$C_0 = -(3qE_p)/2a$$

$$C_1 = (2qE_p)/a$$

and

$$C_2 = -(qE_p)/2a.$$

If we use the transformation:

$$\Psi(x) = e^{-y/2} y^{b/2} F(y),$$

where

$$y = 2dx$$

$$d^2 = (8\pi^2\mu/a^2h^2)(D+C_2)$$

and

$$b^2 = -(32\pi^2\mu/a^2h^2)(W-D-C_0).$$

Equation (3) may be readily solved³ and the energy levels become:

$$W(v) = W^1 + \frac{ah(D - qE_p/a)}{\pi(2\mu)^{1/2}(D - qE_p/2a)^{1/2}} (v + \frac{1}{2}) - \frac{a^2h^2}{8\pi^2\mu} (v + \frac{1}{2})^2 \quad (4)$$

where v is the vibrational quantum number and W^1 is given by:

$$W^1 = D + C_0 - (D - C_1/2)^2 / (D + C_2).$$

Equation (4) is to be compared to the energy expression for the same diatomic group without the perturbing field, namely,

$$W(v) = \frac{ah}{\pi} \left(\frac{D}{2\mu} \right)^{1/2} (v + \frac{1}{2}) - \frac{a^2h^2}{8\pi^2\mu} (v + \frac{1}{2})^2. \quad (5)$$

The result is thence a shifting of all levels with a decrease in the transition energies. A comparison with experimental results may now be made if values for q , E_p and a are chosen.

COMPARISON WITH EXPERIMENT

In order to compare the results of Eq. (4) with experimental values we may evaluate the unbalanced charges by the relation $\mu = qd$ where μ is the dipole moment for a diatomic group, q is the unbalanced charge, and d is the internuclear distance. We shall

³ See, for example, L. Pauling and E. B. Wilson, *Introduction to Quantum Mechanics* (McGraw-Hill Book Company, Inc., New York, 1935), Chapter X.

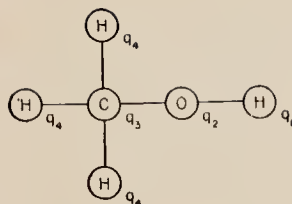


FIG. 2. Charge unbalance designations as applied to methanol.

evaluate q_1 , the charge on the hydrogen atoms, and q_2 , the charge on the oxygen atom from a consideration of methanol and then assume the same values hold for the higher alcohols. Let us consider Fig. 2 where q_1 and q_2 are the unbalanced charges as above and q_3 and q_4 are the unbalanced charges on the carbon atom and on the other hydrogen atoms. From Pauling's tabulations⁴ of covalent radii and of dipole moments we have:

$$\begin{aligned} d(\text{O}-\text{H}) &= 0.96\text{\AA}, & d(\text{C}-\text{H}) &= 1.07\text{\AA}, & d(\text{C}-\text{O}) &= 1.43\text{\AA} \\ \mu(\text{O}-\text{H}) &= 1.51 \times 10^{-18} \text{ e.s.u.}, & \mu(\text{C}-\text{H}) &= 0.4 \times 10^{-18} \text{ e.s.u.}, \\ & & \mu(\text{C}-\text{O}) &= 0.8 \times 10^{-18} \text{ e.s.u.} \end{aligned}$$

We may evaluate q_1 , q_4 , and $(q_2 - q_3)$ directly from $\mu = qd$ obtaining $q_1 = 1.57 \times 10^{-10} \text{ e.s.u.}$, $q_4 = 0.37 \times 10^{-10} \text{ e.s.u.}$, and $(q_2 - q_3) = 0.56 \times 10^{-10} \text{ e.s.u.}$ When these results are combined with the equation

$$q_1 + 3q_4 + q_2 + q_3 = 0,$$

we obtain $q_2 = -1.62 \times 10^{-10} \text{ e.s.u.}$ To evaluate E_p we use 2.70\text{\AA} for the O—H---O distance. The value of E_p at the center of the O—H bond is then $6.47 \times 10^5 \text{ e.s.u.}$ This is due to the contributions from the oxygen on one side and the hydrogen on the other. The constant a may be evaluated by using Eq. (5) for a non-hydrogen-bonded hydroxyl group. For this we consider

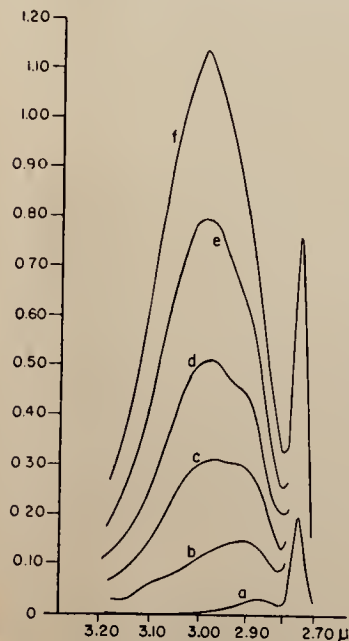


FIG. 3. Plot of optical density versus wave-length for benzyl alcohol in carbon tetrachloride solution at concentrations (a) 0.0486 mole/liter, (b) 0.0972 mole/liter, (c) 0.155 mole/liter, (d) 0.194 mole/liter, (e) 0.243 mole/liter, and (f) 0.278 mole/liter.

benzyl alcohol and use 2.77μ for the "free hydroxyl absorption."⁵ For the dissociation energy D , the value of 110.2 kcal./mole may be used.⁶ When this is done we obtain $a = 2.30 \times 10^8 \text{ cm}^{-1}$. To evaluate the term qE_p/a , the charge unbalance on the hydrogen atom, namely $1.57 \times 10^{-10} \text{ e.s.u.}$ is used with the above values for E_p and a to yield $qE_p/a = 4.42 \times 10^{-13} \text{ erg}$. This is then used with the above value for a in Eq. (4) to calculate the transition energy between the ground and first excited state. From this the wave-length of maximum absorption λ_0 for the hydrogen bonded hydroxyl is determined to be $\lambda_0 = 2.92\mu$.

A comparison with experimental results may be obtained through Fig. 3. It shows the optical density plotted versus the wave-length for several concentrations of benzyl alcohol, ranging from 0.024 to 0.277 mole/liter. The non-bonded hydroxyl absorption occurring at about 2.77μ is shown for the extreme concentrations whereas the absorption in the bonded region, i.e., from 2.85 to 3.10μ is displayed for all.

It is seen that the wave-length of maximum absorption varies with concentration. This is consistent with the explanation of Kempter and Mecke² wherein the distribution of bonded molecules among the various n -fold complexes is a function of the total concentration. It is to be noticed in Fig. 3 that the lower concentrations exhibit a band maxima at about 2.89μ . The shape of the curves for heavier concentrations suggests that they are superpositions of a maximum at about 3.00μ and the maximum at 2.89μ . We thenceforth assume that the 2.89μ point is characteristic of molecules bonded in dimer form and the 3.00μ point is characteristic of molecules bonded in the higher order complexes. Since we used an O—H---O distance from crystal data we should therefore expect our calculated λ_0 to be characteristic of the higher order complexes rather than of the dimer form.

The calculated value of 2.92μ is thence of the correct order of magnitude but is some 0.08μ lower than the observed value. This is perhaps good when it is considered that the perturbation scheme used does not consider van der Waals forces, the polarization of the electron clouds, nor the resonance effects whereby the oxygen is rendered more negative by extraction of electrons from the remainder of the molecule. It must also be borne in mind that the values used for q and E_p are approximate rather than exact.

Catechol provides a simple molecule of well-known structure for a rather direct test of Eq. (4). Overtone data for this material have been published by Wulf and Liddel.⁷ From their Fig. 2 the value of 7060 cm^{-1} may be assigned to the "free" hydroxyl absorption and 6970 cm^{-1} to the bound hydroxyl. The latter value will be compared to one calculated from Eq. (4).

In Fig. 4 are given the geometrical conditions used

⁵ J. J. Fox and A. E. Martin, Proc. Roy. Soc. (London) **162**, 419 (1937).

⁶ See reference 1, Chapter II.

⁷ O. R. Wulf and U. Liddel, J. Am. Chem. Soc. **57**, 1464 (1935).

⁴ See reference 1, Chapters II and V.

to evaluate E_p . The first step is to determine the O---H distance and angle between O—H and O---H. These values were first determined directly from the accepted bond distances and angles. However, that is not sufficient as a correction must be made for the bending of the O—H bond due to the attraction along the O---H line. In order to do this the force constant for O—H bending was evaluated using the value of $\nu = 1340 \text{ cm}^{-1}$ for the O—H bending frequency.⁸ This provides a value of $k = 9.98 \times 10^4 \text{ dynes cm}^{-1}$. When this is used the O---H distance becomes 2.19 Å and the angle between O—H and O---H becomes $61^\circ 57'$. Using this geometry the value of E_p at the center of the O—H bond is evaluated to be $1.59 \times 10^5 \text{ e.s.u.}$ In this the repulsion effect of the unbound proton is neglected in view of the large distance between it and the bound hydroxyl. Equation (5) may be used with the value of 7060 cm^{-1} for the first overtone of the free hydroxyl to obtain $a = 2.31 \times 10^8 \text{ cm}^{-1}$.

When these values are utilized in Eq. (5) we obtain $\nu = 6970 \text{ cm}^{-1}$ as the calculated frequency of the first overtone for the bound hydroxyl. Such excellent agreement with the observed value of 6970 cm^{-1} seems fortuitous in view of the poorer agreement for benzyl alcohol.

IONIC BOND STRENGTH CONSIDERATIONS

It is interesting to observe that a rather simple consideration based on the partial ionic and covalent characteristics of the hydroxyl group also yields frequencies in fair agreement with experiment. Using the postulate of additivity of energies of normal covalent bonds⁹ and the known energies of the O—O and H—H bonds we arrive at the energy of 41.1 kcal./mole as that portion of the hydroxyl bond energy due to the ionic character. Referring back to Fig. 1 we see that in the bonded polymer the oxygen and hydrogen atoms of a particular hydroxyl group are attracted toward neighboring molecules along the dashed lines. This is equivalent to reducing the electrostatic attraction, due to the charge inequality, within the hydroxyl group. A reduction in the electrostatic attraction will reduce the ionic bond character and the dissociation energy. When the dissociation energy is reduced the absorption frequencies are reduced as per Eq. (5). Thence we may calculate the absorption frequency for the bonded hydroxyl if we evaluate the reduction in ionic bond character. In this we assume that the covalent nature of the bond is essentially unaffected by the magnitude of electric field experienced.

For small vibrations the fractional reduction in ionic bond character will just be the ratio between the electrostatic force on a proton due to hydrogen bonding and that due to the charge inequality within the parent hydroxyl group. To calculate these the values of above

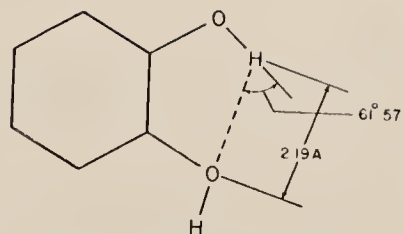


FIG. 4. Distance and angle arrangement as used for catechol calculations.

for q_1 , q_2 and the interatomic spacings are used. Thus F_1 the electrostatic force on a proton due to hydrogen bonding and F_2 the electrostatic force due to the charge inequality in the hydroxyl group are calculated to be:

$$F_1 = (1.57 \times 1.62 \times 10^{-20}) / (1.73 \times 10^{-8})^2 = 8.50 \times 10^{-5} \text{ dyne}$$

$$F_2 = (1.57 \times 1.62 \times 10^{-20}) / (0.97 \times 10^{-8})^2 = 27.0 \times 10^{-5} \text{ dyne.}$$

The fractional decrease of ionic bond character F_1/F_2 is thence 0.315. The new dissociation energy D' is then

$$D' = 110.2 - 0.315 \times 41.1 = 97.2 \text{ kcal./mole.}$$

When this value of D' and the value of a obtained above are used in Eq. (5) we obtain $\lambda = 2.96\mu$ for the bound hydroxyl in a simple alcohol. This is in better agreement with the observed value of $\lambda = 3.00\mu$ than the value obtained by the perturbation method. However, no correction for the constant a as appears in the Morse function was made.

We may now apply the same considerations to catechol, using the geometry and the value of a given above in connection with Eq. (5). When this is done it is found that $F_1/F_2 = 0.0921$ and this leads to a predicted value of 6970 cm^{-1} for the frequency of the first overtone of the bound hydroxyl. This is the same as the observed value.

INTENSITY OF ABSORPTION

There exists a fairly widespread notion that when a hydroxyl group becomes hydrogen bonded the intensity of absorption is enhanced. This may be theoretically checked by solving Eq. (2) and making a comparison with the results for an unperturbed Morse function. This is done by a direct comparison of the squares of matrix elements of the dipole moment for the two cases. The data given in Fig. 3 then may be used as a check on the calculations.

If the earlier calculations are completed for the two cases we get the set of general results given below. The ground and first excited eigenfunctions are:

$$\Psi_0 = a_0 e^{-v/2} y^{b_0/2}$$

$$\Psi_1 = a_1 e^{-v/2} y^{b_0/2} \left(\frac{1}{y} - \frac{1}{b_0 - 1} \right)$$

⁸ G. Herzberg, *Infrared and Raman Spectra* (D. Van Nostrand Company, Inc., New York, 1945), p. 335.

⁹ See reference 1, p. 47.

TABLE I. ΔE values corresponding to increasing polymer order from n to $n+1$.

n	ΔE (kcal./mole)
1	3.94
2	4.39
3	4.52
4	4.58
5	4.60
6	4.61

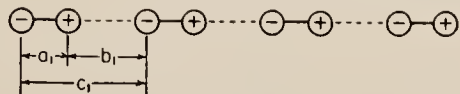


FIG. 5. Simplified model of hydrogen-bonded dipole polymer used in calculating association energy.

where

$$a_0 = (a)^{1/2}/B, \quad a_1 = (ab_0 - 2a)^{1/2}(b_0 - 1)/B$$

and

$$B = \int_0^\infty e^{-y} y^{(b_0-1)} dy.$$

The matrix element, $P(0, 1)$, of the dipole moment for the transition between the ground and first excited state calculates to be:

$$P(0, 1) = (b_0 - 2)^{1/2}/a(b_0 - 1). \quad (6)$$

For the unperturbed Morse function:

$$b_0 = [4\mu(2\mu D)^{1/2}/ah] - 1 \quad (7)$$

and for the perturbed Morse function:

$$b_0 = \frac{4\mu(2\mu)^{1/2}(D - qE_p/a)}{ah(D - qE_p/2a)^{1/2}} - 1. \quad (8)$$

As qE_p/a goes to zero, Eq. (8) reduces to Eq. (7). Also the derivatives of $P(0, 1)$ with respect to qE_p/a is positive. Hence the induced transition probability for the case of the perturbed Morse function is greater than for the unperturbed case.

To make a comparison with experiment through Eq. (6) we shall assume that the value of qE_p/a used earlier was too small. This is based on the fact that it did not give as large a shift of the wave-length of maximum absorption as was observed. We shall evaluate an essentially empirical value of qE_p/a through the use of the observed data and Eq. (4). This is then incorporated in Eqs. (6)–(8) to predict a ratio of absorption intensities. When this is done we obtain:

$$P^2(0, 1) \text{ (perturbed)} / P^2(0, 1) \text{ (unperturbed)} = 1.16. \quad (9)$$

In the data of Fig. 3 the solution of 0.243 mole/liter, i.e., curve e, was chosen for comparison because of the optimum values of optical density. At higher concentrations accurate optical density values are difficult to obtain and at the lower concentrations the absorption band of the bound hydroxyl does not demonstrate the maximum shift.

The optical density \bar{D} is given by:

$$\bar{D} = \log I_0/I = \alpha cl,$$

where I_0 and I are incident and transmitted energy, respectively, α is the extinction coefficient, c is the concentration in moles/liter and l is the length of the absorption cell. The extinction coefficient may be evaluated through the use of dilute concentrations such that appreciable bonding does not occur. When this is done it is found that $(\alpha l) = 5.40$ liter/moles. For curve e the 0.243-mole/liter concentration is thus divided between 0.126 mole/liter of non-bonded hydroxyls and 0.117 mole/liter of bonded material. The predicted optical density for the bonded material is thence:

$$1.16 \times 0.117 \times 5.40 = 0.732$$

which compares to the observed value of 0.795 with a reasonably good agreement, in view of the assumptions involved.

ASSOCIATION ENERGY

We may make a simple calculation of the approximate energy per hydrogen bond using the polymer model as seen in Fig. 1. In Fig. 5 the same model is simplified for the purpose at hand. Here we have replaced each alcohol molecule with a dipole with electrostatic interaction along the dashed lines. Since the length of the hydroxyl dipole is of the order of one-third the O—H—O distance the association must be calculated as the sum of the electrostatic interactions between individual charges rather than as a sum of dipole interactions. If we consider a polymer formed of n interacting dipoles the decrease of potential energy ΔE resulting from adding another dipole to form a polymer of $n+1$ members calculates to be:

$$\Delta E = q_1 q_2 \sum_{m=1}^n \left\{ \frac{1}{mc_1 + a_1} + \frac{1}{mc_1 + b_1 - c_1} - \frac{2}{mc_1} \right\}. \quad (10)$$

If we let $a_1/c_1 = g$, Eq. (10) reduces to:

$$\Delta E = \frac{q_1 q_2}{c_1} \sum_{m=1}^n \frac{2g^2}{m^3 - mg^2}. \quad (11)$$

In Table I may be seen the values of ΔE in kcal./mole for successive values of n . Here we have used the same values of q_1 , q_2 , a_1 , b_1 , and c_1 as above for benzyl alcohol.

The largest change in ΔE occur for the first few members and it is to be seen that for $n > 3$ there is relatively little change. For $n > 2$ the values of Table I agree quite closely with the value of 4.60 kcal./mole for benzyl alcohol in carbon tetrachloride reported by Mecke.¹⁰ This is to be expected if there are negligible volume changes attendant to the bond formation.

¹⁰ R. Mecke, Zeits. f. Electrochemie 52, 269 (1948).

Mecke's values were calculated from data for the free hydroxyl absorption band as a function of temperature and concentration.

By the use of the above equations a relation between ΔE and $\Delta \nu$, i.e., the frequency shift between the free and bonded hydroxyl may now be calculated. From Eqs. (4) and (5) we obtain the approximate expression:

$$\Delta \nu (\text{cm}^{-1}) = \frac{3q_1 E_p}{4\pi c (2\mu)^{1/2} (D)^{1/2}} \quad (12)$$

wherein terms involving quadratic and higher order terms in $(q_1 E_p / a(D)^{1/2})$ have been neglected. Equation (12) may now be rewritten as:

$$\Delta \nu = \frac{3q_1 (q_1 + q_2)}{4\pi c (2\mu)^{1/2} (D)^{1/2} (b_1 + a_1/2)^2},$$

from which we may obtain b_1 as:

$$b_1 = (H/(\Delta \nu)^{1/2} - a_1/2) \quad (13)$$

where

$$H = [3q_1(q_1 + q_2)/4\pi c (2\mu)^{1/2} (D)^{1/2}]^{1/2}.$$

If we use Eq. (13) with the above relations between a_1 , b_1 , and c_1 in Eq. (11), we obtain ΔE in terms of $\Delta \nu$ by the following expression:

$$\Delta E = \frac{2q_1 q_2 a_1^2 (H/(\Delta \nu)^{1/2} - a_1/2)^{-2}}{(H/(\Delta \nu)^{1/2} + a_1/2)} \times \sum_{m=1}^{\infty} \frac{1}{m^3 - m a_1^2 (H/(\Delta \nu)^{1/2} - a_1/2)^{-2}}.$$

Acknowledgment is made to Dr. Paul D. Foote, Executive Vice-President of Gulf Research and Development Company, for permission to publish this material.

[Reprinted from the Journal of the American Chemical Society, **72**, 2836 (1950).]

Copyright 1950 by the American Chemical Society and reprinted by permission of the copyright owner.

[CONTRIBUTION FROM THE GULF RESEARCH & DEVELOPMENT COMPANY]

Absorption Spectroscopic Studies of Hydrogen Bonding and Isomeric Forms in Bis-phenol Alkanes

BY NORMAN D. COGGESHALL

The present report is of infrared and ultraviolet absorption spectroscopic investigations made on a series of bis-phenol alkanes. These compounds are formed by the bridging of two phenolic nuclei through an aliphatic group which may be of various forms. Such materials have been referred to elsewhere as dihydroxyphenols or in some cases as diphenylolmethanes.¹ During some molecular structure determination work it was discovered that the bis-phenol alkanes had unusual hydrogen bonding characteristics. It was found that some members of the species may exist in three states, with regard to the hydrogen bonding. Some molecules may be intermolecularly bonded, some may be in a *cis*-isomeric form and some may be in a *trans*-isomeric form. The *cis*- and *trans*-isomeric forms, as used here, are not true isomeric forms but refer to orientation configurations. The *cis* form is that orientation wherein the two hydroxyl groups on the two phenolic nuclei are close together and hydrogen bonded to each other. The *cis* form hence exhibits intramolecular hydrogen bonding. The *trans* form is that orientation wherein the two hydroxyl groups are sufficiently removed from each other that no hydrogen bond

exists and yet the hydroxyls are not members of intermolecular bonds. The fact that a *trans* form can exist in concentrated solutions of some of the phenols is due to the steric hindrance offered by ortho substituted *t*-butyl groups. The steric hindrance to intermolecular bonding offered by large ortho substituted alkyl groups in the mono-nuclear phenols has been previously discussed^{2,3} and some of the results are applied here.

Experimental Details

Infrared Absorption.—The infrared absorption data were obtained with an automatic recording Perkin-Elmer Model 12B infrared spectrometer. A LiF prism which gives excellent dispersion in the 2.6–3.0 μ region was used. The quantitative data were obtained with a cell-in-cell-out arrangement previously described.⁴

Each compound was examined under four different conditions. As received, the materials were generally a powder of small crystals which had not at any time been exposed to melting temperatures. Since melting sometimes changes the distribution among the various states the materials

(1) N. D. Coggeshall, *THIS JOURNAL*, **69**, 1620 (1947).

(2) N. D. Coggeshall and E. M. Lang, *ibid.*, **70**, 3283 (1948).

(3) E. L. Saier and N. D. Coggeshall, *Anal. Chem.*, **20**, 812 (1948).

(4) H. L. Bender and A. G. Farnham, U. S. Patent 2,464,207.

were examined as mineral oil smears. In addition each material was examined in low and high concentration solutions and in recrystallized form. The latter was prepared by melting the material between two salt plates with subsequent cooling. The solvent used was C.P. carbon tetrachloride.

Ultraviolet Absorption.—The ultraviolet absorption data were obtained with a standard Beckman quartz spectrophotometer. Absolute ethanol was used as the primary solvent. Any effects due to residual traces of benzene were eliminated by the use of the same solvent in both the sample and comparison cells. The most significant data in the ultraviolet absorption were those in which sodium hydroxide in an aqueous solution was added to the ethanol. The same concentration of sodium hydroxide was always used in both the sample and comparison cells.

The bis-phenol alkanes used were kindly supplied by Dr. Donald R. Stevens and Mr. A. C. Dubbs of this Laboratory. They were prepared by condensing various substituted phenols with different aldehydes and ketones in glacial acetic acid. The materials were believed to be better than 99% pure in each case.

Infrared Absorption Results

Bis-(2-hydroxy-3-*t*-butyl-5-methylphenyl)-methane.—The infrared absorption data for this compound may be seen in Fig. 1. Here may be seen the molecular structure diagram as well as the absorption bands for the material under three different condition. These curves, and later ones, are vertically displaced from one another for clarity. They were obtained by automatic scanning and give the amount of transmitting energy as a function of wave length. Curve A is for a solution of 1.0×10^{-2} mole/liter. At this strength it is known from previous work² that negligible intermolecular hydrogen bonding can occur due to the large average separation between molecules. In this spectrum a sharp absorption band at 2.76μ is the characteristic "free" hydroxyl absorption band, *i. e.*, absorption due to hydroxyl groups which are not members of hydrogen bonded complexes. In addition may be seen a strong, broad band centering at 2.85μ . Since the concentration is too low to permit intermolecular bonding this latter band must be ascribed to intramolecular bonding. We hence have the surprising result that this material may exist in two forms in dilute solutions. The 2.76μ band is ascribed to molecular configurations wherein the phenolic groups are so oriented relative to the bridging group that the two hydroxyl groups are widely separated and hence are free of hydrogen bonding effects. This we call the *trans*-isomeric form. The 2.85μ band is ascribed to molecular configurations wherein the phenolic nuclei are so oriented that there is intramolecular bonding between the hydroxyls. This we call the *cis*-isomeric form.

In Curve B may be seen the spectrum for the recrystallized melt. Note that the free hydroxyl

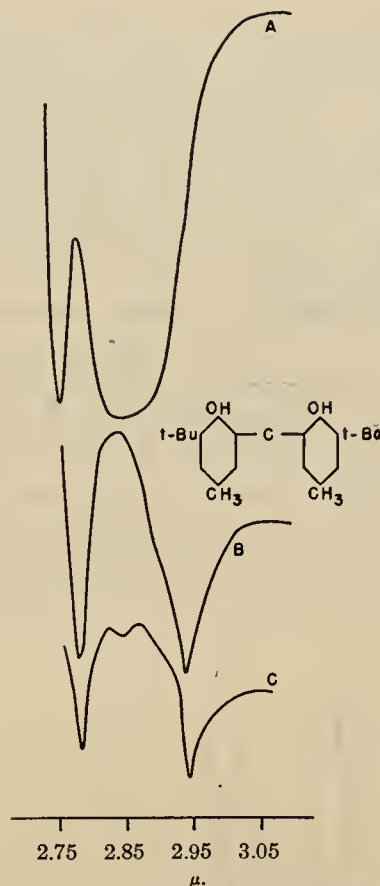


Fig. 1.—Infrared absorption spectra in the hydroxyl region of various forms of bis-(2-hydroxy-3-*t*-butyl-5-methylphenyl)-methane.

band remains strong but that the intramolecular bonding at 2.85μ has disappeared and there is a new band occurring at 2.94μ . The latter is known to be characteristic of hydroxyl groups which are members of strong intermolecular hydrogen bonds. Curve C is the spectrum for the material as a smear. There is, in addition to the free hydroxyl band and the intermolecular bonding band, a faint band characteristic of the *cis*-isomeric form. The wave lengths of the bands and the assignment to the different types for these data may be seen in Table I.

TABLE I

WAVE LENGTHS AT WHICH HYDROXYL ABSORPTION OCCURS IN BIS-(2-HYDROXY-3-*t*-BUTYL-5-METHYLPHENYL)-METHANE

Sample	Wave length, μ	State of existence
Powder (smear)	2.94	Intermolecular bonding
	2.78	<i>trans</i> -Isomer
Recrystallized melt	2.94	Intermolecular bonding
	2.78	<i>trans</i> -Isomer
0.5 m./l. solution	2.85	<i>cis</i> -Isomer
	2.76	<i>trans</i> -Isomer
0.01 m./l. solution	2.85	<i>cis</i> -Isomer
	2.76	<i>trans</i> -Isomer

These data show that this material may exist in three different states. It is to be noted that at a concentration of 0.5 m./l. no intermolecular bonding occurs. This concentration is sufficient to produce strong intermolecular bonding unless the material is sterically hindered. The ortho substituted *t*-butyl groups provide this hindrance in solution. As the material goes into the crystalline phase there is apparently a re-orientation which allows the *cis*-isomeric material to become intermolecularly bonded.

1,1-Bis-(2-hydroxy-3-*t*-butyl-5-methylphenyl)-ethane.—The data for this material are given in Fig. 2. Curves A and B give the spectra of solutions of strength 1.0×10^{-2} and 0.5 m./l., respectively. In each appears the free hydroxyl absorption band representing the *trans*-isomer form. In addition, in each there is the 2.86 μ band due to intramolecular bonding and which represents the *cis*-isomeric form. No intermolecular bonding is evident for the stronger solution indicating the effectiveness of the steric hindrance due to the *t*-butyl groups. Curve C gives the spectrum for the

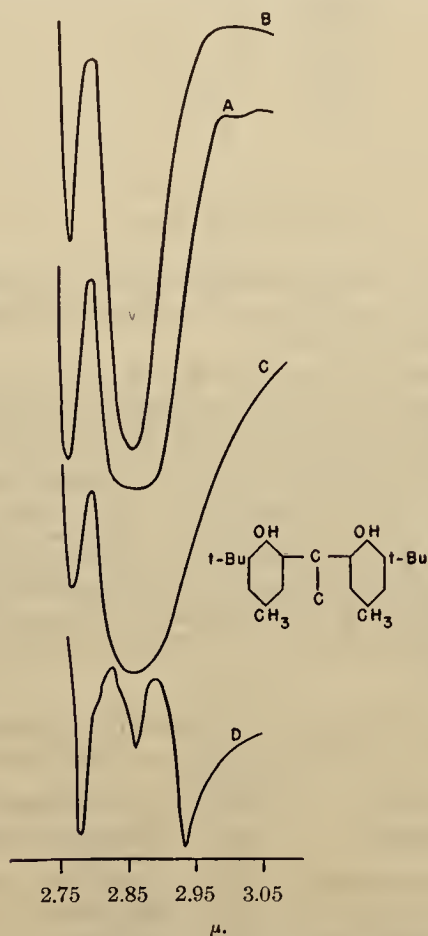


Fig. 2.—Infrared absorption spectra in the hydroxyl region of various forms of 1,1-bis-(2-hydroxy-3-*t*-butyl-5-methylphenyl)-ethane.

material after melting and cooling. Here we observe the presence of the *cis*- and *trans*-isomeric forms and no intermolecular bonding.

The spectrum of the material as a smear is given in Curve D. Note that there is a strong *trans*-isomeric band at 2.78 μ , a weaker *cis*-isomeric form band at 2.86 μ and a strong, sharp intermolecular bonding band at 2.93 μ . Thus, the material exists in substantial proportions in all forms in the original powder state. After the material is melted it does not recrystallize but forms a glass. This is significant in view of the differences between Curves C and D. After melting and cooling there is no intermolecularly bonded form. The conclusion from these differences is that for the original material to crystallize there must be a definite distribution between the three states. When the material is melted this distribution is altered and the material cannot recrystallize. Table II gives the wave lengths at which this compound evidences hydroxyl absorption.

TABLE II

WAVE LENGTHS AT WHICH HYDROXYL ABSORPTION OCCURS IN 1,1-BIS-(2-HYDROXY-3-*t*-BUTYL-5-METHYLPHENYL)-ETHANE

Sample	Wave length, μ	State of existence
Powder (smear)	2.93	Intermolecular bonding
	2.86	<i>cis</i> -Isomer
	2.78	<i>trans</i> -Isomer
Glass	2.86	<i>cis</i> -Isomer
	2.76	<i>trans</i> -Isomer
0.5 m./l. solution	2.86	<i>cis</i> -Isomer
	2.76	<i>trans</i> -Isomer
0.01 m./l. solution	2.86	<i>cis</i> -Isomer
	2.76	<i>trans</i> -Isomer

1,1-Bis-(2-hydroxy)-3-*t*-butyl-5-methylphenyl)-isobutane.—The spectra for this compound will not be shown. It also showed the existence of the *cis*- and *trans*-isomeric forms in a solution of 1.0×10^{-2} m./l. concentration. A spectrum for a solution strength of 0.5 m./l. was not possible due to the low solubility in carbon tetrachloride. In both the recrystallized melt and the smear only one band appeared. This was centered at about 3.12 μ and is ascribed to a very strong type of intermolecular bonding. This is a surprising result as strong bonding would not be expected in view of the *t*-butyl groups substituted ortho to the hydroxyls. This compound is also anomalous in comparison to the above two in that neither *cis*

TABLE III

WAVE LENGTHS AT WHICH HYDROXYL ABSORPTION OCCURS IN 1,1-BIS-(2-HYDROXY-3-*t*-BUTYL-5-METHYLPHENYL)-ISOBUTANE

Sample	Wave length, μ	State of existence
Powder (smear)	3.12	Intermolecular bonding
Recrystallized melt	3.12	Intermolecular bonding
1.0×10^{-2} m./l. solution	2.75	<i>trans</i> -Isomer
	2.86	<i>cis</i> -Isomer

nor *trans* forms are observed for the solid state. The wave lengths observed are given in Table III.

Bis-(2-hydroxy-3-*t*-butyl-5-methylphenyl)-phenylmethane.—The data for this compound may be seen in Fig. 3. Here Curve C is for the smear. It exhibits the absorption of the *cis*-isomeric form as a doublet but shows no evidence for either the *trans* isomer or the intermolecularly bonded form. When the material is examined as a recrystallized melt it again shows no evidence for the latter two forms but shows only the *cis*-isomeric form, although the doublet structure is destroyed. When the material is in solution it is interesting that a weak but definite *trans* absorption band appears.

The fact that the spectrum of the smear shows only the *cis* form implies that either the material was synthesized entirely in the *cis* form or that there is a conversion of the existing *trans* form to the *cis* form at the time of the initial crystallization. The low intensity of the *trans* band for the solutions infers that conversion, through rotation about the saturated valence bonds of the bridging group, of the *cis* isomer to *trans* isomer is possible but not probable. From the size of the phenyl ring group attached to the bridging carbon it would be expected that such rotation might be completely blocked. An investigation with Fisher-Hirschfelder molecular models⁵ shows that this rotation is possible although sterically hindered. The absorption wave lengths for this material are given in Table IV. It is interesting as a type of bis-phenol intermediate between those of above in which the *cis* and *trans* isomers are represented in roughly equal proportions and those to be described immediately below which exist only in the *cis* form.

TABLE IV

WAVE LENGTHS AT WHICH HYDROXYL ABSORPTION OCCURS IN BIS-(2-HYDROXY-3-*t*-BUTYL-5-METHYLPHENYL)-PHENYL-METHANE

Sample	Wave length, μ	State of existence
Powder (smear)	2.83	<i>cis</i> -Isomer
	2.82	<i>cis</i> -Isomer
Recrystallized melt	2.85	<i>cis</i> -Isomer
0.5 m./l. solution	2.85	<i>cis</i> -Isomer
	2.75 (weak)	<i>trans</i> -Isomer
0.01 m./l. solution	2.85	<i>cis</i> -Isomer
	2.75 (weak)	<i>trans</i> -Isomer

2,2-Bis-(2-hydroxy-3-*t*-butyl-5-methylphenyl)-butane, 2,2-Bis-(2-hydroxy-3-*t*-butyl-5-methylphenyl)-propane, and 1,1-Bis-(2-hydroxy-3-*t*-butyl-5-methylphenyl)-cyclohexane.—These three bis-phenols are grouped because they possess the common characteristic of existing only in the *cis* form. The data for one, the 2,2-butane type, may be seen in Fig. 4. Here Curves A and B are solutions of 1.0×10^{-2} m./l. and 0.5 m./l., respectively, Curve C is for the recrystallized melt and Curve D is for a smear. For Curves A,

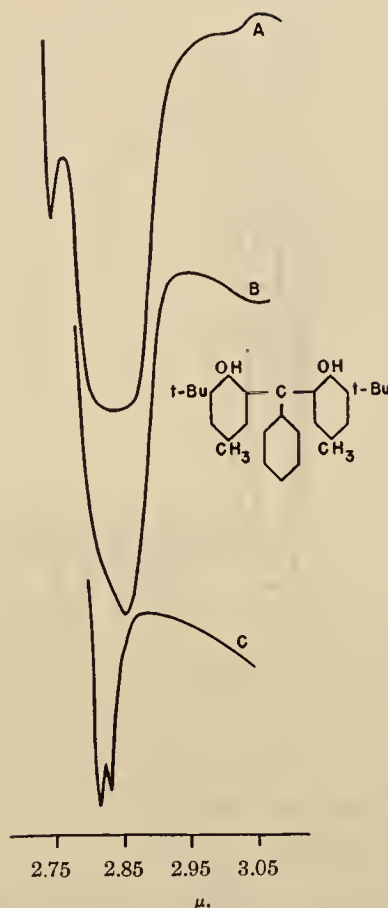


Fig. 3.—Infrared absorption spectra in the hydroxyl region of various forms of bis-(2-hydroxy-3-*t*-butyl-5-methylphenyl)-phenylmethane.

B and C the maximum of absorption occurs at 2.87μ and for Curve D it appears at 2.88μ . It is clear that this band must in every case represent only the *cis*-isomeric form. No *trans* form nor intermolecularly bonded form appears in any state in which the material was examined. This is significant as it implies that the material was originally synthesized in the *cis* form completely.

The behavior of the 2,2-bis-(2-hydroxy-3-*t*-butyl-5-methylphenyl)-propane, for which the data are not shown was very similar to the material above. It was examined as a smear, as the recrystallized melt, in a solution at 0.5 m./l., and in a solution at 1.0×10^{-2} m./l. In each case only one band appeared. This was at 2.87μ in each case and is ascribed to the *cis*-isomeric form.

The data for the third of these compounds, *i. e.*, 1,1-bis-(2-hydroxy-3-*t*-butyl-5-methylphenyl)-cyclohexane are given in Fig. 5. Here Curves A and B are for solutions of 1.0×10^{-2} and 0.5 m./l., respectively, and Curve C is for the original material which in this case was a liquid. Again we observe only the characteristic *cis*-isomeric band. The common center of the band in this case was at 2.85μ .

(5) Available from Fisher Scientific Co., Pittsburgh, Pennsylvania.

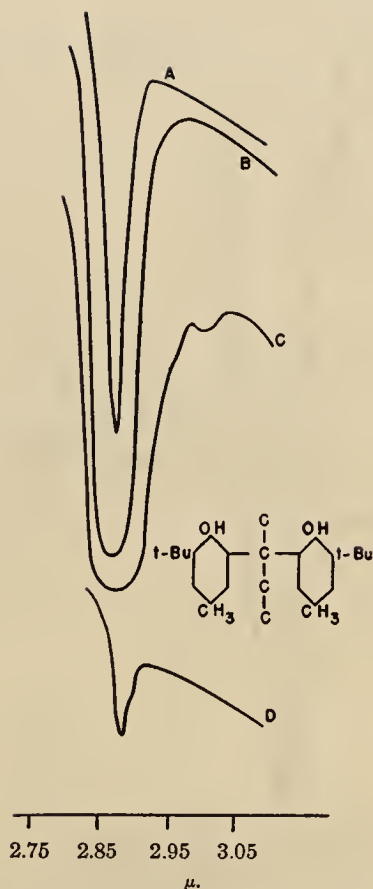


Fig. 4.—Infrared absorption spectra in the hydroxyl region of 2,2-bis-(2-hydroxy-3-*t*-butyl-5-methylphenyl)-butane under various conditions.

The compounds just discussed are remarkable in that they exist in only the *cis*-isomeric form. As was remarked this indicates that in the synthesis only the *cis* form was created. Each of these materials is characterized by the size of the bridging group or the manner of substitution on it. For two of them the bridging is across the number 2 carbon atom in the chain. In the other the effective appendage (the remainder of the cyclohexyl group) on the bridging carbon atom is large due to the unsaturation. These are important items since the materials are found only in the *cis* form. With these types of bridging groups there is so much hindrance to rotation that a *cis* isomer cannot pass to the *trans* form. This may be verified by examination of the corresponding molecular models. These compounds are different in another respect from the earlier ones. There is no tertiary hydrogen atom on the bridging carbon atoms. What effect this has on the molecular properties cannot be conclusively stated. The fact that the materials are synthesized in the *cis* form indicates that the *trans* form is either forbidden because of large steric hindrance effects or that the *cis* form exists in a lower

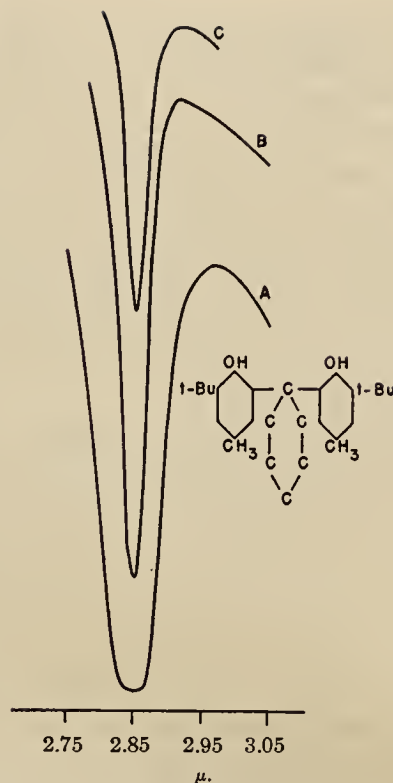


Fig. 5.—Infrared absorption spectra in the hydroxyl region of 1,1-bis-(2-hydroxy-3-*t*-butyl-5-methylphenyl)-cyclohexane under various conditions.

energy state and hence is preponderantly much more probable.

Bis-(2-hydroxy-3-methyl-5-isoöctylphenyl)-methane.—This material is of interest because of the smaller substituents ortho to the hydroxyl groups. As previously remarked^{2,3} large ortho groups are very effective in hindering the formation of intermolecular bonds. We should expect this compound to exhibit very strong intermolecular bonding in the solid state and in the 0.5 m./l. solution. The data are given in Fig. 6. Curve A is for a 1.0×10^{-2} m./l. solution, Curve B is for a 0.5 m./l. solution and Curve C is for the material recrystallized after melting. Note that in the latter case only absorption ascribable to intermolecular bonding is observed. This is also

TABLE V
WAVE LENGTHS AT WHICH HYDROXYL ABSORPTION OCCURS IN BIS-(2-HYDROXY-3-METHYL-5-ISOÖCTYLPHENYL)-METHANE

Sample	Wave length, μ	State of existence
Powder (smear)	2.95	Intermolecular bonding
Recrystallized melt	2.95	Intermolecular bonding
0.5 m./l. solution	2.95	Intermolecular bonding
	2.77	<i>trans</i> -Isomer
1.0×10^{-2} m./l. solution	2.88	<i>cis</i> -Isomer
	2.77	<i>trans</i> -Isomer

true of the spectrum (not shown) of the material when examined as a smear. In a medium strength solution such as 0.5 m./l. there is still very strong intermolecular bonding although a fairly strong *trans* absorption band also appears. This is seen in Curve B. In the weaker solution of 1.0×10^{-2} m./l. (Curve A) such that intermolecular effects are removed the spectrum shows both the *cis* and *trans* form. In Table V are given the wave lengths at which hydroxyl absorption maxima are observed.

Discussion.—From the above data it may be seen that the bis-phenol alkanes wherein the bridging group is ortho to the hydroxyls may be divided into two classes: those that admit of both *cis*- and *trans*-isomeric forms and those that are found only in the *cis* form. It may be further seen that the latter class are those such that the bridging groups offer very large steric hindrance to passage from a *cis* to a *trans* form. Either the bridging is through 2,2-substitution on a chain or the bridging group is very large. As remarked earlier these materials are apparently synthesized directly into the *cis* form as no evidence for the *trans* is found under any of the conditions used.

Among those bis-phenols which exist in both the *cis*- and *trans*-isomeric forms there are large variations in individual behavior. This was exhibited primarily in their hydrogen bonding behavior in the solid state or in concentrated solution as compared to that in dilute solution. For the latter case they all exhibited the *cis* and *trans* forms. However, several variations with respect to the distribution among the *cis* and *trans* forms and intermolecular bonding are observable. From this we may then conclude that the detailed distribution among these forms in the solid state is a specific function of particular bridging group.

The percentages of each compound present in the *cis* and *trans* forms when in dilute solution have been calculated. We may express Beer's law of absorption as

$$D = \log (I_0/I) = ACI$$

where D is the optical density, I_0 and I are the incident and transmitted energies, respectively, A is the extinction coefficient, C is the concentration of absorbing material, and l is the cell thickness. In a previous study of a large number of substituted phenols it has been found that A for the free hydroxyl absorption at about 2.76μ is essentially constant for all. For the present case we therefore assume that the absorption per free hydroxyl group in a *trans* isomer is the same as the absorption per free hydroxyl group in a hindered phenol. For the latter 2,6-di-*t*-butyl-4-methylphenol was used. With the concentration expressed in m./l. it yielded an A with a numerical value of 136.

The optical density for the free hydroxyl band was then determined for each bis-phenol alkane and divided by twice the A obtained for the hindered phenol of above to yield the concentration of *trans*-isomer present. This was then combined

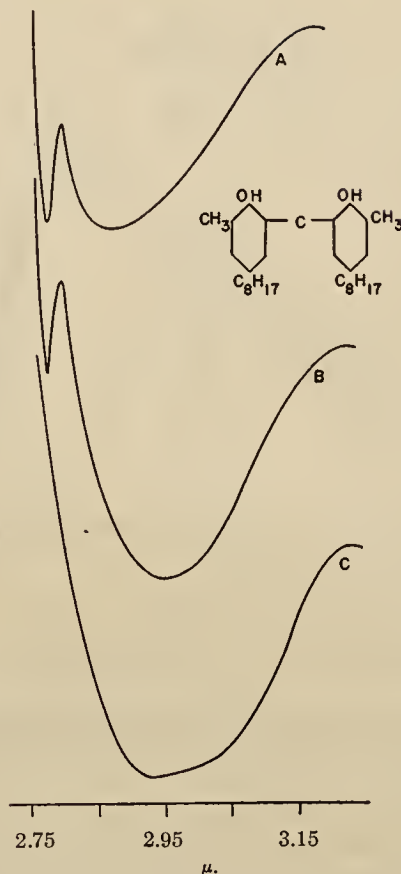


Fig. 6.—Infrared absorption spectra in the hydroxyl region of bis-(2-hydroxy-3-methyl-5-isoctylphenyl)-methane under various conditions.

with the known concentration of the bis-phenol to yield the per cent. of *cis*-isomer present. The results are given in Table VI. The difference per

TABLE VI

DISTRIBUTION BETWEEN *cis*- AND *trans*-ISOMERIC FORMS AND VALUES OF A FOR THE INTRAMOLECULARLY BOUND HYDROXYL GROUP

Compound	% <i>trans</i>	% <i>cis</i>	A
Bis-(2-hydroxy-3- <i>t</i> -butyl-5-methyl-phenyl)-methane	30.3	69.7	202
1,1-Bis-(2-hydroxy-3- <i>t</i> -butyl-5-methyl-phenyl)-ethane	18.3	81.7	229
1,1-Bis-(2-hydroxy-3- <i>t</i> -butyl-5-methyl-phenyl)-isobutane	45.3	54.7	181
Bis-(2-hydroxy-3- <i>t</i> -butyl-5-methyl-phenyl)-phenylmethane	7.7	92.3	102
Bis-(2-hydroxy-3-methyl-5-isoöctyl-phenyl)-methane	55.8	44.2	196
Bis-(2-hydroxy-3- <i>t</i> -butyl-5-methyl-phenyl)-cyclohexane	..	100	82
2,2-Bis-(2-hydroxy-3- <i>t</i> -butyl-5-methyl-phenyl)-propane	..	100	442
2,2-Bis-(2-hydroxy-3- <i>t</i> -butyl-5-methyl-phenyl)-butane	..	100	552

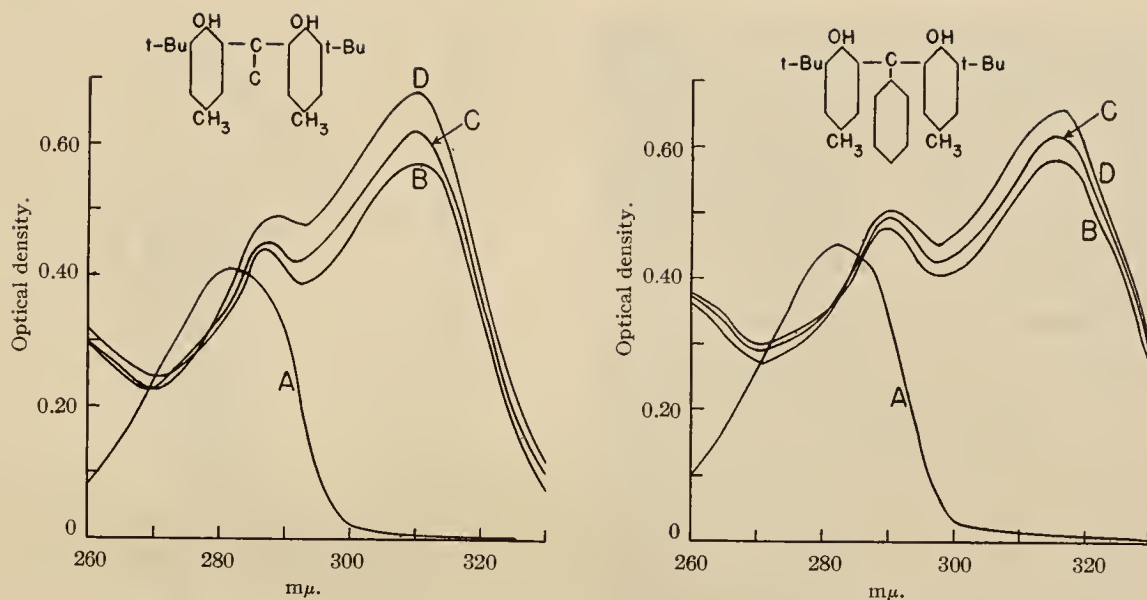


Fig. 7.—Ultraviolet absorption spectra of (a) 1,1-bis-(2-hydroxy-3-*t*-butyl-5-methylphenyl)-ethane and (b) bis-(2-hydroxy-3-*t*-butyl-5-methylphenyl)-phenylmethane in: A, ethanol; B, ethanol plus 1.0×10^{-1} m./l. of sodium hydroxide; C, ethanol plus 5×10^{-1} m./l. of sodium hydroxide; D, ethanol plus 5.0 m./l. of sodium hydroxide.

cent. of *cis*-isomer present is then used with the optical density for the bound hydroxyl band to yield a value of *A* for the latter in each case. These are also given in Table VI.

The validity of the data in Table VI rests upon the assumption that the absorption per free hydroxyl group in a bis-phenol alkane is the same as for the hindered phenol. This assumption was used in the calculation of the per cent. distribution between the two isomeric forms. Those data were in turn used in the determination of the *A* values. With the data obtained there was no way to make an independent check on the above assumption. Since group absorption coefficients are ordinarily reasonably constant in progressing through a series of compounds it is surprising that that *A* values, *i. e.*, the absorption coefficients for the intramolecularly bound hydroxyls, varied as much as they did. They are constant only to within an order of magnitude. The variations exhibited are presumably due to differences in types of bridging groups and the manner of bridging.

The observations above permitted an interesting prediction of the ionization behavior of the two classes of bis-phenols. In the *cis*-isomeric form the two hydroxyl groups are hydrogen bonded to each other. Since material existing totally in the *cis* form exhibits no free hydroxyl absorption it is known that both hydroxyl protons are involved. The assumed model of the bonding is one of dipole-dipole attraction wherein the proton of each hydroxyl group is attracted to the oxygen atom of the other. Such a configuration allows the electrostatic field due to the dipole moment of one hydroxyl group to essentially cancel out the field due to the other. The electrostatic field about the

molecule is at best then a weak quadrupole field. This is in contrast to the two dipole fields attendant to each *trans* isomer. We may therefore expect the *cis*-isomeric form to be less acidic than the *trans* form. We may also expect them to be less acidic for another reason. This is due to the negative potential energy associated with the formation of the intramolecular bond in the *cis* isomer. This results in a higher ionization potential for the *cis* isomers. This expected decrease of acidity is found to be true by ultraviolet absorption measurements which will be discussed below.

The above observations now make available a tool for the determination of substitution in bis-phenols of uncertain structure since their distribution between *cis* and *trans* forms in dilute solution is known to depend on the type and size of the bridging group.

Ultraviolet Absorption Results

When a phenol molecule becomes ionized the ultraviolet absorption due to the phenyl ring chromophore shifts to the red by about 20 mμ. Thus, ultraviolet absorption spectroscopy provides a useful tool for the study of ionization in phenols. In a recent study⁶ of the ionization in a series of substituted phenols it was shown that large alkyl groups ortho to the hydroxyl group are very effective in reducing acidity. Thus the partially hindered phenols are much weaker acids than the unhindered phenols and the hindered phenols are much weaker acids than the partially hindered phenols. This is a result of the smaller differences between energies of solvation of

(6) N. D. Coggeshall and A. S. Glessner, Jr., *THIS JOURNAL*, **71**, 3150 (1949).

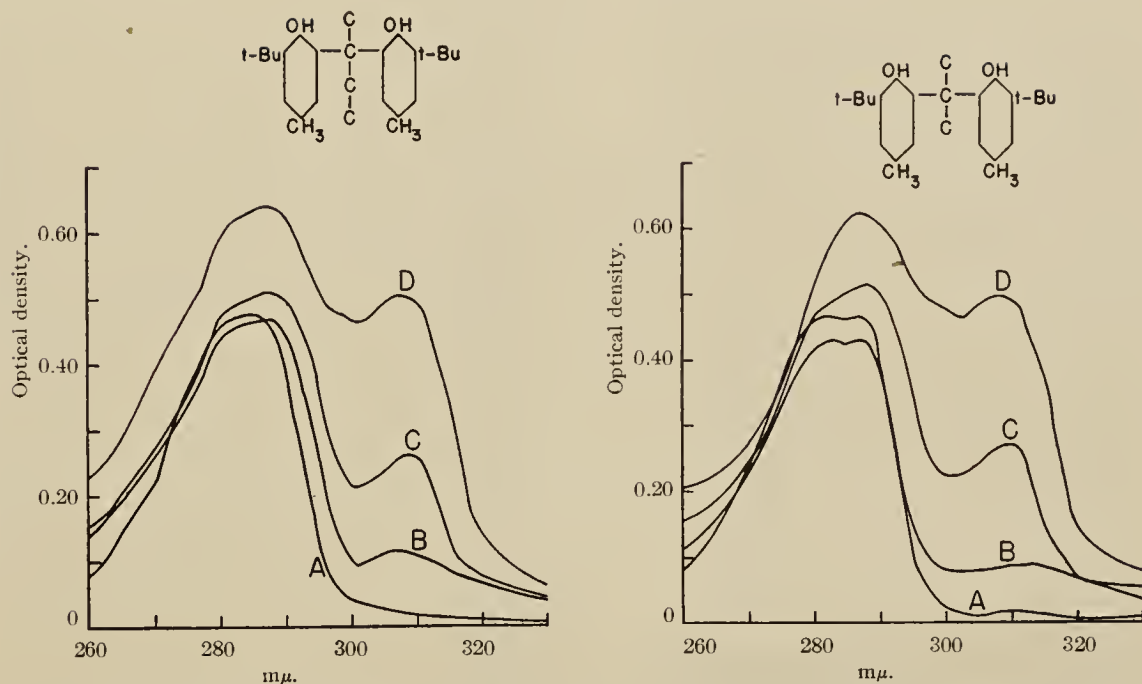


Fig. 8.—Ultraviolet absorption spectra of (a) 2,2-bis-(2-hydroxy-3-*t*-butyl-5-methylphenyl)-butane and (b) 2,2-bis-(2-hydroxy-3-*t*-butyl-5-methylphenyl)-propane in: A, ethanol; B, ethanol plus 1.0×10^{-1} m./l. of sodium hydroxide; C, ethanol plus 5.0×10^{-1} m./l. of sodium hydroxide; D, ethanol plus 5.0 m./l. of sodium hydroxide.

the ions and un-ionized molecules for the hindered materials. In view of the above results we would expect a material existing totally in the *cis* form due to the bridging to remain in the *cis* form after ionization. Thus it would be expected that bis-phenols in the *cis*-isomeric form would be less acidic than those in the *trans*-isomeric form as there would be a large steric hindrance to interaction between the ions and the solvent and hence less increase of energy of solvation upon ionization. The steric hindrance here is due to the *t*-butyl groups ortho to the hydroxyls.

Bis-phenol Alkanes Existing in *cis*- and *trans*-Isomeric Forms.—Typical data for two of these materials, the 1,1-bis-(2-hydroxy-3-*t*-butyl-5-methylphenyl)-ethane and the bis-(2-hydroxy-3-*t*-butyl-5-methylphenyl)-phenylmethane may be seen in Fig. 7(a) and (b). Curve A refers to the material in ethanol solution and Curves B, C and D to ethanol plus 1.0×10^{-1} , 5.0×10^{-1} and 5.0 m./l. of sodium hydroxide, respectively. For each compound characteristic phenol absorption, centering near 280 $m\mu$, is obtained when examined in ethanol. When sodium hydroxide is added a new and very intense band appears at a longer wave length which is due to the phenolate ion. In the present case the presence of the sodium hydroxide is responsible for an apparent shift of the absorption of the un-ionized material about 5 $m\mu$ to the red. This is due to two effects: a virtual shift due to the superposition of absorption due to ionized and un-ionized material and

the usual shift to the red due to a change of solvent properties.

Although the addition of 1.0×10^{-1} m./l. of sodium hydroxide produces a large change of spectra, further increase of sodium hydroxide concentration by factors of 5 and 50 produce little further change. This is interpreted as follows: the addition of 1.0×10^{-1} m./l. of base ionizes most of the *trans*-isomeric material present with little effect on the *cis*-isomeric material; further additions of base have little effect since most of the readily ionizable material is already ionized and the remainder is of the *cis* form which is highly resistant to ionization. This interpretation is consistent with and confirms the predictions of above regarding ionization.

Bis-(2-hydroxy-3-methyl-5-isoöctyl-phenyl)-methane behaves in a class by itself with respect to ionization. Almost complete ionization is achieved with the addition of only 1.0×10^{-1} m./l. of sodium hydroxide. This is ascribed to the unhindered nature of this phenol, *i.e.*, the lack of large alkyl groups, which allows the close approach between the hydroxyl groups and other molecules or ions with subsequent ionization.

Bis-phenol Alkanes Existing in the *cis* Form Only.—Data for two of these materials, the 2,2-bis-(2-hydroxy-3-*t*-butyl-5-methylphenyl)-butane and the 2,2-bis-(2-hydroxy-3-*t*-butyl-5-methylphenyl)-propane, are given in Fig. 8(a) and (b). Curve A refers to the material in pure ethanol and Curves B, C and D to the

material in ethanol plus 1.0×10^{-1} , 5.0×10^{-1} and 5.0 m./l. of sodium hydroxide, respectively. In contrast to the bis-phenols existing in *cis* and *trans* forms the addition of 1.0×10^{-1} m./l. of base produces very little ionization. Also the effects of increasing the base from 1.0×10^{-1} to 5.0 m./l. are relatively much larger. However, even the heaviest concentration of base does not produce strong ionization. These observations confirm the predictions of above that such materials would be highly resistant to ionization. Since in the *cis* form the hydroxyls are bonded together and produce a cross cancellation of dipole fields the molecule as a whole possesses at most only small electric fields. It thus has the property of an essentially non-polar material.

As the hydrogen bonding behavior, as observed by infrared absorption, may be used for structure determination so also may the ionization behavior, as observed by ultraviolet absorption. The above data, for example, demonstrate how differentiation may be made between a bis phenol allowing *cis* and *trans* forms and one allowing the *cis* form only.

Acknowledgment.—Acknowledgment is gratefully made to Dr. Donald R. Stevens and Mr. A. C. Dubbs for kindly furnishing the compounds studied, to Miss E. L. Saier and Mr. A. S. Glessner, Jr., for aid in obtaining the data and to Dr. Paul D. Foote, Executive Vice-President of Gulf Research and Development Company for permission to publish this material.

Summary

A series of bis-phenol alkanes have been examined by infrared and ultraviolet absorption spectroscopy. These materials were found to exist in three distinct states, with regard to their hydrogen bonding characteristics. They exist in *cis*- and *trans*-isomeric forms and with intermolecular hydrogen bonding. This *cis*-isomeric form is one wherein the phenolic nuclei are so oriented relative to each other that there is intramolecular hydrogen bonding between the hydroxyl groups. The *trans* form is one wherein the orientation is such that the hydroxyl groups do not influence each other.

Bis-phenol alkanes with a 2,2-substitution on the bridging group or with a bridging group having a very large appendage are restricted to existence in the *cis* form only. They are shown to have been originally synthesized completely in that form.

The distribution between *cis* and *trans* forms is given for those compounds that exist in both states. The distribution in each case appears to be unique to the compound. On the basis of intramolecular hydrogen bonding whereby the two hydroxyl groups effect a cross cancellation of dipole fields it was predicted that those materials existing in the *cis* form only would be less acidic than those existing in *cis* and *trans* forms. This prediction was confirmed by ultraviolet absorption measurements on the materials in alkaline solutions.

PITTSBURGH 30, PA.

RECEIVED OCTOBER 11, 1949

Solvent Induced Frequency Shifts for Cata-Condensed Aromatics

NORMAN D. COGGESHALL AND ABBOTT POZEFSKY
Gulf Research and Development Company, Pittsburgh, Pennsylvania
(Received May 23, 1951)

BAYLISS¹ has discussed the interaction between solute and solvent whereby electronic transition frequencies are reduced by electrostatic interaction effects. The purpose of the present note is to present certain data on this effect observed for cata-condensed aromatics. These data were obtained with a Beckman DU spectrophotometer.

In the first phase of this work the low frequency band of naphthacene (*circa* 22,000 cm^{-1}) was correlated with the index of refraction of the solvent. For this the solvent was varied to have values of n_D between 1.3915 and 1.6219 by using 2,2,4-trimethylpentane, benzene, styrene, naphthalene, α -methyl-naphthalene, anthracene, and phenanthrene in various combinations and concentrations. The results may be seen in Fig. 1. Here are plotted the observed frequency *versus* $(1/2)(1 - 1/n_D^2)$, which corresponds to Bayliss' Eq. (2), and *versus* $(n_D^2 - 1)/(2n_D^2 + 1)$, which corresponds to his Eq. (3). Here K , the dielectric constant, has been replaced by n_D^2 . It is seen that there is a definite relation between the frequency and the n_D of the solvent. Throughout the central portion of the data the curves are linear in accordance with Bayliss' equations, and the representations are essentially equivalent for the data at hand. It would be necessary to have the vapor phase frequency to obtain a more complete check of the theory. There is a question regarding the appropriateness of the n_D values used rather than index of refraction values for frequencies in the range of the absorption band. This introduces doubt as to the absolute value of the slopes of the curves. However, the dependence of frequency upon index of refraction is definitely displayed, and the concept of the effect as originating in the polarization of the solvent is thereby confirmed.

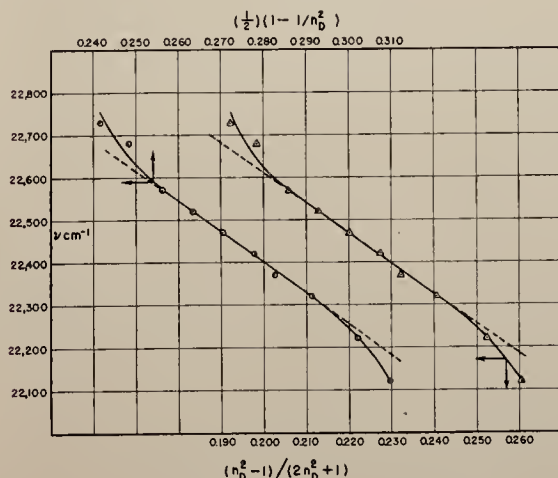


FIG. 1. Dependence of the frequency of naphthacene on the refractive index of the solvent.

TABLE I. Assignment of frequencies in cm^{-1} observed in 2,2,4-trimethylpentane solution.

Compound	' L_a	' L_b	' B_b
Phenanthrene	26670 28090	28900 29540 30300 30960 31700	34130 35590
Anthracene	26670 28090 29500 30960
1,2 benzanthracene	27970 29330 30670 31950	26010 26700	34780 36180
9,10-dimethyl-1,2-benzanthracene	26280 27590 28940	...	33730 35030
1,2,5,6-dibenzanthracene	28740 29990 31250	25410 26080 26810 27510	33610 34970
Methylcolanthrene	27820 29240 30630	25450 26390 26880	33730 35090
Naphthacene	21320 22780 24180	25310	...

The second phase of this investigation was concerned with the correlation of magnitude of frequency shift with type of transition being observed. The terminology used in identifying the transitions is that described by Platt² in his classification of the spectra of cata-condensed hydrocarbons. In this work a series of aromatics was examined in 2,2,4-trimethylpentane solution and in benzene solution. The shifts toward lower frequencies induced by the change of solvent were then correlated with type of transition.

In Table I are given the observed frequencies in the paraffin solution and the tentative assignments using Platt's classification. The transitions are from the ground level to the state indicated. As these data were obtained at wavelength points separated by at least 0.5 $\text{m}\mu$ on the instrument named above, they do not possess

TABLE II. Average frequency shifts between paraffin and benzene solution for the assigned transitions.

Compound	$\Delta\nu('L_a)$	$\Delta\nu('L_b)$	$\Delta\nu('B_b)$
Phenanthrene	295	118	310
Anthracene	275
1,2 benzanthracene	312	155	570
9,10-dimethyl-1,2-benzanthracene	313	...	470
1,2,5,6-dibenzanthracene	297	150	440
Methylcolanthrene	340	210	470
Naphthacene	323	120	...

the precision obtainable with more refined equipment. However, they are adequate for the purposes of this note, which is to point out the order-of-magnitude variations in the shifts observed for the different transitions.

In Table II are given the average values of $\Delta\nu$ for each transition induced by the change in solvent. These are averaged in each case over the individual values obtained for the separate bands as listed in Table I. It is clear from the table that the $\Delta\nu$ for any transition remains of the same order of magnitude throughout the series of materials. Note also that $\Delta\nu('L_a)$ is generally of the order of twice the $\Delta\nu('L_b)$ and that $\Delta\nu('B_b)$ is of the order of three

times $\Delta\nu('L_b)$. The approximate constancy of $\Delta\nu$ for a given transition thus provides a basis for the assignment of the bands to the various transitions for molecules not yet investigated.

Another correlation which may also serve in the assignments for further molecules resides in the separations between individual bands for any particular transition. In Table III are given the values of $\langle\Delta\nu\rangle_{Av}$ for the various transitions for each material. Here $\langle\Delta\nu\rangle_{Av}$ is the average frequency separation between the individual bands for any transition, as examined in the paraffin solution. Here it is evident that $\langle\Delta\nu\rangle_{Av}$ is always of the order of 1300 cm^{-1} for either $'L_a$ or $'B_b$ transitions whereas $\Delta\bar{\nu}$ is always of the order of 700 cm^{-1} for the $'L_b$ transitions.

Following the reasoning of Jones,³ the $\langle\Delta\nu\rangle_{Av}$ values as observed for the $'L_a$ and the $'B_b$ may tentatively be assigned to in-plane C—H bending vibrations. The $\langle\Delta\nu\rangle_{Av}$ values as observed for the $'L_b$ transitions are then tentatively assigned to out-of-plane C—H bending vibrations.

Acknowledgment is made to Mr. A. S. Glessner, who aided in obtaining some of the data.

¹ N. S. Bayliss, J. Chem. Phys. **18**, 292 (1950).

² J. R. Platt, J. Chem. Phys. **17**, 484 (1949).

³ R. N. Jones, Chem. Revs. **41**, 353 (1947).

TABLE III. $\langle\Delta\nu\rangle_{Av}$ values observed for paraffin solutions.

Compound	$\langle\Delta\nu\rangle_{Av}('L_a)$	$\langle\Delta\nu\rangle_{Av}('L_b)$	$\langle\Delta\nu\rangle_{Av}('B_b)$
Phenanthrene	1320	705	1460
Anthracene	1430
1,2-benzanthracene	1350	690	1400
9,10-dimethyl-1,2-benzanthracene	1325	...	1300
1,2,5,6-dibenzanthracene	1250	697	1360
Methylcolanthrene	1410	725	1380
Naphthacene	1430

[Reprinted from the Journal of the American Chemical Society, 73, 5414 (1951).]

Infrared Absorption Study of Hydrogen Bonding Equilibria

By Norman D. Coggeshall and Eleanor L. Saier

[CONTRIBUTION FROM THE GULF RESEARCH & DEVELOPMENT COMPANY]

Infrared Absorption Study of Hydrogen Bonding Equilibria

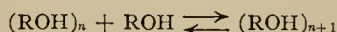
BY NORMAN D. COGGESHALL AND ELEANOR L. SAIER

A study has been made of hydrogen-bonding equilibria using the infrared absorption due to the unassociated hydroxyl group. Sterically unhindered molecules associate in polymeric complexes. Agreement between theory and experiment obtained by the use of two dissociation equilibria constants, one for the dissociation of dimeric complexes and one for the dissociation of higher order complexes is better than that obtained by the single dissociation equilibrium constant scheme of Kempter and Mecke. These constants have been evaluated for a series of simple alcohols and phenols. If a phenol has one ortho position occupied by a large substituent such as a *t*-butyl group it will be sterically hindered and will associate almost entirely in dimeric complexes. The equilibrium constants for several such partially hindered phenols have been evaluated. Hydrogen bonding occurs between hydroxylated materials and proton-acceptor compounds. Equilibrium constants have been evaluated for the systems of benzyl alcohol and methyl ethyl ketone and of benzyl alcohol and 1,4-dioxane.

The present report is of some studies of the equilibrium of hydroxylated materials between the free or unassociated state and the hydrogen-bonded or associated state. The data for this were obtained by infrared absorption measurements wherein the absorption due to the "free" hydroxyl group was correlated with the amount of unassociated material present. Fox and Martin¹ reported in 1937 some studies on phenol from which they concluded that at moderate concentrations an equilibrium is set up between single and double (associated) phenol molecules. More recently Kempter and Mecke² examined phenol using the second overtone of the free hydroxyl stretching frequency. They assumed that complexes of all orders were possible and that all the equilibrium coefficients for the dissociation of complexes were the same, and their data appeared to check the theory satisfactorily. In the present work it was found that better agreement between theory and experiment was obtained if two equilibrium coefficients were used: one for the dissociation of the dimer complexes, and one which was applicable to the dissociation of the higher order complexes. It was found that the association of the partially hindered phenols is almost entirely dimer in nature. In addition, the association between benzyl alcohol and methyl ethyl ketone and between benzyl alcohol and dioxane has been studied.

Equilibrium Equations

Case of a Single Equilibrium Constant.—Kempter and Mecke² considered equilibria of the type



where the subscripts n and $n + 1$ refer to complexes of the n th and $n + 1$ th order. They assumed that the dissociation constants were equal for all orders of complexes and hence derived the equation

$$K_c = \alpha C / (1 - \sqrt{\alpha}) \quad (1)$$

where K_c is the general dissociation constant applicable to each order complex, α is the fraction of hydroxylated mole-

cules which are unassociated, and C is the concentration in moles per liter of hydroxylated material. When they plotted αC vs. $\sqrt{\alpha}$ for phenol, Kempter and Mecke obtained a straight line plot from which they concluded that agreement between their theory and experiment was satisfactory. It has not been possible to obtain agreement between our data and this simple theory and this led to a modification of the theory as given in the next section.

Case of Two Equilibrium Constants.—Here the assumption of equality of all dissociation constants is rejected. Instead we use a distinct constant K_1 for the dissociation of dimer complexes and a general constant K_c for all others, i.e., $K_2 = K_3 = K_4 \dots = K_c$. This procedure is based on evidence from three different considerations: (a) the shape and wave length maxima of the association bands at low concentration, (b) the disagreement with data encountered using the simpler scheme, and (c) the evidence that the potential energy in the formation of a dimer complex is considerably less than the potential energy change when an n -fold complex adds a member to become an $n + 1$ -fold complex. A discussion of these points will be given later.

Utilization of the equilibrium conditions between the various orders of complexes leads to the relation

$$\alpha_n = n\alpha \frac{K_c \{ \alpha C \}^{n-1}}{K_1 \{ K_c \}} \quad (2)$$

where α_n refers to the fraction of hydroxylated molecules bound in complexes of the $n + 1$ th order. With the use of the relation $\sum \alpha_n = 1$ one may then derive the expression for K_c , namely

$$K_c = \frac{\alpha C}{2(K_1 - \bar{K}_1)} \left\{ 2K_1 - \frac{\bar{K}_1}{2} + \sqrt{2K_1\bar{K}_1 + \frac{\bar{K}_1^2}{4}} \right\} \quad (3)$$

where $\bar{K}_1 = 2\alpha^2 C / (1 - \alpha)$. To evaluate K_c from Eq. 3 one must first evaluate K_1 . It may be shown from operations on Eq. 3 that $\lim \alpha^2 C / (1 - \alpha) = \bar{K}_1 / 2$ as $C \rightarrow 0$. Therefore, K_1 may be evaluated by plotting $\bar{K}_1 = 2\alpha^2 C / (1 - \alpha)$ versus C and extrapolating to zero concentration.

Experimental Details

All infrared absorption data were obtained on a Perkin-Elmer Model 12B spectrometer equipped with a LiF prism. The transmission measurements were made manually using a null system previously described.³ Three different cell thicknesses were used. For the study of association between hydroxylated molecules and other materials such as ketones, etc., a cell of 1.4 cm. thickness was used. For the studies on alcohols a cell of 0.036" thickness was used. For the phenols a cell of 0.006" thickness was used. The difference in the latter two cell thicknesses is a result of the wide difference of extinction coefficients for the alcohols as a

(1) J. J. Fox and A. E. Martin, *Proc. Roy. Soc. (London)*, **162**, 419 (1937).

(2) H. Kempter and R. Mecke, *Z. physik. Chem.*, **46**, 229 (1941).

(3) N. D. Coggeshall and E. L. Saier, *J. Applied Physics*, **17**, 450 (1946).

class and for the phenols as a class. The latter two cells were of a design previously described.⁴

The compounds studied were all of C.P. grade and from commercial sources except for the partially hindered phenols. These were supplied by Dr. R. S. Bowman and had been subjected to repeated purifications by recrystallization. In all cases the equilibria were studied in carbon tetrachloride solution.

As the absorption band of the associated hydroxyl group is broad, it might be expected to contribute some absorption at the free hydroxyl band. In order to test this, the data of Fig. 1 were obtained. If the association band (centering between 2.90 and 3.00 μ) is extrapolated through the base of the free hydroxyl band (occurring at 2.77 μ) it provides the contribution from the association band. The extrapolation cannot be done by assuming symmetry of the association band about a center as the long wave length side is raised through contributions from the C-H stretching vibrations. In fact, the extrapolation cannot be done with known precision. If it is done by extending the association band linearly as shown by the dashed line in curve f of Fig. 1, it is obvious that the contribution is at most very small. In view of this, no corrections for such possible contributions were made.

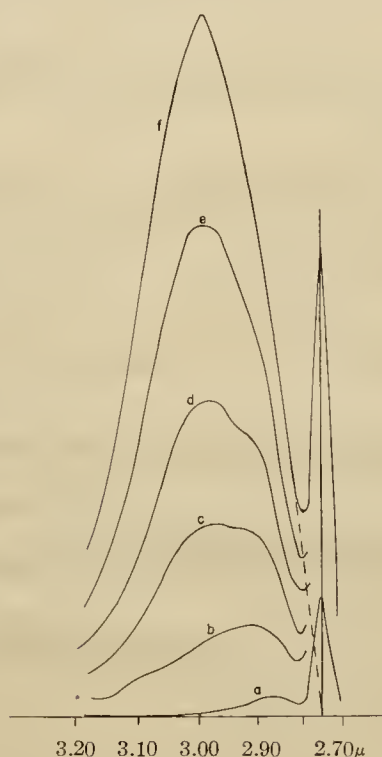


Fig. 1.—Plot of optical density versus wave length for benzyl alcohol in carbon tetrachloride solution at (a) 0.0486 mole/liter, (b) 0.0972 mole/liter, (c) 0.155 mole/liter, (d) 0.194 mole/liter, (e) 0.243 mole/liter and (f) 0.278 mole/liter (from reference 5).

All data used in the equilibrium calculations for any one compound were obtained in the same cell. The absorption measurements were all carried out in an air conditioned room in which the temperature was held constant to about $\pm 2^\circ\text{F}$. It is important that such measurements be made at controlled temperatures as the population of the complexes is affected by temperature. This may be seen in Fig. 2 which shows the association band of a 0.24 m./l. solution of benzyl alcohol over a range of temperatures from 11 to 62°. It is obvious that this temperature increase destroys most of the complexes.

An experimental difficulty generally present in such measurements is the result of the water vapor in the air in the

neighborhood of the absorption cells. The hydroxyl absorption of the water vapor occurs close to that of the hydroxylated materials studied. If the water vapor concentration in this region is constant, the effect will cancel out in the ratio of the incident and transmittal energies. If it is varying, noticeable errors may be introduced. To eliminate this, the ratios were evaluated in duplicate.

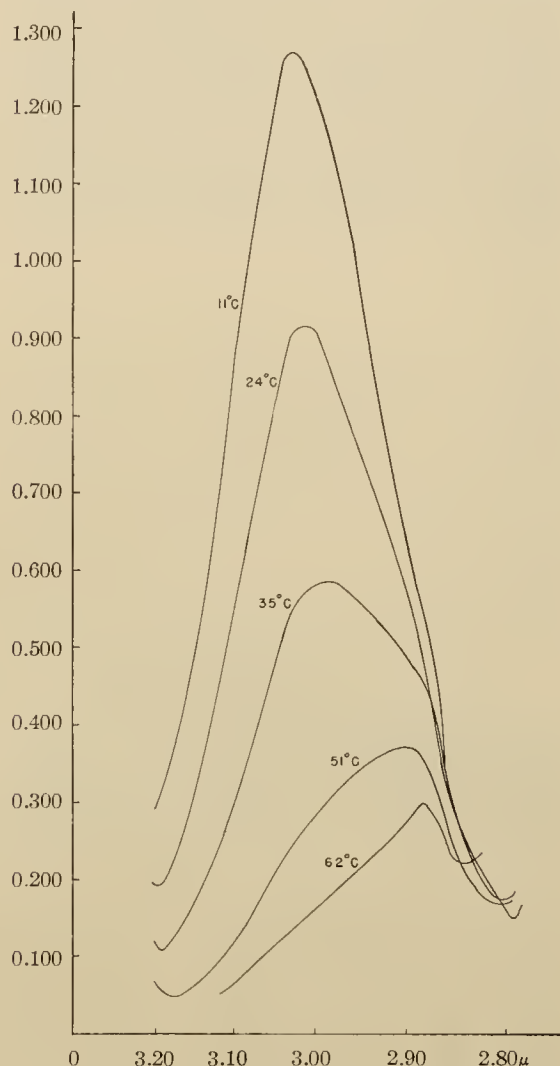


Fig. 2.—Plot of optical density versus wave length through the hydroxyl absorption region for a solution of 0.24 mole/liter of benzyl alcohol in carbon tetrachloride for different temperatures in the 11–61° range.

Compounds Exhibiting Polymeric Association

In this class fall all of the alcohols and the unhindered phenols examined. These were *n*-propyl, *n*-butyl, *t*-butyl, benzyl and *n*-octyl alcohol and phenol and *p*-*t*-butylphenol. The data for these were first examined by the single constant scheme of Kempter and Mecke by the tests described below.

Beer's law of absorption for the hydroxyl absorption band is obeyed for sufficiently dilute solutions. Hence $\log I_0/I = D = hCl$ where I_0 and I are incident and transmitted energy rates, D is the optical density, h is the extinction coefficient and l is the length of the cell. Since constant cell thicknesses were used, one may write $D = gC$ where $g =$

(4) N. D. Coggeshall, *Rev. Sci. Instruments*, **17**, 343 (1946).

hl. With this notation we may calculate α for a solution allowing bonding by the relation $\alpha = D/gC$. We may evaluate g by plotting D/C versus C and extrapolating to zero concentration.

(a) D versus $\sqrt{D/C}$ Plots.—This is equivalent to plotting αC vs. $\sqrt{\alpha}$ which should, according to the simpler theory, provide a straight line. In Fig. 3 may be seen such a curve for phenol. As this curve is typical, others will not be shown. Each was observed to give an approximate straight line plot except for a dropping away of the points in the higher $\sqrt{D/C}$ region and a general concavity to the $\sqrt{D/C}$ axis. Neither of these effects should be present if the single dissociation constant theory were correct.

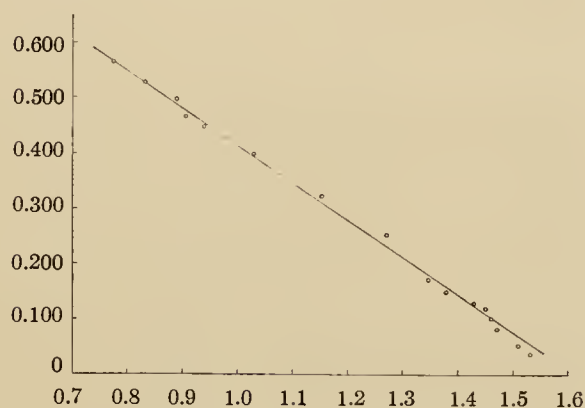


Fig. 3.—Plot of D versus $\sqrt{D/C}$ for phenol.

(b) Direct Evaluation of K_c .—From above K_c may be obtained directly through Eq. 1 over a series of values of α . In Table I are given the values of K_c calculated for a range of concentrations for *n*-octyl alcohol, *n*-butyl alcohol and phenol.

TABLE I

VALUES OF K_c CALCULATED FOR VARIOUS VALUES OF C IN (MOLES/LITER)

<i>n</i> -Octyl alcohol C	K_c	<i>n</i> -Propyl alcohol C	K_c	Phenol C	K_c
0.101	0.680	0.0820	0.672	0.0569	0.690
.202	.610	.154	.630	.158	.549
.244	.560	.205	.497	.237	.523
.303	.510	.410	.472	.474	.485
.504	.493	.615	.443	.758	.463
.576	.460	.714	.432	.948	.456

In each case K_c varied by about 35% over these concentrations. This is contrary to the predictions of the single constant theory. Similar variations of K_c were also observed for the other materials exhibiting polymeric association.

(c) Evaluation of K_c Through Pairs.—By proper operations both K_c and g may be algebraically derived from pairs of data points. When this is done there is found to be a certain amount of scattering in the values of K_c and g which is not correlated with the pairs of points used. Furthermore, this procedure yields values of g which are always larger than the experimentally determined values by approximately 10%.

Résumé for Single Dissociation Constant Calculations.—We have thus seen that each of the

three methods of correlating data with the theory for the single dissociation constant scheme produces discrepancies which are systematic and cannot be ascribed to experimental error. These discrepancies form one basis for rejecting the single constant scheme.

In Fig. 1 it may be observed that the wave length of maximum absorption for the association band varies with concentration. At the lower concentrations it is near 2.90μ and for the higher concentrations it is near 3.00μ . The bands for the intermediate concentrations have the definite appearance of superposition of two such maxima. We must ascribe the lower wave length band to dimer association and the longer wave length band to the higher order complexes. The wave length shift of the perturbed hydroxyl absorption is dependent on the energy of association, the more tightly bound complexes giving rise to greater wave length shifts. We thus have an evident difference of potential energy for molecules in dimer and higher order complexes. This in turn indicates the necessity of considering two dissociation coefficients: one for the dimer complexes, and one for the higher order complexes.

Recent calculations,⁵ employing a linear polymer model of association, have shown that the energy released on forming a dimer is considerably smaller than the energy released on increasing the order of a higher order complex by one. The latter is essentially independent of n for $n > 3$. This is a further indication of the necessity of rejecting a single equilibrium constant.

Calculation of Two Equilibrium Constants.—We have seen earlier that K_1 may be evaluated by extrapolating $2\alpha^2 C/(1 - \alpha)$ to zero concentration. The manner of doing this may be seen from Fig. 4 which shows the extrapolation for K_1 for *n*-butyl alcohol. It is seen that the points scatter rather badly in the low concentration region. This is a consequence of the small $(1 - \alpha)$ term in the denominator and it is a fundamental difficulty in this method of evaluating K_1 . In each case K_1 was determined by drawing a "best curve" through the points, being guided insofar as reasonable by the behavior as it receded from the higher to lower values of the concentration.

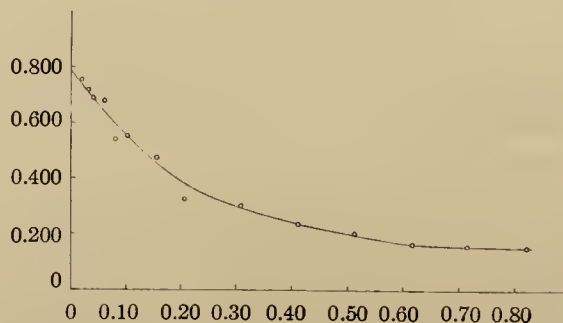


Fig. 4.—Plot of $2\alpha^2 C/(1 - \alpha)$ for *n*-butyl alcohol used to determine K_1 .

With the extrapolated values of K_1 , values of K_c were calculated for each concentration through the use of Eq. 3. In each case there was a certain

amount of scattering in the calculated K_c values. These showed no systematic trend with concentration and the discrepancies are ascribed to limitations in precision of the data and of the extrapolated values of K_1 . The expression for K_c involves

$$(K_1 - \bar{K}_1) = K_1 - 2\alpha^2 C / (1 - \alpha)$$

which is both small and of doubtful reliability for low values of concentration. In view of this the values of K_c calculated for low concentrations were not used in the averages. In Table II may be seen the typical scattering occurring at the higher concentrations.

TABLE II

K_c CALCULATED FOR <i>n</i> -OCTYL ALCOHOL			
<i>C</i> , m./l.	K_c	<i>C</i> , m./l.	K_c
0.244	0.36	0.452	0.35
.303	.33	.504	.36
.352	.33	.576	.34
.403	.36		

In Table III may be seen the extrapolated values of K_1 and the average value of K_c calculated for each of the compounds exhibiting polymeric association.

TABLE III

EXTRAPOLATED AND CALCULATED VALUES OF K_1 AND K_c

Material	K_1	K_c
<i>n</i> -Propyl alcohol	0.89	0.33
Benzyl alcohol	.80	.33
<i>n</i> -Octyl alcohol	.77	.35
<i>n</i> -Butyl alcohol	.78	.33
<i>t</i> -Butyl alcohol	.58	.40
<i>p</i> - <i>t</i> -Butylphenol	.58	.34
Phenol	.72	.34

The data of Table III demonstrate that the equilibrium constants are all of the same order of magnitude and apparently are roughly independent of molecular weight and structure.

In resumé of polymeric association it must be concluded that at least two equilibrium constants are necessary to get satisfactory agreement between theory and experiment.

Compounds Subject to Dimeric Equilibrium

Earlier studies on substituted phenols have shown that large ortho substituents sterically hinder hydrogen-bonding.⁶ Phenols with both ortho positions thus substituted do not form complexes. Phenols with one ortho position thus occupied, otherwise known as partially hindered phenols, are known to form weaker bonds than the simple alcohols and phenols. In view of the molecular geometry it would be expected that the partially hindered phenols would associate in dimer form but would not form the polymeric complexes. This may be determined by examination of the term $2\alpha^2 C / (1 - \alpha)$ over a range of concentrations sufficient for polymeric equilibrium. If this term is essentially constant it may be shown to be a necessary and sufficient condition for dimeric equilibrium.

In Table IV may be seen the values of $2\alpha^2 C / (1 - \alpha)$ for various concentrations for four partially

hindered phenols. The values were not used for the lower concentrations, as they are not so reliable because of the $(1 - \alpha)$ term which is quite small and which appears in the denominator.

TABLE IV

VALUES OF $K = 2\alpha^2 C / (1 - \alpha)$ FOR PARTIALLY HINDERED PHENOLS FOR VARIOUS CONCENTRATIONS

2,4-Di- <i>t</i> -butylphenol		<i>o</i> - <i>t</i> -Butylphenol		2- <i>t</i> -Bu-4-methylphenol		<i>o</i> - <i>s</i> -Butylphenol	
<i>C</i> , m./l.	K	<i>C</i> , m./l.	K	<i>C</i> , m./l.	K	<i>C</i> , m./l.	K
0.200	1.00	0.102	0.62	0.102	1.26	0.201	0.97
.250	1.06	.204	.67	.305	1.47	.315	.81
.333	0.88	.409	.67	.406	1.49	.402	.81
.500	1.06	.545	.62	.508	1.43	.496	.72
.666	0.96	.614	.68	.609	1.26	.603	.63
.750	.94	.700	.69	.678	1.37	.690	.59
1.000	.85	.818	.63	.812	1.34	.801	.56
$K(\text{av}) = 0.96$		$K(\text{av}) = 0.65$		$K(\text{av}) = 1.37$		$K(\text{av}) = 0.73$	

It will be noticed that there is considerable scattering of the K values but, except for *o*-*s*-butylphenol, there is no definite trend with concentration. The scattering is ascribed to limitations of experimental measurements. Excepting *o*-*s*-butylphenol, it may be concluded that the association of the partially hindered phenols is dimeric in nature.

The variation of K with concentration for *o*-*s*-butylphenol indicates that it is not so effectively hindered and that polymeric equilibrium is possible. With this in mind, the methods of the earlier section were used to calculate the values: $K_1 = 1.00$ and $K_c = 1.39$ for this material.

Association Between Unlike Species

Association may occur between hydroxylated materials and proton-acceptor materials. Evidence for this may be seen in Fig. 5. This gives the recorded energy traces for three different solutions, vertically displaced for clarity. Curve A is for 0.015 ml. of ethyl alcohol and the free hydroxyl absorption band may be seen centering on the left-hand dashed line. Curve B is for the same concentration of ethyl alcohol to which has been added 0.235 m./l. of acetone. The energy minimum centering on the center dashed line is due to hydroxyl groups which are in association with the acetone. The other minima seen for this curve are due to the acetone itself. Curve C is for the same concentration of ethyl alcohol to which has been added 0.235 m./l. of 1,4-dioxane. Here the energy minimum centering on the right-hand dashed line is due to hydroxyls in association with the dioxane. The other minima are due to the dioxane.

In these studies quantitative data were obtained for benzyl alcohol in the presence of a methyl ethyl ketone and in the presence of 1,4-dioxane. Each of the latter two compounds have appreciable absorption at the hydroxyl absorption band. Since they are used in concentrations considerably in excess of the benzyl alcohol, it is necessary to accurately evaluate these contributions. This was done by running a series of solutions containing these materials separately.

In order to eliminate the effect of association between alcohol molecules, the latter concentration was held at 0.002 m./l. and the dioxane or ketone concentrations were varied. With this arrange-

(6) N. D. Coggeshall, *TRANS JOURNAL*, **69**, 1620 (1947).

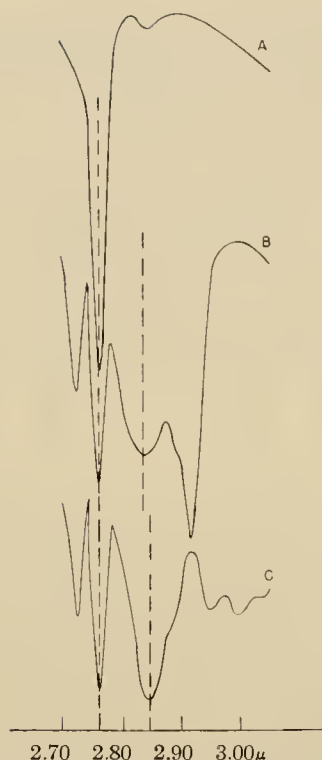


Fig. 5.—Automatic infrared recordings in the 2.7–3.0 μ region showing spectra of (A) 0.015 mole/liter of ethyl alcohol in carbon tetrachloride, (B) 0.015 mole/liter of ethyl alcohol plus 0.235 mole/liter of acetone in carbon tetrachloride and (C) 0.015 mole/liter of ethyl alcohol plus 0.235 mole/liter of 1,4-dioxane in carbon tetrachloride.

ment only binary association involving the alcohol is expected. This is expressed by the equation

$$\alpha\{X - (1 - \alpha)C\} = K(1 - \alpha)$$

where α and C have the same meanings as before, X is the concentration of proton-acceptor material and K is the dissociation constant for the complexes

between hydroxylated and proton-acceptor molecules. Experimentally it is found that for reasonable degrees of association $X \gg C$ so we have

$$\alpha X = K(1 - \alpha)$$

from which K may readily be determined.

In Table V may be seen the values of K calculated for the system of benzyl alcohol and methyl ethyl ketone.

TABLE V
DISSOCIATION CONSTANT K FOR BENZYL ALCOHOL, METHYL ETHYL KETONE SYSTEM

Concn. of methyl ethyl ketone, m./l.	K	Concn. of methyl ethyl ketone, m./l.	K
0.03	0.24	0.18	0.18
.06	.26	.21	.15
.09	.30	.24	.13
.12	.26	.27	.11
.15	.25		

It may be seen that the values of K scatter within a definite range for concentrations of methyl ethyl ketone up to 0.15 m./l. and then drop sharply for higher values. The first five values yielded an average of $K = 0.26$. It is believed that the value of $K = 0.30$ among the first five values is in error as it is erratically displaced when a plot of the data is made.

It is assumed that the decrease of the calculated value of K for the larger concentrations of proton-acceptor material is due to solvent effects. A similar behavior was also observed for the benzyl alcohol, 1,4-dioxane system. For this system the lower concentration range of proton-acceptor material yielded an average value for the dissociation value of $K = 0.20$.

Acknowledgment.—Acknowledgment is made to Dr. Paul D. Foote, Executive Vice-President of Gulf Research & Development Company for permission to publish this material.

PITTSBURGH, PENNA.

RECEIVED MAY 28, 1951

Infrared Absorption Studies of Carbon-Hydrogen Stretching Frequencies

In Sulfurized and Oxygenated Materials

ABBOTT POZEFSKY AND NORMAN D. COGGESHALL
Gulf Research & Development Co., Pittsburgh, Pa.

Reprinted from
ANALYTICAL CHEMISTRY
Vol. 23, Page 1611, November 1951

Infrared Absorption Studies of Carbon-Hydrogen Stretching Frequencies

In Sulfurized and Oxygenated Materials

ABBOTT POZEFSKY AND NORMAN D. COGGESHALL

Gulf Research & Development Co., Pittsburgh, Pa.

A study has been made of the carbon-hydrogen stretching frequencies as observed with a lithium fluoride prism for a series of sulfur-containing compounds comprising mercaptans, sulfides, and disulfides and a series of oxygenated materials comprising alcohols, ethers, ketones, acids, aldehydes, esters, and formates. The purpose has been to see if the Fox and Martin hydrocarbon assignments apply to these sulfurized and oxygenated materials, to determine if and when such assignable frequencies are perturbed by the introduction of the sulfur or oxygen atoms into the molecule, and to see how certain can be the interpretation of such spectra using the selected assignments. It has been found that the band appearing at approximately 2960 cm^{-1} is assignable to a methyl group fundamental in all cases. In the region of approximately 2930 cm^{-1} both methyl and methylene groups absorb and the absorption bands are seldom resolved. Comparison with other bands, however, sometimes allows the presence of either type group to be determined. In the region

between 2850 and 2890 cm^{-1} the absorption must be attributed to the methyl and methylene groups. The bands were often poorly resolved, the methyl absorption being more intense and occurring at the higher frequencies. No uniformly appearing band assignable to tertiary hydrogen was found. For the sulfur-containing molecules the presence of the sulfur atom does not introduce significant perturbations of the observed frequencies. However, for the oxygenated compounds the frequencies in the 2960 cm^{-1} region allow classification by which the attachment of ethyl, isopropyl, or *sec*-butyl groups to the functional group containing the oxygen atom may be assessed. The aldehydic C—H stretching frequency is assigned to one or the other of the two bands appearing uniformly for aldehydes at about 2720 and 2820 cm^{-1} . The formate C—H stretching frequency is tentatively assigned at approximately 2935 cm^{-1} . The results are compared to those obtained by Fox and Martin for hydrocarbons and the assignments are found to be in general agreement.

IN RECENT years a great deal of interest has centered around the qualitative and quantitative determination of types of C—H groups in organic molecules. Rose (11) investigated the $1.7\text{-m}\mu$ absorption of C—H groups and found near constancy of extinction coefficients within a group. Hibbard and Cleaves (8) worked in the second overtone region (8000 to 9000 cm^{-1}) and were able to estimate "the amount of chain branching in paraffins and the degree of substitution on naphthene and aromatic rings." Fox and Martin (3, 4), using a grating spectrometer, investigated the C—H stretching fundamentals of hydrocarbon molecules in the 2800 to 3100-cm^{-1} region. By a judicious choice of molecules, they succeeded in correlating certain observed frequencies with different vibrational modes of the following groups:



The molecules were chosen in such a way that either one or two functional units predominated, and their absorption bands were generally easily discerned. Plyler and Aequista (10) investigated 19 cyclohydrocarbons in the $3.4\text{-m}\mu$ region and extended the data on the >CH_2 vibration frequencies.

The present paper reports the results of an investigation undertaken on aliphatic sulfurized and oxygenated molecules. This investigation had a threefold purpose: to see if the Fox and Martin hydrocarbon assignments apply to these sulfurized and oxygenated materials; to determine if any of the established C—H frequencies were appreciably perturbed by the introduction of the sulfur or oxygen atoms into the molecule and to see how certain one could be in the interpretation of such spectra using the selected assignments.

EXPERIMENTAL

A Perkin-Elmer Model 12-C automatic recording spectrometer equipped with a lithium fluoride prism was used. The sulfur

compounds were mercaptans (thiols), sulfides, and disulfides obtained from either Eastman Kodak or Columbia Chemical; the oxygenated compounds were alcohols, ethers, ketones, aldehydes, acids, esters, and formates obtained from Eastman Kodak or Matheson. The samples were used as received, appropriately diluted in carbon tetrachloride. Either a 0.05- or a 0.15-mm. cell was used, although in several instances a 1.4-cm. cell was employed in an attempt to minimize interaction effects by studying dilute solutions. It is recognized that commercial chemicals of the highest purity may at times contain a sufficient quantity of impurities to give spurious absorption bands, but the number of compounds investigated made any purification procedures impractical.

DISCUSSION OF DATA

Figure 1 is a reproduction of a diagram previously formulated (12) from the group averages given by Fox and Martin (4). Several relative intensity changes have been made in conformity

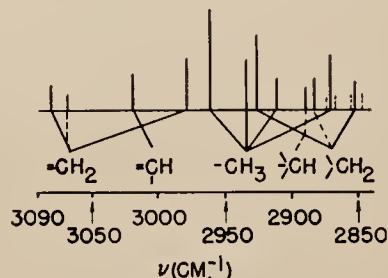


Figure 1. C-H Absorption Frequency Diagram for Hydrocarbons (12)

Dashed lines. Below base line indicate bands infrequently observed. Above base line indicate cases where single band might split into a doublet.

Table I. Observed Absorption Bands for Mercaptans, Sulfides, and Disulfides

Compound	2965 Cm. ⁻¹	2930 Cm. ⁻¹	2910 Cm. ⁻¹	2875 Cm. ⁻¹	2861 Cm. ⁻¹	Others
Mercaptans						
Ethyl	2972	2930	2872	^a ~2857 Sh ^b
n-Propyl	2967	2932	2876	2858
Isopropyl	2968	2927	2868
n-Butyl	2965	2932	2875	~2865 Sh
Isobutyl	2965	2928	2874
n-Amyl	2965	2935	2878	2864
Isoamyl	2967	2935	2878	~2867 Sh
n-Hexyl	2965	2933	2878	2863
n-Heptyl	2965	2933	2878	2863
n-Octyl	2961	2929	2872	2860
n-Dodecyl	2960	2928	~2875 Sh	2858
n-Hexadecyl	2960 Sh	2928	~2873 Sh	2856
Sulfides						
Methyl	2992	2922	2860	2840
Ethyl	2972
Methyl ethyl	2974	2923	2876	2858	2836
Methyl n-butyl	2965	2932	2874	2865	~2844 Sh
Ethyl	2976	2924
Ethyl n-butyl	2965	2928	2876	2858	~2837
n-Propyl	2965	2930	2877	~2865 Sh	~2836 Sh
n-Amyl	2961	~2922 Sh	2877	~2845 Sh
Isobutyl	2963	2931	~2907	2873	2864
Disulfides						
Methyl	2991	2920	2848	2820
Ethyl	2975	2928	~2914 Sh	2873	2820
n-Propyl	2967	2935	2910	2876
n-Butyl	2965	2932	~2910 Sh	2876	~2869 Sh
Isobutyl	2965	2933	~2910	2875	~2854 Sh

^a ~ indicates band positions are approximate.^b Sh refers to bands appearing as shoulders on more intense bands.

with the results of the present investigation. In both the 2930- and 2860-cm.⁻¹ regions there is a possibility of band overlap due to the presence of methyl and methylene groups, and it was of interest to observe when two bands could be resolved in either region. In Figures 2 to 12 the displaced spectra of the various series are reproduced from the actual recording tracings, with transmitted energy as the ordinate. In Figures 13 to 22 graphical representations of the absorption bands which were observed in the 2800 to 3100-cm.⁻¹ region are also presented for the various series. These latter figures are included to facilitate the ease of intercomparison of absorption bands for the reader. The heights of the lines represent a visual estimate of the relative intensities of the different bands which were not normalized to a unit concentration basis. An umbrella over a line designates an absorption band which appears either as a shoulder or with a

broad minimum. The dashed vertical lines connect C—H frequencies that are assigned to the same vibrational mode of the methyl or methylene groups. In Tables I and II the observed frequencies for the sulfurized and oxygenated molecules are tabulated, and only those bands are listed which are unequivocally recognized.

Only the first few members of each series were investigated; if the presence of the sulfur or oxygen atom in the molecule is to affect drastically any of the C—H frequencies as assigned by Fox and Martin (4) for hydrocarbon molecules, the modification would be detected more readily in these small molecules. In the following discussion, the first member of the various series is in most cases excluded because of its extreme departure from the general spectral characteristics of the remaining members. However, the data have been included in the tables and figures.

2960-CM.⁻¹ REGION

This frequency region was assigned to the unsymmetrical —CH₃ stretching by Fox and Martin (4), and the present study agrees with this for the following reasons: The relative intensity of this band compared to the neighboring 2930-cm.⁻¹ band decreases as the ratio of CH₂/CH₃ groups increases; the relative intensity of this band is high for the more highly methyl-branched molecules; and the high intensity of this band compared to other absorption bands in the C—H region must be related to the unsymmetrical —CH₃ stretching mode, which can be shown, by simplified calculations, to have the greatest net dipole moment change of any mode of oscillation of the isolated —CH₃ or >CH₃ groups.

The unsymmetrical methyl stretching frequency for each compound studied appears in the 2960- to 2990-cm.⁻¹ range. As the

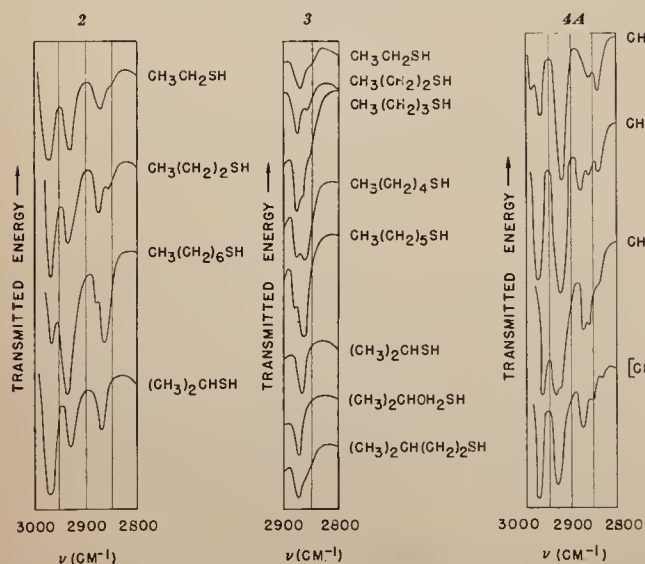


Figure 2. Recorded Spectra of Mercaptans

Figure 3. Symmetrical >CH₂ and —CH₃ Stretching Region

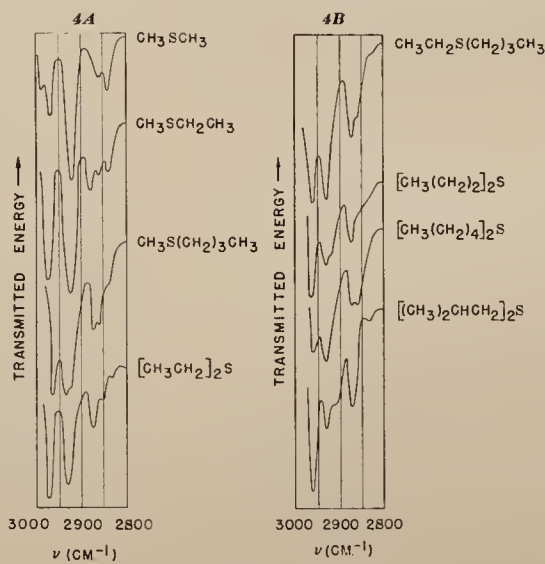


Figure 4. Recorded Spectra of Sulfides

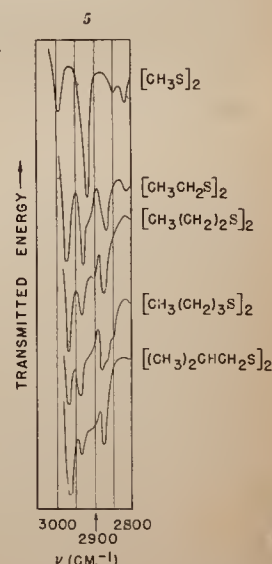
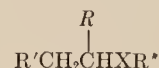


Figure 5. Recorded Spectra of Disulfides

molecule increases in molecular weight and the methyl group is moved away from the sulfur or oxygen atom, the observed frequency decreases and approaches a value of approximately 2960 cm^{-1} . As the ratio of CH_2 to CH_3 groups is increased, the intensity of this band relative to that at approximately 2930 cm^{-1} decreases. A consequence of the experimental data is that a methyl group is still distinguishable in liquid solution when the ratio of CH_2 to CH_3 groups has reached the value of 15 to 1 (spectrum of hexadecyl mercaptan not shown).

It was suspected that unsymmetrically substituted molecules such as methyl *n*-propyl sulfide and methyl *n*-amyl ketone might exhibit two absorption bands in this region, one due to the methyl group adjacent to the sulfur or oxygen atom and the other to the more remote methyl group. However, only in the case of methyl *n*-butyrate were two bands observed (2970 and 2957 cm^{-1}). Except for methyl *n*-butyrate, it was not possible to distinguish a splitting of this methyl band into components that could be characteristic of the different methyl attachments in the molecule. Except for the first members, the unsymmetrical methyl stretching absorption band is easily recognized by its frequency and intensity.

In the sulfurized molecules when an ethyl group is attached to the sulfur atom, the observed frequency is usually in the 2970 to 2980- cm^{-1} interval (ethyl *n*-butyl sulfide is an exception). The remaining sulfurized molecules all absorbed in the 2960 to 2969 interval. However, for the oxygenated molecules, it is convenient to consider the compounds in relation to the following general formula:



where X represents the functional group which is defined as —OH for alcohols, —O— for ethers, —CO— for ketones, —COOH for acids, —CHO for aldehydes, HCOO— for formates, and —COO— for esters. For some of these R'' is obviously nonexistent. The oxygenated compounds are divided into three classes with an assigned frequency interval as follows:

- A. $R=R'=H$ giving the ethyl group (2980 to 2990 cm^{-1}).
 B. $R=CH_3$ and $R'=H$ or $R=R'=CH_3$ giving, respectively, the isopropyl and *sec*-butyl groups (2973 to 2979 cm^{-1}). The *tert*-butyl group is also considered a member of this class.

Table II. Observed Absorption Bands for Oxygenated Aliphatic Molecules

Compound	3000 cm^{-1}	2960 cm^{-1}	2930 cm^{-1}	2910 cm^{-1}	2880 cm^{-1}	2860 cm^{-1}	Others
Alcohols							
Methyl	^a ~2983 Sb	2948	~2918 Sb	2836
Ethyl	2976	2927	~2886
<i>n</i> -Propyl	2968	2939	2880
Isopropyl	2976	2933	2882
<i>n</i> -Butyl	2965	2935	2878
Isobutyl	2961	2932	~2914 Sh	2876
<i>sec</i> -Butyl	2974	2931	2883
<i>n</i> -Heptyl	2961	2933	~2876	2863
<i>tert</i> -Butyl	2976	2935	~2912 Sh	2875
β,β' -Dihydroxyethyl ether	{ 3086	2931	2875 ^c
Allyl alcohol	{ 3014	2924	2871 ^c
Ethylene glycol	{ 2989	2939	2878 ^c
Ethers							
Diethyl	2981	2935	2867	~2897 Sb, 2810, 2778
<i>n</i> -Propyl	2968	2939	2878	2859	2801
Isopropyl	2976	2935	2878
Methyl isobutyl	2965	2932	2874
Ketones							
Acetone	3007	2964	2925	2853	2781
Methyl ethyl	2983	2941	2910	2884
Methyl <i>n</i> -propyl	2968	2939	2908	2878
Methyl isopropyl	2974	2939	2914	2878
Methyl <i>n</i> -butyl	2965	2937	2876	~2869 Sb
Methyl <i>n</i> -amyl	2961	2933	2875	2864
Diethyl	2983	2943	2907	2884	~2812
Diisobutyl	2961	2935	2902	2874
Acids							
Formic	3081	2944	2864
Acetic	~3027, ~3012 Sh	2987	2928
Propionic	2989	2948, ~2929	2891
<i>n</i> -Butyric	2972	2939	2882	~2855 Sb
Isobutyric	2979	2939	2880	~2850 Sb
<i>n</i> -Valeric	2967	2935	2877
Isovaleric	2968	2935	2877	~2855 Sb
Aldehydes							
Acetaldehyde	3005	2961	2914	2830, 2724, ~2750 Sb
Propionaldehyde	2987	2946	2897	2816, 2718, 2772
<i>n</i> -Butyraldehyde	2969	2939	2882	2818, 2718
Isobutyraldehyde	2976	2936	2876	2810, 2712, 2783
Isovaleraldehyde	2968	2936	2901	2878	2820, 2715
<i>n</i> -Heptaldehyde	2961	2933	~2873 Sb	2863	2820, 2716
Esters							
Methyl acetate	~3028 Sb, 3001	2955	~2930 Sb	~2907	2847
Ethyl acetate	2987	2941	2907	2876	2855
<i>n</i> -Propyl acetate	2972	2943, ~2930 Sb	2884	~2863	~2897
Isopropyl acetate	2985	2941, ~2927 Sb	~2907	2884
<i>n</i> -Butyl acetate	2965	2937	2876	~2853 Sb
Isobutyl acetate	2969	~2939 Sh	2912	2878	~2895
Methyl propionate	2989	2952	2886	2846
Ethyl propionate	2987	2946	2912	2886
<i>n</i> -Propyl propionate	2975	2946, ~2926 Sb	2884	~2862 Sb	~2893
Isopropyl propionate	2987	2944, ~2926 Sh	2886
Methyl <i>n</i> -butyrate	2970, 2957	~2939 Sh	~2911 Sh	2880	2848
Ethyl <i>n</i> -butyrate	2972	2938	~2910	2878
<i>n</i> -Propyl <i>n</i> -butyrate	2972	2939	2882
Formates							
Methyl	3106, 3034, 3005	2957	2934	~2900 Sh	2840
Ethyl	3107	2987	2931	~2912 Sb	~2880 Sb
<i>n</i> -Propyl	3104	2972	2931	~2904	2885	~2862 Sb
<i>n</i> -Butyl	3104	2965	2935	2878	~2853 Sb
Isobutyl	3104	2968	2931	2878
<i>sec</i> -Butyl	3104	2978	~2934 Sb, 2928	2907	2884	~2860

^a ~ indicates band positions are approximate.

^b Sh refers to bands appearing as shoulders on more intense bands.

^c These frequencies are definitely methylene.

C. Other structures which are not included in either A or B (2960 to 2972 cm^{-1}).

In the ether, ketone, and ester series it is possible for the molecule to fall into more than one class, depending on R". When this situation arises, the simplest classification is to be used. For example, isopropyl propionate falls into classes A and B, but is considered of class A. Using these classifications for the oxygenated materials it was found that of thirteen compounds which contained an ethyl group attached to the functional group, class A, ten absorbed in the assigned interval of 2980 to 2990 cm^{-1} . Of nine class B type molecules, eight absorbed in the assigned interval of 2973 to 2979 cm^{-1} . The remaining compounds all fall in class C and all absorb in the 2960- to 2972- cm^{-1} interval. The use of these three classes is somewhat arbitrary, but it does give increased orderliness to the data.

If the first member in each series is excluded, the vibrational mode under discussion provides frequency values for the sulfurized and oxygenated compounds in reasonably good agreement

with the Fox and Martin (4) assignment for hydrocarbons. In Table III the averages of the frequencies observed in each absorption region are tabulated along with the averages found by Fox and Martin in their hydrocarbon study. The average oxygenated frequency in this region is 2974 cm^{-1} compared to a sulfurized average of 2966 cm^{-1} and a hydrocarbon average of 2962 cm^{-1} . Thus the sulfur atom does not produce a perturbation great enough to cause frequency shifts that can be distinguished as unique evidence for the presence of the sulfur atom. If care is exercised, it is possible to use the oxygenated frequencies as a means of detecting the probable position of the oxygen functional group in the molecule.

The effects of the introduction of the sulfur and oxygen atoms into the molecule can be seen by noting the unsymmetrical methyl stretching frequencies for molecules where the ethyl group is attached to the functional group. The range for the oxygenated compounds is 2980 to 2990 cm^{-1} , and for the sulfurized molecules it is 2970 to 2980 cm^{-1} . Thus the C—H force constants are

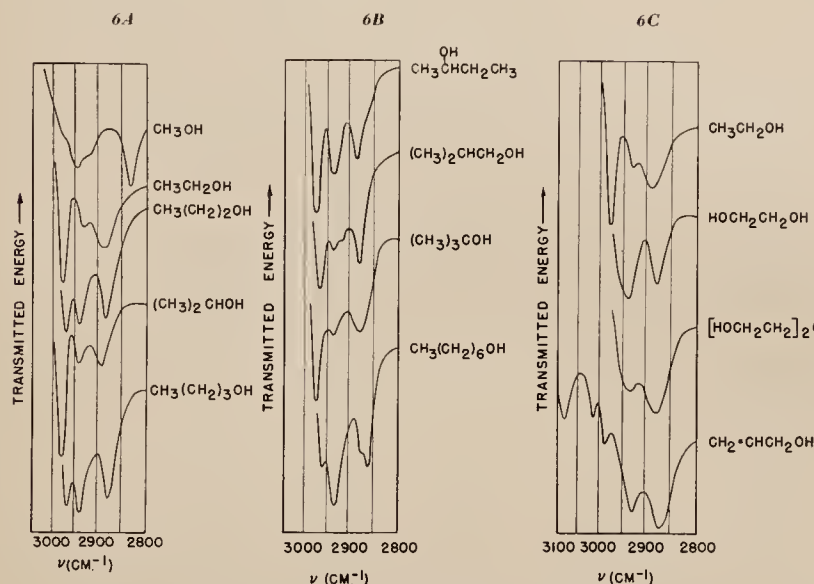


Figure 6. Recorded Spectra of Alcohols

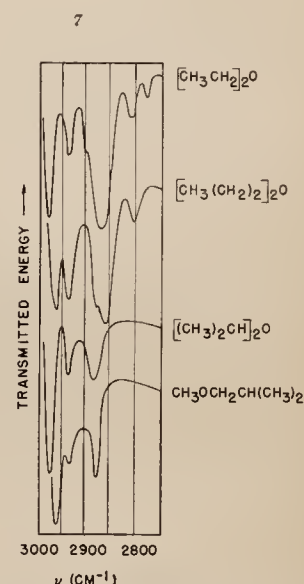


Figure 7. Recorded Spectra of Ethers

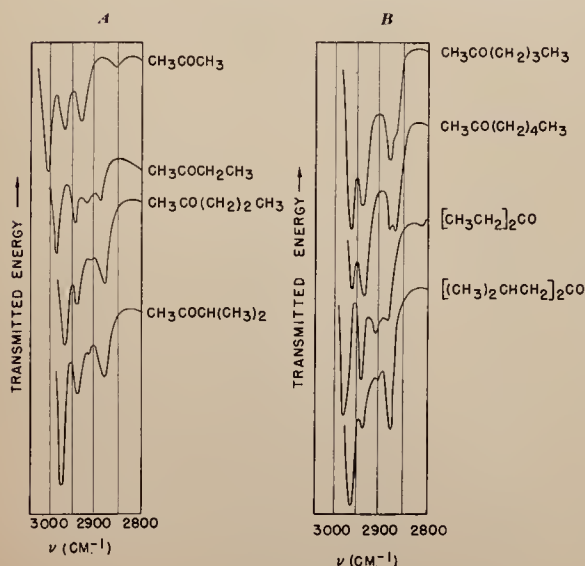


Figure 8. Recorded Spectra of Ketones

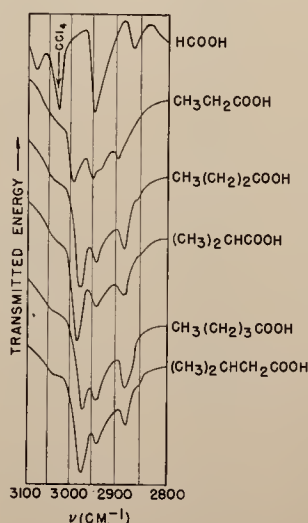


Figure 9. Recorded Spectra of Acids

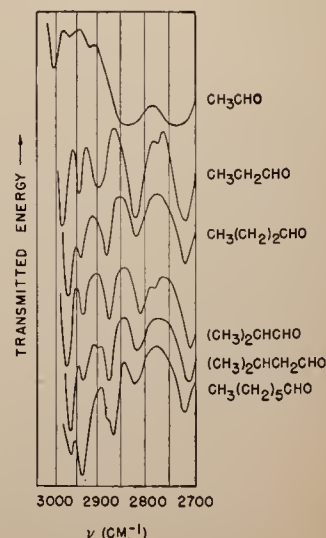


Figure 10. Recorded Spectra of Aldehydes

Table III. Band Frequency Averages

(First members not included)

	2960 Cm. ⁻¹	2930 Cm. ⁻¹	2910 Cm. ⁻¹	2880 Cm. ⁻¹	2860 Cm. ⁻¹
Sulfurized	2966	2930	2910	2875	2861
Oxygenated	2974	2936	2909	2880	2861
Hydrocarbons (F and M)	2962	2934	2912	2872	2853
		2926			

greater when the more electronegative oxygen atom is present. This effect also appears for the isopropyl group.

The relative intensity of this band with respect to the approximately 2930-cm.⁻¹ band increases greatly with branching and this fact is sometimes useful in determining if an unknown molecule is branched or straight chain.

Allyl alcohol, ethylene glycol, and β,β' -dihydroxyethyl ether do not contain methyl groups, and there is correspondingly no methyl band in the spectra of these compounds in this region. Allyl alcohol contains a terminal olefinic group, and a reasonably strong absorption band occurs at 3086 cm.⁻¹ in agreement with the Fox and Martin assignment for this type of group. This band is the unsymmetrical $=CH_2$ stretching frequency, with possibly the 2989-cm.⁻¹ frequency due to the less intense sym-

metrical stretching. The $=C-H$ grouping appears to account for the 3014-cm.⁻¹ band.

Acids of low molecular weight generally do not have as well defined absorption in the C—H region as the acids of higher molecular weight; in more concentrated solutions the strong hydrogen bonding that occurs results in a broad band which partially overlaps the C—H region (2), and the hydrocarbon group absorptions are superimposed on this broad hydroxyl background. When acetic and propionic acids were run in dilute solutions of carbon tetrachloride (~ 0.01 mole per liter in a 1.4-cm. cell), the bands were weak and rather broad, indicating that hydrogen bonding with dimer formation (5) was still occurring at these high dilutions (see Figure 9; acetic acid not shown). Under the present experimental conditions the monomeric acid molecules were probably never the only species present. However, interaction through hydrogen bonding should not be expected to shift the methyl frequencies appreciably, except possibly in acetic acid.

Formic acid was run in very dilute solution, in which both the monomer and dimer forms might be expected. The rather broad band at 3081 cm.⁻¹ is assigned to the hydroxyl frequency of the dimer (for spectral data in the vapor phase see 6). A much more intense and sharp absorption band appeared at 3524 cm.⁻¹, which is the monomer hydroxyl absorption. The remaining bands of formic acid will be briefly discussed at this point. An intense band appears at 2944 cm.⁻¹ and a weaker one at 2864 cm.⁻¹. The former with its high intensity must be

correlated with the high intensity free OH band at 3524 cm.⁻¹, and so is probably the monomeric C—H stretching frequency (7); the 2864-cm.⁻¹ band is then believed to be the dimeric C—H frequency. This latter conclusion is supported by the ratio of the optical density of the 2944-cm.⁻¹ band to that at 2864 cm.⁻¹ in various concentrations of carbon tetrachloride. This ratio increased with decreased concentration, indicating that more monomer was being formed at the expense of the dimer.

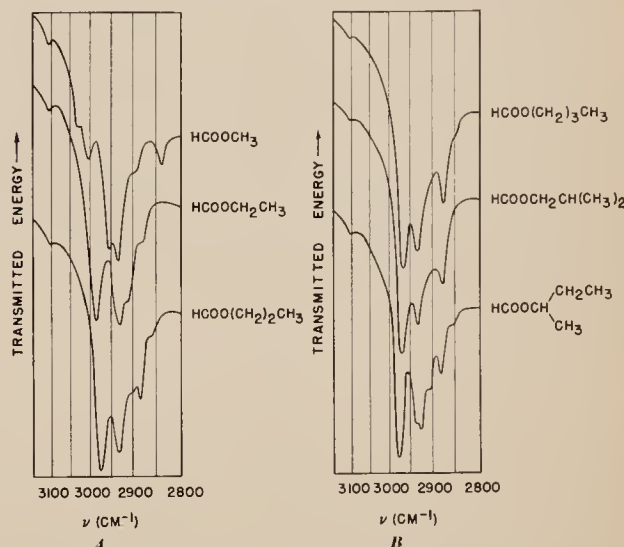


Figure 12. Recorded Spectra of Formates

Methyl acetate contains two methyl groups in different environments, and it is possible that the 2955- and 3001-cm.⁻¹ bands can be attributed to an unsymmetrical stretching mode of each of these methyl groups (see Figure 11, A). Acetic acid and methyl formate represent modifications of methyl acetate wherein one of the methyl groups has been replaced by a hydrogen. However, the observed spectrum of acetic acid was too diffuse to permit reasonable comparisons to be made; methyl formate has a very clean spectrum in this region. Methyl formate absorbs at 3005 and 2957 cm.⁻¹ (see Figure 12, A), while methyl acetate has equivalent bands at 3001 and 2955 cm.⁻¹. The appearance of these bands in both compounds appears to contradict an assignment of them to the different methyl groups.

2930-CM.⁻¹ REGION

For hydrocarbon molecules Fox and Martin found two absorption bands in this region, one at 2934 cm.⁻¹ characteristic of methyl groups and the other at 2926 cm.⁻¹ characteristic of methylene groups (see Figure 1). The latter frequency arises from the unsymmetrical stretching mode of the $>CH_2$ group; the origin of the former frequency has not been definitely established. It was of interest to see if these two bands could be resolved when both groups appear in the same molecule, and in addition to determine the effect of the sulfur and oxygen atoms. In the following discussion the series first member is not included unless specifically mentioned.

All compounds showed at least one absorption band which fell

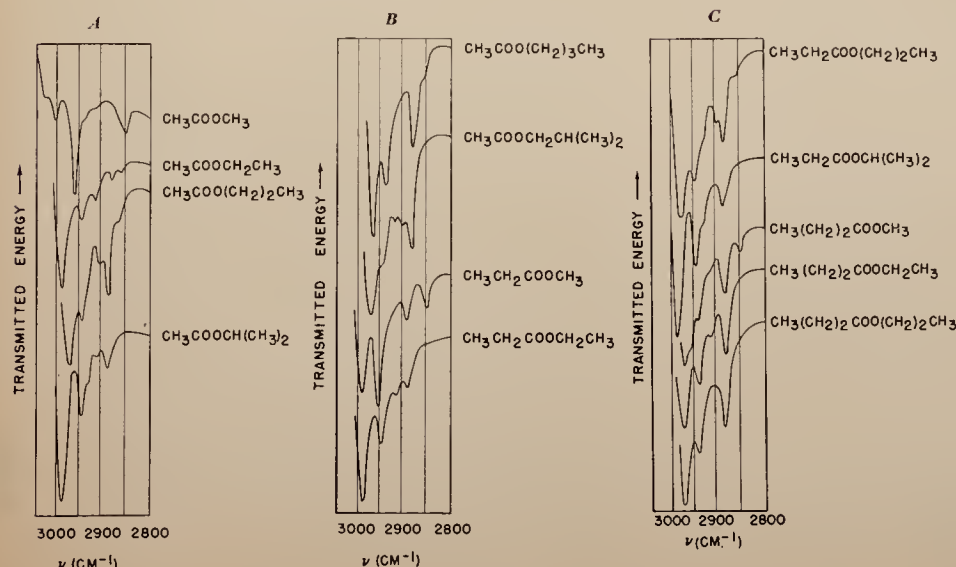


Figure 11. Recorded Spectra of Esters

in the 2922- to 2948-cm.⁻¹ interval. The methyl and methylene absorption bands apparently overlap to such an extent that their resolution was generally not achieved under the experimental conditions of this investigation. In the sulfurized molecules methyl *n*-butyl sulfide has a doublet in this region and *n*-propyl sulfide shows two overlapping bands (see Figure 4). These are the only two instances in the sulfur-containing compounds where two bands were definitely observed. In the oxygenated series only propionic acid and *sec*-butyl formate showed two distinct bands of appreciable intensity in this region. In the esters a slight shoulder sometimes appeared on the low frequency side of the more intense band. This slight shoulder appeared in four esters, and it does not seem possible to assign it definitely to a methyl or methylene group or to correlate its appearance with some other type of hydrocarbon structure. Thus in general only one absorption band was found; sometimes a weak shoulder appeared on the low frequency side of this more intense band.

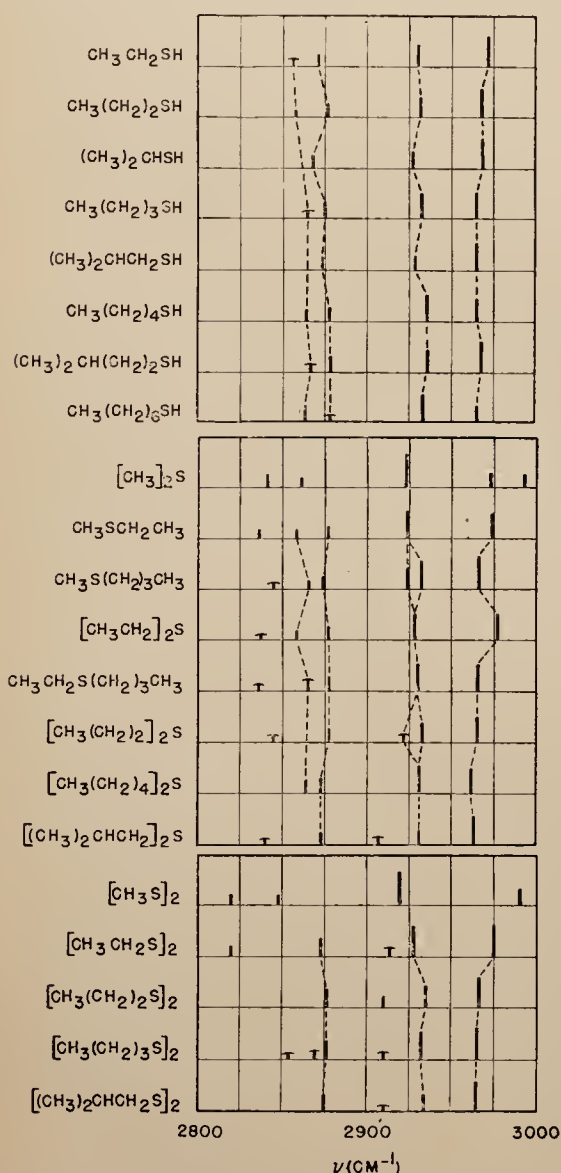


Figure 13 (upper). Observed Frequencies of Mercaptans

Figure 14 (center). Observed Frequencies of Sulfides

Figure 15 (lower). Observed Frequencies of Disulfides

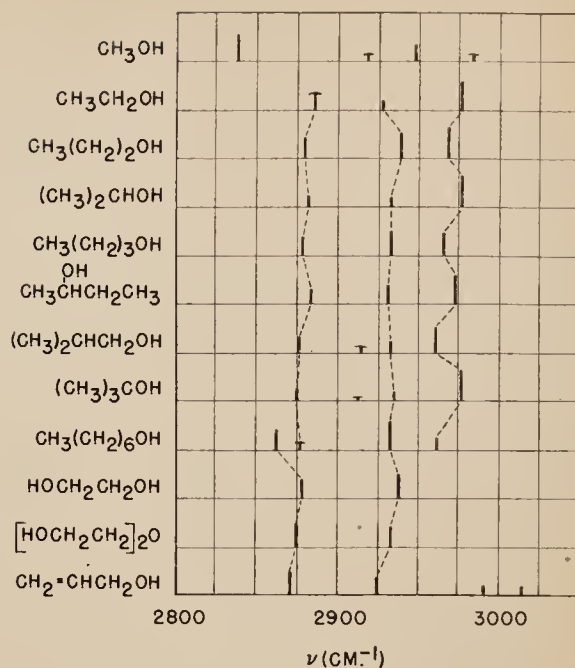


Figure 16. Observed Frequencies of Alcohols

The difficulty that might arise in an attempted interpretation of a single band that appears in this region for an unknown material is illustrated by the following. Isopropyl alcohol has a weak but definite band at 2933 cm.⁻¹, and isobutyl alcohol has the same type of band at 2932 cm.⁻¹. On the other hand, *sec*-butyl alcohol absorbs much more strongly than the above two molecules at 2931 cm.⁻¹ (see Figure 6). Here is a situation where a molecule containing no methylene groups has a weak band, and so does a molecule containing only one methylene group, but an isomer of the latter still containing only one methylene group absorbs much more strongly. *tert*-Butyl alcohol has no methylene groups and a weak band appears at 2935 cm.⁻¹. This indicates the uncertainty one might have in an attempt to identify a lone methylene group in an unknown material by the frequency and intensity of the absorption in the 2930-cm.⁻¹ region. A reasonably strong band must be exhibited to indicate this type of group. As the ratio of CH₂ to CH₃ increases, the intensity of the 2930-cm.⁻¹ band increases relative to that at 2960 cm.⁻¹ and identification of >CH₂ groups becomes more positive.

The 2930-cm.⁻¹ bands do not offer a unique means of detecting unambiguously the presence of either methyl or methylene groups in the compounds of lower molecular weight. The intensity of this band is weak relative to the 2960-cm.⁻¹ region for the more highly methyl-branched materials examined and positive evidence for the presence of a methylene group might not be attainable from the spectra in this region. However, the straight-chain compounds, wherein the CH₂ to CH₃ ratio is high (order of magnitude of approximately 5 to 1), show stronger absorption relative to the 2960-cm.⁻¹ band. The spectrum of such a material represents good evidence for the presence of the methylene group, whose absorption intensity obscures any methyl absorption—e.g., *n*-heptyl mercaptan (Figure 2).

The average absorption frequencies observed for the oxygenated and sulfurized molecules in this region are tabulated in Table III. The oxygenated materials absorbed at 2936 cm.⁻¹, compared to a sulfurized average of 2930 cm.⁻¹. The oxygenated functional groups appear to strengthen the force constants of the C—H bonds, but not enough to cause any serious deviation from the Fox and Martin hydrocarbon assignment.

The intensity of the 2930-cm.⁻¹ band in formates appears visually to be greater relative to the 2960-cm.⁻¹ band than do the

equivalent bands of analogous compounds of other series. The increased intensity of the formate bands in this region compared to other series presented a new question. Possibly this could be caused by the C—H stretching vibration of the formate group. In formic acid a C—H frequency was found to occur at 2944 cm^{-1} in dilute carbon tetrachloride solution where the monomeric molecule appears to predominate (see Figure 9). This

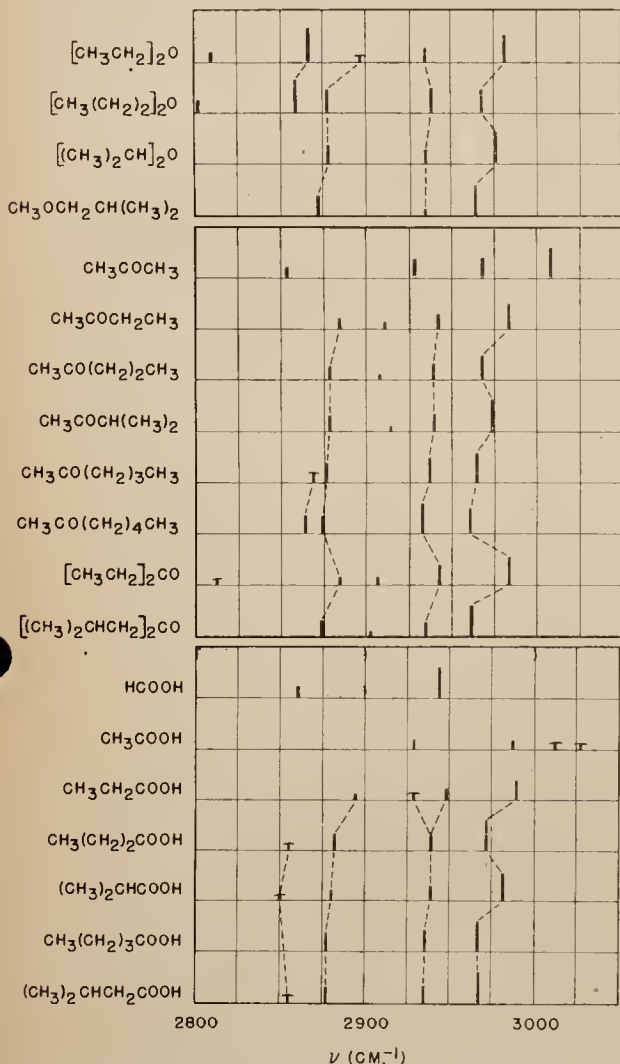


Figure 17 (upper). Observed Frequencies of Ethers
 Figure 18 (center). Observed Frequencies of Ketones
 Figure 19 (lower). Observed Frequencies of Acids

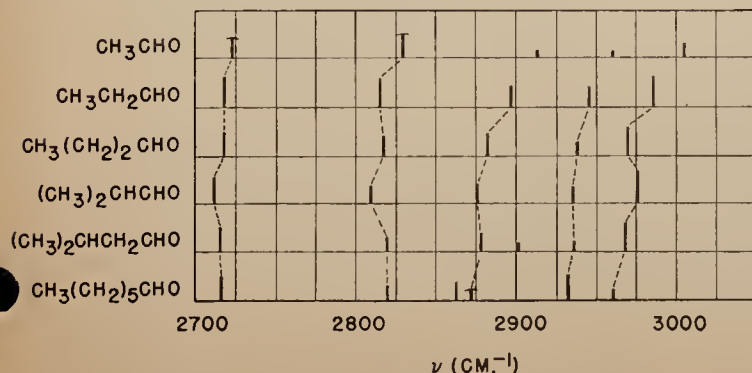


Figure 20. Observed Frequencies of Aldehydes

value compares to 2940 cm^{-1} found by Bonner and Hofstadter (1) for monomeric formic acid vapor. Methyl acetate has its most intense absorption band at 2955 cm^{-1} (Figure 11, A), and this must be assigned to the methyl group. Methyl formate has two very intense bands at 2957 and 2934 cm^{-1} . If the high frequency be assigned to the methyl group by analogy with methyl acetate, then the other might well be the formate C—H stretching frequency. The 2957- cm^{-1} component disappears in the remaining formates and might conceivably be a shifted first member methyl band. In Figure 6, C, it is seen that *sec*-butyl alcohol exhibits one absorption band in this region while *sec*-butyl formate exhibits two (see Figure 12, A). This might also be taken as further evidence that the formate C—H frequency is at approximately 2935 cm^{-1} .

The evidence presented above indicates that the formate C—H frequency could possibly occur in the 2930- cm^{-1} region. However, this possibility has not been shown to be incontrovertibly true, and further experimental data are necessary either to confirm or refute this. If this assignment is correct, in all but *sec*-butyl formate a new near-degeneracy occurs, with the result that only one band is observed. Three groupings would then absorb in the same frequency range, and resolution of these was generally not realized.

The generally slightly high frequencies observed for the esters as compared to the other classes of materials are possibly due to the hydrocarbon groups on the functional group. These are on the average smaller than in the other series and more affected by the functional group.

Allyl alcohol, β,β' -dihydroxyethyl ether, and ethylene glycol all contain methylene groups and absorb at 2924, 2931, and 2939 cm^{-1} , respectively (see Figure 6, C).

2850 TO 2890- CM^{-1} REGION

In this region the symmetrical methyl and methylene C—H stretching frequencies appear. The methylene absorption occurs at approximately 2853 cm^{-1} , while that of the methyl group appears at approximately 2872 cm^{-1} . These assignments are the result of the Fox and Martin investigation.

It was observed that usually two bands could be found in this region for the straight-chain molecules, one at approximately 2875 cm^{-1} and the other at approximately 2860 cm^{-1} . In the branched-chain molecules usually only one band appears. It was of interest to see when two bands appear and when only one band appears, and to check the assignments. In Figure 3 the 2800 to 2900- cm^{-1} region of mercaptan molecules is reproduced. For the straight-chain mercaptans two bands were always observed. Up to *n*-butyl mercaptan the higher frequency band was the more intense. As the number of methylene groups increases, the lower frequency component begins to play a more dominant intensity role, until in *n*-amyl mercaptan both components are approximately of the same intensity. In *n*-heptyl mercaptan the low frequency component is definitely the more intense and can be correlated with the high intensity of the 2930 cm^{-1} band (see Figure 2); the high relative intensities of these two bands can be associated with a large CH_2 to CH_3 ratio. The last three spectra in Figure 3 are of branched-chain molecules and it is seen that only one band is found in the isopropyl and isobutyl mercaptans. In isoamyl mercaptan a faint indication of methylene absorption is evident as a weak shoulder on the low frequency side of the more intense band. Thus the more intense high frequency band is assigned to the methyl group and the low frequency band to the methylene group.

In the alcohol series the same general type of behavior would be expected to exist as in the mercaptan series. In *n*-butyl alcohol an absorp-

tion band appears at 2878 cm^{-1} with enough dissymmetry on its low frequency side to suggest the possibility of another band (see Figure 6, A). In 1-heptanol the 2876-cm^{-1} absorption is now the weaker component; the 2863-cm^{-1} component is somewhat more intense. It appears that by analogy with the mercaptan series, the methyl absorption accounts for the single absorption band generally observed at approximately 2878 cm^{-1} and that the methylene absorption, when observable, occurs at approximately 2863 cm^{-1} . Comparing the analogous mercaptan and alcohol molecules, it is seen that the methylene absorption appeared more frequently in the mercaptan series than for the alcohols. In the alcohols of lower molecular weight this could occur by an increased force constant for the C—H groups adjacent to the functional group—i.e., the methylene groups would be most affected. Thus the methylene frequency for the first few members of the alcohol series would be shifted toward higher values, with the result of sufficient overlap with the methyl band so that only one band could be found. In 1-heptanol the effect of the hydroxyl group on the methylene force constants is limited to the first and possibly second methylenes. The remaining methylenes are practically unaffected; overlap is not so pronounced and good resolution of two bands is again observed. These conclusions seem to apply for the other oxygenated materials.

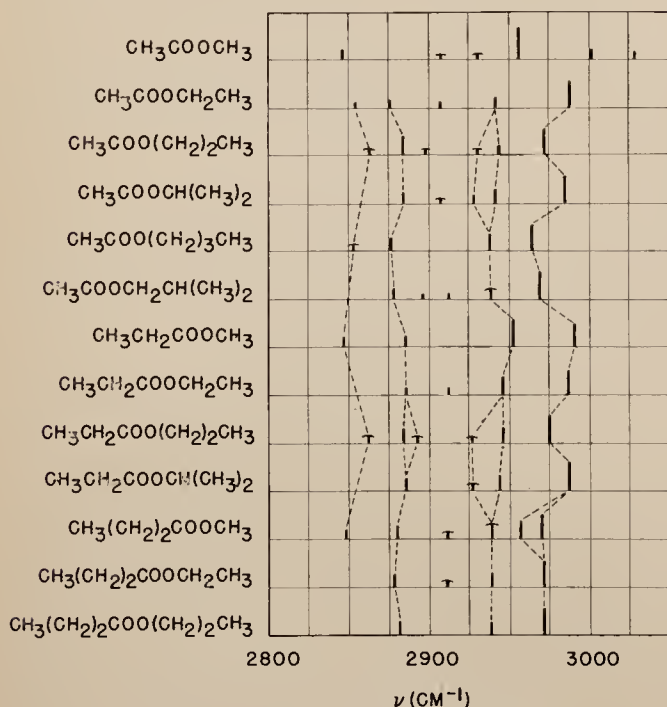


Figure 21. Observed Frequencies of Esters

It appears that the symmetrical stretching mode of the methyl group entails a greater net dipole moment change than the same mode of vibration of the methylene group (if one neglects the effect of the phase relationship of the symmetrical stretching mode between the individual methylene groups along the chain). This results in a high frequency band attributable to the methyl group and a weak band or shoulder on the low frequency attributable to the methylene group for the smaller molecules. Fox and Martin had determined the absorption coefficients for these two groups in this region and found them to be of the same order of magnitude for hydrocarbon molecules. In this study it appears that this is not the case and that the methyl group absorption coefficient is appreciably greater than that of the methylene group.

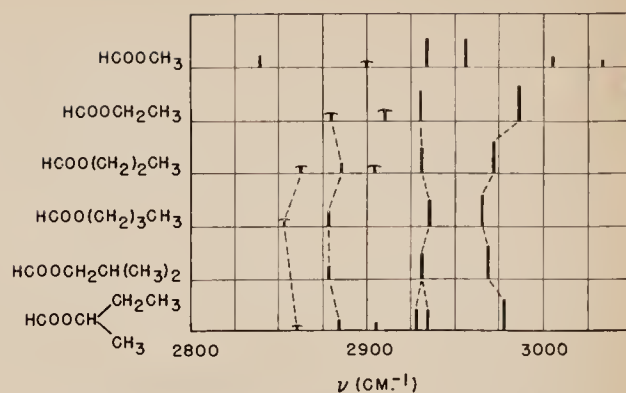


Figure 22. Observed Frequencies of Formates

The average methyl frequency is 2880 cm^{-1} for the oxygenated molecules compared to 2875 cm^{-1} for the sulfurized series (see Table III). The methylene average was 2861 cm^{-1} for both the oxygenated and sulfurized series. (The methylene average for the oxygenated series would probably be somewhat higher if the values for the compounds of lower molecular weight could be obtained and included in the average.) It was more difficult to detect methylene absorption in the oxygenated series.

The observed frequencies in this region agree reasonably well with the Fox and Martin hydrocarbon assignments. With the proper caution these assignments can be applied to unknown materials. The absence of detectable methylene absorption does not necessarily indicate the absence of methylene groups in the molecule. The appearance of two bands is reasonably good evidence for the presence of both groups, but the appearance of only one band must be interpreted with caution.

For relatively small molecules of the type studied, a single band in this region must be interpreted in conjunction with the bands that might appear in the other two frequency regions already discussed. For example, in ethylene glycol, β,β' -dihydroxyethyl ether, and allyl alcohol, a single band appears at approximately 2874 cm^{-1} and no band appears in the 2960 cm^{-1} region. Consequently, the interpretation can be made that a methylene group is giving rise to these 2874-cm^{-1} absorption bands. It is seen that the effect of the oxygen atoms on the C—H force constants of these three compounds is to increase them slightly to give a higher observed methylene frequency.

In the acid series a weak shoulder frequently appeared at approximately 2855 cm^{-1} . This shoulder has been tentatively assigned to methylene absorption, although its appearance in isobutyric acid contradicts such an assignment.

All the methyl esters—i.e., acetate, propionate, and butyrate—have distinct nonoverlapping bands at approximately 2850 cm^{-1} (see Figure 11). The other esters which have bands near this frequency are distinctive in that these appear as shoulders on the more intense higher frequency band. These approximately 2850 cm^{-1} bands of the methyl esters are probably not due to methylene absorption alone.

OTHER REGIONS

Frequently a weak band appears at approximately 2910 cm^{-1} , and this was assigned to the methyl group by Fox and Martin (see Figure 1). The present data offer no definite information concerning this assignment, in so far as it is not observed for all the materials examined which contain the methyl group. The same investigators report an infrequently occurring band at approximately 2893 cm^{-1} which they ascribe to the >CH group.

This band was observed so infrequently that again nothing more can be said concerning its assignment. For the sulfides studied, a weak band occurring at approximately 2840 cm^{-1} was gener-

ally observed. It was not found for any of the mercaptans and was observed for only one disulfide. No explanation is given for these bands.

All the formates exhibited a weak band at approximately 3104 cm^{-1} (not included in Figure 22, but visible in Figure 12), and this might be a useful frequency in formate identification.

A very surprising set of bands arose in the aldehyde series. In each aldehyde two bands always appeared simultaneously, centering around 2720 and 2820 cm^{-1} (Figure 20). Even in very dilute carbon tetrachloride solution (~ 0.01 mole per liter) these absorption bands were present. Thompson and Harris (13) studied acetaldehyde vapor in the infrared, but did not assign a definite frequency to the aldehydic C—H stretching. Morris (9) investigated acetaldehyde and acetaldehyde- d_4 vapors in the infrared and assigned their observed 2710-cm^{-1} band for acetaldehyde to the symmetrical methyl stretching and an observed 2788-cm^{-1} band to the aldehydic C—H stretching. This latter band does not appear in the infrared spectrum of the carbon tetrachloride solution. The point to be made is that two bands appear throughout the aldehyde series, and in the compounds of higher molecular weight a symmetrical methyl stretching frequency has been assigned (approximately 2880 cm^{-1}). Consequently, the two bands that appear in the liquid solutions must be explained as a fundamental and an overtone or combination band whose intensity is enhanced by Fermi resonance with the fundamental. The result of this investigation is that one of these two frequencies (which one is not definite) must be assigned to the aldehydic C—H stretch whose unperturbed frequency would be expected to appear at approximately 2775 cm^{-1} . The other band might tentatively be explained as the first overtone of the symmetrical methyl bending frequency at approximately 1380 cm^{-1} . Benzaldehyde, which contains no methyl groups, also has these two bands when observed in carbon tetrachloride solution. The appearance of these bands in a spectrum is excellent evidence for the presence of an aldehydic molecule.

SUMMARY AND CONCLUSIONS

The frequencies observed for the methyl and methylene groups are on the average highest in the oxygenated series, intermediate in the sulfurized series, and lowest in the hydrocarbons (see Table III). The variations from the Fox and Martin assignments are generally not great enough to cause serious difficulty in using these assignments, but care must be taken to stay within established limits of applicability.

Excluding first members, the unsymmetrical methyl stretching frequencies of the sulfurized molecules fall in the 2960 - to 2976-cm^{-1} interval. (When an ethyl group is attached to the sulfur atom, the observed frequency is generally in the 2970 - to 2976-cm^{-1} interval.) In the oxygenated series the range was 2960 - to 2990 cm^{-1} , with further subclassification possible: an ethyl group (class A) generally absorbing in the 2980 - to 2990-cm^{-1} interval; an isopropyl or *sec*-butyl (class B) generally absorbing in the 2973 - to 2979-cm^{-1} interval; the remaining groups absorbing in the 2960 - to 2972-cm^{-1} interval (class C.).

In the 2930-cm^{-1} region the unsymmetrical methylene stretching frequency appears; a methyl group absorption also occurs

here. In carbon tetrachloride solution it seldom was possible to resolve the two bands. When the ratio of CH_2 to CH_3 groups is approximately 5 to 1, the contribution of the methylene groups to this band is appreciable and can generally be identified as such by comparison of the band intensity with respect to the unsymmetrical methyl stretching band. Otherwise, an absorption band in this region cannot be positively identified as due solely to a methyl or methylene group.

It is suggested that the formate C—H stretching frequency occurs at approximately 2935 cm^{-1} .

In the 2850 - to 2890-cm^{-1} region the symmetrical methyl and methylene stretching frequencies occur. Generally only one relatively strong absorption band appears; this has been identified with the methyl group. Frequently a weak band or shoulder appears on the low frequency side of this band, and is believed to be the methylene absorption. As the ratio of CH_2 to CH_3 groups increases, the intensity of the shoulder increases relative to the main band, and at a ratio of approximately 6 to 1 becomes the dominant absorber.

The absorption frequencies of the first member of a series usually are shifted appreciably from the mean values of the remaining members of the series, and the Fox and Martin assignments are then very uncertain when applied to these.

A weak band at approximately 2840 cm^{-1} was generally observed for sulfides.

No band was observed that could definitely be ascribed to the >CH group.

Carbon tetrachloride solutions of aldehydes show two absorption bands at approximately 2720 and 2820 cm^{-1} . These are assigned to the C—H stretching vibration of the aldehydic group and to some combination or overtone band whose intensity is enhanced by Fermi resonance.

Sufficient differences in detail exist to allow spectra in this region to be used for the identification of specific compounds.

LITERATURE CITED

- (1) Bonner, L. G., and Hofstadter, R., *J. Chem. Phys.*, **6**, 531 (1938).
- (2) Davies, M. M., and Sutherland, G. B. B. M., *Ibid.*, **6**, 755 (1938).
- (3) Fox, J. J., and Martin, A. E., *Proc. Roy. Soc.*, **A167**, 257 (1938).
- (4) *Ibid.*, **A175**, 208 (1940).
- (5) Herman, R. C., and Hofstadter, R., *J. Chem. Phys.*, **6**, 534 (1938).
- (6) Herman, R. C., and Williams, V., *Ibid.*, **8**, 447 (1940).
- (7) Herzberg, G., "Infrared and Raman Spectra of Polyatomic Molecules," p. 321, New York, D. Van Nostrand Co., 1945.
- (8) Hibbard, R. R., and Cleaves, A. P., *ANAL. CHEM.*, **21**, 486 (1949).
- (9) Morris, J. C., *J. Chem. Phys.*, **11**, 230 (1943).
- (10) Plyler, E. K., and Acquista, N., *J. Research Natl. Bur. Standards*, **43**, 37 (1949).
- (11) Rose, F. W., *Ibid.*, **20**, 129 (1938).
- (12) Saier, E. L., and Coggeshall, N. D., *ANAL. CHEM.*, **20**, 812 (1948).
- (13) Thompson, H. W., and Harris, G. P., *Trans. Faraday Soc.*, **38**, 37 (1942).

RECEIVED May 23, 1951. Presented at the Pittsburgh Conference on Analytical Chemistry and Applied Spectroscopy, Pittsburgh, Pa., March 5 to 7, 1951.

Ultraviolet Absorption Determination of C₉ and C₁₀ Aromatics

MATTHEW S. NORRIS and NORMAN D. COGGESHALL
Gulf Research & Development Co., Pittsburgh, Pa.

Reprinted from
ANALYTICAL CHEMISTRY
Vol. 25, Page 183, January 1953

Ultraviolet Absorption Determination of C₉ and C₁₀ Aromatics

MATTHEW S. NORRIS AND NORMAN D. COGGESHALL

Gulf Research & Development Co., Pittsburgh, Pa.

METHODS of analyzing gasoline and other hydrocarbon fractions for the lower molecular weight aromatics are well known (2, 4). For example, a gasoline may be accurately analyzed for benzene, toluene, and the individual xylene isomers by precision distillation followed by multicomponent analyses of the cuts. To extend determination of the individual aromatics to the higher molecular weight members becomes increasingly difficult because of the proximities of their boiling points and the close similarity of the spectra. Fortunately, many cases do not require a detailed knowledge of the concentrations of the individual aromatics but require a total aromatic concentration or concentrations by classes.

The method presented in this paper is an extension of previous methods and is a method for the analysis of hydrocarbon cuts boiling between 150° and 180° C. for different classes of C₉ and C₁₀ aromatics. These results may then be combined to yield the total concentration of aromatics. This method is based on the close similarities in absorption characteristics of monosubstituted aromatics as a class, ortho- and meta-substituted aromatics as a class, and para-substituted aromatics as a class.

EXPERIMENTAL

The instrument used was the Beckman quartz spectrophotometer, equipped for ultraviolet absorption measurements, as manufactured by the National Technical Laboratories, South Pasadena, Calif. The solvent used was spectro grade iso-octane (2,2,4-tri-

methylpentane) obtained from the Special Products Division, Phillips Petroleum Co., Bartlesville, Okla. The aromatics used for calibration were American Petroleum Institute standard samples obtained from the Department of Chemistry, Carnegie Institute of Technology, Pittsburgh, Pa. Glassware was cleaned in all cases by washing with Drene solution, followed by oven drying.

Samples containing olefinic materials were treated with an alkaline permanganate treatment to remove possible interference. This treatment is widely used in the treatment of samples prior to ultraviolet analyses for C₈ and lighter aromatics. The solution of sample is agitated in iso-octane with a strong aqueous solution of potassium permanganate and potassium hydroxide for a period approximately 15 minutes at room temperature.

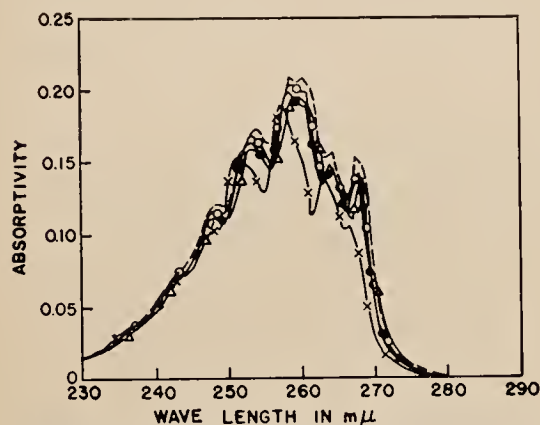
SPECTRAL BEHAVIOR

The absorption of radiation in the ultraviolet range by mononuclear aromatics is due to the electronic system of the benzene ring. This electronic system is affected by variations in direct substitution on the ring—i.e., ortho versus para, and conjugation with olefinic or other active groups. However, variations in hydrocarbon substitution of carbons not directly attached to the ring produce only minor changes. For example, the spectra of *n*-propylbenzene and of isobutylbenzene are very similar in shape and intensities, as shown in Figure 1.

An examination of the physical constants of the hydrocarbons compiled by the American Petroleum Institute Research Project No. 44 (1) showed that 14 of the possible C₉ and C₁₀ aromatics possess boiling points in the 150° to 180° C. range. These have

Table I. C₉ and C₁₀ Aromatics Classified According to Spectral and Structural Characteristics

Mono-Substituted	Ortho- and Meta-Substituted	Para-Substituted
<i>n</i> -Propylbenzene Isopropylbenzene Isobutylbenzene <i>sec</i> -Butylbenzene <i>tert</i> -Butylbenzene	<i>o</i> -Ethyltoluene <i>m</i> -Ethyltoluene 1-Methyl-3-isopropylbenzene 1,3-Diethylbenzene 1,2,3-Trimethylbenzene 1,3,5-Trimethylbenzene 1-Methyl-2-isopropylbenzene	1-Methyl-4-isopropylbenzene <i>p</i> -Ethyltoluene 1,2,4-Trimethylbenzene

**Figure 1. Ultraviolet Absorption Spectra for Monosubstituted Benzenes, Boiling Range 150° to 180° C.**

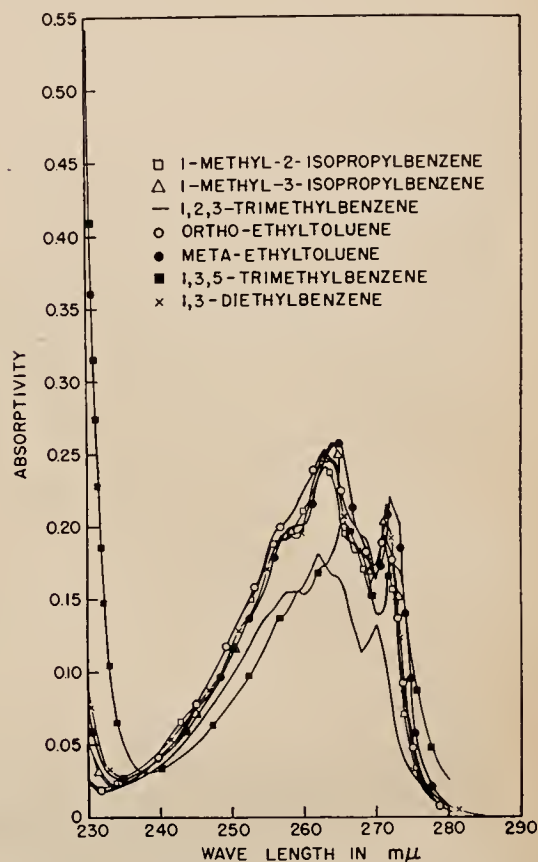
x *tert*-Butylbenzene
 Δ Isopropylbenzene
 --- *n*-Propylbenzene
 ○ Isobutylbenzene
 ● *sec*-Butylbenzene

been classified in Table I according to their spectral and structural characteristics. In addition, 1,3-diethylbenzene, boiling point 181.1° C., has been included.

In Figure 1 are shown the spectra of the mono-substituted aromatics. These are plotted as absorbivity calculated with the concentration expressed in moles per ml. The data are representative of absorption per molecule throughout the class. These materials not only possess very similar spectra in terms of shapes and positions of maxima but also in terms of equivalent intensities. Of these compounds, *tert*-butylbenzene is a bit distinct from the others but is still similar enough to be included in this class. Maximum absorption for this class occurs at about 259 mμ, which is considerably removed from the principal maxima displayed for the other classes of aromatics (Figures 2 and 3).

The spectra of di- or trisubstituted aromatics which are characterized by either or both of ortho and meta substitution but not para substitution are shown in Figure 2. For simplicity, in this paper these are referred to as ortho- or meta-substituted aromatics.

There are two compounds—1,2,3-trimethylbenzene and 1,3,5-trimethylbenzene—that are markedly dissimilar from the others. They do, however, fit the ortho and meta classification better than the mono- or para-substituted classes and are included in the former class for the sake of simplicity. The absorbivity

**Figure 2. Ultraviolet Absorption Spectra for Ortho- and Meta-Substituted Benzenes, Boiling Range 150° to 180° C.****Table II. Molar Absorptivities of C₉ and C₁₀ Substituted Benzenes, 150° to 180° C. Boiling Range**

Wave Length mμ	Molar Absorptivities of Substituted Benzenes, Moles/Liter						Average	
	Class A						Parts/1000	
	<i>n</i> -Propyl	Iso-propyl	<i>tert</i> -Butyl	Isobutyl	<i>sec</i> -Butyl			
259	205	198	173	189	194	192	1.27	
272	27.6	18.6	13.1	25.0	16.9	20.3	0.135	
274	12.1	8.31	5.63	10.0	7.50	8.70	0.059	
276	4.74	2.87	1.25	3.75	1.88	2.90	0.019	
	Class B							
	1,3,5-Tri-methyl	<i>m</i> -Ethyl-toluene	<i>o</i> -Ethyl-toluene	1,2,3-Tri-methyl	1-Methyl-3-isopropyl	1,3-Di-ethyl	1-Methyl-2-isopropyl	
259	153	200	212	154	194	192	200	1.26
272	173	220	184	86.4	210	200	166	1.19
274	133	133	80.2	40.0	85.4	91.3	64.4	0.610
276	80.1	43.9	26.4	22.1	28.0	31.1	23.1	0.250
	Class C							
	<i>p</i> -Ethyl-toluene	1-Methyl-4-isopropyl						
259	290	302						1.96
272	216	283						1.64
274	465	396						2.87
276	219	130						1.18
	Class D							
	1,2,4-Tri-methyl							
259	260							1.86
272	350							2.50
274	329							2.35
276	449							3.21

Table III. Analysis of Synthetic Aromatic Blends

Sample		Concentration, Moles/Liter				Concentrations, Volume %				
		A	B	C	D	Total aromatics	A	B	C	D
1	Blended	1.02	1.06	0.35	0.36	2.79	15.0	15.0	5.0	5.0
	Found	0.96	0.88	0.48	0.38	2.70	14.4	13.4	7.1	5.4
	Difference	-0.06	-0.18	0.13	0.02	-0.09	-0.6	-1.6	2.1	0.4
2	Blended	0.42	0.92	0.21	0.74	2.29	6.0	12.9	2.9	10.4
	Found	0.34	0.79	0.32	0.78	2.23	5.0	12.0	4.8	10.9
	Difference	-0.08	-0.13	0.11	0.04	-0.06	-1.0	-0.9	1.9	0.5
3	Blended	0.96	2.08	0.78	0.65	4.47	15.1	30.3	11.4	9.1
	Found	0.83	1.90	0.94	0.69	4.36	12.1	29.0	14.1	9.5
	Difference	-0.13	-0.18	0.16	0.04	-0.11	-3.0	+1.3	2.7	0.4
4	Blended	0.28	0.72	0.08	0.74	1.82	4.2	10.2	1.2	10.4
	Found	0.28	0.63	0.15	0.77	1.83	4.2	9.5	2.2	10.8
	Difference	0.0	-0.09	0.07	0.03	0.01	0.0	-0.7	1.0	0.4

is calculated for concentrations expressed on a moles per milliliter basis.

In Figure 3 are shown the spectra of the three para-substituted aromatics boiling in the 150° to 180° C. range. These are generally similar. However, for purposes of the calculations, it is necessary to group the two very similar ones, *p*-ethyltoluene and 1-methyl-4-isopropylbenzene, as one subclass and the 1,2,4-trimethylbenzene as another subclass. Therefore, there are four classes of aromatics, based on spectra: mono-substituted ortho- and meta-substituted, and two subclasses of para-substituted members.

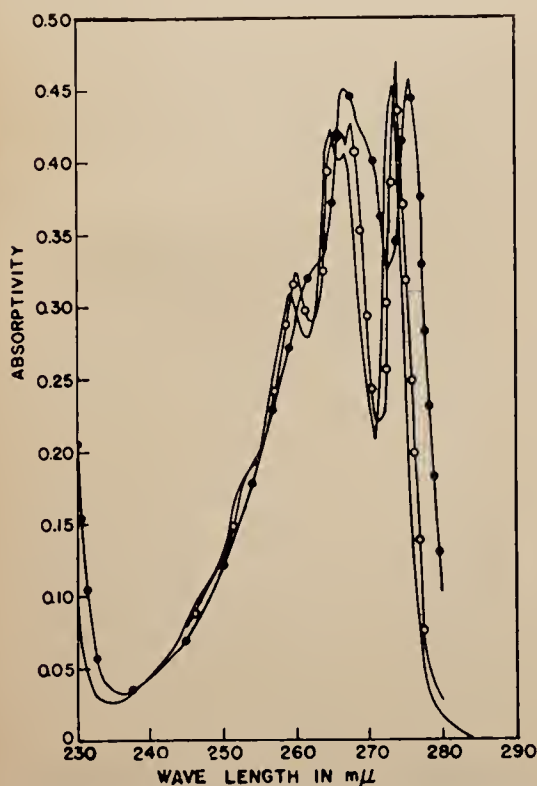


Figure 3. Ultraviolet Absorption Spectra for Para-Substituted Benzenes, Boiling Range 150° to 180° C.

● 1,2,4-Trimethylbenzene
○ *p*-Ethyltoluene
— 1-Methyl-4-isopropylbenzene

The average absorptivities at each wave length for each class were calculated and are plotted in Figure 4. These spectra would not indicate that a multicomponent analysis for the different classes would be feasible. The para compounds dominate the

other classes at all points and the ortho- and meta-substituted compounds dominate the mono-substituted ones almost throughout the entire range. However, a multicomponent analysis scheme was formulated and was found to give satisfactory results.

SCHEME OF ANALYSIS

A four-component matrix system using average values for the different classes was formulated. In Table II are given the molar absorptivities (calculated with concentrations expressed in moles per liter) for all of the 15 aromatics, the wave lengths chosen for each class, and

the classification symbols. With a few exceptions, the absorptivities for a given class at a particular wave length do not deviate too severely from an average value. Those members which show the largest deviations from the averages for their classes are the same ones that show distinct differences in spectra in Figures 1, 2, and 3.

Of the fifteen aromatics examined, eight are C₉'s and seven are C₁₀'s. This suggests that the deviations from average values of the absorptivities calculated with concentrations expressed in volume fractions would be small enough to allow satisfactory analyses on a volume per cent basis. This was found to be the case. This is fortunate, as the volume concentrations of aromatics are frequently needed, and it is desirable to be able to calculate them directly. The average absorptivities for concentrations expressed in parts per thousand are also given in Table II.

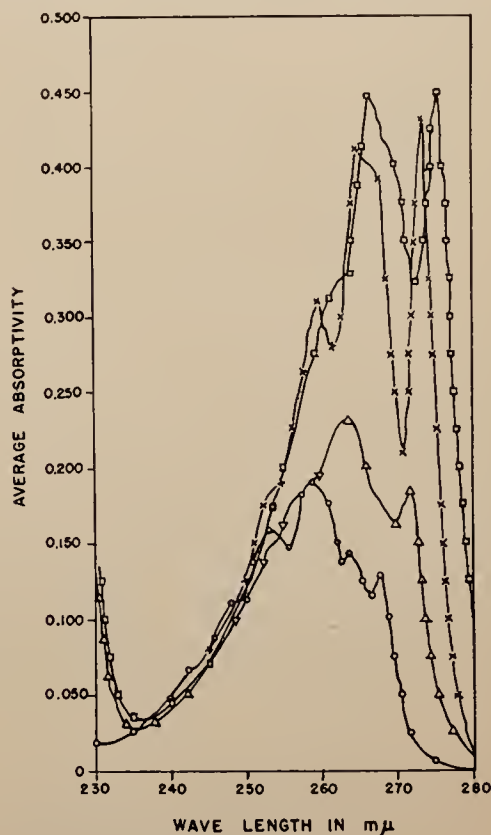


Figure 4. Average Absorptivities of Four Classes of Substituted Benzenes

○ Class A
△ Class B
× Class C
□ Class D

Table IV. Total Aromatic Concentrations Determined by Ultraviolet Absorption and Chromatographic Adsorption

Sample	Concentration, Volume %	
	Ultraviolet absorption	Chromatographic adsorption
1	19.9	20.9
2	24.6	23.0
3	45.6	45.7

RESULTS

The first test of the accuracy of the scheme was made by analyzing synthetically prepared samples. These samples were blended to include various amounts of the different individual aromatics used to provide the calibration data. Since both C_6 's and C_{10} 's are involved, direct volume analyses seemed feasible. The synthetic samples were calculated on both a moles per liter and direct volume concentration basis. The results for four typical synthetic samples are given in Table III.

For the individual classes, there is only fair accuracy as compared to the accuracy for individual components in the ultraviolet analyses for C_6 , C_7 , and C_8 aromatics. However, the calculated total aromatic concentration is always close to the known total aromatic concentration. In fact, the maximum difference between known and calculated total aromatic concentration is less than 3% of the amount present. This is true in either system of calculation—on a moles per liter or a volume per cent basis.

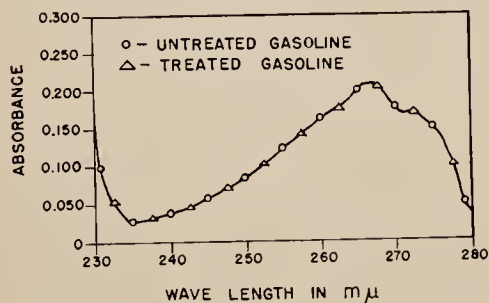


Figure 5. Ultraviolet Absorption Spectra of Straight-Run Gasoline Fraction

A further test of accuracy for total aromatic content was made by comparing results on the same samples by this method and by a chromatographic method (3). The results of this comparison are seen in Table IV. The samples used for this comparison are actual gasoline cuts. The agreement is fairly good in that the two methods yield concentrations which agree to within an average discrepancy of 4% of the aromatics present.

The distribution as obtained in some typical examinations of gasoline cuts boiling between 150° and 180° C. is shown in Table V. The distribution is qualitatively the same in the various types. In Figures 5, 6, and 7 the spectra of three gasoline fractions before and after the alkaline permanganate treatment are shown. The straight-run gasoline is so "clean" that such a treat-

Table V. Distribution of Aromatics in Gasoline Cuts, 150° to 180° C.

	Concentration, Volume %				Total
	Class A	Class B	Class C	Class D	
Straight-run gasoline	0.0	9.7	3.5	6.7	19.9
Thermally cracked gasoline	0.0	12.3	7.4	4.9	24.6
Catalytically cracked gasoline	0.0	19.9	14.7	11.0	45.6

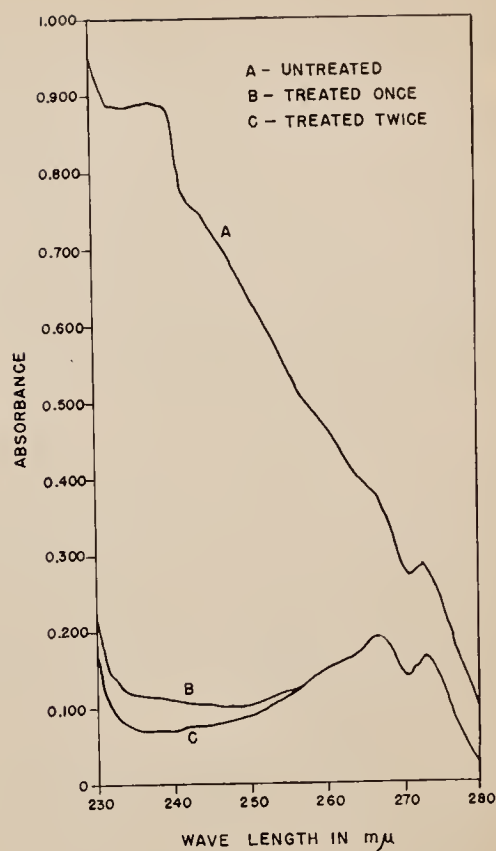


Figure 6. Ultraviolet Absorption Spectra of Thermally Cracked Gasoline Fraction

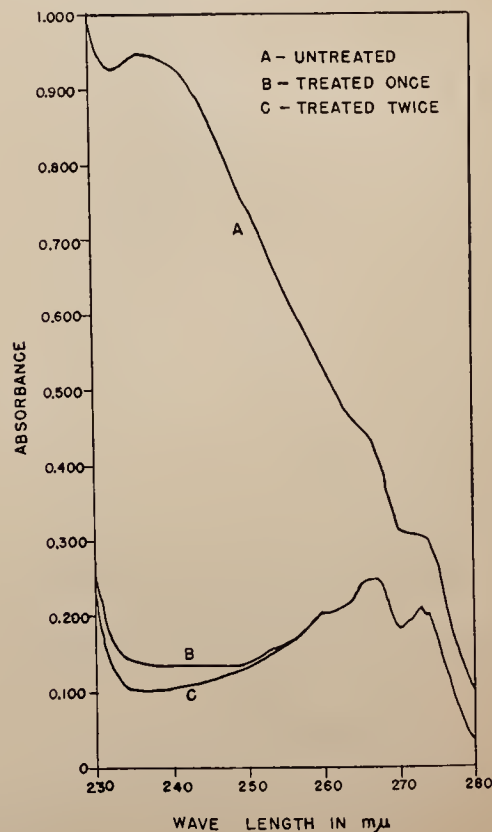


Figure 7. Ultraviolet Absorption Spectra of Catalytically Cracked Gasoline Fraction

ment is unnecessary. The thermally and catalytically cracked gasoline cuts, on the other hand, show very large interference effects that must be removed by the treatment. One treatment does not completely remove the interfering compounds but does eliminate the background at the wave lengths used in this analysis.

In view of the spread that occurs among the absorptivities for a particular class at a specific wave length, it is believed that the success of the method rests primarily upon the extensive averaging that is utilized. The method is only fairly accurate for the determination of concentrations of the individual classes; it is believed to be satisfactory for total aromatic concentrations. Since this method requires only data at four wave lengths and no particular deviation from established procedures, it may be done as rapidly as a routine analysis of a sample for xylenes and ethylbenzene.

ACKNOWLEDGMENT

The authors are indebted to R. E. Snyder for performing the chromatographic analyses. They would also like to express appreciation to the management of Gulf Research & Development Co. for permission to publish this material.

LITERATURE CITED

- (1) Am. Petroleum Inst., "Selected Values of Properties of Hydrocarbons," Research Project 44, Washington, D. C., U. S. Govt. Printing Office, Nov. 1947.
- (2) Coggeshall, N. D., "Physical Chemistry of Hydrocarbons," ed. by A. Farkas, New York, Academic Press, 1950. Chap. 5.
- (3) Criddle, D. W., and LeTourneau, R. L., *ANAL. CHEM.*, **23**, 1620 (1951).
- (4) Tunnicliff, D. D., Brattain, R. R., and Zumwalt, L. R., *Ibid.*, **21**, 890 (1949).

RECEIVED June 26, 1952. Accepted September 23, 1952.

PRINTED IN U. S. A.

Determination of Olefin Group Types

Chromatographic and Infrared Absorption Techniques

ELEANOR L. SAIER, ABBOT POZEFSKY, AND NORMAN D. COGGESHALL
Gulf Research & Development Co., Pittsburgh, Pa.

Reprinted from
ANALYTICAL CHEMISTRY
Vol. 26, Page 1258, August 1954

Determination of Olefin Group Types

Chromatographic and Infrared Absorption Techniques

ELEANOR L. SAIER, ABBOT POZEFSKY¹, and NORMAN D. COGGESHALL
Gulf Research & Development Co., Pittsburgh, Pa.

In the spectroscopic determination of functional group types there are fundamental limitations due to variations in position and intensity of functional group absorption. A detailed study has been made of the limitations and applications of the analysis for functional group-type olefins. A high degree of accuracy is not possible, owing to variations in absorption behavior among olefins of the same class, although very useful results may be obtained. A method of working in dilute carbon disulfide solutions with thick cells has been developed to eliminate the dependence on specific absorption cells. Chromatographic procedures were employed to obtain olefin-rich mixtures for direct examination. The procedure has been employed as an integral portion of a complete analysis for certain problems wherein specific paraffins, group-type olefins, and specific aromatics are determined.

THE realization that the absorptivity of a given functional group often is reasonably constant in a series of compounds has given impetus to the development of infrared spectroscopic methods for quantitative group-type analysis. Johnston and coworkers (8) applied this technique to the determination of several olefinic classes of compounds in gasolines. Anderson and Seyfried (3) extended the method to include five olefinic classes in addition to a group-type analysis for oxygenated compounds. In the past few years the literature on the application of this approach to the quantitative determination of C-H groups in hydrocarbon mixtures has been increasing (5-7, 10). The usefulness of group-type analyses using infrared absorption techniques is evidenced by the increased development and application of these methods in various laboratories. This paper concerns itself with such an analysis for the olefinic functional groups $\text{RCH}=\text{CH}_2$, $\text{RR}'\text{C}=\text{CH}_2$, $\text{RCH}=\text{CHR}'$ (*cis* and *trans*), and $\text{RR}'\text{C}=\text{CHR}''$, using chromatographic separations as a means of concentrating the olefins and minimizing interferences by nonolefinic components. This method does not yield direct information on the concentrations of tetrasubstituted and cyclic olefins. In the development of this method, the following points have been investigated and the results are discussed below:

The utilization of dilute carbon disulfide solutions of the olefins and a comparatively thick cell (approximately 1.5 mm.). This technique has a long-term convenience not encountered with methods using thinner cells.

Use of four analytical wave lengths for the $\text{RR}'\text{C}=\text{CHR}''$ group which shows variable absorption in the 11.9 to 12.7-micron region.

Evaluation of the accuracies of the present method.

Procedure for the chromatographic separation of paraffins, olefins, and aromatics, and the quantitative evaluation of the volume fractions of these three classes of materials from the chromatogram.

Effect of the chromatographic separation on the relative distribution of the five olefinic classes.

Desirability of separating the olefins and aromatics from the paraffins in order to improve the accuracy of any analysis of the paraffinic fraction.

Accuracy of the olefin analysis in the presence of moderate amounts of paraffins present as contaminants.

Application of the olefin matrix as determined for one cell to other thick cells.

The present method has been applied to gasolines and to paraffin-olefin-aromatic mixtures of dehydrogenation experiments, and the results are also discussed. The data presented permit a more critical evaluation of the limitations and accuracies of the present group-type olefin analysis than now appears in the literature.

EXPERIMENTAL

Spectra. A Perkin-Elmer model 12A spectrometer equipped with rock salt optics was used to obtain the quantitative spectral data. The Perkin-Elmer Model 21 spectrophotometer was also used qualitatively to examine samples and fractions from chromatographic separations. The olefins used for calibration in all instances were obtained from American Petroleum Institute Project 6, Carnegie Institute of Technology. Elmer and Amend Purity carbon disulfide was used as the solvent. The pure olefins generally were diluted at least 1 to 100 by volume in order to obtain a cell plus solvent corrected absorbance of 0.4 to 0.5 at their major analytical wave lengths. The absorbance of the same cell filled with the solvent only was taken as the correction at all analytical wave lengths. The limited availability of olefins from API Project 6 resulted in either four or five compounds of each class being used for calibration.

Chromatographic. The chromatographic column employed in concentrating the olefins is illustrated in Figure 1.

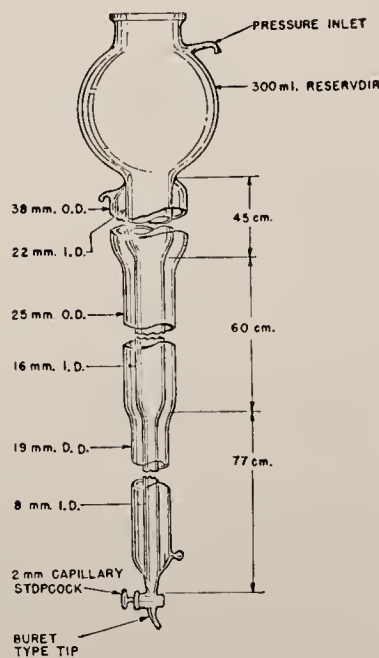


Figure 1. Chromatographic Column Used in Concentrating Saturates, Olefins, and Aromatics

Davison silica gel (Code 923) was used as the adsorbent. It is important to stress the use of this particular silica gel, as it is believed to be the most favorable one in repressing olefin isomerization and polymerization (9). In making a separation on a sample for which only the olefinic content was of interest, 10 ml. of spectral grade iso-octane (2,2,4-trimethyl pentane) was employed to prewet the column. The sample was added as soon as the iso-octane was into the adsorbent zone. (The ratio of

¹ Present address, General Electric Co., Waterford, N. Y.

grams of adsorbent to milliliters of olefins plus aromatics was approximately 10 to 1.) After all the sample had entered this zone, approximately a half inch of fresh adsorbent was added to the column and followed with ethyl alcohol eluent. A sufficient pressure of nitrogen was maintained so that approximately 1 ml. per minute of sample issued from the bottom of the column. The effluent was collected in 0.9-ml. portions using the collector illustrated in Figure 2. The complete separation of a 100-ml. sample takes approximately 4 to 5 hours. The refractive indices are obtained for all cuts and plotted *vs.* cut number. In cases where the paraffinic fraction is to be analyzed, it is advisable not to use a separate prewetting agent. [An excellent discussion of chromatographic procedures and applications has appeared in this journal (2)].

CALIBRATION AND PROCEDURE

Spectral. Originally a 0.15-mm. cell was used with *n*-heptane as the solvent. However, as part of a more general investigation using comparatively thick cells, all the calibration data were re-determined in a 1.5-mm. cell with carbon disulfide as the solvent. (In changing from the 0.15-mm. cell with *n*-heptane as solvent to the 1.5-mm. cell using carbon disulfide as solvent, several synthetic solutions were tested by both methods. An analysis by either technique was usually within the accuracy of the general

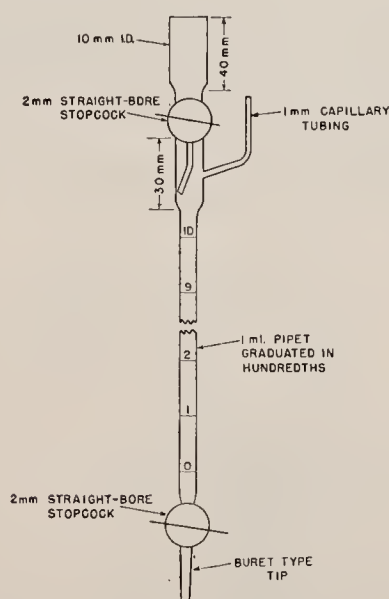


Figure 2. Receiver for Obtaining Measured Volumes of Liquid Issuing from Chromatographic Column

method. There was, however, a definite improvement in the results for the *cis*-RCH=CHR' type resulting from the elimination of the considerable absorbance of heptane at the *cis*-RCH=CHR' point.) In all olefin calculations the concentrations were expressed on a moles per liter basis. The detecting system of the spectrometer requires the use of comparatively wide slit widths, and there was reason to suspect deviations from Beer's law owing to instrumental effects. Consequently, each pure olefin was checked for these deviations within the practical absorbance range using the 1.5-mm. cell. In every case a plot of absorbance *vs.* concentration in moles per liter gave a straight line within experimental error up to an absorbance of approximately 0.45 to 0.5. Beer's law deviations due to solution effects are expected to be at a minimum. Since the olefin concentrations used in calibration at the dominant points were at most 1% by volume, the absorbance of the cell filled with solvent was taken as the correction at all analytical points. This procedure is a very close approximation to the true cell plus solvent correction.

RCH=CH₂, RR'C=CH₂ AND RCH=CHR' (*trans*) CLASSES. For the RCH=CH₂, RR'C=CH₂, and RCH=CHR' (*trans*) classes, the group analytical wave lengths are approximately 11, 11.2, and 10.4 microns, respectively. The constancy of band positions and near-constancy of absorptivities are good. Thirteen olefins were used to calibrate for these three classes, and the average deviation of the absorptivities from the average of the class was 7.6% for RCH=CH₂, 4.4% for RR'C=CH₂, and 4.8% for RCH=CHR' (*trans*). The maximum deviation of absorptivity of any member from the appropriate average of its class was approximately 11%. It is for these three classes then that one would expect to observe the better accuracy on synthetics, and this is the case. The use of carbon disulfide as the solvent gave some trouble with the RR'C=CH₂ class. At 11.2 microns one is on the side of a carbon disulfide absorption band, and it was necessary to obtain scanning data for the solution through this wave length and to correct each point for the cell plus solvent in order to find the absorption maximum. For the three classes above the analytical points for all, samples were obtained by scanning to find the absorption maxima.

RR'C=CHR' CLASS. The RR'C=CHR' class shows a variable region of maximum absorption (3). Five compounds (2-methyl-2-butene, 3-methyl-*cis*-2-pentene, 3-methyl-*trans*-2-pentene, 2-methyl-2-pentene, and 2,4,4-tri-methyl-2-pentene) were used for calibration, and the individual absorption maxima were found to occur at one of four wave lengths which were approximately 12.0, 12.1, 12.3, and 12.5 microns. The absorptivities of each olefin of this class were obtained at these four wave lengths. Two of the procedures employed in utilizing these calibration data in analyses were: (1) The class absorptivity was obtained by averaging the maximum absorptivity of each member regardless of wave length. The spectra of synthetic samples were obtained and the absorption maximum was located in the 11.9 to 12.7-micron region. Absorbance data were taken at this point and used in conjunction with the class absorptivity (2). The absorptivities of each compound at the four wave lengths mentioned above were averaged (four absorptivities were used per compound). This average was taken as the effective absorptivity of the compound in this region. The average of the effective absorptivities of the five pure compounds was taken as the class absorptivity. In practice, data are obtained at these four wave lengths for samples and the resultant absorbances are averaged and used in the calculations. Other schemes of utilizing the calibration data for calculations of the RR'C=CHR' concentration were also tried. The results on synthetic samples indicated that in general the second method above gave the better results more consistently, and hence this procedure has been incorporated into the method.

RCH=CHR' (*cis*) CLASS. Four compounds were used in calibrating for RCH=CHR' (*cis*). The absorption maximum characteristic of this class was found to fall at approximately 14.4 microns for three of the compounds, and the maximum for the fourth one appeared at 13.9 microns. The latter band is close to the methylene wagging frequency characteristic of chain hydrocarbons. Consequently this point was not considered as a good one for which to take data. This would be especially true in the case of samples containing long chain olefins. Hence, the absorbance data were obtained at the absorption maxima of the other three compounds. The absorption maxima of these three compounds are rather broad and 14.44 microns was chosen as the analytical point for all samples. Carbon disulfide is to be preferred as the solvent as its absorbance at this point is very much smaller than that of *n*-heptane. The absorptivities of the members of the RR'C=CHR' and RCH=CHR' (*cis*) classes do not remain as constant as was found for the first three classes discussed above. One expects and finds that the accuracies for these two classes are the poorest.

TESTS ON SYNTHETICS AND ACCURACY. A five-component matrix was set up using the average absorptivity of each class at

its own analytical wave length or wave lengths, and the average absorptivities of the other classes at the same points. This matrix as obtained with a 1.5-mm. cell is seen in Table I.

In solving the above matrix, the concentrations of the different olefin classes are found in moles per liter. The total olefin, in moles per liter, is then used to find the percentage distribution of each class. Synthetic blends of olefins were analyzed in order to obtain information on the expected accuracy of this analysis. Some typical results are shown in Table II.

Table I. Matrix Used in Group-Type Olefin Calculations

Wave Length, μ	(Molar absorptivities in arbitrary units)				
	trans-RCH=CHR'	RCH=CH_2	RR'C=CH_2	RR'C=CHR'	cis-RCH=CHR'
10.36	16.7	0.789	0.456	0.738	0.719
10.95	0.703	14.9	1.31	0.764	0.556
11.24	0.626	1.63	17.3	0.376	0.312
Av. of 4, 12.0-12.5	0.228	0.253	0.353	2.11	0.328
14.44	0.064	0.266	0.108	0.094	3.80

Table II. Analyses of Synthetic Blends^a of Pure Olefins
(Concentrations in mole per cent)

Sample ^b	RCH=CH_2		RR'C=CH_2		RR'C=CHR'		trans-RCH=CHR'		cis-RCH=CHR'	
	Known	Calcd.	Known	Calcd.	Known	Calcd.	Known	Calcd.	Known	Calcd.
1	18.6	19	34.3	34	10.8	8	14.5	12	21.8	27
2	17.2	18	28.9	31	20.3	16	11.2	12	22.4	24
3	27.2	31	19.1	22	16.9	23	12.3	14	24.5	10
4	23.2	26	16.3	18	29.0	34	10.6	13	20.9	9
5	17.1	20	28.8	30	20.4	19	11.2	14	22.5	17

^a Each blend was prepared to contain several members of each class.

^b Samples 1 and 2 were analyzed using the 1.5-mm. cell and CS_2 as solvent. Samples 3, 4, and 5 were analyzed in a 0.15-mm. cell with *n*-heptane as the solvent.

Considering the complexity of this type of analysis, the results of Table II show a reasonable accuracy for all classes except the cis-RCH=CHR' . The poor accuracy for this latter class must be considered an inherent limitation of the present method. In Table III are given the average errors based on the results of Table II and three other synthetics in terms of mole per cent of total sample.

Table III. Average Errors of Total Sample for Various Classes of Olefins, Based on Results of Synthetic Blends

	(Mole %)				
	RCH=CH_2	RR'C=CH_2	RR'C=CHR'	trans-RCH=CHR'	cis-RCH=CHR'
Average error	2.5	1.7	3.6	1.3	5.0

The agreement between blended and calculated compositions is fairly good for the RCH=CH_2 , RR'C=CH_2 , and trans-RCH=CHR' classes, and that the RR'C=CHR' and cis-RCH=CHR' classes contribute the major discrepancies. This analysis was originally set up using a 0.15-mm. cell and *n*-heptane as the solvent. In terms of accuracy, the 0.15-mm. and 1.5-mm. cell procedures were equivalent. However, for reasons discussed in the next section the authors prefer the thicker cell technique.

USE AND INTERCHANGE OF COMPARATIVELY THICK ABSORPTION CELLS. In quantitative infrared analysis the tendency has been to use liquid cells of approximately the same path length as required for obtaining good qualitative spectra of paraffins—i.e., path lengths in the range of 0.1 to 0.2 mm. When using these thin cells, some or all of the following difficulties are frequently encountered:

When a given thin cell is used and dilutions are not employed, the cell absorbance contributes to the "apparent" absorptivities. These will therefore change if there is cell fogging or deterioration and frequent recalibrations may be necessary.

When dilutions are necessary in order to obtain good absorbance data at some of the analytical wave lengths, the problem arises of properly correcting for the solvent and cell and recalculating all the data to a common dilution basis.

Deviations from Beer's law are more likely to occur in concentrated solutions.

The use of comparatively thick cells offers a means of minimizing most of the above difficulties. The thicker the cell, the closer one can approach the situation that exists in ultraviolet spectrometry where it is possible to obtain relatively absolute data. At present the obtaining of calibration data in the infrared for nonroutine liquid analysis accounts for an appreciable part of the time spent in making such an analysis. If calibration data can be obtained with the cell and solvent properly corrected out, these data should have a long-term utility.

A cell approximately 1.5 mm. thick (cell A) was used to obtain all the calibration data which were incorporated into the matrix of Table I. Then a second cell (cell B) was assembled, and its thickness relative to the first cell was found by placing the same

solution in both cells and obtaining absorbances at five or six wave lengths. The ratio of the absorbances of each cell at a given wave length, corrected for the absorbance of the appropriate cell filled with solvent, gave the ratio of the path lengths. A 2-mm. cell (cell C) was purchased from the Perkin-Elmer Corp. and compared in the same way to the original cell A. In no case was the absolute path length determined. The ratio of cell lengths were found to be as follows:

	Cell B	Cell C
Ratio of path length (relative to cell A)	0.84	1.28

It was of interest to see how readily the matrix which had been determined for one cell could be used on other cells. Absorbance data were obtained for several olefin mixtures in each of the three cells, and these data were corrected only for the appropriate cell plus solvent absorbance. Then the original matrix that appears in Table I was used with the corrected absorbance data for each cell to calculate the olefinic content. Of course, the total calculated moles of olefin differed with each cell because of varying path lengths, but the group-type distributions based on total observed olefins are as shown in Table IV.

Table IV indicates the feasibility of switching cells which are approximately of the same path length, and the continued use of the original matrix. The results from cells A and B, which differ in thickness by approximately 16%, agree fairly well. The agreement between cells A and C, which differ in thickness by approximately 28%, is somewhat poorer. This indicates the advisability of using cells of approximately the same thickness. The absolute olefin content as determined in one cell is related to that as determined in the other cell by the ratio of the path lengths (provided that the dilutions for both cells are placed on a common basis). For samples which are mixtures of olefins and nonolefins, the authors prefer to determine the relative olefin distribution spectrally and to report a separate total olefin content as determined by the capillary tube method for Criddle and LeTourneau (4) or by the chromatographic procedure described here.

Chromatographic. This analysis was applied to two types of samples—namely, products of dehydrogenation experiments and to gasolines. The samples contained saturates, olefins, and aromatics. For reasons outlined above, a chromatographic separation was employed. Sufficient sample was charged to the column so that approximately 10 or more 0.9-ml. cuts in the olefin region could be obtained. These cuts were selected by obtaining their spectra and observing when the characteristic olefin bands were present or from a plot of refractive index vs. cut number. The

Table IV. Analysis of Olefin Mixtures Using a Given Matrix on Data Obtained in Three Relatively Thick Absorption Cells of Differing Path Lengths

Type	Synthetic 1				Synthetic 2				Olefin Concentrate			Gasoline		
	Cell ^a A	Cell ^a B	Cell ^a C	Known	Cell A	Cell B	Cell C	Known	Cell A	Cell B	Cell C	Cell A	Cell B	Cell C
RCH=CH ₂	19	19	24	17.6	18	19	20	17.2	46	46	48	21	20	20
RR'C=CH ₂	34	32	28	32.5	31	30	25	28.9	23	25	23	11	11	8
RR'C=CHR'	8	9	8	11.3	16	16	18	20.3	24	22	24	34	35	35
RCH=CHR' (<i>trans</i>)	12	13	16	13.7	12	12	14	11.2	5	4	5	11	10	11
RCH=CHR' (<i>cis</i>)	27	27	25	24.9	23	23	24	22.4	2	3	0	23	24	26

^a Data for matrix of Table I obtained using cell A. See text for ratios of cell path lengths.

selected cuts were reblended in equal volumes and then analyzed for olefins.

EFFECT OF COLUMN ON OLEFIN DISTRIBUTION. It was important to see if the chromatographic separation affected the olefinic distribution by such things as selective separation, isomerization, or polymerization. Several synthetic samples were prepared and analyzed before and after chromatographic separation.

The olefin mixture was analyzed spectrally, then blended with Philips spectral grade iso-octane and Merck reagent grade xylenes and chromatographically separated. In Table V the results of these analyses are presented.

The results in Table V give no definite evidence to indicate a general trend toward any separation within the olefins themselves on the column if the olefin cuts are reblended. The overall average difference between the before and after results generally is of the same magnitude as the over-all average error in the olefin analysis. Thus, any change in olefin distribution due to the chromatographic separation is not much different from the inherent inaccuracies of the olefin analysis itself. The results tend to confirm the conclusions of Johnston and coworkers (8) that "there is little, if any, change in the olefin skeletal structure or double bond position."

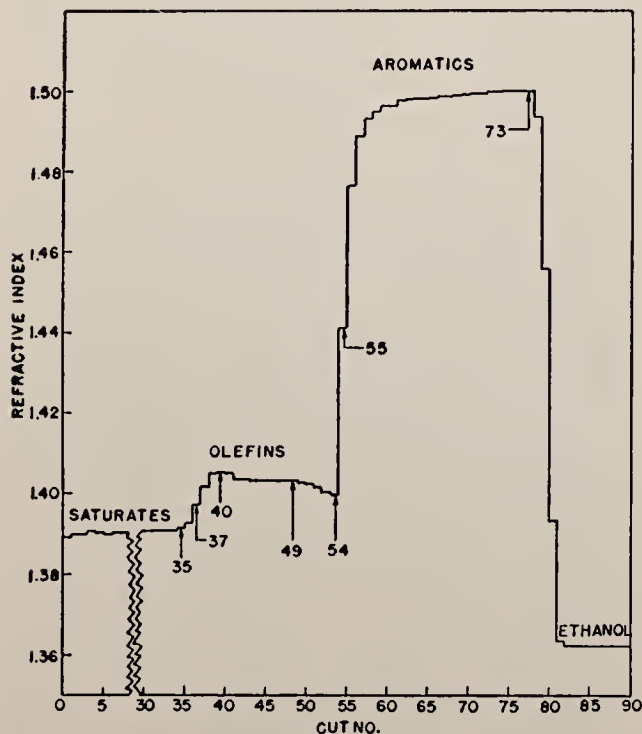
Table V. Comparison between Olefin Portions of Synthetic Blends before and after Chromatography

Sample	RCH=CH ₂		RR'C=CH ₂		RR'C=CHR'		<i>trans</i> -RCH=CHR'		<i>cis</i> -RCH=CHR'	
	Before	After	Before	After	Before	After	Before	After	Before	After
1 ^a	44	46	19	23	29	24	5	5	3	2
2 ^b	4	4	54	50	33	38	7	5	3	3
3 ^b	20	22	30	32	14	13	14	15	22	18
4 ^b	49	55	22	23	21	18	7	4	1	0

^a 1.5-mm. cell with CS₂ solvent.

^b 0.15-mm. cell with *n*-heptane solvent.

USE OF CHROMATOGRAM FOR RECOMBINATION AND CALCULATION OF TOTAL SATURATES, OLEFINS, AND AROMATICS. Figure 3 is a plot of refractive index *vs.* cut number of a typical chromatographic separation. The sample used for this separation was a synthetic blend, and it differed from other synthetic blends that were chromatographed in that a complex mixture of paraffins and aromatics was used with the olefins instead of only iso-octane and xylenes. In previous separations the chromatogram was used to calculate total paraffin, olefin, and aromatic content on a volume per cent basis. The chromatogram of Figure 3 illustrates the calculation procedures for all chromatographic separations. The refractive indices of the truly paraffinic cuts will remain almost constant if the paraffins have approximately the same molecular weight. When the first olefin starts to issue from the column, the refractive index of this cut will show a definite increase unless the saturate portion contains a very high concentration of cycloparaffins. This is the beginning of the transition zone where the separation between paraffins and olefins is incomplete and in Figure 3 occurs at cut 35. At cut 55 the second sharp break in refractive index occurs and this indicates that aromatics are beginning to issue from the column, and an olefin-aromatic mixing zone is encountered. Spectra of the cuts in each transition zone confirm the point where olefins and aromatics first begin to come through the column. This spectral test should be applied if the saturates are very rich in cycloparaffins as the latter may have higher refractive indices than the olefins. In Figure 3 cuts 1 to 34 are considered pure paraffins. From cut 35 onward the cuts contain olefins and decreasing amounts of paraffins and the relative concentrations are computed assuming additivity of refractive indices. The refractive index of cut 34 is taken as typical of the paraffins and the refractive index of cut 40 is taken as typical of the olefins. In the chromatogram the refractive indices of cuts 54 and 73 are taken as typical of the olefins and aromatics, respectively, for the calculations of distribution in the second transition zone. On occasion it has been found that the refractive index of the olefin cuts will rise to a maximum and then fall off slightly until the aromatics start to come through. For chromatograms of this type the maximum refractive index of the olefin fraction is taken as typical of the olefins up to that cut, and the following cuts are assumed to be all olefin until the cut where aromatics start to become apparent. The refractive index of the cut just before the point is used in the calculation of olefin-aromatic distribution. The chromatogram in Figure 3 is an example of this behavior, and cuts 41 through 54 were assumed to be pure olefins in the calculation. This dropping off of refractive index in the olefin

**Figure 3. Chromatogram of Synthetic Sample Containing Complex Mixture of Saturates, Olefins, and Aromatics**

region is due in large part to a partial separation of the olefins on the column. In Figure 4 the spectra of cuts 37, 49, and 54 (see Figure 3 for the chromatogram) are shown in the 9.8- to 11.5-micron region. It is seen that there is an appreciable separation of olefins, and this is the reason why the olefin cuts are reblended instead of using a central heart cut as representative of the distribution. In Table VI results of the chromatographic analysis for total paraffin-olefin-aromatic are given for several synthetic samples.

If it is necessary to obtain an olefin fraction for spectral analysis, the use of this chromatographic method gives data which permit the above type of calculation. However, if only a total paraffin-olefin-aromatic determination is desired, the capillary tube method (4) is to be preferred, as it is much more rapid. In reblending olefinic cuts for spectral analysis, it has been found best to blend from the point where olefins begin to come through to the point just before aromatics are present. This procedure does result in some error as olefins are lost in the transition zone between olefins and aromatics, although this is not too serious, as seen in Table V. The first cuts used in reblending for the spectral analysis of group-type olefins contain some paraffins. In Figure 3 cuts 35 through 54 would be considered the usable olefin fraction, and by assuming additivity of the refractive indices the paraffin content in these cuts is calculated to be 13%. The group-type olefin bands generally have a much larger absorptivity than do paraffins at the same wave lengths. The presence of paraffins will introduce some error, but this has been found to be relatively small (see applications for further evaluation).

Several of the synthetic samples in Table V were also analyzed for total olefins and aromatics (which were xylenes) using ASTM Method D 875 (1). The results were in excellent agreement with those obtained from the chromatographic analyses. However, the same two methods, when applied to gasolines, gave the results tabulated in Table VII.

The agreement between olefin and aromatic contents is not good. It appears that in the chemical method more than just the olefins are being brominated, and this accounts for the higher olefin content as determined chemically. The authors' findings are

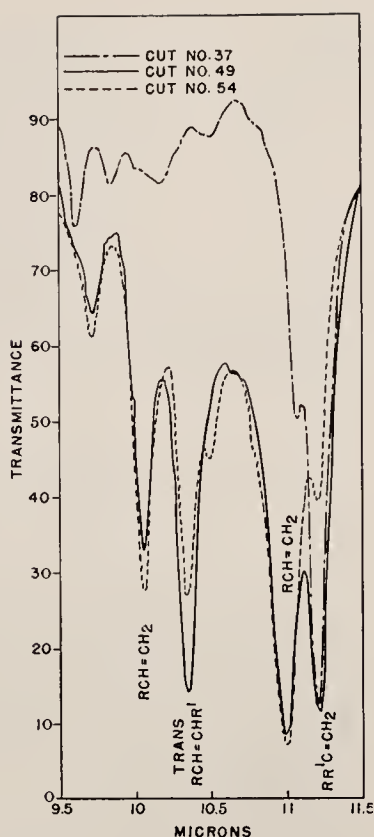


Figure 4. Region of 9.5 to 11.5 Microns of Selected Olefin Cuts

See Figure 3 for chromatogram. Illustrating partial separation of olefins on chromatograph column

Table VI. Comparison between Blended Concentrations of Saturates, Olefins, and Aromatics and Concentrations Obtained by Chromatographic Fractionation

Sample	(Results in volume %)					
	Saturates (Iso-octane), %		Olefins, %		Aromatics (Xylenes), %	
	Blended	Calcd.	Blended	Calcd.	Blended	Calcd.
1	60.0	61.4	20.0	19.3	20.0	19.3
2	55.5	55.3	20.0	19.3	24.5	25.4
3	70.0	69.5	5.0	5.9	25.0	24.6
4	69.6	70.0	8.7	7.8	21.7	22.2

Table VII. Comparison of Chemical and Chromatographic Determination of Volume Per Cent Olefins and Aromatics in Gasolines

Gasoline	Olefin		Aromatics	
	ASTM D 875	Chromat.	ASTM D 875	Chromat.
Polyform distillate	39.8	26.9	8.9	17.3
Thermal cracked	54.1	36.9	0.0	11.8
Cat. blending stock	59.2	44.7	3.8	18.5

similar to those reported and discussed by Criddle and Le Tourneau (4), and it is concluded that the chromatographic method gives a better analysis than the chemical method used above for samples as rich in olefins as these.

APPLICATIONS

In the application of these methods to dehydrogenation products, the saturates used as the reactants were analyzed by conventional infrared methods. The reaction products contained paraffins, olefins, and aromatics. An attempt was made to analyze distillation cuts of the total mixture using the group-type olefin method in conjunction with a specific paraffin analysis. Analysis of synthetic samples blended to simulate the actual samples showed that this procedure gave results for the paraffins which were in error by as much as 10% on total sample, although the olefin analysis was of the accuracy discussed above. These same synthetics were also analyzed as a pure olefin mixture, neglecting all paraffins. In the two cases the olefin analyses agreed very well. Apparently the approximation of the olefin

Table VIII. Olefin Analysis of a Synthetic and a Dehydrogenation Experiment Sample Containing Paraffins and Olefins

(Olefin content expressed as mole % of total olefin content).

	Synthetic			Sample	
	Known	Paraffin-olefin matrix calcd.	Olefin matrix calcd.	Paraffin-olefin matrix calcd.	Olefin matrix calcd.
RCH=CH ₂	20.4	19	20	14	13
RR'C=CH ₂	13.8	13	15	5	5
RR'C=CHR'	13.9	12	16	11	10
RCH=CHR' (trans)	27.3	22	26	41	41
RCH=CHR' (cis)	24.6	34	23	29	31

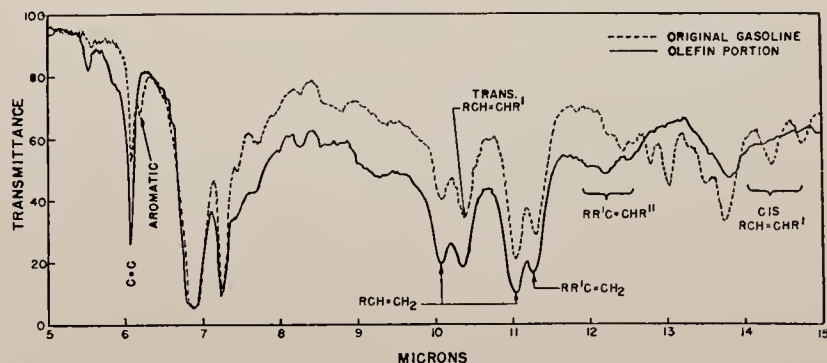


Figure 5. Infrared Spectra of Total Thermally Cracked Gasoline and Olefin Portion of Same Gasoline as Isolated Chromatographically

Table IX. Olefin Data for Three Representative Gasolines

(Different olefin types are given in mole % of the olefin portion. Total olefin portion given as volume % of total gasoline)

Gasoline	Total Olefins, %	RCH= CH ₂ , %	RR'C= CH ₃ , %	RR'C= CHR', %	<i>trans</i> - RCH= CHR', %	<i>cis</i> - RCH= CHR', %
Polyform distillate	27	21	6	35	22	16
Thermal cracked	37	32	10	30	14	14
Cat. blending stock	45	9	13	42	20	16

absorbances at the paraffin points was rather poor and resulted in poor paraffin results. It was evident that the neglect of moderate paraffin contamination did not seriously affect the olefin analysis. Table VIII shows the olefin results of a synthetic sample in which paraffins are present to the extent of 38% by volume, and of an olefin concentrate from a dehydrogenation experiment in which the paraffin content was of the order of 20% by volume. A group-type olefin-specific paraffin matrix was used in one instance, and the calculation was repeated using the group-type olefin matrix alone.

Table VIII shows that moderate paraffin contamination in the olefin cuts of a chromatographic separation will not seriously affect the ordinary accuracy of the olefin analysis. However, in order to obtain better information on the paraffins, chromatographic separation was used. It was then possible to improve the paraffin accuracy so that the average error was approximately $\pm 1\%$ of total sample. The results for specific paraffins before and after reaction permitted the evaluation of any isomerization accompanying the dehydrogenation.

In the application to gasolines, only the olefinic distributions were determined spectrally. The chromatogram permitted the determination of total saturates, olefins, and aromatics. The results for three gasolines are presented in Table IX.

In Figure 5 the spectra of a total thermal cracked gasoline

and of the olefin portion of the chromatographically separated gasoline are shown. The marked changes of absorption in the RR'C=CHR' and RCH=CHR' (*cis*) regions are to be noted.

In any concentration procedure, of which chromatography is an example, errors made in the spectral analysis of the concentrated produce are reduced by the concentration factor when re-

lated back to total sample. Thus in Table IX the absolute error in the determination of any class of the polyform distillate is reduced by the factor of 0.27 when related back to total sample. This assumes that there is no error in the determination of the concentration factor.

ACKNOWLEDGMENT

The aid of the Analytical Section in providing the ASTM analyses of particular samples is gratefully acknowledged.

LITERATURE CITED

- (1) Am. Soc. Testing Materials, "Tentative Method for Test for Olefins and Aromatics in Petroleum Distillates," (Issued 1946), Designation ASTM D 875-46T, Petroleum Book D-2.
- (2) ANAL. CHEM., **22**, 850-81 (1950).
- (3) Anderson, J. A., Jr., and Seyfried, W. D., *Ibid.*, **20**, 998 (1948).
- (4) Criddle, D. W., and Le Tourneau, R. L., *Ibid.*, **23**, 1620 (1951).
- (5) Francis, S. A., *J. Chem. Phys.*, **19**, 942 (1951).
- (6) Hastings, S. A., *et al.*, ANAL. CHEM., **24**, 612 (1952).
- (7) Hibbard, R. R., and Cleaves, A. P., *Ibid.*, **21**, 486 (1949).
- (8) Johnston, R. W. B., Appleby, W. G., and Baker, M. O., *Ibid.*, **20**, 805 (1948).
- (9) Mair, B. J., private communication.
- (10) Rose, F. W., *J. Research Natl. Bureau Standards*, **20**, 129 (1938)

RECEIVED for review February 18, 1954. Accepted April 29, 1954.



Temperature Dependence of Infrared Absorption

R. H. HUGHES, R. J. MARTIN, AND N. D. COGGESHALL

Temperature Dependence of Infrared Absorption

R. H. HUGHES, R. J. MARTIN, AND N. D. COGGESHALL
Gulf Research & Development Company, Pittsburgh, Pennsylvania
(Received November 21, 1955)

A RECENT publication¹ has prompted us to publish the following material on the temperature dependence of infrared absorption intensities. Several years ago while studying hydrogen bonding equilibria one of us observed that the intensity of the unassociated OH band decreased with increasing temperature. This effect was apparently first reported by Davies and Sutherland² who called it a solvent effect. Slowinski and Claver¹ recently observed the effect in pure liquids. In our work the effect was observed in dilute solutions.

A Perkin-Elmer Model 12B instrument equipped with a LiF prism and densitometer attachment was used to obtain absorbance values. Accurate temperature control was accomplished by placing the infrared cell in a specially constructed metal compartment through which water from a regulated bath was circulated. A thermocouple was used to measure the temperature inside the cell compartment. All absorption bands were scanned manually to obtain the maximum absorbance as a slight shift to longer wavelength was observed with increasing temperature. For a 50°C temperature rise this shift amounted to about 0.002 μ . Hexachlorobutadiene was used as the solvent because of its low vapor pressure.

By taking the data rapidly after the previously heated temperature compartment was put into place, the temperature dependence was shown not to result from heating of the instrument. It was verified that the decrease in intensity with increase in temperature was not due to a chemical change caused by heating, as the

TABLE I. Change in absorptivity with temperature.

Compound	Wavelength (μ)	α (liters/mole mm)	T_0 (°C)	ΔT (°C)	$-\Delta\alpha$ (%)
OH stretching					
2,6-di-tert-butyl-4-methylphenol	2.75	16.0	25	46	9
2,4-di-tert-butylphenol	2.78	15.5	24	47	11
2-tert-butyl-4-methylphenol	2.78	14.3	25	46	12
phenol	2.77	16.6	26	43	10
n-pentanol	2.75	5.70	24	45	15
n-heptanol	2.75	5.53	25	46	10
4-heptanol	2.76	4.07	26	45	12
n-decanol	2.75	5.77	26	43	8
n-dodecanol	2.75	5.63	26	45	10
CH stretching					
2,6-di-tert-butyl-4-methylphenol	3.38	31.0	23	49	2
n-decane	3.38	30.2	23	48	5
n-heptanol	3.38	18.9	26	46	4

absorbances returned to the original values on cooling the samples. A small temperature-dependent contribution from the solvent was removed by correcting the absorbance of the sample at each temperature for the absorbance of the cell filled with solvent at that temperature.

The absorbance measurements on the unassociated OH stretching band were all run at solute concentrations of the order of 3×10^{-3} M/l or less which ensures that hydrogen bonding is negligible.³

Figure 1 is a plot of absorbance vs temperature for the unassociated OH bands of three phenols. Part of the decrease in absorbance is due to a decrease in concentration resulting from expansion of the solvent. This amounts to 4% over the range 25° to 71°C. It is interesting to note that the absorbance decreases monotonically with temperature increase over the range studied.

Table I lists absorptivities as measured for the unassociated OH bands of several phenols and alcohols and for the CH stretching bands of several compounds at two widely separated temperatures. The absorptivity values have been corrected at each temperature for the absorbance of the solvent at that temperature and for the change in concentration due to expansion of the solvent. The fact that the change for the OH bands is greater than for the CH bands tends to indicate that the phenomenon is not simply related to a change in dielectric constant or volume.

We do not have an explanation for this temperature dependence of the infrared absorption bands which can be subjected to experimental test. We believe, however, that it most probably is the result of the decrease of the force field on a molecule due to its neighbors.⁴ As the temperature rises the intensity of the force field will decrease owing to the greater average distance between molecules. Furthermore, the rate of decrease will be quite pronounced owing to the fact that the interaction field varies inversely with a large power of the intermolecular distance.

¹ E. J. Slowinski and G. C. Claver, J. Opt. Soc. Am. 45, 396 (1955).

² M. M. Davies and G. B. M. Sutherland, J. Chem. Phys. 6, 767 (1938).

³ N. D. Coggeshall and E. L. Saier, J. Am. Chem. Soc. 73, 5414 (1951).

⁴ This explanation was suggested to us by Professor Bryce Crawford of the University of Minnesota.

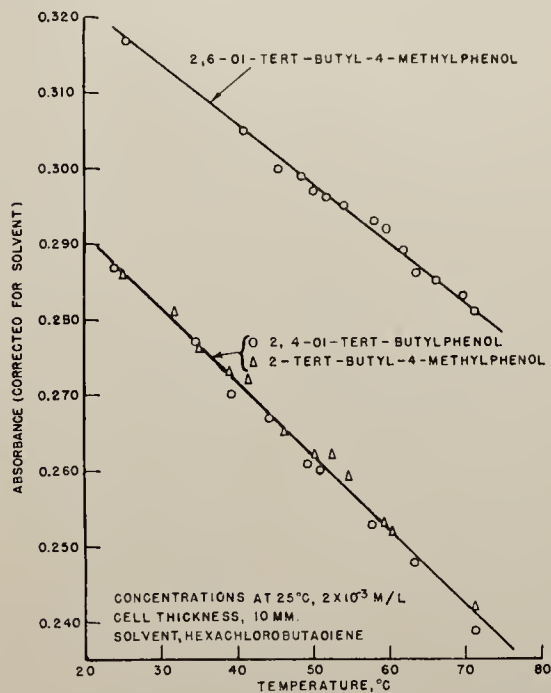


FIG. 1. Temperature dependence of the OH band of three phenols.

Gas Partition Analysis of Light Ends in Gasolines

D. H. LICHTENFELS, S. A. FLECK, F. H. BUROW, AND N. D. COGGESHALL
Gulf Research & Development Co., Pittsburgh, Pa.

Reprinted from
ANALYTICAL CHEMISTRY
Vol. 28, Page 1376, September 1956

Reprinted from **ANALYTICAL CHEMISTRY**, Vol. 28, Page 1376, September 1956
Copyright 1956 by the American Chemical Society and reprinted by permission of the copyright owner

Gas Partition Analysis of Light Ends in Gasolines

D. H. LICHTENFELS, S. A. FLECK, F. H. BUROW, and N. D. COGGESHALL

Gulf Research & Development Co., Pittsburgh, Pa.

The technique of gas-liquid partition chromatography is rapidly establishing itself as a fast and accurate method for analyzing gases and volatile liquids. A modification was developed to provide rapid separation and identification of the light components in gasolines and similar products. The modified apparatus consists of two chromatographic columns in series. The first column acts as a stripping column to separate the light fraction and the second provides a more complete analysis of this fraction. The heavier components retained in the stripping column are removed or prevented from interfering with the light components in subsequent runs by backflushing with gas during the regular chromatographic separation of the light fraction.

ONE of the most important analytical problems in the petroleum industry is the determination of the light components in gasolines and similar samples. A frequently used technique is a combination of low temperature distillation to obtain a C_6 and lighter fraction plus an additional mass or infrared spectrometer analysis of this fraction. These procedures require considerable operator and instrument time and are subject to errors and delays in obtaining the desired analytical data. The solution to this problem was the development and application of a modified gas-liquid partition chromatographic apparatus.

The modified apparatus consists of two chromatographic columns in series. The first is a short column used for stripping the light fraction from the heavier components. The second column then provides a more complete analysis of the lighter

fraction. The use of the stripping column prevents the heavy components of the gasoline from entering the second column, from which they would be very slow to emerge. The results obtained by this technique in less than an hour per sample are comparable to those from the former method of distillation plus mass spectrometer analysis, which required 2 to 3 hours per sample.

The technique of gas-liquid partition chromatography was first suggested by Martin and Synge in 1941 (3). This suggestion was neglected until 1951, when James and Martin developed the technique for the analysis of gases and volatile liquids (1). This technique has been pursued in Europe for the past few years, but only recently have similar works been published in the United States (2).

The method involves separation of components with a narrow column packed with an inert granular support which has been coated with a high boiling organic liquid. When a small amount of a mixture to be analyzed is injected into the end of this column, each component will partially go into solution in the high boiling organic coating and partially exist as a gas phase in the pore spaces. The column is then eluted with an inert carrier gas, which causes the components to move forward with individual velocities less than that of the carrier gas. The velocity with which a component moves is dependent on its partition coefficient. As the partition coefficient varies for different components, a separation into zones results within the column. The different components are detected with a thermal conductivity cell as they emerge from the column.

For this problem of analyzing gasolines, the technique of gas-liquid partition chromatography was first applied for the analysis of the C_5 and lighter fraction as obtained by low temperature distillation of the original sample. The application of this technique provided a rapid and frequently more complete analysis of this fraction than could be obtained by other techniques. However, the man-hours per sample were still excessive, because of the time required for the low temperature distillation.

An attempt was made to analyze gasoline samples by injecting them into a single chromatographic column. This provided a determination of the light components but required excessive time to elute the heavier components from the column before another sample could be injected. The modified chromatographic apparatus eliminated these difficulties.

APPARATUS

A schematic diagram of the modified apparatus is shown in Figure 1.

Carrier Gas Accessories. Accessories include a high pressure tank of helium, coarse and fine pressure regulators, a surge tank, a rotameter, and a wet-test meter.

Detector. The detector is a double-pass thermal conductivity cell, connected electrically to form a Wheatstone bridge. The output of the bridge current is connected directly to a modified Brown recorder having a 0- to 5-mv. range.

Chromatographic Columns. The chromatographic columns are constructed from copper tubing $1/4$ inch in outside diameter and approximately $3/16$ inch in inside diameter. The granular support used in this work consisted of a crushed insulating firebrick, Sil-O-Cel C-22 (Johns-Manville Co., Pittsburgh, Pa.), that was screened to a 40-80 mesh and coated with approximately 30% by weight of a high boiling organic liquid. Column I is the short stripping column and column III provides a more complete

resolution of the lighter fraction. Column I is equipped with a self-sealing serum bottle cap through which the sample to be analyzed is injected.

Air Bath. The chromatographic columns, detector, preheater, etc., are all enclosed in a constant-temperature air bath. This bath is equipped with a mercury-type thermoregulator, circulating fan, and heater for maintaining these components at the desired operating temperature.

Sampling Syringe. The sample to be analyzed is injected into the chromatographic column by means of a modified microsyringe (Figure 2), which is made by sealing a No. 27 hypodermic needle to a short length of fine-bore glass tubing containing an enlarge-

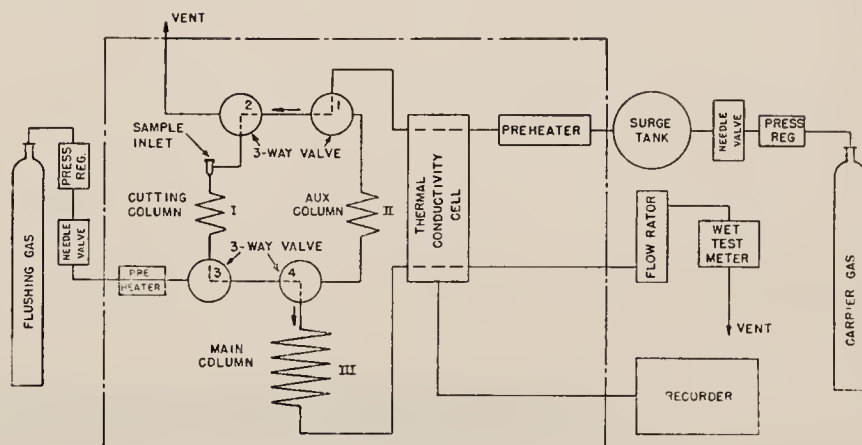


Figure 1. Schematic diagram of apparatus

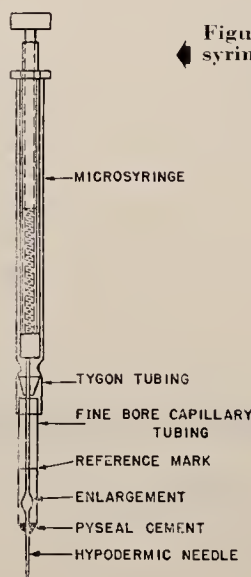


Figure 2. Micro-syringe for charging samples

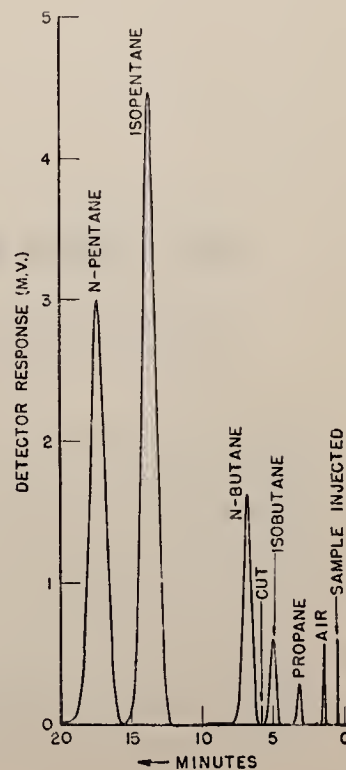


Figure 3. Chromatogram of light components in unstabilized gasoline sample

ment as shown. This pipet arrangement is attached to a micro-syringe equipped with a micrometer screw and metal plunger. A sample is drawn into this special pipet by turning the micrometer screw until it is filled to the reference mark. The liquid is injected into the column by pressing the plunger.

PROCEDURE

In operation, a constant flow of carrier gas is passed through the system in the direction indicated by the arrows in Figure 1.

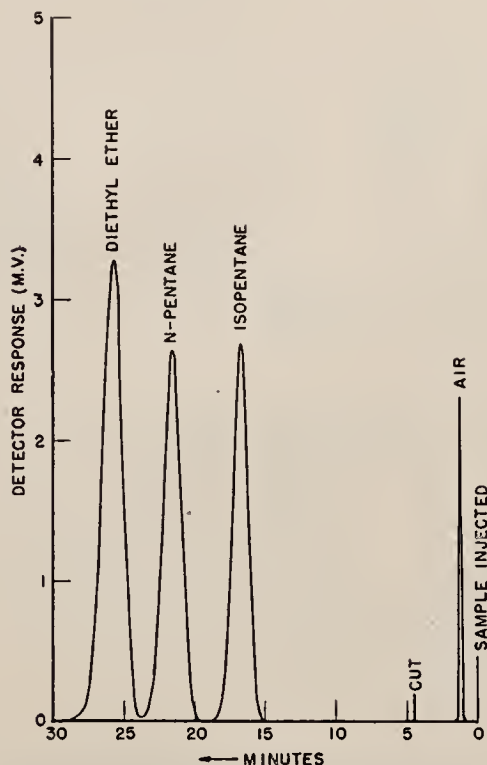


Figure 4. Chromatogram of light components in gasoline using diethyl ether as internal standard

The carrier gas is drawn from a cylinder through the reducing valves, surge tank, and preheat coil before passing through the reference side of the thermal conductivity cell. The carrier gas passes through columns I and III in series, then the sample side of the thermal conductivity cell, and finally the rotameter and wet-test meter, before it is vented. The flow of carrier gas is indicated by the rotameter and is accurately measured by the wet-test meter. After equilibrium has been established with carrier gas passing through the system, the electrical bridge of the thermal conductivity cell is balanced and the recorder pen base line is established.

Before the sample is charged to the apparatus, the three-way valve, 2, is turned to shut off the flow of carrier gas momentarily. This also vents the column to atmospheric pressure to prevent loss of sample during charging. By means of the modified micro-syringe, a calibrated volume of the gasoline sample is injected into column I through the rubber serum bottle cap. Valve 2 is then opened to allow carrier gas to flow through the system in the direction indicated by the arrows, until the faster moving components are eluted from column I. Valves 1 and 4 are turned to bypass column I and allow carrier gas to flow through columns II and III. The flow continues in this direction until all of the light fraction that entered column III is eluted.

In order to maintain the same carrier gas flow rate through both paths, it was necessary to install column II, which has the same pressure drop as column I. The installation of a surge tank in the carrier gas line also provided a means of smoothing out the pressure disturbances resulting from turning the valves. At the same time the light fraction is eluted from column III, valves 2 and 3 are turned to allow carrier gas from another cylinder to backflush through column I. In this manner, the heavier components that are retained in the short column I are eluted, while the regular chromatographic separation of the light fraction is continuing in column III. As soon as the light fraction is eluted from column III, the flow of carrier gas is again passed in the direction indicated by the arrows. The apparatus is then ready to be charged with another sample.

Because some samples may contain components that are not eluted from the stripping column by the backflushing procedure, it may be necessary to change this column occasionally to prevent variations in retention times. However, more than 100 gasoline samples having distillation end points of approximately 400° F. have been analyzed by this technique in the same stripping column with no apparent change in retention times.

The choice of column lengths, liquid coatings, and operating conditions will depend on the particular analytical problem.

As an illustration, a unit was operated at a temperature of 45° C. with a carrier gas flow rate of 30 ml. per minute using di-2-ethylhexyl sebacate (Octoil S, Consolidated Vacuum Corp., Rochester, N. Y.) as the liquid phase in both columns. Column I was approximately 1 foot long and column III was 7 feet long. It was determined by calibration that *n*-pentane and lighter components were eluted from column I in 4.5 minutes under these conditions. Thus, the flow of carrier gas was passed in the direction indicated by the arrows in Figure 1 for at least 4.5 minutes. Then valves 1 and 4 were turned and carrier gas was passed through columns II and III for approximately 20 more minutes to elute the *n*-pentane and lighter components. For this type of sample, the entire run is complete in less than 30 minutes' instrument time and approximately 10 to 15 minutes' operator time.

RESULTS

A chromatogram of the C_6 and lighter components for an unstabilized gasoline is shown

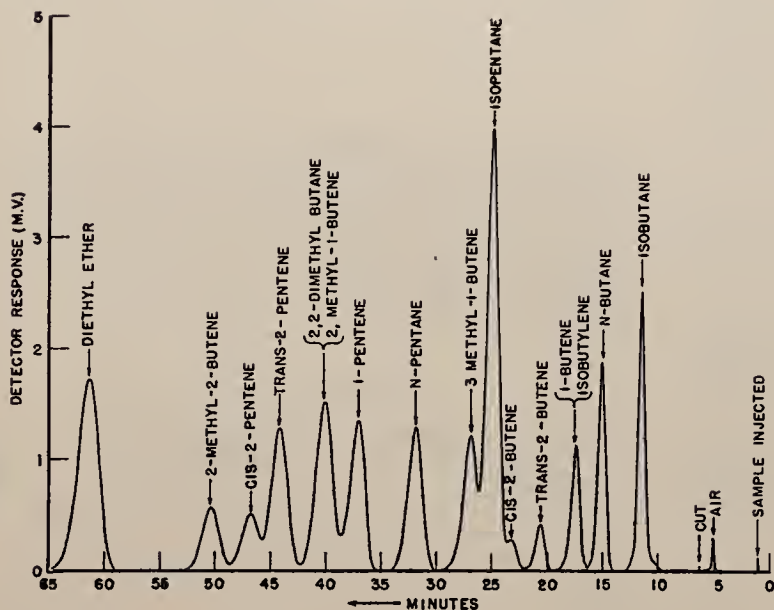
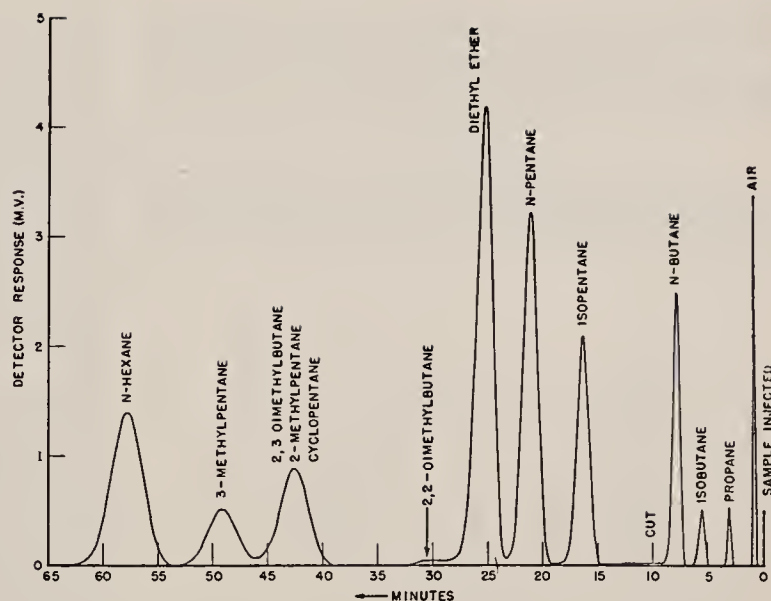


Figure 5. Chromatogram of light components in unstabilized cracked gasoline sample

Figure 6. Chromatogram of *n*-hexane and lighter components in unstabilized gasoline sample



in Figure 3. This curve shows a continuous plot of the signal from the thermal conductivity cell sampling the gases leaving the column *vs.* time of elution. From previous calibration data for retention times, it is evident that the sample contained propane, isobutane, *n*-butane, isopentane, and *n*-pentane. The heavier components are retained in the stripping column. The concentration of each eluted component is calculated from the area under the peaks. The peak areas are usually determined with a planimeter or by multiplying peak heights by the half-band widths. Recently the application of a continuous integrator is providing a fast and accurate method for determining peak areas. In order to relate these calculations to the total sample, the practice of adding a known amount of internal standard is used. The line marked "cut" indicates the time when the flow of carrier gas was discontinued through the stripping column.

One of the first applications of this technique was the determination of isopentane and *n*-pentane in a typical gasoline sample. The chromatogram of one of these samples containing a known amount of diethyl ether as an internal standard is shown in Figure 4. Using the weight and peak area of the internal standard, the percentages of the other eluted components can be calculated from their peak areas. For this calculation, known weights of sample and ether are first blended. From the weight of ether added, the number of moles can be calculated. The moles of ether are then related to the moles of the different hydrocarbons by use of the peak areas. From the moles of each hydrocarbon, the weight of each hydrocarbon in the original sample is calculated. This weight divided by the weight of the original sample yields the results in weight per cent.

The accuracy of this method was tested using synthetic samples similar in composition to the regular gasoline samples. In order to prepare these synthetic samples, several regular gasoline samples were distilled to remove the *n*-pentane and lighter components. Using the residues from these distillations, several blends containing different amounts of isopentane and *n*-pentane plus the internal standard were prepared and analyzed. The results obtained by this method were comparable to those obtained by distillation techniques.

Table I shows the comparative results obtained on three unstabilized straight-run gasoline samples analyzed by this technique compared to the former method of low temperature distillation plus mass spectrometer analysis of the C_5 and lighter fraction.

Figure 5 shows the application of this technique for the determination of the C_5 and lighter components in a cracked gasoline sample. This sample was analyzed in an apparatus containing tri-*m*-tolyl phosphate saturated with silver nitrate as the liquid coating in the second column.

Although this technique was developed mainly for the determination of C_5 and lighter components, the same technique can be used for hydrocarbons of higher molecular weight. This is illustrated in Figure 6, which shows the determination of the *n*-hexane and lighter components in a gasoline sample.

The advantage of speed makes this technique very useful for control purposes. By maintaining a constant temperature, flow

Table I. Comparison of Results by Different Methods

Component	(Weight per cent)					
	Sample 1		Sample 2		Sample 3	
	A ^a	B ^a	A ^a	B ^a	A ^a	B ^a
Propane	0.22	0.21	0.14	0.16	0.05	0.06
Isobutane	0.43	0.35	0.72	0.59	0.07	0.10
<i>n</i> -Butane	1.09	1.27	1.48	1.74	0.29	0.40
Isopentane	2.22	2.06	5.37	5.60	4.19	4.04
<i>n</i> -Pentane	1.93	2.06	4.80	4.96	3.50	3.59
Hexane + (by diff.)	94.11	94.05	87.49	86.95	91.90	91.81

^a A. Analysis by distillation plus mass spectrometry.
B. Analysis by gas-liquid partition method.

Table II. Results for a Synthetic Sample without Use of an Internal Standard

Component	% by Blend	% Determined			
		(Weight per cent)			
		Run 1	Run 2	Run 3	Run 4
Isopentane	4.25	4.24	4.06	4.21	4.21
<i>n</i> -Pentane	4.64	4.69	4.77	4.74	4.70
Hexane +	91.11	91.07 ^a	91.17 ^a	91.05 ^a	91.09 ^a

^a Determined by difference.

rate, and sample size, it is possible to analyze routine samples for control purposes without the addition of an internal standard to each sample. For these samples, the amount of each component is determined by a comparison of peak areas for the unknown with the areas obtained on previously analyzed synthetic samples of known composition.

Table II shows the results of four separate determinations on a synthetic sample analyzed over a period of several days.

LITERATURE CITED

- (1) James, A. T., Martin, A. J. P., *Biochem. J.* 50, 679 (1952).
- (2) Lichtenfels, D. H., Fleck, S. A., Burow, F. H., *ANAL. CHEM.* 27, 1510 (1955).
- (3) Martin, A. J. P., Synge, R. L. M., *Biochem. J.* 35, 1358 (1941).

RECEIVED for review March 28, 1956. Accepted May 21, 1956. Pittsburgh Conference on Analytical Chemistry and Applied Spectroscopy, Pittsburgh, Pa., 1956.

1

2,767,320

METHOD OF GEOCHEMICAL PROSPECTING

Norman D. Coggeshall, Verona, and William E. Hanson, Pittsburgh, Pa., assignors to Gulf Research & Development Company, Pittsburgh, Pa., a corporation of Delaware

No Drawing. Application November 24, 1952,
Serial No. 322,362

15 Claims. (Cl. 250—43.5)

This invention relates to a method of geochemical prospecting for hidden hydrocarbon deposits by analyzing subsurface brines or other waters for the presence of dissolved hydrocarbon components, in particular aromatic hydrocarbons and specifically benzene.

Heretofore, one method of geochemical prospecting has been conducted by making systematic collection of soil samples over an area to be mapped. The soil samples have been tested for a variety of components indicative of the presence of hydrocarbon deposits. Methods of extracting the components from the soil samples have included the use of organic solvents or simply the application of heat to remove hydrocarbon gases trapped in the soil samples. Among the components for which these samples have been tested are the lighter paraffinic hydrocarbons which are presumed to have migrated from deep subsurface hydrocarbon deposits. One of the difficulties encountered with this method of prospecting is that generally there is a wide variation of the sorptive and retentive capacities of the soil samples taken over a plurality of locations. This is due primarily to the differences in chemical and physical properties of the soil itself. A pattern of such concentration values may thus not give a true indication of the proximity of hydrocarbon deposits. Another difficulty encountered is that some of the lower molecular weight paraffinic hydrocarbons may arise from the recent decay of organic or vegetable matter instead of from petroleum deposits.

In other known methods of geochemical prospecting, techniques have been used for detecting extremely small concentrations of crude hydrocarbons dispersed in drilling fluids. These methods have involved subjecting the fluid or cuttings samples to ultraviolet light to produce fluorescence by means of which it is possible to detect extremely small concentrations of crude oil which would ordinarily be invisible to the unaided eye. One of the problems which has been encountered in this type of prospecting for crude oil deposits is that positive indications are obtained when the drilling fluid is contaminated with refined petroleum products, such as pipe-thread grease or lubricating oils.

The present invention is directed to overcome the problems encountered in the type of geochemical prospecting which involves the sampling of soils or formation waters for the detection of paraffinic hydrocarbons as components indicative of the presence of hydrocarbon deposits and to overcome the difficulties involved in detecting hydrocarbon deposits by analyzing formation water samples obtained by drill-stem tests or bottom-hole samplers. This invention therefore has as an object the detection of dissolved aromatic hydrocarbons in formation waters as components related to the proximity of hydrocarbon deposits. Another object of this invention is the detection of dissolved aromatic hydrocarbons in formation waters by radiation from the electromagnetic spectrum. A further object of this invention is the detection of benzene dissolved in formation brine waters. Further objects of this invention will become apparent from the subsequent description.

2

The objects of the present invention are achieved by a method of geochemical prospecting wherein information concerning the proximity of hydrocarbon deposits or source beds is derived by collecting aqueous subterranean samples from prospect areas and wildcat wells and extracting the hydrocarbon components dissolved in these samples with a suitable extracting agent and determining the concentration of these hydrocarbons by the use of electromagnetic radiation. The presence of these dissolved hydrocarbons is an indication that these subterranean waters have been in contact with or are near a petroliferous deposit.

Aromatic hydrocarbons are universal components of crude petroleum and furthermore this class of hydrocarbons is more soluble in water or brine than any other type of hydrocarbon which occurs in crude petroleum. Benzene and a considerable number of benzene homologues have been recognized in crude petroleum. The best established are benzene, toluene, the three xylenes, ethylbenzene, naphthalene and the two methyl naphthalenes. The actual percentages of these components depend on the geographical area where the petroleum is found, but they are always present. The aqueous solubility of these aromatic hydrocarbons found in petroleum decreases rapidly with an increase in molecular weight. For this reason, the lower molecular weight members of this series, such as benzene, are favored as criteria for the proximity of petroleum deposits. This is based on the observation that brines or other waters when brought into contact with petroleum will preferentially dissolve out a portion of the aromatics and particularly benzene and retain them in solution, although the waters may have been later physically separated from the crude petroleum.

A number of investigations have been carried out in an attempt to develop a simple and positive method of distinguishing between the hydrocarbons from pipe-thread grease or other lubricants that may have contaminated sample waters from drill-stem tests or bottom-hole samplers and hydrocarbon from crude oil as they occur in the brines. The basis of this distinction lies in the fact that certain hydrocarbons such as benzene are more soluble in brine than any of the other constituents of crude oil. Furthermore, since benzene has a low boiling point it is virtually absent from most refined products used around a drilling rig with the exception of light fuel oils and gasoline. It is therefore possible that these light fuel oils, gasolines or even natural gas which are commonly used as fuels for powering drilling equipment, may contain light aromatics such as benzene. Precautions should therefore be taken that contaminants from these sources are not present or if they are present they must be capable of removal. If a well or drill hole is contaminated with benzene from a source other than sub-surface waters, the well can be flowed or pumped for a time sufficient to remove all contaminated brine, so that all the benzene from the fresh brine would arise from the contact of the brine with underground crude hydrocarbon deposit. However, the sources of contamination mentioned above are not likely to occur unless careless procedures are used. In actual practice on a series of tests on several wells we have found that the wells gave no evidence of contamination from such sources and we believe that such special precautions or preliminary swabbing prior to obtaining test samples are unnecessary.

By measuring the concentration of dissolved aromatic hydrocarbons, specifically that of dissolved benzene, in fluid samples obtained for instance from wildcat wells, even though considered to be "dry" holes, it is possible to determine whether a particular formation is completely barren or whether nearby portions may be petroliferous. Such information obtained by detecting aromatic hydrocarbons in the subsurface waters or brines from wildcat

wells may guide further drilling activity in the area. Benzene in varying concentrations has been found in tests on "dry" holes and increasing benzene concentration is interpreted as indicating the direction toward petroleum deposits.

In practicing our invention any suitable method of extracting aromatic hydrocarbons and particularly benzene as the component for analysis may be employed. Solvent extraction of the brine or other waters with subsequent distillation to further concentrate and remove interfering material from the aromatic hydrocarbons, followed by infrared or ultraviolet spectroscopic examination of the extract, permits the detection of aromatic components in the brine in concentrations of less than one part per million.

A method based on our procedure to be discussed below and using a strong ultraviolet absorption band of benzene has given positive results and there have been no indications of benzene whatever in synthetic brines given prolonged exposure to pipe-thread grease and lubricating oil.

The samples for analysis may comprise formation waters obtained by swabbing, drill-stem test fluids obtained from a drill-stem test, or samples or underground waters obtained by an convenient means. The preferred method of analyzing the water samples for benzene content will now be described.

If the sample is a swab water, it may be extracted directly after filtering. If it is a mixture of water and mud such as from a drill-stem test, the water for testing may be the supernatant liquid after settling, or satisfactory water may be obtained from the mixture by centrifuging, filtration, or a combination of the two.

A preferred procedure for this invention is to extract a definite volume of the sample water with aromatic-free iso-octane (2,2,4-trimethylpentane). In the extraction a two-liter sample is conveniently used. The water is placed in a glass container with 25 ml. of iso-octane (2,2,4-trimethylpentane) of spectroscopic grade. This is then vigorously agitated in a mechanical shaker for 30 minutes. After the two phases separate, the iso-octane may in some cases be recovered directly by means of a pipette. In other cases emulsions of varying strength will be obtained. These may be broken chemically or by means of a centrifuge. The iso-octane will contain a major portion of the total amount of benzene originally present in the sample water.

In the preferred form of our invention in which benzene is to be detected, we prefer to concentrate the benzene from the extract by distillation. Subsequently a selected fraction of the distillation is quantitatively analyzed for benzene by ultraviolet-absorption spectroscopy. Chromatographic fractionation, however, may also be employed for concentration of the benzene from the extract, and should a suitable colorimetric method for determination of benzene become available such method may be employed.

The iso-octane recovered from the extraction is measured and charged to a still with a still pot volume of approximately fifty ml. and with an efficiency equivalent to about five theoretical plates. The charge is heated slowly until condensation is observed at the take-off point. The still is then allowed to operate at total reflux for one-half hour. At this point the sample is continuously removed until 3 ml. of distillate has accrued. This 3 ml. will contain most of the benzene in the original charge.

The distillate of the above step is then examined in an ultraviolet spectrophotometer with radiation whose wave length is between 220 and 280 millimicrons. The resulting data are plotted to yield an ultraviolet-absorption spectrum. If benzene is present, it is identified by its characteristic pattern of absorption bands. When benzene is found to be present, its concentration in the distillate is calculated from the intensity of one of the characteristic benzene absorption bands.

The amount of benzene in the charge to the still is

calculated from the observed benzene content in the distillate and the ratio of distillate volume to still-charge volume. The amount of benzene in the original water sample is then calculated from the benzene concentration in the charge to the still, the ratio of the volume of iso-octane used for extraction to the volume of the original water sample, and a correction factor discussed below. If less than 25 ml. of iso-octane are recovered from the extraction, it is assumed that the benzene is uniformly distributed between the recovered and non-recovered octane. As the extraction and distillation steps do not yield complete recovery it is necessary to evaluate a correction factor. This is done by introducing known concentrations of benzene into water. These samples are then extracted and processed as above. The results may thus be used to provide the necessary correction factor.

The distillation step in our procedure is important in effecting the removal of material which would interfere with the spectroscopic examination of the benzene extract. In the extraction step described above the benzene is transferred from the water phase to the hydrocarbon phase and as a consequence is concentrated in a smaller volume of liquid. The distillation step serves a twofold purpose and for this reason it is believed important. The first purpose is to remove any material that may interfere with the spectroscopic examination. The second purpose of the distillation step is to further concentrate the benzene in the extract to a smaller volume. It is essential, therefore, that the charge be heated slowly and that it should be refluxed until it is certain that most of the benzene can be removed free from the materials that would interfere with its spectroscopic examination. In our preferred procedure referred to above the refluxing time is one-half hour. At that point it has been found that the removal of approximately 3 ml. of the material serves to remove most of the benzene from the extract and the benzene is essentially free of spectrally-interfering material.

We have found that the above-described distillation step permits benzene to be detected when it occurs in brines in amounts of less than one part per million. However, we do not wish to be restricted to such a procedure in view of the fact that other methods may be practiced. Chromatographic fractionation for example affords the basis for a very effective method of concentrating and separating mixtures, and this method may be used in the detection and determination of benzene and other aromatic hydrocarbons occurring in subsurface waters which have been in contact with buried hydrocarbon deposits.

The numerical values of volumes of water and solvent, of extraction time, of still volume, distillation time, theoretical plates, and volume of distillate used are not critical and may be varied. The only requirement is that once a set of conditions are established that it be adhered to for all calibration and sample runs.

One of the advantages of our invention in using formation waters as the sampling media is that they are more easily handled and sampled than soil samples or soil gases. Another advantage is that there is no evidence in the literature that benzene is a product of recent vegetable or animal decomposition and further that benzene is virtually absent from contaminants arising from lubricating oils and greases employed in drilling machinery.

Having thus described our invention in terms of certain specific embodiments, we intend to cover all changes and modifications of the example of the invention herein chosen for purposes of the disclosure, which do not constitute departure from the spirit and scope of the invention.

What we claim as our invention is:

1. In the art of geochemical prospecting for buried hydrocarbon deposits which comprises collecting aqueous subterranean samples in a prospect area and analyzing these for hydrocarbon components indicative of the presence of hydrocarbon deposits, the improvement which

comprises extracting the aromatic components dissolved in said aqueous samples, and testing the extract for the presence of aromatic hydrocarbons as a measure of the relative amounts of said aromatic hydrocarbons originally present in said aqueous samples, and correlating these results as an indication of the proximity of buried hydrocarbon deposits.

2. In the art of geochemical prospecting for petroliferous deposits which comprises collecting samples of subsurface formation waters in a prospect area and analyzing these for hydrocarbon components indicative of the presence of petroliferous deposits, the improvement which comprises extracting the dissolved hydrocarbon components in said samples and passing electromagnetic radiation through the extract containing the dissolved hydrocarbons for the purpose of detecting the presence of aromatic hydrocarbons identified by their characteristic pattern of absorption bands, and determining their concentration in the original water sample as an indication of the nearness of petroliferous deposits.

3. The method of exploration for petroleum deposits which comprises a systematic collection of brine water samples from a prospect area, extracting the dissolved hydrocarbon content and passing ultraviolet radiation through the extract containing the dissolved hydrocarbons for the purpose of detecting the presence of aromatic hydrocarbons identified by their characteristic pattern of absorption bands, and determining their concentration in the original brine samples as an indication of the proximity of petroleum deposits.

4. In the art of geochemical prospecting for buried hydrocarbon deposits which comprises collecting aqueous subterranean samples in a prospect area and analyzing these for hydrocarbon components indicative of the presence of hydrocarbon deposits, the improvement which comprises extracting the dissolved aromatic components in said samples, and determining the concentration of benzene in the original samples as a component indicative of the presence of hydrocarbon deposits.

5. In the art of geochemical prospecting for petroliferous deposits which comprises a systematic collection of samples of subsurface formation waters in a prospect area and analyzing these for hydrocarbon components indicative of the presence of petroliferous deposits, the improvement which comprises extracting the dissolved hydrocarbon components in said samples, passing electromagnetic radiation through the extract containing the dissolved hydrocarbons for the purpose of detecting the presence of benzene as identified by its characteristic pattern of absorption bands as a component indicative of the proximity of petroliferous deposits.

6. The method of exploration for petroleum deposits which comprises a systematic collection of brine water samples over a prospect area, extracting the dissolved aromatic content therein and passing ultraviolet radiation through the extract containing the dissolved aromatic hydrocarbons in solution for the purpose of detecting the presence of benzene identified by its characteristic absorption bands, and determining the concentration of benzene in the original brine sample as an indication of the proximity of petroleum deposits.

7. In the art of geochemical prospecting for buried hydrocarbon deposits which comprises collecting aqueous subterranean samples in a prospect area and analyzing these for hydrocarbon components indicative of the presence of hydrocarbon deposits, the improvement which comprises extracting the dissolved aromatic components from said aqueous samples, passing ultraviolet radiation through the extract containing the aromatic hydrocarbons in solution for the purpose of detecting the presence of benzene identified by its characteristic absorption bands and for determining its concentration in the original samples, and correlating these results as an indication of the proximity of buried hydrocarbon deposits.

8. In the art of geochemical prospecting for petroliferous deposits which comprises collecting samples of formation waters in a prospect area and analyzing these for hydrocarbon components indicative of the presence of petroliferous deposits, the improvement which comprises extracting the dissolved benzene in said samples with a suitable non-aromatic solvent of spectroscopic grade, concentrating the benzene contained in said solvent and passing ultraviolet radiation through the solvent containing the benzene to determine the concentration of benzene in the original samples as an indication of the nearness of petroliferous deposits.

9. In the art of geochemical prospecting for petroliferous deposits which comprises collecting samples of formation water in a prospect area and analyzing these for hydrocarbon components indicative of the presence of petroliferous deposits, the improvement which comprises extracting the dissolved benzene in said samples with 2,2,4-trimethylpentane, concentrating the benzene contained in said solvent and passing ultraviolet radiation of wave length in the region 220 to 280 millimicrons through the solvent containing the benzene to determine the concentration of benzene in the original samples as an indication of the nearness of petroliferous deposits.

10. The method of exploration for petroleum deposits which comprises collecting samples of brine waters from wells, extracting the benzene content dissolved therein, passing ultraviolet radiation of wave length in the region 220 to 280 millimicrons through the extract containing the benzene and determining the resulting absorption spectrum, the concentration of benzene as a component indicative of the presence of petroleum deposits.

11. The method of detecting subsurface petroleum deposits by analyzing subsurface brines which comprises extracting the aromatic components dissolved in the brine samples, passing ultraviolet radiation through the extract containing the aromatics, and determining the concentration of the aromatic hydrocarbon components in the samples as an indication of the proximity of petroleum deposits.

12. The method of detecting subsurface petroleum deposits by analyzing subsurface brines which comprises extracting the benzene dissolved in the brine samples, passing ultraviolet radiation through the extract containing the benzene, determining from the resulting absorption spectrum the concentration of benzene as an indication of the proximity of petroleum deposits.

13. The method of detecting subsurface petroleum deposits by analyzing subsurface brines which comprises extracting the benzene dissolved in the brine samples with 2,2,4-trimethylpentane, passing ultraviolet radiation of wave length in the region 220 to 280 millimicrons through the extract containing the benzene and determining through its absorption spectrum the concentration of benzene as an indication of the proximity of petroleum deposits.

14. The method of detecting subsurface petroleum deposits by analyzing subsurface brines which comprises extracting the benzene dissolved in the brine samples with 2,2,4-trimethylpentane, passing ultraviolet radiation of wave length in the region 220 to 280 millimicrons through the extract containing the benzene, measuring the absorption spectrum of the extract for said radiation whereby the concentration of benzene in the brine sample may be determined, and correlating the benzene concentration with the source location of the brine sample.

15. The method of exploration for petroleum deposits which comprises a systematic collection of subsurface water samples over a prospect area, extracting the benzene dissolved in the water sample with 2,2,4-trimethylpentane, distilling the hydrocarbon extract to further concentrate benzene and to remove spectrally-interfering materials, and passing ultraviolet radiation of wave length in the region of 220 to 280 millimicrons through the extract

2,767,320

7

containing the benzene, and determining through its absorption spectrum the concentration of benzene as an indication of the proximity of petroleum deposits.

2,406,611
2,500,213

References Cited in the file of this patent

5

114,477

UNITED STATES PATENTS

2,403,631 Brown ----- July 9, 1946

8

Kennedy ----- Aug. 27, 1946
Stevens ----- Mar. 14, 1950

FOREIGN PATENTS

Australia ----- Jan. 15, 1942

Reprinted from

ANALYTICAL CHEMISTRY

Application of Total Ionization Principles to Mass Spectrometric Analysis

G. F. CRABLE and N. D. COGGESHALL

Gulf Research & Development Co., Pittsburgh, Pa.

Volume 30, Number 3

Pages 310-313, March 1958

Copyright 1958 by the American Chemical Society and reprinted by permission of the copyright owner

Application of Total Ionization Principles to Mass Spectrometric Analysis

G. F. CRABLE and N. D. COGGESHALL

Gulf Research & Development Co., Pittsburgh, Pa.

► An expression relating total ionization per mole of hydrocarbons in a homologous series to molecular weight is shown to be a consequence of the principle of additivity of atomic cross sections for ionization. Total ionization data for homologous series will form a family of parallel straight lines when plotted as a function of molecular weight. As a result of the relative invariance of the densities of hydrocarbons, particularly in the high molecular weight range, the total ionization per unit liquid volume is essentially independent of molecular weight. Through the use of total ionization curves and published spectral patterns, sensitivities applicable to any instrument can be calculated.

THE investigation of relationships between molecular structures and the total of all ions produced per unit quantity of material in a mass spectrometer has been a subject of interest to mass spectrometrists for some time. The earliest work was reported in a series of papers by Mohler and coworkers (1, 4-6) at the National Bureau of Standards. They showed that (1) paraffin isomers had essentially the same total ionization (total divisions per unit of pressure), (2) total ionization tends to increase with increasing number of carbon atoms within the same series up to C_{10} , and (3) total ionization decreases with decreasing number of hydrogen atoms for an equal number of carbon atoms. The basic problem in their work was obtaining accurate experimental data with respect to pressure measurements, a problem which is still serious today in obtaining data on high molecular weight total ionization.

Clerc, Hood, and O'Neal (3) first applied the principle of total ionization to a mass spectrometric analytical procedure. They overcame the difficulty of obtaining sensitivities for ion summations used in analysis of saturated hydrocarbons of high molecular weight, by basing the summations on the sum of all ion intensities in the C_4 to C_{11} ion fragment region. Solutions of their matrix were in the form of contributions of specific compound types to the total C_4 to C_{11} ion intensity for the sample. Results as liquid volume percentages

were obtained by assuming equal sensitivities per unit volume for the C_4 to C_{11} portion of the spectrum of the hydrocarbon types considered.

Total ionization as applied to mass spectrometry was given a firmer foundation by the work of Otvos and Stevenson (7). They showed that relative total ionization cross sections of atoms are given to a good approximation by the weighted sum of the valence electrons of the atoms, and that relative total ionization cross sections of molecules are the sums of the atomic cross sections of the atoms contained in the molecule. This additivity rule was shown to be valid for ionization by low energy electrons as employed in mass spectrometry. Sums of all ion intensities in the mass spectra of a number of compounds, including hydrocarbons in the C_1 to C_7 range, were found to be directly proportional to calculated relative molecular cross sections for ionization by electrons. Of particular interest is that the additivity of the relative ionization cross sections of hydrocarbons was found to apply without correction for rings or unsaturation in the molecule.

In the present work an analytical expression in terms of molecular weight is given as a more usable form of the work of Otvos and Stevenson. Predictions from this equation as to slope and y intercepts for several hydrocarbon series agree with experimental data. Applications of total ionization principles to a naphtha group-type analysis and to high molecular weight spectra are presented.

RELATION OF TOTAL IONIZATION TO MOLECULAR WEIGHT

The principle of additivity of atomic cross sections can be expressed for hydrocarbons as follows:

$$T_p = k[n_H Q_H^i + n_C Q_C^i] \\ = k[n_H(1.00) + n_C(4.16)] \quad (1)$$

where Q_H^i and Q_C^i are the relative ionization cross sections for hydrogen and carbon, respectively, while n_H and n_C are the number of hydrogen and carbon atoms in the molecule. The relative cross-section values are from the work of Otvos and Stevenson. T_p is the sum of the specific intensities of all ions in

the mass spectrum in divisions per unit of pressure in the inlet system reservoir. The instrumental constant, k , is a function of the particular mass spectrometer and has the dimensions

$$\frac{\text{(unit of pressure)}}{\text{(unit cross section)}}$$

For applications to mass spectrometric analysis of hydrocarbons, it is convenient to have total ionization expressed as a function of molecular weight. As each homologous series of hydrocarbons is equivalent to a basic structure, or nucleus, plus an increasing number of CH_2 groups, Equation 1 can be rewritten for any hydrocarbon series as:

$$T_p = k[Q_B^i + (6.16) \times n_{CH_2}] \quad (2)$$

where Q_B^i is the ionization cross section for the basic structure of the series and n_{CH_2} is the number of added methylene groups. Substituting for n_{CH_2} ,

$$n_{CH_2} = \frac{M - M_B}{14}$$

where M is the molecular weight of any compound in a homologous series and M_B is the molecular weight of the first member of the series, we obtain

$$T_p = kQ_B^i + k(6.16) \times \frac{M - M_B}{14} \\ = k\left(Q_B^i - \frac{6.16}{14} \times M_B\right) + k \times \frac{6.16}{14} M \quad (3)$$

Equation 3 predicts that plots of total ionization as a function of molecular weight for hydrocarbon series should be a family of parallel straight lines. This, of course, is true only if all data are obtained by the same mass spectrometer having a constant over-all sensitivity as measured by the instrumental constant, k . Data from different instruments should be comparable, if suitable correction factors are applied to the sensitivity factor.

From the constant portion of Equation 3, the y intercepts for different homologous series can be calculated. A number of such calculated values with k assigned a value of unity are given in Table I. These results, with the previous consideration of slopes, show

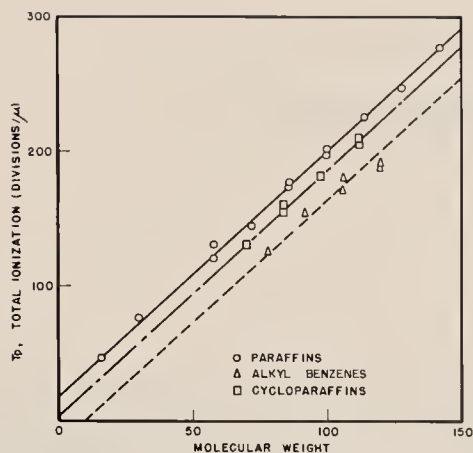


Figure 1. Total ionization data for a number of paraffins, cycloparaffins, and alkyl benzenes as a function of molecular weight

that plots of hydrocarbon total ionization data in terms of partial pressure should be a series of parallel lines separated by factors dependent upon respective hydrogen to carbon atom ratios. Thus, in a plot of T_p for a number of paraffins, cycloparaffins, and alkyl benzenes, the line through the paraffins should be the highest with the cycloparaffin and alkyl benzene lines below it in that order.

In Figure 1 experimental data from a number of paraffins, cycloparaffins, and alkyl benzenes are plotted. These data were obtained by using a modified Consolidated Electrodynamics Corp. Model 21-102 mass spectrometer. As predicted, the straight lines drawn through these data are in the order: paraffins, cycloparaffins, and, lowest, alkyl benzenes. Data obtained for a series of olefins coincide exactly with the cycloparaffin data. In Table I experimental γ intercepts from these plots are shown after normalization of the paraffin intercept to a value of 1.1. The lack of quantitative agreement between the calculated and experimental γ intercepts for the alkyl benzenes cannot be considered significant because of errors in extrapolation of the curves.

TOTAL IONIZATION APPLIED TO NAPHTHA GROUP-TYPE ANALYSIS

The following material shows the application of total ionization to a group-type naphtha analysis. This procedure incorporates the use of ion summations introduced by Brown (2) and the general principles of total ionization as applied to a saturate fraction of high molecular weight by Clerc, Hood, and O'Neal.

This particular analytical scheme was designed to determine paraffins, cycloparaffins, bicyclic paraffins, and alkyl benzenes as groups in mixtures having an upper boiling point of 400° F. The

following characteristic ion sums were used:

$$\text{Paraffins. } \Sigma 43 = 43 + 57 + 71 + 85$$

$$\text{Cycloparaffins. } \Sigma 41 = 41 + 55 + 67 + 83$$

$$\text{Bicyclic paraffins. } \Sigma 67 = 67 + 68 + 81 + 82 + 95 + 96$$

$$\text{Alkyl benzenes. } \Sigma 77 = 77 + 78 + 79 + 91 + 92 + 105 + 106 + \dots 147 + 148$$

The four independent equations required for the determination of these four compound types are:

$$\Sigma 43 = \left(\frac{\Sigma 43}{T}\right)_p \times C_p + \left(\frac{\Sigma 43}{T}\right)_c \times C_c + \left(\frac{\Sigma 43}{T}\right)_b \times C_b + \left(\frac{\Sigma 43}{T}\right)_a \times C_a$$

$$\Sigma 41 = \left(\frac{\Sigma 41}{T}\right)_p \times C_p + \left(\frac{\Sigma 41}{T}\right)_c \times C_c + \left(\frac{\Sigma 41}{T}\right)_b \times C_b + \left(\frac{\Sigma 41}{T}\right)_a \times C_a$$

$$\Sigma 67 = \left(\frac{\Sigma 67}{T}\right)_p \times C_p + \left(\frac{\Sigma 67}{T}\right)_c \times C_c + \left(\frac{\Sigma 67}{T}\right)_b \times C_b + \left(\frac{\Sigma 67}{T}\right)_a \times C_a$$

$$\Sigma 77 = \left(\frac{\Sigma 77}{T}\right)_p \times C_p + \left(\frac{\Sigma 77}{T}\right)_c \times C_c + \left(\frac{\Sigma 77}{T}\right)_b \times C_b + \left(\frac{\Sigma 77}{T}\right)_a \times C_a$$

Subscripts p , c , b , and a refer to paraffins, cycloparaffins, bicycloparraffins, and alkyl benzenes, respectively. T is the total ion summation observed for calibration runs on pure compounds. Each calibration coefficient, $(\Sigma 43/T)_p$, etc., is the ratio of a characteristic ion summation to the total ionization for a particular compound type. The solutions to this system of equations, C_p , C_c , C_b , and C_a , are the contributions of the paraffins, cycloparaffins, bicycloparraffins, and alkyl benzenes, respectively, to the total ion summation of

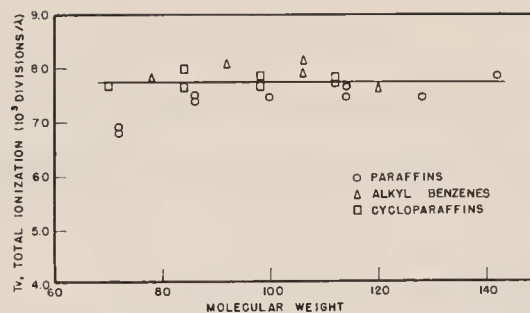


Figure 2. Total ionization per unit liquid volume as a function of molecular weight for a number of paraffins, cycloparaffins, and alkyl benzenes

Table I. γ Intercepts for Hydrocarbon Series

Compound Type	γ Intercepts	
	Calcd. ^a	Exptl. ^b
Paraffins	1.1	1.1
Cyclopentanes	0.0	0.0
Cyclohexanes	0.0	0.0
Olefins	0.0	0.0
Diolefins	-1.2	...
Alkyl benzenes	-3.3	-1.7
Naphthalenes	-6.8	...

^a Relative values.

^b Relative values normalized to paraffin value of 1.1 with respect to cycloparaffins.

a specific sample being analyzed. In a perfect analysis, the total ion summation observed for a sample is equal to the sum of C_p , C_c , C_b , and C_a .

Coefficients for the appropriate sets of equations were obtained from a large number of typical compound patterns. Average coefficient data for the carbon number range of interest were then obtained for each compound type. Table II shows the average coefficient data as percentages of total ionization. The tabulated data show that a single matrix which is approximately independent of carbon number can be developed for the C_7 to C_{10} range. Because the naphthas analyzed at this laboratory were known to contain only small concentrations of olefins, only cycloparaffin data, rather than mixed cycloparaffin and mono-olefin data, were used at $\Sigma 41$. Bicyclic paraffin data were used in place of the coda group data for the $\Sigma 67$. (The coda group includes the cyclomono-olefins, diolefins, and acetylenes.) The small loss of accuracy from the use of a single matrix for a rather wide range of molecular weights was justified by the practical consideration that a large number of samples received contained compounds having a relatively wide range of molecular weights.

To interpret the significance of these calculated total ion summation contributions, C_p , C_c , C_b , and C_a , and convert them to mole percentages, some assumption about the distribution of

Table II. Group-Type Analysis Coefficients

Type of Compound	C No.	$\frac{\Sigma 43}{T}$	$\frac{\Sigma 41}{T}$	$\frac{\Sigma 67}{T}$	$\frac{\Sigma 77}{T}$
Paraffins	C ₅	30.3	14.8	0.0	...
	C ₆	35.8	14.3	0.1	0.0
	C ₇	43.4	13.5	0.2	0.0
	C ₈	46.9	12.8	0.2	0.1
	C ₉	48.8	13.1	0.3	0.1
	C ₁₀	49.6	11.9	0.3	0.2
	Av. C ₇ to C ₁₀	47.2	12.8	0.3	0.1
Cycloparaffins	C ₅	2.3	21.4	0.8	...
	C ₆	4.2	27.6	1.5	0.3
	C ₇	4.0	35.2	2.1	0.3
	C ₈	5.2	36.0	5.4	0.5
	C ₉	6.7	39.0	8.5	0.5
	C ₁₀	7.0	37.8	14.7	0.6
	Av. C ₇ to C ₁₀	5.7	37.0	7.7	0.5
Bicycloparaffins	C ₈	0.3	11.1	47.6	2.1
	C ₉	0.4	12.5	48.9	2.3
	C ₁₀	0.7	17.4	43.6	2.0
	Av. C ₈ to C ₁₀	0.5	13.7	46.7	2.1
Alkyl benzenes	C ₆	0.1	0.1	0.0	47.7
	C ₇	0.9	0.7	0.0	58.4
	C ₈	0.3	0.5	0.2	60.5
	C ₉	0.7	1.7	0.1	63.5
	C ₁₀	0.7	2.6	0.2	63.1
	Av. C ₇ to C ₁₀	0.7	1.4	0.1	61.4

compound types with respect to molecular weight must be made. If the usual assumption of gasoline group-type analyses is made—i.e., the effective molecular weights of all compound types are the same, a molecular weight determination of the sample is required and the total ion summation contributions are divided by appropriate sensitivity data obtained from curves such as those shown in Figure 1.

If, however, the total ionization data are plotted in terms of total ionization per unit liquid volume of material introduced into the mass spectrometer, a much simpler calculation scheme becomes evident. In Figure 2 total ionization data in the form of divisions per liquid volume of 1 μ l. (0.001 ml.) are shown as a function of molecular weight for a number of paraffins, cycloparaffins, and alkyl benzenes. These data were calculated from the experimental total ionization data in divisions per micron of pressure by using the ideal gas law. The equation for conversion from divisions per micron, T_p , to divisions per microliter, T_v , is

$$T_v = \frac{\text{divisions}}{\text{microliter}} = T_p \left(\frac{dRT}{MV} \right)$$

where

- d = liquid density
- R = gas constant
- M = molecular weight
- V = volume of expansion reservoir

or,

$$T_v = \left(\text{constant term} + k \frac{6.16}{14} \times M \right) \times \left(\frac{dRT}{MV} \right) \quad (4)$$

Table III. Total Ionization per 1 μ l. of Liquid

Compound Type	Average Total Ionization, T_v , 10^3 Div./ μ l.	Av. Dev. from Mean, %
Alkyl benzenes	7.83	2.5
Paraffins	7.57	1.8
Cycloparaffins	7.78	1.3
Olefins	7.52	2.5
Diolefins	7.63	Insufficient data
Bicycloparaffins	8.03	Insufficient data
Average, div./ μ l.		7.73×10^3
Average deviation from mean, %		2.0

As T_p in divisions per micron is a linear function of molecular weight, Equation 4 shows that T_v in divisions per unit liquid volume (or microliter) should be to a first order independent of molecular weight. Although dependent on density, the changes in densities over the molecular weight range considered are small. Average values of T_v and per cent deviations from the mean are shown in Table III for six compound types of general interest in naphtha group-type analyses. Pentane data were not included in the paraffin average. Although the data of Table III show differences in T_v with compound type, the spread of data in Figure 2 indicates that these differences are not significant.

Because the value of T_v is essentially independent of compound type, normalization of the calculated total ion summations, C_p , C_c , C_b , and C_a , gives concentrations directly in liquid volume percentages. Further, because

of relative independence of T_v with respect to molecular weight, no assumptions concerning either effective molecular weights for each compound type, or the molecular weight range of the individual compounds of a group type are required within the C₇ to C₁₀ range.

APPLICATION OF TOTAL IONIZATION TO HIGH MOLECULAR WEIGHT MASS SPECTROMETRY

One of the more difficult problems facing a laboratory planning to use a mass spectrometer for studies of compounds of high molecular weight is obtaining calibration data. Compounds of high purity having more than 12 carbon atoms per molecule are, in general, obtainable only through the American Petroleum Institute. Furthermore, it is difficult to obtain good absolute sensitivity data, once pure compounds are available.

Probably the second best source of such data is the large number of mass spectra contained in the API RP 44 spectral files. When high mass work was started at this laboratory, a study was made of the spectra of a number of compounds to determine whether there was agreement between sensitivities for spectra of a given compound obtained in different laboratories, and whether the spectral patterns obtained by several laboratories were in agreement. Absolute sensitivities were found to differ by rather large amounts, enough to show that a result based on the sensitivity of a particular spectrum could be off by almost an order of magnitude. Spectral patterns were in fair agreement, as might be expected, as the same model of mass spectrometer was used by all the laboratories contributing spectra. Thus, if some general means of standardizing spectral data with respect to a known physical property of the compounds could be devised, the large number of spectral patterns in the API spectral file would become available for calibration purposes.

In Equation 3, the total ionization in divisions per micron was expressed as a constant term plus a term which was a linear function of molecular weight. The constant term, or y intercept, differs for each hydrocarbon type, while the slope is independent of compound type. The experimental total ionization data for three compound types were shown in Figure 1 to agree well with the results predicted. If it is now assumed that such data can be extrapolated to compounds of higher molecular weight, the constant term of Equation 3 becomes small in comparison with the variable term. At a molecular weight of 300, the calculated error resulting from neglecting the constant term is 3% for paraffins and 2% for alkyl benzenes. Such errors are smaller than the usual

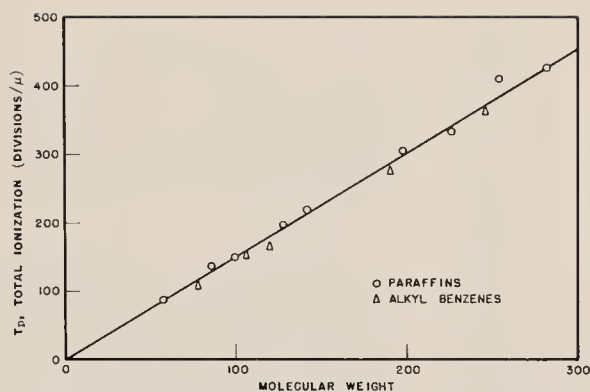


Figure 3. Total ionization per mole as a function of molecular weight for paraffins and alkyl benzenes

errors encountered in absolute sensitivity data for high molecular weight compounds. The total ionization data (divisions per micron) can thus be expressed as

$$T_p = k' \times M \quad (5)$$

where k' is a constant independent of compound type. Figure 3 shows total ionization data obtained for a range of compounds extending from C_{10} to C_{20} . Each experimental point represents the average of data selected from a number of separate runs, all made at the same temperature. Individual results that differed greatly from the average were discarded.

Table IV. Relative Total Ionization per Unit Liquid Volume

Compound Type	Relative Total Ionization
Paraffins	1.00
Noncondensed cyclohexanes	1.03
Alkyl benzenes	1.05

To show the relationship between total ionization per unit liquid volume and molecular weight, the data of Figure 3 were converted from total ionization per unit of pressure to total ionization per unit liquid volume. Figure 4 shows data for paraffins and alkyl benzenes, calculated by obtaining a value of total ionization in divisions per micron for a specific molecular weight from Figure 3 and using the density of a particular compound of that molecular weight in converting to total ionization in divisions per microliter. Considering that the curve of Figure 3 can be expressed as $k' \times M$ and that the conversion from ionization per unit pressure to ionization per unit volume requires the multiplication by a factor involving density/ M as the only variable, we see that the calculated data of Figure 4 actually show only the variation in densities of paraffins and alkyl benzenes

with molecular weight. However, as the densities of paraffins (and other hydrocarbons) approach an asymptote with increasing molecular weight, the total ionization per unit volume appears to approach a limit in molecular weight above which it is a constant independent of molecular weight.

These results show that total ionization per unit liquid volume for each hydrocarbon series is fairly constant for the molecular weight range of approximately 200 and above. Table IV shows average relative sensitivities per liquid volume calculated for several compound types in the 200 to 500 molecular weight range.

The values in Table IV or curves such as those in Figure 4 can be combined with a spectral pattern for any compound to determine the absolute sensitivity of any spectral peak, or sum of peaks as follows:

$$\text{Sensitivity of peak } A = \frac{\text{pattern of } A}{\text{total pattern}} \times (\text{total ionization sensitivity}) \quad (6)$$

Thus, the large amount of spectral data in the American Petroleum Institute Spectral Catalog becomes available for calibration purposes. Published analytical methods and data can be transferred from one mass spectrometer to another with relative ease.

CONCLUSIONS

An equation relating total ionization per mole to molecular weight has been derived from the relative ionization cross-section study of Otvos and Stevenson. This equation predicts that total ionization data for homologous hydrocarbon series are linear functions of molecular weight having the same slope. Experimental data substantiate this prediction.

A naphtha group-type analysis based on total ionization was developed. A consideration of the invariance of total ionization per unit liquid volume with molecular weight over the carbon

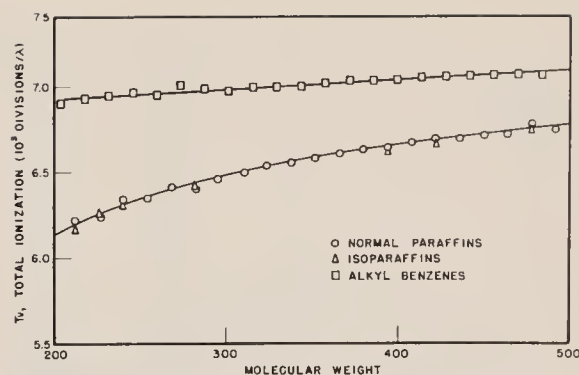


Figure 4. Total ionization per unit liquid volume for high molecular weight paraffins and alkyl benzenes

number range C_7 to approximately C_{10} permits results to be calculated as liquid volume percentages without reference to molecular weight. The coefficients of the system of equations for this analysis were essentially independent of carbon number for C_7 's and higher.

Extrapolation of the equation of total ionization per mole vs. molecular weight to compounds of high molecular weight indicates that a single straight-line plot should fit the data. Experimental data confirm this conclusion. A consequence of this result is the relative independence of total ionization per unit volume of liquid with respect to molecular weight. From total ionization data of this type obtained on a particular mass spectrometer, published spectral patterns can be standardized in terms of sensitivities in either divisions per micron or divisions per unit liquid volume.

ACKNOWLEDGMENT

The authors wish to thank Hildegard A. Gray, H. Thomas Best, and Gerard L. Kearns for their work in obtaining the experimental data used in this report.

LITERATURE CITED

- (1) Bloom, E. G., Mohler, F. L., Lengel, J. H., Wise, C. E., *J. Research Natl. Bur. Standards* **41**, 129 (1948).
- (2) Brown, R. A., *ANAL. CHEM.* **23**, 430 (1951).
- (3) Clerc, R. J., Hood, A., O'Neal, M. J., Jr., *Ibid.*, **27**, 868 (1955).
- (4) Dibeler, V. H., Cordero, F., *J. Research Natl. Bur. Standards* **46**, 1 (1951).
- (5) Mohler, F. L., Bloom, E. G., Williamson, L. M., Wise, C. E., Wells, E. J., *Ibid.*, **43**, 533 (1949).
- (6) Mohler, F. L., Williamson, L., Wise, C. E., Wells, E. J., Dean, H. M., Bloom, E. G., *Ibid.*, **44**, 291 (1950).
- (7) Otvos, J. W., Stevenson, D. P., *J. Am. Chem. Soc.* **78**, 546 (1956).

RECEIVED for review June 26, 1957.
Accepted October 9, 1957.

JUL 31 1958

L.P.

July 1, 1958

N. D. COGGESHALL

2,841,005

CHROMATOGRAPHIC METHOD AND APPARATUS

Filed Dec. 11, 1956

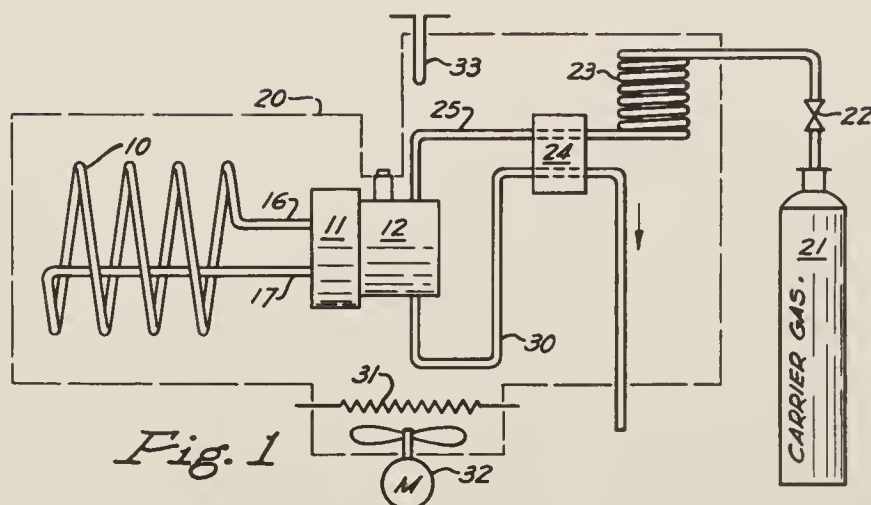


Fig. 1

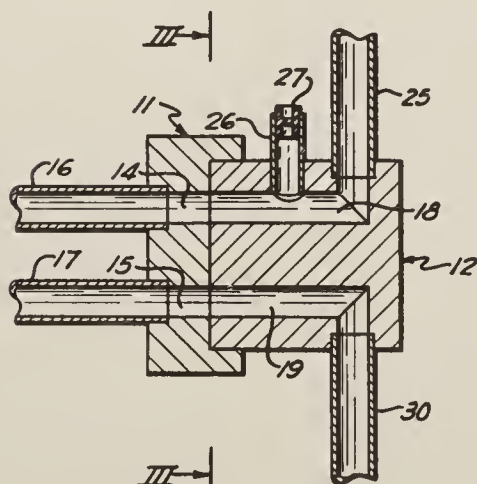


Fig. 2

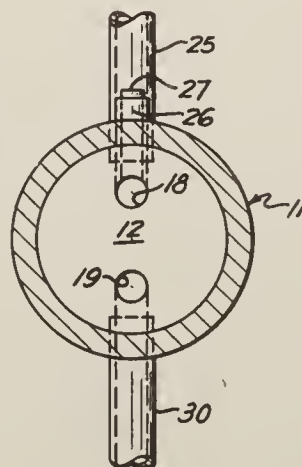


Fig. 3

INVENTOR.
NORMAN D. COGGESHALL
BY

Norman D. Coggeshall

HIS ATTORNEY

1

2,841,005

CHROMATOGRAPHIC METHOD AND APPARATUS

Norman D. Coggeshall, Verona, Pa., assignor to Gulf Oil Corporation, Pittsburgh, Pa., a corporation of Pennsylvania

Application December 11, 1956, Serial No. 627,598

4 Claims. (Cl. 73—23)

This invention relates to a method and apparatus for separating fluid mixtures and more particularly to an improved partition chromatography method and apparatus adapted for high temperature analytical separations.

Partition chromatography has been widely used for the separation and analysis of fluid mixtures. Its principles have been described in the literature, for example, in the article by D. H. Lichtenfels et al., *Analytical Chemistry*, volume 27, number 10, October 1955, pages 1510-13. The article describes the analytical separation of a fluid mixture by gas-liquid partition chromatography. A small sample of a mixture to be separated and analyzed is injected into the end of a long, narrow column packed with inert, granular solid particles on which have been deposited a thin film or coating of a non-volatile solvent. The solvent is usually a high-boiling organic liquid and is referred to as a partitioning liquid. The column is eluted with an inert carrier gas such as helium. Components of the volatile mixture partition between a moving gas phase in the vapor space between the solid particles and a stationary liquid phase absorbed in the liquid coating of the granular particles. This causes the components of the mixture to move through the partitioning media within the column at individual velocities less than that of the carrier gas. The velocity at which each component moves is dependent on its partition coefficient, the latter being a measure of the solubility of the component in the stationary liquid phase. Since different compounds have different partition coefficients, the components of the mixture move through the column at different speeds and, if the column is long enough, they emerge one by one from the column usually in the order of boiling points for homologous series of compounds. The emerging components are detected by suitable means for detecting vapor concentrations in a gas stream. The most commonly used detecting means is a thermal conductivity cell connected with a recording potentiometer. The plot of potentiometer deflection against time provides a quantitative and qualitative analysis of the mixture.

I have referred to the liquid coating on the solid particles of the partition column as being "a non-volatile solvent" and as forming a "stationary" liquid phase. The partitioning liquid is commonly referred to in this way. However, as a matter of fact, none of the available partitioning liquids are completely stationary. During partition chromatography separations carried out at room temperature or at only slightly elevated temperatures the partitioning liquid is stationary for all practical purposes. But, even at low temperature the liquid has at least a slight tendency to flow. The flow is induced by gravity and by the drag of the moving carrier gas. When a gas-liquid partition chromatography column is operated at high temperatures, for example, above 100° C., the liquid coating on the granular material shows a marked tendency to migrate. This is due to the decreased viscosity at higher temperatures of the organic liquids commonly used as partitioning liquids. Movement of the partitioning liquid can have serious disadvantages. It may cause

2

troublesome accumulation of the liquid in the low parts of the partition column and near the exit. The permeability of the column then differs at various points in the column and the volume of stationary liquid per unit length of column is no longer uniform throughout the column. As a result, the interpretation of the recorded plots of thermal conductivity cell responses to the effluent from the column becomes difficult. The reproducibility of measurements is destroyed and it is difficult to compare one run with another. The present invention provides a partition chromatography method and apparatus by means of which these disadvantages of the flow of the partitioning liquid can be reduced or eliminated.

The apparatus of the invention in general comprises a tubular partition column packed with solid particles having a surface coating of a partitioning liquid. The ends of the column are rigidly mounted on one face of a rotatable head and communicate respectively with two channels which extend through the head to an opposite face. On its opposite face the head is rotatably mounted on a stationary charge inlet block. This block has passing through it a carrier fluid channel and an effluent channel. The openings of these channels on the surface of contact between the stationary block and the rotatable head are so positioned that when the carrier fluid channel communicates with either one of the channels in the rotatable head the effluent channel communicates with the other channel in the rotatable head. A carrier fluid line connects the other end of the carrier fluid channel with a source of carrier fluid and an effluent line connects the other end of the effluent channel with a detecting means. The stationary block is also provided with means for injecting charge mixture into the carrier fluid channel.

The method of the invention in general comprises flowing a carrier fluid through the elongated partition column packed with solid particles having a surface coating of a partitioning liquid, injecting a fluid mixture to be analyzed into the stream of carrier fluid, recovering the effluent from the column at an exit point which is positioned preferably in the vicinity of the inlet point and detecting components of the charge mixture in the effluent. Subsequently, this procedure is repeated in additional cycles of introduction of charge mixture and analysis of effluent. At least once between cycles, the partition column is rotated to place the inlet end of the column for the previous cycle in the position of the outlet end of the column for the previous cycle and carrier fluid is flowed into the end of the column which was the exit end for the previous cycle.

The method and apparatus of the invention will be described in more detail by referring to the drawing of which:

Figure 1 is a schematic diagram of one embodiment of the partition chromatography apparatus of the invention;

Figure 2 is an enlarged sectional view of the charge inlet region of the apparatus of Figure 1; and

Figure 3 is a sectional view along line III—III of Figure 2.

In the embodiment of my apparatus shown schematically in Figure 1 the partition column is a long narrow tube 10 in the form of a coil or helix which is packed with an inert, granular material such as granular kieselguhr of 20-100 mesh particle size. The solid particles have a surface coating of a non-volatile solvent such as dioctyl phthalate.

In the preferred embodiment of my apparatus the two horizontal ends of column 10 are positioned relatively close together. They are spaced apart a short distance relative to the length of the column and are rigidly mounted in a rotatable head member 11. The head 11 is rotatably mounted on a circular face of a stationary

charge inlet block 12. This is shown more clearly in Figures 2 and 3.

As they show, channels 14 and 15, which are generally parallel, pass through the rotatable head 11. The end 16 of column 10 is rigidly mounted in channel 14 and the end 17 is rigidly mounted in channel 15 so that the channels, in effect, are extensions of the column. The block 12 has a carrier gas channel 18 and an effluent channel 19. The openings of these channels in the circular face of the stationary block, which forms the surface of contact of the block with the rotatable head, are so positioned that when the carrier gas channel communicates with either one of the channels in the rotatable head the effluent channel communicates with the other channel in the rotatable head. A carrier gas line 25 communicates with carrier gas channel 18. An effluent line 30 communicates with channel 19 and connects channel 19 with a detecting means. For example, as shown in Figure 1, line 30 passes the effluent gas from the partition column through the testing channel of the thermal conductivity cell 24 and then to the atmosphere or to suitable collecting means.

Stationary block 12 is also provided with means for injecting the fluid charge mixture into the carrier gas channel. In the apparatus of the drawing this takes the form of a short tube 26 having at its upper end a puncturable, self-sealing rubber cap, similar to the self-sealing caps used on serum bottles, and communicating at its lower end with the carrier gas channel 18.

In the apparatus of Figure 1 the carrier gas source is the gas cylinder 21. Carrier gas passes from cylinder 21 through a pressure or flow control valve 22, through the reference channel of the thermal conductivity cell 24 and then via line 25 into the carrier gas channel 18 of the stationary block 12. The carrier gas then flows either into end 16 or end 17 of column 10 depending upon which end is aligned with channel 18 for that particular cycle.

As I have mentioned, the apparatus of the invention is particularly suited for separations carried out under conditions at which the viscosity of the partitioning liquid is low enough to cause it to flow excessively. When certain low-viscosity partitioning liquids are used, this problem may occur even at low temperature. Normally, however, in partition chromatography the partitioning liquid is a high-boiling, viscous liquid and the problem of flow of the partitioning liquid is encountered when it is desired to use high temperature for the separation or analysis. Accordingly, the apparatus of the invention would normally include suitable means for providing and maintaining elevated temperatures. For example, means can be provided for preheating the carrier gas and for maintaining the partition column at elevated temperature. Thus, as shown schematically in Figure 1, the apparatus can be provided with a constant temperature air bath which encloses the partition column and the thermal conductivity cell and is adapted to maintain these elements at a desired elevated temperature. The air bath includes an insulated enclosure 20, a heating means such as an electrical resistance heater 31, a blower 32, and a thermostat 33 to control the heater. In the apparatus of the drawing, the means for preheating the carrier gas is the preheater coil 23. This is simply a coiled portion of the carrier gas line 25 through which the carrier gas passes before passing to the reference channel of the thermal conductivity cell. The coil 23 is maintained at the desired elevated temperature by being enclosed within the heated air bath 20. Optionally, the column and the thermal conductivity cell can have individual air baths maintained at the same or different temperatures. These various possible temperature control means are shown only in a highly schematic way in the drawing because their structure and employment is well known and because considerable variations in their structure is possible.

I will describe the method of the invention, as carried out with the apparatus of the drawing, by describing a particular analytical separation for which high temperature is used, namely, the analysis of a crude iso-octyl aldehyde for impurities. The use of carrier gas temperatures above 100° C. is advantageous or necessary in analyzing this mixture by gas-liquid partition chromatography because of the low vapor pressures of its components.

A 0.05 ml. sample of the liquid is drawn into a micro-syringe. The needle of the syringe is inserted through the self-sealing rubber cap 27 and the charge mixture is injected through tube 26 into carrier gas channel 18. Carrier gas preheated to a temperature of 125° C. sweeps the charge mixture through channels 18 and 14 into column 10. This column is in the form of a coiled tube of $\frac{3}{16}$ inch inside diameter and is packed with a crushed fire brick (specifically, a material known commercially as Johns-Manville Corp., Insulated Firebrick Sil-O-Cel, C₂₂) of 40-80 mesh particle size coated with ethyl-hexyl sebacate. The column is also maintained at the temperature of 125° C. The carrier gas successively elutes the components of the mixture from column 10 through channel 15 of the head member, through channel 19 of the block, through line 30 and through the testing channel of the thermal conductivity cell 24. The thermal conductivity cell with its recording potentiometer, not shown in the drawing, provides an analysis of the mixture. When all components of the charge mixture have been eluted from the column the apparatus is ready for the injection of another charge mixture in another analytical cycle.

At the temperature of 125° C. the viscosity of the ethyl-hexyl sebacate coated on the solid particles in column 10 is lowered so much that the liquid shows a tendency to flow to lower parts of column 10 and toward the exit end 17 of the column. Therefore, after each cycle or after several cycles of operation at this elevated temperature the head 11 is rotated 180° on a horizontal axis lying between ends 16 and 17 and on the same plane therewith to align end 16 of column 10 with effluent channel 19 and align end 17 of column 10 with carrier gas channel 18. When the carrier gas flow is resumed in the next cycle the direction of flow in column 10 is opposite to the direction of flow in the previous cycle. Thus, the tendency of flow of the partitioning liquid toward the exit of column 10 is reversed. Furthermore, the 180° rotation of column 10 on a horizontal axis inverts the column and changes the direction of the gravitational force with respect to the liquid coating on the solid particles within the column. Accordingly, the flow of partitioning liquid induced by gravity is reversed. After head 11 is rotated 180° and is locked in position, it provides a gas tight communication between channels 14 and 19 and channels 15 and 18. The flow of carrier gas is resumed and another fluid mixture sample to be analyzed is injected into the charge inlet cap 27.

Column 10 as shown in the drawing is essentially U-shaped and its intermediate portion is in the form of a coil. The coil form is advantageous because of its compactness and because it can be rotated easily on a horizontal axis. Other arrangements having these same advantages can also be used. Whatever the form of column, it is normally preferred that its two ends be close together, or in other words, spaced apart only a short distance relative to the length of the column. This contributes to the compactness of the apparatus and makes it possible for both ends to be mounted in a rotatable head which is conveniently small and yet provides communication for the ends of the column with both the carrier gas line and the effluent line.

The structure of the rotatable head and the stationary block can also, within the scope of the invention, differ from that shown in the drawing. An essential feature

is that the openings of the channels in the rotatable head and in the stationary block should be positioned on the surfaces of contact between the head and the block in such a way as to provide communication between one of the channels in the head and one of the channels in the block when the other channel in the head and in the block are in communication. An example of another form of head and block structure which meet these requirements is found in an apparatus comprising an annular rotatable head member mounted on a cylindrical block and having the column ends mounted 180 degrees apart on the outer circumference of the annular rotatable head. In this apparatus the surface of contact between the block and head is a cylindrical surface rather than a circular face as in the embodiment shown in the drawing.

In the specification and claims when I refer broadly to the rotation of the column I mean to include rotation on a horizontal, vertical or inclined axis. In the form of the column shown in Figure 1 wherein the column is essentially U-shaped the rotation of the column on a horizontal axis inverts the column and thus changes the direction of the gravitational force. It also reverses the direction of the carrier gas flow. In preferred embodiments of the apparatus and method both of these effects are obtained. However, it should be understood that the principles of the invention include rotation of the column to obtain either one of the effects alone. Thus, for example, certain forms of the column can be rotated in such a manner as to invert the column and thus change the direction of the gravitational effect without reversing the direction of carrier gas flow. This inversion of the column will always occur when the column is rotated on a horizontal axis. The rotation of certain forms of the column on a vertical axis will cause reversal of the direction of carrier gas flow but will not change the gravitational effect. The rotation of the column on an inclined axis will cause some change in the gravitational effect and, with certain forms of the column, will change the direction of carrier gas flow. It should be understood, therefore, that the rotation of the column, as used in the broadest sense in the specifications and claims, means (1) a rotation that merely inverts the column to change the gravitational effect or (2) a rotation that merely reverses the direction of flow of carrier gas without inverting the column, or (3) a rotation that both inverts the column and reverses the direction of flow of carrier gas. The latter result is obtained in the preferred embodiments of the apparatus such as the apparatus shown in Figure 1 of the drawing.

In the example above I have described one particular separation in accordance with the invention. It should be understood, however, that the principles of the invention can be applied to the separation or analysis of many types of fluid mixtures, including petroleum naphthas and heavier hydrocarbon fractions. Normally, any of the carrier fluids, partitioning liquids and solids materials that are suitable for partition chromatography can be employed. For example, although I have described separation of a high-boiling liquid mixture for which high temperature separation is advisable, the method and apparatus of the invention will have advantages whenever the possibility of flow of the partitioning liquid is a problem. This problem may occur, depending on the viscosity of the partitioning liquid, at either low or high temperatures and in the separation of either a liquid or gaseous fluid mixture. Therefore, the method of the invention can be applied to the separation of such high-boiling liquid mixtures as described or to the separation of more volatile liquids or to the separation of gases.

The partitioning liquid for coating the solid particles in the process and apparatus of the invention can be selected from the many solvents that are suitable for use in partition chromatography. The partitioning liquid is

applied as a surface coating to the granular solid material in the partitioning column. Suitable liquids include high-boiling organic solvents such as dioctyl phthalate, dinonyl phthalate, dioctyl sebacate, paraffin wax, silicone fluids, etc., but, as I have mentioned, the method and apparatus of the invention are particularly advantageous when a partitioning liquid of low viscosity is used. It is also possible to use volatile partitioning liquids (for example, water) if any such liquids have desirable solvent properties. When using a volatile partitioning liquid the carrier gas should be saturated with vapor of the partitioning liquid so that the liquid will not be removed by evaporation.

I have mentioned granular kieselguhr as a suitable solid material. As a general rule, any of the granular solid materials used for partition chromatography can be used. Preferably the solid particles are non-porous materials which are not chromatographically active adsorbents, as otherwise the effects of adsorption chromatography and partition chromatography may be superimposed upon each other and this might prevent the obtaining of sharply defined fractions.

I have described the use of a gas as the carrier fluid for the process of the invention, in which case the process is a gas-liquid partition chromatography process. Any inert gases that can be separated readily from the components of the charge mixture can be used. Examples of suitable carrier gases include hydrogen, nitrogen, helium, etc. The principles of the invention also extend to the use of a liquid as the carrier fluid, in which event the process is a liquid-liquid partition chromatography process and separation occurs as components of the charge mixture partition between the stationary liquid phase on the solid particles and the moving liquid phase formed by the carrier fluid. In such a process the carrier liquid should be substantially immiscible with the stationary partitioning liquid.

I have described a thermal conductivity cell with a recording potentiometer as a preferred means for analyzing the effluent from the partition chromatography column. However, other known detecting means with high sensitivity can be used in the process and apparatus of the invention.

Obviously many modifications and variations of the invention as hereinbefore set forth may be made without departing from the spirit and scope thereof and therefore only such limitations should be imposed as are indicated in the appended claims.

I claim:

1. A partition chromatography apparatus which comprises an elongated tubular partition column containing a partitioning media, the two ends of said column being rigidly mounted on a rotatable head, said rotatable head having two channels passing therethrough which communicate respectively with the two ends of said column, said rotatable head being rotatably mounted on a stationary charge inlet block, said block having a carrier fluid channel and an effluent channel passing therethrough, the openings of such channels on the surface of contact of said block with said rotatable head being so positioned that when the carrier fluid channel communicates with either of the channels in the rotatable head the effluent channel communicates with the other channel in the rotatable head, a carrier fluid line connecting the carrier fluid channel with a source of carrier fluid, an effluent line connecting the effluent channel with a detecting means and means for introducing a fluid charge mixture into the carrier fluid channel.

2. A partition chromatography apparatus adapted for high temperature use which comprises an elongated tubular partition column, the two ends of said column being spaced apart a short distance relative to the length of the column and rigidly mounted on a rotatable head, said rotatable head having two channels passing therethrough

which communicate respectively with the two ends of said column, said rotatable head being rotatably mounted on a stationary charge inlet block, said block having a carrier gas channel and an effluent channel passing therethrough, said channels having openings on the surface of contact of said block with said rotatable head, such openings being so positioned that when the carrier gas channel communicates with either of the channels in the rotatable head the effluent channel communicates with the other channel in the rotatable head, a carrier gas line connecting the carrier gas channel with a source of carrier gas, a thermal conductivity cell having a reference channel and a testing channel, said reference channel communicating with said carrier gas line between said carrier gas source and said partition column, an effluent line connecting the effluent channel with the testing channel of said thermal conductivity cell, means in said stationary block for injecting a fluid charge mixture into the carrier gas channel and means for maintaining said partition column at an elevated temperature.

3. A method for separating a fluid mixture by partition chromatography under conditions such that the partitioning liquid tends to flow, which comprises flowing a carrier fluid at elevated temperature through an elongated partition column packed with solid particles having a surface coating of a flowable partitioning liquid, injecting a fluid mixture to be analyzed into the stream of carrier fluid, recovering the effluent from the exit end of the column, detecting components of the charge mixture in the effluent, subsequently repeating this procedure in additional cycles of introduction of charge mixture and recovery of effluent, at least once and between said cycles rotating the partition column to place the inlet end of the column for the previous cycle in the position of the exit end of the col-

umn for the previous cycle, flowing carrier fluid into the end of the column which was the exit end for the previous cycle and injecting a fluid mixture to be separated into the stream of carrier fluid.

4. A method for separating a fluid mixture by partition chromatography, under conditions such that the partitioning liquid tends to flow which comprises, flowing a carrier gas at a temperature at least about 100° C. through an elongated partition column packed with solid particles having a surface coating of a flowable partitioning liquid, injecting a fluid mixture to be analyzed into the stream of carrier gas, recovering the effluent from the column at an exit end of the column in the vicinity of the inlet end thereof, detecting components of the charge mixture in the effluent, subsequently repeating this procedure in additional cycles of introduction of charge mixture and recovery of effluent, at least once and between cycles rotating the partition column 180 degrees on a horizontal axis to invert said column and to place the inlet end of the column for the previous cycle in the position of the exit end of the column for the previous cycle, flowing carrier gas into the end of the column which was the exit end for the previous cycle and injecting a fluid mixture to be separated into the stream of carrier gas.

References Cited in the file of this patent

UNITED STATES PATENTS

2,757,541 Watson et al. ----- Aug. 7, 1956

OTHER REFERENCES

"Gas-Liquid Partition Chromatography," by D. H. Lichtenfels et al., *Analytical Chemistry*, volume 27, number 10, October 1955, pages 1510-13.

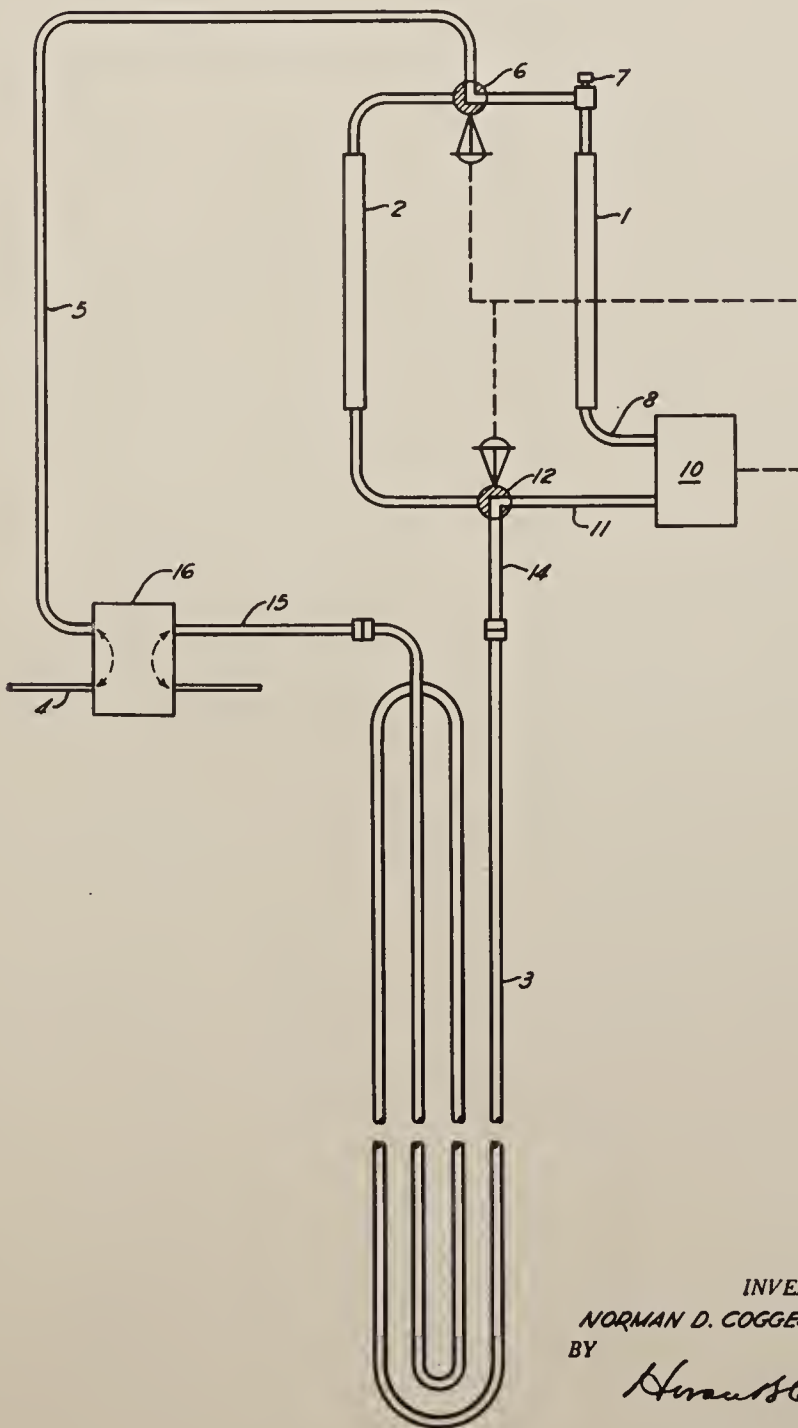
Jan. 13, 1959

N. D. COGGESHALL

2,868,011

MULTIPLE-COLUMN CHROMATOGRAPHIC APPARATUS

Filed Dec. 16, 1955



INVENTOR.

NORMAN D. COGGESHALL

BY

Herbert H. Cooke

HIS ATTORNEY

1

2,868,011

MULTIPLE-COLUMN CHROMATOGRAPHIC APPARATUS

Norman D. Coggeshall, Verona, Pa., assignor to Gulf Research & Development Company, Pittsburgh, Pa., a corporation of Delaware

Application December 16, 1955, Serial No. 553,571

3 Claims. (Cl. 73—23)

This invention relates to apparatus for separating fluid mixtures and more particularly to multiple-column chromatographic apparatus whereby a fluid mixture is fractionated by partition chromatography in order to identify the components of the mixture.

It is known that the principles of partition chromatography can be applied to the separation and analysis of multi-component fluid mixtures (see, for example, the article by N. H. Ray, *Journal of Applied Chemistry*, vol. 4, page 21, February 1954). In a gas-liquid partition chromatography a fluid mixture is separated by selectively partitioning its components between a stationary liquid phase and moving gas phase. The stationary liquid phase is formed as a coating of a non-volatile solvent on a column of granular solid material and the gas phase is formed by flowing a carrier gas such as helium or hydrogen through the column. The manner in which the separation of a mixture is accomplished in partition chromatography can be explained by considering first what happens when a single pure compound is introduced to one end of the partition chromatography column. The compound will immediately partition itself into two portions, one of which will be in solution in the stationary liquid phase and the other of which will be in the gas phase. When the flow of carrier gas is initiated it moves that portion in the gas phase forward. As this occurs there is a continual partitioning between the material in the gas phase and that in the liquid phase. As a result the pure material moves along the column but at a slower speed than the carrier gas. The rate of movement is dependent upon the partition coefficient. Different materials have different partition coefficients and hence move at different speeds. This is the basis for the separation by this technique. A complex mixture of materials injected into the partition chromatography column will separate into components moving at different speeds so that, if the column is long enough, the components will emerge one by one from the column, usually in the order of boiling points for a homologous series.

In analytical methods using the gas-liquid partition chromatography technique the components of the mixture which emerge successively from the partition column are identified in various suitable ways. For example the effluent from the column is passed through a thermal conductivity cell connected with a recording potentiometer. The plot of potentiometer deflection against time provides a quantitative and qualitative analysis of the components of the mixture.

Although the partition chromatography method of analysis has proved to be valuable for many uses, it does have disadvantages in certain separations. Thus, if it is desired to analyze or to separate precisely only those components of a multi-component mixture which are readily removable from a partition chromatography column, a considerable length of time may be required

2

to remove the remaining components of the mixture from the column in order to restore it to its original condition for the next cycle of analysis or separation. For example, if it is desired to analyze precisely only the C_4 - C_6 hydrocarbons of a gasoline sample, these hydrocarbons can be carried through a long partition chromatography column in a period of an hour or less. However, to remove the rest of the gasoline range hydrocarbons could require a period of many hours, for example, 20 hours or more. If a crude oil is being analyzed for light hydrocarbons, these components will emerge from the column in a reasonably short time but it may require many days to remove the rest of the crude oil. As a practical matter it may be impossible to remove all of the heavy components of the crude with carrier gas alone. Therefore, if a column used for such separations is used in subsequent runs the heavier components remaining in the column from previous runs will continue to emerge slowly from the column and will make it difficult or impossible to analyze accurately the light components of the subsequent runs.

The apparatus of the present invention enables avoidance of the problem referred to above and includes a principal chromatographic partition column that can be used for a large number of separations without becoming fouled by heavy materials which would pass through the same slowly.

The apparatus of the invention in general comprises a first partition chromatography column, a parallel by-pass column and a principal chromatographic column. A line is provided for introducing carrier gas into the system and this line has an automatically controlled valve for directing the flow of carrier gas either to the first column or to the by-pass column. The first column is provided with means for introducing feed mixture and a means for withdrawing the effluent from the column for delivery to the principal chromatographic column. In the preferred embodiment the inlet line to the principal column is provided with a valve automatically operable in coordination with the first mentioned valve for receiving flow from either the first column or from the by-pass column. The effluent line from the first column passes through gas analysis means adapted to operate the valves to switch the flow of carrier gas from the first column to the by-pass column upon the appearance of predetermined substances in the effluent from the first column. The principal chromatographic column is provided with an effluent line which passes through a thermal conductivity cell.

Further understanding of the invention can be obtained from the drawing, the sole figure of which shows diagrammatically a preferred embodiment of the apparatus used for analyzing fluid mixtures.

The apparatus of the drawing comprises a first partition column 1, a by-pass column 2 and the principal partition chromatographic column 3. Columns 1 and 2 are arranged in parallel flow with respect to each other and in series with the principal column 3. As the drawing shows, the principal column 3 has greater capacity than the first column. In the modification of the drawing it is in the form of a long coiled tube.

Columns 1 and 3 are filled with a granular solid which has a surface coating of a high boiling liquid. Column 2 may be filled with the same permeable solid material or with any other packing that will provide the same flow resistance as the material in column 1. A carrier gas inlet line 4 passes the carrier gas through one of the two gas channels of a thermal conductivity cell 16. The gas then passes by line 5 to a diaphragm-operated valve

3

6 which is at a bifurcation in line 5. This valve directs the carrier gas either to column 1 or to the by-pass column 2. Column 1 has a feed inlet which, in the apparatus of the drawing, is a serum cap 7 into which a mixture to be analyzed is injected with a hypodermic syringe.

Column 1 has an effluent line 8 for withdrawing the mixture of carrier gas and the lighter components of the feed mixture. In the apparatus shown in the drawing, line 8 passes through a gas analysis means 10. The analyzer 10 can be, for example, a thermal conductivity cell and recording potentiometer. In this case, an operator switches the flow of carrier gas from column 1 to column 2 by operating valves 6 and 12 when the recorder shows that a predetermined component of the feed mixture has emerged from column 1. In another modification of the invention, the analysis means 10 is an analyzing control means such as an infrared absorption spectrometer cell which can identify a particular component of the feed mixture and actuate a valve operating means when such component appears in the effluent from column 1. Line 11 from the gas analysis means passes the effluent of column 1 to valve 12. This is a diaphragm-operated valve for receiving flow from either column 1 or column 2 and directing such flow into line 14 which is the inlet means for the principal column 3.

As I have indicated, both valves 6 and 12 can be automatically operable valves. In the apparatus of the drawing, they are operated to switch the flow of carrier gas from the first column 1 to the by-pass column 2 in response to changes in the effluent from column 1 as detected by the analyzer 10. When a predetermined heavy component of the feed mixture which it is desired to keep out of column 3 appears in the effluent from column 1, the analyzer 10 passes a signal to an actuating means for the air-operated diaphragm valves. Also in accordance with the invention, instead of operating in response to the analyzer 10, valves 6 and 12 can be actuated manually or by a timing device at a predetermined time after introducing the feed mixture. This predetermined time can be at any point between the known time at which the last of the desired light components will be swept from the first column and the known time at which the first of the undesired heavy components will begin to emerge.

Valves 6 and 12 switch the flow of carrier gas from column 1 to column 2. Thereafter, carrier gas alone is passed into column 3 and it successively elutes the lighter components of the feed mixture. These materials emerge from column 3 via line 15 and pass through the testing channel of thermal conductivity cell 16. This cell is connected with a recording potentiometer, not shown in the drawing, which continuously plots potentiometer deflections against time. This plot can be used for a qualitative and quantitative analysis of the lighter components of the feed mixture.

Although thermal conductivity cells are well known in the art, a brief description of their operation can be given. The conventional thermal conductivity cell employs a Wheatstone bridge, two arms of which are heated platinum wires. One of the wires extends into a reference region through which a reference gas flows and the other extends into a testing region through which the gas being analyzed flows. In the process and apparatus of the invention the inlet stream of carrier gas flows through the reference region and the effluent stream from the chromatographic column, consisting of carrier gas and the components of the feed mixture that are eluted from the column, flows through the testing region. When a gas is in contact with a heated platinum wire of the cell, the wire is cooled to an extent that depends on the thermal conductivity of the gas, and, when the composition of the gas flowing through the testing region changes, its thermal conductivity changes and the temperature of the platinum wire changes correspondingly. As a result of the temperature change of the wire its electrical

4

resistance changes. The variations in the difference between the resistances of the platinum wires in the testing and reference regions are reflected in the unbalance of the Wheatstone bridge as indicated by a recording potentiometer. The recorded deviations can be related to the composition of the gas being analyzed.

I have mentioned above that in a preferred embodiment of the apparatus the by-pass column is a column packed with granular material in such a manner that its resistance to gas flow is substantially equal to that of the first column. This is important when a thermal conductivity cell is used as the means for analyzing the effluent from the principal column because it insures that the pressure of the carrier gas at the inlet to the principal chromatographic column will not change substantially when the carrier gas flow is switched from the first column to the by-pass column. Thermal conductivity cells are sensitive to changes in flow rates and to obtain uniform results from the cell, the flow rate of carrier gas through the principal column and therefore its pressure at the inlet to the column should be kept substantially constant.

A further understanding of the invention can be obtained from the following illustrative example of the process of the invention.

Example

A Kuwait crude oil having an API gravity of 32, a 10 percent boiling point of 280° F. and a 70 percent point of 655° F. is analyzed for light ends in an apparatus as illustrated in the drawing. The purpose is to identify qualitatively and quantitatively the lower molecular weight hydrocarbons in the oil, that is to say, the C₆ and lower hydrocarbons. The chromatographic columns are filled with granular kieselguhr. In the principal chromatographic column, column 3 of the drawing, the partitioning liquid which coats the kieselguhr is dioctyl phthalate. In the first column, column 1 in the drawing, the kieselguhr is coated with paraffin wax. The by-pass column 2 is also filled with granular kieselguhr but this body of granular material is not coated with a liquid. However, its resistance to gas flow is substantially equal to that of the body of granular material in column 1. At the start of the process, the carrier gas, helium, is flowed through the first column 1 and the principal column 3 at room temperature. A uniform temperature for the entire apparatus including the chromatographic columns and the detecting means is maintained by the use of a constant temperature air bath. The principal chromatographic column, 3, for this separation is a coiled stainless steel tube 14 feet in length and having an inside diameter of 4.5 mm. The primary column and the by-pass column are similar tubes, each having a length of 3 feet. A charge of the order of 0.08 gram of the crude oil to be analyzed is introduced by a hypodermic syringe into the rubber serum bottle cap which serves as the feed inlet for the first column. In accordance with the principles of partition chromatography, the more volatile components of the crude oil begin to emerge successively from the primary column from whence they pass through a gas analyzing means and then into the principal chromatographic column. The gas analyzer is set to detect the first emergence of hydrocarbons of more than 6 carbon atoms. When the detecting apparatus indicates the first heptanes in the effluent from the primary column, a valve control means automatically operates the diaphragm valves 6 and 12 to switch the flow of carrier gas from the first column to the by-pass column 2. The light constituents of the charge mixture are then successively swept from the principal chromatographic column 3 by the carrier gas. The thermal conductivity cell 16 and its recording potentiometer provide a quantitative and qualitative analysis of the emerging light components of the crude oil charge. The introduction of C₇ and heavier hydrocarbons which move very slowly through a partition chromatography column is avoided. The light hydro-

carbons are completely removed from the principal column 3 by the carrier gas and the column can then be used for another run. The first column 1 containing the heavy ends of the crude oil is replaced by a freshly prepared first column.

Although I have described the embodiment of my apparatus in which an analyzing control means is used to switch the flow of carrier gas from the first partition column to the by-pass column, the switching of the flow at the proper point can also be accomplished without actually analyzing the effluent from the first column. After experience in analyzing a particular type of mixture, one can determine the time after introduction of the feed mixture at which the flow of carrier gas should be switched. For instance, when a gasoline fraction is analyzed for hydrocarbons in the C_4 - C_5 range, there will be normally a substantial period between the times at which the tail end of the last C_5 compound and the head end of the first C_6 compound emerge from the first column. These times will be known after experience with the particular type of mixture and therefore at any desired time during the period the flow of carrier gas can be switched from the first column to the by-pass column without the necessity of analyzing the effluent from the first column. The switching of valves at the predetermined time can be done manually or automatically by a timing device which actuates the valve operating means.

I have used a wide boiling range hydrocarbon mixture as an example of a mixture which can be separated or analyzed by the process of the invention. It should be understood, however, that the process can be applied advantageously to the separation or analysis of a great number of mixtures where it is desired to prevent the entry of the more strongly-held components of the mixture into the main chromatographic column.

In the example above I have described the use of the same granular material in the first column and in the principal column. It is within the scope of the invention to use any of the granular materials known in the art for use in partition chromatography. Furthermore, either the same or different solid materials can be used for the first column and the principal column.

As a general rule, the solid materials used for partition chromatography are non-porous, granular materials. Preferably they are not chromatographically active adsorbents, as otherwise the effects of adsorption chromatography and partition chromatography would be superimposed upon each other and this might prevent the obtaining of sharply defined fractions. The partitioning liquid, that is, the high boiling liquid which is coated on the granular material, can be the same in both columns or, advantageously, different liquids can be used. In the latter case a partitioning liquid adapted for the particular separation being carried out in each column can be selected. Samples of suitable partitioning liquids include dioctyl phthalate, dinonyl phthalate, dioctyl sebacate, paraffin wax, silicone fluids, etc.

The carrier fluid in the process of the invention preferably is a gas, although the principle of the invention extends to the use of a liquid carrier fluid, in which case the process would be a liquid-liquid partition chromatography process. A carrier liquid should be immiscible or partially immiscible with the partitioning liquid. Examples of suitable carrier gases include hydrogen, helium, nitrogen, etc. Preferably a low molecular weight carrier gas is used when the detecting means used for the process is a thermal conductivity cell.

In the foregoing description of the invention I have described a thermal conductivity cell with a recording potentiometer as a preferred means for analyzing the effluent from the principal column. However, other known continuous analyzers with similarly high sensitivity can also be used in the process and apparatus of the invention.

In the description above and in the claims I have referred to "heavy" components and "lighter" components

of the feed mixture and have indicated that the process of the invention prevents the fouling of the principal partition column by such heavy components. The terms heavy and light are used for convenience to distinguish between components of a mixture which move slowly through a partition column and those which move more rapidly. In most mixtures, for example, in mixtures of a homologous series of compounds, the light components or lower molecular weight components will pass more rapidly through a partition column than the heavy or higher molecular weight components. This may not be true, however, of some mixtures of compounds of different molecular types. Therefore it should be understood that, as used in this specification, a heavy component of a mixture is one which has a partition coefficient which favors retention of the component in the liquid phase of a partition column and results in slow movement of the component through the column while a light component is one which has a partition coefficient which favors its entry into the moving gas phase and thus results in more rapid movement of the component through the column.

Obviously many modifications and variations of the invention as hereinbefore set forth may be made without departing from the spirit and scope thereof and therefore only such limitations should be imposed as are indicated in the appended claims.

I claim:

1. A partition chromatography apparatus which comprises a first partition column and a parallel by-pass column, means to introduce a carrier gas into said parallel columns, a principal partition column in series with the first column and the by-pass column, means between said first column and said principal column for analyzing the effluent from said first column, valve means responsive to said analyzing means for switching the flow of carrier gas from said first column to said by-pass column on the appearance of a predetermined constituent in the effluent from the first column, means intermediate the valve means and the first column for introducing a fluid mixture to be analyzed, and means for analyzing the effluent from said principal column.

2. An apparatus for analysis of fluid mixtures which comprises a first partition column and, in parallel flow relation therewith, a by-pass column having substantially the same resistance to gas flow as said first column, a principal partition column, a thermal conductivity cell having channels for the flow of gas, a line for receiving a stream of carrier gas from a reference channel of said cell, said line having a bifurcation at the exit end thereof, one fork of which leads to said first column and the other fork of which leads to said by-pass column, a valve at said bifurcation automatically operable for switching the flow of carrier gas from the first column to the by-pass column, means to introduce the fluid mixture to be analyzed into the said one fork, effluent lines from each of said parallel columns, said lines joining to form an inlet line for said principal column, a valve at the juncture of said effluent lines automatically operable in coordination with said first mentioned valve for switching the flow into the principal column from the the first column to the by-pass column, an analyzing means in the effluent line from said first column between said column and the second mentioned valve, said analyzing means being operably connected with a valve control means adapted to operate said valves to switch the flow of carrier gas from said first column to said by-pass column when a predetermined substance is identified in the effluent from said first column, and an effluent line from said principal column which leads to a testing channel of said thermal conductivity cell.

3. In partition chromatography apparatus, a first partition column having an inlet and an outlet, a by-pass for the first column having an inlet and an outlet, said by-pass affording substantially the same resistance to the flow of

7

fluids therethrough as the first column, means for selectively directing a carrier fluid into the inlets of the first column and the by-pass, means for introducing a fluid mixture to be analyzed into carrier fluid selectively directed to the inlet of the first column, a principal partition column having an inlet and an outlet, means for selectively communicating the inlet of the principal column with the outlets of the first column and the by-pass, and means for analyzing the effluent from the outlet of the principal column.

5

8

References Cited in the file of this patent

UNITED STATES PATENTS

2,398,818 Turner ----- Apr. 23, 1946

OTHER REFERENCES

Gas Chromatograph II: N. H. Ray in Journal of Applied Chemistry, vol. 4, February 1954.

Article: Thermal Conductivity Gauge for Use in Gas Liquid Partition Chromatography, Ambrose et al., in Journal of Scientific Instruments, vol. 32, August 1955.

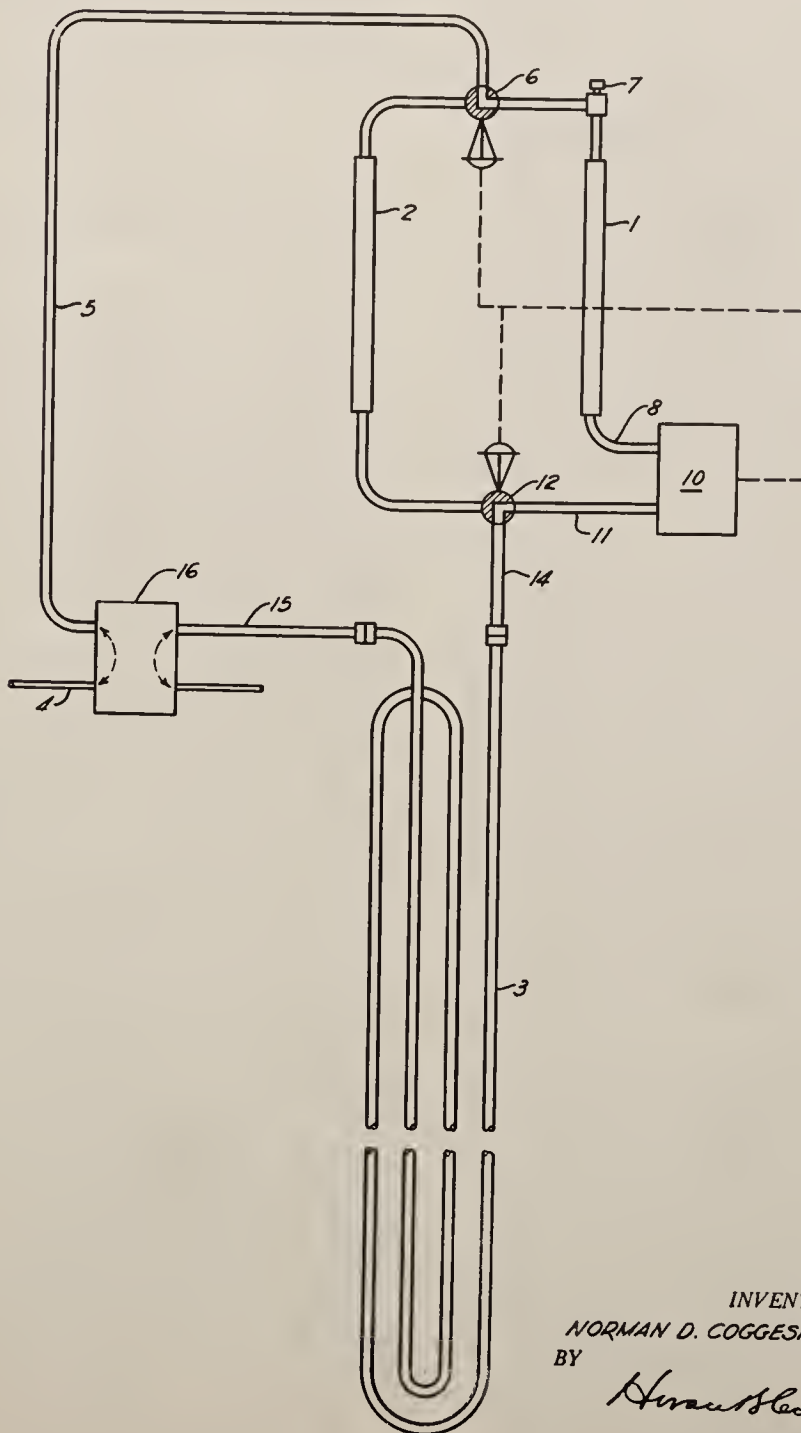
Sept. 27, 1960

N. D. COGGESHALL

Re. 24,876

MULTIPLE COLUMN CHROMATOGRAPHIC APPARATUS

Original Filed Dec. 16, 1955



INVENTOR.
NORMAN D. COGGESHALL
BY *Harold H. Cooke*
HIS ATTORNEY

1

24,876

MULTIPLE COLUMN CHROMATOGRAPHIC
APPARATUS

Norman D. Coggeshall, Penn Hills, Pa., assignor to Gulf
Research & Developing Company, Pittsburgh, Pa., a
corporation of Delaware

Original No. 2,868,011, dated Jan. 13, 1959, Ser. No.
553,571, Dec. 16, 1955. Application for reissue Dec.
28, 1959, Ser. No. 862,434

4 Claims. (Cl. 73—23)

Matter enclosed in heavy brackets [] appears in the
original patent but forms no part of this reissue specifi-
cation; matter printed in *italics* indicates the additions
made by reissue.

This invention relates to apparatus for separating fluid
mixtures and more particularly to multiple-column chro-
matographic apparatus whereby a fluid mixture is frac-
tionated by partition chromatography in order to identify
the components of the mixture.

It is known that the principles of partition chromatog-
raphy can be applied to the separation and analysis of
multi-component fluid mixtures (see, for example, the
article by N. H. Ray, Journal of Applied Chemistry,
vol. 4, page 21, February 1954). In a gas-liquid partition
chromatography a fluid mixture is separated by selec-
tively partitioning its components between a stationary
liquid phase and moving gas phase. The stationary liquid
phase is formed as a coating of a non-volatile solvent on
a column of granular solid material and the gas phase
is formed by flowing a carrier gas such as helium or
hydrogen through the column. The manner in which
the separation of a mixture is accomplished in partition
chromatography can be explained by considering first
what happens when a single pure compound is introduced
to one end of the partition chromatography column. The
compound will immediately partition itself into two por-
tions, one of which will be in solution in the stationary
liquid phase and the other of which will be in the gas
phase. When the flow of carrier gas is initiated it moves
that portion in the gas phase forward. As this occurs
there is a continual partitioning between the material
in the gas phase and that in the liquid phase. As a result
the pure material moves along the column but at a
slower speed than the carrier gas. The rate of move-
ment is dependent upon the partition coefficient. Dif-
ferent materials have different partition coefficients and
hence move at different speeds. This is the basis for
the separation by this technique. A complex mixture
of materials injected into the partition chromatography
column will separate into components moving at different
speeds so that, if the column is long enough the com-
ponents will emerge one by one from the column, usually
in the order of boiling points for a homologous series.

In analytical methods using the gas-liquid partition
chromatography technique the components of the mix-
ture which emerge successively from the partition column
are identified in various suitable ways. For example the
effluent from the column is passed through a thermal
conductivity cell connected with a recording poten-
tiometer. The plot of potentiometer deflection against
time provides a quantitative and qualitative analysis of
the components of the mixture.

Although the partition chromatography method of
analysis has proved to be valuable for many uses, it
does have disadvantages in certain separations. Thus,
if it is desired to analyze or to separate precisely only
those components of a multi-component mixture which
are readily removable from a partition chromatography

2

column, a considerable length of time may be required
to remove the remaining components of the mixture
from the column in order to restore it to its original con-
dition for the next cycle of analysis or separation. For
example, if it is desired to analyze precisely only the
 C_4 - C_6 hydrocarbons of a gasoline sample, these hy-
drocarbons can be carried through a long partition
chromatography column in a period of an hour or less.
However, to remove the rest of the gasoline range hydro-
carbons could require a period of many hours, for ex-
ample, 20 hours or more. If a crude oil is being an-
alyzed for light hydrocarbons, these components will
emerge from the column in a reasonably short time but
it may require many days to remove the rest of the crude
oil. As a practical matter it may be impossible to re-
move all of the heavy components of the crude with
carrier gas alone. Therefore, if a column used for such
separations is used in subsequent runs the heavier com-
ponents remaining in the column from previous runs will
continue to emerge slowly from the column and will
make it difficult or impossible to analyze accurately the
light components of the subsequent runs.

The apparatus of the present invention enables avoid-
ance of the problem referred to above and includes a
principal chromatographic partition column that can be
used for a large number of separations without becoming
fouled by heavy materials which would pass through the
same slowly.

The apparatus of the invention in general comprises
a first partition chromatography column, a parallel by-
pass column and a principal chromatographic column.
A line is provided for introducing carrier gas into the
system and this line has an automatically controlled
valve for directing the flow of carrier gas either to the
first column or to the by-pass column. The first column
is provided with means for introducing feed mixture and
a means for withdrawing the effluent from the column
for delivery to the principal chromatographic column. In
the preferred embodiment the inlet line to the principal
column is provided with a valve automatically operable
in coordination with the first mentioned valve for re-
ceiving flow from either the first column or from the by-
pass column. The effluent line from the first column
passes through gas analysis means adapted to operate the
valves to switch the flow of carrier gas from the first
column to the by-pass column upon the appearance of
predetermined substances in the effluent from the first
column. The principal chromatographic column is pro-
vided with an effluent line which passes through a thermal
conductivity cell.

Further understanding of the invention can be ob-
tained from the drawing, the sole figure of which shows
diagrammatically a preferred embodiment of the ap-
paratus used for analyzing fluid mixtures.

The apparatus of the drawing comprises a first parti-
tion column 1, a by-pass column 2 and the principal parti-
tion chromatographic column 3. Columns 1 and 2 are
arranged in parallel flow with respect to each other and
in series with the principal column 3. As the drawing
shows, the principal column 3 has greater capacity than
the first column. In the modification of the drawing it
is in the form of a long coiled tube.

Columns 1 and 3 are filled with a granular solid which
has a surface coating of a high boiling liquid. Column 2
may be filled with the same permeable solid material
or with any other packing that will provide the same
flow resistance as the material in column 1. A carrier
gas inlet line 4 passes the carrier gas through one of the
two gas channels of a thermal conductivity cell 16. The
gas then passes by line 5 to a diaphragm-operated valve
6 which is at a bifurcation in line 5. This valve directs
the carrier gas either to column 1 or to the by-pass col-

umn 2. Column 1 has a feed inlet which, in the apparatus of the drawing, is a serum cap 7 into which a mixture to be analyzed is injected with a hypodermic syringe.

Column 1 has an effluent line 8 for withdrawing the mixture of carrier gas and the lighter components of the feed mixture. In the apparatus shown in the drawing, line 8 passes through a gas analysis means 10. The analyzer 10 can be, for example, a thermal conductivity cell and recording potentiometer. In this case, an operator switches the flow of carrier gas from column 1 to column 2 by operating valves 6 and 12 when the recorder shows that a predetermined component of the feed mixture has emerged from column 1. In another modification of the invention, the analysis means 10 is an analyzing control means such as an infrared absorption spectrometer cell which can identify a particular component of the feed mixture and actuate a valve operating means when such component appears in the effluent from column 1. Line 11 from the gas analysis means passes the effluent of column 1 to valve 12. This is a diaphragm-operated valve for receiving flow from either column 1 or column 2 and directing such flow into line 14 which is the inlet means for the principal column 3.

As I have indicated, both valves 6 and 12 can be automatically operable valves. In the apparatus of the drawing, they are operated to switch the flow of carrier gas from the first column 1 to the by-pass column 2 in response to changes in the effluent from column 1 as detected by the analyzer 10. When a predetermined heavy component of the feed mixture which it is desired to keep out of column 3 appears in the effluent from column 1, the analyzer 10 passes a signal to an actuating means for the air-operated diaphragm valves. Also in accordance with the invention, instead of operating in response to the analyzer 10, valves 6 and 12 can be actuated manually or by a timing device at a predetermined time after introducing the feed mixture. This predetermined time can be at any point between the known time at which the last of the desired light components will be swept from the first column and the known time at which the first of the undesired heavy components will begin to emerge.

Valves 6 and 12 switch the flow of carrier gas from column 1 to column 2. Thereafter, carrier gas alone is passed into column 3 and it successively elutes the lighter components of the feed mixture. These materials emerge from column 3 via line 15 and pass through the testing channel of thermal conductivity cell 16. This cell is connected with a recording potentiometer, not shown in the drawing, which continuously plots potentiometer deflections against time. This plot can be used for a qualitative and quantitative analysis of the lighter components of the feed mixture.

Although thermal conductivity cells are well known in the art, a brief description of their operation can be given. The conventional thermal conductivity cell employs a Wheatstone bridge, two arms of which are heated platinum wires. One of the wires extends into a reference region through which a reference gas flows and the other extends into a testing region through which the gas being analyzed flows. In the process and apparatus of the invention the inlet stream of carrier gas flows through the reference region and the effluent stream from the chromatographic column, consisting of carrier gas and the components of the feed mixture that are eluted from the column, flows through the testing region. When a gas is in contact with a heated platinum wire of the cell, the wire is cooled to an extent that depends on the thermal conductivity of the gas, and, when the composition of the gas flowing through the testing region changes, its thermal conductivity changes and the temperature of the platinum wire changes correspondingly. As a result of the temperature change of the wire its electrical resistance changes. The variations in the difference between the resistances of the platinum wires in the testing

and reference regions are reflected in the unbalance of the Wheatstone bridge as indicated by a recording potentiometer. The recorded deviations can be related to the composition of the gas being analyzed.

I have mentioned above that in a preferred embodiment of the apparatus the by-pass column is a column packed with granular material in such a manner that its resistance to gas flow is substantially equal to that of the first column. This is important when a thermal conductivity cell is used as the means for analyzing the effluent from the principal column because it insures that the pressure of the carrier gas at the inlet to the principal chromatographic column will not change substantially when the carrier gas flow is switched from the first column to the by-pass column. Thermal conductivity cells are sensitive to changes in flow rates and to obtain uniform results from the cell, the flow rate of carrier gas through the principal column and therefore its pressure at the inlet to the column should be kept substantially constant.

A further understanding of the invention can be obtained from the following illustrative example of the process of the invention.

EXAMPLE

A Kuwait crude oil having an API gravity of 32, a 10 percent boiling point of 280° F. and a 70 percent point of 655° F. is analyzed for light ends in an apparatus as illustrated in the drawing. The purpose is to identify qualitatively and quantitatively the lower molecular weight hydrocarbons in the oil, that is to say, the C₆ and lower hydrocarbons. The chromatographic columns are filled with granular kieselguhr. In the principal chromatographic column, column 3 of the drawing, the partitioning liquid which coats the kieselguhr is dioctyl phthalate. In the first column, column 1 in the drawing, the kieselguhr is coated with paraffin wax. The by-pass column 2 is also filled with granular kieselguhr but this body of granular material is not coated with a liquid. However, its resistance to gas flow is substantially equal to that of the body of granular material in column 1. At the start of the process, the carrier gas, helium, is flowed through the first column 1 and the principal column 3 at room temperature. A uniform temperature for the entire apparatus including the chromatographic columns and the detecting means is maintained by the use of a constant temperature air bath. The principal chromatographic column, 3, for this separation is a coiled stainless steel tube 14 feet in length and having an inside diameter of 4.5 mm. The primary column and the by-pass column are similar tubes, each having a length of 3 feet. A charge of the order of 0.08 gram of the crude oil to be analyzed is introduced by a hypodermic syringe into the rubber serum bottle cap which serves as the feed inlet for the first column. In accordance with the principles of partition chromatography, the more volatile components of the crude oil begin to emerge successively from the primary column from whence they pass through a gas analyzing means and then into the principal chromatographic column. The gas analyzer is set to detect the first emergence of hydrocarbons of more than 6 carbon atoms. When the detecting apparatus indicates the first heptanes in the effluent from the primary column, a valve control means automatically operates the diaphragm valves 6 and 12 to switch the flow of carrier gas from the first column to the by-pass column 2. The light constituents of the charge mixture are then successively swept from the principal chromatographic column 3 by the carrier gas. The thermal conductivity cell 16 and its recording potentiometer provide a quantitative and qualitative analysis of the emerging light components of the crude oil charge. The introduction of C₇ and heavier hydrocarbons which move very slowly through a partition chromatography column is avoided. The light hydrocarbons are completely removed from the principal column 3 by the carrier gas and the column can then be

used for another run. The first column 1 containing the heavy ends of the crude oil is replaced by a freshly prepared first column.

Although I have described the embodiment of my apparatus in which an analyzing control means is used to switch the flow of carrier gas from the first partition column to the by-pass column, the switching of the flow at the proper point can also be accomplished without actually analyzing the effluent from the first column. After experience in analyzing a particular type of mixture, one can determine the time after introduction of the feed mixture at which the flow of carrier gas should be switched. For instance, when a gasoline fraction is analyzed for hydrocarbons in the C_4 - C_5 range, there will be normally a substantial period between the times at which the tail end of the last C_5 compound and the head end of the first C_6 compound emerge from the first column. These times will be known after experience with the particular type of mixture and therefore at any desired time during the period the flow of carrier gas can be switched from the first column to the by-pass column without the necessity of analyzing the effluent from the first column. The switching of valves at the predetermined time can be done manually or automatically by a timing device which actuates the valve operating means.

I have used a wide boiling range hydrocarbon mixture as an example of a mixture which can be separated or analyzed by the process of the invention. It should be understood, however, that the process can be applied advantageously to the separation or analysis of a great number of mixtures where it is desired to prevent the entry of the more strongly-held components of the mixture into the main chromatographic column.

In the example above I have described the use of the same granular material in the first column and in the principal column. It is within the scope of the invention to use any of the granular materials known in the art for use in partition chromatography. Furthermore, either the same or different solid materials can be used for the first column and the principal column.

As a general rule, the solid materials used for partition chromatography are non-porous, granular materials. Preferably they are not chromatographically active adsorbents, as otherwise the effects of adsorption chromatography and partition chromatography would be superimposed upon each other and this might prevent the obtaining of sharply defined fractions. The partitioning liquid, that is, the high boiling liquid which is coated on the granular material, can be the same in both columns or, advantageously, different liquids can be used. In the latter case a partitioning liquid adapted for the particular separation being carried out in each column can be selected. Samples of suitable partitioning liquids include dioctyl phthalate, dinonyl phthalate, dioctyl sebacate, paraffin wax, silicone fluids, etc.

The carrier fluid in the process of the invention preferably is a gas, although the principle of the invention extends to the use of a liquid carrier fluid, in which case the process would be a liquid-liquid partition chromatography process. A carrier liquid should be immiscible or partially immiscible with the partitioning liquid. Examples of suitable carrier gases include hydrogen, helium, nitrogen, etc. Preferably a low molecular weight carrier gas is used when the detecting means used for the process is a thermal conductivity cell.

In the foregoing description of the invention I have described a thermal conductivity cell with a recording potentiometer as a preferred means for analyzing the effluent from the principal column. However, other known continuous analyzers with similarly high sensitivity can also be used in the process and apparatus of the invention.

In the description above and in the claims I have referred to "heavy" components and "light" components of the feed mixture and have indicated that the process of the invention prevents the fouling of the principal parti-

tion column by such heavy components. The terms heavy and light are used for convenience to distinguish between components of a mixture which move slowly through a partition column and those which move more rapidly. In most mixtures, for example, in mixtures of a homologous series of compounds, the light components or lower molecular weight components will pass more rapidly through a partition column than the heavy or higher molecular weight components. This may not be true, however, of some mixtures of compounds of different molecular types. Therefore it should be understood that, as used in this specification, a heavy component of a mixture is one which has a partition coefficient which favors retention of the component in the liquid phase of a partition column and results in slow movement of the component through the column while a light component is one which has a partition coefficient which favors its entry into the moving gas phase and thus results in more rapid movement of the component through the column.

Obviously many modifications and variations of the invention as hereinbefore set forth may be made without departing from the spirit and scope thereof and therefore only such limitations should be imposed as are indicated in the appended claims.

I claim:

1. A partition chromatography apparatus which comprises a first partition column and a parallel by-pass column, means to introduce a carrier gas into said parallel columns, a principal partition column in series with the first column and the by-pass column, means between said first column and said principal column for analyzing the effluent from said first column, valve means responsive to said analyzing means for switching the flow of carrier gas from said first column to said by-pass column on the appearance of a predetermined constituent in the effluent from the first column, means intermediate the valve means and the first column for introducing a fluid mixture to be analyzed, and means for analyzing the effluent from said principal column.

2. An apparatus for analysis of fluid mixtures which comprises a first partition column and, in parallel flow relation therewith, a by-pass column having substantially the same resistance to gas flow as said first column, a principal partition column, a thermal conductivity cell having channels for the flow of gas, a line for receiving a stream of carrier gas from a reference channel of said cell, said line having a bifurcation at the exit end thereof, one fork of which leads to said first column and the other fork of which leads to said by-pass column, a valve at said bifurcation automatically operable for switching the flow of carrier gas from the first column to the by-pass column, means to introduce the fluid mixture to be analyzed into the said one fork, effluent lines from each of said parallel columns, said lines joining to form an inlet line for said principal column, a valve at the juncture of said effluent lines automatically operable in coordination with said first mentioned valve for switching the flow into the principal column from the first column to the by-pass column, an analyzing means in the effluent line from said first column between said column and the second mentioned valve, said analyzing means being operably connected with a valve control means adapted to operate said valves to switch the flow of carrier gas from said first column to said by-pass column when a predetermined substance is identified in the effluent from said first column, and an effluent line from said principal column which leads to a testing channel of said thermal conductivity cell.

3. In partition chromatography apparatus, a first partition column having an inlet and an outlet, a by-pass for the first column having an inlet and an outlet, said by-pass affording substantially the same resistance to the flow of fluids therethrough as the first column, means for selectively directing a carrier fluid into the inlets of the first column and the by-pass, means for introducing a fluid

mixture to be analyzed into carrier fluid [selectively] directed to the inlet of the first column, a principal partition column having an inlet and an outlet, means for selectively communicating the inlet of the principal column with the outlets of the first column and the by-pass, and means for analyzing the effluent from the outlet of the principal column.

4. In partition chromatography apparatus, a first partition column having an inlet and an outlet, a by-pass for the first column having an inlet and an outlet, means for selectively directing a carrier fluid into the inlets of the first column and the by-pass, means for introducing a fluid mixture to be analyzed into carrier fluid directed to the inlet of the first column, a principal partition column having an inlet and an outlet, means for selectively communicating the inlet of the principal column with the outlets of the first column and the by-pass, and means

for analyzing the effluent from the outlet of the principal column.

References Cited in the file of this patent
or the original patent

UNITED STATES PATENTS

2,398,818 Turner ----- Apr. 23, 1946

OTHER REFERENCES

- 10 Article: Thermal Conductivity Gauge for Use in Gas Liquid Partition Chromatography, Ambrose et al., in Journal of Scientific Instruments, vol. 32, August 1955.
Gas Chromatography II: N. H. Ray in Journal of Applied Chemistry, vol. 4, February 1954.
- 15 Article: Chromatographic Analysis of Hydrocarbon Mixtures by Bradford et al., published in Journal of Institute of Petroleum, vol. 41, 1955, pages 80-87.

Ionization of *n*-Paraffin Molecules

NORMAN D. COGGESHALL

Reprinted from THE JOURNAL OF CHEMICAL PHYSICS, Vol. 30, No. 2, pp. 595-596, February, 1959

Ionization of *n*-Paraffin Molecules

NORMAN D. COGGESHALL

Gulf Research and Development Company, Pittsburgh, Pennsylvania

(Received August 25, 1958)

THE purpose of this note is to show that the mass spectral patterns of *n*-paraffins as predicted by an extension of the Lennard-Jones and Hall¹ theory of molecular orbitals do not agree with experiment.

Lennard-Jones and Hall have provided a method of calculating the molecular orbital coefficients for *n*-paraffins. The molecular orbital energy values are given by the solutions of the following equation:

$$\begin{vmatrix} c+2e \cos 2\theta - E & \sqrt{2}d \cos \theta \\ \sqrt{2}d \cos \theta & a+b-E \end{vmatrix} = 0 \dots, \quad (1)$$

where $\theta = r\pi/2s$, $r=1, 2, \dots, s$; s =number of carbon atoms in the molecule. After the energies are calculated the coefficients in the expansion of the molecular orbitals of the paraffin in terms of equivalent CC orbitals are,

$$R_{2n} = R \sin 2nr\pi/2s \dots, \quad (2)$$

where R is a constant.

The values in electron volts of the parameters which can be applied to any paraffin are, $(a+b)=-12$, $c=-12.978$, $e=-1.458$, and $d=-0.698$.

Lennard-Jones and Hall reasoned that when a molecule is ionized the resultant positive charge is distributed according to the molecular orbital of the electron which is removed. Therefore, the square of the molecular orbital gives the distribution of net positive charge when an electron is removed from an otherwise uniform distribution.

It has been postulated² that there is a relation between these net positive charge distributions and the manner in which a molecule ion fragments to produce its mass spectrum. The reasoning is that the probability of dissociation of a particular CC bond is dependent on the concentration of net positive charge which weakens the bond. The value of E chosen for the calculation of the coefficients is the lowest ionization potential as calculated from Eq. (1).

The extension of the Lennard-Jones and Hall theory may be compared to the experimental mass spectra of the paraffins. The procedure is as follows: (a) The lowest ionization potential yielded by Eq. (1) is determined. This sets the corresponding value of r . (b) The values of R_{2n} from Eq. (2) are calculated using the value of r from (a) and varying n . (c) The values of R_{2n} from (b) are squared to provide the net positive charge for each CC bond. (d) Relative probability of fragmentation values are obtained by taking twice the $(R_{2n})^2$ values from (c) except when the

value of n corresponds to the center of the molecule. (e) The relative probability of fragmentation values from (d) are then compared directly with the distribution of ions as experimentally observed in the mass spectrum.

When the values of the parameters are used, Eq. (1) may be rewritten in the form,

$$2E = -(22.6 + 5.83 \cos^2 \theta) \pm \{3.73 + (34.01 \cos^2 \theta - 18.71) \cos^2 \theta\}^{1/2} \dots \quad (3)$$

Examination of this equation shows that the lowest ionization potential is obtained for the smallest allowable value of $\cos^2 \theta$. This therefore specifies the value of $r=s-1$ for application of this procedure for all *n* paraffins. We may use this in Eq. (2) for R_{2n} and the net positive charge on each successive CC bond, starting from the end of the molecule is, after simplification of Eq. (2), therefore proportional to,

$$\sin^2(n\pi/s) \quad n=1, 2, \dots \text{to center of molecule.}$$

With the above assumptions, this theory would therefore predict that the intensity of the ions of *n* carbon atoms in the mass spectrum of an *n*-paraffin of *s* carbon atoms would be proportional to $2 \sin^2 n\pi/s$. This would have its maximum value for $n=s/2$ or $(s-1)/2$ depending on whether *s* is even or odd. This would then predict that the ion peaks would progressively increase from a value for a single carbon ion to a maximum for ions of $(s-2)/2$ or $(s-1)/2$ carbon atoms. In other words, the most abundant ions would be those of approximately one-half the molecular weight of the parent molecule.

This is contrary to well-established experimental evidence. It is well known from the mass spectra of *n*-paraffins in the C_7 to C_{26} range³ that the probability of C—C bond rupture is small for the bonds at the ends; it increases to a maximum for the third or fourth C—C bond from the ends and then decreases for bonds further from the ends. It is believed only fortuitous that the extension of Lennard-Jones and Hall's theory to *n* octane produces approximate agreement with experiment.

The author expresses gratitude to Dr. G. F. Crable and Professor Robert G. Parr for discussions on this subject and for checking through the steps presented.

¹ J. Lennard-Jones, and G. G. Hall, *Trans. Faraday Soc.* **48**, 581 (1952).

² F. H. Field, and J. L. Franklin, *Electron Impact Phenomena* (Academic Press, Inc., New York, 1957), p. 171.

³ Mass Spectral Data, American Petroleum Institute Project 44, Carnegie Institute of Technology, Pittsburgh, Pennsylvania.

LANCASTER PRESS, INC., LANCASTER, PA.

Concentration of Impurities from Organic Compounds by Progressive Freezing

Joseph S. Matthews and Narman D. Caggeshall, Gulf Research & Development Co., Pittsburgh, Pa.

OFTEN it is necessary to determine trace amounts of impurities in organic compounds. Mass spectrometry and ultraviolet or infrared spectroscopy have limits of sensitivity and are not always applicable. The usual procedure, when concentrations are low, is to concentrate the impurities by distillation or extraction prior to instrumental analysis. These methods have certain limitations.

Crystallization by fractional freezing, fractional melting, or zone melting techniques has come to the fore as a means of obtaining ultrahigh purity. Starting with Schwab and Wichers (9, 10) various workers have shown that such methods may be used to purify organic compounds (1, 2, 4-6, 8). Goodman (3) suggested that they might also be used to concentrate impurities that occur in high dilution. In 1957 Schildknecht and Mannl (7) concentrated small quantities of biological material from aqueous solution by zone melting the frozen solution. Progressive freezing can conveniently be used to concentrate impurities from organic liquids.

APPARATUS

The apparatus consists of a lowering mechanism and a cooler. The lowering mechanism is a small synchronous motor with a speed of 1800 r.p.m., geared down through a worm drive which passes the torque on to a ball and disk integrator that serves as a variable speed reducer. The ball cage of the integrator is attached to a calibrated micrometer screw, so that the ball can be moved across the face of the disk to vary the output speed. The torque from the speed reducer is transferred through a worm drive to the output shaft, which can be regulated between 0.25 and 2.87 revolutions per hour. A spirally grooved drum attached to the output shaft carries a very thin metal cable for lowering the sample tube into the cooling bath. The range of speeds at which the cable is unwound can be controlled by the size of the cable drum. With a drum of 1-inch diameter, the speed of the cable can be regulated between 4 and 16 cm. per hour.

Attached to the end of the cable is a

wire frame which holds the sample tube and allows it to be stirred while being lowered into the cooling bath. The stirrer motor remains in a fixed position. The top of the sample tube is closed by a rubber stopper fitted with a Teflon sleeve to serve as a bearing for the stirrer shaft.

The cooling bath consists of a copper pipe, 2 inches in outside diameter by 14 inches long, insulated on the outside with glass fiber pipe insulation, and cooled by circulating acetone cooled by a dry ice-acetone bath. The temperature is regulated by adjusting the coolant flow rate. The coolant is maintained at a constant level by an overflow through which the circulating acetone returns to a reservoir.

frozen is lowered into the freezing bath, while the unfrozen part is stirred by a motor-driven glass stirrer. The tube is lowered until 1 ml. or less of liquid remains unfrozen at the top of the tube. If all the liquid solidifies, a small amount is melted. The liquid is withdrawn with a long dropper pipet, transferred to a vial, weighed, and analyzed. After removal of the fraction, the tube contents are melted and the cycle is repeated if desired.

Several parameters were studied: effect of stirring, lowering speed, temperature of cooling, and size of fraction removed, and effect of impurity concentration on efficiency of separation of impurities.

EXPERIMENTAL

The tube containing the liquid to be

RESULTS AND DISCUSSION

Stirring was necessary for increasing

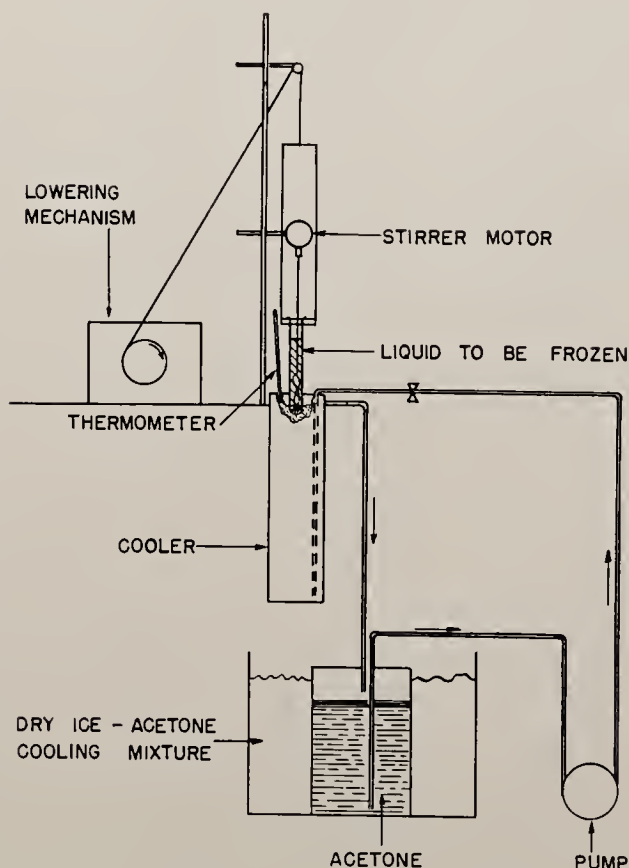


Figure 1. Freezing apparatus

the efficiency of separation; without stirring impurity concentration was only slightly enhanced. Slower lowering speeds were more efficient than faster. Variations of 10° in the cooling temperature had little effect on the efficiency of concentration. Removing relatively small samples (1/40 to 1/60 of charge) obtained higher impurity concentrations in the samples removed. This takes advantage of the impurity distribution in a liquid which is progressively frozen. This process, however, is best suited for low initial concentrations of impurities, as efficiency decreases as impurity concentration increases.

The primary purpose of these studies is the concentration of impurities for identification.

In the identification of impurities in a sample of reagent grade benzene, benzene containing 0.25 weight % impurities was placed in a tube 28 mm. in inside diameter and stirred while being lowered at 5 cm. per hour into the freezing bath at -25° C. As a preliminary concentration step, a large (20%) fraction was removed from the first cycle of the benzene charge. Analysis showed that it contained 65% of the total impurities in the charge. This fraction was then recycled in a tube 22 mm. in inside diameter and about 1 gram was removed and analyzed. This small fraction contained 44% of the impurities present at the start of the cycle and the concentration of impurities had been raised to 5.14 weight %, equal to a 20-fold increase over the original concentration of impurities.

Analysis of the initial benzene charge revealed no detectable quantities of C₇ paraffins or C₈ and C₉ aromatics (Table I). The small sample removed from the second cycle, however, reveals that all these were present in the original charge, although at undetectable concentrations. As the material balance for the over-all experiment was

Table I. Concentration of Impurities in Reagent Grade Benzene

	First Cycle		Second Cycle		Calcd. Initial Concn., Wt. %
	Initial charge	1st fraction	Charge	1st fraction	
Weight, g.	73.3315	14.3033	13.6777	0.9487	...
Impurities, wt. %	0.25	0.81	0.81	5.14	...
Impurity composition, wt. %					
Toluene	0.05	0.22	...	1.25	0.06
Minimum C ₆ cyclics and/or mono-olefins	0.06	0.27	...	1.46	0.07
Minimum C ₇ cyclics and/or mono-olefins	0.03	0.13	...	0.66	0.03
Minimum C ₆ paraffins	0.11	0.19	...	0.45	0.02
Minimum C ₇ paraffins	0.00	0.00	...	1.29	0.06
C ₈ aromatics	0.00	0.00	...	0.01	0.0005
C ₉ aromatics	0.00	0.00	...	0.02	0.001

98.8%, it is possible to calculate the concentration for these groups in the original charge stock. It is assumed that in the concentration procedure all impurities are affected equally—i.e., the relative composition of the mixed impurities remains the same and no impurity is concentrated preferentially. On this basis, the calculated concentrations for C₈ and C₉ aromatics in the initial charge are about 0.0005 and 0.001 weight %, respectively. This explains why these groups were not detected in the initial charge by mass spectrometry.

The C₇ paraffins are calculated to be at an initial concentration of 0.06 weight %, but they are not detected in the initial charge, because the parent mass spectral peak for the C₇ paraffins ($m/e = 100$) is masked by the mercury peak ($m/e = 100$) when the C₇ paraffin concentrations are low. (Mercury is present, because of its use in the sample introduction system of the spectrometer.) However, progressive freezing raised the concentration of the C₇ paraffins to a level where the peak was distinct and easily measured. The parent peak for the C₆ paraffins was contributed to by the undetected C₇ paraffins; this explains why the calculated value

for the C₆ paraffins is much lower than what was found. The total of the impurity concentrations calculated to be initially present in the charge (excluding the very low values for C₈ and C₉ aromatics) is 0.24%, while that actually found in the initial charge is 0.25%.

ACKNOWLEDGMENT

The authors thank the Geophysical Development Division, Gulf Research & Development Co., for the design and construction of the lowering mechanism.

LITERATURE CITED

- (1) Dickinson, J. D., Eaborn, C., *Chem. & Ind. (London)* 1956, 959.
- (2) Glasgow, A. R., Ross, G., *J. Research Natl. Bur. Standards* 57, 137 (1956).
- (3) Goodman, C. H. L., *Research* 7, 177 (1954).
- (4) Handley, R., Herington, E. F. G., *Chem. & Ind. (London)* 1956, 304.
- (5) Herington, E. F. G., Handley, R., Cook, A. J., *Ibid.*, 1956, 292.
- (6) Rock, H., *Naturwissenschaften* 43, 81 (1956).
- (7) Schildknecht, H., Mannl, A., *Angew. Chem.* 69, 634 (1957).
- (8) Schumacher, E. E., *J. Metals* 5, 1428 (1953).
- (9) Schwab, F. W., Wichers, E., *J. Research Natl. Bur. Standards* 25, 747 (1940).
- (10) *Ibid.*, 32, 253 (1944).

Coggeshall

July 7, 1959

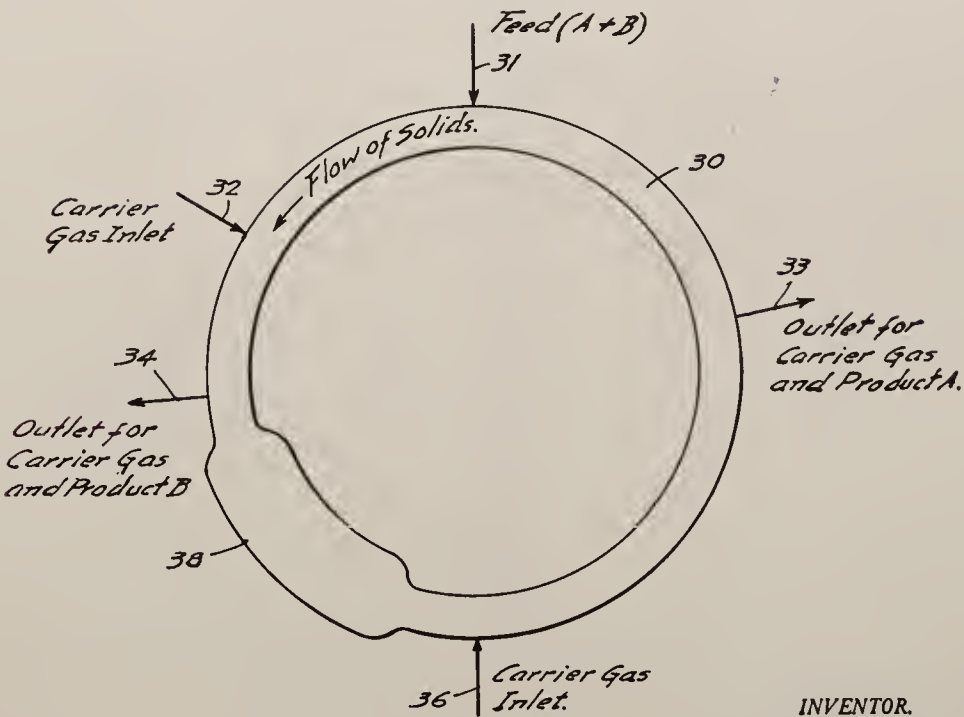
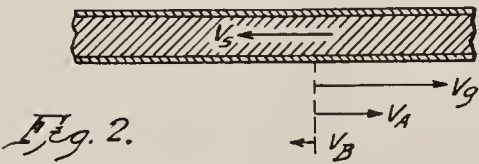
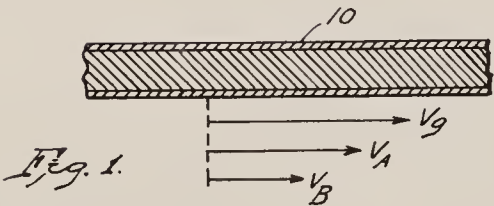
N. D. COGGESHALL

2,893,955

CONTINUOUS SEPARATION PROCESS

Filed May 11, 1956

2 Sheets-Sheet 1



INVENTOR.

Norman D. Coggeshall.

BY

Attorney

July 7, 1959

N. D. COGGESHALL
CONTINUOUS SEPARATION PROCESS

2,893,955

Filed May 11, 1956

2 Sheets-Sheet 2

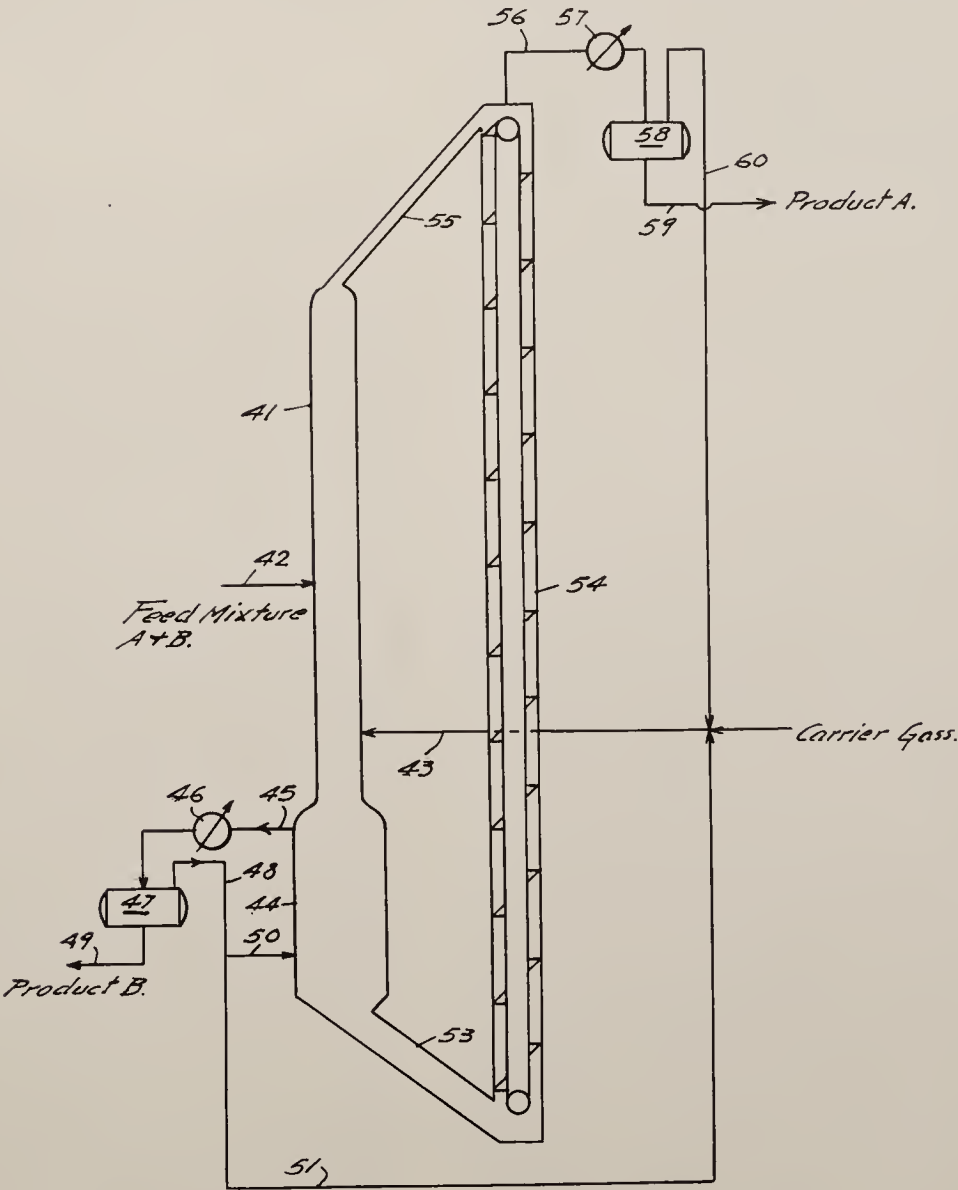


Fig. 4.

INVENTOR.
Norman D. Coggeshall.
BY
Dana H. Hootch
ATTORNEY

CONTINUOUS SEPARATION PROCESS

Norman D. Coggeshall, Verona, Pa., assignor to Gulf Research & Development Company, Pittsburgh, Pa., a corporation of Delaware

Application May 11, 1956, Serial No. 584,367

7 Claims. (Cl. 208—310)

This invention relates to a method of separating fluid mixtures and more particularly to a method in which a fluid mixture stream is continuously separated by partition chromatography.

It is known that the principles of partition chromatography can be applied to the batch separation of fluid mixtures. See for example, the article by D. H. Lichtenfels et al., *Analytical Chemistry*, volume 27, Number 10, October 1955, pages 1510-13. This article describes the separation of a fluid mixture by gas-liquid partition chromatography for analytical purposes. In the method described a sample of a volatile mixture to be separated and analyzed is injected into the end of a narrow column packed with an inert, granular material on which has been deposited a coating of a high boiling organic liquid such as dioctyl phthalate. The column is then eluted with an inert carrier gas such as helium or nitrogen. The individual components of the volatile mixture to be analyzed partition between a gas phase in the vapor space between particles and a liquid phase absorbed in the high boiling organic solvent coating of the particles. This causes the components of the mixture to move forward with individual velocities which are less than that of the carrier gas. The velocity with which a particular component moves is dependent upon its partition coefficient which, for a compound injected into a gas-liquid partition chromatography column can be defined as the ratio of the concentration of the compound in the stationary liquid phase to its concentration in the moving gas phase. Since the partition coefficient varies for different compounds, the components of the mixture move through the column at different speeds and, if the column is long enough, the components emerge one by one from the column, usually in the order of boiling points for a homologous series. In the analytical procedure described in the above article the separated components are detected as they emerge from the partition column by means of a thermal conductivity cell.

The batch separation of fluid mixtures by partition chromatography has proved to be valuable for analytical purposes. I have now discovered a method and an apparatus by means of which the principles of gas-liquid partition chromatography can be used for continuous separation of a fluid mixture stream. My apparatus and process can be used for continuous analysis or for the continuous recovery of desired products from a fluid mixture. The process of my invention in general comprises flowing in a cyclic path a stream of solid particles coated with a partitioning liquid, introducing a stream of fluid feed mixture to be separated into said stream of solid particles and introducing a first stream of carrier gas into the flowing stream of solid particles at a point in the cyclic path downstream from the point of introduction of the feed mixture whereby a portion of the carrier gas flows countercurrently to the flowing stream of particles and another portion flows concurrently therewith, the rate of flow of the stream of solid particles being selected in relation to the partition coefficients of components of the feed mix-

ture and in relation to the carrier gas countercurrent flow rate so that one component of the feed mixture of relatively low partition coefficient is caused to move with the carrier gas countercurrently to the direction of flow of the stream of solid particles and another component of higher partition coefficient is caused to move in the opposite direction concurrently with the stream of solid particles. At a point further along the cyclic path of solid particles flow a gaseous stream comprising carrier gas is withdrawn from the stream of solid particles. Still further along the path of solid particles flow a second stream of carrier gas is introduced into the stream of solid particles whereby a portion thereof flows countercurrently to the stream of solid particles and is withdrawn from the stream of solid particles with said component of higher partition coefficient at the last-mentioned point of withdrawal of a gaseous stream and another portion of said second stream of carrier gas flows concurrently with the stream of solid particles. Between the point of introduction of the second stream of carrier gas and the point of introduction of the feed mixture another gaseous stream comprising carrier gas and the component of the feed mixture having a relatively low partition coefficient is withdrawn from the stream of solid particles.

An apparatus of my invention in which my process can be carried out comprises in general an elongated chamber adapted for flow therethrough (preferably gravity flow) of a stream of solid particles coated with a partitioning liquid and means for conveying the stream of solid particles from the lower end of said chamber to the upper end thereof, the elongated chamber and the conveying means thereby forming a continuous cyclic path for flow of the stream of solid particles. The cyclic path is provided with inlet and outlet conduits for fluid streams comprising a feed inlet means, at least two gas inlets and at least two gas outlets. Along said cyclic path each gas inlet is followed by a gas outlet and each gas outlet is followed by a gas inlet whereby there is concurrent flow of carrier gas and solid particles in each section of the cyclic path following a gas inlet and before a gas outlet and countercurrent flow in each section following a gas outlet and before a gas inlet. In the preferred apparatus of the invention the feed inlet means is positioned in a section of countercurrent flow of carrier gas and solid particles of the cyclic path and an enlarged cross-sectional area of the elongated chamber is provided in the countercurrent section next after the countercurrent section in which the feed inlet is positioned.

To describe further the process and apparatus of the invention reference will be made to the drawings, of which Figures 1 and 2 are vector diagrams of velocities and directions of flow in the separation of a two-component mixture by partition chromatography with a stationary bed and a moving bed of solid particles respectively. Figure 3 is a highly schematic flow diagram of my continuous, moving bed process and Figure 4 is a diagrammatic illustration of one form of apparatus of my invention.

I have explained above that a mixture of fluids injected into a partition chromatography column will separate in components moving at different speeds through the column because of their differences in partition coefficients. The partition coefficient of a compound is the ratio of its concentration in the liquid phase formed as a coating on the solid particles of the partition column to its concentration in the gas phase formed by the carrier gas flowing through the column. The process of the invention uses a moving stream of solid particles coated with a partitioning liquid and relies on the fact that the components of a mixture flow through a partition chamber at different velocities depending on their parti-

tion coefficients, whereby to cause one component of the mixture to move in the direction of flow of the carrier gas and countercurrently to the direction of flow of the solid particles and another component to move in the opposite direction with the moving solid particles. Figures 1 and 2 illustrate this phenomenon vectorially. In Figure 1, numeral 10 designates a partition chamber containing a stationary body of liquid-coated solid particles. The vector V_g represents the direction and velocity of movement of a carrier gas flowing through the partition chamber. V_A represents the direction and velocity of movement of a component A of a binary fluid mixture of compounds A and B that is introduced into the chromatographic chamber. V_B represents the direction and velocity of compound B of the feed mixture.

Figure 2 shows vectorially the result of moving the body of solid particles countercurrently to the direction of carrier gas flow and at a velocity V_B which is opposite in direction to V_A and V_B and numerically less than V_A but greater than V_B . The result is that compound A continues to move in the direction of the carrier gas but at an absolute velocity which is less than its original velocity as shown in Figure 1 by the amount of the negative velocity of the moving stream of solid particles. Compound B reverses its direction of flow and flows in the direction of the flow of the stream of moving particles at a velocity equal to the algebraic difference between its original velocity V_B and the velocity of the moving stream of solid particles.

In accordance with my invention I take advantage of the phenomenon discussed above to separate continuously a mixture such as a mixture of compounds A and B whereby compound A is continuously removed from the separation system at one point and compound B at another point. Figure 3 shows in a highly diagrammatic manner the flow of my process. The annulus 30 represents the cyclic path of a moving stream of solid particles coated with a non-volatile partitioning solvent. The solid particles and the partitioning liquid can be any of the materials which are known for use in fixed bed partition chromatographic columns. For example, the solid particles can be granular kieselguhr. The partitioning liquid can be a high boiling point organic solvent such as dinonyl phthalate. In the process of the invention the stream of solid particles coated with partitioning liquid is caused to circulate, for example, in a counterclockwise direction in the flow diagram of Figure 3, by any suitable procedure for causing cyclic flow of particulate solids. Specific ways of providing this flow will be described in more detail hereinafter.

In accordance with the invention a feed mixture of compounds A and B is continuously introduced into the body of solid particles by means of feed inlet 31. A carrier gas such as nitrogen is introduced at carrier gas inlet 32. The stream of solid particles is flowed in a counterclockwise direction at a velocity relative to the velocities of compounds A and B under the impetus of the carrier gas at its particular clockwise velocity between 31 and 32 whereby to cause component A, the compound of lower partition coefficient of the two components, to move in a clockwise direction with carrier gas while component B, the compound of higher partition coefficient, moves counterclockwise with the stream of solid particles, in accordance with the principle suggested above in connection with Figures 1 and 2.

The carrier gas entering via inlet line 32 flows in two directions. One portion flows clockwise and countercurrently to the direction of flow of the stream of solid particles, carrying with it compound A of the feed mixture. Another portion flows counterclockwise in the direction of flow of the stream of solid particles. The portion of carrier gas flowing in a clockwise direction is withdrawn at the carrier gas and product outlet 33 carrying with it substantially all of compound A of the feed mixture. The other portion of carrier gas introduced via

line 32 is withdrawn substantially entirely via carrier gas and product outlet 34, carrying with it a portion of the more difficultly removable compound B.

A second stream of carrier gas is introduced to the system via carrier gas inlet 36. A portion of this carrier gas flows in a clockwise direction and is withdrawn through outlet 34 carrying with it the remainder of compound B. The other portion of the carrier gas introduced at inlet 36 flows in a counterclockwise direction and is withdrawn at outlet 33. In order to insure complete removal of the more difficultly removable compound B from the partitioning solids, the difference between the velocities of the streams of solid particles and the countercurrently flowing carrier gas between outlet 34 and inlet 36 can be increased. This can be done either by reducing the velocity of the solid stream in the specified interval or by increasing the velocity of the carrier gas or by doing both of these things. The velocity of the solids can be reduced by passing the stream of solids through a chamber of increased cross-sectional area as shown at 38 in the drawing, thereby reducing the linear velocity of the stream. The carrier gas introduced via inlet 36 can be introduced at a greater velocity than the carrier gas introduced at inlet 32.

The discussion above in connection with Figure 3 explains in general the flow of the various streams in my process and the selection of velocities for the solid particles and the carrier gas streams to provide a separation of compounds having different partition coefficients. Figure 4 shows diagrammatically a specific apparatus of my invention in which the process of my invention can be carried out, showing more particularly a specific means for providing continuous flow for a stream of solid particles and such commercially important features as means for recovering carrier gas from the product streams for return to the separation system.

The separation apparatus of Figure 4 comprises a main partition chromatographic chamber 41 which is arranged for gravity flow therethrough of the stream of solid particles coated with a partitioning liquid. At an intermediate point of the chamber 41 a feed inlet line 42 for the fluid mixture of A and B to be separated is provided. Below the feed inlet 42 a carrier gas inlet 43 enters the chamber. Below the carrier gas inlet 43 the cross-sectional area of chamber 41 is enlarged in section 44 thereof. At the upper end of enlarged section 44 is provided a fluid outlet line 45. The fluid outlet line 45 passes to means for separating carrier gas from the separation product B. This means can include a cooling means 46 for condensing the product B from the non-condensable carrier gas and a gas-liquid separation drum 47. A line 48 is provided for withdrawing carrier gas and a line 49 for withdrawing the condensed product B from drum 47. Line 48 divides into a line 50 which returns carrier gas to the lower end of section 44 of chamber 41 and a line 51 which returns another portion of carrier gas to the carrier gas inlet line 43.

The apparatus of the invention includes a means for delivering solid particles from the lower end of chamber 41 to the upper end thereof. In the apparatus illustrated in Figure 4 this means comprises the inclined conduits 53 and 55 and the vertical conduit 54 which contains an elevating or solids lifting means. The solids pass by gravity flow from the lower end of chamber 41 through conduit 53 to the elevating means enclosed in the conduit 54. This elevating means can take the form of a continuous chain drive, bucket-type elevator of well-known design enclosed in the sealed conduit 54. The elevating means delivers the stream of solid particles to the inclined conduit 55 through which the particles pass by gravity flow into the chamber 41.

A second gas outlet means is provided at the upper end of chamber 41, suitably at the top of conduit 54 in the form of the line 56. This line delivers carrier gas flowing upwardly from column 41 and from the solids

elevating conduit 54 and vaporized separation product A to suitable means for separating carrier gas from the product. The separating means in the apparatus of Figure 4 comprises the cooler 57 and the separating drum 58. Condensed product A is withdrawn by line 59. Carrier gas is withdrawn by line 60 and is recirculated to the carrier gas inlet line 43.

The process of the invention is particularly suited for separating mixtures of volatile organic compounds such as the lower molecular weight components of petroleum oil, that is to say C_{10} and lighter hydrocarbons. The process can also be applied to the higher molecular weight less volatile components of petroleum oil provided that conditions under which vaporization of the components of the mixture will occur are used. These conditions can include elevated temperature and/or reduced pressure. The partitioning liquid for coating the solid particles in my process can be selected from the many solvents that are suitable for use in partition chromatography. In some instances one particular partitioning liquid may be superior to another for separating a particular mixture. The partitioning liquid is applied as a surface coating to a granular solid material that forms the stream of solid particles in the process. Liquids that are most suitable for partition chromatography include high boiling organic solvents such as dioctyl phthalate, dinonyl phthalate, dioctyl sebacate, paraffin wax, silicone fluids, etc. It is also possible to use more volatile partitioning liquids in partition chromatography (for example, water) if any such liquids have particularly desirable solvent properties. When using a volatile partitioning liquid the carrier gas should be saturated with vapor of the partitioning liquid so that the liquid will not be removed from the solids by the carrier gas.

I have mentioned granular kieselguhr as an example of a suitable solid material for my process. As a general rule any of the granular solid materials used for partition chromatography can be used in my process, although since in my process a moving stream of particles is used the solids should be resistant to attrition. Preferably the solid particles are nonporous materials which are not chromatographically active adsorbents, as otherwise the effects of adsorption chromatography and partition chromatography would be superimposed upon each other and this might prevent the obtaining of sharply defined fractions.

The carrier gas for the process of the invention can be any inert gaseous material that can be separated readily from the separation products. Examples of suitable carrier gases include hydrogen, helium, nitrogen, etc.

In the specification and claims I have for convenience referred to compounds with high or low partition coefficients. The definitions are of course relative. What is meant by a compound of high or relatively high partition coefficient is one that is more strongly retained in the liquid phase coating on the solid particles than other components of the mixture and a component of low or relatively low partition coefficient is one that passes more readily than other components into the moving gas phase with the carrier gas.

A further understanding of the invention can be obtained from the following illustrative example of the separation of a binary mixture of hydrocarbons according to the process of the invention.

Example

A mixture of n-pentane and iso-pentane is separated by the process of the invention in an apparatus like that of Figure 4 comprising a principal chromatographic chamber 41, six feet in height and one foot in diameter, and having at its lower end an enlarged section 44, three feet in height and two feet in diameter. Granular kieselguhr is circulated through the apparatus at a rate to provide a linear velocity in section 41 of 0.4 foot per minute. The kieselguhr particles range in size from about 75 to

150 microns average diameter and are coated with a thin film of dioctyl phthalate as partitioning liquid. The weight ratio of the partitioning liquid to solid particles is approximately 1 to 2. The coated kieselguhr is maintained in chamber 41 with an overall density of approximately 0.3 gram per cc. The feed mixture of n-pentane and iso-pentane is continuously introduced via line 42. The carrier gas, helium, is introduced via line 43 at a temperature of 130° F. and the circulating stream of kieselguhr particles in the separation apparatus is maintained at a temperature of 130° F. The rate of flow of carrier gas in section 41 is adjusted so that the counter-current flow relative to the coated kieselguhr is 126 cubic centimeters per minute per square centimeter of area in section 41 or, in other words, the linear velocity of the carrier gas flowing countercurrently to the stream of solids in section 41 is about 4.1 feet per minute relative to the stream of solids calculated on a free volume basis, i.e. the flow rate if no solids were present. Carrier gas and substantially pure n-pentane are withdrawn at the first gas outlet 45. The stream is cooled to a temperature of -94° F. in condenser 46 and the condensed n-pentane is withdrawn from drum 47 while carrier gas is returned by line 48 to the separation apparatus. Solids from the bottom of section 44 are continuously lifted by the bucket elevator in conduit 54 and flow back into the top of column 41. Carrier gas and the product iso-pentane are withdrawn via line 56 and cooled by condenser 57 to a temperature of -94° F. The condensed iso-pentane is withdrawn from the drum 58. The carrier gas is recirculated via line 60 and line 43 to the separation apparatus.

Obviously many modifications and variations of the invention as hereinbefore set forth may be made without departing from the spirit and scope thereof and therefore only such limitations should be imposed as are indicated in the appended claims.

I claim:

1. A method for continuously separating a fluid mixture by partition chromatography which comprises flowing in a cyclic path a stream of solid particles coated with a partitioning liquid, introducing a stream of fluid feed mixture into said stream of solid particles and introducing a first stream of carrier gas into the flowing stream of solid particles at a point in the cyclic path downstream from the point of introduction of the feed mixture whereby a portion of the carrier gas flows countercurrently to the flowing stream of particles and another portion flows concurrently therewith, the rate of flow of the stream of solid particles being selected in relation to the partition coefficients of components of the feed mixture and in relation to the carrier gas countercurrent flow rate so that a component of the feed mixture of low partition coefficient is caused to move with the carrier gas countercurrently to the flow of solid particles and another component of higher partition coefficient is caused to move in the opposite direction concurrently with the solid particles, at a point further along the cyclic path withdrawing a first gaseous stream from the stream of solid particles, still further along said cyclic path introducing a second stream of carrier gas whereby a portion thereof flows countercurrently to said stream of solid particles and is withdrawn with said component of higher partition coefficient at said point of withdrawal of the first gaseous stream and another portion thereof flows concurrently with the stream of solid particles, thereafter at a point further along the cyclic path between the point of introduction of the second stream of carrier gas and the point of introduction of the feed mixture withdrawing another gaseous stream comprising carrier gas and said low partition coefficient component of the feed mixture.

2. A method according to claim 1 in which the stream of solid particles is flowed along a section of the cyclic path between said point of withdrawal of a first gaseous stream and said point of introduction of the second

stream of carrier gas at a lower linear velocity than along other sections of the path before and after said section.

3. A method according to claim 1 in which said second stream of carrier gas is introduced at a higher velocity than said first stream of carrier gas.

4. A method according to claim 2 in which said second stream of carrier gas is introduced at a higher velocity than said first stream of carrier gas.

5. The method of effecting a separation by partition chromatography of substances having partition coefficients greater than and less than a predetermined value comprising the steps of moving a partitioning medium in one direction through a column at a constant velocity relative thereto while moving a carrier gas through the column in the opposite direction and at a constant velocity relative thereto, introducing a mixture of the substances to be separated into the column, said velocities being selected so that substances having a partition coefficient higher than the predetermined value move relative to the column in one direction, with the substances having a partition coefficient lower than the predetermined value moving relative to the column in the opposite direction.

6. A method for continuously separating a fluid mixture by partition chromatography which comprises continuously moving a partitioning medium along a prescribed course, introducing a stream of fluid feed mixture into said moving partitioning medium and introducing a stream of carrier gas into said moving partitioning medium at a point along the course of the latter downstream from the point of introduction of the feed mixture, the rate of movement of said partitioning medium being selected in relation to the partition coefficients of components of the feed mixture and in relation

to the carrier gas flow rate so that a component of the feed mixture of low partition coefficient is caused to move with the carrier gas countercurrently to the flow of the partitioning medium and another component of higher partition coefficient is caused to move concurrently with the partitioning medium, and recovering from said carrier gas said component of low partition coefficient and from said partitioning medium the component of higher partition coefficient.

7. In the separation of fluid mixtures by partition chromatography in which a fluid mixture is introduced into a body of solid particles having thereon a liquid coating and in which a carrier gas is caused to flow through said body of coated solid particles whereby components of said mixture are caused to partition between the liquid coating of said solid particles and said carrier gas, the improvement which comprises causing said body of coated solid particles to move with a velocity selected to cause one component of said mixture to move in one direction with said carrier gas and another component having a higher partition coefficient than said first-mentioned component to move in another direction with said coated solid particles.

References Cited in the file of this patent

UNITED STATES PATENTS

2,631,727	Cichelli	Mar. 17, 1953
2,731,149	Findlay	Jan. 17, 1956
2,743,818	Higuchi	May 1, 1956

OTHER REFERENCES

Practical Chromatography, Brimley and Barrett, pp. 61, 71-77, Reinhold Pub. Co. (1954).

Karnofsky: "Let's Look at Selective Adsorption," Chemical Engineering, 1954, vol. 61, No. 9, pp. 189-192.

Ionization Potentials and Electrostatic Polarization

NORMAN D. COGGESHALL

Reprinted from THE JOURNAL OF CHEMICAL PHYSICS, Vol. 32, No. 4, pp. 1265-1266, April, 1960

Ionization Potentials and Electrostatic Polarization

NORMAN D. COGGESHALL

Gulf Research & Development Company, Pittsburgh, Pennsylvania

(Received March 17, 1959)

It is assumed that the difference of ionization potential between two molecules differing only by a methyl substitution will be given approximately by the electrostatic polarization energy of the methyl group. The electric field results from the unbalanced charge at the center of the orbit of the electron removed to produce the ionization. If we add a methyl group at a distance r from the charge site, the field E there will be proportional to $1/r^2$. The energy of polarization will be αE^2 where α is the polarizability of the group. The difference of ionization potential should therefore be proportional to $1/r^4$.

It is not known whether or not the ionization of n -paraffins results from the removal of electrons from preferred sites. However, the addition of a further methyl group in going from a n -paraffin of $(n-1)$ carbon atoms to n carbon atoms will result in the addition of further polarizable C—H groups at a distance which will be a function of the total number of carbon atoms. The increment of ionization potential $\Delta E(n, n-1)$ should then be proportional to the inverse fourth power of a function of n . We may write this as $\Delta E(n, n-1) = k/[f(n)]^4$. By using Honig's values,¹ the $\Delta E(n, n-1)$ were obtained and the inverse fourth roots calculated. When plotted *vs* n the points all fell near a straight line except the one representing the difference in ionization potential of n -octane and n -heptane. This discrepancy corresponds to an apparent discrepancy in Honig's experimental results. Using the graph to determine the slope and making it

TABLE I. $\Delta E(n, n-1)$ values for n -paraffins in ev.

n	$\Delta E(n, n-1)$ calc	$\Delta E(n, n-1)$ (Honig's data)
4	0.43	0.41
5	0.21	0.25
6	0.12	0.12
7	0.07	0.08
8	0.05	0.11
9	0.03	0.03
10	0.02	0.02

TABLE II. ΔE values for different types of addition (Honig's data^a).

A. Methyl group on olefinic carbon		B. Methyl group alpha to bond	
propene		propene	
butene-2 (<i>cis</i> or <i>trans</i>)	0.55 ev	1-butene	0.08 ev
propene		2-butene	
2-methyl propene	0.49	2-pentene	0.13
2-methyl propene		2-pentene	
3-methyl-2-butene	0.50	3-hexene	0.04

^a Reference 1.

a fit on the $n=6$ value, we may calculate the $\Delta E(n, n-1)$ values and compare them with those obtained from Honig's work (see Table I).

In olefins we would expect ionization to remove a pi electron from the double bond. Substitution at a definite distance from the double bond should result in an approximately constant increment of ionization potential. In Table II are given the changes in ionization potential for two different types of substitutions in several cases.

Olefin isomers with equal spatial distribution of C—H bonds from the double bond should have approximately equal ionization potentials. *Cis*-2-butene, *trans*-2-butene, and 2-methyl propene have ionization potentials of 9.31, 9.29, and 9.35 ev, respectively,¹ which confirms this.

If valid, this simple model should yield a value of polarizability of the right order of magnitude. We use the results under A of Table II to get an average of ΔE of 0.51 ev for a methyl group added to an olefinic carbon. We may use $\Delta E = \alpha q^2/r^4$ to calculate α . Using accepted bond distances and angles we obtain $\alpha = 0.42 \times 10^{-24}$ cm³. This compares with $\alpha = 1.82 \times 10^{-24}$ cm³ from molar refraction for a methylene unit.

The center of the benzene ring may be taken as the charge site for an alkyl benzene. From Morrison and Nicholson's data² we get a ΔE value of 0.29 ev for

benzene and toluene. This should represent the polarization energy of substituting a methyl group on the benzene ring. This agrees quite well with a ΔE of 0.27 ev from Field and Franklin's data³ for 1,3-dimethylbenzene and 1,3,5-trimethylbenzene.

By using Morrison and Nicholson's data for toluene and ethylbenzene,² we may calculate α . This gives $\alpha = 1.57 \times 10^{-24}$ cm³ in better agreement with the molar refraction value of 1.82×10^{-24} cm³ than obtained in the foregoing. Using the calculated value of α and applying it to 1,3-dimethylbenzene and 1,3,5-trimethylbenzene gives a predicted ΔE value of 0.30 ev which compares quite well with the experimental value of 0.27 ev.

With two methyl groups on a benzene ring, the interaction resulting from the induced dipoles will provide a positive increment $\Delta(\Delta E)$ to the ionization potential. The order of decreasing ionization potential should be *ortho*; *meta*; *para*. With one methyl group attached, the total field at the *ortho*, *meta*, and *para* positions can be calculated as the resultant of the coulomb field and the dipole field from the polarized methyl group.

Comparison of this field with the coulomb field allows the calculation of the positive increment due to the second methyl substitution as a fraction of the negative increment ΔE due to adding the first methyl group. The total effect will be double due to the mutual effect of the two methyl groups upon each other. Using accepted molecular geometry and the molar refraction value of α we obtain $\Delta(\Delta E)_{ortho} = 0.34\Delta E$; $\Delta(\Delta E)_{meta} = 0.11\Delta E$; $\Delta(\Delta E)_{para} = 0.03\Delta E$. Using $\Delta E = 0.29$ ev from the foregoing, the calculated difference in ionization potential between *ortho* and *para* xylene should be 0.09 ev which agrees with the difference observed by Field and Franklin.³ Their value for *m*-xylene does not fit the predicted trend. However, data obtained by Crable *et al.*⁴ fit the predicted trend for the isomeric xylenes, phenols, and toluidines.

¹ R. E. Honig, J. Chem. Phys. **16**, 105 (1948).

² J. F. Morrison and A. J. C. Nicholson, J. Chem. Phys. **20**, 1021 (1952).

³ F. H. Field and J. L. Franklin, J. Chem. Phys. **22**, 1895 (1954).

⁴ G. F. Crable, G. L. Kearns, and M. S. Norris, Anal. Chem. **32**, 13 (1960).

LANCASTER PRESS, INC., LANCASTER, PA.

THE COMBINATION OF METHODS IN THE ANALYSIS OF COMPLEX HYDROCARBON SYSTEMS

By NORMAN D. COGGESHALL¹ AND WALTER HUBIS¹

The last decade and a half has witnessed enormous strides in the technology of determining the composition of complex hydrocarbon systems. On the whole, the progress has been continuous and each year has seen important advances achieved and new areas penetrated. The complete problem is so vast that many techniques and many variations within techniques are employed. However, in looking back one can recognize three major landmarks of progress. These have been the advents of infrared spectroscopy, mass spectrometry, and, more recently, gas-liquid partition chromatography, respectively.

It has been several years since the last of the major techniques came upon the scene. Nevertheless, the intense pace is continuing with significant progress in all important techniques in terms of instrumentation, a better understanding of the fundamental nature of the phenomena involved, and in empirical correlations. Parallel with this progress within techniques there has been a growing potential realizable by the combination of techniques for handling different aspects of major problems. The maximum utility of the different important techniques requires the services of professional specialists. The extensive utilization of various tech-

niques on a teamwork approach to major problems therefore requires that a new degree of attention be applied to the segmentation of major problems and to effective technical coordination and communications.

The vastness of the field of hydrocarbon analysis is a result of the thousands upon thousands of individual compounds that are inherently involved. It is well known that the number of possible isomers for any hydrocarbon class increases rapidly with the number of carbon atoms per molecule. This is displayed in Fig. 1, which gives the number of alkane isomers possible *versus* carbon number [11].² This extremely rapid rise effectively closes the door for comprehensive methods of analysis for specific compounds past the C₇ or C₈ range. The limitation is not so much a result of deficiencies in the techniques for resolving isomers as it is of the very high cost of synthesizing all the reference compounds. Another aspect is that a complete analysis of a C₁₀ alkane cut, for example, involving information on each of the 75 isomers would not be very practical information to the process research or operations engineer. For other classes of hydrocarbons—olefins, for example—the number of possible isomers goes up even faster with carbon number.

¹ Gulf Research and Development Co., Pittsburgh, Pa.

² The italic numbers in brackets refer to the list of references appended to this paper.

Hydrocarbon analysis in the range of C_8 and higher is therefore predominantly concerned with the determina-

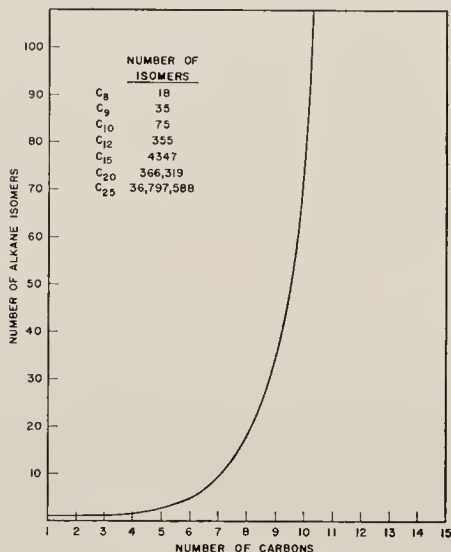


FIG. 1.—Number of Alkane Isomers as a Function of the Number of Carbon Atoms [11].

The fractions of petroleum range from the light gases into the heavy residua. There is no single set of unambiguous terms that covers all mixtures and fractions of interest. In Fig. 2 is given a histogram with the terms sometimes used for straight run fractions with various carbon number ranges. Here the heights of the blocks refer to the percentage of that class found in a particular domestic crude oil. Note that the classes thus displayed overlap carbon numbers and that certain mixtures such as naphthas (occurring generally in the transition region between gasoline and kerosine) and gas oils (occurring generally in the transition range between furnace oils and lube oils) are not shown in this simple picture. The particular system of names and associated carbon number ranges depends upon terminology used in the company involved, and in some measure upon the use made of the material. The broad scope of hydrocarbon analysis is to

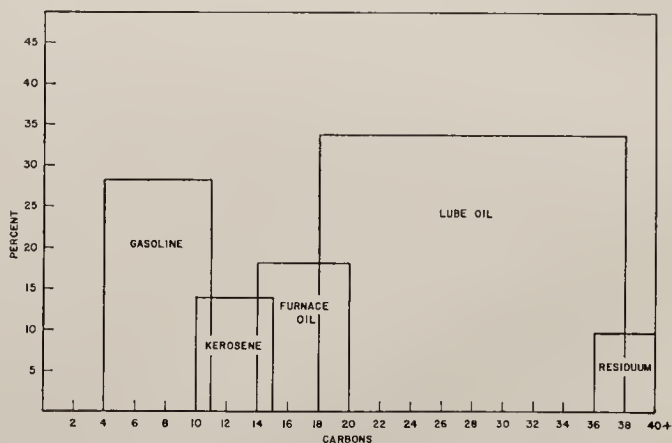


FIG. 2.—Fractions of a Particular Crude in Various Carbon Number Ranges.

tion of group-type compositions and the distribution of subgroups within hydrocarbon classes.

provide as much fine structure as possible, in terms of group types, for each block of such a diagram. Before

describing the attacks possible on such blocks, discussion will be presented on a number of principles and systems encountered throughout the various molecular weight ranges.

zation and fragmentation by electron impact that form the basis for group-type determinations. These are: (a) selective cleavage of carbon-carbon bonds, (b) differences in parent ion


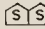
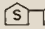

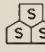



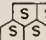
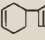
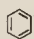
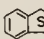
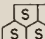
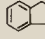
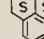
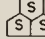
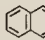
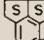
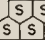
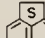
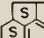
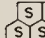
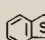
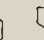

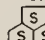
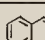

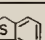
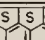
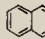
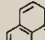
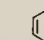
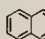
DISTINCTIVE ION SERIES	SERIES	POSSIBLE STRUCTURES OF NUCLEI
C_nH_{2n+1}	C_nH_{2n+2}	R-R
C_nH_{2n-1}	C_nH_{2n}	 R•R
C_nH_{2n-3}	C_nH_{2n-2}	   $R \equiv R$ $R = R = R$
C_nH_{2n-5}	C_nH_{2n-4}	  
C_nH_{2n-7}	C_nH_{2n-6}	  
C_nH_{2n-9}	C_nH_{2n-8}	 $R \cdot R$  
C_nH_{2n-11}	C_nH_{2n-10}	  
C_nH_{2n-13}	C_nH_{2n-12}	  
C_nH_{2n-15}	C_nH_{2n-14}	  
C_nH_{2n-17}	C_nH_{2n-16}	   
C_nH_{2n-19}	C_nH_{2n-18}	   
C_nH_{2n-21}	C_nH_{2n-20}	 ETC. TO 11 RING NAPHTHENES
C_nH_{2n-23}	C_nH_{2n-22}	  ETC. TO 12 RING NAPHTHENES
C_nH_{2n-25}	C_nH_{2n-24}	 ETC.

FIG. 3.—Stoichiometric Relations for Different Types of Hydrocarbon Structures.

MASS SPECTRAL PRINCIPLES

Since mass spectrometry plays a dominant role in the group-type analysis of hydrocarbon systems, this separate discussion is included. The experimental and operational details of this technique can be found in a number of references [2,23] and, hence, are not covered here. At present, there are four phenomena involved in ioni-

sensitivities, (c) selective cleavage at a tertiary carbon bond, and (d) the production of parent ions only by using ionizing voltages just above the ionization thresholds.

The selective cleavage of carbon-carbon bonds in a paraffin results in ions of stoichiometry C_mH_{2m+1} (where m varies between 1 and $n - 1$ and where n is the number of carbons in

the parent molecule) being produced more abundantly than ions with the same carbon number m but minus a greater number of hydrogen atoms. Thus, the sum of ions of C_mH_{2m+1} stoichiometry represents a discriminatory parameter for paraffins [6]. Every hydrocarbon class can be represented by the general formula C_nH_{2n+z} , where z characterizes one or more classes and has integral values downwards from +2. Thus, the sums of C_mH_{2m+z-1} ($m \leq n-1$) type ions provide discriminatory parameters for the corresponding classes. This is illustrated in Fig. 3 where the stoichiometric formulae are given for many classes of hydrocarbons along with the distinctive ion series used. In the structural diagrams shown, the existence of alkyl groups on the structural nuclei is implied. The saturate rings are all shown as 5-membered. The same formulae also apply to 6-membered saturate rings.

The discrimination afforded by these distinctive ion series provides the basis for the group-type analysis of gasolines for alkanes, cycloalkanes plus olefins, cyclo-olefins, diolefins plus acetylenes, and aromatics. It also provides the basis for the group-type analysis of saturate systems in the furnace oil and lube oil range for alkanes, noncondensed cycloalkanes, and condensed cycloalkanes with a breakdown of the latter class according to the number of rings [20]. The distinctive ion series principle is also the basis for the methods developed for the different classes of complex molecules in the aromatic fractions of gas oils or other hydrocarbon systems in that general boiling range [9].

A limited utility can be gained from differences in the intensity of the parent ion formation as dependent on hydrocarbon class. The intensities for

parent mass ions from isoalkanes are very low. For cycloalkanes they will generally be higher, and for n -alkanes they will be still higher [6]. These relations may be employed for certain saturate systems to provide some information on class concentration and, for the n -alkanes, distribution by molecular weight. For the alkylbenzenes the intensities of the parent mass ions are not only relatively pronounced but also fairly constant within a particular carbon number subclass. This makes possible a direct examination for aromatics by molecular weight in complex systems in the gasoline range [19].

In isoalkanes the selective cleavage at tertiary carbon atoms [6] produces strong local maxima of ion intensities at the corresponding mass values. This provides a discriminatory feature that is useful in assaying the presence and degree of branching in certain saturate systems.

If the energy of the ionizing electrons is kept just above the ionization potential but below that necessary for fragmentation, only the parent ion is produced for any compound. All compounds of the same molecular weight may contribute to this one-ion peak, but there will be no contribution from compounds of other molecular weights. This branch of mass spectrometry is now commonly referred to as low-voltage mass spectrometry. A spectrogram of a mixture by this technique, therefore, consists of a series of peaks, each representing materials of corresponding molecular weights. The mass value not only gives the molecular weight, but from the stoichiometry rules such as given in Fig. 3, allows an assignment to the appropriate class. In a mixture of various saturate and unsaturate classes some stoichiometric overlapping is possible. At present,

the technique is not fully quantitative due to incomplete data and understanding of the relations of the ion sensitivities (which are directly related to the ionization potentials) and to all of the structural features of the unsaturates. Despite this, the technique is a powerful tool allowing, for example, a mixture of aromatics from kerosine to be analyzed in terms of alkylated benzenes, indanes, indenenes, naphthalenes, acenaphthenes, acenaphthylenes, and anthracenes [13]. Each class, in turn, is broken down into a distribution by carbon number.

TECHNIQUES FOR OLEFINS

The number and diversity of techniques for determining total olefin content or for getting subclass information on olefin fractions merits separate discussion. For total olefin content, there are several methods with various advantages and disadvantages. A standard procedure is to obtain a bromine number and to calculate the olefin content (ASTM Method D 875).³ The method, which is based on the consumption of bromine by reaction with olefins, is fast and simple. However, it is not highly accurate and suffers from several interferences based on the reaction of bromine with other compound types.

A very popular and widely used method for total olefin content is the Fluorescent Indicator Adsorption Method (ASTM Method D 1319)⁴ commonly referred to as the FIA method. This method is based on silica gel chromatography coupled with the use of fluorescent dyes which

makes the determination of zone lengths for saturates, olefins, and aromatics readily feasible. The method is simple, uses inexpensive equipment, and can be made quite reliable. Raman spectroscopy will yield total olefin content [10], but this requires quite expensive equipment for a job that can be done as satisfactorily otherwise. Catalytic hydrogenation can be used in assaying olefin content; however, its greatest utility will probably emerge as a technique for removing ambiguity in certain analyses, as will be discussed below. Nuclear magnetic resonance can be made to yield a quite satisfactory analysis for total olefinic hydrogen (hydrogens attached to olefin groups) [22]. However, unless this technique is being applied for other studies, this would involve an unreasonably high equipment investment for such information.

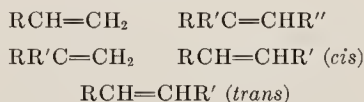
A procedure yielding rather specialized information that can, at times, be of considerable interest is the use of Molecular Sieves to remove normal olefins quantitatively [25]. By normal olefins we refer here to terminal olefins and *cis* and *trans* straight chain olefins. As the sieves will also remove *n*-paraffins, an olefin fraction must first be prepared by silica gel adsorption or other means. The amount of olefins taken up by the sieves can then be quantitatively determined. Unfortunately, the original olefins cannot then be recovered for a breakdown amongst the three subclasses as some isomerization occurs in the sieves.

There are three important spectroscopic techniques for getting subclass information on olefin fractions: the infrared absorption method, the ultraviolet absorption pi complex method, and the low-voltage mass spectral technique. In the infrared absorption procedure, use is made of the fact that

³ Method of Calculation for Olefins and Aromatics in Gasoline (D 875), 1958 Book of ASTM Standards, Part 7.

⁴ Method of Test for Hydrocarbon Types in Liquid Petroleum Products (Fluorescent Indicator Adsorption (FIA) Method) (D 1319), 1958 Book of ASTM Standards, Part 7.

the carbon-hydrogen bending vibrations for olefinic hydrogens are dependent upon the nature of the olefin structure [27]. This allows discriminatory absorption frequencies to be chosen such that group-type analyses can be quite satisfactorily achieved for the following types:



For best results, this should be applied to a fraction relatively free of diolefins and aromatics. Saturates can be tolerated up to some 60 per cent, but better accuracy is obtained if they can also be removed.

The ultraviolet absorption pi complex procedure is based on the fact that when iodine and olefin molecules pi complex they produce absorption bands in the visible and ultraviolet spectral regions [18]. There is a measurable discrimination available wherein the absorption maxima depend upon the olefinic structure. This allows information to be obtained for the same groups as the infrared method provides plus information on tetra substituted olefins. This latter group cannot be assayed by infrared absorption. The two methods are somewhat complementary as the infrared method will not yield the tetra substituted type while the ultraviolet method cannot be applied with comparable accuracy for the other groups.

The foundations for the low-voltage mass spectral method were given in the previous section. In application to olefin analysis, the mass values of the ion peaks allow those representing olefins to be identified from simple stoichiometry. The same stoichiometry also allows the carbon number of the olefin subclass to be identified. This procedure thus gives the break-

down of olefins by carbon number but provides no structural information as yielded by the infrared and ultraviolet methods. The three methods are, therefore, highly complementary. As indicated earlier, there is not at present a completely sound picture on the mass spectral sensitivity values so that the accuracy of the breakdown by carbon number is not as satisfactory as we may expect to see it in the future. The same stoichiometric relations also allow diolefins and triolefins to be identified and distributed by carbon number. Despite the accuracy limitations resulting from inadequate sensitivity values, this newest method can yield extremely important information in specialized cases.

TECHNIQUES FOR AROMATICS

A method that has been extensively used in the past for total aromatic content but which is used much less now is the acid absorption method (ASTM Method D 1019).⁵ This involves treating the sample with a solution of phosphoric pentoxide and concentrated sulfuric acid. It yields the olefin plus aromatic concentration which, with data from the bromine number, may be corrected to yield an aromatic concentration. The FIA method described in the previous section is now used very extensively for total aromatic concentration as well as the other information the procedure supplies.

Ultraviolet absorption spectrometry has been particularly valuable for individual aromatics in the lower molecular weight ranges. With suitable distillation cuts to limit the number of compounds, the procedure yields the individual aromatics through the

⁵ Method of Test for Olefinic Plus Aromatic Hydrocarbons in Petroleum Distillates (D 1019), 1958 Book of ASTM Standards, Part 7.

C₈'s [29]. The ultraviolet absorption is due to the benzene ring, and the effects of substituent changes are, therefore, often of a second order magnitude. This limits the technique for individual compounds but, on the other hand, does provide the basis for certain group-type applications. Thus, the total absorption at 215 m μ can be used to assess the total alkylbenzenes in straight-run gasolines [14]. Application to cracked stocks is impractical because of interferences.

The behavior of alkylbenzenes boiling between 150 and 180 C allows classification into four classes: mono-substituted, *ortho* and *meta* substituted, and two subclasses of *para* substituted [24]. For the naphthalenes, the possibilities are more restricted than for the alkylbenzenes. In this case, it is possible to obtain information on naphthalene and the α - and β -methylnaphthalenes [5]. Beyond that, identification of individual alkyl substituted aromatics in a complex system becomes very difficult by ultraviolet absorption.

The very strong absorbance of aromatic compounds in the ultraviolet region where almost all other hydrocarbons are transparent makes ultraviolet absorption a powerful qualitative tool to determine the presence of aromatics. However, except for such cases as discussed above, the spectra of individual compounds are not dissimilar enough to allow many specific identifications. As one progresses into the condensed ring classes, there are some reasonably diagnostic absorption regions in which certain types of cata-condensed types may be recognized. Even here, the discrimination is poor due to the considerable overlapping and perturbing effects resulting from different types of substitution. If drastic separation procedures

are employed, the technique can be used to recognize various types. Thus, Charlet et al used a silica gel separation for total aromatics followed by alumina adsorption for segregation of types [4]. Using ultraviolet absorption, they obtained evidence for various cata-condensed aromatics up to five condensed rings. Schnurman et al also achieved identification of certain complex classes [28].

Infrared absorption can be of great utility in simple systems, but it has not been of much value for aromatics

TABLE I.—AROMATIC COMPOUND TYPES THAT MAY BE DETERMINED BY DISTINCTIVE ION SERIES TECHNIQUE.

Compound	Formula
Benzenes.....	C _n H _{2n-6}
Indanes-tetralins.....	C _n H _{2n-8}
Dinaphthalenebenzenes-indenes..	C _n H _{2n-10}
Naphthalene-trinaphthalenebenzenes.....	C _n H _{2n-12}
Acenaphthenes.....	C _n H _{2n-14}
Acenaphthylenes.....	C _n H _{2n-16}
Phenanthrenes-anthracenes.....	C _n H _{2n-18}
Pyrenes.....	C _n H _{2n-22}
Chrysenes.....	C _n H _{2n-24}
Benzothiophenes (apparent).....	C _n H _{2n-6}
Dibenzothiophenes (apparent)...	C _n H _{2n-12}
Naphthobenzothiophenes (apparent).....	C _n H _{2n-18}

in complex systems. Schemes utilizing the weak aromatic ring absorption in the 5.0 to 5.85 μ region [15] and the aromatic hydrogen absorption in the 12 to 15 μ region [12] allow some recognition by classes. These are of limited applicability, however, as the various aromatic absorptions are rather strongly influenced by substitutional differences.

Mass spectral techniques are today the most powerful for information on aromatic subclasses. As indicated in a previous section, the group-type procedure applied to gasolines and naphthas yields total aromatics as one

class. An extension of this procedure also allows the determination of the further classes of indanes and tetralins and of naphthalenes. By using the parent ion approach [19] the alkyl-benzenes by carbon number through the C_9 's may be determined. In some cases this may be extended to the C_{12} benzenes. In the higher molecular weight ranges such as for gas oils and higher, the distinctive ion series approach may be used to provide information on classes having different stoichiometry. In Table I are given the different aromatic classes which may be determined in this way with the appropriate stoichiometric formulae [20]. Interference is experienced between classes for which the number of hydrogen atoms differs by 14, which is the molecular weight of a methylene unit as, for example, C_nH_{2n-10} and C_nH_{2n-24} .

As discussed in the section on mass spectral techniques, the new procedure employing electron ionization voltage just above the ionization potentials gives a powerful new tool. No molecule can produce more than one type of ion, that being the parent molecule ion. Thus, each peak observed for an aromatic concentrate may be assigned to a particular class of aromatic of a particular carbon number. This is done through applying the stoichiometric relations such as given in Table I. By identifying each peak as to class and carbon number, the entire composition may then be subdivided in detail by giving all the benzenes *versus* carbon number, all the indanes *versus* carbon number, etc. Examples of some results by this technique will be given later. As indicated in the section on mass spectral techniques, there are at present some questions relative to absolute calibration values that make high accuracy currently

impossible. With time, it is expected that these will be resolved.

GASOLINE AND NAPHTHA RANGE

The gasoline and naphtha range of hydrocarbon systems has experienced the greatest degree of research and development for group-type procedures to date. There is strong economic interest in this work in terms of increased yield of gasoline, upgrading of octane number, and petrochemical problems falling in this region. In addition, it has generally been more feasible to apply new concepts in this simplest of the higher molecular weight systems and to work towards more complex systems from there than to attempt to first set up quantitative procedures for the higher molecular weight systems.

In terms of the older tests, the bromine number gives a measure of olefin content; the acid absorption method (ASTM Method D 1019)⁵ gives a measure of aromatics plus olefins. The n-d-M method [30] using index of refraction, density, and molecular weight gives aromatic, paraffinic, and naphthenic carbon and mean number of naphthene rings per molecule. The PONA method [16] gives paraffins, olefins, naphthenes, and aromatics. This is based on a combination of refractive index and density after separation of saturates from the sample. The FIA procedure discussed in the section on olefins is widely used for rapid and quite accurate analysis for saturates, olefins, and aromatics.

The first mass spectral group-type procedure of importance was developed for materials in the gasoline and naphtha range [3]. It utilizes the distinctive ion series principles outlined earlier, and it yields an analysis for the aliphatic paraffins, for cyclopars-

affins and olefins as a class, for the coda group of cyclo-olefins, diolefins and acetylenes, and for the aromatics.

The above procedures have been quite useful and are still employed extensively today in many applications. However, they only provide information on very broad classes of compounds and cannot generally be pushed for subclass information.

is removed by class separation, it then becomes possible to extract much more information from the spectral observations. The separation into saturate, olefin, and aromatic fractions is accomplished by direct but careful silica gel adsorption techniques [27] or by modifications of the FIA [13] procedures to yield the desired fractions.

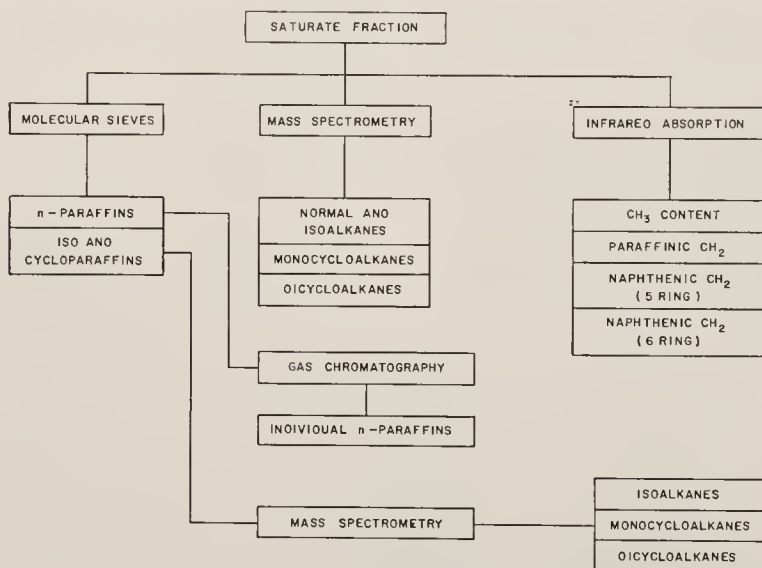


FIG. 4.—Techniques Applied and Information Obtained on Saturate Fractions.

A great step forward was made when it became possible to readily obtain compound class separations by simple physical methods. The separation of a gasoline or naphtha range sample into a saturate fraction, an olefin fraction, and an aromatic fraction makes possible a much greater detail of subclass information than could be obtained on the whole mixture. This is because with the best spectral methods there is generally a considerable degree of interference between classes. If this interference

In Fig. 4 is given a block diagram of the various types of information that can be determined for the saturate fraction using different techniques. The 5-A Linde Molecular Sieves may be employed to quantitatively adsorb the *n*-paraffins. The unadsorbed isoparaffins and cycloparaffins may then be removed to yield the breakdown shown. The *n*-paraffins may be removed [25] from the sieves and charged to a suitable gas chromatograph to yield the concentrations of the individual species. With pure *n*-

paraffin mixtures, this technique can be pushed quite far, yielding individual *n*-paraffins up to the range of 30 carbon atoms. The iso and cycloparaffin fractions may, of course, be examined by mass spectrometry for the breakdown shown. The combination of these two examinations pro-

7.5 μ region to measure the methyl group content and the C-H bending vibrations in the 12.5 to 14.3 μ region to determine the paraffinic methylene group content. The results from these measurements are then applied to remove the corresponding interferences in the C-H stretching region around

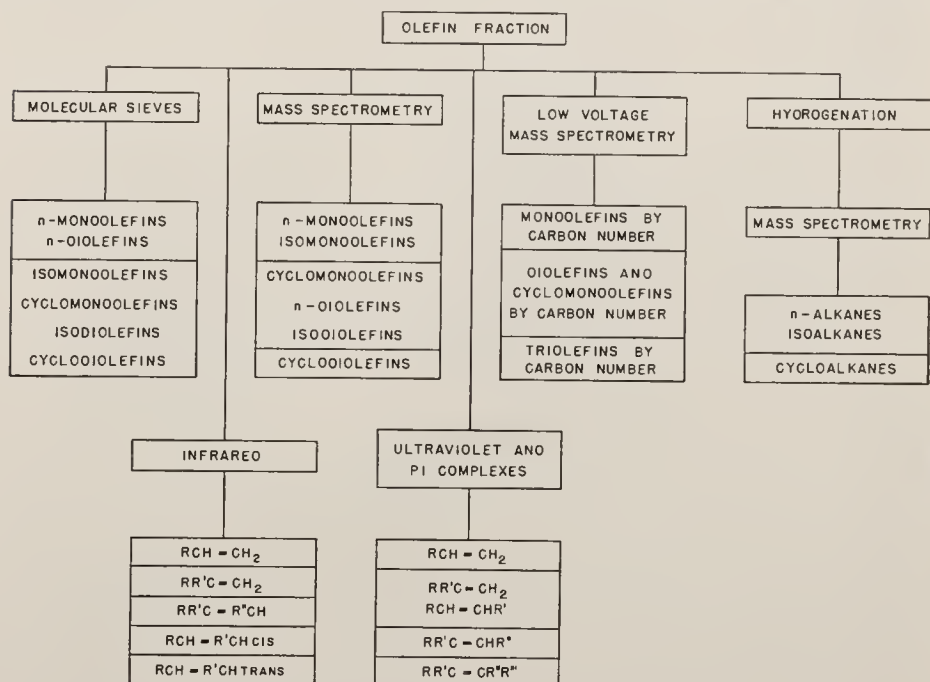


Fig. 5.—Techniques Applied and Information Obtained on Olefin Fractions.

vides the necessary split of the alkanes into normal and iso classes.

The mass spectral operations on the total saturate fraction are very similar to those used on the whole gasoline or naphtha. However, the removal of the olefin and aromatic fractions allows improved accuracy.

The isolation of a saturate fraction removes olefin and aromatic interferences that would effectively block the infrared studies shown. These use the C-H bending vibrations in the 7.1 to

3.4 μ . Use is then made of fine structure behavior in this region to calculate from the spectral remainder the concentration of C₅ and C₆ ring naphthenic methylene groups, respectively [8]. This same infrared method can be applied to advantage to saturate systems extending up into polymers. However, for best results cognizance should be taken of some differences in absorption displayed by pendant *versus* end methyl groups [12].

In Fig. 5 may be seen the various

operations and studies yielding subclass information on the olefin fraction. In the various blocks are shown *n*-mono-olefins, isomono-olefins, cyclomono-olefins, *n*-diolefins, isodiolefins, and cyclodiolefins. In many systems there will not be significant amounts in some of these subclasses and the interpretations may, therefore, be simpler.

The use of 5-A Molecular Sieves [25] allows a quantitative removal and evaluation of the *n*-mono-olefins and *n*-diolefins as a combined subclass. Unfortunately, these cannot be recovered from the sieves for further study without some isomerization occurring. As indicated in the section on techniques for olefins, a direct examination by infrared absorption will yield the structural subclasses shown. It will not give information on the tetra substituted mono-olefins, and the degree of interference that will result from substantial amounts of diolefins has not been evaluated. For systems of mono-olefins where the tetra substituted type is not important, this method often is of great utility for the structural subclass information it furnishes.

Using the principle of the distinctive ion series discussed earlier, a group-type mass spectral examination will yield the *n*-mono-olefins and isomono-olefins as one combined subclass; the cyclomono-olefins, *n*-diolefins, and isodiolefins as another; and, the cyclodiolefins as a separate subclass. The ultraviolet pi complex procedures may be used to get structural subclass information similar to the infrared method and information on the tetra substituted mono-olefins as well. We believe this procedure should only be used for the tetra substituted type and the others obtained by infrared if facilities are available. This is due

to a higher inherent accuracy of the infrared method which is also somewhat simpler than the use of the pi complexes.

The low-voltage mass spectral studies yield subclass information of a different type giving the iso and *n*-mono-olefins as one general class, the iso and *n*-diolefins and cyclomono-olefins as another, and the triolefins and cyclodiolefins as another. For each of these subclasses, there will be a further breakdown according to carbon number. All in all, this approach yields a wealth of quite detailed information although the absolute accuracy cannot reliably be assayed now due to inadequate knowledge of the ionization potentials involved.

If the entire olefin fraction can be carefully hydrogenated without isomerization and then examined by mass spectral group type procedures, it will yield information on the aliphatic *versus* cyclic structures. This combined with the results from the direct mass spectral examination of the olefin fraction should allow the cyclomono-olefin content to be computed.

In materials boiling in the gasoline range, there will not ordinarily be as much interest in further operations on the aromatic fraction as discussed above for the saturate and olefin fractions. This is because this fraction will be predominantly alkylbenzenes. Most information of interest relative to the alkylbenzenes can actually be obtained on the whole gasoline without a silica gel separation, using the technique described above. Using the ultraviolet method mentioned above coupled with distillation, the individual aromatics through the xylenes may be obtained. Using the group-type aromatic ultraviolet method, groupings into mono-substituted, or-

tho and *para*, di- and tri-substituted, and the *para*-substituted subclasses may be obtained directly. Using the mass spectral method employing parent masses, a direct examination can be made to yield alkylbenzenes according to carbon number.

KEROSENE THROUGH GAS OIL RANGE

The kerosene through gas oil range, which also includes furnace oil, extends roughly from C_{12} to C_{25} . If the

the two references cited, this procedure is aided by using the indicator dye technique of the FIA method. The higher the molecular weight, the slower is the development of the zones, sometimes requiring many hours.

The excessive time requirements for zone formation in the FIA procedure for the heavier systems has led to adaptations of elution chromatography over silica gel for making separations in the gas oil range [21]. Here

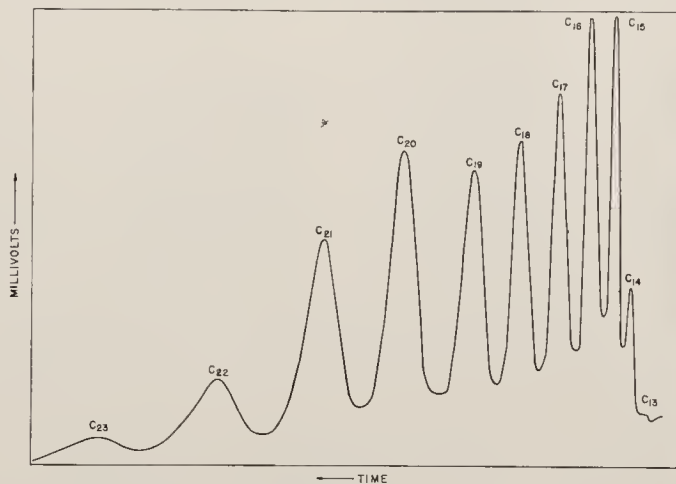


Fig. 6.—Gas-Liquid Partition Chromatogram of *n*-Paraffin Fraction Obtained from Molecular Sieves.

systems are straight-run, then olefins may be expected to be absent. If they are cracked stocks, a high degree of olefinic unsaturation may be expected.

Preliminary separations are generally necessary on these mixtures before one can apply the spectroscopic techniques for detailed class information. In the lighter end of this region, say into the light gas oil range, the displacement chromatographic technique may be used [13,15]. This comprises charging the material to a column of silica gel and displacing the zones that develop with an alcohol. In

the sample is admitted to a pre-wet column of 100 to 200 mesh silica gel (Davison Chemical Co. Code No. 923). The sample is eluted with *n*-pentane to bring out the saturates and then with ether to bring out the aromatics. The eluting solvents can be flashed off to recover the desired fractions. This procedure works well with straight-run materials free of olefins. For cracked stocks with high olefinic content, it is expected that it would be difficult to produce a clean separation between the olefins and aromatics. Samples containing wax up to

about 10 per cent can be handled at room temperature, but higher wax content samples require that the column be heated.

For the information that can be obtained on the saturate fraction, ref-

TABLE II.—DISTRIBUTION BY MOLECULAR WEIGHT OF OLEFINIC CLASSES IN A BLEND CONTAINING CRACKED MATERIALS, VOLUME PER CENT.

	C ₁₁	C ₁₂	C ₁₃	C ₁₄	C ₁₅	C ₁₆	C ₁₇
Mono-olefins.....	0.7	0.9	1.1	0.7	0.4	0.4	0.3
Diolefins.....	0.4	0.7	0.7	0.6	0.5	0.3	0.2
Triolefins.....	0.3	0.2	0.1	0.3	0.1	0.1	0.1

Sieves and quantitatively recovered. The fractions of *n*-paraffins thus recovered can be charged to an appropriate gas chromatograph for quantitative evaluation of each of the *n*-paraffins. Figure 6 shows such a gas chromatogram of the *n*-paraffins recovered from a gas oil. It is interesting that these are the only individual compounds that may readily and systematically be identified and measured in such a complex system.

The saturate fraction may be examined by the method of distinctive ion series [13] to yield information on the alkanes, noncondensed alkanes,

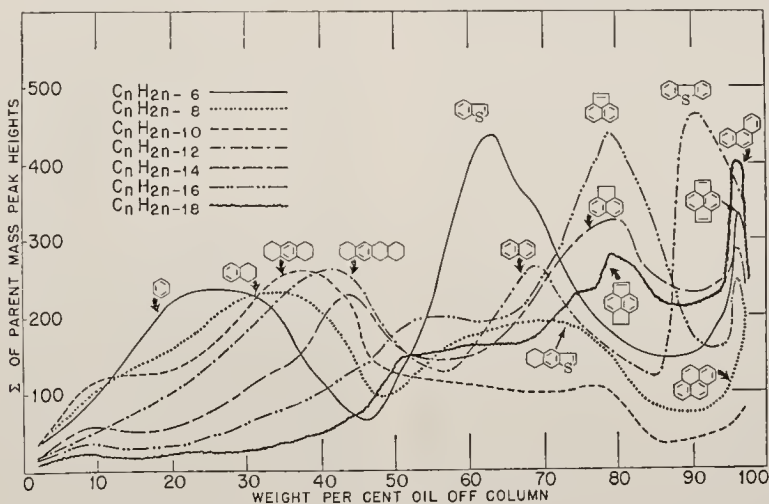


FIG. 7.—Various Types of Aromatic Structures Obtained by Mass Spectrometry for a Heavy Gas Oil (after Hastings et al [9]).

erence is again made to Fig. 4. The same operations will be possible and the same type information will be available, except that there will be more classes to account for in this higher molecular weight region. As has been shown by O'Connor and Norris [25], *n*-paraffins through this region may be quantitatively removed from a system by the use of 5-A Molecular

and condensed cycloalkanes. The condensed cycloalkane class may be further broken down to give information on the two, three, four, etc., ring subclasses. The infrared method referred to in a previous section may also be applied to yield information as to methyl content, paraffinic methylene, cyclopentyl methylene, and cyclohexyl methylene. In this molecular

weight range, it is important in using the infrared method to be cognizant of the differences in methyl absorption depending on position on the

sorption can be satisfactorily applied for the determination of the structural olefin classes. No publication is known to the authors describing at-

TABLE III.—AROMATIC CLASSES BY MOLECULAR WEIGHT IN A WIDE-BOILING AROMATIC FRACTION, VOLUME-PER CENT.

	C ₆	C ₇	C ₈	C ₉	C ₁₀	C ₁₁	C ₁₂	C ₁₃	C ₁₄	C ₁₅	C ₁₆	C ₁₇	C ₁₈
Benzenes.....	1.4	1.9	2.6	2.6	2.4	2.1	1.4	1.0	1.0	0.7	0.4	0.3	0.1
Indanes.....	0.4	0.6	0.6	0.4	0.3	0.2	0.2	0.2	0.1	...
Indenes.....	0.3	0.6	1.0	0.9	0.6	0.3	0.2	0.1	0.1	...
Naphthalenes.....	0.5	1.4	2.1	1.9	1.0	0.6	0.6	0.4	0.1
Acenaphthenes.....	0.4	0.4	0.4	0.2	0.1	0.1
Acenaphthylenes.....	0.2	0.5	0.6	0.4	0.2	0.1
Anthracenes.....	0.2	0.4	0.4	0.2	0.1

TABLE IV.—CLASS INFORMATION FROM MASS SPECTRAL METHODS FOR TWO DISSIMILAR MIXTURES IN THE KEROSENE RANGE, VOLUME PER CENT [13].

	Mixture A	Mixture B
Alkanes.....	2.7	34.0
Noncondensed Cycloalkanes.....	44.6	34.1
Condensed Cycloalkanes:		
2 ring.....	26.9	12.5
3 ring.....	14.6	3.7
4 ring.....	2.3	0.3
5 ring.....	0.2	...
Benzenes.....	5.7	9.0
Indanes.....	0.5	2.6
Indenes.....	...	0.3
Naphthalenes.....	...	3.0
Acenaphthenes.....	...	0.1
Mono-olefins.....	0.3	...
Diolefins.....	0.5	0.1
Triolefins.....	1.7	0.3
Average substitutions per benzene ring.....	1.0	1.9

molecule as observed by Hughes and Martin [12].

If the material under study is a cracked stock and, hence, has olefinic components that may be separated in an olefin fraction, the same type of operations may be made on the latter as diagrammed in Fig. 5. Infrared ab-

tempts to use the pi-complex method in this molecular weight range. Ordinary mass spectral observations will yield the *n*- and isomono-olefins as a class, the cyclomono-olefins, the *n*-diolefins, and the isodiolefins as a class, and the cyclodiolefins as another class. It is expected that severe recovery problems would be experienced in attempting the quantitative hydrogenation procedures that may be used for lighter materials. The low-voltage mass spectral studies can be of exceptional value for such fractions especially when information is needed about the distribution of olefins with molecular weight. In Table II are given in volume per cent the distributions of olefin classes by molecular weight for a particular blend containing cracked material. Without the low-voltage mass spectral technique, this information would be virtually impossible to obtain.

For the aromatic fraction a series of chromatographic separations may be made and ultraviolet absorption interpretation applied to yield identification on condensed aromatic types [4]. However, the mass spectral techniques are generally easier to apply if adequate calibration data are available, and they yield much more in-

formation. The distinctive ion series method may be applied for the different stoichiometric classes to yield an analysis of the classes enumerated in Table I. Figure 7 gives a plot of the concentration of various classes emerging in various cuts from a chromatographic separation. In using this procedure, information concerning the source of the material and the relative behavior in a chromatographic column is important to remove the interferences that would otherwise result from more than two classes having the same stoichiometric formula.

The low-voltage mass spectral method may be used with great success to give a breakdown by molecular weight of the different classes of aromatics in this range. In Table III is given, in volume per cent, such a breakdown for wide-boiling aromatic fractions.

Information such as in these tables may be of particular interest in some cases and, in others, constitute a degree of detail beyond what is usable. Combining the various mass spectral approaches in this region allows more general type of class information such as given in Table IV to be assembled. Here the composition of two rather dissimilar mixtures in the kerosine range are compared.

LUBE OIL AND HEAVIER RANGE

The amount of information currently available in this region is not comparable to that available in the lower molecular weight regions. One reason is that some of the problems are more difficult, another is that fewer reference compounds are available to establish correlations, and a third is that there has not been as much need for more detailed information in this region.

If the material is straight-run, it is

believed [14] that a silica gel elution technique could be used with some success to separate aromatics from saturates. We would expect considerable smearing and overlapping to occur if the material has experienced some cracking and therefore has a relatively high olefinic content.

Certain of the processing steps such as solvent extraction yield saturate fractions relatively free of aromatics. Some of the same techniques discussed earlier may be applied to these fractions, such as the infrared examination for methyl, paraffinic methylene, cyclopentyl methylene, and cyclohexyl methylene. Here again, cognizance of the effect of position on the methyl absorption is important.

If the saturate material is a specialized type like a wax, a distribution with molecular weight by mass spectrometry is possible [26]. The results of O'Connor and Norris indicate that Molecular Sieves can be used in this region to extract the *n*-paraffins. High-temperature gas chromatography [17] can then provide a good distribution of these with carbon number.

A very important analysis of the saturate fractions can be achieved by mass spectrometry using the distinctive ion series technique [7]. This yields information on the normal and iso alkanes as a class, the noncondensed cycloalkanes as a class, and the condensed cycloalkanes as a class with a further breakdown of the latter in terms of 2, 3, 4, 5 etc. condensed rings. This is an important tool in correlating lube oil performance with compound types [1].

Nuclear magnetic resonance [22] can be used to provide information on methyl, methylene, and aromatic hydrogen in these high molecular weight systems. The proton resonances for paraffinic methylene and naphthenic methylene groups overlap so severely,

however, that distinction cannot be reliably made between them. Williams [31] has used the ratio of the heights of the NMR absorption bands due to the methyl groups *versus* the methylene groups to define a "branchiness index." He reports that the branchiness index correlates linearly with the naphthene ring carbon content in saturates from a variety of crude oil sources.

REMARKS ON COORDINATION

In the preceding sections we have been detailing the specific information that can be obtained in various hydrocarbon molecular weight ranges. If there were some convenient way to superimpose the complete detailed picture in all of the blocks of Fig. 2, it would provide an impressive display of the very extensive group-type information that can now be determined for petroleum systems. Although we have only discussed hydrocarbon systems, many parallel investigations can now be conducted on petrochemical and other organic systems.

Progress in this field is quite rapid. Some of the things discussed above are well established to the point of being routinely applied while others are representative of very recent developments. By the time this appears in print, it will, no doubt, be possible to represent additional progress in various areas. The technical know-how presented in the above sections may be regarded as that achieved at a particular time.

Industrial research of a chemical nature is becoming more and more critically dependent upon having detailed information on the chemical systems of interest. The availability of this information can spell the difference between being the first or a

runner-up on a new process or product. It is, therefore, highly important to a large research organization to have an organizational setup which allows them to have not only the last word in technical know-how available, such as discussed above, but also mechanisms which will ensure that this expanding technology is being constantly applied to current problems. This area deserves considerable attention, since having and applying the most up-to-date technology involves a close coordination of specialists and problems and is inseparable from an active research program in the techniques involved.

A major problem in putting current technology to work in a large research organization is that of technical communication. A chemist or engineer making a career in process research, for example, needs to have the best science possible applied to the composition, structure or chemical identity problems inherent in the process research and development. For his own success he will need to concentrate on the process elements, and he cannot possibly keep up with the various physical and chemical techniques and the modes whereby they are applied.

Conversely, the specialists responsible for basic research and application of such techniques as mass spectrometry, nuclear magnetic resonance, gas chromatography, infrared absorption, electron spin resonance, separation techniques, etc., cannot possibly know much about the details of process problems nor the changing trends and needs. Their fields are changing rapidly and their own optimum utility as scientists is dependent upon their being abreast of current basic research and their being able to apply it.

This problem of technical commu-

nication is a serious one, and we are sure that many investigators can, in retrospect, recall various instances where important projects were stalled or impaired for the lack of scientific information that could have been developed if the proper steps of problem segmentation and coordination had been achieved. There seems to be but one satisfactory solution to this problem and that is to have professional manpower explicitly assigned to this communication function. In the Gulf

composition and structure division wherein the investigative work is done. This staff position provides a comprehensive and simple mechanism for technical liaison and the benefits have been marked.

Another major problem is that of creating a professional environment whereby first class scientists can be attracted and stimulated to making specialized contributions to large projects and to doing the research and development necessary to maintain a

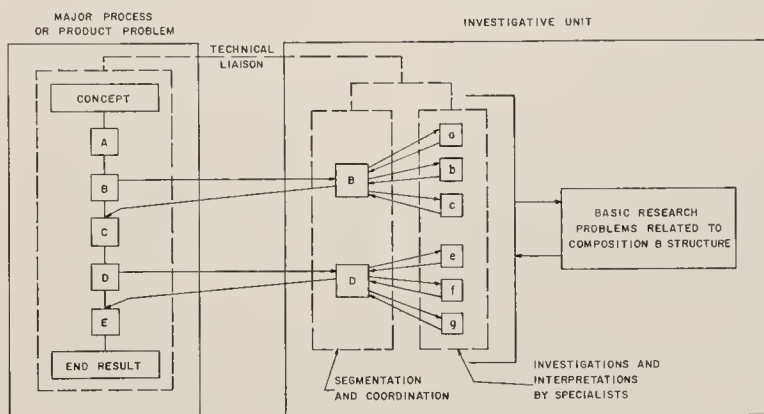


FIG. 8.—Schematic Diagram Representing Project Segmentation and Technical Coordination.

Research and Development Co., this job is the full time assignment of an individual who not only has had supervisory experience in analytical operations but has also been given special training relative to the various branches of spectroscopy, separation investigations, physicochemical investigations, etc. He is available for discussion and guidance to all investigators having problems in composition, structure, or identification which need special studies made. He is also present in progress report discussions within the research divisions wherein the problems arise and within the

fore-front position in their respective fields. A basic ingredient in this is recognition, both professional and salary-wise, for good work. We believe a major step in achieving this is accomplished if the investigative unit where work such as discussed is done is put on a par, organizationally, with the units in which the process, product, chemical, etc., projects are pursued. This makes it easy to delineate clearly to the specialists their very important function to the company of providing and applying the very best in scientific developments. Too often, when the investigative unit is a seg-

ment of a larger unit with a primary responsibility such as process or product development, there is a tendency of the personnel in the investigative unit to have a feeling of secondary importance to the company. This can be debilitating in a very real way to the morale necessary to attract and stimulate first class scientists.

If the organizational structure is such as to provide satisfactory solutions to the two major problems of above, many other organizational problems can be solved, and it is possible to apply very effective teamwork to company problems. In Fig. 8 is a functional flow diagram of how specialized problems may be solved and fed back into the primary company projects. Almost any major company project can be segmented into a set of problems that must be solved or developments that must be achieved. In the figure these are labeled *A*, *B*, *C*, *D*, and *E*. In petroleum or chemical research some of these will be in composition, structure, or identity. In the figure these are labeled *B* and *D*. Those in charge of the primary project will benefit most effectively if these complete segments can be transferred to the investigative unit responsible for solving such problems. Such segments, when representing complex problems as discussed in the technical part of this paper, can be further segmented for handling by specialists in the various techniques. The further segments are labeled *a*, *b*, *c*, *e*, *f*, and *g*. These latter segments can be attacked with undivided attention by the specialists and the results from them all can be coordinated to provide over-all answers to the original problems. These can then be fed back into the stream of progress of the original primary project.

In all of these steps discussed so far, the element of technical liaison

is of primary importance and the individual assigned to it should have free access to those responsible to the primary project and to the specialists responsible for all phases of solving the composition, etc., problems.

This system has another important benefit in addition to getting current problems solved and that is in the direct tie-in with basic research. Basic research can be likened to a powerful horse hitched to a plow. If properly guided, it can plow up a lot of ground that can be put to work by the company. If not properly guided, it may readily veer in different directions and plow up the same amount or more ground. Unfortunately, in the latter case the results can be so disconnected and randomly placed that the company may realize virtually no gain from it. The system outlined in the figure allows a very direct contact between the current company problems and the basic research problems that it is most profitable to solve. The specialists should probably either be engaged in portions of the basic research or in the organizational unit wherein it is done. Today there are literally hundreds of scientifically interesting and valuable problems to be solved in the phenomena employed in such fields as surface chemistry, ion exchange, mass spectrometry, nuclear magnetic resonance, physical adsorption, partitioning mechanisms, infrared absorption, electron-spin resonance, etc. For a good return on its basic research dollar, the selection of the problems within a company chosen for attack should be closely coordinated with its needs. Another additional benefit from the above system is that occasionally discoveries made in the research in the investigative unit are of direct interest to those charged with the primary projects and can readily be made available there.

REFERENCES

- [1] M. L. Andre and M. J. O'Neal, "Mass Spectrometric Analyses of Medium-Viscosity Lubricating Oils," *Analytical Chemistry*, Vol. 31, p. 164 (1959).
- [2] G. P. Barnard, "Modern Mass Spectrometry," *The Institute of Physics*, London, Eng. (1953).
- [3] R. A. Brown, "Compound Types in Gasoline by Mass Spectrometric Analysis," *Analytical Chemistry*, Vol. 23, p. 430 (1951).
- [4] E. M. Charlet, K. P. Lanneau, and F. B. Johnson, "Analysis of Gas Oil Feed and Cycle Stocks from Catalytic Cracking," ACS Division of Petroleum Chemistry Symposium on the Composition of Petroleum, etc., Cleveland Meeting, April, 1951.
- [5] N. D. Coggeshall and A. S. Glessner, Jr., "Ultraviolet Absorption Analysis for Naphthalenes," *Analytical Chemistry*, Vol. 21, p. 550 (1949).
- [6] N. D. Coggeshall, "Organic Analysis," edited by J. Mitchell, Jr., et al, Interscience Publishers, New York, N. Y., (1953), p. 403.
- [7] G. F. Crable and N. D. Coggeshall, "Application of Total Ionization Principles to Mass Spectrometric Analysis," *Analytical Chemistry*, Vol. 30, p. 310 (1958).
- [8] S. H. Hastings, A. T. Watson, R. B. Williams, and J. A. Anderson, "Determination of Hydrocarbon Functional Groups by Infrared Spectroscopy," *Analytical Chemistry*, Vol. 24, p. 612 (1952).
- [9] S. H. Hastings, B. H. Johnson, and H. E. Lumpkin, "Analysis of the Aromatic Fraction of Virgin Gas Oils by Mass Spectrometer," *Analytical Chemistry*, Vol. 28, p. 1243 (1956).
- [10] J. J. Heigl, J. F. Black, and B. F. Dudenbostel, "Determination of Total Olefins and Total Aromatics in Hydrocarbon Mixtures by Raman Spectrometry," *Analytical Chemistry*, Vol. 21, p. 554 (1949).
- [11] H. R. Henze and C. M. Blair, "The Number of Isomeric Hydrocarbons of the Methane Series," *Journal, Am. Chem. Soc.*, Vol. 53, p. 3077 (1931).
- [12] R. H. Hughes and R. J. Martin, Symposium on Composition of Petroleum Oils, Am. Soc. Testing Mats., p. 127 (1958). (Issued as a separate publication ASTM STP No. 224.)
- [13] G. L. Kearns, N. C. Maranowski, and G. F. Crable, "Analysis of Petroleum Products in C_{12} to C_{20} Range. Application of FIA Separatory and Low Voltage Mass Spectrometric Techniques," *Analytical Chemistry*, Vol. 31, p. 1646 (1959).
- [14] J. F. Kinder, "Determination of Total Alkyl Benzenes in Selected Crude Fractions," *Analytical Chemistry*, Vol. 23, p. 1379 (1951).
- [15] H. S. Knight and S. Groennings, "Fluorescent Indicator Adsorption Method for Hydrocarbon Type Analysis," *Analytical Chemistry*, Vol. 28, p. 1949 (1956).
- [16] S. S. Kurtz and C. E. Headington, "Analysis of Light Petroleum Fractions," *Industrial and Engineering Chemistry*, Analytical Edition, Vol. 9, p. 21 (1937).
- [17] D. H. Lichtenfels and F. H. Burow, unpublished work.
- [18] D. R. Long and R. W. Neuzil, "Determination of Olefins by Means of Iodine Complexes," *Analytical Chemistry*, Vol. 27, p. 1110 (1955).
- [19] H. E. Lumpkin and B. W. Thomas, "Aromatic Molecular Weight Distribution and Total Aromatic Content Determination by Mass Spectroscopy," *Analytical Chemistry*, Vol. 23, p. 1738 (1951).
- [20] H. E. Lumpkin and B. H. Johnson, "Identification of Compound Types in a Heavy Petroleum Gas Oil," *Analytical Chemistry*, Vol. 26, p. 1719 (1954).
- [21] N. C. Maranowski, unpublished work.
- [22] R. J. Martin, R. H. Hughes, and G. F. Crable, "Quantitative Determination of Aromatic, Olefinic, and Saturate Hydrogen in Hydrocarbons by High Resolution Proton Magnetic Resonance," presented at the annual Pittsburgh Conference on Analytical Chemistry and Applied Spectroscopy, March 2-6, 1959.
- [23] J. J. Mitchell, "Physical Chemistry of Hydrocarbons," edited by A. Farkas, Academic Press, Inc., New York, N. Y. (1950), Ch. 3.
- [24] M. S. Norris and N. D. Coggeshall, "Ultraviolet Absorption Determination of C_6 and C_{10} Aromatics," *Analytical Chemistry*, Vol. 25, p. 183 (1953).
- [25] J. G. O'Connor and M. S. Norris, *Analytical Chemistry*, in preparation.
- [26] M. J. O'Neal and T. P. Wier, "Mass

- Spectrometry of Heavy Hydrocarbons," *Analytical Chemistry*, Vol. 23, p. 830 (1951).
- [27] E. L. Saier, A. Pozefsky, and N. D. Coggeshall, "Determination of Olefin Group Types," *Analytical Chemistry*, Vol. 26, p. 1258 (1954).
- [28] R. Schnurmann, W. F. Maddams, and M. C. Barlow, "Spectrophotometric Identification of Polynuclear Aromatic Components in High Boiling Petroleum Fractions," *Analytical Chemistry*, Vol. 25, p. 1010 (1953).
- [29] D. D. Tunnicliff, R. R. Brattain, and L. R. Zumwalt, "Benzene, Toluene, Ethylbenzene, *o*-Xylene, *m*-Xylene, and *p*-Xylene Determination by Ultraviolet Spectrophotometry," *Analytical Chemistry*, Vol. 21, p. 890 (1949).
- [30] K. Van Nes and H. A. Van Westen, "Aspects of the Constitution of Mineral Oils," Elsevier Publishing Co., New York, N. Y. (1951).
- [31] R. B. Williams, Symposium on Composition of Petroleum Oils, Am. Soc. Testing Mats., p. 168 (1958). (Issued as a separate publication *ASTM STP No. 224*.)

Quantitative Relations in the Mass Spectra of *n*-Paraffins

NORMAN D. COGGESHALL

Reprinted from THE JOURNAL OF CHEMICAL PHYSICS, Vol. 33, No. 4, pp. 1247-1252, October, 1960

Quantitative Relations in the Mass Spectra of *n*-Paraffins

NORMAN D. COGGESHALL

Gulf Research & Development Company, Pittsburgh, Pennsylvania

(Received May 9, 1960)

The mass spectra of *n*-paraffins in the C_6 to C_{30} range have been examined for quantitative relations that must be predicted by any theory of ion formation by electron impact. An ion sum $C(M, n)$ is defined as the sum of the normalized intensities of all ions of *n* carbon atoms from a *n*-paraffin of *M* carbon atoms. The molar yield $Y(M, n)$ per unit of ionizing current will be $MC(M, n)$. It has been observed that for large ions from large molecules the yield is independent of *M* or *n* but proportional to $(M-n)$. Yields for smaller ions, i.e., *n* between 3 and 15, are linear with *M* but not proportional to *M*. The yields in this region may be expressed as

$$Y(M, n) = An'e^{-bn}(M-n')$$

where *A* and *b* are constants, one set applying for $3 \leq n \leq 10$ and another set applying for $10 \leq n$; the *n'* values are constants, each depending upon the associated *n*. The observations indicate that the details of the fragmentation process for *n*-paraffins depend primarily upon the type of molecular skeleton, i.e., straight chain, single valence carbon-carbon linkages and secondarily upon the size of the molecule.

THE statistical theory¹ of mass spectra has been applied to the lower alcohols and alkanes^{2,3} with varying degrees of success. It is not believed that this theory in its present form can be effectively used for higher molecular weight compounds. This is based on the disagreements observed between predicted and experimental results³ and on the computational difficulties of applying it to larger molecules. A simpler theory, even though it might be usable only in a semiquantitative manner, is highly desirable. The present study was conducted to determine the general quantitative relations such a theory would have to predict for the *n*-paraffins. The studies encompass the *n*-paraffins from C_6 to C_{30} inclusive, excepting C_{19} for which no data were available.

SOURCE AND TREATMENT OF DATA

The data used were taken from the mass spectral data issued by the American Petroleum Institute Re-

search Project 44 and from experimental work done in this Laboratory. All data were taken with Consolidated Electrodynamics Model 21-103 type instruments. It is known that a direct comparison of data between such instruments cannot be made because of all the factors that influence sensitivity. However, the normalized patterns obtained from these instruments agree well enough to allow extensive analytical applications.^{4,5}

In covering the mass range necessary for the higher molecular weight compounds, it is customary to scan portions at two different magnetic fields. To produce a normalized spectrum from the low and high mass scans means that they must be quantitatively adjusted to agree at a particular mass value or cross-over point. The choice of this point could preferentially weight one end of the spectrum. Discrimination and other effects on pattern can result from the fields used and the magnitude of electron current. The values of these parameters as used for each spectrum are given in Table I.

¹ H. M. Rosenstock, M. B. Wallenstein, A. L. Wahrhaftig, and H. Eyring, Proc. Natl. Acad. Sci. U.S. **38**, 667 (1952).

² L. Friedman, F. A. Long, and M. Wolfsberg, J. Chem. Phys. **27**, 613 (1957).

³ L. Friedman, F. A. Long, and M. Wolfsberg, J. Chem. Phys. **30**, 1605 (1959).

⁴ See, for example: American Society for Testing Materials, Committee D-2; Proposed Tentative Method—Hydrocarbon Types in Low Olefinic Gasoline by Mass Spectrometry.

⁵ G. F. Crable and N. D. Coggeshall, Anal. Chem. **30**, 310 (1958).

TABLE I. Operating conditions used for spectra employed.

Carbon no.	Laboratory	Electron current in μ a	Initial magnet current in ma	Final magnet current in ma	Isatron temperature $^{\circ}$ C	Cross-over point (C_nH_{2n-1})	API ser. no.
6	GR&DC ^a	19.5	0.7	...	250
7	GR&DC	19.5	0.7	...	250
8	GR&DC	19.5	0.7	...	250
9	GR&DC	19.5	0.7	...	250
10	GR&DC	19.5	0.7	...	250
11	GR&DC	19.5	0.7	...	250
12	NBS	9.0	b	b	245	...	404
13	NBS	9.0	b	b	245	...	523
14	Shell Oil	50.0	0.9	1.3	265	C ₆	1255
15	Shell Oil	50.0	0.9	1.3	265	C ₆	1318
16	GR&DC	10.5	0.2	0.375	250	C ₃	...
17	Shell Oil	50.0	0.9	1.3	265	C ₆	1351
18	Shell Oil	13.5	0.6	1.3	250	C ₄	574
20	Shell Oil	10.0	0.9	1.3	265	C ₄	705
21	Shell Oil	50.0	0.9	1.3	265	C ₆	1310
22	Shell Oil	50.0	0.9	1.3	265	C ₆	1311
23	Shell Oil	50.0	0.9	1.3	265	C ₆	1312
24	Shell Oil	13.5	0.6	1.3	250	C ₄	575
25	Shell Oil	50.0	0.9	1.3	265	C ₆	1313
26	Atlantic Ref. Co.	9.0	0.56	1.08	250	C ₃	PSC 106
27	Shell Oil	50.0	0.9	1.3	265	C ₆	1314
28	Shell Oil	10.0	0.9	1.3	265	C ₄	886
29	Shell Oil	50.0	0.9	1.3	265	C ₆	1315
30	Shell Oil	50.0	0.9	1.3	265	C ₆	1316

^a Gulf Research & Development Company.^b Not listed.

The work of Otvos and Stevenson⁶ has shown that the total relative ionization cross-section of a compound is a constitutive molecular property, i.e., the sum of the atomic cross sections. Although their work was necessarily done in the lower molecular weight ranges, we are assuming the same results for higher molecular weight compounds. This assumption is somewhat confirmed by the work of Crable and Coggeshall.⁵ If we denote the total ionization of a n -paraffin C_MH_{2M+2} by $T(M)$ we have

$$T(M) = k[M(Q_C + 2Q_H) + 2Q_H], \quad (1)$$

where Q_C and Q_H are the relative ionization cross sections for carbon and hydrogen, respectively, and k is a constant depending upon experimental conditions and the units used for $T(M)$. Since, for compounds of interest here, $2Q_H$ will be small compared to $M(Q_C + 2Q_H)$, we may with adequate accuracy express $T(M)$ as

$$T(M) = KM, \quad (2)$$

where K is a constant.

Let us denote by $P_{M,n,i}$ the normalized ion intensity for an ion of stoichiometry C_nH_{2n+2-j} , $n \leq M$ which appears in the normalized mass spectral pattern for a n -paraffin of M carbon atoms. By normalization we mean that the sum of all intensities is equal to unity,

or in this case, to 100%, i.e.,

$$\sum_n \sum_i P_{M,n,i} = 100.$$

Let us define an ion sum $C(M,n)$ as the summation of intensities of all ions of n carbon atoms appearing in the normalized spectrum. Thus,

$$C(M,n) = \sum_i P_{M,n,i}; \quad \sum_n C(M,n) = 100.$$

Since the total ionization is proportional to M , the product $MC(M,n)$ therefore represents in a manner independent of experimental conditions or units the yield, $Y(M,n)$, per unit of ionizing electron current and per mole, of all ions of n carbon atoms being produced by electron impact on a normal paraffin of M carbon atoms.

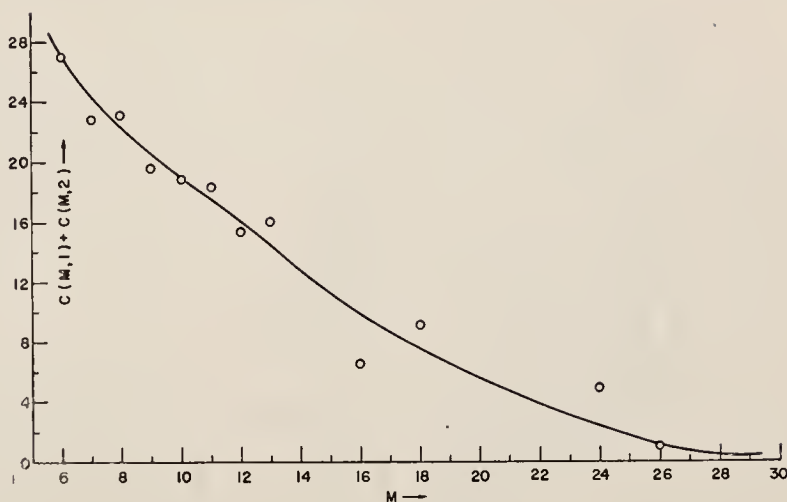
$$Y(M,n) = MC(M,n). \quad (3)$$

Such an approach requires a complete mass spectrum. Many of the API spectra were lacking pattern data for the one and two carbon atom ions. Interpolation and extrapolation were done by utilizing the available data. In Fig. 1 is given a plot of $C(M,1) + C(M,2)$ versus M as obtained from our own and API spectra for which such data were presented. From the curve drawn through these points were obtained the values used for normalizing other spectra.

In Table II are given the $Y(M,n)$ values calculated from the spectra. Note that they are not arranged in a

⁶ J. W. Otvos and D. P. Stevenson, J. Am. Chem. Soc. **78**, 546 (1956).

FIG. 1. Plot of $C(M, 1) + C(M, 2)$ used to interpolate for values not obtainable otherwise.



manner to display the variation with n but rather the variation with M and $(M-n)$. Obviously $(M-n)$ represents the number of carbon atoms going into neutral fragments in the process of creating ions of n carbon atoms from a molecule of M carbon atoms.⁷

DISCUSSION OF DATA

Looking across a row, constant $(M-n)$ value, in Table II, we have the yields from different compounds of ions all characterized by leaving behind the same size neutral fragment. In the upper left-hand part of the table, i.e., for the higher molecular weight compounds for $2 \leq (M-n) \leq 11$ (approximately) two surprising observations may be made. One is that, within this region, the probability or yield of ions created by casting off the same size neutral fragment is approximately constant and independent of the mass of the parent molecule. Thus, the yields are about the same for C_{26}^+ ions from C_{30} , for C_{25}^+ ions from C_{29} , for C_{24}^+ ions from C_{28} , etc.

The other observation, which is particularly well seen from the ions from C_{30} , is that, excepting the cases for $M-n=0$ and $M-n=1$, the yields of ions are approximately proportional to the number of carbon atoms $(M-n)$ in the neutral fragment expelled. For C_{30} this proportionality prevails up to a neutral fragment size of C_{15} .

These observations therefore indicate that the processes whereby large ions are created from the higher molecular weight *n*-paraffins are dominated by the size of the neutral fragment expelled and independent of the total mass of the molecule. This behavior is further demonstrated in Fig. 2 where the yields are plotted versus $(M-n)$ for the higher mass ions for the last eight members of the entire series. The ordinate scale for each successively lighter compound is uniformly

shifted upwards to pull the curves apart for display. In this series these curves are generically the same except for C_{26} which shows appreciable deviation. It is not known whether this is a real effect unique to this compound or whether its origin lies in some different experimental conditions. These deviations are also noticeable in Table II.

In contrast to this behavior it is clear from Table II that the yields of the lower mass ions, C_3^+ and C_4^+ , for example, depend markedly upon the mass of the parent compound. In Fig. 3 are plotted the yields of several different ions characterized by n versus the mass of the parent molecule. A primary observation is that, excepting for the low ends of the curves and for the pronounced scatter for the C_3^+ ions, the yields are linear with M but not proportional to M .

In Fig. 4 are plotted further yields versus M . The data for such curves are progressively poorer for increasing n and certain points and regions were excluded from the figure to eliminate overlapping of points. Although the scatter is bad, these ion types also display a linear dependence upon M . Despite the scatter, there is evidence for this linear dependence for ions as heavy as C_{24} when the data are plotted in a larger form.

It is clear that the yield may generally be represented as

$$Y(M, n) = f(n)(M - n'), \quad (4)$$

where $f(n)$ represents the slope of the curve for ions of n carbon atoms, and n' is the value of M at the point where the curve intercepts the M axis. We, therefore, have n' as a function of n . In Table III are given the values of $f(n)$ and n' as dependent on n up to $n=15$ as extracted from the data examined.

These values of n' cannot be regarded as very accurate as the value depends critically upon how a straight line is fitted to the data in each case. Excepting for $n=3$ they are of the same order of magnitude as n . This correlates with the behavior observed for the heavy ion

⁷ It is assumed in this treatment that during the process of impact and ionization that one ionized and one neutral fragment are created.

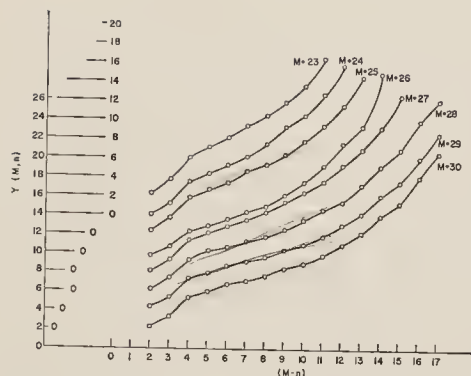


FIG. 2. Yield values versus $(M-n)$ for different values of M . Note the progressively shifted vertical scale.

classes wherein a direct dependence of intensity upon $(M-n)$ was noted.

The conclusions drawn here are based on the assumption that the available mass spectral patterns have absolute significance independent of experimental conditions. The exact status of their absolute significance is not known. It is known that CEC Model 21-103 type instruments give quite reproducible patterns, and this is the basis for extensive analytical applications.⁴ On the other hand, the nature of the scatter observable in the above figures indicates that it most likely arises

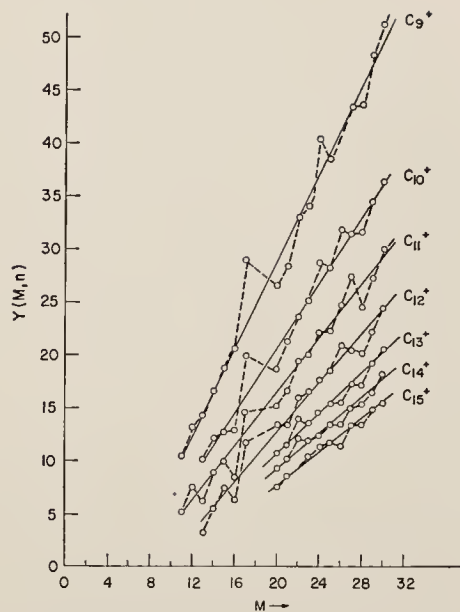


FIG. 4. Further yield plots versus M for the higher values of n .

from experimental conditions rather than unique molecular behavior. Discrimination between ions of different initial kinetic energies can occur in the ion source⁸ and between the ion source and the collector.⁹ It is not possible to correct the data used here for discrimination; however, it is believed that the data used here are fairly reliable in one sense. The discrimination between ion source and collector is independent of mass and dependent on accelerating voltage.⁹ Most investigators generally use about the same range of accelerating and magnetic field values to cover the same mass range. The pattern values used for ions of n carbon atoms will therefore have been obtained with a range of field values independent of M . This condition leads to internally consistent results for the behavior of any $Y(M, n)$ (M variable, n constant). However, the

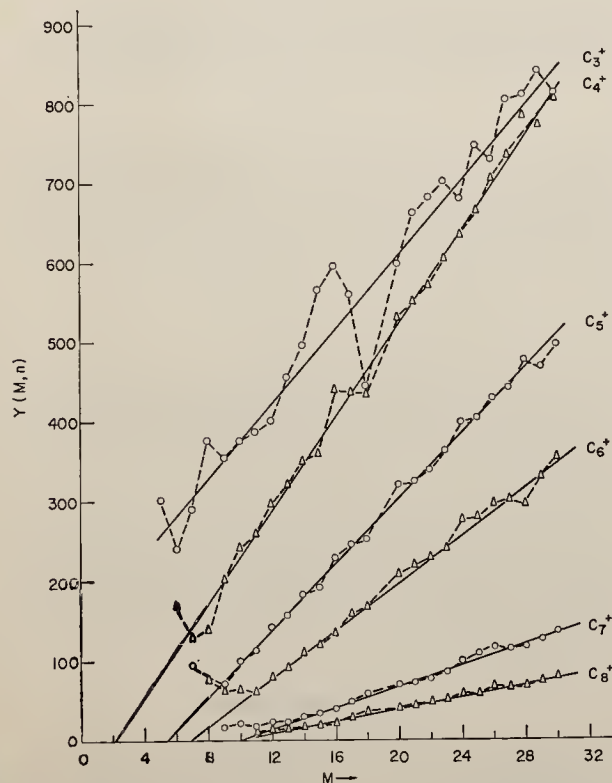


FIG. 3. Plots of yields, $Y(M, n)$ versus M and for different values of n .

TABLE III. Values of $f(n)$ and n' as determined from the data examined.

n	$f(n)$	n'
3	23.2	-6.3
4	28.9	2
5	20.6	5.4
6	14.9	6.8
7	6.8	10
8	3.6	10.4
9	2.1	6.0
10	1.6	6.4
11	1.3	6.5
12	0.94	8.5
13	1.1	8.5
14	0.9	8.5
15	0.8	10.0

⁸ N. D. Coggeshall, J. Chem. Phys. 12, 19 (1944).

⁹ C. E. Berry, Phys. Rev. 78, 597 (1950).

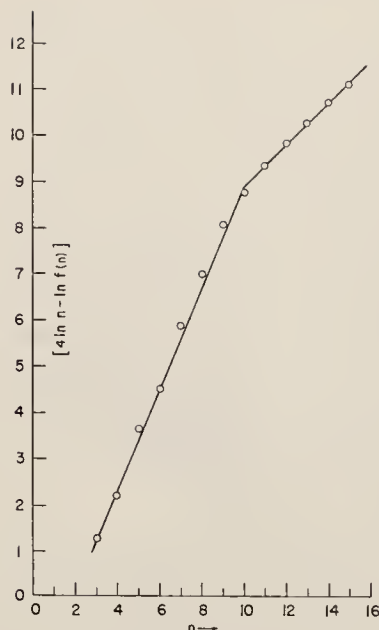


FIG. 5. Plot of $[4 \ln n - \ln f(n)]$ versus n .

effects of discrimination undoubtedly attenuate the intensities of the ions in the higher mass range. If correction could be made for discrimination, it is believed that it would change the slopes of the curves but not the nature of the behavior. The quantitative conclusions made here must then be regarded as subject to change when better data are available. It is expected that such changes would affect the numerical results but not the observed qualitative nature of the spectral behavior.

It is interesting to note that the $f(n)$ values as a function of n have the same general characteristics as the mass spectrum for a n -paraffin, i.e., the greatest values for 3 and 4 carbon atoms, a rapid decrease in value down to about 9 carbon atoms and then a more gradual decrease with increasing carbon number. In Fig. 5 is seen a plot of $[4 \ln n - \ln f(n)]$ versus n . The straight line behavior shows that $f(n)$ may be represented by

$$f(n) = An^4 e^{-bn}, \quad (5)$$

where A and b are constants. One set of constants applies for $2 < n \leq 10$ and another set applied for $10 \leq n$. No explanation is given for this functional behavior of $f(n)$. From these relations it is clear that yields $Y(M, n)$ may therefore be represented for any n -paraffin in the 3 carbon to 15 carbon ion range by

$$Y(M, n) = An^4 e^{-bn} (M - n'). \quad (6)$$

CONCLUSIONS

In summarizing the observations, it is important to restate the mode of handling the data. The spectra

were first normalized. An ion sum $C(M, n)$ was defined as the summation of intensities of all ions of n carbon atoms occurring in the spectrum of a n -paraffin of M carbon atoms. The yield of such ions per unit of ionizing electron current and per mole charged is given as $Y(M, n) = MC(M, n)$. The proportionality with M results from the fact that the total ionization is a constitutive property of the ionization cross sections of the constituent atoms. The data were assembled and studied for n -paraffins ranging from C_6 to C_{30} .

It has been tentatively observed that:

(1) For large ions, i.e., n of the order of 15 or larger, from large molecules the yield of ions is independent of n and M and dependent only on $(M - n)$, the size of neutral fragment created.

(2) The yields of the large ions, as expressed in (1) above, are approximately proportional to $(M - n)$. The extent to which this applies depends, of course, on the size of the molecule; for C_{30} this applies for n between about 15 and 28.

(3) Yields for smaller values of n , for example from 3 to 15, depend upon both M and n .

(4) For any value of n in the region expressed in (3) the yield is linear with M but not proportional to M .

(5) For values of n in this region the yield $Y(M, n)$ can be expressed as

$$Y(M, n) = f(n) (M - n').$$

(6) The values of n' are positive for all values of n observed except for $n=3$ which yields a negative value.

(7) The function $f(n)$ may be represented by

$$f(n) = An^4 e^{-bn}$$

where A and b are constants; one set of these constants applies for $3 \leq n \leq 10$ and another applies for $10 \leq n$.

(8) Combining the above results the yield $Y(M, n)$ may be expressed as

$$Y(M, n) = An^4 e^{-bn} (M - n')$$

for values of n between 3 and 15.

It is realized that these observations are approximate and tentative. It is expected that improved data will change some of the relations quantitatively but not qualitatively.

It is believed that the observations made here on n -paraffin spectra indicate that the details of the fragmentation process depend primarily upon the type of molecular skeleton, i.e., straight-chain, single valence carbon-carbon linkages and secondarily upon the size of the molecule.

ACKNOWLEDGMENTS

Appreciation is expressed to Mr. H. T. Best for the computation work done on the mass spectral data and to Dr. G. F. Crable for various discussions on the subject.

LANCASTER PRESS, INC., LANCASTER, PA.

Effect of Dissolved Oxygen on the Spin-Lattice Relaxation Time of Free Radicals
in Petroleum Oils

A. J. SARACENO AND N. D. COGGESHALL

Reprinted from THE JOURNAL OF CHEMICAL PHYSICS, Vol. 34, No. 1, pp. 260-263, January, 1961

Effect of Dissolved Oxygen on the Spin-Lattice Relaxation Time of Free Radicals in Petroleum Oils

A. J. SARACENO AND N. D. COGGESHALL

Gulf Research & Development Company, Pittsburgh, Pennsylvania

(Received June 14, 1960)

Electron paramagnetic resonance studies of free radicals in petroleum oils reveal that the presence of dissolved oxygen significantly affects the free radical spin-lattice relaxation time, T_1 . Changes in T_1 can occur upon: (a) dilution with solvents, (b) exposure to light, (c) bubbling with oxygen, and (d) stripping of dissolved oxygen. In this investigation it is shown that these changes all result from the influence of dissolved oxygen. Dilution with ordinary cp solvents results in a decrease of T_1 . If the solvent is first stripped of dissolved oxygen, there will be no changes in T_1 . The effect is reversible, i.e., the value of T_1 for free radicals in a petroleum oil may be arbitrarily decreased or increased by adding or removing dissolved oxygen, respectively. It was observed that free radicals in oil, or in oil in solution, experienced an increase in spin-lattice relaxation time when allowed to remain sealed in a quartz tube. This change was traced to the effect of light and appears to occur for wavelengths of the order of 5400 Å and lower. It is concluded that this phenomenon is due to the photochemical takeup of dissolved oxygen whose presence decreases T_1 . This is based on the fact that T_1 may be lowered to its original value merely by adding molecular oxygen to the petroleum oil. Depending upon the degree of saturation being effected, changes in T_1 will be reflected as changes in "apparent" free radical content. The true free radical content was unchanged by the processes studied.

MANY full crudes, petroleum bottoms, and oil distillates have been observed to yield a single paramagnetic resonance peak near a g value of 2.00¹⁻³. The resonance is in addition to and superimposed upon that arising from the presence of any V^{+4} as vanadyl.^{2,3} Nickel porphyrin also occurs in petroleum oils but it exists in a diamagnetic state. Hence, the single resonance can only be explained by the presence of free radicals in petroleum oils. The fact that a large number of free radicals become trapped during the carbonization of organic matter⁴⁻⁶ is probably related to the mechanism by which free radicals were formed in petroleum.

Previous EPR measurements on petroleum crudes^{1,2} reveal no hyperfine structure which may arise from the nuclear moments of surrounding atoms such as hydrogen.

While engaged in the measurement of the free radical content of petroleum oils by EPR, we observed that saturation of the free radical resonance occurred at relatively low rf levels (~ 1 mw). Subsequently, it was found that the degree of saturation (and hence the value of the spin-lattice relaxation time) depended greatly upon the manner in which a given petroleum oil was treated prior to examination. This investigation is concerned with the variation of the spin-lattice relaxation time T_1 for the free radical resonance which was systematically studied with respect to effects of

solvents, dissolved oxygen, and radiation in the visible and ultraviolet region.

APPARATUS AND EQUIPMENT

A Varian Associates X-band spectrometer, model V-4500, employing audiomagnetic field modulation and phase-sensitive detection was used. The standard 6-in. diam pole face magnet (V-4007) with a 2.00-in. air gap and matching power supply (V-2200A) comprised the magnet system. The derivative of the absorption line was traced out in all cases by a pen recorder.

Special, clear fused quartz tubing (General Electric Lamp Glass Department, Cleveland, Ohio) was used in making tubes for holding oil samples in the resonant cavity. The tubes, sealed at one end and about 4.5 in. in length, had the following tolerance specifications: $3 \text{ mm} \pm 12\%$ i.d. $\times 4.75 \text{ mm} \pm 0.25 \text{ mm}$ o.d.

Ultraviolet and Visible Radiation

Petroleum oils were exposed to relatively narrow frequencies in the visible and ultraviolet region through the use of glass color filters with nominal wavelengths of 600, 540, 500, 420, and 400 m μ . The light source was direct (through window glass) or reflected sunlight.

EXPERIMENTAL RESULTS

Saturation Behavior

Electron resonance experiments were conducted at rf power levels varying from about 1 to 80 mw. The general saturation behavior of free radicals in petroleum can be seen in Fig. 1. This curve is also characteristic of asphaltene. The latter saturate easily even at 1.0 mw and, for this reason, it is difficult to obtain an accurate measure of spin concentration in this case. In the low microwave power region, there is only a negligible

¹ H. S. Gutowsky, B. R. Ray, R. L. Rutledge, and R. R. Unterberger, *J. Chem. Phys.* **28**, 744 (1958).

² D. E. O'Reilly, *J. Chem. Phys.* **29**, 1188 (1958).

³ A. J. Saraceno, D. T. Fanale, and N. D. Coggeshall, *Anal. Chem.* (to be published).

⁴ J. E. Bennett, D. J. E. Ingram, and J. G. Tapley, *Defects in Crystalline Solids* (Physical Society, London, 1954), p. 65; *Phil. Mag.* **45**, 545 (1954); *Nature* **174**, 797 (1954).

⁵ J. Uebersfeld, A. Etienne, and J. Combrisson, *Nature* **174**, 614 (1954).

⁶ D. E. G. Austen, D. J. E. Ingram, and J. G. Tapley, *Trans. Faraday Soc.* **54**, 400 (1958).

saturation of the free radicals in oils. A nonsaturating resonance, in the region of rf levels employed, is indicated by the dotted line for V^{+4} as vanadyl ion.

The saturation method is generally used in measuring T_1 .^{7,8} This consists of measuring the absorption at high (saturating) rf levels and at relatively low power. From the variation of signal with microwave power a saturation parameter, defined as the ratio of the complex susceptibility under saturating conditions to the complex susceptibility under nonsaturating conditions, can be determined and, together with a knowledge of the spin-spin relaxation time (T_2), T_1 can be calculated. T_2 is approximated from the linewidth at very large dilution and at lower power. Since precise and absolute determinations of T_1 are difficult, relative values of the spin-lattice relaxation time are emphasized here.

Depending upon the degree of saturation being effected, changes in T_1 will be reflected as changes in "apparent" free radical content. The true free radical content was unchanged by the processes studied. The larger T_1 becomes, the smaller becomes the observed or "apparent" free radical content. Such changes have been at times interpreted as a real change in free radical content.

Portis⁵ treats different types of homogeneous and inhomogeneous broadening and gives four cases for the variation of the saturation parameter with the variable s where $s = \frac{1}{2}\gamma^2 H_1^2 T_1 T_2$. We compared our data with each of the four cases and found about equally good fit for either of Portis' cases 2 or 3. Since case 2 is simple, giving the saturation parameter b_1 as

$$b_1 = 1/(1+s),$$

it was used to determine the order of magnitude of T_1 which is 10^{-6} sec. Spin-lattice relaxation times of smaller

TABLE I. Effect of reflected sunlight on the relative value of spin-lattice relaxation time for free radicals in a Kuwait fuel oil containing 10^{16} spins/g.

Time of exposure (hr)	Relative relaxation time (arbitrary units)	Relative relaxation time of oil shielded from light (arbitrary units)
0	0.22	0.22
1	0.59	0.22
2	0.80	0.22
3	0.98	0.23
4	1.00	0.23

magnitude are difficult to evaluate because of limitations of the klystron power output in obtaining saturation data. The linewidth of the free radical resonance is approximately 6.0 gauss which corresponds to 10^{-9} sec for the value of T_2 .

In each case the signal divided by $P^{\frac{1}{2}}$, where P is microwave power, was extrapolated to zero power. This provided a base point for determination of saturation parameter b_1 as a function of power. Since none of Portis⁵ cases matched the data exactly, we may take $b_1 = f(s)$ wherein the exact functionality of f is unknown. In each experiment we interpolate the data to determine the power for $b_1 = \frac{1}{2}$. From the foregoing we have $s = kPT_1$ where k is a constant. We may then use this expression to calculate relative values of T_1 as s will necessarily have the same value in all cases where $b_1 = \frac{1}{2}$. Parameters such as the volume of the cavity, klystron frequency, etc., which are involved in computing the absolute value of T_1 remain constant and need not be evaluated.

For a given type of treatment (dilution with solvents, exposure to sunlight, etc.) the longest observed T_1 in each case was assigned an arbitrary value of unity. Changes in T_1 are with reference to the oil subjected to the specific treatments listed in Tables I-V.

Effects on Free Radical Concentration

We may briefly state the observations (conducted at nonsaturating rf levels) as follows: exposure of the oils to sunlight or ultraviolet radiation caused no change in the free radical concentration; the addition of either benzene, carbon disulfide, *n*-hexane, or isooctane similarly produced little or no observable effects; and, bubbling molecular oxygen into a petroleum oil had no effect on the radical concentration.

Changes in Spin-Lattice Relaxation Time

Table I contains a tabulation of approximate relative values of T_1 for a fuel oil which was exposed to reflected sunlight for varying periods of time. Corresponding values of T_1 for the oil sample retained in complete darkness are also listed. Values of T_1 for the same oil

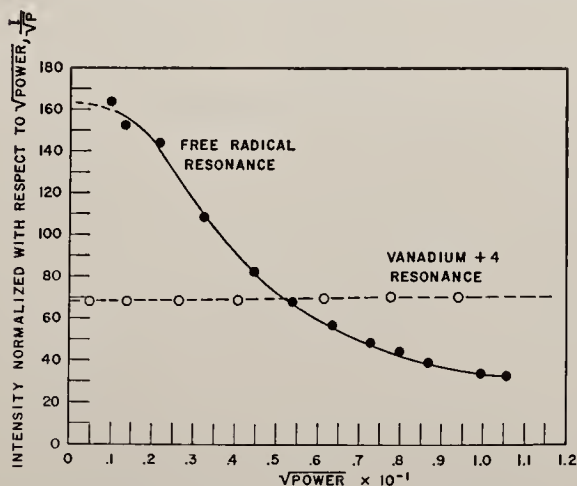


Fig. 1. Typical saturation curve for free radical resonance.

⁷ D. J. E. Ingram, *Free Radicals as Studied by Electron Spin Resonance* (Butterworths Scientific Publications, Ltd., London, 1958).

⁸ A. M. Portis, *Phys. Rev.* **91**, 1071 (1953).

TABLE II. Effect of different wavelengths on the relative value of spin-lattice relaxation time for free radicals in a Kuwait fuel oil containing 10^{16} spins/g.

Wavelength ($m\mu$)	Time of exposure (hr)	Relative relaxation time (arbitrary units)
600	1	0.22
540	1	0.28
500	1	0.60
420	1	0.64
400	1	0.80
Direct sunlight	1	1.00
Complete darkness	1	0.22

exposed to specific wavelengths of light for a time of 1 hr are given in Table II. The oil was exposed to radiation while sealed in quartz tubes which could be immediately scanned for the free radical resonance.

The variation of T_1 as a function of the type of solvent added is summarized in Table III for a Kuwait petroleum residue. Analogous data are presented in Table IV for the residue and an asphalt containing ordinary cp benzene at three concentrations.

The effect of oxygen on T_1 is illustrated in Table V for the residue and its benzene solution (50% by weight). Since little or no change in T_2 was observed throughout this work, its value is not tabulated.

DISCUSSION OF RESULTS

No effects on the free radical concentration were observed as due to light, oxygen, and organic solvents. Consequently, we may conclude that the free radical species in oil are stable and are not created through dissociation of diamagnetic molecules upon dilution with solvents. This is in contrast to the results reported for coal asphaltenes.⁹

Striking changes in the spin-lattice relaxation time were observed for the free radicals in petroleum oils when subjected to the various treatments described. These changes are so pronounced that, at high rf levels

TABLE III. Effect of oxygen-containing solvents on relative spin-lattice relaxation time for a free radical in a Kuwait residue containing 10^{17} spins/g.

Solvent	Wt %	Relative relaxation time (arbitrary units)
Methylene chloride	50	0.26
Benzene	50	0.24
Carbon disulfide	50	0.10
n-Hexane	50	0.97
Original oil sample	...	1.00

TABLE IV. Influence of oxygen-containing benzene on relative value of T_1 at various concentrations of solvent.

Kuwait residue (10^{17} spins/g)	
Wt % benzene (cp)	Relative relaxation time (arbitrary units)
0	1.00
10	0.32
50	0.23
90	0.22
Asphalt (10^{18} spins/g)	
Wt % benzene (cp)	Relative relaxation time (arbitrary units)
0	1.00
10	0.14
50	≈ 0.012
90	≈ 0.010

(~ 80 mw), the free radical signal can differ by as much as an order of magnitude.

When a petroleum oil was sealed in a quartz tube and exposed to sunlight, a progressive increase in the spin-lattice relaxation time is easily detected. When the same oil was kept in the dark, however, little or no change in T_1 was observed (Table I). By contrast, the addition of ordinary cp solvents to a petroleum oil had the effect of shortening the relaxation time. Not only was the decrease in T_1 initially proportional to the concentration of solvent (Table IV), but the net change in T_1 differed considerably for each solvent (Table III).

Shortening of T_1 was found for petroleum oils saturated with molecular oxygen, whereas purging the same

TABLE V. Effect of oxygen on spin-lattice relaxation time of free radicals in a Kuwait residue containing 10^{17} spins/g.

Original oil sample	
Environment	Relative relaxation time (arbitrary units)
Under nitrogen	1.00
Air exposed	0.44
Bubbled with oxygen	0.31
Diluted 50% by weight in benzene	
Environment	Relative relaxation time (arbitrary units)
Under nitrogen	1.00
Air exposed	0.11
Bubbled with oxygen	≈ 0.05

⁹ R. A. Friedel, J. Chem. Phys. **31**, 280 (1959).

oils with either hydrogen or nitrogen resulted in an increase. Since oxygen was found to play such an important role in reducing T_1 , the experiments on oil diluted with solvents were repeated after both had been purged free of dissolved oxygen. Very little change in T_1 was observed upon dilution in this instance. Upon exposure to air, however, T_1 became appreciably shorter (Table V). Again it was found that benzene, carbon disulfide, and methylene chloride solutions of the oil displayed much greater changes than *n*-hexane with respect to T_1 . The addition of nitric oxide, another simple paramagnetic molecule, also results in a shortening of T_1 for the free radical species in a petroleum oil.

Qualitative experiments on photochemical effects, mentioned previously, showed that a spin-lattice relaxation time, which had been increased by exposure to light, could be reduced by bubbling molecular oxygen through the oil. Re-exposure of the oil to light of appropriate wavelength was found to result in an increase of T_1 .

Only wavelengths of light below $600\text{ m}\mu$ are responsible for altering T_1 , as observed with the use of filters (Table II). As can be seen from Table II, there is a greater change of T_1 in going from a light-shielded environment to one exposed to progressively shorter wavelengths. These observations can be explained in the following manner. First, the presence of dissolved oxygen shortens the spin-lattice relaxation time as noted in Table V. Second, it is postulated that, during exposure of oils to light of suitable wavelengths, a chemical reaction between atmospheric or dissolved oxygen and certain photochemically sensitive materials in the oil is accelerated. The free radical species, as well as diamagnetic hydrocarbons, are probably involved in the chemical reaction with dissolved oxygen but, because of the large excess of the latter, a radical change is presumably too slow to be detected. The photochemical uptake of dissolved O_2 results in the removal of a magnetic environment within the spin system and this in turn lengthens T_1 . The effect of light on T_1 is therefore an indirect influence acting by a mechanism involving oxidation of the oil. Since many hydrocarbons undergo

very slow autoxidation even in the absence of light, we may expect that slight changes in T_1 will occur for the free radical species in an oil upon standing in air.

This phenomenon offers an indirect method for detecting, measuring, and following the content of dissolved oxygen, provided that the radical concentration remains constant over a sufficiently long period of time.

The details of the saturation behavior of a spin system depend markedly on the nature of the broadening mechanism. Two types of broadening are recognized⁷: (1) homogeneous broadening in which the line shape is altered by interactions within the spin system or from external interactions which fluctuate rapidly compared with the time taken for a spin transition (e.g., dipolar spin-spin interaction, spin-lattice interaction, and exchange narrowing); (2) inhomogeneous broadening arising from interactions which come from outside the spin system and which vary slowly in time compared with the spin transition. It is possible to distinguish between these two general types by observing any changes accompanying the linewidth upon variation in power. Homogeneous broadening is characterized by an increase in linewidth on saturation, while to a first approximation inhomogeneous broadening does not result in such a change of line shape but only in a reduction of expected power absorption which will be proportional across its whole width. Measurements on linewidth changes at various stages of saturation do not show line broadening between points of maximum slope for the free radical resonance in petroleum oils. This would appear to indicate, therefore, that the shape of the line is remaining constant and inhomogeneous saturation is occurring. This is consistent with the idea that the linewidth of the free radical resonance in petroleum oils is governed by hyperfine interaction with protons.

ACKNOWLEDGMENTS

The authors wish to acknowledge the assistance of J. F. Itzel in obtaining experimental data and the benefit of discussions on this subject with Dr. D. E. O'Reilly and Dr. C. P. Poole, Jr.

Reprinted from

ANALYTICAL CHEMISTRY

An Electron Paramagnetic Resonance Investigation of Vanadium in Petroleum Oils

A. J. SARACENO, D. T. FANALE, and N. D. COGGESHALL
Gulf Research & Development Co., Pittsburgh, Pa.

Volume 33, Number 4

Pages 500-505, April 1961

Copyright 1961 by the American Chemical Society and reprinted by permission of the copyright owner

An Electron Paramagnetic Resonance Investigation of Vanadium in Petroleum Oils

A. J. SARACENO, D. T. FANALE, and N. D. COGGESHALL

Gulf Research & Development Co., Pittsburgh, Pa.

► Electron paramagnetic resonance (EPR) spectra of petroleum oils containing vanadium show the presence of hyperfine splitting which serves to identify part of the resonance with that of porphyrin complexes of vanadium. Quantitative electron paramagnetic resonance spectroscopy was performed to establish the amount of total vanadium existing in the +4 oxidation state for a large number of oils. Using vanadyl etioporphyrin(I) complex as a standard, nominal EPR vanadium determinations were obtained on a series of distillates, residues, and full crudes having a total vanadium content in the range of 0.1 to 200 p.p.m., and the results were compared to values obtained by chemical analysis. Good agreement between the EPR determinations and the chemical results was found. The presence of light ends in full crudes alters the line shape of the vanadyl resonance as compared to viscous media, requiring the use of different standards or the removal of the lighter fractions by distillation. Based on the petroleum oils examined, the conclusions from these studies are that with very few exceptions all the vanadium in petroleum oils whether they be distillates, residues, or full crudes exists in a single valence state, namely, the +4 oxidation state; the crystal field environment around

vanadium in petroleum oils is essentially the same. Quantitative determination of vanadium in oil distillates in the range of 0.1 p.p.m. and higher is feasible by EPR spectroscopy.

PETROLEUM CRUDES, charge stocks, and heavy distillate oils almost invariably contain trace metals such as vanadium, nickel, copper, and iron. Vanadium and nickel are known to be combined at least partly in the form of porphyrin complexes (16). Interest in this respect has centered, on one hand, among geologists who are concerned with any facts which might shed light on questions related to petroleum geology, and, on the other, among chemical engineers in the petroleum refining industry who are interested in the relationship of these trace elements to the technology of refinery operations. Several aspects of the nature of vanadium compounds in oil have been revealed by investigations based largely on chemical and spectrophotometric techniques. These studies have included the identification or isolation of vanadium porphyrin in certain crudes (13, 15) and investigations of physical properties (1, 17). Chemical evidence for the existence of three classes of metallic complexes in oils has been presented (7) and the discrepancy to the effect that there exists only 10 to 40% enough porphyrin

in oil to satisfy the metals content has been pointed out (7, 11). With regard to asphaltenes, the existence of vanadium as a metallo-organic compound (2) and its probable association with large molecules have been indicated (5).

Synthetically prepared vanadyl etioporphyrin(I) complex (4) when dissolved in a high viscosity petroleum oil exhibits a characteristic electron resonance spectrum (12) consisting of a hyperfine pattern with an over-all spread of approximately 1000 gauss. The presence of a single unpaired electron in the 3d orbital of the central quadrivalent vanadium is responsible for the paramagnetism of the metal porphyrin complex. It is not surprising that crude oils, distillates, and residues containing significant amounts of vanadium also exhibit an EPR spectrum similar to that of vanadyl etioporphyrin(I). This resemblance, in fact, indicates that part of the vanadium is present in the +4 oxidation state.

This investigation was undertaken with three specific objectives in mind: First, to determine if the vanadium in petroleum oils is present in a single oxidation state using EPR as a tool. Second, in view of the high sensitivity of electron paramagnetic resonance, to evaluate a possible rapid and accurate quantitative method for the determination of vanadium, and third, to gain

knowledge in the application of EPR for analytical purposes.

Quantitative analysis by EPR of materials containing trace metals has not been as extensive as the determination of spin concentration in various free radical systems, the most widely exploited quantitative use of EPR (8). Considering the analytical rapidity of the technique, the small amount of sample required, and extremely high sensitivity obtainable, development work on electron spin resonance spectroscopy has not kept pace with the newer instrumental methods of analysis.

ELECTRON PARAMAGNETIC RESONANCE (8, 9)

An electron in an atom has an intrinsic spin angular momentum and an orbital angular momentum due to circulation about the nucleus. Both of these angular momenta may have only quantized values in an atom and can be assigned specific quantum numbers. Each of these motions of the electron gives rise to a magnetic moment. The total magnetic moment is the vector sum of these separate magnetic moments. Atoms or ions having closed electron shells and paired electrons have zero moments and quantum numbers. Thus, only relatively few of the common elements are paramagnetic, since to be paramagnetic an atom must have one or more unpaired electrons.

In paramagnetic resonance experiments, only the spin component of angular momentum can usually orient freely in the magnetic field since the orbital component is locked by the electric field existing in the complex. The orbital component is thus said to be quenched. There are several methods of detecting and measuring electron spin moments (9). The method employed here depends upon the fact that, when unpaired spins are placed in a direct current magnetic field, a resonant condition can exist when a microwave field of proper frequency is applied. If compared with a suitable standard, the absorption of microwave energy is a measure of the number of unpaired electrons present in a sample.

Transition elements occur when electrons enter an outer *s* shell before completely filling inner *d* or *f* shells; the first atom showing this effect is titanium. The fact that a metal ion possesses an unfilled shell, and hence a permanent magnetic moment, which can have its energy altered by an external field, does not necessarily mean that paramagnetic resonance can be observed in its compounds. Two additional factors govern the observation of paramagnetic resonance. It is possible for all the degeneracy of the energy levels to be removed before application of the external field due to the action

of the very strong electric fields present in the crystal. In this case, although the applied magnetic field will change the energy of the levels, it may never bring them close enough together for transitions to be induced between them by frequencies in the microwave region. A very general theorem by Kramers (9) states that if there is an odd number of unpaired electrons in the ion no electric field can completely remove the degeneracy. Paramagnetic resonance is always theoretically possible in such cases, the bottom energy level always being at least twofold degenerate in spin.

The other main factor governing the observation of paramagnetic resonance is the question of line width. The two major causes of broad lines in paramagnetic resonance are spread of energy levels by spin-lattice and spin-spin interactions. The latter is associated with the proximity of the neighboring paramagnetic ions and can always be reduced by diluting with an isomorphous salt. The former, on the other hand, is due to the splitting of the orbital levels of the paramagnetic ions themselves, those with relatively close energy levels having short spin-lattice relaxation times and wide absorption lines. It is evident that the crystal field around a metal ion has a profound effect on whether paramagnetic resonance can be observed under usual conditions.

Vanadium (+4), with an odd electron in the *d*-orbital, by virtue of Kramers' theorem can theoretically be observed in any crystal environment. Whether V^{+4} can be observed at room temperature depends essentially on the degree to which the orbital levels are split. An orbital splitting of the order of $10,000\text{ cm}^{-1}$ is required to maintain a sufficiently long spin-lattice relaxation time at room temperature and can occur when the symmetry of the field departs strongly from cubic symmetry. Since the reference compound used in this investigation was in the form of $> V=O$, the presence of oxygen would produce a strongly noncubic field (12). This type of electrostatic field would account for the fact that the vanadyl resonance is observable at room temperature with a relatively narrow line width.

Apparatus. All EPR measurements were made with Varian Associates X-band spectrometer, Model V-4500, employing audio-frequency magnetic field modulation and phase sensitive detection. The standard 6-inch diameter pole face magnet (V-4007) with a 2.00-inch air gap and matching power supply (V-2200A) comprised the magnet system.

QUANTITATIVE EPR MEASUREMENTS

The information obtainable experimentally from electron spin resonance

includes line width, saturation behavior, electron spin concentration, and *g*-factor.

The line width is defined as the width (in gauss) between deflection points on the derivative absorption curve. The normal absorption curve is converted approximately to the first derivative in a phase sensitive detection method which is employed in the Varian Associates EPR spectrometer.

With ideal experimental conditions, the number of spins in an unknown sample may be obtained by direct comparison with a sample of known concentration. For the case of vanadium in oils, vanadyl etioporphyrin(I) complex, which contains one unpaired spin/molecule as expected for the +4 valence state, was used as a reference. Known amounts of the complex were dissolved in an oil distillate free of trace metals. The quantity which measures the number of spins is the area beneath the absorption curve, or in the case of first derivative presentation, the first moment divided by the modulation amplitude. If a series of similar samples is being compared, relative intensities can be obtained by measuring the height of the normal absorption curve, or, in the case of first derivative recording, the height between points of maximum deflection. It must be understood that obtaining relative intensities in this manner is valid only if the line width and shapes are alike. This condition is fulfilled if the environmental viscosity of the standard and unknown solution are equal. The best choice of solvent for the standard was, therefore, a metal-free heavy oil distillate when EPR derivative intensities were being compared.

Some of the important factors which affect intensity or for which corrections must be made are as follows: 1, sample geometry; 2, modulation amplitude; 3, power level, which has to be set so as not to cause saturation; and 4, degradation of the *Q* of the cavity by the sample.

The sample geometry was easily maintained constant by using special clear fused quartz tubing having especially uniform diameter.

The modulation amplitude was kept constant during the entire series of experiments. It was adjusted to a value of 200 c.p.s. for maintaining sweep amplitudes at about 5 gauss in the coils located inside the Varian cavity. An excessive modulation, greater than the line width of resonance line, leads to distorted derivative spectra and artificially broadened lines.

A high power output is desirable to obtain maximum sensitivity. However, power saturation which is possible in resonance spectroscopy can result at certain regions of radio-fre-

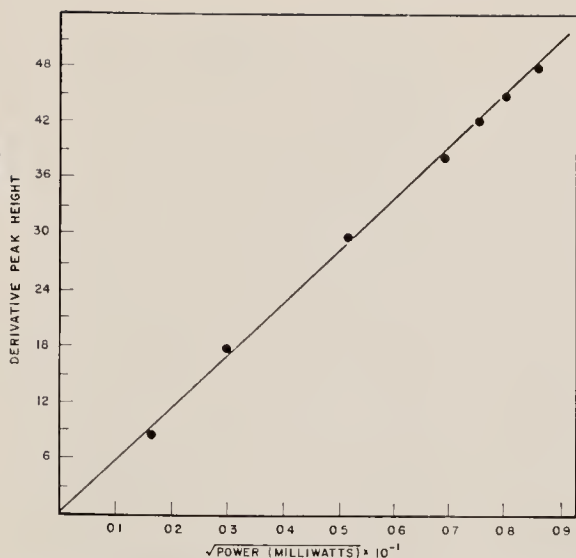


Figure 1. Saturation behavior of vanadyl resonance in viscous oil

quency power. A check against this phenomenon was performed by plotting signal intensity against the square root of the microwave power (Figure 1) for the vanadyl resonance in a high viscosity petroleum oil. The linear relationship shows that it is safe to do quantitative work at the power levels employed for this system.

Changes in the *Q* of the cavity can result with samples that have different dielectric properties or surface areas. Since all samples were of similar type, no serious changes in the efficiency (*Q*) of the resonant cavity were expected.

EXPERIMENTAL PROCEDURE

Special clear fused quartz tubing was used in making sample containers for insertion in the resonant cavity. The tubes, sealed at one end and about 11 cm. in length, had the following tolerance specifications: 3 mm. ± 12% inner diameter × 4.75 mm. ± 0.25 mm. outer diameter. Volume calibrations were performed on a series of tubes to determine if any varied sufficiently to produce experimental errors greater than 10%. Each tube was appropriately labeled and could be positioned to the same point and orientation in the resonant cavity.

After heating to approximately 160° F. with thorough agitation, the oil samples were transferred to the quartz tube by a syringe or eye dropper and allowed to cool to room temperature. Exceedingly viscous samples, such as some visbroken tars, were first diluted with a metal-free heavy oil distillate to facilitate handling. Care was taken to remove air bubbles which became entrapped or dispersed in the oil when placed in the quartz tubes. This was done by reheating the oil in the tube and allowing air bubbles to rise to the surface. The quartz tubes could be easily cleaned for reuse by heating, drawing out the oil by suction with a capillary,

rinsing several times with benzene, and finally drying in a stream of air.

Volume calibration for tubes would have sufficed if all the materials examined had similar densities or if results were being reported in weight per unit volume. Since chemical results were being reported in parts per million by weight, density variations had to be checked. The density of the petroleum oils did not vary by more than 6% (0.93 gram per milliliter being the average). However, several asphalt-*enes* had packing densities of anywhere from 0.5 to 0.9 gram per milliliter and suitable corrections were applied.

Standards were prepared by dissolving known amounts of vanadyl etioporphyrin(I) complex in a Tapanito heavy oil distillate which yielded no EPR spectrum and contained no trace metals. Portions of each standard were then transferred to quartz tubes and sealed. These were retained for use in checking the spectrometer sensitivity from time to time. The standards prepared covered the range of 0.1 to 50 p.p.m. of vanadium.

The magnetic field was slowly altered to obtain the value at which resonance occurred for electronic precession in a microwave field. Since only one line of the hyperfine pattern is necessary for obtaining the relative intensities, just a narrow portion of the vanadium (+4) resonance needs to be scanned. Figure 2 shows a series of four concentrations and the derivative peak height of the most intense peak at room temperature. The magnetic field ranged from about 3300 to 3400 gauss during this scanning time which was about 4 to 5 minutes. At slightly higher fields the free radical peaks occur.

A series of samples can be processed in a relatively short time by simply exchanging tubes in the resonant cavity. Rebalancing of the microwave bridge was usually not necessary be-

STANDARDS OF VANADYL ETIOPORPHYRIN I
AT VARIOUS CONCENTRATIONS

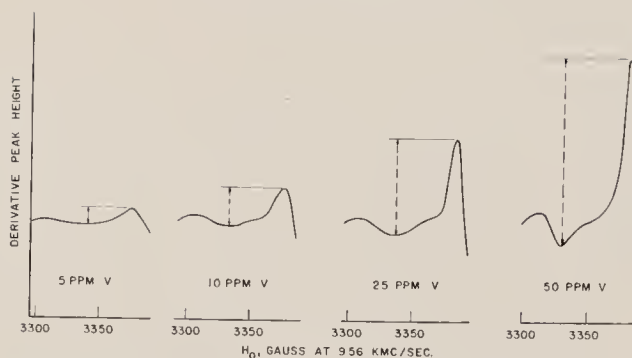


Figure 2. Measurement of intensity using derivative peak height

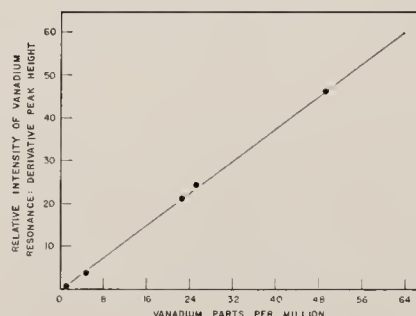


Figure 3. Vanadyl etioporphyrin(I) as standard dissolved in heavy oil distillate containing less than 0.1 p.p.m. V (0-50 p.p.m. V)

cause all samples were of a similar dielectric nature. If slight changes in leakage did occur, rebalancing was done with the slide screw tuner.

Before any quantitative work could be undertaken at all, it was essential to confirm the linearity of the EPR spectrometer with concentration of vanadium. Figure 3 depicts a plot of the derivative EPR peak height of vanadyl etioporphyrin(I) against the concentration of vanadium in the range of 1 to 50 p.p.m. The solvent used in these standards was a heavy oil distillate which was known to contain no trace metals. The solvent was chosen to maintain the environmental medium of the standards constant with respect to the oil distillates and bottoms, thus keeping the line widths and shape similar. It is in this manner that intensities can be obtained simply and quickly by comparing derivative peak heights. Linearity in the high sensitivity setting of the spectrometer is shown in Figure 4 where the 0.1- to 1.0-p.p.m. concentration range is covered. This latter graph is exceedingly important in these studies because it demonstrates that vanadium can easily be detected down to at least 0.1 p.p.m. and, therefore, make EPR spectroscopy applicable to practically all distillates. The method of obtaining relative in-

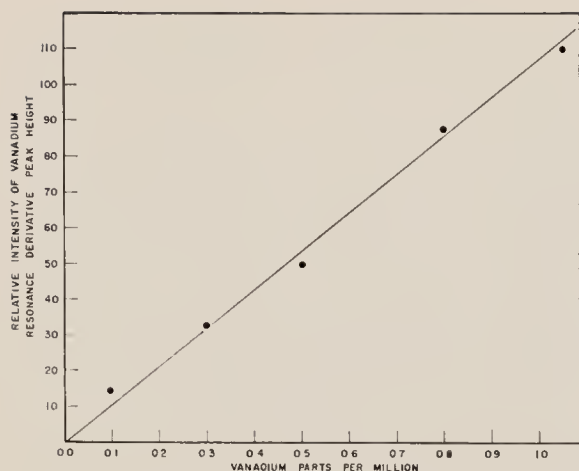


Figure 4. Vanadyl etioporphyrin(I) as standard dissolved in heavy oil distillate containing less than 0.1 p.p.m. V (0.1–1.0 p.p.m. V)

tensity consists of measuring the distance between deflection points of the strongest vanadium line and the opposite weaker component as indicated by the dotted arrows in Figure 2. This is the best peak height to use to avoid interference with free radicals and to obtain maximum sensitivity.

Using the above plots as calibration curves, a number of oil distillates were scanned for the vanadium resonance and the intensities were measured in the manner described to obtain concentration of vanadium in the distillates.

EXPERIMENTAL RESULTS

Figure 5 shows the complete EPR spectrum of a petroleum residue containing 52.0 p.p.m. of V and that of a solution of vanadyl etioporphyrin(I) complex dissolved in a heavy oil distillate free of trace metals. The spectra are similar except for the overlapping of the free radical peak with the intense, central line caused by the vanadium. In all cases, the oil samples showed this spectrum of vanadium and free radicals. In some cases, the free radical peak was nearly absent.

Oil Distillates. If the vanadium signal intensity of the oil distillates is simply plotted against total vanadium as obtained by chemical analysis, a good calibration curve in itself is possible. Figure 6 shows the linear plot obtained. Distillates originating from eight different crudes were purposely chosen in this correlation. A comparison of the slope of the straight line in Figure 6 with that of Figure 3 on the same scale would show that the latter is slightly lower. Using the vanadyl etioporphyrin(I) as a standard could, therefore, lead to slightly higher EPR results by 10%. This similarity in the slopes of the two curves shows that vanadium in distillates is totally present at +4 and also that it exists

as a type of vanadyl complex with essentially the same crystal field environment as vanadyl etioporphyrin(I). Table I lists a number of "unknown" oil distillates for which vanadium determinations had been made by EPR and checked by chemical analysis. The calibration curves shown in Figures 3 and 4 were used in obtaining these results. Table II indicates the repeatability of these results is ± 0.1 p.p.m. of V at the 1-p.p.m. level.

Oil Residues. Essentially a similar procedure was applied here as in the case of the oil distillates. Figure 7 depicts a plot of the EPR signal intensity against the total vanadium as obtained chemically. A scatter of points was obtained averaging to a straight line with a deviation of 13.5%. The most significant feature of this curve is, however, that its slope is close to that of the standard calibration plot of Figure 3. This

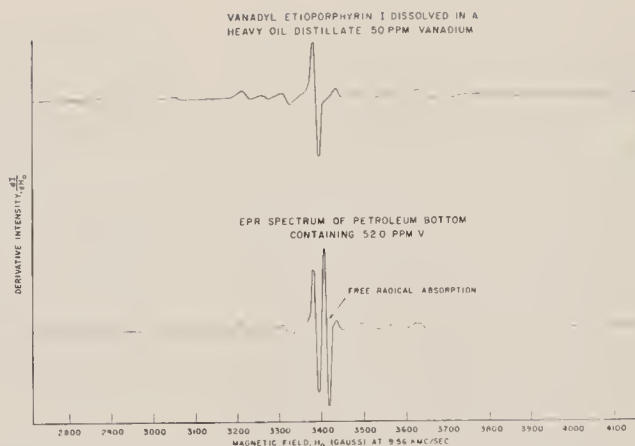


Figure 5. Complete EPR spectra of vanadium resonance in viscous oils

shows that the vanadium in the oil bottoms existed in the same valance state and crystal field environment as in the porphyrin compound used for a reference. Table III lists some types

Table I. Comparison of EPR and Chemical Vanadium Results on Oil Distillates

Sample No.	Vanadium, P.P.M.	
	Chemical	EPR
1-D	0.6	0.7
2-D	11.4	13.5
3-D	0.1	0.1
4-D	1.4	1.7
5-D	0.5	0.5
6-D	0.8	0.7
7-D	2.4	2.4
8-D	0.2	0.1
9-D	21.4	22.8
10-D	0.1	0.2
11-D	0.07	<0.1
12-D	1.1	0.9
13-D	0.9	0.8
14-D	2.5	2.6
15-D	0.4	0.3
16-D	0.07	0.1
17-D	0.6	0.5

Table II. Heavy Gas Oils

Sample No.	Date Sampled	Vanadium, P.P.M.			
		EPR ^a	EPR ^b	Chemical ^a	Chemical ^b
RS-1	11/17/59	0.93	1.02	1.12	1.16
RS-2	11/18/59	0.83		0.95	
RS-5	11/24/59	0.93		1.02	
RS-9	11/25/59	0.91		0.94	
RS-13	11/26/59	2.6		2.51	
RS-17	11/27/59	0.50	0.58	0.61	
RS-20	11/28/59	0.70		0.83	
RS-25	12/7/59	0.30	0.45	0.38	
RS-29	12/8/59	0.10	<0.10	0.06	
RS-33	12/9/59	0.12		0.07	
RS-37	12/10/59	0.30	0.40	0.41	0.42
RS-41	12/11/59	0.50		0.56	
RS-45	12/21/59	1.15	1.16	1.24	
RS-49	12/22/59	1.38		1.31	
RS-53	12/23/59	0.90	0.90	0.87	0.95
RS-57	12/24/59	0.68	0.69	0.66	0.59
RS-59	12/25/59	0.71		0.75	
A	5/10/60		2.0, 2.2		2.23
B	5/11/60		0.5		0.65

^a Analyses made January 1960.

^b Analyses made June 1960.

of oil residues studied together with some EPR results obtained.

Full Crudes. When full crudes are examined directly, one additional factor must be taken into consideration if the same standards which are employed for the distillates and residues are to be used. Differences in viscosity will alter the line shape or width of the vanadium resonance with the result that one cannot make use of derivative peak height as a reliable comparison of relative intensities. Full crudes, therefore, require either the use of a different standard or removal of the lighter fractions. Removal of lighter ends from full crudes by distillation was found to leave a residue for which chemical and EPR vanadium results agreed satisfactorily. Table IV compares chemical and EPR results obtained on full crudes prior to and after distillation. The effect of lighter ends is a decrease in sensitivity of the vanadium signal.

This solvent effect can be deliberately created by merely diluting a residue with a lower boiling solvent. A vacuum tower bottom, which gave 50.0 p.p.m. of V (chemical) and 53.5 p.p.m. (of V (EPR), was successively diluted with benzene and the decrease of vanadium signal intensity was plotted against vanadium concentration. The plot actually obtained was not a straight line but a curve passing through the

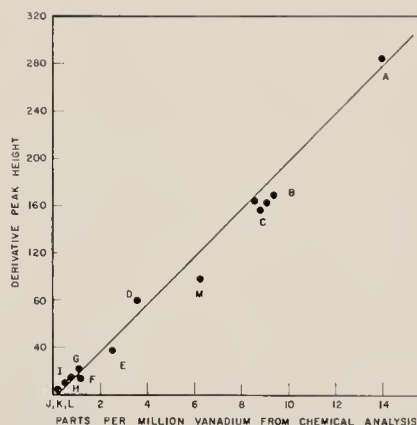


Figure 6. Heavy oil distillates

- A. Taparito heavy gas oil
- B. Virgin Taparito gas oil
- C. Taparito blend gas and furnace
- D. Virgin Kuwait 11% red
- E. Kuwait (distillate)
- F. West Venezuela Ceuta
- G. 50% Kuwait + 10-15 other crudes from East Venezuela
- H. West Venezuela Ceuta
- I. Virgin Kuwait gas oil
- J. South Louisiana (distillate)
- K. Vengref gas oil
- L. West Texas furnace oil
- M. Mara gas oil

origin (Figure 8). In the case of full crudes which contain light ends, a similar effect is encountered and, hence, use of the original standards (of high viscosity) is not possible. The addi-

tion of either *n*-hexane, toluene, or benzene will also cause this phenomenon but, when a high viscosity oil such as a distillate was added, no anomaly was observed.

This solvent effect is probably due to the fact that a change in correlation time of molecular rotation occurs. The hyperfine structure in the spectrum of vanadyl etioporphyrin(I) in benzene and a high viscosity oil shows significant differences attributable to this phenomenon (12).

DISCUSSION OF RESULTS

The degree of hyperfine splitting in the EPR spectrum of vanadyl etioporphyrin(I) is equal to that observed for the petroleum oils while the intensity of the resonance absorption in the reference VO^{+2} compound corresponds quantitatively to that observed for the full crudes, residues, and distillates for which total vanadium was obtained chemically. From the above observations the following conclusion is believed warranted: The vanadium in the petroleum oils examined exists wholly in the paramagnetic $+4$ state; the environment of the vanadium, i.e., the atoms which are immediately coordinated to the metal, is essentially similar, being of the noncubic type with axial symmetry. Only two apparent exceptions to this generality were observed. These were Bachaquero and Lagunillas crudes in which 11 and 29%, respectively, of the vanadium appeared to be in a valence state other than $+4$. It is not known whether these represent true deviations or whether they result from compositional effects.

The common valence states of vanadium are $+2$, $+3$, $+4$, and $+5$. The $+5$ state is diamagnetic and hence cannot be observed by EPR. The $+3$ state, although paramagnetic with two unpaired electrons per vanadium ion, can be completely removed of its degeneracy if sufficiently strong crystal fields are present. Paramagnetic resonance of V^{+3} has been observed only at low temperatures (10).

The remaining valence states of $+2$ and $+4$ are both detectable at room temperature. However, as pointed out earlier, the $+4$ state requires a noncubic field (6, 12), and this condition is fulfilled in vanadyl (VO^{+2})-type complexes. The V^{+2} compounds are generally unstable with respect to the higher valence states of vanadium. The paramagnetic resonance spectrum of V^{+2} differs considerably from that of VO^{+2} in regard to the degree of hyperfine splitting. V^{+2} is, in fact, isoelectronic with Cr^{+3} and these ions are expected to behave similarly in various crystal fields.

It is entirely possible to have a variety of compounds of vanadium in the $+4$ valence state which exhibit different chemical and physical properties.

Table III. Comparison of EPR and Chemical Vanadium Results on Residues

Sample No.	Description	Vanadium, P.P.M.		
		EPR	Chemical	% Error
1-B	Heptane Kuwait extract	20.4	16.1	+26.7
2-B	Kuwait vacuum reduced crude	34.2	23.7	+44.3
3-B	Hydrogenated Kuwait vacuum tower residues	8.9	8.3	+ 7.2
4-B	West Texas visbroken tar	13.5	9.5	+42.1
5-B	West Texas visbroken tar	14.8	12.2	+21.3
6-B	Kentucky crude residues	121	118	+ 3
7-B	Kuwait maltenes, full range	0.1	0.1	0
8-B	Hydrogenated Kuwait vacuum tower residues	0.3	0.3	0
9-B	Kuwait raffinate from heptane extraction	389	391	+ 0.3
10-B	Kuwait composite residues	191	205	- 7
11-B	Liquid product from gasoline fraction of Kuwait visbroken tar	21.6	20.3	+ 6.4
12-B	Heptane precipitation of visbroken tar	13.2	11.7	+12.8

Table IV. Vanadium Results. Chemical vs. EPR on Untopped and Topped Crudes

	Chemical	Vanadium, P.P.M.		
		EPR untopped	EPR topped (based on crude)	% Light ends removed
Santa Barbara crude	21.9	13.7	20.2	27.7
South Louisiana	0.58	0.28	0.40	25.9
Mixed Light Canadian	1.1	0.24	2.0	36.0
Semisweet West Texas	1.5	0.15	1.8	36.7
Ceuta Western Venezuela	10.5	4.0	8.9	36.3
Lagamar	177	101	166	24.5
Composite West Venezuela tar oil (Mara) ^a	936	954

^a Viscous crude diluted with oil distillate.

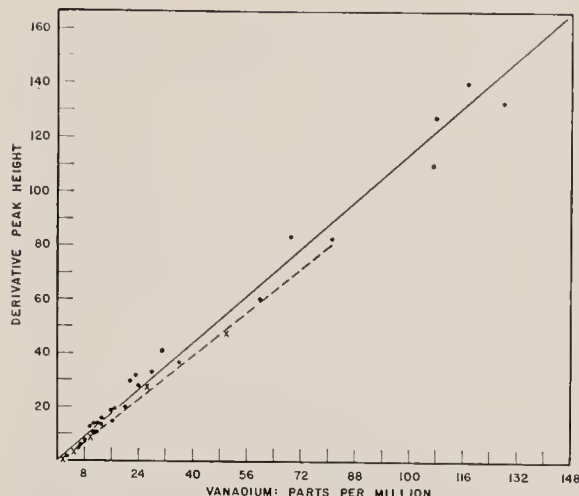


Figure 7. Petroleum residue

● — Oil residues and some asphaltene: p.p.m. from chemical analysis vs. EPR intensity
X — Standards of vanadyl etioporphyrin(I) in heavy gas oil

Thus, one can have inorganic and organic vanadium or vanadium compounds which differ in molecular weight of the porphyrin ring system, but all containing the metal in the +4 state as vanadyl. The presence of one unpaired electron per vanadium ion endows the metal with at least one very characteristic feature: a magnetic moment due to the uncompensated spin motion of the odd electron. Regardless of how the vanadium is bound, this investigation indicates that the metal exists in the same electronic configuration.

Results have been presented to the effect that vanadium in distillates and other petroleum oils does not exist entirely as vanadyl (3). Since a different standard was used in that work and crudes of a different origin and vanadium content were examined, it is not possible to specify any single cause for this discrepancy. Our results on oil distillates are, however, in agreement with other studies (1, 17) regarding the nature of vanadium compounds in petroleum.

With regard to EPR spectroscopy, it may definitely be stated that it is a valuable analytical tool for sensitive and rapid quantitative work provided all the species of interest exist totally in some suitable electronic state. The results obtained on the oil distillates demonstrate this convincingly (Tables I and II).

The scatter of points in Figure 7 is caused by slight variations in the viscosity and/or composition of the oils or by a scatter of the accuracy in chemical values. Since the differences in viscosity influence the sensitivity coefficient for residues and full crudes, EPR is unsuitable for quantitative use for these types of samples. For residues, EPR might be used to rapidly establish the level of vanadium content.

We have found one possible source of interference in the determination of vanadium in oil distillates by EPR spectroscopy. Two or three of the oil residues and one distillate displayed an intense and broad low field resonance which partly overlapped the vanadium spectrum. This is believed to be due to iron and corrections for the interference are readily made. Since iron in significant amounts is rarely found in distillates, no interference should be encountered for these types of oils. The absence of paramagnetism in nickel porphyrin-type compounds (14) prevents their detection by EPR and possible overlap with the vanadium resonance signal.

Scope and Application of EPR. For reasons already discussed (viscosity, Q of the cavity, etc.) the present development in the use of EPR is probably limited to heavy distillate oil samples. If EPR were to be applied, for example, to the quantitative detection of vanadium deposited on catalysts or full crudes, another calibration curve would be necessary, assuming that all of the metal existed in a suitable oxidation state. Although the vanadium concentrations of the various oils examined were no higher than 200 p.p.m., there is no reason why the technique cannot be extended to any value desired by applying a dilution technique. At sufficiently high concentration of vanadium the hyperfine structure smears out because of spin-spin interaction, and the method which was used in measuring relative intensities for this investigation will not be applicable.

ACKNOWLEDGMENT

The authors are grateful to D. E. O'Reilly for valuable advice and to J.

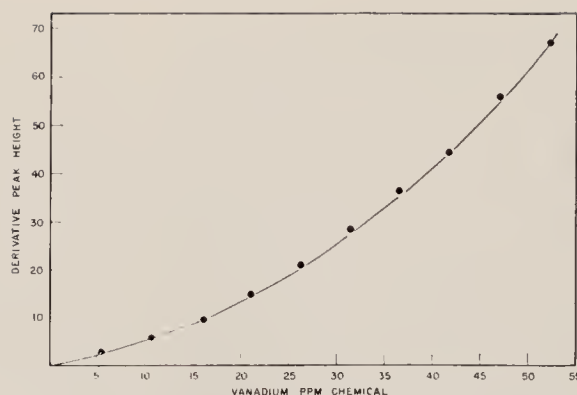


Figure 8. Effect of successive addition of benzene on derivative peak height of vanadium resonance in viscous oil

Gordon Erdman for kindly supplying synthetic samples of vanadyl etioporphyrin(I).

LITERATURE CITED

- (1) Beach, L. K., Shewmaker, J. E., *Ind. Eng. Chem.* **49**, 1157 (1957).
- (2) Bestougeff, M., *Chem. & Ind. (London)* **1948**, 60, 137; *World Petrol. Congr. Proc. 3rd Congr. Hague* **6**, 116 (1951).
- (3) Dunning, H. N., Moore, J. W., Bieber, H., Williams, R. B., Division of Petroleum Chemistry, 137th Meeting, ACS, Gen. Papers, 169, Cleveland, Ohio, April 1960.
- (4) Erdman, J. G., Ramsey, V. G., Kalenda, N. W., Hanson, W. E., *J. Am. Chem. Soc.* **78**, 5844 (1956).
- (5) Garner, F. H., Green, S. J., Harper, F. D., Pegg, R. E., *J. Inst. Petrol.* **39**, 278 (1953).
- (6) Gerritsen, H. J., Lewis, H. R., *Phys. Rev.* **119**, 1010 (1960).
- (7) Howe, W. W., Williams, A. R., Preprints, Division of Petroleum Chemistry, 134th Meeting, ACS, p. 87, Chicago, Ill., September 1958.
- (8) Ingram, D. J. E., "Free Radicals as Studied by Electron Spin Resonance," Butterworths, London, 1958.
- (9) Ingram, D. J. E., "Spectroscopy at Radio and Microwave Frequencies," pp. 138-91, Butterworths, London, 1955.
- (10) Low, W., *Z. Phys. Chem. (Frankfurt)* **13**, 107 (1957); Zverev, G. M., Prokhorov, A. M., *J. Exptl. Theoret. Phys. (U. S. S. R.)* **34**, 707 (1958).
- (11) Moore, J. W., Dunning, H. N., *U. S. Bur. Mines, Rept. Invest. No. 5370*, p. 8, November 1957.
- (12) O'Reilly, D. E., *J. Chem. Phys.* **29**, 1188 (1958).
- (13) Overberger, C. G., Damshefsky, I., "Isolation of Vanadium Porphyrins from Crude Venezuelan Zaguillitas Oil," Tech. Rept. II, Project No. 46, ORN 263 T/O IV, NR-057-089, 1952.
- (14) Pauling, L., Coryell, S., *Proc. Natl. Acad. Sci. (U.S.A.)* **22**, 159 (1936).
- (15) Skinner, D. A., *Ind. Eng. Chem.* **44**, 1159 (1952).
- (16) Triebels, A., *Ann.* **509**, 103 (1934); *Ibid.*, **517**, 172 (1935); *Angew. Chem.* **49**, 682 (1936).
- (17) Woodlee, R. A., Chandler, W. B., *Ind. Eng. Chem.* **44**, 2591 (1952).

RECEIVED for review August 15, 1960.
Accepted November 23, 1960. Division of Petroleum Chemistry, 138th Meeting, ACS, New York, N. Y., September 1960.



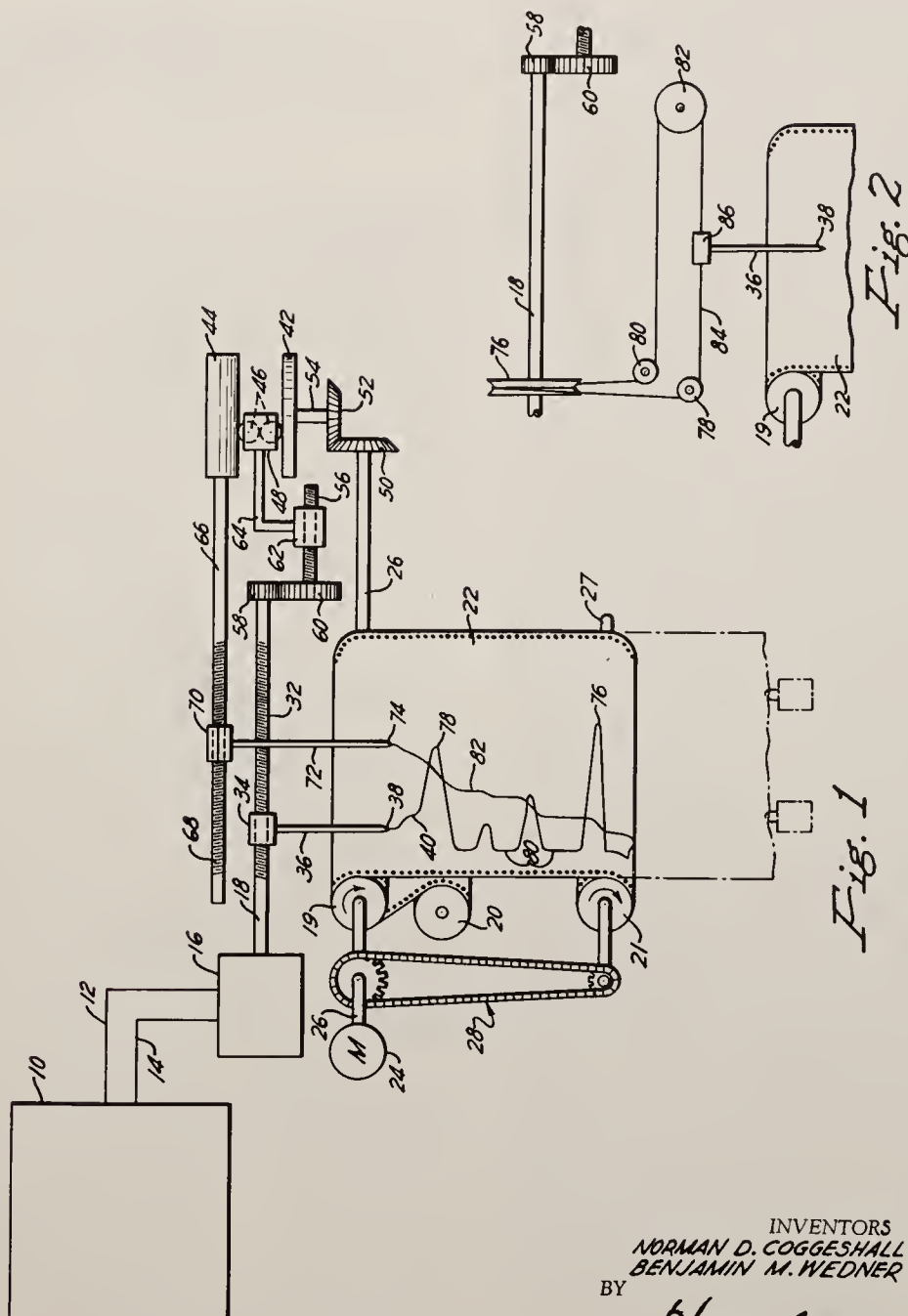
Aug. 29, 1961

N. D. COGGESHALL ET AL

2,998,291

RECORDING INTEGRATOR

Filed Nov. 1, 1957



INVENTORS
 NORMAN D. COGGESHALL
 BENJAMIN M. WEDNER

BY

Harold H. Harker

ATTORNEY

1

2,998,291

RECORDING INTEGRATOR

Norman D. Coggeshall, Verona, and Benjamin M. Wedner, Pittsburgh, Pa., assignors to Gulf Research & Development Company, Pittsburgh, Pa., a corporation of Delaware

Filed Nov. 1, 1957, Ser. No. 693,827

1 Claim. (Cl. 346—13)

This invention pertains to new and useful improvements in recording systems, and more particularly relates to apparatus for recording upon a single chart both the manner in which a particular variable changes with respect to time and the manner in which the integral of such variable with respect to time varies with time.

Broadly, the invention pertains to the combination of a recorder of the class wherein a pen contacting the chart is driven by the motor of a self-balancing potentiometer with a mechanical integrating device of the class wherein a disk is drivingly coupled by ball means to the cylinder; wherein the disk is rotated at a velocity proportional to the velocity of the chart, the potentiometer is drivingly connected to the ball means of the integrator so that displacements of the pen and ball means occur according to a fixed ratio, and the cylinder is drivingly connected to a further pen contacting the chart so that movement of such further pen is proportional to the angular position of the cylinder.

Apparatus employing the principles of the invention is particularly well suited for use with analytical equipment, such as partition chromatography apparatus of the character that produces an electrical signal having a magnitude dependent upon the value of a variable, such as the concentration of eluted substances carried by the carrier gas in the effluent stream of a partition chromatography column.

The invention will be best understood upon reference to the accompanying drawing, wherein FIGURE 1 is a diagrammatic illustration of a preferred embodiment and wherein FIGURE 2 is a diagrammatic illustration of an alternative pen driving arrangement.

In FIGURE 1, the apparatus of the invention is shown associated with partition chromatography apparatus. The numeral 10 indicates a diagrammatic representation of partition chromatography apparatus which, for example, can be of the type that includes a pair of thermal conductivity cells to produce a voltage having a magnitude substantially proportional to the percentage of eluted material present in the effluent gas stream. Such electrical signal is fed by electric leads 12 and 14 from the chromatography apparatus 10 to a conventional electric self-balancing potentiometer 16. The potentiometer 16 includes an electric balancing motor, not shown, having an output shaft 18.

A chart and drive therefor are provided which comprise a driving roll 19, a supply roll 20, and a take-up roll 21. A sheet of chart paper 22 is wound on the roll 20 and is entrained over the driving roll 19 to the take-up roll 21. The roll 19 is driven at a constant rate of rotation by a synchronous electric motor 24, the output shaft 26 of which is secured to the roll 19. The take-up roll 21 is mounted on a shaft 27 and is driven so as to maintain the chart paper 22 taut between rolls 19 and 21 by means of a sprocket and chain drive indicated at 28 and a slip clutch (not shown) connecting the drive 28 to the shaft 27. As clearly apparent in the

2

drawing, the chart paper 22 has perforations along its edges that engage complementary protuberances on the roll 19 that prevent slipping. Rotation of the rolls 19 and 21 causes the strip chart paper 24 to travel downwardly, as viewed in FIGURE 1.

In practice, the chart paper 22 need not be wound on the roll 21, but simply suspended from the roll 19 with weights attached, as indicated in dashed lines.

The output shaft 18 of the self-balancing potentiometer 16 is threaded, as shown at 32, and a traveling nut 34 is disposed on the threaded portion 32 of the shaft 18. While the shaft 18 is free to rotate in the traveling nut 34, the latter is itself secured against rotation and carries a pen arm 36. The pen arm 36 is provided at its outer extremity with a pen 38 that contacts the chart 22 so as to trace a line 40 on the chart 22.

A mechanical integrating device of conventional character is provided which includes a rotatable disk 42, a cylinder 44 having its axis normal to the axis of rotation of the disk 42, and a variable ratio driving connection between the disk 42 and the cylinder 44 comprising a pair of balls 46 between the disk 42 and the cylinder 44. The balls 46, which constitute a motion transferring means are positioned in a sleeve 48, and are constrained to travel along a path parallel to the axis of the cylinder 44 and normal to the axis of rotation of the disk 42. The mechanical integrating device described is well known and is of the character produced commercially by Librascope Incorporated of Glendale, California.

The disk 42 of the integrating device is provided with means for imparting a constant rotational velocity thereto which comprises a pair of meshing beveled gears 50 and 52 fixed to the shaft 26 and a shaft 54 carried by the disk 42, respectively. It will be readily appreciated that the illustrated arrangement causes the chart 22 to be driven at a constant velocity, as well as causing the disk 42 to be given a constant rate of rotation.

Means are provided for establishing a driving connection between the balancing motor of the potentiometer 16 and the sleeve 48 that controls the position of the balls 46 relative to the radius of the disk 42, such that angular displacement of the shaft 18 is directly proportional to the linear displacement of the sleeve 48. In the preferred construction, such means comprises a threaded shaft 56 and meshing spur gears 58 and 60 establishing a driving connection between the shafts 18 and 56. A traveling nut 62 is positioned on the threaded shaft 56. The threaded shaft 56 is free to rotate in the traveling nut 62, but the latter is otherwise secured against rotation by conventional means, not shown. The threaded shaft 56 is parallel to the axis of the cylinder 44, and it is secured to the sleeve 48 of the integrating device by an L-shaped arm 64.

The cylinder 44 is secured to a shaft 66 that is parallel to the shaft 18, and the shaft 66, which constitutes an output shaft of the integrating device, has a threaded portion, as shown at 68. A traveling nut 70 is positioned on the threaded portion 68 of the shaft 66. While the shaft 66 is free to rotate in the traveling nut 70, the latter is secured against rotation by conventional means, not shown. The traveling nut 70 carries a pen arm 72 that is provided with a pen 74 at its outer extremity that is in contact with the chart 22. The traveling nut 70 is preferably a split nut so that the same can be engaged in any selected position on the threaded portion 68 of the shaft 66.

Inasmuch as translation of the traveling nut 62 must be less than the diameter and normally less than the radius of the disk 42, and inasmuch as the radius of the disk 42 is substantially less than the translation normally imparted to the traveling nut 34 upon rotation of the shaft 18, it will be noted that the spur gear 60 is substantially larger than the spur gear 58 so that the shaft 56 rotates to a substantially lesser extent than the shaft 18, whereby the extent of translation of the balls 46 is conveniently reduced.

The operation of the apparatus will now be readily understood. The self-balancing potentiometer 16 causes the shaft 18 to be rotated to an angular displacement that is linear with respect to the magnitude of the electrical signal produced by the chromatography apparatus. Accordingly, the traveling nut 34 and the pen 38 carried thereby are displaced to the right, as seen in the drawing, to an extent that is linear with respect to the magnitude of the electrical signal fed to the potentiometer 16 by the chromatography apparatus 10. Thus, the line 40 traced upon the chart 22 by the pen 36 represents variations in the magnitude of the electrical signal fed to the potentiometer 16 with respect to time. The time axis is of course the direction of travel of the chart 22. Portions of the line 40, such as those indicated at 76 and 78 represent peaks in the magnitudes of the electrical signal fed to the potentiometer 16, while the portions of the line 40, such as those indicated at 80, represent time intervals during which the electrical signal fed to the potentiometer 16 was of zero magnitude.

The traveling nut 62 is so positioned on the shaft 56 that the balls 46 are at the center of the disk 42 when the shaft 18 is in the angular position that is assumed by the same when the electrical signal fed to the potentiometer 16 is zero. It will be seen that rotation of the shaft 18 from the angular position that it occupies when the magnitude of the electrical signal is zero to that which it occupies when the electrical signal has a positive value will cause the ball 46 to be translated radially outward from the center of the disk 42 to an extent directly proportional to the angular displacement of the shaft 18. It will further be understood that the driving ratio between the disk 42 and the cylinder 44 is zero when the balls 46 are at the center of the disk 42, but that the driving ratio increases upon translation of the balls 46 from the center of the disk 42 in direct proportion to the extent of such translation.

With the particularly illustrated arrangement of the gears 50, 52, 58, and 60 and the particularly illustrated threads on the shaft 18, 56, and 66, the balls 46 are translated to the left during translation of the traveling nut 34 to the right. Also, translation of the balls 46 to the left will result in the shaft 66 being rotated in such a direction that the traveling nut 70 moves to the right. It will also be evident that the integrating function of the disk 42, the balls 46, and the cylinder 44 is such that the extent of translation of the traveling nut 70 to the right is proportional to the integral of the translation of the balls 46 to the left of the center of the disk 42 with respect to time, and is therefore also directly proportional to the integral of the magnitude of the electrical signal fed to the potentiometer 16 with respect to time.

Though only positive values of the electrical signal fed to the potentiometer 16 have been considered in describing the integrating function of the illustrated embodiment of the invention, it will be clear that the integral of negative values for the electrical signal fed to the potentiometer 16 with respect to time are simply subtracted and represented by translation of the traveling nut 70 to the left.

The position of the traveling nut 70 with respect to time is indicated on the chart 22 by the pen 74 tracing the line 82 on the chart 22. It will be appreciated that the pen 74 is positioned slightly below the pen 38 as viewed in the drawing and that the pen arm 72 is

so shaped as to avoid any interference between the pen arm 72 on one hand and the traveling nut 34, pen arm 36 and pen 38 on the other. Whenever the pen 74 approaches to near the right-hand side of the chart paper 22, the traveling split nut 70 can be repositioned on the shaft 66 so that the pen 74 is near the left-hand side of the chart paper 22.

In FIGURE 2, there is illustrated an alternative arrangement for driving the pen 38. In this arrangement, the shaft 18 is provided with a pulley 76. Idler pulleys 78, 80, and 82 are provided as shown, with an endless flexible wire or cable 84 constituting a driving belt being entrained over the pulleys 76, 78, 80, and 82 in such a manner that the portion of the cable 84 intermediate the pulleys 78 and 82 is parallel to the driving roll 19. The arm 36 of the pen 38 is secured to cable 84 by a clamping element 86. With this construction, linear movement of the pen is directly proportional to the angular movement of the shaft 18, as in the embodiment of FIGURE 1.

It will be evident that the illustrated embodiment of the invention is susceptible to numerous variations without departing from the scope of the invention. For example, means other than those illustrated can be provided for establishing a driving connection between the motor of the potentiometer 16 and the pen 38, such as is provided in the Leeds and Northrup Recorder—Model G. Also, the driving connection between the shaft 66 and the pen 74 can be such as that shown in FIGURE 2 or that employed between the potentiometer and the pen in the Leeds and Northrup Recorder. If desired, cam means can be employed to establish the described essential driving connection between the motor of the potentiometer 16 and the sleeve 48 such as is employed in the recording system of the commercially available Fisher-Gulf Partitioner. It will be apparent that a substantial variety of alternative means can be provided for driving the disk 42 at a constant rotational velocity such as the provision of a separate synchronous motor, not shown. With any of the modifications suggested, it is only essential that the described relation between the driving element and the driven element be maintained.

Although the illustrated embodiment of the invention has been described in substantial detail, this has been done only for the purpose of conveying a clear conception of the inventive principles involved, rather than to imply a limited scope of the invention. Accordingly, reference should be made to the appended claim in order to ascertain the actual scope of the invention.

We claim:

Recording apparatus comprising in combination a self-balancing potentiometric recording system and a mechanical integrating device; said system including a chart and means for driving the latter at a constant velocity, a first recording pen contacting the chart and means for displacing the first recording pen along a straight path that is transverse to the travel of the contacted portion of the chart by an amount that is linear with respect to the magnitude of a signal fed to the system, such displacing means including a first threaded shaft and a first traveling nut on the first threaded shaft carrying the first recording pen; said mechanical integrating device comprising a rotatable disk and means for rotating the latter at a constant velocity, an output shaft rotatable about an axis normal to the axis of rotation of the disk, motion transferring means establishing a variable ratio frictional driving connection between the disk and the output shaft, said motion transferring means being translatable along a course parallel to the axis of the output shaft and normal to the axis of rotation of the disk; means for translating the motion transferring means comprising a second threaded shaft mounted for rotation, reduction gear means drivingly connecting the first threaded shaft to the second threaded shaft, a second traveling nut on the second threaded shaft operatively connected to the motion transferring means; a second recording pen mov-

ably contacting the chart upon a travel path that is parallel to and in closely spaced relation to the straight path of the first recording pen, means for moving the second recording pen comprising a third threaded shaft parallel to the first threaded shaft, said output shaft being drivingly connected to the third threaded shaft, a third traveling nut on the third threaded shaft carrying the second recording pen, and means for selectively positioning the third traveling nut along the length of the third threaded shaft.

5

10

References Cited in the file of this patent

UNITED STATES PATENTS

1,041,107	Ledoux	Oct. 15, 1912
1,699,807	Pierce	Jan. 22, 1929
1,947,731	Nehls	Feb. 20, 1934
2,387,563	Chapple	Oct. 23, 1945
2,481,039	Ross	Sept. 6, 1949
2,724,631	Ruhland	Nov. 22, 1955
2,834,247	Pickels	May 13, 1958

Note on the Statistical Theory of Mass Spectra

JOHN C. SCHUG AND NORMAN D. COGGESHALL

Note on the Statistical Theory of Mass Spectra

JOHN C. SCHUG AND NORMAN D. COGGESHALL

Gulf Research & Development Company, Pittsburgh, Pennsylvania

(Received March 30, 1961)

THE statistical theory of mass spectra¹ permits one to make reasonable predictions if appropriate values are chosen for its parameters.¹⁻⁴ But interpretation of these parameters in terms of transition complexes¹ has proven difficult. Since the theoretical expressions cannot be analytically integrated, it has been necessary to use trial and error calculations to determine the parameters. In this note, we present a simplification, through which the parameters can be studied without trial and error methods.

The theory expresses dissociation rate constants in terms of state density functions.¹ When the molecule is treated as a collection of oscillators, the expressions become

$$k_i = \nu_i (1 - \epsilon_i/E)^s, \quad (1)$$

where ν_i is a frequency factor, ϵ_i is the activation energy for dissociation, E is the excess internal energy of the decaying ion, and s is the number of vibrational degrees of freedom in the activated complex. If secondary dissociations are neglected, the fractional abundance of the i th fragment is

$$F_i = \int_{\epsilon_i}^{E_m} (dF_i/dE) dE = \int_{\epsilon_i}^{\epsilon_j} (dF_i/dE) dE + \int_{\epsilon_j}^{E_m} R_{ij}(E) (dF_i/dE) dE, \quad (2)$$

where E_m is the maximum excess parent-ion energy, and

$$R_{ij}(E) = dF_i/dF_j = (\nu_i/\nu_j) [(E - \epsilon_i)/(E - \epsilon_j)]^s.$$

The mean value theorem for integrals⁵ permits the removal of $R_{ij}(E)$ from beneath the integral sign, provided that it be evaluated at a particular energy inside the integration range. Thus

$$F_i \geq R_{ij}(E_1) F_j; \quad \epsilon_j \leq E_1 \leq E_m. \quad (3)$$

This equation can be rearranged to

$$E_1 \geq [(F_i \nu_j / F_j \nu_i)^{1/s} \epsilon_j - \epsilon_i] / [(F_i \nu_j / F_j \nu_i)^{1/s} - 1], \quad (4)$$

which is applicable when $(F_i \nu_j / F_j \nu_i) > 1$. Alternatively, if it is possible to specify an energy, E_2 , such that $E_2 \geq E_m \geq E_1$, then it follows that

$$\nu_i/\nu_j \leq (F_i/F_j) [(E_2 - \epsilon_j)/(E_2 - \epsilon_i)]^s. \quad (5)$$

Relative abundances of $C_n H_{2n+1}^+$ ions in low-voltage patterns of n -paraffins^{2b} have been examined in the light of these relations. First, Eq. (4) was applied by assuming that activation energies correspond exactly with appearance potentials, and that (ν_i/ν_j) is unity for pairs of simple C—C bond dissociations; s was taken

TABLE I. Parameters necessary to interpret abundances of indicated ions (j) relative to that of $C_6 H_{13}^+(i)$ in low-voltage pattern of n -octane.^{2b}

s	Ion (j)	Minimum E_1	Maximum ν_i/ν_j
$3n-7=71$	$C_3 H_7^+$	22.1 ev	1×10^{-14}
	$C_4 H_9^+$	12.5	1×10^{-5}
	$C_5 H_{11}^+$	6.55	5×10^{-2}
$71/3=23.7$	$C_3 H_7^+$	7.20	1×10^{-4}
	$C_4 H_9^+$	4.35	8×10^{-2}
	$C_5 H_{11}^+$	2.45	8×10^{-1}
$71/5=14.2$	$C_3 H_7^+$	4.55	1×10^{-2}
	$C_4 H_9^+$	2.72	5×10^{-1}
	$C_5 H_{11}^+$	1.54	1

as $(3n-7)$, the total number of vibrational degrees of freedom in the transition complex. For the various pairs of ions, Eq. (4) showed that $E_1 \geq 6$ to 31 ev. These results contradict the theory, for the spectra were obtained with ionizing voltages 1.5 to 2.0 v above parent-ion appearance potentials.^{2b}

Equation (5), applied to the same data by setting $E_2 = 2.0$ ev, showed that the ratios of the several pairs of frequency factors had to be smaller than 10^{-2} to 10^{-17} . Most values in this range are unrealistic. For example, a number of frequency factors were estimated from skeletal frequencies based on a zig-zag chain model⁶ and allowing for small differences in force constants between radicals and ions. Ratios of these estimated frequency factors were always in the neighborhood of unity.

Some typical results are given in Table I, which also indicates how the data can be made more acceptable by reducing the number of active vibrational degrees of freedom.⁷ In many of the cases examined, it was necessary to reduce s to $\frac{1}{10}$ th its original value in order for Eqs. (4) and (5) to produce reasonable results.

Such inconsistencies are not limited to lower n -paraffins. Calculations based on the spectrum of n -pentadecane, obtained at this laboratory, encounter the same difficulties.

Although it appears that low-voltage mass spectra are not amenable to interpretation by the simplified statistical theory, there remains the possibility that some fragment-ions may result from two-step processes.⁸ Also, we should point out that identical treatments of high-energy spectra give much more reasonable results.

¹ H. M. Rosenstock, M. B. Wallenstein, A. L. Wahrhaftig, and H. Eyring, Proc. Natl. Acad. Sci. U. S. 38, 667 (1952).

² L. Friedman, F. A. Long, and M. Wolfsberg, (a) J. Chem. Phys. 27, 613 (1957); (b) *ibid.* 30, 1605 (1959); (c) *ibid.* 31, 755 (1959).

³ A. Kropf, E. M. Eyring, A. L. Wahrhaftig, and H. Eyring, J. Chem. Phys. 32, 149 (1960).

⁴ E. M. Eyring and A. L. Wahrhaftig, J. Chem. Phys. 34, 23 (1961).

⁵ I. S. Sokolnikoff, *Advanced Calculus* (McGraw-Hill Book Co., Inc., New York, 1939), p. 113.

⁶ K. S. Pitzer, J. Chem. Phys. 8, 711 (1940).

⁷ W. A. Chupka, J. Chem. Phys. 30, 191 (1959).

⁸ J. H. Beynon, R. A. Saunders, A. Topham, and A. E. Williams, J. Phys. Chem. 65, 114 (1961).

Initial Kinetic Energy Discrimination Effects in Crossed-Field Ion Sources

NORMAN D. COGGESHALL

Reprinted from THE JOURNAL OF CHEMICAL PHYSICS, Vol. 36, No. 6, pp. 1640-1647, March 15, 1962

Initial Kinetic Energy Discrimination Effects in Crossed-Field Ion Sources

NORMAN D. COGGESHALL

Gulf Research & Development Company, Pittsburgh 30, Pennsylvania

(Received June 30, 1961)

Previously developed differential equations for crossed-field trajectories are particularly suitable for investigating the characteristics of the orbits in crossed-field ion sources of mass spectrometers. At low repeller voltages there can be enormous initial kinetic energy discrimination due to the cycloidal orbits turning around before reaching the plane of the first slit. Energy relations for collectible orbits will be presented. A transformation of angle may be made between the isotropic distribution of initial velocity components to the anisotropic distribution of orbits that applies in the beam defined by the first slit. The latter will depend upon the operating conditions and may be studied by deflecting the beam across the exit slit by varying the deflection voltages. The signal reaching the detector then represents a progressive lateral sampling of the beam. The width and maximum intensity in this beam are functions of operating conditions and it is shown how very misleading results may be obtained depending upon how the exit slit samples this beam. Collection efficiency can be defined and set up as an integral of a function of the projected initial kinetic energy components on the plane of motion. The area under the curve obtained by progressively pushing the beam from the first slit across the exit slit represents the flux of ions collected by the first slit. This is dependent on operating conditions and may be conveniently used to investigate initial kinetic energies.

DISCRIMINATION effects due to initial velocity components in a mass spectrometer ion source which has no superposed magnetic field have been previously treated.¹ Also, the discrimination in the region between the ion source and detector due to initial velocity components parallel to the magnetic field scattering ions out of the beam has been described.² The latter type of discrimination operates in mass spectrometers which have or do not have magnetic fields superposed on the ion source. Even if the ion source has a superposed magnetic field, the relations derived in reference 1 may be used qualitatively if the trajectories before the first slit are sufficiently dominated by the electric field in contrast to the effects of the magnetic field.

There is now an increased activity involving low repeller voltages (repeller voltage here will refer to the voltage between the repeller electrode and first slit) such as the determination of ionization and appearance potentials and the application of low-voltage mass spectral techniques for the determination of molecular group types. In view of this, it is important to examine carefully what initial velocity discrimination effects operate in a crossed-field ion source of a mass spectrometer when operated at low or moderate repeller voltages.

TRAJECTORY CONDITIONS BEFORE THE FIRST SLIT

In Fig. 1 is provided a schematic diagram of a crossed-field ion source. The repeller electrode, the first slit, and the exit slit are represented by a, b, and f, respectively. The deflection electrodes used to achieve optimum focus are represented by c and c'. The cross-hatched region represents the ionization region, i.e., a cross section of the electron beam path.

The potential difference between this region and the first slit is V_1 , and the distance between this region and the first slit is d . The uniform magnetic field is perpendicular to the plane of the figure and in a direction to make positive ions bend concave downwards. We neglect field penetration at the first slit and, hence, may treat the region behind this slit as one of crossed, uniform fields.

The differential equations of the trajectories for orthogonally crossed fields in which both fields vary with but one and the same variable have been previously derived.³ In this it was shown that the differential equation for trajectories in crossed uniform fields is given by

$$\frac{dy}{dx} = \pm \frac{(Hx + \bar{c})}{[hV_0 + hEx - (Hx + \bar{c})^2]^{1/2}} \quad (1)$$

where E and H are the electric and magnetic fields, respectively; V_0 is the initial kinetic energy of the velocity component in the plane of motion, expressed as potential; and \bar{c} is a constant of integration correlatable with initial conditions. The term h is given by $h = 2mc^2/e$, where m is the mass of the ion in grams, c is the velocity of light in cm/sec and e is the electronic charge in esu. It is well known that this field configuration produces periodic cycloid orbits.^{4,5}

Referring to Fig. 1, we take the x and y coordinates as marked on the plane perpendicular to the magnetic field and parallel to the electric field. It is the initial velocity components in this plane that constitute a starting condition. Let us specify the angle of the initial velocity vector in this plane with the x axis as

³ N. D. Coggeshall, Phys. Rev. **70**, 270 (1946).

⁴ W. Bleakney and J. A. Hipple, Jr., Phys. Rev. **53**, 521 (1938).

⁵ E. B. Jordan and N. D. Coggeshall, J. Appl. Phys. **13**, 539 (1942).

¹ N. D. Coggeshall, J. Chem. Phys. **12**, 19 (1944).

² C. E. Berry, Phys. Rev. **78**, 597 (1950).

ϕ . When we evaluate \bar{c} , we find Eq. (1) becomes

$$\frac{dy}{dx} = \frac{\pm [Hx - (hV_0)^{\frac{1}{2}} \sin \phi]}{\{hV_0 + hEx - [Hx - (hV_0)^{\frac{1}{2}} \sin \phi]^2\}^{\frac{1}{2}}}. \quad (2)$$

This form of the differential equation of a cycloid is particularly useful for deducing some of the trajectory properties.

Let us consider a crossed-field region wherein the field values are such that the trajectories of the ions could trace out complex periods of cycloids without interference from any physical boundaries such as slits or electrodes. We take the region of ion production, i.e., the electron beam as $x=0$. Consider an ion that leaves this beam with angle ϕ . After traversing a portion of its cycloid, it will return and cross $x=0$ with a value of $(dy/dx)_{x=0}$, which is the negative of the starting value. Progressing on, it will then trace out another portion of the cycloid and again cross $x=0$. At this latter point it will be one cycloid period displaced in the y direction from its starting position and it will start another period with the original value of

$$(dy/dx)_{x=0}.$$

Thus, in terms of angular orientation with respect to the electric field, ions leaving $x=0$ with slopes of equal magnitude but opposite signs will produce equivalent orbits. Thus, angular-wise, orbits originating with angle ϕ will have equivalent counterparts originating with $\pi - \phi$.

It is obvious from the numerator in Eq. (2) that values of x such that

$$Hx - (hV_0)^{\frac{1}{2}} \sin \phi = 0 \quad (3)$$

provide the x loci for turning points for $(dy/dx)=0$. It is an interesting observation that Eq. (3) does not depend upon the electric field strength and, thus, varying the electric field will either swell or shrink the cycloid orbits without changing the x loci for

$$(dy/dx)=0.$$

It is also obvious from the denominator in Eq. (2) that values of x such that

$$hV_0 + hEx - [Hx - (hV_0)^{\frac{1}{2}} \sin \phi]^2 = 0 \quad (4)$$

will give $(dy/dx) = \pm \infty$ and hence represent, for particular orbits, points of maximum and minimum penetration in the x direction.

The roots of Eq. (4) are given by the equation

$$x = (1/2H^2) \{hE + 2H(hV_0)^{\frac{1}{2}} \sin \phi \pm \{h^2E^2 + 4H^2hV_0 + 4hEH(hV_0)^{\frac{1}{2}} \sin \phi\}^{\frac{1}{2}}\}. \quad (5)$$

It is clear that for $E > 0$ and a particular V_0 , those orbits which penetrate to the largest x values are those for $\phi = \frac{1}{2}\pi$. Those which penetrate the least will be for $\phi = -\frac{1}{2}\pi$. Intermediate ϕ values will yield intermediate values of penetration.

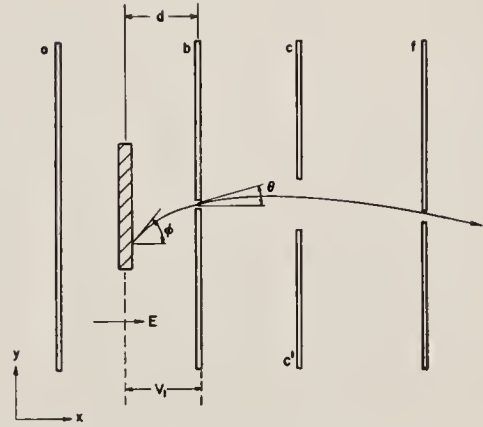


FIG. 1. Electrode and coordinate configuration for a crossed-field ion source. The magnetic field is normal to the plane of the figure.

We shall, at this point, denote an orbit as collectible at the first slit solely on the basis of whether it actually reaches a value of $x=d$. Orbits which barely reach $x=d$ will do so tangentially and for them $(dy/dx) = \pm \infty$. These will be orbits possessing V_0 and ϕ values that satisfy Eqs. (4) and (5) when $x=d$. Let us first consider the region $E > 0$ and determine the value of V_0 that satisfies Eqs. (4) and (5) with $x=d$ and $\phi = -\frac{1}{2}\pi$. Using $\phi = -\frac{1}{2}\pi$ gives an orbit of smallest x penetration for the particular value of V_0 . Hence, all other orbits of the same V_0 but different ϕ 's are collectible. The analytical expression for V_0 defined as above is given by

$$V_0 = (hV_1 - H^2d^2)^2 / 4H^2d^2h. \quad (6)$$

Smaller values of V_0 than given by Eq. (6) result in a weaker interaction with the magnetic field and hence all are collectible. This may also be demonstrated by solving for x in Eq. (5) when values of V_0 less than those given by Eq. (6) are used.

Since $\phi = \frac{1}{2}\pi$ when $E > 0$ gives the maximum x penetration, a value of V_0 obtained from Eq. (5) when $x=d$ and $\phi = \frac{1}{2}\pi$ gives an orbit tangent to the first slit plane. For this value of V_0 , all other values of ϕ give orbits which do not penetrate to $x=d$ and hence are not collectible. The conditions for which this can apply for $E > 0$ occurs only in the region $0 \leq V_1 \leq H^2d^2/h$. The analytical expression which gives the limiting V_0 is algebraically equivalent to Eq. (6). Thus, in the V_1 region specified, Eq. (6) gives the value of V_0 such that orbits having a lower V_0 will be completely non-collectible.

For $V_1 < 0$ we will have the same limiting value of V_0 given by Eq. (6) for a small negative range of V_1 . However, as V_1 becomes more negative $\phi = \frac{1}{2}\pi$ will cease to define the orbit having the greatest x penetration. To determine the value of ϕ giving the greatest penetration, we differentiate Eq. (5) with respect to

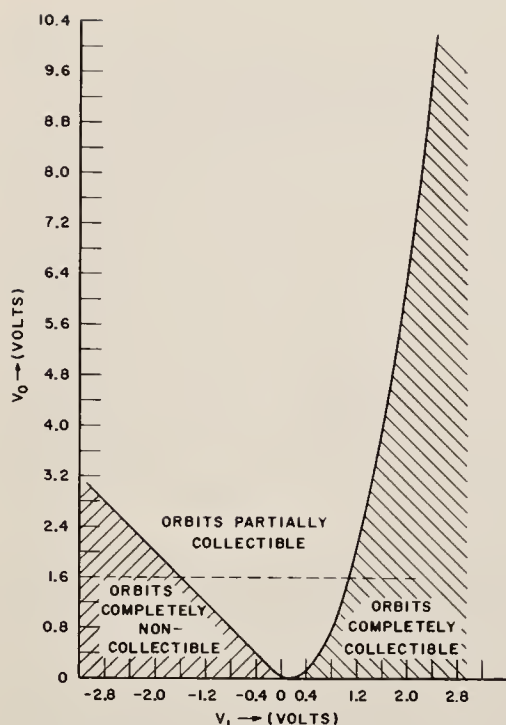


FIG. 2. Limitations on orbits completely noncollectible, partially collectible, or completely collectible as set by the voltage V_1 .

ϕ and equate to zero. This yields

$$\sin\phi = -HV_0/E(hV_0)^{1/2}. \quad (7)$$

Using this relation in Eq. (5), with $x=d$ we derive the limiting value of V_0 as $V_0 = -V_1$. The changeover from Eq. (6) to this relation will occur at

$$V_0 = -V_1 = H^2 d^2 / h,$$

which is also the smallest value of V_1 for which $\phi = \frac{1}{2}\pi$ defines a maximum x penetration.

The above limitations are plotted in Fig. 2 for an ion of $m/e=43$, a magnetic field of 3500 gauss and a distance d to the first slit of 1.0 mm. These are representative conditions for actual mass spectral operations. Here the right-hand portion of the curve represents the upper V_0 limitation on totally collectible orbits and the left-hand portion represents the upper V_0 limitation on totally noncollectible orbits. Let us consider, for example, ions of a particular V_0 ; the value shown by the dashed line represents 1.6 ev. If the V_1 is greater than about 1.1 v, all of these ions are collectible as well as those of lower V_0 . As we go to lower values of V_1 , we pass into a region where progressively fewer of these ions are collectible. When we reach a V_1 value of -1.6 v, all ions of $V_0 \leq 1.6$ ev are completely noncollectible.

On the assumption that the electron ribbon passes through the ionization region about one-half way be-

tween electrodes a and b (Fig. 1), we see that V_1 will be approximately one-half the repeller voltage.

From the above relations it is clear that at repeller voltages near zero, the number of ions collected of a particular type will depend upon the actual repeller voltage value and upon the distribution of the ions with initial kinetic energy. Experiments with low repeller voltages and in which the interpretation depends upon ion intensities thus must be analyzed very carefully.

BEAM FORMATION AT THE FIRST SLIT

Let us designate by θ the angle with which an orbit strikes the plane of the first slit (see Fig. 1). To describe the flux of ions through the first slit we must relate θ to V_0 and ϕ . This may be done by using Eq. (2) with $x=d$ from which we derive

$$\sin\theta = -[Hd - (hV_0)^{1/2} \sin\phi] / [h(V_0 + V_1)]^{1/2}. \quad (8)$$

As the distribution of ions emerging between θ and $\theta+d\theta$ will depend upon the distribution of ions created between ϕ and $\phi+d\phi$, we must derive the distribution function for the latter. In this we shall use the projected velocity u in the plane of motion rather than V_0 , the initial kinetic energy of that velocity component; these are related through $mu^2 = 2eV_0$. We define a distribution function $F(u)$ such that the number of ions created per unit time and per unit volume with u between u and $u+du$ and with ϕ between ϕ and $\phi+d\phi$ will be $F(u)du d\phi / 2\pi$.

Referring to Fig. 3, the above expression will be the summation of all initial velocity vectors that terminate in the incremental volume defined by the dashed lines extending perpendicularly on both sides of the ϕ, u plane. Let us denote by $\rho(c)dc$ the number of ions created per unit time and per unit volume with initial velocity c lying between c and $c+dc$ and which are isotropically distributed. The number in an increment

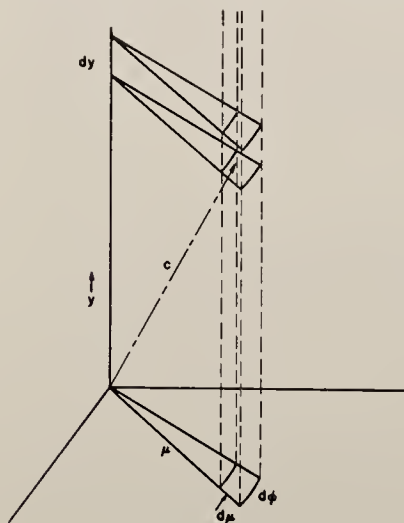


FIG. 3. Incremental arrangement as used in the derivation of the $F(u)$ function.

$d\omega$ of solid angle will be $\rho(c)dc d\omega/4\pi$. From this we may determine a distribution function $f(c)$ such that $f(c)dV$ gives the number of initial velocity vectors terminating in the incremental volume of dV in vector space. This gives $f(c)$ as

$$f(c) = \rho(c)/4\pi c^2. \quad (9)$$

We may use this expression to derive $F(u)$ via the route indicated by Fig. 3. Here, the incremental volume in vector space is given by $u dy d\phi du$, and we have the relation $c^2 = y^2 + u^2$. From this we find

$$F(u) \frac{du d\phi}{2\pi} = 2 \int_0^\infty f(c) dV = \frac{u}{2\pi} du d\phi \int_0^\infty \frac{\rho(y^2 + u^2)^{\frac{1}{2}}}{y^2 + u^2} dy,$$

which may be transformed to give

$$F(u) = u \int_u^\infty \frac{\rho(c) dc}{c(c^2 - u^2)^{\frac{1}{2}}}. \quad (10)$$

For ions created from a gas with a Maxwellian distribution $F(u)$ becomes

$$F(u) = 2Nau \exp(-au^2), \quad (11)$$

where N is the total number of the particular ions created per unit time per unit volume and $a = m/2kT$, where m here is the mass of the parent molecule, k the Boltzmann factor, and T the absolute temperature.

We may describe the beam formed at the first slit by determining the distribution function that will give the number of ions between θ and $\theta + d\theta$ that were created per unit time per unit volume with initial velocity component between u and $u + du$. To get the distribution with θ we regard the area in the electron beam in which ions are formed as essentially infinite in two dimensions compared to the dimensions of the slit. The number of orbits of any particular type created per unit area in the electron beam will, therefore, be the same as the number of the same particular type striking the plane of the first slit, per unit area. This then allows us, for a fixed u , to obtain the relation between $d\theta$ and $d\phi$ by way of Eqs. (8) and (10). When this is done, we may then equate

$$\begin{aligned} F(u) \frac{du d\phi}{2\pi} &= \frac{1}{2\pi} \frac{(h_1^2 u^2 + h_1^2 v^2)^{\frac{1}{2}} \cos \theta d\theta du}{\{h_1^2 u^2 - [Hd + (h_1^2 u^2 + h_1^2 v^2)^{\frac{1}{2}} \sin \theta]^2\}^{\frac{1}{2}}} \\ &\quad \times u \int_u^\infty \frac{\rho(c) dc}{c(c^2 - u^2)^{\frac{1}{2}}}, \quad (12) \end{aligned}$$

where $h_1^2 = m^2 c^2 / e^2$ and we have replaced the potentials V_0 and V_1 by corresponding velocities u and v . The expression on the right, therefore, gives the number of ions of original velocity component between u and $u + du$, found between θ and $\theta + d\theta$ in the beam emerging

from the first slit. The total number of ions in a particular $d\theta$ is, of course, obtained by integrating the right-hand expression in Eq. (12) over u from 0 to ∞ .

If the electrode geometry is such that a uniform field exists between the first slit and the exit slit, the methods and Eq. (16) of reference 3, with appropriate parameter values, could be used to trace every orbit from the first slit through this region. However, in CEC model 21 type instruments, on which a great deal of work has been done, there are two deflecting electrodes (c and c' , see Fig. 1) between these slits. It is the usual practice to impose between these electrodes a voltage selected to maximize a particular reference peak. Such a potential arrangement obviously does not provide a uniform field although the perturbations from uniformity may be small. It is not felt practical, therefore, to attempt a tracing of individual orbits between the slits.

The voltage difference between the deflection electrodes may be employed to qualitatively examine the beam emerging from the first slit. Since the voltage difference between the deflecting electrodes is ordinarily small, compared to the total accelerating voltage between the slits, we may assume that a change in deflection voltage results in a uniform lateral shift of the beam as it strikes the plane of the exit slit. Therefore, by progressively changing the deflection potential, we may push the beam across the exit slit. The ion beam passing through the exit slit and through the analyzer to the detector will then be a measure of the flux density in the portion of the beam falling on the exit slit.

This procedure was employed on a series of ion peaks. A circuit was devised which, while allowing the deflection voltage to vary over a considerable range, both $+$ and $-$, kept the midpoint voltage between the deflection electrodes at a constant potential relative to the first and exit slits.

Equation (8) provides the foundation for two predictions relative to the nature of the beam from the first slit, as determined by the scanning procedure of the above. One is that as the repeller voltage is increased, the angular spread of the beam should decrease. This should be observable as a decrease in beamwidth as a function of increased deflection voltage. The decrease results from the fact, evident in Eq. (8), that for a particular value of V_0 , and for $V_1 > 0$ maximum and minimum values θ occur for $\phi = \frac{1}{2}\pi$ and $-\frac{1}{2}\pi$. The difference between these extremum values of θ decreases as V_1 increases. The other prediction is that an ion with most of its beam flux occurring for low values of V_0 will show an asymmetrical angular shift as V_1 increases. This results from the fact [see Eq. (8)] that for low V_0 ions, all θ values are negative. Increasing V_1 will move all such θ values towards zero. This is equivalent to a general shift of the beam in one direction with increasing V_1 .

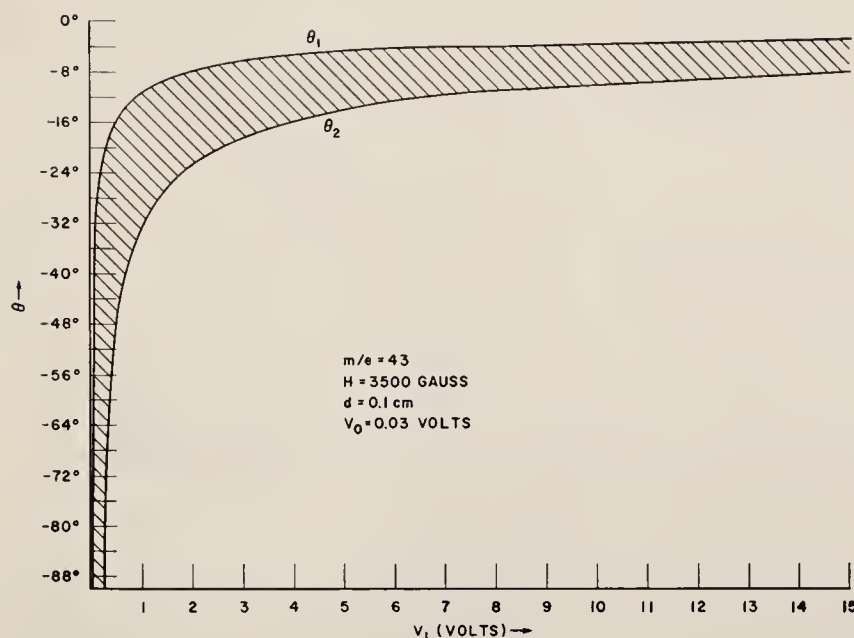


FIG. 4. Limitations on limiting values of θ , i.e., θ_1 and θ_2 imposed by V_1 . Case applies to an $m/e=43$ ion with $V_0=0.03$ v.

Starting with Eq. (11) we may calculate the average projected velocity component \bar{u} for a Maxwellian distribution. This is derived to be

$$\bar{u} = (\frac{1}{2}\pi)^{\frac{1}{2}} (2kT/m)^{\frac{1}{2}}. \quad (13)$$

The thermal distribution for ions originating from n -hexane at 500°K gives a value of \bar{u} corresponding to an average V_0 of 0.034 v. This is low enough to expect the shift in one direction of the beam with increasing V_1 .

In Fig. 4 may be seen a plot derived from Eq. (8) of θ_1 and θ_2 , the maximum and minimum values of θ for an ion of $m/e=43$, $H=3500$ gauss, $d=0.1$ cm, $V_0=0.03$ v, as a function of V_1 . Note that for $V_1=0$, no orbits are collectible and that in a range between $V_1=0$ and $V_1=0.25$ v, the orbits become suddenly collectible and are completely so for $V_1 \geq 0.25$ v. Note also that the spread between θ_1 and θ_2 decreases steadily as V_1 increases.

In Fig. 5 may be seen a series of scans, obtained by varying the deflection voltage of the $m/e=43$ peak from n -hexane. Here we see the predicted narrowing of the beam with increasing repeller voltage. Also, we see the progressive shifting of the beam in a direction representative of more positive values of θ . These curves have all been normalized to a value of 100 at their maxima.

From the relations and behavior demonstrated here it is evident that any measured ion intensity, which of course can only be a particular flux sampling of the beam emerging from the first slit, is highly dependent upon repeller and deflection voltages.

EFFICIENCY OF COLLECTION BY THE FIRST SLIT

It is clear at this point that the ions emerging from the exit slit and hence collected by the detector are generally only a fraction of those in the beam from the first slit. With the complexity involved in attempting to integrate Eq. (12) and to follow the orbits through the inter-slit region, it is not practical to attempt to relate single ion peak measurements to the collection conditions in the ion source. However, we may scan the peak as done for the data in Fig. 5 and thereby experimentally obtain relative total flux values for the beam emerging from the first slit by integrating under the resulting curve.

We may also set up the equations to calculate the total flux in the beam from the first slit. Recalling the reasoning of above, we know that for ions characterized by an initial velocity component u and angle ϕ , the number collected per unit area on the plane of the first slit is equal to the number created per unit area in the ionization region. Defining collectibility as we have, i.e., advancing in the x direction to the plane of the first slit, allows us to calculate those which cannot be collected. We may, therefore, define the collection efficiency of the first slit as the ratio of the number of ions collected per unit area by the first slit to the number created per unit area in the electron beam.

Let us first consider the case for which $V_1 \geq H^2 d^2 / h$. We have seen (see Fig. 2) that for V_0 values equal to or less than those given by Eq. (6), the orbits are totally collectible. However, for larger V_0 values some orbits are excluded. The easiest way to calculate the total number of excluded ions is to determine the

ranges of ϕ for which exclusion occurs and to take advantage of the isotropic distribution of initial velocity components with ϕ . For a given V_1 the collection efficiency $P(V_1)$ may thus be defined as

$$P(V_1) = \int_0^\infty F(u) \frac{(2\pi - \Delta\phi)}{2\pi} du \bigg/ \int_0^\infty F(u) du, \quad (14)$$

where $\Delta\phi$ is a function of u and is the excluded range of ϕ for a particular V_1 . We may determine $\Delta\phi$ from Eq. (8) by substituting the value of $\theta = -\frac{1}{2}\pi$. We get a factor of 2 due to the mirror-image equivalence of excluded ϕ 's and thus obtain (for $V_1 \geq H^2 d^2/h$)

$$\Delta\phi = \pi - 2 \sin^{-1} \left\{ \frac{[h(V_0 + V_1)]^{\frac{1}{2}} - Hd}{(hV_0)^{\frac{1}{2}}} \right\}. \quad (15)$$

Equation (14) then becomes, recalling the relation between u and V_0 ,

$$P(V_1) = \frac{1}{2} + \left(\frac{1}{2} \int_0^{\bar{u}} F(u) du + \frac{1}{\pi} \int_{\bar{u}}^\infty F(u) \times \sin^{-1} \left\{ \frac{[h(V_0 + V_1)]^{\frac{1}{2}} - Hd}{(hV_0)^{\frac{1}{2}}} \right\} du \right) \bigg/ \int_0^\infty F(u) du, \quad (16)$$

where \bar{u} is here the minimum projected velocity at which discrimination starts and which is evaluated via Eq. (6).

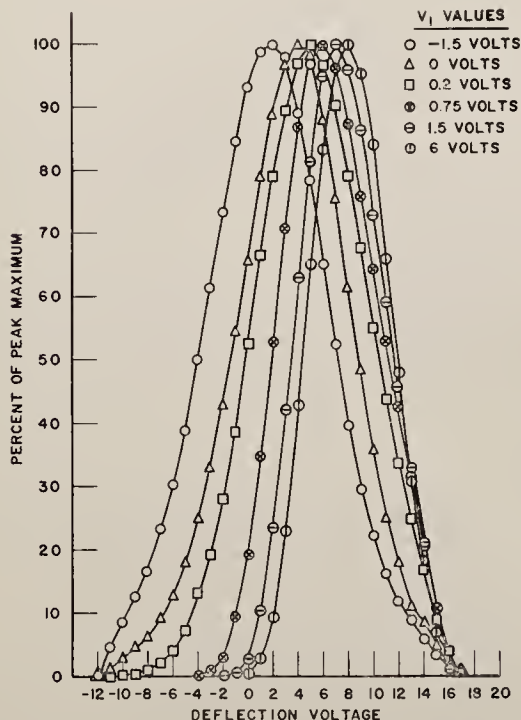


FIG. 5. Normalized scans obtained by pushing the ion beam across the exit slit by means of the deflection voltage. Data apply to $m/e = 43$ peak from *n*-hexane.

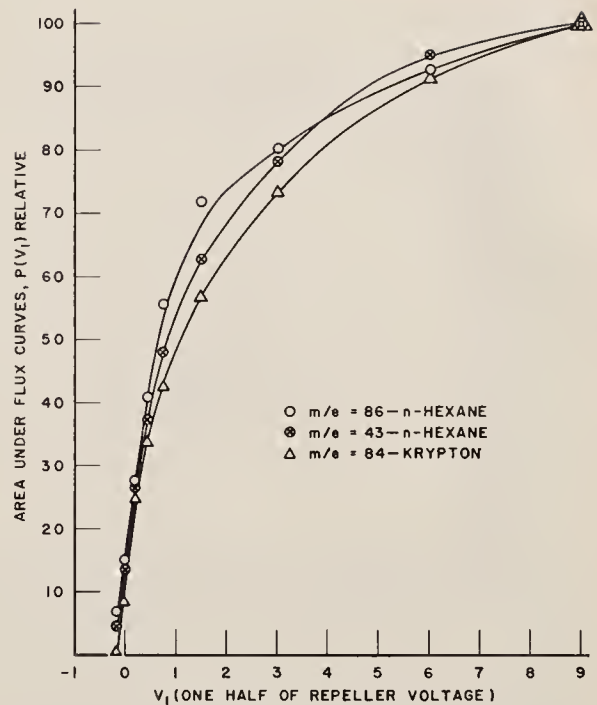


FIG. 6. Variation of integrated ion flux from first slit as a function of V_1 for three ions.

For $V_1 \leq H^2 d^2/h$, we have the situation that for no value of u are all orbits collectible. For this case we can more conveniently define $P(V_1)$ by

$$P(V_1) = \frac{1}{2\pi} \int_0^\infty F(u) \bar{\Delta}\phi du \bigg/ \int_0^\infty F(u) du,$$

where $\bar{\Delta}\phi$ represents the range of ϕ from which collectible orbits of original projected velocity component u may originate. We may derive $\bar{\Delta}\phi$ from Eq. (8) as the difference in ϕ when solving for ϕ in the two cases of $\theta = \frac{1}{2}\pi$ and $\theta = -\frac{1}{2}\pi$. This gives

$$P(V_1) = \frac{1}{2\pi} \int_{\bar{u}}^\infty F(u) \left\{ \sin^{-1} \left[\frac{Hd + (h_1^2 u^2 + hV_1)^{\frac{1}{2}}}{(h_1^2 u^2)^{\frac{1}{2}}} \right] - \sin^{-1} \left[\frac{Hd - (h_1^2 u^2 + hV_1)^{\frac{1}{2}}}{(h_1^2 u^2)^{\frac{1}{2}}} \right] \right\} du \bigg/ \int_0^\infty F(u) du, \quad (17)$$

where \bar{u} is also evaluated via Eq. (6) for the range $-H^2 d^2/h \leq V_1 \leq H^2 d^2/h$ and is given by $\bar{u} = (-2eV_1/m)^{\frac{1}{2}}$ for $V_1 \leq -H^2 d^2/h$.

For any given value of V_1 the collection efficiency may be evaluated, on a relative basis, as the area under the curve generated by pushing the beam from the first slit across the exit slit and recording the ion current reaching the detector as a function of the deflection voltage. Thus, the areas under the original curves (before normalization) used to construct Fig. 5, would provide the relative collection efficiencies in that case.

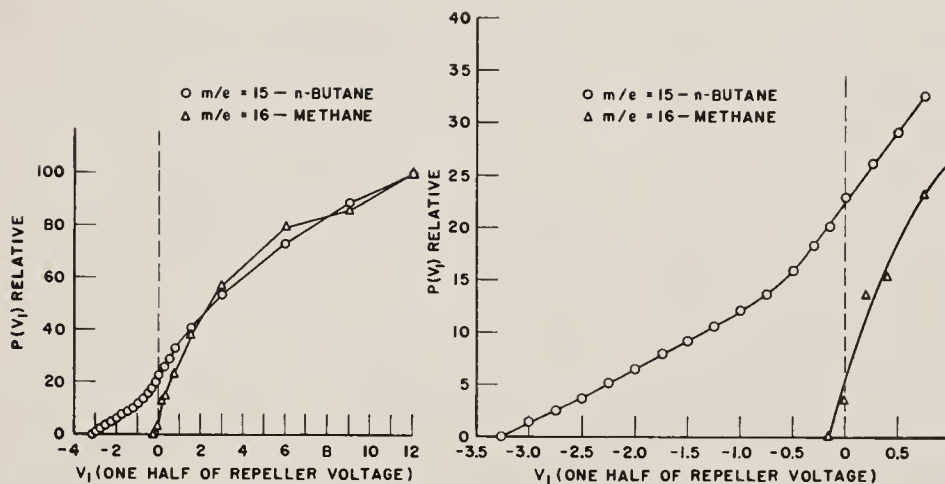


FIG. 7. $P(V_1)$ (relative) curves for $m/e=15$ from *n*-butane and $m/e=16$ from methane as a function of V_1 . The large negative intercept seen for $m/e=15$ results from the large initial kinetic energy.

To derive the $F(u)$ function analytically from such data and Eqs. (16) and (17) would be very difficult because of the complexity of the integrals.

However, even in the absence of analytic evaluations, important relations may be derived from the experimental values of relative collection efficiency. For ions of equal mass and obtained under the same operation conditions, the variables in Eqs. (16) and (17) are all numerically the same except for the projected initial velocities. Thus, direct comparisons may be made between fragmentation ions and those known to possess only thermal energies such as parent ions. Furthermore, it provides a test for the concept that ions from polyatomic molecules spontaneously dissociate. This has been assumed as part of the mechanism of ionic fragmentation and it has been argued that the decreased yield of certain ions with decreased repeller voltage was due to their dissociation as a result of a longer residence time in the ion source.

In Fig. 6 are plotted the areas under flux curves obtained in the manner described vs repeller voltage for the $M/e=84$ peak for krypton and the $m/e=86$ and $m/e=43$ peaks from *n*-hexane. The curves produced, therefore, represent relative collection efficiencies for the different ions as a function of repeller voltage. For comparison purposes all three curves were adjusted to a common value for a repeller voltage of 18 v.

There is no evidence here to substantiate the concept that a parent ion dissociates into fragments with a dependence upon residence time in the ion source. We would expect to see $m/e=86$ from *n*-hexane dropping much faster at the lower voltages than the $m/e=84$ peaks from krypton. This does not occur. We would also expect to see $m/e=43$, one of the dissociation fragments, drop much more slowly, due to enrichment from the dissociation, at lower voltages. This is not observed. This indicates that either the above concept is invalid or that the residence time was not sufficiently altered in the present experiments.

It is clear from the nature of Eq. (17) that $P(V_1)$ must go to zero as $-V_1$ becomes equal to the maximum kinetic energy exhibited by the ions. The V_1 axis intercept of $P(V_1)$ therefore conveniently provides a maximum kinetic energy which may be used to classify the type of ion. For example, the curves in Fig. 6 can be extrapolated and all will yield approximately the same maximum energy. It is known that $m/e=86$ from *n*-hexane and $m/e=84$ from krypton are ions possessing only thermal energy. It was actually surprising to observe that the $m/e=43$ ion from *n*-hexane contains essentially only the kinetic energy of the parent ion.

A much better illustration of the utility of the relative $P(V_1)$ curves is seen in Fig. 7. Here are plotted the data for $m/e=16$ from methane and $m/e=15$ from *n*-butane. The latter has been shown by other methods² to possess considerable initial kinetic energy. In the left-hand portion of the figure is shown the relative behavior over a wide repeller voltage range. The two curves were adjusted to a common value at a repeller voltage of 24 v. In the right-hand portion of the figure is given an expanded plot of the behavior for below-zero repeller voltage.

Machine computation methods could be employed with Eq. (17) and data such as seen in Fig. 7 to derive relative $F(u)du$ curves for different ions. The data as given in Fig. 7 are very readily obtained by the scanning procedure given above.

CONCLUSIONS

With the field conditions normally used in 180° mass spectrometers where the ion source is immersed in the magnetic field there will be severe initial kinetic energy discrimination at low repeller voltages for the ions collected by the first slit. The discrimination due to the first slit may be removed by operating at sufficiently high repeller voltages. The angular distribution of ions emerging from the first slit is dependent on the repeller voltage. The portion of the beam sampled by

the second slit depends upon the repeller voltage and upon the deflector plate voltages. The portion sampled, relative to the maximum flux, will, for constant deflector plate voltages, change with repeller voltage. It is therefore hazardous to interpret results obtained at low repeller voltages with those at higher repeller voltages. A curve representing the flux through the first slit may be obtained by plotting the detector signal as the deflector plate voltages are changed so as to push the beam across the exit slit. The area under this curve can

thus be taken as a measure of the total ion flux through the first slit for a given repeller voltage. Data obtained in this way provide a convenient way to investigate the initial kinetic energy of ions.

ACKNOWLEDGMENTS

The author wishes to express appreciation to Dr. G. F. Crable for various discussions of the subject and to Dr. John Schug for checking the derivations presented here.

Oct. 23, 1962

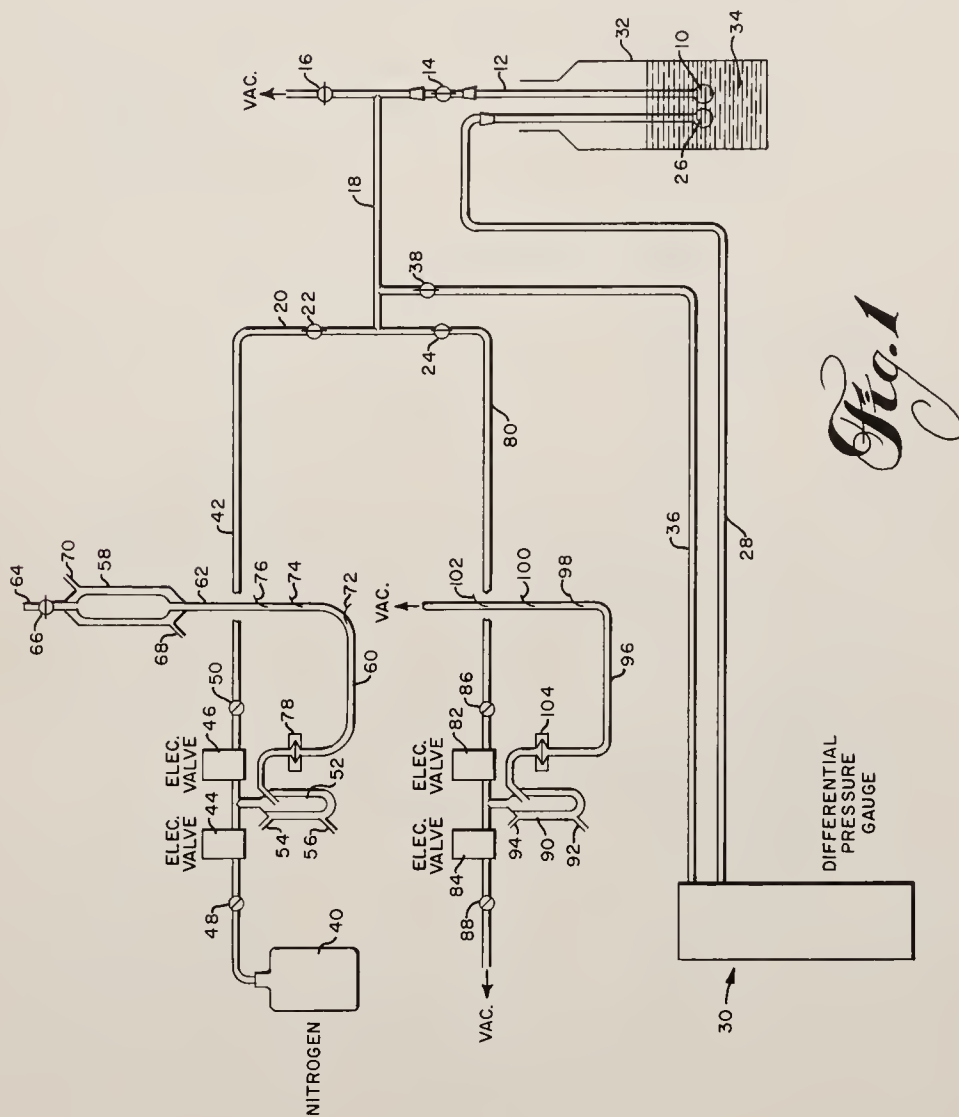
N. D. COGGESHALL ET AL

3,059,478

SORPTION-DESORPTION METHOD AND APPARATUS

Filed Sept. 8, 1959

3 Sheets-Sheet 1



INVENTORS
NORMAN D. COGGESHALL
ORVILLE K. DOOLEN
RALPH D. WYCKOFF

BY

Norman D. Coggeshall

ATTORNEY

Oct. 23, 1962

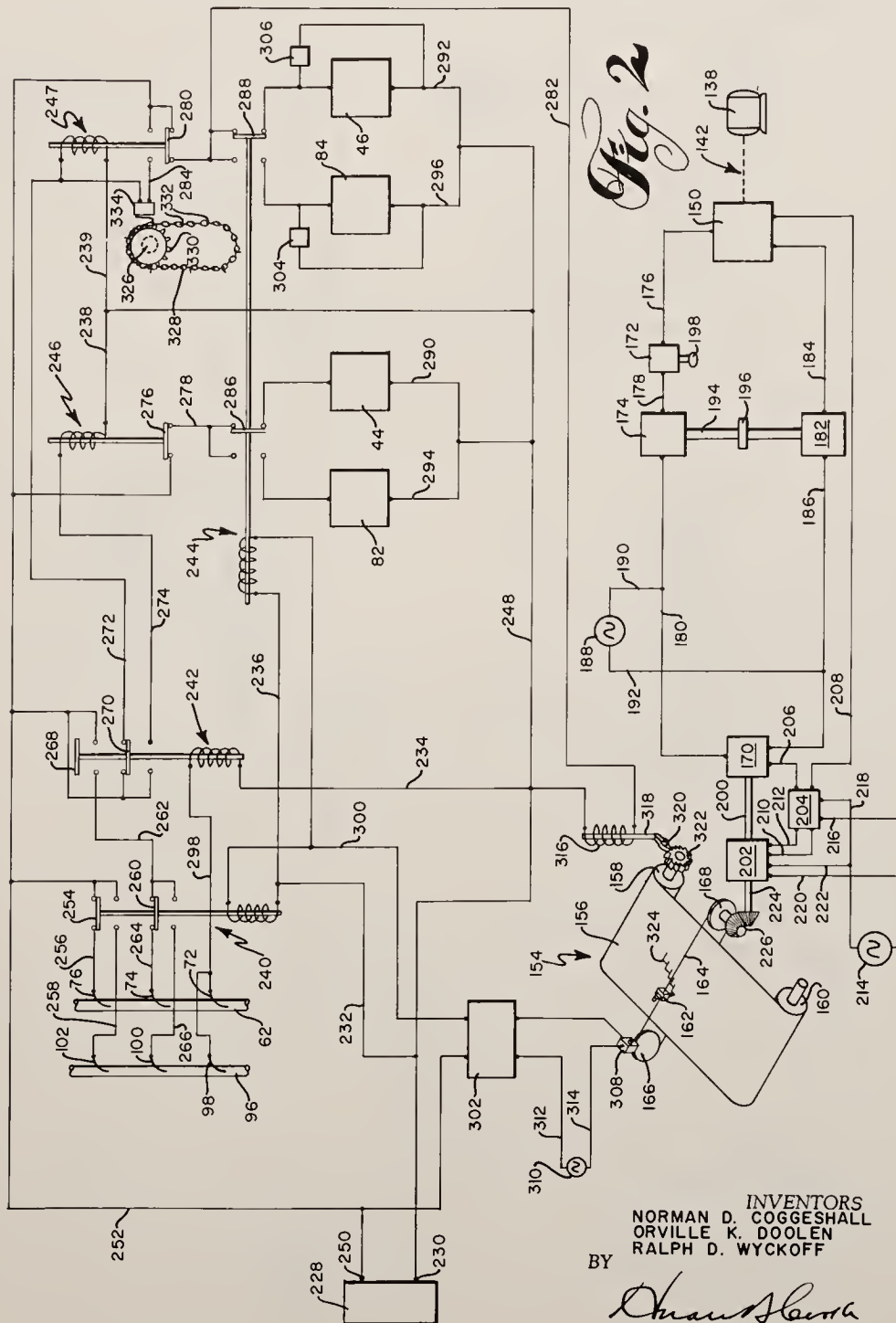
N. D. COGGESHALL ET AL

3,059,478

SORPTION-DESORPTION METHOD AND APPARATUS

Filed Sept. 8, 1959

3 Sheets-Sheet 2



INVENTORS
NORMAN D. COGGESHALL
ORVILLE K. DOOLEN
RALPH D. WYCKOFF

BY

Norman D. Coggeshall

ATTORNEY

1

3,059,478

SORPTION-DESORPTION METHOD AND APPARATUS

Norman D. Coggeshall, Verona, and Orville K. Doolen and Ralph D. Wyckoff, Oakmont, Pa., assignors to Gulf Research & Development Company, Pittsburgh, Pa., a corporation of Delaware

Filed Sept. 8, 1959, Ser. No. 838,553

12 Claims. (Cl. 73—432)

The present invention relates to obtaining data characteristic of the physical surfaces of finely divided or porous solids, and more specifically the present invention is concerned with obtaining data having to do with the isotherms both on the sorption and desorption phases.

Broadly, the invention involves conducting the sorption phase in such a manner that equal mass increments are introduced at timed intervals, each of such timed intervals being of substantially sufficient duration for establishment of pressure equilibrium. The timed intervals can all be equal throughout the sorption phase but are not necessarily equal. The desorption phase is conducted in a similar manner and preferably, though not necessarily, the mass increments withdrawn on desorption are equal to the mass increments introduced during the sorption phase. Also according to the invention, the pressure is recorded versus the total mass of gas introduced and removed during the sorption and desorption phases.

One broad aspect of the invention involves either introducing or removing from the sample volume equal mass increments of gas according to a predetermined timing schedule. Another aspect of the invention involves automatically continuing the introduction of equal increments of gas into the sample vessel until the pressure within the sample vessel rises to a predetermined level, preferably remaining continuously at least at such pressure level for a predetermined time interval, and then automatically discontinuing the sorption phase and initiating the desorption phase by the incremental removal of equal masses of gas from the sample vessel.

In general, the apparatus of the invention for the transfer of equal mass increments of a gas from a first zone of relatively high pressure to a second zone of relatively low pressure, as the case may be for either the sorption or desorption phases, comprises a metering vessel having an inlet provided with a normally closed inlet valve for communication with the first zone and an outlet provided with a normally closed outlet for communication with the second zone, means for maintaining the vessel at a constant temperature, pressure-responsive electric switch means connected to the vessel, said switch means including first, second, and third contacts, with the first and second contacts being closed solely upon the pressure in the vessel exceeding a fixed, relatively high value and with the first and third contacts being closed solely upon the pressure in the vessel exceeding a fixed, relatively low value, a first electrical means connected to the switch means for opening the inlet valve solely during intervals initiated by the opening of the first and third contacts and terminated by the closing of the first and second contacts, and a second electrical means connected to the switch means for opening the outlet valve solely during intervals initiated by the closing of the first and second contacts and terminated by the opening of the first and

2

third contacts. In the preferred construction, there is also provided a third electrical means including a control switch for delaying initiation of the interval of operation of the second electrical means until such control switch is actuated, together with timer means for actuating the control switch according to a predetermined timing schedule.

Substantially identical means such as described in the preceding paragraph is provided for introducing gas to the sample vessel on one hand and for removing gas from the sample vessel on the other hand, such two means employing a common timing means and control switch; such combination additionally being provided with means for preventing concurrent operation of such two means and also for terminating operation of the means for introducing gas and simultaneously initiating operation of the means for removing gas from the sample vessel upon the pressure within the sample vessel rising to a predetermined value.

Another aspect of the invention involves an electromechanical pressure measuring system for measuring the pressure within the sample vessel in such a manner that the volume of gas in the vessel is unchanged.

Basically, the pressure measuring apparatus according to the invention is a servo-operated differential pressure gauge wherein a gas pressure differential is measured by an arrangement involving a pair of bellows mechanically coupled back to back. The connection between the pair of bellows is connected to a sensitive balance employing a thin strip or ligament as a fulcrum. A differential transformer is associated with the balance in such a manner as to actuate a servo-operated nulling system that operates through a mechanical linkage against the balance so as to maintain the juncture between the pair of bellows in a fixed position. The mechanical connection to the balance is coupled to a counter and to a potentiometric system associated with a recorder whereby the differential pressure is recorded. The recorder is associated with the means for either introducing or removing gas from the sample vessel in such a manner that the chart drive is actuated an equal increment of distance in a forward direction upon the occurrence of each increment of gas being either introduced or removed from the sample vessel.

Practice of the invention as broadly outlined above results in automatically producing in graphical form the manner in which the pressure within the sample vessel varies with the mass of gas in the sample vessel throughout both the sorption and the desorption phases. The graphical representation thereby obtained is of interpretive value as to the surface characteristics of a sample undergoing analysis such as to pore size distribution, etc. The theory underlying the interpretation of such data is given in an article entitled "The Determination of Pore Volume and Area Distributions in Porous Substances" by E. P. Barrett, L. G. Joyner, and P. P. Halenda, J. Am. Chem. Soc., 73, 373 (1951). Further statements of theory underlying isotherm phenomena are given in U.S. Patent No. 2,692,497, issued October 26, 1954, to Van Nordstrand, and U.S. Patent No. 2,729,969, issued January 10, 1956, to Innes.

The invention will be better understood upon reference to the accompanying drawings illustrative of a preferred embodiment of the invention, wherein:

FIGURE 1 is a schematic illustration of the gas handling apparatus in general;

FIGURE 2 is a schematic diagram of the electromechanical system associated with the gas handling apparatus shown in FIGURE 1;

FIGURE 3 is a front elevational view of the differential pressure measuring apparatus;

FIGURE 4 is a side elevational view of the differential pressure measuring apparatus shown in FIGURE 3; and

FIGURE 5 is a schematic illustration of the pressure measuring system shown in FIGURES 3 and 4.

Referring to FIGURE 1, a sample vessel, which is small in size, is designated by the numeral 10, such sample vessel being provided with a conduit 12, which is in turn provided with stopcocks 14 and 16. The conduit 12 is provided with a lateral branch 18 intermediate the stopcocks 14 and 16 that is connected to a conduit 20 intermediate a pair of stopcocks 22 and 24 in the conduit 20. Disposed adjacent the sample vessel 10 is a small vessel 26 that is connected by a conduit 28 to a differential pressure measuring gauge designated generally at 30. The vessels 10 and 26 are both disposed within a Dewar flask 32 containing liquid nitrogen 34. Such arrangement affords a constant temperature bath for the vessels 10 and 26 at the temperature of liquid nitrogen boiling at atmospheric pressure. The conduit 18 is provided with a branch conduit 36 communicating with the differential pressure measuring gauge 30, such conduit 36 being provided with a stopcock 38.

One end of the conduit 20 is connected to a nitrogen bottle 40 by a conduit 42. Normally closed, electrically actuated inlet and outlet valves 44 and 46, respectively, are interposed in the conduit 42. Throttle valves 48 and 50 are disposed respectively upstream and downstream of the valves 44 and 46 in the conduit 42.

A jacketed metering vessel 52 communicates with the conduit 42 intermediate the valves 44 and 46, as shown, and the vessel 52 is provided with connections 54 and 56 by means of which a fluid, such as water, can be circulated at a constant temperature so as to maintain the jacketed vessel 52 and its contents at a substantially constant temperature.

A jacketed vessel 58 is provided which is connected to the vessel 52 by way of a conduit 60 that includes a section 62 depending from the vessel 58. The upper end of the vessel 58 is connected to a short vertical conduit 64 that is provided with a normally closed, stopcock 66. The vessel 58 is provided with connections 68 and 70 through which a fluid such as water can be circulated at a constant temperature to maintain the vessel 58 and its contents at a constant temperature. Disposed in the conduit 60 are three electrical contacts 72, 74, and 76 that are insulated from each other, and which are adapted to be electrically connected to each other by mercury in the conduit 60. The mercury in the conduit 60 is isolated from the vessel 52 by an enlarged chamber 78 in the conduit 60. The conduit 60 is of small internal diameter so that only slight vertical movement of the mercury surface in the enlarged chamber 78 accompanies movement of the mercury surface from the contact 74 to the contact 76. The arrangement is such that a substantially fixed volume of a gas, such as air or nitrogen, trapped in the vessel 58 bears against one end of the mercury column in the conduit 60, while the gas pressure in the chamber 52 is applied against the other end of the mercury column in the conduit 60 in enlarged chamber 78. It will be appreciated that two fixed and relatively high and low gas pressures in the vessel 52 are required to place the surface of the mercury column in the conduit 60 at vertical positions just sufficiently high to contact the contacts 76 and 74. It will also be appreciated that a fixed difference in the mass of gas contained in the vessel 52 exists for any particular gas composition (nitrogen in this instance) when the pressure therein is just sufficient for the mercury in the col-

umn 60 to contact the contact 76 on one hand and contact 74 on the other hand; it being recalled that the vessel 52 is jacketed and a fluid at constant temperature is circulated through the jacket. It is assumed of course that sufficient time is allowed for the gas content of vessel 52 to approach temperature equilibrium with the circulated fluid.

Inasmuch as the gas volume in the conduit 42 intermediate the valves 44 and 46 and the connection to the vessel 52 is small, and as the gas volume in conduit 60 intermediate the vessel 52 and the enlarged chamber 78 is also very small compared to the volume of the vessel 52, the comments of the preceding paragraph as to the fixed difference in mass also apply with a high degree of accuracy when such additional volumes of gas are considered along with the volume of gas in the vessel 52. In fact, it is the fixed difference in mass of gas existing in the latter instance that constitutes the amount of gas introduced as a fixed and discreet increment into the sample vessel 10 through the conduits 42, 20, 18, and 12 during the adsorption or as it is sometimes called the absorption cycle or phase. If desired, heat exchange means, not shown, can be provided to maintain the volumes of gas additional to the volume within the vessel 52 at a constant temperature. This provision can generally be dispensed with in practice when room temperature is maintained at a relatively constant level and at a value approximately that of the circulating fluid.

In addition to the above-described apparatus for transferring equal mass increments of gas from the nitrogen supply 40 to the sample vessel 10, apparatus quite similar in principle is provided for withdrawing gas from the vessel 10 in an incremental fashion wherein the increments all have equal masses. This latter apparatus includes a conduit 80 connected to the conduit 20, wherein valves 82, 84, 86, and 88 are provided, these valves corresponding as to type and purpose to the previously described valves 44, 46, 48, and 50.

A metering vessel 90 basically similar to the vessel 52 is provided and connected to the conduit 80 intermediate the normally closed electric valves 82 and 84. The vessel 90 includes connections 92 and 94 through which a fluid at constant temperature can be circulated in the jacket portion thereof. A conduit 96 (corresponding to the conduit 60) is connected to the vessel 90, and the same is provided with electric contacts 98, 100, and 102 (corresponding to the contacts 72, 74, and 76) and an enlarged chamber 104 (corresponding to the chamber 78). Conduit 96 also contains mercury for the same purpose as the mercury in column 60. The upper end of the conduit 96 is connected to a vacuum pump, not shown, or a zone or fixed low pressure to serve a purpose analogous to that previously described in connection with the vessel 58. The conduits 12 and 80 are also connected to vacuum, as shown, the former connection being for the purpose of initially evacuating the vessel 10 and the conduits connected thereto prior to conducting the adsorption (or absorption) phase, with the latter connection simply constituting a low pressure connection for discharging the vessel 90 to its lower pressure limit.

Attention is now directed to FIGURES 3, 4, and 5, wherein there is shown the means 30 for measuring pressure differential existing between the conduits 28 and 36.

Secured to a wall member 106 by means of brackets 108 and 110 is a pair of bellows 112 and 114. The bellows 112 and 114 are secured back to back to a plate 116. As viewed in FIGURE 3, the right ends of the bracket 110 and of the plate 116 are connected by a thin strip or ligament 118, preferably metallic, as shown. Disposed below the bellows 112 and 114 is a lever arm 120. A fulcrum arrangement for the lever arm 120 is provided that is constituted of a bracket 122 secured to the wall 106, and a thin strip or ligament 124, preferably metallic, secured at one end to the bracket and at the other end to an intermediate position along the length of the lever

arm 120, as shown. A thin strip or ligament 126, preferably metallic, is secured at its opposite ends to the left ends of the plate 116 and the lever arm 120, as shown in FIGURE 3.

As viewed in FIGURE 3, the right end of the lever arm 120 (which is preferably of a nonmagnetic metal such as aluminum) has fixed thereto an armature 128, preferably of magnetically soft iron, that constitutes the movable part of a differential transformer 130 otherwise fixed to the wall 106.

The conduits 28 and 36 are coupled to the fixed ends of the bellows 114 and 112, respectively, and communicate with the interiors thereof. With this arrangement, the action of the bellows 112 and 114 is to urge the plate 116 upwardly when the pressure in the conduit 28 exceeds that in the conduit 36, and vice versa. It will be understood that the bellows 112 and 114 are sufficiently flexible about their central axes to allow transference of such forces through the ligament 126 to the lever arm 120.

Means is provided for applying a sufficient torque to the lever arm 120 so as to maintain the plate 116 in fixed position. This torque is applied by a tension spring 132 applying an upward force to the lever arm 120 intermediate the ligament 124 and the armature 128. The neutral position to be maintained by the plate 116 is such that is occupied by the plate 116 when the pressures in the conduits 28 and 36 are equal, with sufficient tension being applied through the spring 132 to maintain all the ligaments 118, 124 and 126 under tension.

The means for applying the torque by way of the spring 132 will be more readily appreciated upon consideration of FIGURE 5. The plate 116 is shown as directly connected to the lever arm 120 for application of force thereto for movement about the schematically illustrated fulcrum constituted of the ligament 124. Motion of the lever arm 120 caused by movement of the plate 116 is communicated to the armature 128, with movement of the latter from its neutral position with respect to the fixed portion of the differential transformer 130 being sensed by the latter, with the result of an error signal being produced by the latter and transmitted to a servo amplifier 134 by way of electrical connecting means 136. The output of the servo amplifier 134 is fed to a servo motor 138 by way of electrical connecting means 140.

The servo arrangement is essentially conventional and functions to drive the motor 138 at a speed generally proportional to the displacement of the armature 128 from its neutral position, and in a direction dependent upon the direction of the displacement of the armature 128. Gearing means designated generally at 142 drives a micrometer screw 144 from the servo motor 138 in a direction such that the spring 132 attached to the screw 144 acts upon the lever arm 120 in a direction tending to return the armature 128 to its neutral position. The neutral position of the armature 128 corresponds to the neutral position of the plate 116 by virtue of the mechanical connections therebetween. Consequently, the servo system described above serves to continuously maintain the system in balance with the plate 116 in its neutral position. The tension applied to the lever arm 120 by the spring is linear with respect to the pressure differential between the conduits 28 and 36.

Since the spring 132 is essentially linear, the rotational position of the servo motor 138 and the gearing means 142 connected thereto at any instant is also linear with respect to the aforementioned pressure differential.

The gearing means 142 is mechanically coupled by means schematically illustrated at 146 and 148, respectively, to a command potentiometer 150 and a mechanical counter 152. The purpose of the potentiometer will be explained presently in connection with FIGURE 2.

Referring now to FIGURE 2, a recorder is designated generally at 154. Said recorder includes a movable chart 156 that is entrained over a drive roller 158 from a sup-

ply roller 160. A recording pen 162 is fixed to a continuous flexible wire or element 164 that is entrained over pulleys 166 and 168. Means is provided for driving the pulley 168 so as to move the recording pen 162 as a linear function of the extent that the servo motor 138 is rotated. The previously mentioned command potentiometer 150 is provided for this purpose. The one terminal of the potentiometer 150 is connected in series to a terminal of a further potentiometer 170 through rheostats 172 and 174 by leads 176, 178, and 180. The other end terminal of the potentiometer 150 is connected to the other end terminal of the potentiometer 170 through a rheostat 182 by leads 184 and 186. A source of 6.3 volts alternating current 188 is provided that is connected to the leads 180 and 186 by leads 190 and 192. The alternating current source 188 provides excitation for the potentiometers 150 and 170. The movable elements of the rheostats 174 and 182 are secured to a common control shaft 194, whereby such rheostats can be jointly adjusted by the single control knob 196. The rheostat 172 is provided with an adjustment knob 198 to be used in conjunction with the knob 196 in adjusting the overall system in a manner to be specified subsequently. The potentiometer 170 includes a control shaft 200 that is connected to a servo motor 202. The numeral 204 designates a servo amplifier, one input connection being connected to the center tap of the potentiometer 170 by a lead 206, and the other input connection being connected to the center tap of the potentiometer 150 by a lead 208. The output connections of the servo amplifier 204 are connected to the servo motor 202 by leads 210 and 212. The numeral 214 designates a source of 110 volts alternating current which is connected to the servo amplifier 204 by leads 216 and 218, and to the servo motor 202 by leads 220 and 222. The servo motor 202 in addition to driving the potentiometer 170 also drives the pulley 168 by means of a shaft 224 and gearing 226.

The described electromechanical means for driving the pulley 168 from the servo motor 138 and its connection to the command potentiometer 150 is conventional and is known to those skilled in the art as a command follow-up system. It will be readily understood by those skilled in the art that the control knob 196 affords a zero adjustment for the trace afforded by the recording pen 162, while the adjustment afforded by the knob 198 affords a provision for scale length adjustment.

The means for scheduling the operation of the valves 44, 46, 82, and 84, as well as the means for driving the chart will now be described. A source of direct current 228 is provided suitable for relay actuation. The negative or ground terminal 230 of the source 228 is connected by leads 232, 234, 236, 238, and 239 to the solenoids of relays 240, 242, 244, 246, and 247, respectively, from a common negative or ground lead 248.

The positive terminal 250 of the supply 228 is provided with a principal lead 252. The relay 240 includes a contact 254, that normally closes a lead 256 between the contact 76 and the lead 252, but which closes a lead 258 between the contact 102 and lead 252 upon energization of the relay 240. The solenoid 240 includes another contact 260 that normally completes a connection between a lead 262 and a lead 264 connected to the contact 74, such contact 260 completing a connection between the lead 262 and the lead 264 connected to the contact 100 during energization of the solenoid 240.

The relay 242 includes a contact 268 that completes a connection between the lead 262 and the lead 252 solely upon energization of the relay 242. The relay 242 includes a further contact 270 that normally connects the lead 252 to a lead 272, with such contact 270 completing a connection between the lead 252 and a lead 274 upon energization of the solenoid 242.

The relay 246 includes a contact 276 that normally connects a lead 278 to the lead 252, with such connection being broken upon the relay 246 being energized.

The relay 247 includes a contact 280 that normally electrically connects the lead 252 to a lead 282, but which connects the lead 252 to a lead 284 upon energization of the solenoid 247.

The relay 244 includes a contact 286 that normally connects the lead 278 to the inlet valve 44, but which connects the lead 278 to the electric valve 82 upon energization of the relay 244. The relay 244 also includes a contact 288 that normally connects the lead 282 to the electric valve 46, but which connects the lead 282 to the electric valve 84 upon energization of the relay 244.

The electric valves 44, 46, 82, and 84 in addition to their connections to the contacts 286 and 288 have their other terminals connected to the negative or ground lead 248 by leads 290, 292, 294, and 296, respectively.

The solenoid of the relay 242 is connected to the contacts 72 and 98 by a lead 298. The solenoids of the relays 246 and 247 are respectively connected to the leads 274 and 272. The solenoids 240 and 244 are arranged to be concurrently energized and can, in fact, be a single relay if desired in practice, such relays being shown as separate entities for the sake of simplicity in the drawings. The relays 240 and 244 are connected through a common lead 300 to a time delay relay 302 that is described more fully hereinafter.

A pair of electrical counters 304 and 306 are connected in parallel with the electric valves 86 and 46, as shown, so that individual counts of the number of times that each of such valves is opened is obtained.

The time delay relay 302 is of a conventional type such that continuous closure of a normally open micro switch 308 for a predetermined time completes a circuit between the leads 252 and 300 so as to energize the relays 240 and 244. A source of 110 volts alternating current 310 is connected to the time delay 302 by leads 312 and 314, the micro switch 308 being disposed in series in the lead 314. As stated previously, the time delay relay 302 is conventional and can be of the type manufactured by A. W. Haydon Company of Waterbury, Connecticut bearing manufacturers No. L11419.

Attention is now directed to the means for advancing the chart 156 an equal increment of distance upon each occasion of either of the valves 46 or 84 being opened. Such means comprises a solenoid 316 connected to the leads 282 and 248, it being apparent that the solenoid 316 is energized whenever the relay 247 is not energized. An armature 318 is associated with the solenoid 316 so that the former is depressed from a normally raised position during the energization of the solenoid 316. The lower extremity of the armature 318 is provided with a pivoted pawl 320 that engages with a tooth of a ratchet wheel 322 mounted on the shaft of the roller 158 during downward movement of the armature 318. The arrangement is such that each successive energization of the solenoid 316 results in the roller 158 being rotated a fixed amount in a forward direction so as to advance the chart 156 in a corresponding manner.

As described thus far, the chart 156 is driven by incremental jumps so that varying differential pressure in the conduits 28 and 36 will record an inked line or trace of the nature indicated at 324. The general form of the inked line 324 made by the recording pen 162 is explained fully later.

For the purpose of timing the introduction into or the removal of equal mass increments from the vessel 10, there is provided an electric timing motor 326 having power connections, not shown. An endless chain 328 is entrained over a sprocket wheel 330 driven by the electric timing motor 326. The endless chain 328 is provided at spaced intervals along its length with laterally extending pins or extensions 332. Disposed along the travel path of the chain 328 is a normally closed micro switch 334, the arrangement being such that micro switch 334 is engaged by and opened during the time interval that

each of the pins 332 travels by the micro switch 334. Hence, the micro switch 334 can be intermittently opened according to any predetermined timing schedule desired dependent upon the spacing of the pins 332 on the chain 328. Of course, a number of chains can be provided of various lengths and a variety of pin spacings (either regular or irregular) thereon that can be interchangeable on the sprocket wheel 330 to afford swift and convenient versatility in adjusting timing schedules. The micro switch 334 is connected between the leads 284 and 272.

The operation of the illustrated apparatus will now be described. Initially, with a sample of material to be analyzed in the vessel 10, the valves 44, 46, 82, and 84 are closed and the stopcocks 14, 16, 22, and 24 are in their customarily closed positions. The stopcocks 16 is opened and the system is evacuated after which the stopcock 16 is closed. The conduit 28 contains nitrogen gas and the vessel 26 contains liquid nitrogen, so that the pressure in the conduit 28 is that of the vapor pressure of liquid nitrogen at the temperature prevailing in the sample vessel 10. It is assumed that the interior of the conduit 42 and the vessel 52 have previously been flushed free of all other gases than nitrogen. The introduction of increments of nitrogen gas into the vessel 10 is now commenced and is accomplished by opening the valve 44 until sufficient nitrogen gas enters the vessel 52 that the mercury in the column 60 makes contact with the contact 76. The throttling valve 48 limits the rate of gas entering the vessel 52 to prevent pressure surges. Then the valve 44 is closed after which the valve 46 is opened and gas allowed to leave the vessel 52 until the pressure in the vessel 52 falls to such a value that the mercury just breaks contact with contact 74 at which time the valve 46 is closed. The throttling valve 50 prevents too rapid gas movement and any harmful pressure surges. As described previously, such action results in the delivery of a fixed mass of nitrogen from the vessel 52. This operation of the valves 44 and 46 is then repeated in a cyclic manner to the conclusion of the adsorption phase of the analysis.

The operation of the valves 44 and 46 is performed automatically by the apparatus shown in FIGURE 2. The description of such automatic operation will be most readily understood if it is assumed initially that the vessel 52 is filled to the extent that the mercury contacts the contact 76. It will be further assumed that the relays 240 and 244 are de-energized and that none of the pins 332 are engaging the micro switch 334 so as to open the latter. Also, it is assumed that the relay 247 is energized through the contact 280 and the switch 334. Under these circumstances, the relay 242 is energized through the contact 254, the contact 76, the mercury in the conduit 60, the contact 72, and the lead 298.

As both the relays 246 and 247 are energized, the contacts 276 and 280 open the circuit to the valves 44 and 46 so that they are de-energized and closed. It will be noted that valves 82 and 84 cannot be energized unless relay 244 is energized. This situation will continue until such time as the switch 334 is actuated open by one of the pins 332 which deenergizes relay 247, with the result that contact 280 moves to close the circuit to the valve 46, opening the latter to permit discharge of gas from the vessel 52.

This situation will continue until the mercury breaks contact with the contact 74, it being noted that relay 242 is kept energized during this interval by the contact 268, contact 260 and contact 74. However, upon the mercury breaking contact with the contact 74, the circuit holding the relay 242 energized is broken and the relay 242 is de-energized, whereupon the contact 270 moves to a position energizing the relay 247 and de-energizing relay 246. Energization of the relay 247 de-energizes the valve 46 closing the latter, while de-energization of relay 246 allows the contact 276 to complete a circuit affording ener-

gization of the valve 44 opening the latter. It should be noted at this time that the relays 246 and 247 both are of the character that move the contacts controlled thereby swiftly on energization but allow such contacts to return to their normal positions more slowly upon de-energization. This prevents the valves 44 and 46 being concurrently open.

This situation will continue until the mercury again makes contact with the contact 76. It will be observed that when the relay 247 is energized with the micro switch 334 closed, the relay is held energized by the contact 280 until such time as the micro switch 334 is opened by one of the pins 332. Upon the mercury contacting the contact 76, the relay 242 is energized and the apparatus has returned insofar as an adsorption dosing cycle is concerned to the initially assumed set of conditions, whereupon a subsequent dosing cycle will be initiated by one of the pins 332 opening the micro switch 334. It will be appreciated that the time intervals between actuations of the micro switch 334 are adjusted so as to be longer than the time required for the vessel 52 to discharge and then be recharged. Consequently, the vessel 52 is in readiness to be discharged upon each opening of the micro switch 334.

During the period of time that the vessel 52 and the valves 44 and 46 are metering increments of gas to the vessel 10, the chart is being advanced a fixed amount at the beginning of each discharge of the vessel 52 through the action of the previously described solenoid 316, pawl 320, and ratchet wheel 322 arrangement. Also, the recording pen 162 constantly occupies a position transverse to the travel path of the chart 156 that is linear with respect to the pressure differential existing between the conduits 28 and 36. This latter function is achieved by virtue of the previously described command follow-up system and the pressure differential measuring apparatus. Eventually, as the adsorption phase is continued, the pressure differential reaches a predetermined value at which the adsorption phase is to be discontinued. Such predetermined pressure differential corresponds to a certain position of the recorder pen 162, and the micro switch 308 is arranged to be engaged by the pen 162 or its mount when the pen occupies such certain position. Inasmuch as the differential pressure may reach and thence withdraw from the predetermined value several times before it is safe to conclude that the adsorption phase should be terminated, there is provision for automatically terminating the adsorption phase and initiating the desorption phase solely after the differential pressure has reached the predetermined value without withdrawal for a predetermined time. Actuation of the micro switch 308 to its closed position for the predetermined uninterrupted time interval by the pen 162 or its mount completes a circuit between leads 252 and 300 so as to energize the relays 240 and 244. Such circuit remains closed until manually reopened.

Energization of the relays 240 and 244 terminates the adsorption phase by moving the contacts 286 and 288 so that the valves 44 and 46 cannot be energized open, but so that valves 82 and 84 can respectively be energized open in their stead upon the relays 246 and 247 respectively being de-energized. Energization of the relay 240 moves the contacts 254 and 260 so that contacts 100 and 102 electrically assume the role previously played by the contacts 74 and 76, respectively, it being noted that contacts 72 and 98 are directly connected. Therefore, it will be seen that energization of the relays 240 and 244 effectively substitutes the elements 82, 84, 98, 100, and 102 for the elements 44, 46, 72, 74, and 76 electrically so that the valves 82 and 84 are now cyclically operated in an analogous manner to the previously described operation of the valves 44 and 46. Such change in mode of operation results in the metering vessel 90 exhausting equal masses of nitrogen from the sample vessel 10 upon the occurrence of each instance of one of the pins 332 open-

ing the micro switch 334. It is to be understood that the valves 86 and 88 serve the same functions during the desorption phase as the valves 48 and 50 serve during the adsorption phase, and that the time consumed for the vessel 90 to discharge and to be charged again is less than the time interval between successive openings of the micro switch 334 by the pins 332.

From the foregoing it will be evident that the recorder 154 operates to produce a continuous record of the adsorption phase followed by the desorption phase wherein the trace 324 plots the differential pressure versus mass of gas either introduced or removed. It will be noted that the mass scale of each phase will be the same if the apparatus is adjusted so that the mass increments discharged from the vessel 10 (each of which is, of course, equal to each other) are each equal to the mass increments introduced to the vessel 10 (each of which is, of course, equal to each other) during the adsorption phase.

The trace or record 324 closely approximates the continuous equilibrium isotherm curve and furnishes the basic data for calculating the physical surface characteristics of the sample analyzed. Of course, the mode of chart drive results in the trace 324 being irregular or steplike. It is contemplated that the chart 156 can be, as is conventional in recorders, driven at a constant rate; however, the illustrated mode of chart drive is preferred in the interest of minimizing the length of the record obtained and for the reason that positions at which the outlet valves 46 and 84 are opened are very plainly marked; also, the transverse portions of the trace 324 made while the chart 156 is not moving afford an easily interpreted measure of the extent that the pressure in the vessel 10 changes in approaching equilibrium pressure for each introduction or removal of an increment of nitrogen. Such measure of equilibrium pressure adjustment is also of interest with respect to the average slope of the trace 324 and can serve as a guide to the sufficiency of the spacing of the pins 322 for the trace 324 to closely approximate the true isotherm.

It is believed that the foregoing is amply sufficient to afford a full and complete understanding of the principles of the invention. Obviously, the apparatus for employing the principles of the invention is susceptible to numerous variations without departing from the spirit of the invention, and therefore the actual scope of the invention should be ascertained upon inspection of the appended claims.

We claim:

1. The method of producing isotherm data with respect to surface characteristics of a solid sample comprising, placing the sample in an evacuated zone, maintaining the zone at the temperature of liquid nitrogen, periodically introducing equal mass increments of nitrogen into the zone, the introduction of the increments being sufficiently spaced apart in time for the nitrogen to closely approach equilibrium pressure in the zone, exposing the pressure in the zone and the vapor pressure of liquid nitrogen at the same temperature as the zone, respectively, to opposing sides of a pressure differential measuring means to measure the pressure differential, and recording such pressure differential versus the mass of nitrogen introduced into the zone.

2. The method of claim 1, wherein the differential pressure is continuously recorded versus the number of increments of nitrogen introduced, whereby the differential pressure immediately following introduction of a nitrogen increment can be compared directly with the resulting equilibrium pressure attained.

3. The method of producing isotherm data with respect to surface characteristics of a solid sample comprising, placing the sample in an evacuated zone, maintaining the zone at the temperature of liquid nitrogen, periodically introducing equal mass increments of nitrogen into the zone, the introduction of the increments being sufficiently spaced apart in time for the nitrogen to

closely approach equilibrium pressure in the zone, after a predetermined equilibrium pressure in the zone has been attained, periodically removing equal mass increments of nitrogen from the zone, the removal of the increments being sufficiently spaced apart in time for the nitrogen to closely approach equilibrium pressure in the zone, exposing the pressure in the zone and the vapor pressure of liquid nitrogen at the same temperature as the zone respectively, to opposing sides of a differential pressure measuring means to measure the pressure differential, and recording such differential pressure versus the number of increments of nitrogen that have been introduced and removed from the zone.

4. Apparatus for the transfer of equal mass increments of a gas from a first zone of relatively high pressure to a second zone of relatively low pressure comprising a metering vessel having an inlet provided with a normally closed inlet valve for communication with the first zone and an outlet provided with a normally closed outlet valve for communication with the second zone, means for maintaining the vessel at a constant temperature, pressure responsive electric switch means connected to the vessel, said switch means including first, second and third contacts with the first and second contacts being closed solely upon the pressure in the vessel exceeding a fixed relatively high value and with the first and third contacts being closed solely upon the pressure in the vessel exceeding a fixed relatively low volume, a first electrical means connected to the switch means for opening the inlet valve solely during intervals initiated by the opening of the first and third contacts and terminated by the closing of the first and second contacts, and a second electrical means connected to the switch means for opening the outlet valve solely during intervals initiated by the closing of the first and second contacts and terminated by the opening of the first and the third contacts.

5. Apparatus for the transfer of equal mass increments of a gas from a first zone of relatively high pressure to a second zone of relatively low pressure comprising a metering vessel having an inlet provided with a normally closed inlet valve for communication with the first zone and an outlet provided with a normally closed outlet valve for communication with the second zone, means for maintaining the vessel at a constant temperature, pressure responsive electric switch means connected to the vessel, said switch means including first, second and third contacts with the first and second contacts being closed solely upon the pressure in the vessel exceeding a fixed relatively high value and with the first and third contacts being closed solely upon the pressure in the vessel exceeding a fixed relatively low value, a first electrical means connected to the switch means for opening the inlet valve solely during intervals initiated by the opening of the first and third contacts and terminated by the closing of the first and second contacts, a second electrical means connected to the switch means for opening the outlet valve solely during intervals initiated by the closing of the first and second contacts and terminated by the opening of the first and the third contacts, and a third electrical means including a control switch for delaying initiation of the interval of operation of the second electrical means until such control switch is actuated.

6. The combination of claim 5 including timer means for successively actuating the control switch according to a predetermined time schedule.

7. Apparatus for the transfer of equal mass increments of a gas from a first zone of relatively high pressure to a second zone of relatively low pressure comprising a metering vessel having an inlet for communication with the first zone and an outlet for communication with the second zone, said inlet and said outlet being provided with normally closed inlet and outlet valves respectively, means for maintaining the vessel at a constant temperature, pressure-responsive electric switch means connected to

said vessel, said switch means including first, second and third contacts, with the first and second contacts being closed solely upon pressure within the vessel being in excess of a fixed relatively high pressure in the vessel and with the first and third contacts being closed solely upon pressure within the vessel being in excess of a fixed relatively low pressure, a first locking relay means operatively connected to the pressure switch means for energization during closure of the first and second contacts and for remaining energized during uninterrupted closure of the first and third contacts, said means connected to the first locking relay means for opening the inlet valve solely during intervals that the first locking relay means is de-energized, a normally closed control switch, a second locking relay means operatively connected to the first locking relay means for energization during deenergization of the first locking relay means and remaining energized during uninterrupted closure of the control switch, and electrical means for opening the outlet valve solely during intervals that the second locking relay means is de-energized, whereby the increments can be transferred according to a predetermined timing schedule.

8. The combination of claim 7 including means for measuring the pressure in one of said zones in relation to a reference standard, and means for recording the measured pressure versus the number of increments transferred.

9. The combination of claim 8, wherein said reference standard is a gas under pressure, said measuring means comprising a pair of bellows arranged back to back with their opposite ends being fixed and communicating with the reference standard gas pressure and the said one zone, first and second ligaments each having one end connected to the juncture of the bellows, with such connections being spaced apart, the first ligament having the remote end thereof fixed, a lever arm and a third ligament constituting a fulcrum for such arm, said second ligament having the end thereof remote from the bellows juncture secured to the lever arm, a differential transformer arranged to sense displacement of the lever arm from a neutral position thereof, a tension spring connected to the lever arm and a micrometer screw connected to the spring for varying the tension of the spring, a servo system coupled to the transformer for driving the micrometer screw in a direction that the tension of the spring returns the lever arm to its neutral position, said servo system including a servo motor, said recording means including a command follow-up operatively coupled to the servo motor.

10. The combination of claim 9, wherein the recording means includes a chart and an intermittent driving means therefor that translates the chart a unit distance at the initiation of each increment transfer.

11. Differential gas pressure measuring means comprising a pair of bellows arranged back to back with their opposite ends being fixed and communicating with the gas pressures, the differential pressure between which is to be measured, first and second ligaments each having one end connected to the juncture of the bellows, with such connections being spaced apart, the first ligament having the remote end thereof fixed, a lever arm and a third ligament constituting a fulcrum for such arm, said second ligament having the end thereof remote from the bellows juncture secured to the lever arm, a differential transformer arranged to sense displacement of the lever arm from a neutral position thereof, a tension spring connected to the lever arm and a micrometer screw connected to the spring for varying the tension of the spring, a servo system coupled to the transformer for driving the micrometer screw in a direction that the tension of the spring returns the lever arm to its neutral position, said servo system including a servo motor, means for recording rotational displacement of the servo motor as a measure of the pressure differential including a command follow-up system coupled to the servo motor.

12. Apparatus comprising a sample vessel, first and

13

second conduits connecting the sample vessel to a gas source and sample vessel evacuating means respectively, means in each of said conduits for transferring equal mass increments of a gas from a first zone of relatively high pressure to a second zone of relatively low pressure, means for preventing concurrent operation of the means in the first conduit and the means in the second conduit, means for periodically causing the operative one of the means in the first and second conduits to transfer a mass of gas, means for terminating operation of the means in the first conduit and also for initiating operation of the means in the second conduit upon the pressure in the sample vessel rising to a predetermined level, and means for recording the pressure in the sample vessel versus the number of gas transfers.

5

10

14

References Cited in the file of this patent

UNITED STATES PATENTS

2,692,497	Von Nordstrand	Oct. 26, 1954
2,694,927	Coulbourn et al.	Nov. 23, 1954
2,729,969	Innes	Jan. 10, 1956
2,816,443	Gomez et al.	Dec. 17, 1957
2,910,870	Schaefer	Nov. 3, 1959

OTHER REFERENCES

Schlosser et al.: German application, 1,057,798, printed May 21, 1959.



Studies of Metastable Ion Transitions with a 180° Mass Spectrometer

NORMAN D. COGGESHALL

Reprinted from THE JOURNAL OF CHEMICAL PHYSICS, Vol. 37, No. 10, pp. 2167-2175, November 15, 1962

Studies of Metastable Ion Transitions with a 180° Mass Spectrometer

NORMAN D. COGGESHALL

Gulf Research & Development Company, Pittsburgh, Pennsylvania

(Received June 25, 1962)

The decay of metastable ions through transitions giving an ionized fragment and a neutral radical has been investigated with a 180° mass spectrometer. Four aspects of the main problem have been studied. These are: (a) the decay of metastable ions within the ion source to produce a continuous distribution of "metastable ions"; (b) an examination of the mathematical conditions relating dissociation beyond the ion-source exit slit to the formation of a "metastable" peak, to the shape of such a peak, to the cutoff imposed by the analyzer walls and to the length of travel during which detectable dissociation may occur; (c) an examination of the conditions for determining lifetimes with a 180° instrument; and (d) a consideration of the elements leading to the broadness of metastable peaks.

The distribution function resulting from dissociation within the slit drops very rapidly and is ordinarily hidden within the peak due to the daughter ion. The formation of a metastable peak

in a 180° instrument results from a low-order dependence of where the ion fragment resulting from dissociation hits the focal plane on the position of dissociation beyond the exit slit. The cutoff mass due to ions striking the walls of the analyzer tube may be readily calculated. In a CEC model 21-103 instrument there is adequate distance of free travel beyond the exit slit to allow the instrument to be used for lifetime measurements. Using repeller voltages up to 120 V, shorter lifetimes than those previously reported have been observed. For the $m^*=31.9$ metastable peak from *n*-butane, for example, there is evidence that the metastable ions are created in at least three classes, each with its own lifetime. The shortest lifetime observed was of the order of 9×10^{-8} sec. Evidence has been obtained to indicate that the broadness of the observed metastable peaks is probably the result of the perturbation of focusing conditions by the increased angular spread in the ion beam.

THE existence and interpretation of ions arising from the dissociation of metastable ions are of great importance in constructing a theory of mass spectra. The present report gives some results from a quantitative examination of metastable transition ions as observed in a 180° mass spectrometer. The ions resulting from the dissociation of metastable ions are usually observed at nonintegral mass units. For simplicity these peaks are referred to as metastable ion peaks and the mass in each case is referred to as the metastable mass. The relationship between the metastable mass, the mass of the metastable ion from which it originates, and the mass of the dissociation fragment bearing the charge was first given by Hipple and Condon.¹

Unless otherwise stated, all data examined were determined with Consolidated Electrodynamics Corporation model No. 180° mass spectrometers, equipped with Isotron ion sources. In some cases, a metastable suppressor was used. Slitwidths and electrode separations utilized were those normally used and recommended by the manufacturer.

DISSOCIATION OF METASTABLE IONS WITHIN THE ION SOURCE

Let us denote by n_0 the total number of ions of mass m created per unit area in the electron beam. We assume that a fraction of these are created in a metastable state with a decay constant λ . We denote by m_1 the mass of the charged fragment resulting from dissociation. The apparent mass possessed by these ions when collected at the detector, otherwise referred to as the metastable mass, is denoted by m^* . The geometry and symbols used for the ion source are

given in Fig. 1. Here, the electron beam passes through the ionization region approximately one-half way between the repeller and the first slit. Ions will reach the first slit at a time t_1 after being formed and with a potential of V_1 . Ions will reach the second slit a time t_2 after passing through the first slit and with a total potential of $V = V_1 + V_2$.

The focusing conditions in a 180° instrument are given by

$$mV = r^2 e H^2 / (2c^2), \quad (1)$$

where r is the radius of curvature in centimeters, e is the charge of the electron in electrostatic units, H is the magnetic field in gauss, and c is the velocity of light in centimeters per second. The potentials used in Eq. (1) must be in electrostatic units. The apparent mass of a metastable ion is calculated by inserting in Eq. (1) the value of V at which it is observed and calculating for m^* .

Metastable ions which dissociate immediately upon creation will yield normal ions of mass m_1 . Metastable ions which dissociate at the exit slit will yield ions of the usual apparent mass m^* given by

$$m^* = m_1^2 / m. \quad (2)$$

Metastable ions dissociating between the plane of the electron beam and the exit slit appear at apparent masses lying between m_1 and the m^* of Eq. (2). It is the purpose of this section to derive the distribution function for these metastable ions as a function of m^* .

Let us consider a metastable ion created at $t=0$ in the electron beam. Let us further consider the case wherein this ion dissociates at a time t before the ion has passed out of the source. The m_1^+ ion emerging from the exit slit has an equivalent potential V_e which is less than

¹ J. A. Hipple and E. U. Condon, Phys. Rev. 68, 54 (1945).

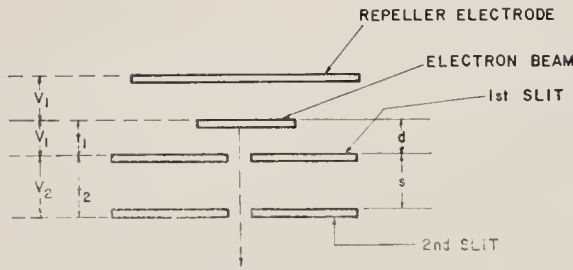


FIG. 1. Schematic ion source geometry and symbols.

the instrument potential $V = V_1 + V_2$. When V_e is equal to the potential which normally focuses normal ions of mass m_1 , the m_1^+ ion resulting from dissociation of a metastable ion is collected and has an apparent mass m^* derived from Eq. (1). As is seen later, we may calculate V_e as a function of t and invert the function to evaluate t in terms of V_e . This, in turn, may be transformed to provide t as a function of m^* , i.e., $t = t(m^*)$.

The number of metastable ions which dissociate in the interval between t and $t + \Delta t$ and which can be collected by the detector is given by

$$f(m^*) dm^* = \lambda A a n_0 \exp(-\lambda t) dt, \quad (3)$$

where $f(m^*)$ is the intensity distribution function for the number of ions from metastable transitions as a function of m^* , and A is a collection and transmission factor which relates the number of ions issuing from the exit slit to the internal geometry and discrimination of the source.

Using $t = t(m^*)$ we transform Eq. (3) to

$$f(m^*) dm^* = \lambda A a n_0 \exp[-\lambda t(m^*)] (dt/dm^*) dm^*,$$

from which we may express $f(m^*)$ as

$$f(m^*) = - (d/dm^*) \{ A a n_0 \exp[-\lambda t(m^*)] \}. \quad (4)$$

The exact evaluation of $t(m^*)$ for a 180° instrument would be based on the equations of cycloidal motion.² However, for the sake of tractability we ignore the magnetic field. For large values of V_1 (one-half the repeller voltage) this will be a good approximation, whereas for low values of V_1 , it is very poor. We also assume uniform electric fields between the repeller electrode and the first slit and between the first and second slits. This ignores the field penetration through the first slit but it is impossible to account for it in a simple analytical treatment. The above approximations dictate that numerical results calculated from the following treatment should only be used to establish the qualitative and semiquantitative nature of the behavior.

Let us first consider a metastable ion which dissociates before the first slit at time t ($0 \leq t \leq t_1$), where t_1

is the time it takes an ion of mass m to reach the first slit. We use the common operating conditions such that V_1/V_2 is constant so that $V_1 = d_1 V$ and $V_2 = d_2 V$, $d_1 + d_2 = 1$. Applying the equations of motion to a charge particle in a uniform field, we find

$$\frac{m_1 v^2(2)}{2} = e \left[V - \left(\frac{m - m_1}{m} \right) \frac{e d_1^2}{2 m d^2} V^2 t^2 \right], \quad (5)$$

where $v(2)$ is the velocity of the charged fragment resulting from the dissociation as it emerges from the second slit. If this ion is collected at the detector, it appears at a mass m calculated from Eq. (1) by inserting the total instrument accelerating voltage V . We may use this with Eq. (1) to get

$$m^* V = \frac{H^2 e r^2}{2 c^2} = \frac{m_1}{e} \left[\frac{m_1 v^2(2)}{2} \right]. \quad (6)$$

This allows us to replace the $m_1 v^2(2)/2$ term and the V and V^2 terms in Eq. (5) as functions of m^* . When this is done and the resulting equation solved for t , we get

$$t = [(m_1 m^* - m^{*2}) / a_1 a_2 m_1 d_1^2]^{\frac{1}{2}}, \quad (7)$$

where $a_1 = H^2 e r^2 / 2 c^2$ and $a_2 = (e / 2 m d^2) [(m - m_1) / m]$. We may evaluate t_1 as

$$t_1 = d(2 m / e d_1 V)^{\frac{1}{2}}.$$

When this is inserted in Eq. (7), we may solve for the $m^*(1)$ which applies to ions dissociating at the first slit. This is given by

$$m^*(1) = m_1 \left[1 - \left(\frac{m - m_1}{m} \right) d_1 \right]. \quad (8)$$

Utilizing Eq. (4), we may then evaluate $f(m^*)$ between m_1 and $m^*(1)$ as

$$f(m^*) = - A a n_0 \frac{d}{dm^*} \exp \left[-\lambda \frac{(m_1 m^* - m^{*2})}{a_1 a_2 m_1 d_1^2} \right]. \quad (9)$$

For the evaluation of $f(m^*)$ corresponding to the dissociation time occurring between t_1 and $t_1 + t_2$, let us denote $t' = t - t_1$. When this is done, we find for $0 \leq t' \leq t_2$ that

$$\begin{aligned} & \frac{m_1 v^2(2)}{2} \\ &= \left\{ \frac{m_1}{m} e V_1 + e V_2 - \frac{e V_2 (m - m_1)}{s} \left[v(1) t' + \frac{e V_2 t'^2}{2 m s} \right] \right\} \end{aligned} \quad (10)$$

where $v(1)$ is the velocity of the undissociated metastable ion as it passes through the first slit. We may proceed through the same type steps as used above to transform Eq. (5) to derive an expression relating m^* and t . This is

$$m^* / m_1 = \{ a_3 - [a_4 / (m^*)^{\frac{1}{2}}] - a_5 t^2 - a_6 t (m^*)^{\frac{1}{2}} + a_7 m^* \}, \quad (11)$$

where a_3, a_4, a_5, a_6 , and a_7 are constants which may be

² N. D. Coggeshall, Phys. Rev. **70**, 270 (1946).

evaluated in terms of m , m_1 , s , d , d_1 , d_2 , a , and a_2 . Equation (11) is quadratic in t so that it may be solved explicitly in terms of m^* to obtain the $t(m^*)$ function to use in Eq. (4). Using this and Eq. (9), the complete $f(m^*)$ function may be evaluated for the distribution between m_1 and m_1^2/m , of the ions resulting from dissociation within the source.

The $f(m^*)$ function discussed above drops very rapidly in progressing from m_1 to lower masses. When observable at all it is in the form of an asymmetric tailing on the low mass side of the normal fragment peak. This tailing is normally not seen in the peaks from CEC model 21 instruments used without metastable suppressors. In these the ion-source dimensions and normally used values of the d_1/d_2 ratio favor a very sharp drop of the $f(m^*)$ function. However, the ion source geometry and d_1/d_2 ratios effective in the sector-type instrument, employed by Hipple, Fox, and Condon,³ favor a less steep descent of $f(m^*)$ and the low-mass asymmetric tailing may be observed in Figs. 1 and 8 of their article.

The reason $f(m^*)$ drops so fast is that the metastable ion spends most of its residence time in the ion source in the initial stages of its acceleration and, hence, most of the fragment ions from dissociation of metastable ions in the source have m^* values so close to m_1 that their contribution cannot be detected. The $f(m^*)$ function cannot be graphically displayed without an arbitrary normalization at some mass value lower than m_1 . This is because the $f(m^*)$ function possesses a singularity at $m^*=m_1$. To appreciate how the major contribution from $f(m^*)$ is hidden within the experimental peak width of the m_1^+ peak, let us consider $C_4H_{10}^+(58) \rightarrow C_3H_7^+(43) + 15$; $m^*=31.9$, where m^* designates the normally observed metastable peak mass. We use the representative operating conditions of $V=1610$ volts, $V_1=2$ volts. For these conditions $t_1=1.01 \times 10^{-6}$ sec and $t_1+t_2=1.17 \times 10^{-6}$ sec. Assuming the metastable ion to have a half-life of 2×10^{-6} sec, we find that 34% of the metastable ions dissociate within the source but that 30% dissociate by the time they reach the first slit. Using the above relation for $m^*(1)$ we therefore find that of the total area under the $f(m^*)$ curve, 88% of it lies within the extremely narrow mass interval (unobservable) between $m_1(43)$ and $0.99996m_1(43)$.

It would be of value to achieve experimental conditions such that the $f(m^*)$ curve could be unambiguously recognized and measured on the low-mass side of the m_1^+ peaks. This could provide further information as to the approximate lifetimes of the metastable states dissociating to particular ions. We may obtain guidance on the physical conditions required by examining the above equations. Since the observations are in the immediate neighborhood of m_1 , we may express $m^*=$

$m_1 - \Delta m_1$. Ions dissociating as they pass through the first slit give $\Delta m_1(1)$ calculated from Eq. (8) as

$$\Delta m_1(1) = m_1 d_1 (m - m_1) / m.$$

The fraction of the total accelerating voltage, represented by d_1 , which operates behind the first slit, may thus be adjusted to make those ions dissociating at the first slit appear at a Δm_1 value outside the natural width of the m_1^+ peak. If we neglect Δm_1^2 relative to $m_1 \Delta m_1$, we may simplify Eq. (7) to

$$t = [(\Delta m_1)^{1/2} / d_1 (a_1 a_2)^{1/2}].$$

The area under the $f(m^*)$ curve appearing between $\Delta m_1'$ and $\Delta m_1''$ when both are smaller than $\Delta m(1)$ but preferably lying outside the natural peak width are

$$\int_{\Delta m_1'}^{\Delta m_1''} f(m^*) dm^* = A a n_0 \left\{ \exp \left[-\lambda \frac{(\Delta m_1')^{1/2}}{d_1 (a_1 a_2)^{1/2}} \right] - \exp \left[-\lambda \frac{(\Delta m_1'')^{1/2}}{d_1 (a_1 a_2)^{1/2}} \right] \right\}. \quad (12)$$

This area is increased by decreasing the numerical values of a_1 and a_2 which correspond to reducing the value of $(H^2 r^2)$ and increasing the value of d (see Fig. 1), respectively. It should be remembered that the above derivations are based on the assumption of uniform electric fields, of no magnetic field, and of no field penetration. The latter effect, particularly, makes the above relations useful only for qualitative guidance.

An experimental difficulty that may negate the effects of increasing d_1 is the broadening of the m_1^+ peak as the repeller voltage is increased. This may occur if the effect of increasing repeller voltage is to thicken the electron beam so that ions may be created at points of different potential. The m_1^+ peak may also broaden due to changes in focus conditions. This broadening of the m_1^+ peak may, therefore, completely obscure the $f(m^*)$ contribution.

DISSOCIATION OF METASTABLE IONS BEYOND THE ION SOURCE

Ion peaks resulting from the dissociation of metastable ions within the magnetic analyzer region of a 180° instrument would not appear if it were not for a fortuitous mathematical relationship. This is that the lateral displacement with which the fragment ions strike the focal plane has a low-order dependence upon the position at which the metastable ion dissociates for some distance beyond the exit slit. This is inherent in the derivation made by Hipple⁴ who showed that such a peak should be observed in a 180° instrument.

We may derive, in the same manner as Hipple,⁴ the $f(m^*)$ curve for ions resulting from the dissociation of metastable ions past the exit slit in the same general procedure as before. We let $t=0$ at the exit slit and derive $t=t(m^*)$ for substitution in Eq. (4). Let us

³ J. A. Hipple, R. E. Fox, and E. U. Condon, Phys. Rev. **69**, 347 (1946).

⁴ J. A. Hipple, Phys. Rev. **71**, 594 (1947).

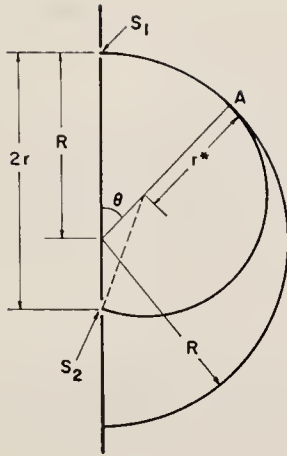


FIG. 2. Geometrical conditions required for a fragment ion to be collected at the detector.

refer to Fig. 2 which refers to a 180° instrument. Here, S_1 refers to the exit slit of the ion source and S_2 refers to the entrance slit to the detector. Here, an m^+ ion path has a radius R , the m_1^+ fragment path has a radius r^* , and r is the radius for the paths of ions normally focused. From the geometry we see that when a metastable ion dissociates after traversing an angle θ , the conditions for the fragment to be collected dictate that

$$r^{*2} = (R - r^*)^2 + (2r - R)^2 + 2(R - r^*)(2r - R) \cos \theta. \quad (13)$$

To simplify this we may use [from Eq. (1)]:

$$\frac{m_1^2}{m} \frac{V}{r^{*2}} = \frac{mV}{R^2} = \frac{m^*V}{r^2} = \frac{H^2 e}{2c^2}. \quad (14)$$

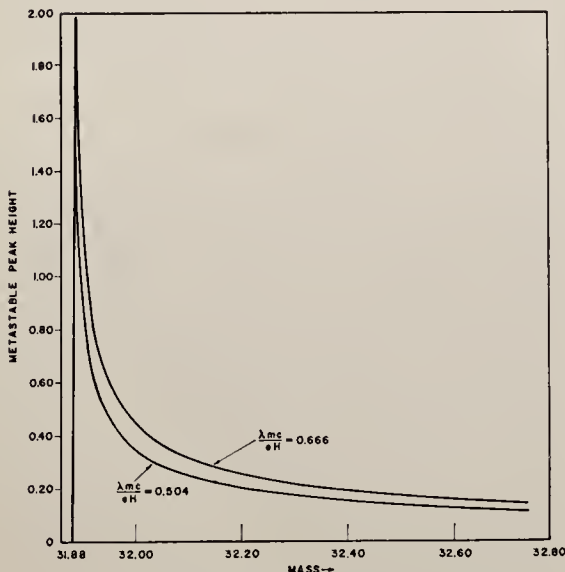


FIG. 3. Computed shapes of the peaks from metastable ions for $m_1^* = 31.9$ shown for two different parameter values.

Denoting $m - m_1 = \Delta m$, this leads to:

$$\cos \theta = \frac{[2(m^*)^{\frac{1}{2}} m^{\frac{1}{2}} - 2m^* - \Delta m]}{[2(m^*)^{\frac{1}{2}} - m^{\frac{1}{2}}](\Delta m/m^{\frac{1}{2}})}. \quad (15)$$

We may combine Eq. (15) with results from Eq. (14) to obtain

$$t(m^*) = \frac{mc}{eH} \cos^{-1} \left\{ \frac{[2(m^*)^{\frac{1}{2}} m^{\frac{1}{2}} - 2m^* - \Delta m]}{[2(m^*)^{\frac{1}{2}} - m^{\frac{1}{2}}](\Delta m/m^{\frac{1}{2}})} \right\}. \quad (16)$$

Using various results from above we, therefore, have

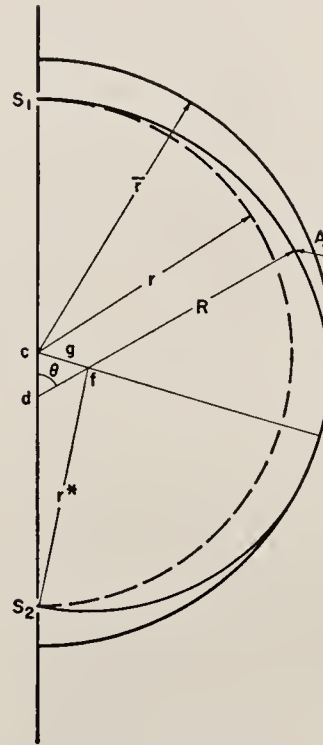


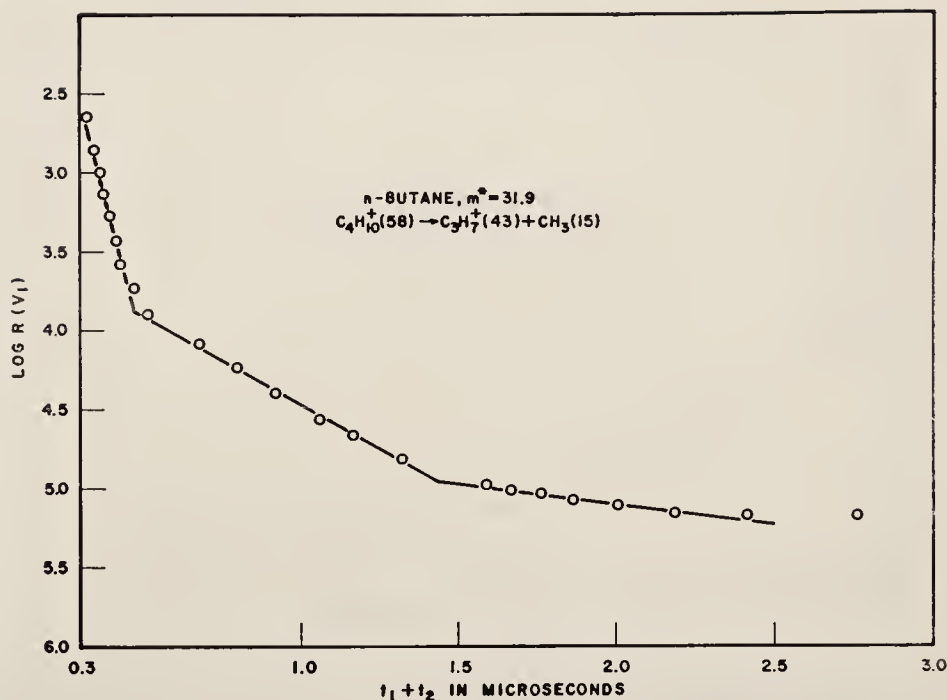
FIG. 4. Geometrical conditions representing cutoff conditions for fragment ions reaching the detector.

for the distribution function of apparent metastable mass

$$f(m^*) = A a n_0 \exp[-\lambda(t_1 + t_2)] (d/dm^*) \times \exp \left(-\lambda \frac{mc}{eH} \cos^{-1} \left\{ \frac{[2(m^*)^{\frac{1}{2}} m^{\frac{1}{2}} - 2m^* - \Delta m]}{[2(m^*)^{\frac{1}{2}} - m^{\frac{1}{2}}](\Delta m/m^{\frac{1}{2}})} \right\} \right). \quad (17)$$

In Eq. (17) only the derivative portion of the right-hand side need be considered to define the shape of $f(m^*)$. This is plotted in Fig. 3 for two cases: for $(\lambda mc/eH) = 0.666$ and 0.504 . These correspond to $m^+(58)$ dissociating to $m^+(43) + m(15)$ with half-life of 1.5×10^{-6} sec and an impressed magnetic field of 4600 G for the first case and with half-life of 2.5×10^{-6} sec and an impressed magnetic field of 3300 G for the second case. These curves were determined by machine calculation. The calculations thus predict a sharp asymmetric peak which tails off towards higher mass.

FIG. 5. Data used to determine the lifetimes for the metastable ion transition giving $m^* = 31.9$ for *n*-butane.



Hipple⁴ determined the same type of results to explain the existence of a metastable peak in a 180° instrument. He discussed the effect of baffles, sometimes used in a 180° instrument, which would cut out those ions which are not displaced very far from m_1^2/m . In the CEC instruments used here, there are no baffles between the exit slit of the source and the detector slit. It is, therefore, possible to calculate at what mass there would be a cutoff due to the ions hitting the walls of the analyzer tube. When we examine in detail *how this cutoff operates*, we find it does so for the ions resulting from dissociation of metastables rather than on the metastable ions before dissociation.

Referring to Fig. 4, \bar{r} is the radius of the outer inside wall of the analyzer tube and we consider a metastable ion progressing on a circle of radius R until it dissociates at point A . Ordinarily, it would then progress in a circular path of radius r^* unless it encounters interference from the wall. This first occurs for the fragment paths that tangentially encounter the wall. In the figure c is the center of the tube, d is the center of the circle of radius R , and f is the center of the circle of radius r^* . Interference occurs when the distance g between points c and f is such that

$$r^* + g = \bar{r}.$$

We may evaluate g from the relation

$$g^2 = (R - r^*)^2 + (R - r)^2 - 2(R - r^*)(R - r) \cos \theta. \quad (18)$$

Let us denote the ratio \bar{r}/r as h . Then using the rela-

tionships in Eq. (14) we transform Eq. (18) to

$$\frac{[h(m^*m)^{\frac{1}{2}} - m_1]^2}{m} = [m^{\frac{1}{2}} - (m^*)^{\frac{1}{2}}]^2 + \frac{\Delta m^2}{m} - 2[m^{\frac{1}{2}} - (m^*)^{\frac{1}{2}}] \frac{\Delta m}{m^{\frac{1}{2}}} \cos \theta. \quad (19)$$

We may find the effective m^* at which wall interference occurs by inserting the appropriate value of h in Eq. (19) and find the proper values of m^* and $\cos \theta$ from the use of Eq. (15). In our instruments h was approximately 1.1.⁵ For the mass 58 ion from *n*-butane, for example, decaying through a metastable transition to a mass 43 ion to give the mass 31.9 metastable peak, the predicted cutoff is calculated by the above procedure as mass 32.23. This corresponds to a limiting θ of 0.310 rad and an allowable travel distance in the analyzer tube of 3.94 cm. The quantities evaluated for this particular metastable transition will, in general, not be exactly applicable to other transitions. However, they serve adequate order-of-magnitude values.

The upper mass limit of the 31.9 peak from *n*-butane was experimentally evaluated by extrapolating the high mass side of the peak to the base line. This gave an upper limit to the metastable peak of 32.27 which is in good agreement with the value predicted above of 32.23.

LIFETIME MEASUREMENTS WITH 180° INSTRUMENT

We show here that lifetime measurements may be made with a 180° machine and we provide several examples.

⁵ C. E. Berry, (private communication).

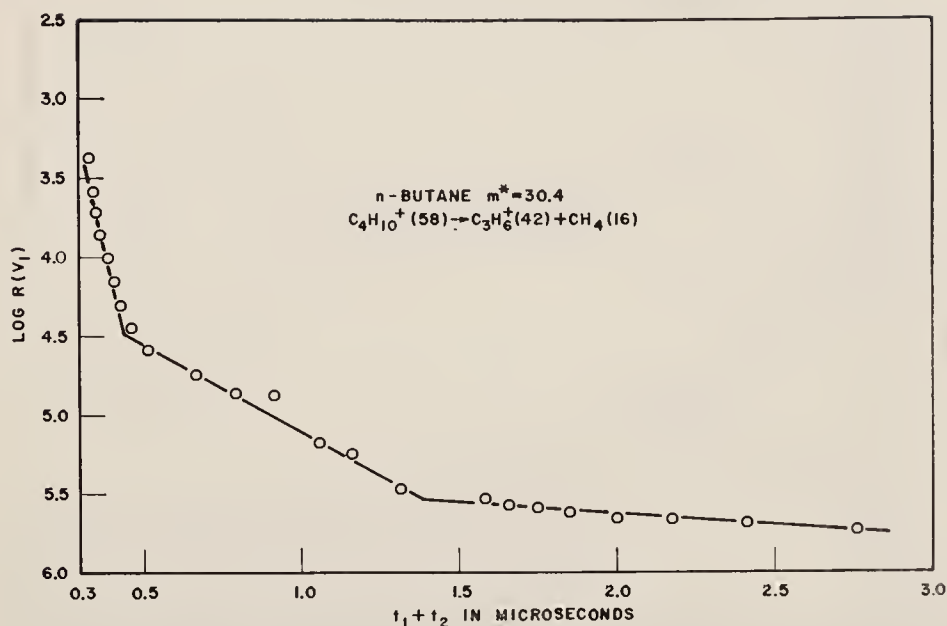


FIG. 6. Data used to determine the lifetimes for the metastable ion transition giving $m^* = 30.4$ for *n*-butane.

Let us assume that ions of mass m are formed in the electron beam at a density of n_0 per unit area. Let us assume as in Eq. (3) that a fraction a of them are in the metastable state at the instant of formation. The number of ions of apparent mass $m^* = m_1^2/m$ is given by the following equation:

$$I(m^*) = an_0 A(V_1, V_2, V) \exp[-\lambda(t_1 + t_2)] \times [1 - \exp(-\lambda s/v)] D_v(V) D_s. \quad (20)$$

Here, $A(V_1, V_2, V)$ represents a collection-transmission factor, dependent on the potentials, which relates the number of metastable ions which emerge from the exit slit, available for dissociation, to the number created per unit area in the electron beam. Here, s is the distance such ions may travel with velocity v in the analyzer tube before effective cutoff. $D_v(V)$ is a discrimination function which measures the beam attenuation due to initial kinetic-energy components parallel to the magnetic field.⁶ D_s is a discrimination function which measures the beam attenuation due to kinetic energy components which are imparted to the ions by the process of dissociation of metastable states. Similarly, the intensity of the m^+ ion peak are given by

$$I(m) = (1-a)n_0 A(V_1, V_2', V') D_v(V'), \quad (21)$$

where V_2' and V' indicate the different voltages for focusing the m^+ ion than were used for the m^* ion. Here we omit any contribution due to undissociated metastable ions reaching the collector. This is due to the facts that with the accelerating voltages used and with the analyzer radius used, the total transit time is of the

order of 10 μ sec. This is adequate for essentially complete dissociation for lifetimes of the order of 10^{-6} sec.

Let us denote the ratio of these peak intensities as $R(V_1)$, where

$$R(V_1) = I(m)/I(m^*) = B \exp[\lambda(t_1 + t_2)],$$

where

$$B = \frac{(1-a) A(V_1, V_2', V') D_v(V')}{a[1 - \exp(-\lambda s/v)] D_v(V) D_s A(V_1, V_2, V)}. \quad (22)$$

Consider a set of runs, using constant magnetic field, in each of which a different V_1 is used. The total accelerating voltages for parent ions and fragment ions from metastable transitions are always the same and, hence, B is essentially constant. All terms in B are constant under the conditions defined except the ratio $A(V_1, V_2', V')/A(V_1, V_2, V)$. This ratio is that of the collection-transmission factor for the undissociated ion for the values of V corresponding to m and m^* . Since the collection-transmission value will depend primarily on V_1 , which is the same in both terms of the ratio, we may treat the latter as constant. We may, therefore, plot $\log R(V_1)$ vs $t_1 + t_2$ to obtain information on metastable lifetimes.

A number of such experiments have been run in our Laboratory and the results are plotted in Figs. 5, 6, and 7. In these experiments, V_1 (one-half of repeller voltage) values up to 60 volts were used to reduce the total residence time $t_1 + t_2$ to the submicrosecond values seen. The metastable peak intensities were taken from the maxima of the metastable peaks. With each successive increase of V_1 , the electron voltage (nominally 70 volts) was decreased a corresponding amount so that the ionizing electron energy would be essentially con-

⁶ C. E. Berry, Phys. Rev. **78**, 597 (1950).

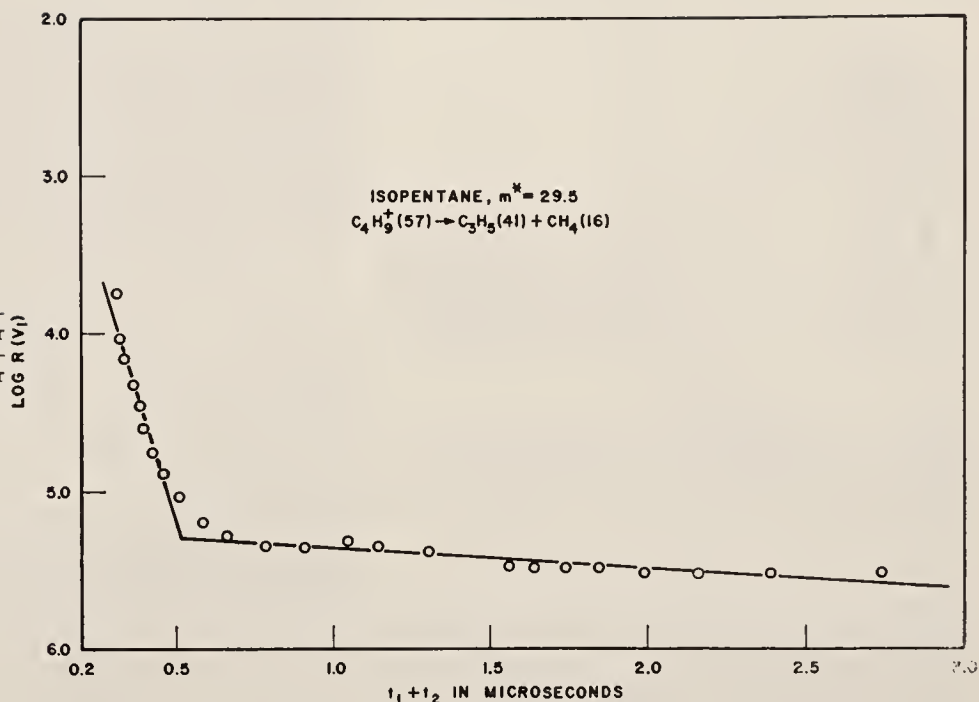


FIG. 7. Data used to determine the lifetimes for the metastable ion transition giving $m^* = 29.5$ for isopentane.

stant for all points. Straight lines may be drawn through different segments of the curve with the immediate interpretation that the metastable ions are distributed in different species characterized by different lifetimes. An examination of Hipple's measurement of the half-life for one of the metastable transitions for *n*-butane shows that the shorter half-lives were not found then as the residence times achieved were not short enough.

It could be argued that the data presented represent a continuous distribution of half-lives. However, the straight-line portions are rather distinct. There is some evidence in these data to indicate that shorter half-lives than those observed would be found with a further reduction of residence time. In Table I are given the half-lives as calculated from the straight-line portions.

TABLE I. Metastable transition half-life values.

Compound	Transition	Half-life values
<i>n</i> -butane	$C_4H_{10}^+(58) \rightarrow C_3H_7^+(43) + CH_3(15)$	8.9×10^{-8} sec
		6.1×10^{-7} sec
		2.7×10^{-6} sec
<i>n</i> -butane	$C_4H_{10}^+(58) \rightarrow C_3H_6^+(42) + CH_4(16)$	8.1×10^{-8} sec
		5.8×10^{-7} sec
		4.8×10^{-6} sec
isopentane	$C_4H_9^+(57) \rightarrow C_3H_5^+(41) + CH_4(16)$	1.03×10^{-7} sec
		5.4×10^{-6} sec

CONSIDERATIONS ON METASTABLE PEAK SHAPE

In many cases, the peaks resulting from a metastable ion transition occur so close to the normal ion peaks that the complete peak shape cannot be observed. An example, however, where the metastable peak lies apart from neighboring peaks is the $m^* = 31.9$ peak for *n*-butane. In examining such metastable peaks it is seen that there is tailing on the high-mass side as predicted in Fig. 3. However, the peaks do not rise abruptly on the low-mass side as predicted by Fig. 3, but show a surprising amount of tailing towards lower mass (see Fig. 9).

It is important to determine, if possible, the origin of the low mass tailing. Let us first consider the effects of the incremental velocity changes imparted to the fragment ion in the process of dissociation. We may consider two extremes: the one in which an increment of velocity Δv is imparted perpendicular to the velocity v of the parent ion, and the other in which the increment is added to or subtracted from the parent ion velocity. In Fig. 8 we have a diagram, with exaggerated conditions, which applies to the first case for an ion which dissociates just as it passes through the exit slit. Let us suppose that the angle between the new velocity after dissociation and the velocity before dissociation is θ . Then $\theta = \Delta v/v$.

For the purposes of this calculation we may neglect the change of absolute value of velocity. Using the same absolute value of v we may determine the center of the orbit of fragment ion after dissociation. This is swung out from the focal plane by a distance s , where $\theta = s/r$.

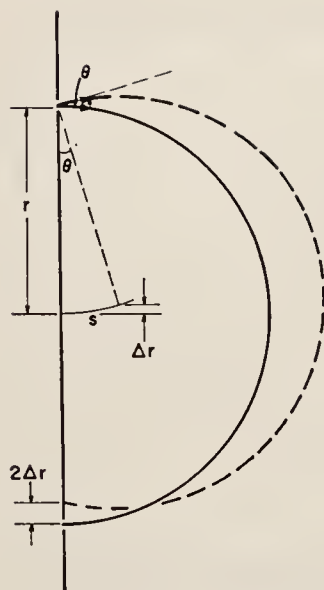


FIG. 8. Schematic diagram of the incremental velocity effect in metastable ion peak broadening.

This center is shifted parallel to the focal plane and relative to the original center by a distance Δr where $\theta = \Delta r/s$. This deflection of orbit is equivalent to an apparent change of mass by Δm . To determine Δm we use the relations above plus the relations

$$mV = Dr^2, \text{ where } D \text{ is constant,}$$

$$|\Delta V/V| = |\Delta m/m|,$$

$$|\Delta V| = |2V\Delta r/r|,$$

to obtain

$$|(\Delta m/m)| = 2(\Delta v/v)^2.$$

Dissociations with the incremental velocity change opposite to that shown will produce the same value of Δm .

For dissociations wherein the incremental velocity completely adds to or subtracts from the original velocity, we may use

$$mv = Her/c,$$

$$|\Delta v| = v |\Delta r/r|,$$

to obtain $|\Delta m/m| = |2(\Delta v/v)|$.

Thus, we see that the spread of apparent mass due to velocity additions perpendicular to the original velocity depends upon the square of the small quantity

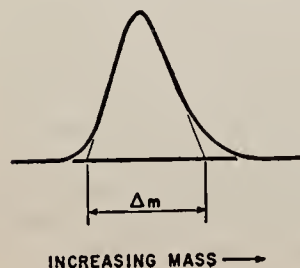


FIG. 9. Method of extrapolating the sides of the $m^*=31.9$ peak to determine Δm .

$(\Delta v/v)$, whereas, the apparent mass spread due to additions or subtractions of the velocity increment to the original velocity depends upon the first power of $(\Delta v/v)$. Thus, if the broadening of the peak were due to velocity additions, it should be dominated by the latter type. However, this argument is based on the assumption that the perpendicular type of dissociations would not sufficiently alter the solid angle of the beam to disturb focusing conditions.

Let us assume, for the moment, that the broadening is due to dissociations of the latter type, wherein there is numerical addition or subtraction of the energy of dissociation to the kinetic energy of the fragment ion. Since the processes that produce the metastable ions are the same, by the statistical theory of mass spectra, then we should observe the same kinetic energy spread

TABLE II. $(\Delta m/m)$ values for $m^*=31.9$ and $m_1=43$ for *n*-butane. (V^* refers to the accelerating voltage for m^* and V refers to the accelerating voltage for $m_1=43$.)

Repeller ($2V_1$)	V^*	$\Delta m^*/m^*$	V	$\Delta m_1/m_1$	$\Delta m^*/m_1$
$\frac{1}{2}\%$ of V^* or V	737	0.0256	547	0.0089	2.88
$\frac{1}{2}\%$ of V^* or V	1180	0.0223	875	0.0049	4.55
$\frac{1}{2}\%$ of V^* or V	1505	0.0200	1116	0.00473	4.23
$\frac{1}{2}\%$ of V^* or V	1880	0.0198	1387	0.00393	4.00
$\frac{1}{2}\%$ of V^* or V	2260	0.0181	1676	0.00366	4.95
$\frac{1}{2}\%$ of V^* or V	2635	0.0177	1955	0.00340	5.21
30	737	0.0278	547	0.01325	2.10
30	1180	0.0202	875	0.00612	3.30
30	1880	0.0175	1387	0.00426	4.11
30	2635	0.0173	1955	0.00367	4.72

or equivalently, mass spread, in the normal m_1^+ ion peak.

A comparison was made between the observed $(\Delta m/m)$ for the $m^*=31.9$ and the $m_1=43$ peaks for *n*-butane under a number of operating conditions. The $(\Delta m/m)$ values were obtained by making, for each run, a plot of m vs chart distance and determining the width of the base of each peak. The width of the metastable peak was determined in each case by linearly extrapolating the sides of the peak to the base line, as in Fig. 9. The results of these determinations are given in Table II.

Examination of the conditions applied in Table II show that the observations were taken across a wide range of accelerating voltages with both small and large repeller voltages. The results show that the $(\Delta m/m)$ values decrease with increased accelerating voltage as expected but not to changes in repeller voltage. In all cases, $(\Delta m/m)$ for m^* is larger than $(\Delta m/m)$ for m , whereas, the relation would be reversed

if the broadening were due only to the kinetic energy spread effective for the m_1^+ peak.

Let us assume that the dissociation of the metastable ions is of a different type than the one that produces the normal m_1^+ ions and that an extra increment of kinetic energy ΔV^* is imparted to the fragment ions. Let ΔV be the energy spread of the normal m_1^+ ions and assume that the energy spread of the metastable ions can be represented by $\Delta V + \Delta V^*$. Then

$$|(\Delta m^*/m^*)| = |(\Delta V + \Delta V^*)/V^*|.$$

We may then derive the relation

$$\begin{aligned} |(\Delta m^*/m^*)/(\Delta m_1/m_1)| \\ = |(m^*/m_1) + (m^*/m_1)(\Delta V^*/\Delta V)|. \end{aligned}$$

This predicts that the ratio $(\Delta m^*/m^*)/(\Delta m_1/m_1)$ should remain constant with increasing accelerating voltage. We see in Table II that rather than remain constant, the ratio changes by a factor of two over the range studied. We thus conclude that the abnormal broadening in the metastable peak is not due to an extra increment of energy ΔV^* imparted to the fragment ions during dissociation. Since we find no basis for an explanation based on incremental kinetic energy change, we conclude that the breadth of the metastable peak results from the details of the focusing action and its dependence on angular scatter, i.e., an instrumental effect.

In an earlier section it is shown that the metastable transitions studied exhibited species of different lifetimes. It is of interest to ascertain, if possible, if shape of the metastable peak depends upon the species making the major contribution to the metastable peak. When low repeller voltages are used so that the residence time in the ion source is long (of the order of $1.5 \mu\text{sec}$), the metastable peak is dominated by transitions of lifetimes of the order of $2 \mu\text{sec}$. If the repeller voltage is high so that the residence time is of the order of several tenths of a microsecond and if the short lifetime species predominate in the ion source (as was seen for the three cases studied), the metastable peak is dominated by transitions of lifetimes of the order of hundredths of microseconds. If the metastable transitions of short lifetime gave ions of a different kinetic energy spread, it would be expected that the shape of the metastable peak obtained with high repellers would be significantly different from the shape obtained with low repellers.

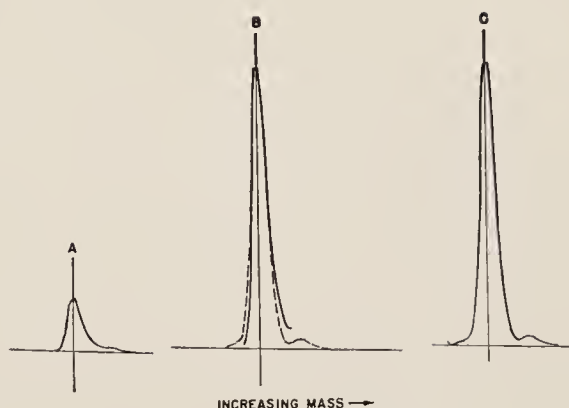


FIG. 10. Comparison of the shape of metastable peaks, $m^* = 31.9$, obtained at different repeller voltages. A is for a peak obtained at low-repeller voltage. C is for a peak obtained with high-repeller voltage. B is the superposition of curve A distended in the vertical direction to the same height as curve C onto curve C.

In order to get information on this, a metastable peak obtained with low-repeller voltage was graphically expanded to the same height as a peak obtained with high-repeller voltage. The results are shown in Fig. 10. Here, A represents the $m^* = 31.9$ peak as observed with a repeller voltage of 3 volts and C is the same peak as observed with a repeller voltage of 120 volts. Curve B is that produced by the one-dimensional expansion of curve A traced on top of curve C. Here, the dashed portion at the bottom refers to lower portion from curve C. On the whole, the curves are identical except for the departure as seen in the base. It is believed that this resulted from error in the expansion of the smaller portions of curve A. This latter step was made by measuring peak to the nearest 0.001 in. at points separated by $\frac{1}{64}$ in. and multiplying by a normalizing factor. Until this experiment can be done with greater accuracy, we must conclude that the factors affecting peak shape, such as kinetic energy and angular spread, are the same for transitions of short and long half lives.

ACKNOWLEDGMENT

Appreciation is due to Dr. J. C. Schug for various discussions on these topics and to Mr. J. P. Klems and Mr. H. T. Best for obtaining data and making calculations.

[Reprinted from the Journal of Physical Chemistry, **67**, 183 (1963).]

Comparison of Mass Spectral Regularities for n -Paraffins and n -Terminal Olefins

By Norman D. Coggeshall

COMPARISON OF MASS SPECTRAL REGULARITIES FOR n -PARAFFINS AND n -TERMINAL OLEFINS¹

BY NORMAN D. COGGESHALL

Gulf Research & Development Company, Pittsburgh, Pennsylvania

Received August 1, 1962

The mass spectra of n -paraffins and n -terminal olefins in the C_{10} to C_{20} range, inclusive, have been studied to establish the quantitative relationships that must be predicted by a satisfactory theory of mass spectra. The n -terminal olefin spectra are generically similar to those for the n -paraffins but systematically have a higher center of gravity (based on $C(M,n)$ plots). The linear behavior of classes upon M (carbon number of parent molecule) previously observed for n -paraffins has been confirmed by this investigation. The same type of class dependence upon M was observed for the olefins. Subclasses defined by $Y(M,n,j)$, each of which represents specific ions, showed, for both classes of compounds, a linear dependence on M expressible as $Y(M,n,j) = f_j(n) \cdot (M - n_j')$. The postulate that the molecules first dissociate into C_nH_{2n+1} ions with subsequent dissociation into ions of different stoichiometry is shown to be untenable for some classes of ions but not for others. The data indicate that the presence of the double bond probably affects the molecule as a whole in all its dissociation modes rather than just those modes involving the double bond. Classes of ions defined by particular stoichiometric relationships and summed over all n are shown to be independent of or linearly dependent upon M . This suggests that the molecules may first dissociate to a particular stoichiometry and then to the final values of n .

The theoretical studies aimed at formulating and quantitatively testing a complete theory of the fragmentation and ionization by electron impact need systematically obtained data obtained under controlled conditions. Steiner,^{2a} *et al.*, and Schug,^{2b} *et al.*, discussed some of the difficulties in the application of the statistical theory prior to its reformulation.³ It is believed that the data taken for events near and just beyond onset of fragmentation should be supplemented by observations at higher electron voltages wherein the structure type or molecular weight of the molecule are systematically varied. The purpose of this is to establish the quantitative relationships between mass spectral parameters and structural parameters. This report constitutes an extension of studies previously reported⁴ on n -paraffin spectra.

Source and Treatment of Data.—In the previous study⁴ the data were largely taken from existing API Research Project 44 spectral files. In this study, the data were taken at this Laboratory on a C.E.C. Model 21-103 instrument. The conditions were as follows: electron current = 10.5 μ a.; ionizing voltage = 70 volts; ion chamber temperature = 250°; vapor temperature = 200°; first scan, m/e 12 through 90, magnet current 230 ma. (2200 gauss); second scan, m/e 60 through 500, magnet current 530 ma. (5067 gauss); and collector slit width = 7 mils.

The compounds examined comprised the n -paraffins and the normal terminal olefins, C_{10} through C_{20} , excepting the C_{19} members of both types which were unavailable. The compounds were obtained from the Phillips Petroleum Company, the Aldrich Chemical Company, and the American Petroleum Institute. Infrared examination indicated the possibility of several per cent of olefin types other than the n -terminal olefins in the higher molecular weight members. However, this test⁵ is not highly accurate, and it cannot be reli-

ably calibrated in this range due to the unavailability of reference compounds. There was no mass spectral evidence for any isoolefins. In consideration of all the data obtained, it is believed that if impurity olefins were present that they were of the *cis* and *trans* n -olefin type.

Relative to the latter point, an examination of the API data for terminal *vs.* internal double bond n -olefins of the C_7 , C_8 , and C_9 classes showed spectral variations for the internal bond types which were not observed in the present studies. To our knowledge the spectra obtained therefore represent the best that can be obtained for the normal terminal olefins in the mass range studied until further, more highly purified materials become available.

As in the previous study⁴ we denote by $P_{M,n,j}$ the normalized ion intensity for an ion of stoichiometry C_nH_{2n+2-j} coming from a compound of M carbon atoms. An ion sum $C(M,n)$ is the summation of normalized intensities of all ions of n carbon atoms. The yield $Y(M,n) = MC(M,n)$ represents the yield of all ions of n carbon numbers being produced from a compound of M carbon atoms per unit of ionizing current and per mole.

A C.E.C. Mascot digitized the data for punching onto IBM cards. The cards were handled by machine calculations and tabulation to yield the data in a variety of forms. The intensities were given as percentages of total ionization, as monoisotopic peak heights, and as monoisotopic percentages of total ionization. Also, the ion summations ($C(M,n) = \sum_j P_{M,n,j}$) by carbon number on a monoisotopic basis were calculated.

General Behavior.—In Fig. 1 may be seen plotted the $C(M,n)$ values for both n -octadecane and octadecene-1. The relative behavior seen here is typical of the entire series of paraffins and olefins. The differences always observed comprised the olefin $C(M,n)$ values being lower through $n = 4$, being higher for the region $n = 5$ to 9, and lower throughout the remainder. Clearly the centers of gravity of the $C(M,n)$ plots are shifted to higher values for the olefins. In Table I are given the n values for the centers of gravity (CG) of all members and the shift for each carbon number. It is interesting to note that the CG is shifting progressively to larger n values for both classes but that the difference between

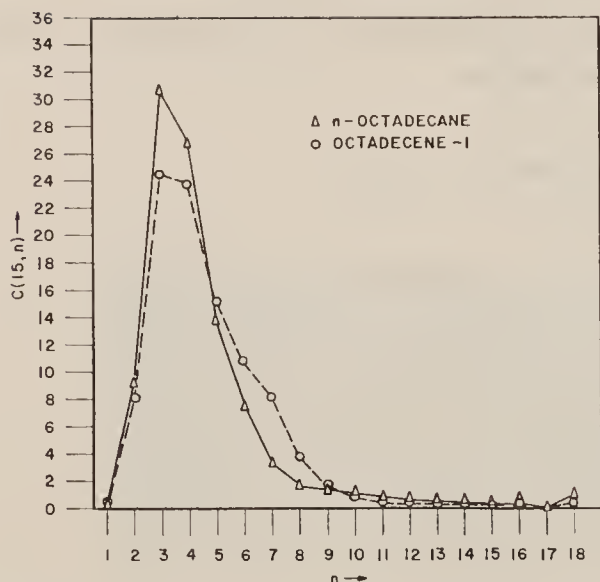
(1) This material was presented at the 1961 meeting of ASTM E-14, Mass Spectrometry, Chicago, Ill., as paper no. 26.

(2) (a) B. Steiner, C. Giese, and M. Inghram, *J. Chem. Phys.*, **34**, 189, (1961); (b) J. C. Schug and N. D. Coggeshall, *ibid.*, **35**, 1146 (1961).

(3) M. Vestal, A. Wahrhaftig, and W. Johnson, paper no. 19 presented at the 1961 meeting of ASTM E-14 on Mass Spectrometry at Chicago, Ill., 1961.

(4) N. D. Coggeshall, *J. Chem. Phys.*, **33**, 1247 (1960).

(5) E. L. Saier, A. Pozefsky, and N. D. Coggeshall, *Anal. Chem.*, **26**, 1258 (1954).

Fig. 1.— $C(M,n)$ values for n -octadecane and for 1-octadecene.

corresponding members reaches a maximum for $n = 16$ and then progressively decreases.

TABLE I
CENTERS OF GRAVITY OF THE $C(M,n)$ PLOTS

Carbon no.	n -Paraffin	n -Terminal olefin	Difference
C_{10}	3.73	3.89	0.16
C_{11}	3.83	4.02	.15
C_{12}	3.94	4.13	.19
C_{13}	4.04	4.26	.22
C_{14}	4.15	4.37	.22
C_{15}	4.24	4.48	.24
C_{16}	4.36	4.57	.31
C_{17}	4.47	4.67	.20
C_{18}	4.55	4.73	.18
C_{20}	4.82	4.96	.12

$Y(M,n)$ values were plotted vs. M and the types of relations observed previously for the n -paraffins⁴ again were obtained and the same generic type behavior also was obtained for the olefins. The data for the latter are seen in Fig. 2. Here it may be seen that the $Y(M,n)$ approximately obey the general type relation

$$Y(M,n) = f(n)(M - n') \quad (1)$$

In Table II are given the $f(n)$ values for both classes from this work as determined from the curve slopes, the $f(n)$ values from the previous work, and the n' values for the olefins. The latter were algebraically determined from the straight lines in Fig. 2. These were not determined for the paraffins as it is believed the larger range of M covered previously provides better n' values. Values of $f(n)$ and n' were not determined for $n > 9$ as the limited spread of M and the low $Y(M,n)$ values do not permit adequate accuracy.

It is interesting to note that for the paraffins the present $f(n)$ values are in fair agreement with those previously determined except for $n = 6$. In this case it is believed the previous value should be preferred due to the greater spread in M . A large difference in $f(n)$ behavior between the paraffins and olefins may be noted with $f(n)$ peaking at $n = 4$ for the latter and decreasing much more slowly with increasing n .

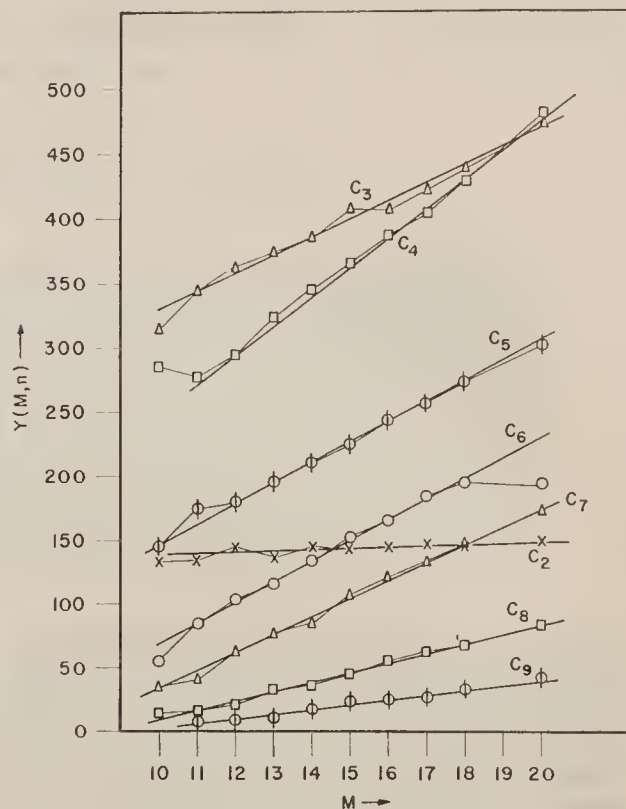
Fig. 2.— $Y(M,n)$ plots for various n 's for the n -terminal olefins.

TABLE II
 $f(n)$ VALUES FOR THE n -PARAFFINS AND n -TERMINAL OLEFINS
AND n' VALUES FOR THE LATTER

n	Paraffins— $f(n)$ values		Olefins	
	(This work)	Previous ⁴	$f(n)$	n'
2	2.0	..	0.55	...
3	21.6	23.2	13.9	-13.7
4	27.1	28.9	22.9	-0.9
5	19.8	20.6	16.2	0.9
6	10.3	14.9	16.0	5.6
7	6.4	6.8	14.0	7.6
8	3.4	3.6	7.3	8.6
9	2.5	2.1	3.7	8.8

The data of this study provided the behavior for the C_1 and C_2 type ions which could not be determined in the previous study. This is because data for these ions have been left out of most of the API spectra. In Table III are given the $Y(M,n)$ values for $n = 1$ and 2. When these are expressed as $C(M,n)$ values, it is clear that the data used to construct Fig. 1 of reference 4 were not very accurate and that curve which was used to interpolate for $C(M,1) + C(M,2)$ dips too steeply with increasing M . It is of interest to note for both types that the increase of $Y(M,n)$ with M is very small for $n = 2$ and that there is actually a negative slope for $n = 1$.

Subclass Behavior.—In the previous section we discussed the behavior of ion classes wherein a class was defined as all ions having a particular number, n , of carbon atoms. In this section will be compared the behavior of the types: C_nH_{2n+1} , C_nH_{2n} , C_nH_{2n-1} , C_nH_{2n-2} , and C_nH_{2n-3} which in each case account for practically all of the ions in a class. The comparative behavior of corresponding types within a class should reflect differences in dissociation behavior between a n -paraffin and a n -terminal olefin. For example, we may

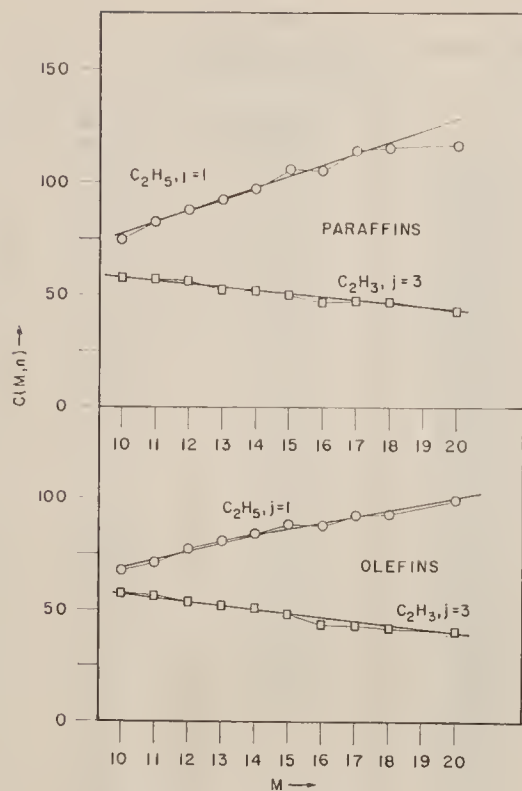
Fig. 3.—Subclass behavior for the principal ions for $n = 2$ for the paraffins and olefins.

TABLE III

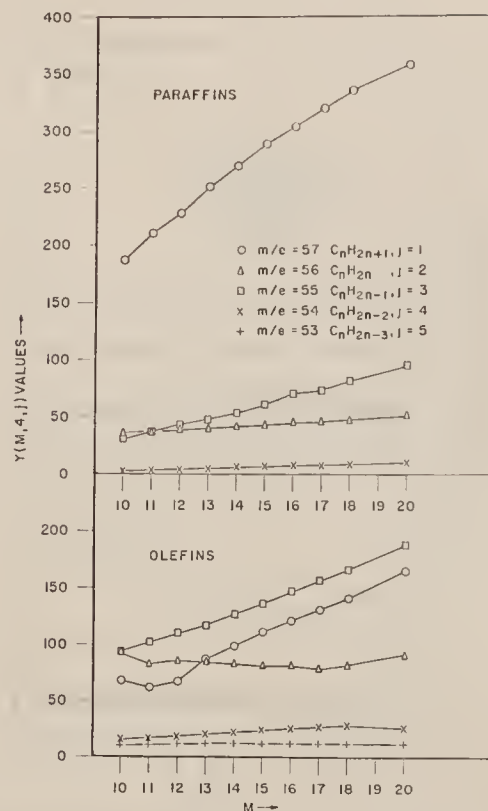
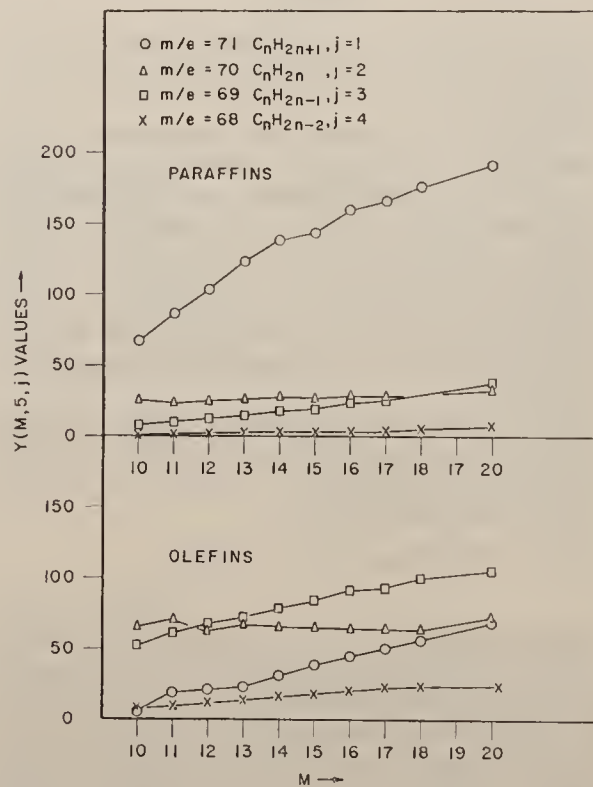
VALUES OF $Y(M,1)$ AND $Y(M,2)$ FOR *n*-PARAFFINS AND *n*-TERMINAL OLEFINS

<i>M</i>	Paraffins		Olefins	
	$Y(M,1)$	$Y(M,2)$	$Y(M,1)$	$Y(M,2)$
10	3.8	136	4.8	132
11	3.6	146	4.2	134
12	3.4	154	4.0	144
13	3.0	159	3.5	138
14	2.7	155	3.4	144
15	2.3	159	2.9	143
16	2.2	156	2.7	144
17	2.6	164	3.2	148
18	2.3	164	2.9	146
20	1.9	165	2.4	150

postulate that the dissociation proceeds as follows: (1) first, a carbon-carbon bond is broken to yield C_nH_{2n+1} ions, and (2) the C_nH_{2n+1} ions then dissociate to yield C_nH_{2n} , C_nH_{2n-1} , etc., ions. If this were true, the yields of the C_nH_{2n+1} ions from olefins would be expected to be only one-half of the yields of the corresponding types from paraffins of equal molecular weight.

In Fig. 3 is given the behavior of the mass 29 and 27 ions (C_nH_{2n+1} and C_nH_{2n-1}) for the paraffins and olefins. It is to be noted that between types they are about equal in both magnitude and slope with increasing M . This would not be the case if the above postulate were true.

In contrast to the quite similar behavior of paraffins and olefins for the principal 2-carbon ions seen in Fig. 3, we may see large but systematic differences in the subclass behavior shown in Fig. 4 and 5. These give the subclass behavior for the 4- and 5-carbon ion types, respectively. One important observation which may be made immediately is that the individual ions are linear but not proportional to M . Thus, a subclass yield specified by $Y(M,n,j) = MP(M,n,j)$ is expressible as

Fig. 4.—Subclass behavior for paraffins and olefins for $n = 4$.Fig. 5.—Subclass behavior for paraffins and olefins for $n = 5$.

$$Y(M,n,j) = f_i(n)(M - n_i')$$

Thus, we have the observation that the intensity of a subclass ion is linearly dependent, but not proportional to M , the total number of carbon atoms in the molecule. This general type of behavior is observed for both paraffins and n -terminal olefins. However, the numerical

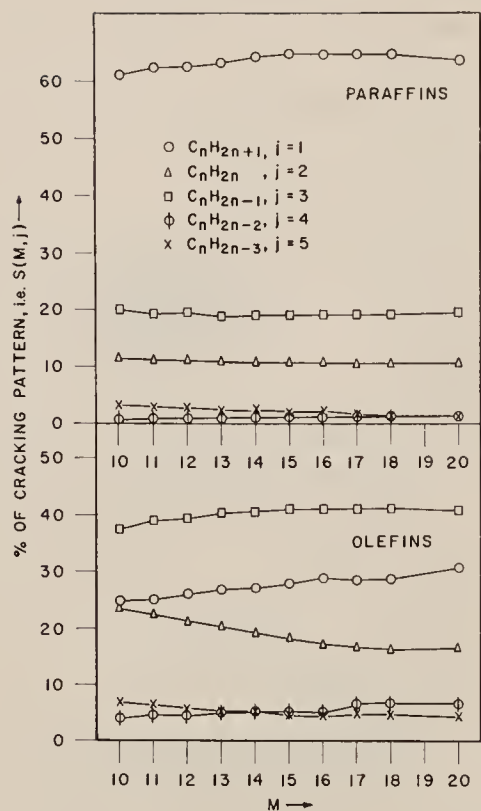
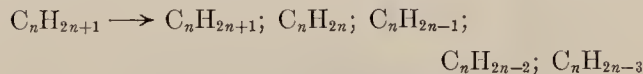


Fig. 6.— $S(M, j)$ behavior as dependent on M for paraffins and olefins.

values, $f(n)$ and n_j' , obviously differ widely for ions of the same type and mass originating from the two classes of compounds.

Slopes, i.e., $f_j(n)$ values, were determined for subclasses up to $n = 7$, inclusive. These are given in Table IV. Due to the scatter of points and the limited mass range, these values should not be regarded as highly accurate, especially for ions of low intensity. Also included in Table IV are the Y values for the two C_{15} compounds, pentadecane and pentadecene-1. Using these and the $f_j(n)$'s, one can readily calculate the Y for any subclass type for any other molecule among those examined.

These data also provide evidence against the simple dissociation model postulated above. By it we would expected the initially formed C_nH_{2n+1} ions to divide into the various subclasses as



A simple ancillary postulate to this model would be that C_nH_{2n+1} ions would always divide into the subclasses with the same relative relationships. Since the yield of the C_nH_{2n+1} ions increases with molecular weight M of the parent molecule, each subclass would also increase with M . Thus all $f_j(n)$ values would be positive. Negative values have been clearly obtained for some classes and they constitute evidence against the above model and the ancillary postulate.

It seems very significant that the wide differences in slope occur within a subclass. In the previous work it was shown that class yields in terms of ions produced per unit of ionizing electron current and per mole of compound in the observation region are dependent in

TABLE IV
SLOPES FOR PRINCIPAL SUBCLASS IONS AND Y VALUES FOR IONS FROM C_{15} MOLECULES

Class n	Subclass	Ion mass	Slopes, f values		Y values, C_{15}	
			Paraffins	Olefins	Penta- decane	Penta- decene-1
2	C_nH_{2n+1}	29	5.1	3.3	106	88.9
	C_nH_{2n-1}	27	-1.4	-1.7	50.3	48.8
3	C_nH_{2n+1}	43	15.5	10.1	289	164
	C_nH_{2n}	42	0.6	-0.5	36.1	34.5
	C_nH_{2n-1}	41	7.6	6.2	139	168
	C_nH_{2n-2}	40	0.0	0.0	3.4	4.6
	C_nH_{2n-3}	39	-1.1	-1.3	21.6	36.2
4	C_nH_{2n+1}	57	17.9	11.4	289	111
	C_nH_{2n}	56	1.4	-1.0	43.4	81.3
	C_nH_{2n-1}	55	6.5	9.5	61.1	136
	C_nH_{2n-2}	54	1.0	1.8	6.4	24.0
	C_nH_{2n-3}	53	0.1	0.0	6.1	12.0
5	C_nH_{2n+1}	71	13.0	6.1	144	38.3
	C_nH_{2n}	70	0.3	-0.3	26.9	65.3
	C_nH_{2n-1}	69	3.0	6.1	19.6	84.8
	C_nH_{2n-2}	68	0.5	2.0	3.3	17.9
	C_nH_{2n-3}	67	0.5	2.0	3.7	16.8
6	C_nH_{2n+1}	85	8.0	3.3	77.0	15.6
	C_nH_{2n}	84	0.33	0.5	13.1	34.1
	C_nH_{2n-1}	83	2.1	8.4	8.3	75.5
	C_nH_{2n-2}	82	..	2.3	2.0	18.3
	C_nH_{2n-3}	81	..	1.2	0.6	5.9
7	C_nH_{2n+1}	99	2.5	1.2	18.4	1.7
	C_nH_{2n}	98	1.3	0.25	13.4	23.8
	C_nH_{2n-1}	97	2.4	9.1	6.9	69.0
	C_nH_{2n-2}	96	..	1.8	1.0	9.2
	C_nH_{2n-3}	95	0.5	3.1

some cases directly upon the size of the neutral fragments produced. However, in all cases observed there, the class yields varied linearly with total mass of the molecule. In Fig. 4 and 5 and in Table IV we see subclass yields which increase linearly with M or which are essentially independent of M as is the case for the C_nH_{2n} ions from both paraffins and olefins. In Fig. 3 we see, for the C_nH_{2n-1} ions from both compound types, an example of a decrease of yield with M . Other examples may be seen in Table IV. Thus, we see instances where increasing the size of the molecule may increase or decrease the probability of creation of particular ions.

The fact that subclasses depend differently upon M , or equivalently upon total mass, suggests that the subclass types each arise through different dissociation mechanisms. This in turn suggests that the summation of a particular subclass type over n should show a regular trend with M . We define such a summation as $S(M, j)$ which is given by

$$S(M, j) = (1/M) \sum_n Y(M, n, j) = \sum_n P_{m, n, j}$$

$S(M, j)$ thus represents the fraction, expressed in per cent, of all ions from a molecule of M carbon atoms that have the stoichiometry C_nH_{2n+2-j} , $n = 1, 2, 3, \dots, M$. In Fig. 6 are plotted the $S(M, j)$'s for the paraffins and olefins. By definition, $\sum_j S(M, j) = 100$. From

the observed behavior in Fig. 6, it is clear that $S(M, j)$ is approximately constant or a linear function of M in all cases. Thus, we may express

$$S(M, j) = a_j M + b_j$$

From above we know that

$$\frac{\partial}{\partial M} \sum_j S(m,j) = 0$$

so that $\Sigma a_i = 0$, which states that the negative slopes balance out the positive slopes. This is quite evident in both sets of curves in Fig. 6.

The data in Fig. 4, 5, and 6 and in Table IV all demonstrate the rather extensive differences in detail between the characteristics of *n*-paraffin and *n*-terminal olefin spectra. Let us assume that the existence of the terminal double bond did not in any way affect the dissociation mechanism involving bonds apart from the double bond itself. With this assumption it would be possible to calculate much of the olefin spectra from the *n*-paraffin spectra as the effect of the double bond would be a mere stoichiometric change for many ions. The observed differences are much more profound than this and they indicate that the presence of the terminal olefin bond affects the whole molecule in its dissociation behavior.

Conclusions

The observations of above may be summarized as follows: (a) the spectra plotted as $C(M,n)$ vs. M of the *n*-terminal olefins are generically similar to those of the *n*-paraffins in demonstrating the universal maxima in the C_3 - C_4 region with general decrease of intensities with increasing carbon number, (b) the $Y(M,n)$ for *n*-terminal olefins also depend linearly upon M , (c) the center of gravity of the $C(M,n)$ plots are always higher for the olefins than for the corresponding paraffins, (d)

the subclass behavior, expressible through $Y(M,n,j)$, for both paraffins and olefins was shown to be represented by

$$Y(M,n,j) = f_i(n)(M - n_i')$$

(e) the differences in subclass behavior between the two types of compounds show the invalidity of the postulate that the molecules first dissociate into C_nH_{2n+1} ions and these in turn dissociate further into C_nH_{2n} , C_nH_{2n-1} , C_nH_{2n-2} , etc., ions, (f) the subclass differences between the olefins and paraffins show that the double bond in the olefins has a general effect on the dissociation pattern that cannot be explained by a mere difference in stoichiometry, and (g) the subclass behavior for both types of compounds indicates that a molecule C_MH_{2M+2} may first dissociate into C_MH_{2M+1} , C_MH_{2M} , C_MH_{2M-2} , or C_MH_{2M-3} ions with further dissociations into ions of different *n* values but of the same stoichiometry; suitable changes in stoichiometry apply to the consideration of olefins.

Although some speculation is offered relative to dissociation mechanisms, the main purpose of this work has been to find and describe mass spectral regularities that have regular dependence on M , n , or j , as used above. Such regularities must be quantitatively explained by the unimolecular theory as it develops and they serve to guide the development and to provide tests of validity.

Acknowledgment.—Grateful acknowledgment is due to Dr. J. C. Schug for worthwhile discussions of this subject.

RELEASE AFTERNOON PAPERS TUESDAY, MAY 14

Paper for Presentation to a Session on Plant and Laboratory Analyzers during the 28th Midyear Meeting of the American Petroleum Institute's Division of Refining, in the Benjamin Franklin Hotel, Philadelphia, Pa., May 14, 1963.

A PROCESS ANALYZER FOR VANADIUM IN GAS OILS ‡

N. D. COGGESHALL,* F. A. NELSON,† O. K. DOOLEN,* AND G. A. BAKER ‡

ABSTRACT

The poisoning of the catalysts used for catalytic cracking by metals in concentrations of a few parts per million in the charge stocks emphasizes the need for continuous analyzers for these metals. An onstream process analyzer for vanadium in gas oils has been built and successfully applied. This analyzer employs electron spin resonance. In this phenomenon, unpaired electrons in molecular systems have the property of responding to certain frequencies in the microwave region in the presence of a magnetic field.

Vanadium in gas oils was shown to exist in the +4 valence state which produces (for vanadium) an elec-

tron spin resonance signal. An electronic system was devised to utilize this signal to produce a continuous output which is proportional to the content of vanadium in the gas oil in the 1-ppm range. The accuracy and reliability of the system are very good and the instrument has been in almost continuous operation in the refineries for over one year. Discussion is given of the phenomenon, the initial feasibility study, the requirements of the instrument, the electronic system, the auxiliary equipment, the trailer mounting of the system, and of the performance of the system.

The catalysts used in catalytic cracking can be poisoned by metals occurring at levels of a few parts per million in the gas oil charge stock. As it is very expensive to replace the poisoned catalyst or to remove the metals, it is necessary that the level of metals which are exceptionally bad catalyst poisons, such as nickel or vanadium, be kept down to 1 ppm or less in the catalytic cracking charge stock. Many metals may poison catalysts but nickel and vanadium are usually of most interest because of their frequent occurrence in crude oils.

It is well known that, for a crude oil having a high metal concentration, the deeper the crude oil is cut, the higher will be the metal concentration in the gas oil. In Fig. 1, for example, the vanadium concentrations in the overhead are given as a function of equilibrium flash temperature for several crude oils. If a particular value of vanadium in the catalytic cracking charge stock is set as a maximum acceptable value, it is obvious that different flash temperatures will be required for different crude oils and that different yields will be obtained.

In a refinery charging crude oils of varying metal content there is, therefore, a continuing problem in the optimum operation of the primary vacuum towers. If operations are conducted with a single equilibrium flash temperature, one of two difficulties will result. If the flash temperature is set low enough that a safe metals content is obtained on the gas oils from all crude oils, there will be a serious loss of potential charging stock from those crude oils of low metals content. If the flash temperature is set high enough for a safe metals content for the gas oil from a crude oil of intermediate metals content, catalyst poisoning will occur when crude oils of high metals content are processed.

Ideally, the vacuum towers would be operated to adjust the flash temperature so that the maximum amount of charge stock of acceptable metals content is obtained for each crude oil or crude blend as it is being processed. For this to be realized in practice requires a very rapid determination of metals content. For adequately accurate results the laboratory techniques which have been found to be satisfactory, such as colorimetry, emission spectroscopy, or x-ray emission, require a preliminary ashing to concentrate the metals. The necessity for taking a sample, ashing, making the analysis, and reporting the results introduces a time lag of several hours. In addition, optimum operation requires the availability of round-the-clock laboratory operations. Clearly, what is needed is an instrument that can con-

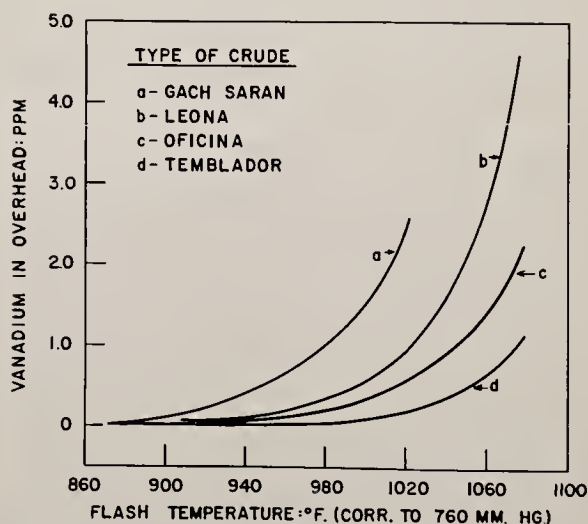


FIG. 1—Vanadium (Parts per Million) in the Overhead (Gas Oil) as a Function of Flash Temperature for Four Different Crude Oils.

* Gulf Research and Development Co., Pittsburgh, Pa.

† Varian Associates, Palo Alto, Calif.

‡ Presented, by N. D. Coggeshall, to a session on plant and laboratory analyzers during the 28th Midyear Meeting of the American Petroleum Institute's Division of Refining, in the Benjamin Franklin Hotel, Philadelphia, Pa., May 14, 1963; presiding, R. D. Bent, The Atlantic Refining Co., Philadelphia, Pa.

tinuously sample the heavy gas oil from a vacuum tower, produce an immediate instrumental analysis of one or several of the metals of interest in the gas oil, and transduce the information obtained for continuous recording.

When work was started on this problem, a number of instrumental approaches were considered. These included emission spectroscopy, x-ray fluorescence, automation of wet-chemical methods, activation analysis, flame photometry, and optical absorption spectroscopy. The requirements for such a device are quite severe. The metal level to be accurately determined is at the 1-ppm level; the time lag between sampling and analysis should at most be only an hour or less; the approach must be one that can be made very free of maintenance and checking as it will be used in round-the-clock service and the investment cost must not be too high. The use of electron spin resonance for vanadium was the only approach that gave the promise of meeting the requirements in a practical way.

Electron Spin Resonance

Electron spin resonance (ESR), often referred to as electron paramagnetic resonance (EPR), is a technique of microwave spectroscopy whereby information is obtained about unpaired electrons as they occur in molecules, ions, radicals, or in the solid state.^{1a, 2}

The properties of an electron are such that it possesses intrinsic spin angular momentum. In connection with this, it possesses a magnetic moment and on a classical picture it has properties analogous to a sub-microscopic bar magnet. By the rules of quantum mechanics the electron magnetic moment will align, in the presence of an applied magnetic field, in only two orientations, i.e., parallel or antiparallel to the applied magnetic field. There will be a slight energy difference between these alignments and an electron may flip from one alignment to the other with the absorption or emission of this energy in the form of electromagnetic radiation. The energy differences associated with these electron spin reversals correspond to wave lengths in the microwave region.

If a material possessing unpaired electrons is subjected to a uniform magnetic field, there will be a particular frequency of radiation capable of adding the exact energy to the electron to change its spin orientation. When the sample is subjected to this radiation, the energy absorption will be selective and analogous to classical resonance absorption in vibrating systems; hence, the term "electron spin resonance."

The energy difference between spin orientation states is directly proportional to the applied magnetic field; hence, the resonant absorption frequency depends upon magnetic field. The resonance absorption of a sample could be observed if the microwave absorption were measured as a function of frequency. A more convenient method, however, is to operate with a fixed microwave frequency and to vary the intensity of the applied magnetic field. The technical problem of measuring the microwave absorption is handled by the measurement

of unbalance of a microwave equivalent of a Wheatstone bridge. The unbalance is measured by a crystal detector. It is common practice to sweep across the resonance line by slowly varying the applied magnetic field. Superimposed upon this field variation is a rapid modulation of the total field by a few gauss. This modulates the signal picked up by the crystal detector which permits a-c amplification which is of a great benefit. The modulation of the signal to the crystal detector is such that the amplified signal represents the derivative of the time microwave absorption curve. Equipment to perform these functions is in a relatively advanced state of development.^{1, 2}

There will only be certain materials that exhibit electron spin resonance. The electrons in the filled shells in atoms will occur in pairs. The spin orientation of one electron in each pair will be exactly opposite to the spin orientation of the other electron of the pair, and there will be no net magnetic moment to interact with applied fields. When atoms with unfilled shells combine to form valence bonds, they will generally do so by the pairing of electrons from the unpaired shells. Materials that may exhibit electron spin resonance due to unpaired electrons will comprise free radicals, certain ions, atoms with an unpaired spin such as can occur in transition element compounds, and metals or semiconductors showing unpaired spins in the conduction electrons.

Fortunately, for our problem, vanadium in the +4 valence state possesses an unpaired electron in the unfilled 3d electron shell. By virtue of this, compounds containing +4 valent vanadium such as the vanadyl porphyrins exhibit a strong ESR absorption. In Fig. 2 may be seen the ESR derivative spectrum for a gas oil containing free radicals and vanadium in the +4 valence state.

Feasibility Study

The results of the feasibility studies needed to establish electron spin resonance as a suitable analytical tool for vanadium in charge stocks have been published.³ In these studies it was necessary to establish a number of points such as the linearity of response between the ESR signal and the concentration of vanadium, the practical limits of sensitivity, and the reproducibility of the method. Details of these studies are given in the previously mentioned paper but suffice it to say that operating conditions were established for linearity, that sensitivity to as low as 0.1 ppm of vanadium is easily achieved, and that the reproducibility is superior to the wet-chemical method.^{4, 5, 6}

The only forms of organometallic compounds containing vanadium which give the electron spin resonance for vanadium are those in which the vanadium occurs in the +4 valence state. It is well known that this is true for vanadyl porphyrins which occur in crude oil. However, it had to be established that either all of the vanadium in the oils of interest was in the +4 valence state or that a constant percentage was in this form. The equipment was calibrated for vanadium in the +4 valence state using synthetic blends of vanadyl etio-

^a Figures refer to REFERENCES on p. 9.

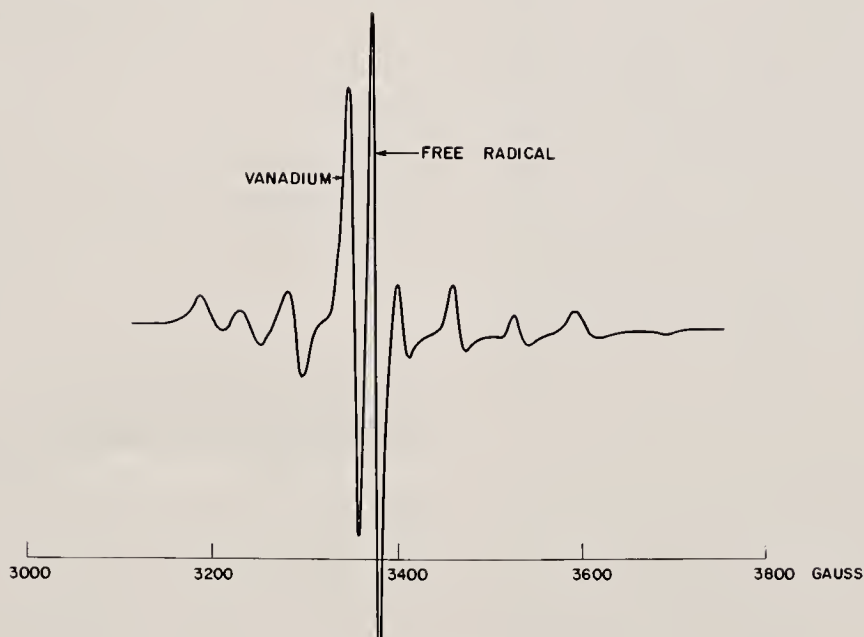


FIG. 2—Electron Spin Resonance Spectrum of a Gas Oil Showing Vanadium and Free-Radical Peaks.

porphyrin (I). A large number of reduced crude oils, gas oils, and residues were examined and the total vanadium (+4) calculated by use of the calibration coefficient as obtained previously herein. The vanadium values were then compared to the total vanadium anal-

yses as determined by wet-chemical methods. This procedure showed that with the possibility of rare exceptions the vanadium is in the +4 valence state in the natural heavy oils and the ESR values can be used with reliability. Some of these results are shown in Fig. 3.

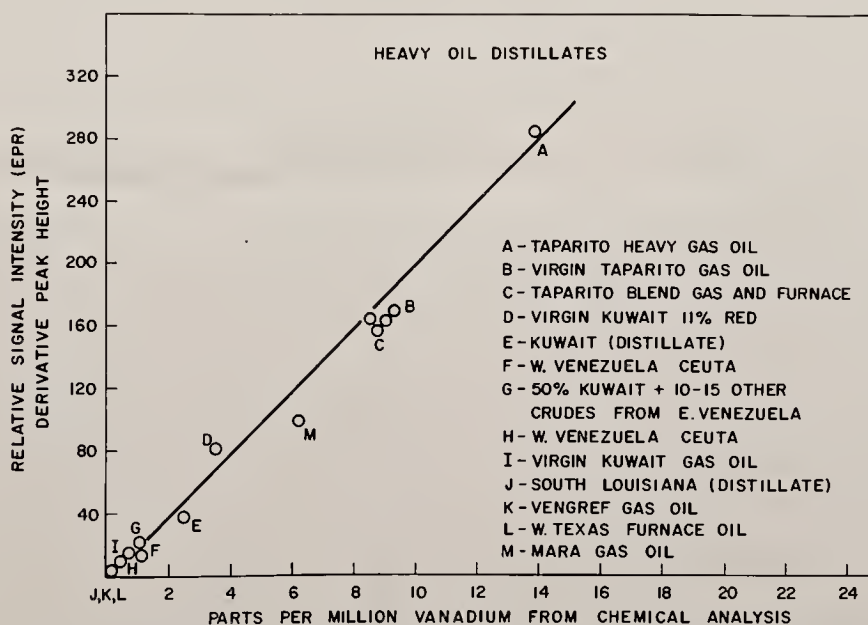


FIG. 3—Comparison of Vanadium Results by Electron Spin Resonance Versus Chemically Determined Values for a Series of Heavy Oils.

Differences in viscosity alter the ESR line shape and width. This causes deviations in calibration for total vanadium content. A heavy gas oil at room temperature has a semisolid gelatinous consistency. There is essentially no change in resonance sensitivity at lower temperatures and stiffer consistencies. However, at approximately 80 F, at which temperature the viscosity becomes significantly lower, the sensitivity begins to drop and a considerable loss of sensitivity occurs at temperatures around 100 F. Dilution with light materials which produce like reductions in viscosity produces corresponding reductions in sensitivity. Because of this viscosity effect the sample is forced through the measuring cell in the onstream instrument at reduced temperatures.

Requirements of the Total Instrument

The requirements which it was felt desirable to meet for a satisfactory onstream vanadium analyzer designed for our problem were as follows:

1. It should be continuous or, if batchwise, it should not have a time lag of more than an hour.
2. It should be capable of unattended round-the-clock operation.
3. It should measure vanadium in the 1-ppm level to an accuracy of at least ± 0.2 ppm.
4. It should be explosionproofed or explosion-protected for use in the refinery.
5. It must be capable of handling the hot oil direct from the vacuum tower, cooling it, measuring the vanadium, and returning the oil to the line.
6. The total cost should not be incompatible with the economies it would afford.

In the material to follow, it will be shown explicitly or implicitly how these requirements were met. One exception to this is that no discussion is given of item 6. With the economies the instrument affords, this requirement was met manyfold. Information relevant to this point is given in the paper by Donaldson, Murphy, McBride, and Story.⁷

Mode of Vanadium Measurement

The quantity of vanadium is determined by a measurement of the difference in the signal output at the positive peak of the strongest line and at the negative peak of an adjacent weaker line of the vanadium derivative absorption curve. The concentration is determined by a comparison of this value with the amplitude of the signal from a reference sample.

Fig. 4(A) shows the lines to be measured. The magnetic field is adjusted to have a fixed value H_A and is periodically biased up to the value H_B . The magnetic field values H_A and H_B are such as to give resonance conditions illustrated for the klystron frequency used which is approximately 9,500 Mc. Fig. 4(B) shows the derivative absorption curve for the reference sample, which is locally biased to also produce resonance at H_B . This biasing is achieved through the use of iron shims. Normally, the resonance for the reference sample would occur at a slightly higher value of the applied magnetic

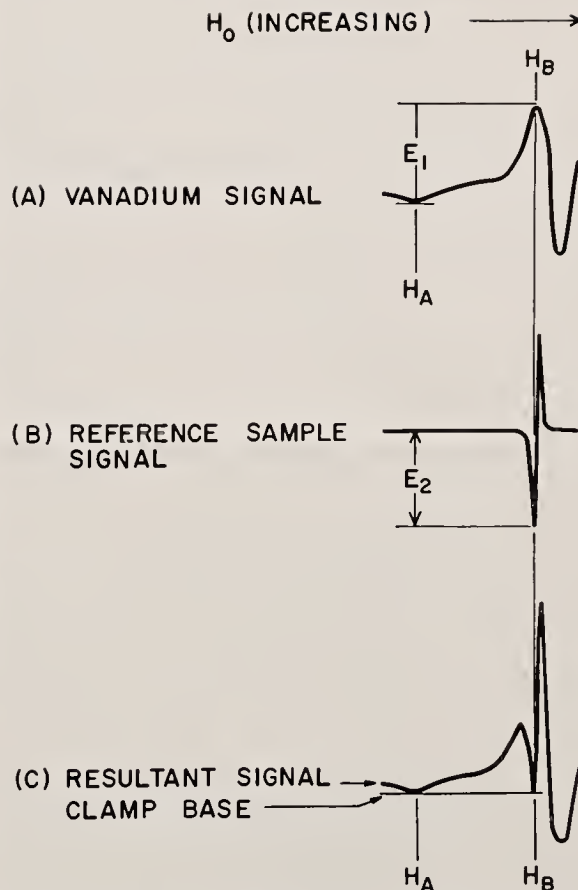


FIG. 4—Mode of Balancing the Vanadium Signal Against the Signal Obtained from a Standard Reference Sample.

field, H_0 . The phase of the signal from the reference sample has been reversed 180 deg relative to the vanadium signal by adjusting the phase of the field modulation at the reference sample.

Signals from the vanadium and reference sample are obtained simultaneously and the difference obtained as shown in Fig. 4(C). When the reference signal amplitude is equal to the vanadium signal amplitude at H_B , the two signals cancel as a result of the phase difference. If the two signals are not the same amplitude, then a signal voltage will be obtained at H_B . This voltage will be positive or negative with respect to the voltage obtained at point H_A as the reference signal is increased or decreased from the null condition. Because the two signals are of equal amplitude when a null signal is obtained, the reference signal amplitude becomes a measure of the vanadium signal.

The major variables in the system which affect the signal amplitude are klystron power, klystron frequency drift, cavity Q, amplifier gain, and sweep modulation amplitude. As both samples are affected by these variations in a similar manner, the effects on calibration are minimized.

Circuit Description and Operation

A block diagram of the electronic components is shown in Fig. 5. A klystron oscillator delivers microwave power to the resonant cavity which is located in the gap of the magnet. The klystron frequency is locked to this cavity frequency by means of an automatic frequency control circuit. The oil sample is pumped through the center of the cavity and the reference sample is fixed in a helix attached to the cavity. The helix is electrically coupled to the cavity so that signals from both samples are transmitted to the same microwave crystal detector.

The magnetic field at the two samples is modulated independently at the same frequency by separate sets of sweep coils. A 100-kcps sine wave generator furnishes output directly to the oil sample sweep coils. This output also is fed through a phase shifter to a motor-driven potentiometer which controls the amplitude of the reference sample field modulation. The phase shifter is adjusted so that the two field sweeps are 180 deg apart in phase. The output from the potentiometer is amplified by the gain-stabilized, reference sweep amplifier before it finally is fed to the sweep coils at the reference sample.

The ESR signals from the microwave detector are modulated at the 100-kcps rate of the field modulation. These a-c signals are amplified and then fed into a phase detector which produces a d-c output proportional to the amplitude of the 100-kcps input signal. When the magnitude of the field modulation is small

compared with the width of the ESR absorption line, the signal from a sample is proportional to the magnitude of the modulation. This phenomenon is used as a means of controlling the reference signal size. The reference ESR signal is therefore controlled by the motor-driven potentiometer, whereas the signal from the oil sample with its constant sweep depends only upon vanadium concentration.

The programmer controls the cycle bias so that the field of the magnet is periodically stepped between H_A and H_B , Fig. 4(A). If the ESR signal is nulled, the output from the phase detector is unchanged as the field is shifted from H_A to H_B and no signal goes into the servo amplifier. If there is a signal difference, the phase detector will produce a square wave output which is coherent with the magnet shifts. The d-c component of this square wave, after amplification by the signal servo amplifier, runs the motor that turns the potentiometer and thereby adjusts the size of the reference signal so as to again null the system. The sign of the error is determined by a clamping function of the programmer. This operates as follows: The output from the phase detector is coupled through a capacitor to the signal servo amplifier. While the field is at H_A , the output of the capacitor is shorted to ground by relay K_2 . This allows the capacitor to charge to the voltage present at this point. When the field is biased up to H_B , the clamp or ground is removed and the signal voltage is coupled to the input of the signal servo amplifier. The input to the servo amplifier is therefore the

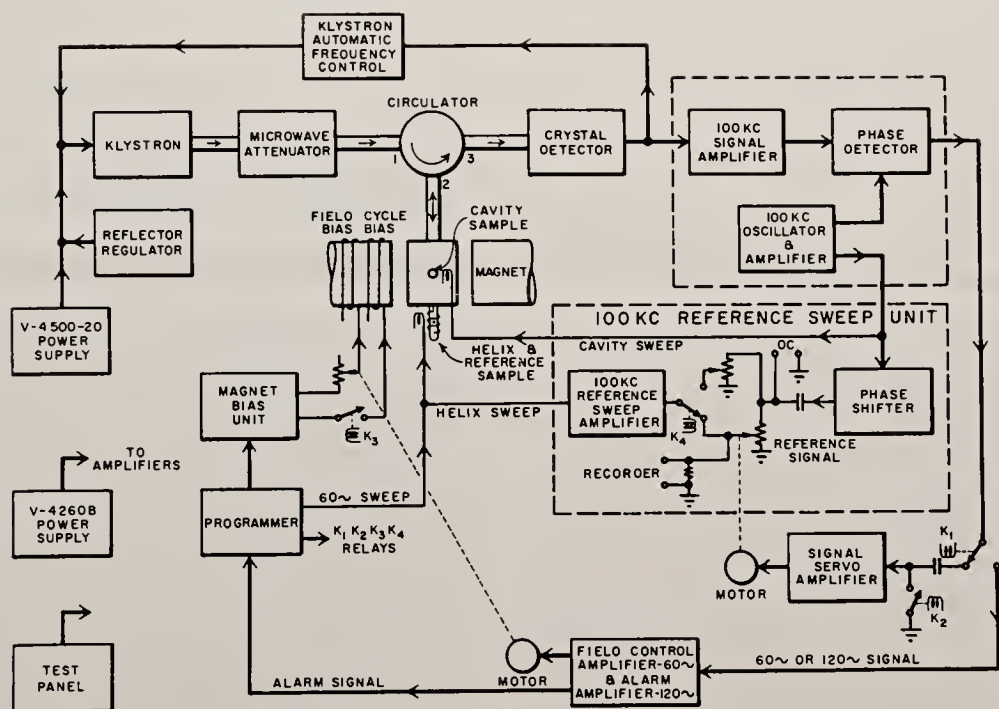


FIG. 5—Schematic Diagram of the Various Electronic and Electromechanical Components and of Their Interconnections.

signal at H_B relative to that at H_A and the system is balanced when E_1 of Fig. 4(A) equals E_2 of Fig. 4(B).

During the excursion from H_A to H_B , there is a transient signal resulting from the fact that the reference sample does not have the same line width as the major resonance line of the vanadium and, therefore, there is not a complete cancellation of the signals during the switching of the field. A null signal condition is only established at H_B , the peak of the derivative absorption curve. This transient signal is eliminated by the programmer which de-energizes relay K_1 to open the signal lead momentarily during the switching of the field.

Periodically, the programmer switches on the field control circuits to correct any drift in the magnetic field. The magnet is biased up to H_B by applying a steady value of cycle bias through relay K_3 , and the output from the phase detector is switched to the field control amplifier by relay K_1 . Relay K_2 grounds the input to the servo amplifier. The 100-kcps field modulation to the reference sample is increased by relay K_1 and a 60-cps sweep is superimposed. Fig. 6 shows the resulting signals for three different values of H_0 with a 60-cps sweep applied. When the applied field is adjusted for resonance at the peak of the derivative absorption curve, the 60-cps modulation produces a signal which is predominately second harmonic or 120-cycle. Any deviation from the correct value of H_0 gives a 60-cps signal whose phase depends upon the direction of the error. This 60-cps signal is amplified to drive the field control servomotor which corrects the magnet field bias. The magnitude of the cycle bias is constant and is not changed by the field control cycle. For the range of field variations encountered, the required cycle

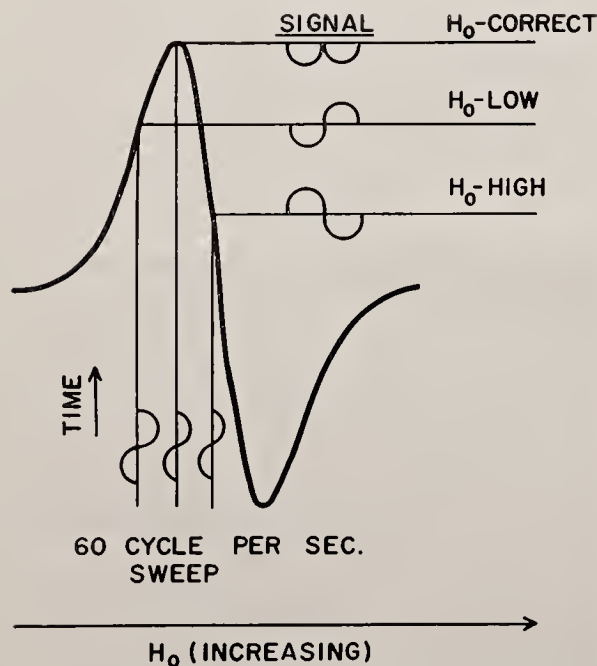


FIG. 6—Sensing Method Used to Establish Correction for Magnetic Field Bias.

bias may be considered independent of the absolute value of H_0 . The field bias is corrected with the cycle bias applied to establish the field at H_B . When the cycle bias is removed, the field is at H_A and the two required field values have been established.

The 120-cps signal, which occurs at resonance during the field control period, controls the alarm circuit. At the beginning of the field control cycle an alarm time delay relay is energized and is held off by the 120-cps signal which results when the field is correctly set at the peak of the absorption curve. If a loss of the ESR signal occurs the alarm relay will be locked down during the field control cycle and the alarm light will come on. External contacts on the alarm relay are connected to a terminal strip to allow connection to an external alarm circuit.

Other Significant Components

Reference Sample

The reference sample is a minute quantity of the free-radical diphenylpicrylhydrazyl (DPPH) which has a very strong free-radical line. By virtue of its line strength, the reference sample can be closely coupled to the cavity and the small sample size minimizes the problem of magnetic field homogeneity for the reference sample. Also, the sample does not saturate at the radio frequency power level used, and the strong line makes possible a signal which is linear with sweep modulation over a range greater than 100 to 1. This is important because the amplitude of the reference signal is controlled by the applied 100-kcps sweep modulation amplitude. The reference sample resonance occurs at a field approximately 25 gauss above the strongest vanadium line. To obtain resonance from both lines simultaneously the reference sample must be locally biased to increase the field. This is accomplished by two small iron rings located on either side of the reference coil plus a small direct current through the reference sample sweep coils.

The Permanent Magnet

An electromagnet is normally a part of an ESR spectrometer system. The field of this magnet is often swept from near zero to the maximum strength available but the situation is different with the vanadium analyzer because, in this instrument, the field is never changed more than 100 gauss from the nominal value of 3,400 gauss. For this reason a permanent magnet seemed practical and it had the advantage of requiring a smaller power supply and, consequently, had much less heat to dissipate.

The major uncertainty about a permanent magnet was whether it would withstand the continuous stepping of 50 gauss without gradually losing its field strength. A test run which included temperature changes and 200,000 cycles of such field switching showed that, if the magnet had previously been stabilized, the field strength would not sag. Of course, the field of a normal permanent magnet is quite sensitive to temperature

and, therefore, the magnet in this instrument had to be adjustable over the range of an additional 40 gauss.

This vanadium analyzer magnet has 4-in.-diameter pole caps with an air gap of 1 in. The field uniformity requirement makes it necessary to use specially compensated pole caps which are adjusted during manufacture to give a homogeneous field at both the oil and reference samples. The resulting 3,400-gauss field has a maximum inhomogeneity of 0.1 gauss over the 0.4-ml flowing sample volume being measured.

There are two small sets of windings on the permanent magnet. One set carries the current which steps the field back and forth between the vanadium lines; the other windings carry the field regulating current and are also used for the initial energizing and stabilizing of the magnet. The regulation is required for two reasons: First, the magnetic field must be corrected for shifts caused by magnet temperature or external field changes; and, second, this field must be changed to keep the field-to-frequency ratio constant whenever the microwave frequency changes. The information obtained by the periodic measurement of the ESR resonance of the reference sample is used to keep the permanent magnet within one part in 10^4 of the correct field.

The control cabinet and the permanent magnet in its housing may be seen in Fig. 7. This photograph was taken before this and other auxiliary equipment were installed in the trailer in which the entire unit is mounted.

The Sample Pumping System

Earlier it was stated that the viscosity of the oil affects the vanadium line signal intensity. For simplicity, it is easier to work with the gas oil at a semi-solid or grease-like consistency at a cool temperature than to have to correlate signal strength with viscosity as would be necessary for the higher temperatures that would keep the gas oil in a liquid state. At the cooler temperatures (approximately 75 F and below) there is essentially no dependence of signal strength on temperature. The equipment was, therefore, designed to pass the gas oil through the resonant ESR cavity in a semisolid condition and at a cool temperature. This is accomplished by cooling the hot oil coming from the sampling slipstream at the same time as it is being moved under pressure toward the cavity.

In Fig. 8 may be seen a cutaway drawing that demonstrates the pump action. The displacement mechanism is a helical screw that forces the oil forward. Intimate contact is afforded between the oil and the pump case. The latter is submerged in a low-temperature, refrigerated bath. This arrangement achieves several things. It reduces the temperature of the oil as it is being forced forward. As the oil cools inwardly from the case, this provides an effective seal against bypassing contrary to the motion imparted by the screw threads. The pump moves approximately 12 ml of gas oil per minute through the resonant cavity.

Trailer Mounting

In considering a housing for a complex instrument, such as the vanadium analyzer, a number of factors must be considered such as safety precautions, access to components for maintenance, and the control of ambient conditions. When these factors, plus a consideration of constructing a small permanent building for the device and the desirability of making the device available to different processes, were examined it was decided to install the analyzer in a trailer constructed with particular specifications.

The trailer is of the ordinary house trailer variety with the particular specifications built into it. A large window-type air conditioner of three-ton refrigeration capacity is built into one end. The vents are arranged so that during normal operation no outside air is brought in. This condition may be altered when desired. The doors are gasketed and there is only one window which, itself, is equipped with louvers which can be made quite tight. Connections for refinery instrument air are provided so that a positive pressure of instrument air can be maintained in the trailer during operation. An electric heater and fan arrangement maintain the interior temperature at a preset value during cold weather. Both the air conditioner and electric heater are controlled by thermostatic sensors inside the trailer.

The necessary transformers to step down the voltage from the usual 440 v in the refinery lines to the 220 v and 115 v needed by the air conditioning, heater, instrument, refrigeration equipment, etc. are an integral part of the trailer. A device for monitoring explosive gases is maintained in the interior of the trailer and

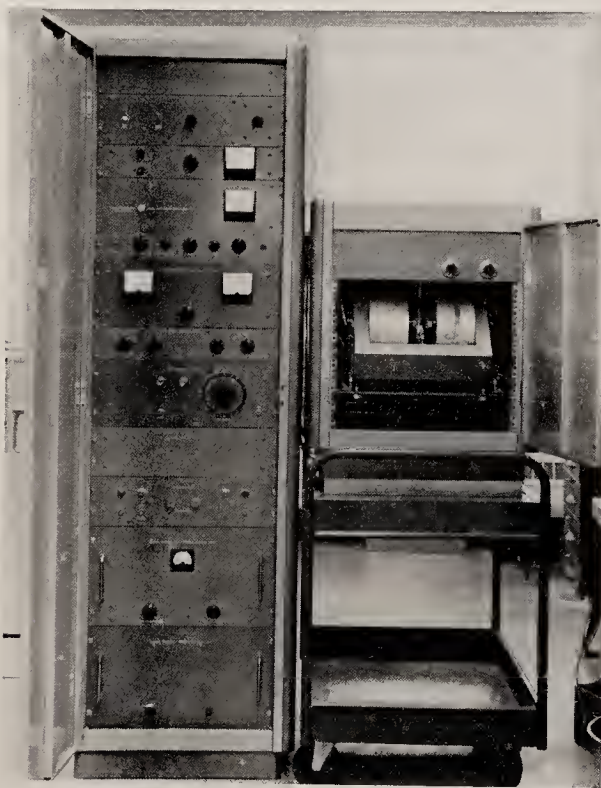


FIG. 7—Photograph of Magnet Assembly Case and Electronic Control Panel Prior to Trailer Installation.

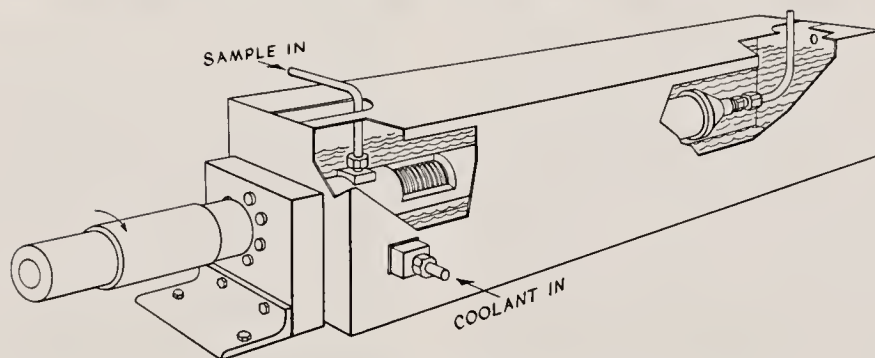


FIG. 8—Perspective, Cutaway Figure of Oil Pump and Associated Heat Exchange Equipment.

is connected to a circuit breaker that will deactivate all electrical equipment if necessary. An extra temperature sensor with circuit breaker provisions is also in the trailer. This will deactivate the equipment if the temperature starts to rise as a result of air-conditioner failure or other causes.

All instrumentation is grounded to a rod that is driven into the ground adjacent to the trailer. A telephone and necessary connections are provided so that communications may be joined with the refinery telephone system. In order to reduce the radio frequency noise and its effects on the instrument components, the interior lighting system is of the incandescent instead of the fluorescent type. The sample line bringing the hot oil to the instrument is steam-traced up to the

trailer. The line that allows the oil to be pumped back into the process line is similarly steam-traced.

Operation

The equipment has proven itself to be quite stable, dependable, and very free of troubles. To illustrate this point, the first seven months of refinery use (extending up to the time of this writing) may be reviewed. After preliminary testing and development at the Gulf Research Center in Pittsburgh was completed, the trailer was hauled to the Gulf refinery at Toledo, Ohio. It was put into operation and utilized there for nine weeks. It was then hauled to Philadelphia for use in the Gulf refinery there. At this site it was used for eight weeks

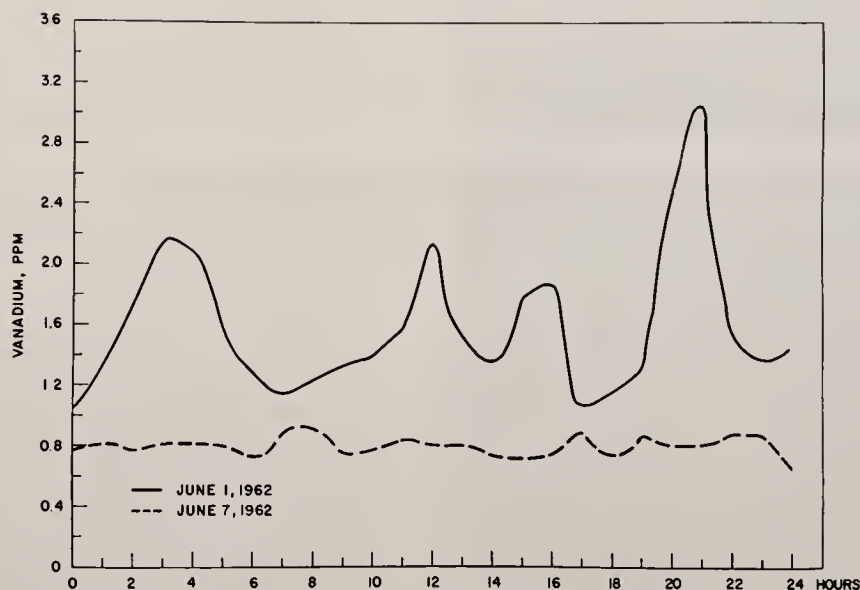


FIG. 9—Continuous Vanadium Analyses Obtained for Different Types of Operating Conditions over Separate 24-Hr Periods.

after which it was hauled back to Toledo and used for seven weeks. It was then again hauled to Philadelphia where it has been in use for four weeks up to the end of the first seven months.

During the time the instrument was considered to be "onstream," the downtime has been estimated to have been less than 2 percent. The response calibration has not been changed by the various over-the-road trips. As an extra guarantee that no change in calibration occurs from such a move, one or more grab samples are taken and analyzed chemically for each new installation. This type of checking could also be achieved by putting a reference sample of gas oil through the analyzer.

In Fig. 9 may be seen some typical data as obtained with the equipment. In this figure are shown continuous vanadium analyses over two separate 24-hr periods. For convenience, both have been plotted against the same time scale. The solid curve gives the vanadium analysis for a 24-hr period during which experimental changes were being made in the operation of the vacuum tower. The dashed curve gives the vanadium analysis over a 24-hr period of "lined-out" stable operations which had been adjusted to yield heavy gas oil of approximately 0.8 ppm of vanadium content. In the solid curve it is of interest to note the rather wide ranges of vanadium content (from 1.1 to 3.1 ppm) that may be encountered in a very few hours if vacuum tower operating conditions are changed. It also shows that the vanadium content may change by as much as 1 ppm in an hour, despite the huge operational inertia of a refinery unit.

Availability of the Instrument

The equipment was developed through the joint efforts of the Gulf Research Center and Varian Associates. Patent rights, held by Gulf Research and Development Company, have been licensed to Varian Associates; and the latter have an active program to make the equipment available to interested parties on a lease arrangement.

ACKNOWLEDGMENT

Grateful acknowledgment for valuable aid is due many individuals in both companies, with especial acknowledgment to Mr. R. D. Wyckoff, of Gulf Research and Development Company, and Dr. Emery Rogers, of Varian Associates.

REFERENCES

- ¹D. J. E. Ingram, *Free Radicals as Studied by Electron Spin Resonance*, Butterworth and Co., London (1958).
- ²D. J. E. Ingram, *Spectroscopy at Radio and Microwave Frequencies*, Butterworth and Co., London (1955).
- ³A. J. Saraceno, D. T. Fanale, and N. D. Coggeshall, "An Electron Paramagnetic Resonance Investigation of V in Petroleum Oils," *Anal. Chem.* **33** 506-5 (1961).
- ⁴J. T. Horeczy, B. N. Hill, A. E. Walters, H. G. Schmitze, and W. H. Bonner, "Determination of Trace Metals in Oils," *Anal. Chem.* **27** 1899-1903 (1955).
- ⁵E. B. Sandell, *Colorimetric Determination of Traces of Metals*, 3rd edn., 928, Interscience Publishers, Inc., New York (1959).
- ⁶John E. Shott, Jr., Thomas J. Garland, and Ralph O. Clark, "Determination of Traces of Ni and V in Petroleum Distillates. An X-Ray Emission Spectrographic Method Based on a New Rapid-Ashing Procedure," *Anal. Chem.* **33** 506-10 (1961).
- ⁷R. E. Donaldson, J. R. Murphy, W. R. McBride, and D. O. Story, "Process Control Using the Continuous Vanadium Analyzer," paper to be presented at session on plant and laboratory analyzers during 28th Midyear Meeting of API Division of Refining, Philadelphia, Pa., May 14 (1963).

Feb. 18, 1964

N. D. COGGESHALL ETAL

3,121,677

PROCESS FOR CONTROLLING CARBON RESIDUE CONTENT OF OIL

Filed Oct. 28, 1960

3 Sheets-Sheet 1

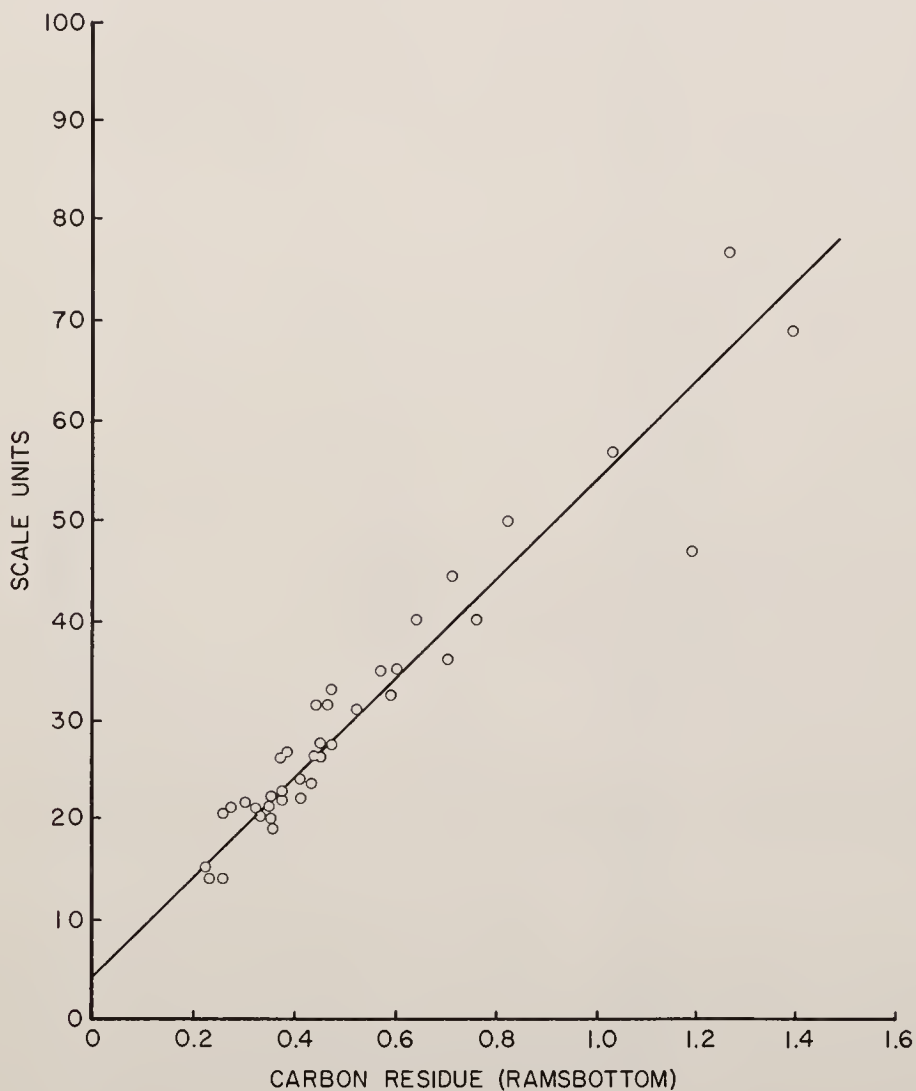


FIG. 1

INVENTORS
NORMAN D. COGGESHALL
MATTHEW S. NORRIS
BY

Shaul Horne
ATTORNEY

Feb. 18, 1964

N. D. COGGESHALL ETAL

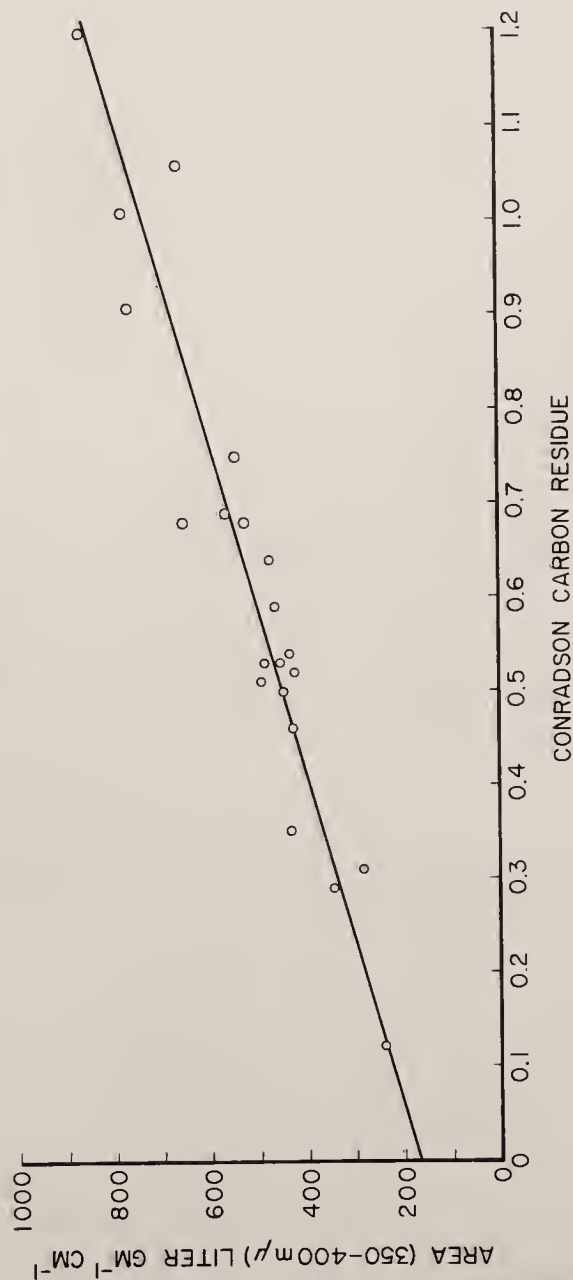
3,121,677

PROCESS FOR CONTROLLING CARBON RESIDUE CONTENT OF OIL

Filed Oct. 28, 1960

3 Sheets-Sheet 2

FIG. 2



INVENTORS
NORMAN D. COGGESHALL
MATTHEW S. NORRIS
BY

Matthew S. Norris

ATTORNEY

Feb. 18, 1964

N. D. COGGESHALL ETAL

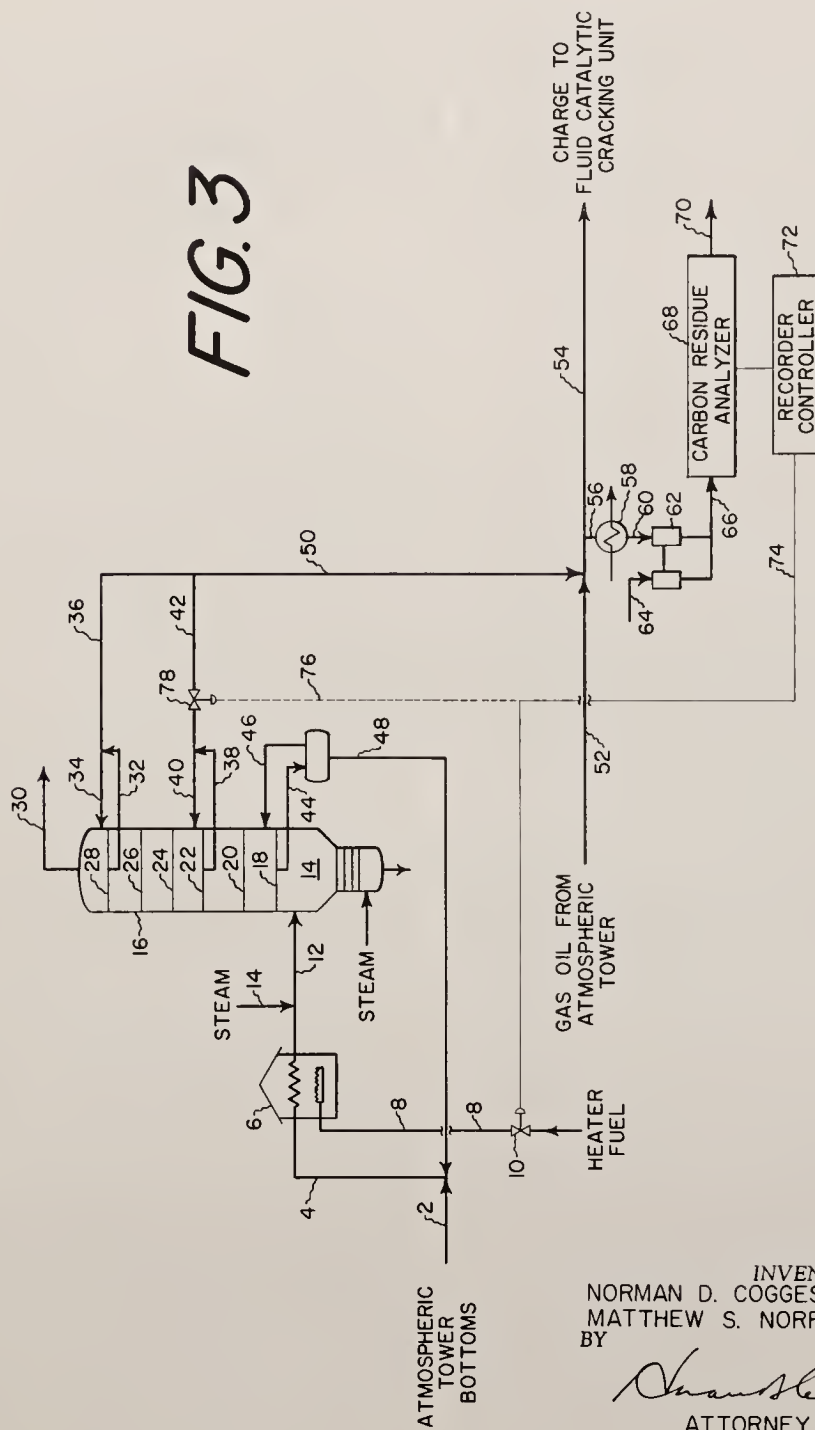
3,121,677

PROCESS FOR CONTROLLING CARBON RESIDUE CONTENT OF OIL

Filed Oct. 28, 1960

3 Sheets-Sheet 3

FIG. 3



INVENTORS
NORMAN D. COGGESHALL
MATTHEW S. NORRIS
BY

Norman Coggeshall
ATTORNEY

1

3,121,677

PROCESS FOR CONTROLLING CARBON RESIDUE
CONTENT OF OIL

Norman D. Coggeshall, Verona, and Matthew S. Norris,
Gibsonia, Pa., assignors to Gulf Research & Develop-
ment Company, Pittsburgh, Pa., a corporation of Del-
aware

Filed Oct. 28, 1960, Ser. No. 65,778

12 Claims. (Cl. 203—178)

This invention relates to a rapid method for quantitatively determining the presence in hydrocarbon oils of materials that are indicative of the carbon residue content of such oils, and particularly to the use of such method as a basis for the control of petroleum refining operations.

The carbon residue content of hydrocarbon oils is used frequently in petroleum refining or process operations as an index of the quality of such oils. The term "carbon residue" is defined as the carbonaceous residue formed after evaporation and pyrolysis of a petroleum product under controlled conditions. The residue is not entirely composed of carbon but is a coke that can be further changed by pyrolysis. Carbon residue values are normally reported in terms of percent by weight on the oil sample subjected to the test.

As an example of the use of the carbon residue content of an oil as an index of the quality of an oil, the carbon residue of the side stream of a vacuum distillation unit in which is prepared the heavy gas oil portion of the feed to a catalytic cracking unit can be used as an index of the amount of coke that will be formed by the feed on the cracking catalyst. The carbon residue of the combined feed to a catalytic cracking unit also can be used in the same way. Similarly, the carbon residue of various other hydrocarbon oil processing streams, for example, the products of primary or finishing distillation operations carried out on lubricating oil stocks, or the product streams obtained from the solvent treating of lubricating oil stocks can be used as an index of the efficiency of the particular processing operation in question. In each case, in the event of deviation from a preselected optimum carbon residue value, one or more appropriate processing variables can be modified in such a way as to change the carbon residue content of the product stream to the desired level, or alternatively, to compensate for the particular carbon residue content found.

Heretofore it has been necessary from a practical standpoint to determine carbon residues by one or both of two laboratory methods, the so-called Conradson method (ASTM D-189) and the Ramsbottom method (ASTM D-524). Each of these methods involves essentially evaporating and partially coking under control conditions the oil to be analyzed, weighing the residue, and determining the proportion of the original sample represented by the residue. Each method normally requires at least about two hours to carry out. As such, neither method is adapted for close monitoring and process control. By the time oil samples are taken, analyses run, and results returned to the operator, many barrels of product having too high or too low a carbon residue may have been produced by the unit. As a consequence, it frequently has been the practice to carry

2

out petroleum refining operations that are dependent on carbon residue determinations, not at the optimum level, but rather at carbon residue levels that are well within the maximum permissible or optimum limits. This practice is not entirely satisfactory for the reason that the carbon residue content is maintained at a safe level only with a proportionate sacrifice of a portion of the potential yield of upgraded products that would be obtainable if the particular process in question were operated at or above the maximum permissible carbon residue level.

The present invention relates to controlling a hydrocarbon oil refining process in response to changes in the carbon residue content of an oil stream in such process. It has now been found that certain components of a hydrocarbon oil that are indicative of the carbon residue content of the oil can be rapidly determined quantitatively by spectrometric methods, whereby oil streams in refining operations can be closely monitored for changes in carbon residue and whereby improved yields of upgraded products can be obtained from such operations without undue sacrifice in the quality of such product. In accordance with the present invention a plurality of oil samples taken at different times from the hydrocarbon oil stream to be analyzed are subjected to spectrometric analysis by passing light therethrough of a wavelength that is selectively absorbable by the components of the oil that are indicative of carbon residue content, in a proportion related to the quantity of such components in the oil samples. Excellent results have been obtained by the use of light radiation having a plurality of wavelengths that are at least representative of a wavelength band of about 350 to 400 millimicrons, but the invention is not limited to the use of light of this broad wavelength band, as good results have also been obtained with light radiation having a wavelength of only about 400 millimicrons. The radiation that is not absorbed by the oil samples, that is, the transmitted light, is electrically detected and converted to output signals whose intensity is related to the amount of radiation absorbed by the oil samples, and consequently, under Beer's law, to the concentration in the oil samples of the components that are indicative of carbon residue content. In connection with the use of light of wavelengths representative of the wavelength band of about 350 to 400 millimicrons, the integrated absorptivity in the indicated wavelength band, that is, the area under the absorptivity curve over the wavelength band indicated, has been found to correlate with carbon residue in excellent fashion. However, the present invention is not limited to the use of the integrated absorptivity as an index of carbon residue content, as other functions of the absorption signal intensity that are related to the concentration in the oil of components that are indicative of carbon residue can be used. For example, good correlation with carbon residue can also be obtained from the integrated absorbance in the 350 to 400 millimicron wavelength band, or directly from the absorptivity, the absorbance, or indeed, the absorption signal intensity itself, with light of a single wavelength of about 400 millicrons. For purposes of hydrocarbon oil refining process control, one or more variable conditions of a selected operation of the process, for example, the conditions under which the oil stream is prepared, e.g., distillation conditions, or alternatively, the conditions of

a process operation to which the oil stream undergoing analysis is to be conducted, e.g., a catalytic cracking operation, are adjusted in response to changes in the intensity of the absorption signal or a function thereof that is also related to the concentration in the oil samples of the components that are indicative of carbon residue, so as to correct the carbon residue content of the stream to a preselected level, or alternatively, to compensate for the change in carbon residue. Although the invention is especially adapted for controlling hydrocarbon oil processing operations, it involves not only the method for controlling such processes, but also various combinations of such method, including the particular analytical method disclosed herein for determining carbon residue.

The exact nature of the components of the oil that are responsible for the carbon residue of the oil is not definitely known. Nor is it definitely known whether the components that are responsible for the characteristic absorption of light upon which the analytical method of the present invention is based are the same as or different from the components that actually are responsible for carbon residue. However, it is clear from experiments carried out upon a large number of hydrocarbon oil samples having a wide range of carbon residues that the components that exhibit a characteristic absorption for light of the wavelengths disclosed herein are at least present in an amount that varies with the amount of the components that are responsible for the carbon residue of the oil, and more than likely, the components are substantially the same.

It is to be emphasized that the chemical compounds in the oil that are responsible for the characteristic light absorption utilized in the analytical method of the present invention comprise a complex mixture of materials of chemical structure that is not precisely known, the individual components of which apparently differ but slightly from member to member over a relatively broad range of compounds. This fact is important as it renders the measurement of the amount of such compounds by spectrophotometry completely different from the spectrophotometric methods heretofore used for quantitative measurement of other materials, for example, single compounds or other mixtures. Thus, whereas pure compounds and many mixtures are usually found to exhibit one or more characteristic absorption peaks that are typical of such compound or compounds, the complex mixtures of compounds with which the present invention is concerned exhibit no such characteristic peaks. Rather, because of the presence in the mixture of a relatively large number of compounds that differ but slightly from member to member and that therefore absorb adjacent wavelength of light, the absorption curve for the compounds in question and for the compounds adjacent thereto is ordinarily a more or less smooth curve, frequently approaching a straight line. Thus, the eye is normally unable to distinguish any significant difference between the portion of the absorption curve that is responsible for the characteristic absorption utilized in the analytical method of the present invention and the portion of the absorption curve that bears no relation to the carbon residue of the oil. The present invention is based on the discovery of the fact that specific portions of the light absorption curve for a hydrocarbon oil that are not characterized by any distinguishing shape, furnish a quantitative index of components in the oil that are indicative of the carbon residue content of the oil.

Referring now briefly to the drawings, in FIGURE 1 there is shown a calibration curve plotting absorption signal intensity for light having a wavelength of about 398 millimicrons against Ramsbottom carbon residue content for a variety of petroleum gas oils. FIGURE 2 is a calibration curve plotting Conradson carbon residue content against the integrated absorptivity per liter per gram

centimeter for light of a plurality of wavelengths representative of the 350 to 400 millimicron band for a number of petroleum gas oils. FIGURE 3 is a simplified flow diagram of a vacuum distillation tower of the kind used in the preparation of a gas oil charge stock for a fluid catalytic cracking unit, wherein certain conditions of the distillation are controlled in response to changes in light absorption, that is, changes in carbon residue, of an oil stream subjected to analysis in accordance with this invention.

In accordance with the analytical method disclosed herein, there is first obtained a sample of a hydrocarbon oil having unknown carbon residue characteristics. Sampling may be carried out in any convenient way. Thus, in the case of a process stream, the oil may be sampled intermittently and the thus-obtained samples placed in the test cell of a spectrophotometer and the desired measurement obtained on a batch-wise basis. Alternatively, the hydrocarbon oil stream can be sampled continuously and a continuous stream of the oil can be circulated through the test cell. In either case, when the oil is quite dark it is desirable to dilute the oil prior to analysis with a solvent that will not itself absorb a significant proportion of the radiation of the wavelength employed in the analysis, that is, that will not interfere with the selective absorption by the components in the oil that are indicative of carbon residue, so that a measurable amount of radiation will be transmitted to form a detectable electrical output signal. Clear naphtha has been used successfully, but other solvents that do not interfere with the selective absorption of radiation by the oil being tested can be used. Specific examples of other solvents include mononuclear aromatic solvents such as benzene and toluene and paraffinic solvents such as kerosene. The proportion in which the solvent is employed will depend upon the absorptivity of the oil and the length of the radiation path through the test cell of the spectrophotometer. Good results have been obtained, for example, with dilutions of 9 to 24 parts naphtha solvent per part of a heavy gas oil that prior to dilution is opaque to radiation of the wavelength employed in the analysis, using test cell path lengths varying from 0.5 millimeter to 2 centimeters in length, but other dilutions and other test cell path lengths can be used. In the event that continuous sampling, as well as dilution, are desired, these objectives can be achieved by the use of conventional proportioning pump means designed to pump and blend two fluids in a predetermined ratio. Examples of suitable proportioning pumps are shown in United States Patent No. 2,873,889 to Mori, but other functionally equivalent pumps can be used.

The temperature at which the oil is subjected to spectrometry is not critical in principle, except of course that the temperature should be sufficiently low that portions of the oil will not be volatilized, although not so low that the oil will solidify. However, the limitations of commercially available spectrophotometric apparatus are presently such that best results are obtained when the oil is at a temperature not greater than about 200° F. Excellent results have been obtained with diluted oil samples at ambient atmospheric temperature, but of course, good results also can be obtained at other temperatures. It will be understood that the oil streams in many processing operations for which the carbon residue is to be determined will be at temperatures greater than 200° F. and accordingly, samples obtained from these streams for analysis in accordance with the present invention must be cooled before subjecting them to analysis in accordance with the herein-disclosed method. However, this requirement poses no real problem, and cooling of the stream to the desired test temperature can be effected rapidly and continuously, when desired, by conventional heat exchange devices, condensers, or the like.

The radiation to which the oil is subjected should be

of a wavelength that is selectively absorbed by the components that are indicative of carbon residue, that is to say, of a wavelength that will be absorbed by the aforesaid components without at the same time being appreciably absorbed by other components of the oil that are not indicative of carbon residue. As indicated, excellent results have been obtained by the use of light having a plurality of wavelengths representative of the band of about 350 to 400 millimicrons. Light of somewhat higher and lower wavelength can be used, but the accuracy of the correlation between carbon residue and light absorption decreases rather rapidly outside the wavelength band indicated. Preferably, the wavelength of the light is not appreciably less than 350 millimicrons as inclusion of light of such shorter wavelengths appears unduly to distort the carbon residue values obtained by the present method. Inasmuch as the light absorption for the materials in question varies less greatly with changes in wavelength near the 400 millimicron limit of the wavelength band, a somewhat greater departure from the above-indicated upper limit, for example, up to 405 millimicrons and possibly even as high as 425 millimicrons, can be tolerated. When using light in the 350 to 400 millimicron wavelength band, for the purpose disclosed, excellent results can be obtained by scanning the test oil with light having a plurality of wavelengths that are representative of the wavelength band indicated, plotting absorption signal intensity for each such wavelength, or a function thereof, such as absorbance or absorptivity that is also related to the concentration in the oil of the components that are indicative of carbon residue, as a function of the wavelength, and integrating the thus-obtained curve to determine the area thereunder. Absorptivity is defined as absorbance per unit concentration of the material subjected to analysis in grams per liter, per unit test cell path length in centimeters. Absorbance is defined as the logarithm to the base 10 of the reciprocal of the transmittance. The area under the absorptivity curve in the 350 to 400 millimicron wavelength band has been found to be related quantitatively to the carbon residue of the oil undergoing analysis. With some oils slight peaks of varying intensity sometimes have been observed in the absorption curve in the 350 to 400 millimicron wavelength band that are not attributable to components indicative of carbon residue. However, by correlating carbon residue with a function of the absorption signal intensity over the entire 350 to 400 millimicron wavelength band, inaccuracies resulting from absorption of radiation by substances that are not indicative of carbon residue are minimized.

Although good accuracy has been obtained from the correlation of carbon residue and integrated absorptivity, that is, a function of the absorption signal intensity reflecting absorption over the entire wavelength band of 350 to 400 millimicrons, this particular correlation is not absolutely essential to the invention, and good results also can be obtained by correlation between carbon residue and the integrated absorbance over the wavelength band indicated, or the absorption signal intensity at a single wavelength of light, or other functions of such signal intensity that are related to the concentration in the oil of components that are indicative of carbon residue content, for example, absorptivity. Especially good results are obtainable from the absorption signal intensity at a single wavelength of about 400 millimicrons, but some deviation from this wavelength can be tolerated. For direct correlation of carbon residue at a single absorption signal intensity, we prefer to use light having a wavelength of about 393 to 405 millimicrons, with light having a wavelength of about 398 to 400 millimicrons being especially useful.

For purposes of hydrocarbon oil refining process control, it is not absolutely necessary that the carbon residue content for the particular oil undergoing analysis actually

be determined. Once the desired efficiency in the processing operation in question has been obtained, whatever the carbon residue of the stream undergoing analysis at that time may be, it is sufficient thereafter merely to effect control of the desired processing operation according to whether the absorption signal intensity or the selected function thereof increases or decreases. As indicated the amount of the process adjustment will preferably be governed either by the integrated absorptivity using light having a wavelength band of 350 to 400 millimicrons, or directly with the absorption signal intensity using light having a wavelength of about 400 millimicrons.

Although it is not necessary for purposes of process control to determine the actual numerical carbon residue value of the oil undergoing analysis, it is sometimes desirable to do so as a partial indication of the quality of such oil. In these instances the actual numerical carbon residue content of the oil can easily be obtained by the use of a preestablished correlation between carbon residue content and absorption signal intensity or a function thereof that is also related to the concentration in the oil of components that are indicative of carbon residue. This correlation can conveniently take the form of a calibration curve, table or equivalents thereof.

In determining the absorption of light by the oil samples for purposes of this invention, conventional spectrophotometric apparatus can be used. Thus, when light having a single wavelength is to be used, either conventional filter-type or dispersion-type spectrophotometers can be used. When absorption of light having a plurality of wavelengths over a wavelength band is to be determined, the dispersion-type spectrophotometer is usually most convenient, but the filter-type spectrophotometer can be used provided that a filter capable of transmitting light of the desired wavelength band is available. In the latter instance a single absorption signal intensity or a function thereof representing the combined absorption signal intensities over the entire wavelength band will be obtained rather than a curve of absorption signal intensities or functions thereof over the wavelength band.

The analytical process of the present invention is useful as such merely to determine carbon residue, but it finds especial utility as a means of process control in hydrocarbon oil refining operations. For example, the analytical process described herein can be used to control the cut-point in the vacuum distillation of topped crude oil to obtain a heavy gas oil component of the charge to a catalytic cracking unit. As the boiling point of the highest boiling side stream from the vacuum distillation tower increases, so also does the carbon residue content of that stream and the carbon residue content of the total catalytic cracking unit feed of which it forms a part. As the carbon residue of the feed to the catalytic cracking unit increases, so also does the amount of coke deposited upon the catalyst, usually on a percent for percent basis, the coke on catalyst in this comparison being measured as percent coke based on the weight of the fuel. An increase in the amount of coke that is deposited upon the cracking catalyst that cannot be compensated for by reserve regeneration capacity, as is the usual case, is accompanied by a reduction in cracking catalyst activity. In accordance with the present invention, as the carbon residue content of the heavy gas oil and/or catalytic cracking unit feed stock increase to an undesirable level, the absorption signal intensity of such feed stock will also increase and such increase can be caused by means of conventional recorder-controller equipment to effect a change in a processing available to correct or compensate for the change in carbon residue content of the oil. For example, in one embodiment the fuel flow to the heater for the vacuum tower feed can be reduced so as to reduce the cut-point, i.e., reduce the boiling point of the highest boiling side stream of the vacuum distillation tower. Alternatively, the severity of the cracking conditions can

be reduced, or, when some reserve regeneration capacity is available, an increase in the absorption signal intensity can be used to increase the regeneration air, regeneration time, and/or regeneration temperature during the regeneration of the cracking catalyst, so as to burn off the additional amount of coke deposited on the catalyst by the feed. Conversely, as the carbon residue of the hydrocarbon oil stream undergoing analysis decreases, the cut-point of the highest boiling vacuum tower side stream can be raised, or alternatively, the severity of the cracking conditions can be increased, or the severity of the regenerating conditions can be reduced, so as to maintain the optimum conversion depth. The analytical method of the present invention can also be used in a similar manner to control other hydrocarbon oil processing operations. For example, it can be used to control the cut-point in the vacuum distillation of lubricating oil stocks, or to control the exhaustiveness of solvent treatment in the solvent refining of lubricating oil stocks.

The operability of the analytical method of the present invention has been demonstrated by calculating the carbon residue values of a number of gas oils in accordance with the present method and comparing the values obtained with carbon residue values obtained by conventional laboratory methods. In carrying out some of these experiments, an Analytical Systems Inc. filter-type spectrophotometer was employed utilizing a Baird-Atomic Interference Filter with a band pass at 393 millimicrons and cut-off transmission at 393 and 405 millimicrons. A 4-97 Corning glass color filter was used in conjunction with the Baird filter to block out transmission of the Baird filter about 690 millimicrons. In these experiments the output signal from the spectrophotometer was set to vary between 0 and 5 millivolts for 100 to 0 percent transmission.

In accordance with the experimental procedure followed, one milliliter of each gas oil to be analyzed was diluted to 25 milliliters with a heavy Kuwait naphtha so that some light of the wavelength selected would be transmitted through the otherwise opaque gas oil samples. Each diluted gas oil sample was then placed in the absorption cell of the spectrophotometer. The test cell in this instance had a path length of 0.5 millimeter, and the absorption signal intensity scale reading was observed on the recording scale of a Speedomax (Leeds & Northrop, Inc.) 0-5 millivolt recorder.

The absorption signal density at a wavelength of 398 millimicrons in the scale units of the recording instrument was obtained for 39 different gas oils having Ramsbottom carbon residues from 0.22 to 1.39 percent. A calibration curve was established by plotting the absorption signal intensity in recorder scale units as a function of Ramsbottom carbon residues for the oils undergoing analysis. The Ramsbottom carbon residues employed in the preparation of the calibration curve were averages of three or more laboratory determinations. A straight line was drawn through the thus-plotted points, using the so-called "least squares" method. A plot of the calibration curve obtained in this manner is shown in FIGURE 1.

To determine the accuracy of the method described herein, the absorption signal intensity in recorder scale units for each of the 39 gas oils tested was applied to the calibration curve obtained as described above to obtain a "calculated" carbon residue value. The difference between the thus-obtained calculated carbon residue value and the average Ramsbottom carbon residue value for the same oil was then determined and the percent deviation from the laboratory value was calculated. The recorder scale units, which are an index of percent light absorption, obtained for each gas oil sample in the above-described analysis, the corresponding Ramsbottom carbon residue values, the calculated carbon residue values, the difference between calculated and Ramsbottom carbon residues, and the percent deviation between the calculated

values and the laboratory values are shown in the following table:

Table A

Sample No.	Scale units	Ramsbtm. carbon residue	Calc. carbon residue	Δ carbon residue	Percent deviation
001	27.5	0.47	0.46	-0.01	2.1
002	35.0	0.60	0.62	+0.02	3.3
003	26.5	0.45	0.44	-0.01	2.2
004	22.0	0.41	0.36	-0.05	12.2
005	27.5	0.45	0.47	+0.02	4.4
006	20.0	0.35	0.32	-0.03	8.6
007	36.0	0.65	0.64	-0.01	1.5
008	21.0	0.32	0.34	+0.02	6.3
009	26.0	0.37	0.44	+0.07	18.9
010	21.0	0.35	0.34	-0.01	2.9
011	22.0	0.37	0.36	-0.01	2.7
012	33.0	0.47	0.58	+0.11	23.4
013	26.5	0.38	0.45	+0.07	18.4
014	26.5	0.44	0.45	+0.01	2.3
015	21.0	0.27	0.34	+0.07	25.9
016	15.0	0.22	0.22	0.00	0.0
017	20.5	0.26	0.32	+0.06	23.1
018	14.0	0.23	0.19	-0.04	17.4
019	21.5	0.30	0.31	+0.01	3.3
020	14.0	0.25	0.20	-0.05	20.0
021	40.0	0.64	0.71	+0.07	10.9
022	23.5	0.43	0.38	-0.05	11.6
023	32.5	0.59	0.56	-0.03	5.1
024	19.0	0.35	0.30	-0.05	14.3
025	35.0	0.57	0.61	+0.04	7.0
026	20.5	0.33	0.32	-0.01	3.0
027	31.0	0.52	0.53	+0.01	1.9
028	22.5	0.37	0.36	-0.01	2.7
029	31.5	0.44	0.54	+0.10	22.7
030	22.0	0.36	0.35	-0.01	2.8
031	31.5	0.46	0.54	+0.08	17.4
032	24.0	0.41	0.39	-0.02	4.9
033	57.0	1.03	1.06	+0.03	2.9
034	50.0	0.82	0.91	+0.09	11.0
035	69.0	1.39	1.30	-0.09	6.5
036	40.0	0.76	0.71	-0.05	6.6
037	47.0	1.19	0.85	-0.34	28.6
038	44.5	0.71	0.80	+0.09	12.7
039	77.0	1.26	1.45	+0.19	15.1

From the foregoing table it will be seen that the standard, or average, deviation of the calculated carbon residue values from the laboratory carbon residue value is about 13 percent. This compares favorably with the standard deviation between successive determinations by laboratory methods on the same oil.

To demonstrate the correlation between carbon residue content and integrated absorptivity over the 350 to 400 millimicron wavelength band, integrated absorptivity values in the wavelength band indicated were obtained for 20 different gas oil samples having Conradson carbon residues of 0.21 to 1.23 percent. A calibration curve was obtained from these data by plotting the integrated absorptivity as a function of Conradson carbon residues, and by drawing a straight line through the thus-plotted points, again using the least squares method. The carbon residue contents of the different gas oils were then calculated from the integrated absorptivities for these oils using the thus-prepared calibration curve. The calculated carbon residues were then compared with the laboratory carbon residues as described above. The calibration curve for this series of experiments is demonstrated in FIGURE 2. The term "absorptivity area" employed in FIGURE 2 corresponds to the integrated absorptivity and refers to the area under the curve obtained by plotting absorptivity against wavelength.

In the series of experiments referred to in the preceding paragraph, a Cary Model 11 dispersion-type spectrophotometer, manufactured by the Applied Physics Corporation was employed, using a one-centimeter path-length quartz sample tube. Unlike the Analytical Systems Inc. spectrophotometer described hereinabove, which produces light of the desired wavelength by the use of a filter capable of transmitting only light of the desired wavelength, the dispersion-type spectrophotometer produces light of the desired wavelength by dispersing individual wavelengths of light from a source of mixed wavelengths by means of a suitable prism. The prism is rotated to focus light of the desired wavelength upon a mirror which reflects the desired wavelength of

light through suitable monochromating means to eliminate radiation of undesired wavelength and thence through the test samples to a photomultiplier for detecting the transmitted light and converting it to an electrical output signal. Since the wavelength of the light passed through the test sample can be easily varied by rotating the dispersing prism in appropriate fashion, the dispersion-type spectrophotometer is well-suited both for determining absorption by the test sample of light of a number of wavelengths that are representative of a broad wavelength band, as well as of light having a single wavelength.

The Conradson carbon residue values, calculated carbon residue values, and the percent deviation of the calculated carbon residue values from the Conradson carbon residue values are shown in the following Table B:

Table B

Sample	Description	Conradson Carbon Residue (C.R.)	350-400 Millimicrons	
			Calc. C.R.	Δ percent
1.....	Mid-Continent Gas Oil.....	0.53	0.52	-2
2.....	West Texas Gas Oil.....	0.68	0.87	+28
3.....	Heavy Overhead Distillate.....	0.50	0.49	-2
4.....	Blend of Three Kuwait Gas Oils.....	0.75	0.67	-11
5.....	G.O. fr. Normal Vac. Reduction of Gasoline-Free Reduced Mara-W. Venez. Crude.....	0.52	0.46	-12
6.....	West. Venez. Virgin Gas Oil.....	1.06	0.88	-17
7.....	Composite Typical Chg. Stock to Fluid Unit Still.....	0.46	0.46	0
8.....	Virgin Kuwait Gas Oil.....	0.59	0.53	-10
9.....	Fluid Unit Chg. Stock.....	0.64	0.55	-14
10.....	Virgin Mid-Cont. Gas Oil.....	0.51	0.21	-32
11.....	Virgin Kuwait Gas Oil.....	0.54	0.48	-11
12.....	Virgin West Texas Gas Oil.....	0.29	0.32	+10
13.....	S. Louisiana Overhead (721-953° F.).....	0.53	0.54	+2
14.....	S. Louisiana Overhead (721-1,000° F.).....	0.68	0.63	-7
15.....	Centa (Eocene) Ovhd. (720-950° F.).....	1.01	1.08	+7
16.....	Centa (Eocene) Ovhd. (730-972° F.).....	0.91	1.07	+18
17.....	Centa (Eocene) Ovhd. (725-1,000° F.).....	1.20	1.23	+3
18.....	Ovhd. from Ragusa Crude.....	0.35	0.47	+34
19.....	do.....	0.51	0.58	+14
20.....	do.....	0.69	0.71	+3

From the foregoing table it will be seen that the standard or average percent deviation of the carbon residue values obtained by the herein-disclosed spectrophotometric analytical method from the laboratory carbon residues was about 16 percent. Again, this deviation compares favorably with the percent deviation between repeated laboratory determinations on the same gas oil. A still smaller percent deviation can be obtained by correlating the absorptivity area as obtained above with Ramsbottom carbon residues instead of Conradson carbon residues, as the dispersion of the results obtained by the former laboratory method is relatively smaller.

In a working embodiment, with particular reference to FIGURE 3, 346.5 barrels per hour of the distillation bottoms from an atmospheric distillation tower, not shown, are passed through line 2 and blended with 13.8 barrels per hour of recycle oil from line 43, obtained from the bottom tray 18 of the fractionation zone of vacuum distillation tower 16, and the mixture of atmospheric tower bottoms and vacuum recycle oil is charged through line 4 to a vaporizing heater 6 whose burner is supplied with fuel from line 8. The heated feed is then passed into line 12 where it is mixed with steam from line 14 to assist in vaporizing the heavier components of the oil, and the over-all feed is then passed to the flash zone 14 of the vacuum tower 16 at a temperature of 757° F. In the flash zone 14, which is maintained at an absolute pressure of about 74 millimeters Hg, the vaporizable components of the feed stock are flashed off from the unvaporized bottoms and are passed upwardly

into the fractionation zone. As the vapors pass upwardly, they are washed with liquid retained in fractionation trays 18, 20, 22, 24, 26, and 28, the heavier portion of the oil vapors being condensed in the liquid in the trays contacted thereby. Two oil side streams, in the respective amounts of 107.1 barrels per hour and 97.5 barrels per hour are withdrawn by way of lines 38 and 42 and 32 and 36, respectively, and passed into line 50 and thence into line 54 where the combined side streams are blended with 341.3 barrels per hour of a light gas oil stream obtained from line 52 and from the atmospheric distillation tower, not shown. Reflux streams from the respective side streams 38 and 32 are returned to the vacuum tower 16 by way of lines 40 and 34 at rates of 489 and 280 barrels per hour, respectively. A side stream of oil is also removed from fractionation tray 18 by way of line 44. A portion of this oil is returned to the space above tray 18 by way of line 46, and the remainder is passed through line 48 as recycle oil.

During the operation of the unit as described above, a sample stream is withdrawn from line 54 through line 56 and cooled to 100° F. in cooler 58. The cooled oil is then passed by way of line 60 through one side of a gear-type proportioning pump 62 and thence into line 66 where each volume of cooled oil is blended with 24 parts by volume of naphtha drawn from line 64 by the other side of the proportioning pump 62. The cooled and diluted gas oil sample is then continuously passed through the sample tube of the carbon residue analyzer of spectrophotometer 68. In this instance the carbon residue analyzer is a spectrophotometer of the non-dispersion-type employing an interference filter with a band pass at 398 millimicrons and cut-off transmission at 393 and 405 millimicrons, employed in conjunction with a Corning 4-97 glass color filter to block out transmission of the first described filter above 690 millimicrons. In this embodiment the output signal from the analyzer is set for 0 to 5 millivolts corresponding to 100 to 0 percent transmission. The light transmitted through the sample tube of the analyzer 68 is electrically converted to an electrical signal whose magnitude is proportional to the amount of light absorbed by the diluted gas oil in the sample tube. After passing through the analyzer the cooled diluted gas oil sample can be passed to waste oil storage through line 70, or alternatively, since it is relatively small in amount, the diluted gas oil can be returned to line 54 through a conduit not shown.

The signal from analyzer 68 is passed to a recorder-controller 72 of conventional construction where the magnitude of the signal is recorded quantitatively on the recording scale. In the present embodiment the unit is set to operate with a total catalytic cracking feed Ramsbottom carbon residue of about 0.50, which corresponds to a yield of about 1.07 coke on cracking catalyst based on the weight of the oil at a conversion depth of 50 percent, a reactor temperature of 925° and at a carbon-on-regenerated catalyst level of 0.2 weight percent. In the embodiment described, this operation corresponds to a scale reading on the recorder of approximately 30 scale units. Under these conditions, the quantity of fuel passed through line 8 into vacuum tower heater 6 is controlled at the desired rate by means of pneumatic diaphragm motor valve 16 which in turn is controlled by the supply of instrument air from line 74, which in turn is governed by the recorder-controller 72, which is of the recording potentiometer-pneumatic controller type.

As the carbon residue of the total catalytic cracking unit feed through line 54 varies upwardly or downwardly a proportionate and compensatory adjustment in the amount of heater fuel passed through valve 10 is brought about.

Under an alternative method of operation, instrument air from recorder-controller 72 and line 74 is directed through dashed line 76 from which it is caused to con-

trol pneumatic diaphragm motor valve 78. As valve 78 is urged to a more closed position, the amount of recycled oil through line 40 to the upper surface of tray 22 is increased. As the amount of liquid returned to tray 22 increases, so also the amount of liquid flowing downwardly to the trays lower in the column increases, as a consequence of which the amount of recycled oil through line 48 is increased. As a result of this operation the proportion in the total catalytic cracking charge stock represented by the highest boiling side stream of the vacuum tower 16 is reduced, whereby the carbon residue of the total catalytic cracking charge stock is also reduced. Conversely, urging of valve 78 to a more open position will increase the proportion in the total catalytic cracking feed of the highest boiling side stream of the vacuum tower, whereby the carbon residue of the catalytic cracking feed will be increased.

The analytical method of the present invention is adaptable to the hydrocarbon oil refining process control by virtue of the fact that it can be carried out rapidly and continuously without destruction of the sample undergoing analysis. Although the method is readily adaptable to automatic control, it is also useful per se as a laboratory analytical method in place of presently used laboratory methods for determining carbon residue values.

The expression "hydrocarbon oil" is employed herein in its usual sense to define oils that are composed chiefly of components containing essentially carbon and hydrogen, of which petroleum oils and fractions derived therefrom are typical samples. The expression is not intended to exclude oils that contain minor proportions of elements other than carbon or hydrogen such as sulfur, oxygen, nitrogen, etc., as is the usual case with petroleum oils and fractions thereof.

By the expression "hydrocarbon oil refining process" and the like is meant any process for upgrading hydrocarbon oils or fractions thereof, including processes involving distillation, blending, solvent treating, and chemical and catalytic treating processes.

The invention is not limited to the embodiments shown and described herein. Many other modifications will occur to those skilled in the art, and such modifications can be resorted to without departing from the spirit or scope of this invention. Accordingly, only such limitations should be imposed as are indicated in the appended claims.

We claim:

1. A method for controlling a hydrocarbon oil refining process in response to changes in the carbon residue content of an oil stream of said process, comprising subjecting a plurality of samples taken at different times from said oil stream to spectrometric analysis by passing light therethrough of a wavelength that is selectively absorbable by components of the oil that are indicative of the carbon residue content of the oil, in a proportion related to the quantity of said components in the oil, detecting the intensity of the light transmitted through the oil samples, and converting the transmitted light to at least one output signal whose intensity is related to the quantity of said components in the oil samples, and modifying a variable in said hydrocarbon oil refining process in response to changes in at least one of (a) the absorption signal intensity, and (b) a function thereof that is also related to the quantity of said components in the oil samples.

2. A method for controlling a hydrocarbon oil refining process in response to changes in the carbon residue content of an oil stream of said process, comprising subjecting a plurality of samples taken at different times from said oil stream to spectrometric analysis by passing light therethrough having a plurality of wavelengths that are representative of the wavelength band of about 350 to 400 millimicrons and that is selectively absorbable by components of the oil that are indicative of the carbon residue content of the oil, in a proportion related to the

quantity of said components in the oil, detecting the intensity of the light of such wavelengths transmitted by the oil samples, and converting the transmitted light to output signals whose intensity is related to the quantity of said components in the oil samples, and modifying a variable in said hydrocarbon oil refining process in response to changes in at least one of (a) the absorption signal intensities for the respective oil samples, and (b) a function thereof that is also related to the quantity of said components in the oil samples.

3. A method for controlling a hydrocarbon oil refining process in response to changes in the carbon residue content of an oil stream of said process, comprising subjecting a plurality of samples taken at different times from said oil stream to spectrometric analysis by passing light therethrough having a plurality of wavelengths that are representative of the wavelength band of about 350 to 400 millimicrons and that is selectively absorbable by components of the oil that are indicative of the carbon residue content of the oil, in a proportion related to the quantity of said components in the oil, detecting the intensity of the light of such wavelengths transmitted by the oil samples, and converting the transmitted light to output signals whose intensity is related to the quantity of said components in the oil samples, plotting one of (a) the absorption signal intensity, and (b) a function thereof that is also related to the quantity of said components in the oil samples, for said wavelengths of light to obtain a curve indicative of the light absorption in the wavelength band indicated, determining the area under said curve, and modifying a variable in said hydrocarbon oil refining process in response to changes in said area for said oil samples.

4. A method for controlling a hydrocarbon oil refining process in response to changes in the carbon residue content of an oil stream of said process, comprising subjecting a plurality of samples taken at different times from said oil stream to spectrometric analysis by passing light therethrough having a wavelength of about 400 millimicrons and that is selectively absorbable by components of the oil that are indicative of the carbon residue content of the oil, in a proportion related to the amount of said components in the oil, detecting the intensity of the light transmitted by the oil samples, and converting the transmitted light to output signals whose intensity is related to the quantity of said components in the oil samples, and modifying a variable in said hydrocarbon oil refining process in response to changes in at least one of (a) the absorption signal intensity and (b) a function thereof that is also related to the quantity of said components in the oil samples.

5. A method for controlling a hydrocarbon oil refining process in response to changes in the carbon residue content of a distillate oil stream of said process, comprising subjecting a plurality of samples taken at different times from said distillate oil stream to spectrometric analysis by passing light therethrough having a wavelength that is selectively absorbable by components of the oil that are indicative of the carbon residue content of the oil, in a proportion related to the quantity of said components in the oil, detecting the intensity of the light transmitted by the oil samples and converting the transmitted light to output signals whose intensity is related to the quantity of said components in the oil samples, and modifying the distillation conditions under which said distillate hydrocarbon oil stream is produced in response to changes in at least one of (a) the absorption signal intensity, and (b) a function thereof that is also related to the quantity of said components in the oil samples.

6. A method for quantitatively analyzing a hydrocarbon oil for carbon residue content comprising subjecting a sample of the hydrocarbon oil to spectrometric analysis by passing light therethrough having a wavelength that is selectively absorbable by components of the

oil that are indicative of the carbon residue content of the oil, in a proportion related to the quantity of said components in the oil, detecting the intensity of the light transmitted by the oil and converting the transmitted light to at least one output signal whose intensity is related to the quantity of said components in the oil, and determining the carbon residue content that corresponds to one of (a) the absorption signal intensity, and (b) a function thereof that is also related to the quantity of said components in the oil, as shown by a pre-established correlation therebetween.

7. A method for quantitatively analyzing a hydrocarbon oil for carbon residue content comprising subjecting a sample of the hydrocarbon oil to spectrometric analysis by passing light therethrough having a plurality of wavelengths representative of the wavelength band of about 350 to 400 millimicrons and that is selectively absorbable by components of the oil that are indicative of the carbon residue content of the oil, in a proportion related to the quantity of said components in the oil, detecting the intensity of the light of such wavelengths transmitted by the oil and converting the transmitted light to output signals whose intensity is related to the quantity of said components in the oil, and determining the carbon residue content of the oil that corresponds to one of (a) the absorption signal intensity, and (b) a function thereof that is also related to the quantity of said components in the oil, as shown by a pre-established correlation therebetween.

8. A method for quantitatively analyzing a hydrocarbon oil for carbon residue content, comprising subjecting a sample of the hydrocarbon oil to spectrometric analysis by passing light therethrough having a plurality of wavelengths representative of the wavelength band of about 350 to 400 millimicrons and that is selectively absorbable by components of the oil that are indicative of the carbon residue content of the oil, in a proportion related to the quantity of said components in the oil, detecting the intensity of the light of such wavelengths transmitted by the oil, and converting the transmitted light to output signals whose intensity is related to the quantity of said components in the samples, plotting one of (a) absorption signal intensity, and (b) a function thereof that is also related to the quantity of said components in the oil, for said wavelengths of light to obtain a curve indicative of light absorption in the indicated wavelength band, determining the area under said curve, and determining the carbon residue content that corresponds to the thus-determined area as shown by pre-established correlation between carbon residue and the area under the absorption curve.

9. A method for quantitatively analyzing a hydrocarbon oil for carbon residue content comprising subjecting a sample of the hydrocarbon oil to spectrometric

analysis by passing light therethrough having a wavelength of about 400 millimicrons and that is selectively absorbable by components of the oil that are indicative of the carbon residue content of the oil, in a proportion related to the amount of said components in the oil, detecting the intensity of the light transmitted by the oil, and converting the transmitted light to an output signal whose intensity is related to the quantity of said components in the oil, and determining the carbon residue content of the oil that corresponds to one of (a) the absorption signal intensity, and (b) a function of absorption signal intensity that is also related to the quantity of said components in the oil as shown by a pre-established correlation therebetween.

10. An on-line analytical apparatus for quantitatively analyzing a hydrocarbon oil process stream for carbon residue content, comprising hydrocarbon oil refining apparatus provided with conduit means for conducting a hydrocarbon oil stream in said refining apparatus, sampling means associated with said conduit means for withdrawing hydrocarbon oil samples from the oil stream transported thereby, spectrophotometric means provided with an absorption cell connected to said sampling means so as to permit flow of said oil samples into said absorption cell, said spectrophotometric means also being provided with a source of light having a wavelength that is selectively absorbable by components of the oil that are indicative of the carbon residue content of the oil, and that is selectively absorbable by such components in a proportion related to the quantity of said components in the oil, said spectrophotometric means also including detecting means for sensing the intensity of the light of said wavelength transmitted by the oil, and means for converting the transmitted light to an output signal whose intensity is related to the intensity of the transmitted light and thus to the quantity of said components in the oil, and recording means for indicating at least one of (a) the absorption signal intensity, and (b) a function thereof that is also related to the quantity of said components in the oil.

11. The apparatus of claim 10 where said source of light has a plurality of wavelengths representative of the wavelength band of about 350 to 400 millimicrons.

12. The apparatus of claim 10 where said source of light has a wavelength of about 400 millimicrons.

References Cited in the file of this patent

UNITED STATES PATENTS

2,047,985	Weir	July 21, 1936
2,753,292	Porter et al.	July 3, 1956
2,766,265	Goldsmith et al.	Oct. 9, 1956
2,906,798	Starnes et al.	Sept. 29, 1959
2,910,523	Montgomery et al.	Oct. 27, 1959
2,994,646	Kleiss	Aug. 1, 1961

Aug. 31, 1965

N. D. COGGESHALL ET AL

3,203,250

SAMPLING APPARATUS

Filed Nov. 29, 1962

2 Sheets-Sheet 1

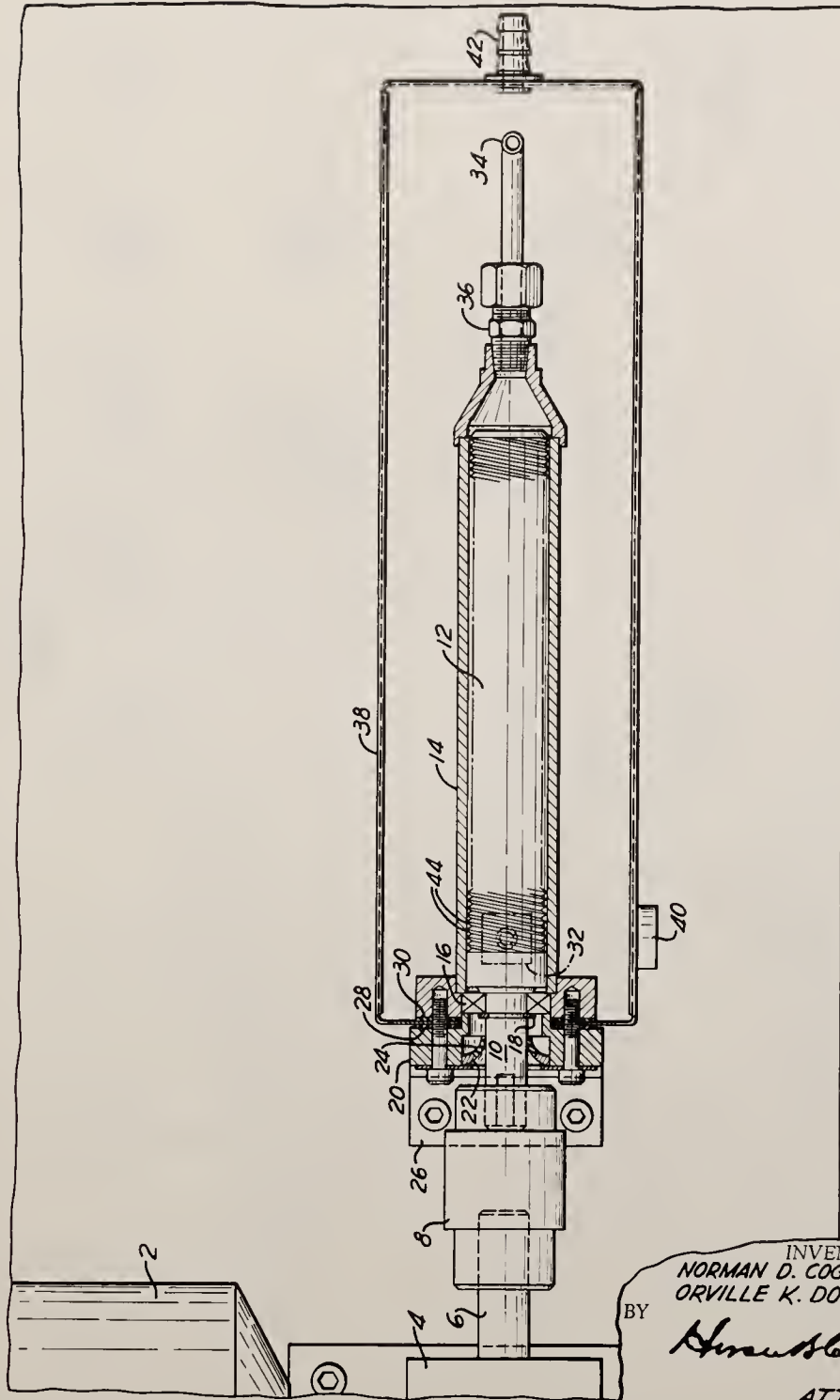


Fig. 1

INVENTORS,
NORMAN D. COGGESHALL
ORVILLE K. DOOLEN

BY

Herbert H. ...

ATTORNEY

Aug. 31, 1965

N. D. COGGESHALL ET AL

3,203,250

SAMPLING APPARATUS

Filed Nov. 29, 1962

2 Sheets-Sheet 2

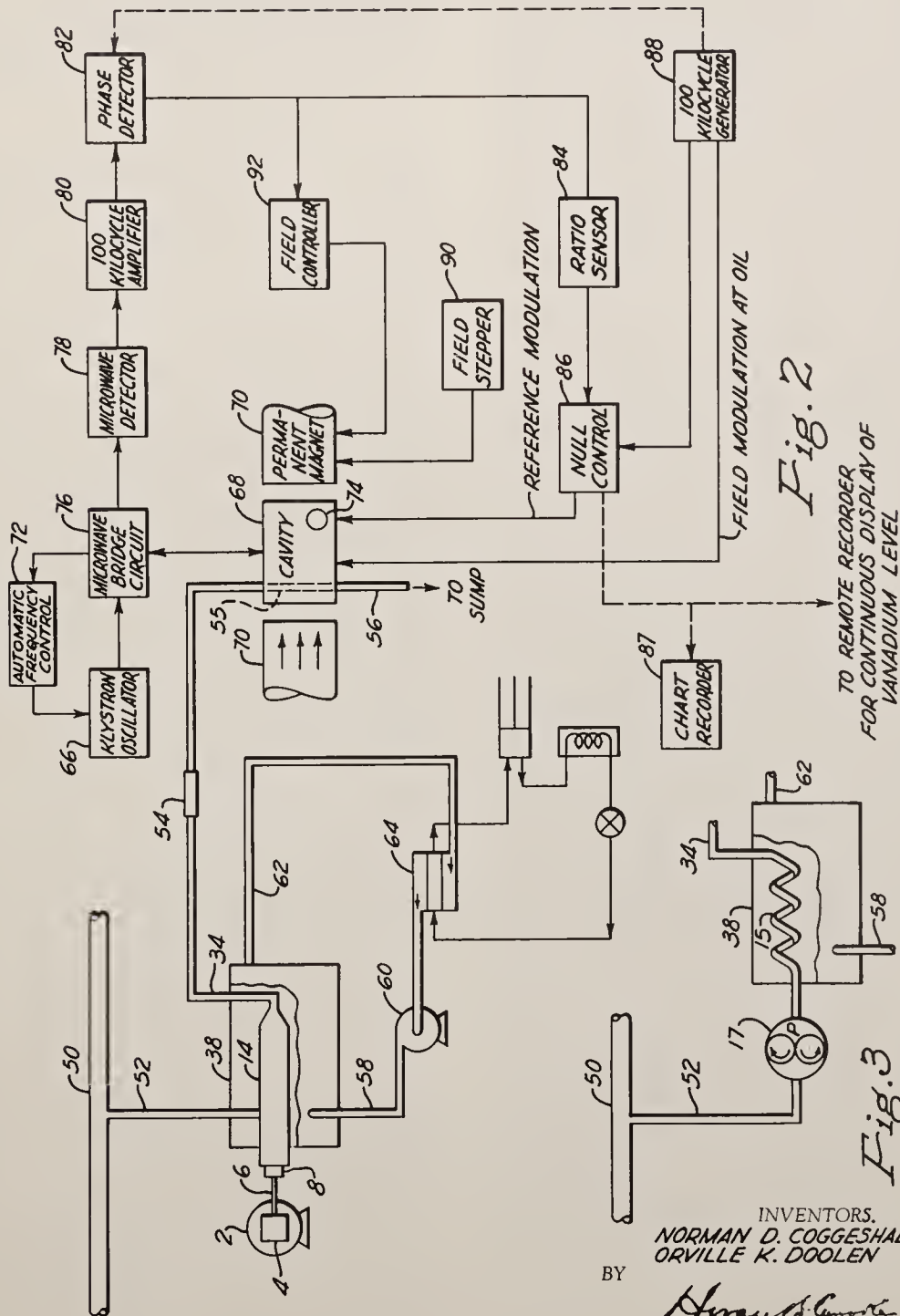


Fig. 2

TO REMOTE RECORDER
FOR CONTINUOUS DISPLAY OF
VANADIUM LEVEL

Fig. 3

INVENTORS.
NORMAN D. COGGESHALL
ORVILLE K. DOOLEN

BY

Howard S. Cooke

ATTORNEY.

1

3,203,250

SAMPLING APPARATUS

Norman D. Coggeshall, Verona, and Orville K. Doolen, Oakmont, Pa., assignors to Gulf Research & Development Company, Pittsburgh, Pa., a corporation of Delaware

Filed Nov. 29, 1962, Ser. No. 240,882

4 Claims. (Cl. 73-422)

This invention relates to apparatus for sampling a body of liquid and for analyzing the samples taken therefrom, and more particularly, to apparatus for on-line sampling of a flowing liquid stream where said analysis is carried out at temperatures, pressures and flow rates that are different from those of the flowing liquid stream.

Automatic, on-line analysis of liquid process streams frequently presents problems that are not encountered when the analysis is carried out by routine laboratory procedures. For example, the temperature, pressure and flow rate of the process stream being subjected to analysis are functions of the process conditions, and these conditions may not be those best suited for the particular method of analysis required. This difficulty may be compounded when the viscosity of the liquid subjected to analysis is significantly different at the desired analytical conditions from its viscosity in the process stream.

By way of illustration, in the on-line analysis of a hydrocarbon oil refinery process stream, such as a vacuum distillation tower gas oil side stream, for vanadium content using an electron paramagnetic resonance spectrometric technique, it has been found that the process stream temperature pressure and flow rate are not well-suited for measurement of the particular physical property on which the analytical method depends. Thus, a typical temperature for a vacuum distillation tower gas oil side stream might be about 400° F., and a typical stream pressure might be about 125 p.s.i.g. At this temperature and pressure, the viscosity of the oil would be so low that accurate monitoring could not be obtained.

The problem of flow rate through the sample chamber of the analytical instrument is complicated by the fact that the flow rate of the process stream, on which the flow rate through the sample chamber ordinarily depends, is not constant but varies with changes in the process conditions and with changes in the properties of the oil being processed. Accurate monitoring cannot be achieved when the flow through the instrument pulsates.

Moreover, the sample chamber of the analytical instrument may not be able to withstand pressures of the magnitude encountered in a process stream. For example, the fused quartz sample chambers employed in EPR spectrometry are not adapted to withstand high pressures.

Finally, the physical property measured in accordance with the particular analytical method employed may be affected by high temperatures, as is the case with the paramagnetic resonance of vanadium in hydrocarbon oils. Thus, the vanadium resonance signal intensity for a particular oil was found to be about 0.9 as great at 100° F. as at 70° F., about 0.76 as great at 110° F. as at 70° F., and about 0.62 as great at 120° F. as at 70° F.

The foregoing difficulties are not satisfactorily solved merely by cooling the sample stream, as the increase in viscosity experienced by the oil upon cooling may be so great as to interfere with the liquid flow. When the change in viscosity is so great as to approach or achieve a change of flow, difficulties may also be encountered in obtaining a uniform temperature throughout the oil stream. Moreover, it will be recognized that the flow rate of the liquid sample stream, even in a relatively viscous state, may still be subject to change with changes

2

in the processing conditions and/or changes in the nature of the oil being processed.

The present invention relates to apparatus for sampling a body of liquid, e.g., a refinery process stream, and for analyzing the samples taken therefrom at temperature, pressure and flow conditions other than those existing in the body of liquid from which the samples are taken, whereby improved analytical accuracy, and continuous, automatic monitoring are made possible. In accordance with the present invention, there is provided, inter alia, the combination of analysis means for detecting and measuring a physical property of the liquid to be analyzed and a sampling conduit connecting the analysis means and the main body of liquid to be analyzed for delivering representative portions of the liquid in said main body to the analysis means. An electron paramagnetic resonance spectrometer capable of detecting and measuring the intensity of a resonance signal for paramagnetic vanadium in petroleum hydrocarbon oils is an example of a particular analysis means contemplated in the present invention, but other analytical instruments utilizing analytical methods dependent upon detection and measurement of physical properties that are affected by temperature, pressure and/or flow rate also can be used. Heat exchange means are also provided intermediate of the main body of liquid and the analysis means for adjusting the temperature of the liquid in the sampling conduit to the temperature desired in the analysis means, irrespective of the normal range of temperatures of the main body of liquid. The apparatus of this invention also includes means intermediate of the main body of liquid and the analysis means for adjusting the flow conditions, that is, the fluid pressure and flow rate, of the liquid in the sampling conduit to the conditions desired in the analysis means, irrespective of the normal range of temperatures and flow conditions in the main body of liquid. In a preferred embodiment, the means for adjusting the temperature and flow conditions of the liquid in the sample conduit may comprise a screw conveyor assembly comprising an elongated cylindrical pump tube containing a coaxially positioned pump screw. The pump screw is provided with alternate helical flights or lands and grooves, the latter forming a path of flow for liquid introduced into the pump tube. The outer peripheries of the flights of the pump screw are in close proximity to the inner surfaces of the pump tube. Drive means are also provided for rotating the pump screw and forcing the sample liquid from one end of the pump tube to the other. The preferred means for adjusting the temperature and flow conditions of the sample liquid also involves heat exchange means comprising a jacket spaced apart from and surrounding the pump tube of the screw conveyor assembly. This jacket is provided with inlet and outlet means, which are in turn provided with conduit means fluidly connecting said jacket with the heat exchange chamber of a refrigerating means. Pump means serve to circulate a heat exchange fluid from the heat exchange chamber to the jacket and back to the heat exchange chamber. The use of a flexible coupling between the outlet of the screw conveyor assembly and the analysis means is especially advantageous, and such use is included in the present invention.

Referring briefly to the drawings, FIGURE 1 is a plan view, partly in horizontal section, of a preferred means for adjusting the temperature and flow conditions of the sample liquid. FIGURE 2 is a flow diagram showing a preferred combination of the sampling means, analysis means and means for adjusting the temperature and flow conditions of the sample liquid included by the present invention. FIGURE 3 is an alternative embodiment of sampling means and means for adjusting the temperature

3

and flow conditions of the sample liquid included by the present invention. In the several figures of the drawing, like numerals refer to the same or similar elements.

The present invention can be best understood by detailed reference to the drawings. Referring first to FIGURE 1, a power train composed of electric motor 2, change speed mechanism 4 and drive shaft 6 is connected through flexible coupling 8 to shaft 10 of the pump screw element 12 of a screw conveyor assembly. The screw conveyor assembly is mounted on the same supporting surface as the motor 2 and change speed mechanism 4 by means of angle mount 26. The base of angle mount 26 is bolted to the supporting surface. The vertical portion of angle mount 26 is bolted first to support plate 20 and then to an anchoring member positioned against the inside wall of jacket 38. Support plate 20 is provided with a stepped annular opening, through which passes shaft 10 of pump screw 12. The larger annular space in support plate 20 contains a shaft seal member 22 which has embedded therein a synthetic rubber seal 24. Seal 24 bears upon shaft 10 and prevents leakage of the liquid passed through the screw conveyor along shaft 10. Numeral 16 denotes an annular ball-bearing and race forming a bearing member for shaft 10. Bearing race 16 is maintained in proper position by retaining ring 18 which is seated in an annular recess in shaft 10. Pump screw 12 mounted coaxially within pump tube 14, together with the latter element, forms a screw conveyor assembly for causing liquid introduced into the pump tube to advance therethrough. The outer peripheries of the flights or lands 44 of pump screw 12 are in close proximity to the inside surface of pump tube 14 so as to facilitate removal of any solid material formed on the inside surface of pump tube assembly 14 with each revolution of pump screw 12. Numeral 32 designates an inlet saddle mounted on the upper surface of pump tube assembly 14. An annular orifice positioned in the center of inlet saddle 32 forms inlet means permitting passage of the liquid sample whose temperature and flow conditions are to be adjusted from the sample conduit, to which the orifice is connected, into the helical, grooved recesses between the flights 44 of pump screw 12. These grooved recesses form a path of flow through the pump tube for liquid introduced therein. Numeral 34 designates the outlet of the screw conveyor mechanism through which the liquid sample passes following the desired adjustment of its temperature and flow conditions in said screw conveyor. Outlet line 34 is connected to the screw conveyor proper through a suitable coupling 36. The pump tube assembly 14 is surrounded by a jacket 38 which is spaced apart therefrom. Gaskets 28 and 30 form a liquid tight seal between the interior and exterior of jacket 38 in the vicinity of the mounting bolts. Numeral 40 designates a pipe fitting forming an inlet for a heat exchange fluid. While cooling water is specifically disclosed as the heat exchange fluid in the embodiment described hereinafter, it will be appreciated that a heated fluid can be used where the analysis temperature is greater than the temperature of the liquid body from which samples are taken for analysis. Numeral 42 designates a nipple providing an outlet for the heat exchange liquid from jacket 38. A top, not shown, for jacket 38, having slots through which pass the inlet conduit for pump tube 14, and the outlet conduit 34, is also provided.

Referring now to FIGURE 2, which as stated, illustrates a preferred combination of sampling means, temperature and flow condition adjustment means, and analysis means, numerals up to and including numeral 64 refer to the sampling, and temperature and flow condition adjustment portions of the apparatus combination. With particular reference to these portions of the drawing, numeral 50 designates a main conduit, through which is caused to flow a stream of liquid to be analyzed. Numerals 52 and 34 refer to separate portions of a sample conduit

4

adapted to deliver a representative portion of the liquid stream flowing through main conduit 50 to the sample chamber 55 of the analysis means shown schematically on the right-hand side of the figure. Inlet conduit 58 and pump 60 form means for circulating a refrigerated heat exchange liquid to the jacket 38 from the heat exchange chamber 64 of a conventional, vapor-compression refrigerating unit, shown schematically. Numeral 62 denotes an outlet conduit for returning heat exchange liquid from jacket 38 to the inlet side of heat exchange chamber 64.

In the alternative embodiment of the sampling, and temperature and flow condition adjustment means shown in FIGURE 3, numeral 15 designates a tubular cooling coil connected in series between portions 52 and 34 of the sample conduit. Numeral 17 designates a gear pump for adjusting the flow conditions of the liquid in the sample line irrespective of those existing in main conduit 50.

In operation, with particular reference to FIGURE 2, a representative portion of a liquid stream to be analyzed, for example, a vacuum tower gas oil side stream, flowing through a main conduit 50 at a temperature of about 400° F. and under a fluid pressure of about 125 p.s.i.g. is diverted through sample conduit 52 into the grooved recesses of a pump screw 12 positioned within pump tube 14 and having a thread length of about 21 feet. The liquid in these grooved recesses is caused to move toward the outlet 34 of pump tube 14 by the rotational motion imparted to pump screw 12 by means of motor 2, change speed mechanism 4 and drive shaft 6. As the liquid progresses along a helical path along the inside surface of pump tube 14, the liquid loses heat to a refrigerated heat exchange liquid, such as a water-ethylene glycol mixture, circulated through jacket 38. As the temperature of the oil within the pump tube assembly falls below the pour point of the oil, about 120° F. in the present instance, the oil assumes a semisolid or soft grease-like consistency along the surface of the pump tube. This semisolid film forms an insulating layer that retards the removal of heat from the remaining liquid oil. However, the scraping action of the flights of pump screw 12 against the inside surface of pump tube 14 with each revolution of pump screw 12 causes the film of semisolid material to be scraped from the tube surfaces and mixed with any unsolidified liquid whereby uniform temperature and homogeneous consistency is achieved. Thus, a homogeneous semisolid stream of uniform temperature, in this instance, about 70° F., is continuously extruded through outlet 34 of pump tube 14, in this instance, at a constant, pulsationless rate of about 12 ml. per minute. The temperature of the stream is adjusted below the maximum temperature (80° F.) desired in the analysis means, as some reheating of the oil takes place in the sample chamber 55 of the analytical instrument.

The semisolid condition of the oil, together with the resistance to flow of the screw conveyor assembly, provides an effective seal against liquid flow. Consequently, where it is desired to stop flow through the analytical instrument for any reason, for example, mechanical adjustment of the instrument, all that is necessary to take the instrument out of service is to switch off motor 2. When the liquid being analyzed is not sufficiently viscous to stop liquid flow, a conventional flow regulating device can be employed in the sample line downstream of the screw conveyor assembly.

The extruded material is forced through flexible coupling 54 and through the sample chamber 55 of the analytical device, where the desired physical property, e.g., vanadium electron paramagnetic resonance, is detected and measured, and from this point through line 56 to a sump. Alternatively, the oil from line 56 can be returned to main conduit 50 through conduit means not shown. Refrigerated heat exchange liquid is circulated through jacket 38 from the heat exchange chamber of a conventional vapor-compression refrigerating system by means of pump 60, inlet 58 and outlet line 62.

With further reference to FIGURE 2, numerals 66 and following indicate generally the component elements of a model X-4800 EPR Vanadium Process Monitor, manufactured by Varian Associates. While the particular analytical instrument illustrated is preferred for continuous monitoring of vanadium in hydrocarbon oils for the reason that it is especially designed for this purpose, the use of this instrument is not essential to the present invention, and other analytical instruments can be used. For example, a conventional, Varian X-band model V-4500 electron paramagnetic resonance spectrometer can be employed in the apparatus of the present invention, not only to detect and measure resonance due to the paramagnetic vanadium in hydrocarbon oils but also to detect resonance due to other paramagnetic substances in the same or other liquid media. In fact, analytical instruments based on the detection and measurement of properties entirely different from electron paramagnetic resonance can be used. For example, a spectrophotometer can be employed as the analysis means of the herein disclosed combination apparatus, where the property to be measured in the sample liquid is dependent upon light transmission rather than paramagnetic resonance.

Inasmuch as the invention in its broader aspects does not depend for novelty upon the use of any particular analytical instrument, it will be seen that the structural or functional details of the model X-4800 EPR Process Monitor shown in FIGURE 2 form no part of the present invention. However, in order that the invention may be fully understood it may be stated generally that the principles of EPR analysis are generally described in Bloch et al. Reissue Patent No. 23,950, and the principles of such analysis as applied to the determination of vanadium paramagnetic resonance in petroleum oils are described in application Serial No. 36,381, filed June 15, 1960, in the name of A. J. Saraceno, now Patent No. 3,087,888. More particularly, the model X-4800 EPR Process Monitor illustrated in FIGURE 2 is a null-seeking system in which the resonance signal from paramagnetic vanadium in a sample to be analyzed is compared with a resonance signal from a reference sample. Referring in detail to the diagram in FIGURE 2, a klystron oscillator 66 connected to a source of electrical power, not shown, delivers microwave power to a cavity 68, located between the poles 70 of a permanent magnet. The klystron frequency is locked to the cavity frequency by an automatic frequency control circuit 72. In operation, any difference in amplitude between the signal strength at zero resonance, and the resultant signal amplitude at the vanadium resonance peak, between the signal from the oil sample in sample chamber 55 and an opposite phase signal from reference sample 74, manifests itself as an output from the microwave bridge circuit 76. This output is detected by microwave detector 78, amplified by 100 kc. amplifier 80, and passed to phase detector 82. The output of the phase detector 82 is fed to a ratio sensor 84. This element in turn transmits an electrical output proportional to the aforesaid difference in signal amplitude to a servo motor component of a motor-driven potentiometer component of null control 86. The motor effects an adjustment of the potentiometer output, so that this output—in amplified form—can be used to modulate the reference sample signal and eliminate the aforesaid difference in signal amplitude. The degree of adjustment of the potentiometer is calibrated against the degree of adjustment required for an oil of comparable viscosity and having a known vanadium content, in terms of the vanadium content of the oil. A D.C. voltage is applied to the potentiometer to drive the recorder 87 and also any remote recorder, controller, or recorder-controllers that may be employed. Power for 100 kc. sweep modulation of both reference sample 74 and the oil sample in sample chamber 55 is supplied by the 100 kilocycle generator 88. A

phase shifter, not shown, is provided in the reference modulation circuit so that this sweep is 180 degrees out of phase with the sweep of the oil sample, whereby opposite phase signals are obtained from the oil sample and the reference sample.

The magnetic field strength is varied from the point of zero resonance to the point of the vanadium resonance peak by field stepper 90 in response to a programmer, not shown. Periodically, another programmer switches on the circuits of field controller 92 to correct any drift in the magnetic field.

The functioning of the embodiment shown in FIGURE 3 is similar to that of the embodiment of FIGURE 2. The embodiment of FIGURE 3, however, is less satisfactory when used in connection with a liquid that is to be cooled below its pour point, for the reasons indicated.

It will be understood that the herein described specific embodiments are intended as illustrative only and not as limiting the scope of the invention. Good results can also be obtained by the substitution of equivalent elements included within the scope of the present invention for the corresponding elements of the foregoing specific embodiments.

For the reasons stated, the scope of the present invention is not to be limited by the foregoing description but only by the scope of the appended claims.

We claim:

1. Apparatus for sampling a liquid stream flowing in a main conduit and for analyzing the samples so obtained at temperature, fluid pressure and flow conditions other than those existing in said main conduit, comprising analysis means for continuously detecting and measuring a physical property of the liquid to be analyzed, a sampling conduit connecting the analysis means and said main conduit for delivering representative portions of the liquid stream flowing through said main conduit to said analysis means, heat exchange means intermediate of said main conduit and the analysis means for adjusting the temperature of the liquid in the sampling conduit to the temperature desired in the analysis means, irrespective of the temperature of said liquid stream, means intermediate of said main conduit and said analysis means for adjusting the fluid pressure and the flow rate of the liquid in the sampling conduit to the conditions desired in the analysis means, irrespective of the fluid pressure and flow rate of said liquid stream, said means for adjusting the fluid pressure and flow rate comprising a cylindrical pump tube, a pump screw positioned coaxially within said cylindrical pump tube and having alternate, helical flights and grooves, the latter forming a path of flow through said pump tube, the outer peripheries of the flights of said pump screw being in close proximity to the inside surface of said pump tube, and drive means for causing rotation of said pump screw within said pump tube, whereby liquid introduced into said pump tube is caused to advance therethrough.

2. Apparatus for sampling a liquid stream flowing in a main conduit and for analyzing the samples so obtained at temperature, fluid pressure and flow conditions other than those existing in said conduit, comprising analysis means for detecting and measuring a physical property of the liquid to be analyzed, a sampling conduit connecting the analysis means and said main conduit for delivering representative portions of the liquid stream flowing through said main conduit to said analysis means, flow regulating means intermediate of said main conduit and said analysis means for adjusting the fluid pressure and flow rate of the liquid in the sampling conduit to the conditions desired in the analysis means, said flow regulating means comprising a cylindrical pump tube, a pump screw positioned coaxially within said cylindrical pump tube and having alternate, helical, flights and grooves, the latter forming a path of flow through said pump tube, the outer peripheries of the flights of said pump screw

being in close proximity to the inside surface of said pump tube, and drive means for causing rotation of said pump screw within said pump tube, whereby liquid introduced into said pump tube is caused to advance therethrough, cooling means comprising a jacket surrounding said pump tube and spaced apart therefrom, said jacket having an inlet and an outlet, said inlet and outlet being provided with conduit means fluidly connecting said jacket with the heat exchange chamber of a refrigerating means, means for circulating heat exchange fluid from said heat exchange chamber to said jacket and back to said heat exchange chamber.

3. Apparatus for sampling a liquid stream flowing in a main conduit and for analyzing the samples so obtained at temperature, fluid pressure and flow conditions other than those existing in said main conduit, comprising electron paramagnetic resonance spectrometric analysis means for continuously detecting and measuring the intensity of a resonance signal for a paramagnetic substance in the liquid to be analyzed, a sampling conduit connecting the analysis means and said main conduit for delivering representative portions of the liquid stream flowing through said main conduit to said analysis means, heat exchange means intermediate of said main conduit and the analysis means for adjusting the temperature of the liquid in the sampling conduit to the temperature desired in the analysis means, irrespective of the temperature of said liquid stream, means intermediate of said main conduit and said analysis means for adjusting the fluid pressure and the flow rate of the liquid in the sampling conduit to the conditions desired in the analysis means, irrespective of the fluid pressure and flow rate of the liquid stream in said main conduit, said means for adjusting the fluid pressure and flow rate comprising a cylindrical pump tube, a pump screw positioned coaxially within said cylindrical pump tube and having alternate, helical flights and grooves, the latter forming a path of flow through said pump tube, the outer peripheries of the flights of said pump screw being in close proximity to the inside surface of said pump tube, and drive means for causing rotation of said pump screw within said pump tube, whereby liquid introduced into said pump tube is caused to advance therethrough.

4. Apparatus for sampling a liquid stream flowing in a main conduit and analyzing the samples so obtained at temperature, fluid pressure and flow conditions other

than those existing in said conduit, comprising electron paramagnetic resonance spectrometric analysis means for detecting and measuring a resonance signal for a paramagnetic substance in the liquid to be analyzed, a sampling conduit connecting the analysis means and said main conduit for delivering representative portions of the liquid stream flowing through said main conduit to said analysis means, flow regulating means intermediate of said main conduit and said analysis means for adjusting the fluid pressure and flow rate of the liquid in the sampling conduit to the conditions desired in the analysis means, irrespective of the fluid pressure and flow rate of the liquid stream in said main conduit, said flow regulating means comprising a cylindrical pump tube, a pump screw positioned coaxially within said cylindrical pump tube, said pump screw having alternate, helical flights and grooves, said grooves forming a path through said pump tube for liquid introduced therein, the outer peripheries of the flights of said pump screw being in close proximity to the inside surface of said pump tube, and drive means for causing rotation of said pump screw within said pump tube, whereby liquid introduced into said pump tube is caused to advance therethrough, cooling means comprising a jacket surrounding said pump tube and spaced apart therefrom, said jacket having an inlet and an outlet, said inlet and outlet being provided with conduit means fluidly connecting said jacket with the heat exchange chamber of a refrigerating means, means for circulating heat exchange fluid from said heat exchange chamber to said jacket and back to said heat exchange chamber.

References Cited by the Examiner

UNITED STATES PATENTS

1,649,399	11/27	Gard	73—422
2,637,211	5/53	Norman	73—422
2,306,606	12/42	Hirsch	73—422 X
2,955,252	10/60	Williams	324—0.5

OTHER REFERENCES

Dunda et al.: Oil and Gas Journal, vol. 54, No. 55, May 21, 1956, pages 251-253.

RICHARD C. QUEISSER, *Primary Examiner*.

JOSEPH P. STRIZAK, *Examiner*.

Reprinted from

Geochimica et Cosmochimica Acta, 1967, Vol. 31, pp. 1155 to 1166. Pergamon Press Ltd. Printed in Northern Ireland

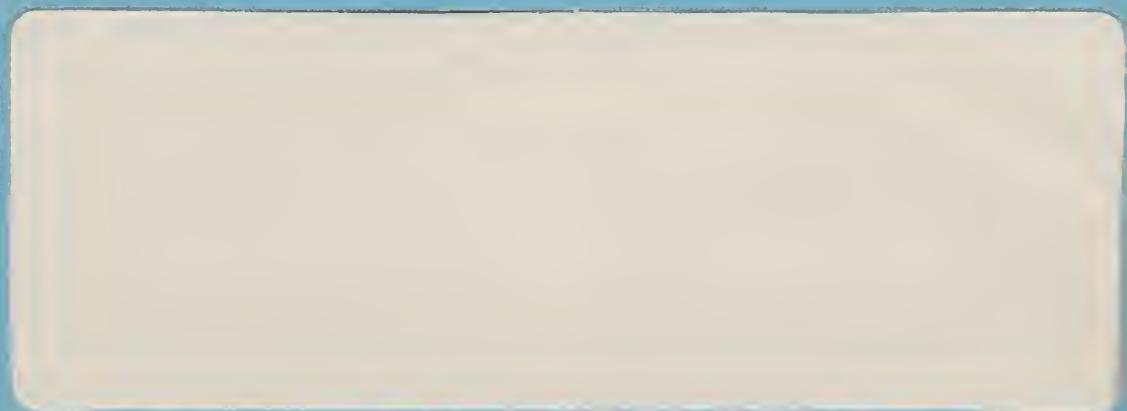
Analysis and significance of hydrocarbons in subsurface brines

W. M. ZARRELLA, R. J. MOUSSEAU, N. D. COGGESHALL,
M. S. NORRIS and G. J. SCHRAYER

Gulf Research & Development Company, P.O. Drawer 2038,
Pittsburgh, Pennsylvania 15230



PERGAMON PRESS
OXFORD NEW YORK LONDON PARIS



Analysis and significance of hydrocarbons in subsurface brines

W. M. ZARRELLA, R. J. MOUSSEAU, N. D. COGGESHALL,
M. S. NORRIS and G. J. SCHRAYER

Gulf Research & Development Company, P.O. Drawer 2038,
Pittsburgh, Pennsylvania 15230

(Received 17 February 1967; accepted 10 March 1967)

Abstract—Spectrophotometric and gas chromatographic methods for the analysis of minute concentrations of hydrocarbons dissolved in water and brines are described. These methods have been applied to studies of the quantities and distributions of dissolved hydrocarbons in subsurface waters. Criteria for the collection of representative formation fluids and for minimizing loss of the hydrocarbons before analysis are outlined. The results of analyses of brines from petroleum-producing wells are presented to indicate the variability in the concentration of benzene in waters surrounding different types of hydrocarbon accumulations. Additional data for brines from development wells indicate that the benzene concentration decreases, in an aquifer, with increasing distance from the correlating oil pool. Finally, benzene data for brines from a number of formations in a single well show that this hydrocarbon is specific for reflecting the occurrence of a petroleum accumulation in the tested formation: i.e. vertical migration of benzene between aquifers is restricted. The results of this study have culminated in a direct detection method for petroleum exploration and in research techniques for the evaluation of petroleum migration and accumulation mechanisms.

INTRODUCTION

RESEARCH on the presence and significance of hydrocarbons dissolved in subsurface brines has been in progress for the past several years. The aims of this research have been to develop methods for the recognition of petroleum-bearing rock units, for the detection of undiscovered petroleum accumulations, and to seek an understanding of the natural processes operating in the migration and accumulation of petroleum. The results of a portion of this research are summarized in this paper.

Several reports in the literature describe attempts to utilize information on the composition of formation brines in petroleum exploration and in the evaluation of subsurface fluid movements. Initially, the studies were centered on the qualitative and quantitative aspects of the salts dissolved in these brines (SAGE, 1958; SCHOELLER, 1955). Although the salt compositions of underground waters have resulted in a partial understanding of the movement of this fluid in rocks, no direct relationship of brine composition to the constitution of petroleum has yet been uncovered. Consequently, the utilization of the salt composition of brines for the detection of petroleum accumulations has had very limited application. Recent publications (BUCKLEY *et al.*, 1958; KORTSENSHTEIN, 1961; LONDON *et al.*, 1961) show that emphasis is currently being placed on the composition and quantities of gaseous components dissolved in oil field brines in the search of direct detection methods for exploration and in the study of petroleum migration processes. These studies have depended on the collection of brine samples in high-pressure bottom-hole samplers in order to

prevent loss of the dissolved gases on reaching the surface. The results of these investigations indicate that the quantities of dissolved gases in subsurface brines increase with depth. The data of BUCKLEY (1958) suggest that local enrichment of the brines in the dissolved gaseous hydrocarbons may occur in the vicinity of some oil or gas fields.

The investigations reported in this paper were carried out using subsurface samples recovered at the surface of drilling and producing wells. Large proportions of the normally gaseous hydrocarbons escape from the brines with changes in the temperature and pressure conditions from the subsurface to the surface. Consequently, greatest emphasis was placed on the concentration of benzene dissolved in formation brines (COGGESHALL and HANSON, 1956) since this hydrocarbon is the most soluble in water and, thus, is expected to be present in greatest amounts and least susceptible to release from solution at the surface.

EXPERIMENTAL

Sample collection and handling

The formation brine samples examined were obtained from drill stem test recoveries in wildcat and development wells. All the samples used in this study were collected by field personnel. In order to minimize dilution from mud filtrate, the instructions for sample collection requested that the brine be obtained from the drill stem test tool or from the lowest portion of the drill stem consistent with obtaining a brine sample free of bottom sediments settling out of the recovery column. The instructions also indicated that the sample should be caught in clean buckets on opening the pipe string and immediately transferred to new narrow-necked glass or metal containers. Filling of the containers to within one-eighth inch of the top was also requested. The samples were then kept under seal until ready for analysis.

Analytical methods

Extraction and u.v. absorption analysis of benzene. A rapidly filtered 2-l. sample of brine is shaken with 25 ml of spectrally pure isooctane for $\frac{1}{2}$ hr, and the isooctane layer is then separated. The isooctane extract is charged to a small, all-glass, vacuum-jacketed Vigreux still and, after reflux, a 3-ml sample of distillate is collected for u.v. absorption measurement at the analytical wave lengths for benzene and toluene. The absorbance values in the benzene absorption region are corrected for toluene and background absorbances, and the resultant benzene concentration in the isooctane extract is adjusted for the various quantitative steps. A final correction is made for the over-all efficiency in the recovery of benzene in the isooctane distillate. This efficiency factor was determined by repeated runs on synthetic brine samples having known concentrations of benzene and processed under identical conditions.

Gas chromatographic analysis of hydrocarbons. In the gas chromatographic analysis of hydrocarbons in subsurface brines, the sample is charged to a glass inlet tube ($\frac{1}{4}$ -in. O.D.) packed with 30–60 mesh Chromosorb P and 16–32 mesh Drierite. The Chromosorb packing in the upper portion of the inlet serves to increase the surface area of the fairly large samples, permitting more rapid charging and elution of the hydrocarbons. The lower Drierite section is used to remove water from the sample before entering the analytical column.

A dual unit is employed for the analysis of aromatic and saturated hydrocarbons. The aromatics unit consists of the glass inlet tube containing $3\frac{1}{2}$ in. Chromosorb and $1\frac{1}{2}$ in. Drierite and an analytical column of 1 ft \times $\frac{1}{4}$ in. O.D. copper tubing packed with 27 wt. % of β, β' -oxydipropionitrile on 30–60 mesh Chromosorb P. Helium is used as a carrier at a rate of approximately 100 ml/min. A 0.5 ml brine sample is used for the aromatics analysis.

The inlet tube of the saturates unit, containing $1\frac{1}{2}$ in. Chromosorb and $3\frac{1}{2}$ in. Drierite, is heated by an outside winding of nichrome wire. The analytical column is a 10 ft \times $\frac{1}{4}$ in. O.D. copper tubing packed with 5% by weight of the methylene chloride-soluble fraction of

Dow-Corning High Vacuum silicone grease on Chromosorb P. A nitrogen carrier flow rate of 90 ml/min and a sample size of about 0.1 ml is used.

The aromatics and the saturates units are equipped with hydrogen flame ionization detectors, and the detector output is amplified with a Keithley Model 610A Electrometer. The hydrogen flow to each detector is adjusted to give maximum response for the carrier flow rate used. The amplified signal from the electrometer is recorded on a Bristol or a Texas Instruments Recorder. The peak areas of the chromatograms are used to calculate the quantities of the components present in the brine sample.

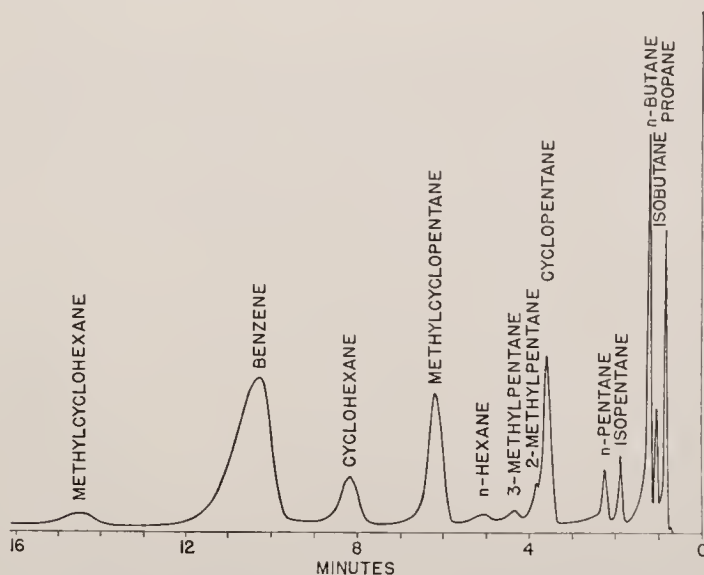


Fig. 1. Chromatogram of hydrocarbons in water; silicone column. Peaks identified by major component.

RESULTS AND DISCUSSION

Accuracy and comparison of analytical methods

In the studies of hydrocarbons dissolved in subsurface brines, initial emphasis was placed on the determination of benzene. In the extraction procedure, the slow filtration of those samples containing suspended matter resulted in substantial losses of benzene on handling. With the advent of the hydrogen flame ionization detector it became possible to overcome this problem by the development of the more rapid and more reliable direct gas chromatographic analysis. As seen in the sample chromatograms shown in Figs. 1 and 2 the gas chromatographic method can also give results on the saturated light hydrocarbons. Unanswered questions remain, however, in regard to the reliability of the sample handling methods when applied to the saturates. (When their low solubility per unit vapor pressure is considered, it might be anticipated they would be more susceptible to losses.) In view of this and the fact that most of the results have been obtained by the extraction-u.v. absorption method, further discussion will be limited to the significance of benzene.

The accuracy of the gas chromatographic method has been checked by running

samples prepared by diluting a saturated solution of benzene in water. The concentrations measured by the chromatograph, after calibration with a benzene in iso-octane solution, are shown in Table 1, column 2. The concentration of benzene in the undiluted sample, calculated from the measured concentration and the dilution factor, is shown in column 3 of the table. The results are seen to be linear with dilution factor with an average deviation from the mean of 1.2% (the last two concentrations were not taken into the average because of their proximity to the

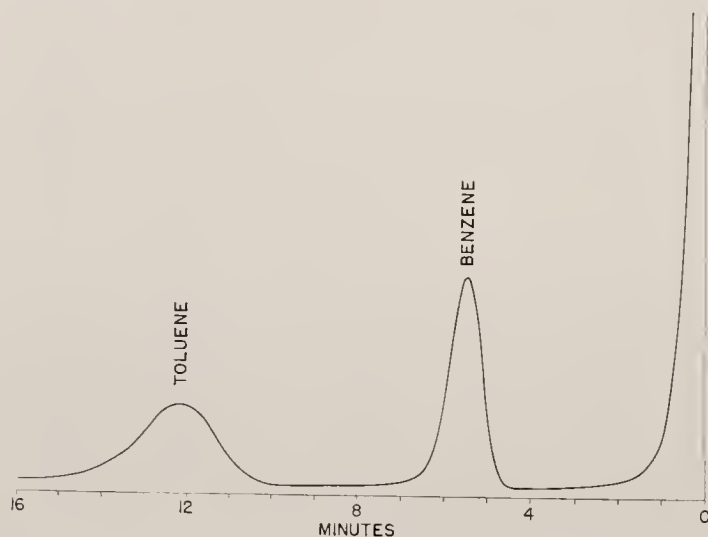


Fig. 2. Chromatogram of hydrocarbons in water; β,β' -oxydipropionitrile column.

Table 1. Test of benzene analysis by gas chromatographic method

Dilution factor	Concentration (ppm by volume)	Equivalent undiluted concentration (ppm by volume)
1:203	9.56	1940
1:501	3.91	1960
1:2044	0.980	2010
1:5040	0.393	1980
		av. 1976 ± 23
1:20460	0.101	2070
1:20460	0.097	1980

detection limit of about 0.01 ppm). However, the results are 2% lower than the value of 2011 ppm obtained when the saturated solution (room temperature, not thermostated) is injected directly into the instrument. The value of 2011 ppm agrees with the reported values of 2030, 2050, and 1990 ppm (McDEVIT, 1952; BOHON, 1951; ANDREWS, 1949). The difference is probably due to losses during dilution.

The extraction-u.v.-absorption method has been refined to the point where it can yield duplicate results to within less than 5%. The accuracy of this method is less, however, as is illustrated in Table 2. This table gives a comparison between results obtained by the gas chromatographic method and the extraction-u.v. method on a series of field brine samples and solutions made by contacting 1 N sodium chloride with different crude oils.

Sampling precautions

In the early stages of this work, it was recognized that three potential difficulties arise in the study of dissolved hydrocarbons in formation brines, namely, contamination of the recovered fluid with hydrocarbon containing materials used on the drilling rig, recovery of fluid which is not representative of the formation brine and loss of

Table 2. Comparison of analytical methods

Type of sample	Concentration (ppm by volume)	
	Gas chromatography	extraction-u.v. absorption
Field sample	0.03	0.04
Field sample	0.38	0.60
Field sample	1.91	1.99
Prepared sample	1.99	1.91
Prepared sample	2.58	2.14
Prepared sample	3.62	3.33
Prepared sample	4.62	3.86
Prepared sample	6.53	6.43

hydrocarbon from the brine during handling and storage of the sample. Each of these problems has been investigated and, although they cannot be thoroughly controlled, the errors arising from these factors can be minimized with the exercise of proper precautions.

Hydrocarbon contamination. The petroleum products commonly used on drill rigs are pipe thread greases, lubricants and diesel oils. These compositions are devoid of benzene and other low molecular weight hydrocarbons; consequently, their use should not lead to contamination of formation brines. All tests of the typical products used on drill rigs have shown no detectable benzene in the brines exposed to them.

Occasionally virgin or untopped crude oils are added to drill holes, e.g. in oil-base drilling muds, in releasing stuck drill pipe, etc. In addition, petroleum shows or petroleum accumulations are occasionally penetrated when drilling for deeper objectives. Formation fluids obtained on tests after the introduction of crude oil into the well or below the occurrence of crude oil zones would, therefore, be subject to serious contamination. However, such contamination can be minimized, or even eliminated, if the interval to be drill stem tested is well isolated with packers and if adequate recovery is obtained to yield a representative formation fluid.

Examples are given in Table 3 of benzene analyses of formation fluids obtained from tests made after penetration of a crude oil zone. The brines were collected from

Table 3. Benzene content of formation brines below oil bearing zones in same well

Area	Approximate depth of test interval (ft)	Formation	Benzene content of brine (ppm)
1. Alberta, Canada	5700	Permo Pennsylvanian	(crude oil)
	5900	Rundle	0.1
	8700	Woodbend	(crude oil)
2. Alberta, Canada	6400	Triassic	(crude oil)
	11,300	Granite Wash	0.0
3. Saskatchewan, Canada	4500	Midale	(crude oil)
	6700	Souris Valley	0.0

the lowermost portion of drill stem test recoveries which yielded 1000 ft, or more, of fluid on test. The first example shows the presence of a relatively low level of benzene from a brine obtained only 200 ft below a penetrated crude oil column. It cannot be stated with certainty whether the benzene represents contamination from the crude oil occurring in the Permo Pennsylvanian horizon or whether it reflects the presence of crude oil in the Rundle formation in the area of the test. The remaining two examples, however, indicate that no detectable benzene (less than 0.01 ppm) is present in brines obtained below a crude oil zone. In these instances the presence of crude oil in the well did not cause contamination of brines from subsequently sampled formations. The results, therefore, indicate that it is possible to control this type of contamination.

Mud contamination. As suggested above, fluids recovered on drill stem tests may not be representative of the formation brine except in the lower portion of a drill stem test recovery, which yields sufficient fluid. This is a consequence of the weighting of drilling muds to give pressures in excess of hydrostatic in order to prevent fluid blow-out from the well. The excess pressure results in the invasion of porous zones by filtrate from the mud. When the pressure in the porous rock unit is released on drill stem test, the invading fluid enters the drill pipe first, followed by mixtures of filtrate and formation fluid and finally, on successful tests, true formation fluid enters the pipe string. This zonation of fluids in the drill stem is commonly noted from salt analyses of samples taken at successive depths.

As expected, the dilution of drill stem test recovery fluids also results in benzene concentrations below those of the actual formation brines. This is shown by the examples recorded in Table 4; the benzene contents of the bottom fluids are substantially higher than the values for the fluids in the upper zones. In order to minimize dilution effects, therefore, the dissolved hydrocarbon studies have been carried out on clear brines collected at the lowest possible depth in the recovery column.

Sample handling. The problem of handling and storing drill stem test fluids has received some attention in these studies. Since the hydrocarbons found in subsurface brines are volatile and of limited solubility, they exhibit great tendencies to escape from water solution. Consequently, exposure of the brines to the atmosphere or incomplete filling of sample containers results in serious loss of the hydrocarbons to the atmosphere or to the vapor space in the container. Three typical experiments

Table 4. Variation of benzene content of drill stem test recoveries with depth in pipe

Area	Approximate depth of test interval (ft)	Formation	Position in recovery	Benzene content of brine
1. New Mexico	5900	Paradox B	Top	0.15
			Middle	0.26
			Bottom	2.0
2. New Mexico	6100	Paradox B	Top	0.15
			Middle	0.20
			Bottom	2.7
3. Mississippi	14,100	Sligo	Top	0.25
			Middle	3.4
			Bottom	6.5

carried out to indicate the magnitude of the loss of dissolved hydrocarbons through improper handling follow:

1. Two quarts of a formation brine containing 6.2 ppm benzene were placed in a loosely covered 1-gal bottle. The sample was stored at room temperature for a period of three days. Subsequent analyses of the brine showed the presence of only 2.0 ppm benzene. Under these conditions, an apparent loss of 68% of the benzene occurred.
2. A brine sample containing finely divided suspended matter was examined by the extraction and gas chromatographic methods described above. The direct gas chromatographic analyses of a fresh sample of the unexposed brine yielded a value of 2.8 ppm benzene. In the analyses by the extraction procedure, a period of 4 hr was required for filtration. The apparent benzene concentration of the brine after this long exposure to the atmosphere was 1.5 ppm; almost one-half of the dissolved benzene had escaped from the brine.
3. A 1 N NaCl solution containing 4.3 ppm benzene was placed in a polyethylene bottle and set aside for one month. Analysis of the brine after this period showed a concentration of only 0.46 ppm benzene. Adsorption and diffusion of benzene through the polyethylene reduced the benzene concentration by almost 90%.

Duplicate tests. The extreme test of the reproducibility of the benzene content in subsurface brines was performed using fluids obtained from independent drill stem tests of a single porous horizon from a single well. During the course of this study six of these tests have been made. In each of the six examples (Table 5), the subsurface units were tested immediately after penetration; the wells were subsequently drilled to deeper objectives and, before plugging and abandoning, the same units were retested.

The time interval between the repeat tests in five of the examples in Table 5 was a few weeks. In example No. 5, the second test was made 3 months after the first. The duplicate test samples for four of the examples yielded reproducible benzene

Table 5. Benzene content of brines from multiple tests of a single horizon

	Approximate depth of tested interval (ft)	Horizon tested	Benzene content of brine (ppm)	
			1st test	2nd test
1.	10,300	Permo Penn Sandstone	0.0	0.0
2.	7500	Mississippian Dolomite	0.2	0.2
3.	4500	Lower Mississippian Ls.	1.1	0.6
4.	1900	Lower Cretaceous Ss.	1.5	1.8
5.	5600	Lower Cretaceous Dolomite	2.3	2.3
6.	9700	Middle Devonian Reef	7.6	7.6

values. The benzene concentrations of only two of the duplicate brine sets showed discrepancies beyond the average repeatability of the analytical methods.

The results of the above tests argue strongly for the validity of the benzene content of subsurface brines when proper precautions are taken in the collection, preservation and analysis. The data are all the more striking when it is considered that each of the duplicate samples was subjected to all of the possible hazards noted in this section. A note of caution must be made however, by pointing out that one of the samples in example No. 3 had an apparent benzene content of little more than one-half that of its duplicate.

Occurrence and significance of hydrocarbons in formation brines

Benzene in oil field brines. The contact of petroleum with water results in a partitioning of the hydrocarbons between the two phases. This partition is dependent on the activities of the hydrocarbons in each phase. In practice, only the aromatic hydrocarbons, and possibly the lowest molecular weight saturated hydrocarbons, partition favorably enough towards water to result in a significant release of hydrocarbons from the crude oil. In principle, an analogous situation should exist in the subsurface at the oil-water contact.

In order to determine the magnitude of the concentration of dissolved hydrocarbons in oil field waters, samples of brines co-produced with crude oils from a number of oil fields have been examined. The samples were collected from drill stem tests or from wells producing crude oil and brine. The precautions in sampling drill stem test fluids have already been discussed; samples from producing wells were obtained at the well head prior to any treatment. The water was immediately separated from the crude oil and handled in the same manner as drill stem test brines.

The benzene concentrations of a number of co-produced brines, Table 6, give an indication of the extent of variability of the hydrocarbon contents in the waters in immediate contact with crude oil accumulations; two examples are also given of the absence of benzene in brines from gas fields. Although the magnitude of the benzene concentrations may be expected to be related to the benzene concentrations in the contacting crude oil, considerable variability in brine-benzene/crude oil-benzene ratios exist on comparison of the data obtained from a number of petroleum regions. A more accurate expression of the partition of benzene between the crude oil and water is dependent on the activity of this hydrocarbon in each phase. Thus, the

Table 6. Benzene content of brines co-produced with crude oil

Field	Area	Formation	Type of production	Benzene content of brine (ppm)
1. Gwinville	Mississippi	Eagle Ford	Condensate	18.6
2. Bough	Lea Co., N.M.	Pennsylvanian	Crude oil	10.7
3. Golden Spike	Alberta, Can.	Basal Quartz	Crude oil	7.1
4. Lampman	Saskatchewan, Canada	Frobisher-Alida	Crude oil	7.0
5. Keystone	Crane Co., Texas	Holt	Crude oil	5.6-4.7
6. Stettler	Alberta, Canada	Leduc	Crude oil	6.0-4.8
7. Stettler	Alberta, Canada	Nisku	Crude oil	6.0-4.9
8. Darst Cr.	Texas	Edwards Ls.	Crude oil	0.21
9. Braeburn	Alberta, Canada	Permo Penn	Gas	0.0
10. Hereford	Alberta, Canada	Viking	Gas	0.0

chemical compositions of the crude oils, the salts and their concentrations in the brine, and the temperature-pressure conditions in the subsurface are all factors which enter into this expression. Research aimed at relating these factors to the results obtained from the field samples are in progress and will be reported in a subsequent publication.

Horizontal distribution in brines of petroleum-bearing formations. Since formation brines at the oil-water contact contain dissolved hydrocarbons released from the crude oil, it can logically be expected that the reflection of the oil pool can also be found in the brines in the general vicinity of the field. Brine samples from tests in several petroliferous regions, covering barren and producing horizons, from development and wildcat wells have been analyzed to determine the extent of the petroleum-derived hydrocarbon distributions in formation brines. In Table 7, typical variations in the benzene concentrations in brines from producing formations are given. Each series represents samples from the vicinity of a single oil field, or a group of neighboring fields. In these instances, the benzene concentration in the formation brines is seen to decrease with increasing distance from the near-by oil field. The results indicate that the presence of hydrocarbons in the brine not only reflects the presence of an oil field, but also that the concentrations of the hydrocarbons are to some extent related to the distances from the oil fields.

Vertical distribution of benzene in brines. The data given in Table 7 show that measurable quantities of dissolved hydrocarbons occur in subsurface brines in producing horizons at a substantial distance from the oil field. In order to determine whether the hydrocarbons in a brine are specific only to the oil-bearing porous rock unit, a number of brine samples collected from horizons above and below a producing member have been studied. In almost all instances encountered in these studies, brines recovered from horizons which are known to be barren in the general area

Table 7. Variation of benzene content of formation brine with distance from production

Area	Formation	Benzene content of brine (ppm)	Distance to production in equivalent zone (miles)
1. New Mexico	Pennsylvanian	10.7	0
		6.5	2
2. Saskatchewan, Canada	Frobisher-Aldia	7.0	0
		4.5	1
		3.4	$\frac{3}{4}$
		2.2	$1\frac{3}{4}$
		1.6	$1\frac{1}{2}$
		1.0	$5\frac{1}{2}$
3. Alberta, Canada	Leduc	6.0-4.8	0
		3.4	$\frac{1}{2}$
		2.2	$1\frac{1}{2}$
		1.8	$2\frac{3}{4}$
		1.6	$2\frac{3}{4}$
4. West Texas	Wolfcamp	2.5	0
		1.2	$\frac{3}{4}$
		1.3	$2\frac{1}{2}$
		0.9	5
		0.0	16

gave negative tests for benzene. The results obtained on a few typical examples are given in Table 8. The last example is of extreme interest in that the brine sample from a unit separated by only 90 ft of shale from an oil pool contained only a trace (less than 0.02 ppm) of benzene.

It is apparent from the results that the presence of hydrocarbons in formation brines reflects the petroleum potential of the horizon from which the brine was obtained; minimum thicknesses of shale having low permeability appear to prevent

Table 8. Variation of benzene content in brines from wells with multiple tests

Area	Interval tested (ft)	Formation	Benzene content of brine (ppm)	Production in equivalent zone
1. Saskatchewan	2950-2980	Viking	0.0	None
	3265-3436	Blairmore	0.0	None
	3415-3436	Blairmore	0.0	None
	3510-3530	Blairmore	0.0	None
	3858-3875	Jurassic	0.0	None
	3993-4002	Jurassic	0.0	None
	4645-4655	Frobisher-Aldia	(oil)	0 mile
2. Saskatchewan	2929-2969	Blairmore	0.0	None
	3649-3685	U. Shaunavon	0.0	None
	3739-3760	L. Shaunavon	0.0	None
	4220-4230	Frobisher-Aldia	(oil)	0 mile
3. Saskatchewan	4419-4459	Midale	6.8	$\frac{1}{2}$ mile
	4490-4502	Frobisher-Aldia	trace	

the movement of these hydrocarbons from one porous rock unit to another. The lack of transport of the dissolved hydrocarbons across rock boundaries may result from the very tortuously distributed low porosity of the fine-grained shales and from the adsorption of hydrocarbons on the surface of the clay mineral constituents in the shale.

CONCLUSIONS

Methods have been developed for the analysis of dissolved hydrocarbons in subsurface brines. Concentrations of benzene as low as 0.01 ppm can be determined. The application of these methods to the determination of the significance of hydrocarbons in subsurface brines requires the collection of representative formation fluids, and the preservation of the fluids in a manner which will not permit loss of the dissolved hydrocarbon. The precautions which have been outlined are required to minimize sampling and handling errors.

Studies of the occurrence of benzene in oil field brines have shown that the waters in immediate contact with the oil pool contain measurable amounts of this hydrocarbon. Brines from oil-productive horizons in the vicinity of oil fields also show measurable benzene concentrations, whereas no detectable benzene has been found in a number of brine samples from formations which are barren in the areas tested. These observations suggest that the occurrence of benzene in subsurface brines is a direct indicator of the presence of an oil accumulation in the area and that this positive indicator reflects the crude oil potential of the tested horizon. Finally, several instances have been given in which the concentration of benzene dissolved in formation brines decreases with increasing horizontal distance from the nearby oil field.

The results of this study have culminated in a method applicable to exploration for petroleum. This method should provide valuable additional information to the geological and geophysical evaluations of prospective petroleum areas. In addition, knowledge of the horizontal and vertical distribution of hydrocarbons dissolved in subsurface brines have potential value in the evaluation of the natural processes effective in the migration and accumulation of petroleum. The restriction of movement of dissolved benzene across formation barriers, noted in this research study, is an example of this potential.

Acknowledgments—The authors wish to thank Dr. W. E. HANSON for his suggestions on the selection of benzene for this study, and the personnel of the Gulf Oil Corporation and The British American Oil Company for their help in obtaining the brine samples.

REFERENCES

- ANDREWS L. J. and KEEFER R. M. (1949) Cation complexes of compounds containing carbon-carbon double bonds. IV. The argentation of aromatic hydrocarbons. *J. Am. Chem. Soc.* **71**, 3644.
- BOHON R. L. and CLAUSSEN W. F. (1951) The solubility of aromatic hydrocarbons in water. *J. Am. Chem. Soc.* **73**, 1571.
- BUCKLEY S. E., HOCOTT C. R. and TAGGART M. S., JR. (1958) *Habitat of Oil* (editor L. G. Weeks), p. 850. American Association of Petroleum Geologists.
- COGGESHALL N. D. and HANSON W. E. (1956) Method of geochemical prospecting. U.S. Patent 2,767,320.
- KORTSENSHTEIN V. N. (1961) New data on the hydrogeochemistry of ground waters in cretaceous deposits of the Bukhara-Khiva oil and gas Province in connection with problems of the origin of gas Deposits. *Doklady Akad. Nauk USSR* **137**, 162-165.

- LONDON E. E., ZORKIN L. M. and VASILEV E. W. (1961) Principles of evaluating gas-bearing prospects from the composition and pressure of gases dissolved in subsurface waters. *Geol. Nefti i Gaza* **5**, 35-40.
- MCDEVIT W. F. and LONG F. A. (1952) The activity coefficient of benzene in aqueous salt solutions. *J. Am. Chem. Soc.* **74**, 1773.
- SAGE J. F. (1958) *Subsurface Geology in Petroleum Exploration* (editors J. D. Haun and L. W. LeRoy), Pt. 2, p. 251. Colorado School of Mines, Golden, Colorado.
- SCHOELLER H. (1955) Geochimie des eaux souterraines: application aux eaux des gisements de petrole. *Rev. inst. franc. petrole.* **10**, 507, 671.

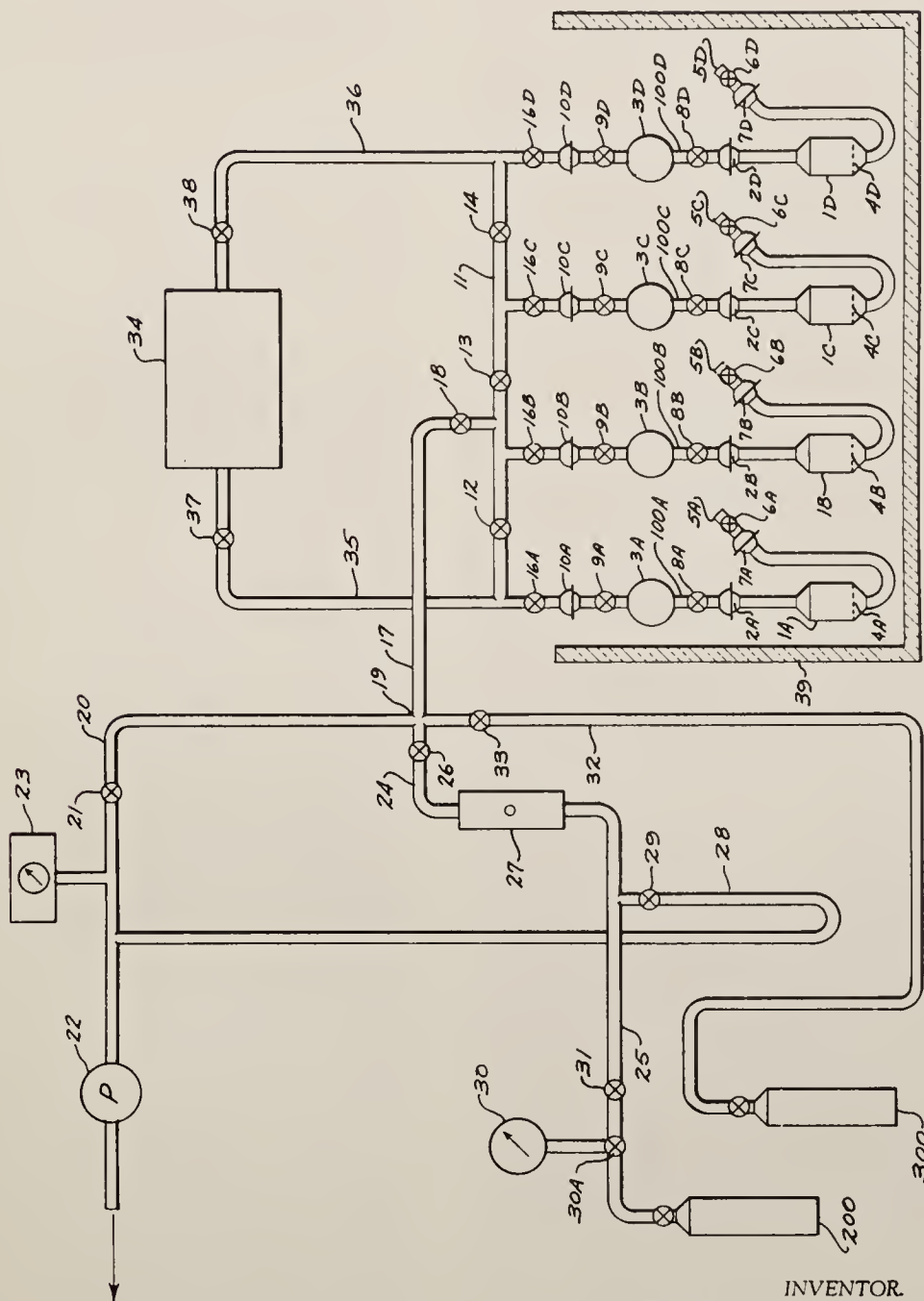
Oct. 31, 1967

W. F. BENUSA ET AL

3,349,625

ADSORPTION MEASURING APPARATUS AND METHOD

Filed Jan. 10, 1964



INVENTOR.
WILLIAM F. BENUSA &
NORMAN D. COGGESHALL
BY

Edward G. Cook
ATTORNEY

1

3,349,625

ADSORPTION MEASURING APPARATUS AND METHOD

William F. Benusa and Norman D. Coggeshall, Verona, Pa., assignors to Gulf Research & Development Company, Pittsburgh, Pa., a corporation of Delaware
Filed Jan. 10, 1964, Ser. No. 336,974
7 Claims. (Cl. 73—432)

Our invention provides a method and apparatus for directly measuring chemisorption of a gas on a solid material which has both chemisorbing and physically adsorbing components. In a particular embodiment, the chemisorption so measured indicates quantitatively the chemical composition of the surface of a solid catalyst, such as a supported platinum catalyst, and thus provides information useful in research on catalysts of that type and in evaluation of catalysts whose purchase and commercial application are under consideration.

Previous to the development of our invention, chemisorption on a solid material which contained both chemically and physically adsorbing components ordinarily has been measured indirectly. The reason is that chemisorption and physical adsorption occur together, and therefore it generally has been thought necessary first to measure both chemical and physical adsorption on the solid material under consideration, then to measure separately on a corresponding sample containing only the physically adsorbing components of the first sample the physical adsorption of the same gas, and finally to subtract the measurement made on the second sample from that made on the first. Not only is this double measurement inconvenient, but, in addition, it may provide results both imprecise and inaccurate. This is particularly true when, as often happens, physical adsorption is responsible for a large proportion of the total absorption—that is, of the sum of physical and chemical adsorption—for the chemisorption must then be calculated by subtracting from the total adsorption (a relatively large number) the physical adsorption of the control sample (a relatively large number) to obtain the chemisorption (a relatively small number). Although differential measurements of some phenomena have been proposed for avoiding some of the difficulties mentioned above, no technique for actually accomplishing this end has been suggested.

In accordance with the present invention, the inconvenience, impreciseness, and inaccuracy of prior practice is overcome by the provision of a method and apparatus for measuring directly the chemisorptive ability of a solid material which comprises both chemisorbing and physically adsorbing components. In our method, we employ a measured first sample representative of the aforesaid solid material, that is, a "chemisorbing" sample, and a measured second sample (preferably of substantially identical magnitude) of a solid material consisting only of non-chemisorbing components of the type and in the relative proportion of those present in the first sample, that is, a corresponding non-chemisorbing or "physically adsorbing" sample. For example, if we wish to measure the chemisorption of hydrogen by the platinum component of a hydrocracking catalyst comprising platinum supported on silica-alumina, we may employ as the first sample one gram of the platinum hydrocracking catalyst and as the second sample one gram of the silica-alumina support.

Further, in accordance with the method of this invention, we contact a measured chemisorbing sample with a measured amount of chemisorbable gas in a first closed system of known constant volume, and, at the same time, we contact a measured sample of the corresponding physically adsorbing material in a second closed system of

2

known and constant volume. These systems, preferably substantially identical, are brought to chemisorption conditions, as, for example, by heating in a furnace, to effect chemisorption on the chemisorbing sample, and the pressure difference between the systems is then measured by a suitable differential pressure-measuring device, for example, a differential oil manometer. The differential pressure so measured is indicative directly of the amount of gas chemisorbed by the first sample. This amount is in turn indicative of the ability of this sample to chemisorb gas and, when divided by the weight of the chemisorptive sample, provides as the quotient the specific chemisorptive ability of the chemisorbing sample. Under assumptions which have been established as correct for supported platinum catalysts, this information can be employed to compute the surface area of the platinum on a gram of catalyst and can be combined with BET (Brunauer-Emmett-Teller) surface-area measurement information to determine the proportion of the surface of the catalyst which is occupied by platinum, and the present invention includes such combination of measurement processes.

In accordance with the apparatus of our invention, there are provided a pair of systems of substantially constant and known volume, each comprising a reservoir of constant and known volume and a sample container of known volume. Each reservoir is connected to its respective sample container by a gas flow means, such as a length of glass tubing, which is provided with valve means, such as a stopcock for alternately connecting and isolating each such reservoir and its corresponding sample container, and conveniently with a separable fitting, such as a spherical glass joint. Each reservoir is also connected to a pressure-measuring device, for example, a mercury manometer. Additionally, each gas reservoir is provided with a gas flow means for connecting the gas reservoir to a source of chemisorbable gas, such as a cylinder of hydrogen. In each last-mentioned gas flow means is positioned a valve means, such as a stopcock, for alternately connecting and isolating said source and said reservoir.

In a preferred embodiment of our invention, the two reservoirs are interconnected by a gas flow means, such as a length of glass tubing, provided with valve means, such as a stopcock for alternately connecting and isolating said reservoirs from each other. During charging of the reservoirs with chemisorbable gas, the last-mentioned valve means is left open. When, after charging, this valve means is closed, the reservoirs will be at equal pressure. By this procedure it is assured that the amounts of chemisorbable gas employed will remain in constant ratio and that when, as we prefer, reservoirs of substantially equal volume are employed, substantially equal amounts of gas will be charged to each system. Further in accordance with the apparatus of our invention, there is provided a differential pressure-measuring means, suitably, for example, of the diaphragm, manometric, or strain-gauge types, so connected to the above-described systems as to measure the difference in pressure between them.

With brief reference to the drawing, the figure is a schematic representation of an apparatus suitable for directly measuring chemisorption of a gas on a solid material having both chemisorbing and physically adsorbing components.

Now with more detailed reference to the figure symbols 1A, 1B, 1C and 1D designated sample containers suitable for containing either chemisorbing or physically adsorbing samples in the practice of our invention. Symbols 3A, 3B, 3C and 3D denote gas reservoirs of known and constant volume, each reservoir being connected by a suitable gas-tight fitting, denoted by symbols

2A, 2B, 2C and 2D to a respective sample container. Attachment means to be suitable must prevent significant leakage of air from the ambient atmosphere to the interior of the reservoirs and sample containers and must, at the same time, allow gas flow between each reservoir and its respective sample container. Conventional ball-and-socket ground-glass joints form suitable and convenient attachment means.

With continuing reference to the figure, symbols 4A, 4B, 4C and 4D designate sample support means, suitably fritted disks, which serve to retain the sample during preparative processing, as will appear below. Symbols 5A, 5B, 5C and 5D designate venting means, fitted with valve means, suitably stopcocks, designated by symbols 6A, 6B, 6C and 6D, for venting the respective sample chambers at appropriate times. Symbols 7A, 7B, 7C and 7D denote gas-tight fittings, such as conventional ball-and-socket ground-glass joints, which allow detachment of venting means from the main body of sample containers 1A, 1B, 1C and 1D. The venting means are used during sample preparation as, for example, during pretreatment of the sample with flowing hydrogen. When the gas being vented is explosive, venting means 5A, 5B, 5C and 5D are advantageously provided with venting hoses, not shown, to conduct the explosive gas away to a safe place.

Symbols 100A, 100B, 100C and 100D denote gas flow means, which connect the reservoirs to their respective sample containers. Symbols 8A, 8B, 8C and 8D designate valve means, suitably stopcocks, for example, for closing off gas flow in, respectively, gas flow means 100A, 100B, 100C and 100D during charging of the reservoirs with gas, and for connecting reservoirs 3A, 3B, 3C and 3D to their corresponding sample containers 1A, 1B, 1C and 1D during the sorption phase of the cycle.

Symbols 9A, 9B, 9C and 9D designate valve means, suitably stopcocks. Said valve means are in the open position during charging and evacuation of the gas reservoirs and during interconnection of the reservoirs with the differential pressure-sensing means to be described below. Symbols 10A, 10B, 10C and 10D denote attachment-detachment means, which may be of the same type as attachment-detachment means 2A, 2B, 2C and 2D and which form gas-tight connections between the reservoirs and the sources of gas and between the reservoirs and the differential pressure-sensing means.

It will be appreciated that each reservoir and the respective sample container to which it is connected constitute a system of known, substantially constant volume. For example, the volume of reservoir 3A is defined by its walls, valve means 8A and valve means 9A.

The use of substantially constant volume systems coupled with measurement of pressure differential between, in accordance with the present invention, is especially advantageous in that it renders the method and apparatus particularly constantly sensitive, accurate, and adaptable to automation. In differential pressure-measuring apparatus, high and essentially constant sensitivity is attainable over large ranges of differential pressure so that the differential pressure-measuring device requires no attention or adjustment of sensitivity between one measurement and the next, thus rendering the method and apparatus of the present invention easily adaptable to automation. Moreover, with apparatus of the highly developed differential pressure-measuring art, readings are obtained which are continuous functions of the differential pressure being measured. In contrast, volume-change measurements have been fraught with problems of highly variable sensitivity and inaccuracy. This highly variable sensitivity sometimes necessitates readjustment of the volume-measuring apparatus after each measurement, thus rendering this apparatus unsatisfactory for automatic operation. Moreover, apparatus for volume-change measurement have produced step-function outputs, only approximating the volume changes whose measurement has

been sought. These disadvantages, highly variable sensitivity and inaccuracy, have not been corrected because measures taken to reduce the one have increased the other and vice versa.

Attempts to measure volume changes in terms of concentration have also encountered difficulty, especially with respect to adaptation to automation, for they involve measurement of a differential change which takes place over a period of time. Such changes are recorded as broad, short peaks on recording charts, which are difficult to integrate accurately. Differential pressure-measurement on the other hand, which is employed in the method and apparatus of the present invention, is easily adapted to automation.

The sizes of the reservoirs and sample containers are chosen to provide a conveniently measurable pressure decrease during sorption of gas by the samples. This pressure decrease will be dependent on the magnitude of the samples of solid materials whose chemisorptive abilities are to be measured, on the specific sorptive (both physically adsorptive and chemisorptive) ability of the said material for the gas being sorbed, on the amount of gas initially charged to the reservoirs, and on the sum of the volumes of the sample containers and their respective reservoirs. For example, in studies of supported platinum catalysts, one gram samples of catalyst and of catalyst support have been employed with satisfactory results in sample containers of 10 ml. volume associated with gas reservoirs of 10 ml. volume filled with hydrogen initially at 200 mm. Hg pressure at ambient temperature (20° C.). The catalysts of these studies had specific sorptive capacities of the order of about 10 micromoles of hydrogen per gram at sorptive conditions pertaining in the system [2 hours at 250° C. followed by reduction in temperature to ambient (20° C.) before measurement of differential pressures between reservoir-sample container systems]. The amount of hydrogen charged to each reservoir was therefore about 110 micromoles. Sorption, then, resulted in a pressure decrease of the order of 10 mm. Hg, an order of magnitude easily measured manometrically.

It will be appreciated, of course, that the value measured in the method of this invention is a pressure difference between two sample container-reservoir systems and that this difference will generally be less, and may be much less, than the greater of the pressure decreases brought about by sorption in each of the systems.

Numerical 11 designates a valved manifold which provides for connecting closed, constant volume, reservoir-sample container systems 1A-3A, 1B-3B, 1C-3C, and 1D-3D to, in succession, evacuating means 22, source of chemisorbable gas 200, source of inert gas 300, and differential pressure-measuring means 34. Numerals 12, 13, 14, 16A, 16B, 16C, 16D and 18 denote valve means, suitably stopcocks, by which the desired of the said connections is accomplished. Thus, for example, for evacuating systems 1A-3A, 1B-3B, 1C-3C and 1D-3D, valve means 8A, 8B, 8C, 8D, 9A, 9B, 9C, 9D, 16A, 16B, 16C, 16D, 12, 13, 14, and 18 will be in "open" position whereas valve means 6A, 6B, 6C and 6D will be in closed position. For charging reservoirs, 3A, 3B, 3C and 3D with chemisorbable gas, valve means 6A, 6B, 6C, 6D, 8A, 8B, 8C and 8D will be in closed position while the other above-said valves are in their open positions. For measuring the differential pressure between, for example, systems 1A-3A and 1B-3B, valve means 6A, 6B, 12, 16C, 16D and 18 will be closed whereas valve means 8A, 8B, 9A, 9B, 16A, 16B, 13 and 14 (and 37 and 38 described below) will be open.

Numerals 35 and 36 designate branches of manifold 11 which connect manifold 11 to differential pressure-measuring means 34. Numerals 37 and 38 denote valve means, such as stopcocks, by which the differential pressure-measuring means 34 may be isolated from the remainder

of the apparatus when the differential pressure-measuring means is not in use.

Differential pressure-measuring means 34, referred to above, may be of any type suitable for the differential pressure range encountered in carrying out the method of the invention. This differential pressure will always be less than the highest absolute pressure in the systems, 1A-3A, 1B-3B, 1C-3C and 1D-3D, and will generally be less than about 25 mm. Hg. Commercial differential pressure-measuring devices, such as Sanborn Differential Pressure Transducer No. 613 DMS2 together with Sanborn Transducer Amplifier and Indicator Model 311, manufactured by the Sanborn Company of Waltham, Mass., are conveniently employed, but simple differential pressure-measuring devices assembled from standard laboratory equipment, for example, a differential oil manometer or a differential mercury manometer, are also employed with satisfactory results. If the differential pressure-measuring means employed effects during measurement (or effects measurement by virtue of) a change in the volume of each of the systems with which it is connected, then such change in volume should be insignificant with respect to the total volume of each of the systems, so that the volume of the systems remains substantially constant. Particularly, such change in volume should not exceed a value corresponding to the smallest differential measuring instrument sensitivity acceptable for chemisorption measurements for which the apparatus embodying the instant invention is designed.

Evacuating means 22 is suitably an oil diffusion pump backed by a mechanical pump. Numeral 23 refers to a vacuum gauge, such as a cold cathode discharge gauge, which functions to determine whether the apparatus is leak-proof and whether during evacuation of samples in sample containers 1A, 1B, 1C, and 1D all adsorbed gas has been removed.

Numeral 17 denotes a conduit means, a branch of manifold 11, connecting manifold 11 to the gas charging and evacuation sections of the system; numeral 19 denotes a conduit gas flow interconnection means; numeral 20 denotes a conduit means connecting in gas flow relation evacuating means 22 and vacuum gauge 23 through branch 17 to manifold 11. Numeral 21 denotes valve means, suitably a stopcock, for controlling gas flow in conduit means 20. Conduit means 17 and 20 together with manifold 11 allow evacuating means 22 to remove gases from systems 1A-3A, 1B-3B, 1C-3C and 1D-3D, and vacuum gauge 23 to measure the degree of evacuation in those systems.

Numeral 200, briefly referred to above, designates a source of chemisorbable gas, for example, a cylinder of chemisorbable gas, for use in the practice of the invention. The nature of the chemisorbable gas will depend on the type of solid material whose chemisorptive ability is to be determined. Both hydrogen and carbon monoxide are frequently employed as chemisorbable gases. For determining the chemisorbing ability of supported platinum catalysts, hydrogen is very suitable.

Numeral 27 denotes a flow-measuring means, for example, a Flowrotor, manufactured by Fischer-Porter, Warminster, Pa. Numeral 25 designates a conduit means connecting gas source 200 to flow-measuring means 27. Numeral 24 denotes a conduit means connecting flow-measuring means 27 to conduit intersection region 19. Numeral 26 represents a valve means, suitably a stopcock, for controlling flow through conduit 24. Numeral 30 designates a gauge for measuring the delivery pressure of chemisorbable gas from its source, for example, from a high-pressure cylinder. Numeral 30A designates an adjustable valve associated with gauge 30 for adjusting the delivery pressure of chemisorbable gas. Valve 30A and gauge 30, in concert, allow said delivery pressure to be adjusted to a desired value. Numeral 31 designates a flow control valve means, such as the SS 4M Nupro Metering Valve, marketed by Fogleman Company, Inc.,

for fine control of gas flow in conduit 25. Fine control valve 31 and flow-measuring means 27, in concert, allow adjustment and control of rate of gas flow in conduit 24. Conduits 25 and 24 along with flow-measuring means 27 and valve means 26 and 31 provide a gas-flow path by which chemisorbable gas is charged to manifold 11 and thence to systems 1A-3A, 1B-3B, 1C-3C and 1D-3D for sample pretreatment or to reservoirs 3A, 3B, 3C and 3D preparatory to measurement of chemisorptive ability of solid materials.

Numeral 28 designates a pressure-measuring means, suitably a mercury manometer, for determining the pressure of chemisorbable gas in reservoirs 3A, 3B, 3C and 3D. Together with the known volumes of the reservoirs, this pressure indicates (by the gas law) the amount of gas in each reservoir. Numeral 29 denotes a valve means, suitably a stopcock, for controlling access to pressure-measuring means 28.

Numeral 32 designates a conduit means connecting a source designated by numeral 300, of an inert, non-sorbable gas, suitably helium, to interconnection fitting 19 and thence to manifold 11 and systems 1A-3A, 1B-3B, 1C-3C and 1D-3D. Auxiliary elements, not shown, are provided in conduit means 32 to correspond to flow-measuring means 27, pressure-measuring means 28, pressure gauge 30, and valve means 30A and 31 in conduits 24 and 25. The inert gas supply system is therefore essentially similar to the chemisorbable gas supply system. Numeral 33 designates a valve means controlling flow in conduit means 32.

Numeral 39 designates a furnace, for example, an electric furnace whose temperature may be regulated by means not shown. The furnace is withdrawn, by means not shown, from the region of systems 1A-3A, 1B-3B, 1C-3C and 1D-3D when these systems are to be cooled, assembled or disassembled.

For purposes of illustration, the operation of the apparatus of the figure will be described in terms of the determination of the chemisorptive ability of three supported platinum reforming catalysts, the support for each catalyst being the same alumina. In addition, the calculation of the platinum surface area of one of these catalysts will be described. Sample tubes 1A, 1B, 1C and 1D are detached from reservoirs 3A, 3B, 3C and 3D and into each of sample tubes 1A, 1B and 1C is weighed a one gram sample of the appropriate catalyst. A one gram sample of the catalyst support is weighed into sample tube 1D. Next, the sample tubes are connected to their respective reservoirs and the outlet stopcocks 6A, 6B, 6C and 6D on the sample tubes are closed. Furnace 39 is then moved into position. With valves 30A, 31, 29 and 26, and corresponding valves (including valve 33) in the helium supply system closed, and valves 21, 37 and 38 closed, and with valves 8A, 8B, 8C, 8D, 9A, 9B, 9C, 9D, 16A, 16B, 16C, 16D, 12, 13, 14 and 18 open, valve 21 is carefully opened to evacuate reservoirs 3A, 3B, 3C and 3D and sample tubes 1A, 1B, 1C and 1D, oil diffusion pump 22 having been placed into operation.

Electric furnace 39 is then turned on and its temperature adjusted to 500° C. The apparatus is then left in this condition for two hours so that adsorbed vapors are completely removed from the supported catalyst samples in sample tubes 1A, 1B and 1C and from catalyst support in sample tube 1D.

After this two hour evacuation of the sample tubes 1A, 1B, 1C and 1D, stopcock 29 is opened to connect manometer 28 to the hydrogen inlet system and stopcock 21 is closed to isolate the vacuum pumping system from the sample container-reservoir system. Next, stopcock 26 is opened in hydrogen delivery line 24, and valve 30A is adjusted to give a hydrogen delivery pressure of three pounds per square inch as indicated on gauge 30. Fine control valve 31 is opened. Hydrogen is allowed to flow into the system until it reaches atmospheric pressure, as indicated by manometer 28. At that point, sample

tube outlet stopcocks 6A, 6B, 6C and 6D are opened and fine control valve 31 is adjusted to provide a hydrogen flow of 25–50 cc. per minute, as measured on flow-measuring device 27. Advantageously during this reduction of the catalyst samples, vent hoses (not shown) are provided on vent tubes 5A, 5B, 5C and 5D of sample containers 1A, 1B, 1C and 1D.

Reduction of the samples continues in this way for two hours, the temperature of the furnace remaining at 500° C. After that, outlet stopcocks 6A, 6B, 6C and 6D are closed and immediately thereafter fine control valve 31 is closed, as are stopcock 26, stopcock 29 and valve 30A. Then stopcock 21 is carefully opened to avoid damage by a pressure surge to the reservoir-sample container system. This system is then evacuated until a pressure lower than 10^{-4} millimeters of mercury is read on gauge 23. (If such pressure is not attained within a reasonable time, the reduction described above should be repeated and evacuation to 10^{-4} millimeters of mercury attempted again.) As soon as evacuation to 10^{-4} millimeters is successful, stopcocks 8A, 8B, 8C and 8D on reservoirs 3A, 3B, 3C and 3D are closed.

Furnace 39 is turned off and removed from sample tubes 1A, 1B, 1C and 1D to allow the sample-reservoir system to attain ambient temperature, and stopcock 26 in hydrogen line 24 is opened, and stopcock 29 is opened to connect manometer 28 to the hydrogen delivery system. Valve 30A is then adjusted to provide a hydrogen delivery pressure at three pounds per square inch, as indicated on gauge 30, and stopcock 21 is closed. Fine control valve 31 is opened to allow hydrogen to flow until a pressure of 200 millimeters mercury is read on manometer 28, whereupon stopcock 26 is closed as are also valves 30A and 31, to prevent further flow of hydrogen into the system. Stopcock 29 may be closed to protect manometer 28 from accident. At this point, pressure in reservoirs 3A, 3B, 3C and 3D is equal at 200 millimeters of mercury. Stopcocks 9A, 9B, 9C and 9D are then closed to isolate reservoirs 3A, 3B, 3C and 3D from intercommunication with one another.

Stopcocks 8A, 8B, 8C and 8D are next opened to secure gas-flow communication between reservoirs 3A, 3B, 3C and 3D and their respective sample containers 1A, 1B, 1C and 1D. To complete chemisorption of hydrogen, furnace 39 is moved into place around sample tubes 1A, 1B, 1C and 1D, and the temperature in furnace 39 is adjusted to 250° C. The apparatus is left in this condition for two hours to complete chemisorption. After this, furnace 39 is again lowered away from sample containers 1A, 1B, 1C and 1D, and thus the samples in sample containers 1A, 1B, 1C and 1D are allowed to reach ambient temperature.

The temperature of chemisorption, 250° C., has been found to give useful information about platinum on supported platinum catalysts, the chemisorption at this temperature in the pressure range employed corresponding to about one atom of chemisorbed hydrogen per atom of surface platinum. Carbon monoxide is usefully employed at lower temperature. Still lower temperature may be adequate for other types of chemisorptive reactions. For example, chemisorption of carbon dioxide on potassium oxide has been achieved at a temperature of -78.5° C.

The differential measurement characterizing the chemisorptive ability of the samples may be carried out at the temperature of chemisorption. Because, however, the chemisorption is for all practical purposes irreversible at ambient temperature, it is convenient and permissible to measure chemisorption at ambient temperature.

Stopcock 21 is opened, evacuation means 22 being in operation. When a pressure of less than 10^{-4} millimeters mercury, as read on gauge 23, has been achieved, stopcock 21 is closed, and the desired series of differential pressure measurements is begun.

In the apparatus depicted in FIGURE 1, the volume of conduits 35 and 36 and of manifold 11 and of other interconnecting conduits is insignificant with respect to the volume of reservoirs 3A, 3B, 3C and 3D and sample containers 1A, 1B, 1C and 1D. If, in equivalent apparatus, volumes of interconnecting lines are not insignificant, such volumes may be taken into account in the interpretation of the results of the differential pressure measurement. However, such interpretation is simplified when the apparatus of our invention is so constructed as to provide interconnecting conduit means of volume insignificant with respect to the volumes of the reservoirs and sample containers.

To characterize the catalyst sample in sample container 1A with respect to the support sample in sample container 1D, stopcocks 18, 12, 13 and 14 are closed; then stopcocks 9A and 9D are opened, and finally stopcocks 37 and 38 are simultaneously opened. This results in a differential pressure reading on differential pressure-measuring device 34, and this reading may be recorded automatically or manually.

To prepare for a subsequent differential pressure determination, stopcocks 37, 38, 16A and 9A are closed.

When, as in the apparatus of the figure, the volume of conduits 35 and 36, of manifold 11, and of other interconnecting conduits is insignificant with respect to the volume of reservoirs 3A, 3B, 3C and 3D and sample containers 1A, 1B, 1C and 1D, a subsequent differential pressure determination may be undertaken without intermediate operations. When, on the other hand, the volume of interconnecting conduits such as 35 and 36 and manifold 11 is not insignificant with respect to the volume of reservoirs and sample containers, then advantageously the conduits which will connect the differential pressure-measuring system to the catalyst sample container-reservoir system to be employed in the subsequent differential pressure determination are evacuated. In apparatus that functions in the same manner as that of the figure, but that has significantly voluminous interconnecting conduits, such evacuation can be accomplished by opening valves corresponding to stopcocks 12, 18 and 21 and operating evacuation means corresponding to vacuum pump 22. After the evacuation, valves corresponding to stopcocks 12, 18 and 21 are closed. Inasmuch as the volume of conduits 35 and 36 and of manifold 11 and of other interconnecting conduits is insignificant with respect to the volume of the reservoirs and sample containers of the figure, no further reference will be made to evacuation of interconnecting conduits between differential pressure measurements.

To determine the differential pressure between sample container-reservoir system 1B–3B, sample container-reservoir system 1D–3D, stopcocks 9B and 12 are opened. Then, stopcocks 37 and 38 are simultaneously opened to provide a differential pressure reading on gauge 34. This reading may be recorded manually or automatically. To prepare for a subsequent differential pressure reading, valves 37 and 38 are closed and stopcocks 16B and 9B are closed.

To characterize the catalyst sample in sample container 1C with the catalyst support sample in sample container 1D, stopcock 9C is opened and stopcock 13 is opened. Then, stopcocks 37 and 38 are simultaneously opened to provide a differential pressure reading on differential pressure-sensing means 34. This reading is recorded automatically or manually.

For a more nearly exact determination of chemisorptive ability, the differences in intrinsic densities of the catalyst (and hence differences in dead space in their respective systems) may be taken into account. To prepare catalyst and catalyst support samples in sample containers 1A, 1B, 1C and 1D, stopcocks 37 and 38 are closed, and stopcocks 14, 18, 16A, 16B, 9A, 9B and 21 are opened. Furnace 39 is moved into place and adjusted to 500° C. The evacuating means 22 is placed in operation.

When a pressure lower than 10^{-4} millimeters has been attained as indicated by gauge 23, stopcock 21 and stopcocks 8A, 8B, 8C and 8D are closed. The differential pressure resulting from interaction of the samples with helium supplied through line 32 controlled by stopcock 33 is determined in a manner exactly analogous to that described above for hydrogen. As in the above-described procedure for hydrogen, reservoirs 3 should be initially pressured to 200 millimeters of mercury.

In one instance when one gram of a platinum-on-alumina catalyst was in sample tube 1A and one gram of its support was in sample tube 1D, differential hydrogen and helium pressure readings determined as described above were 9.69 millimeters and 0.50 millimeter of mercury, respectively, in each instance the pressure in reservoir 3A exceeding that in 3D. The helium reading reflects, of course, a difference between the volumes of the catalyst and catalyst support samples corresponding to one gram, that is, the difference in their densities. The difference between these differential pressure readings, 9.19 millimeters, may be multiplied by the sum of the volume of reservoir 3A and the volume of sample container 1A, in this instance the sum being 20 millimeters, and that product divided by the product of the gas constant (in appropriate units) and the absolute ambient temperature (in this instance 293.2°K.) to give the specific chemisorption of hydrogen per gram of catalyst, namely 10.07 micromoles per gram. This is attributable to the platinum alone.

Because each surface atom of platinum is associated with a single hydrogen atom, the platinum surface area may be computed from the above-described measurement and the known density of platinum. In particular, this area in square meters per gram is determined by multiplying the specific adsorption due to platinum (micromoles per gram) by 0.1073. For the catalyst described above, this gives a platinum surface area of 1.08 square meters per gram.

It will be apparent that the method and apparatus of the instant invention, disclosed primarily in terms of measurement of the specific chemisorptive ability of solid materials, will also serve for any differential characterization of one solid material with respect to another whenever that characterization is accomplished by interaction of the solid materials with a gas.

Our invention is not to be construed as limited by the embodiment we have described above, but is limited only as defined explicitly or simplicity in the appended claims. We claim:

1. A method for determining directly the chemisorptive ability of a solid material comprising chemisorbing and physically adsorbing components, the method comprising (1) contacting a measured first sample of solid material in a closed system of known, substantially constant volume with a measured amount of chemisorbable gas so as to effect both chemisorption and physical adsorption of said by the sample, contacting in like manner in a second closed system of known, substantially constant volume with a second measured amount of the same chemisorbable gas a second measured sample of a second solid material consisting essentially of non-chemisorbing components of the same kind and in the same relative proportions as in the first sample so as to effect physical adsorption of said gas by the sample, and (2) measuring the difference in gas pressure between the first closed system and the second closed system, the difference in gas pressure so measured being indicative of the amount of gas chemisorbed by the first sample, the amount of gas chemisorbed being, in turn, indicative of the chemisorptive ability of the first solid material.

2. A method for determining directly the specific chemisorptive ability of a first solid material comprising chemisorbing and physically adsorbing components, the method comprising (1) contacting a weighed first sample of said first solid material in a first closed system of known, substantially constant volume with a first measured amount of both chemisorbable gas so as to effect both chemisorp-

tion and physical adsorption of said gas by the sample, and contacting a second sample of a second solid material in like manner in a second closed system of volume substantially equal to that of said first closed system, with a second measured amount of the same chemisorbable gas, this second amount being substantially equal to the first measured amount of this gas, said second sample having a weight substantially equal to that of the first sample and consisting essentially of non-chemisorbing components of the same kind and in the same relative proportions as in the first sample so as to effect physical adsorption of said gas by the sample, and (2) measuring the difference in gas pressure between the first closed system and the second closed system, the difference in gas pressure so measured being indicative of the amount of gas chemisorbed per unit weight of the first sample, this amount of gas, in turn, being indicative of the chemisorptive ability per unit weight of the first solid material.

3. The method of claim 2 where the first solid material is a supported platinum catalyst and the second solid material consists of the support material.

4. A method for determining directly the specific chemisorptive ability of a solid material comprising chemisorbing and physically adsorbing components, the method comprising (1) so contacting a weighed first sample of the solid material in a closed system of known, substantially constant volume with a first measured amount of chemisorbable gas as to effect chemisorption of said gas by the sample, (2) contacting a second sample in like manner in a second closed system of volume substantially equal to that of said first closed system with a second measured amount of the same chemisorbable gas, this second amount being substantially equal to the first measured amount of the same chemisorbable gas, said second sample having a weight substantially equal to that of the first sample and consisting essentially of non-chemisorbing components of the same kind and in the same relative proportion as in the first sample, (3) measuring the difference in gas pressure between the first closed system and the second closed system, (4) contacting the first sample in the first closed system with a first measured amount of non-sorbable gas, (5) contacting in like manner the second sample in the second closed system with a second measured amount of the same non-sorbable gas, this second amount being substantially equal to the first measured amount of this gas, and (6) measuring the difference in gas pressure between the first closed system and the second closed system, this difference and the difference measured in step (3), taken in concert, being indicative of the chemisorptive ability per unit weight of the solid material.

5. The method of claim 4 where the chemisorbable gas is hydrogen and the non-sorbable gas is helium.

6. A method for determining directly the specific chemisorptive ability of a first solid material comprising chemisorbing and physically adsorbing components, the method comprising (1) separating a mass of chemisorbable gas into two portions of equal pressure and substantially equal volume, (2) contacting a weighed first sample of said first solid material in a first closed system with the first of the said portions of chemisorbable gas so as to effect both chemisorption and physical adsorption of said gas by the sample, and contacting in like manner in a second closed system of volume substantially equal to that of the first closed system the second said portion of chemisorbable gas with a second sample of weight substantially equal to that of the first sample and consisting essentially of non-chemisorbing components of the type and relative proportion of those present in the first sample so as to effect physical adsorption of said gas by the sample, and (3) measuring the difference in gas pressure between the first closed system and the second closed system, the difference in gas pressure so measured being indicative of the amount of gas chemisorbed per unit weight of the first sample, this amount of gas, in turn, being indicative of the chemisorptive ability per unit weight of the first solid material.

7. Apparatus for determining directly the chemisorptive ability of a solid material comprising chemisorbing and physically adsorbing components, the apparatus comprising two closed systems of substantially constant volume, a first gas flow means connecting the systems and adapted to permit pressure equilibration between the systems, a pressure-measuring means connected to said gas flow means and adapted to measure the said equilibration pressure therefor between said systems, valve means for closing off the gas flow means thereby isolating said systems from each other and a differential pressure-sensing means connected to each said system and adapted to sense the differential pressure between the systems while said systems are isolated from each other, each system comprising (1) a closed gas reservoir of known volume connected to said first gas flow means, (2) a closed sample container of known volume and adapted to contain a sample of solid material, (3) second gas flow means connecting the reservoir and the sample container and adapted to facilitate rapid flow of chemisorbable gas from the said gas reservoir to the said sample container and subsequently chemisorption of said gas upon said sample, (4) valve means positioned in the second gas flow means for alternately connecting and isolating said reservoir and said sample container, (5) a third gas flow means for connecting a source

of gas to said first gas flow means, and (6) valve means positioned in said third gas flow means for alternately connecting and isolating said source and said reservoir.

References Cited

UNITED STATES PATENTS

3,059,478	10/1962	Coggeshall et al.	73—432
3,203,252	8/1965	Poinski et al.	73—432
3,222,133	12/1965	Ballou et al.	23—230

FOREIGN PATENTS

1,057,798	5/1959	Germany.
-----------	--------	----------

OTHER REFERENCES

Gruber: "An Adsorption Flow Method . . .," published in *Analytical Chemistry*, vol. 34, No. 13, December 1962, pages 1828-1829, 1830, 1831.

Article—Haul et al.—Published in *Chemie-Ingtechn*, August 1963, pages 586-589.

JAMES J. GILL, *Primary Examiner*.

RICHARD QUEISSER, *Examiner*.

C. A. RUEHL, *Assistant Examiner*.

